SpringerWienNewYork

Thomas P. Naidich, Henri M. Duvernoy, Bradley N. Delman,
A. Gregory Sorensen, Spyros S. Kollias and E. Mark Haacke

Duvernoy's Atlas of the Human Brain Stem and Cerebellum

High-Field MRI: Surface Anatomy, Internal Structure, Vascularization and 3D Sectional Anatomy

With contributions by

T. Benner	W. Boonn	F. Cattin
P. Choi	J. Delgado	P. Hof
M. Law	W. Lin	J. Linn
Y. Lui	A. Macedo	E. Manova
M. Sasaki	M. Schwartz	E. Shibata
A. Tai	C. Tang	D. Wolfe
C. Yeo	I. Yousry	T. Yousry

Drawings by Jean-Louis Vannson

SpringerWienNewYork

Thomas P. Naidich, M. D.
Professor of Radiology and Neurosurgery
Irving and Dorothy Regenstreif Research Professor of Neuroscience (Neuroimaging)
Director of Neuroradiology, Mount Sinai School of Medicine of New York University, New York, NY, USA

Henri M. Duvernoy, M. D.
Anatomist, emeritus
Laboratoire d' Anatomie, Faculté de Médecine et de Pharmacie, Université de Franche-Comté, Besançon, France

Bradley N. Delman, M. D.
Associate Professor of Radiology
Department of Radiology, Mount Sinai School of Medicine of New York University, New York, NY, USA

A. Gregory Sorensen, M. D.
Associate Professor in Radiology at Harvard Medical School
Co-Director: Athinoula A. Martinos Center for Biomedical Imaging,
Harvard Medical School, Boston, MA, USA

Spyros S. Kollias, Prof. Dr. med.
Professor of Neuroradiology, Vice-Chairman of the Institute of Neuroradiology
University Hospital of Zurich, Switzerland

E. Mark Haacke, Ph. D.
Professor of Radiology, Director: MR Research Facility
Wayne State University, Detroit, MI, USA

Printed in Austria

SpringerWienNewYork is part of
Springer Science + Business Media
springer.at

Illustrations: Figures 2.2, 2.3, 2.7, 3.6, 4.17–4.19 redrawn by Stefan Kindel
Typesetting and Printing: Holzhausen Druck und Medien GmbH, 1140 Wien, Austria

Printed on acid-free and chlorine-free bleached paper
SPIN: 12061198

With numerous (partly coloured) Figures

Library of Congress Control Number: 2007934675

ISBN 978-3-211-73970-9 SpringerWienNewYork

DEDICATIONS

We dedicate this text to those who gave of themselves to train us and to the trainees who have entrusted us with years of their lives for what we now pass on to them.

Successful completion of this project depended upon real physical and emotional support for us from colleagues, families and friends. We gratefully thank them for their encouragement during the endless hours needed to bring this material together.

Henri M. Duvernoy:	To my family – Odile, Charles and David Duvernoy
Thomas P. Naidich:	To my wife Michele, my daughter Sandra, my brother James, and the loving memory of my parents James and Rose Naidich. May this meet your expectations.
Bradley N. Delman:	To my wife Allissa and young daughter Maya, who lovingly endured my absence through many late nights and even later mornings
A. Gregory Sorensen:	To my family: Kristiina, Rachel, Caroline and Samuel
Spyros S. Kollias:	To the next generation of Neuroradiologists
E. Mark Haacke:	To all those students and faculty who have helped in our quest to take research concepts and put them into clinical practice.

ACKNOWLEDGMENTS

The authors thank the Manhattan HIV and Manhattan Hepatology Brain Banks (R24MH59724) for providing normal control brain stems for 9.4 Tesla imaging.

We deeply thank Dr. Burton P. Drayer, The Dr. Charles M. and Marilyn Newman Professor of Radiology, Chairman of Radiology and President of the Mount Sinai Hospital, Dr. Zvi Lefkovitz, Vice-Chairman of Radiology, and Dr. Zahi Fayad, Director of the Imaging Science Laboratories of the Mount Sinai Medical Center, for their strong support of this project. We give a warm and special thanks to Ronit Gilad, M.D. for her research assistance with Section IX – Cranial Nerves, and acknowledge our very large debt to Drs. Daniel Perl, Susan Morgello, and George Kleinmann of the Section of Neuropathology, Mount Sinai Medical Center for sharing their knowledge of brain stem anatomy.

We also thank Juan Gilberto S. Aguinaldo M. D., Daniel D. Samber P. E. and all of the staff of the Imaging Science Laboratories for their technical help in obtaining the 9.4 Tesla MR images. We gratefully acknowledge the imaging assistance of John C. Gentile R.T., Hanna Oltarzewska R.T., and Frank M. Macaluso R.T., B. S. for their assistance with the 3 Tesla images.

The authors also wish to acknowledge the help of those “who have directly participated in this work”:
Mr. J. L. Vannson, Mrs. J. Euvrard, Mrs. A. Barthelet, Mrs. F. Gillet, Mrs. Asya Volberg, and Ms. Elba Colman.

We greatly appreciate the expertise of Mr. Wolfgang Dollhäubl of Springer Wien New York. We would like to thank him for the very real help he gave us in laying out and producing this volume, for the elegant technical solutions he provided to tricky problems, and for the grace and patience with which he guided us toward the finished work.

CONTENTS

LIST OF CONTRIBUTORS

Thomas P. Naidich, M. D.
Professor of Radiology and Neurosurgery
Irving and Dorothy Regenstreif Research Prof.
of Neuroscience (Neuroimaging)
Director of Neuroradiology
Mount Sinai School of Medicine of New York University
One Gustave L. Levy Place
New York, NY 10029, USA
E-mail: thomas.naidich@mountsinai.org

Henri M. Duvernoy, Prof. Dr. med.
Faculté de Médecine et de Pharmacie
Université de Franche-Comté Besançon
12 chemin des Relancons, 25000 Besançon, France
E-mail: henri.duvernoy@wanadoo.fr

Bradley N. Delman, M. D.
Associate Professor of Radiology
Department of Radiology
Mount Sinai School of Medicine of New York University
One Gustave L. Levy Place
New York, NY 10029, USA
E-mail: bradley.delman@mountsinai.org

A. Gregory Sorensen, M. D.
Associate Professor in Radiology at Harvard Medical School, Co-Director: Athinoula A. Martinos Center for Biomedical Imaging
149 Thirteenth Street, Suite 2301
Charlestown, MA 02129, USA
E-mail: sorensen@nmr.mgh.harvard.edu

Spyros S. Kollias, Prof. Dr. med.
Professor of Neuroradiology
Vice Chairman Institute of Neuroradiology
Chief of Magnetic Resonance Imaging
University Hospital of Zurich
Frauenklinikstr. 10
8091 Zurich, Switzerland
E-mail: kollias@dmr.usz.ch

E. Mark Haacke, Ph. D.
Professor of Radiology
Director: MR Research Facility
Wayne State University
HUM-MR Research
G0301 Radiology
3990 John R. Road
Detroit, MI 48201, USA
E-mail: nmrimaging@aol.com

Thomas Benner, Ph. D.
Instructor in Radiology at Harvard Medical School
Athinoula A. Martinos Center for
Biomedical Imaging
149 Thirteenth Street, Suite 2301
Charlestown, MA 02129, USA
E-mail: benner@nmr.mgh.harvard.edu

William W. Boonn, M. D.
Associate Director of Clinical Imaging Informatics
Department of Radiology
Hospital of the University of Pennsylvania
3400 Spruce Street
Philadelphia, PA 19104, USA
E-mail : bill@medicalpocketpc.com

Françoise Cattin, M. D.
Service de Neuroradiologie
Centre Hospitalier Universitaire J. Minjoz
Besançon, France
E-mail: fcattin@chu-besançon.fr

Paul S. Choi, M. D.
Radiologist, East River Medical Imaging
519 East 72nd Street
New York, NY 10021, USA
E-mail: pchoi@eastriverimaging.com

Josser E. Delgado-Almandoz, M. D.
Department of Radiology, Founders 216
Harvard University School of Medicine
Massachusetts General Hospital
55 Fruit Street
Boston, MA 02114, USA
E-mail: jdelgadoalmandoz@partners.org

Patrick R. Hof, M. D.
Irving and Dorothy Regenstreif Research
Professor of Neuroscience (Neurobiology)
Chairman, Department of Neuroscience
Mount Sinai School of Medicine of New York University
One Gustave L. Levy Place
New York, NY 10029, USA
E-mail: patrick.hof@mssm.edu

Meng Law, M. D., F. R. A. C. R.
Associate Professor of Radiology and Neurosurgery
Department of Radiology
Mount Sinai School of Medicine of New York University
One Gustave L. Levy Place
New York, NY 10029, USA
E-mail: meng.law@mountsinai.org

Wen Lin, M. D.
Mount Sinai School of Medicine of New York University
One Gustave L. Levy Place
New York, NY 10029, USA
E-mail: wen.lin@mssm.edu

Jennifer Linn, Dr. med.
Department of Neuroradiology
University Hospital Munich
Marchioninistr. 15
81377 Munich, Germany
E-mail: jennifer.linn@med.uni-muenchen.de

Yvonne W. Lui, M. D.
Assistant Professor of Radiology
Department of Radiology, Albert Einstein College
of Medicine of Yeshiva University
Montefiore Medical Center
111 East 210th Street
Bronx, NY 10467, USA
E-mail: ylui@montefiore.org

Aisha A. Macedo, M. D.
Department of Ophthalmology
Mount Sinai Medical Center of New York University
One Gustave L. Levy Place
New York, NY 10029, USA
E-mail: aisha.macedo@mssm.edu

Elena Manova, M. S.
Graduate Research Assistant
Biomedical Engineering Department and
MR Research Facility
Wayne State University
818 West Hancock
Detroit, MI 48201, USA
E-mail: nmrimaging@aol.com

Michael B. Schwartz, M. D.
Department of Radiology
Weill-Cornell School of Medicine
525 East 70th Street
New York, NY 10021, USA
E-mail: michael.schwartz01@mssm.edu

Eri Shibata, M. D.
Postdoctoral Fellow
Department of Neuropsychiatry
Iwate Medical University School of Medicine
19-1 Uchimaru, Morioka 020-8505, Japan
E-mail: eshibata@iwate-med.ac.jp

Makoto Sasaki, M. D.
Assistant Professor of Radiology
Iwate Medical University School of Medicine
19-1 Uchimaru, Morioka 020-8505, Japan
E-mail: masasaki@iwate-med.ac.jp

Angela W. Tai, M. D.
Department of Radiology
Brigham and Women's Hospital
75 Francis Street
Boston, MA 02115, USA
E-mail: awtai@partners.org

David E. Wolfe, M. D.
Associate Professor of Pathology
Mount Sinai School of Medicine of New York University
One Gustave L. Levy Place
New York, NY 10029, USA

Christopher H. Yeo, Ph. D.
Professor of Behavioural Neuroscience
Department of Anatomy and Developmental Biology
University College London
London, WC1E 6BT, UK
E-mail: c.yeo@ucl.ac.uk

Cheuk Ying Tang, Ph. D.
Assistant Professor of Radiology
Department of Radiology and Imaging
Science Laboratory
Mount Sinai School of Medicine of New York University
One Gustave L. Levy Place
New York, NY 10029, USA
E-mail: cheuk.tang@mssm.edu

Indra Yousry, Dr. med. Privat Dozent
Department of Neuroradiology
Klinikum Grosshadern
Ludwig Maximilian Universität
81377 Munich, Germany
E-mail: indra.yousry@med.uni-muenchen.de

Tarek A. Yousry, Dr. med. habil, F. R. C. R.
Professor of Neuroradiology
Head, Lysholm Department of Neuroradiology
The National Hospital for Neurology
and Neurosurgery
Institute of Neurology
8-11 Queen Square, London WC1N 3BG, UK
E-mail: t.yousry@ion.ucl.ac.uk

INTRODUCTION

This study of the brain stem and cerebellum builds upon the prior publications [1–491] and presentations [A1–A9] of many investigators, and incorporates portions of our own work on the encephalon (cerebral hemispheres and diencephalon) [125], the brain stem and cerebellum [121, 123, 128], and brain vascularity [120, 122]. Large new sections have been added to reflect the great advances in anatomic MR imaging since the first edition [121]. All sagittal images have been re-oriented and relabelled to conform to standard MR display. As in the first edition, each section is organized so that early images teach the overview, while later images provide the detailed knowledge required for understanding serial anatomic and MR sections and their clinical utility.

Following a brief survey of the methods used:

Section I describes the surface anatomy of the brain stem and cerebellum as well as their location in the posterior cranial fossa.

Sections II–IV describe the internal structure of the brain stem and cerebellum and then summarize their function, to introduce the roles of individual nuclei and fasciculi within and traversing the brain stem and cerebellum.

Section V addresses the anatomy of the mesencephalic-diencephalic junction.

Section VI depicts the vascular network of the brain stem in detail and summarizes the results of the authors' prior research on both the superficial blood vessels and the intrinsic vascular territories of the brain stem [120, 122, 307, 308]. The description of cerebellar vascularization derives predominantly from the literature rather than personal investigation.

Section VII depicts the intrinsic vascular territories of the brain stem, and illustrates these with clinical images of human brain stem infarctions.

Section VIII presents near-histologic sections of the brain stem in three orthogonal planes, obtained using 9.4 Tesla magnetic resonance microscopy (MRM) of formalin-fixed human cadaver specimens. Although some details depicted in these sections are beyond present clinical imaging, we believe that future advances in MR and computer technology will render them clinically useful in the coming years.

Section IX illustrates the intra-axial and cisternal courses of the cranial nerves, to show their complete trajectories from the nuclei of origin to the exit foramina in the skull base.

Section X illustrates advanced MR techniques for depicting neuromelanin, brain iron, and fiber tract orientation, enhancing our understanding of brain stem anatomy.

Section XI correlates serial 2–4 mm thick sections of the brain in axial, coronal and sagittal planes with clinical 3 Tesla T1- and T2-weighted MR images obtained with a 32-channel surface array head coil. All the clinical MR images are of the same volunteer, studied in two sequential sessions, so the anatomic relationships shown may be correlated directly with each other and with the anatomic specimens in all three orthogonal planes. Due to individual variation in head shape (brachycephalic vs. dolichocephalic), some structures shown together on the anatomic sections are seen to lie in adjacent MR sections in vivo, and vice versa. Not all of the strucures indicated on the anatomic images are yet demonstrable on the clinical MR images. However, the locations of these important structures may be inferred on MR images from their known anatomic relationships to other, larger structures. As with the MR microscopic images, these smaller structures will become increasingly easier to display – and increasingly important to appreciate – in the near future.

This text uses the common non-Latin anatomical terminology. Latin terms are used only where common usage has not supplanted the original Latin nomenclature.

METHODS

Differing methods were used to study the surfaces of the brain stem and cerebellum, the structures and vascular networks of these regions, specific features such as neuromelanin, and the serial three-dimensional sections.

The surfaces of the brain stem and cerebellum

Thirty human encephala were examined following fixation in a 10% formalin solution sufficiently voluminous to prevent their distortion. Both cerebral hemispheres were removed. What remained thus comprised the brain stem, cerebellum, and diencephalon. These structures were immersed in a 30% alcohol solution and then dissected under a stereoscopic microscope and photographed in distilled water to prevent degradation of the images by light reflections. So far as possible, each specimen was photographed in three oblique views to provide anatomic references for the specific section illustrated.

The structures and vascular network of the brain stem and cerebellum

The material and methods used in this study are derived from previous works [119, 120, 122, 123, 127, 128, 129, 130, 131]. Sixty brains were examined after having undergone two processes: intravascular injection with India ink and plastics, and Bodian's method of silver impregnation.

Intravascular injection (Capillary maps)

The brains were injected with 400 cm^3 of a solution containing India ink and 5% gelatin. After fixation, dehydration, immersion into toluene, and embedding in paraffin, the relevant portions were cut into serial thick sections (400 μm), which were then cleared in a Spalteholz solution (methylsalicylate and benzyl benzoate). Intravascular injection with low viscosity resin (Mercox) completed the previous study, and further defined the fine vascular network and its spatial organization. After injection, the perivascular tissue was removed and the vascular network was examined with a scanning electron microscope.

The complementary India ink and resin injection techniques provided a "map" of differences in capillary density across the brain stem. The density of injected capillaries varied sustantially from gray matter (higher capillary density) to white matter (lower capillary density) and even varied among different gray matter nuclei. These "capillary maps" enabled specific localization and identification of dense, highly vascular gray matter nuclei and the adjacent less dense, less well vascularized white matter tracts.

Bodian's method of silver impregnation

A specific advantage of the India ink injection technique is that it permits use of subsequent histological techniques, such as the Bodian silver impregnation technique, to confirm the anatomic analysis. Specifically, use of serial thick sections showing the vascular pattern and alternating thin silver-impregnated sections showing the anatomic structures, enabled us to characterize the patterns of vascularization of the gray matter of the brain stem and cerebellum. However, these methods provide only limited depiction of white matter, so only large fasciculi can be appreciated directly (e. g., corticospinal tracts, medial lemnisci, medial longitudinal fasciculi, and central tegmental tracts). The numerous smaller fasciculi of the brain stem (**seen on Figs. 2.7–2.22**) were localized only through their known relationships to the gray nuclei actually displayed.

The superficial blood vessels and brain stem vascular territories

The same India ink injection methods successfully display the overlapping arterial and venous networks of the superificial pial vasculature of the brain stem (**Figs. 6.1–6.36**). Using a stereoscopic microscope to examine

2–3 mm thick sections cleared by the Spalteholz technique, we could localize the points at which the arteries enter – and veins exit – the nervous tissue, and then trace the distribution of each vessel to map the intrinsic arterial and venous teritories of the whole brain stem (**Figs 7.4–7.24**) [122]. The vascular mapping proposed here may vary slightly from individual to individual. However, a less detailed examination of ten other brain stems appears to confirm the initial conclusions reported in this work

MR Microscopy (MRM) at 9.4 Tesla

Ten human cadaver brain stems were fixed in 15% formalin for two weeks, suspended in phosphate buffer, and then imaged in all three orthogonal planes with a Brüker 9.4 Tesla superconducting magnet (Brüker Analytik, Rheinstetten, Germany). The scanner used an 89 mm bore, a 35 mm bird cage coil, and intermediate-weighted pulse sequences: [Repetition time (TR): 1800–2500 msec, Echo time (TE): 20–30 msec, Slice thickness: 500 microns, Field of View: 20–35 mm, and Data matrix: 512 x 512 to 640 x 640 (interpolated to 1024 x 1024)]. This technique achieves images with an in-plane resolution of 30 to 68 microns. The narrow diameter of the bore and the coil often required the specimens to be trimmed or "halved" to fit within the scanner. The resultant intermediate-weighed MRM images were correlated with the injected specimens (capillary maps) (**Figs. 2.7–2.22** and **6.38–6.51**) and with standard atlases of neuroanatomy [4, 7, 15, 39, 78, 79, 99, 101, 106, 107, 109, 120, 122, 124, 125, 147, 155, 164, 167, 179, 231, 243, 294, 322a, 327, 328, 332, 335, 358, 370, 396, 423] to identify the structures depicted.

Serial images of the brain stem were then organized into a detailed atlas of the fiber tracts and nuclei of the brain stem in axial, sagittal and coronal planes (**Figs. 8.1–8.147**). Within each anatomic area (except the midbrain), all of the images displayed are from a single specimen, so the anatomic relationships among structures may be compared directly in all three orthogonal planes. Two different specimens were required to image the midbrain. Different specimens are illustrated for the different anatomic regions.

Advanced MR Imaging

Specific MR techniques have evolved to demonstrate neuromelanin (Figs. 10.1–10.3) [373, 394], susceptibility changes from parenchymal iron and intra-vasculature deoxyhemoglobin (**Figs. 10.4–10.14**) [177], and fiber tract orientation (Figs. 10.15–10.38) [28, 34, 146, 192, 217, 223, 275, 276, 293, 296, 297, 298, 299, 301,302, 303, 306, 316, 317, 345, 371, 407, 447, 453, 459] *in vivo*. These images are presented and correlated with both (i) sections of the whole head, and (ii) 3T images of formalin-fixed whole brains to illustrate the specific aspects of anatomy that they depict. The technical details of these techniques are given in the introduction to each of these sections.

Three-dimensional serial sections of the head

Three preparations, each including the brain stem, cerebellum, and diencephalon were cut into 2 to 4 mm thick sections by a circular-blade electric slicer.

The axial sections (Figs. 11.1–11.29) were obtained in the intercommissural plane of Schaltenbrand, which extends from the mid anterior commissure (AC) to the mid posterior commissure (PC) [1, 377, 378, 423, 424, 425]. This differs slightly from the standard bicommissural plane of Talairach, which is drawn from the top of the anterior commissure to the bottom of the posterior commissure [420, 421]. Coronal plane anatomic sections (Figs. 1.30–11.55) were obtained perpendicular to Schaltenbrand's intercommisural line. The sagittal sections (Figs. 11.56–11.70) were obtained parallel to the median plane.

Although the neuro-orbital plane recommended by Cabanis [69, 70] and the posterior commissure-obex (PC-O) plane of Tamraz [423–425] might have been better adapted to the sectional anatomy of the brain stem, we chose Schaltenbrand's intercommissural plane in order to build upon our previous studies of the sectional anatomy of the brain [125].

The principle of the three-dimensional serial sections is to gradually erode the preparation by sectioning it from inferior to superior for axial sections, from anterior to posterior for coronal sections, and from lateral to medial for sagittal sections. Each section then displays the anatomy of that section in relationship to the remaining portions of uneroded brain.

Each plate demonstrates the surface of the prepared section viewed "en face", plus diverse oblique views of the preparation to orient the viewer.

The serial sections of the eroded brain were correlated with anatomic sections of the head to show the brain *in situ*, and to show the relationship of the brain to the skull. The specific reference plane chosen for the head sections was the suborbito-meatal plane, which passes from the lower margins of the bony orbits to the centers of the external auditory canals. This external plane appears to correlate best with the internal intercommissural plane of Schaltenbrand.

Correlative T1- and T2-weighted clinical magnetic resonance images (MRI) were obtained in vivo at 3 Tesla (Siemens Trio, Erlangen, Germany), along the same reference planes parallel to and perpendicular to Schaltenbrand's intercommissural plane, utilizing a 32-channel surface array custom-built head coil (courtesy of Graham C. Wiggins Ph. D. and Larry L. Wald Ph. D.). These clinical images were then matched as closely as possible to the prepared anatomic specimens. The same volunteer was imaged for the axial, coronal and sagittal planes to enhance the value of correlations among the different planes. Because these lengthy MR sequences required two sessions to complete, the precise plane of section does vary slightly among images.

SECTION I

SURFACE ANATOMY OF THE BRAIN STEM AND CEREBELLUM

This chapter on the surface anatomy of the brain stem and cerebellum is divided into several portions:

A. General remarks on the encephalon
B. Surface of the brain stem
C. Surface of the cerebellum
D. Relationship between brain stem and cerebellum; emergence of the cranial nerves
E. The fourth ventricle
F. Lengths and angular relationships among these structures

A. General remarks

The encephalon comprises:
- The brain itself (prosencephalon) formed by the telencephalon (cerebral hemispheres),
- The diencephalon,
- The cerebellum, and
- The brain stem.

The brain is set in the anterior and middle cranial fossae, while the cerebellum and brain stem are located in the posterior cranial fossa. The anterior and middle cranial fossae are partially separated from the posterior fossa by the tentorium cerebelli, but communicate with the posterior fossa through the tentorial hiatus. The mesencephalon passes through this opening and joins the brain stem and cerebellum below with diencephalon and telencephalon above. **Figures 1.1–1.3** display the anatomic relationships among the different portions of the encephalon. The boundaries of the posterior cranial fossa are described in **Fig. 1.30**.

The brain stem is composed of 3 parts: in ascending order the medulla, the pons, and the mesencephalon.

The cerebellum is also composed of 3 parts: a median vermis and paired right and left cerebellar hemispheres.

The medulla, pons, and cerebellum together form the rhombencephalon, which encloses the fourth ventricle. The fourth ventricle is connected to the third ventricle through the cerebral aqueduct of Sylvius and to the subarachnoid spaces through the median foramen of Magendie and the paired lateral foramina of Luschka.

Fig. 1.1. The encephalon. Ventral aspect.
Bar: 10 mm

Cerebral hemisphere
1 Frontal (orbital) lobe
2 Temporal lobe
3 Olfactory bulb
4 Olfactory tract
5 Anterior perforated substance

Diencephalon
6 Optic chiasm
7 Hypophyseal stalk
8 Tuber cinereum
9 Mammillary body

Brain stem
10 Mesencephalon (crus cerebri)
11 Interpeduncular fossa
12 Pons
13 Medulla

Cerebellum
14 Cerebellar hemisphere
15 Vermis
16 Flocculus

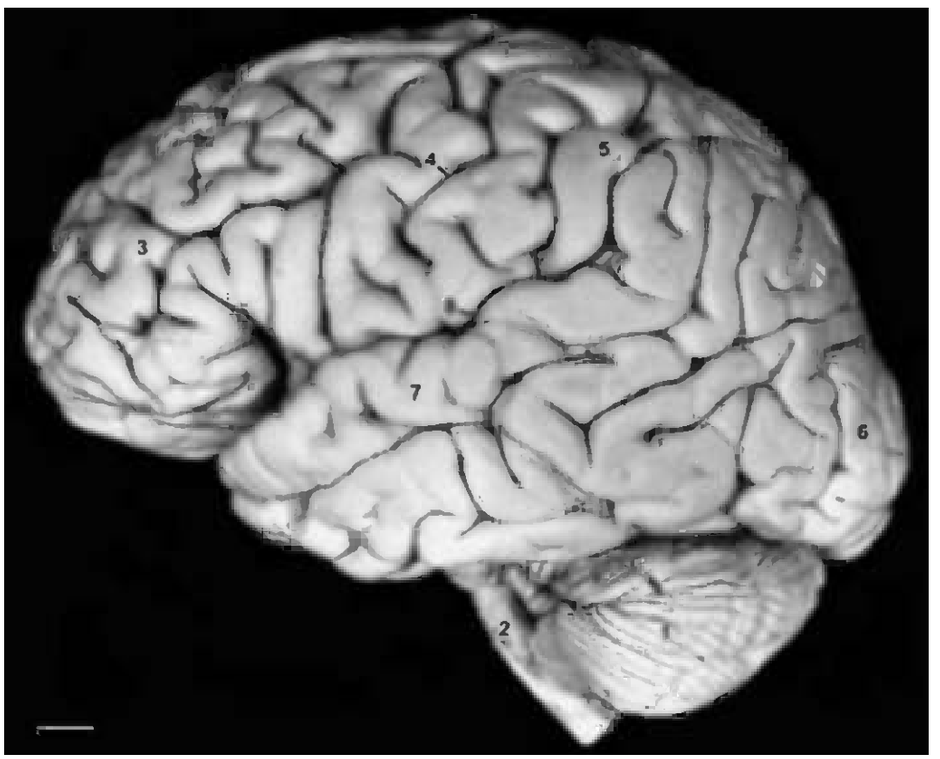

Fig. 1.2. The encephalon. Lateral aspect. Cerebral hemisphere.
Bar: 10 mm.

1 Cerebellar hemisphere
2 Brain stem
3 Frontal lobe
4 Central sulcus
5 Parietal lobe
6 Occipital lobe
7 Temporal lobe
8 Lateral (Sylvian) fissure

Fig. 1.3. The encephalon. Median section.
Bar: 10 mm.

Cerebral hemisphere (medial aspect)
1 Medial aspect of the frontal lobe
2 Medial aspect of the parietal lobe
3 Medial aspect of the occipital lobe
4 Cingulate sulcus
5 Subparietal sulcus
6 Parieto-occipital fissure
7 Calcarine sulcus
8 Corpus callosum
8′ Callosal sulcus
9 Septum pellucidum
10 Fornix

Diencephalon
11 Third ventricle
12 Anterior commissure
13 Posterior commissure
14 Thalamus
15 Mammillary body
16 Optic chiasm

Brain stem
17 Mesencephalon (crus cerebri)
18 Mesencephalon (tectum)
19 Cerebral aqueduct
20 Pons
21 Medulla

Cerebellum
22 Vermis
23 Medial aspect of the cerebellar hemisphere
24 Fourth ventricle

The median axis, composed of the brain stem and diencephalon, is partially covered by the bulk of the hemispheres during brain growth. Because the hemispheres adhere only partially to the diencephalon and mesencephalon, a transverse fissure still separates the fully developed telencephalon from both the diencephalon and mesencephalon.
The transverse fissure has two parts:
(A) A median portion located between the telencephalic commissures (corpus callosum and fornix) above and the diencephalon below the cistern of the velum interpositum, and
(B) Paired right and left lateral portions surrounding the mesencephalon (**Figs. 1.3 and 1.30**).

B. Brain stem surface

Each of the three segments of the brain stem presents anterior, posterior and lateral aspects, which will be described in turn (see [48, 78, 85, 99, 109, 167, 228, 250, 251, 273, 322, 324, 334, 357, 387, 430, 445, 455]).

Figure 1.4 displays the anterior surface of the brain stem including the medullary pyramids, the belly of the pons, the cerebral peduncles, and the origins of all the cranial nerves, except the trochlear (CN IV).

Figure 1.5 displays the posterior surface of the brain stem including the characteristic shape of the fourth ventricle (rhomboid fossa), the surface features of the fourth ventricular floor, the structures of the quadrigeminal plate, and the origin of the trochlear nerve (CN IV).

Figure 1.6 displays the lateral aspect of the brain stem including the relative ventral-dorsal positions of the cranial nerve origins, the dorsally converging angulations of the three cerebellar peduncles, and the relationships among the inferior colliculus, its brachium and the medial geniculate body.

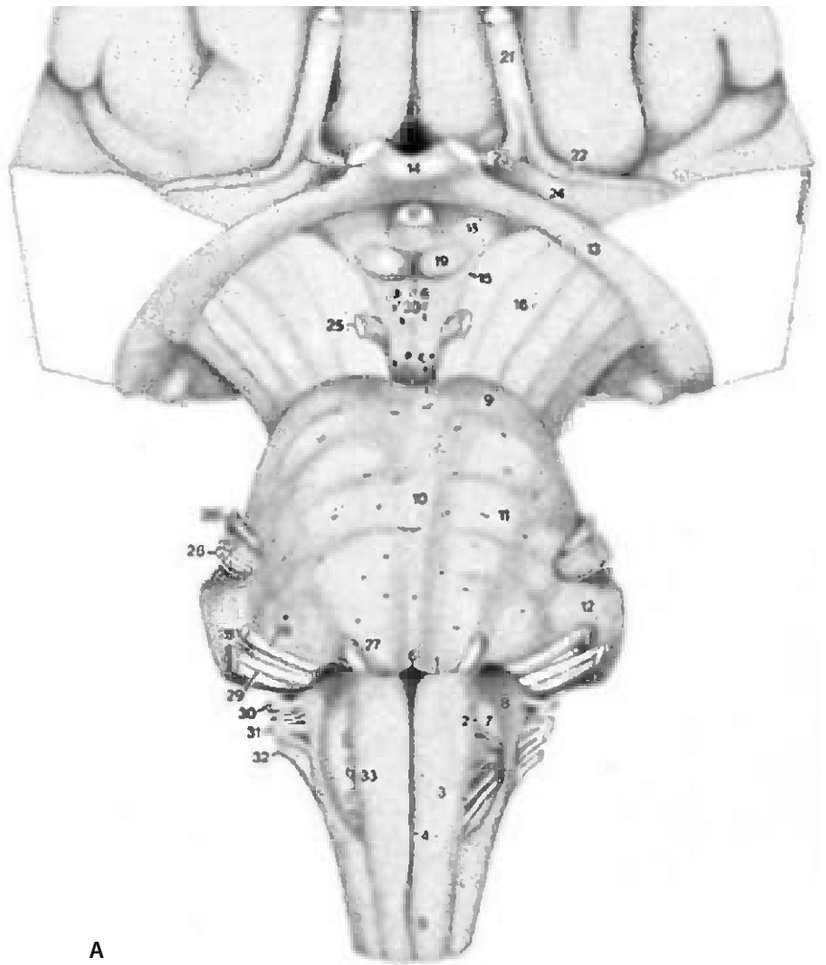

Fig. 1.4 (A–B). The brain stem. Anterior view. Bar: 5 mm.

Medulla

The boundaries between the spinal cord and medulla are noted on **Fig. 1.30.** The pontomedullary sulcus (1) separates the medulla from the pons.

Anterior aspect

1 Pontomedullary sulcus
2 Anterolateral medullary (pre-olivary) sulcus
3 Pyramid of the medulla (including corticospinal tract)
4 Anterior median medullary sulcus
5 Pyramidal decussation (spinomedullary junction)
6 Foramen cecum

Lateral aspect

7 Inferior olive
8 Lateral fossa of the medulla

Pons

The pons is separated from the medulla by the pontomedullary sulcus (1) and from the mesencephalon by the pontomesencephalic sulcus (9).

Anterior aspect

9 Pontomesencephalic sulcus
10 Basilar sulcus
11 Basilar (ventral) portion of the pons

The lateral aspect of the pons (12) merges into the middle cerebellar peduncle (brachium pontis).

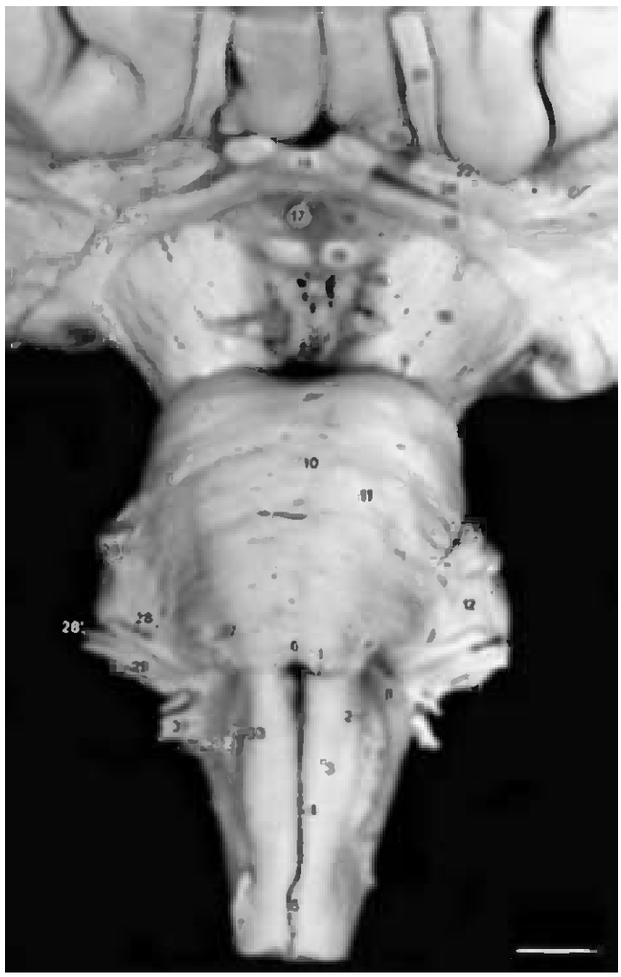

B

Mesencephalon

The mesencephalon is separated from the pons by the pontomesencephalic sulcus (9) and from the brain by the optic tract (13), the optic chiasm (14), and the medial mesencephalic sulcus (15).

Anterior aspect

The mesencephalon consists of the crus cerebri (pes pedunculi or basis pedunculi) (16).

The interpeduncular region, which belongs to the diencephalon, includes the hypophyseal stalk (17), tuber cinereum (18), mammillary bodies (19), and interpeduncular fossa (posterior perforated substance) (20).

Also shown are the olfactory tracts (21), dividing into lateral (22) and medial (23) olfactory striae bordering the anterior perforated substance (24).

Roots of the cranial nerves

25 Oculomotor nerve
26 Trigeminal nerve (sensory root)
26′ Trigeminal nerve (motor root)
27 Abducens nerve
28 Facial nerve
28′ Nervus intermedius
29 Vestibulocochlear nerve
30 Glossopharyngeal nerve
31 Vagus nerve
32 Accessory nerve (medullary root)
33 Hypoglossal nerve

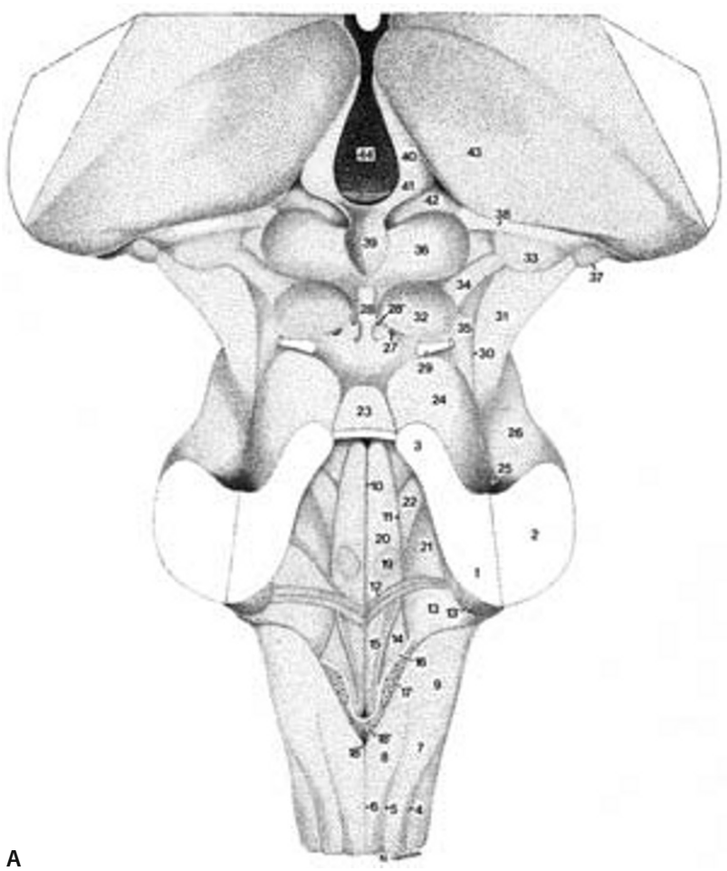

A

Fig. 1.5 (A–B). The brain stem. Posterior view. The cerebellum was removed by section of the three cerebellar peduncles: inferior (restiform body) (1), middle (brachium pontis) (2), and superior (brachium conjunctivum) (3). Bar: 5 mm.

Medulla – posterior aspect

The medulla is divided into superior and inferior levels. The superior level belongs to the floor of the fourth ventricle. The inferior level extends to the posterior aspect of the spinal cord.

Inferior level

4 Posterolateral medullary sulcus
5 Posterior intermediate medullary sulcus
6 Posterior median medullary sulcus

The cuneate tubercle (7) and gracile tubercle (clava) (8) are produced by the subjacent cuneate and gracile nuclei (See Fig. 2.8).

Superior level

The superior level is composed of the medullary portion of the fourth ventricular floor and the right and left inferior cerebellar peduncles (9).

Pons – posterior aspect

This aspect of the pons mostly consists of the pontine (superior) portion of the fourth ventricular floor.

Floor of the fourth ventricle (Rhomboid fossa)

The floor or rhomboid fossa (See Fig. 2.6) shows one median sulcus (10) and paired right and left paramedian sulci limitantes (11). The striae medullares (12) divide the floor into the inferior medullary triangle and superior pontine triangle.

Brain stem surface

The medullary triangle consists of three segments (13, 14 and 15) that run from the lateral region to the median line.

13 Medullary vestibular area (due to the protrusion of the medial vestibular nucleus);
13′ Acoustic tubercle
14 Vagal trigone (fovea inferior) corresponding to the dorsal motor nucleus of the vagus
15 Hypoglossal trigone produced by the subjacent hypoglossal and intercalated nuclei.
16, 17 A thickening of the ependyma, the funiculus separans (16), borders the area postrema (17) (See Fig. 1.21).
18 Obex
18′ Funicular commissure linking the right and left funiculi separantes (16) (See Fig. 1.21).

B

The pontine triangle consists of

19 Facial colliculus (protrusion due to the abducens nucleus- and the facial nerve fibers)
20 Medial eminence
21 Pontine vestibular area
22 Superior fovea (fovea trigemini)
23 Superior medullary velum linking the right and left superior cerebellar peduncles (brachia conjunctiva) (24).
25 Parabrachial recess (**See Figs. 11.18 and 11.19**) situated between the brachium conjunctivum (24) and the brachium pontis (26)

Mesencephalon - posterior and lateral aspects

27 Infracollicular recess (emergence of deep veins [122])
28 Frenulum veli
29 Root of the trochlear nerve
30 Lateral mesencephalic sulcus bordering the crus cerebri (31)
32 Inferior colliculus linked to the medial geniculate body (33) by the brachium of the inferior colliculus (34)
35 Lateral aspect of mesencephalon

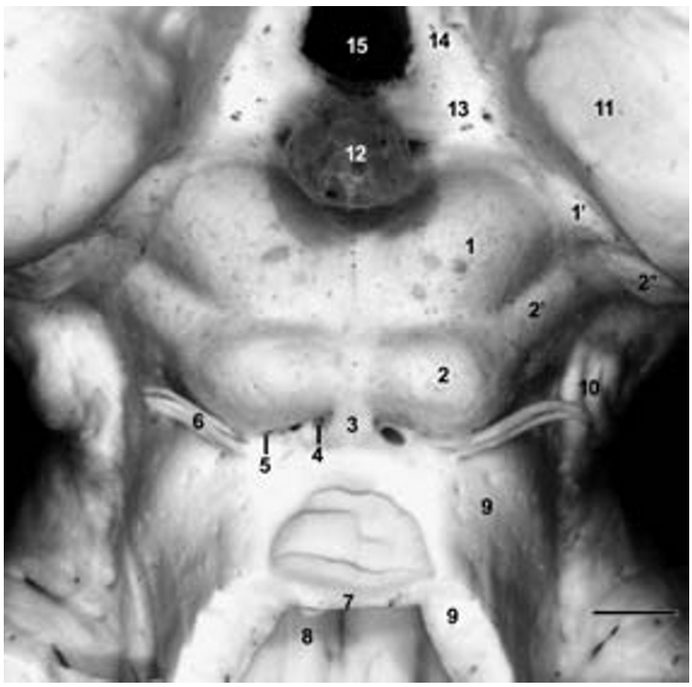

C

36 Superior colliculus linked to the lateral geniculate body (37) by the brachium of the superior colliculus (38)
39 Pineal gland
40 Stria medullaris thalami
41 Habenular trigone
42 Pretectal area
43 Thalamus (pulvinar)
44 Third ventricle

C. The mesencephalon. Enlarged posterior view. Bar: 5 mm.

1 Superior colliculus
1′ Brachium of the superior colliculus
2 Inferior colliculus
2′ Brachium of the inferior colliculus
2″ Medial geniculate body
3 Frenulum veli
4 Recess of the frenulum veli
5 Infracollicular recess
6 Root of the trochlear nerve
7 Superior medullary velum
8 Fourth ventricle
9 Superior cerebellar peduncle (brachium conjunctivum)
10 Crus cerebri (cerebral peduncle)
11 Pulvinar
12 Pineal gland
13 Habenular trigone (site of medial and lateral habenular nuclei)
14 Stria medullaris thalami
15 Third ventricle

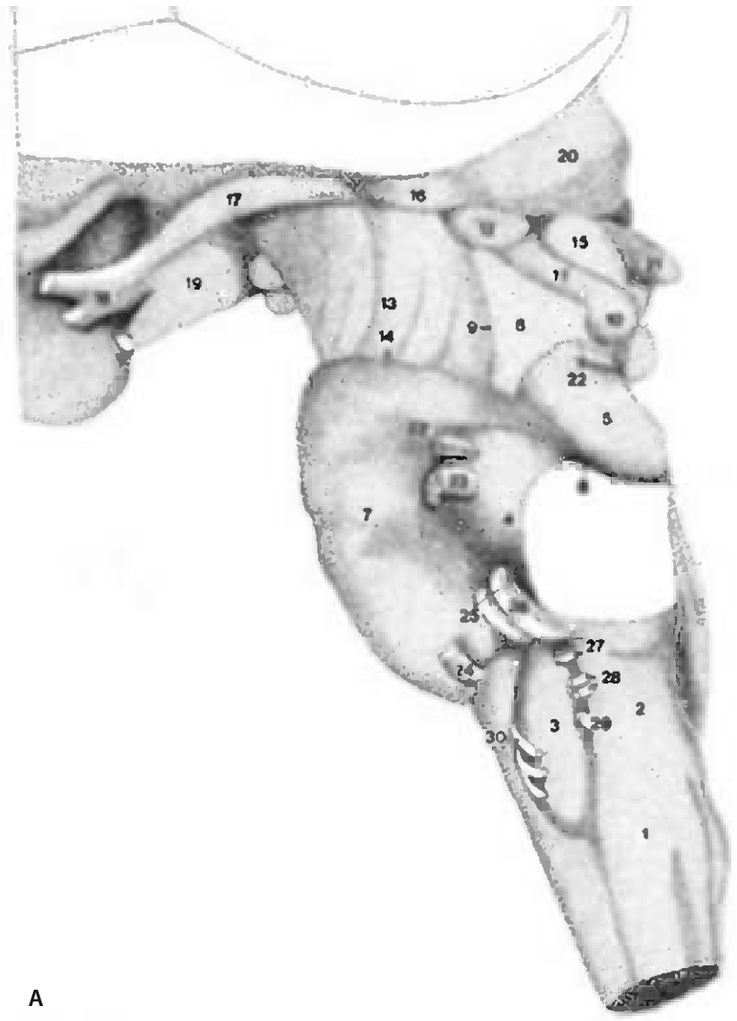

Fig. 1.6 (A–B). The brain stem. Lateral view.
Bar: 5 mm.

Medulla – lateral aspect
Inferior level
1 Lateral medullary funiculus

Superior level
2 Inferior cerebellar peduncle (restiform body)
3 Inferior olive

Pons – lateral aspect
The lateral aspect of the pons is formed by the middle cerebellar peduncle (brachium pontis) (4)
5 Superior cerebellar peduncle (brachium conjunctivum)
6 Parabrachial recess
7 Anterior aspect of the pons

Mesencephalon – lateral aspect
This lateral surface is also called the acoustic or lemniscal trigone due to the underlying lateral lemniscus (auditory fibers).

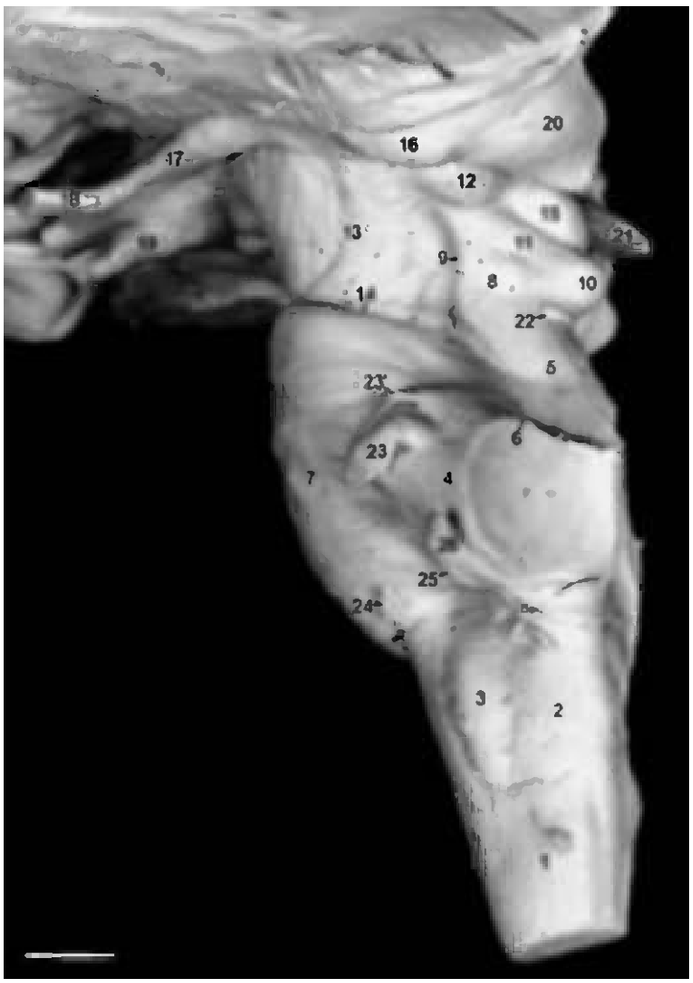

B

The triangular lateral aspect of the mesencephalon (8) is bordered laterally by the mesencephalic sulcus (9), posteriorly by the inferior colliculus (10) and its brachium (11), cranially by the medial geniculate body (12), and caudally by the superior cerebellar peduncle (5) (brachium conjunctivum).

13 Crus cerebri
14 Pontomesencephalic sulcus
15 Superior colliculus
16 Lateral geniculate body
17 Optic tract
18 Optic chiasm
19 Median eminence of the tuber cinereum
20 Pulvinar
21 Pineal gland

Roots of cranial nerves

22 Trochlear nerve
23 Trigeminal nerve, sensory root
23′ Trigeminal nerve, motor root
24 Abducens nerve
25 Facial nerve
26 Vestibulocochlear nerve
27 Glossopharyngeal nerve
28 Vagus nerve
29 Accessory nerve (medullary root)
30 Hypoglossal nerve

C. Cerebellar surface

The cerebellum consists of the median vermis and the paired left and right cerebellar hemispheres. The superior vermis rises above the cerebellar hemispheres, while the inferior vermis is deeply embedded between the two cerebellar hemispheres, within the posterior cerebellar notch and vallecula.

The cortex covering the cerebellum is tightly folded. A single fold is called a folium. Multiple folds are called folia; grouped folia form lobules that are separated by fissures. Each lobule has a median portion belonging to the vermis and paired lateral portions belonging to the two cerebellar hemispheres.

The lobules group together into anterior, posterior, and flocculonodular cerebellar lobes. The anterior lobe is separated from the posterior lobe by the primary fissure. The posterior lobe is separated from the flocculonodular lobe by the posterolateral fissure (**Fig. 1.7**).

Figure 1.7 depicts the cerebellar anatomy as seen from the midline. Figure 1.8 diagrams the cerebellar surface as if it were unrolled and seen, simultaneously, from the ventral, superior, and inferior perspectives (**See arrows in Fig. 1.7**). Table 1.1 summarizes the relationships among the lobules and fissures of the vermis and cerebellum. Figures 1.9 through 1.17 then depict the surface anatomy of the cerebellum. See [15, 48, 55, 61, 78, 85, 92, 99, 109, 155, 167, 218, 228, 248, 251, 253, 254, 255, 273, 322, 324, 334, 342, 343, 350, 357, 387, 430, 445, 474, 475, 476].

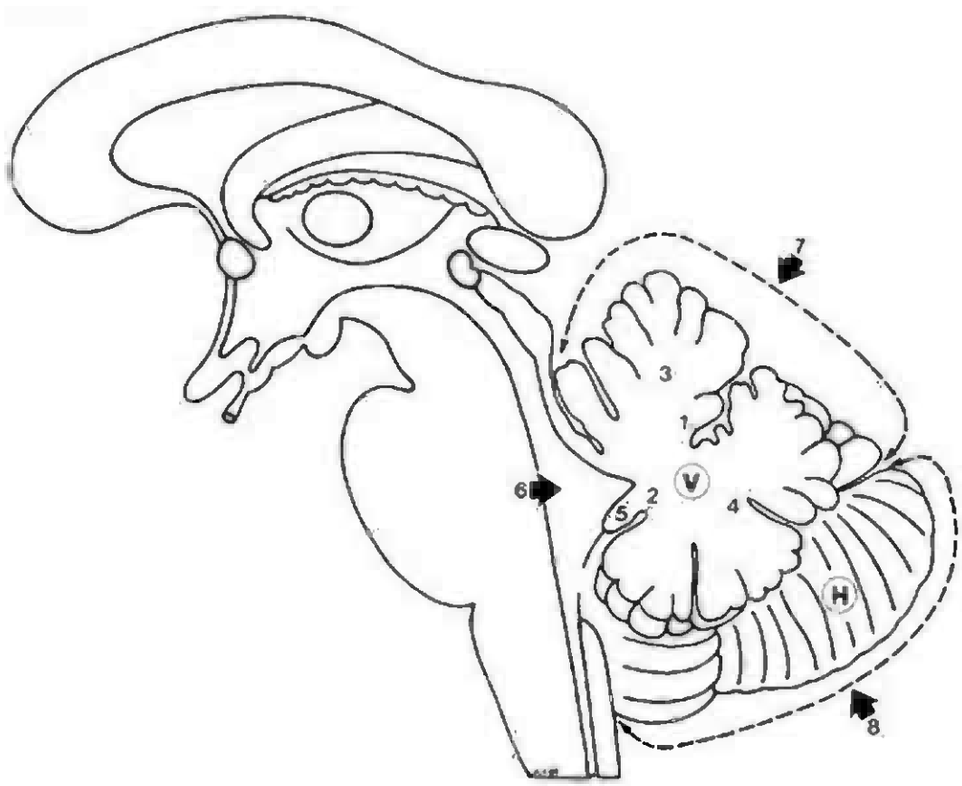

Fig. 1.7. Diagram. Median section of the vermis (V) and medial surface of the cerebellar hemisphere (H).

1 Anterior superior fissure (primary fissure)
2 Posterolateral fissure
3 Anterior lobe
4 Posterior lobe
5 Flocculonodular lobe
6 Viewpoint for the anterior aspect of the cerebellum
7 Viewpoint for the superior aspect
8 Viewpoint for the inferior aspect

The dotted line indicates the superior and inferior aspects of the cerebellum as shown in Fig. 1.8.

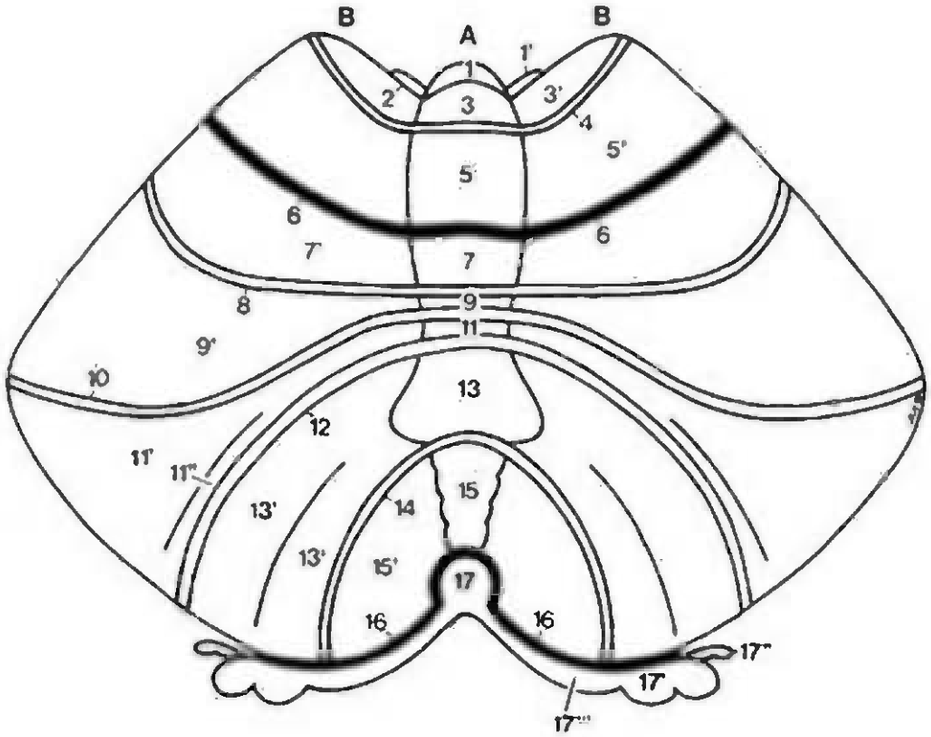

Fig. 1.8. The unrolled surface of the cerebellum. Composite diagram, as seen from the viewpoints shown in Fig. 1.7.
A. Vermis, **B.** Cerebellar hemispheres. The terminology used to describe the cerebellum is particularly complex. This book tries to use the most common terms (and provides synonyms in brackets for comparison with other texts) [218, 255].

I. Anterior lobe

1 Lingula (**lobule I** of Jansen, only applied to the vermis)
1′ Vinculum lingulae (likely vestigial in man)
2 Precentral fissure
3 Central lobule (**lobules II and III** of Jansen)
3′ Wing of the central lobule
4 Preculminate fissure (postcentral fissure)
5 Culmen (**lobules IV and V**)
5′ Quadrangular lobule (anterior quadrangular lobule)
6 Anterior superior fissure (primary fissure)

II. Posterior lobe

7 Declive (**lobule VI**)
7′ Simple lobule (posterior quadrangular lobule)
8 Posterior superior fissure (postclival fissure)
9 Folium (**lobule VII** of Jansen)
9′ Superior semilunar lobule (crus I)
10 Great horizontal fissure (intercrural fissure)
11 Tuber (**also lobule VII** of Jansen)
11′ Inferior semilunar lobule (crus II). The superior and inferior semilunar lobules (crura I and II) together form the ansiform lobule.
11″ Gracile lobule (paramedian lobule). This is sometimes considered to belong to the inferior semilunar lobule, but may be separated from the latter by the ansoparamedian fissure.
12. Prepyramidal fissure. For simplicity, this term is sometimes used for both the vermian and the hemispheric portions of the fissure.
13 Pyramis (pyramid) of the vermis (**lobule VIII** of Jansen)
13′ Biventral lobule (digastric lobule, dorsal paraflocculus) divided into two portions by the intrabiventral fissure
14 Postpyramidal fissure (secondary fissure). For simplicity, this term may also be used for both the vermian and the hemispheric portions of the fissure.
15 Uvula (**lobule IX** of Jansen)
15′ Tonsil (cerebellar amygdala, ventral paraflocculus)
16 Posterolateral fissure (postnodular fissure)

III. Flocculonodular lobe

17 Nodulus (**lobule X**)
17′ Flocculus
17″ Paraflocculus (accessory paraflocculus)
17‴ Floccular brachium (floccular peduncle)

Table 1.1. Lobes, lobules and fissures of the cerebellum

Classical 3 Lobes	Yasargil[476] 4 Lobes	Larsell[253-255] 10 Divisions	Vermis 9 Lobules	Hemispheres 10 Lobules	Intervening Fissure 10 Fissures
			Anterior Medullary Velum		
		I	Lingula	Vinculum	
					Precentral Fissure
Anterior Lobe	Anterior Lobe	II, III	Central	Wing of Central	
					Preculminate Fissure
		IV, V	Culmen	Anterior Quadrangular	
					Primary Fissure
		VI	Declive	Lobulus Simplex	
	Middle Lobe				Posterior Superior Fissure
		VII	Folium	Superior Semilunar	
					Great Horizontal Fissure
		VII	Tuber	Inferior Semilunar	
					Fissura Ansoparamedianus
Posterior Lobe			Prepyramidal Fissure	Lobulus Gracilis	
	Posterior Lobe				Prebiventral Fissure
				Biventral Lobule	
		VIII	Pyramis		Intrabiventral Fissure
				Biventral Lobule	
					Secondary Fissure
		IX	Uvula	Tonsil	
					Posterolateral Fissure
Flocculo-Nodular Lobe	Flocculo-Nodular Lobe	X	Nodulus	Flocculus	
			Posterior Medullary Velum		

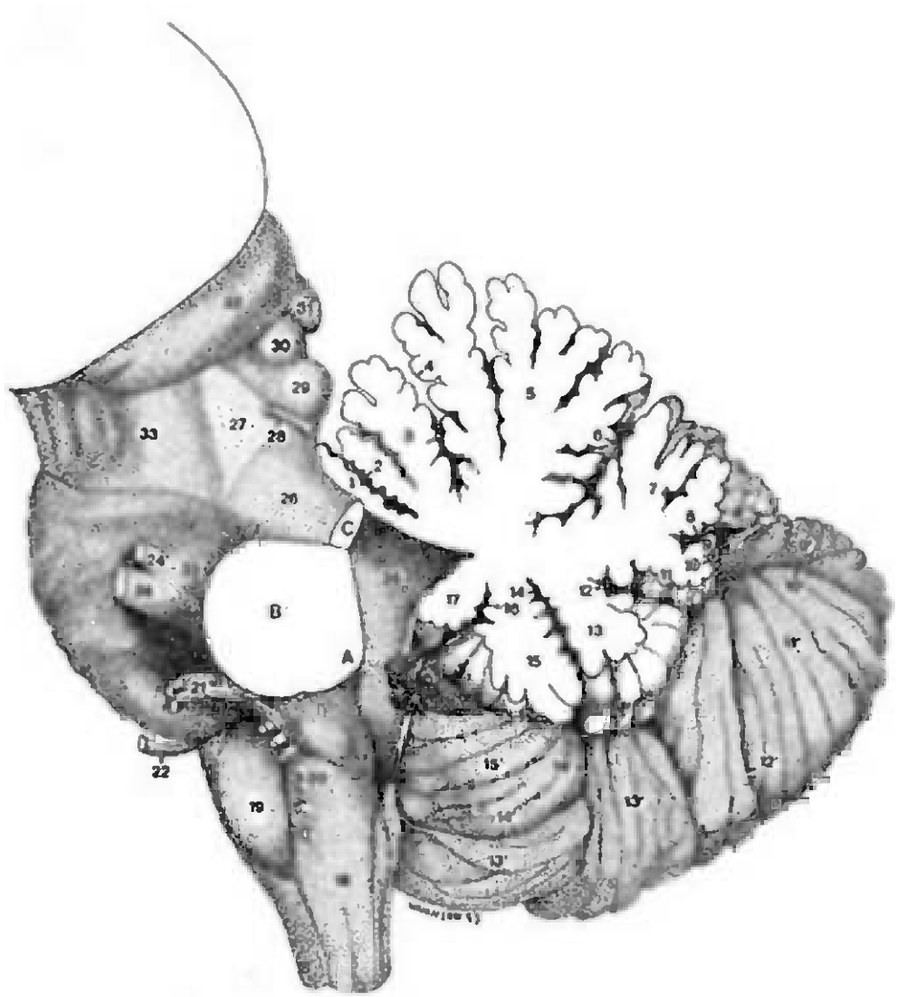

Fig. 1.9 (A–B). The vermis. Median section. Diagram **(A)** and specimen photograph **(B)** display the medial view of the cerebellar hemisphere and the lateral view of the brain stem. The inferior (A), middle (B), and superior (C) cerebellar peduncles have been resected. Bar: 5 mm.

Median section of the vermis

1 Lingula
2 Precentral fissure
3 Central lobule
4 Preculminate fissure
5 Culmen
6 Anterior superior fissure (primary fissure)
7 Declive
8 Posterior superior fissure
9 Folium
10 Great horizontal fissure (the vermian portion of the horizontal fissure is difficult to identify)
11 Tuber
12 Prepyramidal fissure
13 Pyramid of the vermis (pyramis)
14 Postpyramidal fissure (secondary fissure)
15 Uvula
16 Posterolateral fissure
17 Nodulus

Medial view of the left cerebellar hemisphere

7′ Simple lobule
8′ Posterior superior fissure
9′ Superior semilunar lobule
10′ Horizontal fissure
11′ Inferior semilunar lobule
12′ Prepyramidal fissure
13′ Biventral lobule
14′ Postpyramidal fissure
15′ Tonsil

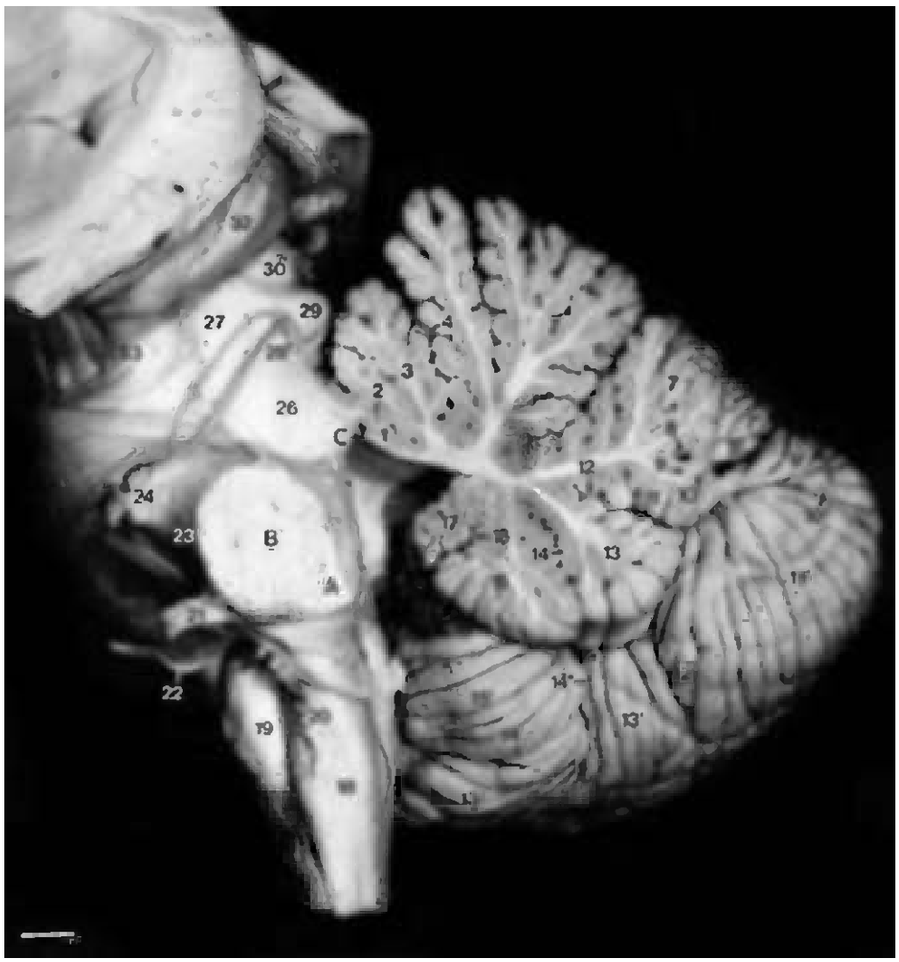

B

Lateral view of the brain stem

18 Lateral aspect of the medulla
19 Inferior olive
20 Roots of glossopharyngeal, vagus, and accessory nerves, in descending order
21 Roots of vestibulocochlear and facial nerves
22 Root of abducens nerve
23 Lateral aspect of the pons (middle cerebellar peduncle)
24 Sensory root of trigeminal nerve
24′ Motor root of trigeminal nerve
25 Fourth ventricle
26 Superior cerebellar peduncle (brachium conjunctivum)
27 Lateral aspect of the mesencephalon
28 Trochlear nerve
29 Inferior colliculus
30 Superior colliculus
31 Pineal gland
32 Pulvinar
33 Crus cerebri

Fig. 1.10. The vermis and cerebellar hemisphere. Medial aspect. Oblique view. The vallecula has been opened by removal of the contralateral cerebellar hemisphere. Bar: 5 mm.

1, 1′	The great horizontal fissure (1) is difficult to see on the vermis, but is easily identified on the hemispheres (1′)
2	Declive
2′	Simple lobule
3, 3′	Posterior superior fissure
4	Folium of the vermis
4′	Superior semilunar lobule
5	Tuber of the vermis
5′	Inferior semilunar lobule
6, 6′	Prepyramidal fissure
7	Pyramid of the vermis
7′	Biventral lobule
8	Postpyramidal fissure (secondary fissure)
9	Tonsil

Fig. 1.11. The cerebellum. Posterosuperior view. Bar: 5 mm.

1 Culmen
1′ Quadrangular lobule
2, 2′ Anterior superior fissure (primary fissure)
3 Declive
3′ Simple lobule
4 Posterior superior fissure
5 Superior semilunar lobule
6 Great horizontal fissure
7 Inferior semilunar lobule (medial portion is visible on the superior aspect of the cerebellum due to the orientation of the great horizontal fissure (**See Fig. 1.16**).
8 Inferior colliculus
9 Trochlear nerve
10 Superior colliculus
11 Pineal gland
12 Habenular trigone
13 Pulvinar

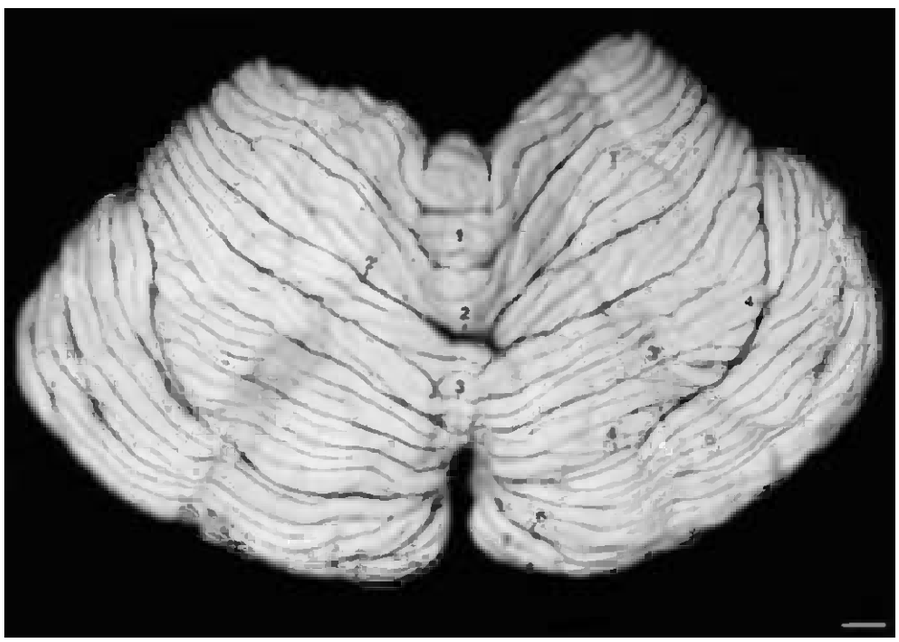

Fig. 1.12. The cerebellum. Superior view. The brain stem and diencephalon have been removed. Bar: 5 mm.

1 Culmen
1′ Quadrangular lobule
2, 2′ Anterior superior fissure (primary fissure)
3 Declive
3′ Simple lobule
4 Posterior superior fissure
5 Superior semilunar lobule
6 Great horizontal fissure
7 Inferior semilunar lobule (visible on the superior aspect of the cerebellum due to the orientation of the great horizontal fissure, **See Fig. 1.16**)

Fig. 1.13. The cerebellum. Antero-inferior view. Bar: 5 mm.

1 Uvula
1′ Tonsil
2, 2′ Postpyramidal (secondary) fissure
3 Pyramid of the vermis
3′ Biventral lobule
4 Prepyramidal fissure
5 Gracile lobule
6 Inferior semilunar lobule
7 Great horizontal fissure
8 Superior semilunar lobule (visible on the inferior aspect of the cerebellum due to the orientation of the great horizontal fissure, **See Fig. 1.16**)
9 Vallecula
10 Medulla

1.13

1.14

Fig. 1.14. The cerebellum. Inferior view. The brain stem has been removed. Bar: 5 mm.

1 Uvula
1′ Tonsil
2, 2′ Postpyramidal (secondary) fissure
3 Pyramid of the vermis
3′ Biventral lobule
4 Prepyramidal fissure
5 Gracile lobule
6 Inferior semilunar lobule
7 Great horizontal fissure
8 Superior semilunar lobule
9 Vallecula
10 Flocculus
10′ Paraflocculus

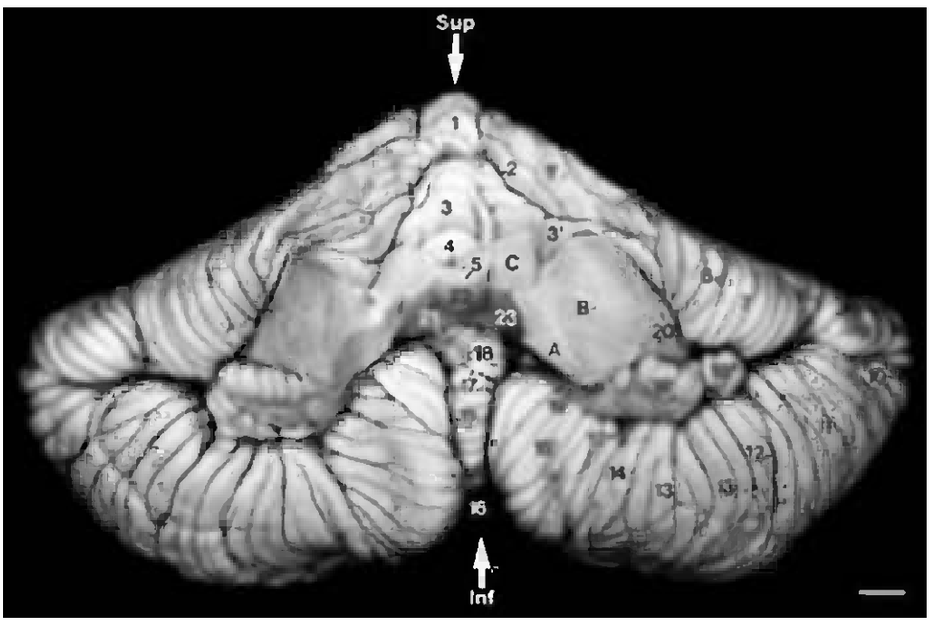

A

Fig. 1.15 (A–B). The cerebellum. Anterior view.
A. Specimen photograph. **B.** Diagram.
The brain stem has been removed by section through the inferior (A), middle (B), and superior (C) cerebellar peduncles. Bar: 5 mm.

The superior vermis rises above the cerebellar hemispheres, while the inferior vermis is deeply embedded within the posterior cerebellar notch and the vallecula.

1 Culmen
1′ Quadrangular lobule
2 Postcentral fissure
3 Central lobule
3′ Ala of the central lobule
4 Lingula
5 Superior medullary velum
6 Anterior superior (primary) fissure
7 Simple lobule
8 Posterior superior fissure
9 Superior semilunar lobule

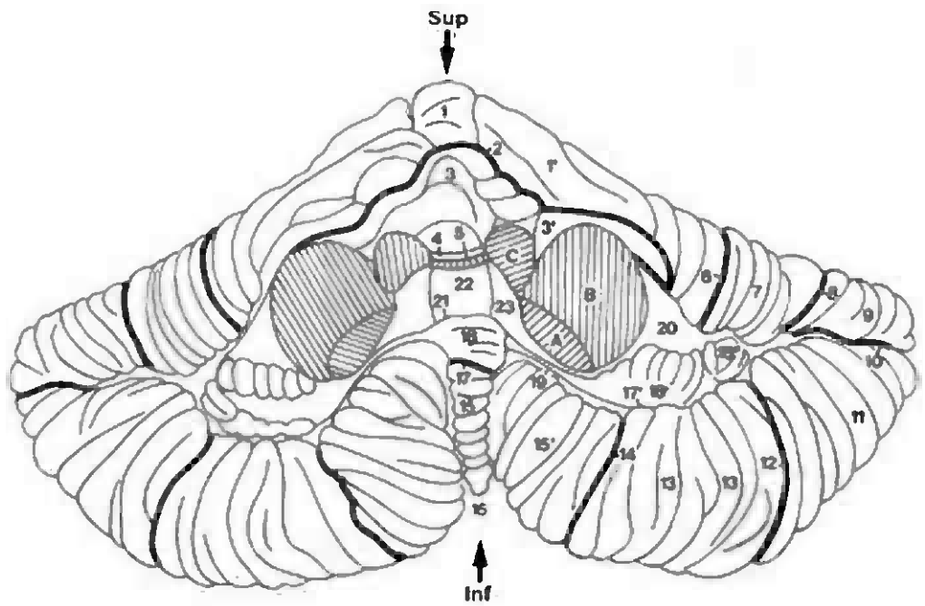

B

10 Great horizontal fissure
11 Inferior semilunar lobule
12 Prepyramidal fissure
13 Biventral lobule
14 Postpyramidal fissure (secondary fissure)
15 Uvula
15′ Tonsil
16 Vallecula
17, 17′ Posterolateral fissure
18 Nodulus
18′ Flocculus
18″ Paraflocculus
19 Brachium of the flocculus (peduncle of the flocculus) and inferior medullary velum
20 Middle cerebellar peduncle (brachium pontis)
21 Fastigial sulcus
22 Superior portion of the ventricular roof (median vermian portion)
23 Superior portion of the ventricular roof (lateral hemispheric portion)

Fig. 1.16. The cerebellum. Posterior view. Bar: 5 mm.

1 Culmen
2, 2′ Anterior superior fissure (primary fissure)
3 Declive
3′ Simple lobule
4, 4′ Posterior superior fissure
5 Folium of the vermis
6 Great horizontal fissure
Due to the sinuous path of the great horizontal fissure, the superior semilunar lobule is visible on the superior aspect (7) as well as on the inferior aspect (7′) of the cerebellum. For the same reason, the inferior semilunar lobule is also visible on both the inferior aspect (8) as well as the superior aspect (8′) of the cerebellum.
9 Vallecula
10 Medulla
11 Mesencephalon
12 Habenular trigone
13 Pulvinar

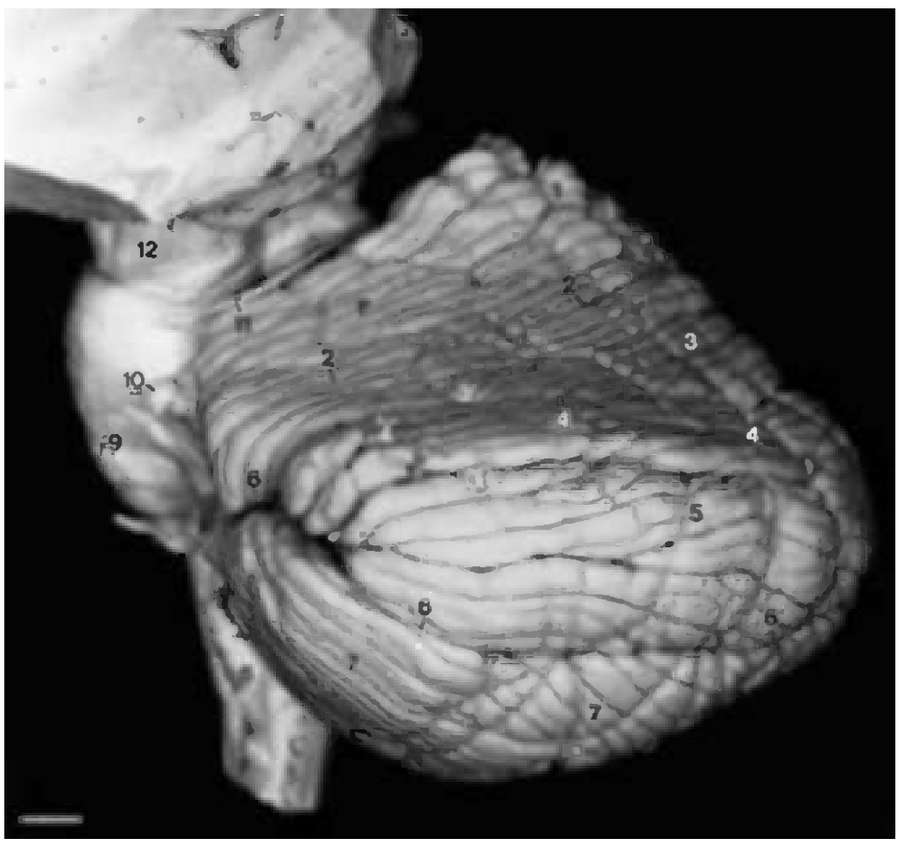

Fig. 1.17. The cerebellum. Lateral view of the cerebellar hemisphere. Bar: 5 mm.

1 Culmen
1′ Quadrangular lobule
2 Anterior superior fissure (primary fissure)
3 Declive
3′ Simple lobule
4 Posterior superior fissure
5 Superior semilunar lobule
6 Great horizontal fissure
7 Inferior semilunar lobule
8 Medulla
9 Pons
10 Root of trigeminal nerve
11 Trochlear nerve
12 Crus cerebri
13 Pulvinar

D. Relationship between brain stem and cerebellum: emergence of the cranial nerve roots

See [32, 48, 71, 78, 85, 99, 235, 251, 258, 271, 322, 330, 337, 357, 387, 430, 455].

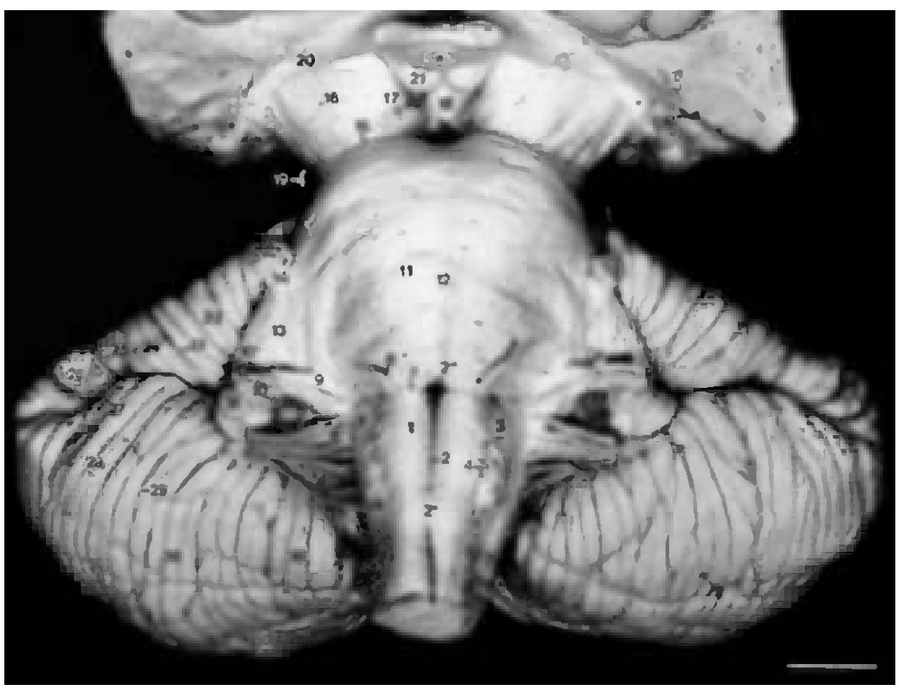

A

Fig. 1.18 (A–B). The brain stem and cerebellum.
A. Anterior view. Bar: 5.7 mm. **B.** Magnified view of A.

Brainstem

Medulla

1 Pyramid of the medulla
2 Anterior median medullary sulcus
2′ Decussation of the pyramids
2″ Foramen cecum
3 Inferior olive
4 Anterolateral (pre-olivary) medullary sulcus and hypoglossal nerve roots
5 Lateral medullary fossa
6 Roots of glossopharyngeal, vagus, and accessory nerves (from upper to lower levels)

Pons

7 Pontomedullary sulcus
8 Abducens nerve
9 Facial nerve
10 Vestibulocochlear nerve
10′ Nervus intermedius
11 Anterior surface of the pons (basilar portion of the pons)
12 Basilar (median pontine) sulcus
13 Lateral aspect of the pons extending into the middle cerebellar peduncle (brachium pontis)
14 Trigeminal nerve

B

Mesencephalon

15 Pontomesencephalic sulcus
16 Crus cerebri
17 Oculomotor nerve
18 Interpeduncular (intercrural) fossa
19 Trochlear nerve
20 Optic tract
21 Mammillary body

Cerebellum

22 Quadrangular lobule
23 Anterior superior fissure (primary fissure)
24 Simple lobule
25 Posterior superior fissure
26 Superior semilunar lobule
27 Great horizontal fissure
28 Inferior semilunar lobule
29 Prepyramidal fissure
30 Biventral lobule
31 Flocculus
32 Lateral aperture and extraventricular choroid plexus of the fourth ventricle

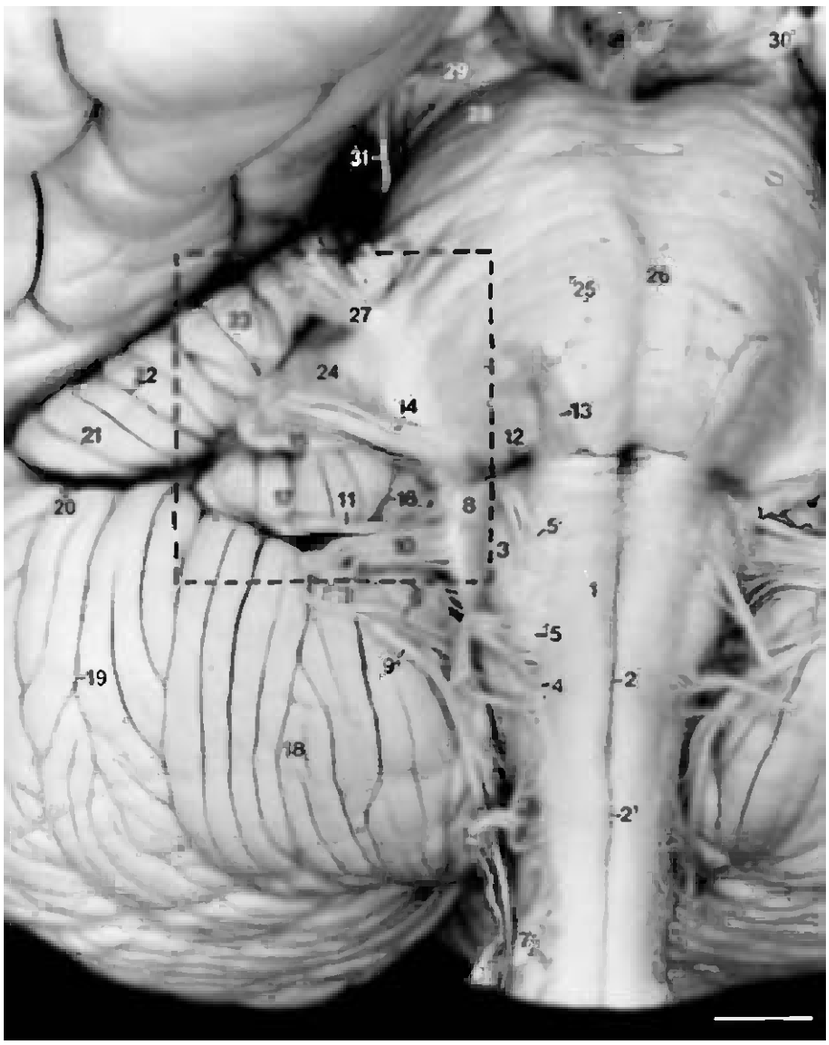

A

Fig. 1.19 (A–B). The brain stem and cerebellum: Emergence of the roots of the cranial nerves.

A. Anterior view. Bar: 5 mm.

B. Magnified view of the foramen of Luschka (16) and the adjoining nerve roots (dashed box in A).

1 Pyramid of medulla
2 Anterior median medullary sulcus
2′ Decussation of the pyramids
3 Inferior olive
4 Anterolateral (pre-olivary) medullary sulcus
5 Roots of the hypoglossal nerve emerging from the anterolateral medullary sulcus
6 Ventral roots of the first cervical nerve
7 Ventral root of the second cervical nerve
8 Lateral medullary fossa

From the lateral aspect of the medulla emerge successively in ascending order:

9′ Spinal root of the accessory nerve
9 Medullary root of the accessory nerve
10 Vagus nerve
11 Glossopharyngeal nerve
12 Pontomedullary sulcus and emergence of:
13 Abducens nerve
14 Facial nerve
15 Vestibulocochlear nerve

B

16 Lateral aperture (of Luschka) and choroid plexus of the fourth ventricle
17 Flocculus
18 Biventral lobule
19 Prepyramidal fissure
20 Great horizontal fissure
21 Simple lobule
22 Anterior superior (primary) fissure
23 Quadrangular lobule
24 Lateral aspect of the pons (middle cerebellar peduncle, brachium pontis)
25 Anterior surface of the pons
26 Basilar sulcus
27 Trigeminal nerve (sensory root)
28 Pontomesencephalic sulcus
29 Crus cerebri
30 Oculomotor nerve
31 Trochlear nerve

The dotted line indicates the area of the cerebellopontine angle. Some researchers restrict this area to the flocculus and the emergence of the facial and vestibulocochlear nerves.

E. The fourth ventricle

The fourth ventricle (rhombencephalic ventricle) is located in the cerebellum, pons, and medulla (which together compose the rhombencephalon). The upper portion of the fourth ventricle communicates with the cerebral aqueduct, while the lower portion communicates with the central canal of the medulla and spinal cord, and with the subarachnoid space. The fourth ventricle is the only ventricular cavity to have apertures allowing the ventricular fluid secreted by the choroid plexi to flow into the subarachnoid spaces.
[See 48, 78, 85, 99, 228, 251, 289, 322, 357, 430, 445, 455].

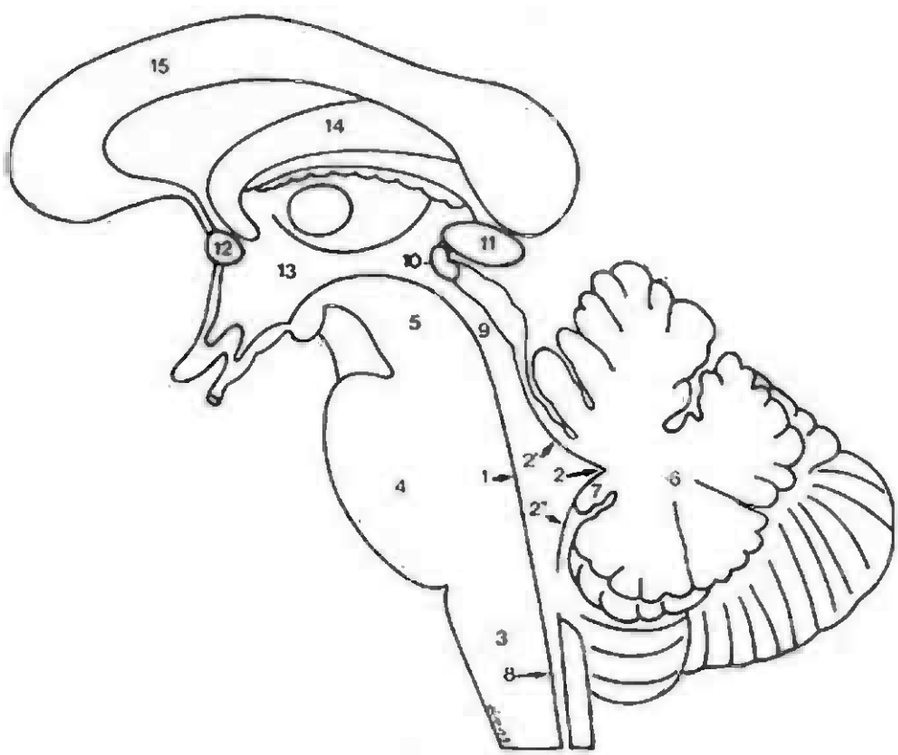

A

B

Fig. 1.20 (A–B). Features of the fourth ventricle.
A. Diagram. **B.** Specimen photograph. On this median section, the fourth ventricle is a triangular cavity with a floor (1) (rhomboid fossa) and a roof. Bar: 10 mm.

The roof has three parts: a fastigium (fastigial sulcus) (2) situated between the superior (2′) and inferior (2″) medullary vela.

3 Medulla
4 Pons
5 Mesencephalon
6 Cerebellum (vermis)
7 Nodulus
8 Central canal
9 Cerebral aqueduct (of Sylvius)
10 Posterior commissure
11 Pineal gland
12 Anterior commissure
13 Third ventricle
14 Fornix
15 Corpus callosum

Fig. 1.21 (A–B). The floor of the fourth ventricle (rhomboid fossa). Right side.
A. Diagram. **B.** Posterior view after removal of the cerebellum by section of the inferior (1), middle (2), and superior (3) cerebellar peduncles. Bar: 3.5 mm.

The floor of the fourth ventricle is rhomboidal. Its superior angle (4) is continuous with the cerebral aqueduct, while its inferior angle (5) is continuous with the central canal. The narrow converging multilayered points of the inferior fourth ventricle resemble the cut ends of an old hollow quill pen, giving the inferior end the name calamis scriptorius.

At each lateral angle (lateral recess) (6), the dorsal cochlear nucleus (6′) raises a small protrusion designated the acoustic tubercle. The floor is grooved vertically by a median sulcus (7) and by paired paramedian sulci limitantes (8). The striae medullares (9) (dorsal pontocerebellar fibers and parts of dorsal acoustic striae) cross the floor from its lateral angle to the median sulcus and divide the ventricular floor into two portions: the inferior medullary triangle and the superior pontine triangle.

Inferior (medullary) triangle

10 Hypoglossal trigone corresponding to the hypoglossal nucleus and nucleus intercalatus
11 Vagal trigone (fovea inferior) corresponding to the dorsal motor nucleus of the vagus and the nucleus of the solitary tract
12 Medullary vestibular area corresponding to the vestibular nuclei
13 Area postrema (See Fig. 1.22) overlying the lower portion of the vagal trigone
14 Funiculus separans (a thickening of ependyma) bordering the area postrema
14′ Interfunicular commissure
15 Ligula (medullary insertion of the membrana tectoria) (See Fig. 1.25)

The posterior ligula (visible on a posterior view of the medulla) is linked (15′) to that of the opposite side at the obex. The anterior ligula prolongs the posterior ligula around the inferior cerebellar peduncle and is visible on an anterior view of the medulla (See Fig. 1.27) [289].

Superior (pontine) triangle

This triangle can be divided into inferior, middle, and superior levels.

Inferior level

16 Facial colliculus, corresponding to the abducens nucleus crossed by the fibers of the facial nerve
17 Pontine vestibular area, corresponding to the vestibular nuclei

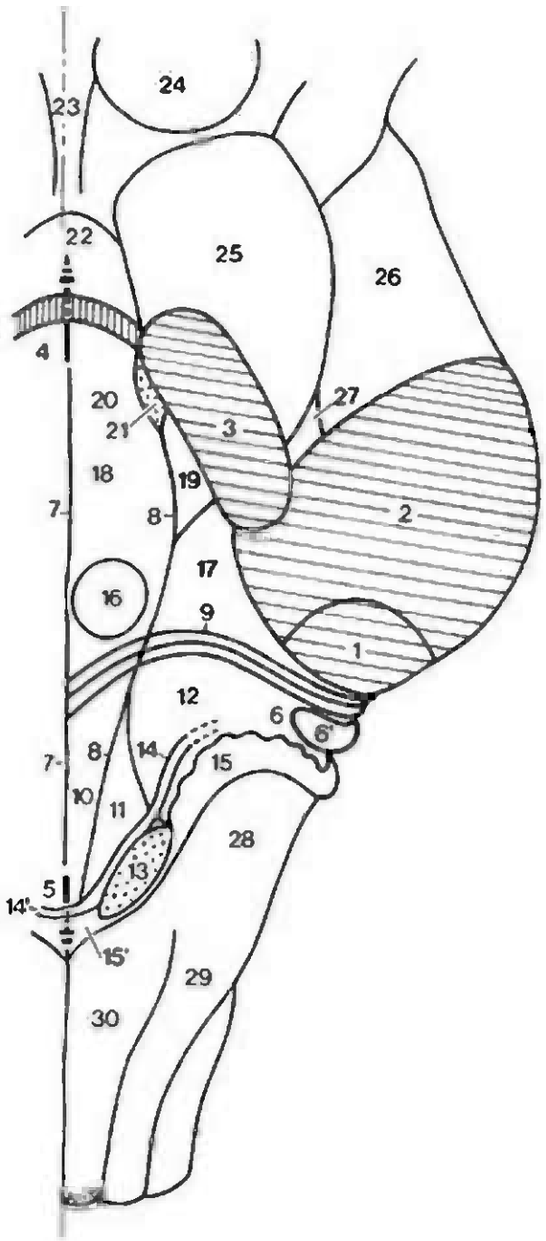

A

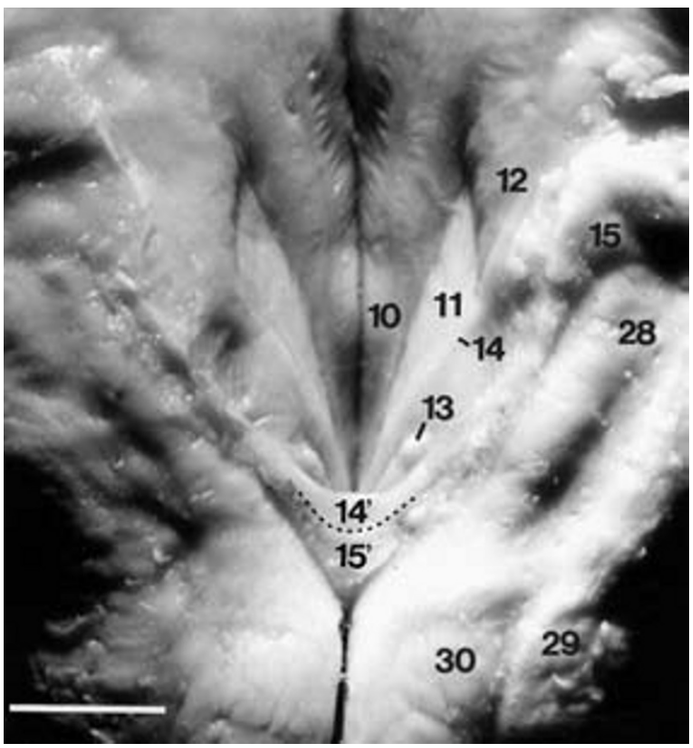

B

Middle level

18 Medial eminence
19 Superior fovea (fovea trigemini) corresponding to the motor trigeminal nucleus

Superior level

20 Medial eminence
21 Locus ceruleus
22 Superior medullary velum overlapping the superior angle of the floor
23 Frenulum veli
24 Inferior colliculus
25 Superior cerebellar peduncle (brachium conjunctivum)
26 Middle cerebellar peduncle (brachium pontis)
27 Parabrachial recess
28 Inferior cerebellar peduncle (restiform body)
29 Cuneate tubercle
30 Gracile tubercle (clava)

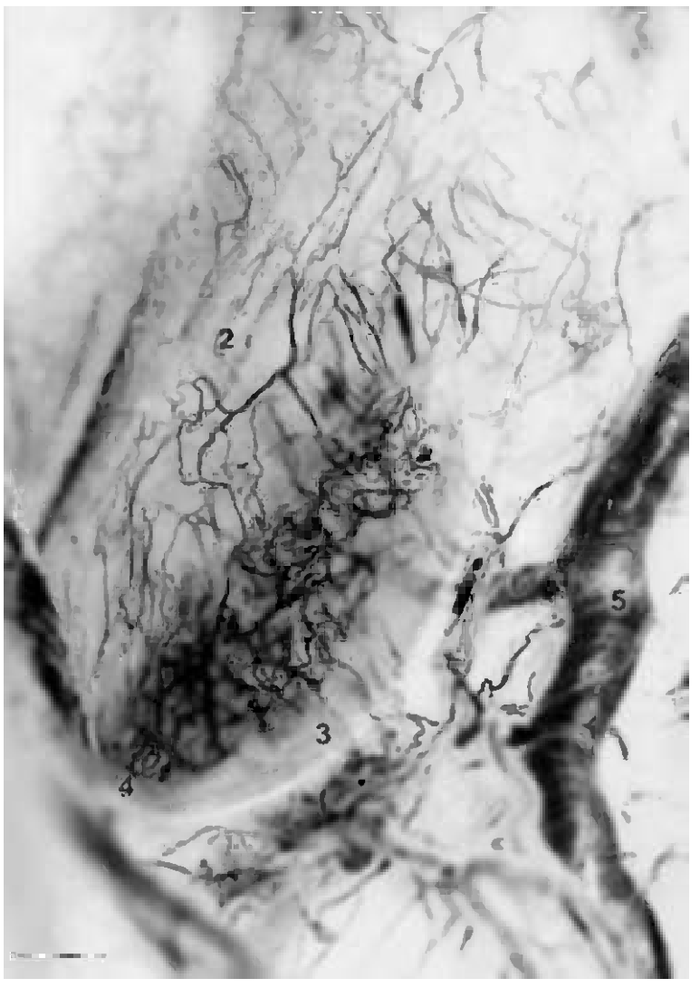

Fig. 1.22. The right area postrema. Endoventricular view. Intravascular India ink injection. Bar: 1 mm.

1 Area postrema (**See also Fig. 1.25A**)
2 Funiculus separans and vagal trigone
3 Posterior ligula
4 Obex
5 Marginal vein of the floor of the fourth ventricle
6 Deep vein draining from the structures of the ventricular floor into the marginal vein

The area postrema belongs to the group of circumventricular organs, whose vessels are devoid of a blood-brain barrier.
(For more information about area postrema vascularization, see [123, 131]).

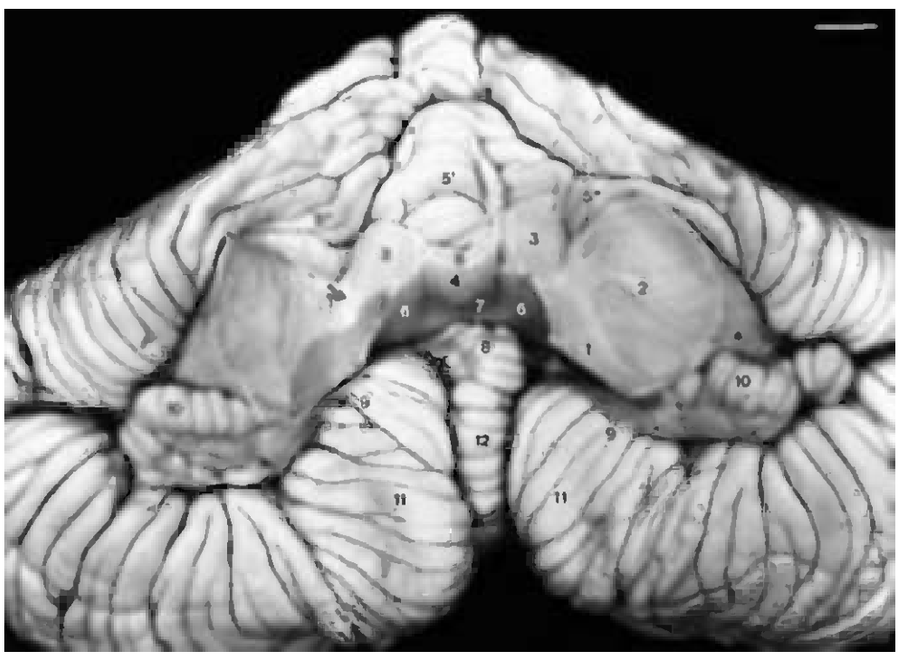

Fig. 1.23. The roof of the fourth ventricle.
Anterior view of the cerebellum after removal of the brain stem by section of the inferior (1), middle (2), and superior (3) cerebellar peduncles. This dissection shows the fastigial sulcus (7) and the superior portion of the ventricular roof (**See Fig. 1.20**). Bar: 5 mm.

Superior portion of the ventricular roof
In the midline, the superior vermis (lingula (5) and central lobule (5′)) form a dorsal median protrusion (4), covered by the superior medullary velum. To each side, the superior cerebellar peduncles (3) and the cerebellar hemispheres (alae of the central lobule, 5″) indent the roof to form right and left dorsal lateral (posterior superior) recesses (6).

7 Fastigium of the roof (fastigial sulcus)
The tectorial membrane belonging to the inferior portion of the roof is fixed medially on the nodulus (8) and laterally on the inferior medullary velum (9) along the brachium of the flocculus.
10 Flocculus
11 Tonsil
12 Uvula

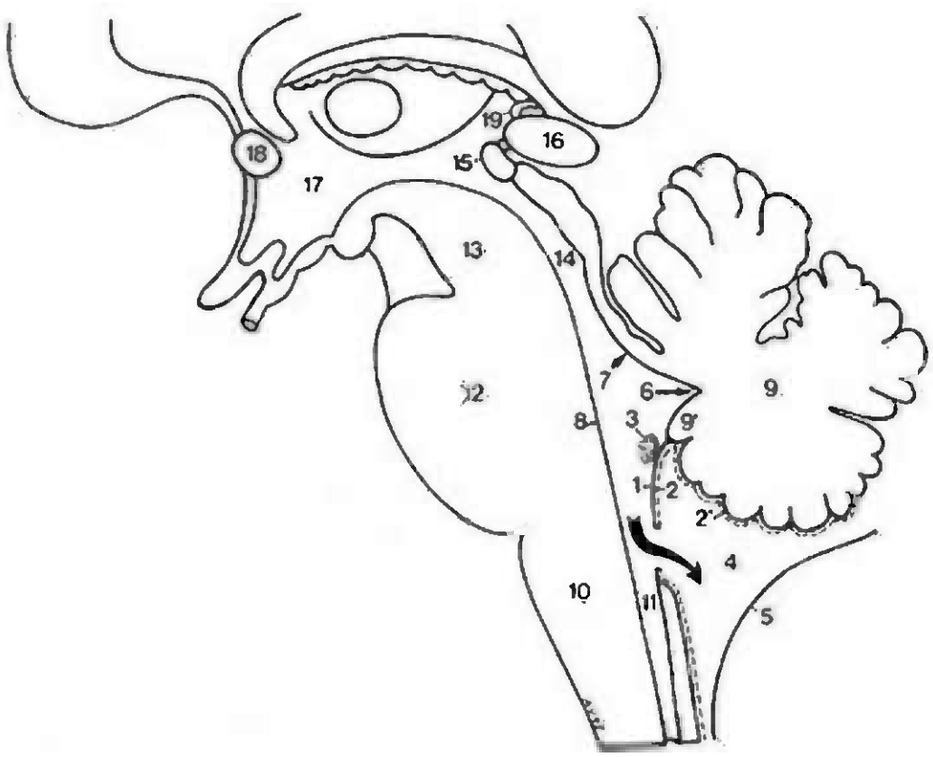

Fig. 1.24. The roof of the inferior fourth ventricle. Diagram of a median section. The inferior portion of the roof is a thin wall made up of two layers:

1 Tectorial membrane (ependyma)
2 Medullary layer of the inferior tela choroidea

The inferior tela choroidea itself is composed of two pial layers: a medullary (2) and a cerebellar (2′) layer. These layers of the tela choroidea delimit the cerebellomedullary cistern (cisterna magna) (4), which is completed posteriorly by the arachnoid mater (5). The arrow indicates the median aperture of the roof (foramen of Magendie), which communicates the ventricular cavity with the subarachnoid spaces.

3 Choroid plexus
6 Fastigial sulcus
7 Superior portion of the roof
8 Floor of the fourth ventricle
9 Vermis
9′ Nodulus
10 Medulla
11 Central canal
12 Pons
13 Mesencephalon
14 Cerebral aqueduct
15 Posterior commissure
16 Pineal gland
17 Third ventricle
18 Anterior commissure
19 Habenular commissure

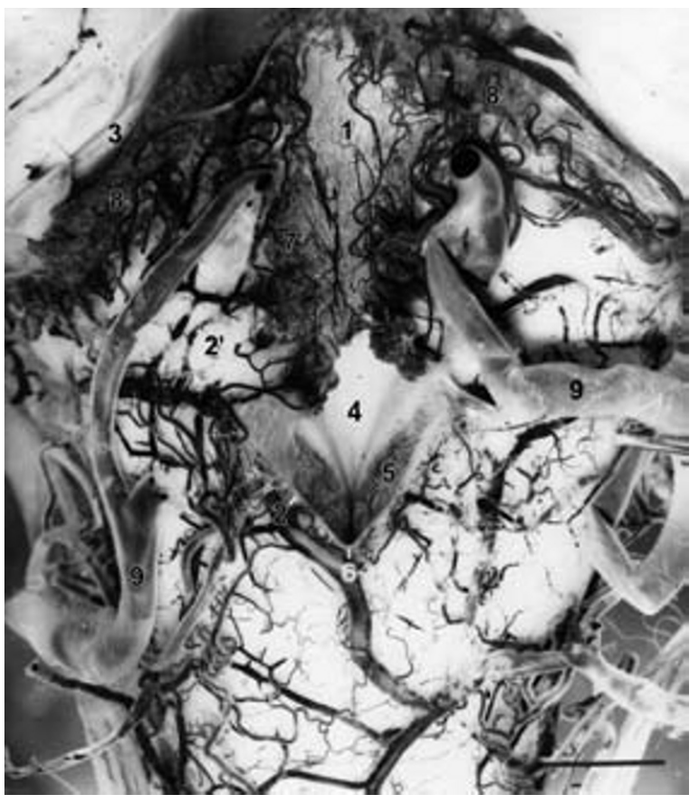

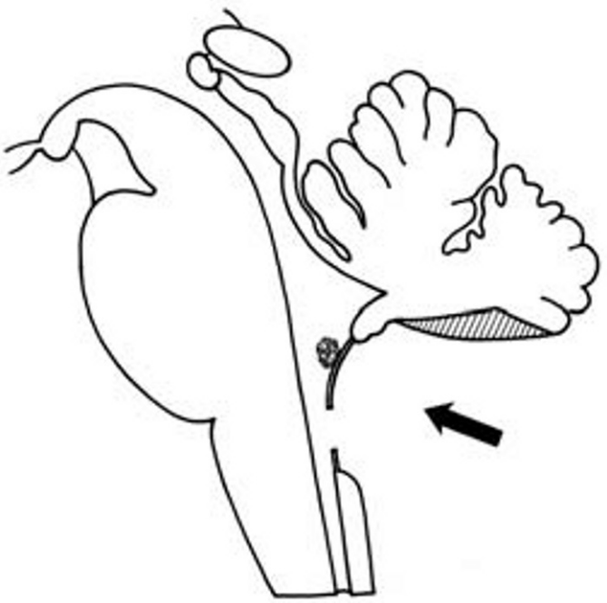

Fig. 1.25 (A–B). The roof of the inferior fourth ventricle, after partial removal of the cerebellum. Gross anatomic specimen and diagram. The arrow in the diagram indicates the point of view for the specimen.

1–3 The tectorial membrane (1), covered with pia mater (**See Fig. 1.24**), is stretched between the medulla and cerebellum. It is attached to the medulla by the ligula (thin medially (2) but substantial laterally (2′)). It is attached to the cerebellum by the inferior medullary velum (3), which is fixed to the brachium of the flocculus laterally and the nodulus medially (**See Fig. 1.23**).

4 Median aperture (foramen of Magendie). The ventricular floor and area postrema (5) are visible through this foramen (**See Fig. 1.22**).

6 Obex

7–8 The paired intraventricular choroid plexi are seen through the transparent tela choroidea. On each side the choroid plexus is formed by a vertical limb (7) and a transverse limb (8) which passes through the lateral aperture and exits from the ventricle to enter the cerebellopontine angle (**See Figs. 1.26–1.28**). The portions of the choroid plexi that protrude into the subarachnoid space are called the extraventricular choroid plexi.

9 Posterior inferior cerebellar arteries

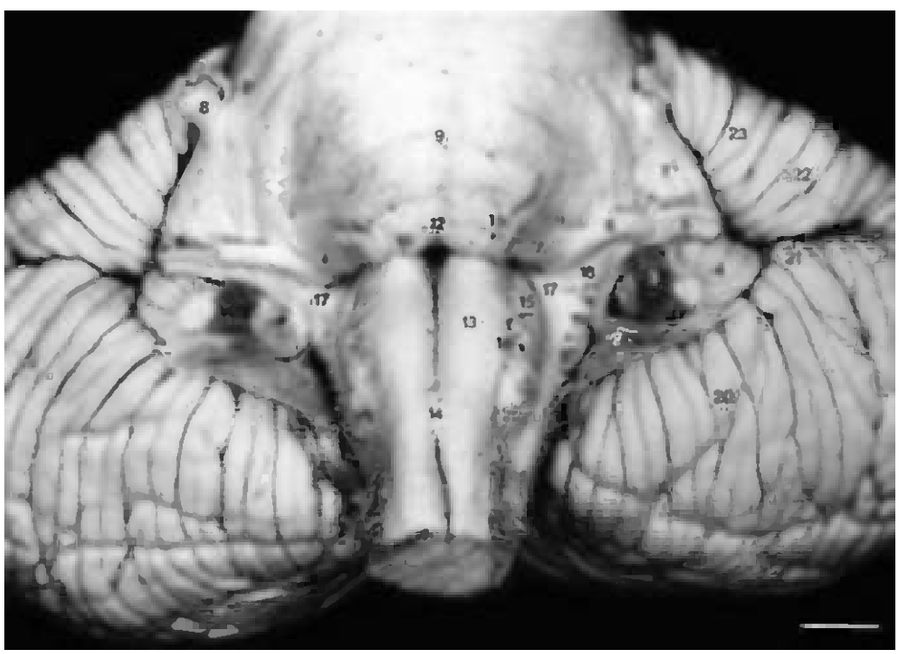

Fig. 1.26. The brain stem and cerebellum. Anterior view. Bar: 5 mm.

1 Lateral aperture of the fourth ventricle (foramen of Luschka)
2 Anterior ligula (anterior extension of the posterior ligula shown in **Figs. 1.21 and 1.25**)
3 Extraventricular choroid plexi
The lateral aperture of the fourth ventricle forms a portion of the cerebellopontine angle (**See Fig. 1.19**).
4 Flocculus
5 Vestibulocochlear nerve
6 Facial nerve
7 Middle cerebellar peduncle
8 Trigeminal nerve (sensory root)
8′ Trigeminal nerve (motor root)
9 Pons
10 Pontomedullary sulcus
11 Abducens nerve
12 Foramen cecum
13 Pyramid of the medulla
14 Decussation of the pyramids
15 Inferior olive
16 Hypoglossal nerve
17 Lateral medullary fossa
18 Glossopharyngeal nerve
19 Vagus nerve
20 Biventral lobule
21 Great horizontal fissure
22 Anterior superior fissure (primary fissure)
23 Quadrangular lobule

Fig. 1.27. The fourth ventricle. Anterior view.
Lateral aperture (foramen of Luschka). Bar: 2 mm.

1 Lateral aperture (right side)
2 Anterior ligula bordering the lateral aperture
2' Free edge of the anterior ligula
3 Extraventricular choroid plexus
The ligula and its free edge embody the old picture of Bochdalek's cornucopia, the fruit being the choroid plexus. (For more information about the anatomy of this region, see [289].)
4 Glossopharyngeal nerve
5 Vagus nerve
Both these nerves have been partially cut to show the ligula.
6 Remnant rootlets of vagus nerve
7 Accessory nerve, medullary root
8 Accessory nerve, spinal root
9 Inferior olive
10 Hypoglossal nerve
11 Vestibulocochlear nerve
12 Cerebellar hemisphere

1.28

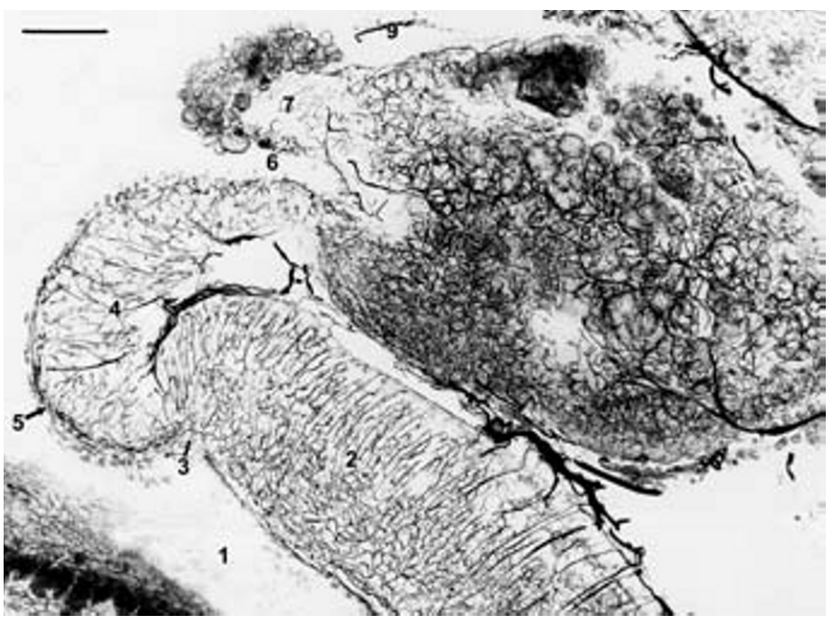

1.29

Fig. 1.28. The cerebellomedullary fissure and lateral aperture of the fourth ventricle. Transverse section. Inferior aspect of the left side. Intravascular India ink injection. Bar: 2 mm.

1 Lateral aperture of the fourth ventricle (foramen of Luschka)
2 Extraventricular choroid plexus
3 Intraventricular choroid plexus
4 Ventricular cavity
5 Tonsil
6 Inferior medullary velum
7 Flocculus
8 Inferior cerebellar peduncle
9 Vagus nerve
10 Anterior ligula covered by both the vagus and glossopharyngeal nerves, depending upon the specific superior-inferior level of section (**See Fig. 1.27**)
11 Inferior olive
12 Lateral medullary fossa

Fig. 1.29. The mesencephalon. Median section. Intravascular India ink injection. Bar: 1 mm.

1 Cerebral aqueduct (of Sylvius)
2 Tectum of the mesencephalon (sectioned between the left and right colliculi)
3 Recessus mesocoelicus (recess at the superior aspect of the cerebral aqueduct (of Sylvius))
4 Posterior commissure
5 Subcommissural organ. Like the area postrema, it belongs to the group of circumventricular organs whose blood vessels are devoid of a blood-brain barrier. The role of the subcommissural organ is controversial (**See Fig. 8.116**).
6 Pineal recess
7 Habenular commissure
8 Pineal gland
9 Suprapineal recess

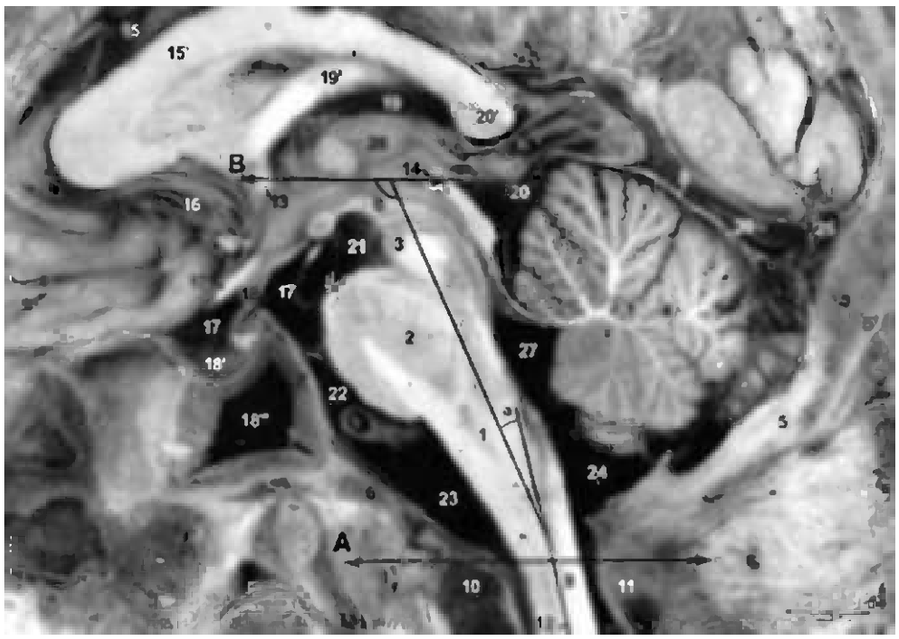

F. Lengths and angular relationships [68–70, 423–425]

Fig. 1.30. Median section of the head. Bar: 10 mm.
The medulla (1), pons (2), mesencephalon (3), and cerebellum (4) are located within the posterior cranial fossa. This is bounded dorsally by the occipital squama (5) (5′ external occipital protuberance), ventrally by the basilar portions of the occipital (6) and sphenoid (7) bones, and superiorly by the tentorium cerebelli (8). The mesencephalon (3) enters the middle cranial fossa through the tentorial hiatus (See Fig. 5.5).

The cervicomedullary junction is defined as the transverse plane just superior to the first pair of cervical spinal nerves. This approximates a plane (A) through the apex of the dens (10) and the middle of the posterior arch of the atlas (11).

Position of the brain stem
The angle (a) between the axis of the spinal cord (12) and the axis of the brain stem averages 15°. The angle (b) between the brain stem and the intercommissural plane (B) of Schaltenbrand [377] (extending from the mid-anterior commissure (13) to the mid-posterior commissure (14)) averages 110°-130°.

Subarachnoid cisterns
The subarachnoid cisterns are enlargements of the subarachnoid spaces due to the disparity between the nervous structures and the skull. They are divided into supra- and infra-tentorial cisterns.

Supratentorial cisterns
15 Supracallosal cistern
15′ Corpus callosum
16 Cistern of the lamina terminalis
16′ Lamina terminalis
17 Chiasmatic cistern (suprasellar or perihypophyseal cistern about the hypophyseal stalk (18)
17′ Optic chiasm
18 Hypophyseal (pituitary) stalk
18′ Anterior lobe of the hypophysis (adenohypophysis)
18″ Posterior lobe of hypophysis (neurohypophysis)
18‴ Sphenoid sinus
19 Cistern of the velum interpositum (See Fig. 1.3) (median portion of the transverse fissure)
19′ Fornix
20 Quadrigeminal plate cistern
20′ Splenium of the corpus callosum
21 Interpeduncular cistern linked to the quadrigeminal cistern by the crural and ambient cisterns situated around the mesencephalon

Infratentorial cisterns
Due to the tentorial hiatus, the quadrigeminal cistern (20) belongs to both the supra- and infra-tentorial cisterns
22 Prepontine cistern, continuous laterally with the cistern of the cerebellopontine angle
23 Premedullary cistern
24 Cerebellomedullary cistern (cisterna magna)
25 Torcular Herophili
26 Sinus rectus (straight sinus)
27 Fourth ventricle
28 Third ventricle

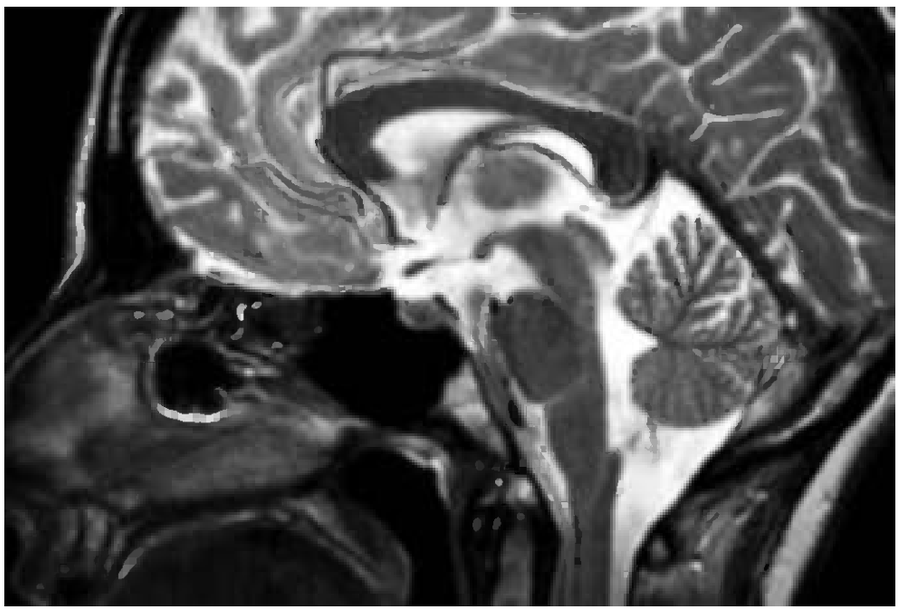

A

Fig. 1.31 (A–B). Standard lengths and angles of the midline. Mid-sagittal T2-MRI (1.5 Tesla).

A Anterior commissure
B Basion
F Folium line (line along the central axis of the arbor vitae directed toward the folium)
N Nasion
O Obex
P Posterior commissure
T Tuberculum

The lengths and angles of midline osseous and parenchymal landmarks were measured on mid-sagittal T2-MRI in 272 normal adult male and female patients evenly distributed across all decades two – nine (17 males and 17 females per decade) [68–70, 377, 423–425]. Statistical analysis provided standard deviations of the measurements, correlations among them, and estimates of the significance of the observations**.**

Skull base lengths and angle:
The skull base was measured from the nasion (N) to the tuberculum (T) to the basion (B) and the basal angle N-T-B determined (**Table 1.2A**). The NT and TB lines are longer in men than women. Their length does not change with age from 10-89 years in either gender ($p < 0.001$) The basal angle of the skull (N-T-B) shows no significant difference between genders or across decades two to nine.

Parenchymal lengths and angle:
Talairach's AC-PC line is measured from the top of the anterior commissure (AC) to the bottom of the posterior commissure (PC). On MRI, *in vivo*, Tailarach's AC-PC line ranges from 22.7 to 30.1 mm (mean 26.9 mm, SD 1.3 mm) **(Table 1.2B).** It is very slightly larger in men (mean 27.2 mm, SD 1.3 mm) than women (mean 26.5 mm; SD 1.2 mm) ($p < 0.001$). Within each gender, the length of Talairach's AC-PC line does not vary significantly with age. These MR measurements correlate well with Talairach's own measurements in 55 brains (Range: 20.5 to 28.5 mm, Modal length: 25 mm, Mean length: 25.07 mm (SD 1.54 mm)). [420, 421].

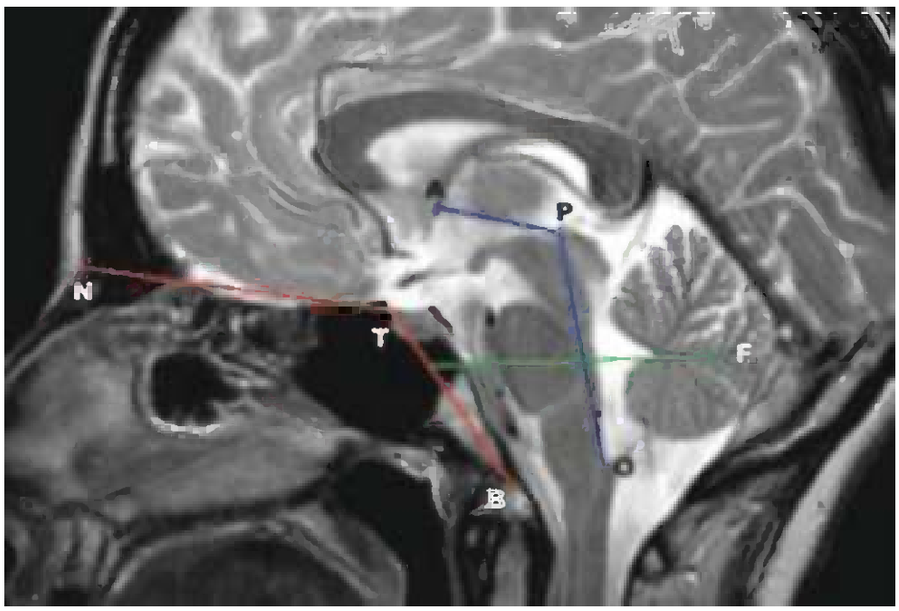

B

Schaltenbrand's line is measured from the midpoint of the AC to the midpoint of the PC. Therefore it is consistently shorter than Talairach's line, by an average of 0.7 mm (standard deviation 0.5 mm). On MRI, *in vivo*, Schaltenbrand's line ranges from 22.0 to 30.0 mm (mean 26.2 mm, SD 1.3 mm) **(Table 1.2B).** Within each gender, the length of Schtenbrand's line does not vary significantly with age. These MR measurements also correlate well with Schaltenbrand's own measurements of 23.5 to 27.5 mm [1, 377, 378].

Tamraz's line extends from the posterior commissure (PC) to the obex (O) [423, 424, 425]. On MRI, *in vivo*, the length of the PC-O line ranges from 40.9 to 58.8 mm and is larger in men (mean 49.5 mm; SD 3.1 mm) than women (mean 47.7 mm; SD 2.5 mm) ($p < 0.001$) (**Table 1.2B**). The PC-O line shortens very slightly with age (0.26 mm per decade, $p = 0.001$). The length of this line has not been reported previously.

The central angle of the brain (AC-PC-O) varies from 102.1 to 128.8° (mean 114.3°, SD 3.8°) **(Table 1-2B).** This angle is slightly larger in males than females, by an average of 1.7° ($p=0.0002$). It increases very slightly with age (0.27° per decade, $p=0.008$). The AC-PC-O angle has not been specifically measured previously, but accords well with a similar angle of approximately 118°, which may be calculated from published data of Tamraz [423, 424, 425]. The basal angle of the skull (N-T-B) is larger than the central angle of the brain (AC-PC-O) in both genders at all ages by an average of 17° (SD 6.8°).
The MRI data reported in Figs. 1.31 and 1.32 plus Tables 1.2 and 1.3 derive from research performed at the Mt. Sinai Medical center by Michael B. Schwartz, M. D.

Arbor vitae cerebelli:
The vermian white matter forms a reproducible branching pattern that identifies each lobule (**See Figs. 1.30 and 1.32**).

Table 1.2A. Lengths and angles of the skull base in the midline. MRI data 1.5 T.

Decade (D)	Age (Years)	Nasion-Tuberculum line Length (mm)		Tuberculum-Basion line Length (mm)		Base of skull (N-T-B) Angle (°)	
		Female	Male	Female	Male	Female	Male
2	10–19	57.4	57.4	46.7	46.4	131.8	133.3
3	20–29	59.5	60.6	46.7	48.2	131.0	130.4
4	30–39	58.1	60.7	47.4	49.3	130.1	134.0
5	40–49	57.6	60.4	46.3	47.8	129.3	129.7
6	50–59	56.7	60.4	46.9	49.9	128.7	129.6
7	60–69	57.6	60.9	45.3	48.1	132.2	131.0
8	70–79	58.2	59.4	45.3	47.0	131.2	133.0
9	80–89	58.4	60.6	45.5	47.1	131.4	132.9

For each gender separately

D		Female	Male	Female	Male	Female	Male
2–9	Mean ± SD	57.9 ± 2.6	60 ± 2.5	46.2 ± 2.8	48 ± 3.0	130.8 ± 5.9	131.7 ± 5.8
	Range	52.2 – 62.6	50.3 – 67.2	40.6 – 54.3	39.9 – 54.2	119.1 – 144.9	115.9 – 143.4

For both genders together

2–9	Mean ± SD	58.9 ± 2.7	47.1 ± 3	131.3 ± 5.9
	Range	50.3 – 67.2	39.9 – 54.3	115.9 – 144.9
	Mean ± 2 SD	53.5 – 64.3	41.1 – 53.1	119.5 – 143.1

Abbreviations:

B = Basion
N = Nasion
T = Tuberculum

Base of skull angle = Nasion-Tuberculum-Basion angle (open anteriorly)

SD = Standard deviation of mean

Table 1.2B. Lengths and angles of the central brain in the midline. MRI data 1.5 T.

Decade (D)	Age (Years)	Talairach Top AC-Bot PC Line Length (mm)		Schaltenbrand Mid AC-Mid PC Line Length (mm)		Tamraz PC-Obex Line Length (mm)		Central AC-PC-Obex Angle (°)		Tamraz Line-Folium Line Angle (°)		T-B Line-Folium Line Angle (°)	
		Female	Male	Female	Male	Female	Male	Female	Male	Female	Male	Female	Male
2	10–19	26.2	26.5	25.5	25.7	46.7	49.1	114.1	113.7	104.8	103.6	128.9	130.3
3	20–29	26.7	27.4	26.3	26.7	49.7	49.2	112.7	114.8	105.0	105.5	130.3	130.4
4	30–39	26.6	27.6	26.1	27.0	48.9	51.2	113.7	112.7	102.0	105.1	127.7	131.2
5	40–49	26.9	27.1	26.1	26.3	48.2	50.6	113.0	115.7	106.1	107.5	129.1	132.6
6	50–59	26.1	27.4	25.5	26.7	47.4	51.5	113.0	115.2	105.8	108.1	130.6	132.4
7	60–69	26.2	27.0	25.4	26.5	47.0	49.2	114.6	116.1	108.1	107.2	134.0	131.0
8	70–79	26.2	27.1	25.5	26.3	47.1	47.2	114.1	115.3	109.4	108.4	135.3	132.3
9	80–89	27.2	27.5	25.9	26.7	46.3	47.9	113.2	117.7	110.1	109.9	134.4	132.6

For each gender separately

D		Female	Male	Female	Male	Female	Male	Female	Male	Female	Male	Female	Male
2–9	Mean ± SD	26.5 ± 1.2	27.2 ± 1.3	25.9 ± 1.2	26.5 ± 1.4	47.7 ± 2.5	49.5 ± 3.1	113.5 ± 3.7	115.1 ± 3.8	106.4 ± 5.8	106.9 ± 5.9	131.4 ± 6.3	131.6 ± 5.5
	Range	22.7 – 29.7	23.7 – 30.1	22.2 – 29.6	22.6 – 30	41.1 – 54.7	40.9 – 58.8	105.2 – 128.8	102.1 – 121.7	92.3 – 122	91.7 – 119.9	115.2 – 145.6	116.3 – 147.5

For both genders together

2–9	Mean ± SD	26.9 ± 1.3	26.2 ± 1.3	48.6 ± 3.0	114.3 ± 3.8	106.7 ± 5.9	131.5 ± 5.9
	Range	22.7 – 30.1	22.2 – 30.0	40.9 – 58.8	102.1 – 128.8	91.7 – 122.0	115.2 – 147.5
	Mean ± 2SD	24.3 – 29.5	23.6 – 28.8	42.6 – 54.6	106.7 – 121.9	94.9 – 118.5	119.7 – 143.3

Abbreviations:

AC = Anterior Commissure
PC = Posterior Commissure

AC-PC-Obex Angle = Central angle open anteriorly between AC-PC and PC-Obex lines
Folium Line = Line through the central branch of the arbor vitae common to the declive, folium and tuber
Schaltenbrand line (Mid AC – Mid PC) = Line taken from the middle of AC to the middle of PC
Talairach Top AC-Bot PC Line = Line taken from the top of AC to the bottom of PC
Tamraz PC-Obex Line = Line from the midpoint of PC to the obex

SD = Standard deviation of mean

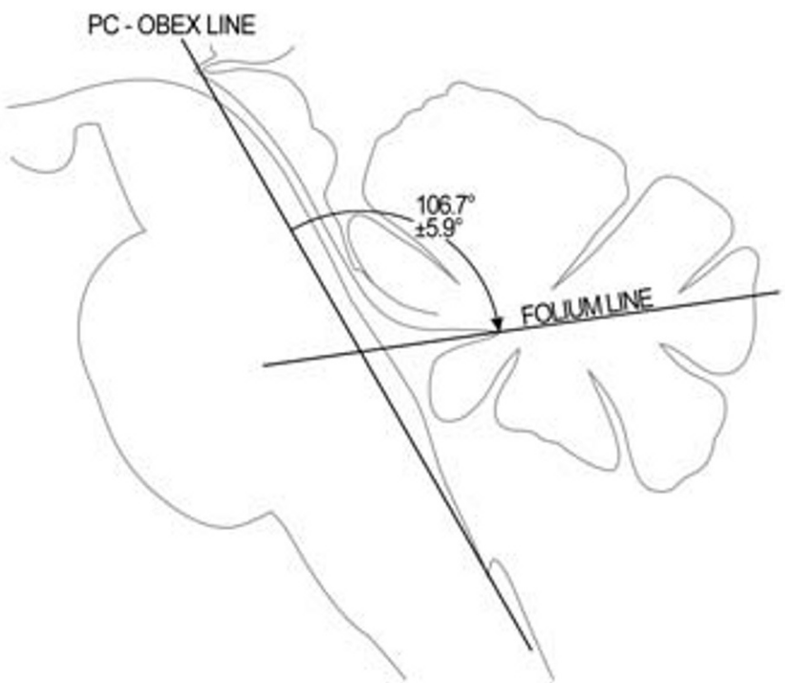

A

Fig. 1.32 (A–B). Angular relationships of the vermian lobules to the posterior commmissure-obex line (PC-O line) of Tamraz.

Prior studies have evaluated vermian areas and volumes, but not the angular relationships of the vermian lobules to the brain stem or to each other [22, 351, 352, 353, 376, 393].

A. Angular relationship of the folium line to the posterior commissure (PC)-obex line. Diagram. The prominent central arm of the arbor vitae common to the declive, folium and tuber (folium line) intersects the PC-O line reproducibly. This angle is easily measured directly from midsagittal T1- or T2-weighted MR images. The folium-angle measured greater than 90° in all patients studied. It averaged 106.7° (standard deviation 5.9°) in 272 men and women in decades 2-9, and increased slightly with age (0.85° per decade) **(See Tables 1.2 and 1.3).**

B. Angular relationships of the other vermian lobules to the PC-O line. Diagram. The angular relationships of the other vermian lobules to the brain stem may be measured by translating the PC-O line to the apex of the fourth ventricle (fastigial sulcus) and measuring the angles there. Alternatively one may simply extend the folium line anteriorly, measure the lobular angles with respect to the folium line, and then adjust arithmetically for the folial angle itself.

The angular relationships of each vermian lobule to the PC-O line, and the angular relationships among the individual vermian lobules, show no substantive difference with gender or age over decades two – nine **(Table 1.3).** Wider angles of anterior lobules do correlate with narrower angles of posterior lobules, however, raising question of possible conservation of substrate destined for construction of the vermis [183].

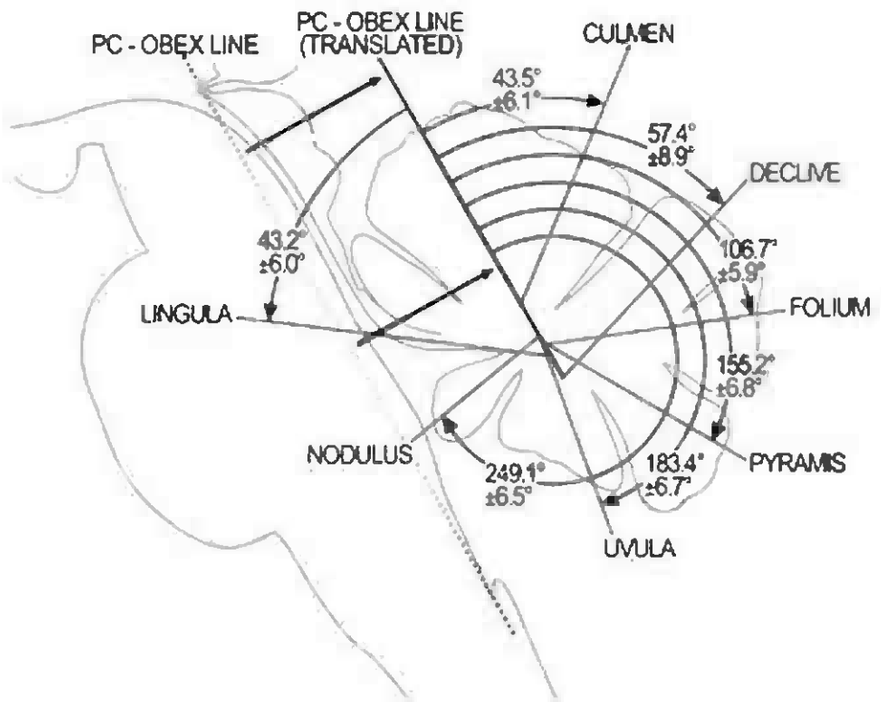

B

The most consistent vermian angles include the

PC-O to Culmen angle:	**Range: 25.3 to 59.1°**	**Mean: 43.5°**	**(SD 6.1°)**
PC-O to Folium angle:	**Range: 91.7 to 122.0°**	**Mean: 106.7°**	**(SD 5.9°)**
PC-O to Pyramis angle:	**Range: 135.7 to 175.0°**	**Mean: 155.2°**	**(SD 6.8°)**
PC-O to Uvula angle:	**Range: 165.3 to 199.1°**	**Mean: 183.4°**	**(SD 6.7°)**
PC-O to Nodulus angle:	**Range: 230.8 to 264.7°**	**Mean: 249.1°**	**(SD 6.5°)**

Measurements of the angles to the lingula, central lobule, declive and tuber proved to be more challenging technically and more difficult to achieve reliably **(Table 1.3).**

Since the vermis forms rostrally along the superior lips of the rhombencephalic vesicle and then rotates caudally, in clockwise fashion, to surround the fourth ventricle, measurement of vermian angles provides one method for quantifying vermian malrotation and hypoplasia. Measurement of a PCO-lobule angle to the culmen of $< 25^{o}$, to the folium of $< 90^{o}$, to the pyramis of $< 135^{o}$, to the uvula of $< 165^{o}$ and to the nodulus of $< 230^{o}$ suggests possible incomplete vermian rotation, since those minimum PC-O to lobule angles represent the *minimum* degree of rotation found in any of the 272 normal individuals aged 10–89 years studied by mid-sagittal MRI.

Table 1.3. Vermian angles: Degrees of clockwise rotation from the PC-Obex Line. MRI data 1.5 T.

Decade (D)	Age (years)	PC-Obex to Lingula* Angle (°)		PC-Obex to Centralis* Angle (°)		PC-Obex to Culmen Angle (°)		PC-Obex to Declive Angle (°)		PC-Obex to Folium Angle (°)		PC-Obex to Tuber Angle (°)		PC-Obex to Pyramis Angle (°)		PC-Obex to Uvula Angle (°)		PC-Obex to Nodulus Angle (°)	
		Female	Male	Female	Male	Female	Male	Female	Male	Female	Male	Female	Male	Female	Male	Female	Male	Female	Male
2	10–19	−44.5	−46.4	−11.5	−11.5	41.9	40.7	54.6	52.5	104.8	103.6	141.1	139.3	151.9	151.0	180.6	179.7	245.8	246.1
3	20–29	−44.9	−43.9	−10.7	−14.3	42.8	42.6	54.0	56.6	105.0	105.5	143.7	141.9	154.6	153.9	181.8	181.3	248.0	246.1
4	30–39	−48.6	−43.9	−14.2	−9.8	38.9	42.4	52.2	56.0	102.0	105.1	138.9	139.8	152.0	152.0	181.1	181.0	245.2	248.2
5	40–49	−43.1	−42.5	−13.4	−11.5	42.2	45.3	56.1	57.7	106.1	107.5	142.4	143.8	156.9	155.1	187.1	182.9	249.9	249.8
6	50–59	−44.5	−41.9	−12.7	−12.4	41.4	44.1	54.0	61.4	105.8	108.1	142.9	143.0	157.7	156.7	183.7	183.8	240.6	249.7
7	60–69	−41.9	−44.2	−12.2	−10.4	44.9	44.8	58.8	56.7	108.1	107.2	144.1	143.8	156.1	155.2	184.6	184.4	249.9	249.7
8	70–79	−40.8	−40.9	−15.6	−12.1	45.3	44.7	62.6	61.6	109.4	108.4	145.7	144.2	159.3	155.8	184.8	185.3	252.2	249.9
9	80–89	−39.8	−39.5	−9.8	−12.1	46.5	46.7	60.4	61.1	110.1	109.9	146.8	145.4	157.9	157.5	185.4	186.1	253.2	251.3

For each gender separately

D		Female	Male	Female	Male	Female	Male	Female	Male	Female	Male	Female	Male	Female	Male	Female	Male	Female	Male
2–9	Mean ± SD	−43.5 ± 5.9	−42.9 ± 6.1	−12.5 ± 7.3	−11.8 ± 7.2	43.1 ± 6.0	43.9 ± 6.2	56.8 ± 8.6	57.9 ± 9.2	106.4 ± 5.8	106.9 ± 5.9	143.1 ± 7.2	142.7 ± 6.9	155.8 ± 7.1	154.7 ± 6.6	183.6 ± 6.7	183.1 ± 6.7	249.3 ± 6.5	248.9 ± 6.5
	Range	−57.9 – −27.7	−57.3 – −28.8	−30.2 – 8.6	−29.1 – 4.6	25.3 – 58.4	29.5 – 59.1	37.0 – 77.4	36.0 – 81.2	92.3 – 122.0	91.7 – 119.9	125.5 – 158.2	118.5 – 158.6	135.7 – 175.0	136.7 – 168.7	165.3 – 199.1	166.1 – 198.4	230.8 – 264.7	231.9 – 264.3

For both genders together

2–9	Mean ±SD	−43.2 ± 6.0	−12.1 ± 7.2	43.5 ± 6.1	57.4 ± 8.9	106.7 ± 5.9	142.9 ± 7.0	155.2 ± 6.8	183.4 ± 6.7	249.1 ± 6.5
	Range	−57.9 – −27.7	−30.2 – 8.6	25.3 – 59.1	36.0 – 81.2	91.7 – 122.0	118.5 – 158.6	135.7 – 175.0	165.3 – 199.1	230.8 – 264.7
	Mean ± 2 SD	−55.2 – −31.2	−26.5 – 2.3	31.3 – 55.7	39.6 – 75.2	94.9 – 118.5	128.9 – 156.9	141.6 – 168.8	170.0 – 196.8	236.1 – 262.1

Abbreviations:

PC = Posterior Commissure
PC-Obex Line = Line from the midpoint of PC to the obex
SD = Standard deviation of mean

* signifies that the angle falls to the left of the PC-Obex line

SECTION II

INTERNAL ARCHITECTURE OF THE BRAIN STEM WITH KEY AXIAL SECTIONS

The structure of the brain stem is presented first in overview (**Figs. 2.1 to 2.6**), including the reticular formation (**Fig. 2.2**), the cranial nerve nuclei (**Fig. 2.3**) and the principal functional pathways (**Figs. 2.4 and 2.5**). The structure is then presented in detail, using a series of 16 axial (transverse or horizontal) sections (**Figs. 2.7 through 2.22**) parallel to Schaltenbrand's intercommissural plane. These may be compared to the the axial anatomic and MRI sections shown in **Figs. 11.1–11.29**.

Structure of the brain stem

This study is based primarily on the works of Riley [358] and Olsewsky and Baxter [327]. See also works by [7, 8, 13, 19, 24, 25, 35, 38, 39, 42, 44, 50, 66, 67, 72, 74, 78, 85, 88, 93, 99, 106, 109, 122, 131, 147, 148, 181, 194, 195, 201, 202, 212, 221, 228, 229, 236, 238, 244, 245, 248, 281, 286, 287, 291, 304, 322, 322a, 324, 329, 360, 372, 382, 386, 396, 398, 405, 434, 441, 443, 454, 455, 466, 486].

References [21, 22, 91, 251, 265, 266, 282, 322, 322a, 330, 337, 357, 387, 452, 455, 474, 475] discuss the brain stem and cerebellum.

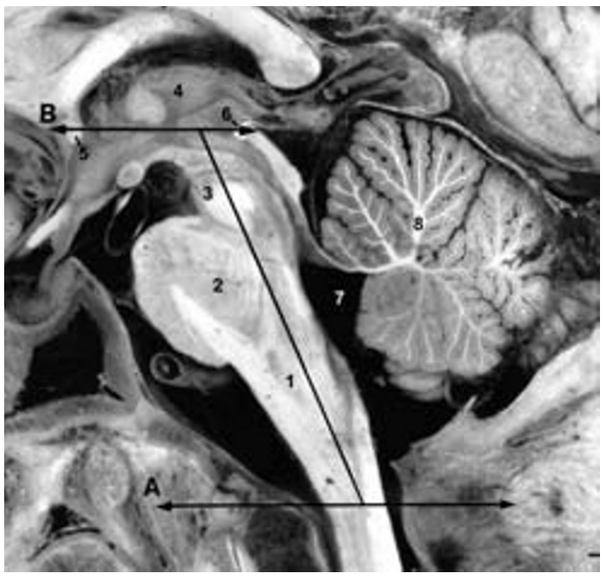

Fig. 2.1. Median section of the head, for orientation of the following figures. (See Fig. 1.30 for more detail)

Structurally, the brain stem is composed of the medulla (1), the pons (2), and the mesencephalon (3), interposed between the spinal cord inferiorly and the diencephalon (4) superiorly. The brain stem contains multiple nuclei for the cranial nerves, multiple nuclei for relaying sensory and motor data to and from the brain and spinal cord, and multiple reticular nuclei including monoamine-producing nuclei with widespread connections to all parts of the brain [321]. Short white matter tracts interconnect structures within the brain stem. Long white matter tracts extend into or through the brain stem from above and below to convey information to the stem, relay information through the stem, or carry information from the brain stem to other centers.

Line A through the cervico-medullary junction and **Line B** (Schaltenbrand's line) through the midpoints of the anterior and posterior commissures indicate the location and orientation of the axial sections illustrated in Figs. 2.7–2.22.

5 Anterior commissure
6 Posterior commissure
7 Fourth ventricle
8 Arbor vitae of the vermis, with the "8" placed on the central portion for the culmen

Fig. 2.2. The reticular formation of the brain stem. The brain stem contains most of the encephalic reticular centers. The brain stem reticular nuclei are divided into three longitudinal columns: median, central (or medial), and lateral. The general arrangement of these columns is depicted diagrammatically in this posterior view of the brainstem (See Figs. 2.7 through 2.22 for more precise localization of the reticular nuclei and pp. 100–101 for their main functions). The reticular nuclei are usually named according to the Latin international nomenclature. However, their specific identification, localization and differentiation are difficult to determine with precision.

Median column (Pink)
The median column is formed by the raphe nuclei (situated on each side of the median raphe, which divides the brain stem into right and left portions).

Medulla
1 Nucleus raphe pallidus, ventrally
2 Nucleus raphe obscurus, dorsally

Pons
3 Nucleus raphe magnus
4 Nucleus raphe pontis
5 Nucleus reticularis centralis superior

Mesencephalon
6 Nucleus raphe dorsalis (dorsal nucleus of raphe)

Central (medial) column (Gray)
Medulla
7 Nucleus reticularis gigantocellularis, extending widely into the pons

Pons
8 Nucleus reticularis pontis caudalis
9 Nucleus reticularis pontis oralis
10 Nucleus reticularis tegmenti pontis (centralis inferior), which may belong to the pontine nuclei

Mesencephalon
11 Nucleus reticularis cuneiformis

Lateral column (Blue)
Medulla
12 Nucleus reticularis medullae oblongatae centralis
13 Nucleus reticularis lateralis (nucleus funiculi lateralis)

Pons
14 Nucleus reticularis parvocellularis (extension of the nucleus reticularis medullae oblongatae centralis into the pons)
15 Medial parabrachial nucleus
16 Lateral parabrachial nucleus

Mesencephalon
17 Nucleus reticularis pedunculopontinus

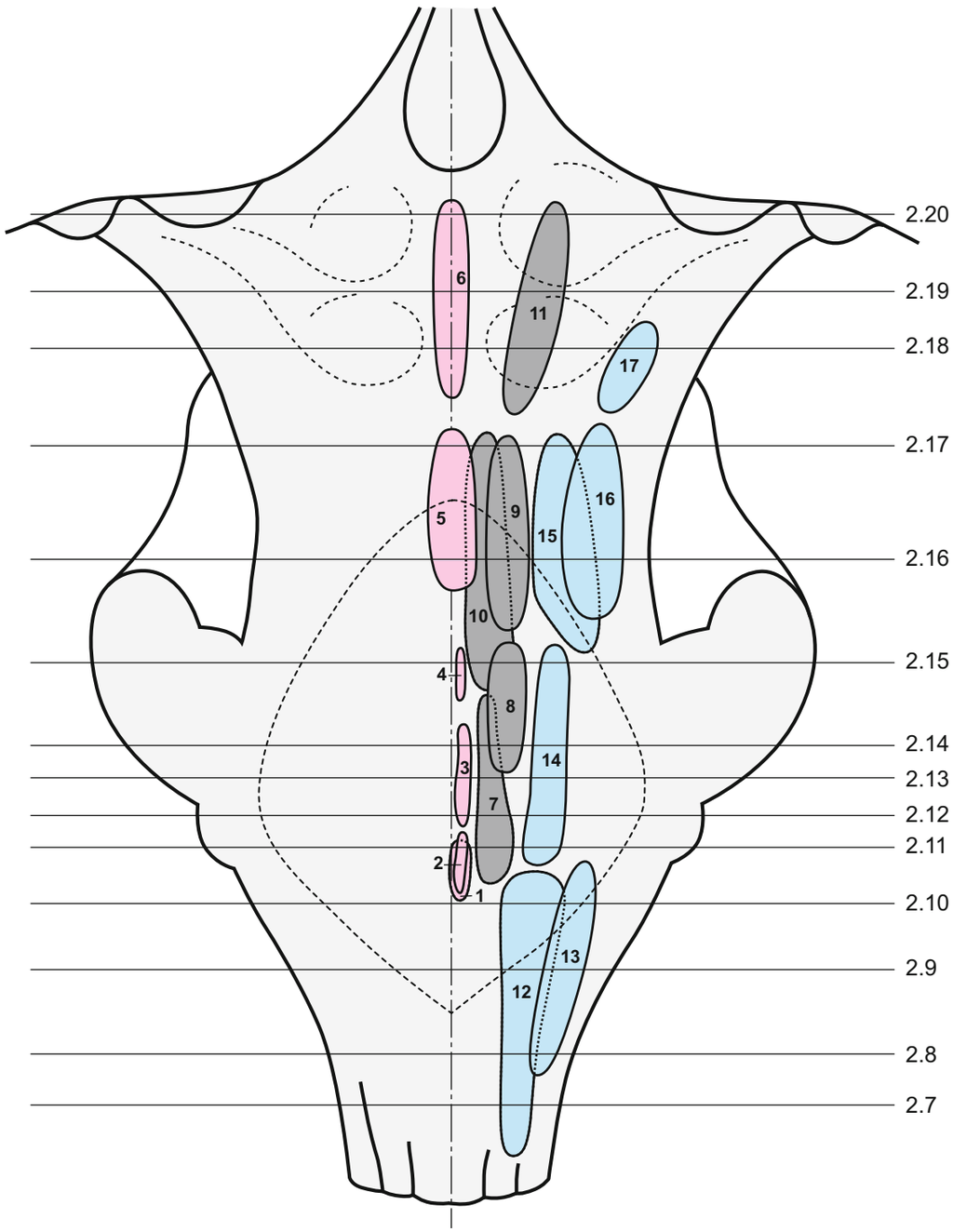

THE RETICULAR FORMATION

Fig. 2.3. The general arrangement of the motor (pink) and sensory (blue) cranial nerve nuclei. The orientation of these nuclei is shown in detail in Figs. 2.7 through 2.22. Most of the cranial nerve nuclei lie within the medulla.

MEDULLA

Motor nuclei

1 **Hypoglossal nucleus (CN XII)**, motor to the muscles of the tongue

2 **Dorsal motor nucleus of the vagus (CN X),** a motor center for parasympathetic autonomic innervation

3 **Inferior salivatory nucleus,** belonging to the glossopharyngeal nerve and involved in parasympathetic motor innervation of the parotid gland

4 **Nucleus ambiguus,** the origin of motor fibers entering several cranial nerves. In descending order, these are the glossopharyngeal nerve (**4**), vagus nerve (**4'**), accessory nerve (medullary root) (**4"**). The nucleus ambiguus innervates the muscles of the pharynx and larynx. The nucleus of the spinal root of the accessory nerve (not shown in this drawing) innervates the sternocleidomastoid and trapezius muscles

5 **Motor nucleus to the first cervical nerve (C1)** (nucleus supraspinalis)

Sensory nuclei

6 **Nucleus of the solitary tract (NST).** Its caudal extremity is linked to the opposite side through the commissural nucleus (**7**). Its slender oral extremity is called the nucleus ovalis. The nucleus of the solitary tract receives, in descending order, fibers of nervus intermedius (**6**), glossopharyngeal nerve (**6'**), vagus nerve (**6"**).
It has two functions:
The middle and lower portions of the nucleus of the solitary tract receive visceral fibers from peripheral receptors situated in visceral organs and blood vessels, transmitted via the glossopharyngeal and vagus nerves. The upper portion of the nucleus of the solitary tract receives gustatory fibers from the nervus intermedius and the glossopharyngeal nerve.

8 **Spinal trigeminal nucleus (CN V).** This long nucleus begins in the cervical spinal cord and ends in the pons. It is divided into three portions, in ascending order: **pars caudalis (8):** protopathic pathways from the face (pain and temperature), **pars interpolaris (8'):** sending fibers to the cerebellum, **pars oralis (8"):** a nucleus situated in the pons (See below). The spinal trigeminal nucleus also receives sensory fibers from the nervus intermedius, and the glossopharyngeal and vagus nerves.

9 **Cochlear nuclei (CN VIII)** dorsal (**9**) and ventral (**9'**), receiving auditory fibers from the internal ear.

10 **Vestibular nuclei (CN VIII)** receive information from the membranous labyrinth. They participate in the control of equilibrium and the oculomotor system. Among the different vestibular nuclei, the medial (**10**) and inferior (**10'**) vestibular nuclei are situated in the medulla.

PONS

Motor nuclei

11 **Abducens nucleus (CN VI),** motor to lateral rectus muscle belonging to the group of extra-ocular muscles

12 **Facial nucleus (CN VII),** motor to cutaneous facial muscles

13 **Lacrimal nucleus,** belonging to the nervus intermedius (**VII bis**) (parasympathetic innervation of the lacrimal, nasal, and palatine glands)

14 **Superior salivatory nucleus,** belonging to the nervus intermedius (**VII bis**) (parasympathetic innervation of sublingual and submandibular glands)
The existence of the lacrimal nucleus is uncertain. At present the superior salivatory nucleus can be considered as the center for the whole automatic innervation that depends on the nervus intermedius.

15 **Motor trigeminal nucleus (CN V)**, motor to masticatory muscles

Sensory nuclei

8" **Spinal trigeminal nucleus (CN V) (pars oralis)** receiving the epicritic pathways from the face

16 **Principal sensory trigeminal nucleus (CN V)** receiving the epicritic pathways from the face (like **8"**)

17 **Lateral vestibular nucleus (CN VIII)**

17' **Superior vestibular nucleus (CN VIII)** The inferior (**10'**) and medial (**10**) vestibular nuclei extend superiorly into the pons

18 **Mesencephalic trigeminal nucleus (CN V),** receiving proprioceptive information from the face

MESENCEPHALON

Motor nuclei

19 **Trochlear nucleus (CN IV),** motor to the superior oblique muscle belonging to the group of extra-ocular muscles

20–23 **Oculomotor nuclei (CN III),** supplying all the extra-ocular muscles except the superior oblique and lateral rectus:

20 **Principal oculomotor nucleus**

21 **Caudal central oculomotor nucleus**

22 **Nucleus of Perlia**

23 **Accessory oculomotor nucleus (of Edinger-Westphal),** parasympathetic center for motor innervation of intra-ocular muscles (constriction of the pupil and accommodation reflex)

Sensory nucleus

24 **Mesencephalic trigeminal nucleus (CN V)**, upper portion

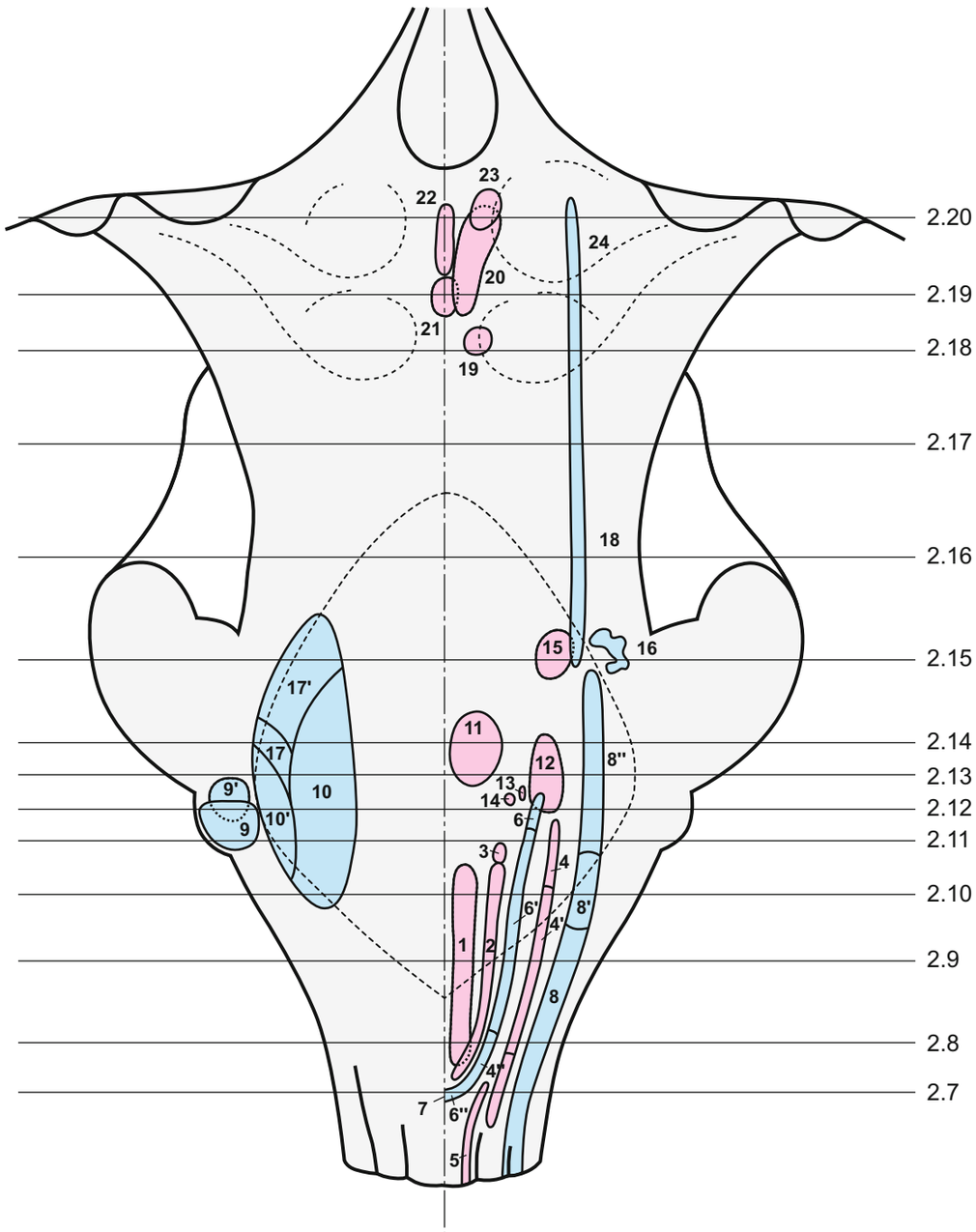

THE MOTOR AND SENSORY CRANIAL NERVE NUCLEI

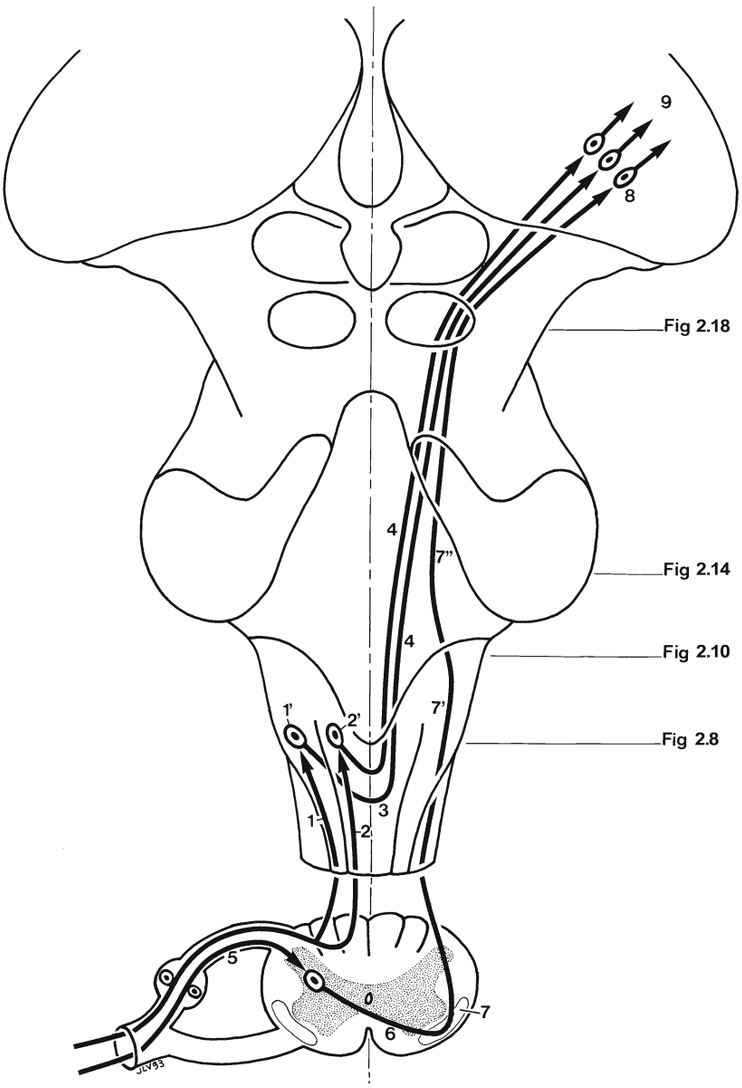

Fig. 2.4. The principal ascending pathways. See **Figs. 2.8, 2.10, 2.14** and **2.18** for their location in the brain stem and pp. 95–97 for their functions.

Epicritic pathways

1 Cuneate fasciculus (first-order neurons of the epicritic pathways connected to the second-order neurons in the cuneate nucleus, 1′)

2 Gracile fasciculus (first-order neurons of the epicritic pathways connected to the second-order neurons in the gracile nucleus, 2′)

3 Sensory decussation

4 Medial lemniscus (ascending route of the second-order neurons of the epicritic pathways towards the thalamus, 8)

Protopathic pathways

5 First-order neurons connected to the second-order neurons in the posterior horn of the spinal cord

6 Second order neurons of the protopathic pathways

7 Spinothalamic tract (containing the second-order fibers of the protopathic pathways) in the lower brain stem (7′). The protopathic fibers of the spinothalamic tract merge (7″) with the epicritic fibers of the medial lemniscus (4) in the upper brain stem

9 Thalamocortical fibers

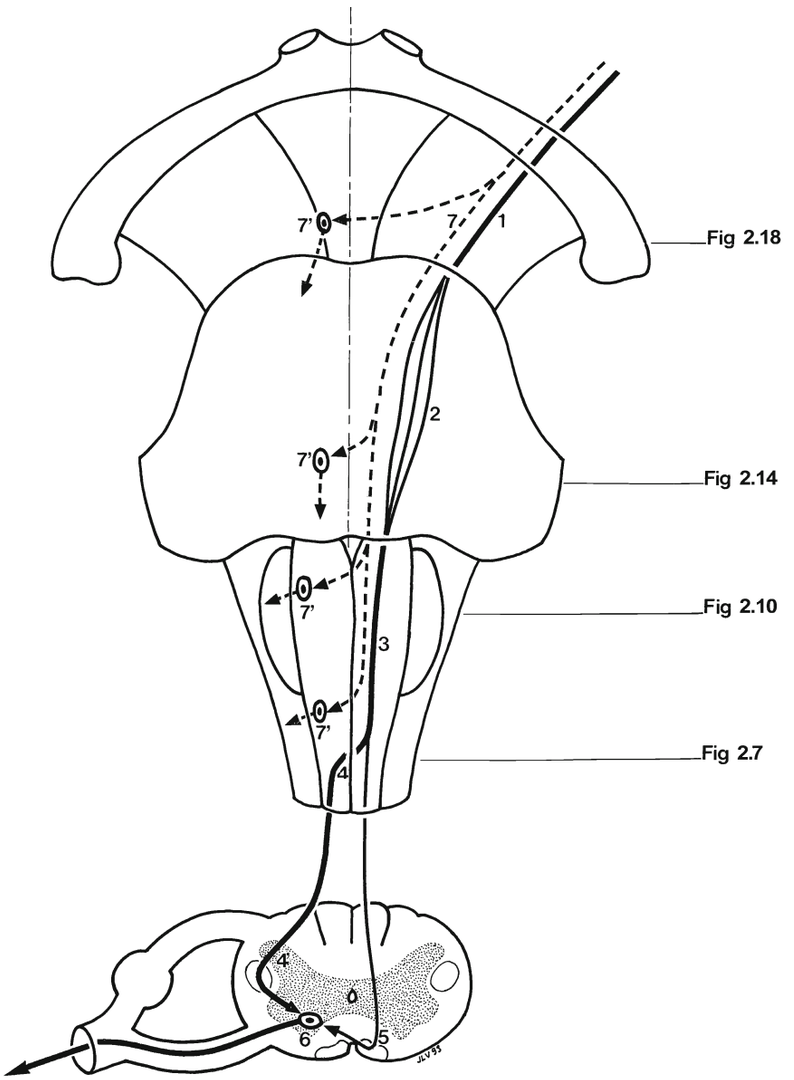

Fig. 2.5. The principal descending pathways. See **Figs. 2.7, 2.10, 2.14** and **2.18** for their location in the brain stem and pp. 97–98 for their functions.

1 Corticospinal (pyramidal) tract situated in the mid-portion of the crus cerebri
2 Corticospinal tract split into small fasciculi along its path through the pons
3 Corticospinal tract in the pyramid of the medulla
4 Decussation of the lateral corticospinal tract (4') at the lower limit of the medulla (decussation of the pyramids)
5 Ventral corticospinal tract (uncrossed fibers)
6 Motoneurons in the spinal anterior horn
7 Corticonuclear (corticobulbar) tract connected after decussation to the motor nuclei of cranial nerves (7')

Fig. 2.6. (Overview and Sections A.-D). The floor of the fourth ventricle (rhomboid fossa). Diagrammatic representations of the right side. Posterior view after removal of the cerebellum by section of the inferior (1), middle (2), and superior (3) cerebellar peduncles. The floor of the fourth ventricle is rhomboidal. At each lateral angle (lateral recess) (6), the dorsal cochlear nucleus (6′) raises a small protrusion designated the acoustic tubercle. The floor is grooved vertically by a median sulcus (7) and by paired paramedian sulci limitantes (8). The striae medullares (9) (dorsal pontocerebellar fibers) cross the floor from the lateral angle to the median sulcus and divide the ventricular floor into two portions: the inferior medullary triangle and the superior pontine triangle. The inferior cerebellar peduncle (restiform body) (28), the cuneate tubercle (29) and the gracile tubercle (clava) (30) form the sides of the inferior medullary triangle.

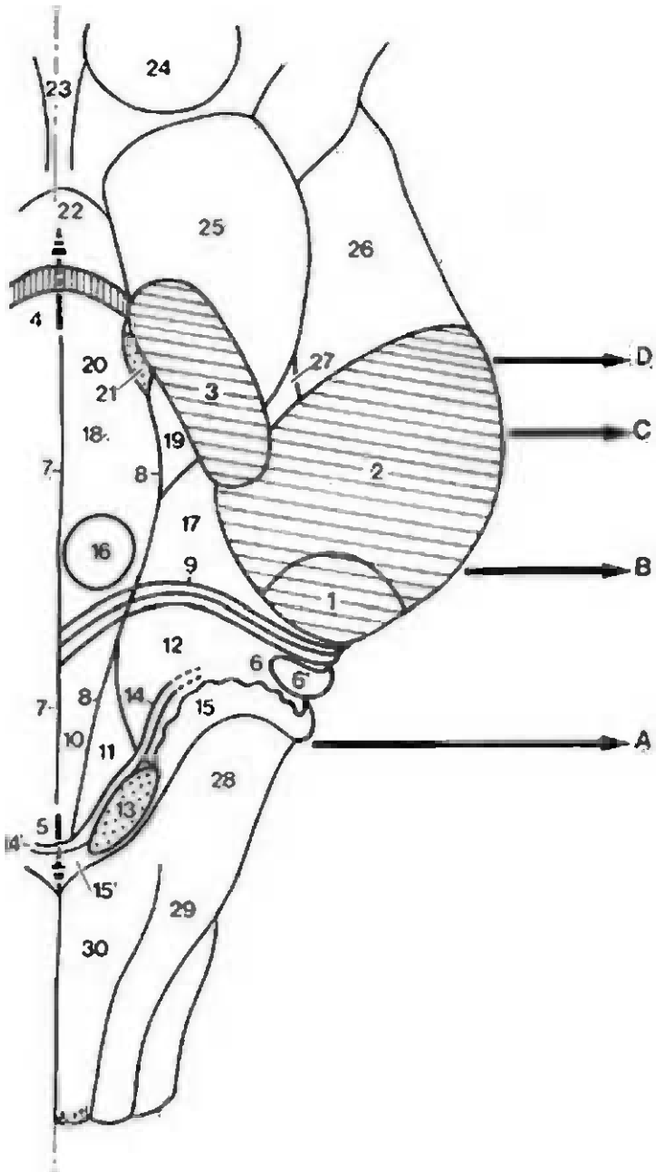

Inferior (medullary) triangle (See Section A)

10 Hypoglossal trigone corresponding to the hypoglossal nucleus (10′) and nucleus intercalatus (10″)
11 Vagal trigone (fovea inferior) corresponding to the dorsal motor nucleus of the vagus (11′) and the nucleus of the solitary tract (11″)
12 Medullary vestibular area corresponding to the vestibular nuclei (12′)
13 Area postrema (**See Figs. 1.21 and 1.22**) overlying the lower portion of the vagal trigone
14 Funiculus separans (a thickening of ependyma) bordering the area postrema
14′ Interfunicular commissure
15 Ligula (medullary insertion of the tectorial membrane) (**See Fig. 1.25**)

The posterior ligula (visible on a posterior view of the medulla) is linked (15′) to that of the opposite side at the obex. The anterior ligula prolongs the posterior ligula around the inferior cerebellar peduncle and is visible on an anterior view of the medulla (**See Figs. 1.26 and 1.27**) [289].

Superior (pontine) triangle

This triangle can be divided into inferior, middle, and superior levels

Inferior level (See Section B)

16 Facial colliculus, corresponding to the abducens nucleus (16′) crossed by the fibers of the facial nerve (16″)
17 Pontine vestibular area, corresponding to the vestibular nuclei (17′)

Middle level (See Section C)

18 Medial eminence (18′ medial longitudinal fasciculus)
19 Superior fovea (fovea trigemini) corresponding to the motor trigeminal nucleus (19′)
19″ Principal sensory trigeminal nucleus

Superior level (See Section D)

20 Medial eminence (20′ medial longitudinal fasciculus)
21 Locus ceruleus (21′ nucleus ceruleus)
22 Superior medullary velum overlapping the superior angle of the floor
23 Frenulum veli
24 Inferior colliculus
25 Superior cerebellar peduncle (brachium conjunctivum)
26 Middle cerebellar peduncle (brachium pontis)
27 Parabrachial recess
28 Inferior cerebellar peduncle (restiform body)
29 Cuneate tubercle
30 Gracile tubercle (clava)

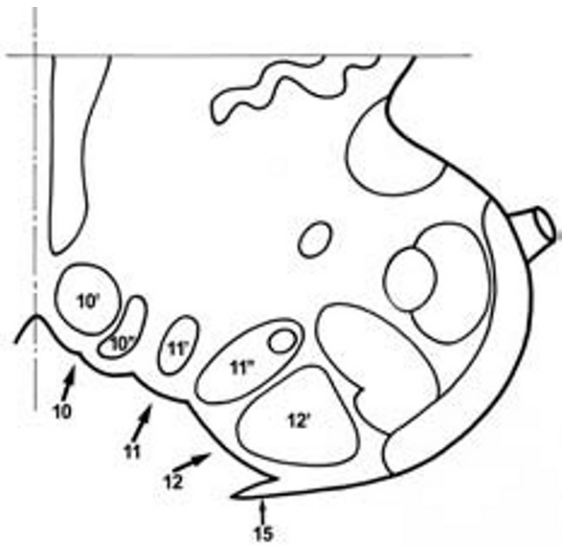
10'
10"
11'
11"
12'
10
11
12
15

A

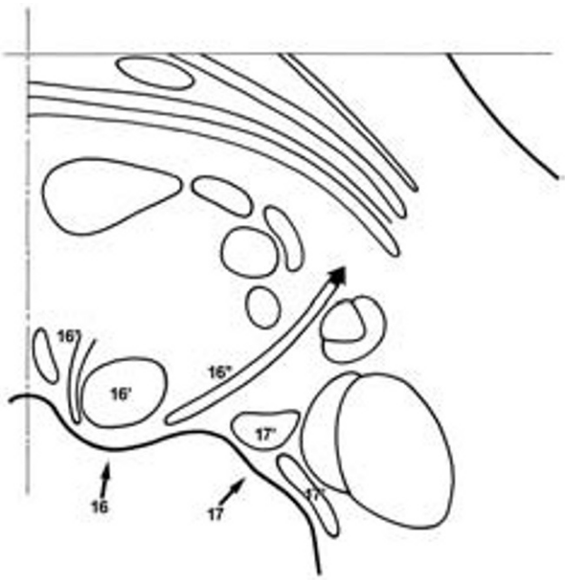
16'
16'
16"
17'
16
17
17"

B


19'
18"
19"
18
19

C

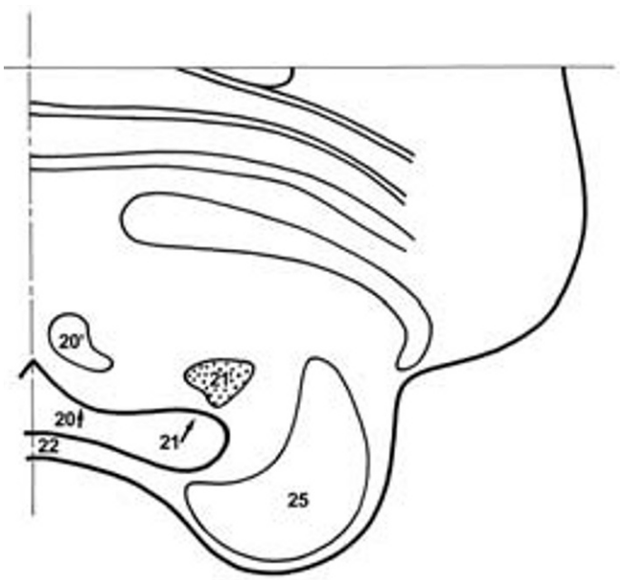
20'
21'
20"
22
21
25

D

Figures 2.7–2.22 display 16 axial (transverse or horizontal) sections of the brain stem, parallel to the intercommissural plane. Each section is seen from below to correspond to the atlas of axial (horizontal) sections and MRI views (Figs. 11.1–11.29**).** Each plane is illustrated by a diagram, an intravascular India ink injection, and post-mortem 9.4 Tesla MR microscopy. Most of the nuclei were localized following the methods described in this work. Large fasciculi, such as the corticospinal, spinocerebellar, spinothalamic, central tegmental and tectospinal tracts, the medial longitudinal fasciculus, the medial lemniscus, and the cerebellar peduncles, could be identified by direct inspection of the anatomic or 9.4 T MR images. The locations of smaller tracts, such as the corticonuclear, rubrospinal and trigeminothalamic tracts, were inferred from the known positions of the dominant tracts in accord with references [4, 39, 78, 99, 106, 164, 179, 218, 322, 328, 332, 335, 396, 430]. Where references disagreed, the authors assigned positions based on anatomic experience.

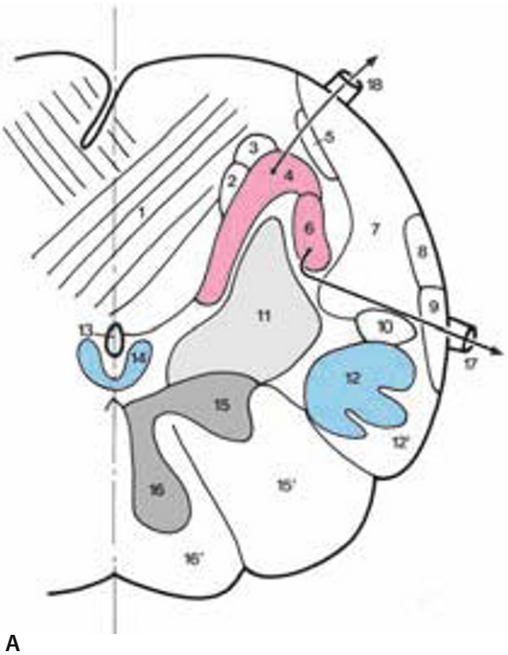

A

Fig. 2.7. Section 1. The medulla. Level of the pyramidal decussation.

See Fig. 11.1 for the general location of this section and the corresponding MRI view.

A. Diagram of an axial (horizontal) section.

B., D. Intravascular India ink injection**.**

B. Bar: 1 mm.

D. Bar: 500 µm.

C., E. Matching MR Microscopy at 9.4 Tesla.

1 Corticospinal tract (decussation of the pyramids)
2 Medial longitudinal fasciculus
3 Tectospinal tract
4 Supraspinal nucleus (motor fibers to the first cervical nerve)
5 Vestibulospinal tract
6 Accessory nucleus (nucleus ambiguus, lowest portion)
7 Spinothalamic tract (anterolateral fasciculus)
8 Ventral spinocerebellar tract
9 Dorsal spinocerebellar tract
10 Rubrospinal tract
11 Nucleus reticularis medullae oblongatae centralis
12 Spinal trigeminal nucleus (pars caudalis)
12′ Spinal trigeminal tract
13 Central canal (also black arrowhead)
14 Nucleus of the solitary tract (commissural nucleus)
15 Medial cuneate nucleus
15′ Cuneate fasciculus
16 Gracile nucleus
16′ Gracile fasciculus
17 Accessory nerve
18 First cervical nerve

Black arrowhead: Central canal (also 13)


7
6
13
11
14
12
15
12'
15'
16'

B

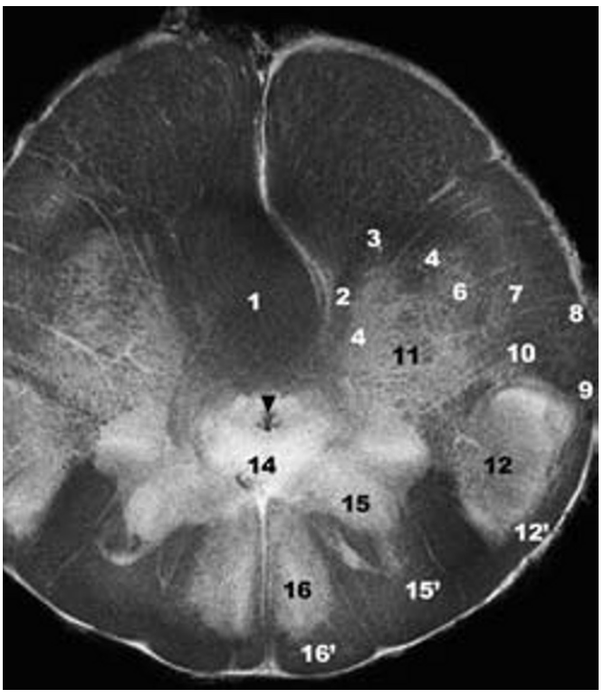
3
4
1
2
6
7
8
4
11
10
9
14
12
15
12'
16
15'
16'

C


12'
15'
16
16'

D

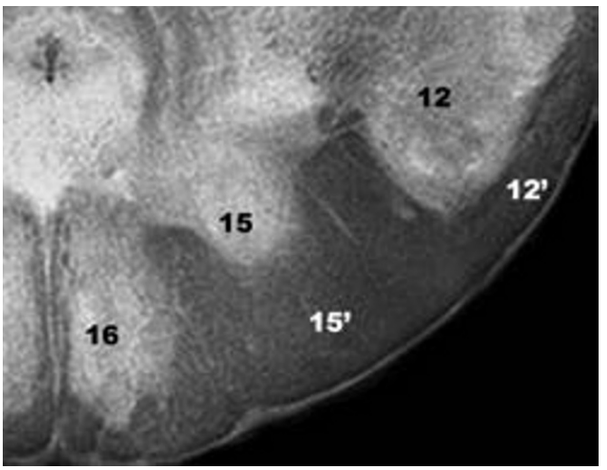
12
12'
15
16
15'

E

Fig. 2.8. Section 2. The medulla. Level of the lower portion of the inferior olivary nucleus.
See Fig. 11.3 for the general location of this section and the corresponding MRI.
See Fig. 7.4 for the intrinsic vascular territories.

A. Diagram of an axial (horizontal) section.
B. Intravascular India ink injection. Bar: 1 mm.
C. Matching MR Microscopy at 9.4 Tesla.

1 Corticospinal tract
2 Corticonuclear tract
3 Medial lemniscus
3′ Internal arcuate fibers (also arrowheads)
3″ Decussation of internal arcuate fibers (also white arrow)
4 Tectospinal tract
5 Medial longitudinal fasciculus
6 Ventral trigeminothalamic tract
7 Medial accessory olivary nucleus
8 Inferior olivary nucleus
8′ Amiculum of inferior olivary nucleus
9 Vestibulospinal tract
10 Nucleus reticularis lateralis
11 Spinothalamic tract
12 Ventral spinocerebellar tract
13 Dorsal spinocerebellar tract
14 Rubrospinal tract
15 Spinal trigeminal nucleus (pars caudalis)
15′ Spinal trigeminal tract
16 Nucleus reticularis medullae oblongatae centralis
17 Nucleus ambiguus
18 A1 noradrenergic and C1 adrenergic centers (ventrolateral medulla)
19 Hypoglossal nucleus
20 Dorsal longitudinal fasciculus (fibers linking the hypothalamus to autonomic centers of the brain stem)
21 Central canal
22 Nucleus intercalatus
23 Dorsal motor nucleus of the vagus
24 Nucleus of the solitary tract
24′ Solitary tract (also black arrow)
25 A2 noradrenergic and C2 adrenergic centers situated in and around the nucleus of the solitary tract (24′)
26 Gracile nucleus
26′ Gracile fasciculus
27 Medial cuneate nucleus
27′ Cuneate fasciculus
28 Lateral cuneate nucleus

Arrowheads: Internal arcuate fibers (also 3′)
White arrow: Decussation of internal arcuate fibers (also 3″)
Black arrow: Solitary tract (tractus solitarius) (also 24′)

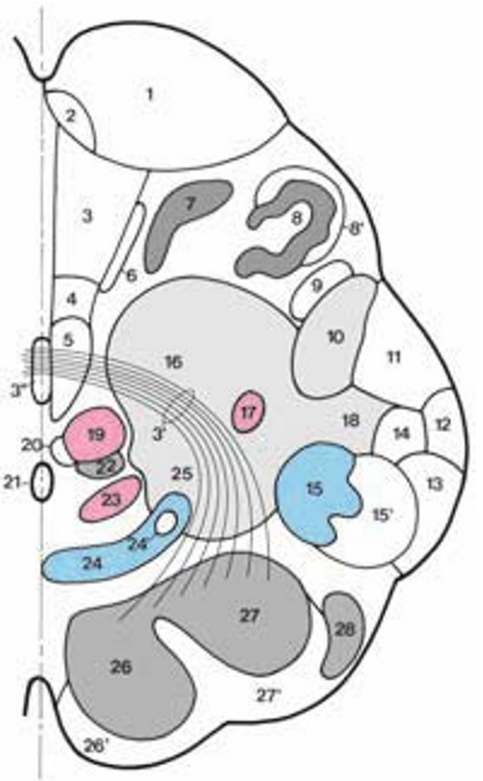

A


1
3
8
10
11
5
16
21
15
24
27
26

B

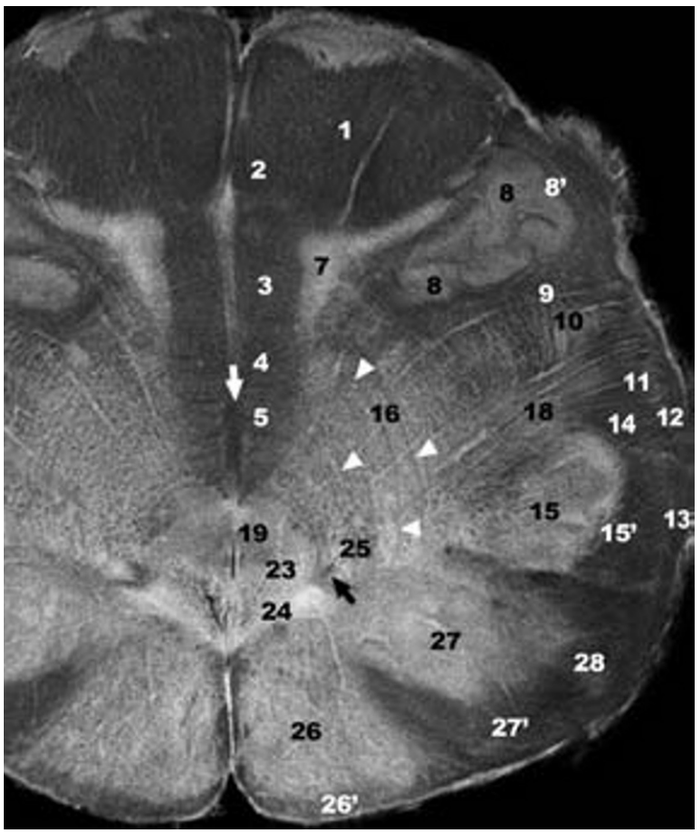
1
2
8
8'
7
3
8
9
10
4
11
5
16
18
14
12
15
15'
19
25
23
24
27
28
26
27'
26'

C

Fig. 2.9. Section 3. The medulla. Level of the inferiormost fourth ventricle and the area postrema.
See Fig. 11.5 for the general location of the section and the corresponding MRI.
See Fig. 7.6 for the intrinsic vascular territories.

A. Diagram of an axial (horizontal) section.
B., D. Intravascular India ink injection.
B. Bar: 1 mm.
D. Bar: 500 µm.
C. Matching MR Microscopy at 9.4 Tesla.

1 Corticospinal tract
2 Corticonuclear tract
3 Medial lemniscus
4 Tectospinal tract
5 Medial longitudinal fasciculus
6 Ventral trigeminothalamic tract
7 Medial accessory olivary nucleus
8 Inferior olivary nucleus
8′ Amiculum of the inferior olivary nucleus
9 Dorsal accessory olivary nucleus
10 Vestibulospinal tract
11 Nucleus reticularis lateralis
12 Spinothalamic tract
13 Ventral spinocerebellar tract
14 Rubrospinal tract
15 Inferior cerebellar peduncle (restiform body) composed mainly of the dorsal spinocerebellar tract and olivocerebellar fibers arising from the contralateral inferior olivary nucleus.
16 Spinal trigeminal nucleus (pars caudalis)
16′ Spinal trigeminal tract
17 Nucleus ambiguus
18 Nucleus reticularis medullae oblongatae centralis
19 A1 noradrenergic and Cl adrenergic centers (ventrolateral medulla, see pp. 110–111)
20 Hypoglossal nucleus
20′ Fibers of the hypoglossal nerve (also white arrowheads)
21 Dorsal longitudinal fasciculus (also white arrow)
22 Nucleus intercalatus
23 Dorsal motor nucleus of the vagus
24 Nucleus of the solitary tract
24′ Nucleus gelatinosus belonging to the nucleus of the solitary tract (for more details about the structure of this nucleus, see [286])
24″ Solitary tract (also black arrow)
25 Area postrema (see Fig. 1.22) (Together, the dorsal motor vagal nucleus, nucleus of the solitary tract and area postrema form the dorsomedial medulla, see p. 114)
26 A2 noradrenergic and C2 adrenergic centers situated in and around the nucleus of the solitary tract
27 Gracile nucleus
28 Medial cuneate nucleus
29 Lateral cuneate nucleus
30 Fourth ventricle

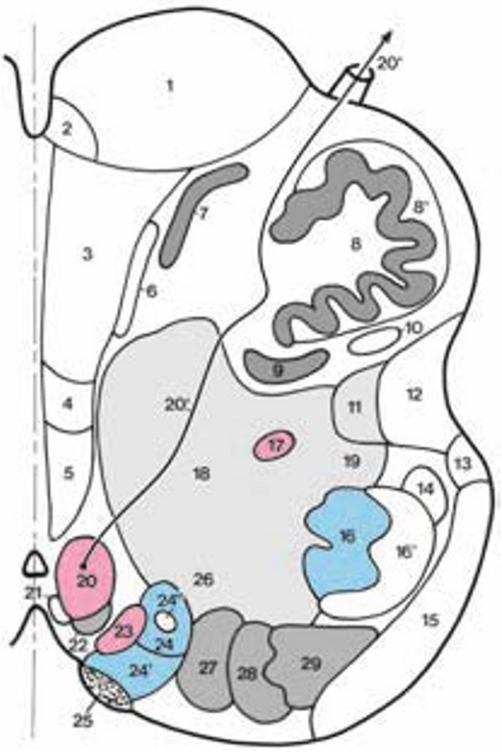

A

White arrowhead: Fibers of the hypoglossal nerve (also 20′)
White arrow: Dorsal longitudinal fasciculus (also 21)
Black arrow: Solitary tract (also 24″)


3
11
12
5
18
20
16
15
25

B

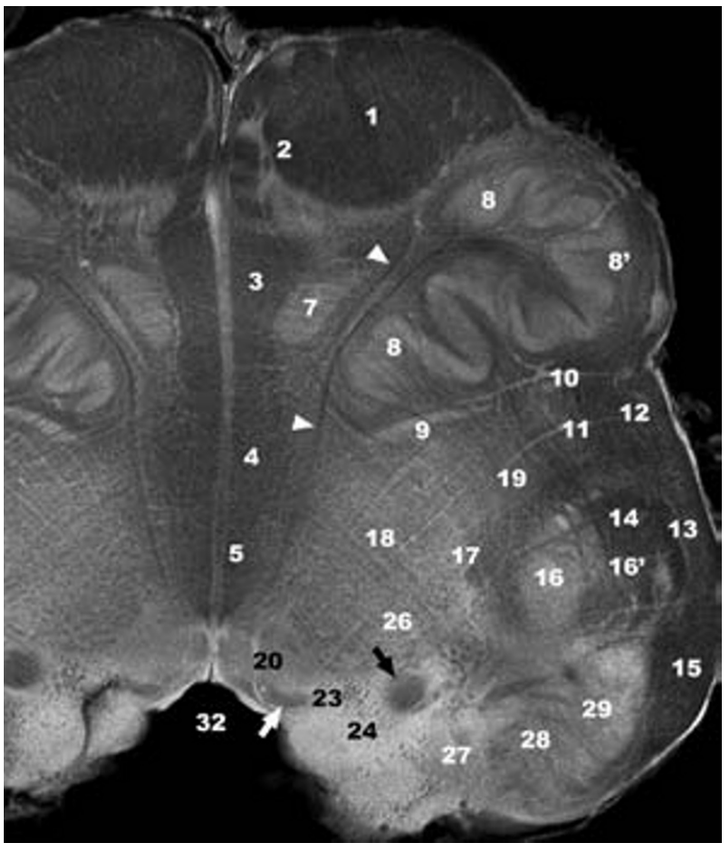
1
2
8
8'
3
7
8
10
12
9
11
4
19
14
13
18
5
17
16
16'
26
20
15
23
29
32
24
28
27

C

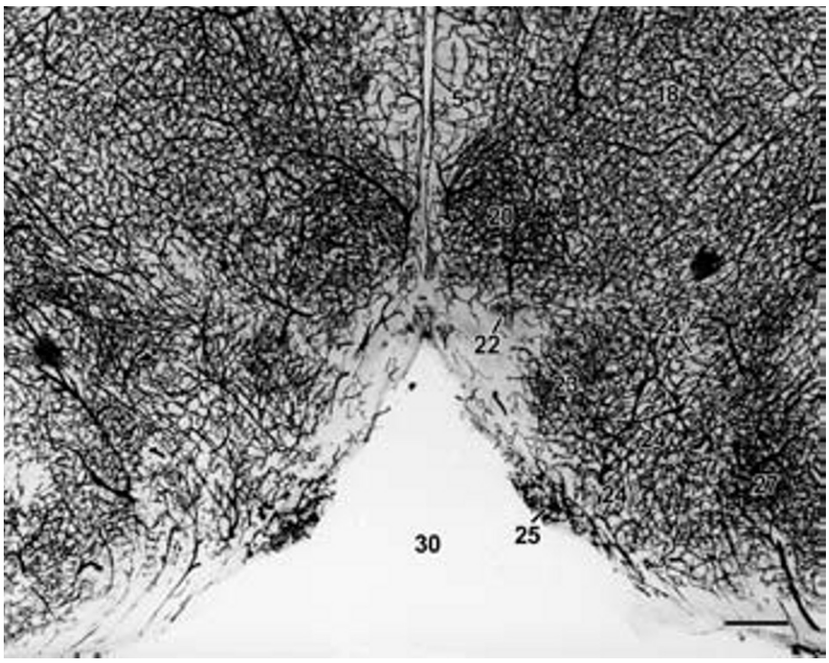
5
18
20
22
24
30
25

D

Fig. 2.10. Section 4. The medulla. Level of the medullary (inferior) portion of the fourth ventricular floor and mid-portion of the inferior olivary nucleus.
See Figs. 11.7 and 11.8 for the general location of the section and the corresponding MRI.
See Fig. 7.8 for the intrinsic vascular territories.

A. Diagram of an axial (horizontal) section.
B., D. Intravascular India ink injection.
B. Bar: 1 mm.
D. Bar: 1 mm.
C. Matching MR Microscopy at 9.4 Tesla.

1 Corticospinal tract
2 Corticonuclear tract
3 Arcuate nucleus (belonging to the pontine nuclei)
4 Medial lemniscus
5 Tectospinal tract
6 Medial longitudinal fasciculus
7 Ventral trigeminothalamic tract
8 Medial accessory olivary nucleus
9 Inferior olivary nucleus
9′ Amiculum of the inferior olivary nucleus
10 Dorsal accessory olivary nucleus
11 Spinothalamic tract
12 Ventral spinocerebellar tract
13 Rubrospinal tract
14 Inferior cerebellar peduncle
15 Spinal trigeminal nucleus (pars interpolaris)
16 Spinal trigeminal tract
17 Nucleus ambiguus
18 Fibers of the vagus nerve (also black arrowheads)
19 Nucleus reticularis lateralis
20 A1 noradrenergic and C1 adrenergic centers (ventrolateral medulla)
21 Nucleus reticularis medullae oblongatae centralis
22 Nucleus sublingualis (of Roller)
23 Hypoglossal nucleus
23′ Fibers of the hypoglossal nerve (also white arrowheads)
24 Dorsal longitudinal fasciculus (also white arrow)
25 Nucleus intercalatus (with the nucleus sublingualis, it belongs to the group of peri-hypoglossal nuclei with unknown function)
26 Dorsal motor nucleus of the vagus
27 Nucleus of the solitary tract
27′ Solitary tract (also black arrow)
27″ Nucleus gelatinosus belonging to the nucleus of the solitary tract
28 A2 noradrenergic and C2 adrenergic centers situated in and around the nucleus of the solitary tract
29 Medial vestibular nucleus
30 Lateral cuneate nucleus
31 Ligula
32 Fourth ventricle

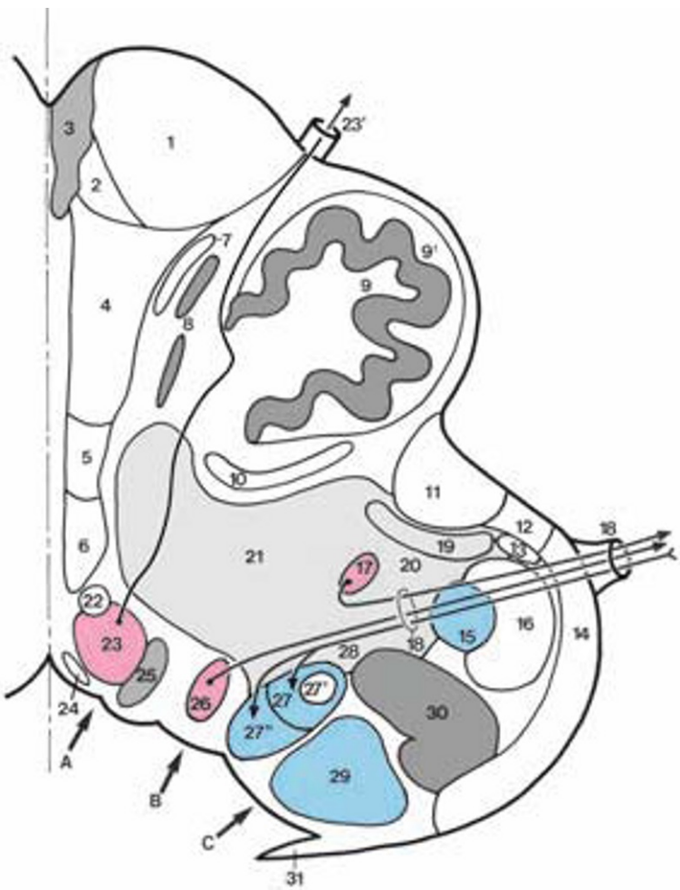

A

A Hypoglossal trigone
B Vagal trigone
C Vestibular area (See Fig. 2.6)

White arrowheads: Fibers of the hypoglossal nerve (also 23′)
Black arrowheads: Fibers of the vagus nerve (also 18)
White arrow: Dorsal longitudinal fasciculus (also 24)
Black arrow: Solitary tract (also 27′)


1
4
8
11
10
15
21
16
6
22
23
25
26
27
14
2
30
A
B
C
32
29
31

B

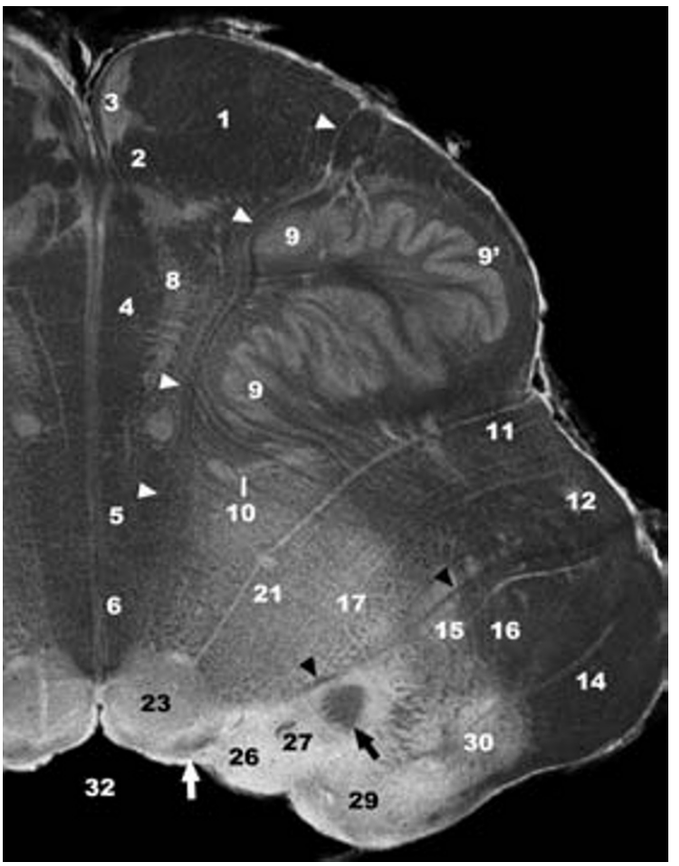
3
1
2
9
9'
8
4
9
11
5
10
12
6
21
17
15
16
14
23
26
27
30
32
29

C

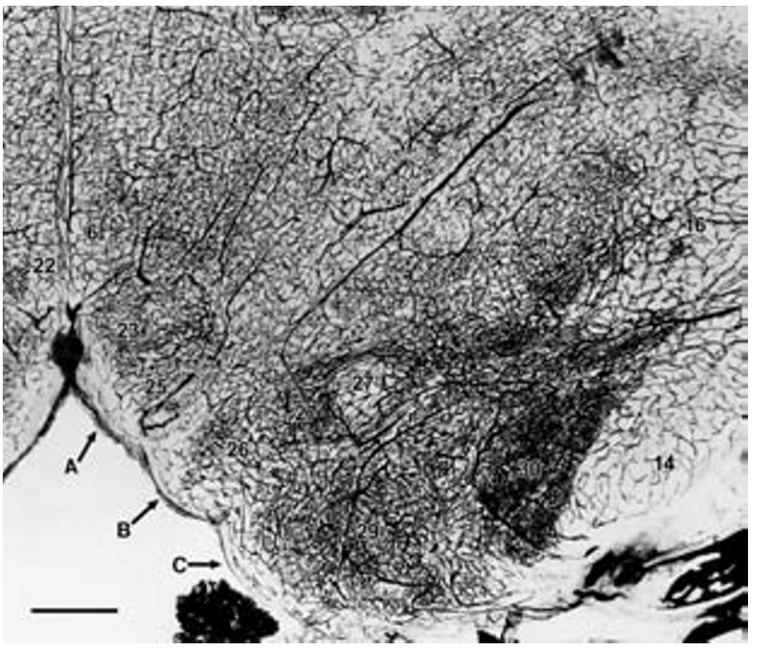
6
16
22
23
27
A
26
14
B
C

D

Fig. 2.11. Section 5. The medulla. Level of the dorsal cochlear nucleus (acoustic tubercle) of the lateral ventricular recess.
See Fig. 11.9 for the general location of the section and the corresponding MRI.

A. Diagram of an axial (horizontal) section.
B., D. Intravascular India ink injection.
B. Bar: 1 mm.
D. Bar: 1 mm.
C. Matching MR Microscopy at 9.4 Tesla.

1 Corticospinal tract
2 Corticonuclear tract
3 Arcuate nucleus (belonging to the pontine nuclei)
4 Medial lemniscus
5 Tectospinal tract
6 Medial longitudinal fasciculus
7 Nucleus raphe obscurus (B2 serotoninergic center)
8 Nucleus raphe pallidus (B1 serotoninergic center)
9 Ventral trigeminothalamic tract
10 Inferior olivary nucleus
11 Central tegmental tract
12 Spinothalamic tract
13 Ventral spinocerebellar tract
14 Rubrospinal tract
15 Corpus pontobulbare (belonging to the pontine nuclei)
16 Inferior cerebellar peduncle
17 Dorsal cochlear nucleus (The lateral extension of the dorsal cochlear nucleus over the restiform body forms a prominence at the dorsolateral angle of the medulla called the acoustic tubercle. A small lateral portion of the acoustic area of the floor of the fourth ventricle and a marginal nucleus of the restiform body contribute to the tubercle) [358].
18 Spinal trigeminal nucleus (pars oralis)
19 Spinal trigeminal tract
20 Nucleus ambiguus
20′ Fibers of the glossopharyngeal nerve
21 Nucleus reticularis parvocellularis (extension of the nucleus reticularis medullae oblongatae centralis)
22 Nucleus reticularis gigantocellularis
23 Dorsal longitudinal fasciculus
24 Nucleus prepositus hypoglossi (sometimes considered as part of the reticular formation; it plays a role in the control of horizontal eye movements. See p. 264)
25 Nucleus of the solitary tract (superior portion: nucleus ovalis)
26 Medial vestibular nucleus
27 Descending vestibular root
28 Inferior vestibular nucleus

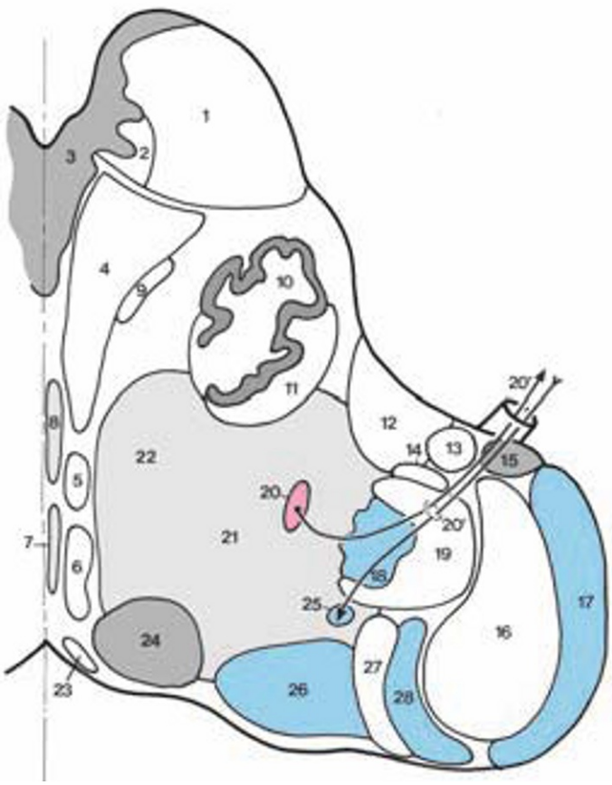

A


1
4
12
15
19
25
16
6
29

B

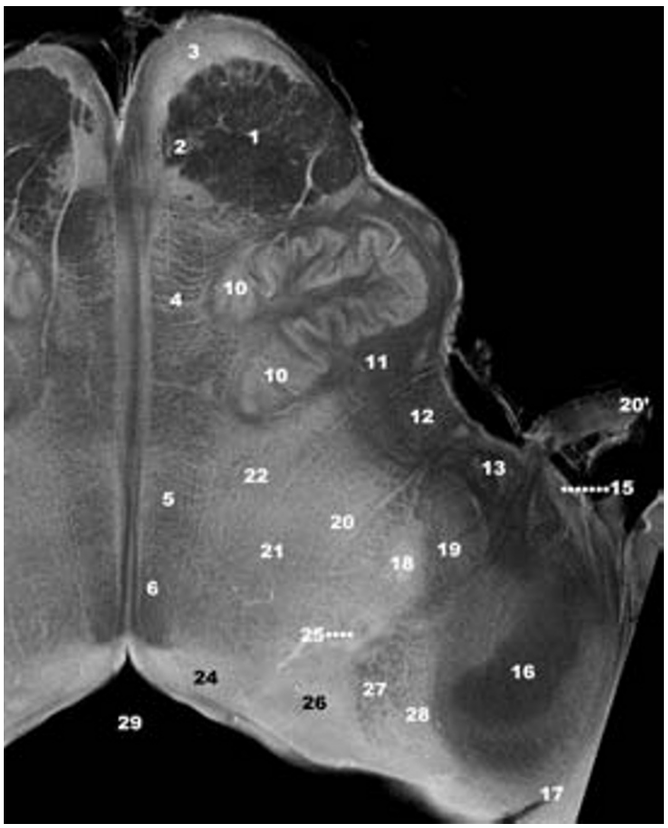
3
2
1
4
10
10
11
12
20'
22
13
15
5
20
21
19
18
6
25
24
16
27
26
28
29
17

C


21
6
27
28
16
26

D

Fig. 2.12. Section 6. The medulla. Level of the pontomedullary sulcus, ventral cochlear nucleus, and superior portion of the inferior olivary nucleus.
See Fig. 11.10 for the general location of the section and the corresponding MRI.
See Fig. 7.10 for the intrinsic vascular territories.

A. Diagram of an axial (horizontal) section.
B., D. Intravascular India ink injection.
B. Bar: 1 mm.
D. Bar: 1 mm.
C. Matching MR Microscopy at 9.4 Tesla.

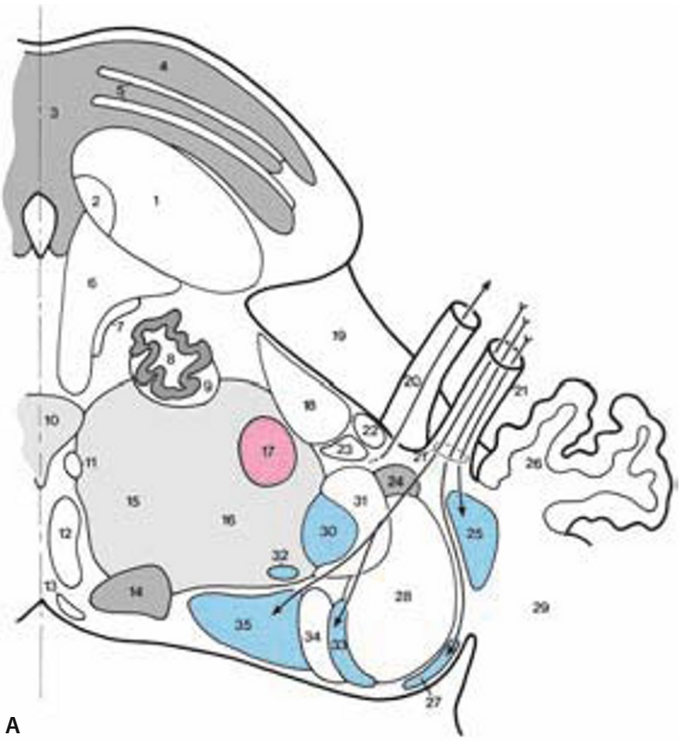

1 Corticospinal tract
2 Corticonuclear tract
3 Arcuate nucleus (belonging to the pontine nuclei)
4 Pontine nuclei
5 Pontocerebellar fibers
6 Medial lemniscus
7 Ventral trigeminothalamic tract
8 Superior portion of the inferior olivary nucleus
9 Central tegmental tract
10 Nucleus raphe magnus (B3 serotoninergic center)
11 Tectospinal tract
12 Medial longitudinal fasciculus
13 Dorsal longitudinal fasciculus (also white arrow)
14 Nucleus prepositus hypoglossi
15 Nucleus reticularis gigantocellularis
16 Nucleus reticularis parvocellularis
17 Facial nucleus
18 Spinothalamic tract
19 Pontomedullary sulcus
20 Facial nerve
21 Vestibulocochlear nerve
21′ Fibers of the vestibulocochlear nerve
22 Ventral spinocerebellar tract
23 Rubrospinal tract
24 Corpus pontobulbare (See Fig. 2.11)
25 Ventral cochlear nucleus
26 Flocculus
27 Dorsal cochlear nucleus
28 Inferior cerebellar peduncle (restiform body)
29 Middle cerebellar peduncle (brachium pontis)
30 Spinal trigeminal nucleus (pars oralis)
31 Spinal trigeminal tract
32 Nucleus of the solitary tract (superior portion: nucleus ovalis)
33 Inferior vestibular nucleus
34 Descending vestibular root
35 Medial vestibular nucleus
36 Fourth ventricle

White arrow: Dorsal longitudinal fasciculus (also 13)


1
6
10
18
17
16
15
31
24
12
32
28
29
14
35
34
36

B

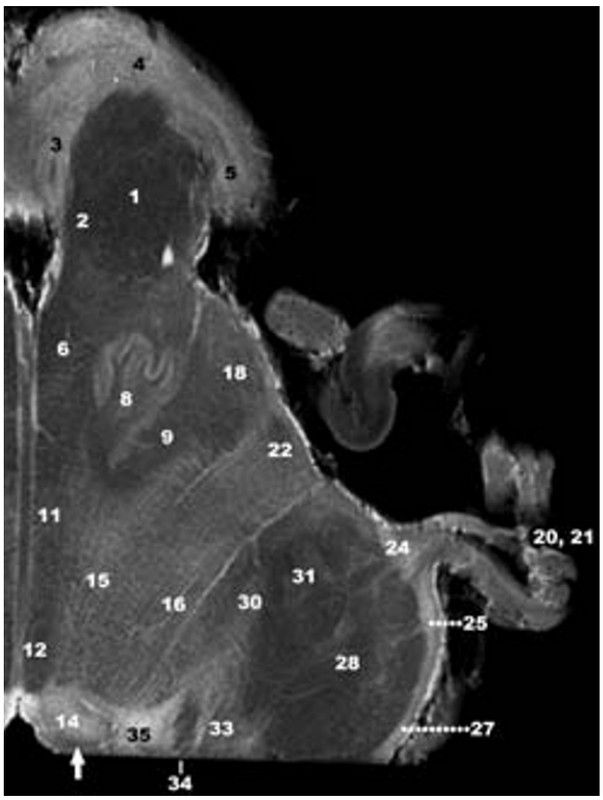
4
3
5
1
2
6
18
8
9
22
11
20, 21
24
15
31
16
30
25
12
28
14
35
33
27
34

C

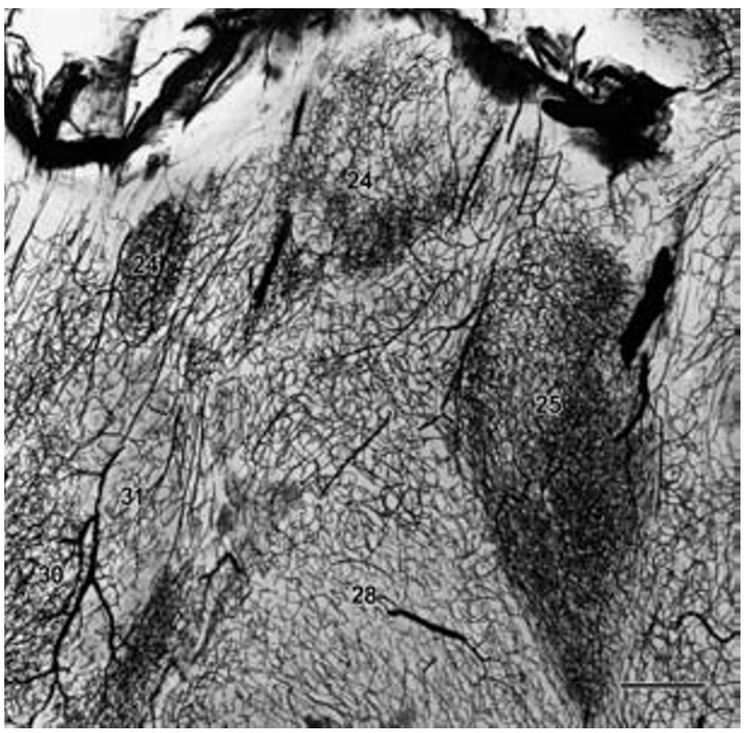
24
24
25
31
30
28

D

Fig. 2.13. Section 7. The low pons. Level of the facial and superior olivary nuclei.
See Fig. 11.12 for the general location of the section and the corresponding MRI.

A. Diagram of an axial (horizontal) section.
B., D. Intravascular India ink injection.
B. Bar: 1 mm.
D. Bar: 1 mm.
C., E. Matching MR Microscopy at 9.4 Tesla.

1 Corticospinal tract
2 Corticonuclear tract
3 Pontine nuclei
4 Pontocerebellar fibers
5 Medial lemniscus
6 Spinothalamic tract moving towards the medial lemniscus
7 Lateral lemniscus (auditory pathways)
8 Trapezoid body composed of fibers arising from the ventral cochlear nucleus
9 Nucleus of the trapezoid body
10 Medial superior olivary nucleus
11 Lateral superior olivary nucleus
12 Rubrospinal tract
13 Ventral trigeminothalamic tract
14 Central tegmental tract
15 A5 noradrenergic center
16 Facial nucleus
16′ Fibers of facial nerve
17 Ventral spinocerebellar tract
18 Pontomedullary sulcus
19 Middle cerebellar peduncle (brachium pontis)
20 Inferior cerebellar peduncle (restiform body)
21 Spinal trigeminal nucleus (pars oralis)
21′ Spinal trigeminal tract
22 Nucleus reticularis parvocellularis
23 Nucleus reticularis gigantocellularis
24 Nucleus raphe magnus (B3 serotoninergic center)
25 Tectospinal tract
26 Medial longitudinal fasciculus
27 Dorsal longitudinal fasciculus (also white arrow)
28 Abducens nucleus
29 Medial vestibular nucleus
30 Descending vestibular root
31 Inferior vestibular nucleus
32 Lateral vestibular nucleus

White arrow: Dorsal longitudinal fasciculus (also 27)

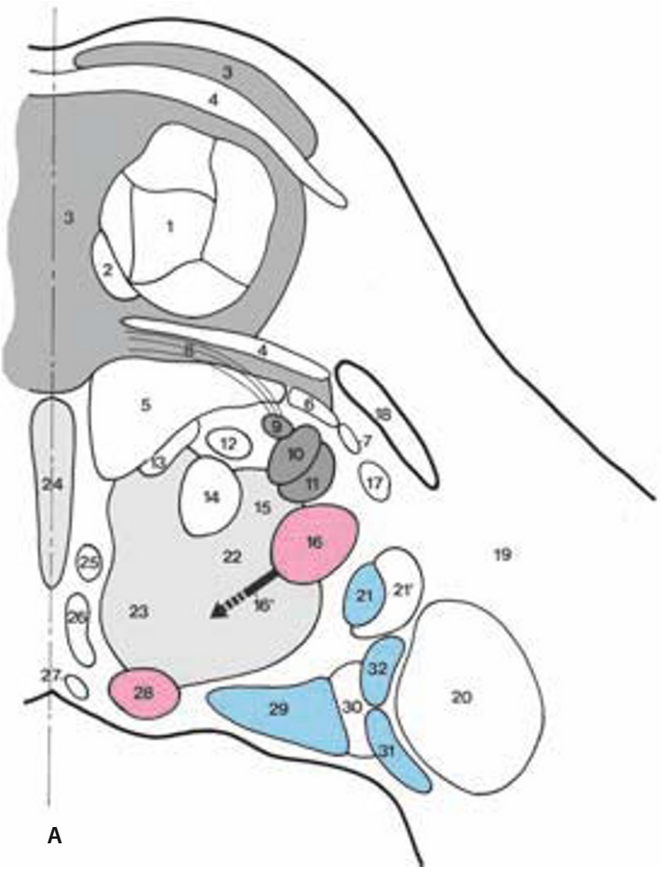


1
18
19
5
23
21
26
32
28
30
31
29
20

B

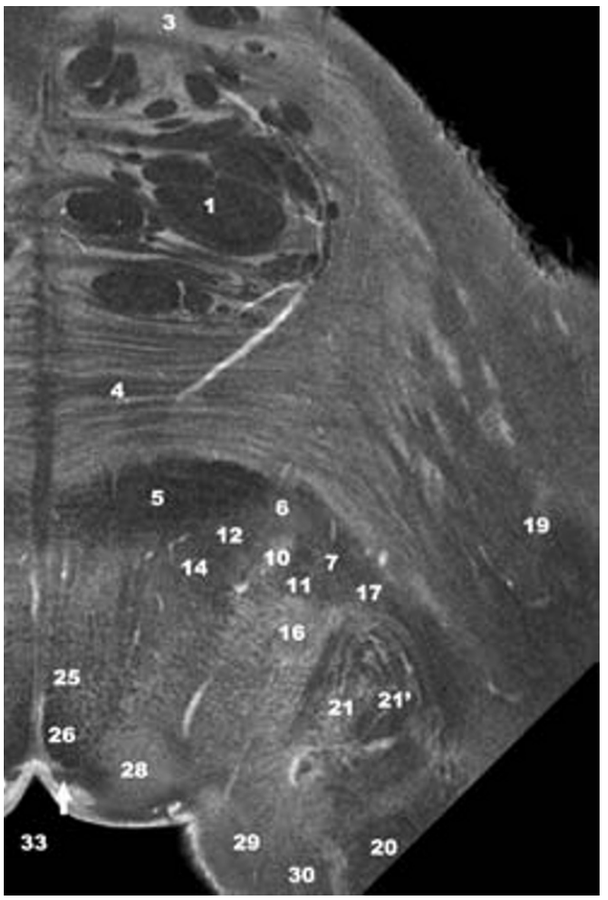
3
1
4
5
6
19
12
14
10
7
11
17
16
25
21
21'
26
28
33
29
20
30

C

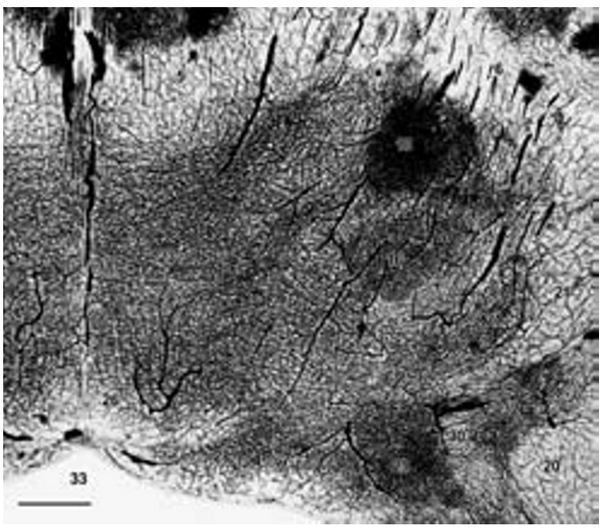
33
20

D

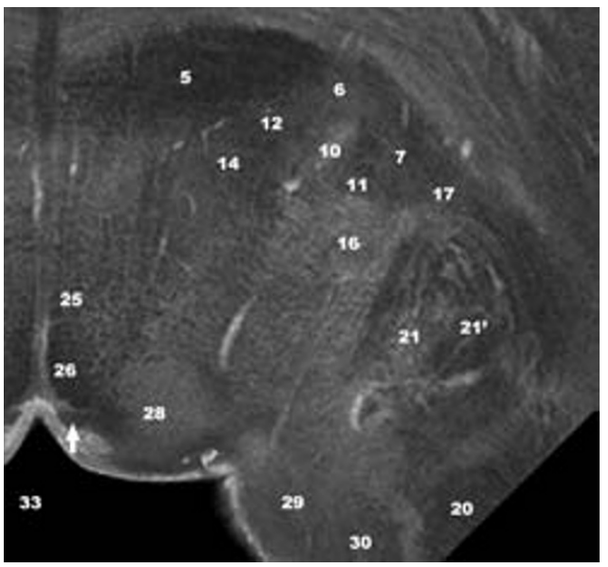
5
6
12
10
7
14
11
17
16
25
21
21'
26
28
33
29
20
30

E

Fig. 2.14. Section 8. The mid pons. Level of the abducens nucleus.
See Fig. 11.13 for the general location of the section and the corresponding MRI.
See Fig. 7.13 for the intrinsic vascular territories.

A. Diagram of an axial (horizontal) section.
B. Diagram of the pontine divisions. A frontal plane passing through the medial lemniscus (a) divides the pons into the tegmentum (b) dorsally and the basilar portion (c) ventrally.
C., E. Intravascular India ink injection.
C. Bar: 1 mm.
E. Bar: 500 µm.
D. Matching MR Microscopy at 9.4 Tesla.

1 Corticospinal tract split into small fasciculi
2 Corticonuclear tract
3 Pontocerebellar fibers
4 Pontine nuclei
5 Medial lemniscus
6 Ventral trigeminal tract
7 Spinothalamic tract
8 Lateral lemniscus (auditory pathways)
9 Medial superior olivary nucleus
10 Lateral superior olivary nucleus
11 Nucleus of the trapezoid body
12 Trapezoid body
13 Rubrospinal tract
14 Central tegmental tract
15 Facial nucleus
16, 16′ Fibers of the facial nerve (also black arrow(head)s)
17 Nucleus reticularis parvocellularis
18 Nucleus reticularis pontis caudalis
19 Nucleus reticularis gigantocellularis
20 Nucleus raphe magnus (B3 serotoninergic center)
21 Tectospinal tract
22 Medial longitudinal fasciculus
23 Dorsal longitudinal fasciculus (also white arrow)
24 Abducens nucleus
24′ Fibers of the abducens nerve (also white arrowheads)
25 Facial colliculus (protrusion into the floor of the fourth ventricle where the facial nerve fibers (genu of the facial nerve) cross over the abducens nucleus)
26 Medial vestibular nucleus
27 Superior vestibular nucleus
28 Lateral vestibular nucleus
29 Inferior cerebellar peduncle (restiform body)
30 Middle cerebellar peduncle (brachium pontis)
31 Spinal trigeminal nucleus (pars oralis)
32 Spinal trigeminal tract
33 Ventral spinocerebellar tract

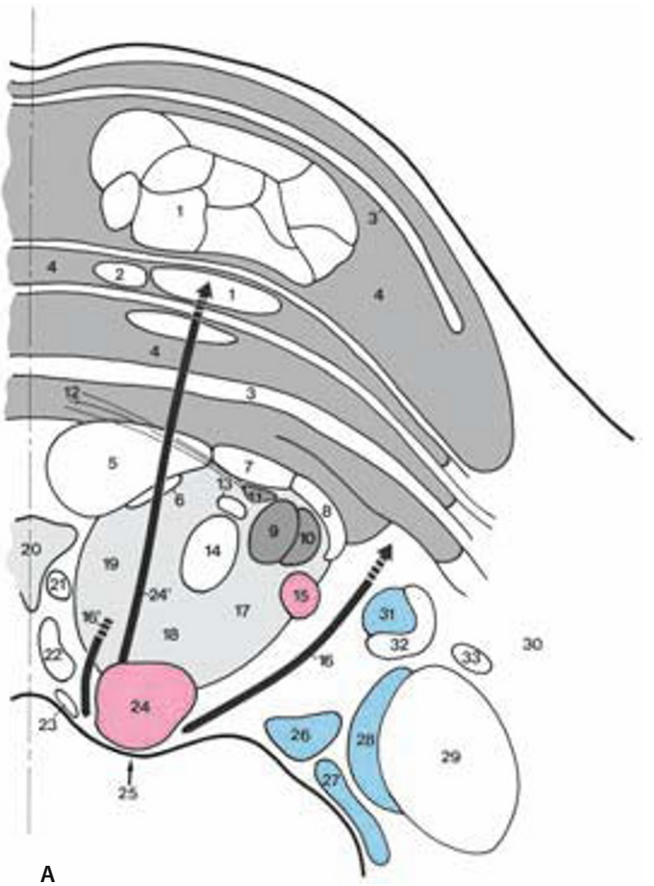

White arrowheads: Fibers of the abducens nerve (also 24′)
White arrow: Dorsal longitudinal fasciculus (also 23)
Black arrowheads: Fibers of the facial nerve, decending segment (also 16)
Black arrow: Fibers of the facial nerve, ascending segment (also 16′)


22
25
34

C

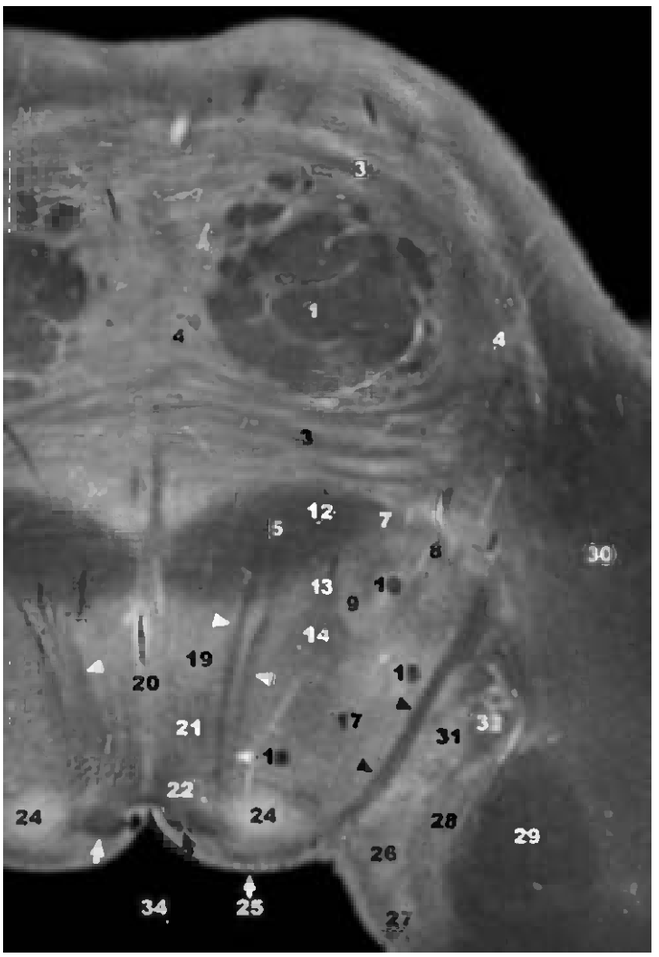
3
1
4
4
3
12
5
7
8
30
13
9
14
19
20
21
17
31
22
24
24
28
29
26
34
25
27

D


16
16
34
25

E

Fig. 2.15. Section 9. The upper pons. Level of the motor and principal sensory trigeminal nuclei.
See Figs. 11.16 and 11.17 for the general location of the section and the corresponding MRI.
See Fig. 7.15 for the intrisic vascular territories.

A. Diagram of an axial (horizontal) section.
B., D. Intravascular India ink injection.
B. Bar: 2 mm.
D. Bar: 500 µm.
C. Matching MR Microscopy at 9.4 Tesla.

1 Corticospinal tract split into small fasciculi
2 Corticonuclear tract
3 Pontocerebellar fibers
4 Pontine nuclei
5 Nucleus reticularis tegmenti pontis
6 Medial lemniscus
7 Ventral trigeminothalamic tract
8 Spinothalamic tract
9 Lateral lemniscus (auditory pathways)
10 Ventral nucleus of the lateral lemniscus
11 Rubrospinal tract
12 Nucleus reticularis parvocellularis
13 Central tegmental tract
14 Dorsal trigeminothalamic tract (arising from the dorsal portion of the principal sensory trigeminal nucleus. (See pp. 96 and 445)
15 Tectospinal tract
16 Nucleus raphe pontis (B5 serotoninergic center)
17 Nucleus reticularis pontis caudalis
18 Medial longitudinal fasciculus
19 Dorsal longitudinal fasciculus (also white arrow)
20 Superior vestibular nucleus
21 Superior cerebellar peduncle (brachium conjunctivum)
22 Ventral spinocerebellar tract
23 Motor trigeminal nucleus
24 Principal sensory trigeminal nucleus
25 Mesencephalic trigeminal nucleus
26 Mesencephalic trigeminal tract
27 Spinal trigeminal tract
28 Fibers of the motor root of trigeminal nerve (28′)
29 Fibers of the sensory root of trigeminal nerve (29′)
30 Middle cerebellar peduncle (brachium pontis)
31 Fourth ventricle

White arrow: Dorsal longitudinal fasciculus (also 19)

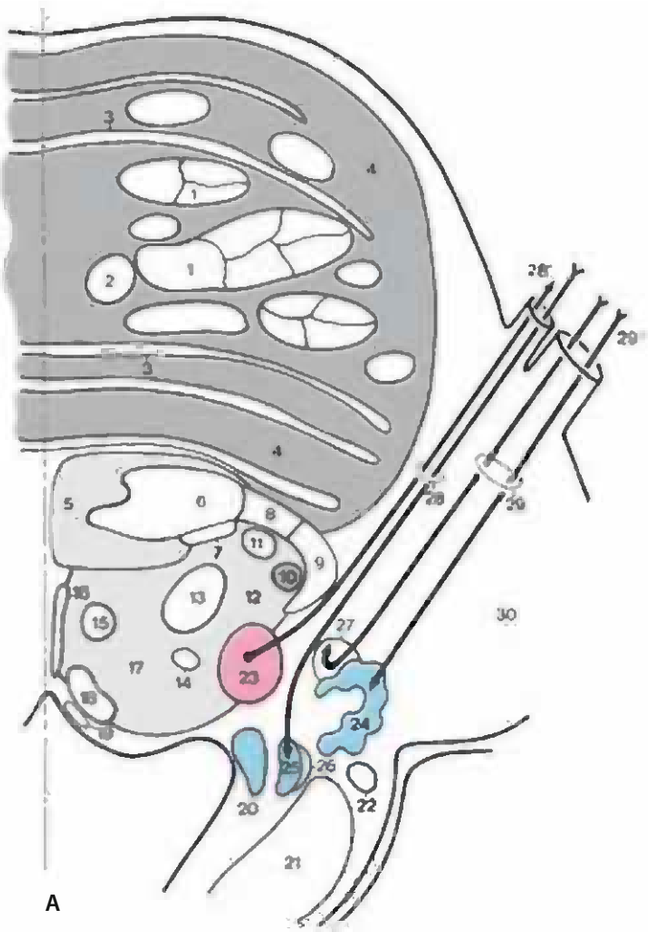

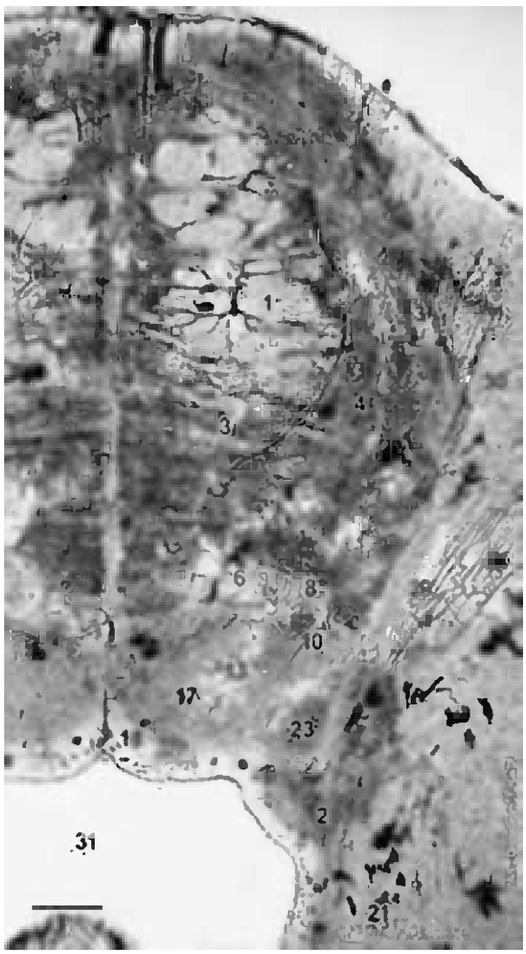
1
3
6
8
10
17
23
1
2
31
21

B

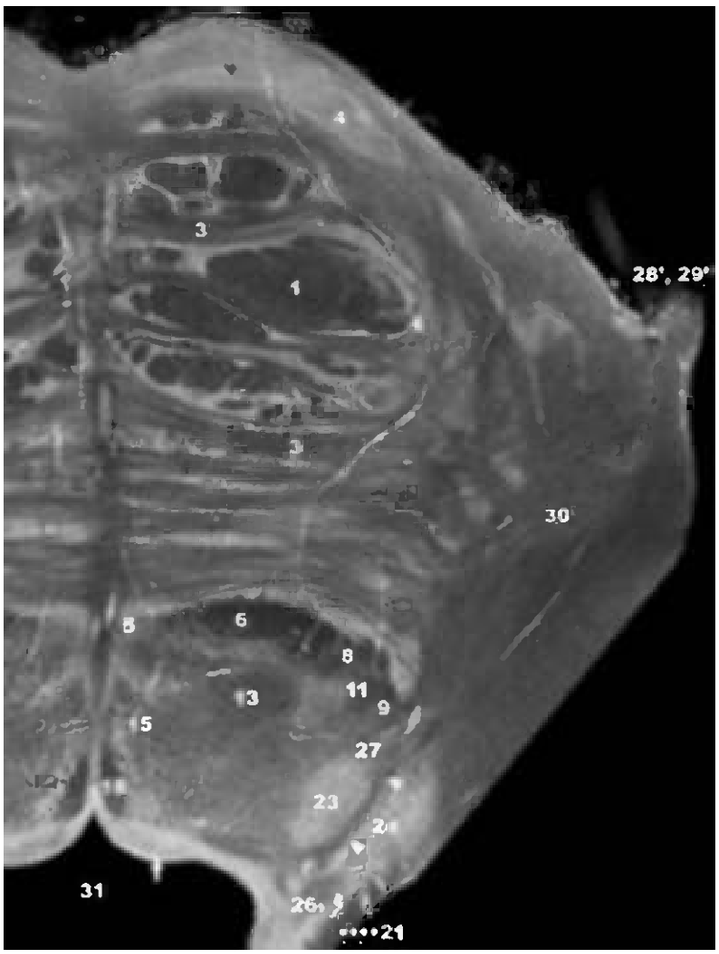
4
3
1
28', 29'
3
30
5
6
8
11
3
9
5
27
23
2
31
26
21

C


6
8
29
9
12
17
18
20
31
21

D

Fig. 2.16. Section 10. The high pons. Level of the nucleus ceruleus.
See Fig. 11.19 for the general location of the section and the corresponding MRI.
See Fig. 7.17 for the intrinsic vascular territories.

A. Diagram of an axial (horizontal) section.
B., D. Intravascular India ink injection.
B. Bar: 2 mm.
D. Bar: 1 mm.
C. Matching MR Microscopy at 9.4 Tesla.

1 Corticospinal tract split into small fasciculi
2 Corticonuclear tract
3 Pontocerebellar fibers
4 Pontine nuclei
5 Dorsolateral pontine nucleus (See pp. 98–99) (belonging to the pontine nuclei)
6 Middle cerebellar peduncle (brachium pontis)
7 Trigeminal nerve
8 Nucleus reticularis tegmenti pontis (nucleus reticularis centralis inferior)
9 Medial lemniscus
10 Ventral trigeminothalamic tract
11 Spinothalamic tract
12 Rubrospinal tract
13 Lateral lemniscus (auditory pathways)
14 Ventral nucleus of the lateral lemniscus
15 Central tegmental tract
16 Dorsal trigeminothalamic tract (See Fig. 2.15, No. 14)
17 Nucleus reticularis pontis oralis
18 Nucleus reticularis centralis superior (B6 and B8 serotoninergic centers)
19 Tectospinal tract
20 Medial longitudinal fasciculus
21 Dorsal longitudinal fasciculus
22 Central gray
23 Nucleus ceruleus (A6 noradrenergic center)
24 Nucleus subceruleus (A6 subceruleus noradrenergic center)
25 CH6 cholinergic center situated in and around the nucleus ceruleus
26 Medial parabrachial nucleus (A7 noradrenergic center)
27 Nucleus of Kölliker-Fuse (its location is not clearly defined in man). The ceruleus, subceruleus, and medial parabrachial nuclei together form the dorsolateral pontine tegmentum.
28 Lateral parabrachial nucleus
29 Ventral spinocerebellar tract
30 Superior cerebellar peduncle (brachium conjunctivum)
31 Mesencephalic trigeminal nucleus
32 Mesencephalic trigeminal tract (also white arrow)
33 Superior medullary velum
34 Upper fourth ventricle

White arrow: Mesencephalic trigeminal tract (also 32)

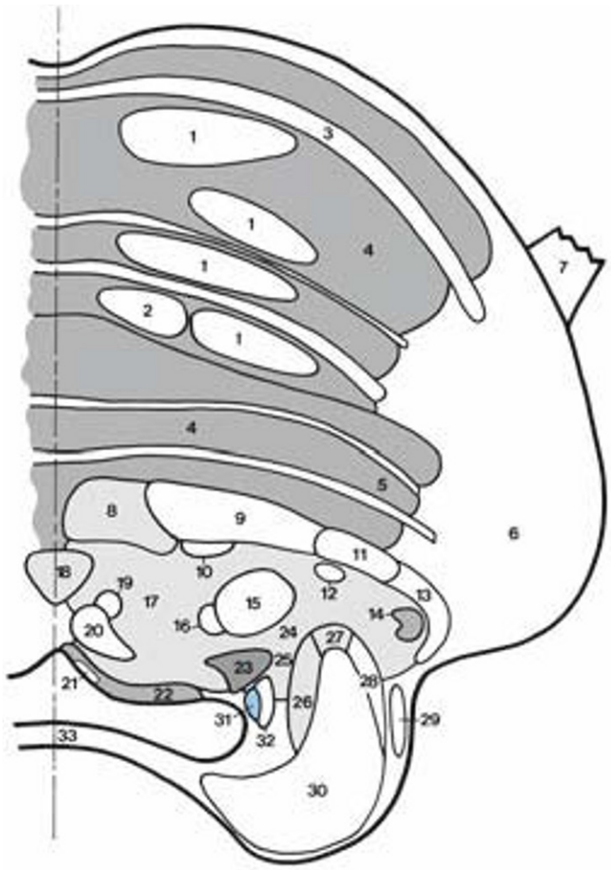

A


1
1
1
6
3
5
9
11
13
1
15
18
17
14
20
23
34
33
25
30

B

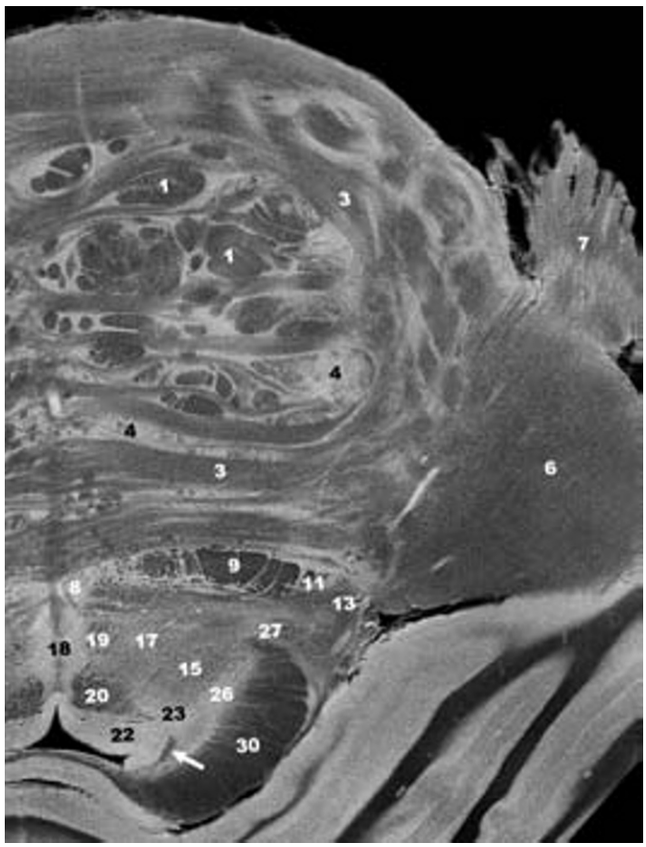
1
3
7
1
4
4
3
6
9
8
11
13
18
19
17
27
15
20
26
23
22
30

C

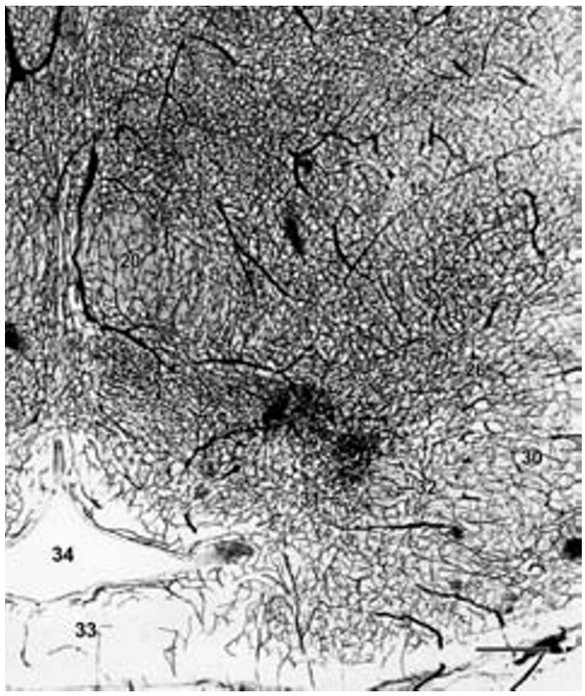
15
20
26
30
32
34
33

D

Fig. 2.17. Section 11. The high pons. Level of the lateral lemniscus and decussation of the trochlear nerves.
See Fig. 11.20 for the general location of the section and the corresponding MRI.
See Fig. 7.19 for the intrinsic vascular territories.

A. Diagram of an axial (horizontal) section.
B., D. Intravascular India ink injection.
B. Bar: 2 mm.
D. Bar: 500 µm.
C., E. Matching MR Microscopy at 9.4 Tesla.

1 Corticospinal tract split into small fasciculi
2 Corticonuclear tract
3 Frontopontine tract
4 Parietotemporopontine tract
5 Pontine nuclei
5′ Dorsolateral pontine nucleus (See pp. 98–99)
6 Pontocerebellar fibers
7 Nucleus reticularis tegmenti pontis
8 Medial lemniscus
9 Spinothalamic tract
10 Lateral lemniscus (auditory pathways)
11 Dorsal nucleus of the lateral lemniscus
12 Ventral trigeminothalamic tract
13 Rubrospinal tract
14 Nucleus reticularis pontis oralis
15 Nucleus reticularis centralis superior (B6 and B8 serotoninergic centers)
16 Tectospinal tract
17 Medial longitudinal fasciculus
18 Dorsal tegmental nucleus (of Gudden)
19 Central gray matter
20 Dorsal longitudinal fasciculus
21 Dorsal trigeminothalamic tract
22 Central tegmental tract
23 Medial parabrachial nucleus (A7 noradrenergic center)
24 Nucleus of Kölliker-Fuse
25 Lateral parabrachial nucleus
26 Superior cerebellar peduncle (brachium conjunctivum)
27 Mesencephalic trigeminal nucleus
28 Mesencephalic trigeminal tract (also white arrow)
29 Nucleus ceruleus (A6 noradrenergic center)
30 Nucleus subceruleus (A6 subceruleus noradrenergic center)
31 CH6 cholinergic center situated in and around the nucleus ceruleus
32 Superior medullary velum containing the decussation of the trochlear nerve fibers (33, black arrow in C.)
34 Upper fourth ventricle

White arrow: Mesencephalic trigeminal tract (also 28)
Black arrow: Decussation of the trochlear nerve fibers (also 33)

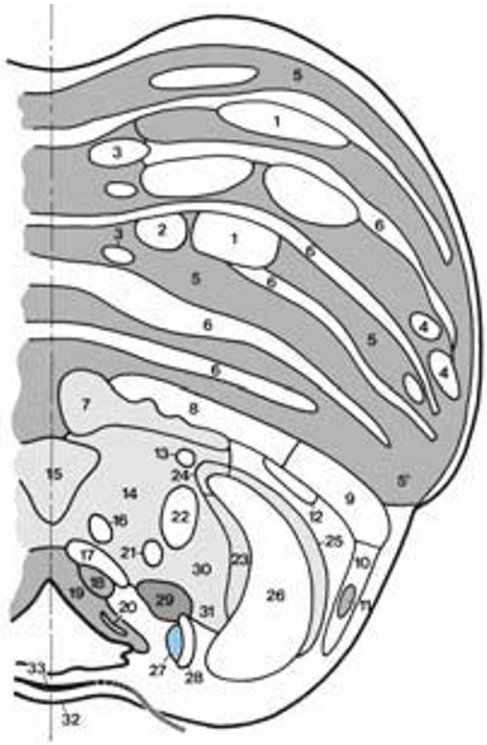

A


1
6
9
10
22
11
18
29
2
28
25
34
32

B

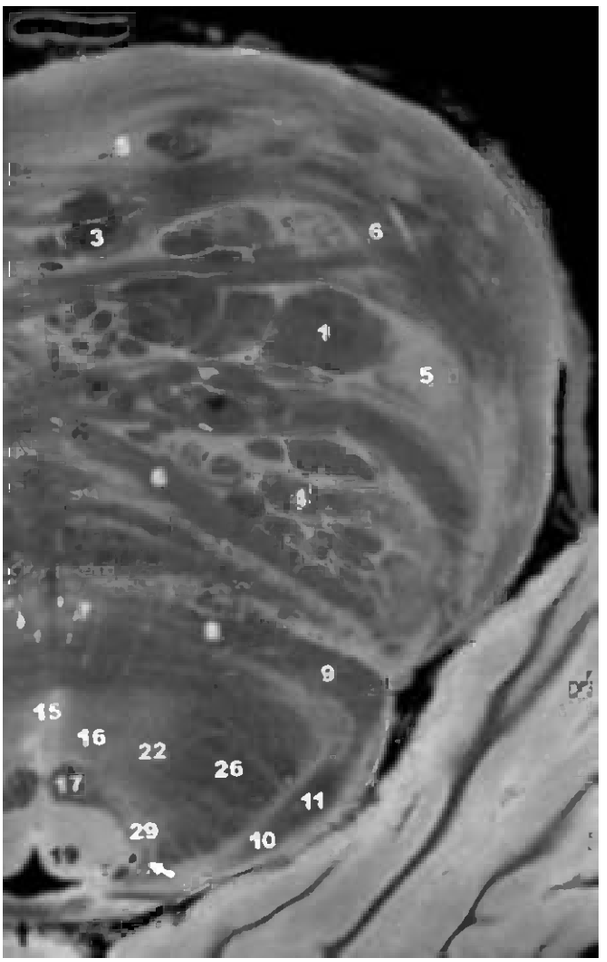
3
6
1
5
9
15
16
22
26
17
11
29
10

C

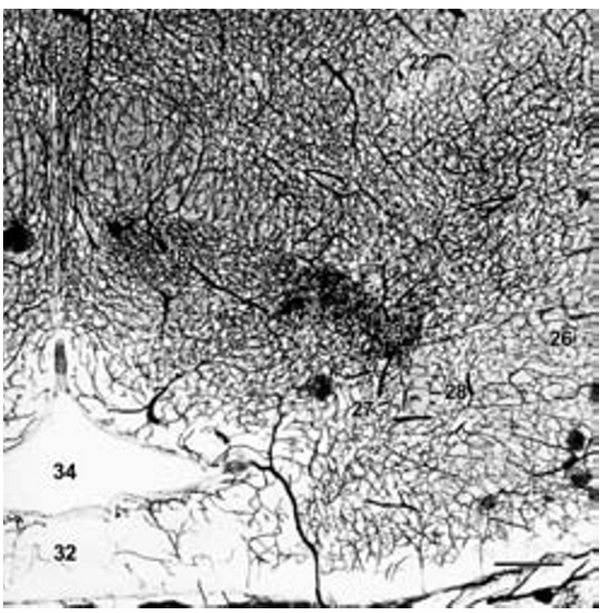
22
26
27
28
34
32

D

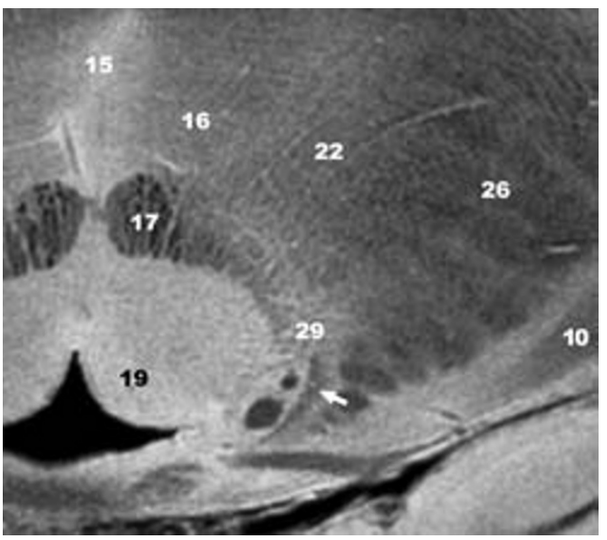
15
16
22
26
17
29
10
19

E

Fig. 2.18. Section 12. The mesencephalon. Level of the inferior colliculus and trochlear nucleus.
See Fig. 11.23 for the general location of the section and the corresponding MRI.
See Fig. 7.21 for the intrinsic vascular territories.

A. Diagram of an axial (horizontal) section.
B., D. Intravascular India ink injection.
B. Bar: 1 mm.
D. Bar: 500 µm.
C., E. Matching MR Microscopy at 9.4 Tesla.

1 Corticospinal tract
2 Corticonuclear tract
3 Frontopontine tract
4 Parietotemporopontine tract
5 Substantia nigra, pars compacta (A9 dopaminergic center related to the striatum by the nigrostriatal fibers)
6 Ventral tegmental area (A10 dopaminergic center related to the limbic system)
7 Interpeduncular nucleus receiving the habenulo-interpeduncular tract (fasciculus retroflexus)
8 Rubrospinal tract
9 Superior cerebellar peduncle (brachium conjunctivum)
9′ Decussation of the right and left superior cerebellar peduncles
10 Dorsal nucleus of raphe
11 Tectospinal tract
12 Medial longitudinal fasciculus
13 Trochlear nucleus (also paired black arrows)
14 Periaqueductal gray matter
15 Cerebral aqueduct
16 Dorsal longitudinal fasciculus
17 Inferior colliculus
18 Mesencephalic trigeminal nucleus
19 Mesencephalic trigeminal tract (also black arrowhead)
20 Dorsal trigeminothalamic tract
21 Central tegmental tract
22 Nucleus reticularis cuneiformis
23 Nucleus reticularis pedunculopontinus (CH5 cholinergic center)
24 Ventral trigeminothalamic tract
25 A8 dopaminergic center (of uncertain location)
26 Medial lemniscus
27 Spinothalamic tract
28 Lateral lemniscus: auditory pathways related to the lateral aspect of the mesencephalon (single black arrow in A.) (lemniscal or acoustic trigone) (See Fig. 1.6)
29 Parabigeminal nucleus (CH8 cholinergic center)

Black arrowhead: Mesencephalic trigeminal tract (also 19)
Single black arrow in A.: Lemniscal trigone
Paired black arrows: Trochlear nuclei (also 13)

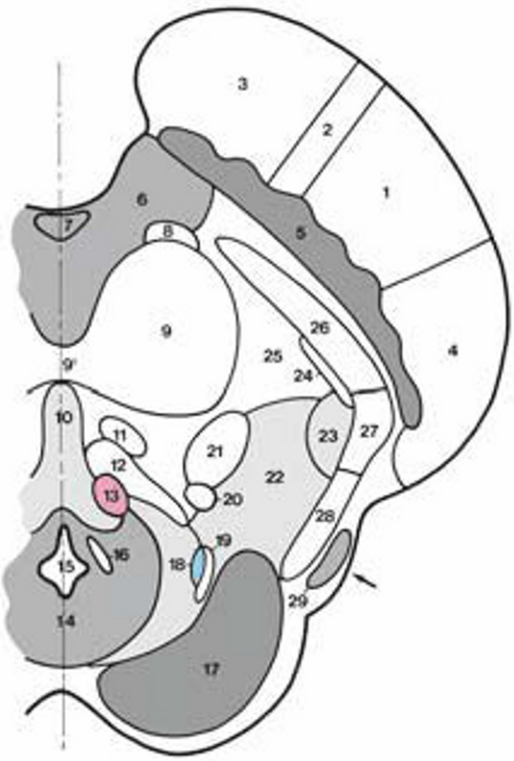

A


3
1
7
6
26
4
9
9
21
12
13
10
18
19
28
15
14

B

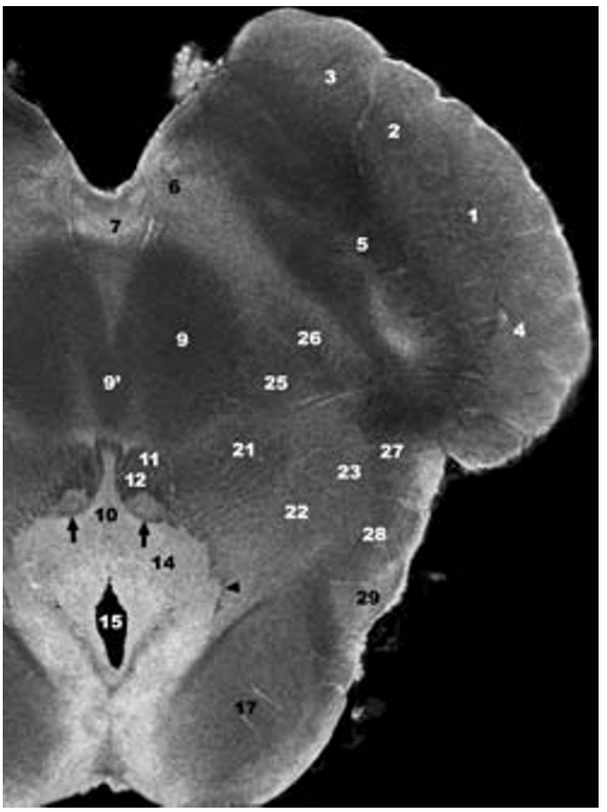
3
2
6
1
7
5
4
9
26
9'
25
11
21
27
12
23
10
22
28
14
29
15
17

C

D

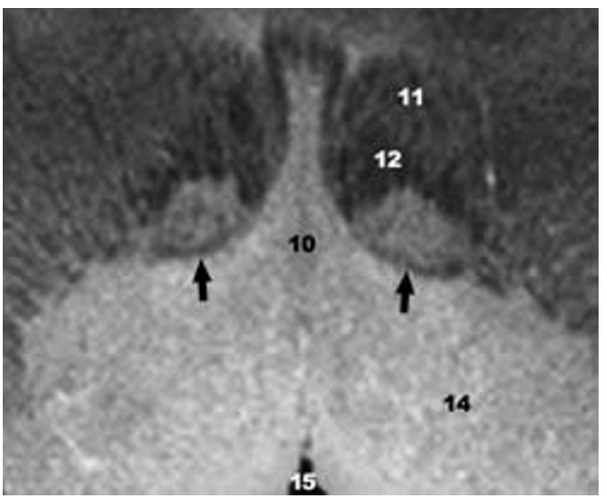
11
12
10
14
15

E

Fig. 2.19. Section 13. The mesencephalon. Level of the inferior pole of the red nucleus.
See Fig. 11.24 for the general location of the section and the corresponding MRI.

A. Diagram of an axial (horizontal) section.
B., D. Intravascular India ink injection.
B. Bar: 2 mm.
D. Bar: 500 µm.
C. Matching MR Microscopy at 9.4 Tesla.
E. Diagram. The overall division of the mesencephalon. A curved line drawn just ventral to the cerebral aqueduct (a) separates the tectum (b) from the tegmentum (c, d). A curved line drawn along the ventral aspect of the substantia nigra (c) separates the basilar portion of the mesencephalon (e) from the tegmentum (c, d).

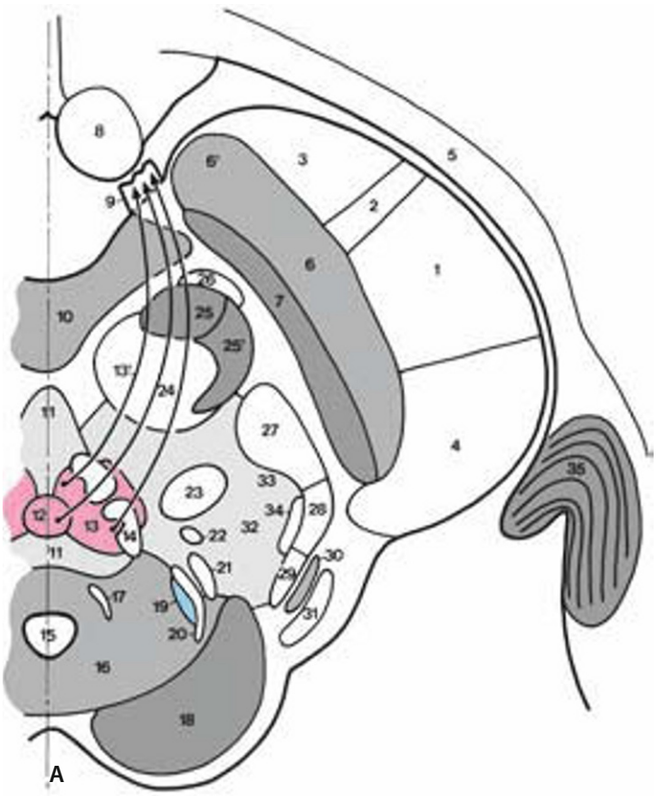

1 Corticospinal tract
2 Corticonuclear tract
3 Frontopontine tract
4 Parietotemporopontine tract
5 Optic tract
6 Substantia nigra, pars reticulata
6′ Extension of the pars reticulata into the crus cerebri ventral portion
7 Substantia nigra, pars compacta (A9 dopaminergic center)
8 Mammillary body
9 Oculomotor nerve
10 Ventral tegmental area (A10 dopaminergic center)
11 Dorsal nucleus of raphe (B7 serotoninergic center)
12 Oculomotor nucleus: caudal central nucleus
13 Principal oculomotor nucleus
13′ Fibers of the oculomotor nerve (also white arrows)
14 Medial longitudinal fasciculus
15 Cerebral aqueduct (of Sylvius)
16 Periaqueductal gray matter
17 Dorsal longitudinal fasciculus
18 Intercollicular nucleus (between superior and inferior colliculi)
19 Mesencephalic trigeminal nucleus
20 Mesencephalic trigeminal tract
21 Tectospinal tract
22 Dorsal trigeminothalamic tract
23 Central tegmental tract
24 Superior cerebellar peduncle (brachium conjunctivum)
25 Red nucleus (magnocellular portion)
25′ Red nucleus (parvocellular portion)
26 Rubrospinal tract
27 Medial lemniscus
28 Spinothalamic tract
29 Lateral lemniscus
30 Nucleus paralemniscalis (unknown function)
31 Brachium of the inferior colliculus
32 Nucleus reticularis cuneiformis
33 A8 dopaminergic center (of uncertain location)
34 Ventral trigeminothalamic tract
35 Lateral geniculate body

White arrows: Fibers of the oculomotor nerve (also 13′)

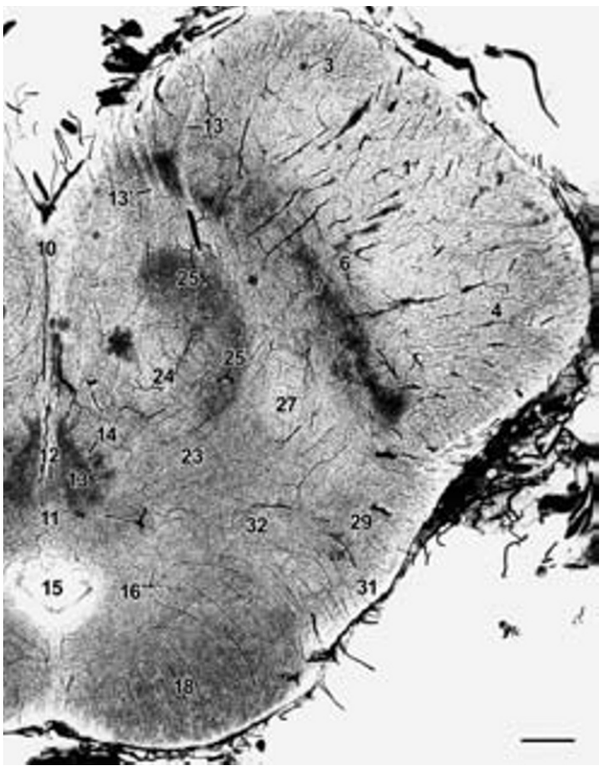
3
13'
1'
13
10
6
25
4
24
25
27
14
12
23
13
11
32
29
15
16
31
18

B

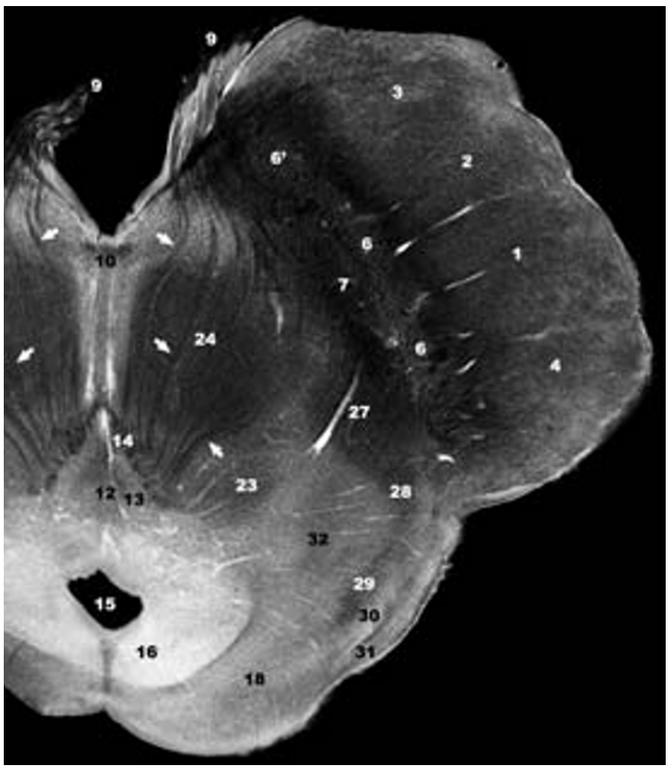
9
9
3
6'
2
6
1
10
7
24
6
4
27
14
12
13
23
28
32
29
15
30
16
31
18

C

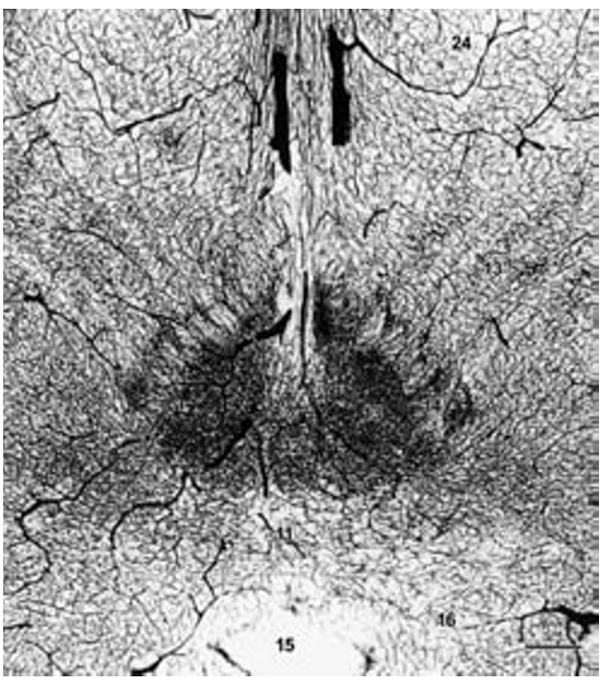
24
15
16

D

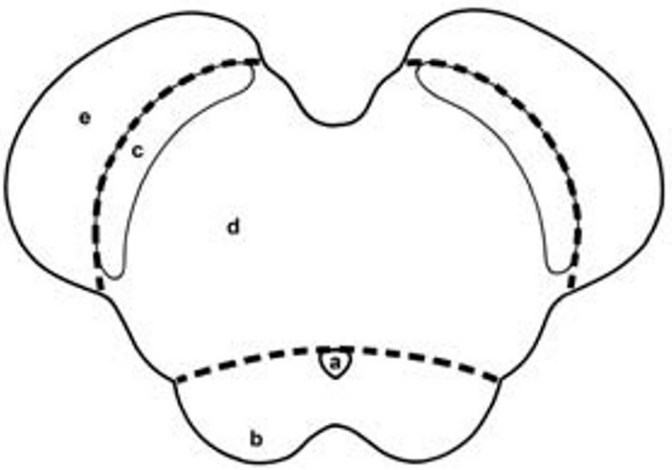
e
c
d
a
b

E

Fig. 2.20. Section 14. The mesencephalon. Level of the red nucleus and oculomotor nucleus.
See Fig. 11.25 for the general location of the section and the corresponding MRI.
See Fig. 7.23 for the intrinsic vascular territories.

A. Diagram of an axial (horizontal) section.
B., D. Intravascular India ink injection.
B. Bar: 2 mm.
D. Bar: 500 µm.
C. Matching MR Microscopy at 9.4 Tesla.

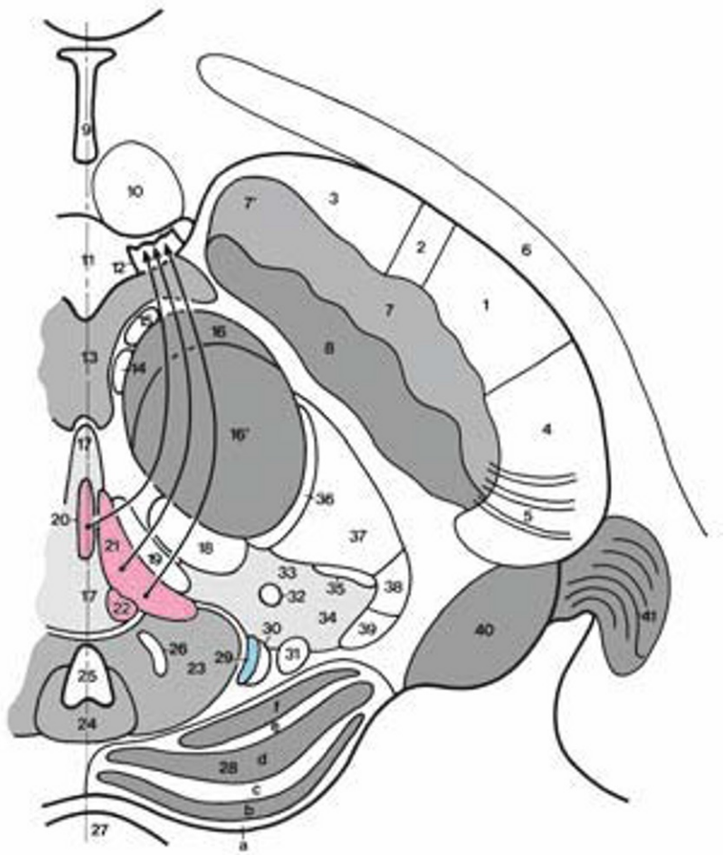

A

1 Corticospinal tract
2 Corticonuclear tract
3 Frontopontine tract
4 Parietotemporopontine tract
5 Nigrostriatal fibers
6 Optic tract
7 Substantia nigra, pars reticulata
7′ Extension of the pars reticulata into the crus cerebri (ventral portion)
8 Substantia nigra, pars compacta (A9 dopaminergic center connected to the striatum through the nigrostriatal fibers)
9 Third ventricle
10 Mammillary body
11 Interpeduncular fossa
12 Oculomotor nerve
13 Ventral tegmental area (A10 dopaminergic center connected with the limbic system)
14 Rubrospinal tract
15 Habenulo-interpeduncular tract (fasciculus retroflexus)
16 Red nucleus, magnocellular portion
16′ Red nucleus, parvocellular portion
17 Dorsal nucleus of raphe (B7 serotoninergic center)
18 Central tegmental tract
19 Medial longitudinal fasciculus
20 Oculomotor nucleus (nucleus of Perlia)
21 Principal oculomotor nucleus
22 Accessory oculomotor nucleus (nucleus of Edinger-Westphal)
23 Lateral periaqueductal gray matter
24 Dorsal periaqueductal gray matter
25 Cerebral aqueduct
26 Dorsal longitudinal fasciculus
27 Pineal gland
28 Superior colliculus
a. stratum zonale
b. stratum griseum superficiale
c. stratum opticum
d. stratum griseum medium
e. stratum lemnisci
f. stratum griseum profundum
29 Mesencephalic trigeminal nucleus
30 Mesencephalic trigeminal tract
31 Tectospinal tract
32 Dorsal trigeminothalamic tract
33 A8 dopaminergic center (of uncertain location)
34 Nucleus reticularis cuneiformis
35 Ventral trigeminothalamic tract
36 Cerebellorubrothalamic fibers
37 Medial lemniscus
38 Spinothalamic tract
39 Lateral lemniscus (auditory pathways)
40 Medial geniculate body
41 Lateral geniculate body

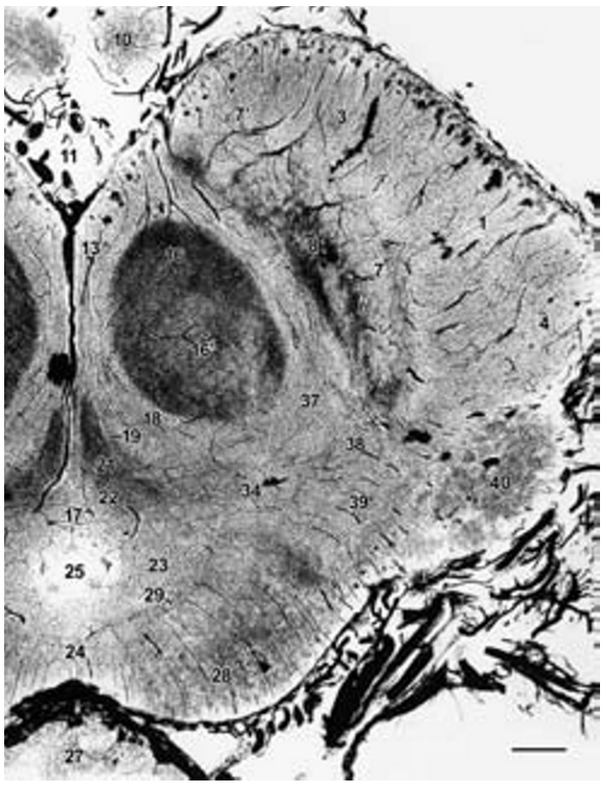
10
7'
3
11
13'
8
7
1
4
16'
37
18
19
38
34
40
39'
17
22
25
23
29
24
28
27

B

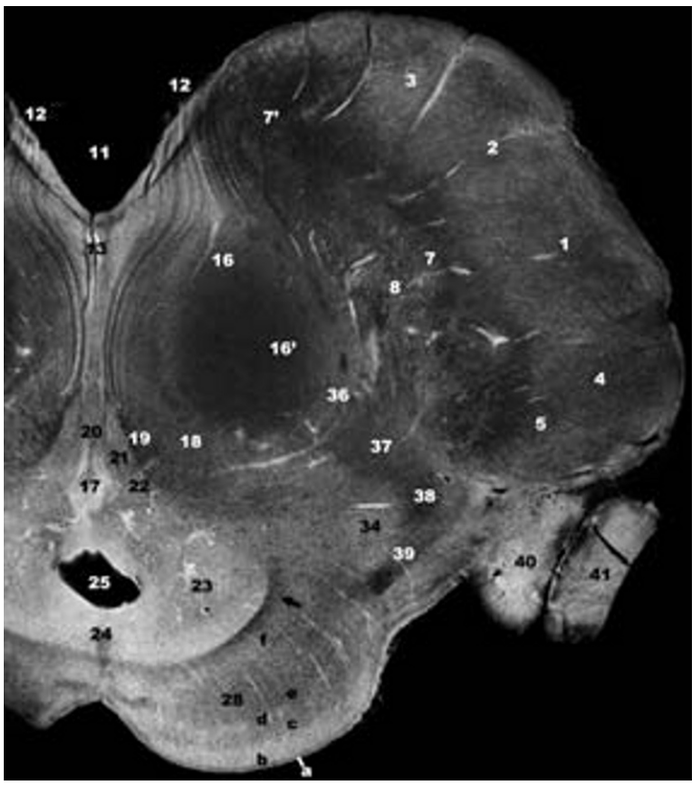
12
12
7'
3
11
2
33
16
7
1
8
16'
4
36
5
20
19
18
37
21
17
22
38
34
39
40
41
25
23
24
f
28
e
d
c
b
a

C

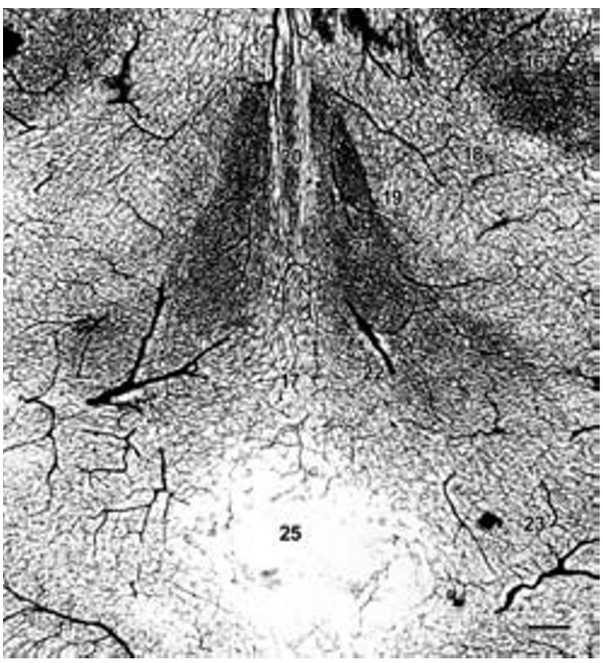
16'
20
18
19
17
25
23

D

Fig. 2.21. Section 15. The diencephalo-mesencephalic junction. Level of the superior pole of the red nucleus and the subthalamic nucleus.
See Fig. 11.27 for the general location of the section and the corresponding MRI.

A. Diagram of an axial (horizontal) section.
B., D. Intravascular India ink injection.
B. Bar: 1 mm.
D. Bar: 1 mm.
C. Matching MR Microscopy at 9.4 Tesla.

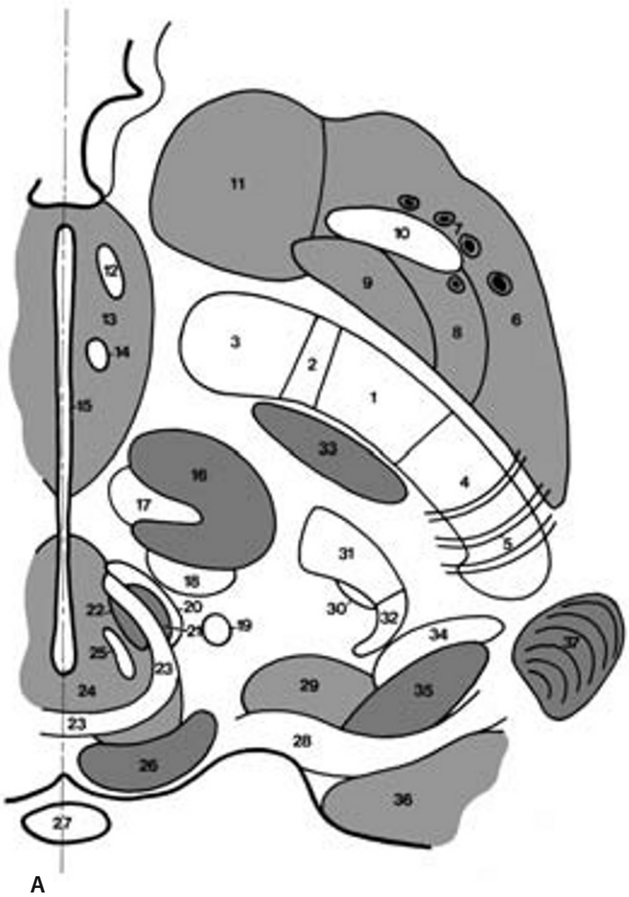

A

1 Corticospinal tract
2 Corticobulbar tract
3 Frontopontine tract
4 Parietotemporopontine tract
5 Nigrostriatal fibers
6 Putamen
7 Striate blood vessels
8 Lateral pallidum (globus pallidus, pars externa)
9 Medial pallidum (globus pallidus, pars interna)
10 Anterior commissure
11 Caudate nucleus (head)
12 Anterior column of fornix
13 Hypothalamus
13′ Paraventricular nucleus of hypothalamus
14 Mammillothalamic tract
15 Third ventricle
16 Red nucleus (superior pole)
17 Habenulo-interpeduncular tract (fasciculus retroflexus)
18 Central tegmental tract
19 Dorsal trigeminothalamic tract
20 Medial longitudinal fasciculus
21 Interstitial nucleus of Cajal
22 Nucleus of Darkschewitsch
23 Posterior commissure
24 Periaqueductal gray matter
25 Dorsal longitudinal fasciculus
26 Superior colliculus
27 Pineal gland
28 Brachium of the superior colliculus
29 Pretectal area
30 Ventral trigeminothalamic tract
31 Medial lemniscus
32 Lateral lemniscus
33 Subthalamic nucleus
34 Brachium of the inferior colliculus
35 Medial geniculate body
36 Pulvinar
37 Lateral geniculate body
38 Hippocampus
39 Caudate nucleus (tail)
40 Cerebral aqueduct (of Sylvius)

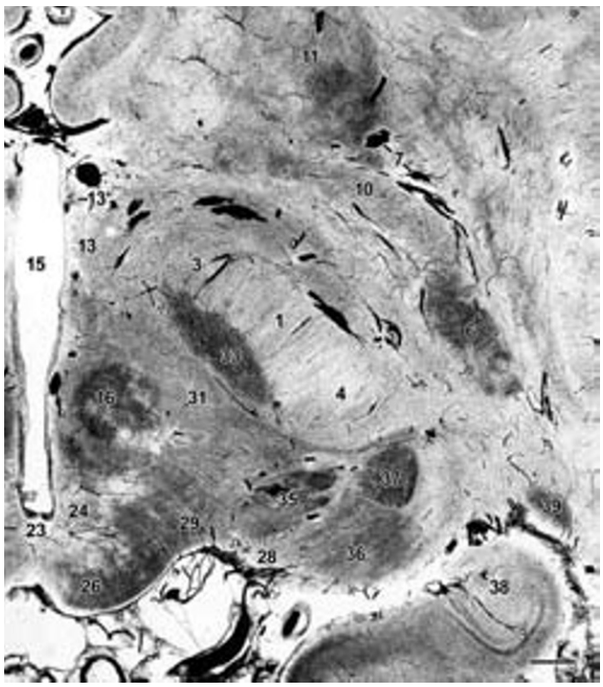
11
7
10
13
13
15
3
1
16
31
4
24
23
29
28
36
26
38

B

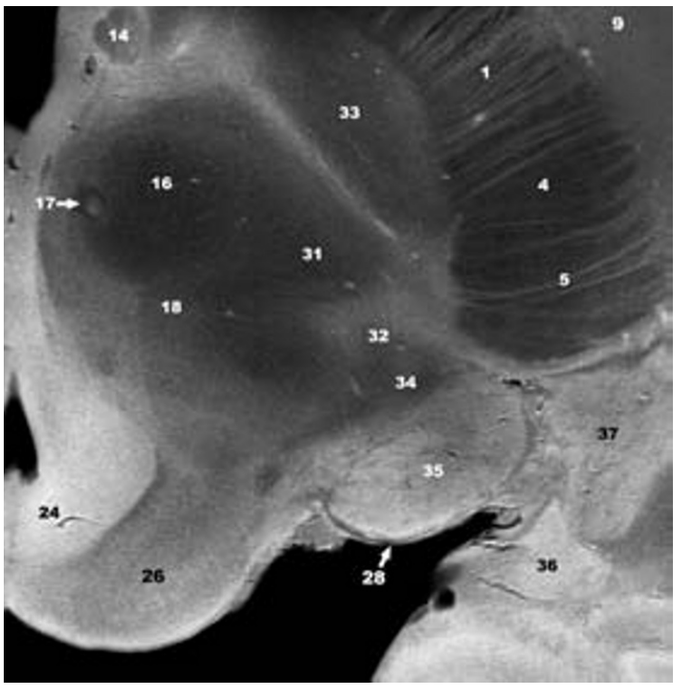
14
9
1
33
16
17
4
31
5
18
32
34
37
35
24
26
28
36

C

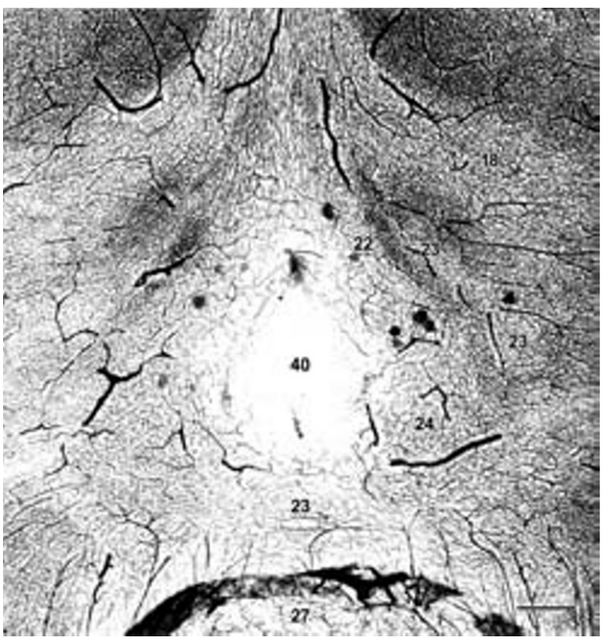
18
22
23
23
40
24
23
27

D

Fig. 2.22. Section 16. The diencephalon. Level of Schaltenbrand's bicommissural plane (from mid-anterior commissure to mid-posterior commissure).
See Fig. 11.29 for the general location of the section and the corresponding MRI.

A. Diagram of an axial (horizontal) section.
B. Intravascular India ink injection. Bar: 1 mm.
C. Matching MR Microscopy at 9.4 Tesla.

1 Internal capsule, posterior limb: corticospinal tract
2 Internal capsule, genu: corticonuclear tract
3 Medial pallidum (globus pallidus, pars interna)
4 Lateral pallidum (globus pallidus, pars externa)
5 Claustrum
6 Putamen
7 Striate blood vessels
8 Caudate nucleus (head)
9 Anterior commissure
10 Third ventricle
11 Anterior column of fornix
12 Hypothalamus
12′ Paraventricular nucleus of hypothalamus
13 Mammillothalamic tract
14 Zona incerta
15 Subthalamic nucleus
16 Ventral posterolateral thalamic nucleus
17 Ventral posteromedial thalamic nucleus
18 Centromedian thalamic nucleus
19 Dorsomedial thalamic nucleus
20 Parafascicular thalamic nucleus
21 Habenulo-interpeduncular tract (fasciculus retroflexus)
22 Posterior commissure
23 Pineal gland
24 Superior colliculus
25 Brachium of the superior colliculus
26 Pretectal area
27 Pulvinar
28 Medial geniculate body
29 Lateral geniculate body
30 Hippocampus
31 Caudate nucleus (tail)

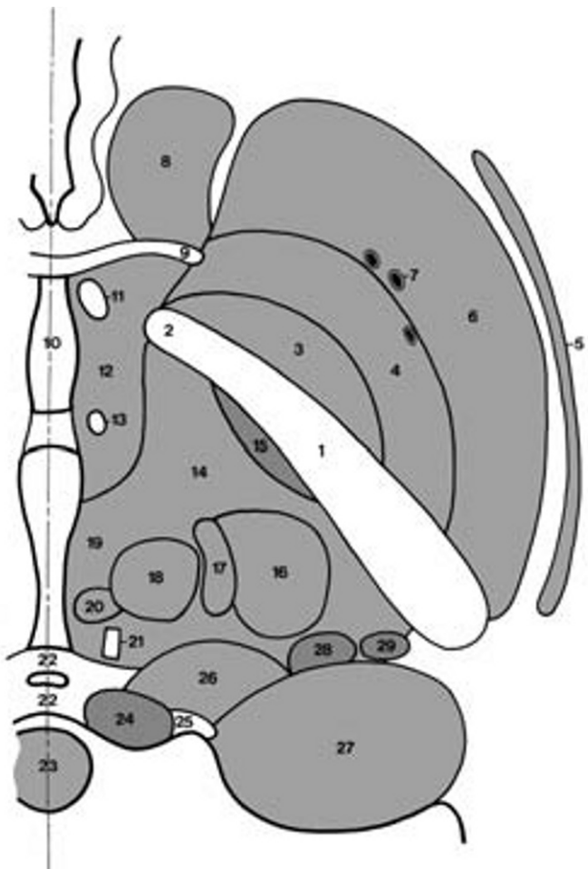

A

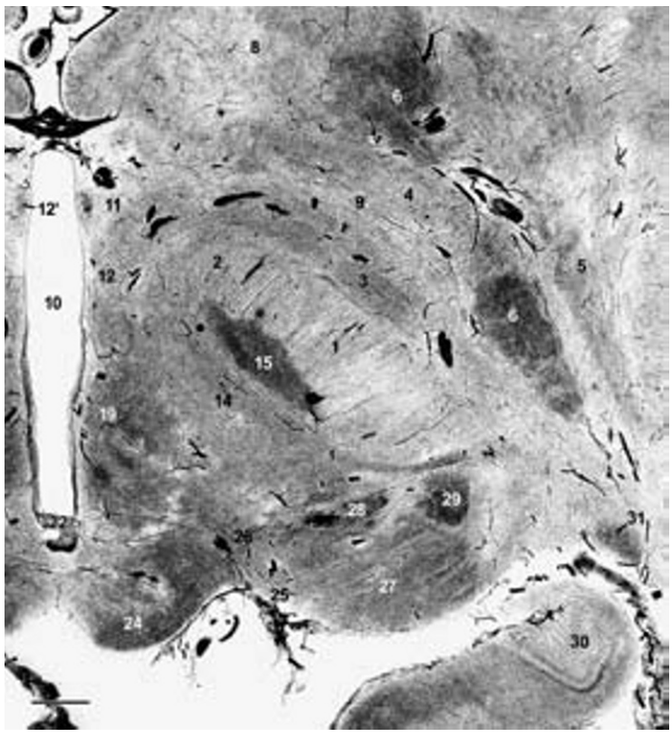
8
6
12'
11
9
4
12
2
3
5
10
15
14
19
1
28
29
31
26
27
25
24
30

B

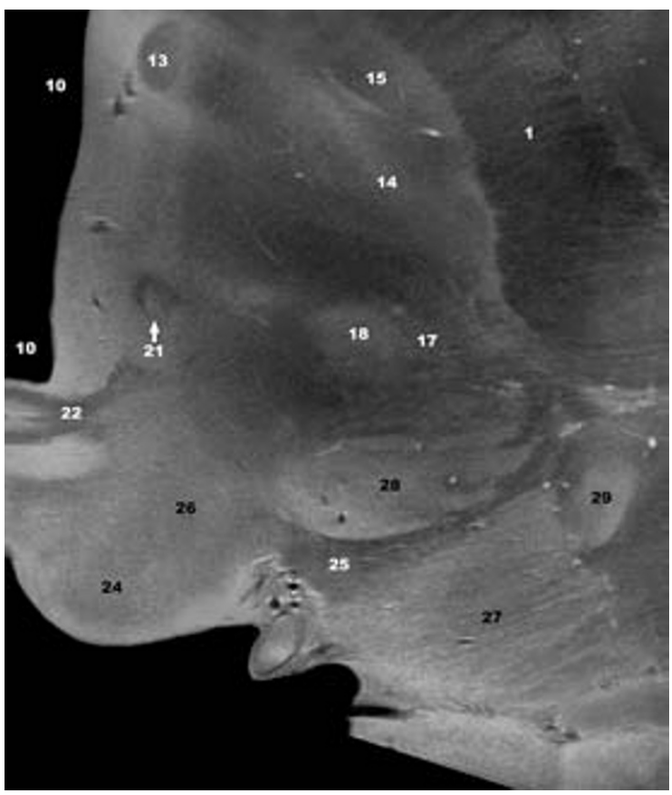
13
10
15
1
14
10
21
18
17
22
28
29
26
25
24
27

C

SECTION III

MAJOR FUNCTIONS OF THE BRAIN STEM

The brain stem is involved in many of the basic functions of the encephalon. This section reviews some of the more important components of the sensory, motor, and autonomic systems, as described in the literature, to assist the reader in understanding the anatomic structures discussed [16, 17, 18, 27, 30, 31, 36, 40, 41, 48, 65, 68, 78, 82, 86, 87, 89, 98, 100, 105, 141, 142, 154, 156, 162, 176, 191, 195, 211, 214, 221, 224, 226, 228, 252, 262, 284, 285, 295, 300, 315, 322, 329, 333, 335, 341, 344, 349, 359, 361, 365, 381, 384, 385, 391, 406, 410, 413, 414, 415, 429, 432, 438, 439. 444, 454, 455, 457, 460, 461, 462, 463, 464, 465, 477, 485].

A. Sensory functions of the brain stem

The brain stem structures that are involved in the general sensory systems and in the special sensory systems will be studied in turn.

General sensory systems

The brain stem contains the general sensory pathways that ascend from the spinal cord to the thalamus and cerebral cortex (**Figs. 2.4 and 3.1**). These pathways are classified into epicritic and protopathic pathways, according to the type of information they convey. They may also be considered as lemniscal (epicritic) and extra-lemniscal (protopathic) pathways, the latter following a path that is not yet clearly defined [See 16, 17, 18, 31, 36, 40, 41, 48, 78, 82, 105, 141, 142, 154, 176, 228, 315, 322, 341, 349, 365, 384, 406, 455, 460, 465, 477, 485].

Epicritic pathways

The epicritic pathways are concerned with discriminative tactile and kinesthetic proprioceptive senses. Epicritic sensations provide the fine tactile location and identification of an object and a precise perception of body location, in particular for the limbs. The large myelinated first order fibers of this system ascend in the dorsal columns of the spinal cord (gracile and cuneate fasciculi) to reach the gracile and cuneate nuclei in the medulla, respectively. Within these nuclei, the primary fibers synapse with neurons that then give off second order (internal arcuate) fibers. The second-order fibers cross the midline in the great sensory decussation of the medulla (decussation of the internal arcuate fibers) and ascend as the medial lemniscus on the contralateral side of the medulla (**Fig. 2.10**), the pons (**Fig. 2.14**) and the mesencephalon (**Fig. 2.20**) to reach the ventral posterolateral nucleus of the thalamus.

Protopathic pathways

The protopathic pathways transmit pain, temperature, and, as opposed to the epicritic system, crude poorly localizing tactile information. The protopathic system may be an early warning system alert to external aggression. The protopathic system includes several named tracts:

Spinothalamic (anterolateral) tract. This tract is concerned with crude tactile and pain sensation. Inferiorly, the spinothalamic tract lies in the lateral portion of the medulla, far from the medial lemniscus (**Fig. 2.10**). Further superiorly, in the pons (**Fig. 2.14**) and the mesencephalon (**Fig. 2.20**), the spinothalamic tract approaches the medial lemniscus more and more closely, until the two tracts reach the ventral posterolateral thalamic nucleus together. Some fascicles of the spinothalamic tract continue to the intralaminar nuclei.

Spinoreticulothalamic tract of the reticular formation (**Fig. 2.4**). This tract transmits diffuse and poorly localized pain and thermal sensations. Its location in the spinal cord and the brain stem is poorly known and controversial. Ultimately, it reaches the reticular nuclei of the thalamus (intralaminar and parafascicular thalamic nuclei).

Spinoreticular tract. These fibers, which have no defined location, reach the reticular centers of the brain stem at different levels and give rise to descending systems (described later).

Brain stem mechanisms for control of pain conduction

The periaqueductal gray matter receives information from the ascending spinoreticular tract and gives rise

to fibers that project to the raphe nuclei (mainly the nucleus raphe magnus). The raphe nuclei of the reticular formation (Fig. 2.2) are the origin of a descending serotoninergic inhibiting system controlling the dorsal horns of the spinal cord. Thus, the brain stem reticular formation has a dual role in the sensory system:

- Conduction of pain sensitivity to the thalamus, and
- Organization of a descending inhibitory system to the spinal cord.

Sensory systems originating from the face (trigeminal system)

The principal sensory trigeminal nucleus and the pars oralis of the spinal trigeminal nucleus receive epicritic innervation from the face. The pars caudalis of the spinal trigeminal nucleus is involved with protopathic sensitivity. The mesencephalic trigeminal nucleus receives proprioceptive impulses from the face. Some sensory fibers belonging to the glossopharyngeal nerve (innervating the middle ear and pharynx) and the vagus nerve (arising from the external acoustic meatus and the lower portion of the pharynx) also reach the trigeminal nuclei.

From the trigeminal nuclei, fibers ascend towards the thalamus, but their route is controversial.

(a) In conventional view, the trigeminal fibers decussate and then form the ventral trigeminothalamic tract (trigeminal lemniscus) along the posterolateral border of the contralateral medial lemniscus.

The dorsal trigeminothalamic tract, whose function is uncertain, arises from the dorsal portion of the principal sensory trigeminal nucleus and is composed of uncrossed fibers.

(b) In more recent views, the epicritic pathways coming from the face are associated with the medial lemniscus, while the protopathic pathways from the face are associated with the spinothalamic system.

General sensory pathways to the cerebellum

The cerebellum receives proprioceptive sensory information from bones, joints, and muscles via several pathways that track through the brain stem:

The dorsal (posterior) spinocerebellar tract arises from the nucleus thoracicus (Clarke's column, nucleus dorsalis). It transmits information from the lower portion of the body to the cerebellum through the inferior cerebellar peduncle.

The cuneocerebellar tract originates in the lateral cuneate nucleus. It transmits proprioceptive information from the upper portion of the body to the cerebellum through the inferior cerebellar peduncle. Functionally it is the upper body equivalent of the dorsal spinocerebellar tract.

The ventral (anterior) spinocerebellar tract arises from lumbar levels of the spinal cord [322]. It conveys information to the cerebellum through the superior cerebellar peduncle about the excitability of spinal interneurons and the spinal locomotor pattern generator [322a].

The rostral spinocerebellar tract is known from animal studies and is the upper body equivalent of the ventral spinocerebellar tract.

Trigeminocerebellar fibers arise mainly from the pars oralis and pars interpolaris of the spinal trigeminal nucleus and supply somatosensory information from the face.

The reticular formation (nucleus reticularis lateralis) also transmits information to the cerebellum.

Special sensory systems

Vision

Visual appreciation and coordination involve multiple visual subsystems (Figs. 3.2–3.5):

Retinogeniculocortical system. The optic tracts conduct visual impulses from the retinae to the lateral geniculate bodies, which relay them to the primary visual cortex (striate cortex) (Brodmann area 17).

Retinocolliculocortical system. The superior colliculus receives visual input through the brachium of the superior colliculus. The superficial layer of the colliculus (stratum griseum superficiale) (Fig. 2.20) belongs to the retinocolliculocortical system, which bypasses the principal retinogeniculocortical system. The functions of the retinocolliculocortical system are not clear in humans. The deeper layers of the superior colliculus (stratum griseum medium and profundum) receive input from the retina. They give rise to descending motor fibers that pass to the spinal cord (tectospinal tract) and to the nuclei of the cranial nerves (oculomotor system, see p. 98).

The accessory optic system is composed of dorsal and lateral terminal nuclei, which play a role in the control of eye and head movements (see p. 98). They are grouped with the nucleus of the optic tract in the pretectal area, but their precise location is not defined. See [27, 48, 65, 86, 87, 89, 98, 100, 156, 162, 214, 228, 322, 333, 341, 361, 381, 432, 455, 457].

Audition

The central auditory pathways include many brain stem structures (Fig. 3.2). The vestibulocochlear nerve fibers arising from the internal ear (cochlea) reach the dorsal and ventral cochlear nuclei (Fig. 2.12).

From the ventral cochlear nucleus, fibers synapse within the ipsi- and contralateral superior olivary complex, formed by the medial and lateral superior olivary nuclei and by the nucleus of trapezoid body (Fig. 2.13). These fibers then ascend in both lateral lemniscus.

From the dorsal cochlear nucleus, fibers cross the midline and join with fibers originating in the ventral cochlear nucleus to form the lateral lemniscus. Although some fibers relay in the nuclei of the lateral lemniscus, most of them reach the inferior colliculus directly and then continue onward to the medial geniculate body via the brachium of the inferior colliculus. From the medial geniculate body, auditory fibers pass to the temporal lobe for audition, and to the frontal premotor areas and the parietal lobes for auditory spatial localization. See [48, 176, 228, 322, 329, 341, 391, 414, 415, 455].

Vestibular responsiveness

The membranous labyrinth of the inner ear sends vestibular information to the vestibular nuclear complex via the vestibulocochlear nerve (Figs. 3.3–3.5). It also projects vestibular fibers directly to the cerebellum. The large vestibular complex is divided into four nuclei:

Inferior vestibular nucleus (of Roller),
Medial vestibular nucleus (of Schwalbe),
Lateral vestibular nucleus (of Deiter),
Superior vestibular nucleus (of Bechterew).

The vestibular nuclei mainly have motor functions:

The descending vestibulospinal tract. This tract links the lateral vestibular nucleus to the spinal cord for control of equilibrium (see p. 98);

The medial longitudinal fasciculus **(MLF).** Within the MLF, fibers from the medial, inferior, and superior vestibular nuclei interconnect with the nuclei of cranial nerves (CN) III (oculomotor), IV (trochlear), and VI (abducens) to control the extra-ocular muscles. Other fibers within the MLF link the vestibular system with the cervical spinal cord for visual fixation and conjugate gaze as the head is turned.

Some ascending fibers appear to reach the thalamus by way of the lateral lemniscus, and then continue on to the parietal cortex. See [48, 157, 322, 341, 455].

Gustation

Gustatory fibers arising from the dorsal surface of the tongue extend through the nervus intermedius, the glossopharyngeal nerve, and the vagus nerve to terminate within the medulla in the upper portion of the nucleus of the solitary tract. This rostral portion of the solitary tract is designated the gustatory nucleus. From this nucleus, central gustatory pathways decussate and pass successively to the thalamus and the taste cortex, a ventral insular extension of the somatosensory cortex (Brodmann 1). Other cortically-directed fibers relay to the cortex through the medial parabrachial nucleus rather than the thalamus. See [48, 221, 322, 341, 344, 438, 455].

B. Motor functions of the brain stem

The brain stem structures that are involved in general and in special motor systems will be studied in turn. See [26, 48, 62, 67, 78, 158, 168, 176, 228, 237, 247, 322, 326, 349, 390, 439, 444, 454, 455].

General motor systems

The long descending motor pathways traverse the brain stem *en route* towards the nuclei of the cranial nerves and the spinal cord (Figs. 2.5 and 3.1) See [48, 62, 67, 78, 145, 168, 176, 228, 247, 322, 326, 349, 455].

Motor tracts reaching the anterior horn of the spinal cord

Corticospinal (pyramidal) tract. These fibers originate in the motor cortex and pass successively downward through the internal capsule (posterior limb), mesencephalon, pons, and medulla. In the mesencephalon, the corticospinal tract is situated in the midportion of the crus cerebri (Figs. 2.20 and 3.1). In the basilar portion of the pons, the corticospinal tract separates into numerous small fascicles (Fig. 2.14). In the medulla it occupies the pyramid (pyramidal tract) (Fig. 2.10). As the corticospinal tract traverses the brain stem, it gives numerous collateral fibers to neighboring structures, in particular the pontine nuclei (See p. 100). At the inferior limit of the medulla, most corticospinal fibers cross the midline (motor or pyramidal decussation) (Fig. 2.7) to form the contralateral lateral corticospinal tract, which terminates on the motoneurons in the anterior horns of the spinal cord. Other fibers do not decussate in the medulla, but continue inferiorly in the ipsilateral ventral and lateral corticospinal tracts.

Other descending tracts. It is currently believed that the corticospinal tract is not the only tract reaching the spinal motor centers and can be bypassed by other small bundles. As a result, the long descending motor systems can be divided into lateral and medial groups [247] as follows:

The lateral motor system is formed mainly by the corticospinal (pyramidal) tract and, to a lesser degree, by the corticorubrospinal tract (whose function is reduced in man). This system terminates in the lateral spinal motoneurons, which help innervate the distal muscles of the limbs, and, in particular, control the prehensile mechanism.

The medial motor system controls the spinal motoneurons that innervate the proximal muscles. It is divided into several small fasciculi: the corticotectospinal tract (involving the superior colliculus), corticovestibulospinal tract, and corticoreticulospinal tract.

The reticulospinal tracts (Fig. 3.1), the main part of this system, are divided into the medial reticulospinal tract and the lateral reticulospinal tract. The medial reticulospinal tract originates from the central pontine reticular formation and is excitatory for the spinal motoneurons. The lateral reticulospinal tract arises from the central medullary reticular formation and has an inhibitory function. The descending reticular tract, arising from the raphe nuclei, controls the sensory pathways at the spinal level (See pp. 95–96). Because their location is not well established, the reticulospinal tracts are not described in this work.

Descending tracts reaching the cranial nerve motor nuclei

The location of the corticobulbar (corticonuclear) tract within the brain stem is uncertain. Overall, it is divided into secondary small fascicles, which decussate at various levels to reach the motor nuclei of the cranial nerves. In fact, however, most of the motor nuclei of the brain stem receive bilateral innervation from the corticobulbar tracts.

Brain stem motor centers in relation to the cerebellum

Numerous structures, such as the red nucleus, the pontine nuclei, and the inferior olivary nucleus connect with the cerebellum. Their functions are described on p. 140.

Brain stem motor centers in relation to the thalamus and basal ganglia

The pars reticulata and pars compacta of the substantia nigra are the main centers of this group. The pars reticulata receives fibers from the striatum and gives rise to two different groups of efferent GABA-ergic fibers: (A) ascending fibers to the thalamus (ventral lateral and ventral anterior nuclei), and (B) descending fibers to the superior colliculus and reticular formation (which play a role in oculomotor control). The pars compacta controls striatal function (see below) through the dopaminergic nigrostriatal fibers.

Special motor systems

The brain stem is involved in numerous complex motor systems such as oculomotor control, respiration, deglutition (swallowing), micturition (urination), and emesis (vomiting).

Oculomotor system

The oldest oculomotor systems (the vestibulo-ocular and optokinetic reflexes) serve to maintain the stability of vision during movements of the head (Figs. 3.2 and 3.3). The more recent oculomotor systems (saccades and smooth-pursuit eye movements) serve to fix and follow a special target. Only the brain stem centers concerned with these systems will be reviewed.

The vestibulo-ocular reflex (***VOR***) provides compensatory eye movements to stabilize retinal images during head motion (Fig. 3.3). The eye movements are opposite to those of the head. The principal pathways for the horizontal VOR extend from the labyrinth to the medial vestibular nucleus and then to the abducens nucleus, which projects to the oculomotor nucleus. The control system is composed of the flocculus, the inferior olivary nucleus, and the nucleus prepositus hypoglossi. The vertical VOR is served by analagous pathways.

The optokinetic reflex **(*OKR*)** is characterized by eye (and head) movements in response to global motion of the visual field (Fig 3.3). The principal pathways of the horizontal OKR begin in the retina and successively link the nucleus of the optic tract (in the pretectal area), the nucleus reticularis tegmenti pontis, and the vestibular nucleus. As with the vestibulo-ocular system, the fibers of the vestibular nucleus reach the abducens nucleus, which controls the oculomotor nucleus. The nucleus prepositus hypoglossi controls the principal pathways.

The saccades consist of rapid eye movements that bring the image of an object situated in the visual field onto the fovea (central portion of the retina) and allow fixation to pass rapidly from one object of interest to another (Fig 3.4). The saccades are divided into horizontal and vertical saccades.

Horizontal saccades. The principal pathways originating from the retina successively involve the deep layers of the superior colliculus, the paramedian pontine reticular formation (nuclei reticularis pontis caudalis and oralis), and the abducens nucleus, which projects to the oculomotor nucleus.

Regulatory circuits. The superior colliculus appears to be controlled by GABA-ergic fibers of the substantia nigra pars reticulata. The paramedian pontine reticular formation receives inputs from the cerebellar vermis (declive: lobule VI; folium and tuber: lobule VII) by way of the fastigial and medial vestibular nuclei.

Vertical saccades. The organization of this system is poorly understood. From the retina, fibers reach the deep layers of the superior colliculus, then the rostral interstitial nucleus of the medial longitudinal fasciculus (riMLF). Together, the riMLF, the interstitial nucleus of Cajal, and the pretectal area may constitute the control center for vertical saccades, from which fibers project to the oculomotor and trochlear nuclei.

Smooth-pursuit eye movements. These concern the pursuit of a target moving in a fixed visual field (Fig 3.5). The cortical pathways mediating smooth-pursuit eye movements are poorly understood. From the occipital and temporal cortex, fibers successively reach the dorsolateral pontine nucleus (Figs. 2.16 and 2.17), and the cerebellum (flocculus and vermis: declive (VI); folium and tuber (VII)). The flocculus is linked to the medial vestibular nucleus. The vermis is linked to the fastigial nucleus. These two nuclei project to the abducens nucleus, which controls the oculomotor nucleus. The medial longitudinal fasciculus is the principal link for the entire oculomotor system. See [38, 67, 74, 77, 87, 89, 100, 133, 145, 158, 162, 168, 191, 211, 237, 241, 262, 305, 322, 323, 340, 341, 343, 384, 385, 390, 432, 439, 444, 454, 455, 457].

Brain stem respiratory centers

The respiratory centers are subdivided into medullary and pontine centers (Fig 3.6) [211].

The medullary centers comprise two groups of cells, which control respiratory rhythm: a dorsal group in the nucleus of the solitary tract, and a ventral group, often called nucleus retroambiguus, situated in the reticular formation around the nucleus ambiguus. (Note: the term nucleus retroambiguus is also sometimes used to designate the lowest portion of the nucleus ambiguus). The medullary centers extend fibers to the phrenic motoneurons.

The pontine center is the pneumotaxic center situated in the medial parabrachial and Kölliker-Fuse nuclei. The pontine center regulates the two medullary centers. See [211, 322, 389].

Brain stem deglutition (swallowing) centers

The swallowing mechanisms depend on afferent centers near the nucleus of the solitary tract and efferent centers near the nucleus ambiguus, which project to the motoneurons located in the nucleus ambiguus and the hypoglossal nucleus (Fig. 3.7). A pontine center near the superior olivary nucleus monitors the motor sequences. See [48, 220, 270, 322, 411].

Brain stem micturition (urination) centers

The dorsolateral pontine tegmentum (Fig. 2.16) is the principal control center for micturition (Fig. 3.8). This zone is indistinctly divided into lateral and medial regions. See [30, 198, 267, 322, 335].

The lateral region (L-region) gives descending fibers that project to the nucleus of Onuf in the central portion of the ventral horn of the first and second sacral segments. This nucleus innervates the striated muscles of the pelvic floor, including the anal and urethral sphincters [322].

The medial region (M-region) is the micturition reflex center. It gives fibers to the parasympathetic sacral centers that innervate the pelvic smooth muscles, in particular the bladder detrusor muscle.

Brain stem emesis (vomiting) centers

These centers are ill-defined and controversial. A medullary vomiting center situated in the reticular formation near the dorsal vagal nucleus is influenced by a chemoreceptor trigger zone situated in the area postrema. See [26, 48, 322, 386].

Fig. 3.1. Diagram. Principal motor and sensory systems of the brain stem reticular formation

Sensory system (Green):

5HT	5-Hydroxytryptamine (Serotonin)
CING. CORTEX	Cingulate cortex
CL	Centrolateral thalamic nucleus
PAS	Periaqueductal gray matter
PF	Parafascicular nucleus of the thalamus
RAPH. MAG.	Nucleus raphe magnus
SPINO. RET. TH. TR.	Spinoreticulothalamic tract. The spinoreticulthalamic tract has an ascending path to the thalamic nuclei (the parafascicular nucleus (PF) and the centrolateral and intralaminar nuclei (CL)) before reaching the cingulate cortex (CING. CORTEX). This tract makes several steps in the reticular formation.
SPINO. RET. TR.	Spinoreticular tract. The spinoreticular tract is involved in the control of pain conduction. It reaches the periaqueductal substance (PAS), which, through the raphe nuclei (nucleus raphe magnus), controls the spinal cord (5HT: serotonergic pathways)
SPINO. TH.	Spinothalamic tract, extending directly to the ventral posterolateral nucleus (VPL) of the thalamus and the sensory cortex.
VPL	Ventral posterolateral nucleus of the thalamus

Motor system (Red):

CORTICO. SP. TR.	Corticospinal tract
GIG. CEL.	Nucleus reticularis gigantocellularis
LAT. CORTICO. RET. SP. TR.	Lateral corticoreticulospinal tract. The lateral corticoreticulospinal tract (1), after a step in the nucleus gigantocellularis (GIG. CEL.) has an inhibitory action on the spinal cord.
MED. CORTICO. RET. SP. TR.	Medial corticoreticulospinal tract. The medial corticoreticulospinal tract (2) relays within the nuclei reticularis pontis oralis (PO) and caudalis (PC), and has an activating action on the spinal cord.
PC	Nucleus reticularis pontis caudalis
PO	Nucleus reticularis pontis oralis

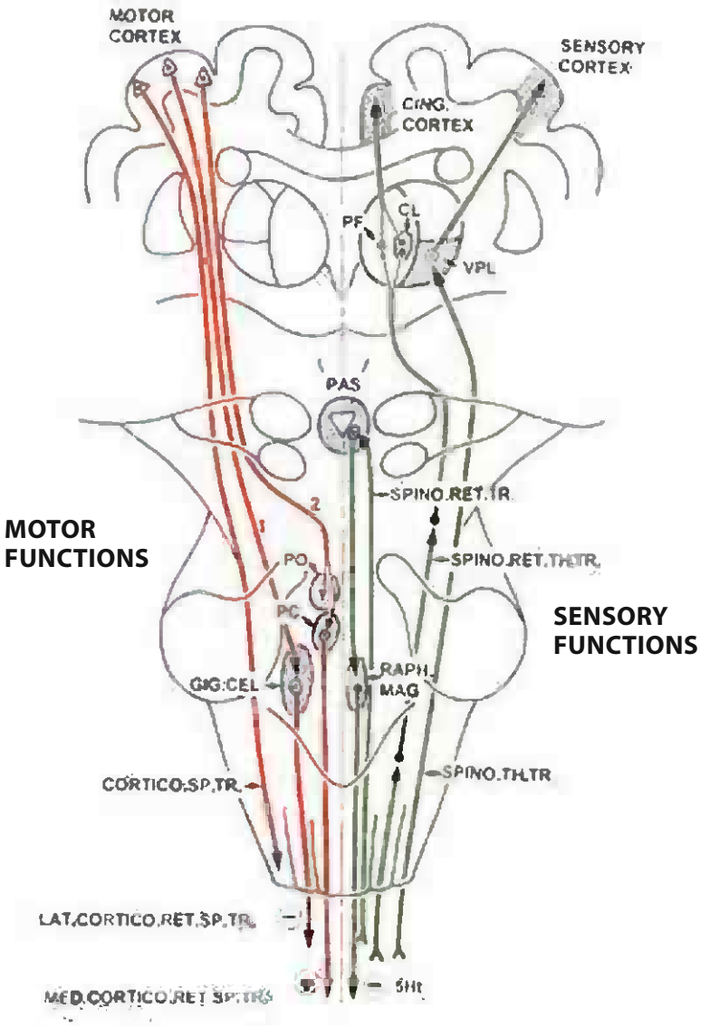

MOTOR AND SENSORY FUNCTIONS

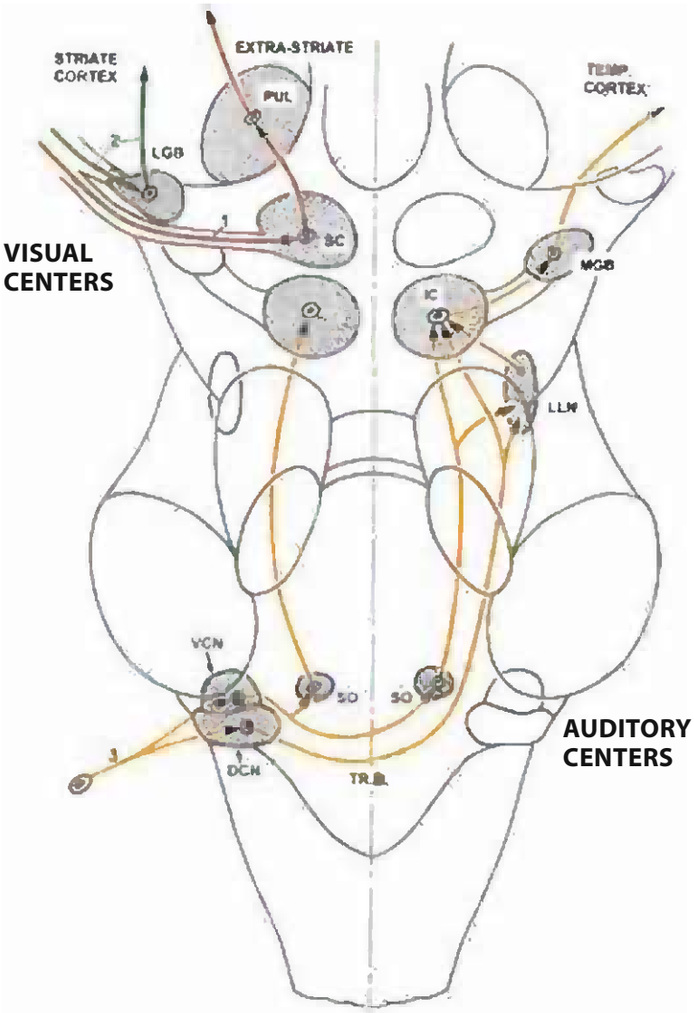

Fig. 3.2. Special sensory functions of the brain stem

Brain stem visual centers

Retinocolliculocortical system (1). The superior colliculus (SC) receives visual input through the brachium of the superior colliculus (1) and projects through the pulvinar (PUL) to the extrastriate cortex (extrastriate).

Retinogeniculocortical system (2). The lateral geniculate body (LGB) receives fibers from the retina and projects directly to the striate cortex, with no intermediate link through the brain stem.

Brain stem auditory centers

The principal auditory centers are at the pontine level. These include:

- The dorsal cochlear nucleus (DCN) and ventral cochlear nucleus (VCN)
- The superior olivary complex (superior olivary nucleus (SO) and the nucleus of the trapezoid body (TR.B.)).

These centers receive information from the internal ear via the vestibulocochlear nerve (3) and send fibers to the inferior colliculi (IC) both directly and via the lateral lemniscal nucleus (LLN). The auditory pathways ascend to the medial geniculate body (MGB), from which the auditory (geniculotemporal) radiations convey information to the temporal cortex (TEMP. CORTEX).

LLN Lateral lemniscal nuclei

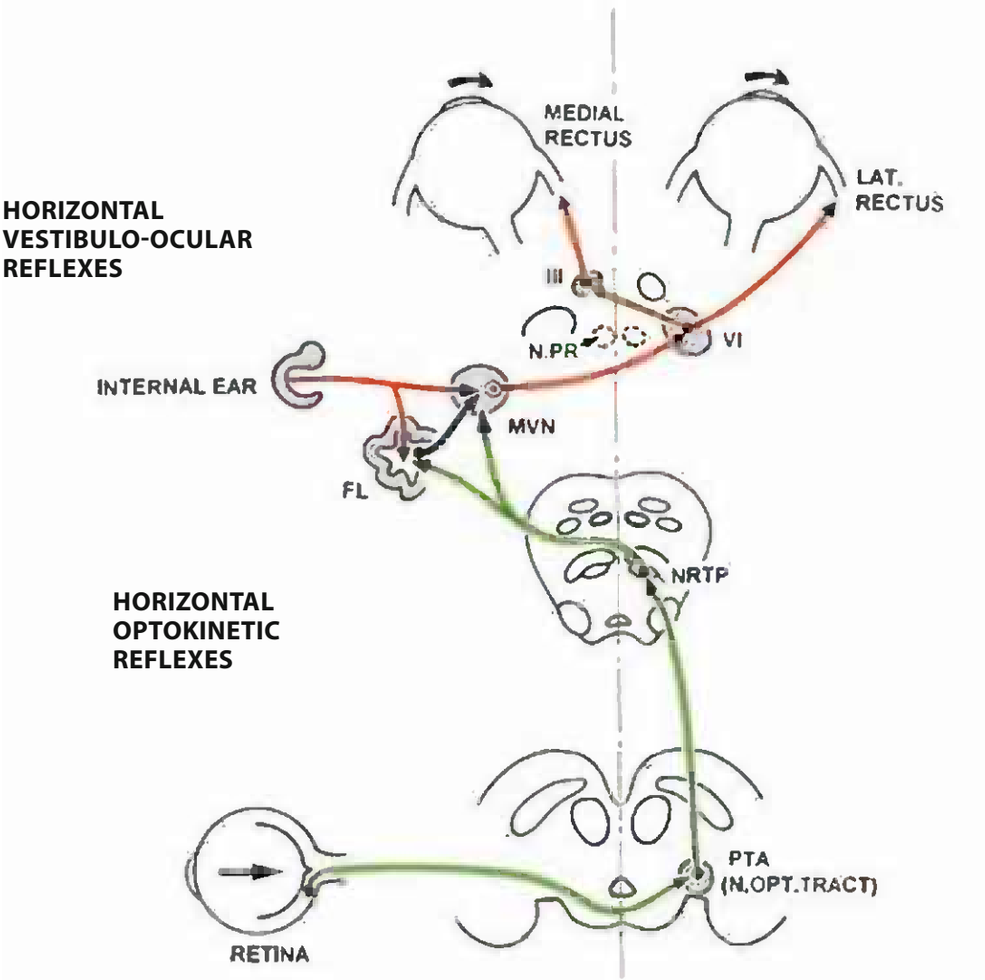

VESTIBULO-OCULAR AND OPTOKINETIC CENTERS

OCULOMOTOR CENTERS

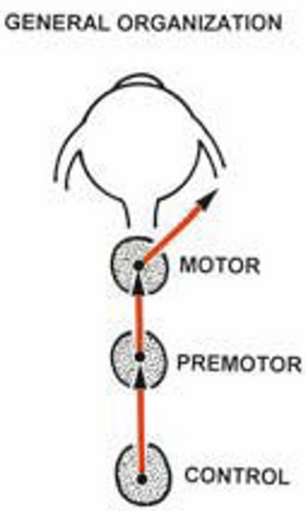

Fig. 3.3. Vestibulo-ocular and optokinetic reflexes

III	Nucleus of cranial nerve III (oculomotor nucleus)
VI	Nucleus of cranial nerve VI (abducens nucleus)
FL	Flocculus
MVN	Medial vestibular nucleus
N. OPT. TRACT	Nucleus of the optic tract
NPR	Nucleus reticularis pedunculopontinis
NRTP	Nucleus reticularis tegmenti pontis
PTA	Pretectal area

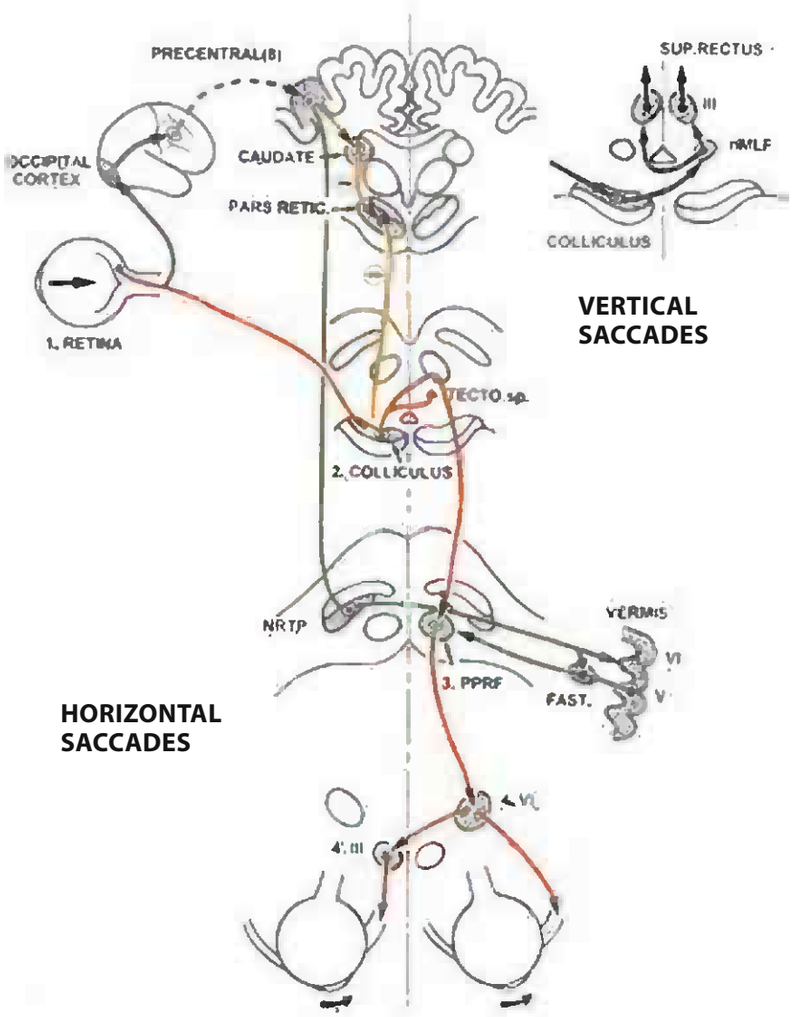

Fig. 3.4. Vertical and horizontal saccades

Vertical saccades

III	Nucleus of cranial nerve III (oculomotor nucleus)
riMLF	Rostral interstitial nucleus of the medial longitudinal fasciculus
SUP. RECTUS	Superior rectus

Horizontal saccades

The sequential steps leading to horizontal saccades follow in order: 1, 2, 3, 4 and 4'.

III	Cranial nerve III (oculomotor nucleus)
VI	Cranial nerve VI (abducens nucleus)
FAST.	Fastigial nucleus
NRTP	Nucleus reticularis tegmenti pontis
PARS RETIC.	Pars reticularis of the substantia nigra
PPRF	Paramedian pontine reticular formation
TECTO. sp.	Tectospinal tract
VERMIS V	Lobule V (of Larsell) (posterior culmen)
VERMIS VI	Lobule VI (of Larsell) (declive)

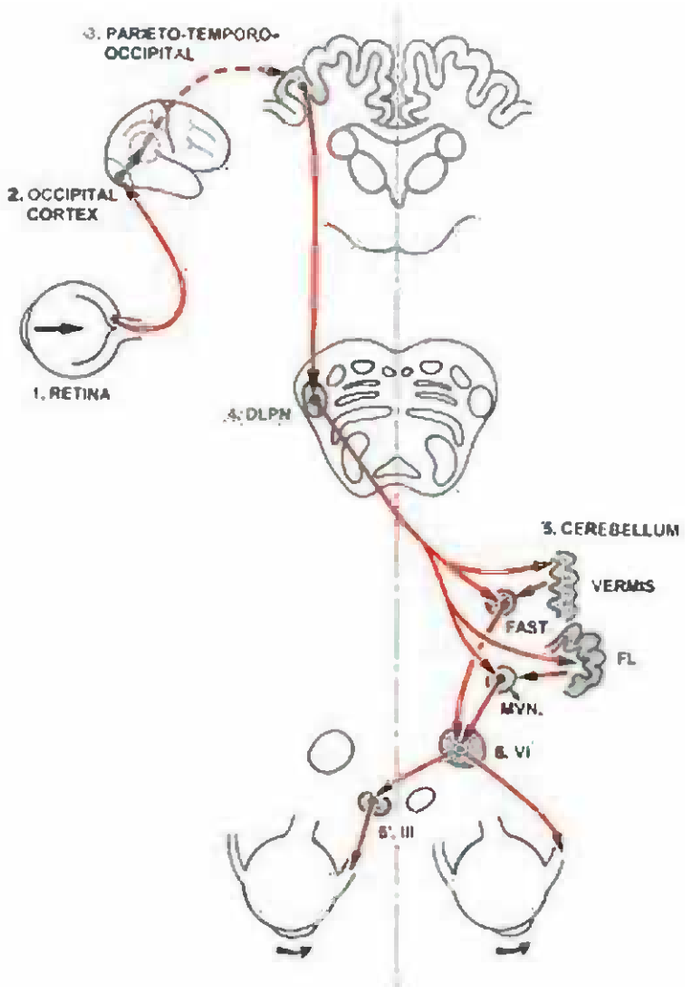

CENTERS FOR SMOOTH PURSUIT EYE MOVEMENTS

Fig. 3.5. Smooth pursuit eye movements.
The sequential steps leading to smooth pursuit follow in order:
1, 2, 3, 4, 5, 6 and 6'.

III	Nucleus of cranial nerve III (oculomotor nucleus)
VI	Nucleus of cranial nerve VI (abducens nucleus)
DLPN	Dorsolateral pontine nucleus
FAST.	Fastigial nucleus
FL	Flocculus
MVN	Medial vestibular nucleus

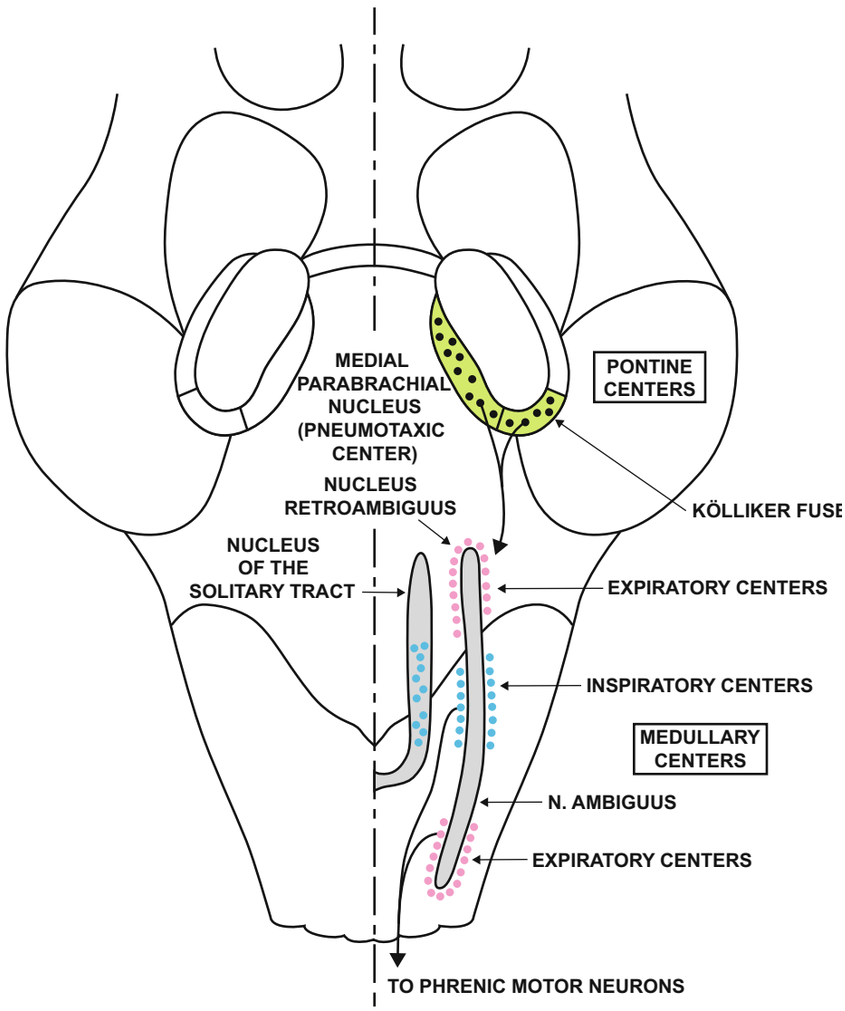

Fig. 3.6. **Brain stem respiratory centers**

Medullary centers
Nucleus ambiguus
Nucleus of the solitary tract
Nucleus retro-ambiguus

Pontine centers
Medial parabrachial nucleus (pneumotaxic center)
Kölliker-Fuse nuclei

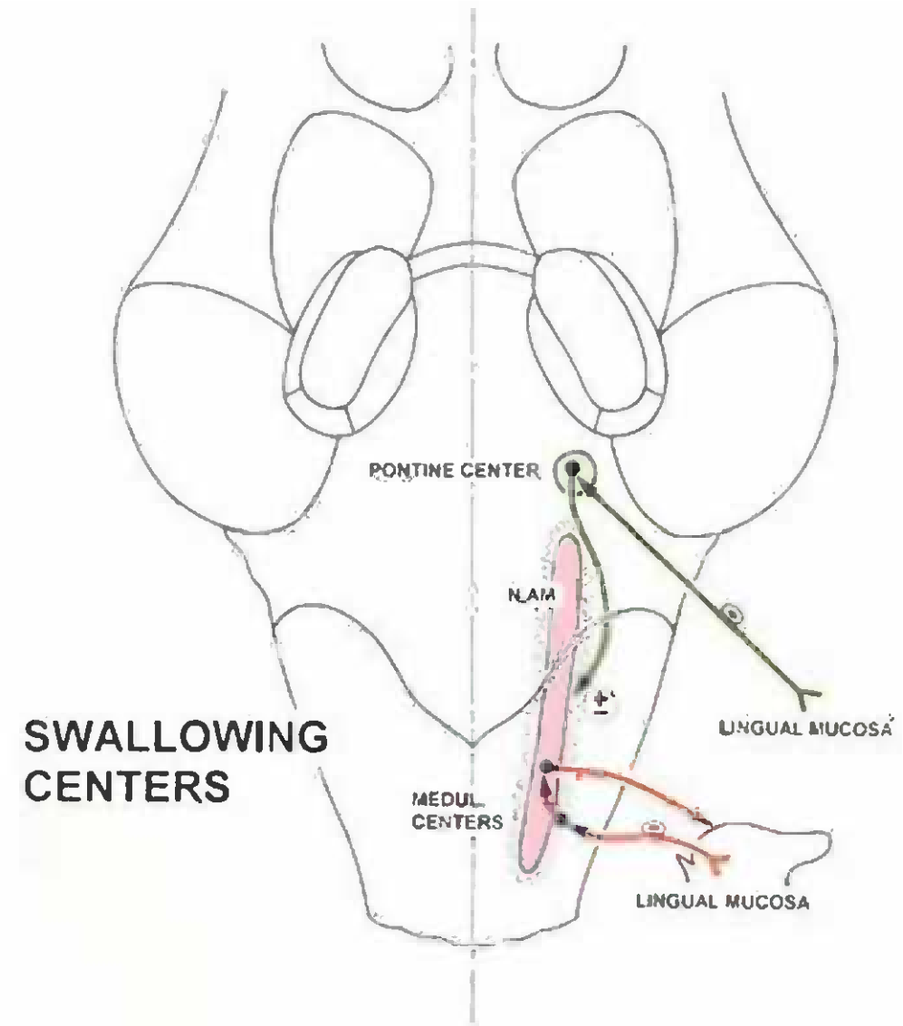

SWALLOWING CENTERS

Fig. 3.7. Swallowing centers

MEDUL. CENTERS Medullary centers
N. AM. Nucleus ambiguus

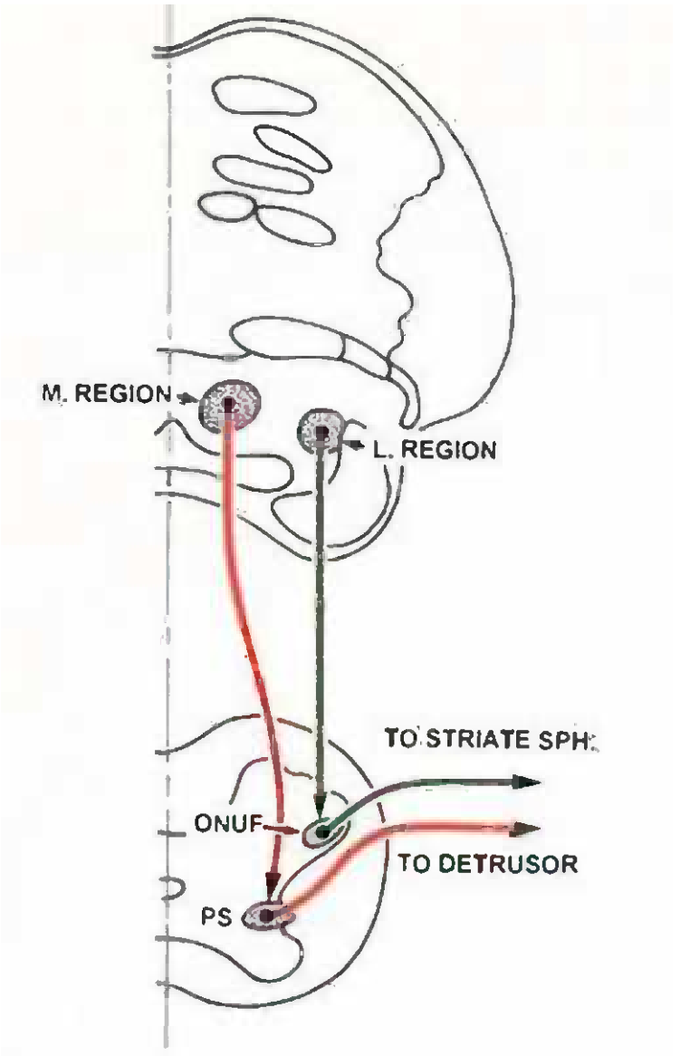

Fig. 3.8. Micturition centers

L. REGION	Lateral region
M. REGION	Medial region
ONUF	Somatomotor nucleus of Onuf in the ventral horn of segments S1 and S2, which innervates the striated muscle of the anal and bladder sphincters.
PS	Parasympathetic neurons that give motor supply to smooth muscle, including the detrusor muscle of the bladder
STRIATE SPH.	Striated muscle sphincters

B. Neurotransmitters in the brain stem

Among the numerous neurotransmitters found in the brain stem, only the monoaminergic and cholinergic centers will be described here (**Figs. 3.9 to 3.13**). For more information, see [19, 36, 41, 45, 84, 88, 113, 181, 199, 212, 219, 269, 287, 300, 321, 322, 341, 359, 364, 386, 395, 412, 443, 466, 486].

Brain stem monoaminergic centers

These centers are divided into three groups on the basis of the neurotransmitter utilized

– noradrenergic (and adrenergic)
– serotoninergic
– dopaminergic

Brain stem cholinergic centers

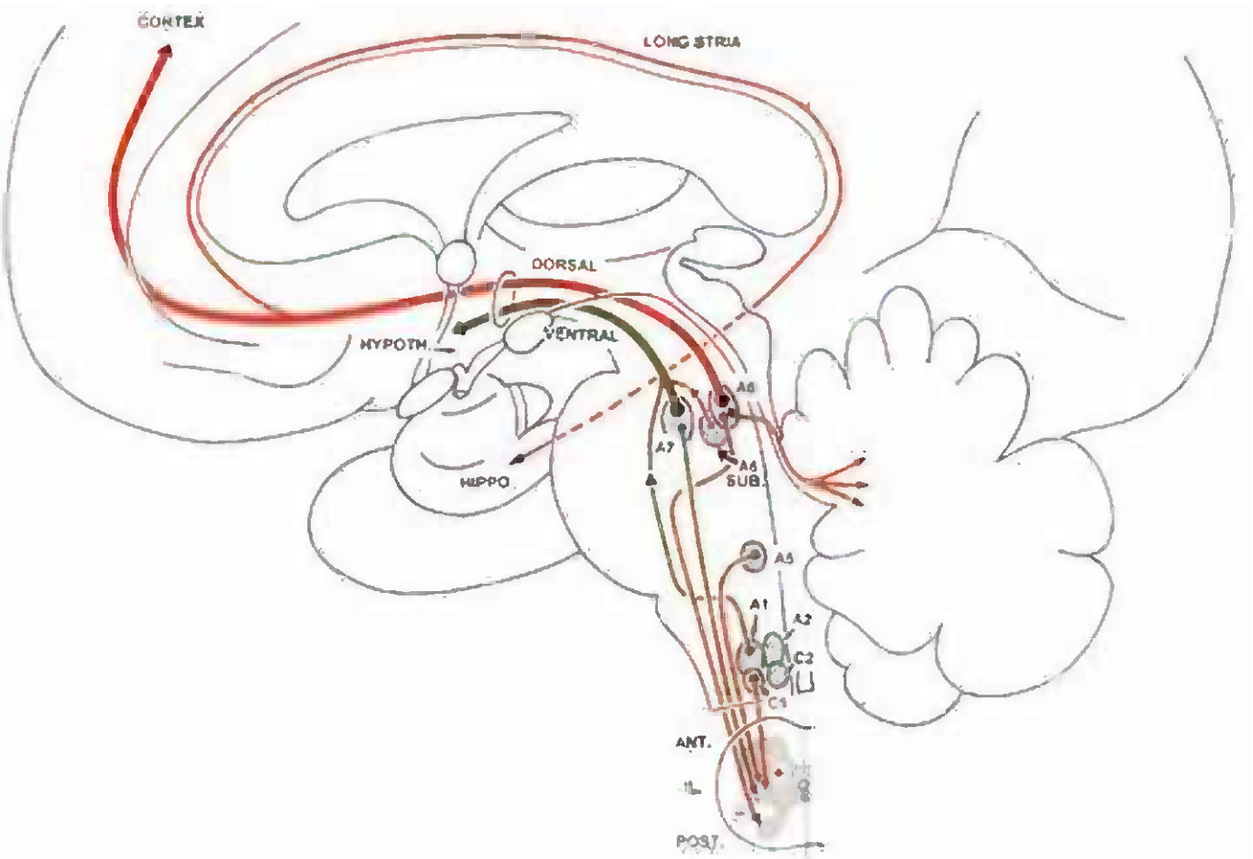

NORADRENERGIC AND ADRENERGIC CENTERS

Fig. 3.9. The brain stem noradrenergic (and adrenergic) centers. Diagram. The dorsal noradrenergic pathway (red) reaches the cortex. The ventral noradrenergic pathway (green) mainly supplies the hypothalamus.

A1 The A1 noradrenergic center (associated with the C1 adrenergic center) is located in the ventrolateral medulla (See p. 114) .

A2 The A2 noradrenergic center (associated with the C2 adrenergic center) lies predominantly within the nucleus of the solitary tract [322].

A5 The A5 noradrenergic center lies near the superior olivary nucleus.

A6 The A6 noradrenergic center is located in the nucleus ceruleus. This is the main source of noradrenaline for the entire brain. A6 gives supply to the cerebellar cortex through the superior cerebellar peduncle. The A6 subceruleus is situated in the ill-defined nucleus subceruleus.

A7 The A7 noradrenergic center is located in the medial parabrachial and Kölliker-Fuse nuclei.

The A6 and A7 noradrenergic centers, together with the CH6 cholinergic center, are situated in the dorsolateral pontine tegmentum (Fig. 2.16).

ANT.	Anterior
HIPPO.	Hippocampus
HYPOTH.	Hypothalamus
IL.	Intermediolateral column of Terni (lateral horn) (Preganglionic outflow to the sympathetic chain ganglia)
LONG.STRIA	Longitudinal striae
POST.	Posterior

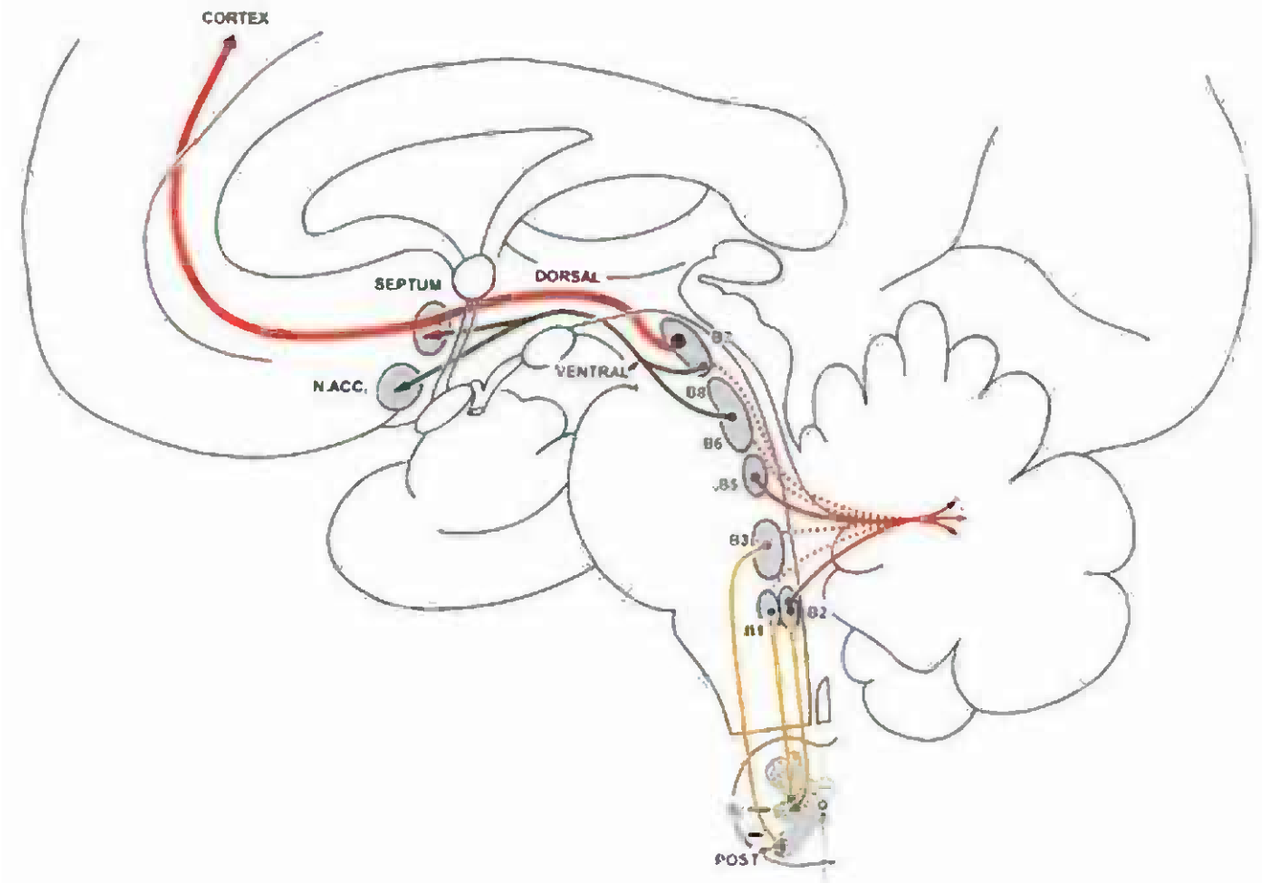

SEROTONINERGIC (5HT) CENTERS

Fig. 3.10. The brain stem serotoninergic centers. Diagram. 5Ht (5-hydroxytryptamine, serotonin) is derived from tryptophan. Serotoninergic centers are situated in the median reticular column (raphe nuclei). The dorsal serotoninergic pathway (red) reaches the cortex. The ventral serotoninergic pathway (green) mainly reaches the septum and the nucleus accumbens septae. Serotoninergic centers also extend (gold) to the posterior horn (POST) and the intermediolateral column (IL) of the spinal cord.

B1 Serotoninergic center: Nu. raphe pallidus
B2 Serotoninergic center: Nu. raphe obscurus
B3 Serotoninergic center: Nu. raphe magnus
B5 Serotoninergic center: Nu. raphe pontis
B6, B8 Serotoninergic centers: Nu. centralis superior
B7 Serotoninergic center: Dorsal nu. raphe

The noradrenergic and serotoninergic centers send numerous ascending fibers to the brain and descending fibers to the spinal cord. The ascending noradrenergic and serotoninergic fibers act in opposition, and may be involved in arousal and sleep, respectively. The supply to the cerebellar hemisphere arises from all raphe nuclei, especially B2 and B5, and enters the cerebellum via the middle cerebellar peduncle [321].

IL Intermediolateral column of Terni (lateral horn)
N.Acc. Nucleus accumbens septae
POST Posterior horn of the spinal cord

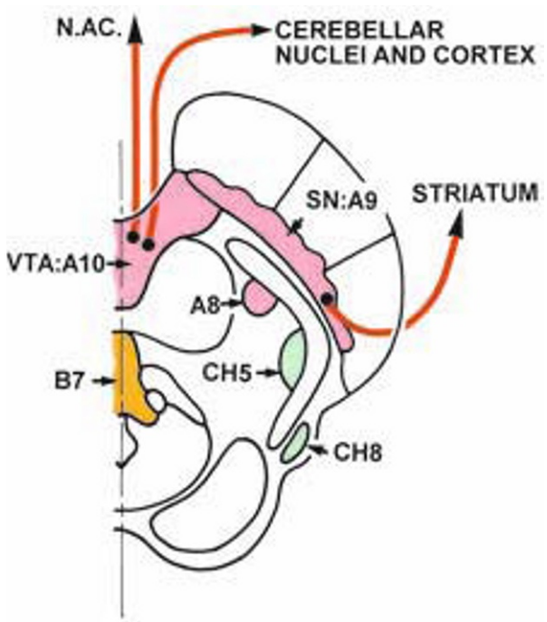

Fig. 3.11. The brain stem dopaminergic centers. Diagram. Dopamine (DA) is derived from tyrosine.
The dopaminergic centers of the brain stem are all situated in the mesencephalon.

A8 Dopaminergic center. This has a debatable location.
A9 Dopaminergic center. This is situated in the substantia nigra, pars compacta. The pars compacta is involved in the control of the striatum via dopaminergic nigrostriate fibers (Fig. 2.20).
A10 Dopaminergic center: The A10 dopaminergic center is situated in the ventral tegmental area (VTA). It projects to the septal nuclei, amygdala, and cortex. Together with the periaqueductal gray matter, dorsal raphe, dorsal tegmental and interpeduncular nuclei, the A10 center forms the mesolimbic and mesocortical systems, which are involved in behavior and environmental adaptation.
B7 Dorsal nucleus of the raphe (Serotoninergic)
CH5 Nucleus reticularis pedunculopontinus (Cholinergic)
CH8 Parabigeminal nucleus (Cholinergic)
N. AC. Nucleus accumbens septae
SN Substantia nigra
VTA Ventral tegmental area

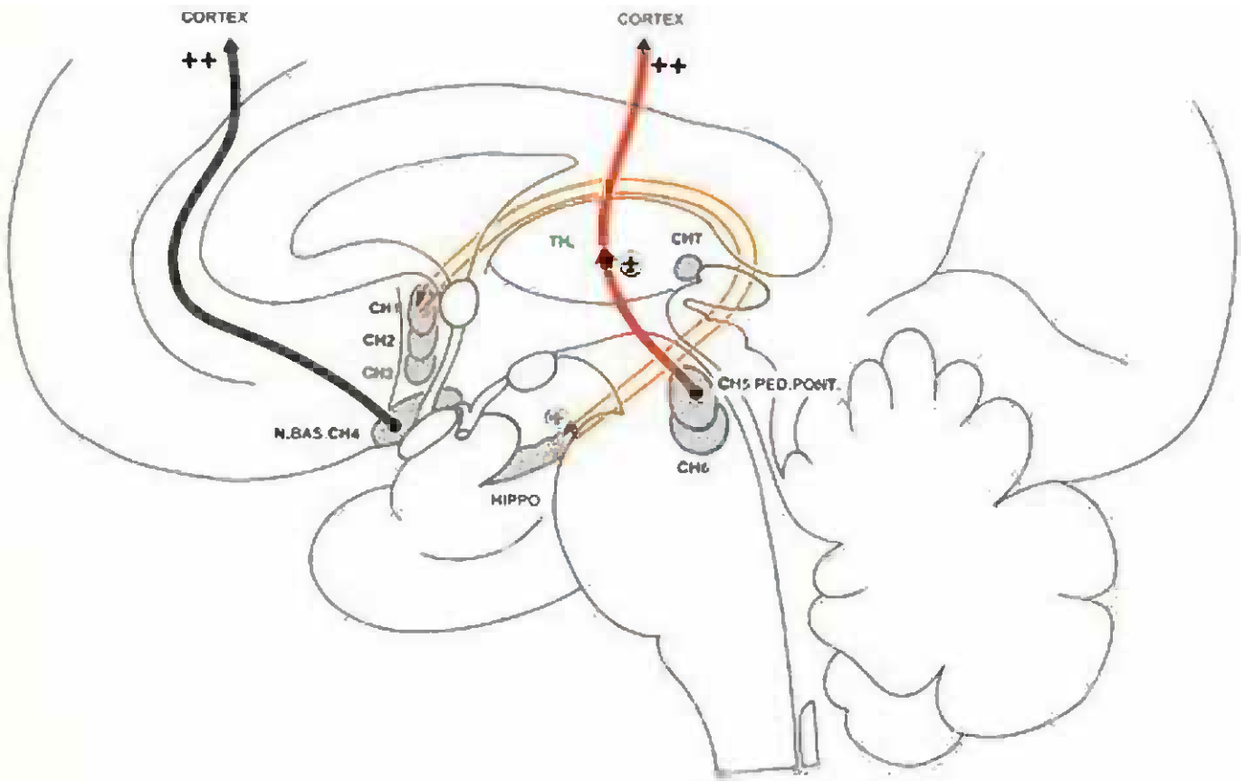

CHOLINERGIC CENTERS

Fig. 3.12. The brain stem cholinergic centers. Diagram. ACH signifies acetylcholine derived from choline.

Cholinergic loci in the basomedial forebrain

CH1 Medial septal nucleus
CH2 Diagonal band of Broca (vertical limb)
CH3 Diagonal band of Broca (horizontal limb)
CH4 Nucleus basalis of Meynert (N.BAS.)

Cholinergic loci in the caudal midbrain and rostral rhombencephalon

CH5 Nucleus reticularis pedunculopontinus (PED. PONT.)
CH6 Situated in the dorsolateral pontine tegmentum (in and around the nucleus ceruleus).
CH7 Situated within the medial habenular nucleus
CH8 This center, situated in the parabigeminal nucleus (**Figs. 2.18 and 3.11**), projects to the superior colliculus. Many cholinergic cells are also scattered throughout the brain stem.

HIPPO Hippocampal formation
TH. Thalamus

C. Autonomic brain stem centers

The autonomic brain stem centers in the medulla, pons and mesencephalon will be described in turn. See [19, 59, 60, 66, 67, 78, 80, 81, 84, 93, 113, 174, 202, 221, 224, 225, 252, 300, 322, 341, 364, 389, 412, 464].

Autonomic medullary centers

The principal autonomic centers of the brain stem are found in the medulla. They are divided into the dorsomedial and ventrolateral medullary centers.

Dorsomedial medullary centers (dorsomedial medulla)

These centers are principally parasympathetic and, to a lesser degree, sympathetic.

Parasympathetic centers: the dorsal vagal complex visceral afferent system

The principal visceral afferent system in the brain stem is formed by the nucleus of the solitary tract (NST). This important nucleus is divided into three portions:

(a) The rostral portion receives fibers from the nervus intermedius and from the glossopharyngeal and vagus nerves. It is an important relay in the gustatory system.
(b) The midportion of the nucleus of the solitary tract mainly receives fibers from the glossopharyngeal nerve and plays an important role in the respiratory and cardiovascular systems (baro- and chemoreflexes).
(c) The caudal portion (commissural and gelatinosus nuclei) mainly receives fibers from the vagal nerve and is involved in gastrointestinal reflexes.

The area postrema is a chemoreceptor center, whose vessels lack a blood-brain barrier (**See Fig. 1.22**).

The dorsal motor nucleus of the vagus, which receives fibers from the afferent system, is the principal autonomic efferent system in the brain stem.

The dorsal longitudinal fasciculus appears to be an important link between the autonomic medullary centers and the superior autonomic centers such as the hypothalamus.

Sympathetic centers:

A2 noradrenergic and C2 adrenergic centers, situated in the vicinity of, or intermingled with, the dorsal vagal complex, have a modulatory function on the parasympathetic centers.

Ventrolateral medullary centers (ventrolateral medulla)

These centers are mainly sympathetic. The sympathetic neurons are scattered in an ill-defined region comprising the lateral reticular nuclei and the reticular formation surrounding the nucleus ambiguus. The A1 noradrenergic and C1 adrenergic neurons (often linked together as ventrolateral medulla) send ascending fibers to the hypothalamus and descending fibers to the spinal sympathetic centers (tractus intermediolateralis). Through these pathways, the ventrolateral medullary centers have a tonic action on the cardiovascular system (in contrast to the dorsal vagal complex). The dorsomedial and ventrolateral centers are strongly interconnected.

Autonomic pontine centers

These centers are composed of parabrachial, salivatory, and lacrimal nuclei.

The parabrachial nuclei (medial and lateral parabrachial nuclei and Kölliker-Fuse nucleus) are arrayed around the brachium conjunctivum. They receive important afferent fibers from the cardiovascular, respiratory, and gustatory systems and give efferent fibers toward superior centers.

The salivatory nuclei are part of the parasympathetic brain stem centers: The inferior salivatory nucleus innervates the parotid gland via the glossopharyngeal nerve.

The superior salivatory nucleus projects to the sublingual and submandibular glands via the nervus intermedius (VII bis).

The lacrimal nucleus, whose identity is controversial (**See Fig. 2.3**), sends fibers through the nervus intermedius to the lacrimal, nasal, and palatine glands. The salivatory and lacrimal nuclei have an imprecise location.

Autonomic mesencephalic centers

The accessory oculomotor nucleus (nucleus of Edinger-Westphal) is the main parasympathetic mesencephalic center. It controls two major ocular functions:

(a) the light reflex (constriction of the pupil in response to increased light intensity);
(b) the accommodation reflex (modification of the form of the lens) in response to cortical centers.

It appears that the major centers of the reticular formation (**Fig. 2.2**) are located in the brain stem. These centers primarily modulate global states such as attention, arousal and sleep. However, they also play specific roles in the sensory system (including pain conduction), in the general motor system (via the reticulospinal tracts), and in special motor mechanisms (such as oculomotor control, respiration, and swallowing). The principal monoaminergic centers as well as important autonomic (mainly sympathetic) nuclei are located in the reticular formation. The main tracts related to the brain stem reticular formation are the spinoreticular tract, the reticulospinal tracts, and the central tegmental tract (which also contains numerous other connections such as rubro-olivary fibers).

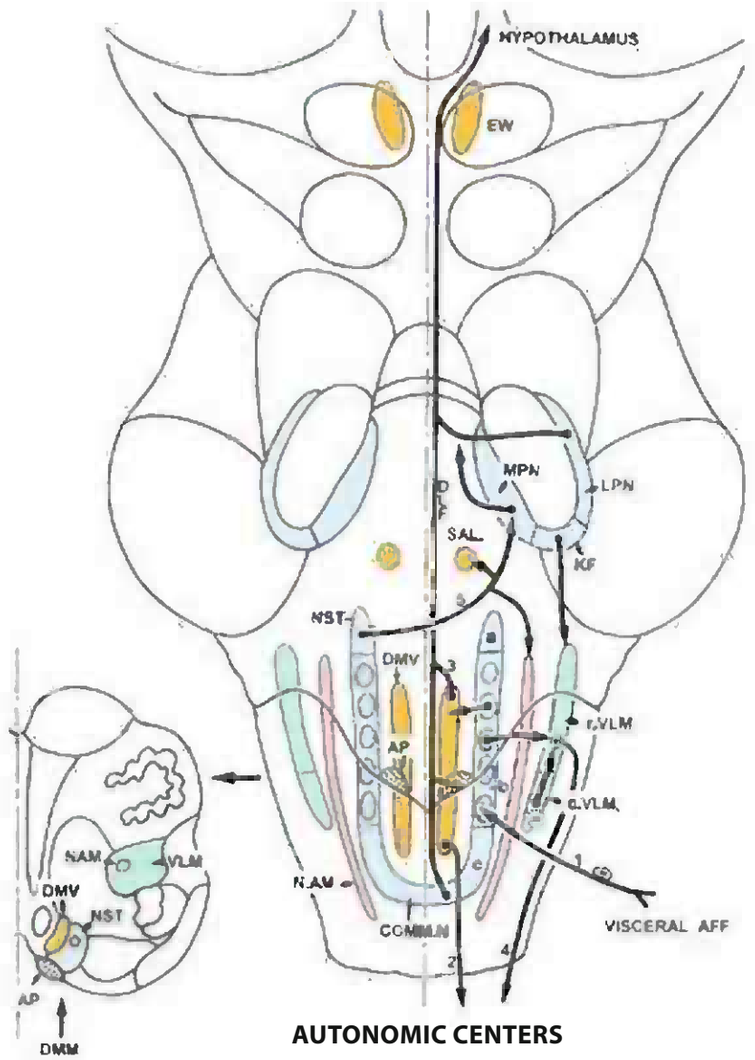

Fig 3.13. The autonomic functions in the brain stem. Diagram. The majority of the autonomic centers of the brain stem lie in the medulla. The medial and lateral parabrachial nuclei lie medial and lateral to the brachium conjunctivum (superior cerebellar peduncle).

I. Medullary autonomic centers

Dorsomedial medullary centers

NST	Nucleus of the solitary tract
a	Rostral portion
b	Midportion
c	Caudal portion
COMM.N	Commissural nucleus
1	Visceral afferent (visceral AFF)
DMV	Dorsal motor nucleus of the vagus sending descending fibers to the spinal cord (2) and ascending fibers to the hypothalamus (3)
AP	Area postrema
DLF	Dorsal longitudinal fasciculus

Ventrolateral medullary centers

rVLM	Rostral portion
cVLM	Caudal portion
4	Fibers to the spinal cord
N. AM	Nucleus ambiguus

II. Pontine autonomic centers

SAL	Salivatory nucleus (receiving fibers (5) from the nucleus of the solitary tract)
MPN	Medial parabrachial nucleus
LPN	Lateral parabrachial nucleus
KF	Nucleus of Kölliker-Fuse

III. Mesencephalic autonomic centers

EW	Accessory oculomotor nucleus (of Edinger-Westphal)
AFF	Afferent inputs

SECTION IV

STRUCTURE AND FUNCTIONS OF THE CEREBELLUM

A. Structure of the cerebellum

This study builds upon on the work of prior authors [1, 4, 31, 48, 51, 57, 67, 71, 72, 78, 85, 89, 99, 109, 132, 136, 142, 151, 167, 175, 180, 182, 187, 218, 228, 245, 247, 248. 280, 304, 322, 324, 331].

Figure 4.1 reviews the general structure of the cerebellum.
Figures 4.2 through 4.10 review the structure of the cerebellar cortex, while
Figures 4.11 through 4.13 address the deep cerebellar nuclei.

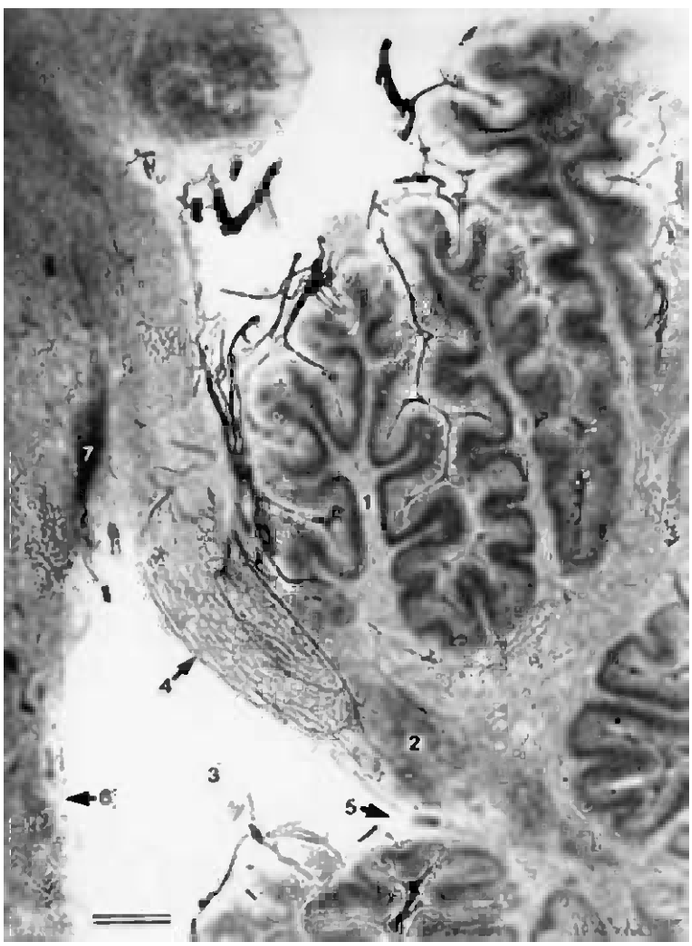

Fig. 4.1. Overview of cerebellar structures.
Sagittal section after intravascular India ink injection.
Bar: 1.5 mm.

1 Cerebellar cortex (a folium of the central lobule)
2 Deep cerebellar nuclei (fastigial nucleus)
3 Fourth ventricle
4 Superior aspect of the ventricular roof (superior cerebellar peduncle)
5 Fastigial sulcus
6 Floor of the fourth ventricle
7 Nucleus ceruleus
8 Inferior colliculus

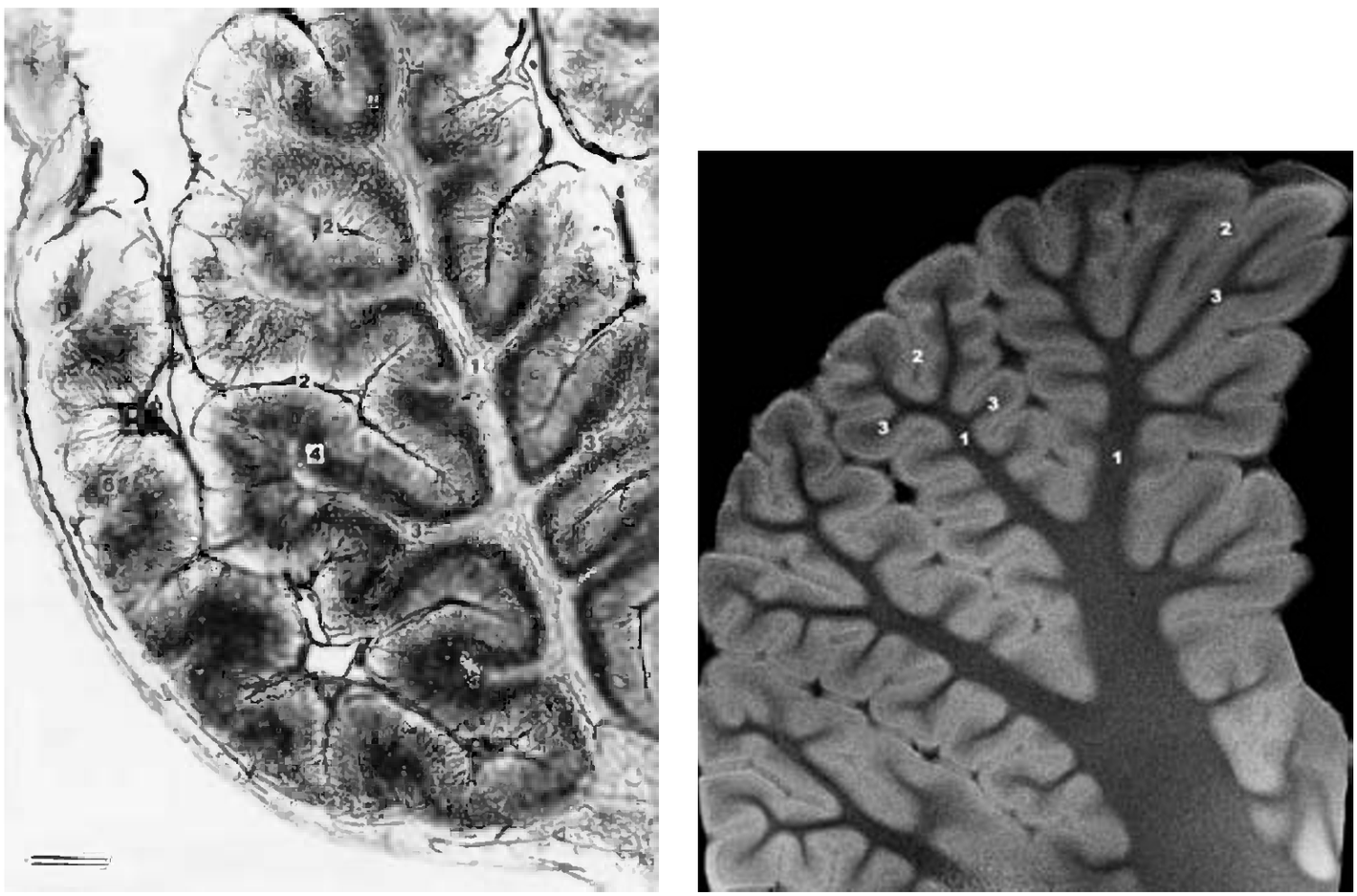

A B

Fig. 4.2 (A–B). The architecture of a folium.

A. Central lobule. Sagittal section. Intravascular India ink injection. Bar: 1 mm.

B. MR Microscopy at 9.4 Tesla

1 Folium axis
2 Secondary sulci
3 Secondary folds
4 Granular layer (note its intense vascular network)
5 Molecular layer
6 Cortex of lingula

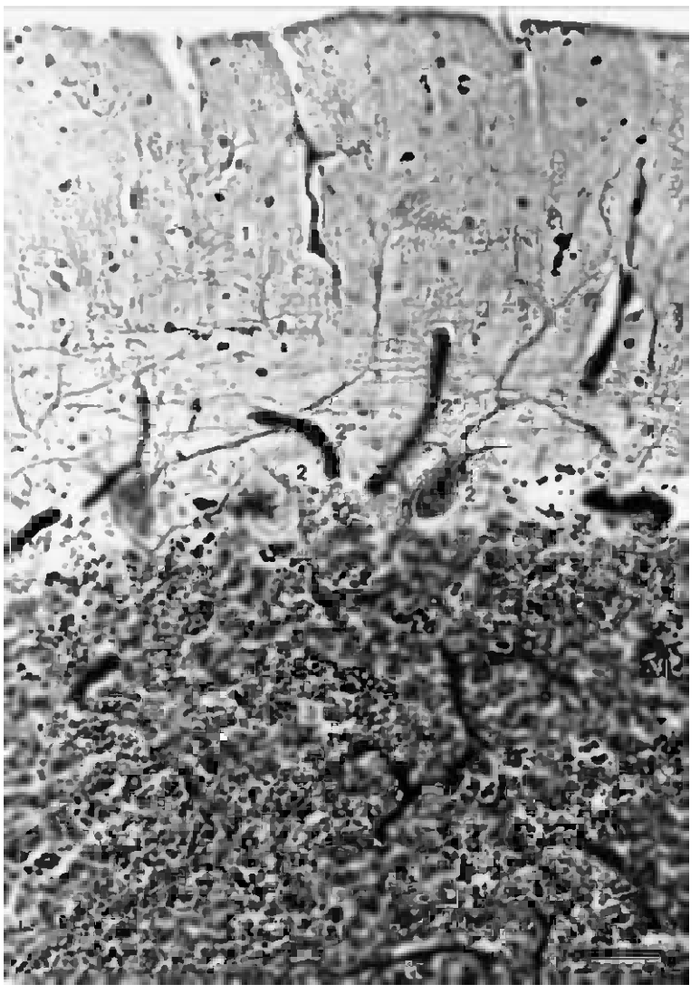

Fig. 4.3. The architecture of the cerebellar cortex.
Intravascular India ink injection and silver impregnation. Bar: 50 µm.

1 Molecular layer
2 Purkinje cell layer (2′ Purkinje cell bodies) and vascular arborization in this layer (2″) (**See Fig 4.8**)
3 Granular layer
4 Parallel fibers

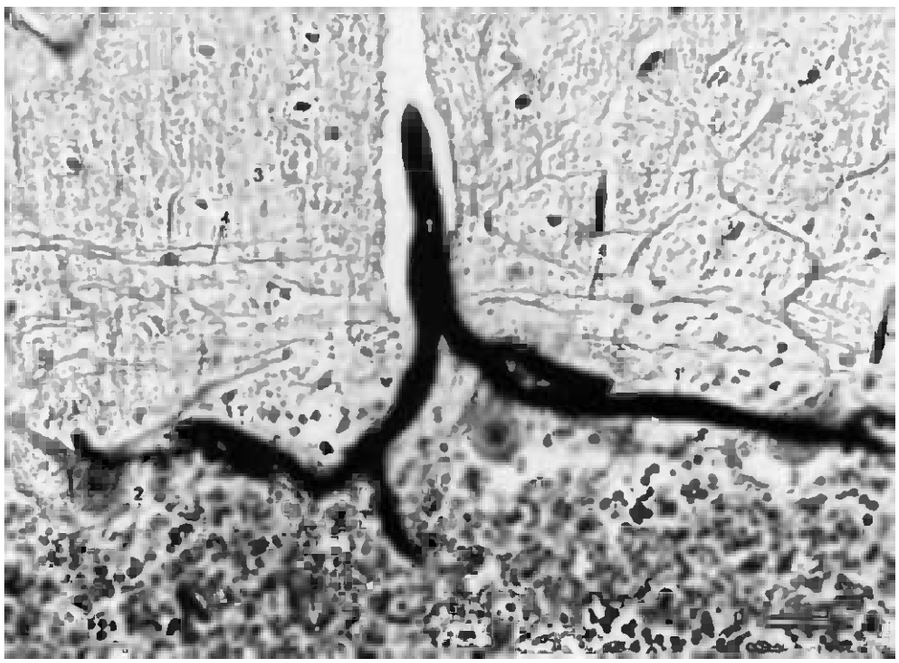

Fig. 4.4. The arterial organization of the cerebellar cortex.
Transverse section across the folium. Intravascular India ink injection and silver impregnation. Bar: 40 μm.

1 Intracortical arteries (Middle A3 artery)
1′ Arterial branches within the Purkinje cell layer run parallel to the surface (parallel arteries)
2 Purkinje cell bodies in close contact with the parallel arteries
3 Molecular layer
4 Parallel fibers coursing parallel to the surface of the cerebellum
5 Granular layer

A

Fig. 4.5 (A–B). The superficial cerebellar vasculature.

A. Intravascular India ink injection showing surface arteries and veins. Bar: 1.2 mm.

B. Corresponding diagram.

The superficial pial arteries give off two types of branches:

1 Large diameter branches penetrating the sulci, and

2 Small diameter branches penetrating the cortical surface.

The cerebellar surface is drained by:

3 Pial veins emerging from the cerebellar surface at the center of the folia.

4 Superficial venous arch.

Black circles indicate the sites of arterial or venous anastomoses.

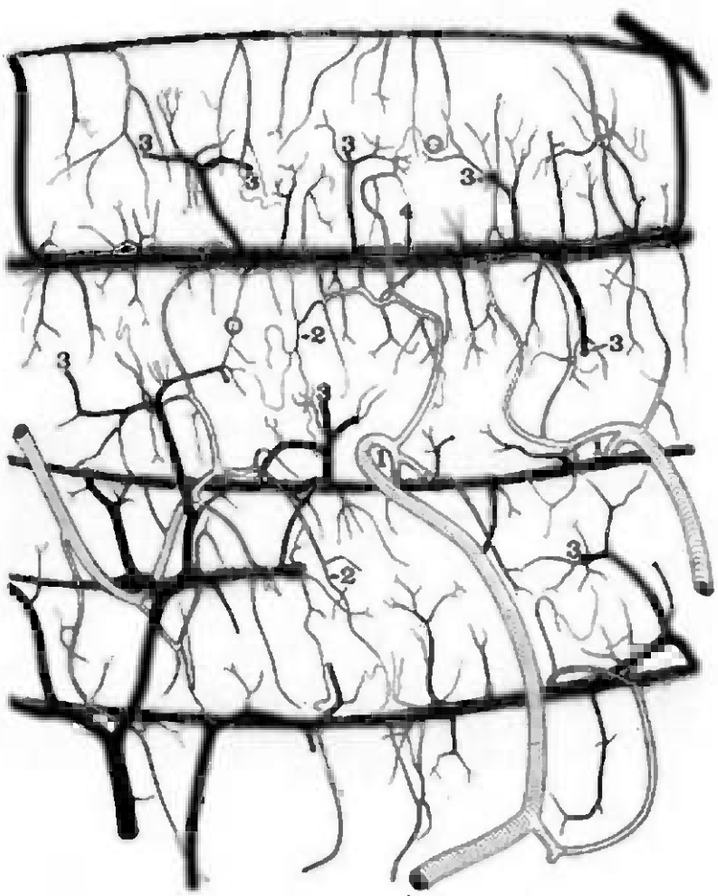

B

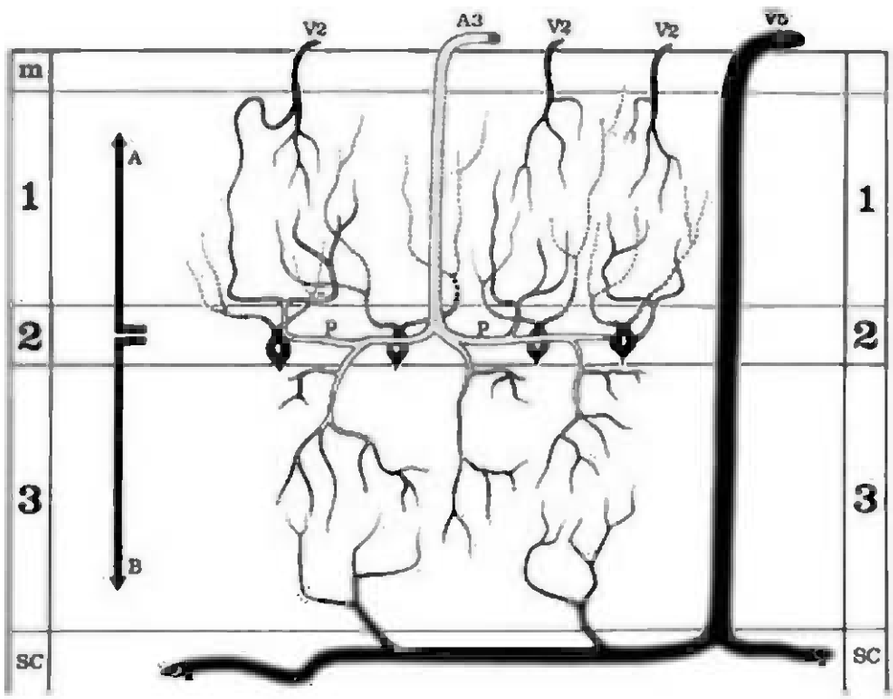

Fig. 4.6. The major components of cortical blood flow. Diagram.

1–3. There are three vascular layers of the cerebellar cortex:
1. Superficial, 2. Middle and 3. Deep
In the superficial circulation, the main arterial supply is provided by the recurrent branches of parallel arteries (P). The main venous drainage is provided by short V2 veins.
In the deep circulation, the main arterial supply is provided by branches of parallel arteries (P). The main venous drainage is provided by long V5 principal veins.

m Marginal zone
sc Subcortical white matter

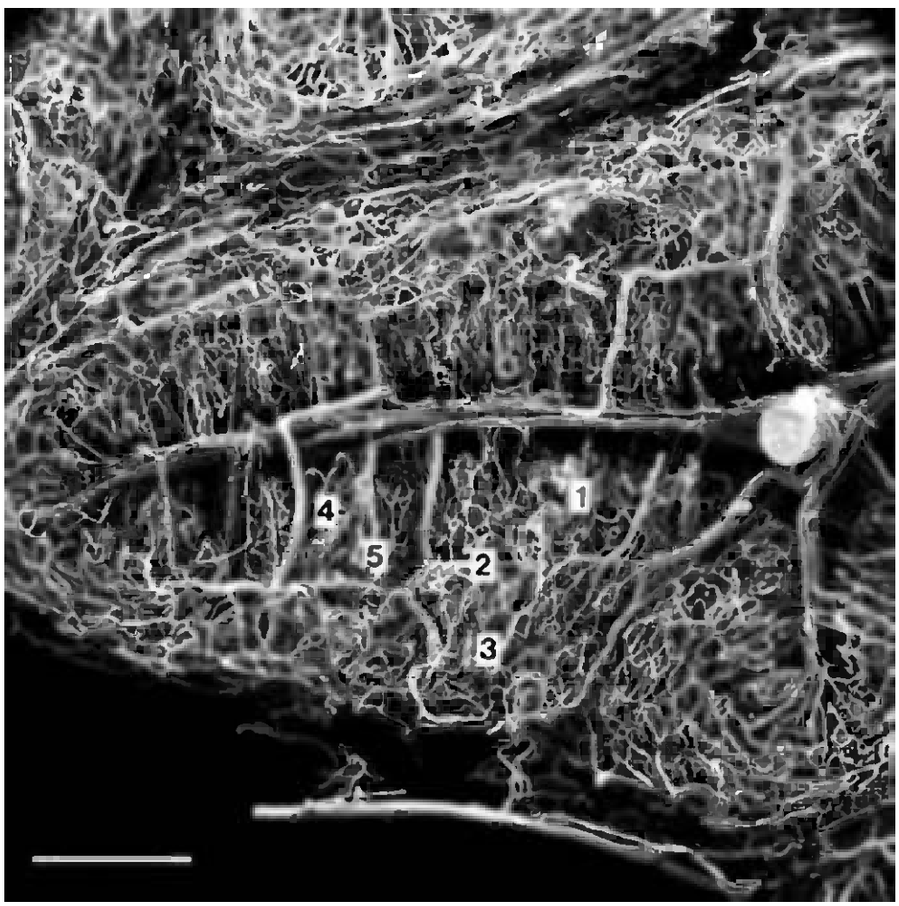

Fig. 4.7. The arterial organization of the cerebellar cortex. Section through a secondary fold of a folium. Intravascular injection of resin (Mercox) and scanning electron microscopy. Bar: 500 μm.

1–3 The molecular (1), Purkinje cell (2), and granular (3) layers show different densities of vascular networks.

4–5 In the Purkinje cell layer, the arterioles run parallel to the cerebellar surface (parallel arteries) (5) and give rise to a prominenent arterial arborization (4).

For more information about the vascularization of the cerebellar cortex, see [128].

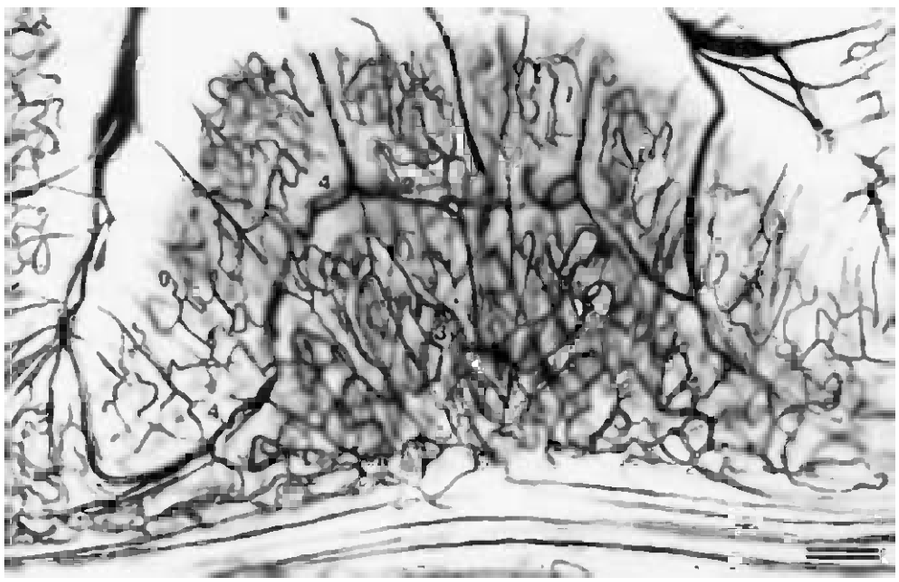

A

Fig. 4.8 (A–B). The arterial organization of the cortex.
Transverse section across the folium. Intravascular India ink injections.

A. **At the convexity.** Bar: 150 μm.

1 Superficial intracortical vascular layer within the molecular layer.

2 Middle vascular layer with ramifications of parallel arteries surrounded by a capillary-free space.

3 Deep vascular layer within the granular layer. This layer is thicker along the convexity of the folium than in the depths of the fissure. Note the vascular density in the granular layer and the special arrangement of the Purkinje cell layer arteries (4).

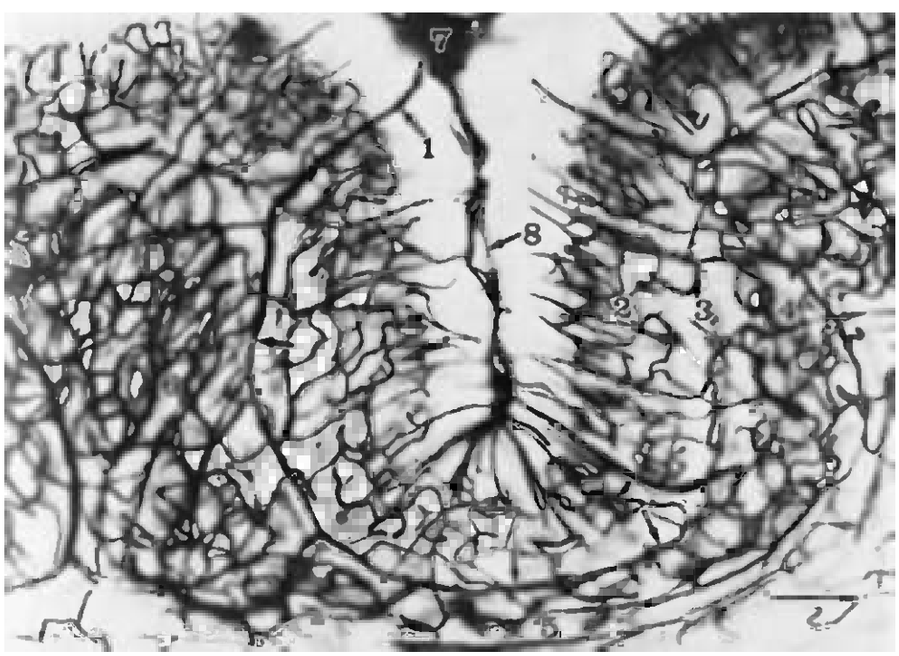

B

B. Within the depth of a furrow. Bar: 160 µm.

1 Middle A3 artery. The parallel artery (arrow) can be traced for a substantial distance under the fissure (arrows).

2 Superficial intracortical vascular layer in the molecular layer.

3 Middle vascular layer with branches of parallel arteries. Because there are few capillaries in this layer, it appears "clearer" than the adjoining superficial and deep vascular layers.

4-6 At the bottom of the sulcus, the granular layer is extremely thin (5). Along the convexity, this layer is particularly thick (6).

7 Pial venous arch.

8 Pial vascular layer in the furrow.

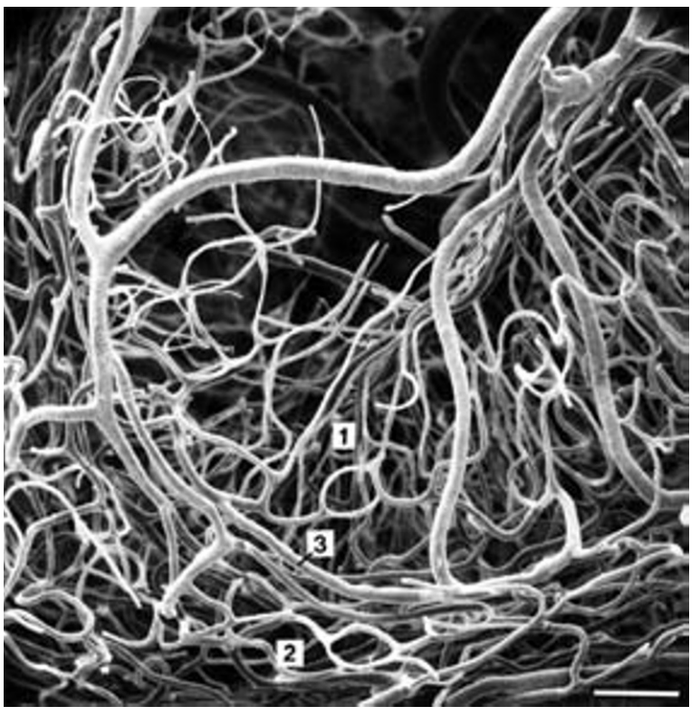

4.9

Fig. 4.9. Cortical arterial organization at the depth of a fissure. Intravascular resin injection (Mercox) and scanning electron microscopy. Bar: 100 µm.

1 Molecular layer
2 Granular layer
3 Middle A3 arteries of the Purkinje cell layer, which follow the curve of the fissure. Note the radial aspect of the trunks of the middle arteries and the arch-like appearance of the parallel arteries.

→

Fig. 4.10 (A–B). The pial vascular lamina within a fissure.

A. Scanning electron microscopy. Intravascular injection of resin (Mercox). Bar: 440 µm.

B. Corresponding diagram with the bottom of the furrow on the right.

1 Principal venous arch.
2 Secondary venous arch.

The deep pial arteries and veins are grouped into several bundles (1) separated by poorly vascularized areas.

A

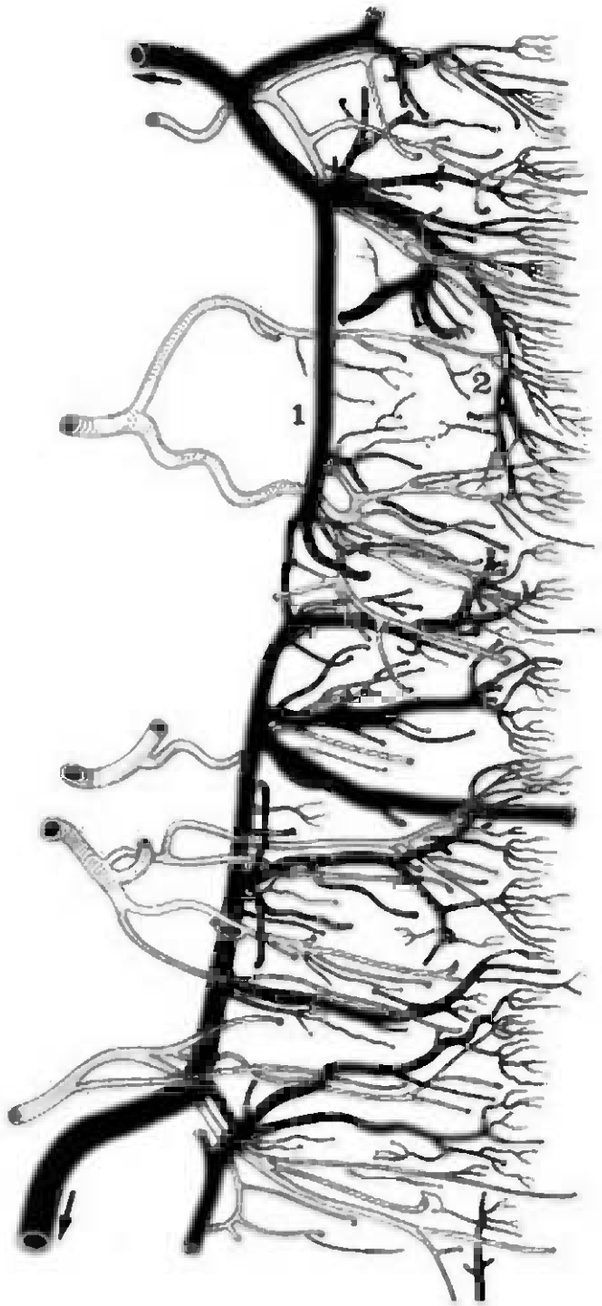

B

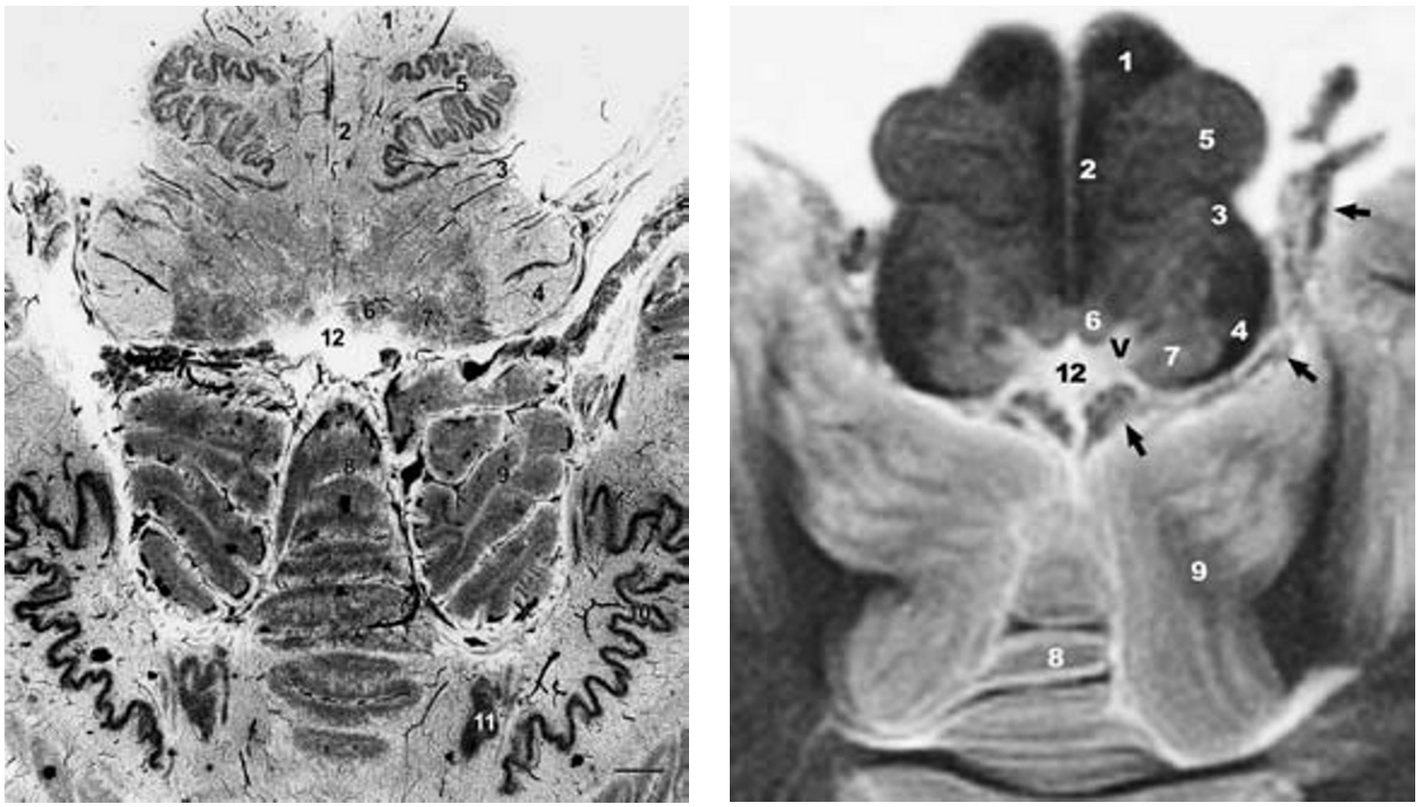

A B

Fig 4.11 (A–B). Cerebellar architecture.

A. Overview. Intravascular India ink injection. Bar: 2 mm.

B. Corresponding axial 3 Tesla MRI of a formalin-fixed human specimen. The deep cerebellar nuclei are shown in Fig. 4.12.

Medulla

White matter

1 Corticospinal tract
2 Medial lemniscus
3 Spinothalamic tract
4 Inferior cerebellar peduncle

Gray matter

5 Inferior olivary nucleus
6 Hypoglossal nucleus (CN XII)
7 Vestibular nuclei (CN VIII)
V Dorsal motor nucleus of the vagus (CN X)

Cerebellum

Cerebellar cortex

8 Vermis
9 Tonsil

Deep nuclei and ventricle

10 Dentate nucleus
11 Emboliform nucleus
12 Fourth ventricle

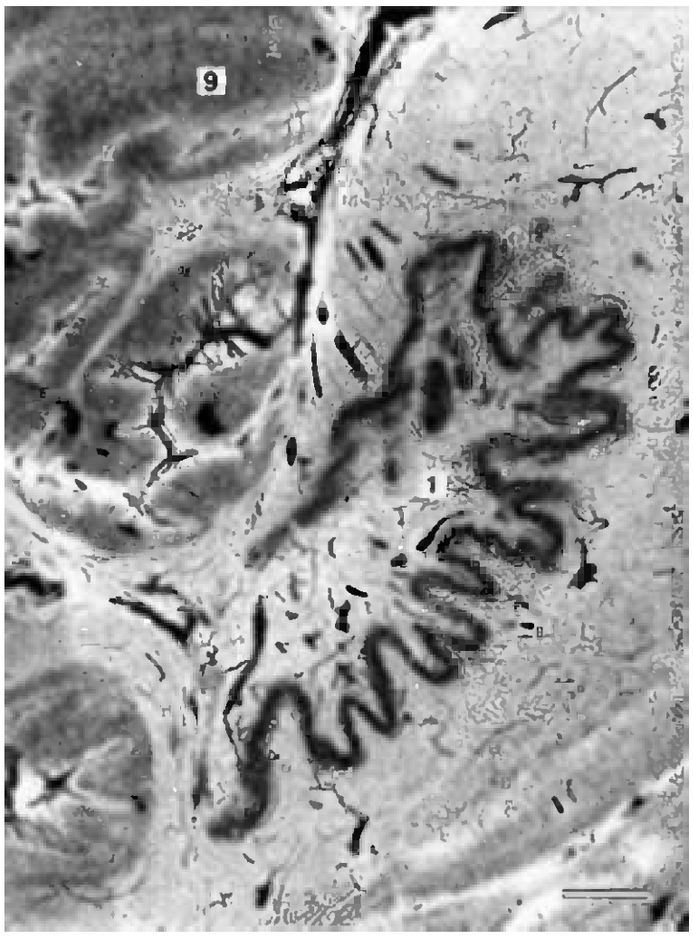

A

B

Structure of the deep cerebellar nuclei

The deep cerebellar nuclei are divided into three cellular groups:

Fastigial nucleus
Nucleus interpositus (composed of the globose and emboliform nuclei) and the
Dentate nucleus

Fig. 4.12 (A–F). The deep cerebellar nuclei. Transverse sections of the cerebellum

A–D. Intravascular India ink injections: Sequential levels from most caudal **(A)** to most cranial **(D)** Bar: 2 mm.
E–F. Matching MR Microscopy at 9.4 Tesla

1 Dentate nucleus
2 Emboliform nucleus
3 Globose nucleus
4 Fastigial nucleus
5 Nodulus
6 Fourth ventricle, including the posterior superior recesses (6′)
7 Corpus medullare (central white matter) of the cerebellar hemisphere
8 Vermis
9 Tonsil (in A.)

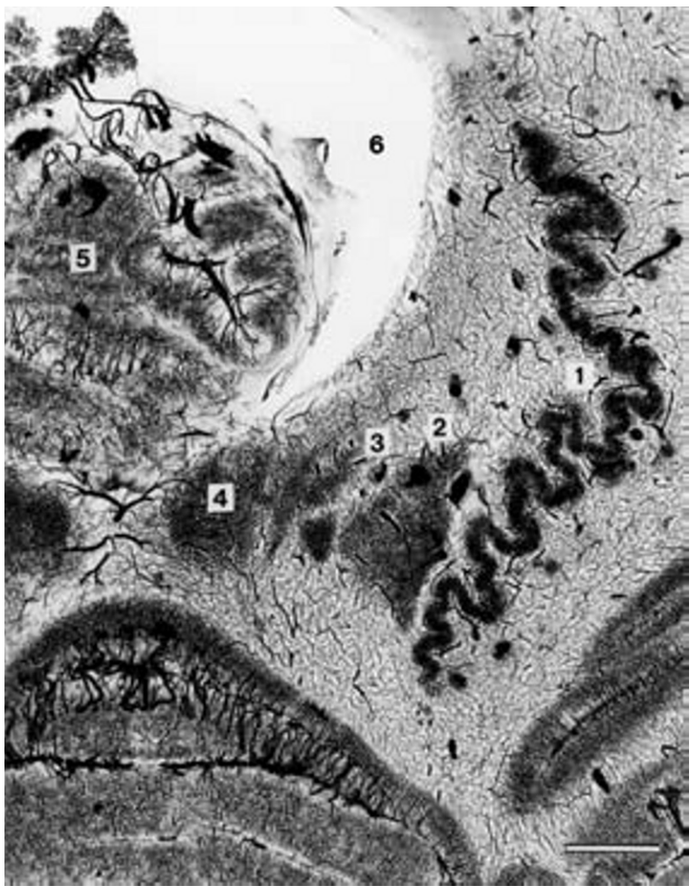

C

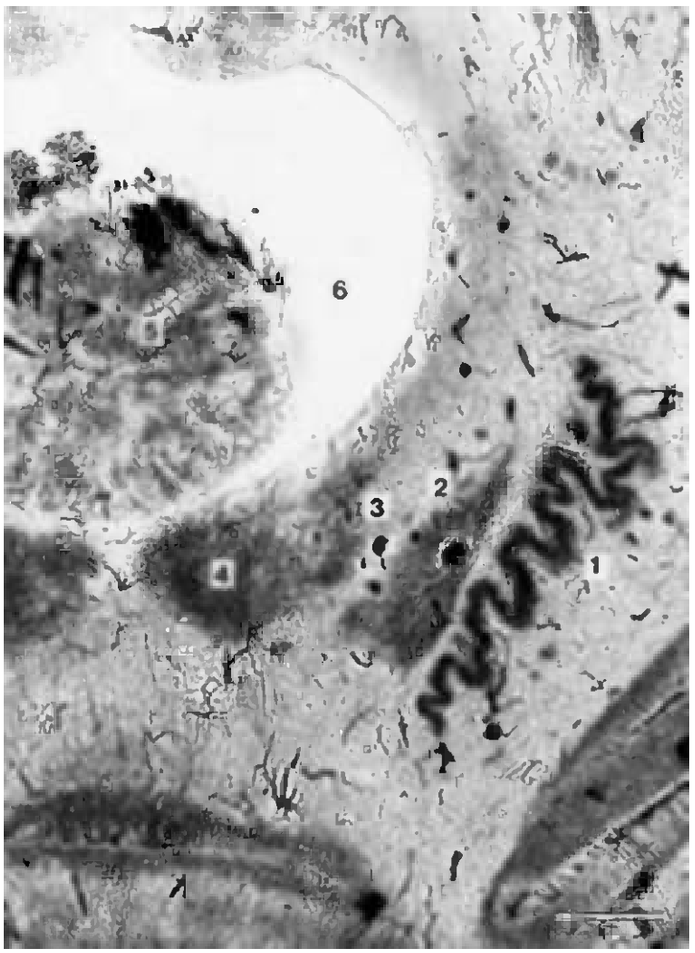

D

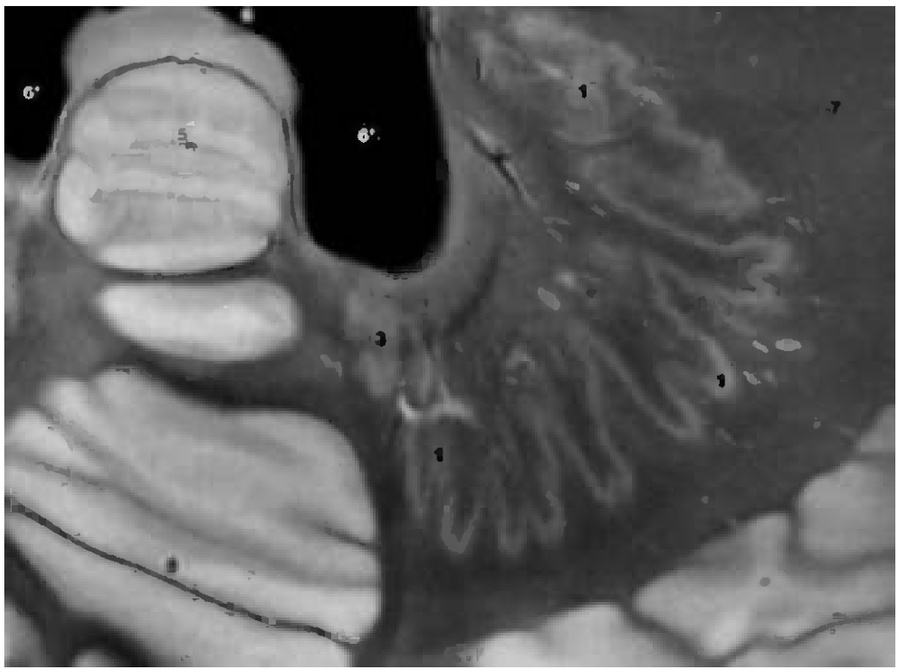

E

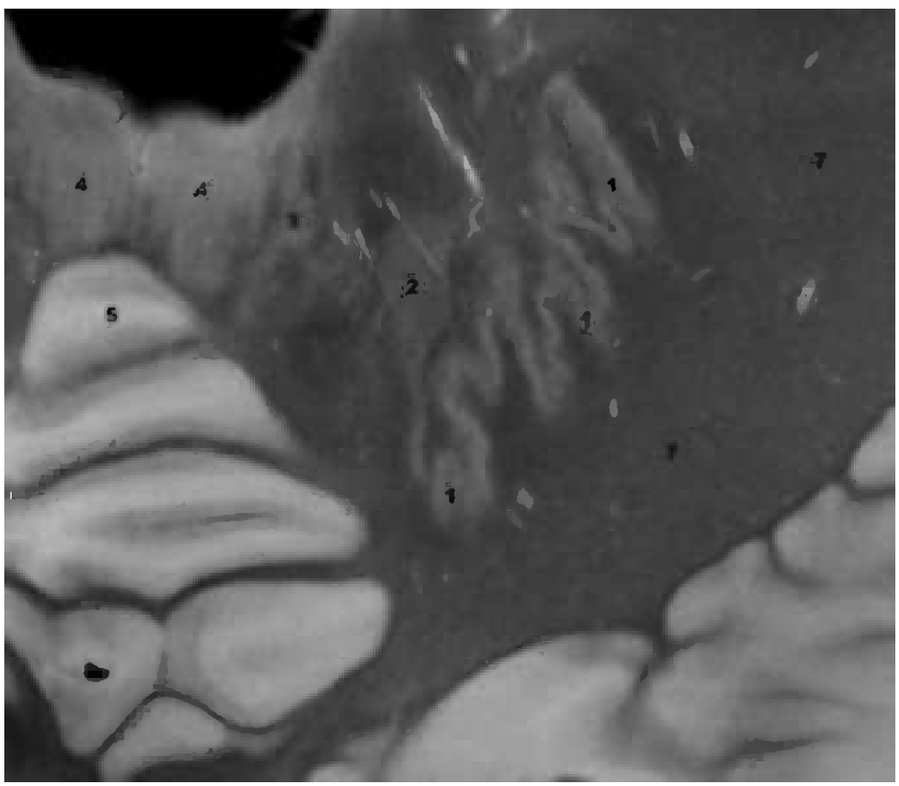

F

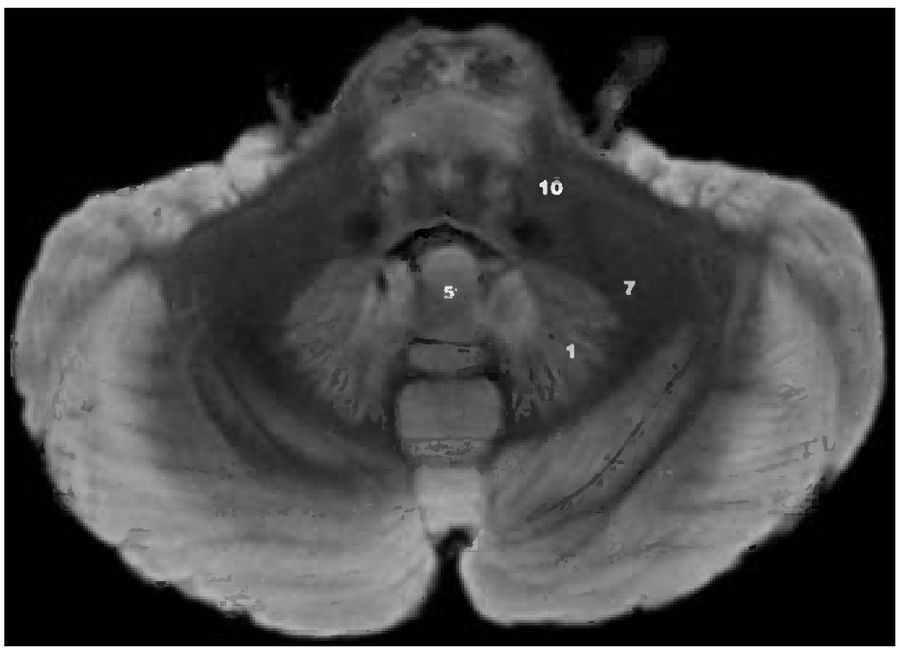

A

Fig. 4.13 (A–C). 3 Tesla Specimen MRI.
Formalin-fixed human cadaver specimen sectioned in the **A.** Axial, **B.** Coronal and **C.** Sagittal planes.
See Fig. 11.14A for the comparable axial gross anatomic section.

1 Dentate nucleus
2 Interposed nucleus (nucleus interpositus)
4 Fastigial nucleus
5 Nodulus
7 Corpus medullare of the cerebellar hemisphere
9 Tonsil
10 Middle cerebellar peduncle (brachium pontis)
11 Superior cerebellar peduncle (brachium conjunctivum)
12 Medulla
13 Pons

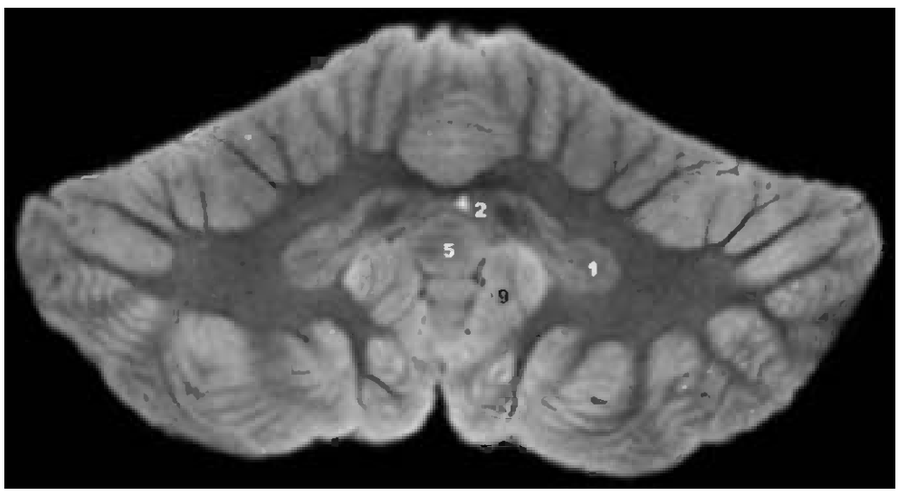

B

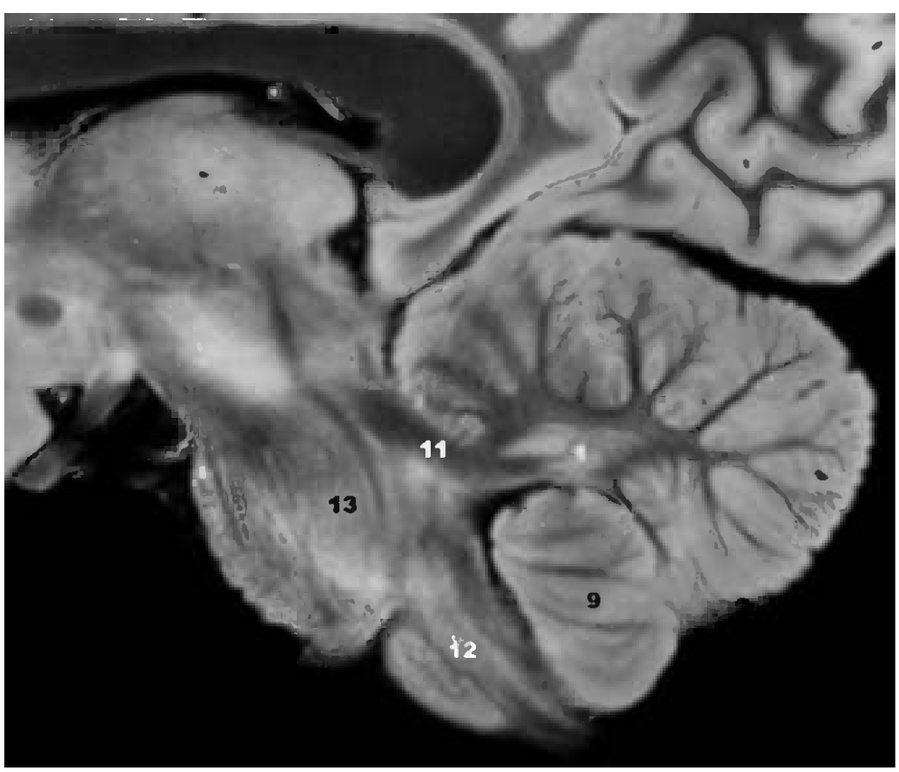

C

B. Functions of the cerebellum

Figures 4.14 through 4.19 presents an overview of the general functional organization of the cortex and deep nuclei (Fig. 4.14) with a description of the functions of the cerebellum. These can be divided between the well known motor and the emerging cognitive functions. See [6, 20, 48, 53, 78, 111, 132, 161, 170, 176, 213, 215, 216, 227, 263, 280, 281, 305, 322, 323, 347, 382a, 382b, 383, 383a, 430a, 455, 458].

General functional organization of the cerebellar cortex and deep nuclei.
Figure 4.14 summarizes the cerebellar circuits, and indicates the excitatory and inhibitory functions of the different neurons.

Deep nuclei (fastigial, globose, emboliform, and dentate nuclei)
The deep nuclei (1), together with parts of the lateral vestibular nucleus, are the only outputs of the cerebellum. Via their axons (1′), they reach the brain and brain stem centers such as the thalamus, red nucleus, and vestibular nuclei.

The cerebellar cortex
The principal neurons of the cerebellar cortex are the Purkinje cells (2). They control the deep nuclei through inhibitory GABAergic fibers (2′). Their dendritic tree (2″) is oriented perpendicular to the axis of the folium. Purkinje cells have numerous synaptic contacts in the molecular layer, particularly with the axons of granule cells whose perikaryons are in the granular layer (3). The granule cell axons ascend to the Purkinje cell dendritic layer and then bifurcate into a T-shape to form parallel fibers (3′) oriented parallel to the folium axis. These fibers pass through, and make excitatory synaptic contact on, the dendritic trees of hundreds of Pukinje cells.

Inputs to the cerebellum
Both the cerebellar cortex and the deep nuclei receive two types of afferent fibers: mossy fibers and climbing fibers.

Mossy fibers
The mossy fibers (4) have excitatory synaptic inputs at two targets: the deep cerebellar nuclei (4′) and the granule cells. In the cerebellar cortex, the endings of the mossy fibers come together with the dendritic tree of granule cells (3) and axonal arborizations of Golgi cells (14) to form the cerebellar glomerulus (5).
The mossy fibers have numerous origins:
The dorsal spinocerebellar tract (6) transmits proprioceptive impulses to the cerebellum from the lowest portion of the body. (The function of the ventral spinocerebellar tract is less well understood, so it is not shown on this diagram.)
The cuneocerebellar tract (7), arising from the lateral cuneate nucleus, transmits proprioceptive information from the upper portion of the body.
The nucleus reticularis lateralis (8) links the reticular formation to the cerebellum.
The trigeminocerebellar fibers (9), arising from the pars oralis and pars interpolaris of the spinal trigeminal nucleus, provide the cerebellum with sensory information from the face.
The vestibular fibers (10) arise from the membranous labyrinth.
The pontocerebellar fibers (11), the most numerous cerebellar input, arise from both the contralateral pontine nuclei (11′) (about 2/3) and the ipsilateral pontine nuclei (about 1/3). These nuclei receive the voluminous corticopontine tracts from all lobes of the cerebrum (11″).

Climbing fibers
The climbing fibers (12) arise from the contralateral inferior olivary nucleus (12′) as olivocerebellar fibers. Each climbing fiber reaches the deep nuclei (13) and the dendritic tree of only a few Purkinje cells (13′). Importantly, each Purkinje cell receives input from only a single climbing fiber, though each climbing fibre makes multiple, excitatory contacts with the Purkinje cell.

The cerebellar cortex also has numerous interneurons, Golgi (14), stellate (15), and basket (16) cells, all of which are inhibitory, regulating the Purkinje and granular cell functions.

Fig. 4.14. General functional organization of the cerebellar cortex and deep nuclei. + and –, respectively, indicate the excitatory and inhibitory functions of the different neurons

1 Deep nuclei
1′ Efferent fibers from the deep nuclei
2 Purkinje cell
2′ Efferent fibers from the Purkinje cell
2″ Dendritic tree of the Purkinje cell
3 Granule cell
3′ Parallel fibers
4 Mossy fibers
4′ Endings of the mossy fibers on the deep cerebellar nuclei
5 Cerebellar glomerulus
6 Dorsal spinocerebellar tract
7 Cuneocerebellar tract
8 Fibers arising from the nucleus reticularis lateralis
9 Trigeminocerebellar fibers
10 Vestibulocerebellar fibers
11 Pontocerebellar fibers
11′ Pontine nuclei
11″ Corticopontine tracts
12 Climbing fibers
12′ Inferior olivary nucleus
13 Endings of the climbing fibers on the deep nuclei
13′ Endings of the climbing fibers on the dendritic tree of the Purkinje cells
14 Golgi cell
15 Stellate cell
16 Basket cell

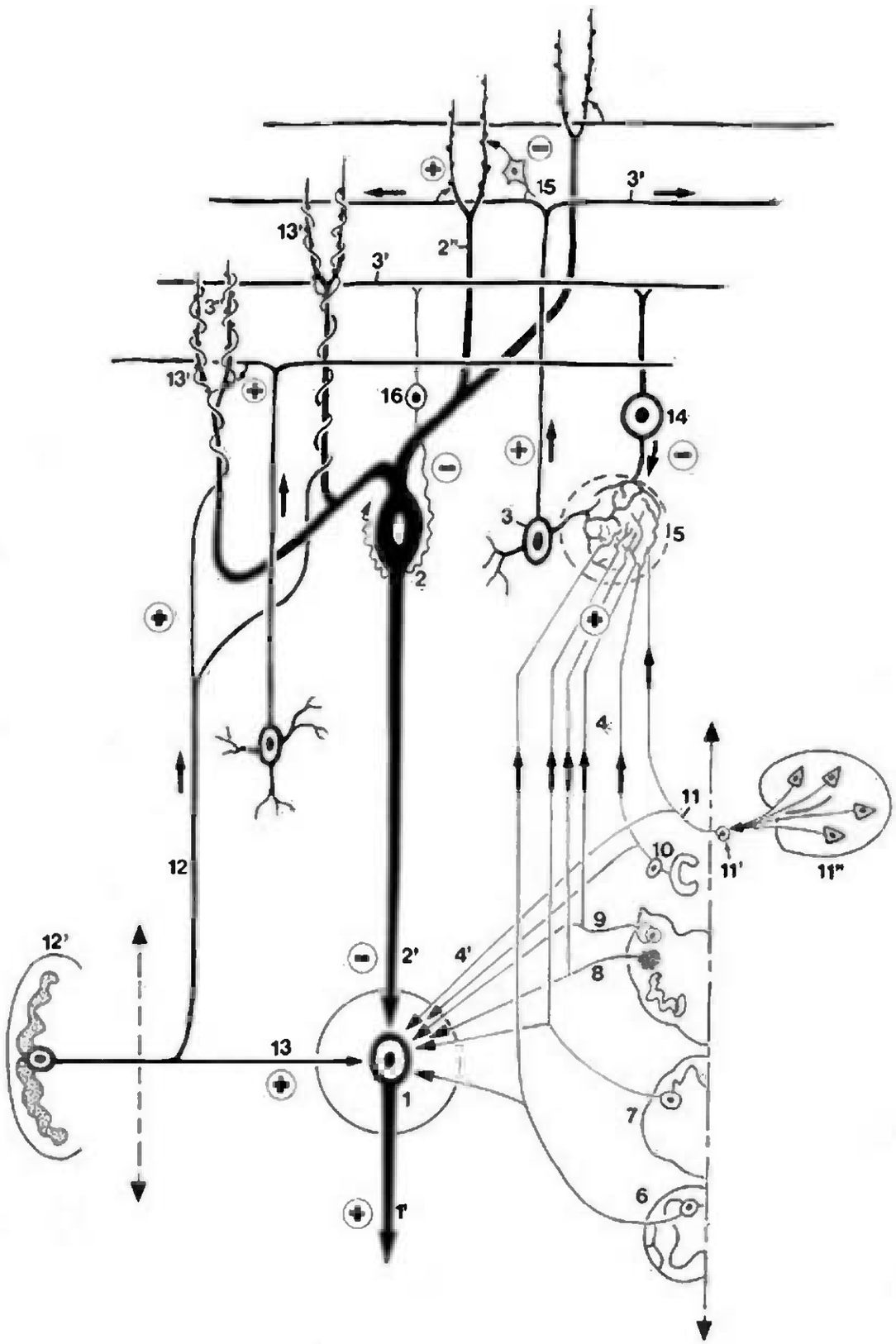
15
3'
13'
2"
3'
3'
13'
16
14
3
5
2
4
11
10
11'
11"
12
9
12'
2'
4'
8
13
1
7
6
1'

Functional divisions of the cerebellum

Although the anatomical divisions of the cerebellum are organized vertically into anterior, posterior, and flocculonodular lobes, the functional divisions are organized transversely into median, intermediate and lateral longitudinal zones (**Fig. 4.15**). Each median, intermediate and lateral zone of the cerebellar cortex relates to the corresponding median-, intermediate- and laterally-situated deep nucleus.

The median cerebellum. The median cerebellum (1) comprises the cortex of the vermis and flocculonodular lobe. The corresponding deep nuclei are the fastigial nuclei (1′) and the vestibular nuclei (which in many ways function as deep cerebellar nuclei). The median cerebellum is the oldest portion of the cerebellum in evolutionary terms, and is called the paleocerebellum.

The intermediate cerebellum. The intermediate cerebellum (2) comprises the most medial portion of the cerebellar hemispheric cortex. It is associated with the globose (2″) and emboliform (2′) nuclei, which are often grouped together as the nucleus interpositus (globose plus emboliform nuclei).

The lateral cerebellum. The lateral cerebellum (3) comprises the major portion of the cerebellar hemispheric cortex, and is highly developed in man. It relates to the dentate nucleus (3′), the largest, most laterally positioned, and newest of the deep cerebellar nuclei.

The intermediate and lateral cerebellum are functionally linked as the neocerebellum.

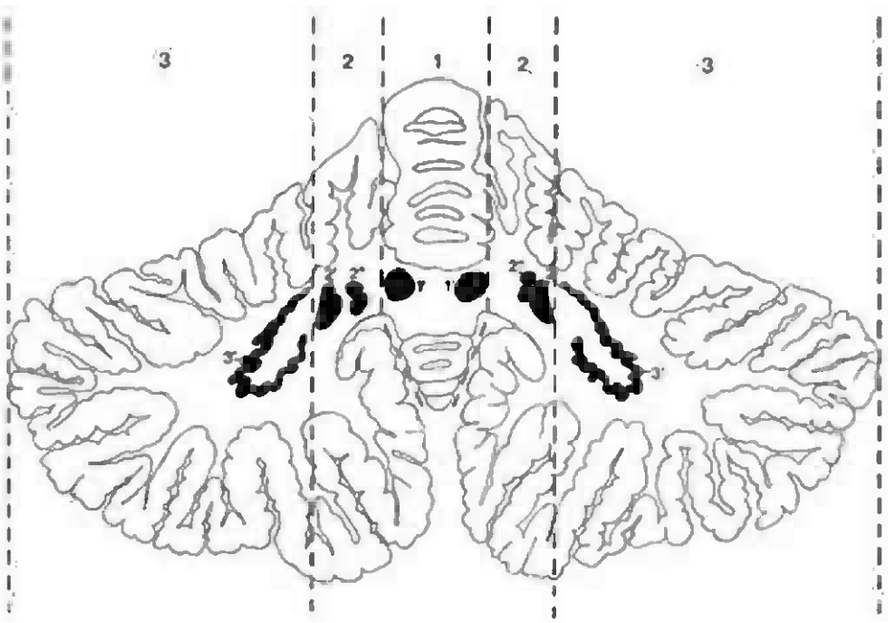

Fig. 4.15. Frontal section of the cerebellum

1 Median cerebellum
1′ Fastigial nucleus
2 Intermediate cerebellum
2′ Emboliform nucleus
2″ Globose nucleus
3 Lateral cerebellum
3′ Dentate nucleus

Motor functions of the cerebellum

Functions of the median cerebellum (paleocerebellum)
(See Fig 4.16).

The median cerebellum controls equilibrium and conjugate eye movements.

Control circuits of equilibrium

The principal circuit: Vestibular fibers originating in the internal ear (membranous labyrinth) reach the brain stem in the vestibulocochlear nerve, and end mainly in the vestibular nuclei. In turn, the vestibular nuclei give rise to two pathways:
From the lateral vestibular nucleus, fibers descend as the lateral vestibulospinal tract to reach the spinal motoneurons. This pathway provides rapid control of posture by action on extensor (antigravity) muscles.
From the medial, superior, and inferior vestibular nuclei, fibers ascend through the medial longitudinal fasciculus to the cranial nerve nuclei and descend to the cervical spinal cord. This pathway helps to control head movements associated with maintenance of posture.
The regulatory circuit: The median cerebellum receives direct inputs from the internal ear. It controls the vestibulospinal tract through the fastigial and lateral vestibular nuclei.

Control of eye movements
The role of the cerebellum in the oculomotor system has been described on p. 98.
In brief, the flocculus controls the vestibulo-ocular and smooth-pursuit reflexes. The vermis (declive (VI), folium and tuber (VII)) regulates the saccades and, along with the flocculus, regulates smooth-pursuit eye movements.

Functions of the intermediate and lateral cerebellum (neocerebellum)
The principal functions of the neocerebellum are concerned with movement control. The intermediate cerebellum is involved in movement execution, whereas the lateral cerebellum is associated with movement planning.

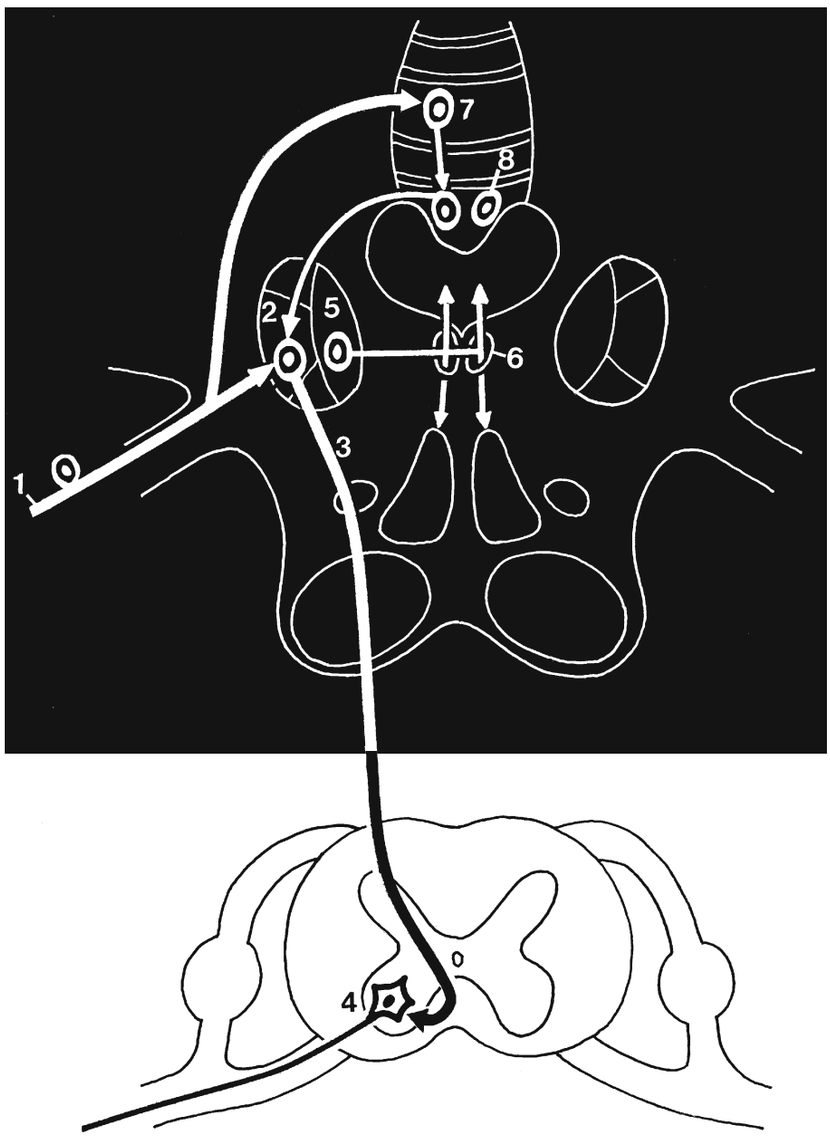

Fig. 4.16. Median cerebellum

1 Vestibular fibers originating in the inner ear
2 Lateral vestibular nucleus
3 Vestibulospinal tract
4 Spinal motoneurons
5 Medial vestibular nucleus
6 Medial longitudinal fasciculus

Control of this system by the:
7 Vermis, and
8 Fastigial nucleus

The intermediate cerebellum

The intermediate cerebellum (Fig 4.17) controls muscle contraction in distal portions of the body, particularly the distal limbs. (By contrast, the median cerebellum controls the muscles of the axial body parts.)
The intermediate cerebellum receives two kinds of information. It receives:

Cortical information through collaterals of the corticospinal tract and, in particular, the large corticopontocerebellar tracts. These fibers inform the cerebellum about intended movements.

Peripheral information through diverse tracts: The dorsal spinocerebellar, cuneocerebellar, and trigeminocerebellar tracts originate from the lowest to the highest parts of the body, respectively. These tracts inform the cerebellum about the execution of a movement. The ventral spinocerebellar tract, whose functions are disputed, appears to send information to the cerebellum on the level of cortical motor signals projecting to the anterior horns.
The intermediate cerebellum compares an intended movement with the actual movement and sends correction outputs to the thalamus, the motor cortex, and the magnocellular portion of the red nucleus.
During the course of a movement, the intermediate cerebellum first has an excitatory action on agonist muscles and an inhibitory one on antagonists. Toward the termination of movements, the intermediate cerebellum stimulates the antagonist muscles to bring the motion to a smooth halt. Thus, the intermediate cerebellum provides smooth and coordinated movements through its action on agonist and antagonist limb muscles.

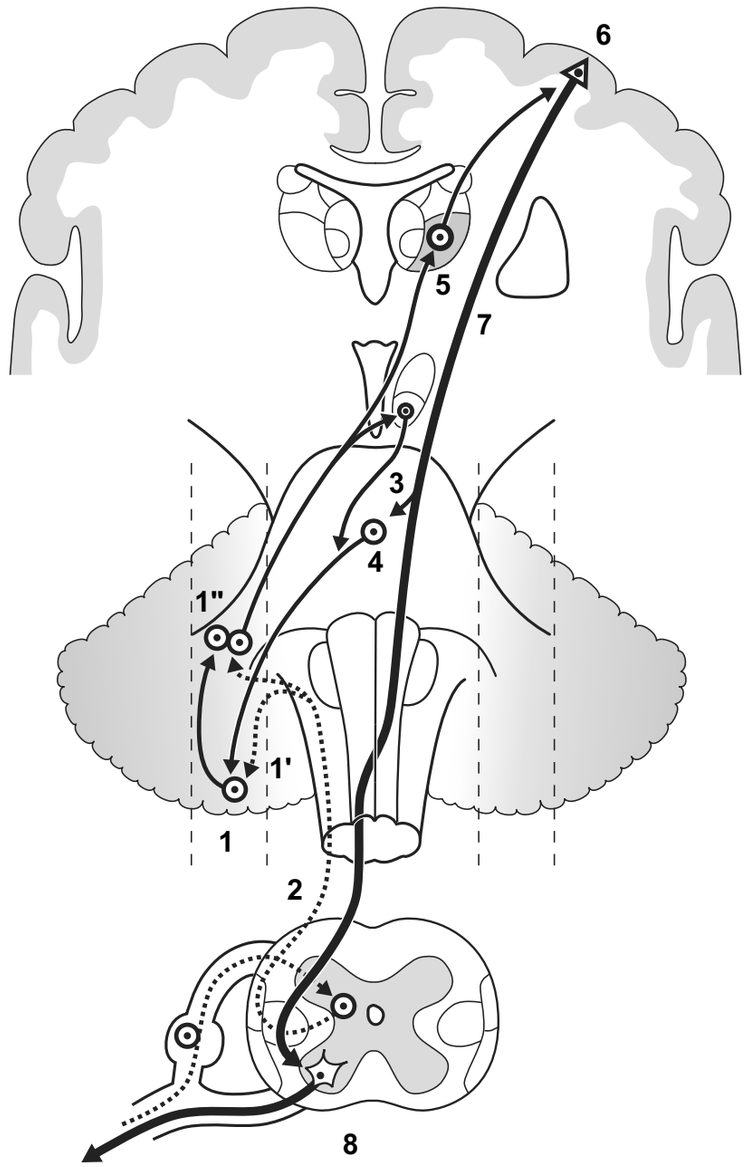

Fig. 4.17. Intermediate cerebellum

1 Intermediate cerebellum
1′ Cortex of the intermediate cerebellum
1″ Interposed nuclei (globose and emboliform nuclei)
2 Afferent fibers from the periphery and spinal cord (dorsal spinocerebellar tract)
3 Afferent fibers from the cortex
4 Pontine nuclei
5 Thalamus (ventral lateral and ventral anterior nuclei)
6 Motor cortex
7 Corticospinal tract
8 Spinal motoneurons

The lateral cerebellum

The lateral cerebellum (Fig 4.18) receives cortical information from the premotor and associative cortical areas by way of the corticopontocerebellar tracts. Its outputs are towards the thalamus and then the motor cortex. Unlike the intermediate cerebellum (which receives both peripheral and cortical inputs), the lateral cerebellum receives only cortical information.
The lateral cerebellum is involved in movement planning. In particular, it prepares the next movement during the course of the present movement, and so permits a smooth and coordinated progression from one movement to the next.

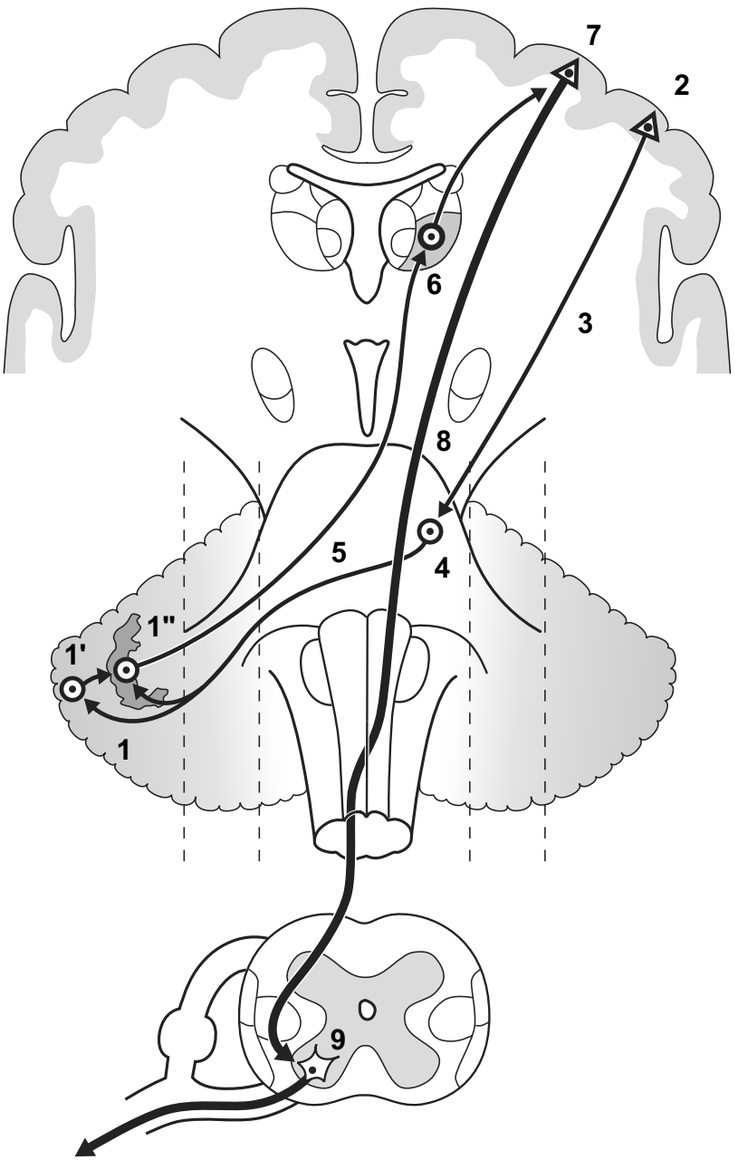

Fig. 4.18. Lateral cerebellum

1 Lateral cerebellum
1′ Lateral cerebellar cortex
1″ Dentate nucleus
2 Premotor cortex
3 Corticopontine fibers
4 Pontine nuclei
5 Pontocerebellar fibers
6 Thalamus (ventral lateral and ventral anterior nuclei)
7 Motor cortex
8 Corticospinal tract
9 Spinal motoneurons

The role of the inferior olivary nucleus on the control of cerebellar functions

The inferior olivary nucleus receives cortical fibers, which have frequent intermediate synapses in the red nucleus (parvocellular portion). These descending fibers are mainly situated within the central tegmental tract. The inferior olivary nucleus also receives peripheral ascending fibers by way of the spino-olivary tract.

Thus, the olivary nucleus (as well as the intermediate cerebellum) compares the intended movement to its results and sends correction signals to the cerebellum through climbing fibers. The climbing fibers can produce long-lasting changes in the circuitry of the cerebellar cortex, especially in the synapses between dendritic trees of Purkinje cells and parallel fibers. Thus, the inferior olivary nucleus can play an important role in motor learning (**Fig. 4.19**).

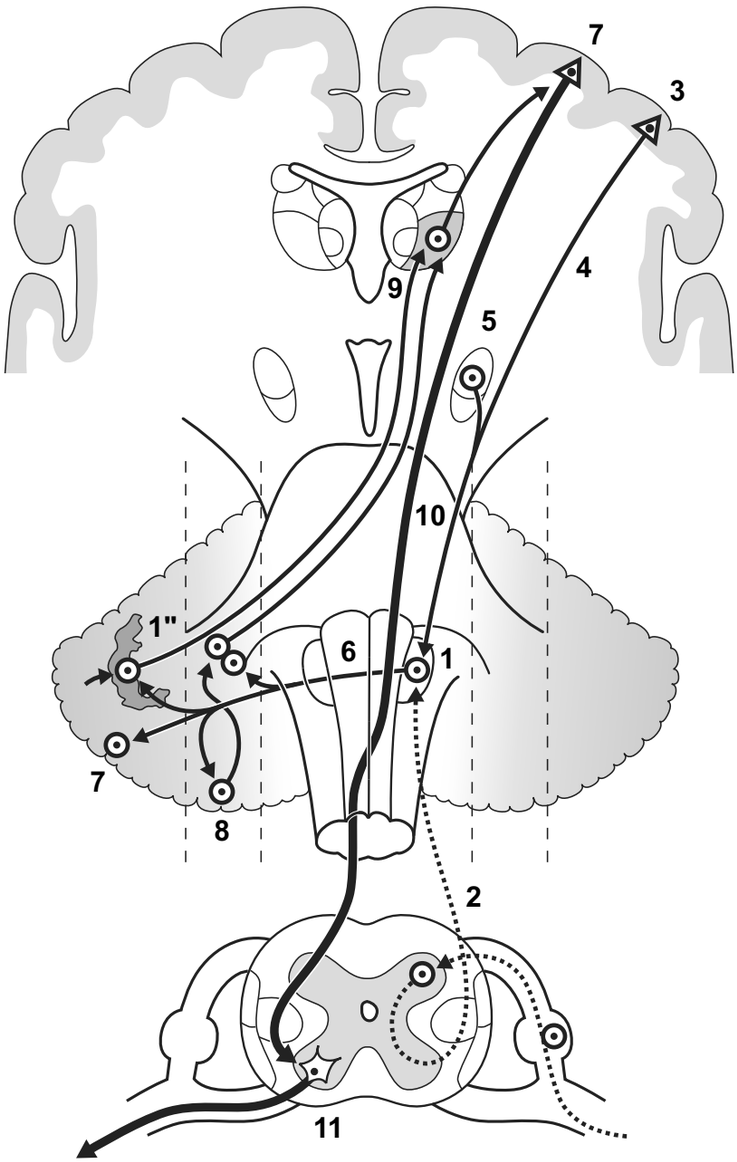

Fig. 4.19. Role of the inferior olivary nucleus in the control of movements and correction of errors.

1 Inferior olivary nucleus
2 Peripheral information to the inferior olive through the spino-olivary tract
3 Central information from the premotor cortex to the inferior olive through the cortico-olivary fibers
4 Cortico-olivary fibers
5 Red nucleus
6 Control of the cerebellum by the inferior olive through the climbing fibers
7 Lateral cerebellum
8 Intermediate cerebellum. The lateral (7) and intermediate (8) cerebellum act together to control the motor cortex via the thalamus (9)
9 Thalamus (ventral lateral and ventral anterior nuclei)
10 Corticospinal tract
11 Spinal motoneurons

The cognitive and affective cerebellum

Increasing evidence now links the cerebellum with cognitive and affective brain function, in addition to the familiar motor control functions [382b]. Anatomical and physiological studies of the cerebellum demonstrate a primary sensorimotor region within the anterior lobe and a secondary sensorimotor region within the medial aspect of the posterior lobe [382b]. A cognitive region has now been shown to lie within the lateral hemispheric portion of the posterior lobe and an affective region in the medial (vermal) portion of the posterior lobe of the cerebellum. Cerebral association areas in the frontal, prefrontal, cingulate and posterior parietal cortices are linked to the cerebellum. Feedforward loops relay to the posterior lobe via nuclei in the basis pontis, and feedback loops return from the deep cerebellar nuclei (dentate and interpositus) through the thalamus to the cerebral association cortices [382b]. These loops, and reciprocal connections between the cerebellum and the hypothalamus, integrate the cerebellum into distributed neural circuits that help modulate intellect, emotion, autonomic function and sensorimotor control. It is postulated that the cerebellum functions by performing a "universal cerebellar transform," in which the parallel fibers of the cerebellar cortex combine stimulus with response to create a stimulus-response linkage [430a]. That linkage then serves to optimize all cognitive, emotional and sensorimotor activities around a homeostatic baseline through trial and error learning, according to context [289a, 382a, 382b, 383, 430a].

Lesions confined to the posterior cerebellum may manifest as the cerebellar cognitive affective syndrome (CCAS) [382b]. When such lesions affect the lateral hemispheric portion of the posterior lobe, the CCAS is characterized by impairments in executive function (planning, set shifting, verbal fluency, abstract reasoning, working memory), spatial cognition (visual spatial organization and memory), and linguistic processing (agrammatism and dysprodia) [382b]. When such lesions encroach on the limbic cerebellum (vermis and fastigial nucleus), the CCAS includes dysregulation of affect [382b, 383a].

SECTION V

STRUCTURAL ORGANIZATION OF THE MESENCEPHALIC-DIENCEPHALIC JUNCTION

The upper mesencephalon expands and transitions into the paired bilateral structures of the diencephalon. The posterior commissure marks the caudal border of the diencephalon and the junction of the mesencephalon with the diencephalon [78]. The diencephalic structures include the epithalamus, thalamus, hypothalamus, subthalamus and metathalamus. The epithalamus consists of the pineal gland, habenular nuclei and commissure, striae medullares thalami, and the habenulo-interpeduncular tract.

The thalami are paired ovoid masses of gray matter containing numerous individual nuclei partially separated by medullary laminae. Generally, the thalami extend from the interventricular foramina anteriorly to the posterior commissure posteriorly and from the walls of the third ventricle medially to the inner aspects of the posterior limbs of the internal capsules laterally. The internal medullary laminae separate the medial thalamic nuclei from the lateral thalamic nuclei, and themselves split to surround the intercalated intralaminar thalamic nuclei.

Inferiorly, the paired hypothalamic sulci (sulci limitantes) delimit the thalami dorsally from the hypothalamus ventrally. The hypothalamus extends from the region of the optic chiasm anteriorly to the caudal border of the mammillary bodies posteriorly [78]. It includes multiple individual nuclei broadly divided into medal and lateral subgroups by arbitrary sagittal planes drawn through the anterior columns of the fornices.

The subthalamus is a transition zone, bounded by the thalamus above, the hypothalamus medially and the internal capsule laterally [78]. It contains the large subthalamic nucleus.

The metathalamus is composed of the medial and lateral geniculate bodies, situated anterolateral to the pulvinar of the thalamus and posterolateral to the subthalamus.

Fig. 5.1. Mid-sagittal section of the mesencephalic-diencephalic junction. Overview. Bar: 10 mm.

1 Floor of fourth ventricle
2 Roof of fourth ventricle (fastigial sulcus) situated between the superior and inferior medullary vela
3 Medulla
4 Pons
5 Mesencephalon
6 Cerebellum (vermis)
7 Nodulus
8 Central canal
9 Cerebral aqueduct (of Sylvius)
10 Posterior commissure
11 Pineal gland
12 Anterior commissure
13 Third ventricle
14 Fornix
15 Corpus callosum

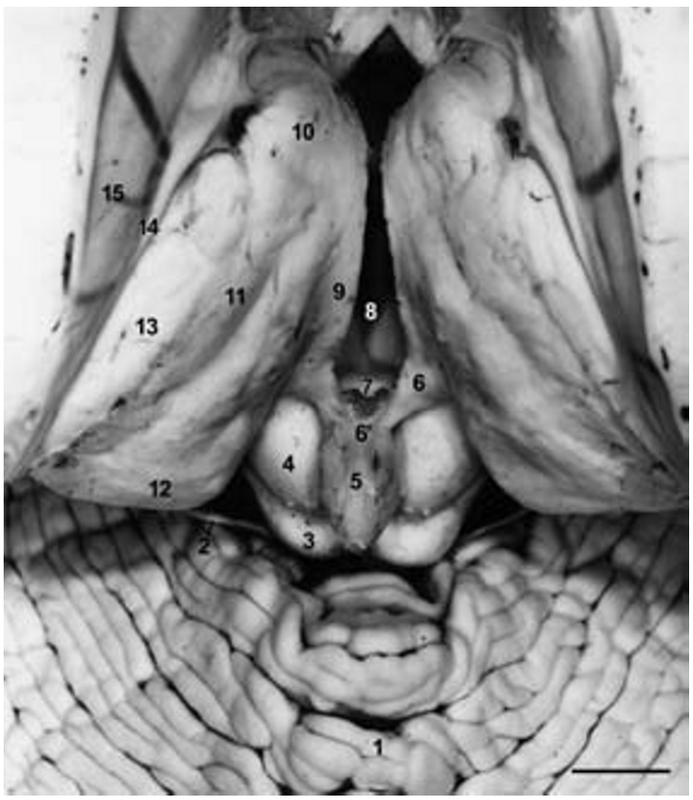

Fig. 5.2. The relationship of the brain stem and cerebellum to the brain. Posterior-superior view of the mesencephalic-diencephalic junction. The corpus callosum, choroid plexus of the third ventricle, and blood vessels have been removed.
Bar: 3.6 mm.

Cerebellum
1 Culmen of vermis

Mesencephalon
2 Trochlear nerve (CN IV)
3 Inferior colliculus
4 Superior colliculus

Diencephalon
5 Pineal gland
6 Habenular trigone (medial and lateral habenular nuclei)
6′ Habenular commissure
7 Posterior commissure
8 Third ventricle
9 Stria medullaris thalami coursing between the septal region and the habenular trigone along the lateral edge of the roof of the third ventricle, where the roof inserts into the medial aspects of the two thalami
10 Anterior nucleus of thalamus
11 Lateral thalamic nuclei
12 Pulvinar
13 Lamina affixa
14 Striothalamic sulcus with the stria teminalis
15 Caudate nucleus

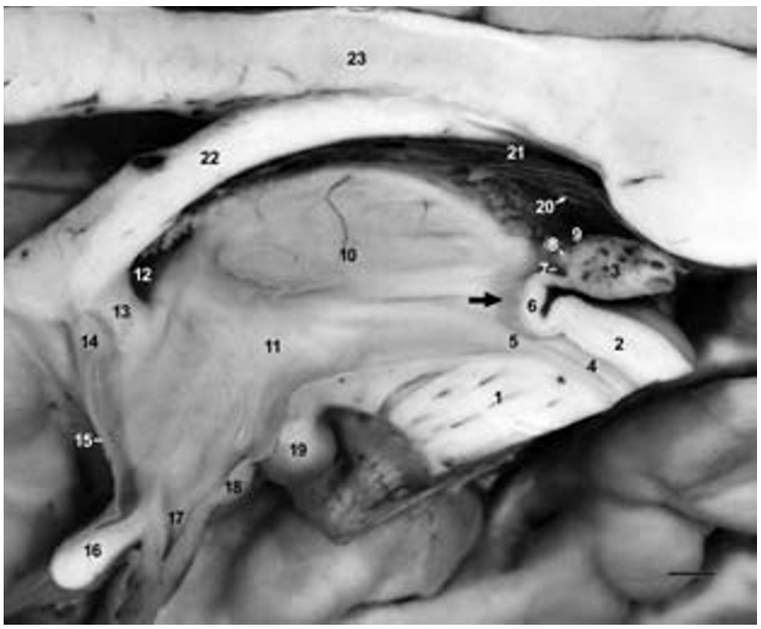

A

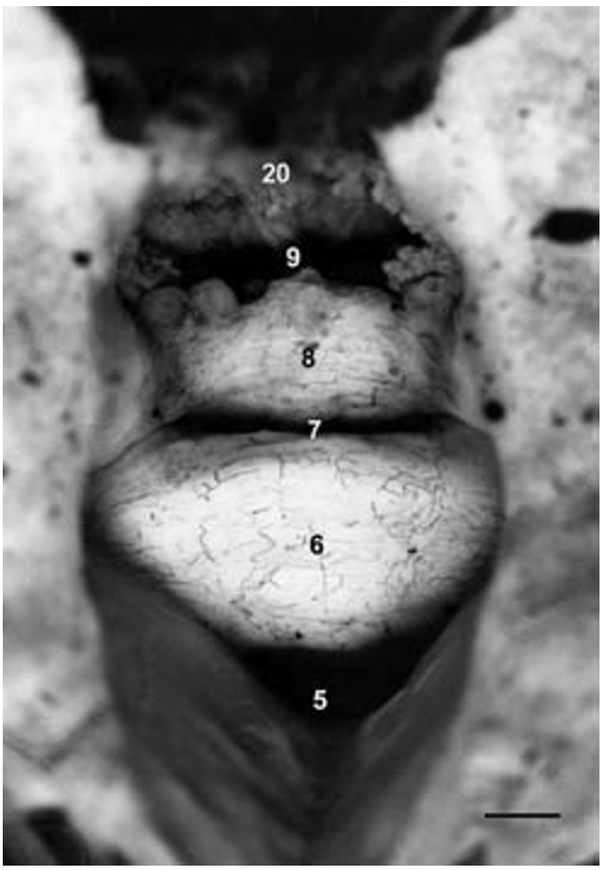

B

Fig. 5.3 (A–B). The relationships of the brain stem to the third ventricle.

A. Mid-sagittal section of the third ventricle. Bar: 3.3 mm**.**

B. Endoventricular view of the posterior wall of the third ventricle as seen from the arrow. Bar: 1.3 mm.

1 Crus cerebri
2 Midbrain tectum (tectal plate, quadrigeminal plate)
3 Pineal gland (body)
4 Cerebral aqueduct (of Sylvius)

Posterior wall of the third ventricle

5 Superior ostium of the aqueduct. The aqueduct exits from the third ventricle just inferior to the posterior commissure (6)
6 Posterior commissure
7 Pineal recess of the third ventricle
8 Habenular commissure
9 Suprapineal recess

Lateral wall of the third ventricle

10 Lateral wall of the third ventricle, thalamic portion, showing the medial wall of the contralateral thalamus
11 Lateral wall of the third ventricle, hypothalamic portion

Anterior wall of the third ventricle

12 Interventricular foramen **(**of Monro)
13 Fornix, anterior column forming the anteromedial wall of the foramen of Monro
14 Anterior commissure
15 Lamina terminalis of the third ventricle

Inferior wall of the third ventricle (floor)

16 Optic chiasm
17 Hypophyseal (infundibular) recess of the anterior third ventricle
18 Tuber cinereum
19 Mammillary body

Superior wall of the third ventricle (roof)

20 Tela choroidea of the third ventricle and choroid plexus
21 Cistern of the velum interpositum (velum transversum)
22 Fornix body
23 Corpus callosum, body

Arrow: Point of view from within the ventricle toward the posterior wall (See B).

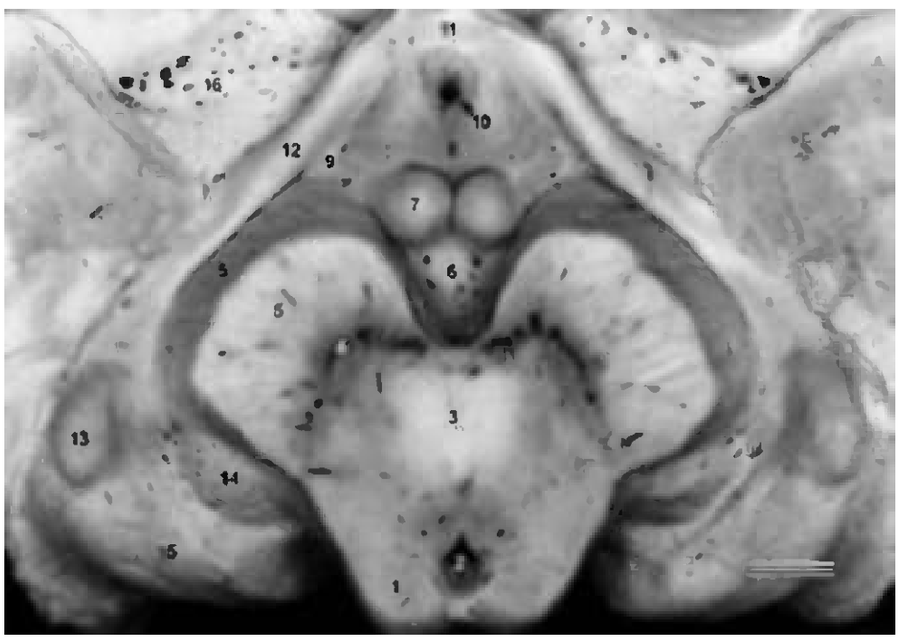

Fig. 5.4. The junction of the mesencephalon with the basal aspect of the brain.
Gross anatomic specimen. Bar: 5.5 mm.

Mesencephalon

1 Inferior colliculus
2 Cerebral aqueduct (of Sylvius)
3 Decussation of the superior cerebellar peduncle (brachium conjunctivum)
4 Substantia nigra
5 Crus cerebri (cerebral peduncle)

Diencephalon

6 Posterior perforated substance (interpeduncular fossa, intercrural fossa)
7 Mammillary body
8 Tuber cinereum (posterior tuber)
9 Lateral tuber and lateral perforated substance
10 Hypothalamic stalk and recess
11 Optic chiasm
12 Optic tract
13 Lateral geniculate body
14 Medial geniculate body
15 Pulvinar

Basal brain

16 Anterior perforated substance

Figures 5.5–5.8 show serial transverse sections of the diencephalo-mesencephalic junction and mesencephalon at progressively more superior levels. Intravascular India ink injections.

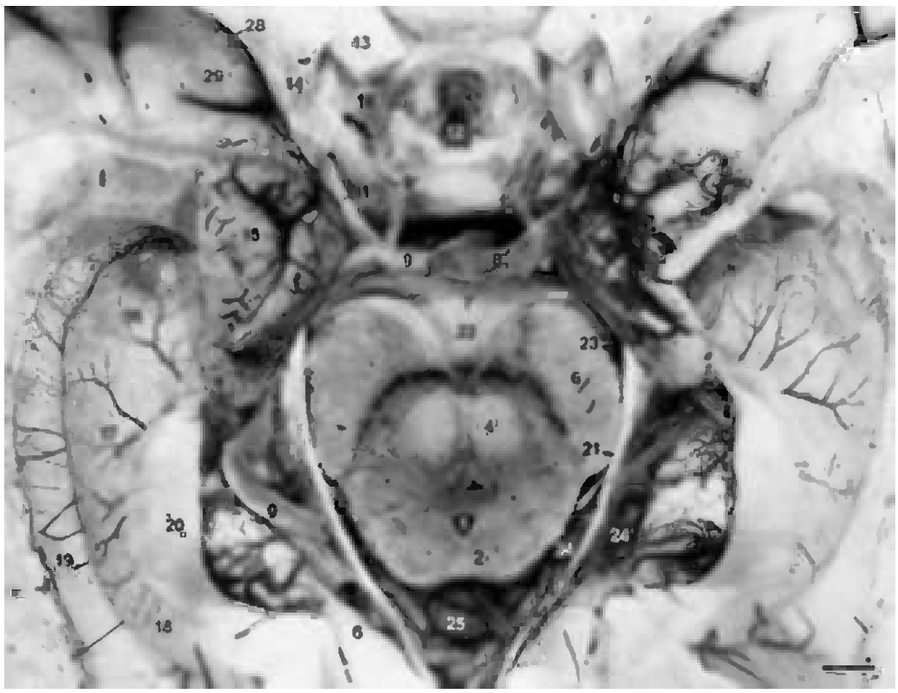

Fig. 5.5. Lower portion of the mesencephalon and tentorial hiatus. Transverse section. Bar: 5 mm.

1 Cerebral aqueduct (of Sylvius)
2 Inferior colliculus
3 Trochlear nucleus (CN IV)
4 Superior cerebellar peduncle (brachium conjunctivum)
5 Substantia nigra, pars compacta
6 Crus cerebri (cerebral peduncle)
7 Pons
8 Basilar artery
9 Posterior cerebral artery
9' Posterior communicating artery
10 Internal carotid artery
11 Oculomotor nerve (CN III)
12 Hypophyseal stalk
13 Optic nerve (CN II)
14 Anterior clinoid process, which anchors the free edge of the tentorium anteriorly
15 Uncus

Opening the temporal horn and removal of the choroid plexus discloses:

16 Head of hippocampus (digitations of the pes hippocampi)
17 Body of hippocampus
18 Tail of hippocampus (the left and right hippocampi encircle the mesencephalon.)
19 Collateral eminence
20 Fimbria
21 Free edge of the tentorium cerebelli and tentorial hiatus crossed by mesencephalon

Perimesencephalic cisterns

22 Interpeduncular cistern
23 Crural cistern
24 Ambient cistern against the lateral mesencephalic surface
25 Quadrigeminal plate cistern and superior vermis

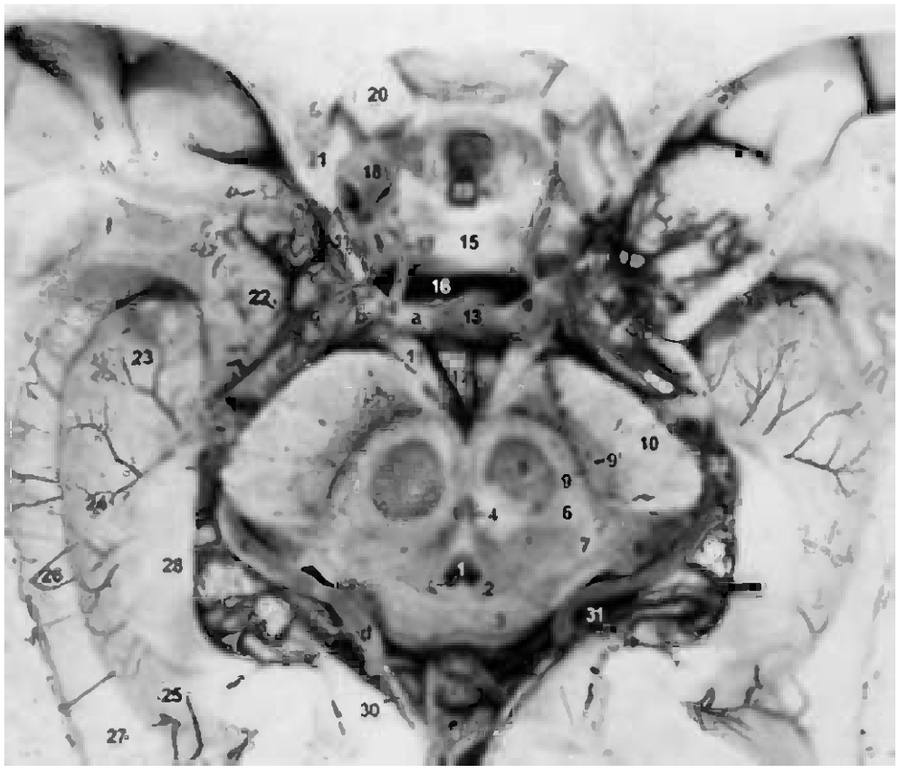

Fig. 5.6. Mid-portion of the mesencephalon. Transverse section. Bar: 5 mm.
(For more information on the hippocampal formation, see references [124] and [125]).

1 Cerebral aqueduct (of Sylvius)
2 Periaqueductal gray matter
3 Superior colliculus
4 Oculomotor nucleus (CN III)
5 Red nucleus
6 Medial lemniscus
7 Lateral lemniscus
8 Medial geniculate body
9 Substantia nigra, pars compacta
9′ Substantia nigra, pars reticulata
10 Crus cerebri (cerebral peduncle)
11 Oculomotor nerve (CN III)
12 Pons and interpeduncular cistern
13 Basilar artery
14 Posterior cerebral artery divided into four segments:
a. P1 Segment
b. P2 Segment
c. P3 Segment
d. P4 Segment
15 Dorsum sellae
16 Prepontine cistern
17 Posterior communicating artery
17′ Anterior choroidal artery
18 Internal carotid artery
19 Hypophyseal stalk
20 Optic nerve (CN II)
21 Anterior clinoid process
22 Uncus

Opening the temporal horn and removal of the choroid plexus discloses

23 Head of hippocampus
(digitations of the pes hippocampi)
24 Body of hippocampus
25 Tail of hippocampus
26 Collateral eminence
27 Floor of the ventricular atrium
28 Fimbria
29 Quadrigeminal plate cistern and superior vermis
30 Free edge of tentorium cerebelli
31 Ambient cistern
32 Crural cistern

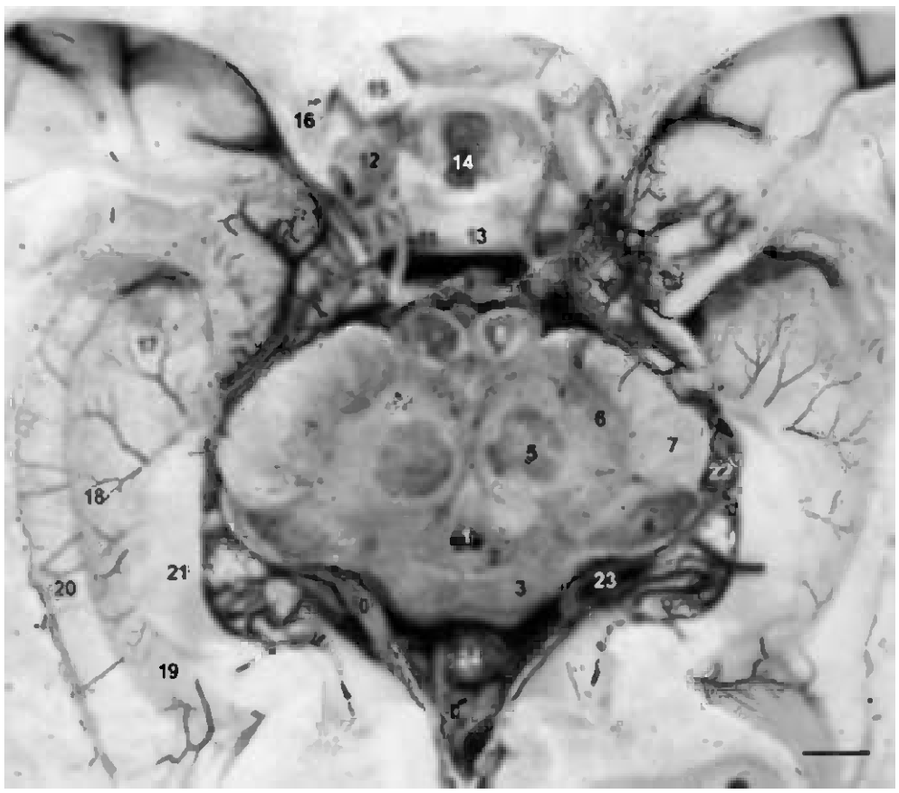

Fig. 5.7. Upper portion of the mesencephalon. Transverse section. Bar: 5 mm.

1 Cerebral aqueduct
2 Periaqueductal gray matter
3 Superior colliculus
4 Medial geniculate body
5 Red nucleus
6 Substantia nigra, pars reticulata
7 Crus cerebri (cerebral peduncle)
8 Mammillary body
9 Basilar artery
10, 10′ Posterior cerebral artery
11 Posterior communicating artery
12 Internal carotid artery
13 Dorsum sellae
14 Hypophyseal stalk
15 Optic nerve (CN II)
16 Anterior clinoid process

Opening the temporal horn and removal of the choroid plexus discloses

17 Head of hippocampus (digitations of the pes hippocampi)
18 Body of hippocampus
19 Tail of hippocampus
20 Collateral eminence
21 Fimbria
22 Crural cistern
23 Ambient cistern
24 Quadrigeminal plate cistern

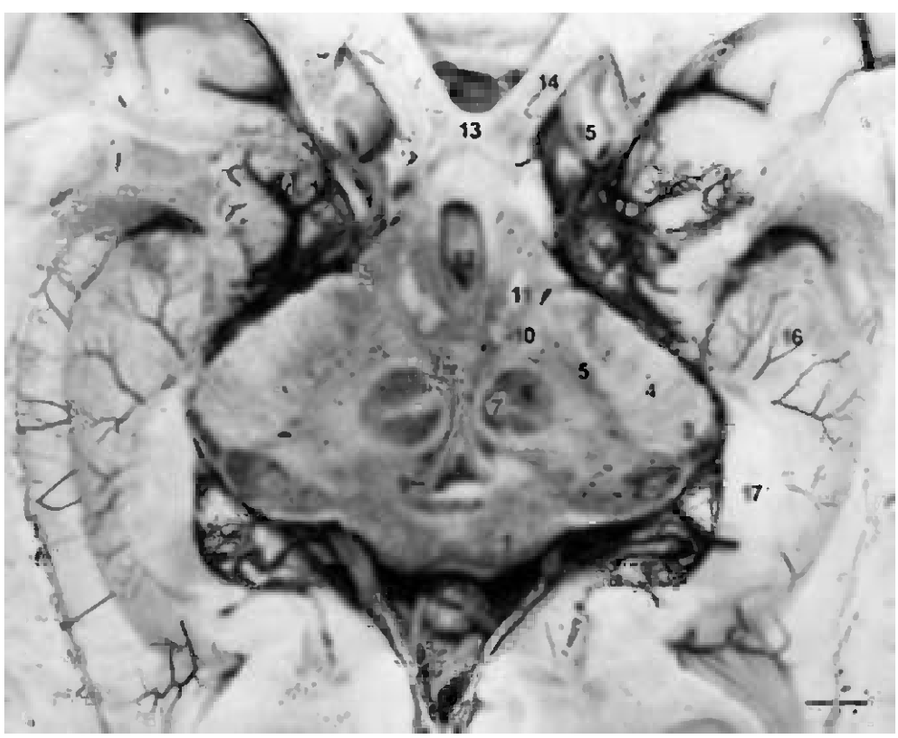

Fig. 5.8. Diencephalo-mesencephalic junction. Bar: 5 mm.

1 Superior colliculus
2 Medial geniculate body
3 Lateral geniculate body
4 Crus cerebri (cerebral peduncle)
5 Subthalamic nucleus
6 Red nucleus
7 Habenulo-interpeduncular tract
8 Cerebral aqueduct (of Sylvius)
9 Periaqueductal gray matter
10 Mammillothalamic tract
11 Fornix (anterior column)
12 Floor of the third ventricle and infundibular recess (infundibulum)
13 Optic chiasm (CN II)
14 Optic nerve (CN II)
15 Internal carotid artery
16 Hippocampus (at the floor of the opened temporal horn)
17 Fimbria

SECTION VI

VASCULARIZATION OF THE CEREBELLUM AND THE BRAIN STEM

This section reviews the vascularization of the cerebellum and brain stem, presenting first the surface vascularity, then the penetrating vessels. The following section (Section VII, p. 219 analyzes the intrinsic arterial and venous compartments of the brain stem in detail.

Additional information is found in the following references:

General vascularity:	37, 73, 76, 118, 120, 127, 172, 184, 231, 239, 241, 242, 251, 257, 282, 314, 338, 339, 369, 370, 379, 399, 404, 417, 418, 472, 473, 474, 475
Brain stem vascularity:	35, 109, 114, 117, 121, 122, 173, 182, 185, 186, 196, 204, 205, 206, 210, 266, 277, 282, 284, 285, 368, 375, 419, 435, 452, 469
Medulla oblongata:	5, 8, 24, 47, 54, 131, 138, 152, 171, 272, 408
Pons varioli:	21, 54, 150, 159, 278, 290, 408
Mesencephalon:	9, 10, 25, 143, 144, 151, 233, 279, 290, 451
Cerebellum:	12, 114, 128, 173, 182, 196, 204, 205, 206, 210, 241, 246, 266, 277, 282, 375, 419, 452
Hypothalamus:	119, 130, 149, 368
Thalamus and basal ganglia:	2, 3, 129, 149, 160, 165, 166, 446, 471
Pineal gland:	29, 126, 139, 261, 268, 356, 392, 422, 426, 427, 448, 449, 473

A. Surface Vascularization (Figs. 6.1–6.37)

Cerebellar arteries

The cerebellar arterial supply derives from the superior, anterior inferior, and posterior inferior cerebellar arteries.

The superior cerebellar artery
(Figs. 6.1, 6.2, 6.8, 6.19 and 6.20).
Originating from the basilar artery just before its division into right and left posterior cerebral arteries, each superior cerebellar artery (SCA) curves around the upper portion of the pons and divides into medial and lateral branches.
The medial branch sends off descending branches to vascularize the superior vermis and the neighboring portion of the surface of the cerebellar hemisphere. The medial branch also sends rami along the superior cerebellar peduncles to reach the deep cerebellar nuclei (especially the dentate nucleus).
The lateral branch vascularizes the most lateral portion of the superior surface of the cerebellar hemisphere (quadrangular, simple, and superior semilunar lobules).

The anterior inferior cerebellar artery
(Figs. 6.1, 6.2 , 6.16 and 6.17)
Arising from the caudal or middle third of the basilar artery, the anterior inferior cerebellar artery (AICA) crosses the roots of the abducens, facial, and vestibulocochlear nerves. Near the opening of the internal acoustic meatus (where it usually forms a characteristic loop), the anterior inferior cerebellar artery often gives rise to the internal auditory artery.
The anterior inferior cerebellar artery loops around the flocculus (floccular loop) and divides into two branches. One descends behind the flocculus within the posterior lateral fissure, while the other ascends into the great horizontal fissure of the cerebellum (Fig. 6.1). The anterior inferior cerebellar artery usually vascularizes the anterior surface of the simple, superior, and inferior semilunar lobules, as well as the flocculus, the choroid plexi of the lateral ventricular recess, and the middle cerebellar peduncles. However, its caliber and cerebellar vascular territory are quite variable.

The posterior inferior cerebellar artery
(Figs. 6.1, 6.8, 6.9, 6.11 and 6.13).
The posterior inferior cerebellar artery (PICA) generally originates from the vertebral artery, and may be the terminal branch of the vertebral artery. It frequently has a tortuous path on the lateral medullary surface, convering the lateral medullary fossa. The posterior inferior cerebellar artery subsequently reaches the inferior cerebellar surface where it divides into medial and lateral branches.
The medial branch, situated in the vallecula, vascularizes the inferior vermis and the choroid plexus of the fourth ventricle.
The lateral branch supplies the inferior and posterior surfaces of the cerebellar hemispheres (tonsil and biventer, inferior and part of superior semilunar lobules). The deep cerebellar nuclei (dentate, globose, emboliform, and fastigial nuclei) have a principal arterial supply coming from the medial branch of the superior cerebellar artery, and an accessory supply by way of the lateral branch of the superior cerebellar artery and the posterior inferior cerebellar artery.
Like the cerebral arteries, the cerebellar arteries have variable importance and territories.

Fig. 6.1. The arteries of the brain stem and cerebellum.
Anterior view: General organization.
A. Medulla; **B.** Pons; **C.** Mesencephalon; **D.** Cerebellum

Brain stem arteries

The arteries of the brain stem arise from the following main arterial trunks

1 Vertebral artery
2 Anterior spinal artery
3 Posterior inferior cerebellar artery (PICA)
4 Basilar artery
5 Anterior inferior cerebellar artery (AICA)
6 Superior cerebellar artery (SCA)
6′, 6″ Medial and lateral branches of the superior cerebellar artery
7 Posterior cerebral artery
8 Posterior communicating artery
9 Anterior choroidal artery

The brain stem arteries arising from the main trunks are divided into anteromedial, anterolateral, lateral, and posterior groups according to their point of penetration into the surface of the brain stem. The arteries of the medulla, pons, and mesencephalon will be studied successively.

Arteries of the medulla

10 Anteromedial group of medullary arteries. Arising from the anterior spinal and vertebral arteries, these arteries penetrate in the anteromedian sulcus (10′).
11 Anterolateral group of medullary arteries. Arising from the anterolateral group, these arteries enter the pyramid and the anterolateral (pre-olivary) sulcus (11′).
12 Lateral group of medullary arteries. These arteries penetrate the lateral medullary fossa (arteries of the lateral medullary fossa). The arteries of the lateral medullary fossa are divided into four groups of rami:
a Inferior rami, arising from the posterior inferior cerebellar artery (3)
b Middle rami, arising from the vertebral artery (1)
c, c′ Superior rami, composed of two distinct groups:
c Arising from the initial segment of the basilar artery (4) and supplying the upper medullary level
c′ Arising from the anterior inferior cerebellar artery (5) and supplying the lowest pontine tegmentum (**See Fig. 7.12A**)
d Posterior rami arising from the anterior inferior cerebellar artery and entering the nervous tissue posterior to the glossopharyngeal and vagus nerves.
The posterior group of medullary arteries is hidden on this anterior view and will be described in **Fig. 6.13**. The vessels of this group arise from the posterior inferior cerebellar arteries and from the posterior spinal arteries.

Arteries of the pons

13 The anteromedial group of pontine arteries branch off from the basilar artery and enter the pons through the basilar sulcus (13) (for the midpontine arteries), the foramen cecum (13′) (for the inferior arteries) and the interpeduncular fossa (13″) (for the superior arteries) (**See Fig. 7.12A** to follow their deep path).
14 The anterolateral group of pontine arteries arise from the basilar artery and penetrate the anterior aspect of the pons.
15–18 The lateral group of pontine arteries arise from two origins: (i) From the lateral pontine arteries. Two lateral pontine arteries are usually found: the superior lateral pontine artery (16) whose branches enter the trigeminal nerve entry point (16′), and the inferior lateral pontine artery (17) whose branches supply the middle cerebellar peduncle (lateral pontine aspect);
(ii) From the anterior inferior cerebellar artery for the middle cerebellar peduncle (18). See also 5′: an AICA variation that loops forward to the trigeminal root.

The posterior group of pontine arteries, hidden on this anterior view (**See Fig. 6.3**), vascularizes the superior cerebellar peduncles (brachia conjunctiva). These arteries arise from the medial and lateral branches of the superior cerebellar artery.

Arteries of the mesencephalon

These arteries arise from arterial trunks which curve around the mesencephalon and are, in ascending order: the superior cerebellar (6) (medial (6′) and lateral branches (6″)), collicular (19), posterior medial choroidal (20), posterior cerebral (7), and anterior choroidal (9) arteries (**See Fig. 6.3**).
The anteromedial group of mesencephalic arteries belongs to the middle group of the interpeduncular fossa arteries.
The interpeduncular fossa arteries are frequently divided into four groups:
Inferior for the pons (13″)
Superior for the thalamus (thalamoperforating arteries, 21)
Middle for the mesencephalon (22), penetrating into both the middle zone of the interpeduncular fossa and the oculomotor nerve exit point (22′).
Anterolateral group of mesencephalic arteries(23). These arteries arise from the arterial trunks that course around the crus cerebri (collicular, posterior medial choroidal, and anterior choroidal arteries).
The lateral and posterior groups of mesencephalic arteries will be described in **Fig. 6.3**.

Cerebellar arteries

24 Rami arising from the lateral branch of the superior cerebellar artery, supplying the superior cerebellar surface
25 Rami from the anterior inferior cerebellar artery supplying the anterior cerebellar surface
26 Internal auditory artery (supplying the internal ear)
27 Rami arising from the posterior inferior cerebellar artery supplying the anterior and inferior cerebellar surfaces

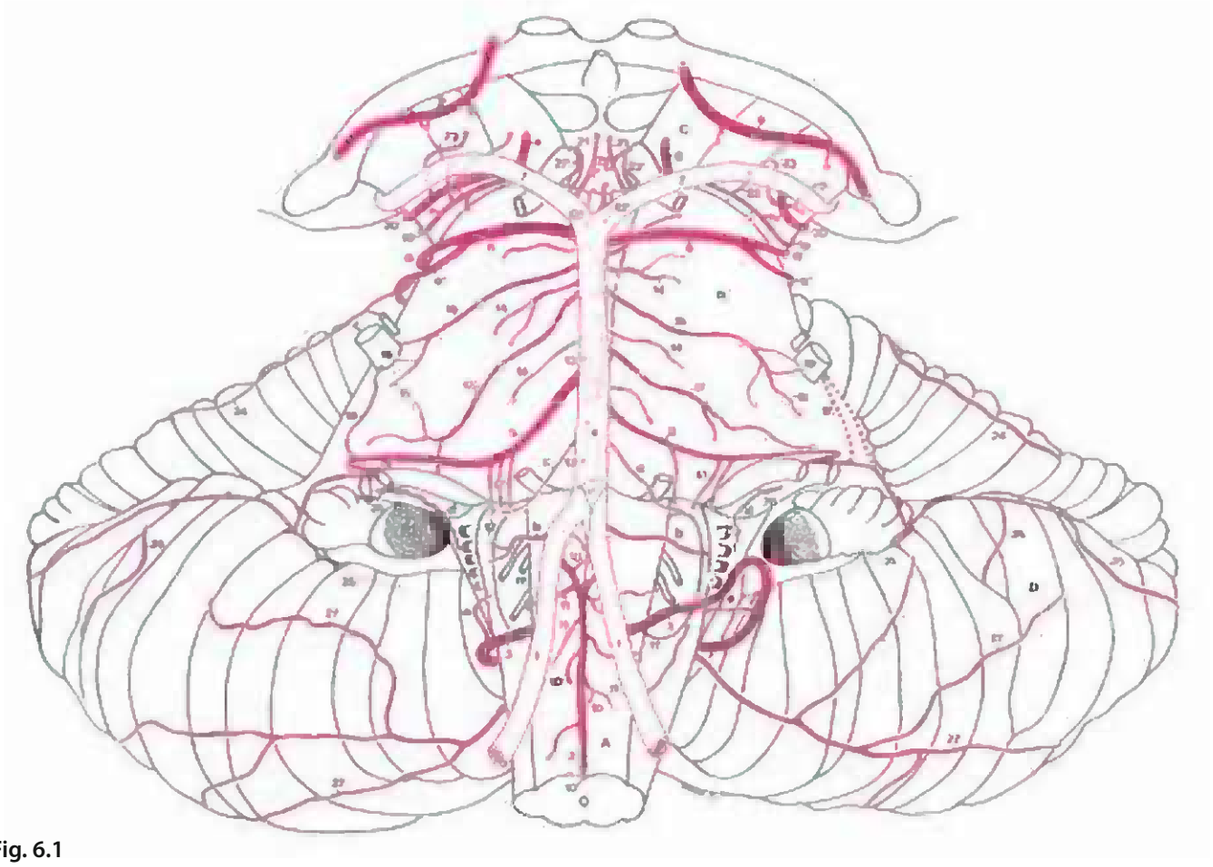

Fig. 6.1

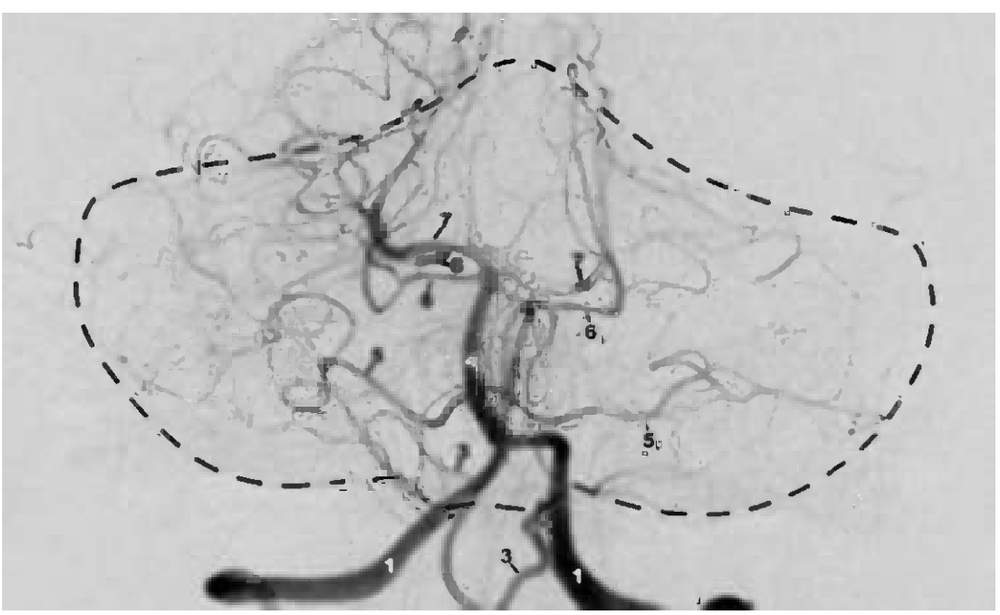

Fig. 6.2

Fig. 6.2. Corresponding right vertebral arteriogram, Arterial phase. Water's projection (perpendicular to the clivus). Labels as in Fig. 6.1.

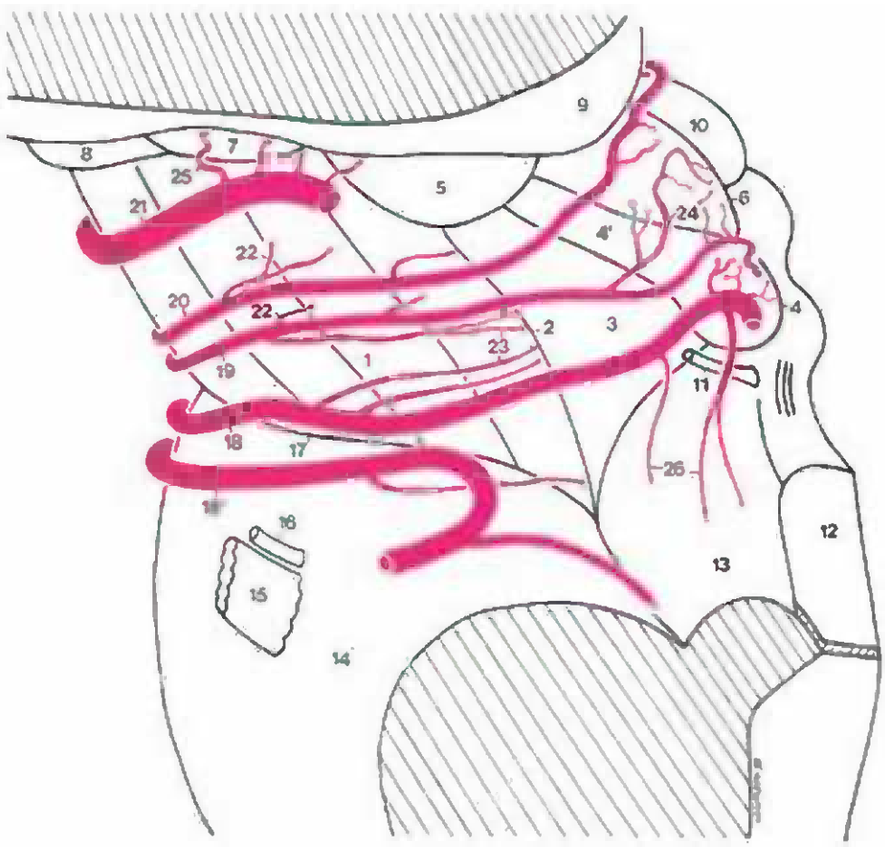

Fig. 6.3. The arteries of the uppermost pons and mesencephalon. Lateral view.

1 Crus cerebri
2 Lateral mesencephalic sulcus
3 Lateral aspect of the mesencephalon
4 Inferior colliculus
4′ Brachium of the inferior colliculus
5 Medial geniculate body
6 Superior colliculus
7 Lateral geniculate body
8 Optic tract
9 Pulvinar
10 Pineal gland
11 Trochlear nerve (CN IV)
12 Superior medullary velum
13 Superior cerebellar peduncle (brachium conjunctivum)
14 Middle cerebellar peduncle (brachium pontis)
15 Trigeminal nerve, sensory root
16 Trigeminal nerve, motor root
17 Pontomesencephalic sulcus

Five arterial trunks give rise to the arteries supplying the mesencephalon, in ascending order:

18 Superior cerebellar artery. The lateral branch (18′) arises inferior to the medial branch (18).
19 Collicular artery
20 Posterior medial choroidal artery
21 Posterior cerebral artery

Mesencephalic arteries

22 The anterolateral group of mesencephalic arteries studied in ventral view (Fig. 6.1) is also visible in a lateral view of the crus cerebri. The anterolateral group of mesencephalic arteries mainly arises from the collicular and posterior medial choroidal arteries.
23 The lateral group of mesencephalic arteries is composed of branches arising from the medial and lateral superior cerebellar, collicular, and posterior choroidal arteries. They mainly enter the lateral mesencephalic sulcus (2).
24 The posterior group of mesencephalic arteries forms a dense network covering the colliculi. It is composed of branches arising from the medial superior cerebellar, collicular and posterior medial choroidal arteries.
25 Thalamogeniculate arteries, supplying the thalamus, arise from the posterior cerebral artery.

Pontine arteries

The posterior group of pontine arteries arises from the medial and lateral superior cerebellar artery and supplies the superior cerebellar penduncle (brachium conjunctivum).

Cerebellar veins

The veins of the superior cerebellar surface

These veins are divided into the vermian and hemispheric veins.

The superior vermian veins drain upward into the precentral vein (**Figs. 6.7 and 11.70**) and the great cerebral vein (of Galen). They drain downward into the straight sinus and the torcular Herophili (confluens sinuum) (**Figs. 11.20 and 11.22**).

The superior hemispheric veins reach the tentorium cerebelli and the transverse and superior petrosal sinuses.

The veins of the inferior cerebellar surface

These veins are also divided into vermian and hemispheric veins. The inferior vermian veins reach the torcular Herophili (confluens sinuum), while the inferior hemispheric veins drain into the neighboring transverse sinus (**Figs. 11.20, 11.50 and 11.52**).

The veins of the anterior cerebellar surface

These veins principally drain into the anterior cerebellar vein situated in the great horizontal fissure (**Fig. 6.5**). The anterior cerebellar vein reaches the superior petrosal vein, which itself drains into the superior petrosal sinus.

Fig. 6.4. The veins of the brain stem and cerebellum. Anterior view: General organization.
A. Medulla; **B.** Pons; **C.** Mesencephalon; **D.** Cerebellum

Brain stem veins

The path of the brain stem veins is quite different from that of the brain stem arteries. The principal venous trunks together form a rectilinear grid of longitudinal and transversal veins Fig. 6.10). Their drainage into the venous sinuses is variable, so this diagram shows only the most common features (See [120–122] for more details). The principal venous trunks drain the deep veins, which emerge from the nervous tissue. As for the arteries, these veins will be subdivided into anteromedial, anterolateral, lateral, and posterior groups.

Veins of the medulla

Anterior aspect

1 Anterior median medullary vein
2 Anterior lateral (pre-olivary) medullary vein
3 Transverse medullary veins
4 The anterior median vein drains the anteromedial group of medullary veins (4).
5 The anterior lateral and transverse veins drain the anterolateral group of medullary veins (5).

Lateral aspect

6 Lateral medullary vein situated behind the glossopharyngeal and vagus nerve roots
6′ Drainage by a bridging vein towards the inferior petrosal sinus
6″ Drainage by a bridging vein towards the sigmoid sinus
7 Retro-olivary vein
8 Vein of the pontomedullary sulcus

These veins together receive the lateral group of medullary veins (9) (veins of the lateral medullary fossa).

Posterior aspect

The veins of the posterior aspect of medulla are seen in transparency (See Fig. 6.13 for more details).

10 Posterior median medullary vein
11 Marginal vein of the ventricular floor draining into the lateral medullary vein (6).

The posterior group of medullary veins drain into the posterior median medullary vein at the lower medullary level and into the marginal veins at the upper medullary level. The marginal vein mainly receives the veins of the ventricular floor (See Fig. 1.22).

Veins of the pons

Anterior aspect

12 Anterior median pontine vein, draining upward into the right and left interpeduncular veins (21)
13 The anterior median pontine vein draining the anteromedial group of pontine veins (13)
14 Transverse pontine veins, draining into the basilar plexus (15) and the superior petrosal vein (16)
17 The transverse pontine veins receive the anterolateral group of pontine veins (17).

Lateral aspect

18 The lateral pontine vein. It receives the lateral medullary vein (6) and drains into the anterior cerebellar vein (19), which is a tributary of the superior petrosal vein (16).

The transverse and lateral veins drain the lateral group of pontine veins (20).

Posterior aspect

The veins of the posterior aspect of the pons (veins of the brachium conjunctivum) are shown in Fig. 6.7.

Veins of the mesencephalon

Interpeduncular fossa

21 Interpeduncular vein draining the anterior median pontine vein and reaching the basal vein of Rosenthal (22)
The interpeduncular veins drain the anteromedial group of mesencephalic veins (24) (veins of the interpeduncular fossa)
23 Posterior communicating vein

Mesencephalon anterior aspect (crus cerebri, cerebral peduncle)

22 Basal vein (ventral segment) (See Fig. 6.19).
25 Vein of the pontomesencephalic sulcus
The basal and interpeduncular veins and the vein of the pontomesencephalic sulcus together drain the anterolateral group of mesencephalic veins (26).

Lateral and posterior aspects

Described in Figs. 6.6 and 6.7, these veins are visible in transparency.

27 Lateral mesencephalic vein
28 Basal vein (laterodorsal segment)
29 Great cerebral vein (of Galen)

Cerebellar veins

30 Veins of the anterior aspect of the cerebellum, drain into the anterior cerebellar vein (19).
31 Veins of the inferior (and adjacent superior) cerebellum drain into the transverse sinus.

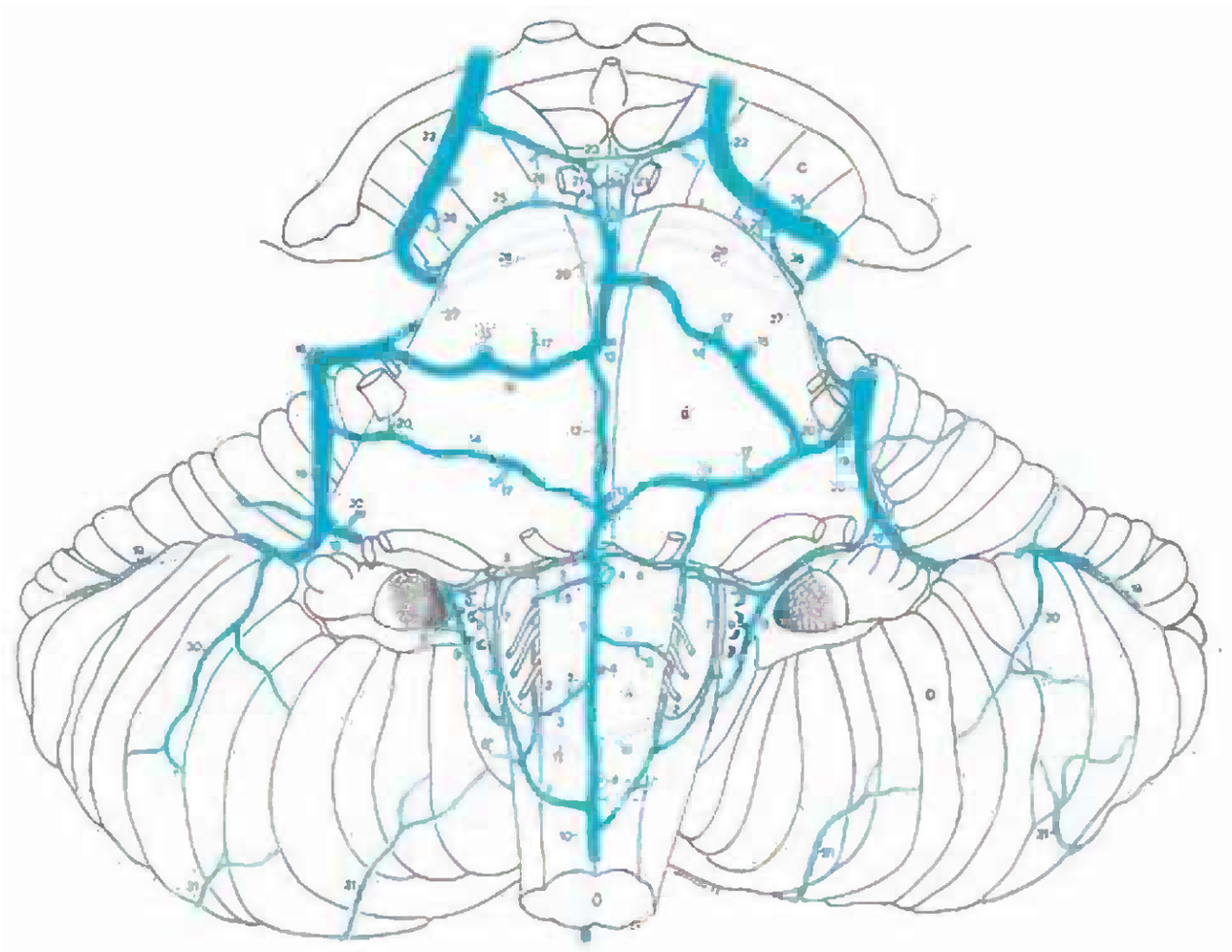

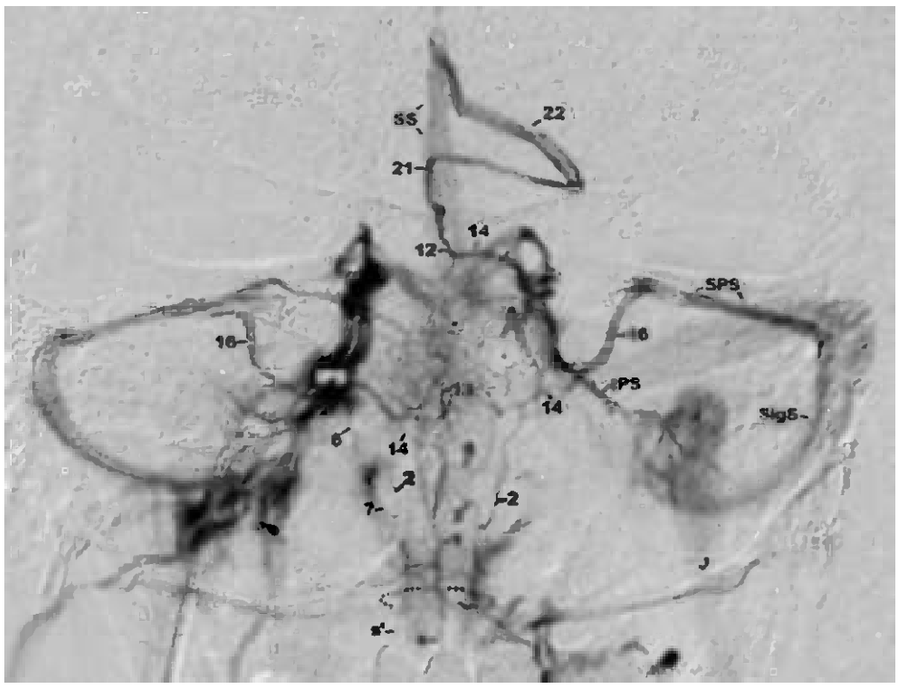

A

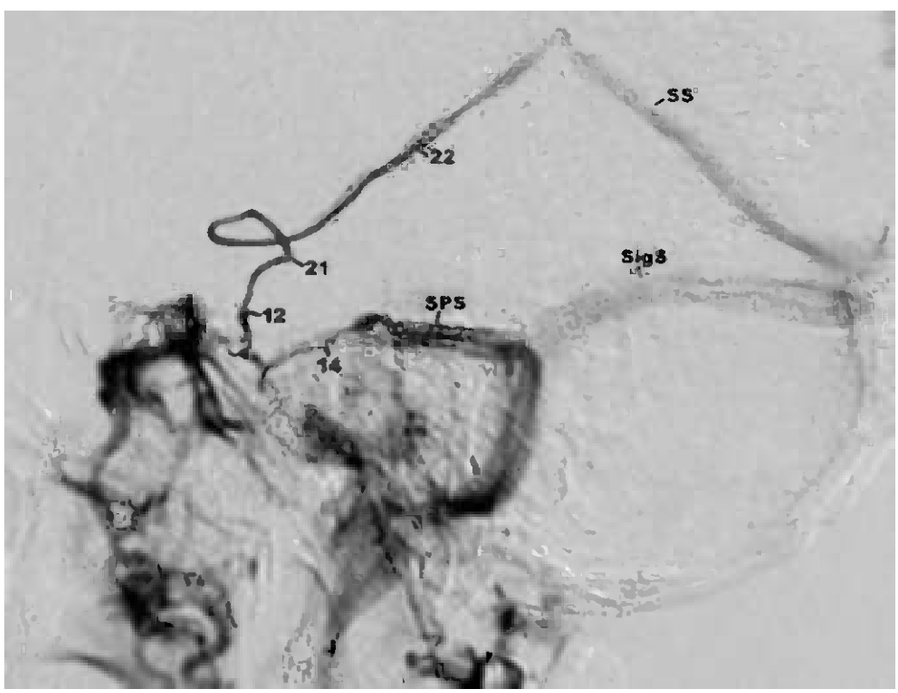

B

Fig. 6.5. Venogram, corresponding to Figs. 6.4 and 6.6.
A. Water's projection (perpendicular to the clivus) and
B. lateral projection performed by contrast injection into the right inferior petrosal sinus.

IPS	Inferior petrosal sinus
J	Jugular bulb and vein
S	Anterior median spinal vein
S'	Posterolateral spinal vein
SS	Straight sinus
SigS	Sigmoid sinus
SPS	Superior petrosal sinus
Dotted ring	Foramen magnum

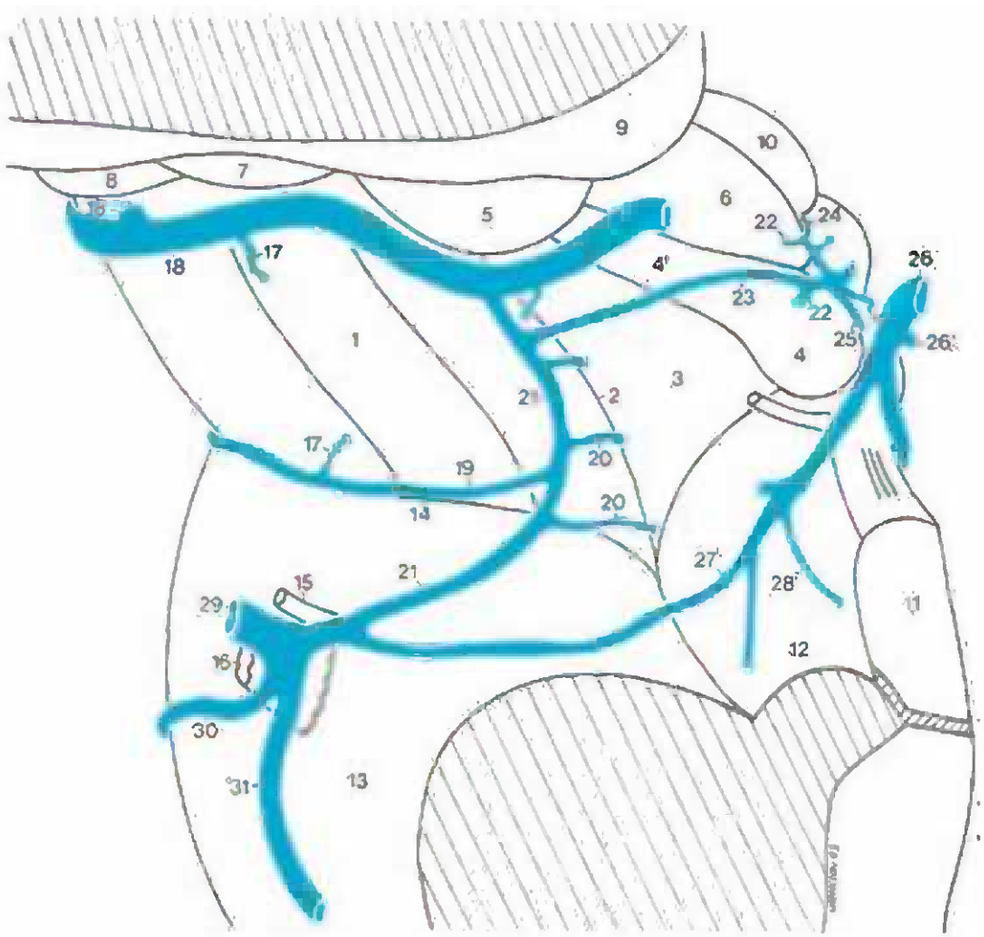

Fig. 6.6. The veins of the uppermost pons and mesencephalon. Lateral view.

1 Crus cerebri
2 Lateral mesencephalic sulcus
3 Lateral aspect of the mesencephalon
4 Inferior colliculus
4′ Brachium of the inferior colliculus
5 Medial geniculate body
6 Superior colliculus
7 Lateral geniculate body
8 Optic tract
9 Pulvinar
10 Pineal gland
11 Superior medullary velum
12 Superior cerebellar peduncle (brachium conjunctivum)
13 Middle cerebellar peduncle (brachium pontis)
14 Pontomesencephalic sulcus
15 Trigeminal nerve, motor root
16 Trigeminal nerve, sensory root

Mesencephalic veins

17 Anterolateral group of mesencephalic veins draining upward into the basal vein of Rosenthal (18) (laterodorsal segment) (18′ vein of the temporal horn of the lateral ventricle) and downward into the vein of the pontomesencephalic sulcus (19)
20 Lateral group of mesencephalic veins mainly draining into the lateral mesencephalic vein (21)
22 Posterior group of mesencephalic veins, draining into the intercollicular veins (23) and the superior (24) and inferior (25) median collicular veins
26 Precentral vein
26′ Superior vermian vein

Pontine veins

27 Veins of the brachium conjunctivum draining the posterior group of pontine veins (28)
29 Superior petrosal vein. This important venous trunk, which flows into the superior petrosal sinus, is formed by the union of the transverse pontine (30), anterior cerebellar (31) and lateral mesencephalic (21) veins

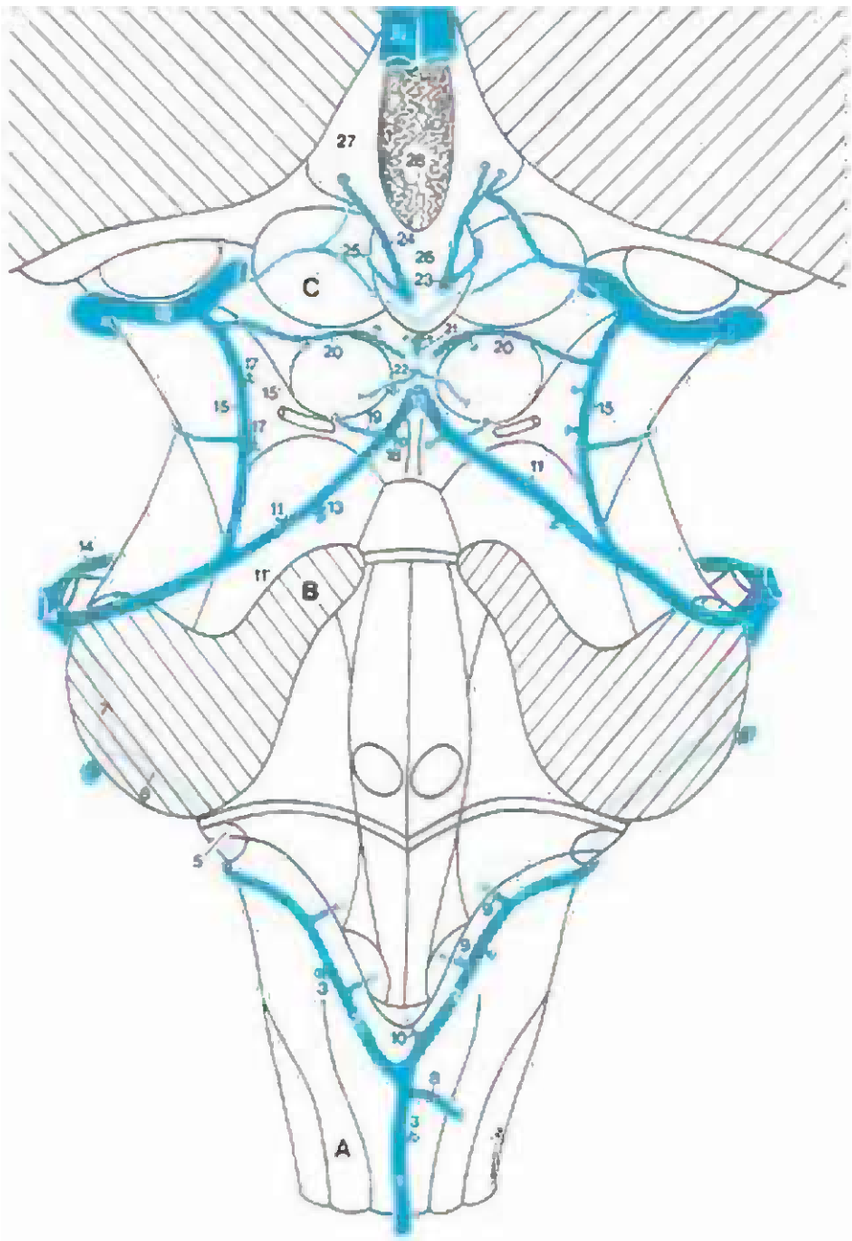

Fig. 6.7. Veins of the posterior surface of the brain stem. Diagram. Dorsal view after resection of the cerebellar hemispheres. **A.** Medulla. **B.** Pons. **C.** Mesencephalon.

Veins of the posterior surface of the medulla.

1 Posterior median medullary vein

2 Marginal vein of the ventricular floor (vein of the inferior cerebellar peduncle)
The marginal vein and the posterior medullary vein receive the *posterior group of medullary veins* (3) and often drain toward the superior petrosal vein (4) successively through the lateral medullary (5), lateral pontine (6), and anterior cerebellar (7) veins.

8 The vein of the cerebellomedullary cistern (8) occasionally drains the posterior medullary venous network toward the marginal sinus, which borders the foramen magnum, or toward the occipital sinus.

9 Internal lateral medullary vein

10 Median posterior medullary vein. The internal lateral and median posterior medullary veins drain the floor of the fourth ventricle (subependymal veins).

Veins of the posterior surface of the pons.

11 Veins of the brachia conjunctiva (superior cerebellar peduncles (11')) link the precentral cerebellar vein (12) to the superior petrosal veins (4), which receive the posterior group of pontine veins *(13)*.

14 Transverse pontine vein

Veins of the lateral and posterior surfaces of the mesencephalon.

15 The lateral mesencephalic vein (15) and the basal vein of Rosenthal (16) (laterodorsal segment) are the major veins of the lateral surface of the mesencephalon. They receive the lateral group of mesencephalic veins (17).
The posterior group of mesencephalic veins drains into the vein of the brachium conjunctivum (11) [vein of the recess of the frenulum veli (18), vein of the infracollicular recess (19)] and into the collicular veins [left and right intracollicular veins (20), superior median collicular vein (21), and inferior median collicular vein (22)].

23 The lateral pineal veins (23) drain the pineal gland (26) and the habenular trigone (27) by superior (24) and inferior (25) branches.

28 Suprapineal recess

29 Internal cerebral vein

Vascularization of the brain stem

The brain stem vessels were studied after intravascular injection of India ink, following the methods described on p. 2. The superficial vessels were dissected and photographed. The deep vessels were traced through the nervous tissue after clearing. The results that are shown here summarize more detailed descriptions that can be found in three previous works [120, 121, 122].
See also [7, 8, 21, 24, 35, 42, 54, 114, 117, 118, 119, 127, 129, 130, 135, 149, 150, 153, 163, 185, 186, 196, 197, 204, 210, 256, 258, 259, 282, 337, 388, 389, 404, 408, 409, 452].

The drawings shown in **Figs. 6.1–6.7** display an overview of the superficial arteries and veins, whereas **Figs. 6.8–6.37** show dissections of injected pial vessels. The superficial pial blood vessels are subclassified into three groups by their point of entrance into (arteries) or emergence from (veins) the nervous tissue:

(a) The anterior group (further subdivided into anteromedial and anterolateral), penetrating into the anterior surface of the brain stem
(b) The lateral group, which penetrates the lateral surface, and
(c) The posterior group, related to the posterior surface of the brain stem.

The vessels of each group may be followed into the deep brain stem structures to specify their corresponding intranervous territories (anteromedial, anterolateral, lateral, and posterior arterial and venous territories) (**Figs. 7.1–7.24**).

Figures 6.8–6.37 show dissections of the superficial vessels of the brain stem after intravascular injection of India ink.

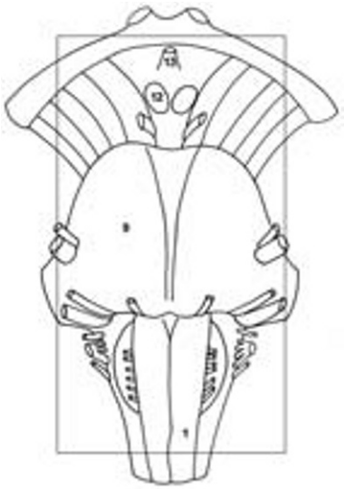

Fig. 6.8. The brain stem. Anterior view. Bar: 2 mm.

1 Medulla
2 Hypoglossal nerve
3 Accessory nerve
4 Vagus nerve
5 Glossopharyngeal nerve
6 Choroid plexus at the lateral aperture of the fourth ventricle (Foramen of Luschka)
7 Facial nerve
8 Abducens nerve
9 Pons
10 Trigeminal nerve
11 Oculomotor nerve
12 Mammillary body
13 Hypophyseal stalk
14 Vertebral artery
15 Anterior spinal artery
16 Posterior inferior cerebellar artery
17 Anterior inferior cerebellar artery
18 Basilar artery
19 Superior cerebellar artery
20 Posterior cerebral artery
21 Posterior communicating artery
22 Internal carotid artery

Fig. 6.9. The medulla. Anterior aspect. Bar: 1 mm.

1 Pyramid of the medulla
2 Inferior olive
3 Hypoglossal nerve
4 Vertebral arteries
5 Anterior spinal artery
6 Trunks of origin of the anterior spinal artery
7 Anterior median medullary vein
8 Transverse medullary veins
9 Anterior lateral (pre-olivary) vein
10 Anteromedial group of medullary arteries
11 Anterolateral group of medullary arteries

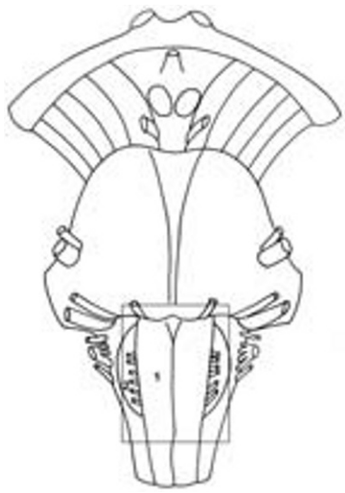

Fig. 6.10. The anterior medullary veins.
The arterial network has been removed. Bar: 2 mm.

1 Pyramid of the medulla
2 Inferior olive
3 Hypoglossal nerve
4 Pons
5 Anterior median medullary vein
6 Anterior lateral medullary vein
7 Transverse medullary vein
7′ In this case, a large transverse medullary vein drains the venous network through a venous trunk (7″, bridging vein), which is a satellite of the hypoglossal nerve (3).
8 Vein of the pontomedullary sulcus
9 Anterior median pontine vein

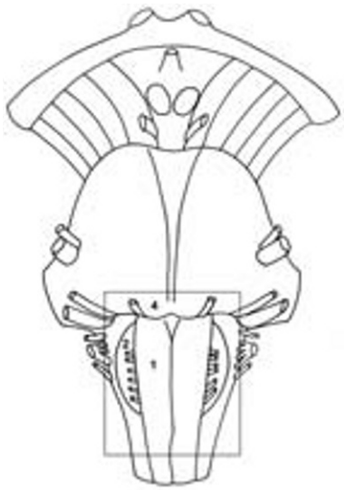

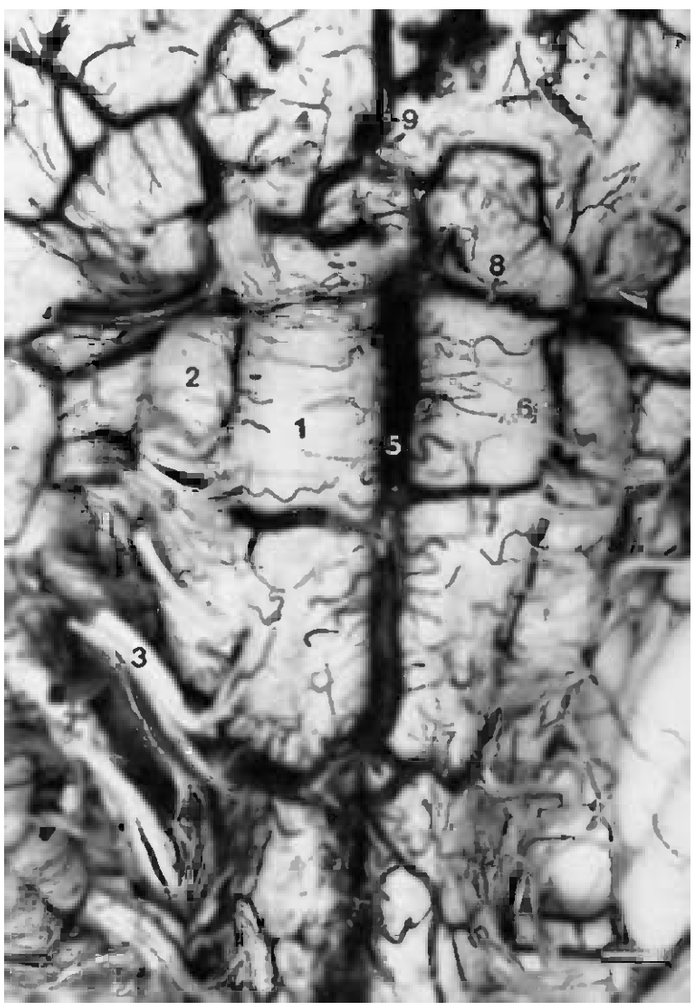

Fig. 6.11. The medulla. Right lateral view. Bar: 1 mm.

1 Pyramid of the medulla
2 Inferior olive
3 Accessory nerve, spinal root
3' Accessory nerve, medullary root
4 Vagus nerve
5 Choroid plexus at the lateral aperture of the fourth ventricle (Foramen of Luschka)
6 Glossopharyngeal nerve
7 Vestibulocochlear nerve
8 Facial nerve
9 Pons, lateral surface
10 Abducens nerve
11 Vertebral artery
12 Posterior inferior cerebellar artery
13 Lateral medullary (retro-olivary) fossa

Arteries of the lateral medullary fossa (Lateral group of medullary arteries)

A Inferior rami originating from the posterior inferior cerebellar artery
B Middle rami arising from the vertebral artery
C Superior rami arising from the basilar artery
C' Superior rami arising from the anterior inferior cerebellar artery (arrow). These arteries enter the pontomedullary sulcus (14) and supply the pontine tegmentum (**See Fig. 7.12A**)
D Posterior rami originating from the anterior inferior cerebellar artery
15 Lateral pontine vein

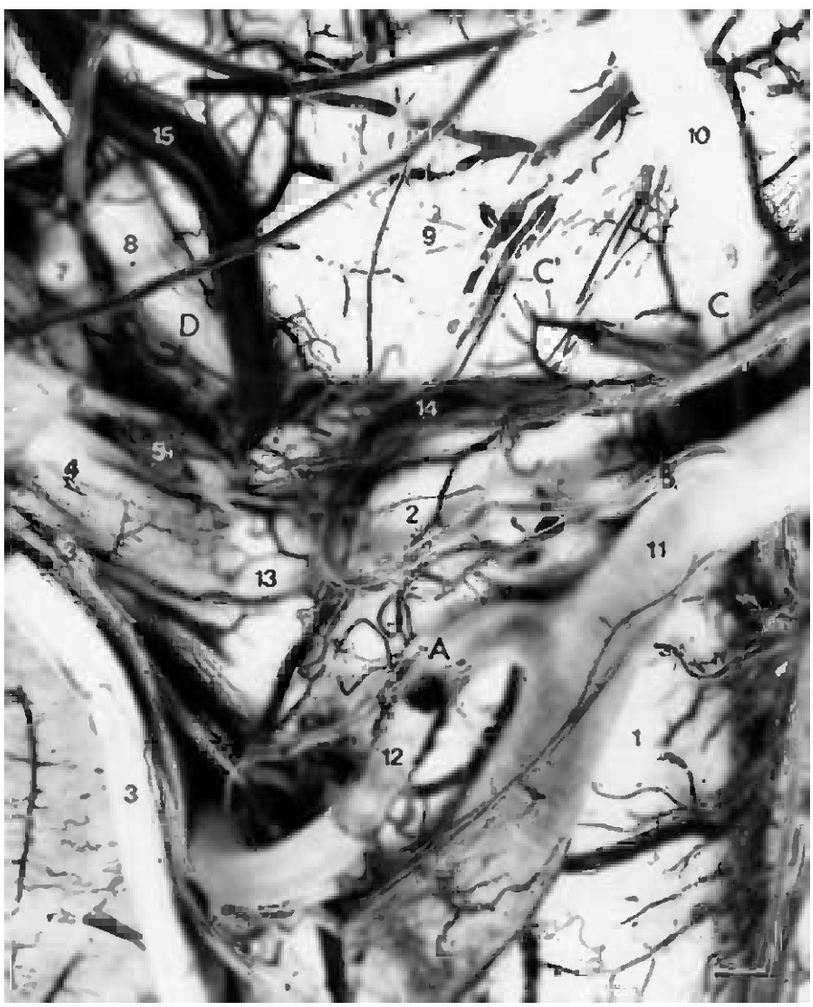

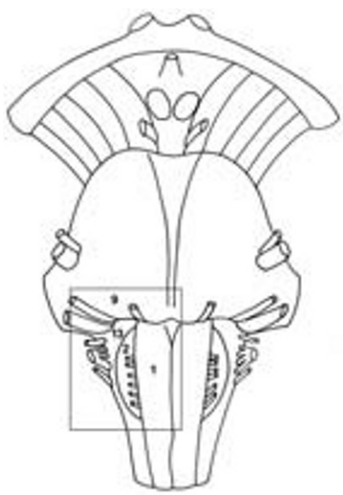

Fig. 6.12. The venous network of the medulla. Left lateral view after removal of the overlapping arterial network. Bar: 2 mm.

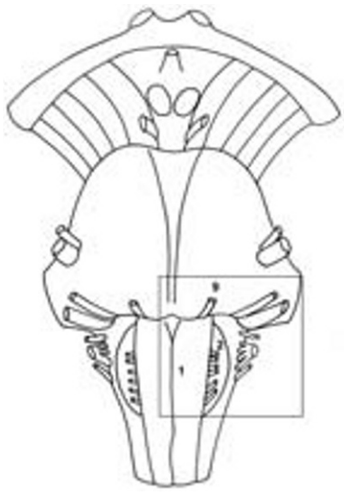

1 Pyramid of the medulla
2 Inferior olive
3 Lateral medullary fossa
4 Extraventricular choroid plexus
5 Lateral aperture of the fourth ventricle (foramen of Luschka)
6 Flocculus
7 Vestibulocochlear nerve
8 Facial nerve
9 Pons
10 Abducens nerve
11 Anterior lateral medullary vein
12 Lateral medullary vein
13 Vein of the pontomedullary sulcus
14 Lateral pontine vein
15 Anterior cerebellar vein

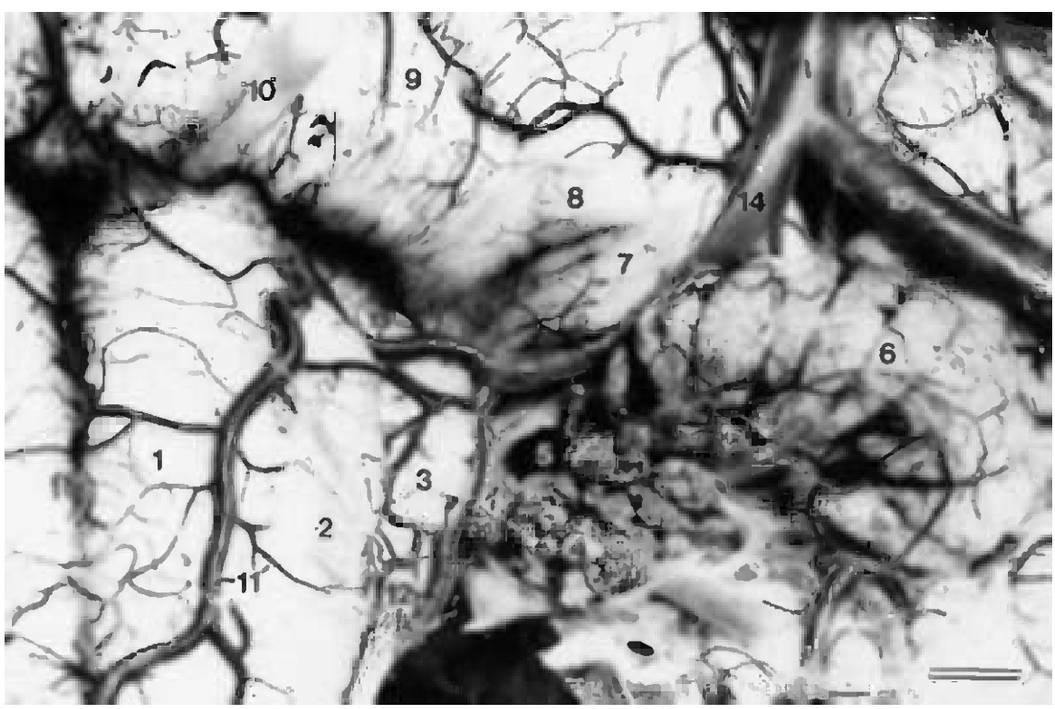

Fig. 6.13. The medulla. Posterior view. Bar: 2 mm.

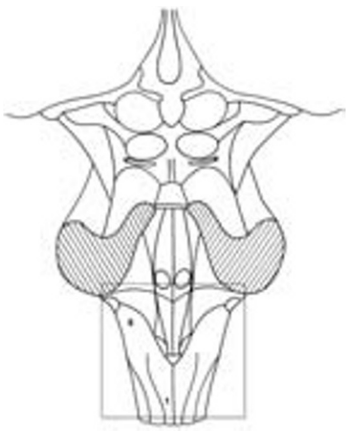

1 Medulla, posterior aspect
2 Accessory nerve, spinal root
3 Choroid plexus of the fourth ventricle
4 Median aperture of the fourth ventricle (foramen of Magendie)
5 Area postrema (5' ligula)
6 Inferior cerebellar peduncle (restiform body)
7 Posterior inferior cerebellar arteries
8 Posterior spinal arteries
9 Posterior median medullary vein
10 Marginal veins of the floor of the fourth ventricle
11 In this specimen the posterior venous network is drained towards the marginal sinus bordering the foramen magnum.
12 Posterior group of medullary arteries arising from the posterior inferior cerebellar arteries
13 Posterior group of medullary arteries arising from the posterior spinal arteries

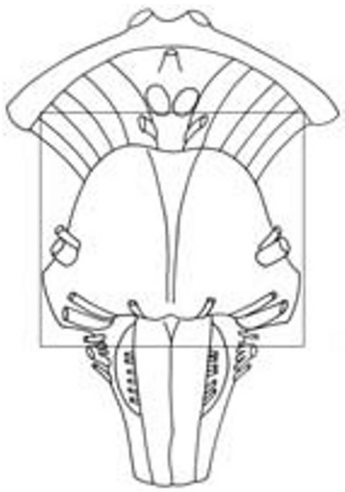

Fig. 6.14. Blood vessels on the anterior aspect of the pons.
Bar: 3.7 mm.

Arteries of the anterior pontine surface

1 Anterior surface of the pons
2 Basilar artery
3 Vertebral artery
4 Posterior inferior cerebellar artery
5 Anterior inferior cerebellar artery
6 Superior cerebellar artery
7 Posterior cerebral artery

Veins of the anterior pontine surface

8 The transverse pontine veins are drained into the superior petrosal vein (9)
10 Abducens nerve
11 Facial nerve
12 Vestibulocochlear nerve
13 Trigeminal nerve (note the density of veins around the root of this nerve)
14 Oculomotor nerve

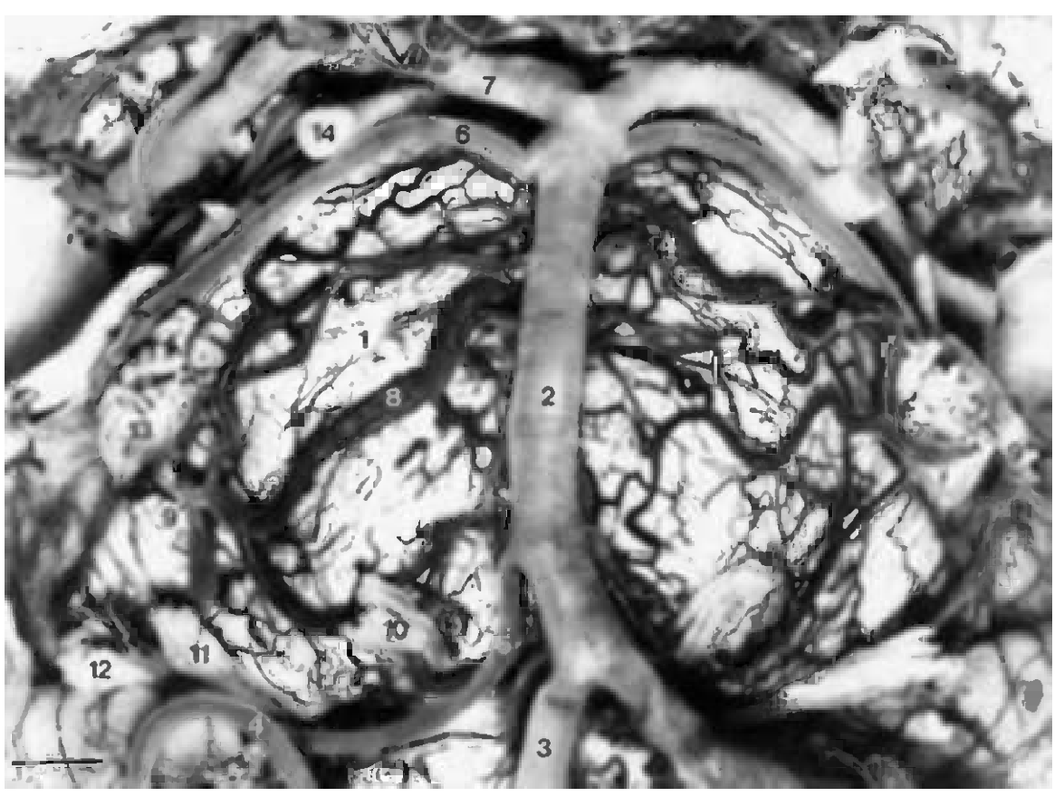

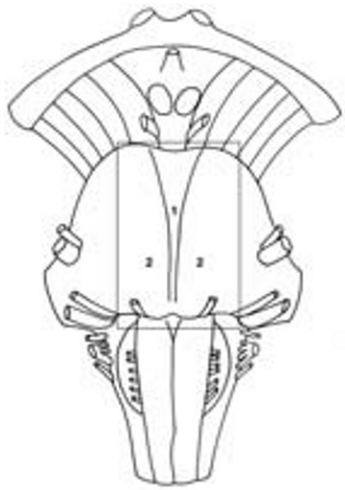

Fig. 6.15. Blood vessels on the anterior aspect of the pons. The basilar artery has been removed. Bar: 2 mm.

1 Basilar sulcus
2 Basilar portion of the pons
3 Abducens nerve
4 Anterior median pontine vein
5 Transverse pontine veins
6 Anteromedial group of pontine arteries entering the basilar sulcus
7 Anterolateral group of pontine arteries entering the basilar portion of the pons
8 Superior lateral pontine artery
9 Inferior lateral pontine artery
10 Anterior inferior cerebellar artery

Fig. 6.16. The pons. Right anterolateral view. Bar: 2 mm.

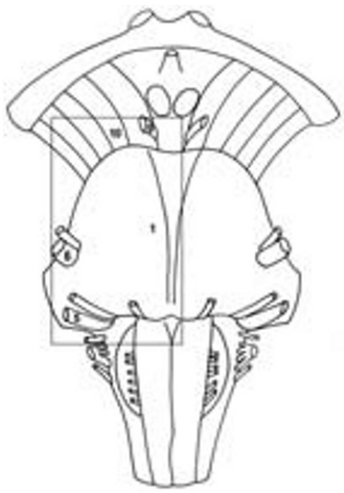

1 Basilar portion of the pons
2 Lateral pontine surface
3 Abducens nerve
4 Facial nerve
5 Vestibulocochlear nerve
6 Trigeminal nerve, sensory root
7 Trigeminal nerve, motor root
8 Trochlear nerve
12′, 12″ Medial and lateral branch of superior cerebellar artery
12‴ Posterolateral pontine artery
13 Basilar artery
14 Anterior inferior cerebellar artery
15 Vertebral artery
16, 16′ Superior (16) and inferior (16′) lateral pontine arteries
17 Transverse pontine vein
18 Transverse pontine veins, drained into the basilar plexus in this specimen
19 Anterolateral group of pontine blood vessels
20 Lateral group of pontine blood vessels

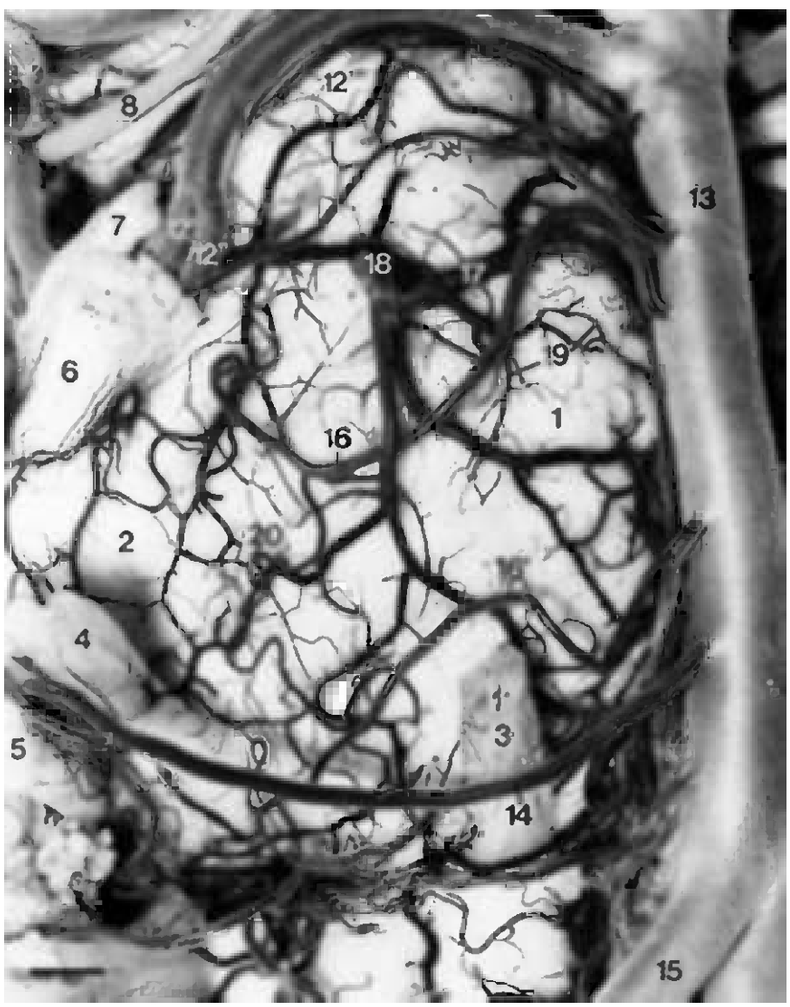

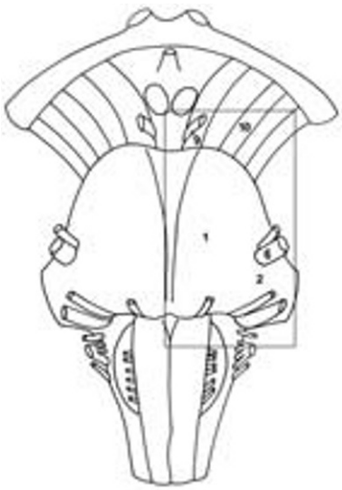

Fig. 6.17. The pons. Left anterolateral view. Bar: 2 mm.

1 Basilar portion of the pons
2 Lateral pontine surface
3 Abducens nerve
4 Facial nerve
5 Vestibulocochlear nerve
6 Trigeminal nerve, sensory root
7 Trigeminal nerve, motor root
8 Trochlear nerve
9 Oculomotor nerve
10 Anterior surface of the mesencephalon (crus cerebri, cerebral peduncle)
11 Basal vein, ventral segment
12 Posterior cerebral artery
13 Posterior medial choroidal artery
14 Collicular artery
15 Superior cerebellar artery
16 Basilar artery
17 Superior lateral pontine arteries
17′ Inferior lateral pontine arteries
18 Anterior inferior cerebellar artery
19 Vertebral artery
20 Posterior inferior cerebellar artery
21 Anterior cerebellar vein
22 Superior petrosal vein
23 Transverse pontine veins
24 Anterolateral group of pontine blood vessels
25 Lateral group of pontine blood vessels

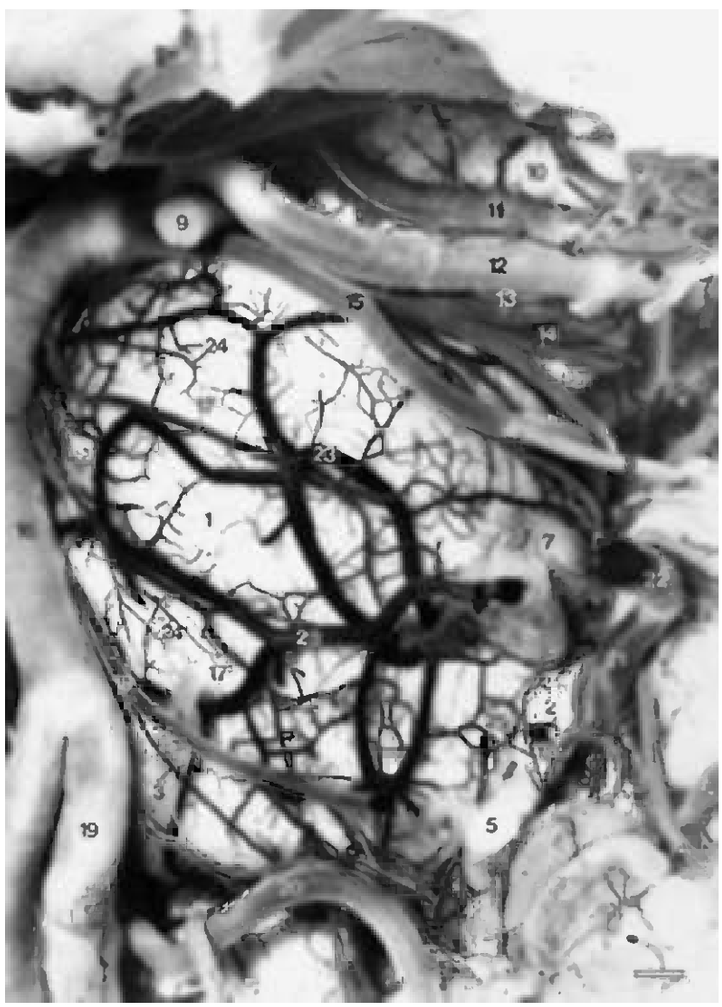

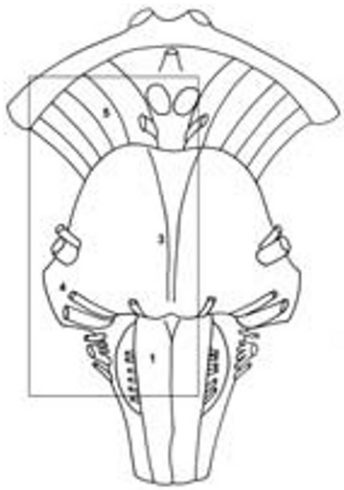

Fig. 6.18. The brain stem. Right anterolateral view of the pial venous network after removal of the overlapping superficial arterial network. Bar: 4 mm.

1 Pyramid of the medulla
2 Inferior olive
3 Basilar portion of the pons
4 Lateral aspect of the pons (brachium pontis)
5 Anterior mesencephalic aspect (crus cerebri, cerebral peduncle)
6 Oculomotor nerve
7 Abducens nerve
8 Facial nerve
9 Vestibulocochlear nerve
10 Trigeminal nerve
11 Anterior median pontine vein
12 Superior petrosal vein formed by the union of 13–15:
13 Transverse pontine veins
14 Anterior cerebellar vein
14′ Lateral pontine vein, and the
15 Lateral mesencephalic vein.
16 Tentorium cerebelli

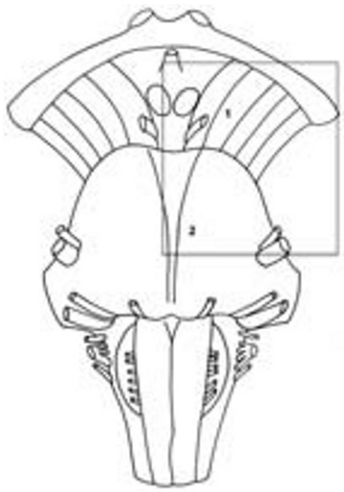

Fig. 6.19. The pontomesencephalic junction. Anterior view.
Bar: 2 mm.

1 Crus cerebri
2 Pons
3 Oculomotor nerve
4 Trochlear nerve

Several arterial trunks curve around the crus cerebri. They are, in descending order:

5 Anterior choroidal artery reaching the choroid plexus of the temporal horn of the lateral ventricle (5′)
6 Basal vein (ventral segment)
6′ Vein of the temporal horn of the lateral ventricle
7 Posterior cerebral artery
8 Superior cerebellar artery

The anterolateral group of mesencephalic vessels supplying the crus cerebri is hidden by these arterial trunks.

Fig. 6.20. The mesencephalon. Left lateral view. The posterior cerebral artery has been removed from this dissection. Bar: 2 mm.

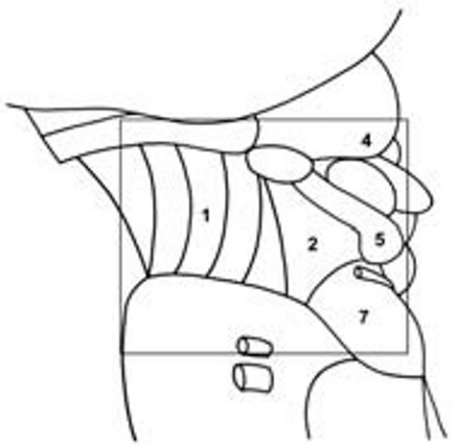

1 Crus cerebri
2 Lateral mesencephalic surface
3 Medial geniculate body
4 Pulvinar
5 Inferior colliculus
6 Trochlear nerve
7 Superior cerebellar peduncle (brachium conjunctivum)
8 Trigeminal nerve

Vascular trunks circling the mesencephalon

9 Basal vein, laterodorsal segment
9′ Vein of the temporal horn of the lateral ventricle
10 Posterior medial choroidal artery
11 Collicular artery
12 Superior cerebellar artery
12′ Lateral branch
12″ Medial branch
12‴ Supernumerary branch
13 Lateral mesencephalic vein
14 Lateral group of mesencephalic blood vessels
15 Thalamic branches arising from the posterior medial choroidal artery
16 Thalamogeniculate arteries (branches of the posterior cerebral artery)

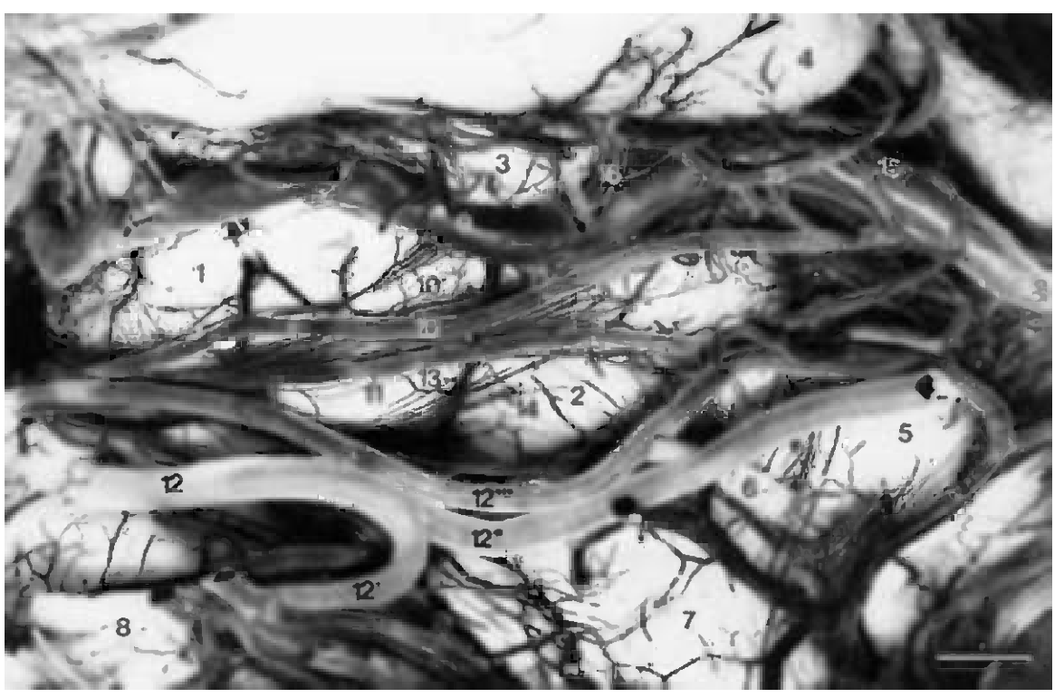

Fig. 6.21. The mesencephalon. Left lateral view of the mesencephalic veins after removal of the overlapping arterial network. Bar: 3 mm.

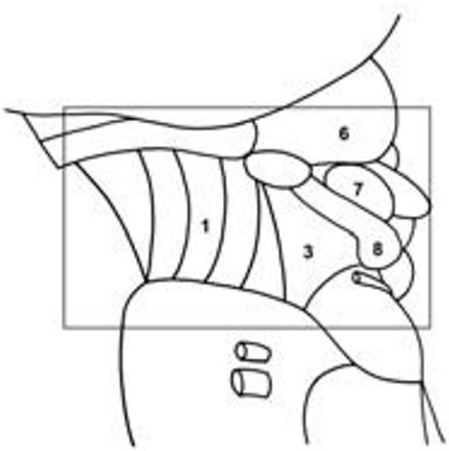

1 Crus cerebri (cerebral peduncle)
2 Pons
3 Lateral mesencephalic aspect
4 Lateral geniculate body
5 Medial geniculate body
6 Pulvinar
7 Superior colliculus
8 Inferior colliculus
9 Trochlear nerve
10 Superior cerebellar peduncle (brachium conjunctivum)
11 Basal vein, ventral segment
12 Vein of the temporal horn of the lateral ventricle
13 Basal vein, laterodorsal segment
14 Lateral mesencephalic vein
15 Internal cerebral vein
16 Great cerebral vein (of Galen)
17 Veins of the brachium conjunctivum

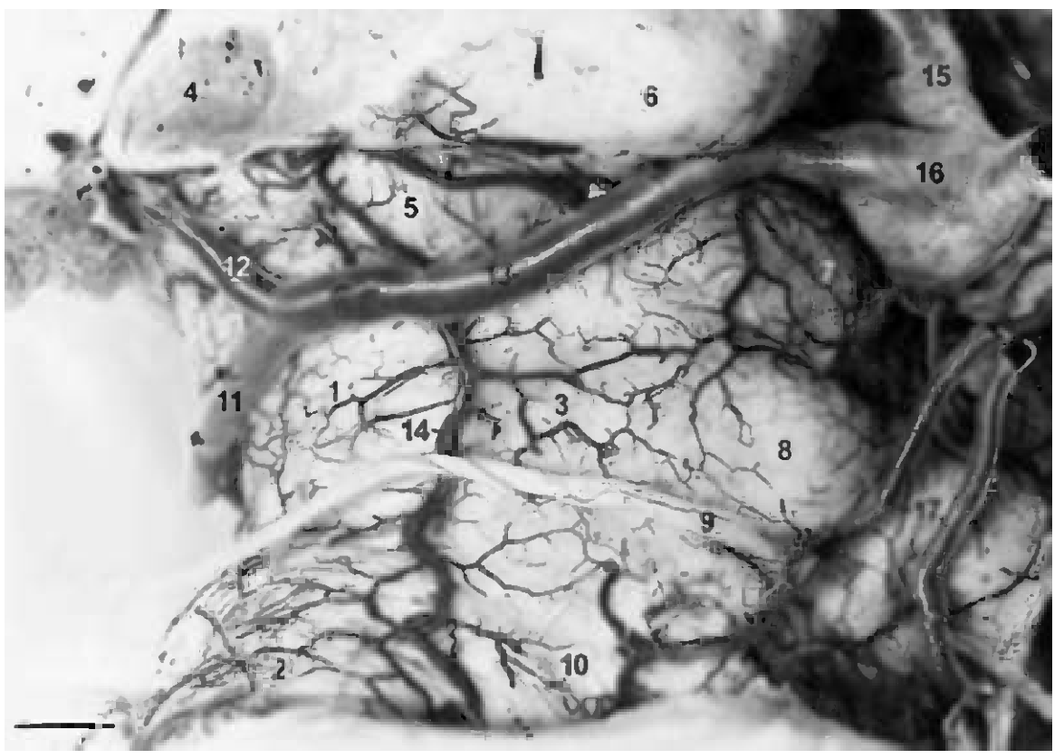

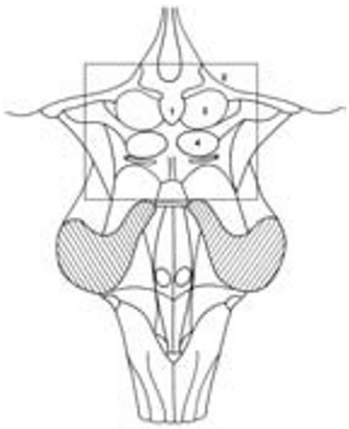

Fig. 6.22. The mesencephalon. Posterior view. The great cerebral vein (of Galen) and the internal cerebral veins were removed. Bar: 3 mm.

1 Pineal gland
2 Pulvinar
3 Superior colliculus
4 Inferior colliculus
5 Habenular trigone
6 Suprapineal recess
7 Basal vein of Rosenthal
The colliculi are almost completely covered by the posterior group of mesencephalic arteries.
8 Posterior medial choroidal arteries
9 Collicular arteries dividing into superior (9′) and inferior (9″) branches, supplying the superior and inferior colliculi, respectively
10 Median collicular vein
11 Right intercollicular vein
12 Veins of the superior cerebellar peduncles (brachia conjunctiva)

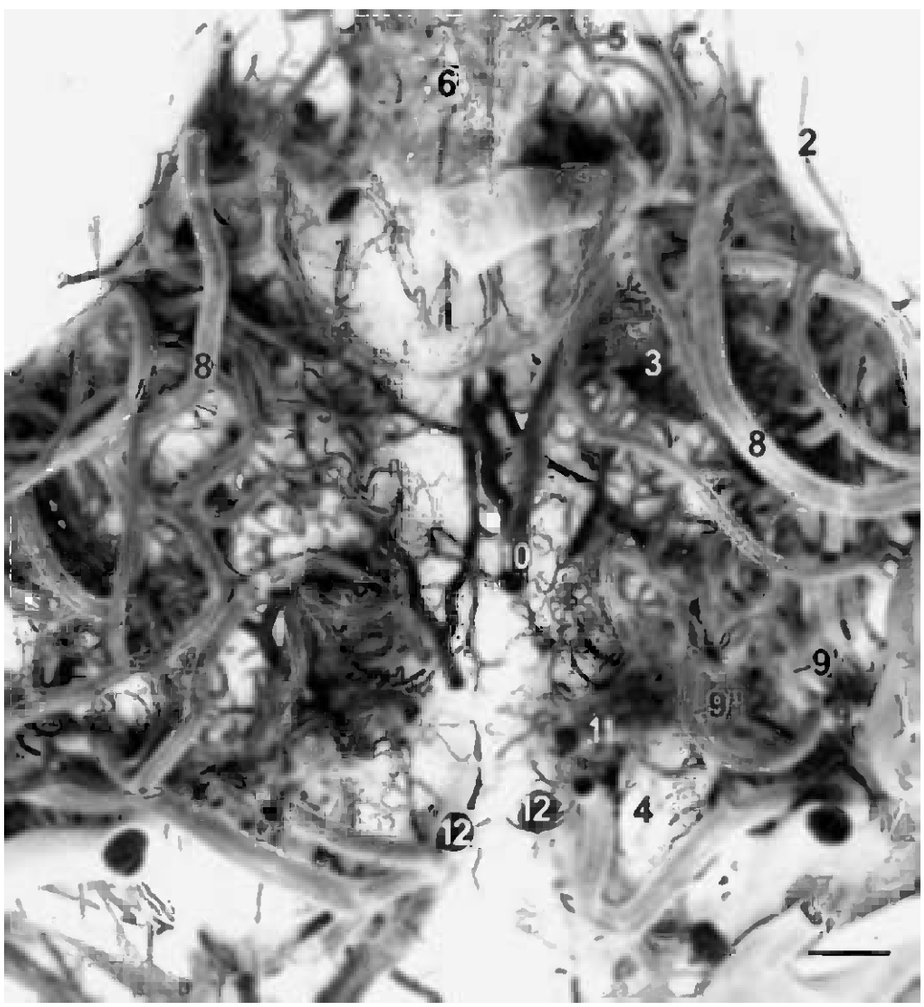

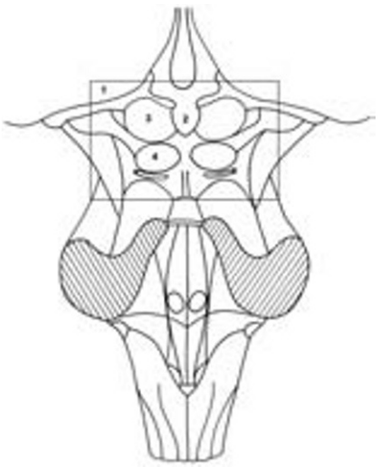

Fig. 6.23. The mesencephalon. Posterior view. The great cerebral vein (of Galen), internal cerebral, and basal veins were removed. Bar: 2 mm.

1 Pulvinar
2 Pineal gland (displaced upward)
3 Superior colliculus
4 Inferior colliculus
5 Precentral vein
6 Veins of the brachium conjunctivum
7 Superior cerebellar artery (medial branch)
8 Collicular artery
9 Posterior medial choroidal artery
10 Superior and median intercollicular vein

Note the density of the posterior group of mesencephalic blood vessels overlying and obscuring the superior and inferior colliculi.

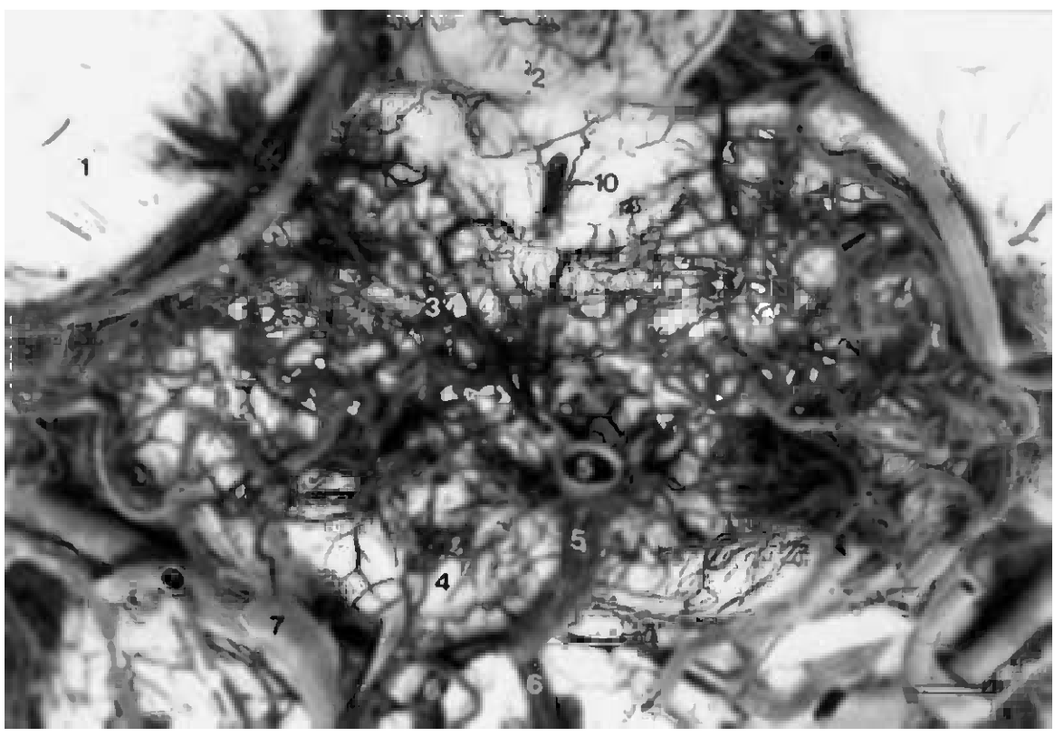

Fig. 6.24. The pineal gland and collicular region. Venous network covering the colliculi. Posterior view. Bar: 4 mm.
The internal cerebral veins, the great cerebral vein (of Galen) and the arterial network have been removed.

1 Pineal gland
2 Pretectal area
3 Superior colliculus
4 Inferior colliculus
5 Superior median collicular vein
6 Intercollicular veins

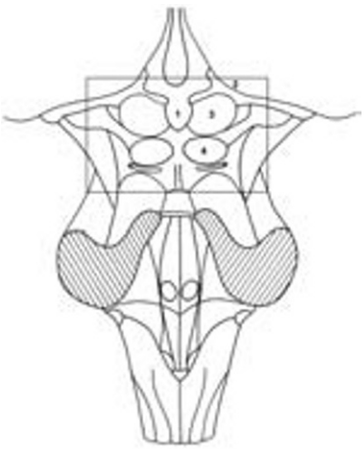

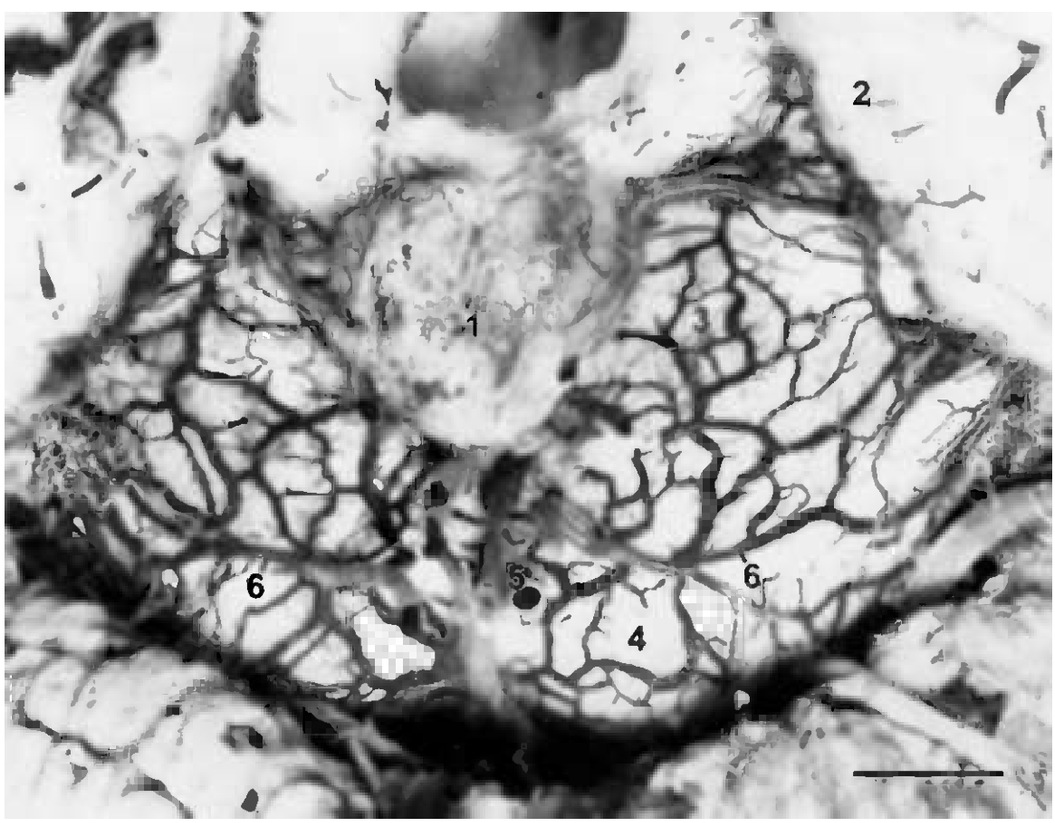

Fig. 6.25. The precentral cerebellar vein. Lateral view.
Bar: 2.5mm.

1-4 The precentral vein is divided into a longitudinal segment (1) and a dorsal segment (2), which meet at a right angle (3). It drains into the great cerebral vein (of Galen) (4).
5 Opening of the left basal vein into the great cerebral vein
6 Internal cerebral vein
7 Pineal gland (inferior aspect)

Tributaries of the precentral vein
8 Left vein of the superior cerebellar peduncle (vein of the brachium conjunctivum)
9 Vein of the precentral lobule (9')
10 Vein of the culmen (10')
11 Left intercollicular vein
12 Median collicular vein
13 Left superior colliculus
14 Left inferior colliculus
15 Trochlear nerve

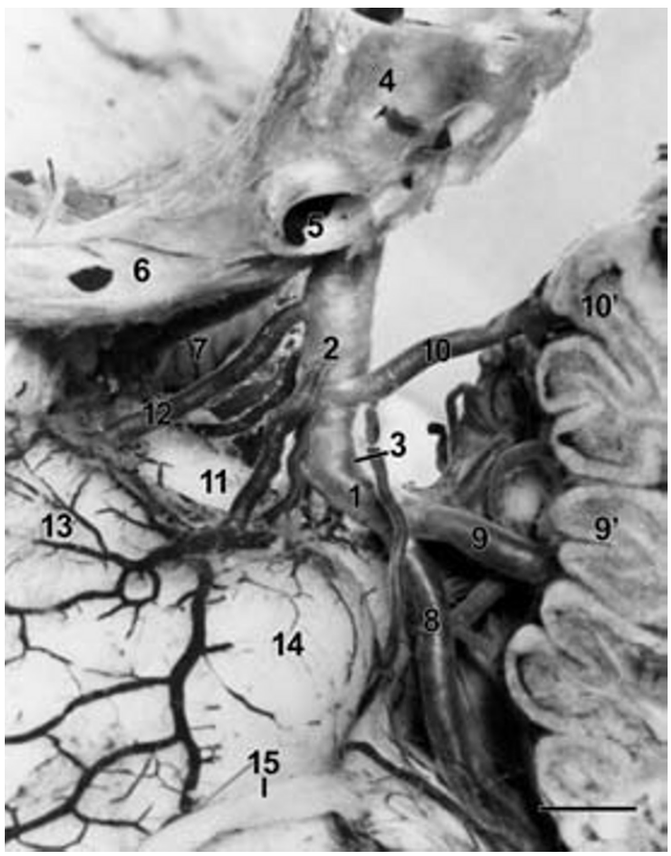

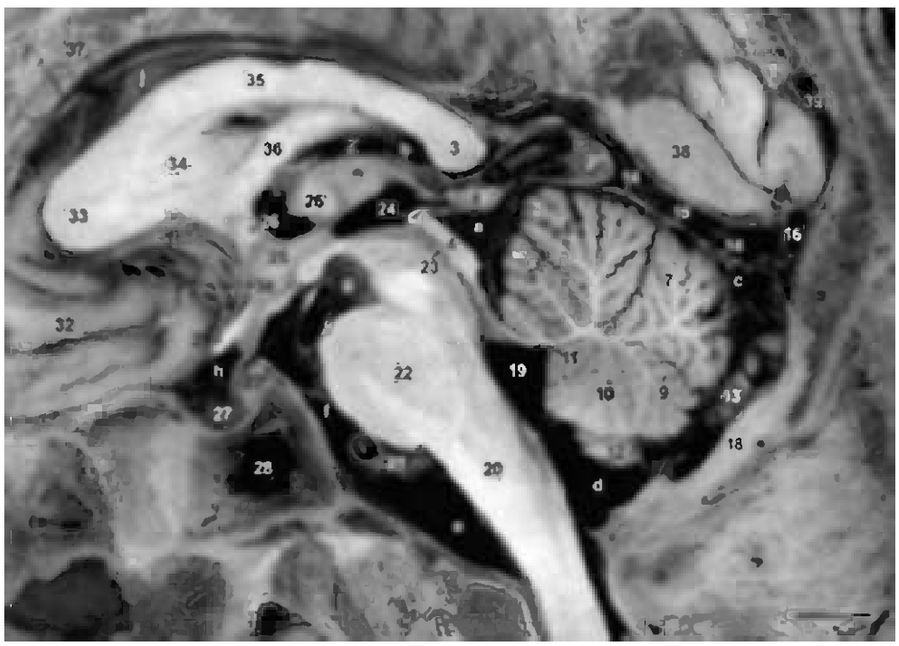

6.26

Figs. 6.26 and 6.27. The relationship of the pineal gland to the surrounding structures. Median sagittal section of the head.
6.26. Gross anatomic specimen. Bar: 12.7 mm.
6.27. Corresponding diagram.

1 Pineal gland
2 Great cerebral vein (of Galen)
2′ Internal cerebral vein
2″ Cavernous body
3 Splenium
4 Quadrigeminal plate

Cerebellar vermis
5 Central lobule
6 Culmen
7 Declive
8 Great horizontal fissure
9 Pyramid
10 Uvula
11 Nodule
12 Tonsil
13 Medial aspect of the right cerebellar hemisphere
14 Tentorium cerebelli
15 Sinus rectus (straight sinus)
16 Torcular Herophili
17 External occipital protuberance
18 Occipital squama
19 Fourth ventricle
20 Medulla
21 Right vertebral artery
22 Pons
23 Cerebral aqueduct
24 Posterior commissure

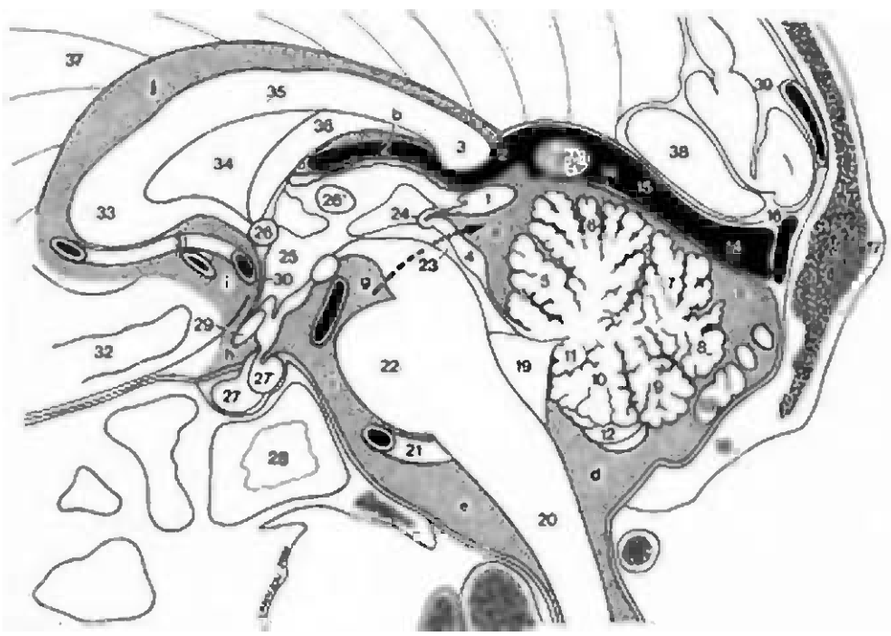

6.27

25 Third ventricle
26 Anterior commissure
26′ Interthalamic adhesion (massa intermedia)
27 Hypophysis (anterior lobe)
27′ Hypophysis (posterior lobe)
28 Sphenoid sinus
29 Optic chiasm
30 Lamina terminalis
31 Anterior cerebral artery
32 Right frontal lobe, medial aspect
33 Genu of corpus callosum
34 Septum pellucidum
35 Body of corpus callosum
36 Fornix
37 Falx cerebri
38 Occipital lobe, medial aspect
39 Superior sagittal sinus

Subarachnoid cisterns

a Quadrigminal plate cistern
b Cistern of the velum interpositum (median portion of the transverse fissure)
c Superior cerebellar cistern
d Cerebellomedullary cistern (cisterna magna)
e Premedullary cistern
f Prepontine cistern
g Interpeduncular cistern linked to the quadrigeminal cistern by the ambient cistern around the lateral aspect of the mesencephalon (arrow in diagram)
h Chiasmatic (perihypophyseal) cistern
i Cistern of the lamina terminalis
j Supracallosal cistern

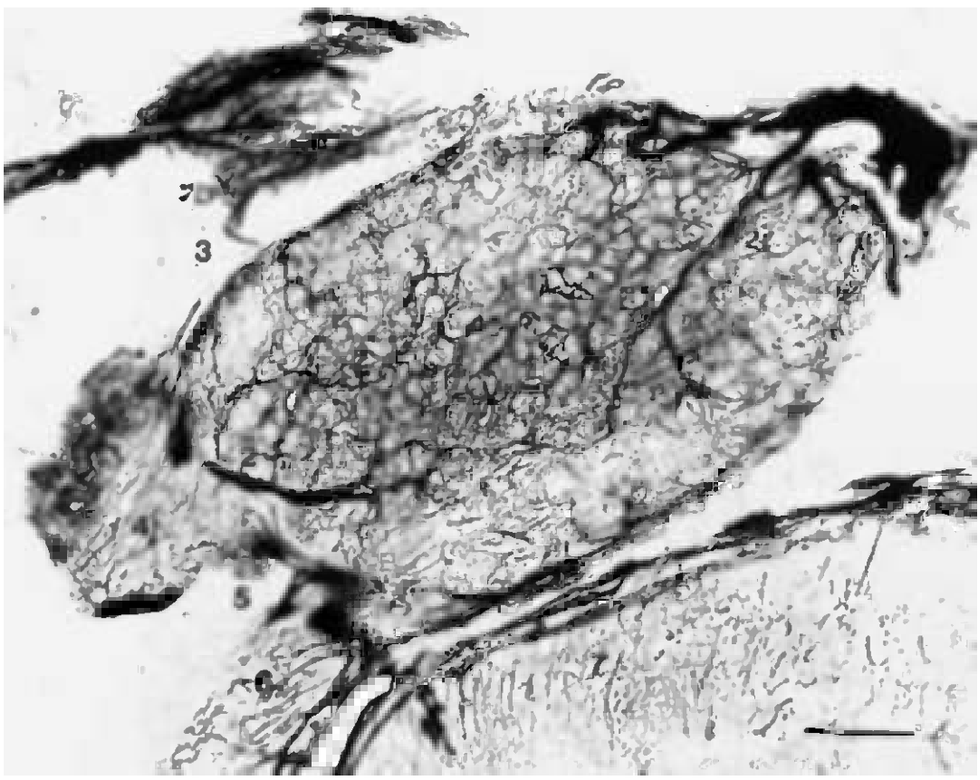

Fig. 6.28. The pineal gland: Median sagittal section.
Bar: 0.8 mm.
The blood supply reaches the pineal gland through vascular pedicles that penetrate its superior, lateral and inferior aspects.

1 Pineal gland
2 Intrapineal vascular pedicles
3 Suprapineal recess
4 Habenular commissure
5 Pineal recess
6 Posterior commissure
7 Quadrigeminal plate

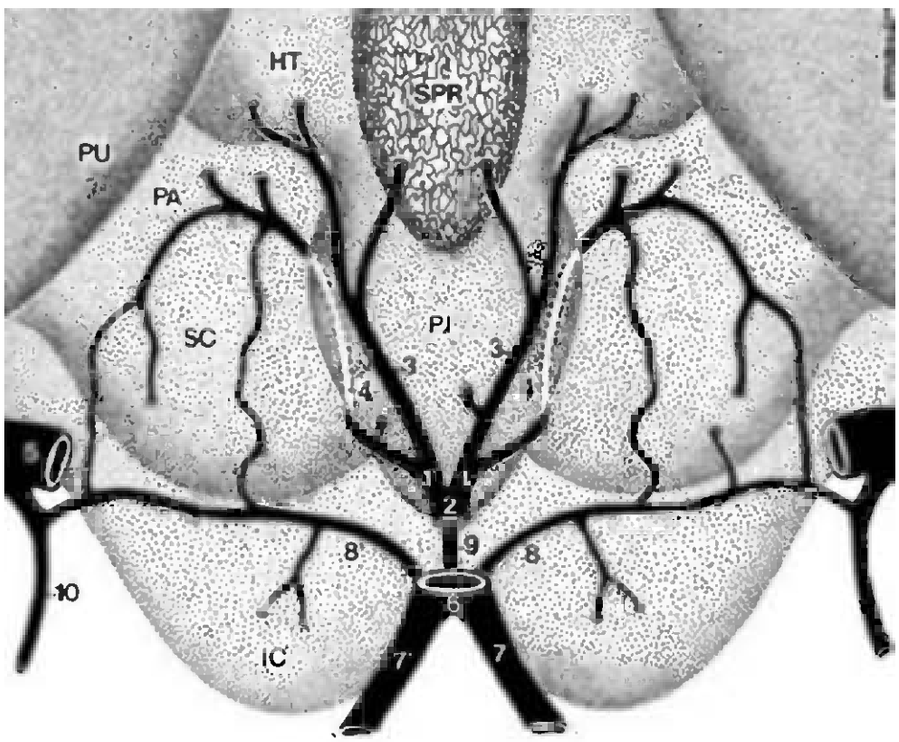

Fig. 6.29. The venous network along the superior aspect of the pineal gland. Diagram after removal of the internal cerebral veins and arteries.

HT Habenular trigone
IC Inferior colliculus
PA Pretectal area
PI Pineal gland
PU Pulvinar
SC Superior colliculus
SPR Suprapineal recess

Pineal veins

The right (1) and left (1′) lateral pineal veins join together to form the medial pineal vein (2) reaching the great cerebral vein (of Galen). Each lateral pineal vein receives a superior (3) and inferior (4) lateral pineal vein draining blood from the pineal gland, habenular trigone, suprapineal recess (for the superior lateral vein), pretectal area, and superior colliculus (for the inferior lateral vein). In practice, this symmetrical arrangement is subject to numerous variations.

5 Basal vein
6 Precentral cerebellar vein
7, 7′ Right and left veins of the superior cerebellar peduncle (veins of the brachium conjunctivum)
8, 8′ Right and left intercollicular veins
9 Superior median collicular vein
10 Lateral mesencephalic vein

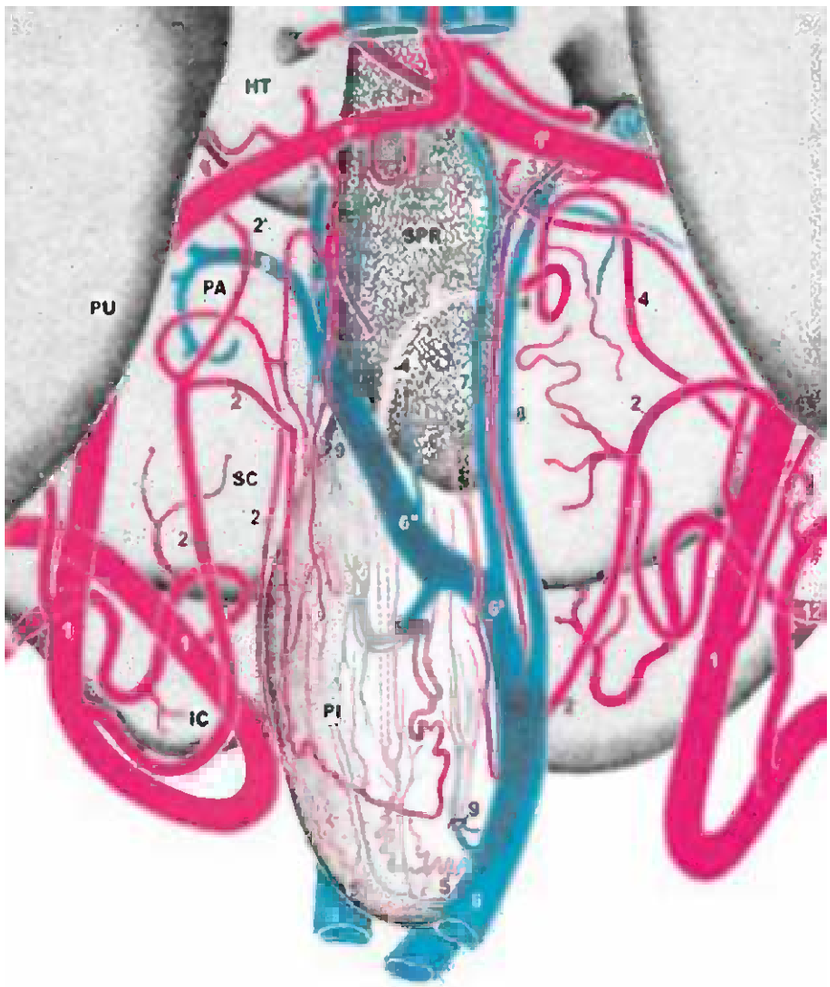

Figs. 6.30 and 6.31. The pineal region.
(Fig. 6.30) **Diagram** and (Fig. 6.31) **Intravascular India ink injection** of the vessels of the pineal region. The splenium of the corpus callosum and the internal cerebral veins have been removed. [126, 139, 261, 356, 426, 427, 448] See also Fig. 6.32

HT Habenular trigone
IC Inferior colliculus
PA Pretectal area
PI Pineal gland
PU Pulvinar
SC Superior colliculus
SPR Suprapineal recess

1 Medial posterior choroidal arteries in the quadrigeminal cistern
1′ Medial posterior choroidal arteries in the cistern of the velum interpositum

Pineal arteries (red)

2 The lateral pineal arteries, the most frequent and important, usually arise from the quadrigeminal segment of the medial posterior choridal arteries (and sometimes from the collicular arteries in the ambient cistern). They reach the gland by frequent recurrent paths. They often supply the pretectal area (2′).
3 The rostral pineal arteries, small in size, arise from the medial posterior choroidal arteries near the cistern of the velum interpositum.
4, 5 An occasional median pineal artery lies on the inferior surface of the gland. All these arteries (2, 3, and 4) converge toward the apex of the pineal gland, where they resolve into a tortuous and anastomotic subpial arterial plexus (5), situated predominantly on the inferior aspect of the gland.

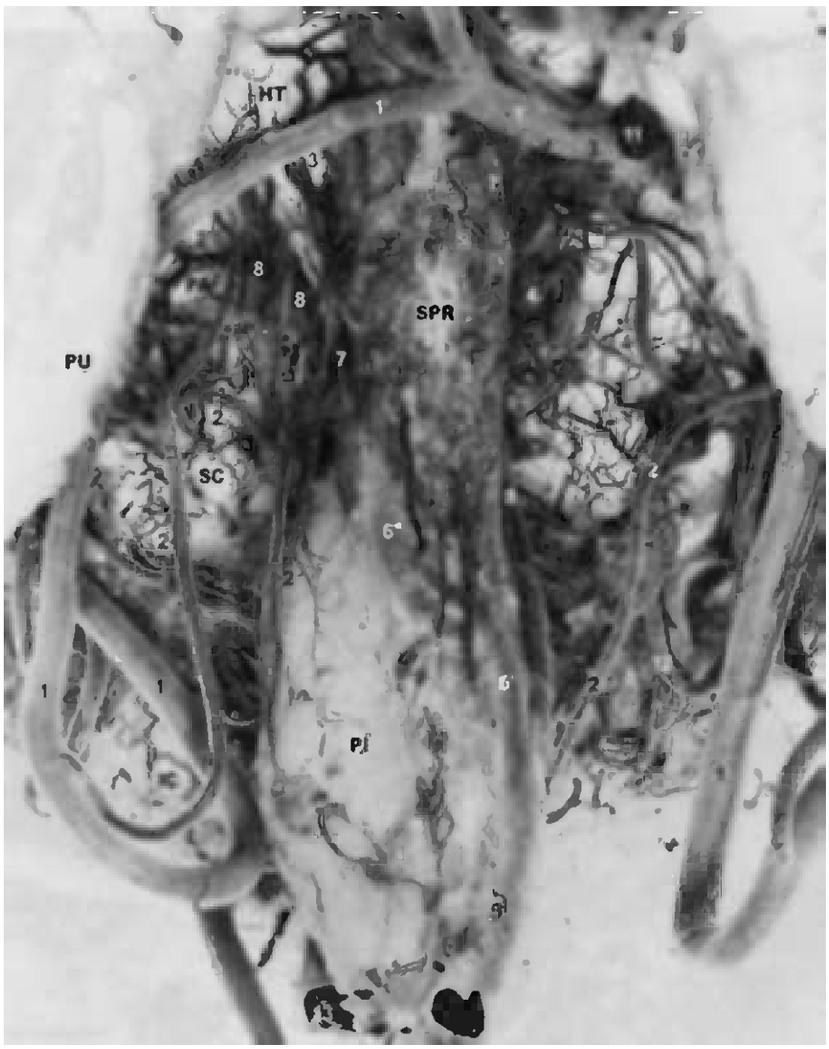

Pineal veins (blue)

6 The median pineal vein draining the right (6′) and left (6″) pineal veins is displaced laterally in this preparation. Each lateral pineal vein receives a superior and inferior lateral pineal vein.

7 The superior lateral pineal veins also drain the choroid plexi and the habenular trigone.

8 The inferior lateral pineal veins also receive drainage from the pretectal area and the neighboring superior colliculus. The pineal arteries and veins are subject to many variations. The pineal gland receives its internal blood supply via penetrating vascular pedicles, which are often composed of a large main artery paired with a small satellite artery (9).

10 Internal cerebral veins

11 Posterior (principal) thalamic vein

12 Collicular arteries

13 Precentral cerebellar vein

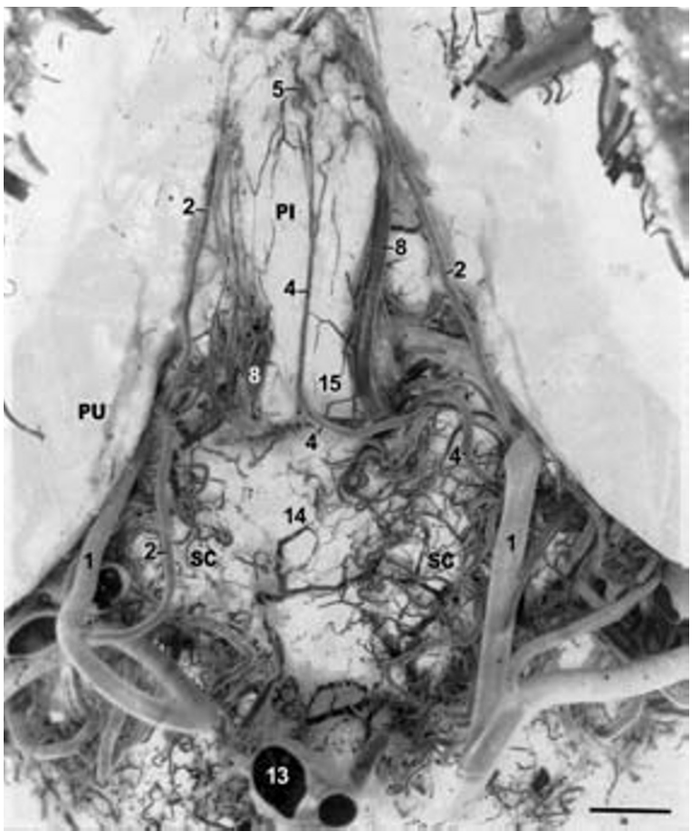

Fig. 6.32. The pineal gland. Inferior surface. The pineal gland (PI) has been reflected superiorly to reveal its inferior surface and the colliculi. Bar: 2.5 mm.
Same specimen as shown in **Figs. 6.30** and **6.31**.

1 Medial posterior choridal arteries
4, 5 Course and branches of the median pineal artery. The pineal arterial branches often resolve into subpial arterial plexi of high density (5) before penetrating the pineal tissue.
8 Inferior lateral pineal vein
13 Precentral cerebellar vein
14 The region between the two superior colliculi (SC), which is normally hidden by the pineal gland, is poorly vascularized. In this preparation the superior median collicular vein is absent.
15 Inferior aspect of the pineal stalk

PU Pulvinar

Fig. 6.33. The venous and arterial relationships of the dorsal surface of the pineal gland. The fibrous trabeculae of the velum interpositum have been removed. Bar: 3 mm.

1 Pineal gland
2 Suprapineal recess
3 Medial posterior choroidal arteries
4 Internal cerebral veins
5 Habenular trigone
6 Posterior ventricular vein (medial atrial vein)
6′ Posterior (principal) thalamic vein
7 Lateral pineal veins
7′ Median pineal vein
8 Great cerebral vein (of Galen)
9 Right basal vein of Rosenthal
10 The left basal vein is small in diameter

Fig. 6.34. The pineal gland. Transverse section. Intravascular India ink injection. Bar: 0.85 mm.

1, 2 The highly vascularized central portion of the gland (1) contrasts with the poorly vascularized periphery (2)
3 Suprapineal recess
4 Lateral pineal veins
5 Internal cerebral veins
6 Splenium of the corpus callosum
7 Superior median collicular vein
8 Superior colliculus

Fig. 6.35. The pineal gland. Transverse section. Intravascular India ink injection. Bar: 2 mm.

1 Pineal gland
1′ The large vascular network in the dorsal and the central portions of the gland is composed of sinusoidal capillaries surrounding the pineal lobules. This contrasts with the fine vascular network irrigating the homogeneous pineocytes (1″) in the ventral portion of the gland. This difference suggests differing exchanges between the blood and pineocytes in the lobules and in the homogeneous portion of the gland.
2 Posterior commissure
3 Cerebral aqueduct
4 Nucleus of Darkschewitsch (accessory oculomotor nucleus)
5 Interstitial nucleus (Cajal)

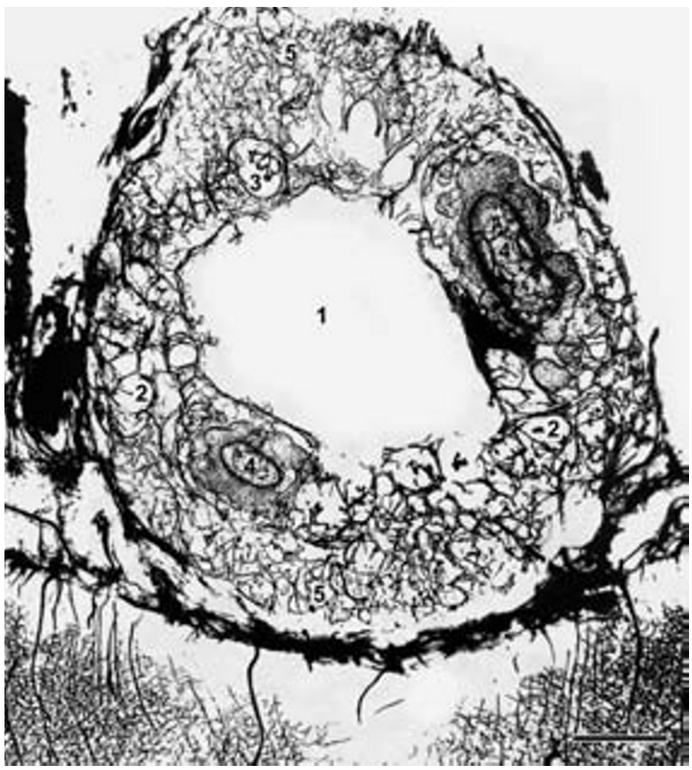

Fig. 6.36. Characteristic structure of the pineal gland. Transverse section. Intravascular India ink injection. Bar: 1 mm.

1 Typical glial cavity surrounded by pineal tissue, formed by lobules (2), some invaded by capillary loops (3)
4 Calcareous concretions
5 Fine peripheral vascular network

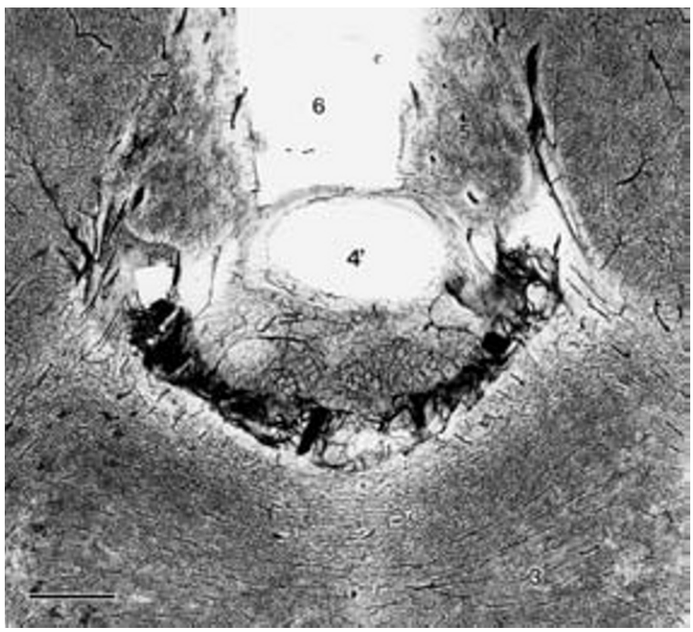

Fig. 6.37. The epithalamus. Posterior superior view. India ink injection. Bar: 2.2 mm.

3 Superior collliculus
4 Pineal gland with intrapineal cyst (4')
5 Habenular trigone, a leaf-like region composed of the medial and lateral habenular nuclei on each side of the posterior third ventricle (6)

B. Deep Vascularization of the Brain Stem with MR I correlation (Figs. 6.38–6.53)

Figures 6.38–6.53 illustrate the deep vascular anatomy of the brain stem in three orthogonal planes, using both intravascular India ink injections and, where possible, corresponding magnetic resonance images at 9.4 Tesla. The far richer capillary network of gray matter vs. white matter provides sufficient contrast to distinguish the capillary-rich brain stem nuclei from the more poorly vascularized major white matter tracts. The "capillary maps" created by India ink injection correlate very well with the differing signal intensities of these structures on intermediate-weighted high resolution MR images.

Fig. 6.38 (A–B). The medulla. Paramedian section.
A. Intravascular India ink injection. Bar: 2 mm.
B. 9.4 T Magnetic resonance microscopy.

1 Decussation of the pyramids
2 Corticospinal tract
3 Medial lemniscus
4 Arcuate nucleus
5 Pontine nucleus
6 Hypoglossal nucleus
7 Sublingual nucleus (of Roller)
8 Dorsal motor nucleus of the vagus
9 Area postrema
10 Nucleus of the solitary tract
11 Gracile nucleus

Arrows: Blood vessels belonging to the internal anteromedial medullary group.

A

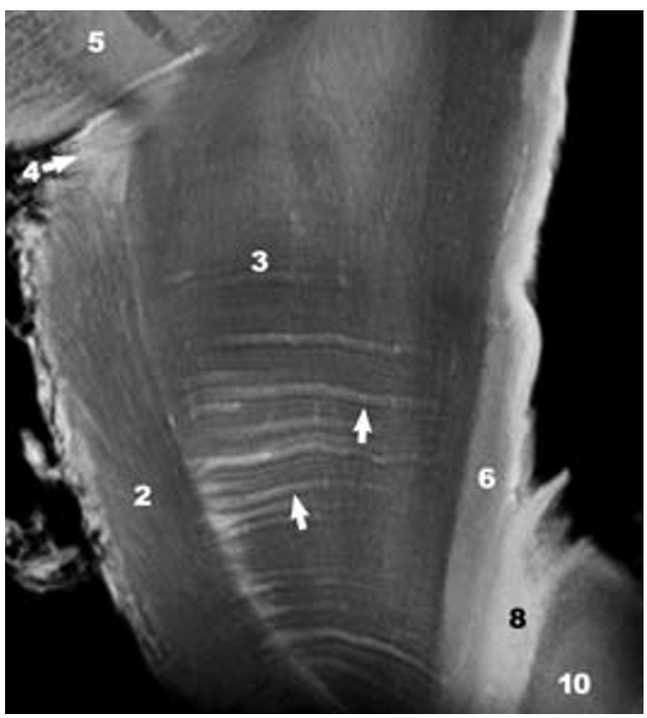

B

Fig. 6.39 (A–B). The medulla. Sagittal section.
A. Intravascular India ink injection. Bar: 2 mm.
B. 9.4 T Magnetic resonance microscopy.

1 Corticospinal tract
2 Medial accessory olivary nucleus
3 Inferior olivary nucleus
4 Dorsal accessory olivary nucleus
5 Hilum of the inferior olivary nucleus
6 Gracile nucleus
7 Dorsal motor nucleus of the vagus
8 Medial vestibular nucleus
9 Pontine nuclei
10 Solitary tract (dark) with surrounding solitary nucleus (light)

A

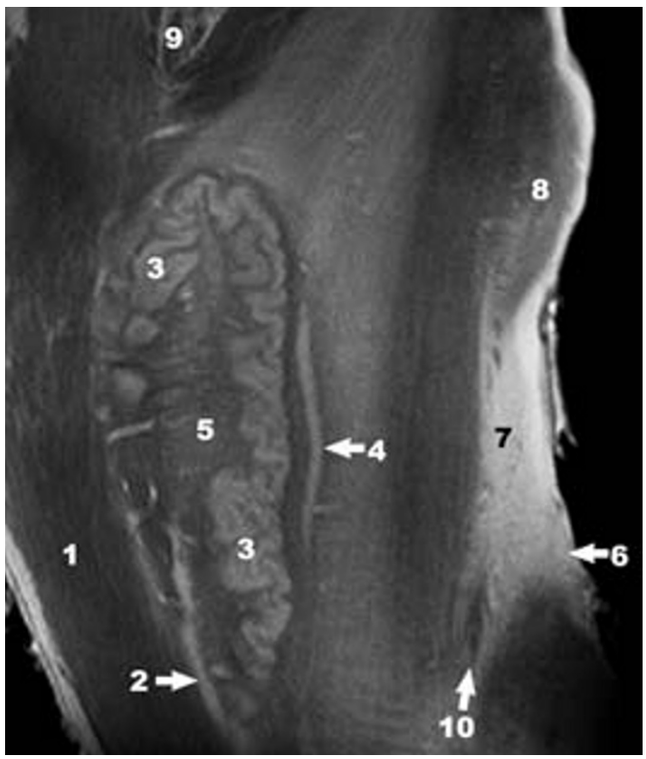

B

A

Fig. 6.40 (A–B). The pontomedullary junction. Sagittal section.

A. Intravascular India ink injection. Bar: 2.5 mm.

B. 9.4 T Magnetic resonance microscopy.

1 Inferior olivary nucleus
2 Pontomedullary sulcus
2′ Abducens nerve emerging from the pontomedullary sulcus
3 Pontine nuclei
4 Spinal trigeminal tract
5 Superior vestibular nucleus
6 Lateral vestibular nucleus
7 Medial vestibular nucleus
8 Accessory cuneate nucleus
9 Spinal trigeminal nucleus (subnucleus oralis)
10 Spinal trigeminal nucleus (subnucleus interpolaris)
11 Solitary tract (dark) with surrounding solitary nucleus (light)

Arrows: Cross-sections of internal lateral medullary vessels

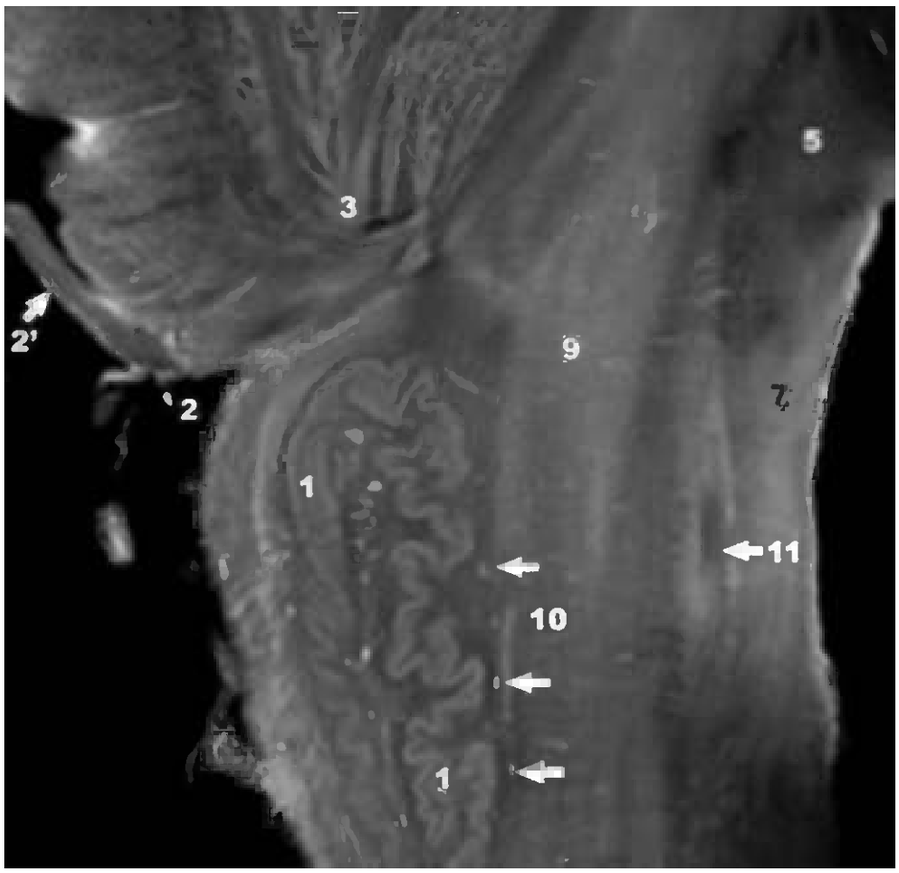

B

A B

Fig. 6.41 (A–B). The ventral medulla. Coronal section.
For more information, see [120, 121].
A. Intravascular India ink injection. Bar: 2 mm.
B. 9.4 T Magnetic resonance microscopy.

1 Hilum of the inferior olivary nucleus
1′ Inferior olivary nucleus
2 Medial accessory olivary nucleus
3 Medial lemniscus
4 Corticospinal tract
5 Arcuate nucleus
6 Decussation of the corticospinal tracts

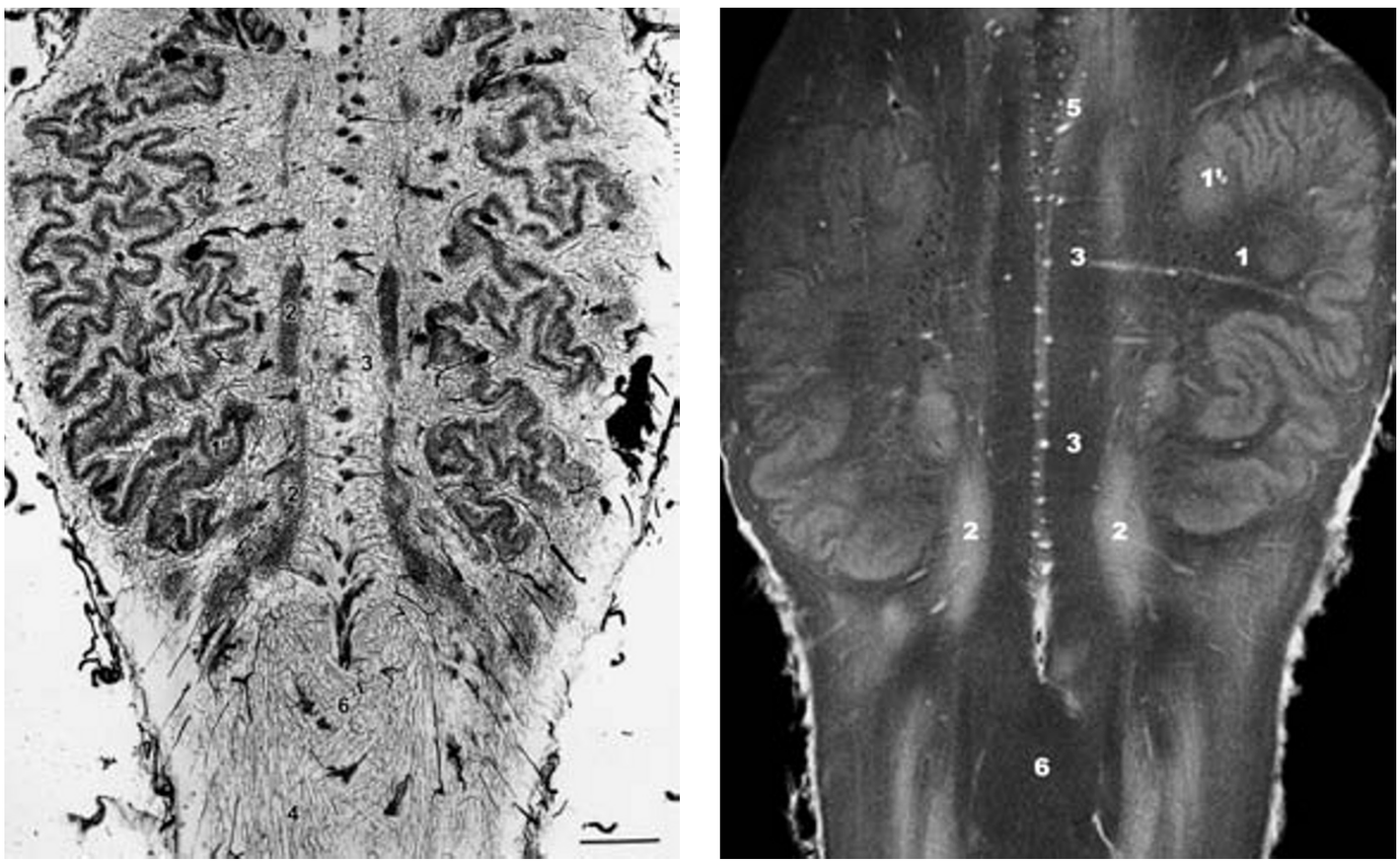

A B

Fig. 6.42 (A–B). The ventral medulla. Coronal section dorsal to Fig. 6.41.

A. Intravascular India ink injection. Bar: 2 mm.

B. 9.4 T Magnetic resonance microscopy.

1 Hilum of the inferior olivary nucleus
1′ Inferior olivary nucleus
2 Medial accessory olivary nucleus
3 Medial lemniscus
5 Arcuate nucleus
6 Decussation of the corticospinal tracts

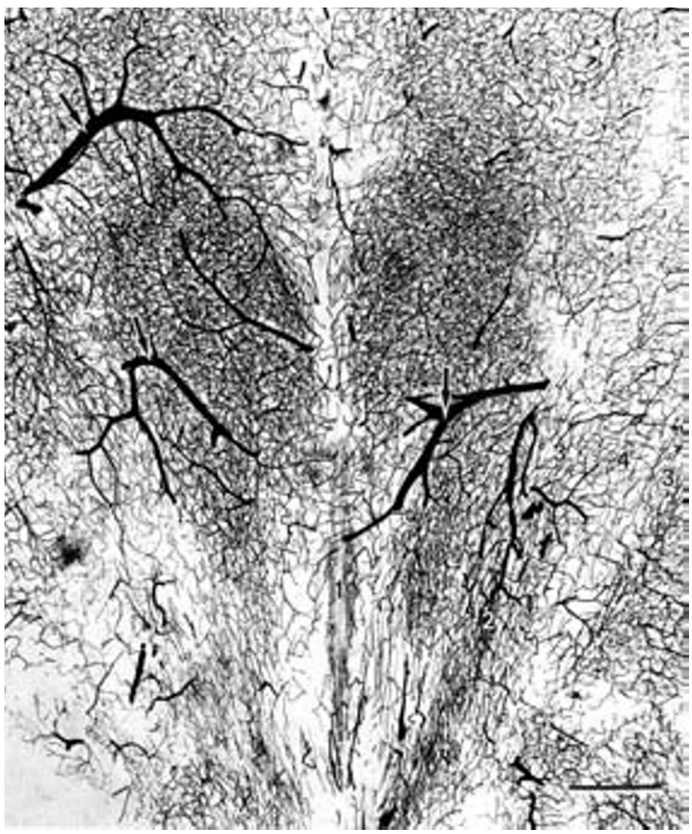

A

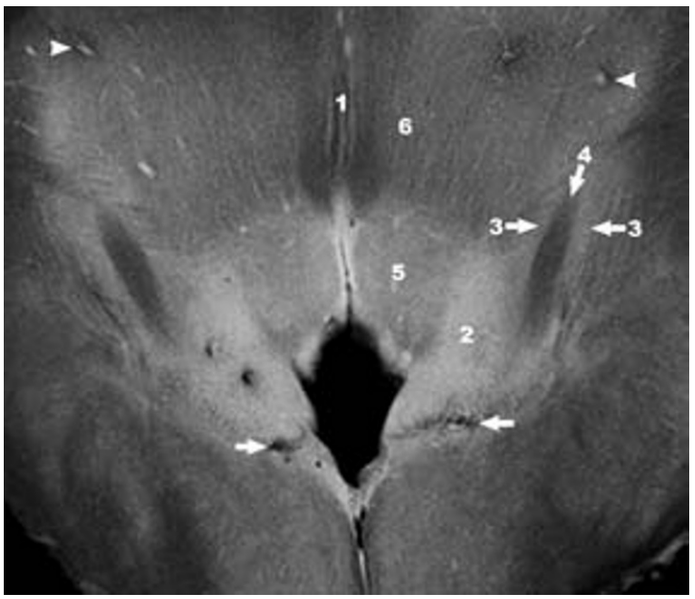

B

Fig. 6.43 (A–B). The dorsal medulla. Coronal section.
A. Intravascular India ink injection. Bar: 930 µm.
B. 9.4 T Magnetic resonance microscopy.

1 Median sulcus of the fourth ventricle
2 Dorsal motor nucleus of the vagus
3 Nucleus of the solitary tract
4 Solitary tract
5 Hypoglossal nucleus
6 Nucleus prepositus hypoglossi

Arrowheads: The internal anterolateral group of vessels
Arrows: Veins of the internal lateral medullary group

A

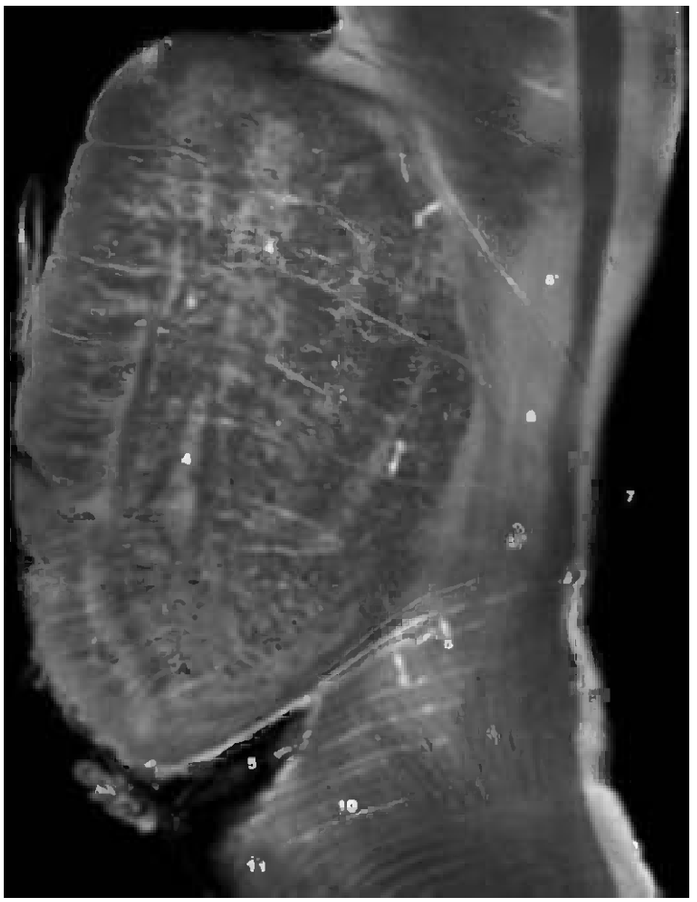

B

Fig. 6.44 (A–B). The pons and adjoining brain stem. Sagittal sections.

A. Intravascular India ink injection. Bar: 2.2 mm.

B. 9.4 T Magnetic resonance microscopy (composite of two specimens, see Fig. 7.1).

General orientation of vessels supplying the pontine tegmentum

1 Interpeduncular fossa
2 Arteries and veins belonging to the inferior pedicle of the interpeduncular fossa with their characteristically-curved downward route toward the superior pontine tegmentum (8′)
3 Internal principal anteromedian vein of the pons
4 Pontine nuclei
5 Foramen cecum
6 Arteries and veins of the foramen cecum (note their characteristically-curved upward course toward the inferior pontine tegmentum) (8″)
7 Fourth ventricle
8 Pontine tegmentum (mid portion)
8′ Superior pontine tegmentum
8″ Inferior pontine tegmentum
9 Basilar portion of the pons
10 Medulla
11 Arcuate nuclei

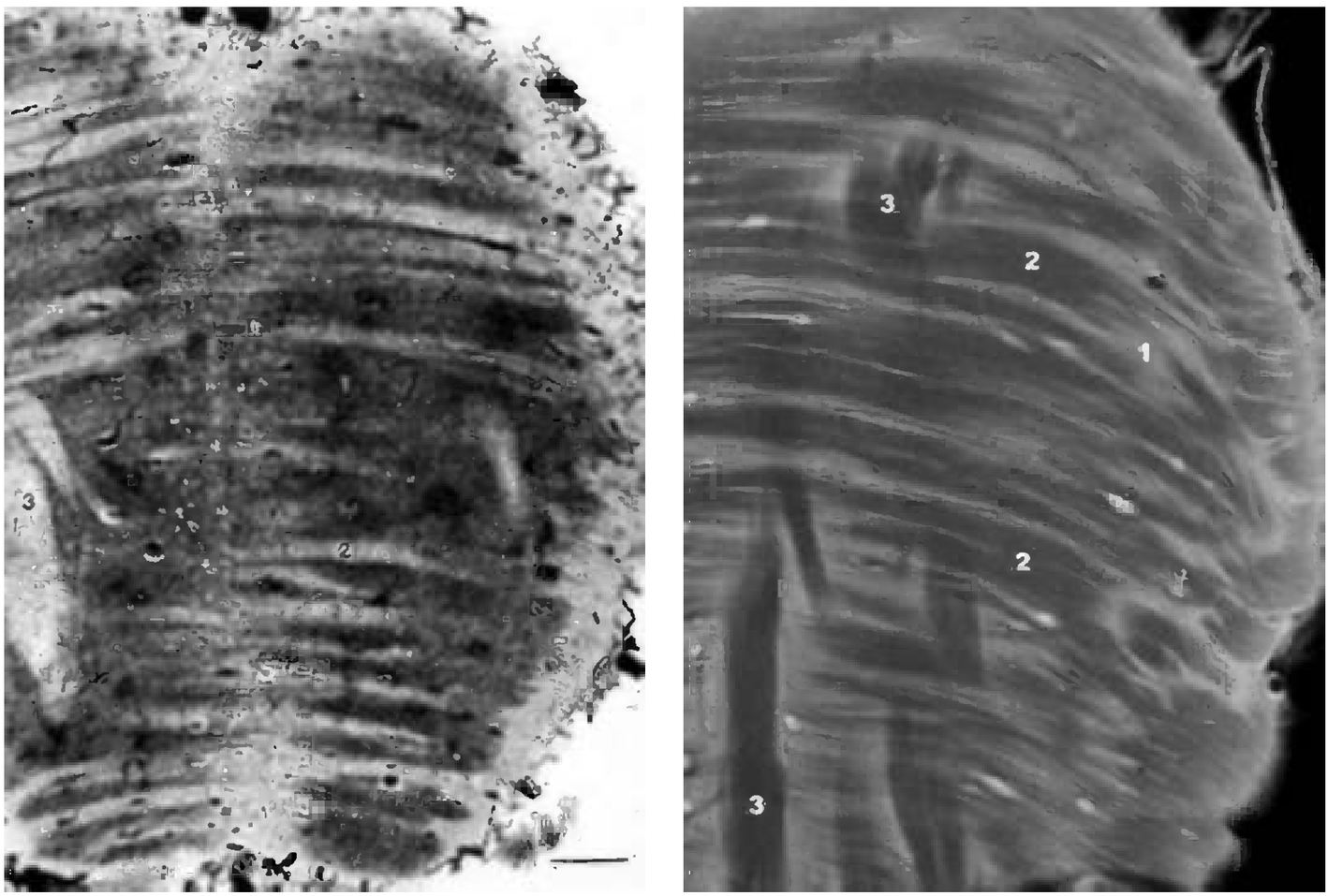

A B

Fig. 6.45 (A–B). The ventral pons. Coronal section.
A. Intravascular India ink injection. Bar: 2.2 mm.
B. 9.4 T Magnetic resonance microscopy.

1 Pontine nucleus
2 Pontocerebellar fibers
3 Corticospinal tract

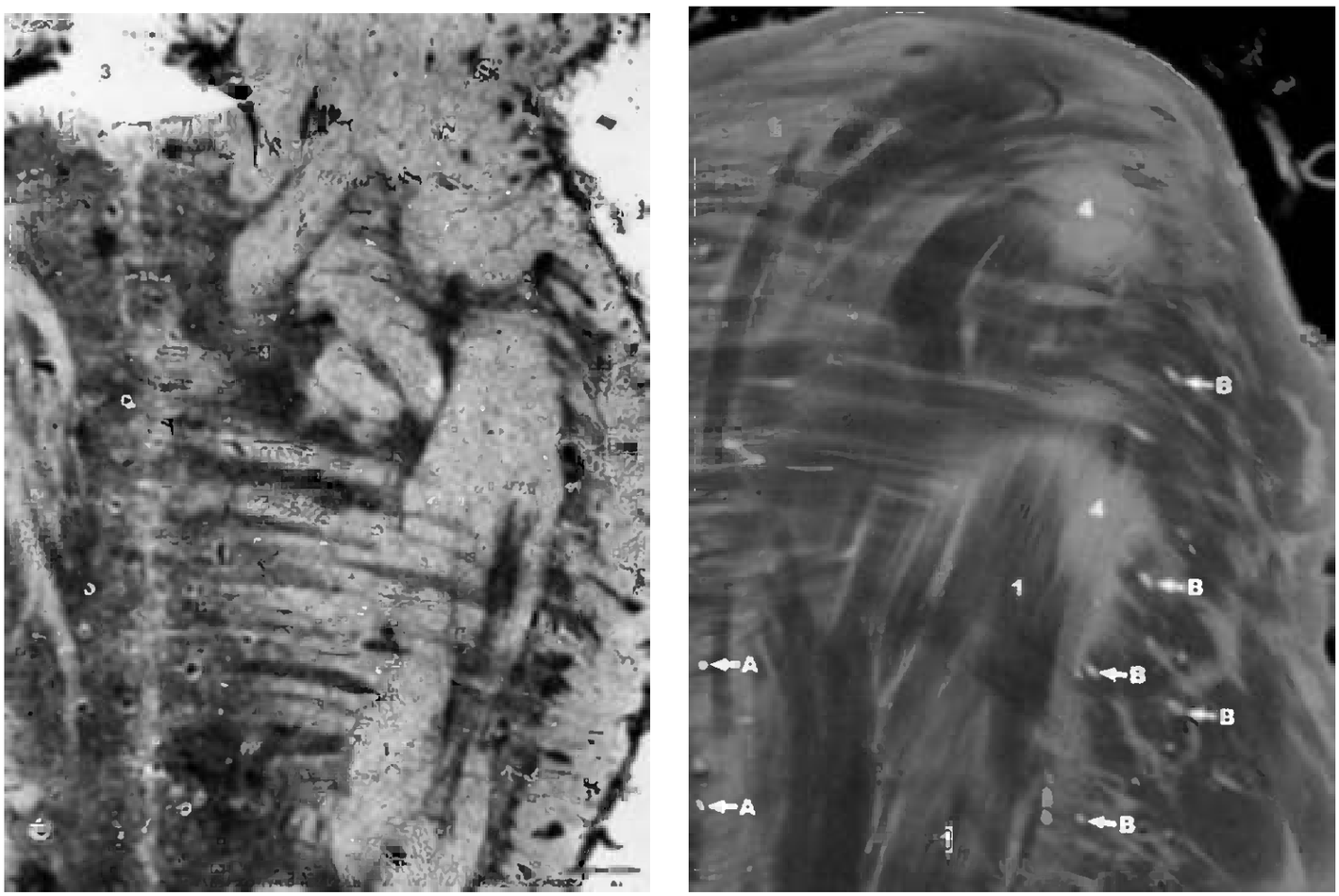

A **B**

Fig. 6.46 (A–B). The ventral pons. Coronal section dorsal to Fig. 6.45.
A. Intravascular India ink injection. Bar: 2.2 mm.
B. 9.4 T Magnetic resonance microscopy.

1 Corticospinal tract
2 Crus cerebri
3 Interpeduncular fossa
4 Pontine nuclei
5 Pontocerebellar fibers

A: Internal anteromedial pontine blood vessels (See p. 222)
B: Internal anterolateral blood vessels (See p. 222)

Fig. 6.47 (A–B). The dorsal pons. Coronal section.

A. Intravascular India ink injection. Bar: 1.9 mm.

B. 9.4 T Magnetic resonance microscopy.

1 Medial lemniscus
2 Nucleus reticularis tegmenti pontis
3 Pontocerebellar fibers
4 Middle cerebellar peduncle (brachium pontis)

A

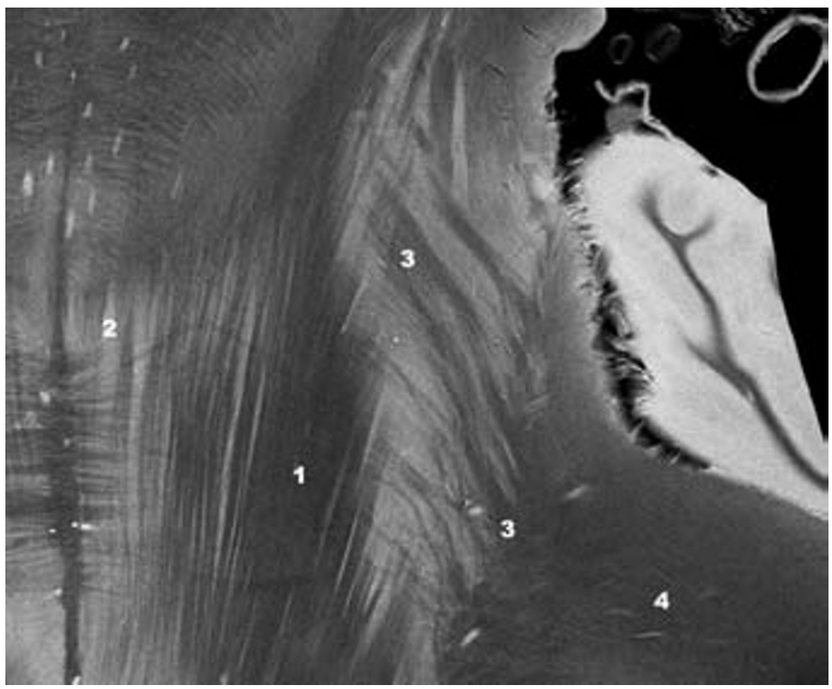

B

Fig. 6.48 (A–B). The dorsal pons. Coronal section.
A. Intravascular India ink injection. Bar: 1.2 mm.
B. 9.4 T Magnetic resonance microscopy.

1 Nucleus ceruleus (stippled locus in B.)
2 Superior cerebellar peduncle (brachium conjunctivum)
3 Nucleus parabrachialis medialis

Arrow in A: Vein of the locus ceruleus

Note the stippled appearance of the locus ceruleus. See also **Fig. 10.1**.

A

B

Fig. 6.49 (A–B). The mesencephalon. Sagittal section.
A. Intravascular India ink injection. Bar: 1.4 mm.
B. 9.4 T Magnetic resonance microscopy.

1 Inferior colliculus (note its rich vascular network)
2 Superior colliculus
3 Mesencephalic trigeminal tract
4 Red nucleus
5 Superior cerebellar peduncle and its decussation
6 Ventral portion of the pons

Arrowheads: Medullary lamina of the inferior colliculus
Arrows: Oculomotor fibers (CN III)

A

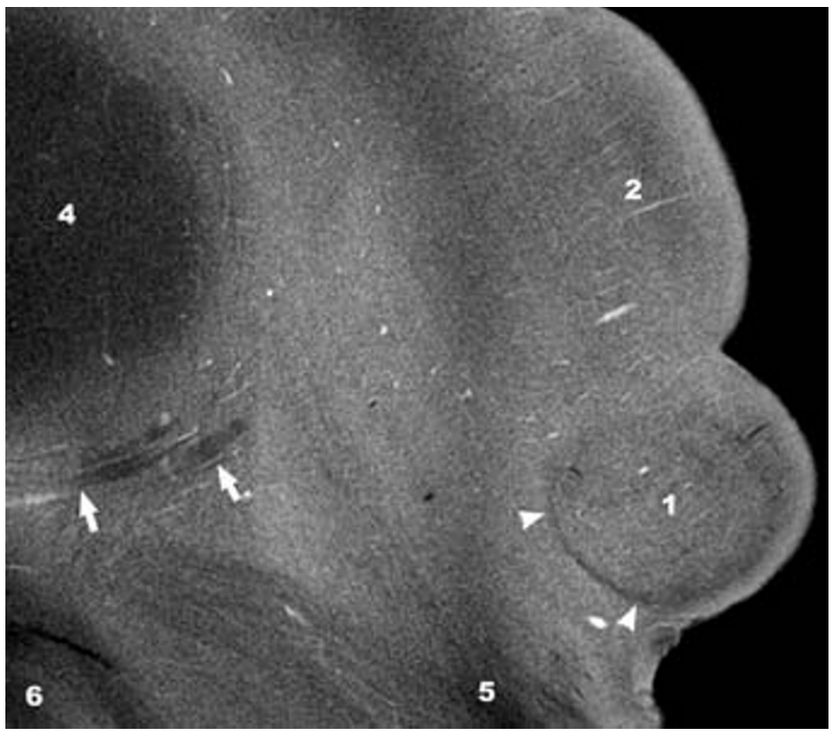

B

Fig. 6.50 (A–B). The mesencephalon. Sagittal section.

A. Intravascular India ink injection. Bar: 3.3 mm.

B. 9.4 T Magnetic resonance microscopy.

1 Inferior colliculus
2 Superior colliculus
3 Red nucleus
4 Substantia nigra
5 Crus cerebri
6 Ventral portion of pons
7 Superior cerebellar peduncle (brachium conjunctivum)

Note the stippled appearance of the substantia nigra.
See also **Figs. 10.1–10.3**.

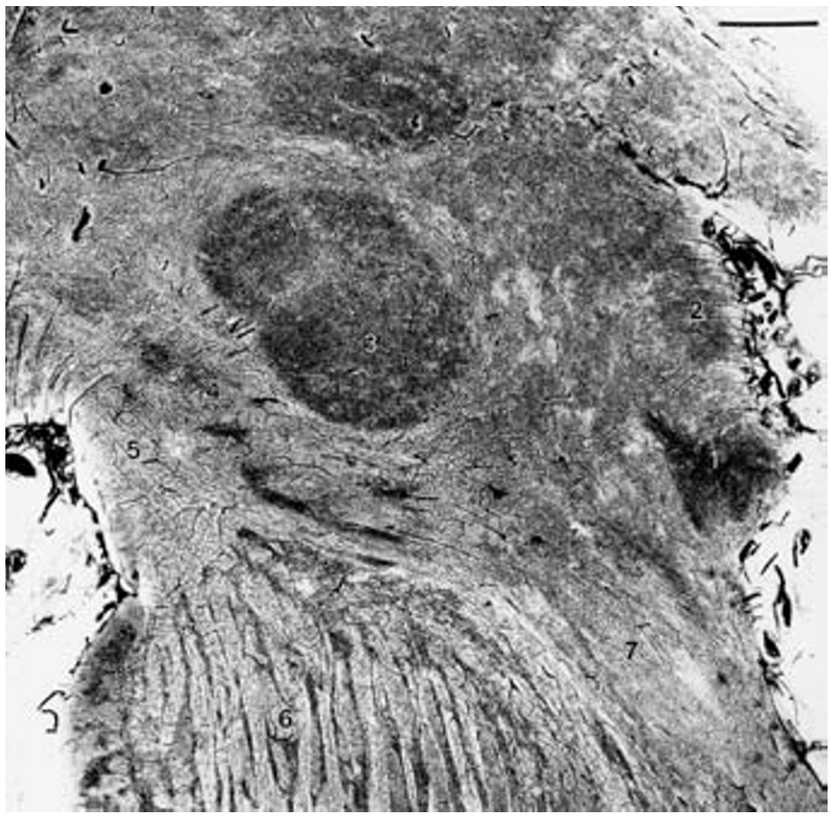

A

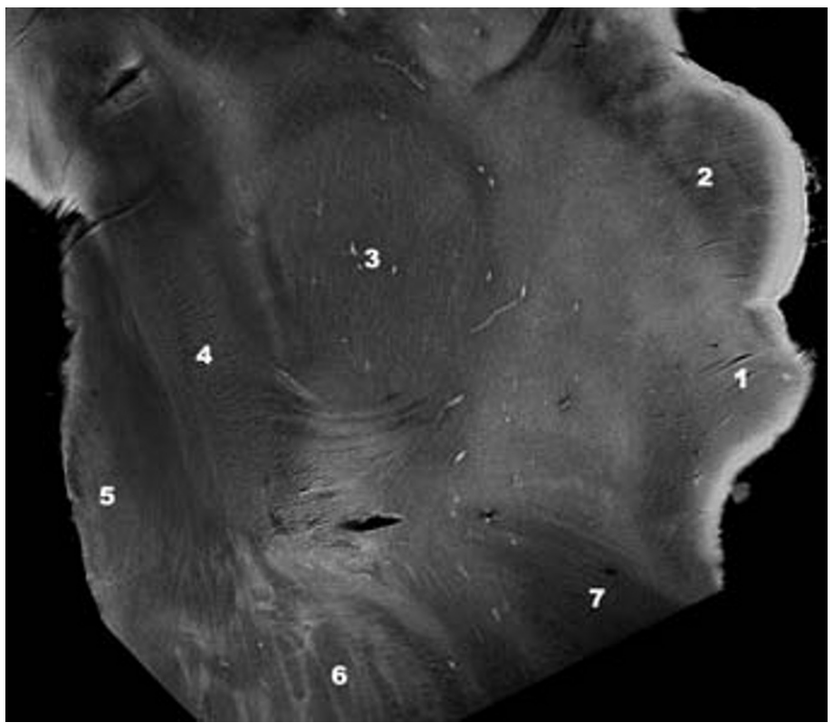

B

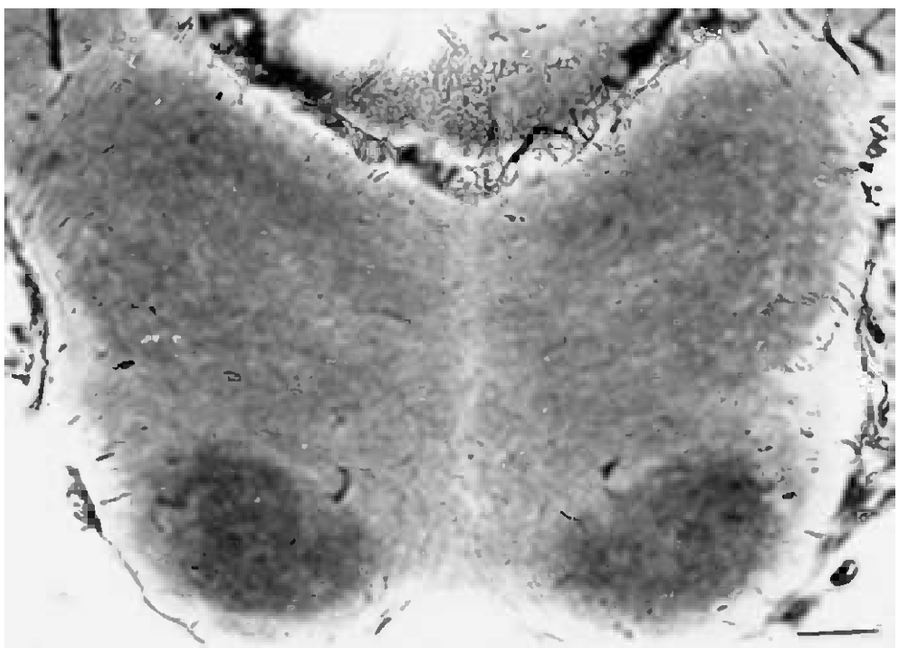

A

Fig. 6.51 (A–C). The mesencephalon. Coronal section.
A. Intravascular India ink injection. Bar: 1.8 mm.
B–C. 9.4 T Magnetic resonance microscopy.

1 Inferior colliculus (note its dense vascular network)
2 Superior colliculus
3 Pineal gland (cystic)
4 Frenulum veli
5 Periaqueductal gray matter

Paired black arrowheads:	Marginal fibers of the periaqueductal gray matter
Single black arrow:	Medullary lamina of the inferior colliculus
Paired white arrows:	Decussation of the trochlear nerves (CN IV) in the superior medullary velum, just caudal to the inferior colliculi

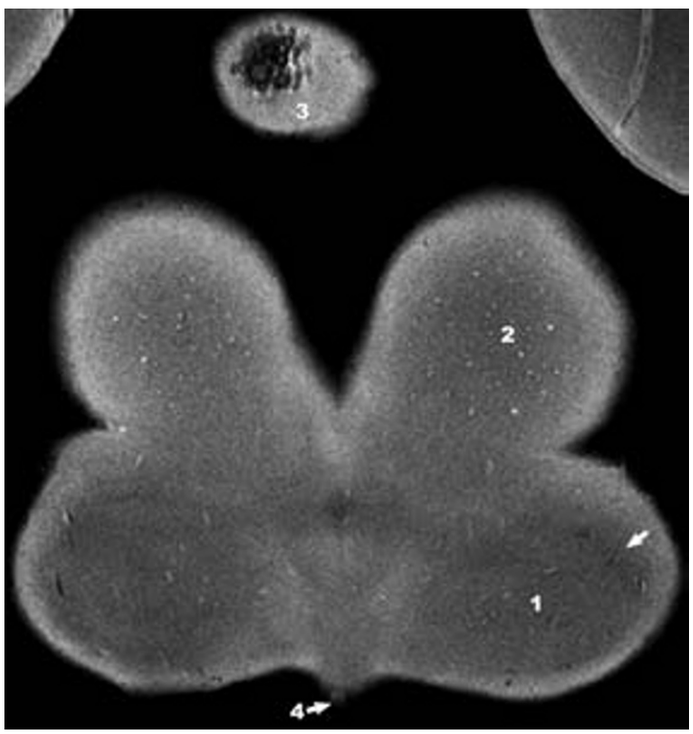

B

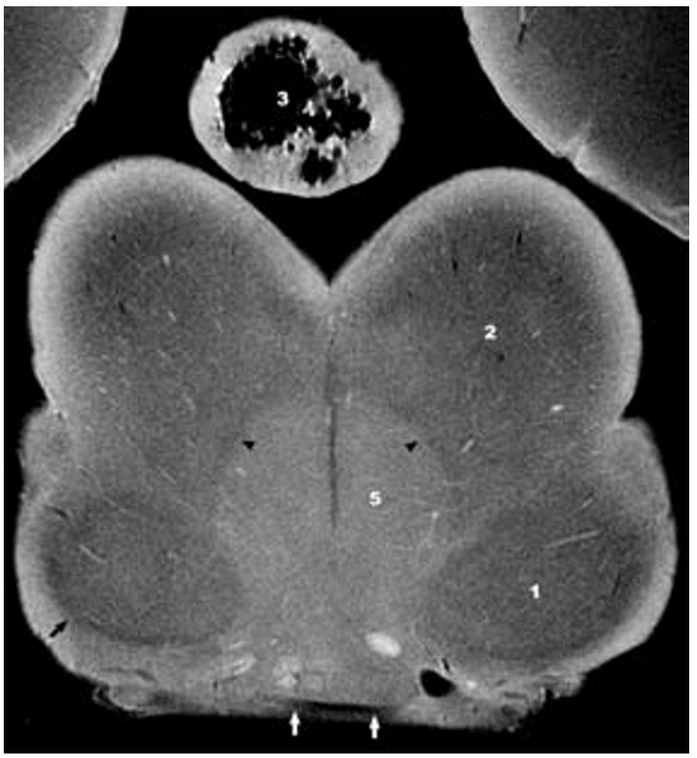

C

Fig. 6.52. The mesencephalon. Coronal section. Bar: 2.5 mm.

1 Nucleus ceruleus
2 Superior cerebellar peduncle (brachium conjunctivum)
3 Medial longitudinal fasciculus
4 Dorsal nucleus of the raphe
5 Trochlear nucleus
6 Main oculomotor nucleus
7 Caudal central oculomotor nucleus
8 Accessory oculomotor nucleus (Edinger-Westphal)
9 Interstitial nucleus (of Cajal)
10 Third ventricle
11 Medial geniculate body
12 Lateral geniculate body
13 Ventral posterolateral thalamic nucleus
14 Centromedian thalamic nucleus
15 Mediodorsal thalamic nucleus
16 Lateral posterior thalamic nucleus

Fig. 6.53. The mesencephalon. Magnified coronal section.

1 Medial longitudinal fasciculus
2 Trochlear nucleus
3 Dorsal nucleus of the raphe
4 Main oculomotor nucleus
5 Caudal central oculomotor nucleus
6 Accessory oculomotor nucleus (Edinger-Westphal)
7 Interstitial nucleus (of Cajal)
8 Third ventricle

SECTION VII

INTRINSIC ARTERIAL AND VENOUS TERRITORIES OF THE BRAIN STEM

Intrinsic vascular territories of the brain stem with infarct correlation

The arteries and veins of the brain stem form four groups of penetrating parenchymal vessels: the anteromedial, anterolateral, lateral, and posterior arterial and venous groups (**Figs. 7.1 to 7.3**). Each group irrigates or drains the corresponding anteromedial, anterolateral, lateral or posterior territory within the substance of the brain stem. These territories were evaluated and demarcated by detailed study of one brain stem whose blood vessels were injected with India ink. Thereafter, serial sections of several millimeters' thickness were cleared by immersion in a methylsalycilate and benzyl benzoate solution (Spalteholz's method), so that the individual arteries and veins could be traced through the parenchyma under a stereoscopic microscope. The results of that study form the basis for the vascular territories illustrated. Since the intrinsic vascular territories were analyzed in detail in only one brain stem, the territories illustrated in this section may not be completely typical. However, further less-detailed examination of ten other brain stems gives reasonable basis to assume that the brain stem studied is a representative example. See [24, 121, 122, 179, 278, 288, 322, 375, 428] for more information about the intrinsic vascular territories of the brain stem and [7, 13, 24, 33, 42, 46, 90, 108, 135, 169, 187, 190, 232, 234, 288, 366, 437, 450, 487] for additional information about brain stem infarctions.

Figures 7.1–7.34 illustrate the major intrinsic vascular territories of the medulla, pons, and mesencephalon.

The extent of these territiories is illustrated in clinical images of focal brain stem infarctions *in vivo*. To the extent possible, examples of brain stem infarction were provided for each territory at each level of the brain stem.

Abbreviations used for the clinical images include:
Territories and vessels:

AM = Anteromedial
AL = Anterolateral
L = Lateral
P = Posterior

MR terminology

T1-WI T1-weighted image
T2-WI T2-weighted image
FLAIR Fluid Attenuated Inversion Recovery T2-weighted image
D-WI Diffusion-weighted image

Fig. 7.1 (A–C). Median sagittal section of the brain stem. General orientation of the penetrating vessels.

A. Intravascular India ink injection. Bar: 2.2 mm.

B. Panoramic sagittal MR image at 9.4 Tesla, formed from multiple individual images

C. Diagram of the segments making up the composite image

1 Medulla
2 Basal portion of the pons
3 Pontine tegmentum
4 Decussation of the superior cerebellar peduncle in the basal portion of the midbrain
5 Medial longitudinal fasciculus
6 Cerebral aqueduct (of Sylvius)
7 Tectal plate of the mesencephalon
8 Superior vermis
9 Fourth ventricle
10 Arteries and veins belonging to the inferior pedicle of the interpeduncular fossa with their characteristic downwardly-curving route toward the superior pontine tegmentum (3)
11 Arteries and veins of the foramen cecum, with their characteristic upwardly-curving course toward the inferior pontine tegmentum (3)
12 Anteromedial group of penetrating vessels extending through the medulla to the floor of the fourth ventricle (9)
12′ Foramen cecum

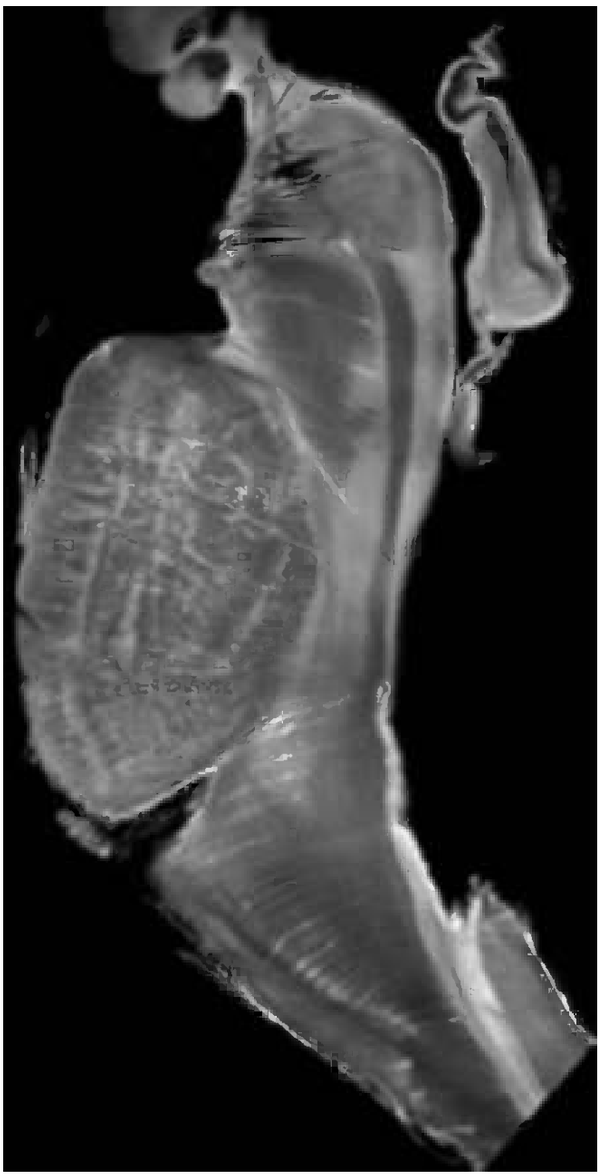

B

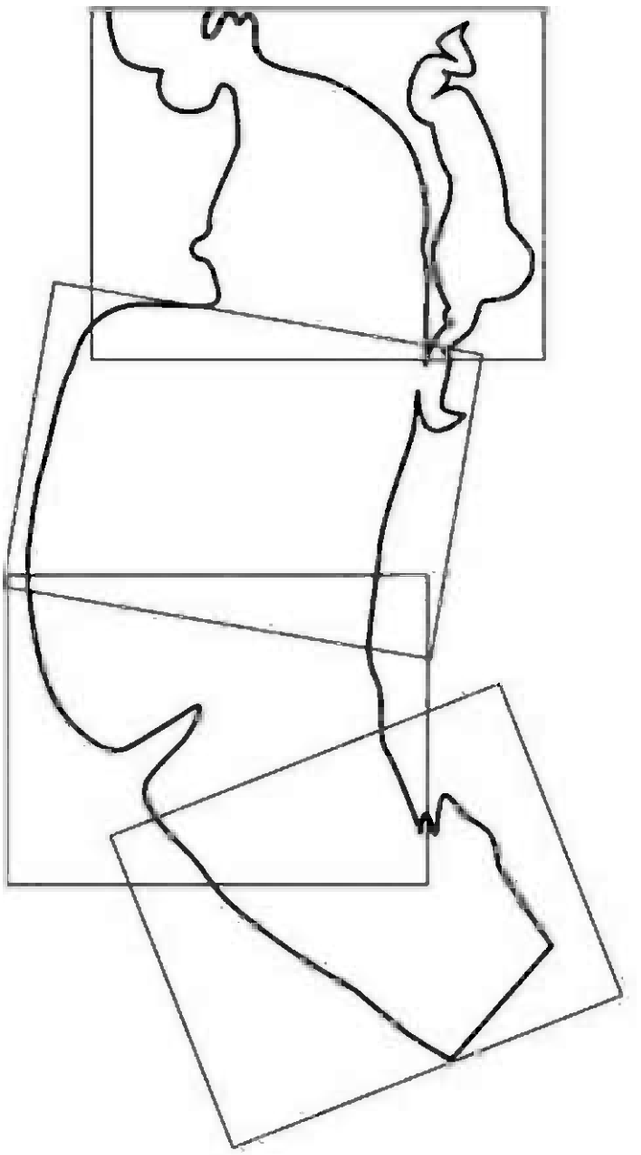

C

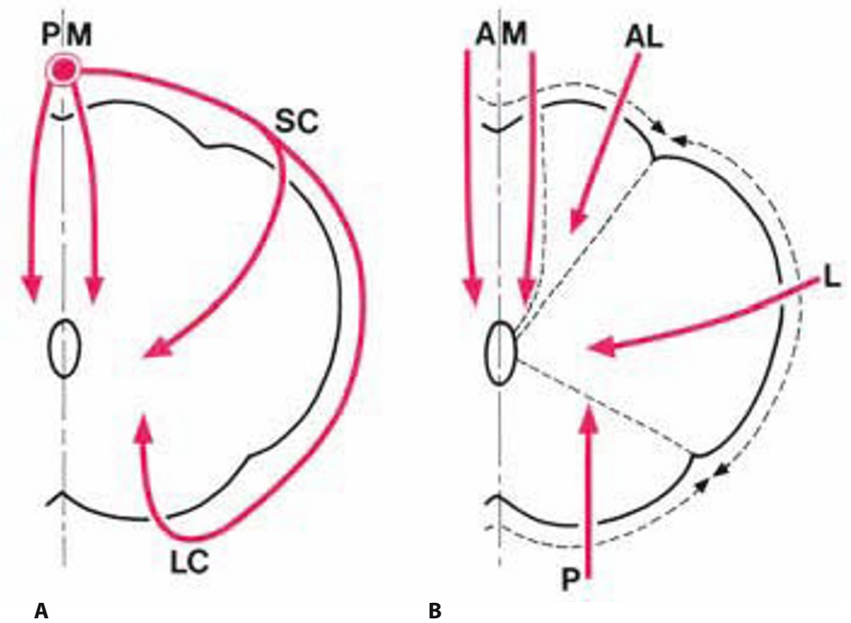

Fig. 7.2 (A–B). Nomenclature of the penetrating vessels. Diagrammatic representations of two possible systems of nomenclature. This text uses B., which is based upon the point of entry (arterial) or exit (venous) of the vessel from the brain stem. Dotted lines indicate the boundaries of the vascular territories.

A. Classification of Foix and Hillemand [107–258, 259]. The penetrating branches arising from the surface vessels are divided into **PM** (paramedian), **SC** (short circumferential), and **LC** (long circumferential) vessels.

B. Classification of Gillilan [163] **and Lazorthes et al.** [257, 258, 259]**,** used in this text.
The penetrating branches arising from the surface vessels are divided into
AM (anteromedial)
AL (anterolateral)
L (lateral) and
P (posterior) groups

Fig. 7.3 (A–D). Penetrating vessels. MR microscopy of the pons at 9.4 Tesla.
A. Parasagittal section of the pons
B. Coronal Section of the pons
C–D. Axial sections of the pons demonstrating the anteromedial **(C)** and anterolateral **(D)** groups of penetrating vessels

On MR microscopy, different segments of a single vessel may exhibit high or low signal signal intensity, depending upon whether that segment is filled with air (dark), Fomblin (Solvay Solexis Thorofare, New Jersey) (dark), formalin (dark), or phosphate buffer (bright).

3 Internal principal anteromedian vein of the pons
5 Foramen cecum
6 Arteries and veins of the foramen cecum (note their characteristically-curved upward course toward the inferior pontine tegmentum) (8″)
7 Fourth ventricle
8 Pontine tegmentum (mid portion)
8″ Inferior pontine tegmentum
9 Basilar portion of the pons
10 Rostral medulla
11 Corticospinal tracts descending through the pons
12 Pyramid of medulla (containing the corticospinal tract)
13 Middle cerebellar peduncle (brachium pontis)

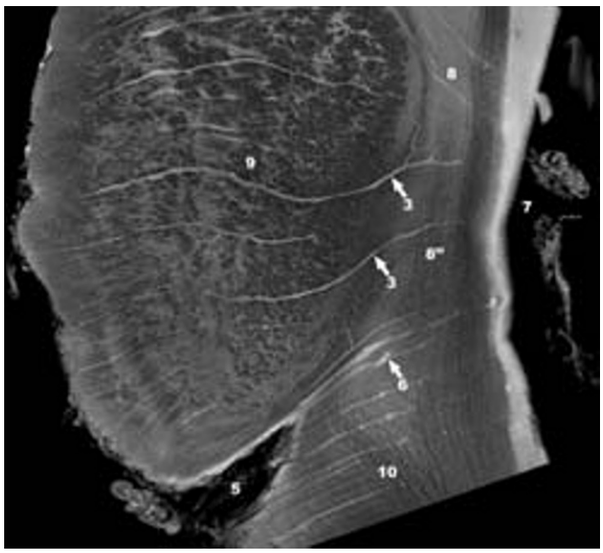

A

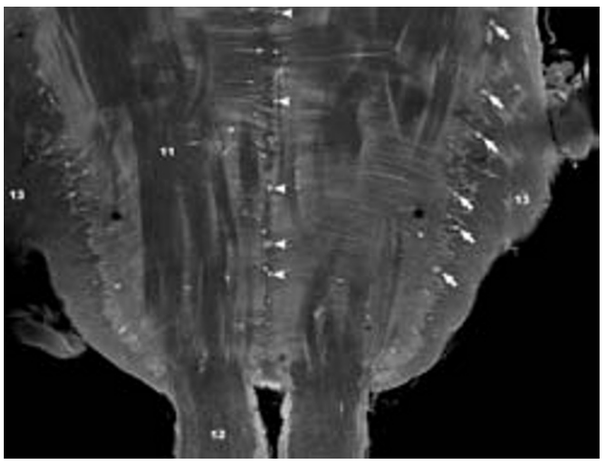

B

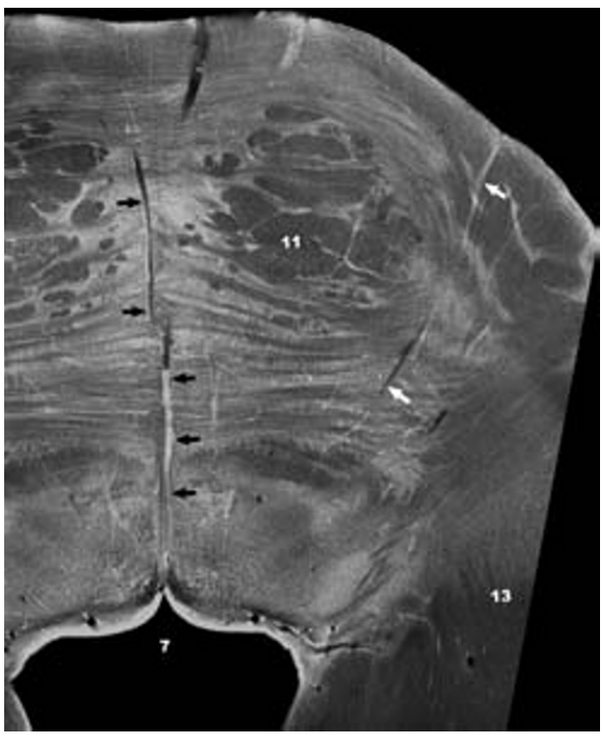

C

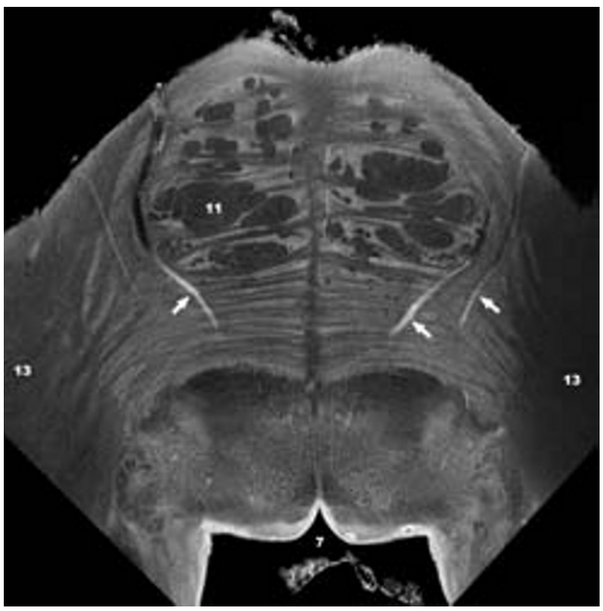

D

White arrowheads: Anteromedial group of penetrating vessels. Their entry points align vertically immediately to each side of midline, but appear to alternate from side to side as the basilar artery ascends cephalically (staggered entries). Their entry points are almost never precisely symmetrical.

White arrows: Anterolateral group of penetrating vessels. Their entry points align vertically toward the lateral edge of the basis pontis. Distally, they curve gracefully posteromedially toward the tegmentum.

Black arrows in C. Within the brain stem, the anteromedial vessels hug the midline or curve gently posterolaterally toward the tegmentum, (See **Fig. 2.16B**).

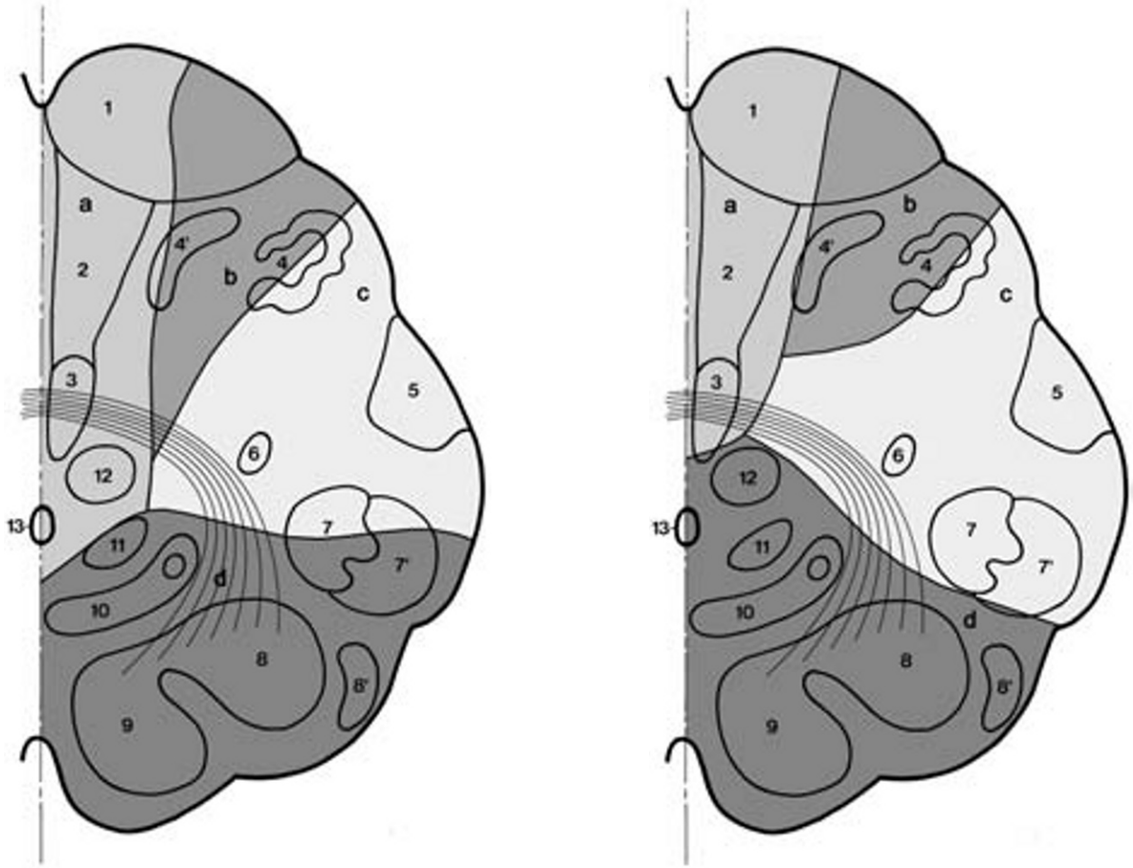

Arterial **Venous**

Fig. 7.4 (A–B). The vascular territories: Lower medulla.
See also Fig. 2.8.

1 Corticospinal tract
2 Medial lemniscus
3 Medial longitudinal fasciculus
4 Inferior olivary nucleus
4′ Medial accessory olivary nucleus
5 Spinothalamic tract
6 Nucleus ambiguus
7 Spinal trigeminal nucleus (pars caudalis)
7′ Spinal trigeminal tract
8 Medial cuneate nucleus
8′ Lateral cuneate nucleus
9 Gracile nucleus
10 Nucleus of the solitary tract
11 Dorsal motor nucleus of the vagus
12 Hypoglossal nucleus
13 Central canal

Arterial territories

a. Anteromedial medullary territory supplied by the anteromedial group of medullary arteries arising from the anterior spinal artery

b. Anterolateral medullary territory supplied by the anterolateral group of medullary arteries arising from the anterior spinal and posterior inferior cerebellar arteries

c. Lateral medullary territory supplied by the lateral group of medullary arteries arising from the posterior inferior cerebellar artery

d. Posterior medullary territory supplied by the posterior group of medullary arteries arising from the posterior spinal arteries

Venous territories

a. Anteromedial medullary territory drained by the anteromedial group of medullary veins, which drain into the anterior median medullary vein

b. Anterolateral medullary territory drained by the anterolateral group of medullary veins, which drain into the anterior lateral (pre-olivary) medullary vein

c. Lateral medullary territory drained by the lateral group of medullary veins, which drain into the lateral medullary vein.

d. Posterior medullary territory drained by the posterior group of medullary veins, which drain into the posterior median medullary vein

A

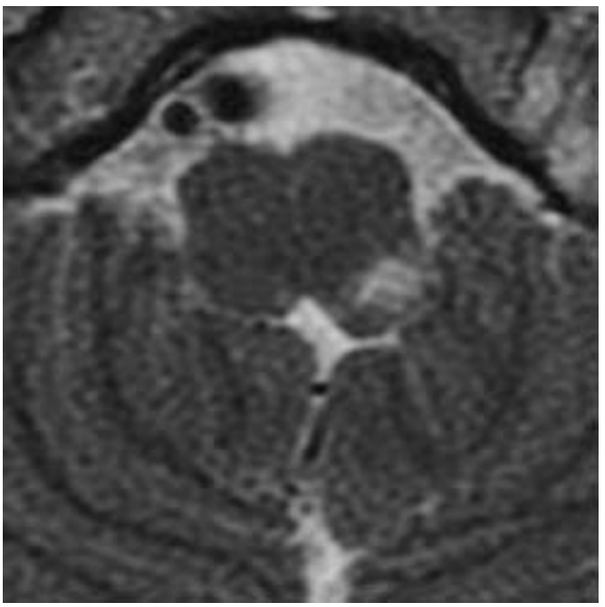

B

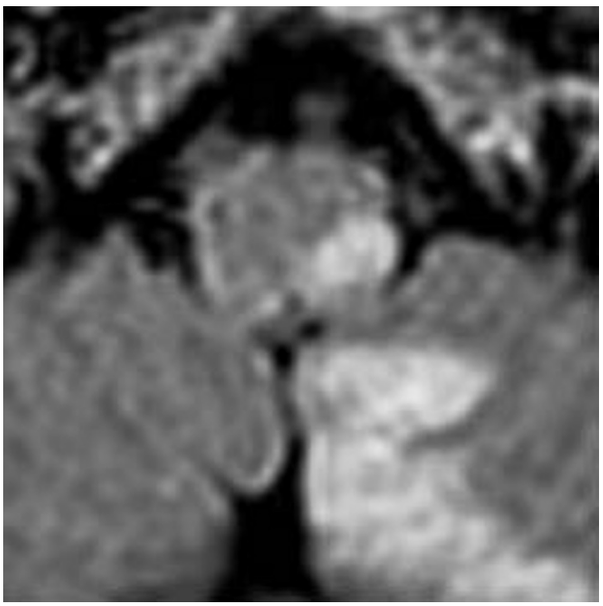

C

D

Fig. 7.5 (A–D). Focal infarctions of the lower medulla. Clinical MR images at 1.5 Tesla.

A. **Territories affected: AM, AL, L.** Note sparing of **P** at this level. Axial FLAIR image

B. **Territory affected: L only**. Axial T2-WI

C–D. Territories affected: L in brain stem. Posterior inferior cerebellar artery in cerebellum.
C. Axial FLAIR and **D.** Sagittal T2-WI (same patient)

Note the separate vascular compartments within the tonsil.

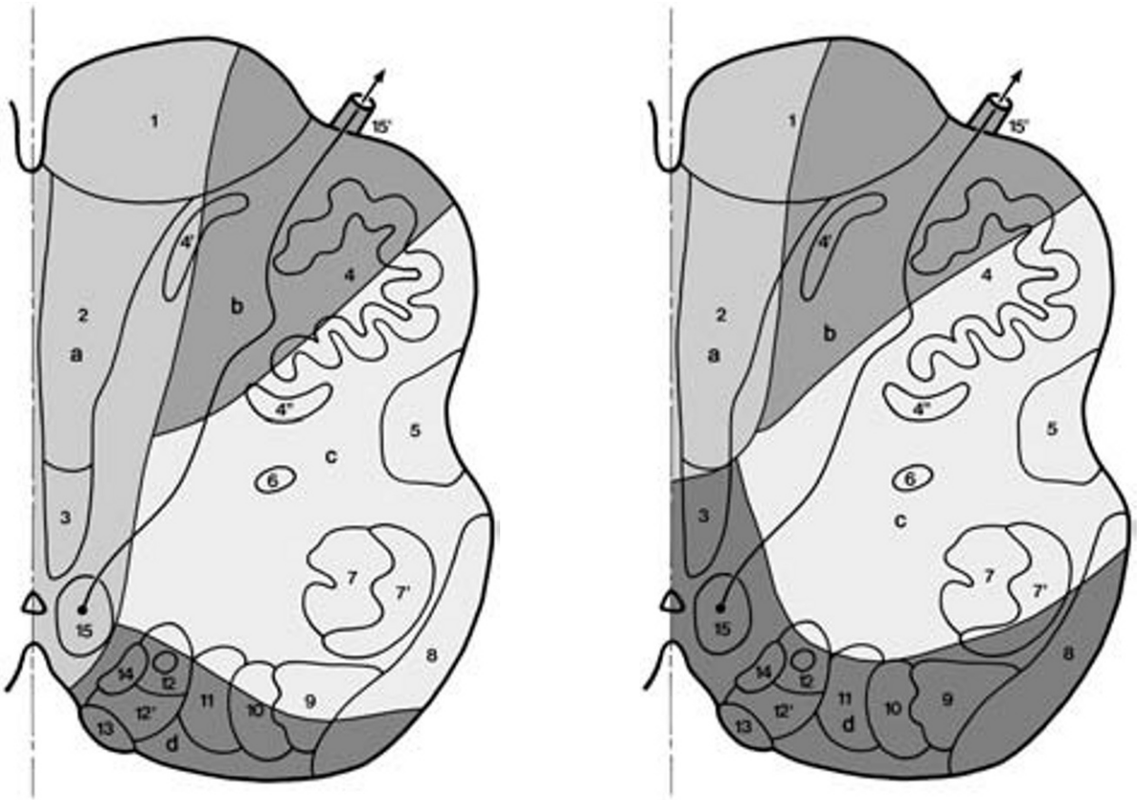

Arterial **Venous**

Fig. 7.6 (A–B). Vascular territories: Lower medulla.
See also Fig. 2.9.

1 Corticospinal tract
2 Medial lemniscus
3 Medial longitudinal fasciculus
4 Inferior olivary nucleus
4′ Medial accessory olivary nucleus
4″ Dorsal accessory olivary nucleus
5 Spinothalamic tract
6 Nucleus ambiguus
7 Spinal trigeminal nucleus (pars caudalis)
7′ Spinal trigeminal tract
8 Inferior cerebellar peduncle
9 Lateral cuneate nucleus
10 Medial cuneate nucleus
11 Gracile nucleus
12 Nucleus of the solitary tract
12′ Nucleus of the solitary tract (nucleus gelatinosus)
13 Area postrema
14 Dorsal motor nucleus of the vagus
15 Hypoglossal nucleus
15′ Hypoglossal nerve

Arterial territories

a Anteromedial medullary territory supplied by the anteromedial group of medullary arteries arising from the anterior spinal artery
b Anterolateral medullary territory supplied by the anterolateral group of medullary arteries arising from the anterior spinal and posterior inferior cerebellar arteries
c Lateral medullary territory supplied by the inferior rami of the lateral medullary fossa, arising from the posterior inferior cerebellar artery
d Posterior medullary territory supplied by the posterior group of medullary arteries arising from the posterior inferior cerebellar artery

Venous territories

a Anteromedial medullary territory drained by the anteromedial group of medullary veins, which drain into the anterior median medullary veins
b Anterolateral medullary territory drained by the anterolateral group of medullary veins, which drain into the anterior lateral (pre-olivary) medullary vein
c Lateral medullary territory drained by the lateral group of medullary veins, which drain into the lateral medullary and retro-olivary veins
d Posterior medullary territory drained by the posterior group of medullary veins, which drain into the marginal veins of the floor of the fourth ventricle

A

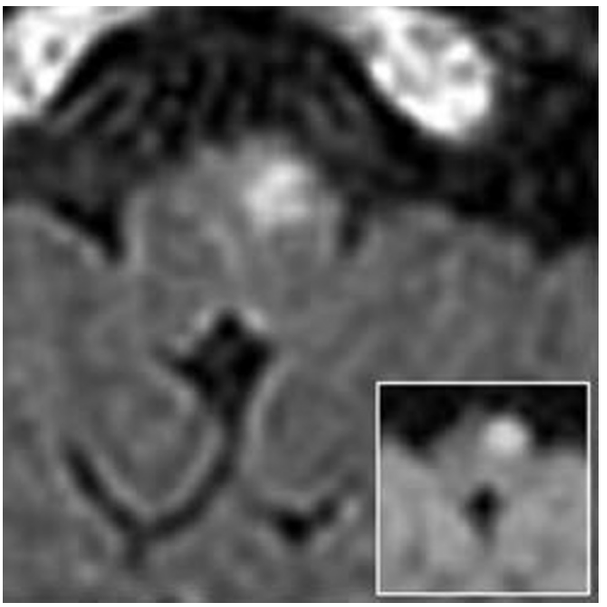

B

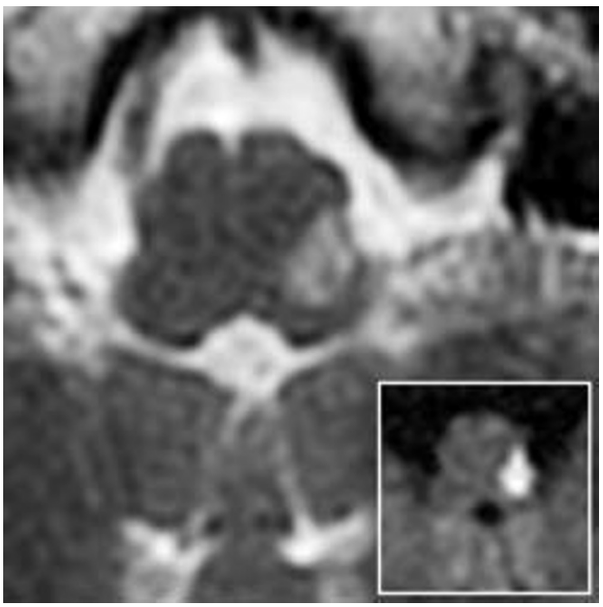

C

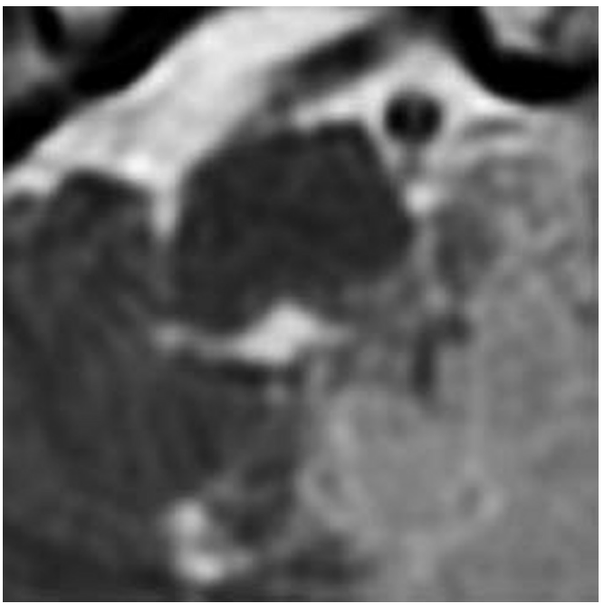

D

Fig. 7.7 (A–D). Focal infarctions of the lower medulla. Clinical MR images at 1.5 Tesla.

A. **Territories affected: AM, AL, L, P.** Axial T2–WI (Same patient as Fig 7.5A). The tonsils and cerebellar hemispheres show infarctions bilaterally.

B. **Territory affected:** **AL.** Axial FLAIR (with D-WI inset)

C. **Territory affected:** **L only.** Axial T2-WI (with D-WI inset), same patient as Fig. 7.5B.

D. **Territory affected:** **P in brain stem.** Posterior inferior cerebellar artery in cerebellum Axial T2-WI

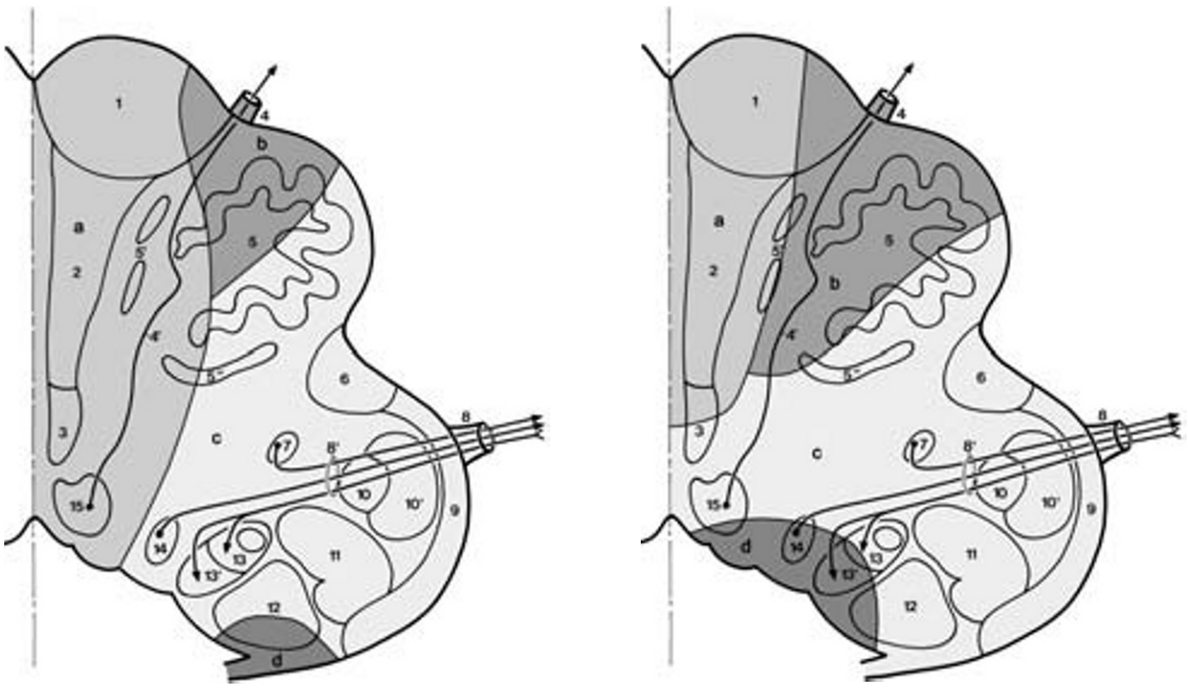

Arterial **Venous**

Fig. 7.8 (A–B). Vascular territories: Mid-medulla.
See also Fig. 2.10.

1 Corticospinal tract
2 Medial lemniscus
3 Medial longitudinal fasciculus
4 Hypoglossal nerve
4′ Intramedullary hypoglossal fibers
5 Inferior olivary nucleus
5′ Medial accessory olivary nucleus
5″ Dorsal accessory olivary nucleus
6 Spinothalamic tract
7 Nucleus ambiguus
8 Vagus nerve
8′ Intramedullary vagal fibers
9 Inferior cerebellar peduncle
10 Spinal trigeminal nucleus (pars interpolaris)
10′ Spinal trigeminal tract
11 Lateral cuneate nucleus
12 Medial vestibular nucleus
13 Nucleus of the solitary tract
13′ Nucleus of the solitary tract (nucleus gelatinosus)
14 Dorsal motor nucleus of the vagus
15 Hypoglossal nucleus

A Arterial territories

a Anteromedial medullary territory supplied by the anteromedial group of medullary arteries arising from the anterior spinal and vertebral arteries

b Anterolateral medullary territory supplied by the anterolateral group of medullary arteries arising from the anterior spinal and vertebral arteries

c Lateral medullary territory supplied by the lateral group of medullary arteries, both:
(i) middle rami of the lateral medullary fossa, arising from the vertebral artery, and
(ii) posterior rami of the lateral medullary fossa, arising from the anterior inferior cerebellary artery.

d Posterior medullary territory supplied by the posterior group of medullary arteries (of minor importance at this level), arising from the posterior inferior cerebellar artery

B Venous territories

a Anteromedial medullary territory drained by the anteromedial group of medullary veins, which drain into the anterior median medullary vein

b Anterolateral medullary territory drained by the anterolateral group of medullary veins, which drain into the anterior lateral (pre-olivary) medullary vein

c Lateral medullary territory drained by the lateral group of medullary veins (veins of the lateral medullary fossa), which drain into the lateral medullary and retro-olivary veins.

d Posterior medullary territory drained by the posterior group of medullary veins, which drain into the marginal vein of the floor of the posterior fossa

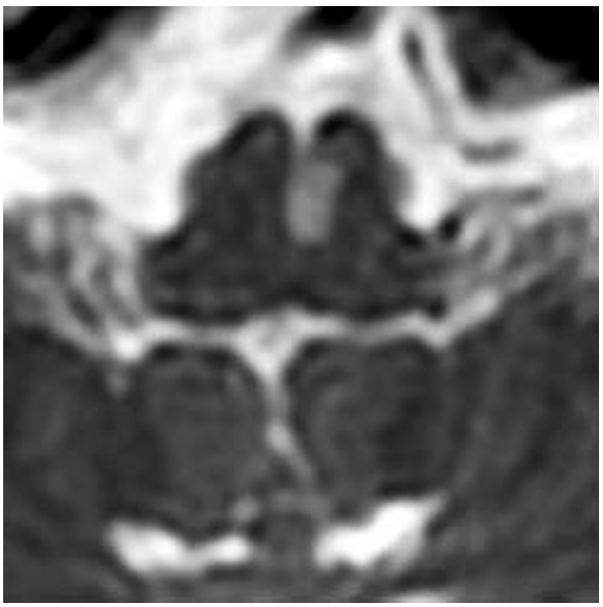

A

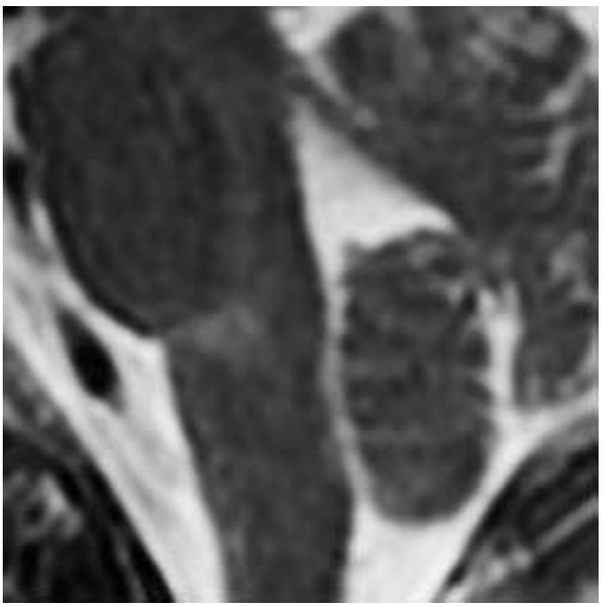

B

C

Fig. 7.9 (A–C). Focal infarctions of the mid-medulla.
Clinical MR images at 1.5 Tesla.

A–**B. Territory affected: AM only. A.** Axial and **B.** Sagittal T2-WI (same patient)

C. Territories affected: Bilateral AM. Note that the AM arterial territory extends to the floor of the fourth ventricle. Axial T2-WI (D-WI inset).

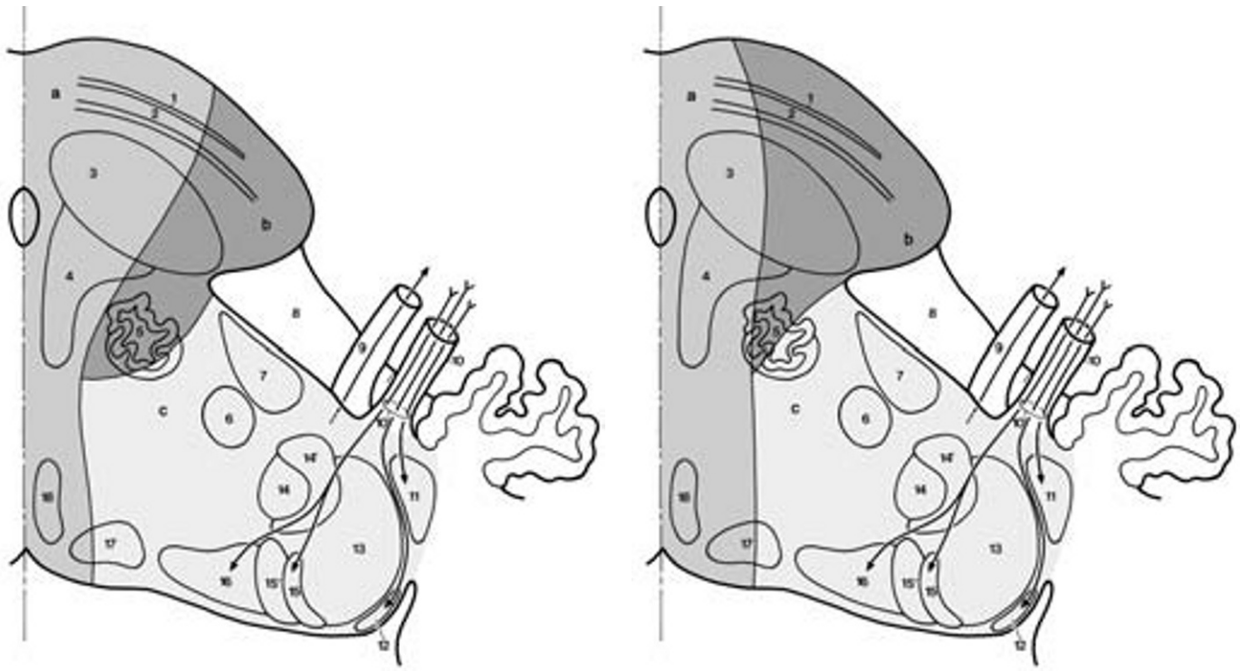

Arterial **Venous**

Fig. 7.10 (A–B). Vascular territories: Pontomedullary junction. See also Fig. 2.12.

1 Pontocerebellar fibers
2 Pontine nuclei
3 Corticospinal tract
4 Medial lemniscus
5 Superior portion of inferior olivary nucleus
6 Facial nucleus
7 Spinothalamic tract
8 Pontomedullary sulcus
9 Facial nerve
10 Vestibulocochlear nerve
10′ Fibers of the vestibulocochlear nerve
11 Ventral cochlear nucleus
12 Dorsal cochlear nucleus
13 Inferior cerebellar peduncle
14 Spinal trigeminal nucleus, pars oralis
14′ Spinal trigeminal tract
15 Inferior vestibular nucleus
15′ Descending vestibular root
16 Medial vestibular nucleus
17 Nucleus prepositus hypoglossi
18 Medial longitudinal fasciculus

Arterial territories

a Anteromedial pontine territory supplied by the anteromedial group of pontine arteries (arteries of the foramen cecum)
b Anterolateral pontine territory supplied by the anterolateral group of pontine arteries arising from the basilar artery
c Lateral pontine territory supplied by the lateral group of pontine and medullary arteries, both
(i) superior rami of the lateral medullary fossa, arising from the vertebral and anterior inferior cerebellar arteries;
(ii) posterior rami of the lateral medullary fossa, arising from the anterior inferior cerebellar artery and supplying the inferior cerebellar peduncle and the cochlear nuclei

Venous territories

a Anteromedial pontine territory drained by the anteromedial group of pontine veins, which drain into the veins of the foramen cecum
b Anterolateral pontine territory drained by the anterolateral group of pontine veins, which drain into the vein of the pontomedullary sulcus
c Lateral pontine territory drained by the lateral group of pontine veins, which drain into the vein of the pontomedullary sulcus medially and into the lateral medullary vein laterally

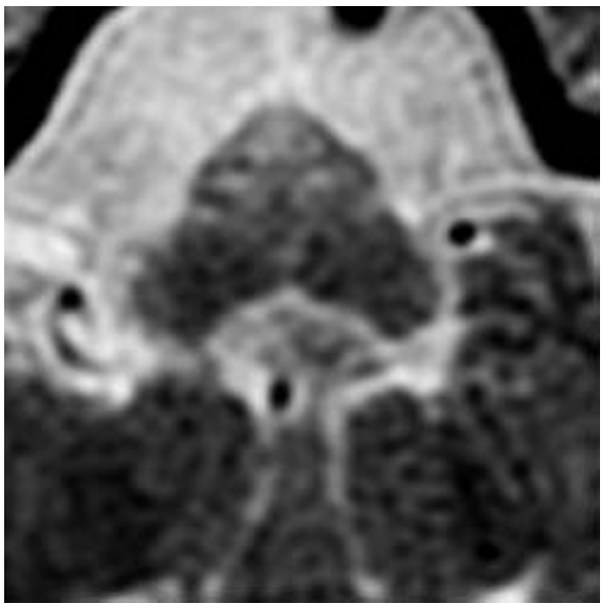

A

B

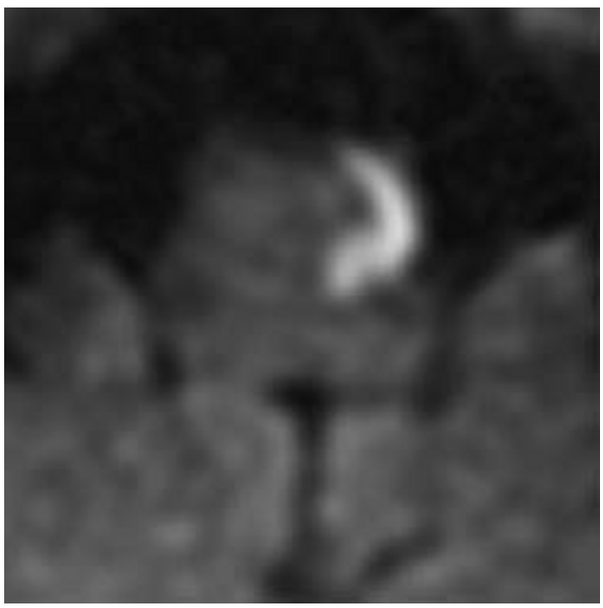

C

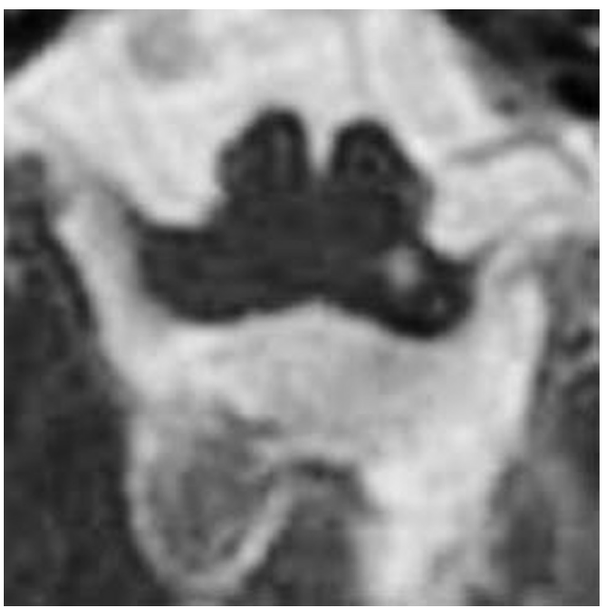

D

Fig. 7.11 (A–F). Focal infarctions of the high medulla and pontomedullary junction. Clinical MR images at 1.5 Tesla.

A.–B. Territories affected: Bilateral AM and AL.
A. Axial and **B.** Sagittal T2-WI (same patient).
C. Territory affected: AL only. Axial D-WI.
D. Territory affected: L only. Axial T2-WI.

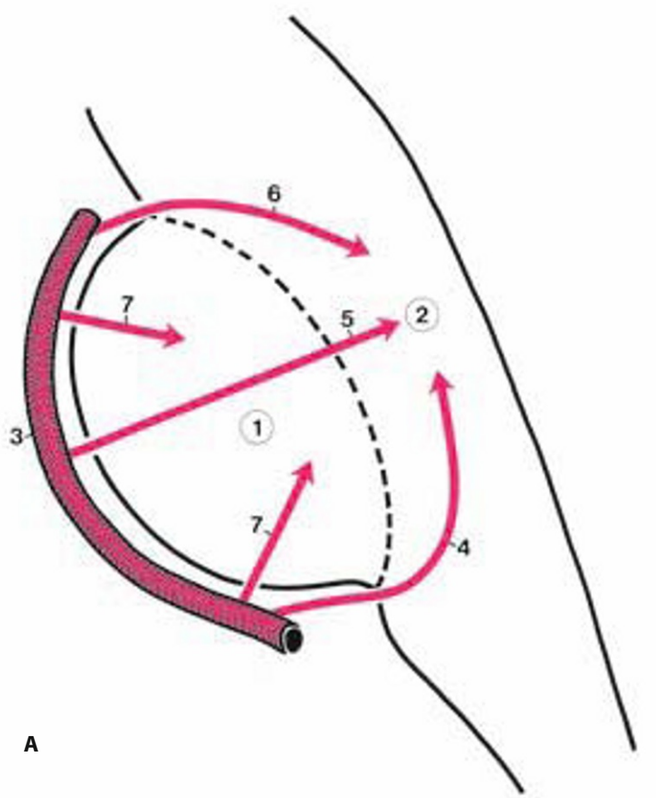

Fig. 7.12 A. Pathways of the arteries (and veins) vascularizing the pontine tegmentum.

A. Diagram of a sagittal section.

1 Basilar portion of the pons
2 Pontine tegmentum
3 Basilar artery
4 Lowest tegmental level: the arteries entering the pontomedullary sulcus (superior rami of the lateral medullary fossa) and the foramen cecum supply the tegmentum by a characteristic, upwardly-curved ascending pathway
5 Middle tegmental level: the arteries reach the tegmentum by a direct penetrating pathway
6 Upper tegmental level: the arteries entering the interpeduncular fossa (inferior pedicle of the interpeduncular fossa) reach the tegmentum by a characteristic, downwardly-curved descending pathway
7 Arteries supplying the basilar portion of the upper and lower pons

Fig. 7.12 (B–E). Pontine infarctions. Sagittal clinical MR images at 1.5 Tesla

B. Territory affected: **Lower pontine AL** infarction. T2-WI (Same patient as Fig. 7.14C)
C. Territory affected: **Midpontine AM** infarction. T2-WI
D. Territory affected: **Lower pontine AM** infarction. T2-WI
E. Territories affected: **Bilateral upper pontine AM** with hemorrhagic conversion. T2-WI (Same patient as Fig. 7.14D)

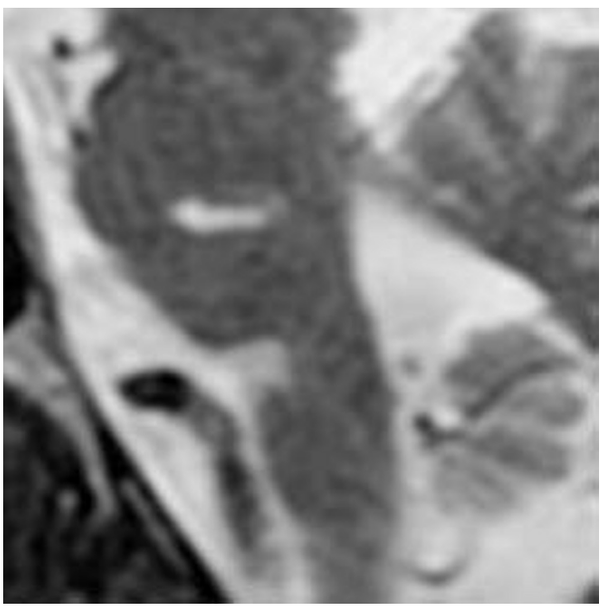

B

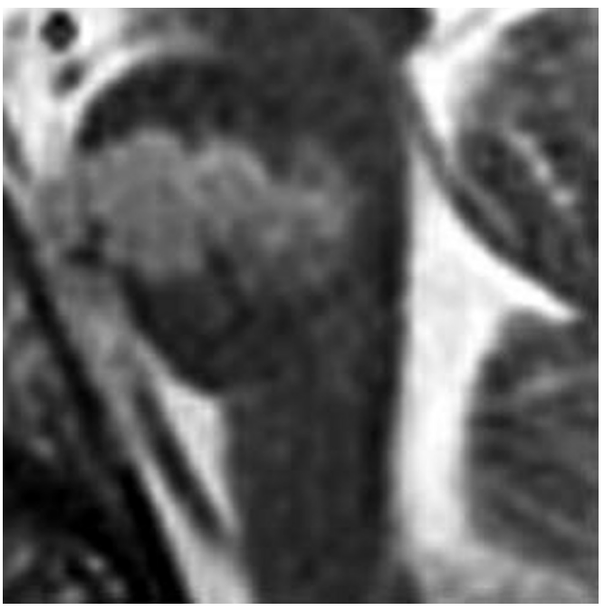

C

D

E

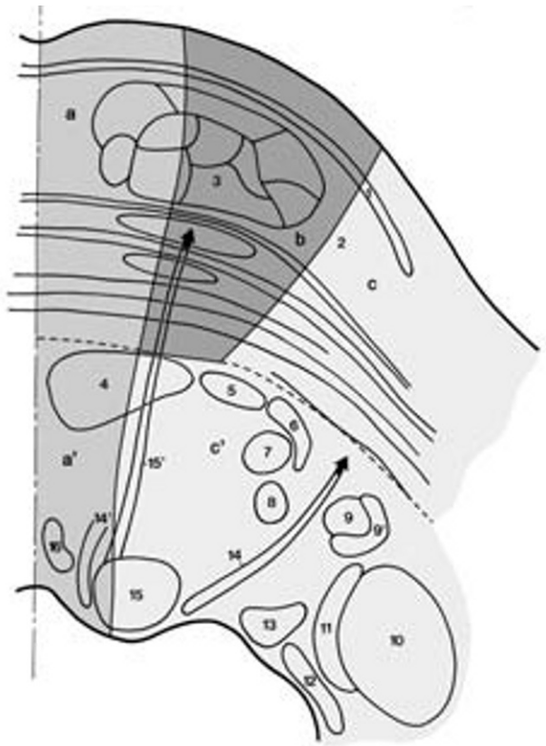

Arterial

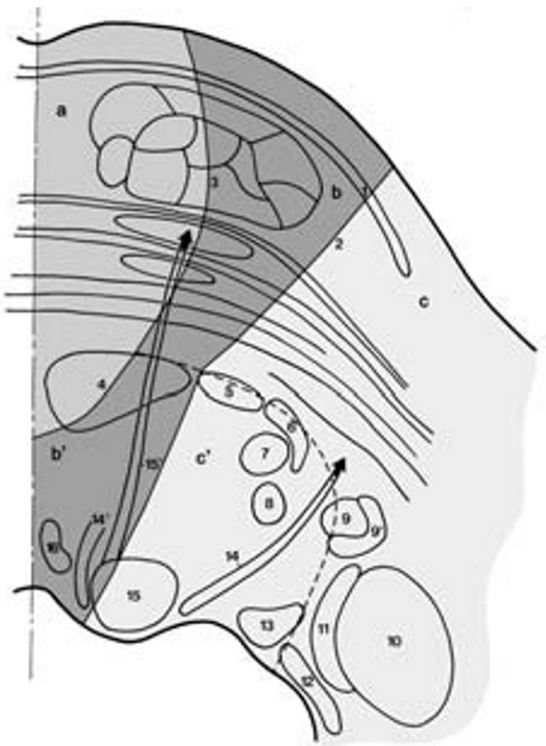

Venous

Fig. 7.13 (A–B). Vascular territories: Low pons.
See also **Fig. 2.14.**

1 Pontocerebellar fibers
2 Pontine nuclei
3 Corticospinal tract
4 Medial lemniscus
5 Spinothalamic tract
6 Lateral lemniscus (auditory fibers)
7 Superior olivary nucleus
8 Facial nucleus
9 Spinal trigeminal nucleus (pars oralis)
9′ Spinal trigeminal tract
10 Inferior cerebellar peduncle
11 Lateral vestibular nucleus
12 Superior vestibular nucleus
13 Medial vestibular nucleus
14, 14′ Fibers of the facial nerve
15 Abducens nucleus
15′ Fibers of the abducens nerve
16 Medial longitudinal fasciculus

Arterial territories

a, a′ Anteromedial pontine territory supplied by the anteromedial group of pontine arteries:
a Arising from the basilar artery and supplying the basilar portion of pons;
a′ Arising from the arteries of the foramen cecum (basilar artery) and supplying the pontine tegmentum by an ascending path (**See Fig. 7.12**)
b Anterolateral pontine territory supplied by the anterolateral group of pontine arteries arising from the basilar artery
c, c′ Lateral pontine territory supplied by the lateral group of pontine arteries:
c Arising from the lateral pontine arteries;
c′ Arising from the superior rami of the lateral medullary fossa (anterior inferior cerebellar artery) and supplying the pontine tegmentum by an ascending path (**See Fig. 7.12**)

Venous territories

a Anteromedial pontine territory drained by the anteromedial group of pontine veins, which drain into the anterior median pontine vein
b, b′ Anterolateral pontine territory drained by the anterolateral group of pontine veins:
b Draining into the transverse pontine veins;
b′ Draining into the vein of the pontomedullary sulcus by a descending path (**See Fig. 7.12**)
c, c′ Lateral pontine territory drained by the lateral group of pontine veins:
c Draining into the lateral pontine vein;
c′ Draining into the vein of the pontomedullary sulcus and into the veins of the lateral medullary fossa by a descending path (**See Fig. 7.12**)

A

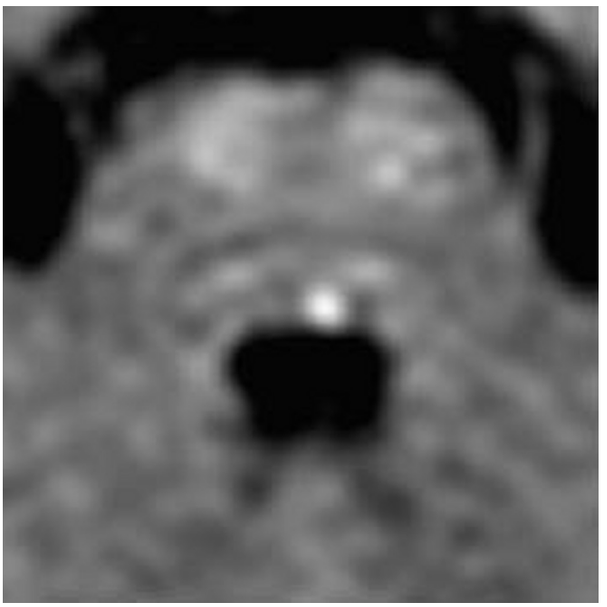

B

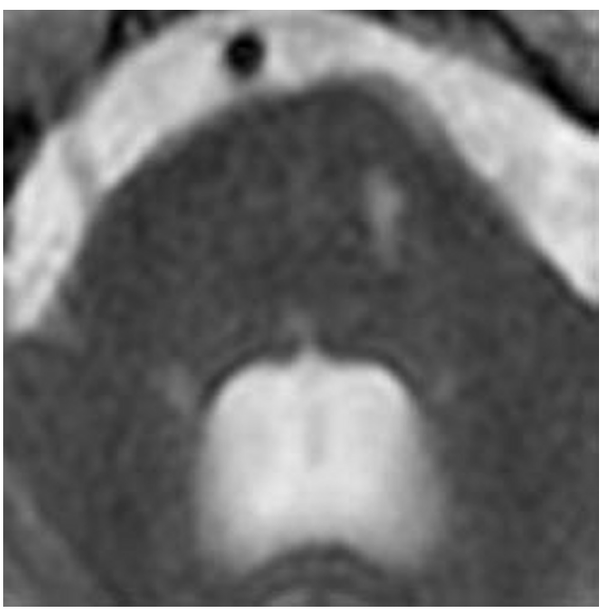

C

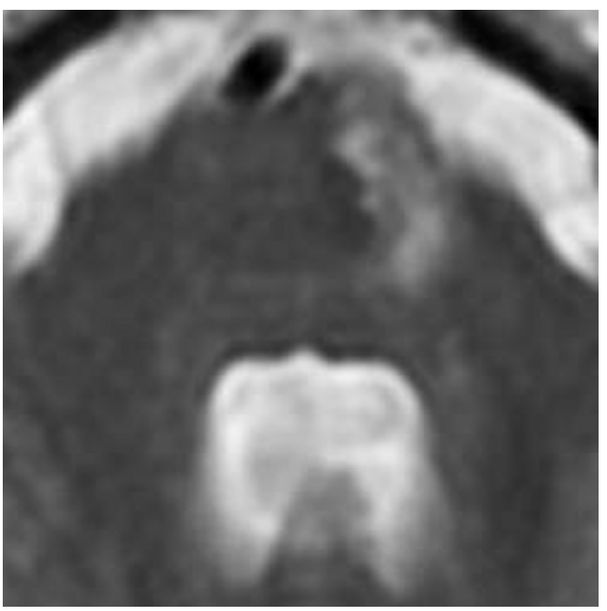

D

Fig. 7.14 (A–D). Focal Low and Mid-pontine infarctions.
Clinical MR images at 1.5 Tesla.

A. **Territory affected:** **AM.** Axial T2-WI (D-WI inset)
B. **Territory affected:** **Distal tegmental AM.** Axial D-WI
C. **Territory affected:** **AL.** Axial T2-WI (Same patient as **Fig. 7.12B**)
D. **Territory affected:** **AL.** Axial T2-WI

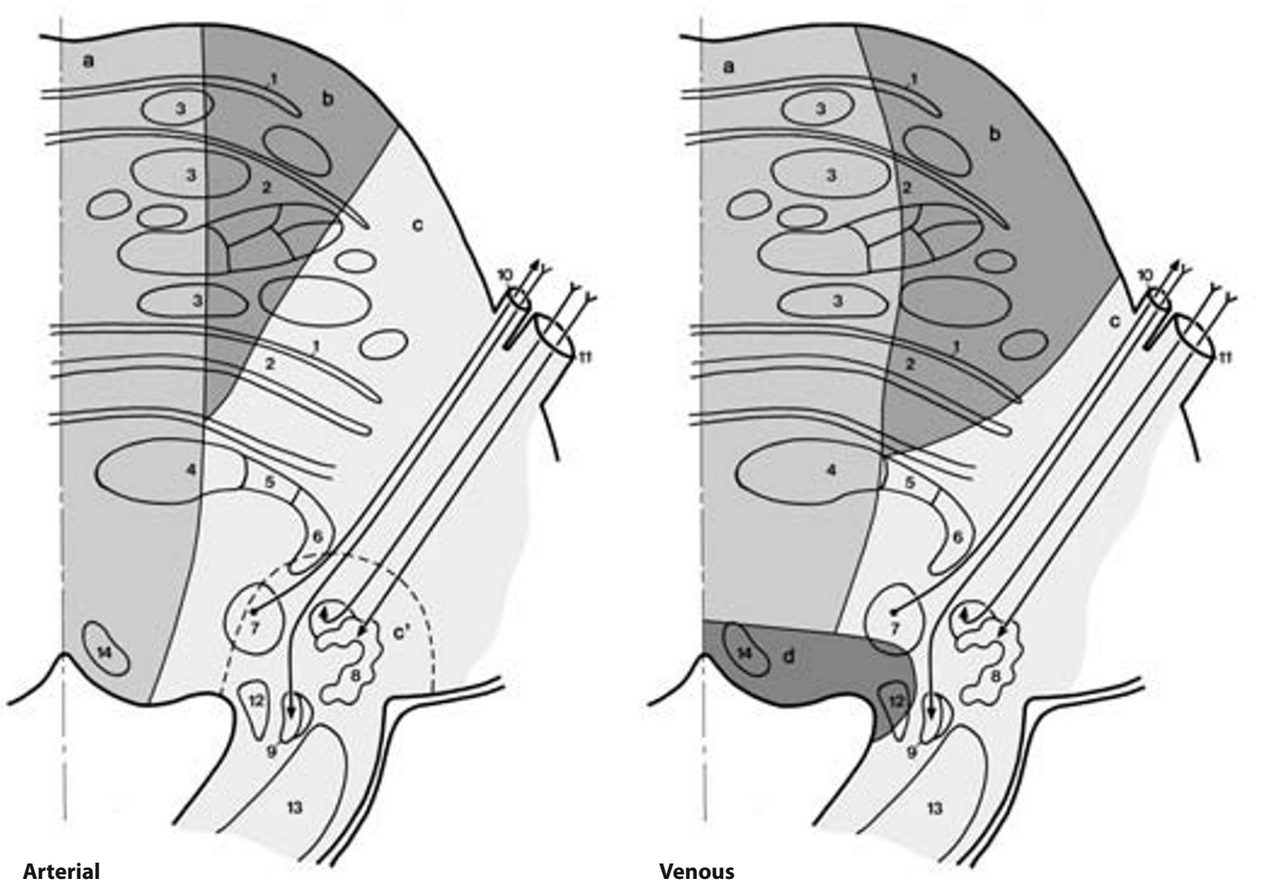

Fig. 7.15 (A–B). Vascular territories: Mid-pons.
See also Fig. 2.15.

1 Pontocerebellar fibers
2 Pontine nuclei
3 Corticospinal tract
4 Medial lemniscus
5 Spinothalamic tract
6 Lateral lemniscus
7 Motor trigeminal nucleus
8 Principal sensory trigeminal nucleus
9 Mesencephalic trigeminal nucleus
10 Fibers of the trigeminal motor root
11 Fibers of the trigeminal sensory root
12 Superior vestibular nucleus
13 Superior cerebellar peduncle (brachium conjunctivum)
14 Medial longitudinal fasciculus

Arterial territories

a Anteromedial pontine territory supplied by the anteromedial group of pontine arteries, arising from the basilar artery (See Fig. 7.12).
b Anterolateral pontine territory supplied by the anterolateral group of pontine arteries arising from the basilar artery
c, c′ Lateral pontine territory supplied by the lateral group of pontine arteries:
c Arising from the lateral pontine arteries;
c′ Arising from the anterior inferior cerebellar artery and from the lateral pontine arteries, and supplying the motor and principal sensory trigeminal nuclei by a route following the intra-axial trigeminal fibers

Venous territories

a Anteromedial pontine territory drained by the anteromedial group of pontine veins which drain into the anterior median pontine vein
b Anterolateral pontine territory drained by the anterolateral group of pontine veins, which drain into the transverse pontine veins
c Lateral pontine territory drained by the lateral group of pontine veins, which drain into the transverse and lateral pontine veins
d Posterior pontine territory drained by the posterior group of pontine veins, which drain into the veins of the brachium conjunctivum by an ascending path

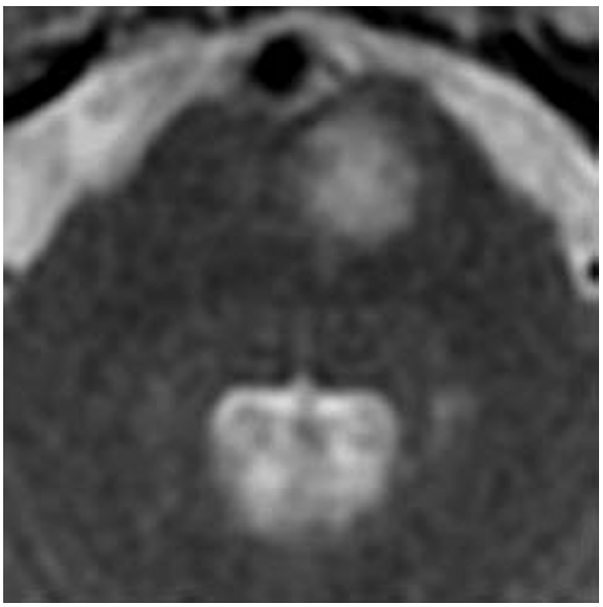

A

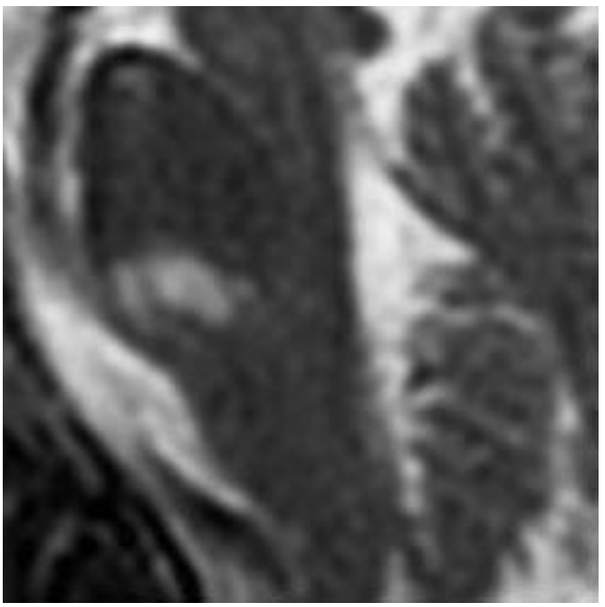

B

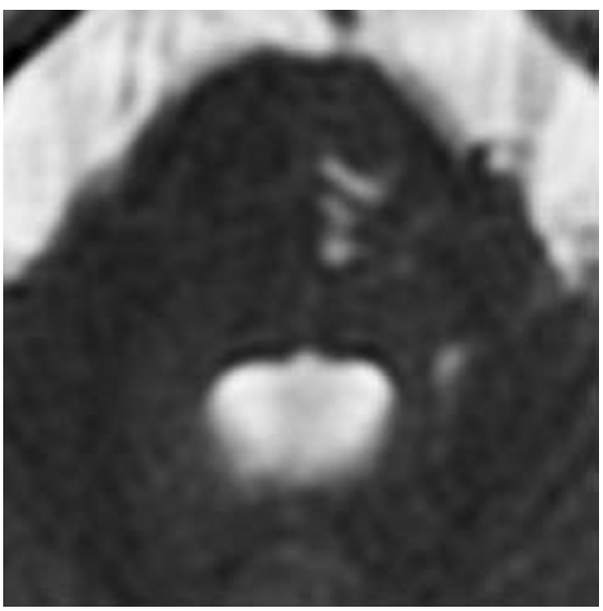

C

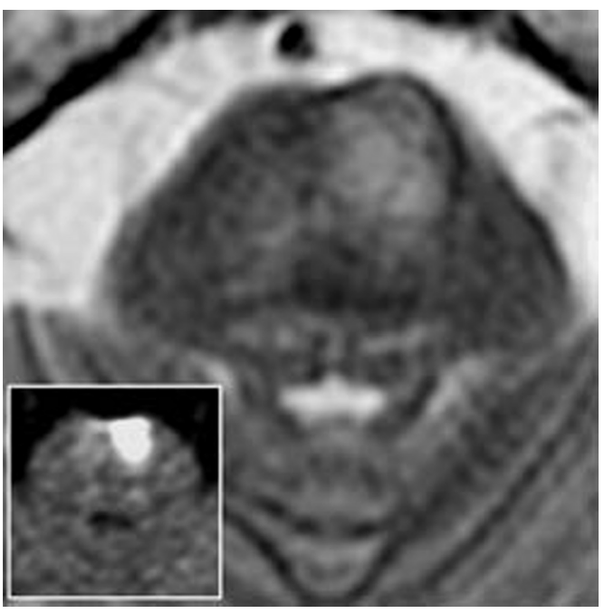

D

Fig. 7.16 (A–D). Focal mid-pontine infarction. Clinical MR images at 1.5 Tesla.

A–B. Territory affected: AM only. A. Axial and **B.** Sagittal T2-WI (same patient).
C. Territory affected: AM. Axial T2-WI.
D. Territory affected: AM. Axial T2-WI (D-WI inset)

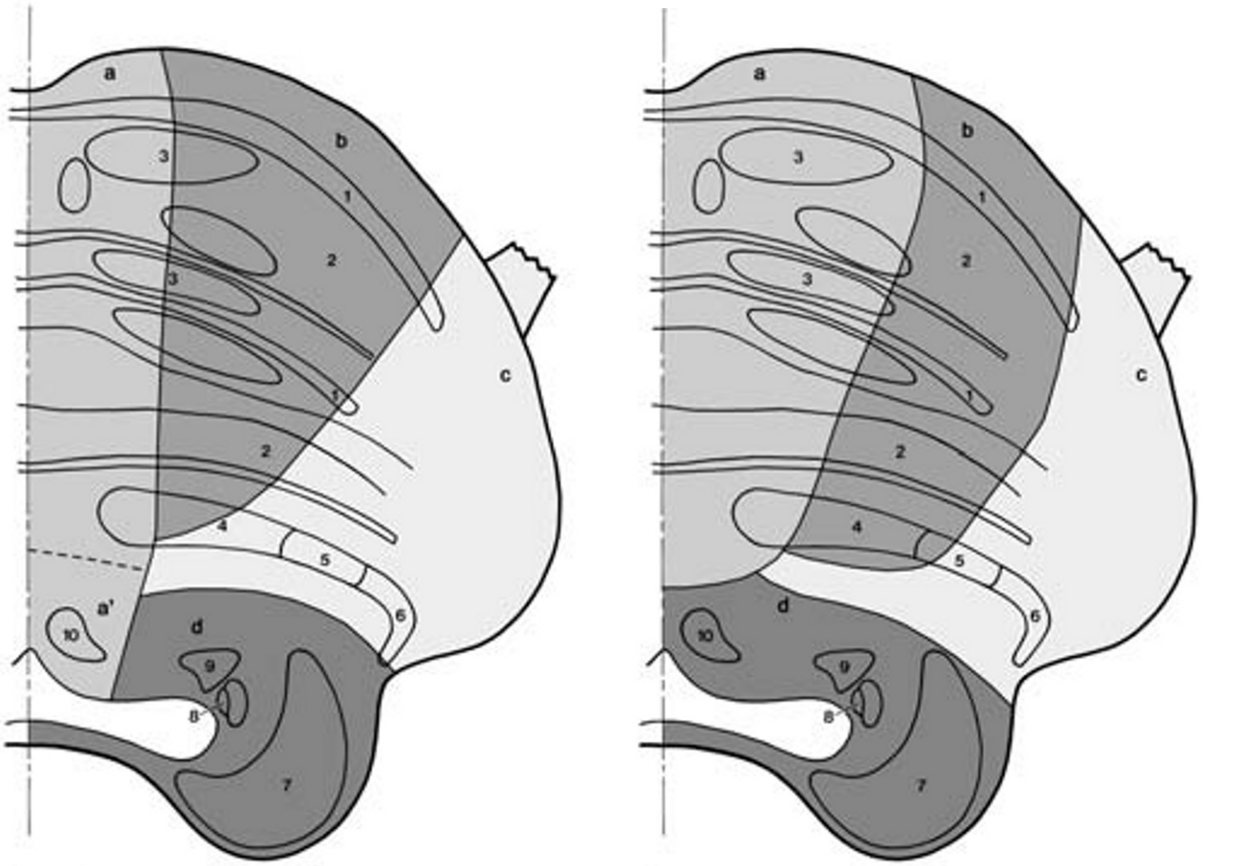

Arterial **Venous**

Fig. 7.17 (A–B). Vascular territories: Upper pons.
See also Fig. 2.16.

1 Pontocerebellar fibers
2 Pontine nuclei
3 Corticospinal tract
4 Medial lemniscus
5 Spinothalamic tract
6 Lateral lemniscus
7 Superior cerebellar peduncle (brachium conjunctivum)
8 Mesencephalic trigeminal nucleus
9 Nucleus ceruleus
10 Medial longitudinal fasciculus

Arterial territories

a, a' Anteromedial pontine territory supplied by the anteromedial group of pontine arteries:
a arising from the basilar artery,
a' arising from the arteries of the interpeduncular fossa (inferior pedicle), and supplying the pontine tegmentum by a descending path (See Fig. 7.12).
b Anterolateral pontine territory supplied by the anterolateral group of pontine arteries arising from the basilar artery
c Lateral pontine territory supplied by the lateral group of pontine arteries arising from the lateral pontine arteries
d Posterior pontine territory supplied by the posterior group of pontine arteries arising from the superior cerebellar artery.

Venous territories

a Anteromedial pontine territory drained by the anteromedial group of pontine veins, which drain into the anterior median pontine vein
b Anterolateral pontine territory drained by the anterolateral group of pontine veins, which drain into the transverse pontine veins
c Lateral pontine territory drained by the lateral group of pontine veins, which drain into the transverse pontine and lateral mesencephalic veins
d Posterior pontine territory drained by the posterior group of pontine veins, which drain into the veins of the brachium conjunctivum.

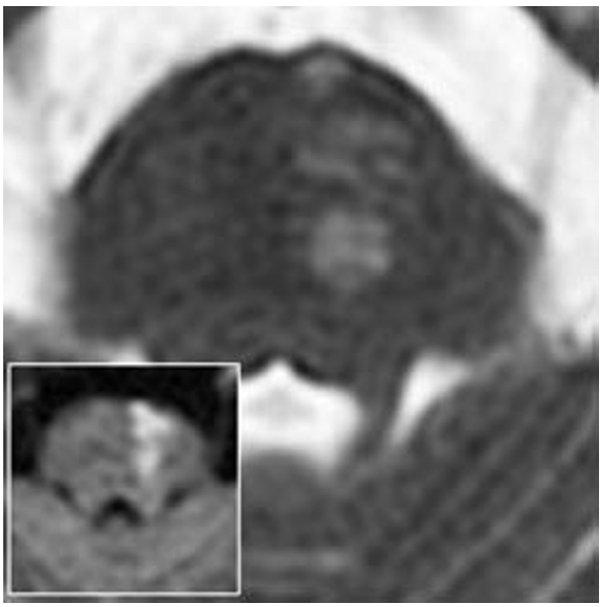

A

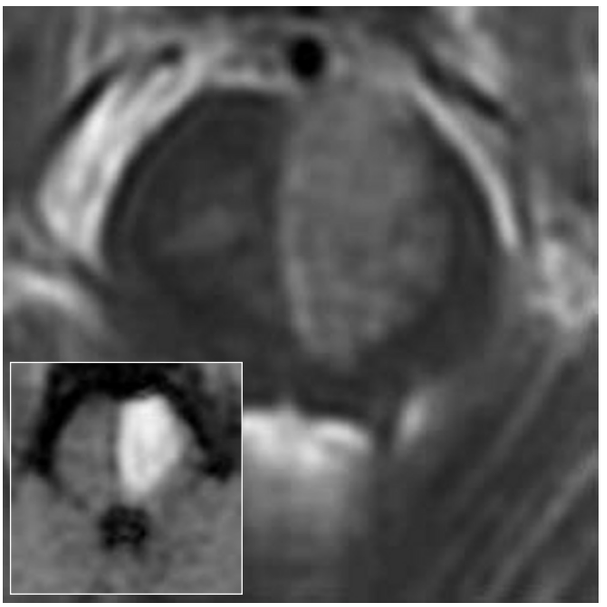

B

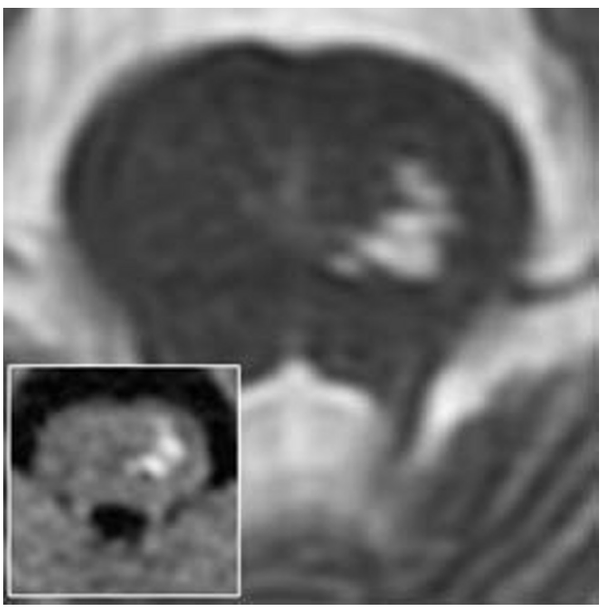

C

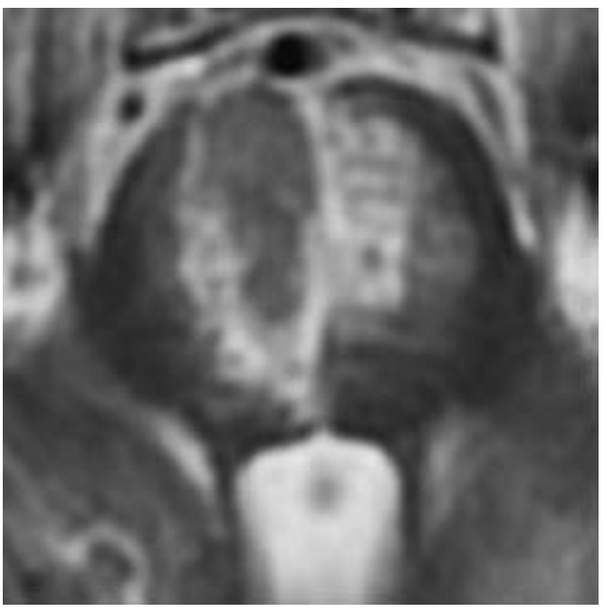

D

Fig. 7.18 (A–D). Focal Mid-Upper pontine infarction.
Clinical MR images at 1.5 Tesla.

A **Territory affected:** **AM.** Axial T2-WI (D-WI inset)
B. **Territory affected:** **AM.** Axial T2-WI (D-WI inset)
C. **Territory affected:** **AL.** Axial T2-WI, (D-WI inset)
D. **Territories affected:** **Bilateral AM** with hemorrhagic conversion on right. Axial T2-WI

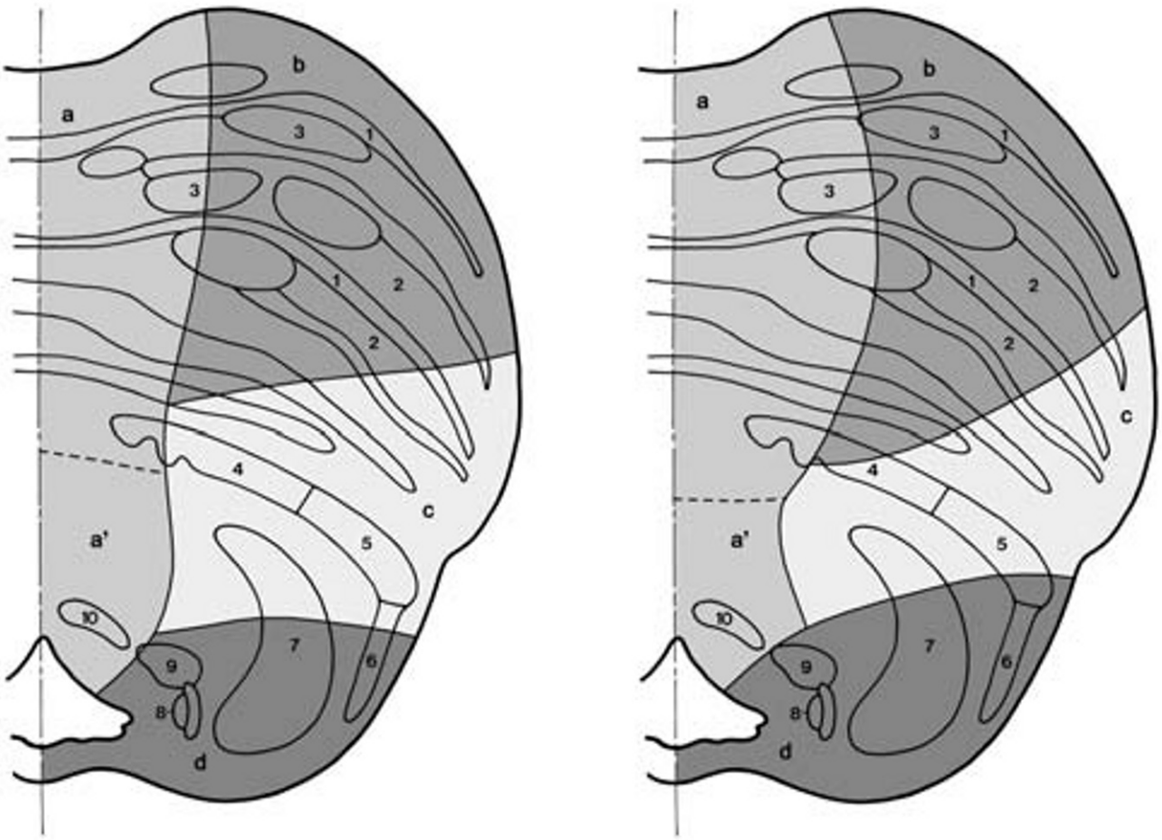

Fig. 7.19 (A–B). Vascular territories: Upper pons.
See also Fig. 2.17.

1 Pontocerebellar fibers
2 Pontine nuclei
3 Corticospinal tract
4 Medial lemniscus
5 Spinothalamic tract
6 Lateral lemniscus (auditory fibers)
7 Superior cerebellar peduncle (brachium conjunctivum)
8 Mesencephalic trigeminal nucleus
9 Nucleus ceruleus
10 Medial longitudinal fasciculus

Arterial territories

a, a' Anteromedial pontine territory supplied by the anteromedial group of pontine arteries:
a Arising from the basilar artery
a' Arising from the arteries of the interpeduncular fossa (inferior pedicle) and reaching the pontine tegmentum by a descending route (See Fig. 7.12).
b Anterolateral pontine territory supplied by the anterolateral group of pontine arteries arising from the basilar artery
c Lateral pontine territory supplied by the lateral group of pontine arteries arising from the superior cerebellar artery
d Posterior pontine territory supplied by the posterior group of pontine arteries arising from the superior cerebellar artery

Venous territories

a, a' Anteromedial pontine territory drained by the anteromedial group of pontine veins:
a Draining into the anterior median pontine vein;
a' Draining into the interpeduncular veins, by an ascending path
b Anterolateral pontine territory drained by the anterolateral group of pontine veins, which drain into the transverse pontine veins
c Lateral pontine territory drained by the lateral group of pontine veins, which drain into the lateral mesencephalic vein
d Posterior pontine territory drained by the posterior group of pontine veins, which drain into the veins of the brachium conjunctivum

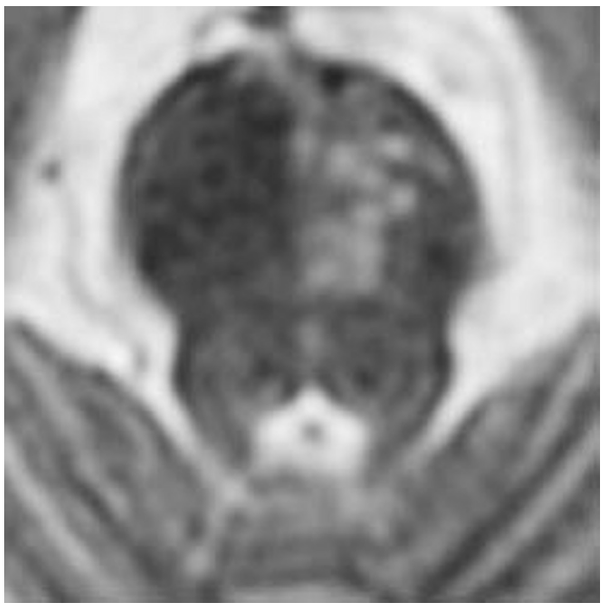

A

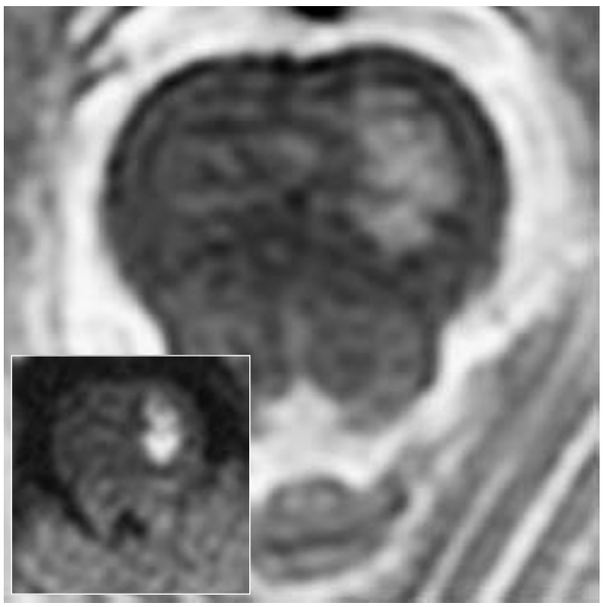

B

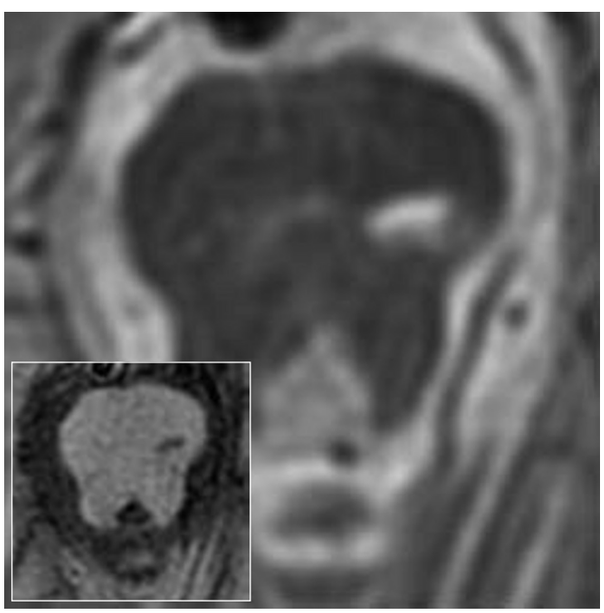

C

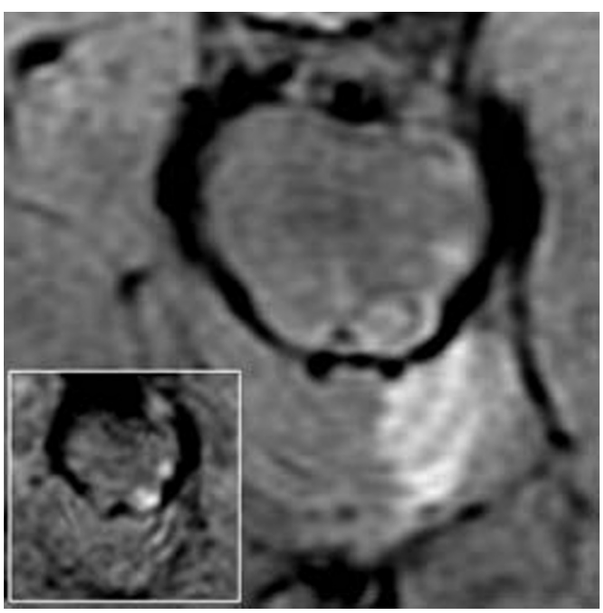

D

Fig. 7.20 (A–D) Focal upper pontine infarctions.
Clinical MR images at 1.5 Tesla.

A. Territories affected: AM. Axial T2-WI
B. Territories affected: AL. Axial T2-WI (with D-WI inset)
C. Territory affected: L. Axial T2-WI (with T1 inset).
D. Territories affected: Predominantly P with some L. Axial FLAIR (with D-WI inset). Concurrent infarction of the brain stem and superior cerebellum.

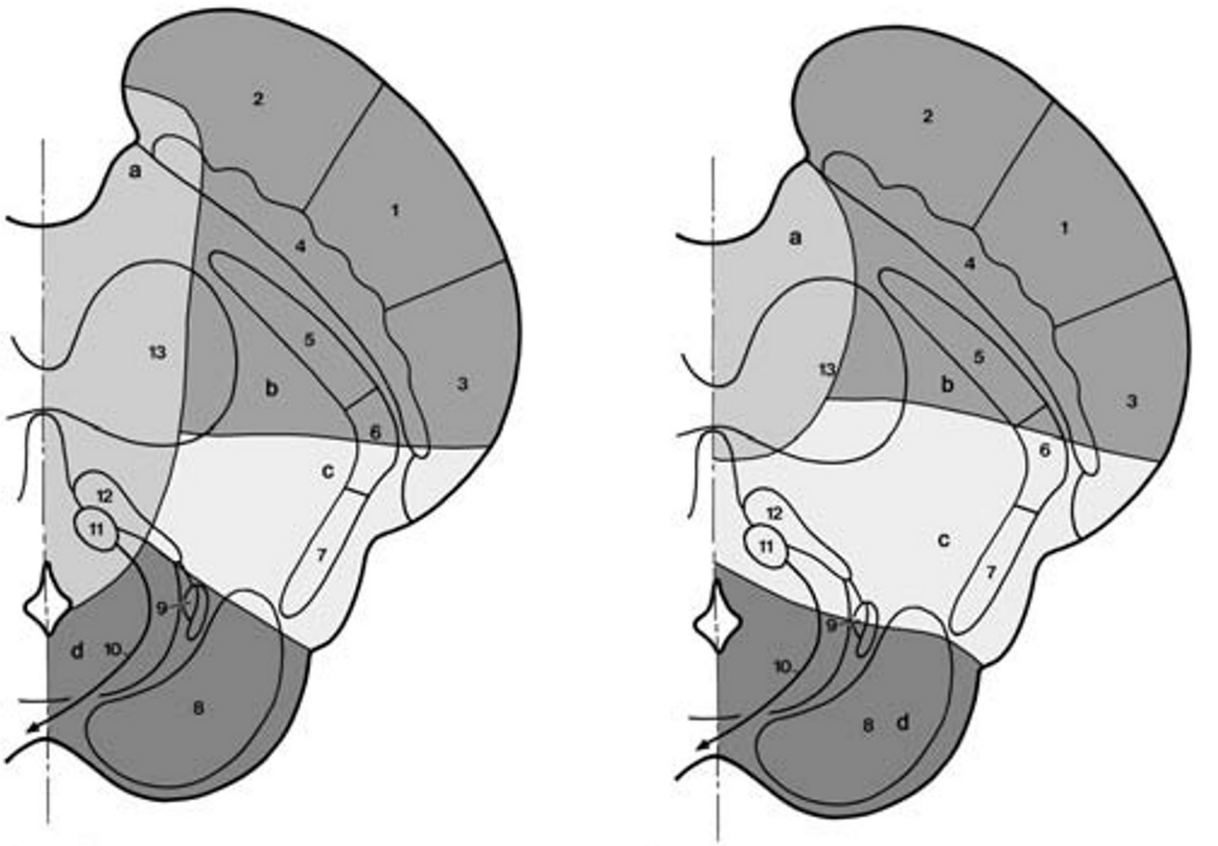

Fig. 7.21 (A–B). Vascular territories: Mesencephalon at the level of the inferior colliculi. See also Fig. 2.18.

1 Corticospinal tract
2 Frontopontine tract
3 Parietotemporopontine tract
4 Substantia nigra, pars compacta
5 Medial lemniscus
6 Spinothalamic tract
7 Lateral lemniscus (auditory fibers)
8 Inferior colliculus
9 Mesencephalic trigeminal nucleus
10 Fibers of the trochlear nerve
11 Trochlear nucleus
12 Medial longitudinal fasciculus
13 Superior cerebellar peduncle (brachium conjunctivum)

Arterial territories

a Anteromedial mesencephalic territory supplied by the anteromedial group of mesencephalic arteries arising from the middle group of the arteries of the interpeduncular fossa: reaching the trochlear nucleus by arteries penetrating near the midline; reaching the superior cerebellar peduncle by arteries penetrating into the exit zone of the oculomotor root

b Anterolateral mesencephalic territory supplied by the anterolateral group of mesencephalic arteries arising from the collicular and posterior medial choroidal arteries

c Lateral mesencephalic territory supplied by the lateral group of mesencephalic arteries arising from the collicular artery

d Posterior mesencephalic territory supplied by the posterior group of mesencephalic arteries arising, in ascending order, from the superior cerebellar and collicular arteries.

Venous territories

a Anteromedial mesencephalic territory drained by the anteromedial group of mesencephalic veins, which drain into the interpeduncular veins and into the veins of the pontomesencephalic sulcus

b Anterolateral mesencephalic territory drained by the anterolateral group of mesencephalic veins, which drain into the interpeduncular veins and into the veins of the pontomesencephalic sulcus

c Lateral mesencephalic territory drained by the lateral group of mesencephalic veins, which drain into the lateral mesencephalic vein

d Posterior mesencephalic territory drained by the posterior group of mesencephalic veins, which drain into the precentral and intercollicular veins.

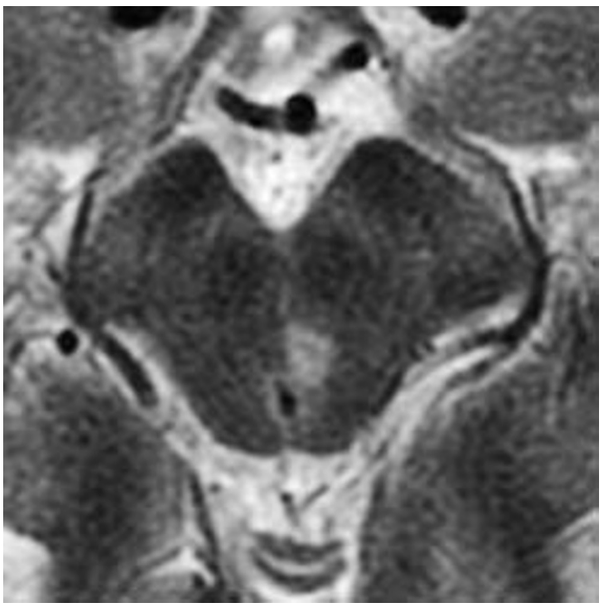

A

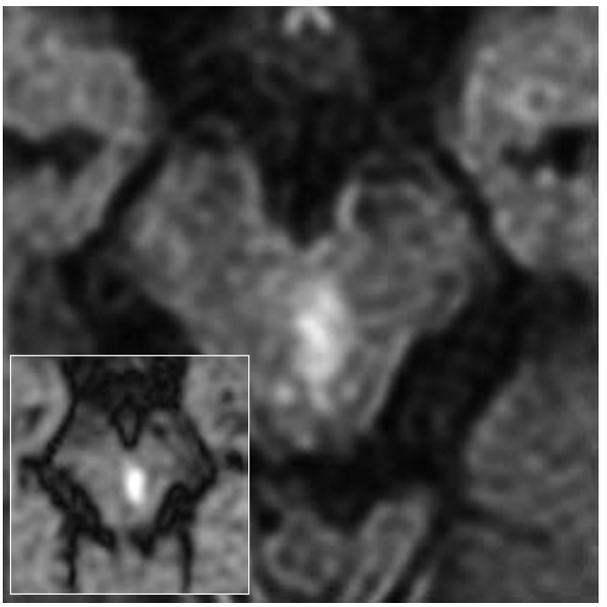

B

C

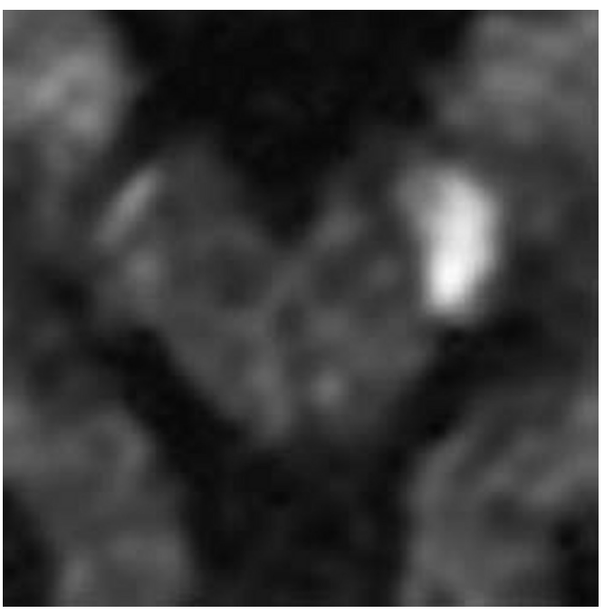

D

Fig. 7.22. (A–D). Focal mesencephalic infarction.
Clinical MR images at 1.5 Tesla.

A. Territory affected: Distal AM. Axial T2-WI
B. Territory affected: Distal AM. Axial T2-WI (D-WI inset)
C. Territories affected: Bilateral AM. Axial FLAIR (D-WI inset)
D. Territory affected: AL. Axial D-WI

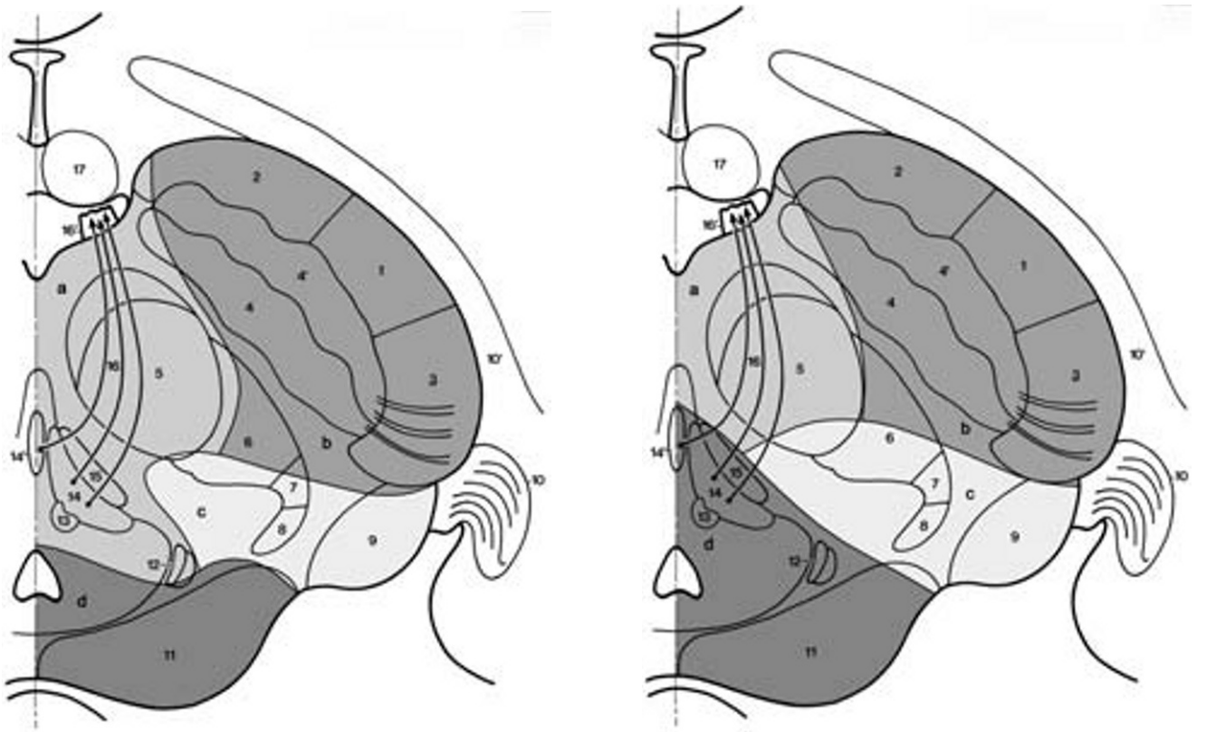

Arterial **Venous**

Fig. 7.23 (A–B). Vascular territories: Mesencephalon at the level of the superior colliculi. See also Fig. 2.20.

1 Corticospinal tract
2 Frontopontine tract
3 Parietotemporopontine tract
4 Substantia nigra, pars compacta
4′ Substantia nigra, pars reticulata
5 Red nucleus
6 Medial lemniscus
7 Spinothalamic tract
8 Lateral lemniscus (auditory fibers)
9 Medial geniculate body
10 Lateral geniculate body
10′ Optic tract
11 Superior colliculus
12 Mesencephalic trigeminal nucleus
13 Accessory oculomotor nucleus (Edinger-Westphal)
14 Principal oculomotor nucleus
14′ Nucleus of Perlia
15 Medial longitudinal fasciculus
16 Fibers of the oculomotor nerve
16′ Oculomotor nerve
17 Mammillary body

Arterial territories

a Anteromedial mesencephalic territory supplied by the anteromedial group of mesencephalic arteries, arising from the middle group of arteries of the interpeduncular fossa: reaching the oculomotor nuclei by arteries penetrating near the midline; reaching the red nucleus by arteries penetrating at the root exit zone of the oculomotor nerve

b Anterolateral mesencephalic territory supplied by the anterolateral group of mesencephalic arteries arising in ascending order from the collicular, posterior medial choroidal, posterior cerebral, and anterior choroidal arteries

c Lateral mesencephalic territory supplied by the lateral group of mesencephalic arteries arising in ascending order from the collicular, posterior medial choroidal, and posterior cerebral arteries

d Posterior mesencephalic territory supplied by the posterior group of mesencephalic arteries arising in ascending order from the collicular and posterior medial choroidal arteries.

Venous territories

a Anteromedial mesencephalic territory drained by the anteromedial group of mesencephalic veins, which drain into the interpeduncular veins

b Anterolateral mesencephalic territory drained by the anterolateral group of mesencephalic veins, which drain into the basal and interpeduncular veins

c Lateral mesencephalic territory, drained by the lateral group of mesencephalic veins which drain into the lateral mesencephalic and basal veins

d Posterior mesencephalic territory drained by the posterior group of mesencephalic veins, which drain into the intercollicular and superior median collicular veins.

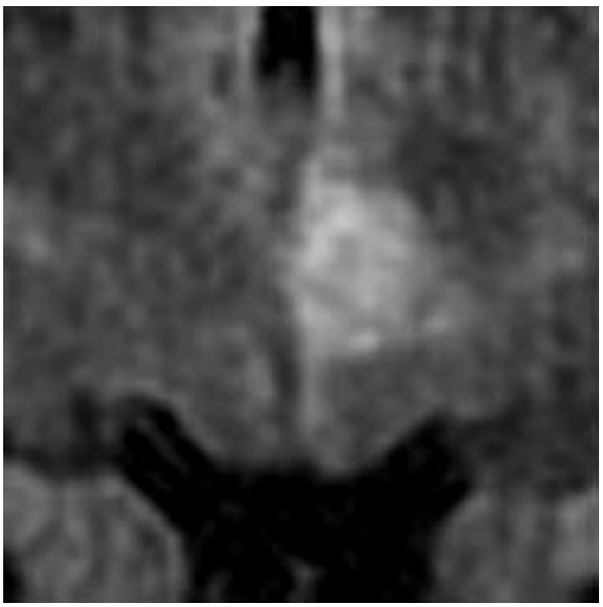

A

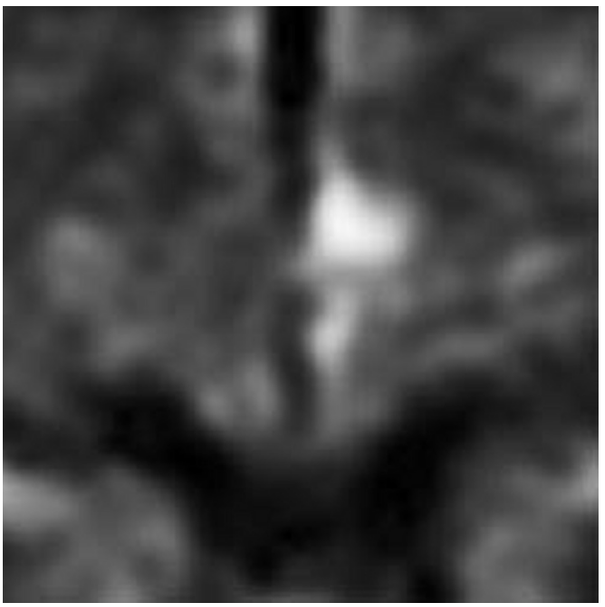

B

C

Fig. 7.24 (A–C). Focal mesencephalic infarction.
Clinical MR images at 1.5 Tesla.

A.–C. Territory affected: AM. A. Axial FLAIR
B. Axial D-WI
C. Sagittal T2-WI

SECTION VIII

MAGNETIC RESONANCE MICROSCOPY AT 9.4 TESLA

Prior imaging studies have depicted the anatomy of the brain stem and spinal cord in some detail [56, 102, 107, 146, 148, 188, 194, 236, 238, 244, 250, 271, 320, 32, 354]. High-field MRI now depicts brain anatomy with increasingly high resolution, both *in vivo* [49, 64, 83, 104, 433] and *in vitro* [136, 137, A1, A2, A3, A4, A5, A6, A7, A8]. In the near future, advancing technology will require comparable advances in anatomic knowledge, in order to make full use of the image detail that will become routine.

For that reason, this section provides a detailed atlas of the gray matter nuclei and the white matter tracts of the brain stem, as seen in formalin-fixed human cadaver specimens at 9.4 Tesla. Each caption indicates the pertinent anatomic relationships displayed in the section and discusses relevant aspects of the structures illustrated.

Technical limitations necessitated dividing the brain stem into segments for higher resolution study of each portion (Fig 8.1). Except in the midbrain, the same specimen was imaged in all three orthogonal planes, so all of the images may be compared within plane and across planes *for each segment*. In the midbrain, the axial plane images were aquired in one specimen, while the coronal and sagittal images were obtained in a second.

A single coherent alphanumeric system was used for all the specimens illustrated in this section, so the same structures may be identified easily in all of the images. This system is given in the list below. In specific instances cited in the list, a given structure was assigned more than one designation, to allow us to place a label within the structure without completely obscuring it. In general, the numbering system begins caudally and ascends cranially, so, on average, lower numbers refer to structures that are encountered more caudally, even if they then extend far cranially.

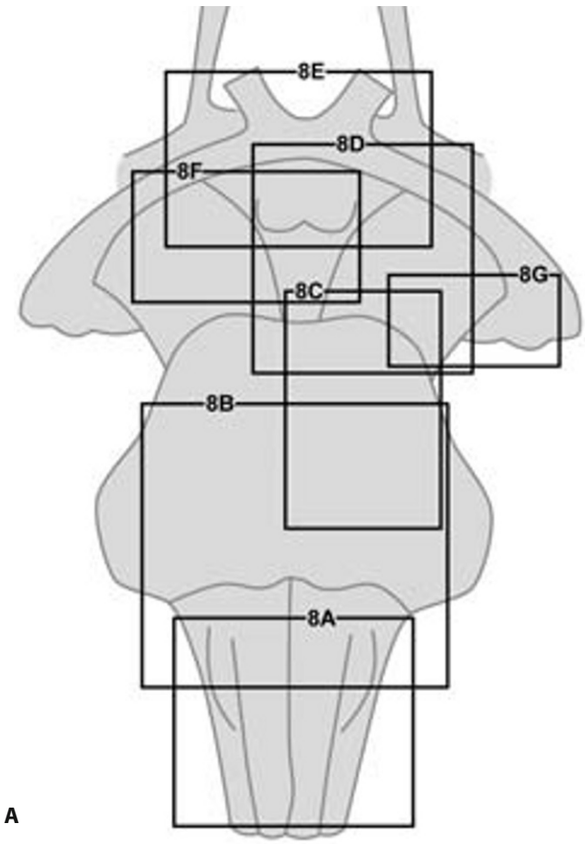

A

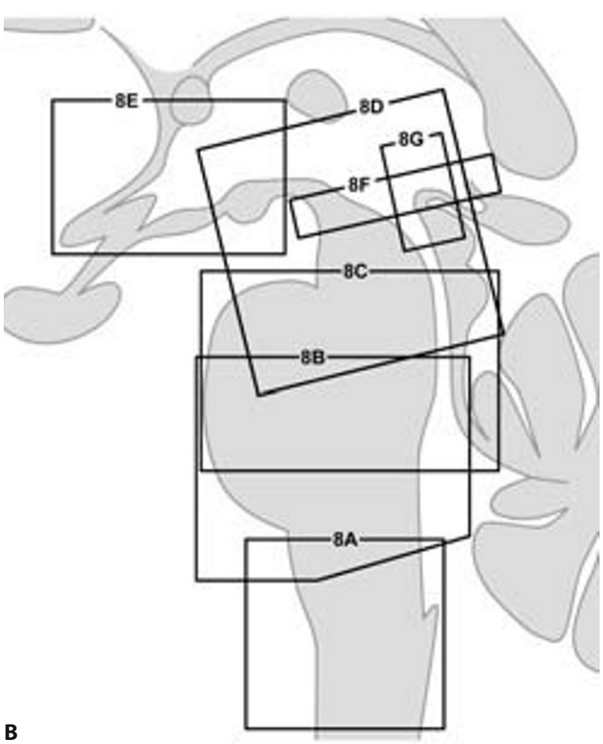

B

Fig. 8.1 (A–B). Diagrams of the segments of the brain stem imaged in each of the following sections A. Composite frontal coronal representation. B. Composite sagittal representation.

The narrow bore (3.5 cm) of the bird cage coil used to obtain the MR images necessitated sectioning the brain stem into portions that fit snugly into the coil without significant distortion. **A.** and **B.** illustrate the overlapping coverage of the brain stem obtained by imaging multiple volumes. In each subsection, individual diagrams illustrate the volume imaged for that section.

Global Number & Letter List for MR Microscopy and Cranial Nerves

This set of Numbers and Letters is a coherent key for the identification of all structures in Section VIII. The arrows and arrowheads are used variably as needed for each figure. The numbers in other sections do not necessarily conform to this nomenclature.

1 Nucleus gracilis
1′ Fasciculus gracilis
2 Nucleus cuneatus
2′ Fasciculus cuneatus
2″ Accessory (lateral) nucleus cuneatus
3 Spinal trigeminal tract
4 Spinal trigeminal nucleus
5 Posterior (dorsal) spinocerebellar tract
6 Anterior (ventral) spinocerebellar tract
7 Rubrospinal tract
7′ Ventral tegmental decussation
8 Extensive reticular formation (light gray)
8′ Lateral reticular nucleus
9 Central gray matter around central canal of spinal cord
9′ Periaqueductal gray matter
10 Spinothalamic tract
11 Ventral horn
12 Lateral spinovestibular tract
13 Medial spinovestibular tract
14 Tectospinal tract (with tectobulbar fibers, this forms part of the predorsal longitudinal fasciculus (55) [358]
15 Lateral corticospinal tract
15′ Decussation of the corticospinal tracts
16 Pyramid containing the corticospinal tract
16′ Anterior corticospinal tract
16″ Corticospinal fibers descending through the pons toward the pyramid
17 Medial longitudinal fasciculus
18 Decussation of the internal arcuate fibers
19 Arcuate nuclei
20 Pontine nuclei
20′ Lateral tegmental process of pontine nuclei
21 Medial lemniscus
21′ Rete of the medial lemniscus, where the fibers assume a reticular relationship with diverse pontine nuclei [358]
21″ Nucleus of the medial lemniscus
22 Ventral trigeminothalamic tract (ventral central trigeminal tract)
23 Superior cerebellar peduncle
23c Cruciate portion of 23 (fiber mass of 23 post decussation) [358]
23′ Decussation of the superior cerebellar peduncle
23′d Dorsal portion of decussation of the superior cerebellar peduncle
23′v Ventral portion of decussation of the superior cerebellar peduncle
24 Central tegmental tract
25 Inferior cerebellar peduncle (restiform body)
26 Medial vestibular nucleus
27 Inferior vestibular nucleus
27′ Descending root of the vestibular nerve (primary sensory neurons of the vestibular nerve extending caudally to synapse in the inferior vestibular nucleus)
28 Superior vestibular nucleus
29 Lateral vestibular nucleus
30 Olivocerebellar tract
31 Glossopharyngeal nerve (CN IX)
31′ Vagal nerve (CN X)
32 Dorsal cochlear nucleus (CN VIII)
33 Ventral cochlear nucleus (CN VIII)
34 Vestibulocochlear nerve (CN VIII)
34′ Vestibular division of CN VIII
34″ Cochlear division of CN VIII
35 Facial nerve (CN VII)
35′ Genu of the facial nerve
36 Tracts of the ventrolateral columns of the spinal cord
37 Trapezoid body (auditory fibers)
38 Middle cerebellar peduncle (brachium pontis)
39 Abducens nucleus (CN VI)
40 Facial nerve nucleus (CN VII)
41 Ventral pontine decussation
42 Dorsal pontine decussation
43 Trigeminal nerve (CN V)
43′ Motor root of the trigeminal nerve (CN V)
44 Mesencephalic nucleus and tract of CN V
45 Motor nucleus of CN V
46 Principal sensory nucleus of CN V
46′ Intrapontine fascicles of the sensory root of CN V
47 Lateral lemniscus
47′ Dorsal nucleus of the lateral lemniscus
48 Ventral nucleus of the lateral lemniscus
49 Supra-olivary nuclear complex (superior olivary nucleus and trapezoid nucleus)
50 Pontobulbar body
51 Pontocerebellar fibers
52 Dorsal trigeminothalamic tract [106]
53 Tegmento-olivary tract
54 Nucleus centralis superior (of Bechterew) (extensive nuclear region on each side of the raphe)
54′ Nucleus centralis superior medialis (medial portion of 54; Synonym: Superior nucleus of the raphe)
54″ Nucleus centralis superior lateralis (lateral portion of 54)
55 Predorsal longitudinal fasciculus (contains tectospinal fibers (14) [358])
56 Inferior colliculus
57 Area parabigemina posterior
58 Pedunculopontine nucleus of the tegmentum
59 Nucleus of the trochlear nerve (CN IV)
59′ Trochlear nerve (CN IV)
60 Cerebral peduncle
61 Interpeduncular nucleus

62 Dorsolateral tegmental fasciculus (fiber bundle in the dorsal portion of the central tegmental tract (24), lying in relation to the tegmento-olivary tract (53) extending superomedially to become part of the area acclinis (A). It may arise from fibers surrounding the red nucleus [358]
63 Oculomotor nucleus (CN III)
63′ Intramesencephalic oculomotor fibers (CN III)
63″ Cisternal segment of the oculomotor nerve (CN III)
64 Substantia nigra
64c Pars compacta of substantia nigra
64r Pars reticulata of substantia nigra
65 Stragulum (layer of gray matter lateral to the superior cerebellar peduncle containing, among other elements, remnants of the inferior cerebellar peduncle and, caudally the ventral spinocerebellar tract) (see also 191 Sagulum)
66 Corpus medullare (central white matter of the cerebellar hemisphere)
67 Brachium of the inferior colliculus
68 Dorsal longitudinal fasciculus
69 Superior colliculus
69′ Commissure of the superior colliculus
70 Brachium of the superior colliculus
71 Mammillary body
72 Fornix (anterior column)
72′ Fornix (body)
73 Principal mammillary fasciculus
74 Mammillotegmental fasciculus (tract)
75 Mammillothalamic fasciculus (tract) (of Vicq d'Azyr)
76 Habenular nuclei
76c Habenular commissure
76m Medial habenular nucleus (also v)
76l Lateral habenular nucleus (also w)
77 Stria medullaris thalami
78 Habenulo-interpeduncular tract (fasciculus retroflexus)
79 Hypothalamo-tegmental fibers, supramammillary commissure and peduncle of the mammillary body
80 Pretectal area
81 Corticobulbar fibers in the medial cerebral peduncle
82 Nuclei mediani thalami (group of the more medial portions of the nucleus medialis thalami and nucleus centri mediani thalami plus the subependymal collections of nuclei) [358] (also p)
83 Nucleus dorsomedialis thalami
83′ Anteroventral nucleus of the thalamus
84 Nucleus medialis thalami, pars dorsolateralis
85 Nucleus medialis thalami, pars ventromedianis
86 Nucleus lateralis thalami
86p Nucleus lateralis posterior thalami
86′ Thalamoparietal fibers
87 Nucleus reticularis thalami (within the lateral (external) medullary lamina of the thalamus)
88 Thalamic peduncles
88c Caudal thalamic peduncle
88d Dorsal thalamic peduncle
88r Rostral thalamic peduncle
88v Ventral thalamic peduncle (also 172)
88vc Ventrocaudal thalamic peduncle
89 Area triangularis of Wernicke
90 Pregeniculate nucleus
91 Centromedian nucleus of the thalamus
92 Pulvinar
92i Nucleus pulvinaris inferior thalami
92l Nucleus pulvinaris lateralis thalami
92m Nucleus pulvinaris medialis thalami
93 Ventral posterior thalamic nuclei
93m Ventral posteromedial nucleus of the thalamus
93l Ventral posterolateral nucleus of the thalamus
94i Ventral intermediate nucleus of the thalamus
94l Ventral lateral nucleus of the thalamus
95 Red nucleus
95′ Capsule of the red nucleus
96 Prerubral radiations (cerebellorubrothalamic tract)
97 Subthalamic nucleus
98 Zona incerta
99 Fields of Forel (H, H1 (thalamic fasciculus) and H2 (lenticular fasciculus))
100 Optic chiasm
100x Optic chiasm (decussating fibers)
100i Optic chiasm (nondecussating fibers
100n Prechiasmal optic nerve
101 Optic tract
102 Hypothalamus
104 Medial geniculate body
104d Dorsal nucleus of the medial geniculate body
104m Medial nucleus of the medial geniculate body
104v Ventral nucleus of the medial geniculate body
104′ Capsule of the medial geniculate body
105 Auditory radiations (geniculotemporal radiations)
106 Lateral geniculate body
106′ Capsule of the lateral geniculate body
107 Optic radiations (geniculocalcarine radiations)
108 Frontal radiations of the red nucleus
109 Nucleus medialis mesencephali
110 Nucleus lateralis mesencephali reticularis [358]
111 Pallidonigral and corticonigral tracts
112 Peripeduncular nucleus
112d Dorsal division of the peripeduncular nucleus
112l Ventral division of the peripeduncular nucleus
113 Pregeniculate nucleus
139 Cistern of the lamina terminalis
140 Gyrus rectus
140′ Medial orbital gyrus
141 Olfactory nerve
142 Medial olfactory stria
143 Lateral olfactory stria
144 Area olfactoria
153 Tuber cinereum
155 Supra-optic recess of the third ventricle
156 Nucleus of the ansa lenticularis
157 Ansa lenticularis

158 Ansa peduncularis
159 Area densa (ventromedial mesencephalic tegmentum medial and ventral to the red nucleus, containing fibers of uncertain nature) [358]
161 Stria semicircularis

170 Caudate nucleus (head)
170′ Caudate nucleus (body)
170″ Caudate nucleus (tail)
171 Nucleus accumbens septi
172 Ventral thalamic peduncle (also 88v)
173 Anterior commissure
174 Cingulate gyrus
175a Anterior limb of the internal capsule
175g Genu of the internal capsule
175p Posterior limb of the internal capsule
175r Retrolenticular portion of the internal capsule
175s Sublenticular portion of the internal capsule
176 Anterior perforated substance
177 Substantia innominata
178 Putamen
178′ Caudato-lenticular bridges of gray matter
179 Globus pallidus
179l Globus pallidus (lateral nucleus, external nucleus)
179m Globus pallidus (medial nucleus, internal nucleus)
179′ Lateral (external) medullary lamina of the lenticular nucleus
179″ Medial (internal) medullary lamina of the lenticular nucleus
181 Fasciculus uncinatus
182 Extreme capsule, claustrum and external capsule

190 Lateral nucleus of the mesencephalon (nuclear mass situated between the medial lemniscus, medial geniculate body and the area tegmentalis) [358]
191 Sagulum (cell poor layer of gray matter lateral to the inferior colliculus, containing the tectopontine tract) [358] (see also 65 Stragulum)
192 Superior longitudinal fasciculus

201 Temporal stem (narrow attachment of the temporal lobe to the central brain)
202 Superior temporal gyrus
203 Middle temporal gyrus
204 Inferior temporal gyrus
205 Lateral occipito-temporal gyrus (partially synonymous with the fusiform gyrus)
206 Parahippocampal gyrus (also PHG)
207 Uncus (also Un)
208 Amygdala

210 Hippocampal formation
211 Transverse temporal gyrus (of Heschl)

213 Cuneus
214 Lingual gyrus
215 Calcarine sulcus

220 Anterior nucleus of the thalamus

Structures of the Anterior Lobe of Cerebellum
221 Lingula of vermis (also Li)
222 Precentral fissure
223 Central lobule of vermis (also Ce)
223′ Wings of the central lobule (also Ce′)
224 Preculminate fissure (postcentral fissure)
225 Culmen of the vermis
225′ Quandrangular lobule (anterior quadrangular lobule)
226 Primary fissure (anterior superior fissure), dividing the anterior lobe from the posterior lobe

Structures of the Posterior Lobe of Cerebellum
227 Declive of the vermis
227′ Simple lobule (posterior quadrangular lobule)
228 Posterior superior fissure (post clival fisssure)
229 Folium of the vermis
229′ Superior semilunar lobule (Crus I)
231 Tuber of the vermis
231′ Inferior semilunar lobule (Crus II). Together Crura I and II may be called the ansiform lobule.
232 Prepyramidal fissure
232′ Fissura ansoparamedianis
233 Pyramis of the vermis (pyramid of the vermis)
233′ Gracile lobule
233″ Biventral lobule (digastric lobule, dorsal paraflocculus)
234 Prebiventral fissure
234′ Intrabiventral fissure
234″ Postpyramidal fissure (secondary fissure)
235 Uvula of the vermis (Also U)
235′ Tonsil of the cerebellum (Also T) (ventral paraflocculus)
236 Posterolateral fissure (postnodular fissure), dividing the posterior lobe from the flocculonodular lobe.

Structures of the Flocculonodular Lobe of Cerebellum
237 Nodulus of the vermis
237′ Flocculus

250 Corpus callosum, rostrum
251 Corpus callosum, genu
252 Corpus callosum, body
253 Corpus callosum, splenium
254 Forceps major, fibers crossing through the splenium

Letter labels (Numbers and Lower Case):

3V Third ventricle
4V Fourth ventricle
a Ventromedial nucleus of the hypothalamus
a′ Dorsomedial nucleus of the hypothalamus
ac Ambient cistern
b Lateral area of the hypothalamus
c Subcommissural organ

cpc Cerebellopontine angle cistern
d Lateral nuclei of the tuber cinereum
e Medial nucleus of the mammillary body
f Lateral nucleus of the mammillary body
g Intercalated nucleus of the mammillary body
h Paraventriculo-hypophyseal tract [358]
i Supra-optic nucleus
j Pre-optic area
k Fasciculus olfactorius
l Paraventricular nucleus of the hypothalamus
lmc Lateral medullary cistern
m Posterior area of the hypothalamus
n Radiations of the corpus callosum
nb Radiations of the body of the corpus callosum
nr Radiations of the rostrum of the corpus callosum
o Dorsomedian nucleus of the hypothalamus
p Nuclei mediani thalami (also 82)
pmc Premedullary cistern
ppc Prepontine cistern
q Lateral pre-optic nucleus
qc Quadrigeminal plate cistern
r Cingulum
s Alveus
sc Suprasellar (chiasmatic) cistern
t Fimbria
u Pallido-hypothalamic tract
v Medial habenular nucleus (also 76 m)
w Lateral habenular nucleus (also 76 l)
x Medial parabrachial nucleus
y Kölliker-Fuse nucleus
z Lateral parabrachial nucleus

Letter labels (Upper Case):

A Vertebral artery
Ac Area acclinus (dorsomedial tegmental zone situated dorsolateral to the medial longitudinal fasciculus and rostral to the hypoglossal and dorsal vagal nuclei, extending the length of the brain stem from the medulla nearly to the diencephalon)
B Basilar artery
C Corpus parabigeminum
Ce Central lobule of vermis (also 223)
Ce′ Wings of the central lobule of vermis (hemispheric analogue of Ce) (also 223′)
Cl Clivus
CP Choroid plexus
CS Corticospinal tract (partial overlap with 16)
D Dorsal accessory olivary nucleus
DC Descending cortical tracts passing to or through the brain stem
De Dentate nucleus
F Frontopontine tract
H Hypoglossal nucleus
H0 Forel field H (area tegmentalis H) (also 99, used generically for any H field)
H1 Forel field H1 (thalamic fasciculus) (also 99)
H2 Forel field H2 (lenticular fasciculus) (also 99)
I Nucleus intercalatus (this merges superiorly into the nucleus prepositus hypoglossi)
ICA Internal carotid artery
IF Inferior foramen cecum (deep midline segment of pontomedullary sulcus)
IP Interpeduncular fossa
IR Infundibular recess of the third ventricle
L Locus ceruleus or site of the locus ceruleus
Li Lingula of the vermis (also 221)
M Medial accessory olivary nucleus
MC Meckel's (trigeminal) cave
NP Nucleus prepositus hypoglossi (Nucleus dorsalis tegmenti inferior) (nucleus situated cephalic to the hypoglossal nucleus, but occuping the same relative position. It receives fibers from the dorsal longitudinal fasciculus) [358]
O Inferior olivary nucleus
O′ Amiculum (capsule of the inferior olivary nucleus)
O″ Hilum of the inferior olivary nucleus
P Pyramid
Pi Pineal gland
Po Area postrema
PB Petrous bone
PC Posterior commissure
PHG Parahippocampal gyrus (also 206)
PS Pontomedullary sulcus (midline portion)
PT Parieto-temporopontine tract
S Nucleus of the solitary tract
SC Suprasellar cistern
SAS Subarachnoid space
Sph Sphenoid sinus
T Tonsil (also 235′)
U Uvula (also 235)
Un Uncus (also 207)
V Dorsal nucleus of the Vagus
Vm Dorsal *motor* nucleus of the Vagus, situated ventromedial to the
Vs Dorsal *sensory* nucleus of the Vagus
VG Vein of Galen

A. Medulla (Figs. 8.2–8.33)

A 1. Axial medulla

Axial sections of the medulla displayed from caudal to cranial (Figs. 8.2 to 8.13).

These cartoons (A–B) display the anatomic region imaged in Figs. 8.2–8.33.

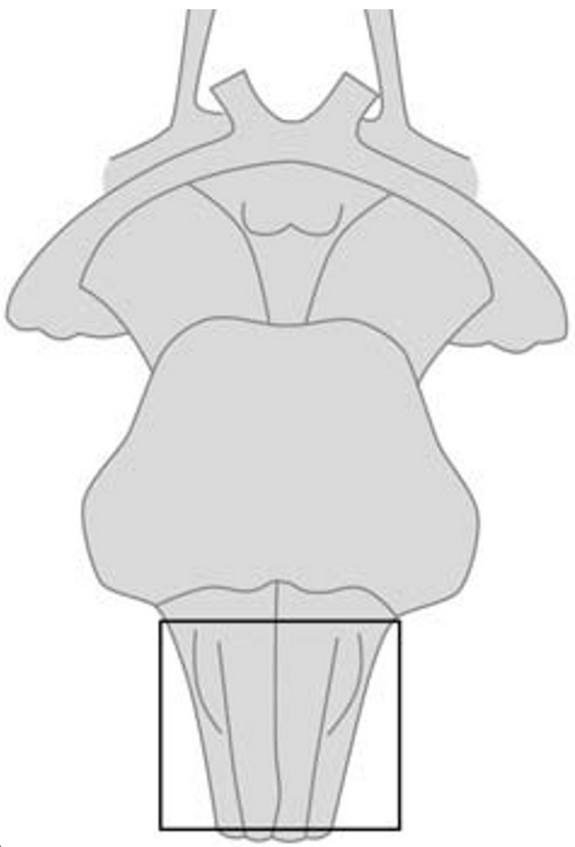

A

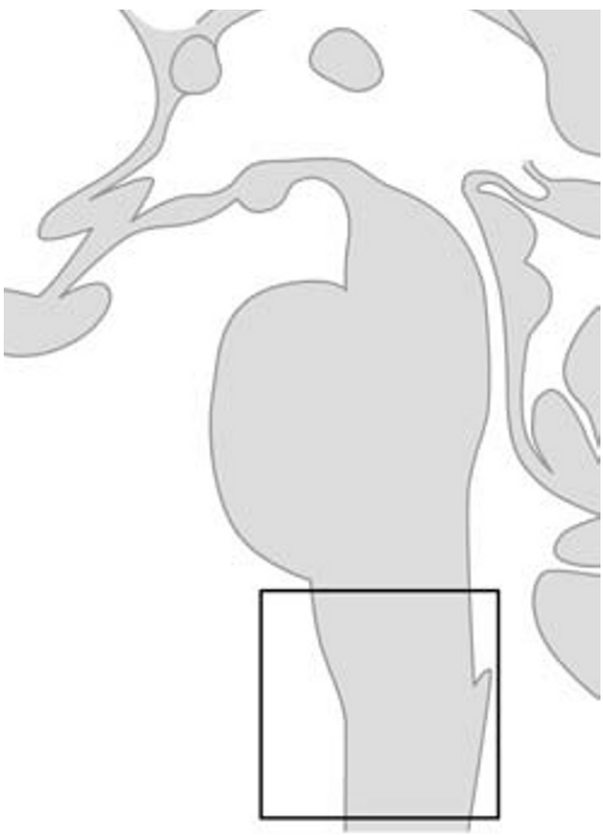

B

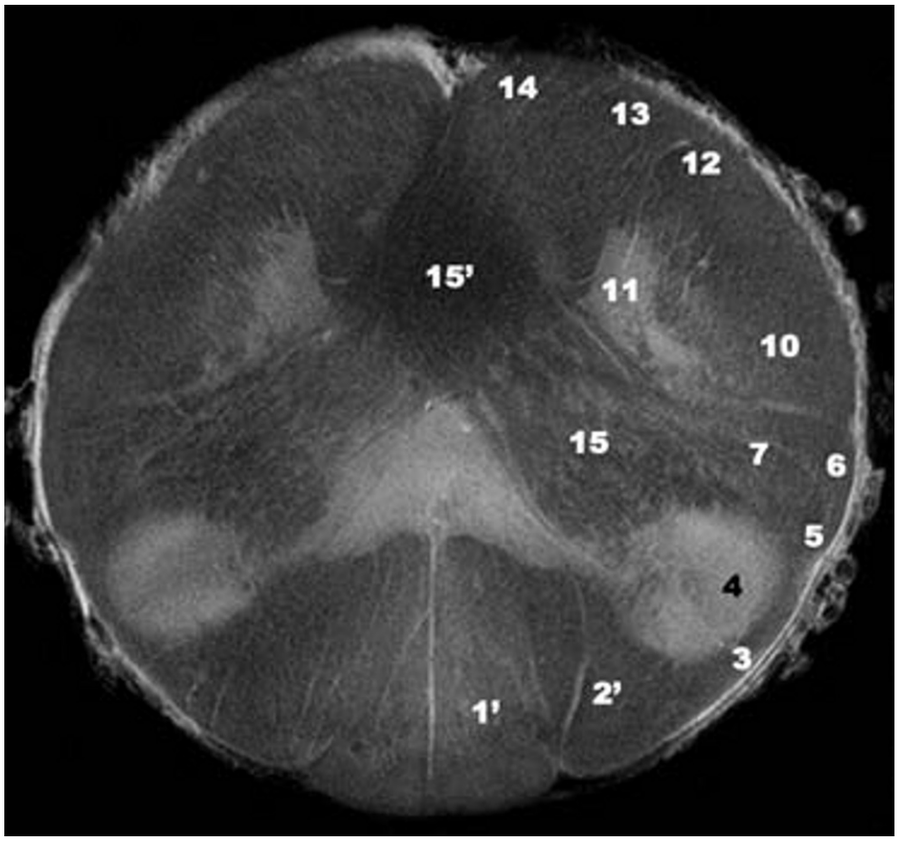

Fig. 8.2. Cervico-medullary junction. Axial section through the decussation of the pyramids.

As the corticospinal fibers approach the bulbospinal junction, most of the fibers decussate (15′), pass laterally (15) to the contralateral lateral columns of the spinal cord, and descend in the *posterior portion* of the lateral columns as the lateral corticospinal tracts (approximately 75–90%) [78, 322]. Other corticospinal fibers continue directly caudally into an oval region along both sides of the anterior median fissure of the spinal cord as the uncrossed anterior corticospinal tracts (approximately 10%) [322]. These descend to thoracic levels [322]. A third group of corticospinal fibers extends directly downward into the *anterior portion* of the ipsilateral lateral column as the uncrossed lateral corticospinal tracts. Perhaps 55% of corticospinal fibers end in the cervical spinal cord, 20% in the thoracic cord and 25% in the lumbosacral segments [78]. Uncrossed fibers predominantly extend to alphamotoneurons of the spinal cord that innervate the proximal musculature of the extremities [78]. Crossed fibers predominantly extend to alphamotoneurons of the spinal cord that innervate the distal musculature of the extremities [78].

1′ Fasciculus gracilis approaching the caudal pole of the nucleus gracilis
2′ Fasciculus cuneatus
3 Spinal trigeminal tract
4 Spinal trigeminal nucleus
5 Posterior spinocerebellar tract
6 Anterior spinocerebellar tract
7 Rubrospinal tract
10 Spinothalamic tract
11 Ventral horn of the spinal cord
12 Lateral spinovestibular tract
13 Medial spinovestibular tract
14 Tectospinal tract
15 Decussated corticospinal tract diverging toward the lateral columns
15′ Decussation of the corticospinal tracts

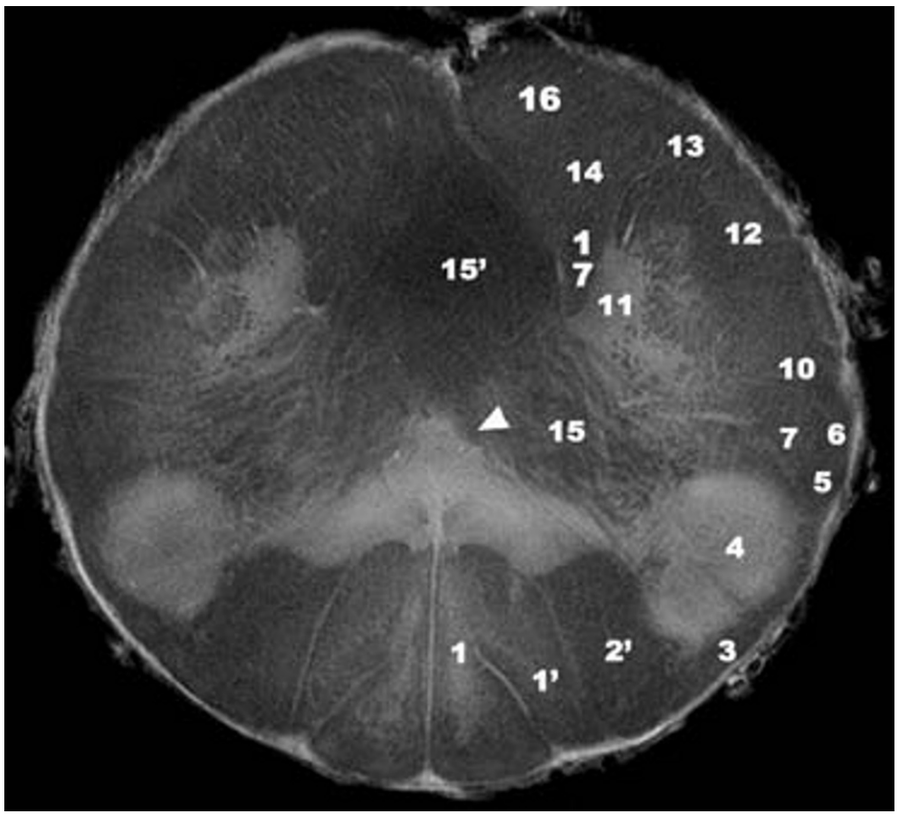

Fig. 8.3. Cervico-medullary junction. Axial section through the inferior pole of the nucleus gracilis.

At this level, the spinal trigeminal tract (3) and nucleus (4) lie near to the surface, with the posterior (5) and anterior (6) spinocerebellar tracts situated ventral to them. The ascending anterior spinocerebellar tract (6) and spinothalamic tract (10) group together as the anterolateral funiculus [358]. The anterolateral funiculus lies ventral and lateral to the spinal trigeminal tract and nucleus (3,4) and lateral to the reticular nuclei, with the anterior spinocerebellar tract (6) at the periphery of the funiculus [322]. Within the anterolateral funiculus, fibers from lower spinal levels lie lateral to fibers from higher levels [322]. The rubrospinal tract (7) descends from the red nucleus into the spinal cord in the lateral funiculus, near to the anterior spinocerebellar (6) and spinothalamic (10) tracts [358].

1 Nucleus gracilis (caudal pole)
1′ Fasciculus gracilis
2′ Fasciculus cuneatus
3 Spinal trigeminal tract
4 Spinal trigeminal nucleus
5 Posterior spinocerebellar tract
6 Anterior spinocerebellar tract
7 Rubrospinal tract
10 Spinothalamic tract
11 Ventral horn
12 Lateral spinovestibular tract
13 Medial spinovestibular tract
14 Tectospinal tract
15 Corticospinal tracts diverging from the decussation
15′ Decussation of the corticospinal tracts
16 Pyramid containing the corticospinal tract
17 Medial longitudinal fasciculus

Arrowheads and arrows
White arrowhead: Central gray matter

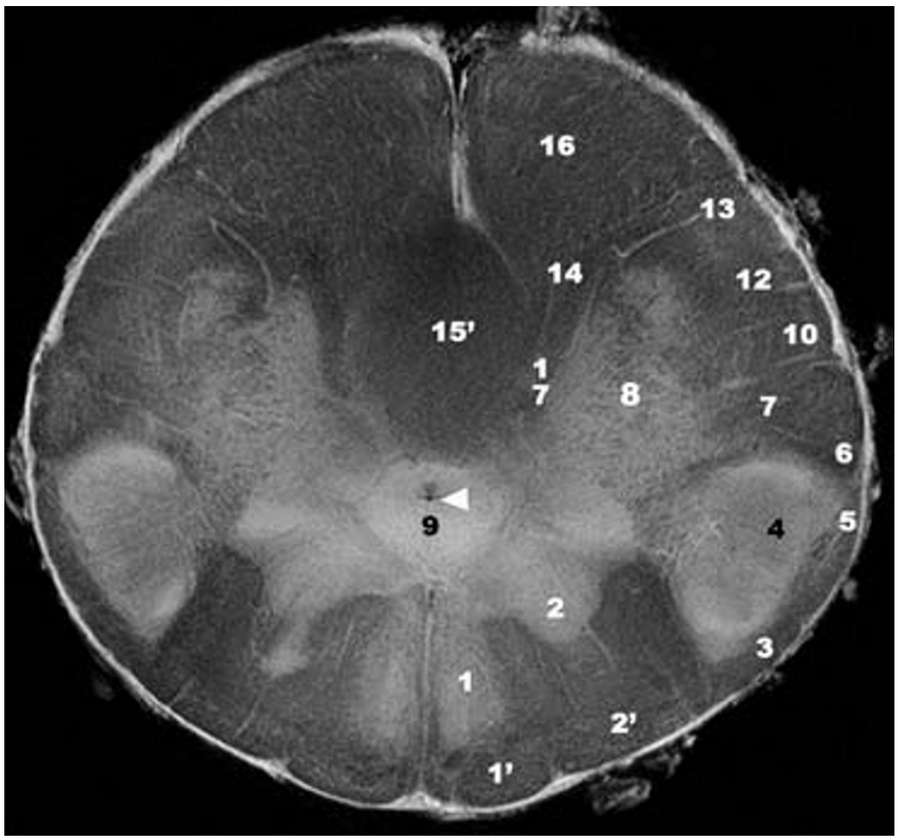

Fig. 8.4. Cervico-medullary junction. Axial section through the inferior pole of the nucleus cuneatus.

As it ascends, the posterior spinocerebellar tract (5) moves dorsally toward and then into the inferior cerebellar peduncle. As a result, the spinal trigeminal tract (3) and nucleus (4) come to lie deep to the surface of the brain stem, and the inferior cerebellar peduncle thickens. Primary somatosensory (dorsal root) fibers that ascend within the fasciculi gracilus and cuneatus are organized somatotopically. Fibers from the sacral and lumbar roots ascend medially within the fasciculus gracilus. Fibers from the thoracic region lie in intermediate position, and fibers from the cervical roots ascend laterally within the fasciculus cuneatus [322]. As they ascend, fibers that arise from adjacent dorsal roots and that innervate the same cutaneous fields become bundled together, so adjacent dermatomes become more sharply defined [322]. The dorsal columns also carry secondary postsynaptic viscerosomatic input from the nucleus proprius of the spinal cord to the nuclei gracilis and cuneatus [322a].

1 Nucleus gracilis (caudal pole)
1′ Fasciculus gracilis
2 Nucleus cuneatus (caudal pole)
2′ Fasciculus cuneatus
3 Spinal trigeminal tract
4 Spinal trigeminal nucleus
5 Posterior spinocerebellar tract
6 Anterior spinocerebellar tract
7 Rubrospinal tract
8 Extensive reticular formation (light gray)
9 Central gray matter (9) around central canal (arrowhead)
10 Spinothalamic tract
12 Lateral spinovestibular tract
13 Medial spinovestibular tract
14 Tectospinal tract
15′ Decussation of the corticospinal tracts
16 Pyramid containing the corticospinal tract
17 Medial longitudinal fasciculus

Arrowheads and arrows
White arrowhead: Central canal surrounded by the central gray matter (9)

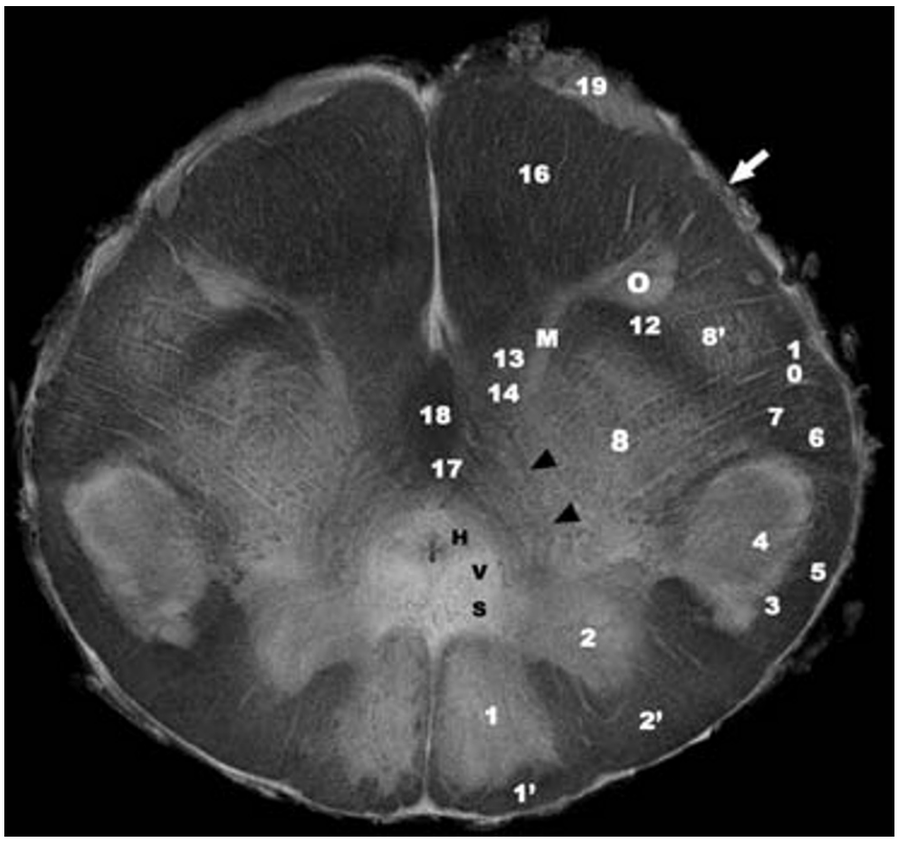

Fig. 8.5. Low medulla. Axial section through the closed portion of the medulla, the inferior pole of the great sensory decussation, and the inferior pole of the olivary nuclear complex.

The somatosensory (dorsal root) fibers ascend to the tops of the dorsal columns of the spinal cord and synapse there somatotopically over the lengths of the nuclei gracilis and cuneatus. Second order fibers originate from the nuclei gracilis and cuneatus, pass circumferentially around the central gray matter as the internal arcuate fibers (black arrowheads), cross the midline in the great sensory decussation (18), and emerge on the contralateral side as the medial lemniscus (See 21 in Section 8.7 and above).
Within the central gray matter, the hypoglossal nucleus (H), dorsal motor nucleus of the vagus (V), and nucleus of the solitary tract (S) align vertically from ventral to dorsal on each side. More superiorly, as the central canal of the closed medulla widens into the fourth ventricle of the open medulla, the posterior end of this vertical nuclear alignment will rotate laterally, and displace these nuclei into a coronal (medial to lateral) alignment.

1 Nucleus gracilis
1′ Fasciculus gracilis
2 Nucleus cuneatus
2′ Fasciculus cuneatus
3 Spinal trigeminal tract
4 Spinal trigeminal nucleus
5 Posterior spinocerebellar tract now covering the spinal trigeminal tract
6 Anterior spinocerebellar tract
7 Rubrospinal tract
8 Extensive reticular formation (light gray)
8′ Lateral reticular nucleus
10 Spinothalamic tract
12 Lateral spinovestibular tract
13 Medial spinovestibular tract
14 Tectospinal tract
16 Corticospinal tract
17 Medial longitudinal fasciculus
18 Decussation of the internal arcuate fibers (arrowheads)
19 Arcuate nuclei

Letter labels
H Hypoglossal nucleus
M Medial accessory olivary nucleus
O Inferior olivary nucleus
S Nucleus of the solitary tract
V Dorsal motor nucleus of the Vagus

Arrowheads and arrows
Black arrowheads: Internal arcuate fibers
White arrow: External arcuate fibers

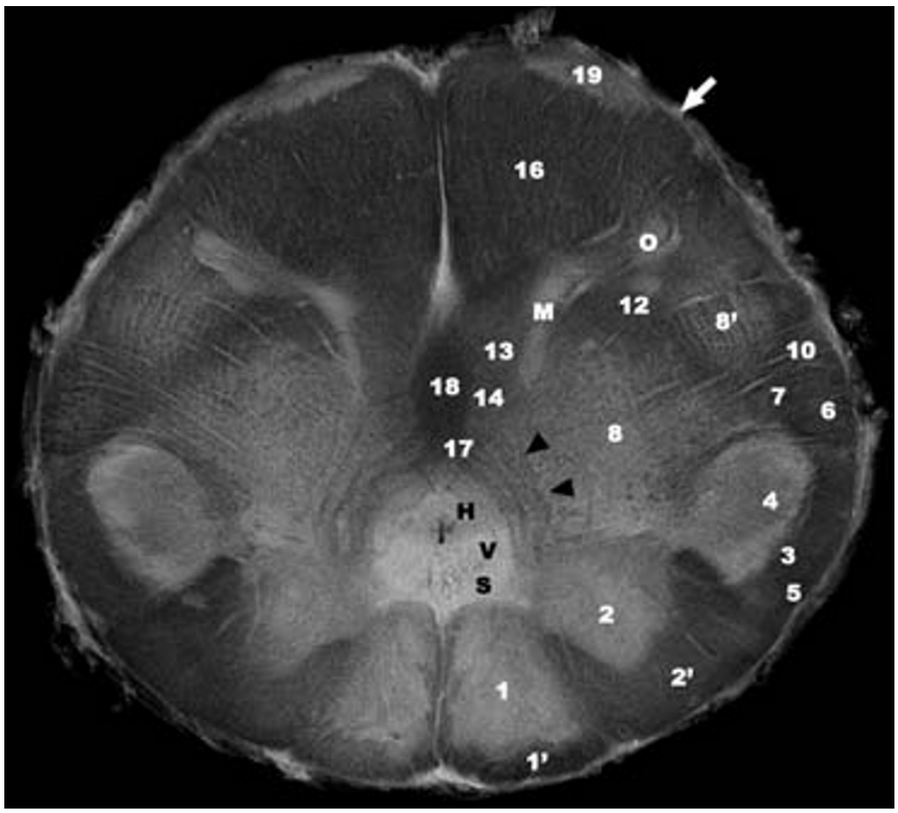

Fig. 8.6. Low medulla. Axial section through the upper end of the closed medulla.

The spinal trigeminal tract (4) and nucleus (3) now lie further from the surface of the medulla, deep to the posterior spinocerebellar tract (5). The medial accessory olivary nucleus (M) is well seen. The signal intensity of the the hypoglossal nucleus (H) is substantially and characteristically lower than the signal intensities of the dorsal motor nucleus of the vagus (V) and solitary nucleus (S). The arcuate nuclei (19) lie along and within the corticospinal fibers (16), and are regarded as separated portions of the pontine nuclei (See 20 in **Figs. 8.34–8.43**). They give rise to a thin superficial layer of external arcuate fibers (white arrow) that pass posteriorly and cranially into the inferior cerebellar peduncle (See 25 in **Fig. 8.10 –8.43**).

1 Nucleus gracilis
1′ Fasciculus gracilis
2 Nucleus cuneatus
2′ Fasciculus cuneatus
3 Spinal trigeminal tract
4 Spinal trigeminal nucleus
5 Posterior spinocerebellar tract covering the spinal trigeminal tract
6 Anterior spinocerebellar tract
7 Rubrospinal tract
8 Extensive reticular formation (light gray)
8′ Lateral reticular nucleus
10 Spinothalamic tract
12 Lateral spinovestibular tract
13 Medial spinovestibular tract
14 Tectospinal tract
16 Pyramid containing the corticospinal tract
17 Medial longitudinal fasciculus
18 Decussation of the internal arcuate fibers
19 Arcuate nuclei

Letter labels
H Hypoglossal nucleus
M Medial accessory olivary nucleus
O Inferior olivary nucleus
S Nucleus of the solitary tract
V Dorsal motor nucleus of the Vagus

Arrowheads and arrows
Black arrowheads: Internal arcuate fibers
White arrow: External arcuate fibers

Fig. 8.7. Low medulla. Axial section through the inferiormost open portion of the fourth ventricle (near foramen of Magendie), and the caudal pole of the accessory cuneate nucleus.

The inferior olivary nucleus (O) and its capsule (the amiculum (O')) bulge outward at the lateral surface of the medulla, forming the olive, the pre-olivary sulcus, and the retro-olivary sulcus. The posterior spinocerebellar tract moves further dorsally. The anterior spinocerebellar tract (6), rubrospinal tract (7) and spinothalamic tract (10) remain together in the ventral lateral aspect of the brain stem, ventrolateral to the spinal trigeminal tract (3) and nucleus (4), and dorsal to the olive.

The medial lemnisci (21) form sagittally oriented paramedian tracts to each side of the midline, dorsal to the pyramids (16) and ventral to the tectospinal tracts (14) and medial longitudinal fasciculi (17). Within the medial lemnisci, fibers from the lowest portions of the body (e.g., foot) lie most ventrally, with progressively more cranial fibers (e.g., leg) leg, thigh, arm) taking progressively more dorsal positions within the lemnisci [294]. The medial lemnisci ascend through the brain stem to the ventral posterolateral nuclei of the thalamus.

Tectospinal fibers (14) descend through the brain stem between the medial longitudinal fasciculi (17) and the medial lemnisci (21). These fibers originate in deep layers of the contralateral superior colliculus, cross the midline in the dorsal tegmental decussation, and descend into the cervical spinal cord with the medial longitudinal fasciculus to influence motor innervation of the neck muscles, for example the spinal accessory nucleus (cranial nerve XI) [488].

The solitary nucleus and tract (S) are moving lateral to the dorsal motor nucleus of the vagus (V). The vagal nuclei remain posterior to the hypoglossal nuclei (H). Hypoglossal nerve fibers (white arrowheads) emerge from the ventral aspect of the hypoglossal nucleus (H) and course ventrally. They pass lateral to the medial lemniscus (21) and then between the medial accessory olivary nucleus (M) and the inferior olivary nucleus (O) to emerge at the pre-olivary sulcus.

The dorsal longitudinal fasciculus (white arrow) is a longitudinal fiber bundle that extends the full length of the brain stem. In this section, it passes dorsal to the hypoglossal nucleus (delimiting its posterior surface) to reach the caudal end of the solitary nucleus and dorsal vagal nucleus. This tract carries ascending and descending fibers that, in part, interconnect the hypothalamus, periaqueductal gray matter and dorsal tegmental nucleus with the solitary and vagal nuclei and the spinal cord [322a, 358].

The accessory cuneate nucleus (2') now appears dorsolateral to the medial cuneate nucleus (2) and expands rostrally into the next two sections (Figs. 8.8 and 8.9). Group Z (asterisk in Fig. 8.8) is a collection of large neurons situated just rostral to the nucleus gracilis (1) and just caudal to the inferior vestibular nucleus [322a]. These nuclei relay somatosensory data to the cerebellum (see below). In addition, neurons in Group Z and the accessory cuneate nucleus send fibers across the midline to join the contralateral medial lemniscus [322a].

1 Nucleus gracilis
2 Nucleus cuneatus
2′ Fasciculus cuneatus
2″ Accessory (lateral, external) cuneate nucleus
3 Spinal trigeminal tract
4 Spinal trigeminal nucleus
5 Posterior spinocerebellar tract passing toward the inferior cerebellar peduncle
6 Anterior spinocerebellar tract
7 Rubrospinal tract
8 Extensive reticular formation (light gray)
10 Spinothalamic tract
12 Lateral spinovestibular tract
13 Medial spinovestibular tract
14 Tectospinal tract
16 Pyramid containing the corticospinal tract
17 Medial longitudinal fasciculus
19 Arcuate nuclei
21 Medial lemniscus
22 Ventral trigeminothalamic tract
24 Central tegmental tract converging on inferior olivary nucleus (O)

Letter labels

H Hypoglossal nucleus
M Medial accessory olivary nucleus
O Inferior olivary nucleus
O′ Amiculum (capsule of the inferior olivary nucleus)
S Solitary nucleus (black S) surrounding the solitary tract (white S)
V Dorsal nucleus of the Vagus

Arrowheads and arrows

White arrowheads: Intramedullary fibers of the hypoglossal nerve passing lateral to and through the medial accessory olivary nucleus (M)
Black arrowheads: Internal arcuate fibers
Short white arrow: External arcuate fibers
Long white arrow: Dorsal longitudinal fasciculus

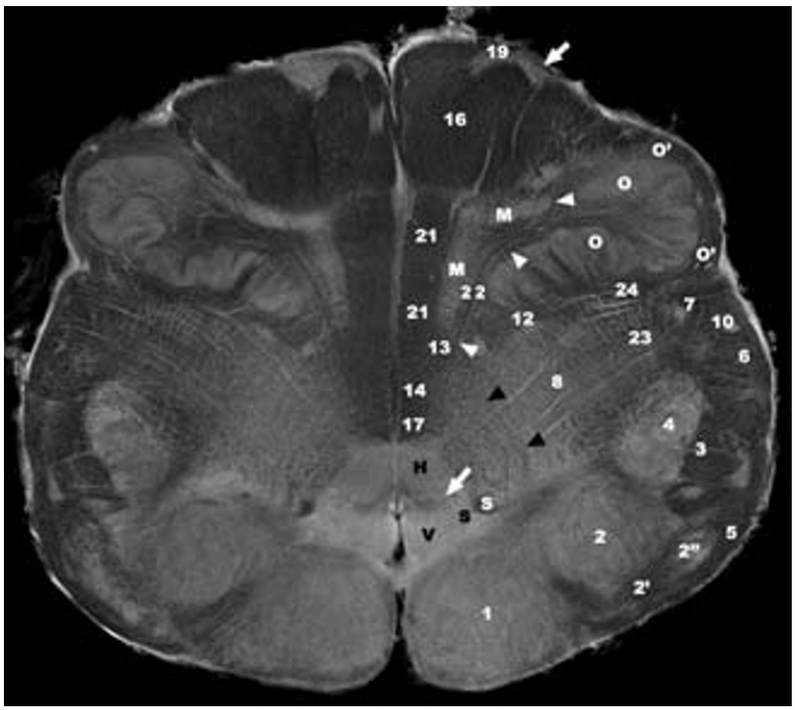

Fig. 8.7.

Four major pathways carry ascending somatosensory data from the extremities to the cerebellum [164, 322a].

(i) Ventral spinocerebellar tract for the lower limbs. Somatosensory data on proprioception (primarily Golgi tendon organs), pain and pressure from the lumbar (and to a lesser extent sacral) levels enter the dorsal horns, synapse with neurons in the intermediate gray matter and base of the dorsal horns, and cross the midline through the ventral white commissure of the spinal cord to ascend as the primarily crossed ventral spinocerebellar tract (6) [164].

(ii) Dorsal spinocerebellar tract for the lower limbs and trunk. Somatosensory data from muscle spindles, cutaneous touch receptors and joint receptors for the trunk and upper limbs enter the dorsal horn and synapse in the ipsilateral dorsal nucleus of Clarke. The dorsal nucleus of Clarke is a long column of gray matter situated at the base of the dorsal horn in spinal segments T1-L2. Afferent fibers from segments S5 to L3 enter the dorsal horns at each level, ascend through fasciculus gracilis and then exit fasciculus gracilis to synapse in the caudal end of Clarke's nucleus at L1 and L2 [322a]. Afferent fibers from the trunk (segments L2-T1) enter the dorsal horn at each level and synapse directly in Clarke's nucleus at the entry level. The efferent fibers from Clarke's column form the ipsilateral dorsal spinocerebellar tract (5) from L2 superiorly [322a]. Collateral afferent fibers from muscle spindles of both lower extremities also ascend to synapse in Group Z neurons (asterisk in Fig. 8.8) [322a].

(iii) Cuneocerebellar tract for the upper extremities. Somatosensory data from muscle spindles, cutaneous touch receptors and joint receptors from T5-C2 enter the dorsal horns and ascend through fasciculus cuneatus to synapse somatotopically in the ipsilateral accessory cuneate nucleus (2") [164, 322a]. The accessory cuneate nucleus is the upper extremity counterpart of Clarke's nucleus [164]. Efferent fibers from the accessory cuneate nucleus form the ipsilateral cuneocerebellar tract.

(iv) Rostral spinocerebellar tract for the upper extermities. Somatosensory data from the upper extremity enter the dorsal horns and synapse in the intermediate zone of the cervical spinal cord. The efferent fibers ascend ipsilaterally as the uncrossed rostral spinocerebellar tract. This tract is the upper extremity counterpart of the ventral spinocerebellar tract. The ascending dorsal spinocerebellar, cuneocerebellar and rostral spinocerebellar tracts enter the cerebellum through inferior cerebellar peduncle [164, 322a]. The ventral spinocerebellar tract ascends further to enter the cerebellum with the superior cerebellar peduncle. All four tracts terminate mainly in the midline vermis and intermediate zones ipsilateral to the tracts [164]. They project predominantly to the anterior lobe, with contributions to the caudal part of the posterior lobe [164].

Fig. 8.8. Mid-medulla. Axial section through the hilum of the inferior olivary nucleus.

The closed portion of the medulla is opening outward, so the solitary nucleus and dorsal vagal nucleus (V) are are now displaced lateral to the hypoglossal nucleus (H), bringing these nuclei into coronal alignment (See subsequent sections). The dorsal curvatures of the hypoglossal and vagal nuclei create the hypoglossal trigone and vagal trigone along the medullary portion of the floor of the fourth ventricle. These are better developed in the next section. (See also **Fig.1.5**).

The accessory cuneate nucleus (2″) lies lateral to the rostral end of the cuneate nucleus (2). Fibers from the red nucleus of the midbrain descend to the ipsilateral inferior olivary nucleus through the central tegmental tract (24), which envelops the outer surface of the olive to form its capsule, the amiculum (O′). The hilum of the olive (O″) faces medially, toward the midline. The hilum of the inferior olivary nucleus (O) and the medial accessory olivary nucleus (M) give rise to the numerous olivocerebellar fibers that cross through the medulla to the contralateral inferior cerebellar peduncle. (See subsequent sections). The caudal pole of the dorsal accessory olive is just visible (See D in the next, more cranial section **Fig. 8.9**).

Fig. 8.9. Mid-medulla. Axial section through the dorsal accessory olivary nucleus and the vestibular nuclei.

The posterior spinocerebellar (5) tract has now moved far dorsally to join the inferior cerebellar peduncle (25). External arcuate fibers (arrows) also enter the inferior cerebellar peduncle (25). The posterior spinocerebellar tract (5), the cuneocerebellar tract, and the olivocerebellar tract are three major components of the inferior cerebellar peduncle (See also next two figures).

The vestibular nuclei form a diamond shaped nuclear mass at the lateral angle of the rhomboid fossa (**See Figs. 2.4 and 2.6**). Of these, the medial vestibular nucleus (26) and the inferior vestibular nucleus (27) lie within the medullary portion of the rhomboid fossa. Primary myelinated axons of the vestibular nerve enter the brain stem at the pontomedullary sulcus and descend (27′) within the inferior vestibular nucleus (27) to synapse in the inferior and medial vestibular nuclei [294]. The myelinated fascicles descending through the gray matter of the nucleus create a stippled appearance that identifies both the descending vestibular fibers (27′) and the inferior vestibular nucleus (27) (See also the next more cephalic section). Fibers from the medial vestibular nucleus *descend* through the medial longitudinal fasciculus (17) to the upper cervical spinal cord, to provide reflexive turning of the head with alterations in body posture. Fibers from all of the vestibular nuclei *ascend* through the medial longitudinal fasciclus to reach the abducens, trochlear and oculomotor nuclei to provide reflexive adjustment of gaze (fixation) with changes in body posture.

1 Nucleus gracilis
2 Nucleus cuneatus
2″ Accessory (lateral, external) nucleus cuneatus
3 Spinal trigeminal tract
4 Spinal trigeminal nucleus
5 Posterior spinocerebellar tract, now part of the inferior cerebellar peduncle
6 Anterior spinocerebellar tract
7 Rubrospinal tract
8 Extensive reticular formation (light gray)
10 Spinothalamic tract
14 Tectospinal tract
16 Pyramid containing the corticospinal tract
17 Medial longitudinal fasciculus
21 Medial lemniscus
22 Ventral trigeminothalamic tract
24 Central tegmental tract converging on inferior olivary nucleus (O)
25 Inferior cerebellar peduncle (restiform body)
26 Medial vestibular nucleus
27 Inferior vestibular nucleus
27′ Descending root of the vestibular nerve

Letter labels

4V Fourth ventricle
D Dorsal accessory olivary nucleus
H Hypoglossal nucleus
I Intercalated nucleus (nucleus intercalatus)
M Medial accessory olivary nucleus
O Inferior olivary nucleus
O′ Amiculum (capsule of the inferior olivary nucleus)
O″ Hilum of the inferior olivary nucleus with emerging olivocerebellar fibers
S Tract of the solitary nucleus, surrounded by the solitary nucleus
V Dorsal nucleus of the Vagus
Vm Dorsal *motor* nucleus of the Vagus, situated ventromedial to the dorsal sensory nucleus (Vs)
Vs Dorsal *sensory* nucleus of the Vagus

Arrowheads, arrows and asterisk

White arrowhead: Intramedullary fibers of the hypoglossal nerve passing medial to and through the medial accessory olivary nucleus
Single white arrow: Dorsal longitudinal fasciculus
Paired white arrows: External arcuate fibers
Asterisk: Group Z (nucleus Z) (approximate location)

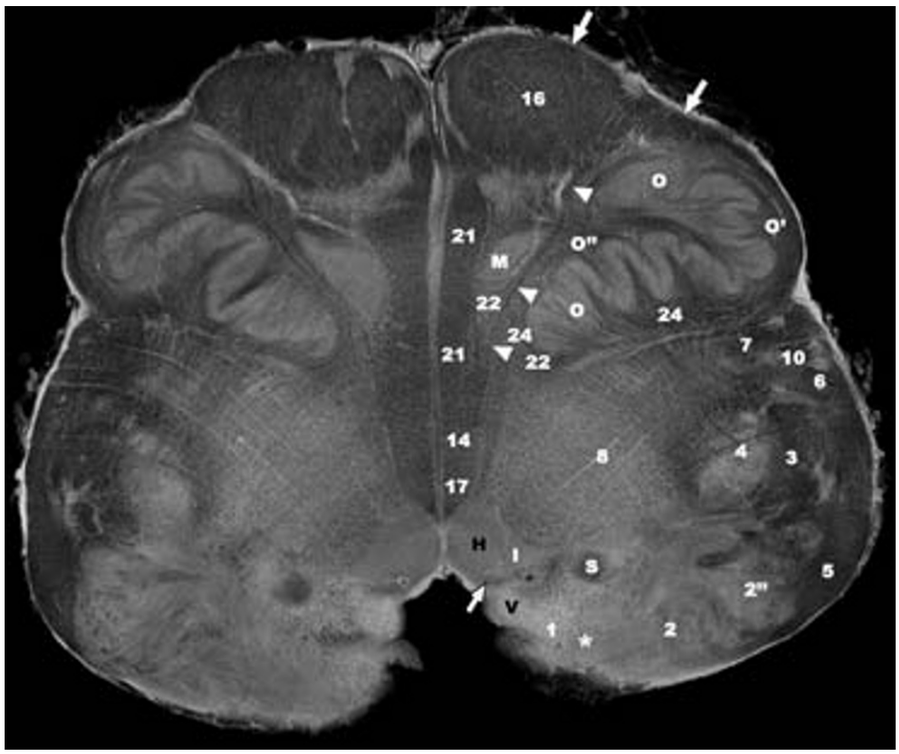
16
O
O'
21
O"
M
22
O
24
24
21
22
7
10
6
14
8
4
3
17
H
I
S
5
2"
V
1
2

8.8.

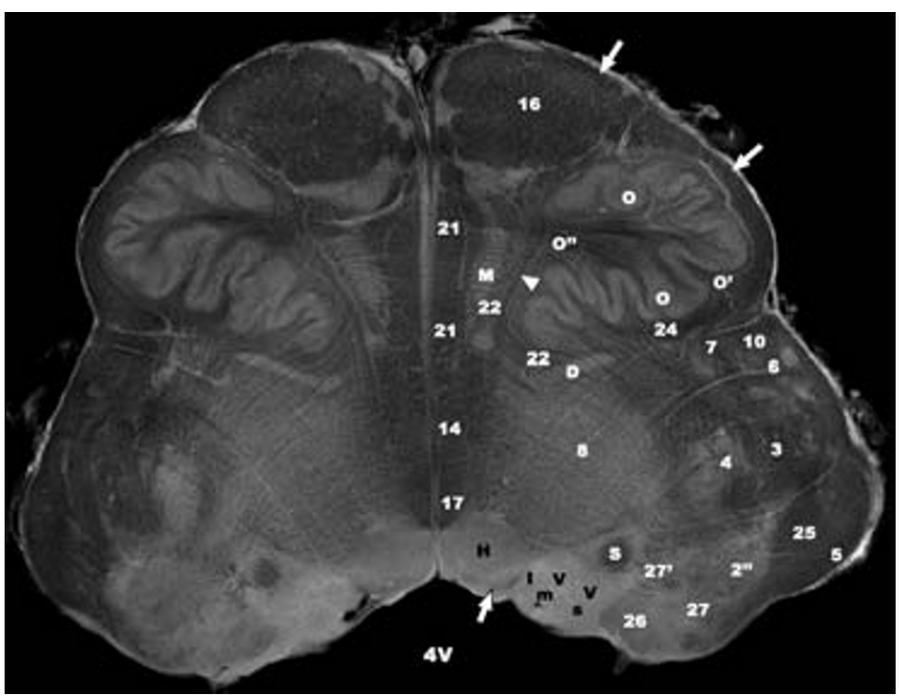
16
O
21
O"
M
O'
22
O
21
24
7
10
22
D
6
14
8
4
3
17
25
H
S
5
27'
2"
I
V
V
m
a
26
27
4V

8.9.

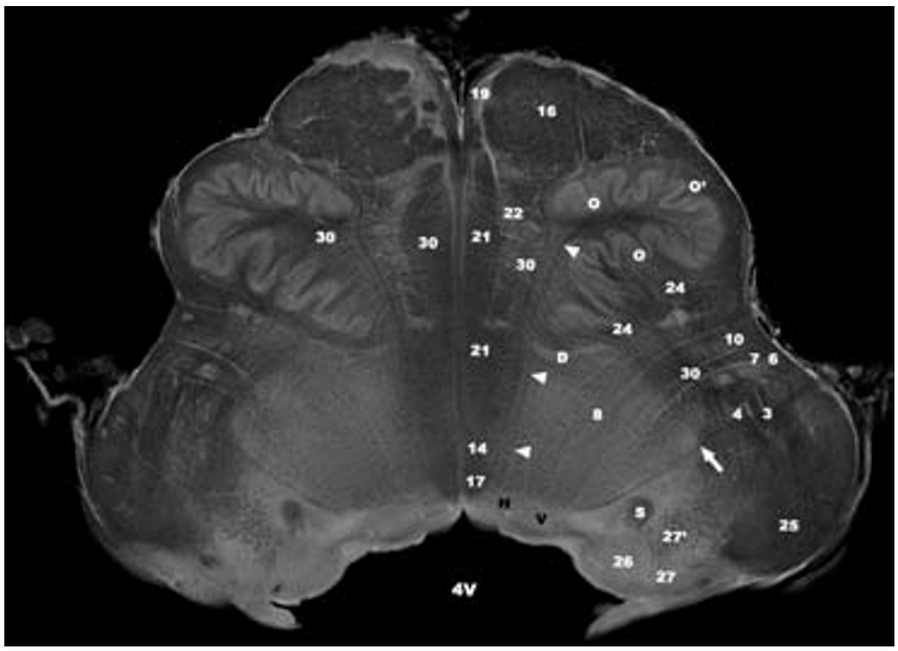

Fig. 8.10. Upper medulla. Vagus nerve. Nucleus ambiguus. Axial section.

In this section and the next, the olivocerebellar tract (multiple 30s) can be followed from the hilum of the contralateral inferior olivary nucleus (O) and the medial accessory olivary nucleus across the midline, directly through the ipsilateral inferior olivary nucleus (O) and the dorsal accessory olivary nucleus (D), into the inferior cerebellar peduncle (25).

At this level, the prominent bundle (single arrow) of nerve fascicles passing anterolaterally toward the surface most likely represents vagal nerve fibers (See Fig. 8.12). Ventral to this bundle, and oriented slightly oblique to it, a stippled band indicates the cut cross-sections of fibers of the nucleus ambiguus. Note the proximity of the nerve bundle (single arrow) to the dorsal vagal nucleus (V), the solitary nucleus and tract (S), and the fibers of the nucleus ambiguus (See Sect. IX, Cranial nerves).

3 Spinal trigeminal tract
4 Spinal trigeminal nucleus
6 Anterior spinocerebellar tract
7 Rubrospinal tract
8 Extensive reticular formation (light gray)
10 Spinothalamic tract
14 Tectospinal tract
16 Pyramid containing the corticospinal tract
17 Medial longitudinal fasciculus
19 Arcuate nuclei
21 Medial lemniscus
22 Ventral trigeminothalamic tract
24 Central tegmental tract converging on inferior olivary nucleus
25 Inferior cerebellar peduncle (restiform body)
26 Medial vestibular nucleus
27 Inferior vestibular nucleus
27′ Descending root of the vestibular nucleus
30 Olivocerebellar tract

Letter labels

4V Fourth ventricle
H Hypoglossal nucleus (rostral pole)
O Inferior olivary nucleus
O′ Amiculum (capsule of the inferior olivary nucleus)
S Solitary tract surrounded by the solitary nucleus (light gray)
V Dorsal nucleus of the Vagus

Arrowheads and arrows

Arrowheads: Intramedullary fibers of the hypoglossal nerve (CN XII) passing medial to and through the medial accessory olivary nucleus
Single white arrow: Intramedullary fibers of the vagus nerve (CN X)

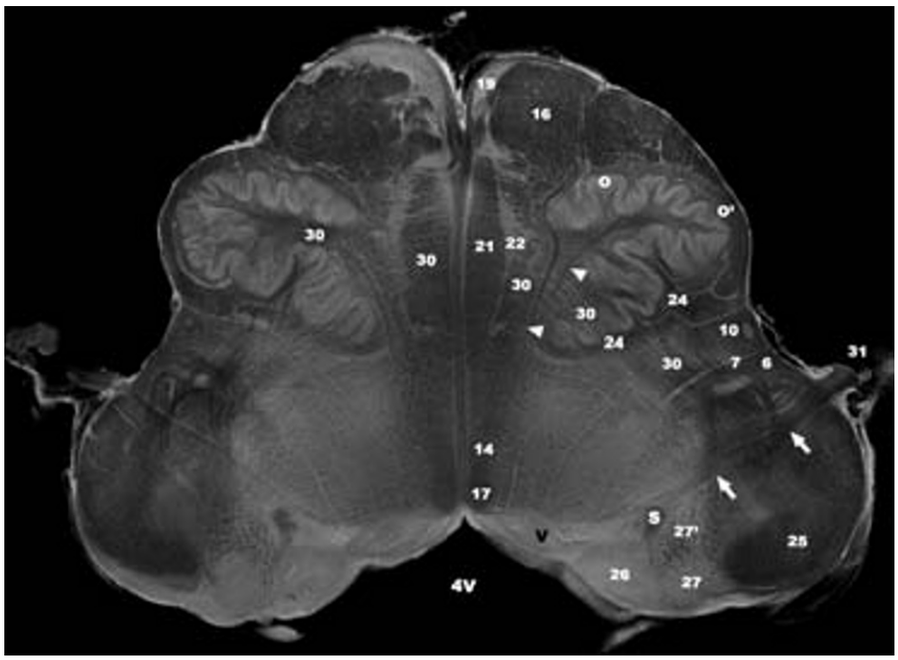

Fig. 8.11. High medulla. Glossopharyngeal and hypoglossal nerves. Axial section.

The glossopharygeal nerves (31) cross the surface of the medulla at the postolivary sulcus between the olive (O) and the inferior cerebellar peduncle (25) (See Sect. IX, Cranial nerves). Prominent fiber bundles (arrow) traverse the dorsal medulla toward the solitary and dorsal vagal nuclei, and at this level appear to represent glossopharyngeal fibers. The anterior spinocerebellar tract (6), rubrospinal tract (7), and spinothalamic tract (10) remain together anterolateral to the spinal trigeminal tract (3) and nucleus (4). The ventral trigeminothalamic tract (22) is composed of fibers that arise from the spinal trigeminal nucleus (4), pass ventromedially through the reticular formation (8), cross the midline, and ascend as a somewhat diffuse fascicle along the lateral aspect of the *contralateral* medial lemniscus to reach the ventral posteromedial nucleus of the thalamus. In this and subsequent images, the number(s) 22 indicate the approximate position of this diffuse ascending fiber system. Serotoninergic raphe nuclei B1 and B2 lie within the thin vertical stripes of unlabeled gray matter between the midline raphe and the paramedian fiber tracts (17, 14, 21) (**See Fig. 3.10**).

6 Anterior spinocerebellar tract
7 Rubrospinal tract
10 Spinothalamic tract
14 Tectospinal tract
16 Pyramid containing the corticospinal tract
17 Medial longitudinal fasciculus
19 Arcuate nuclei
21 Medial lemniscus
22 Ventral trigeminothalamic tract
24 Central tegmental tract converging on the inferior olivary nucleus
25 Inferior cerebellar peduncle (restiform body)
26 Medial vestibular nucleus
27 Inferior vestibular nucleus
27′ Descending root of the vestibular nucleus
30 Olivocerebellar tract
31 Glossopharyngeal nerve (CN IX)

Letter labels

4V Fourth ventricle
O Inferior olivary nucleus
O′ Amiculum (capsule of the inferior olivary nucleus)
S Solitary tract surrounded by the solitary nucleus (light gray)
V Dorsal nucleus of the Vagus

Arrowheads and arrows

Arrowheads: Intramedullary fibers of the hypoglossal nerve (CN XII) passing medial to and through the inferior olivary nucleus
Paired white arrows: Intramedullary fibers of the glossopharyngeal nerve (CN IX). Note the proximity to the dorsal vagal and solitary nuclei

Fig. 8.12. High medulla. Striae medullares. Axial section.

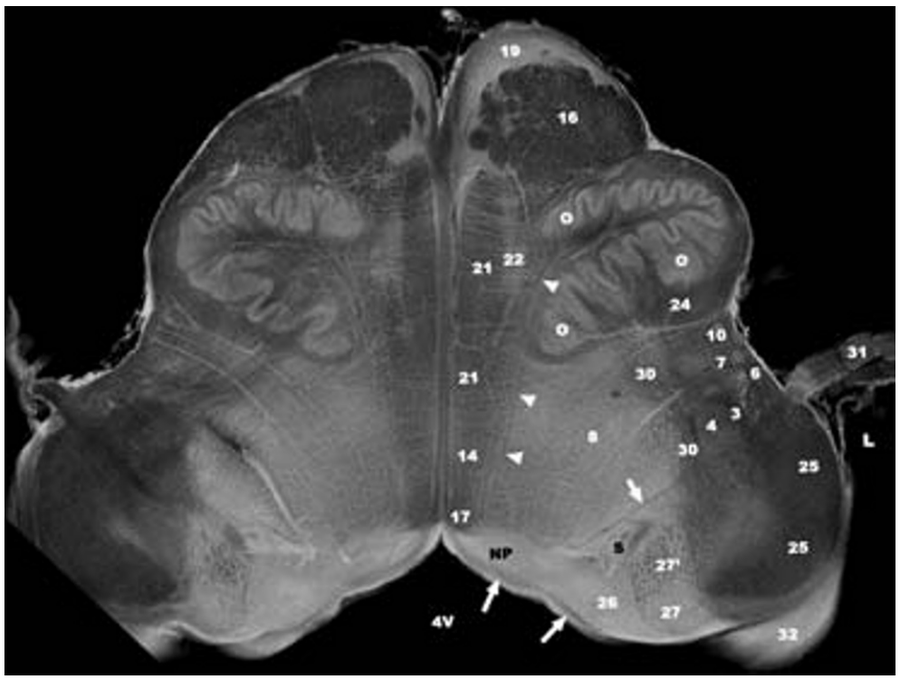

The dorsal medullary striae (paired white arrows) mark the cranial end of the medullary triangle of the floor of the fourth ventricle (See Fig. 1.5). The dorsal cochlear nucleus (32) lies superficial to the inferior cerebellar peduncle (25) at the lateral angle of the fourth ventricle (4V). It bulges into the the floor of the fourth ventricle as the auditory tubercle. Efferent fibers from the dorsal cochlear nuclei form the dorsal acoustic striae, which contribute to the dorsal medullary striae [322a].

The nuclei prepositus hypoglossi (NP) are paired paramedian nuclei that lie just beneath the floor of the fourth ventricle, between the rostral end of the hypoglossal nuclei (caudally) and the abducens nuclei (rostrally). They are links in the oculomotor system that project to the abducens nuclei bilaterally to maintain horizontal gaze position following saccades [322a]. They also project to the cerebellar vermis and fastigial nucleus [78]. They are continuous caudally with the nucleus intercalatus (See Fig. 8.9) [78]. Prominent nerve fascicles (single arrow) pass anterolaterally toward the glossopharyngeal nerve (31). Ventral to this, and oriented slightly oblique to it, a stippled band indicates the cut cross-sections of fibers of the nucleus ambiguus. Note the proximity of this nerve bundle (single arrow) to the dorsal vagal nucleus, the solitary nucleus and tract (S) and the fibers of the nucleus ambiguus (See Sect. IX, Cranial nerves). Serotoninergic raphe nuclei B1 and B2 are still seen within the thin vertical stripes of unlabeled gray matter between the midline raphe and the paramedian fiber tracts (17, 14, 21) (See Fig. 3.10).

3 Spinal trigeminal tract
4 Spinal trigeminal nucleus
6 Anterior spinocerebellar tract
7 Rubrospinal tract
10 Spinothalamic tract
14 Tectospinal tract
16 Pyramid containing the corticospinal tract
17 Medial longitudinal fasciculus
19 Arcuate nuclei
21 Medial lemniscus
22 Ventral trigeminothalamic tract
24 Central tegmental tract converging on the inferior olivary nucleus
25 Inferior cerebellar peduncle (restiform body)
26 Medial vestibular nucleus
27 Inferior vestibular nucleus
27′ Descending root of the vestibular nucleus
30 Olivocerebellar tract
31 Glossopharyngeal nerve (CN IX)
32 Dorsal cochlear nucleus (CN VIII)

Letter labels

4V Fourth ventricle
L Lateral aperture of the fourth ventricle (Foramen of Luschka)
NP Nucleus prepositus hypoglossi
O Inferior olivary nucleus
S Solitary tract surrounded by the solitary nucleus (light gray)

Arrowheads and arrows

Arrowheads: Intramedullary fibers of the hypoglossal nerve (CN XII) passing medial to and through the inferior olivary nucleus
Single white arrow: Intramedullary fibers of the glossopharyngeal nerve (CN IX). Fibers of the adjacent vagal and solitary nuclei enter this nerve
Paired white arrows: Dorsal medullary striae (dorsal pontocerebellar fibers)

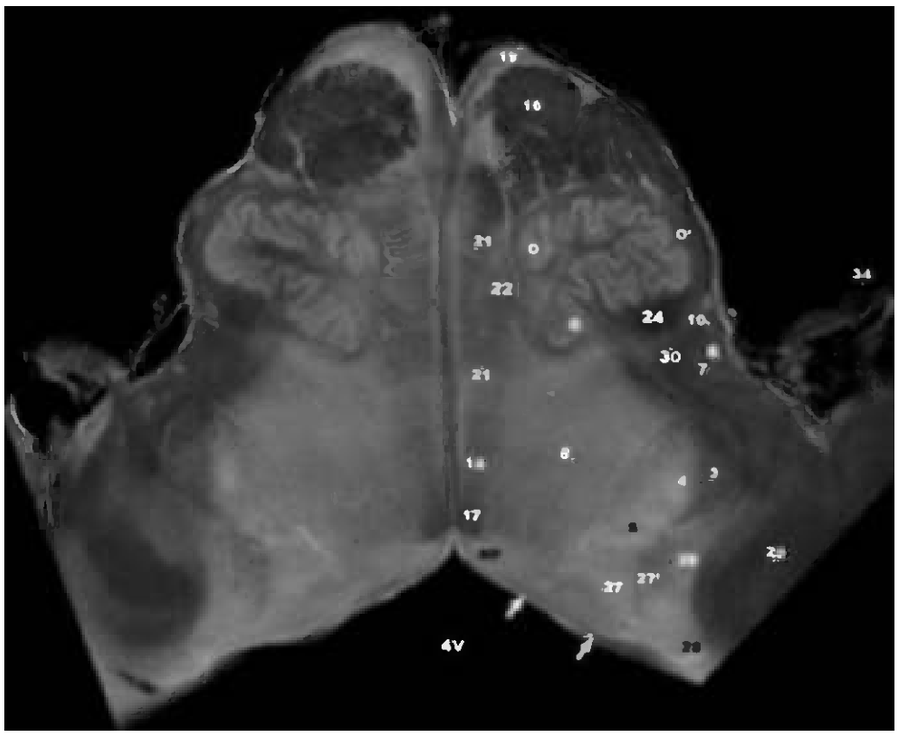

Fig. 8.13. High medulla. Axial section.

This section lies at the cranial limit of the medullary portion of the floor of the fourth ventricle, as indicated by the dorsal medullary striae (white arrows). The caudal pole of the superior vestibular nucleus (28) is just visible. The lateral vestibular nucleus (29) is the most laterally positioned of the four vestibular nuclei. It is best considered to be a cerebellar nucleus, not a vestibular nucleus, because it receives no direct vestibular input, is innervated instead by Purkinje cell axons from the superior vermis, and gives rise to the descending lateral vestibulospinal tract [78, 322a]. The lateral vestibulospinal tract is an uncrossed, somatotopically organized tract that extends the full length of the spinal cord to enhance extensor muscle tone in response to vestibular input data [78]. Serotoninergic raphe nuclei B1 and B2 lie within the thin vertical stripes of unlabeled gray matter between the midline raphe and the paramedian fiber tracts (17, 14, 21) (**See Fig. 3.10**).

3 Spinal trigeminal tract
4 Spinal trigeminal nucleus
6 Anterior spinocerebellar tract
7 Rubrospinal tract
8 Extensive reticular formation (light)
10 Spinothalamic tract
14 Tectospinal tract
16 Pyramid containing the corticospinal tract
17 Medial longitudinal fasciculus
19 Arcuate nuclei
21 Medial lemniscus
22 Ventral trigeminothalamic tract
24 Central tegmental tract
25 Inferior cerebellar peduncle (restiform body)
27 Inferior vestibular nucleus
27′ Descending root of the vestibular nuclei
28 Superior vestibular nucleus
29 Lateral vestibular nucleus
34 Cranial nerves VII (Facial nerve) and VIII (Vestibulocochlear nerve)

Letter labels
4V Fourth ventricle
NP Nucleus prepositus hypoglossi
O Inferior olivary nucleus
O′ Amiculum of the inferior olivary nucleus
S Solitary tract surrounded by the solitary nucleus (light gray)

Arrowheads and arrows
Paired white arrows: Dorsal medullary striae

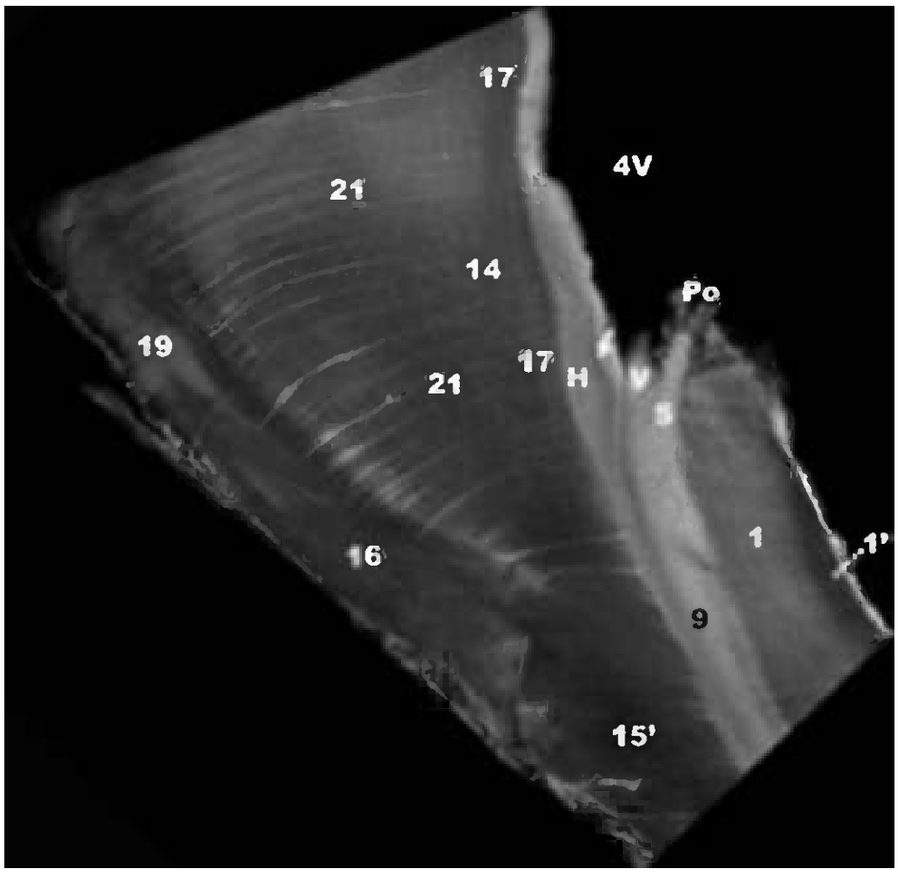

A 2. Sagittal Medulla

Sagittal sections of the medulla displayed from midline to lateral (Figs. 8.14 to 8.23).

Fig. 8.14. Medulla. Medial sagittal section.

Corticospinal fibers within the pyramids (16) of the medulla decussate (15') at the bulbospinal junction. From ventral to dorsal, the longitudinal fibers of the medial lemnisci (21), tectospinal tract (14) and medial longitudinal fasciculus (17) layer vertically just to each side of the midline. The dorsal longitudinal fasciculus (white arrow) courses over the hypoglossal nucleus (H), delimiting its dorsal border. The fasciculus gracilus (1') conveys somatosensory fibers from the lower extremity to the nucleus gracilus (1), where the fibers synapse.

1 Nucleus gracilis
1' Fasciculus gracilis
9 Central gray matter about central canal
14 Tectospinal tract
15' Decussation of the corticospinal tracts
16 Pyramid (corticospinal tract)
17 Medial longitudinal fasciculus
21 Medial lemniscus

Letter labels
4V Fourth ventricle
H Hypoglossal nucleus
Po Area postrema
S Solitary nucleus
V Dorsal motor nucleus of the Vagus

Arrowheads and arrows
Single white arrow: Dorsal longitudinal fasciculus

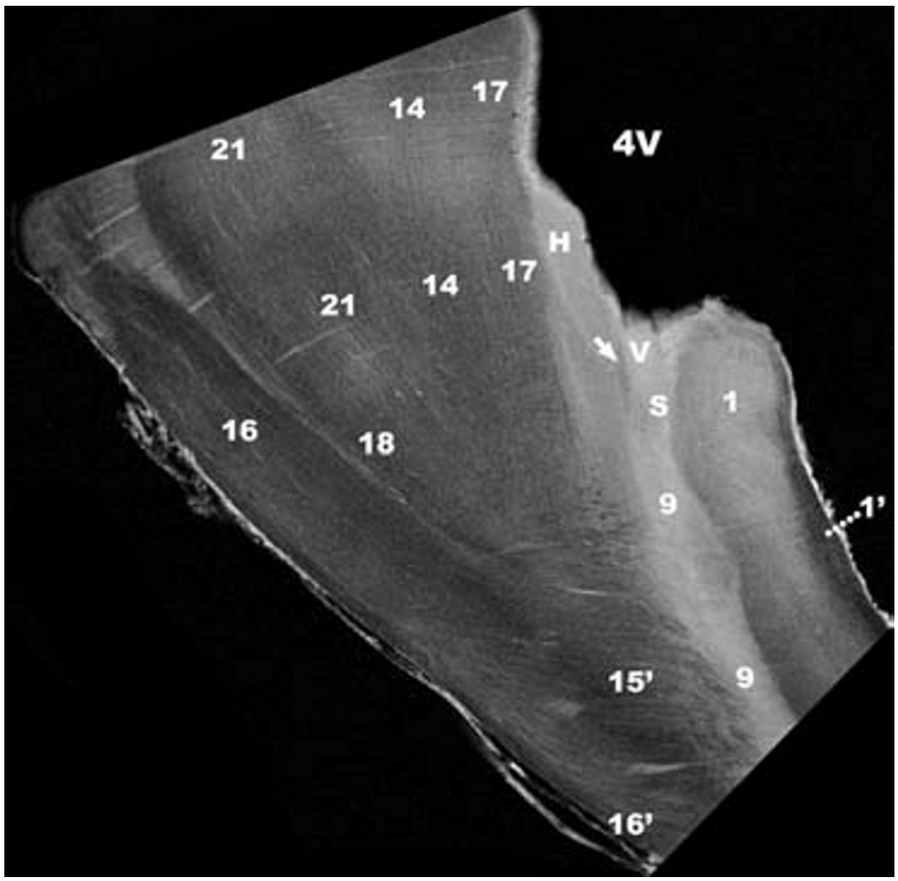

Fig. 8.15. Medulla. Parasagittal section.

From the nucleus gracilus, post-synaptic internal arcuate fibers course ventrally, around the lateral margins of the central gray matter (9), and decussate (18) ventrally, before emerging into the medial lemniscus (21) of the contralateral side. Within the medial lemniscus, fibers are organized somatotopically, with fibers from more caudal portions of the body consistently situated ventral to fibers from more cephalic regions. The descending corticospinal tracts (16) give rise to uncrossed fibers (16′) that enter the anterior columns of the spinal cord, uncrossed fibers that pass into the anterior portions of the lateral columns, and crossed corticospinal fibers (15′) that diverge laterally toward the posterior aspects of the lateral columns of the spinal cord (See also 15 in **Fig. 8.16**).

1 Nucleus gracilis
1′ Fasciculus gracilis
9 Central gray matter around the central canal
14 Tectospinal tract
15′ Decussation of the corticospinal tracts
16 Pyramid (corticospinal tract)
16′ Anterior corticospinal tract
17 Medial longitudinal fasciculus
21 Medial lemniscus

Letter labels
4V Fourth ventricle
H Hypoglossal nucleus
S Solitary nucleus
V Dorsal motor nucleus of the Vagus

Arrowheads and arrows
Single white arrow: Dorsal longitudinal fasciculus

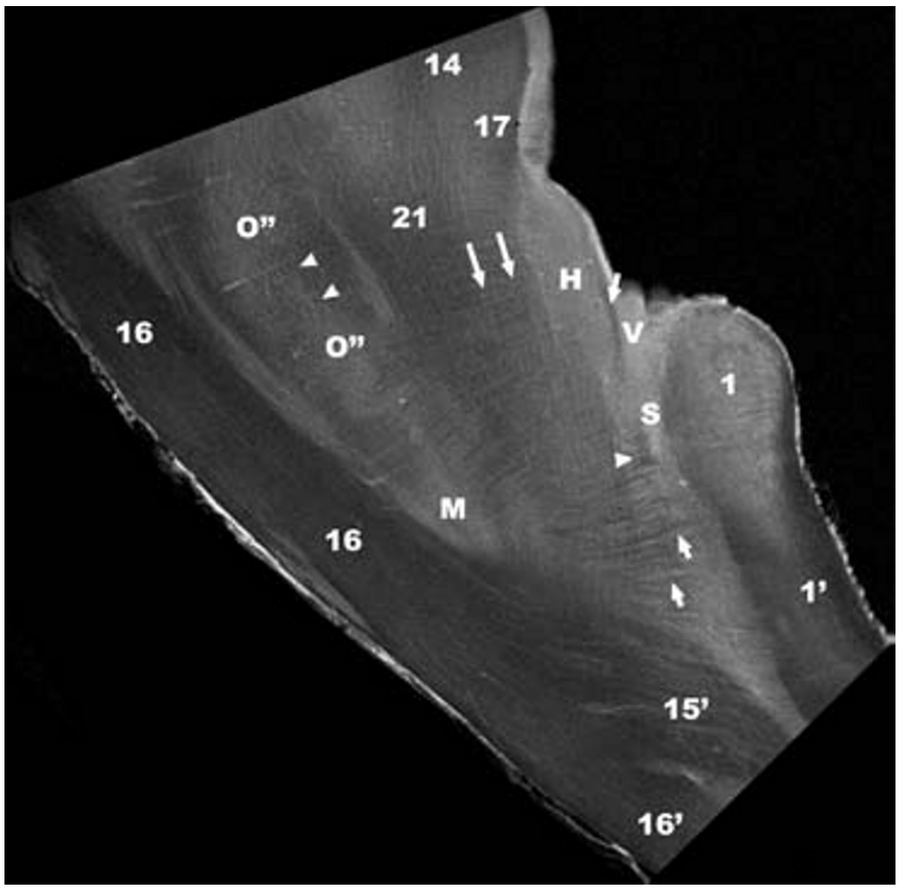

Fig. 8.16. Medulla. Parasagittal section.

The internal arcuate fibers (short white arrows) are prominent in this section. The hypoglossal nucleus (H) bulges into the floor of the fourth ventricle to form the hypoglossal trigone. Multiple hypoglossal fibers (long white arrows) course ventrally and laterally through the medulla toward the pre-olivary sulcus. The dorsal longitudinal fasciculus (single white arrow) descends toward the solitary nucleus (S) and tract (single white arrowhead). The caudal ends of the solitary nucleus and tract converge toward the midline and unite there to form the commissural nucleus (See Fig. 2.4). The most medial part of the hilum (O″) of the inferior olivary nucleus just extends into this section.

1 Nucleus gracilis
1′ Fasciculus gracilis
14 Tectospinal tract
15′ Decussation of the corticospinal tracts
16 Pyramid containing the corticospinal tracts
16′ Anterior corticospinal tract
17 Medial longitudinal fasciculus
21 Medial lemniscus

Letter labels

4V Fourth ventricle
H Hypoglossal nucleus covered dorsally by the dorsal longitudinal fasciculus (single white arrow)
M Medial accessory olivary nucleus
O″ Hilum of the inferior olivary nucleus (with dot-like cross-sections of the emerging olivocerebellar fibers). See also Fig. 6.39
S Solitary nucleus (light gray) surrounding the solitary tract white arrowhead)
V Dorsal nucleus of the vagus

Arrowheads and arrows

Single white arrowhead:	Solitary tract
Double white arrowheads:	Cross-sections of olivocerebellar fibers emerging from the hilum of the inferior olivary nucleus *en route* to the contralateral inferior cerebellar peduncle and hemisphere
Single white arrow:	Dorsal longitudinal fasciculus coursing over the dorsal surface of the hypoglossal nucleus
Lower pair of white arrows:	Internal arcuate fibers
Upper pair of white arrows:	Intramedullary fibers of the hypoglossal nerve passing toward the pre-olivary sulcus

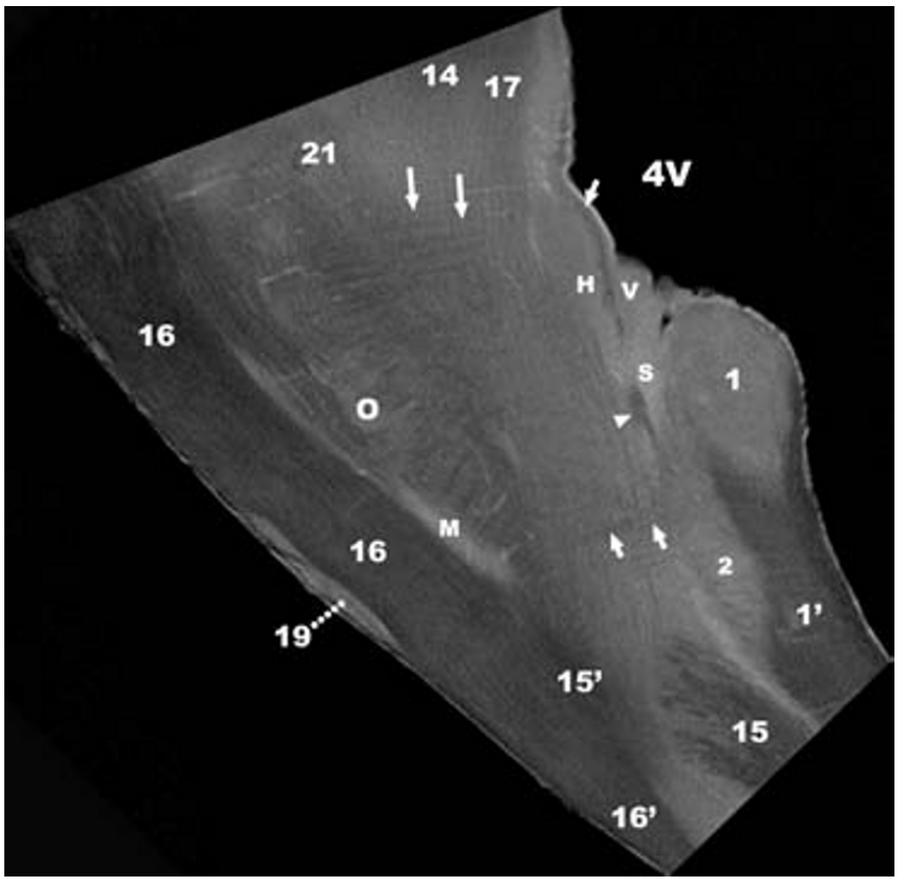

Fig. 8.17. Medulla. Parasagittal section.

The crossed corticospinal fibers (15) diverge laterally toward the lateral columns of the spinal cord, while the uncrossed anterior corticospinal fibers (16′) continue inferiorly into the anterior columns of the spinal cord. The medial portions of the nucleus cuneatus (2) and medial accessory olivary nucleus (M), as well as more cephalic portions of the solitary nucleus (S) and tract (white arrowhead) become visible. The internal arcuate fibers (dual short white arrows) and hypoglossal fibers (dual long white arrows) course ventrally through the medulla. The gray matter of the external arcuate nucleus (19) is seen ventrally. The dorsal longitudinal fasciculus (single white arrow) interconnects the posterior hypothalamus with autonomic centers in the lower medulla and spinal cord [322a].

1 Nucleus gracilis
1′ Fasciculus gracilis
2 Nucleus cuneatus
14 Tectospinal tract
15 Corticospinal tracts diverging infero-laterally from the decussation
15′ Decussation of the corticospinal tracts
16 Pyramid containing the corticospinal tracts
16′ Anterior corticospinal tract
17 Medial longitudinal fasciculus
19 Arcuate nuclei
21 Medial lemniscus

Letter labels

4V Fourth ventricle
H Hypoglossal nucleus covered dorsally by the dorsal longitudinal fasciculus (single white arrow).
M Medial accessory olivary nucleus
O Inferior olivary nucleus (most medial portion)
S Solitary nucleus (light gray) surrounding the solitary tract (white arrowhead)
V Dorsal vagal nucleus

Arrowheads and arrows

White arrowhead: Solitary tract
Single white arrow: Dorsal longitudinal fasciculus
Lower pair of white arrows: Internal arcuate fibers
Upper pair of white arrows: Intramedullary fibers of the hypoglossal nerve passing toward the pre-olivary sulcus

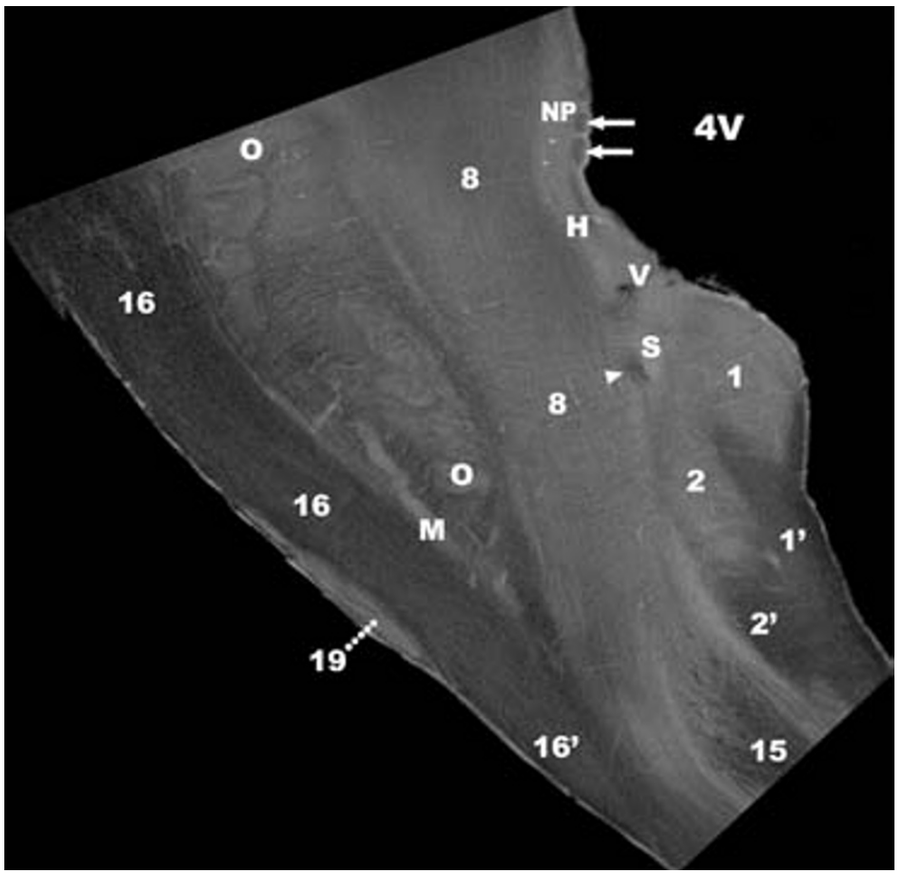

Fig. 8.18. Medulla. Parasagittal section lateral to the medial longitudinal fasciculus, tectospinal tract and medial lemniscus.

The nucleus prepositus hypoglossi (NP) lies rostral to the hypoglossal nucleus and is delimited dorsally by the dark dorsal longitudinal fasciculus. The laterally situated fasciculus cuneatus (2′) ascends to the nucleus cuneatus (2). The spinal trigeminal system (unlabeled) just comes into view between the anterior corticospinal tract (16′) and the diverging lateral corticospinal fibers (15) (See next section).

1 Nucleus gracilis
1′ Faciculus gracilis
2 Nucleus cuneatus
2′ Fasciculus cuneatus
8 Gray matter of the reticular formation
15 Corticospinal tracts diverging infero-laterally from the decussation
16 Pyramid containing the corticospinal tracts
16′ Anterior corticospinal tract
19 Arcuate nuclei

Letter labels

4V Fourth ventricle
H Hypoglossal nucleus
M Medial accessory olivary nucleus
NP Nucleus prepositus hypoglossi
O Inferior olivary nucleus (most medial portion)
S Solitary nucleus (light gray) surrounding the solitary tract (white arrowhead)
V Dorsal nucleus of the vagus

Arrowheads and arrows

White arrowhead: Solitary tract
Paired horizontal white arrows: Dorsal medullary striae (in cross-section)

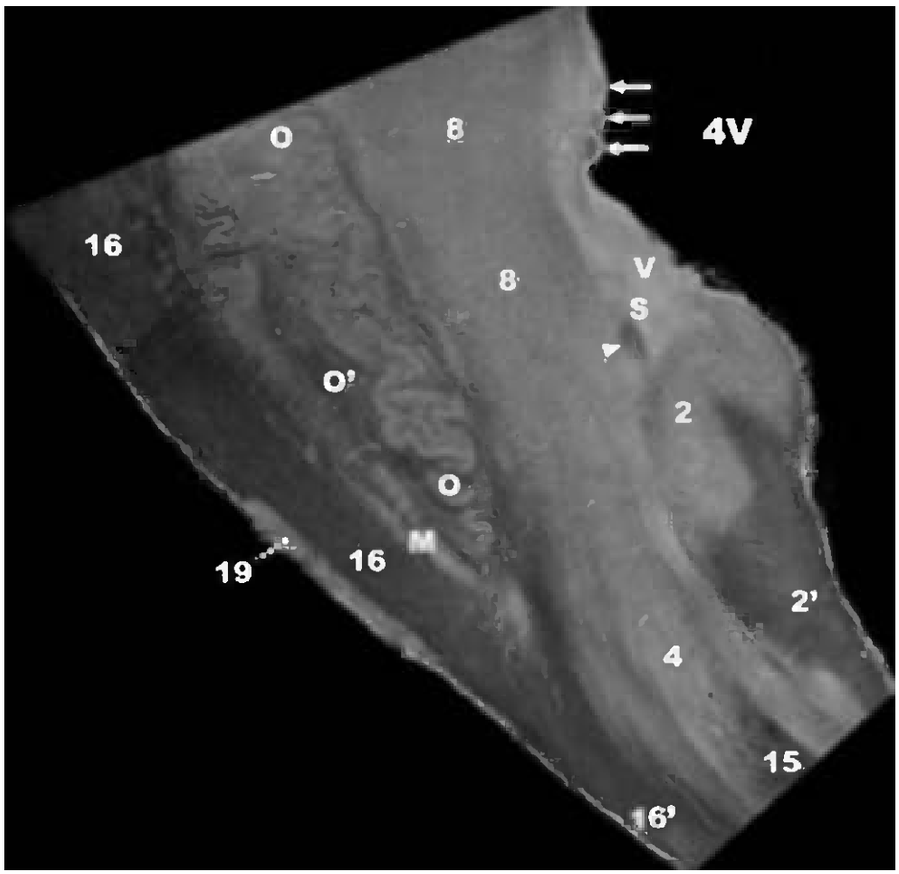

Fig. 8.19. Medulla. Parasagittal section.

The medially situated nucleus and fasciculus gracilus are not included in this section. The laterally situated nucleus and fasciculus cuneatus (2, 2′) are prominent. The spinal trigeminal nucleus (4) is now visible. The spinal trigeminal tract runs along the lateral border of the spinal trigeminal nucleus, so it is better seen in more lateral sections. The inferior olivary nucleus (O) shows extensive folding of its cortex. The dorsal accessory olivary nucleus (see D in the next figure) forms a thin strip of gray matter dorsal to and aligned along the long axis of the inferior olivary nucleus. The dorsal medullary striae (white arrows) extend across the floor of the fourth ventricle at the cephalic end of the inferior (medullary) portion of the fourth ventricle. They mark the transition between medulla and pons on the dorsal surface of the brain stem.

2 Nucleus cuneatus
2′ Fasciculus cuneatus
4 Spinal trigeminal nucleus
8 Gray matter of the reticular formation
15 Corticospinal tracts diverging inferolaterally from the decussation
15′ Decussation of the corticospinal tracts
16 Pyramid containing the corticospinal tracts
16′ Anterior corticospinal tract
19 Arcuate nuclei

Letter labels

4V Fourth ventricle
M Medial accessory olivary nucleus
O Inferior olivary nucleus (most medial portion)
O′ Amiculum (capsule of the inferior olivary nucleus)
S Solitary nucleus (light gray) surrounding the solitary tract (white arrowhead)
V Dorsal vagal nucleus

Arrowheads and arrows

White arrowhead: Solitary tract
Three horizontal white arrows: Dorsal medullary striae (in cross-section)

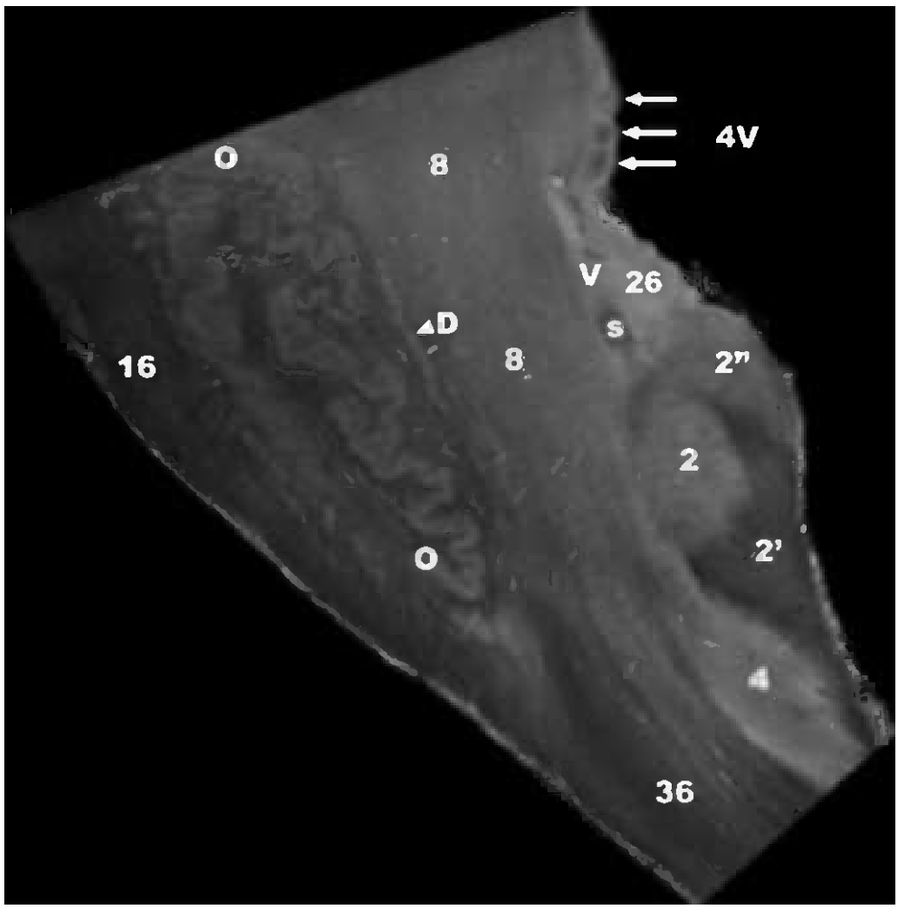

Fig. 8.20. Medulla. Lateral sagittal section.

The dorsal olivary nucleus (D) forms a thin lamina just dorsal to the inferior olivary nucleus (O). A portion of the spinal trigeminal tract now creates the dark band along the spinal trigeminal nucleus (4). Because lateral sections cut through a thinner sagittal dimension of the round brain stem, the spinal trigeminal nucleus appears to lie far posterior in the section. The medial vestibular nucleus (26) and the ventrolateral tracts (36) now enter the section.

2 Nucleus cuneatus
2′ Fasciculus cuneatus
2″ Accessory (lateral) nucleus cuneatus
4 Spinal trigeminal nucleus
8 Gray matter of the reticular formation
16 Pyramid containing the corticospinal tracts
26 Medial vestibular nucleus
36 Tracts of the ventrolateral columns of the spinal cord

Letter labels

4V Fourth ventricle
D Dorsal olivary nucleus
M Medial accessory olivary nucleus
O Inferior olivary nucleus
S Solitary tract (dark) surrounded by the solitary nucleus (light gray)
V Dorsal vagal nucleus

Arrowheads and arrows

Three horizontal white arrows: Dorsal medullary striae (in cross-section)

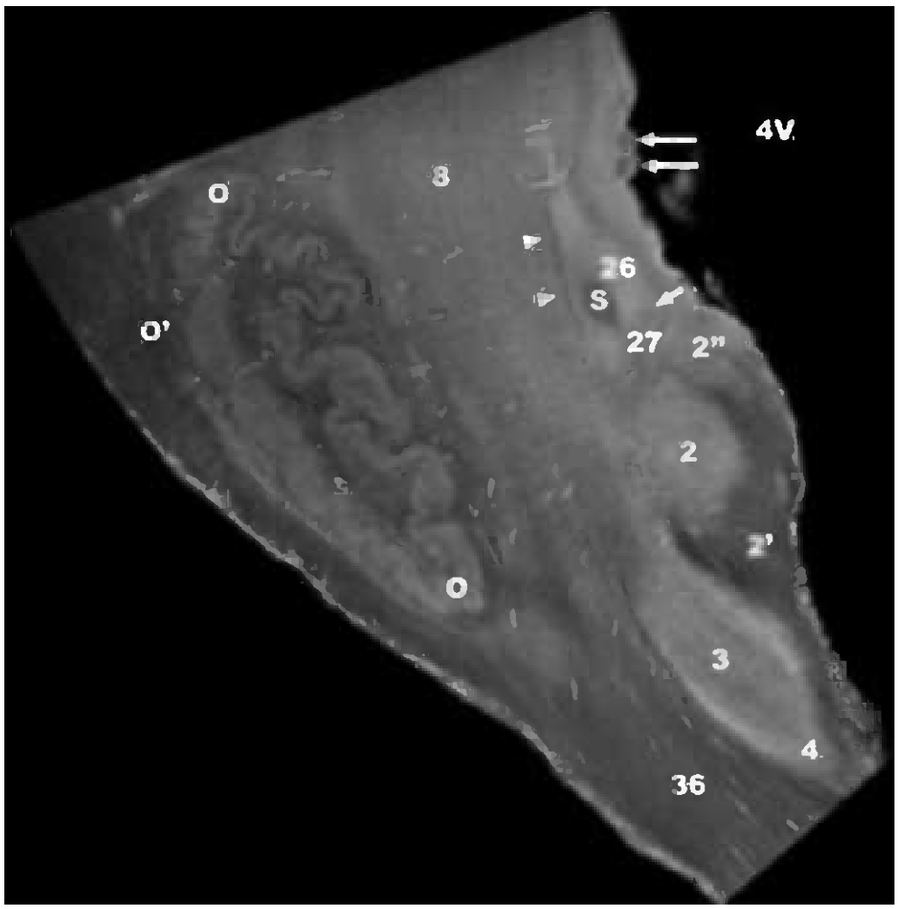

Fig. 8.21. Medulla. Lateral sagittal section.

The laterally positioned accessory cuneate nucleus (2″) lies superior as well as lateral to the cuneate nucleus (2), because lateral structures must ascend higher than medial structures to reach the lower border of the diamond-shaped fourth ventricle. Lateral sagittal sections also show the spinal trigeminal tract (3) along the lateral border of the spinal trigeminal nucleus (4) and cephalic portions of the solitary nucleus and tract. The inferior vestibular nucleus (27) lies inferolateral to the medial vestibular nucleus (26).

2 Nucleus cuneatus
2′ Fasciculus cuneatus
2″ Accessory (lateral) nucleus cuneatus
3 Spinal trigeminal tract
4 Spinal trigeminal nucleus
8 Gray matter of the reticular formation
26 Medial vestibular nucleus
27 Inferior vestibular nucleus (with descending fibers (arrow) of the vestibular nerve)
36 Tracts of the ventrolateral columns of the spinal cord

Letter labels

4V Fourth ventricle
O Inferior olivary nucleus
O′ Amiculum (capsule of the inferior olivary nucleus)
S Solitary tract (dark) surrounded by the solitary nucleus (light gray)

Arrowheads and arrows

Paired white arrowheads: Glossopharyngeal fibers arising from the solitary nucleus
Single white arrow: Descending fibers of the vestibular nerve, entering the inferior vestibular nucleus
Two horizontal white arrows: Dorsal medullary striae (in cross-section)

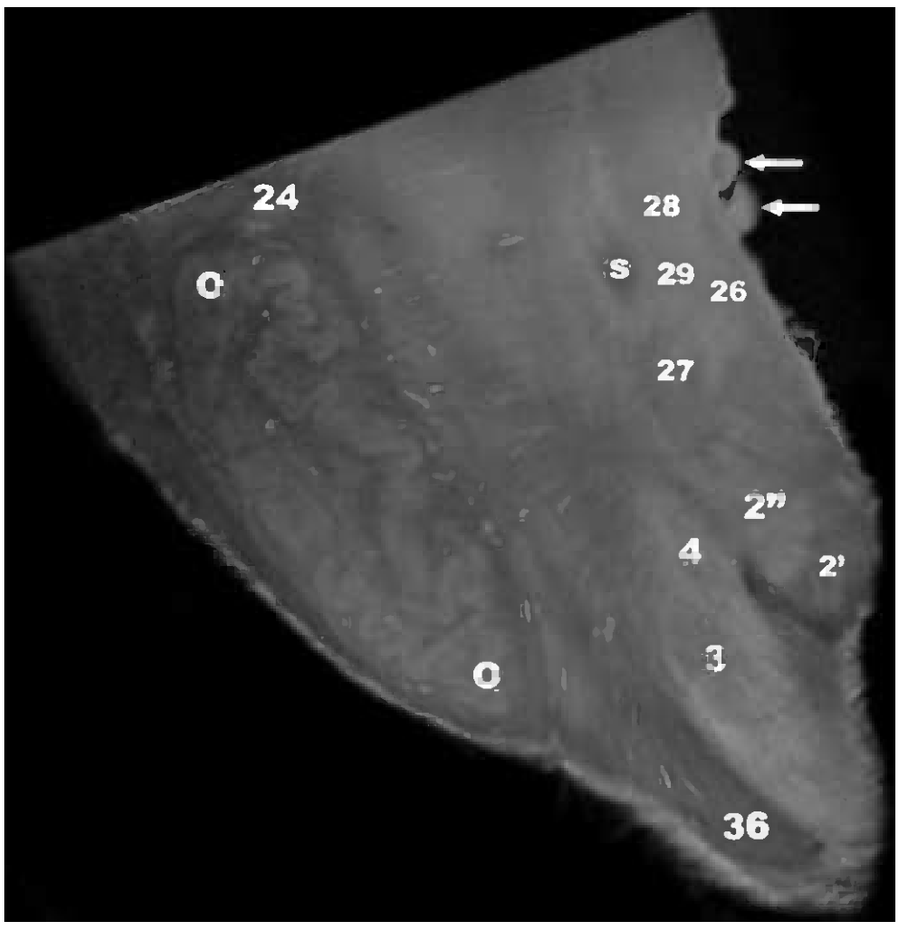

Fig. 8.22. Medulla. Lateral sagittal section.

The central tegmental tract (24) descends to the superior pole of the inferior olivary nucleus (O). The superior (28) and lateral (29) vestibular nuclei lie dorsal to the solitary nucleus and tract (S). The ridges formed by the dorsal medullary striae (white arrrows) may be quite prominent. The ventrolateral columns (36) form the ventral margin of the spinal cord.

2′ Fasciculus cuneatus
2″ Accessory (lateral) nucleus cuneatus
3 Spinal trigeminal tract
4 Spinal trigeminal nucleus
24 Central tegmental tract
26 Medial vestibular nucleus
27 Inferior vestibular nucleus
28 Superior vestibular nucleus
29 Lateral vestibular nucleus
36 Tracts of the ventrolateral columns of the spinal cord

Letter labels

4V Fourth ventricle
O Inferior olivary nucleus
O′ Amiculum (capsule of the inferior olivary nucleus)
S Solitary tract (dark) surrounded by the solitary nucleus (light gray)

Arrowheads and arrows

Two horizontal white arrows: Dorsal medullary striae (in cross-section)

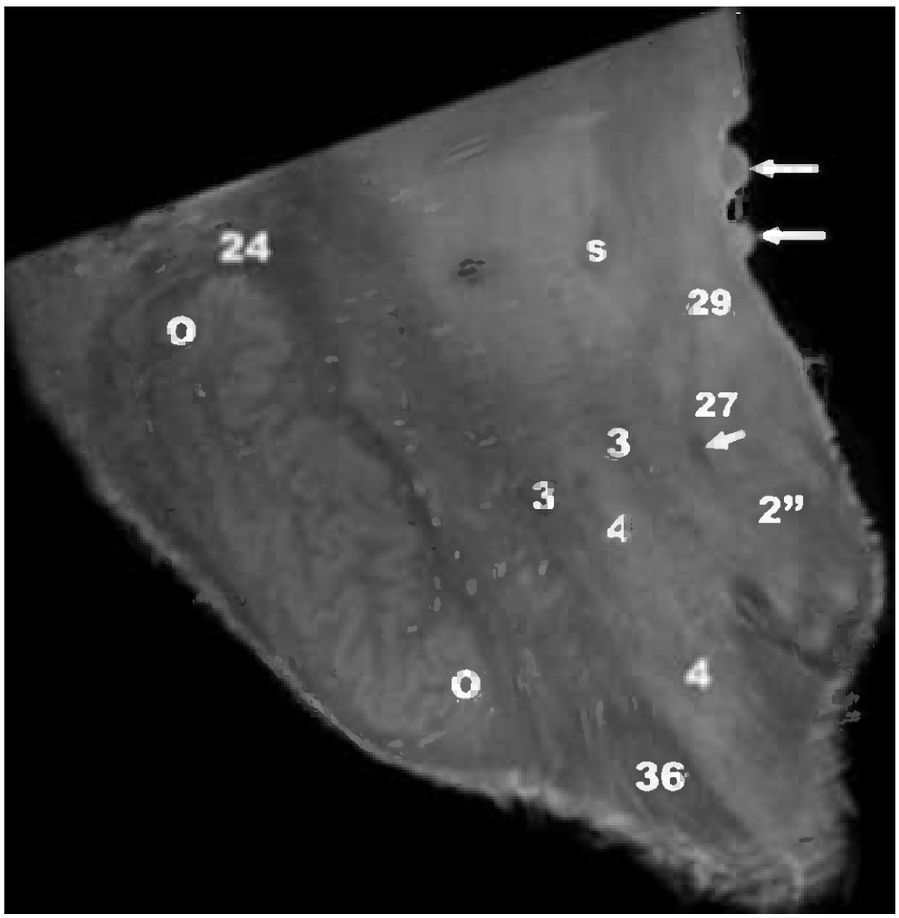

Fig. 8.23. Medulla. Lateral sagittal section.

The fasciculus and nucleus cuneatus are no longer seen. The accessory nucleus cuneatus (2′) and the spinal trigeminal nucleus (4) and tract (3) are prominent. The descending vestibular fibers (single white arrow) lie in relationship to the inferior vestibular nucleus (27). The descending vestibular fibers have a superficial resemblence to the solitary tract (S), but review of sequential sagittal images demonstrates the true course of the solitary tract.

2″ Accessory (lateral) nucleus cuneatus
3 Spinal trigeminal tract
4 Spinal trigeminal nucleus
27 Inferior vestibular nucleus (with descending fibers (white arrrow) of the vestibular nerve)
29 Lateral vestibular nucleus
36 Tracts of the ventrolateral columns of the spinal cord

Letter labels
O Inferior olivary nucleus
S Solitary tract (dark) surrounded by the solitary nucleus (light gray)

Arrowheads and arrows
Single white arrow: Descending vestibular fibers within the inferior vestibular nucleus
Two horizontal white arrows: Dorsal medullary striae (in cross-section)

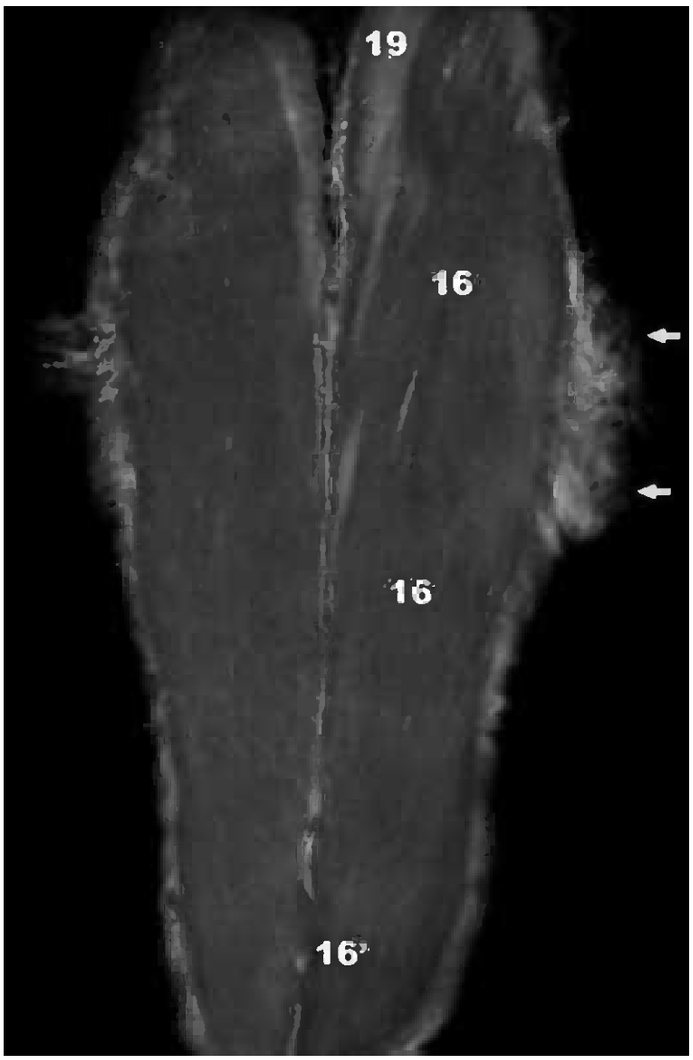

A 3. Coronal Medulla

Coronal sections of the medulla displayed from ventral to dorsal (Figs. 8.24–8.33).

Fig. 8.24. Medulla. Ventral coronal section.

Coronal sections parallel to the ventral medulla show the pyramids containing the corticospinal tracts (16), the arcuate nuclei (19) along the ventral sulcus, and a "brush border" (arrows) representing the cut ends of the hypoglossal nerves emerging into the pre-olivary sulcus.

16 Pyramid containing the corticospinal tracts
16′ Anterior corticospinal tract
19 Arcuate nuclei

Arrowheads and arrows
White arrows: Fibers of the hypoglossal nerve (CN XII) emerging at the pre-olivary sulcus ventral to the olive

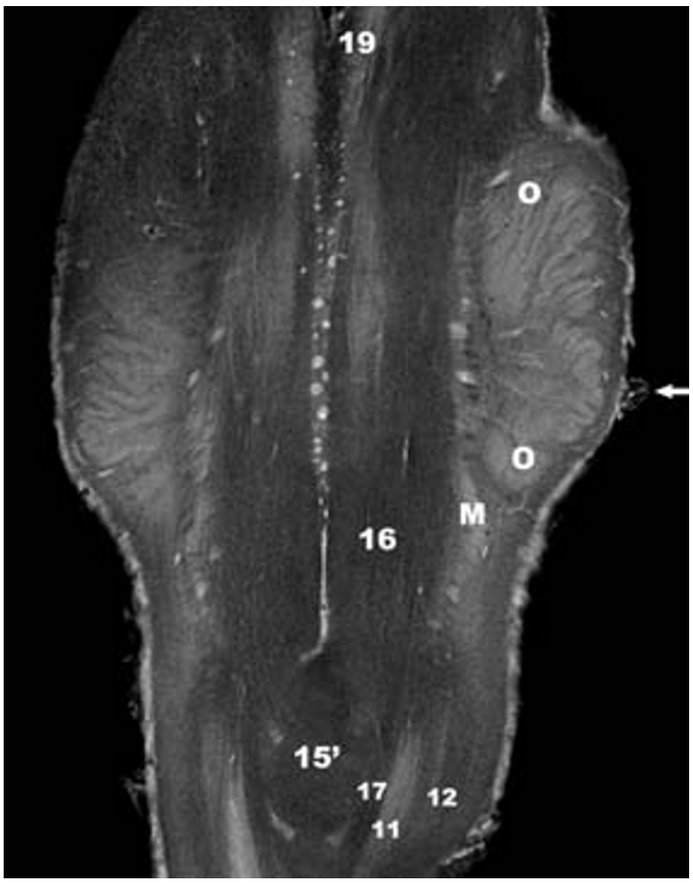

Fig. 8.25. Medulla. Ventral coronal section.

Major portions of the corticospinal tracts that descend through the pyramids (16) decussate (15′) at the bulbospinal junction. At the level of the decussation, the caudal portions of the medial longitudinal fasciculi (17) curve off midline to enter the sulcomarginal region of the anterior columns of the spinal cord. There, descending vestibular fibers within the medial longitudinal fasciculi (17) effect reflex control of head position in response to alterations in body posture. The ventral aspects of the medial accessory (M) and inferior (O) olivary nucleus reach into this section.

11 Ventral horn of the spinal cord
12 Lateral spinovestibular tract
15′ Decussation of the pyramids (corticospinal tracts)
16 Pyramid containing the corticospinal tract
17 Medial longitudinal fasciculus (extending into the cervical spinal cord)
19 Arcuate nuclei

Letter labels

M Medial accessory olivary nucleus
O Inferior olivary nucleus

Arrowheads and arrows

White arrow: Fibers of the hypoglossal nerve (CN XII) emerging at the pre-olivary sulcus ventral to the olive

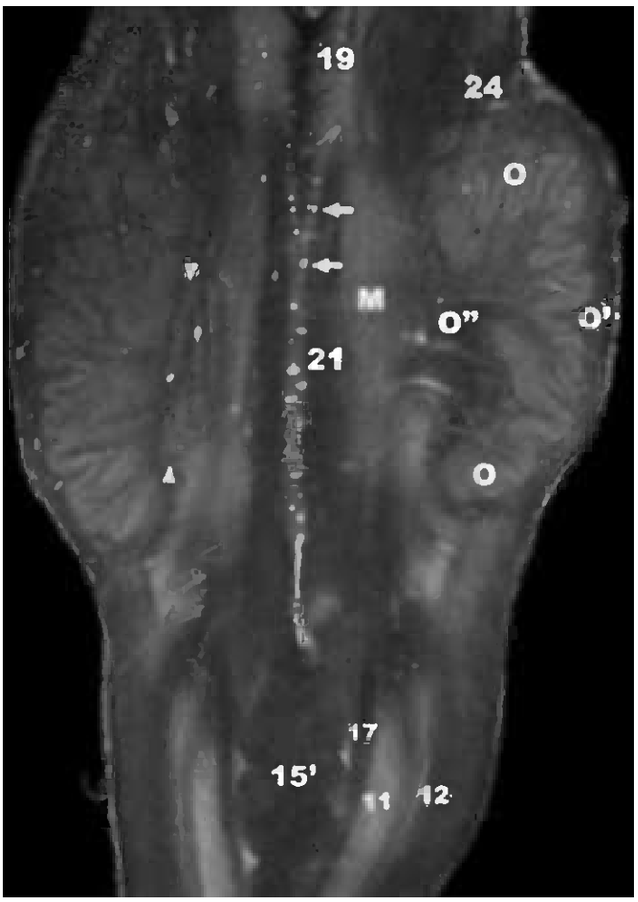

Fig. 8.26. Medulla. Ventral-mid coronal section.

The medial lemnisci (21) form paired paramedian columns of longitudinal fibers which lie just dorsal to the pyramids, between the median raphe medially and the medial accessory olivary nuclei (M) laterally. The cross sections of olivocerebellar fibers and hypoglossal nerve fibers form lines of "dots" as they traverse the interval between the hilum (O") of the inferior olivary nucleus and the medial accessory olivary nucleus (M). The central tegmental tract (24) extends caudally from the ipsilateral red nucleus to the inferior olivary nucleus, forming one leg of the triangle of Guillain-Mollaret. This "triangle" consists of (i) olivocerebellar fibers from the hilum of one olive crossing the midline and traversing the inferior cerebellar peduncle of the contralateral side to reach the contralateral dentate nucleus, (ii) dentatorubral fibers arising in the contralateral dentate nucleus, entering their own superior cerebellar peduncle and decussating in the midbrain to reach the opposite red nucleus (ipsilateral to the original side), and (iii) the ipsilateral central tegmental tract (24) descending from the red nucleus to the original inferior olivary nucleus (O). The descending central tegmental fibers envelop the inferior olivary nucleus to form the amiculum (O') [322a].

11 Ventral horn of the spinal cord
12 Lateral spinovestibular tract
15' Decussation of the pyramids (corticospinal tracts)
17 Medial longitudinal fasciculus (extending into the cervical spinal cord)
19 Arcuate nuclei
21 Medial lemniscus
24 Central tegmental tract

Letter labels

M Medial accessory olivary nucleus
O Inferior olivary nucleus
O' Amiculum (capsule of the inferior olivary nucleus)
O" Hilum of the inferior olivary nucleus

Arrowheads and arrows

White arrowheads: Fascicles of the hypoglossal nerve (CN XII) passing ventrally between the inferior olivary nucleus (O) and the medial accessory olivary nucleus (M)

White arrows: Paramedian perforating branches supplying the anteromedial compartment of the brain stem

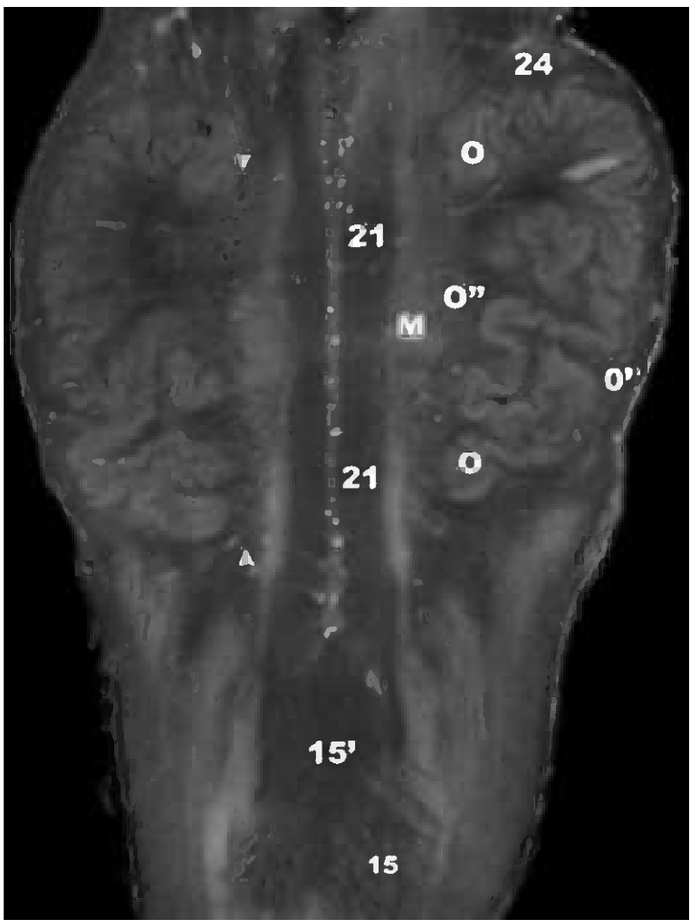

Fig. 8.27. Medulla. Mid coronal section.

The decussated corticospinal fibers (15) now pass laterally toward the contralateral lateral columns of the spinal cord. The inferior olivary nuclei (O), their capsules (O'), the medial accessosry olivary nuclei (M), and the medial lemnisci (21) are well developed. The bulging contours of the inferior olivary nuclei along the lateral borders of the medulla create the gross anatomic feature designated the "olives".

15 Corticospinal tracts descending from the decussation (15')
15' Decussation of the pyramids (corticospinal tracts)
21 Medial lemniscus
24 Central tegmental tract

Letter labels
O Inferior olivary nucleus
O' Capsule of the inferior olivary nucleus
O" Hilum of the inferior olivary nucleus

Arrowheads and arrows
White arrowheads: Fascicles of the hypoglossal nerve (CN XII)

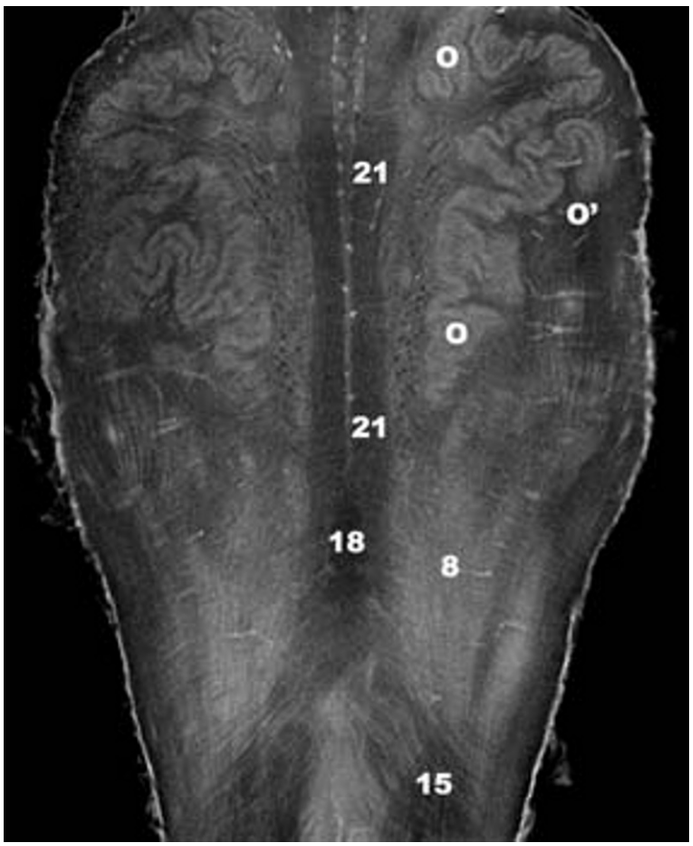

Fig. 8.28. Medulla. Mid coronal section.

The decussated diverging corticospinal fibers (15) are well seen. The reticular nuclei (8) and the spinal trigeminal nuclei (not labeled) are just coming into view (See next section).

8 Reticular formation
15 Corticospinal tracts descending from the ventral pyramidal decussation
18 Decussation of the internal arcuate fibers (great sensory decussation) to form the medial lemnisci (21)
21 Medial lemniscus

Letter labels
O Inferior olivary nucleus
O′ Capsule of the inferior olivary nucleus

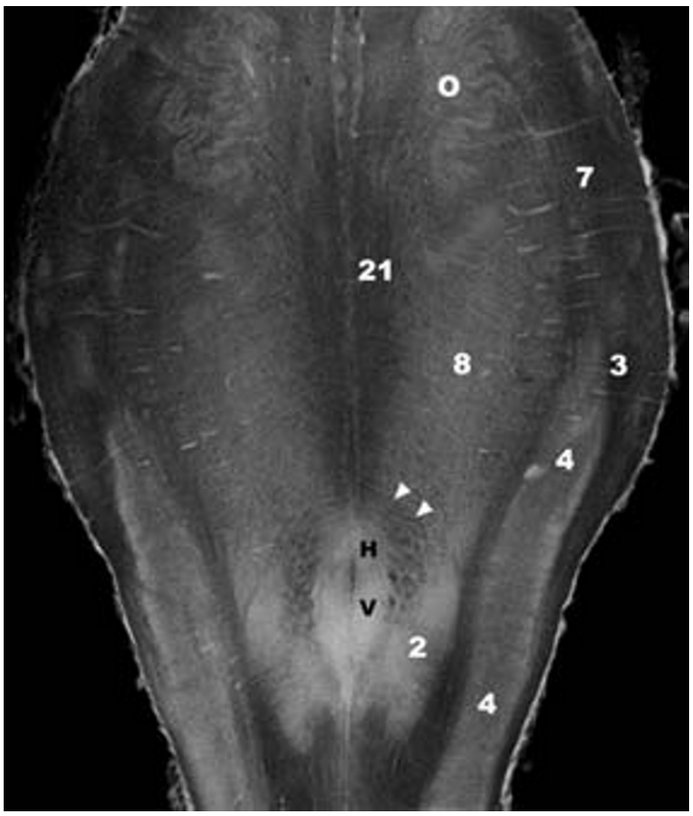

Fig. 8.29. Medulla. Mid-dorsal coronal section.

Dorsally, the hypoglossal (H) and vagal (V) nuclei lie centrally to each side of the midline. The crescents of "dots" (arrowheads) lateral to these nuceli are the cross sections of the internal arcuate fibers, passing around the central gray matter from the dorsally situated nuclei gracilis and cuneatus to the ventrally positioned medial lemnisci (21).

Dorsal to the olives, the spinal trigeminal nuclei (4) and spinal trigeminal tracts (3) form prominent paired columns that align with the lateral borders of the medulla. The spinal trigeminal tract and nucleus are the caudal portion of the trigeminal system. They carry impulses for pain, thermal sense and touch from the head to higher centers, and also receive general somatic afferent (GSA) input from the facial (intermediate), glossopharyngeal and vagal nerves [78]. The long spinal trigeminal system is divided into three subparts. The pars oralis of the spinal trigeminal nucleus extends from the entry of the trigeminal nerve at the pons to the rostral third of the inferior olivary nucleus. Its upper end merges with the principal sensory trigeminal nucleus. The pars interpolaris extends from the caudal end of pars oralis to the decussation of the pyramids. The pars caudalis extends from the caudal end of pars interpolaris to the second cervical segment of the spinal cord. Its caudal end merges with the dorsal gray matter of cervical spinal cord segments 1 and 2 [78].

Fibers from all three divisions of the trigeminal nerve enter the pons and descend within the spinal trigeminal tract (3) to the medulla and spinal cord. These descending trigeminal fibers are organized somatotopically, with fibers from the ophthalmic division (V1) situated ventrally, fibers of the maxillary division (V2) in intermediate position, and fibers of the mandibular division (V3) situated dorsally within the tract [322]. The descending trigeminal fibers leave the solitary tract and synapse nearly immediately with neurons of the surrounding spinal trigeminal nucleus, maintaining the somatotopy. In turn, the spinal trigeminal neurons give rise to secondary fibers that ascend to the thalamus within the ventral trigeminothalamic tracts.

2 Nucleus cuneatus
3 Spinal trigeminal tract
4 Spinal trigeminal nucleus
7 Rubrospinal tract
21 Medial lemniscus

Letter labels

H Hypoglossal nucleus
O Inferior olivary nucleus
V Dorsal vagal nucleus

Arrowheads and arrows

White arrowheads: Internal arcuate fibers

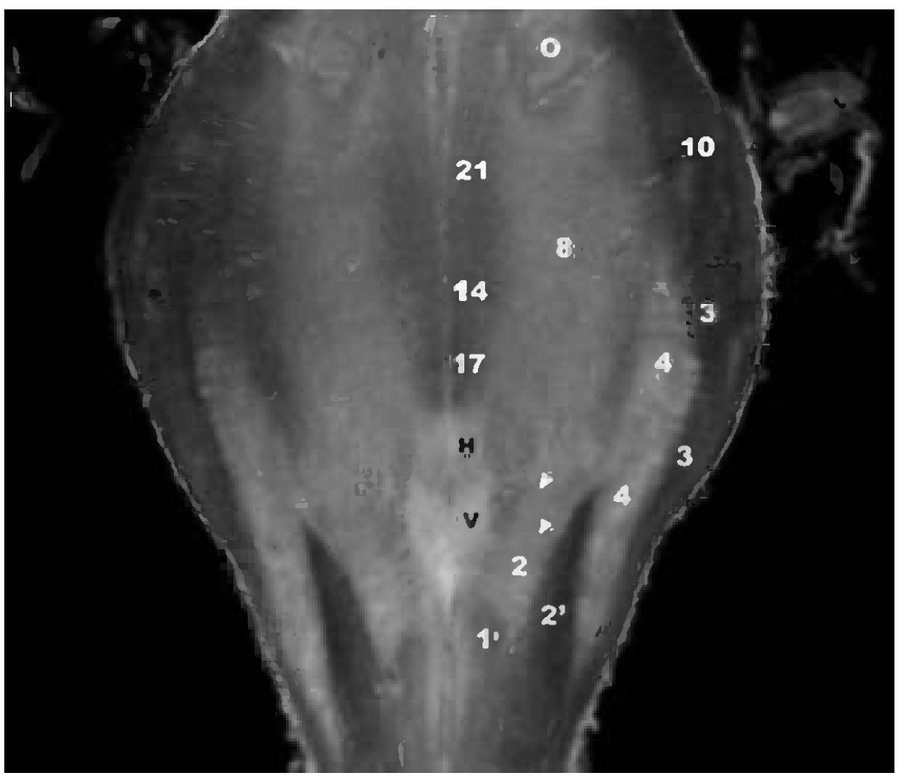

Fig. 8.30. Medulla. Dorsal coronal section.

Further dorsally, the tectospinal tracts (14), the medial longitudinal fasciculi (17), the fasciculus gracilis (1′), the fasciculus cuneatus (2′), and the nucleus cuneatus (2) also enter the section. These structures diverge laterally as they ascend, matching the rhomboid shape of the fourth ventricle.

1′ Fasciculus gracilis
2 Nucleus cuneatus
2′ Fasciculus cuneatus
3 Spinal trigeminal tract
4 Spinal trigeminal nucleus
8 Extensive reticular formation
10 Spinothalamic tract
14 Tectospinal tract
17 Medial longitudinal fasciculus
21 Medial lemniscus

Letter labels
H Hypoglossal nucleus
O Inferior olivary nucleus
V Dorsal vagal nucleus

Arrowheads and arrows
White arrowheads: Internal arcuate fibers

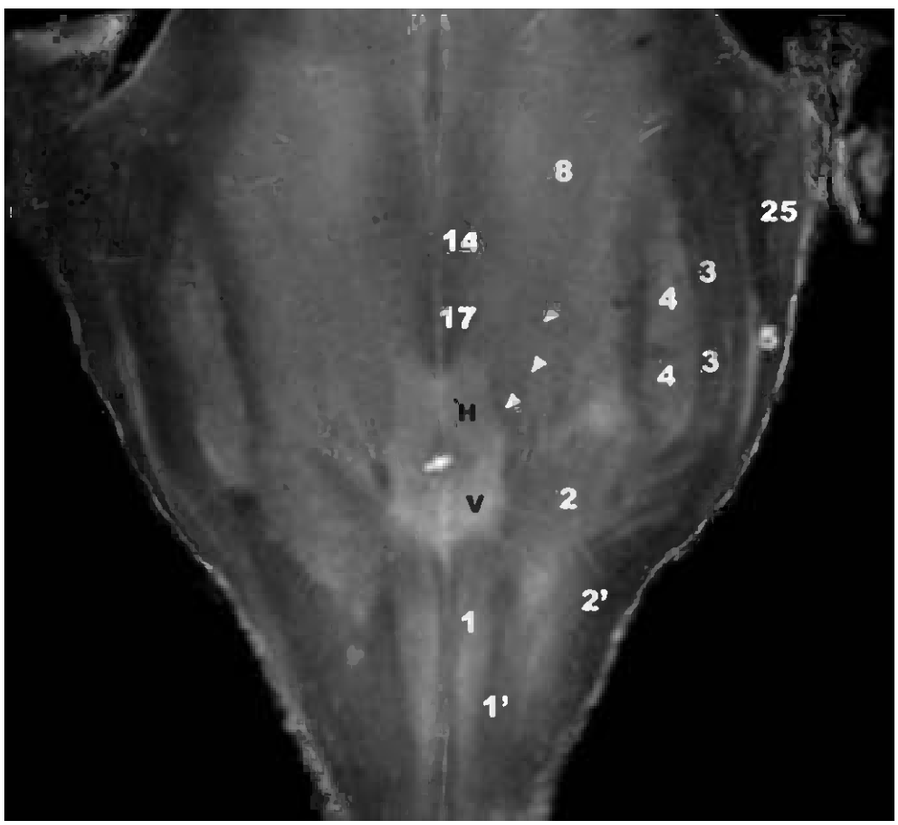

Fig. 8.31. Medulla. Dorsal coronal section.

Dorsal to the medial lemnsici, only the tectospinal tracts (14) and medial longitudinal fasciculi (17) are seen. The posterior spinocerebellar tract (5) enters the inferior cerebellar peduncle (25). The spinal trigeminal tract (3) courses along the lateral border of the spinal trigeminal nucleus (4). The nuclei and fasciculi gracilis and cuneatus (1, 1′, 2, 2′) ascend progressively. Their upper limits conform to the diamond shape of the inferior fourth ventricle. The dorsal longitudinal fasciculus (white arrow) is just visible between the hypoglossal (H) and dorsal vagal (V) nuclei.

1 Nucleus gracilis
1′ Fasciculus gracilis
2 Nucleus cuneatus
2′ Fasciculus cuneatus
3 Spinal trigeminal tract
4 Spinal trigeminal nucleus
5 Posterior spinocerebellar tract
8 Extensive reticular formation
14 Tectospinal tract
17 Medial longitudinal fasciculus
25 Inferior cerebellar peduncle (restiform body)

Letter labels
H Hypoglossal nucleus
V Dorsal vagal nucleus

Arrowheads and arrows
White arrowheads: Internal arcuate fibers
White arrow: Dorsal longitudinal fasciculus

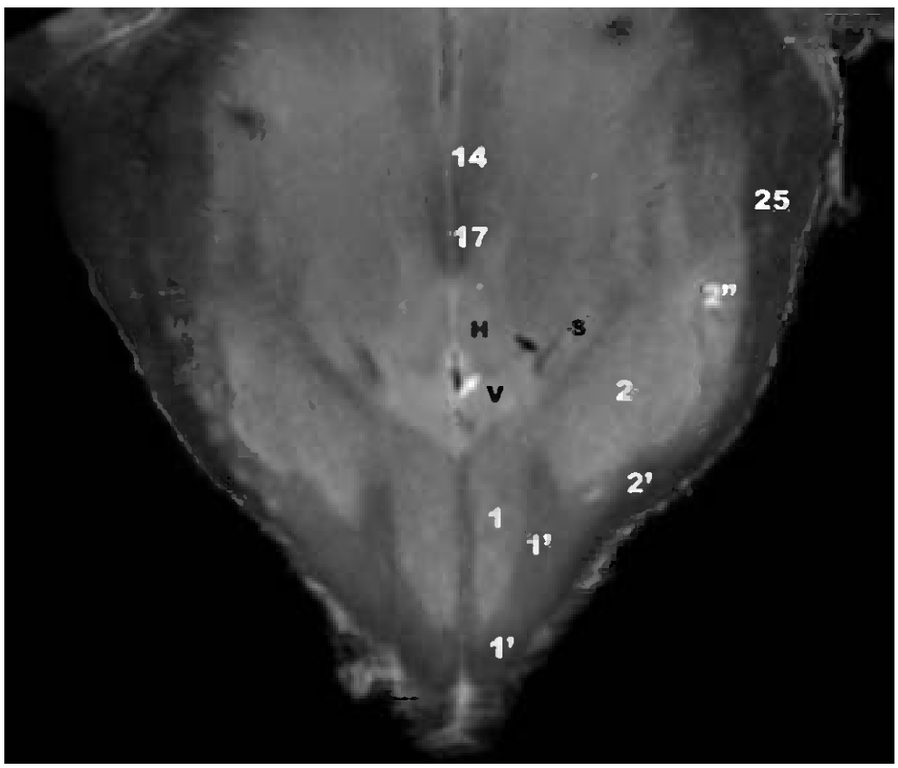

Fig. 8.32. Medulla. Dorsal coronal section

On each side, the solitary nucleus (S) and tract (black arrow) have shifted lateral to the dorsal motor nucleus of the vagus. The higher signal vagal nuclei still lie predominantly inferior to the lower signal hypoglossal nuclei (H). The upper borders of the nuclei gracilis (1), cuneatus (2) and accessory cuneatus (2′) conform to the triangular shape of the medullary portion of the fourth ventricle. The long axes of the solitary nucleus (S) and tract (black arrow) are similarly oblique.

1 Nucleus gracilis
1′ Fasciculus gracilis
2 Nucleus cuneatus
2′ Fasciculus cuneatus
2″ Accessory (lateral) cuneate nucleus
14 Tectospinal tract
17 Medial longitudinal fasciculus
25 Inferior cerebellar peduncle (resitform body)

Letter labels

H Hypoglossal nucleus.
S Solitary nucleus (black S) surrounding the solitary tract (black arrow)
V Dorsal nucleus of the vagus

Arrowheads and arrows

White arrow: Dorsal longitudinal fasciculus
Black arrow: Solitary tract

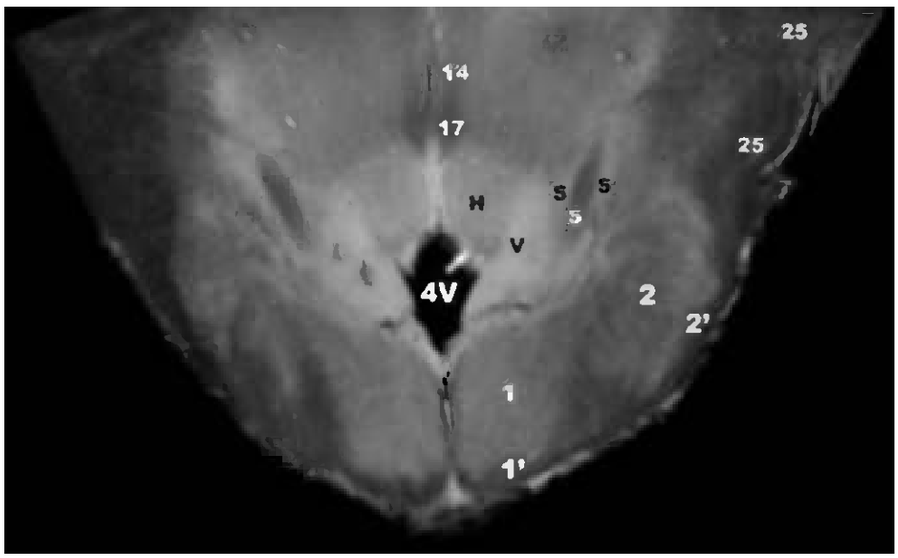

Fig. 8.33. Medulla. Dorsal coronal section.

The section now opens into the fourth ventricle (4V). The higher signal dorsal vagal nucleus (V) lies lateral to the lower signal hypoglossal nucleus (H) along the floor of the fourth ventricle. The solitary nucleus and tract (S) are larger and better developed at this level. The solitary tract is formed by general and special *visceral* afferent fibers (See Sect. IX, Cranial nerves). These fibers enter the brain stem through the facial (intermediate), glossopharyngeal and vagal nerves, descend together as the solitary tract, and then progressively leave the tract to synapse in the surrounding envelope of gray matter designated the nucleus of the solitary tract. Caudally, the slender remnants of the paired solitary tracts and nuclei unite to form the commissural nucleus inferior to the fourth ventricle. (**See Figs. 8.33 back to 8.30**). Special visceral taste fibers of the nervus intermedius synapse in a rostral portion of the solitary nucleus designated the gustatory nucleus [78]. Secondary fibers from this nucleus ascend within the central tegmental tract to the ventroposteromedial nucleus of the thalamus. Special and general visceral afferent fibers of the glossopharyngeal and vagal nerves typically synapse in more caudal (cardiorespiratory) portions of the solitary nucleus and may even cross beneath the obex to the contralateral solitary tract [322]. The secondary fibers from these inputs ascend ipsilaterally to the medial and lateral parabrachial nuclei situated along the superior cerebellar peduncles, to the nucleus ambiguus, to the vagal nucleus and to the ventroposteromedial nucleus of the thalamus [78]. Crossed solitariospinal fibers descend through the dorsal longitudinal fasciculus (white arrow) to autonomic centers in the spinal cord [322a].

1 Nucleus gracilis
1′ Fasciculus gracilis
2 Nucleus cuneatus
2′ Fasciculus cuneatus
14 Tectospinal tract
17 Medial longitudinal fasciculus
25 Inferior cerebellar peduncle (restiform body)

Letter labels

4V Fourth ventricle (caudal end)
H Hypoglossal nucleus.
S Solitary nucleus (black S) surrounding the solitary tract (white S)
V Dorsal vagal nucleus

Arrowheads and arrows

White arrow: Dorsal longitudinal fasciculus

B. Pontomedullary junction (Figs. 8.34–8.65)

B 1. Axial Pontomedullary junction
This series is obtained at a slightly different angle than the prior series and overlaps with it.

Axial sections displayed from caudal to cranial (Figs. 8.34 to 8.43)

The inferior foramen cecum (IF) marks the transition of medulla to pons ventrally. In the zone of transition, axial images display caudal portions of the pons overlapping the medulla ventrally, and paired lateral grooves (**Fig. 8.34**) or slits (**Fig. 8.35**) marking the pontomedullary sulci anterolaterally.

These cartoons (A–B) display the anatomic region imaged in **Figs. 8.34–8.65**.

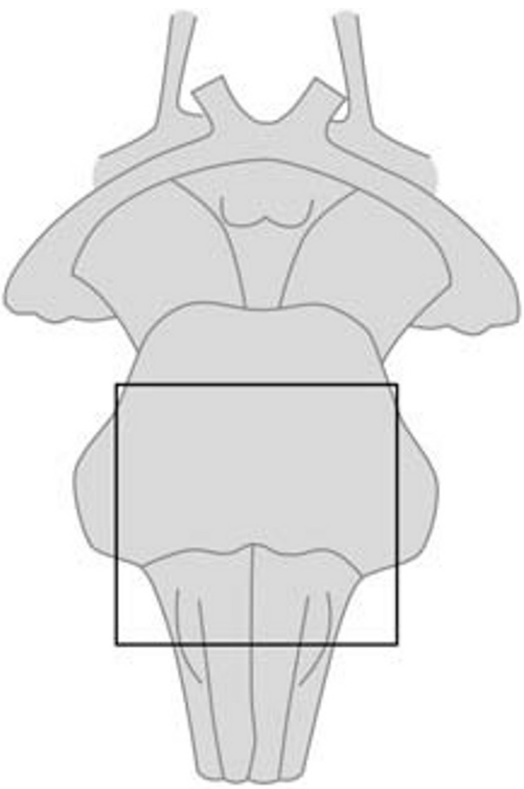

A

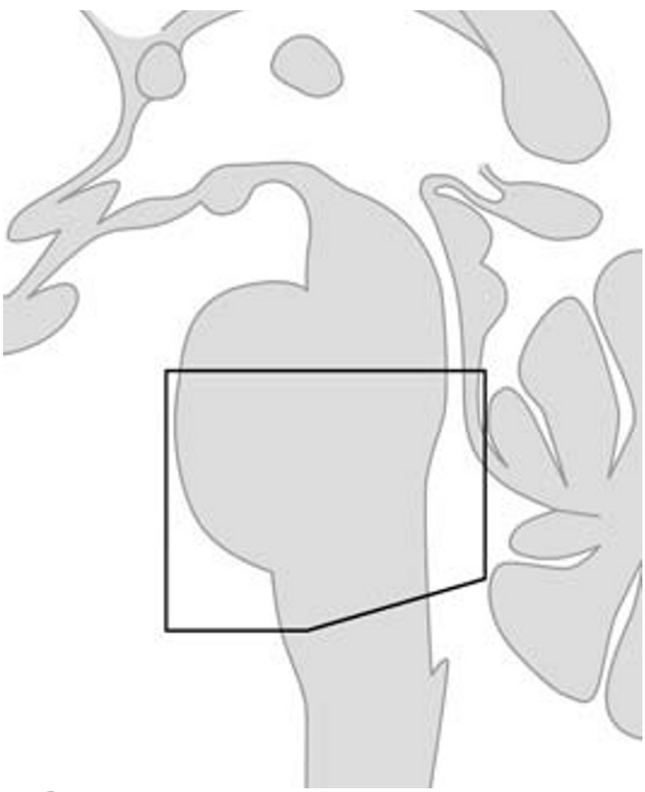

B

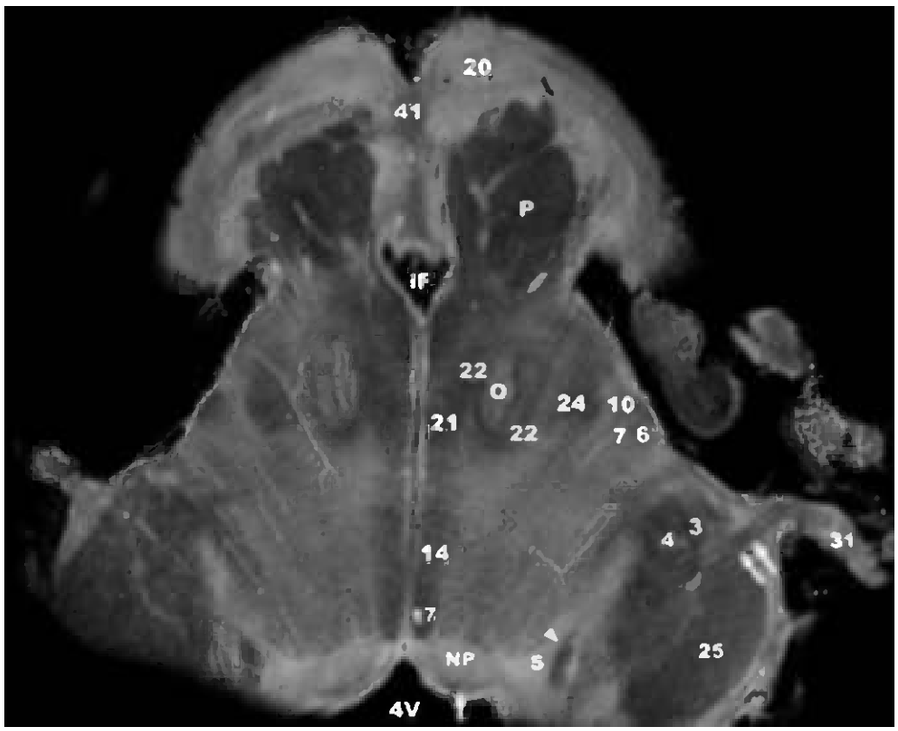

Fig. 8.34. Pontomedullary junction. Axial section.

The belly of the pons bulges anterior to the rostral end of the medulla. The pyramids of the medulla merge into the pyramidal tracts (P) of the pons. The pontine nuclei (20) and the ventral pontine decussation (41) surround the pyramidal tracts. The glossopharyngeal nerve (paired white arrows) crosses the surface of the brain stem between the inferior cerebellar peduncle (25) dorsally and the spinal trigeminal tract (3) and nucleus (4) ventrally. The anterior spinocerebellar tract (6), rubrospinal tract (7) and spinothalamic tract (10) course together anterolaterally. The central tegmental tract (24) is prominent as it approaches the superior pole of the inferior olivary nucleus (O).

3 Spinal trigeminal tract
4 Spinal trigeminal nucleus
6 Ventral spinocerebellar tract
7 Rubrospinal tract
10 Spinothalamic tract
14 Tectospinal tract
17 Medial longitudinal fasciculus
20 Pontine nuclei (pontine counterpart of medullary arcuate nuclei)
21 Medial lemniscus
22 Ventral trigeminothalamic tract
24 Central tegmental tract
25 Inferior cerebellar peduncle (restiform body)
31 Glossopharyngeal nerve (CN IX)
41 Ventral pontine decussation

Letter labels

4V Fourth ventricle
IF Inferior foramen cecum (deepest midline portion of the pontomedullary sulcus)
NP Nucleus prepositus hypoglossi
O Inferior olivary nucleus (superior pole)
P Pyramidal tract
S Solitary nucleus

Arrowheads and arrows

Single white arrowhead: Solitary tract within the solitary nucleus (S)
Single white arrow: Dorsal longitudinal fasciculus
Dual white arrows: Intramedullary portion of the glossopharyngeal nerve (CN IX)

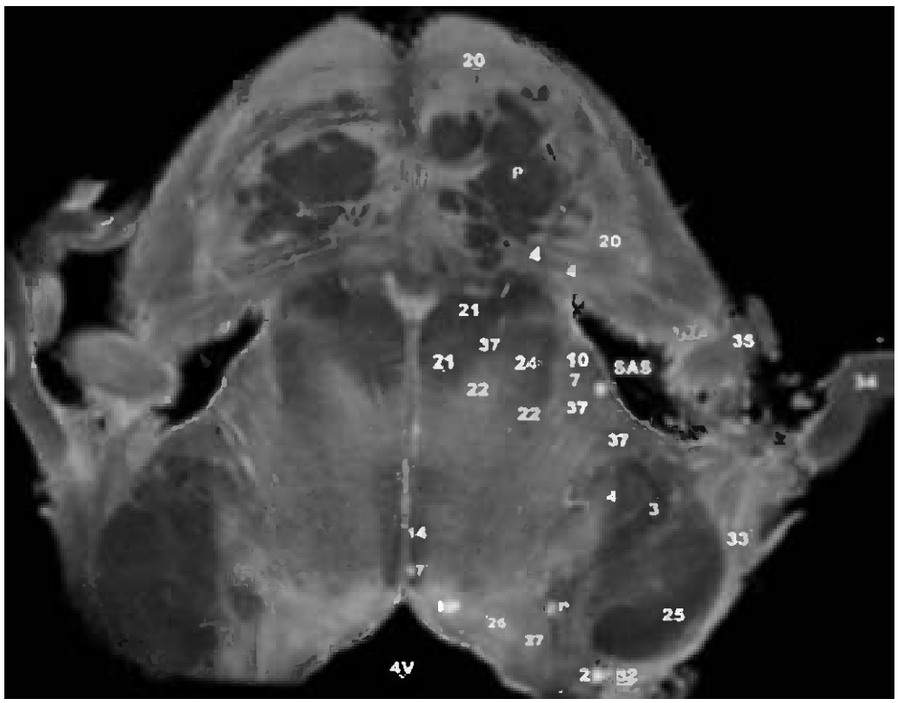

Fig. 8.35. Pontomedullary junction. Axial section.

The subarachnoid spaces (SAS) mark the lateral portions of the pontomedullary sulci and the transition from medulla to pons ventrolaterally. The dorsal medullary striae (unlabeled) on the floor of the fourth ventricle mark this transition dorsally. The vestibulocochlear (34) and facial (35) nerves emerge from the brain stem just caudal to the inferior cerebellar peduncle (25). Fibers arising in the cochlear division of the vestibulocochlear nerve enter the brain stem at the ventral cochlear nucleus and bifurcate there to synapse in the dorsal cochlear nucleus (32) (for high frequencies) and the ventral cochlear nucleus (33) (for low frequencies). The trapezoid body (37) is a complex, transversely oriented fiber stream that carries secondary auditory fibers from the cochlear and related nuclei to the lateral lemnisci bilaterally. (See **Figs. 8.37** and Sect. IX, Vestibulocochlear Nerves). The lateral vestibular nucleus (29) lies along the floor of the lateral angle of the fourth ventricle, and gives rise to the descending lateral vestibulospinal tract. Primary myelinated fibers of the vestibular nerve (27′) descend into the inferior vestibular nucleus (27), causing the stippled appearance.

3 Spinal trigeminal tract
4 Spinal trigeminal nucleus
6 Ventral spinocerebellar tract
7 Rubrospinal tract
10 Spinothalamic tract
14 Tectospinal tract
17 Medial longitudinal fasciculus
20 Pontine nuclei (pontine counterpart of medullary arcuate nuclei)
21 Medial lemniscus (now beginning to curve over to a coronal orientation)
22 Ventral trigeminothalamic tract
24 Central tegmental tract
25 Inferior cerebellar peduncle (restiform body)
26 Medial vestibular nucleus
27 Inferior vestibular nucleus
27′ Descending root of the vestibular nerve
29 Lateral vestibular nucleus
32 Dorsal cochlear nucleus
33 Ventral cochlear nucleus
34 Vestibulocochlear nerve (CN VIII)
35 Facial nerve (CN VII)
37 Trapezoid body (follow the three 37 labels along the transverse course of the auditory fibers.)

Letter labels

4V Fourth ventricle
NP Nucleus prepositus hypoglossi
P Pyramidal tract
SAS Subarachnoid space at the lateral aspect of the pontomedullary junction (supra-olivary fossette)

Arrowheads and arrows

Two white arrowheads: Pontocerebellar fibers passing to the contralateral middle cerebellar peduncle

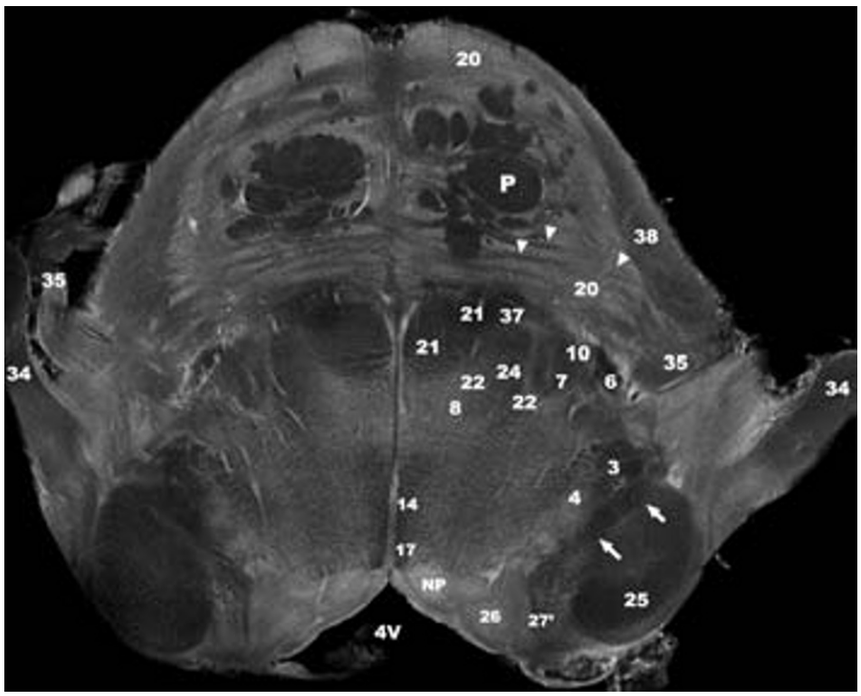

Fig. 8.36. Low pons. Axial section.

In the caudal pons, the medial lemnisci (21) curve laterally and transition (over the next several sections) into a coronal orientation. In this transition, the ventral ends of the medial lemnisci slide laterally, so that the fibers within the medial lemnisci maintain their same relative positions and somatotopy. Thus, in the caudal (vertical) portion of the medial lemniscus, fibers from caudal structures lie ventral to those from more dorsal structures. In the cranial (coronal) portion of the medial lemniscus, fibers from caudal strucures lie lateral to fibers from more proximal structures. The ventral trigeminothalamic tracts (22) maintain their relationship with the medial lemnisci (21) as the medial lemnisci transition from vertical to coronal orientation. Thus, the ventral trigeminothalamic tracts (22) that lay just lateral to the vertical medial lemnisci in caudal sections (see Fig. 8.9) now lie just dorsal to the coronal medial lemnisci in this and more cranial sections.

The separate entry/exit zones of the facial (35) and vestibulocochlear (34) nerves are well shown. The descending afferent vestibular fibers (paired white arrows) form a well developed bundle or "root" that courses lateral *to* the spinal trigeminal tract (3) and nucleus (4). The prominent pyramidal (corticospinal) tracts (P) descend through the pons, surrounded by the pontine nuclei (20) and the crossing pontocerebellar fibers (white arrowheads). The pontocerebellar fibers coalesce laterally into the middle cerebellar peduncles (38).

3 Spinal trigeminal tract
4 Spinal trigeminal nucleus
6 Ventral spinocerebellar tract
7 Rubrospinal tract
8 Reticular formation
10 Spinothalamic tract
14 Tectospinal tract
17 Medial longitudinal fasciculus
20 Pontine nuclei (pontine counterpart of medullary arcuate nuclei)
21 Medial lemniscus (curving over toward a coronal orientation)
22 Ventral trigeminothalamic tract
24 Central tegmental tract
25 Inferior cerebellar peduncle (restiform body)
26 Medial vestibular nucleus
27′ Descending root of the vestibular nerve
34 Vestibulocochlear nerve (CN VIII)
35 Facial nerve (CN VII)
37 Trapezoid body (auditory fibers)
38 Middle cerebellar peduncle

Letter labels

4V Fourth ventricle (with choroid plexus just dorsal to the label)
NP Nucleus prepositus hypoglossi
P Pyramidal tract

Arrowheads and arrows

White arrowheads: Pontocerebellar fibers crossing to the contralateral middle cerebellar peduncle (38)
Two white arrows: Afferent vestibular fibers (27′) descending to the inferior vestibular nucleus

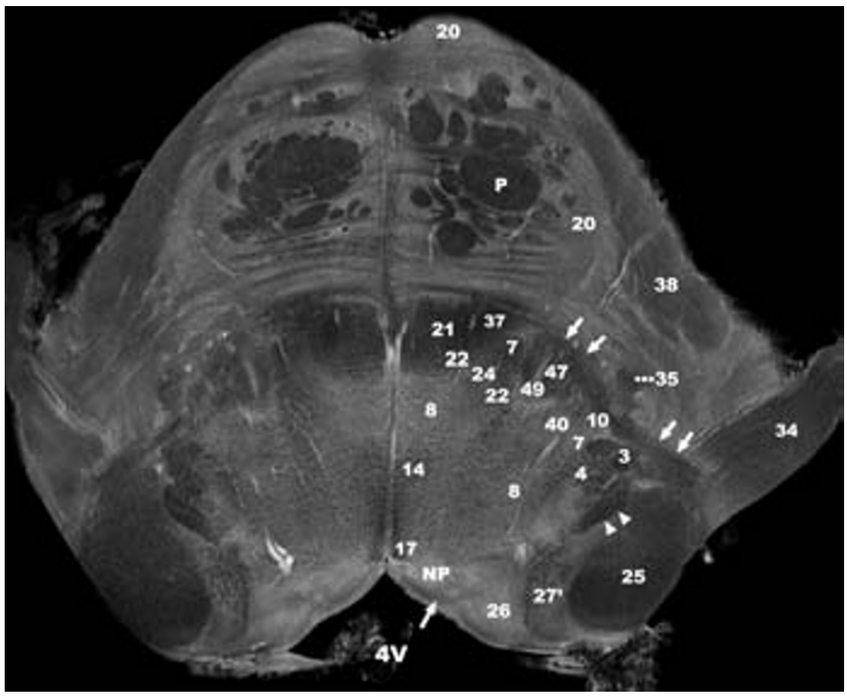

Fig. 8.37. Low-mid pons. Axial section.

The ventral cochlear nucleus (seen in Fig. 8-35) gives rise to a prominent ventral acoustic stria, which courses ventral to the inferior cerebellar peduncle (25) and the spinal trigeminal system (3,4), synapses within the supra-olivary complex (superior olivary nucleus and trapezoid nucleus) (49), and sends auditory fibers to the lateral lemnisci (47) and inferior colliculi bilaterally. The fibers of the ventral stria and secondary fibers arising from the supraolivary complex (49) form the large transversely oriented fiber bundle called the trapezoid body (37, four white arrows). (See also Sect. IX, Cranial nerves). The nucleus of the facial nerve (40) lies in the ventrolateral pontine tegmentum caudal, ventral and lateral to the nucleus of the abducens nerve, and medial to the trigeminal nucleus (4) and tract (3) (**See Figs 8.39 and 9.38**). The ventral trigeminothalamic tract (22) courses along the dorsal aspect of the medial lemniscus (21). The central tegmental tract (24) lies dorsal to the medial lemniscus (21) and to the auditory fibers (37, four white arrows).

3 Spinal trigeminal tract
4 Spinal trigeminal nucleus
7 Rubrospinal tract
8 Reticular formation
10 Spinothalamic tract
14 Tectospinal tract
17 Medial longitudinal fasciculus
20 Pontine nuclei (pontine counterpart of medullary arcuate nuclei)
21 Medial lemniscus (curving toward a coronal orientation)
22 Ventral trigeminothalamic tract
24 Central tegmental tract
25 Inferior cerebellar peduncle (restiform body)
26 Medial vestibular nucleus
27′ Descending root of the vestibular nerve
34 Vestibulocochlear nerve (CN VIII)
35 Descending intrapontine fascicles of the facial nerve (CN VII)
37 Trapezoid body (auditory fibers)
38 Middle cerebellar peduncle
40 Facial nerve nucleus (CN VII)
47 Lateral lemniscus
49 Supra-olivary nucleus complex (superior olivary nucleus and trapezoid nucleus)

Letter labels

4V Fourth ventricle (with choroid plexus just lateral to the label)
NP Nucleus prepositus hypoglossi
P Pyramidal tract

Arrowheads and arrows

Two white arrowheads: Afferent vestibular fibers passing lateral to the spinal trigeminal tract (3) and nucleus (4) as they descend to the inferior vestibular nucleus (27′)
Single white arrow: Dorsal longitudinal fasciculus
Four white arrows: Fibers of the trapezoid tract and body (37) coursing medially from the ventral cochlear nucleus to decussate in the midline

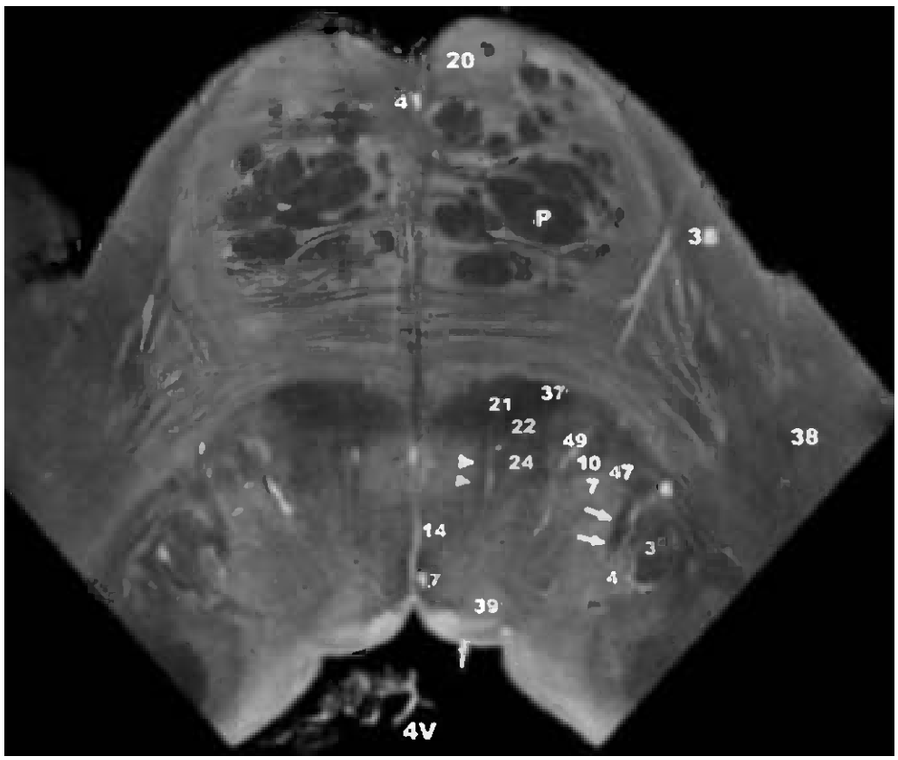

Fig. 8.38. Low-mid pons. Axial section.

The abducens nucleus (39) lies just deep to the floor of the fourth ventricle-rostral, dorsal and medial to the nucleus of the facial nerve. The efferent abducens fibers (white arrowheads) course caudally, ventrally and slightly laterally to their exit zone at the pontomedullary sulcus. (See next **Figs 8.39**, **8.40**, plus Figs. **2.14, 9.7A**). The descending intrapontine segment of the facial nerve (dual white arrows) courses ventrolaterally, *medial to* the spinal trigeminal tract and nucleus (3,4). The descending vestibular fibers (dual white arrowheads in prior **Fig. 8.37**) pass ventrolaterally *lateral to* the spinal trigeminal tract and nucleus. The position of the nerve fibers with respect to the spinal trigeminal system is one criterion for distinguishing the descending intrapontine facial nerve fibers (medially) from the descending vestibular fibers (laterally).

3 Spinal trigeminal tract
4 Spinal trigeminal nucleus
6 Ventral spinocerebellar tract
7 Rubrospinal tract
10 Spinothalamic tract
14 Tectospinal tract
17 Medial longitudinal fasciculus
20 Pontine nuclei (pontine counterpart of medullary arcuate nuclei)
21 Medial lemniscus (now oriented in coronal plane)
22 Ventral trigeminothalamic tract
24 Central tegmental tract
37 Trapezoid body (auditory fibers)
38 Middle cerebellar peduncle
39 Abducens nucleus (CN VI)
41 Ventral pontine decussation
47 Lateral lemniscus
49 Supra-olivary nuclear complex (superior olivary nucleus and trapezoid nucleus)

Letter labels

4V Fourth ventricle
P Pyramidal tract

Arrowheads and arrows

Two white arrowheads: Abducens nerve fibers passing ventrally from the abducens nucleus (39)
Single white arrow: Dorsal longitudinal fasciculus
Two white arrows: Descending intrapontine fascicles of the facial nerve (CN VII)

Fig. 8.39. Mid pons. Axial section.

The fibers that emerge from the facial nucleus (40) first form a diffuse spread of fibers that pass rostral, dorsal and medial to reach the medial aspect of the rostral pole of the abducens nucleus (39). These are poorly resolved. The facial fibers then condense (small black arrowhead) into a tight bundle that courses over the abducens nucleus, raising a distinct bulge – the facial colliculus – in the floor of the medial pontine portion of the fourth ventricle (4V). The now-compact facial nerve bundle recurves ventrally (black arrows) to pass between its own nucleus (40) and the spinal trigeminal tract (3) and nucleus (4). Within the basis pontis, pontine nuclei (20) on each side give rise to pontocerebellar fibers (white arrowheads), which cross the midline to enter the contralateral middle cerebellar peduncles (38) bilaterally. The pontocerebellar fibers are the major fiber bundles within the middle cerebellar peduncles.

Fig. 8.40. Upper pons. Axial section.

The medial lemniscus (21), spinothalamic tract (10) and lateral lemniscus (47) begin to curve dorsally, and, in ascending sections, form distinct, paired crescents or "horns" that arch dorsally to enclose the rostral fourth ventricle and aqueduct. Pontine nuclei extend into the tegmentum lateral to the medial lemnisci and spinothalamic tracts to form the lateral tegmental extension (20′) of the pontine nuclei. The ventral nucleus (open arrowhead) of the lateral lemniscus notches the medial border of the lateral lemniscus just where the lemniscus turns dorsally. The ventral trigeminothalamic tract (22) continues to ascend along the dorsal aspect of the medial lemniscus (21). The dorsal trigeminothalamic tract (52) now appears and ascends within the dorsolateral pontine tegmentum.

In this section, the multiple divisions of the trigeminal system converge [467]. The pars oralis of the spinal trigeminal nucleus merges into the principal sensory nucleus (46) of the trigeminal nerve. Afferent trigeminal fibers (46′) enter the pons medial to the principal sensory nucleus (46) and distribute within the principal sensory nucleus somatotopically. As in the spinal trigeminal nucleus, ophthalmic division (V1) fibers lie ventral within the principal sensory nucleus. The maxillary (V2) fibers are intermediate in positon, and the mandibular (V3) fibers lie dorsally. Secondary fibers that arise from the principal sensory nucleus follow two pathways. Secondary fibers from the ventral portion of the principal sensory nucleus cross the midline, enter the contralateral ventral trigeminothalamic tract (22) and ascend with the crossed secondary fibers of the spinal trigeminal nucleus to reach the ventral posteromedial nucleus of the contralateral thalamus [78, 322]. Secondary fibers from the dorsomedial portion of the principal sensory nucleus enter the ipsilateral dorsal trigeminothalamic tract (52) and ascend as uncrossed fibers to the ventral posteromedial nucleus of the ipsilateral thalamus [78]. The name *portio major* is given to the spinal trigeminal nucleus and tract, the principal sensory nucleus, and the afferent sensory fibers that are distributed to them [322].

The motor nucleus of the trigeminal nerve (masticator nucleus) (45) lies medial to the principal sensory nucleus (46). Its efferent fibers form the small motor root, which passes through the pons to to emerge superomedial to the larger sensory root (**See Fig. 8.42**). These fibers innervate the muscles of mastication (See also Sect. IX, Cranial Nerves). The mesencephalic nucleus of the trigeminal nerve (44) extends cranially from this site into the high pons and midbrain, and is addressed later. The name *portio minor* is given to the mesencephalic nucleus and tract plus the motor nucleus and its nerve [322].

3 Spinal trigeminal tract
4 Spinal trigeminal nucleus
6 Ventral spinocerebellar tract
7 Rubrospinal tract
8 Reticular formation
10 Spinothalamic tract
14 Tectospinal tract
17 Medial longitudinal fasciculus
20 Pontine nuclei
20′ Lateral tegmental extension of pontine nuclei
21 Medial lemniscus
22 Ventral trigeminothalamic tract
24 Central tegmental tract
37 Trapezoid body (auditory fibers)
38 Middle cerebellar peduncle
39 Abducens nucleus (CN VI)
40 Facial nerve nucleus (CN VII)
41 Ventral pontine decussation
42 Dorsal pontine decussation
44 Mesencephalic tract and surrounding mesencephalic nucleus of the trigeminal nerve (CN V)
45 Motor nucleus of the trigeminal nerve (CN V)
46 Principal sensory nucleus of the trigeminal nerve (CN V)
46′ Intrapontine fascicles of the sensory root of CN V
47 Lateral lemniscus
52 Dorsal trigeminothalamic tract

Letter labels

4V Fourth ventricle
F Frontopontine tract
L Site of the locus ceruleus (See Sect. X, Neuromelanin pp. 475–481)
P Pyramidal tract (containing corticospinal fibers)
PT Parieto-temporopontine tract

Arrrowheads and arrows

Open arrowhead: Ventral nucleus of the lateral lemniscus (also 48 in other images)
Single black arrowhead: Genu of the facial nerve at the facial colliculus
Five white arrowheads: Pontocerebellar fibers passing to the contralateral middle cerebellar peduncle (38)
Single white arrow: Intrapontine fascicles of the abducens (CN VI) coursing ventrally
Dual black arrows: Descending intrapontine fascicles of the facial nerve (CN VII)

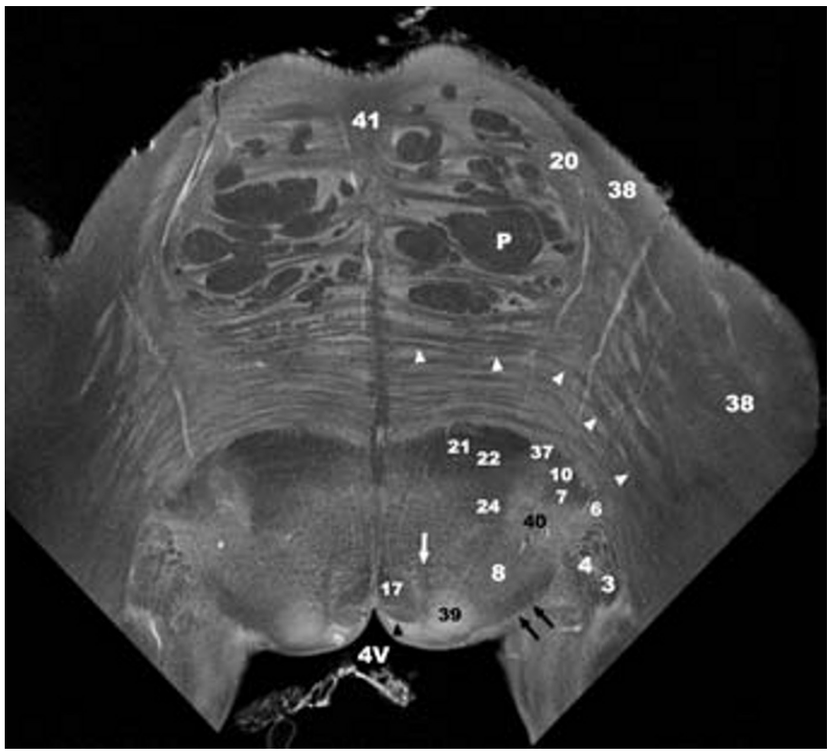
41
20
38
P
38
21
22
37
10
7
6
24
40
4
3
8
17
39
4V

8.39.

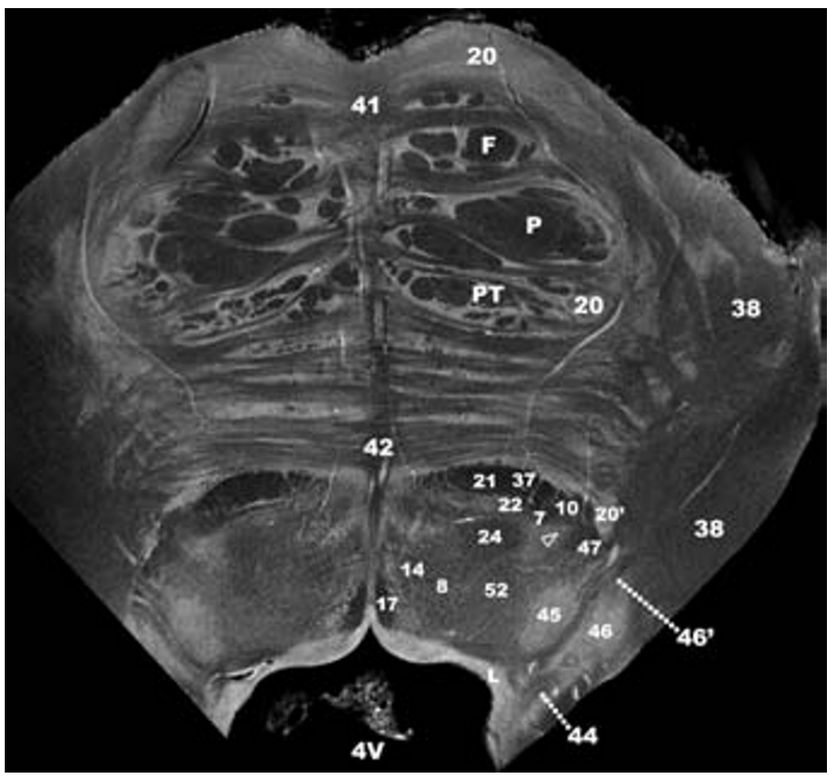
20
41
F
P
PT
20
38
42
21
37
22
7
10
20'
38
24
47
14
8
52
17
45
46
46'
L
44
4V

8.40.

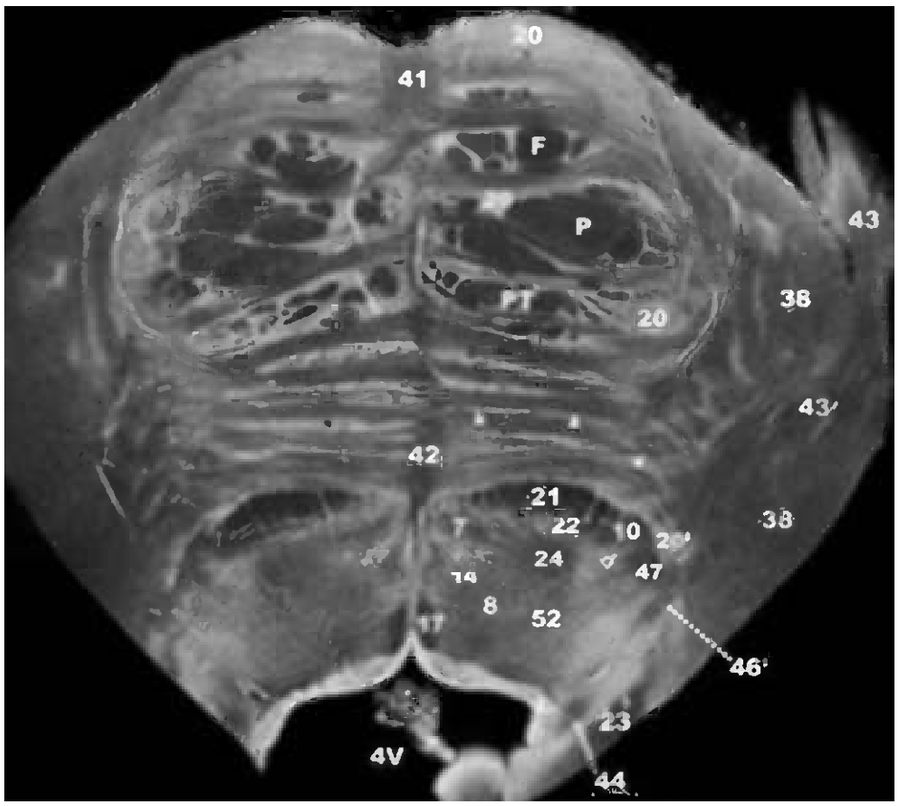

Fig. 8.41. High pons. Axial section.

The sensory trigeminal nerve fibers (43) can be traced from their entry into the ventral brain stem, through the middle cerebellar peduncle (38), toward the principal sensory trigeminal nucleus (unlabeled, but compare with prior section). The mesencephalic nucleus and tract (44) of the trigeminal nerve ascend through the pontine tegmentum toward the midbrain. The locus ceruleus lies just beneath the floor of the fourth ventricle. The dark melanin within the locus is seen grossly as a bluish discoloration of the floor of the fourth ventricle, giving the nucleus its name (See Fig. 10.1). Within the basis pontis, the descending cortical fibers that are grouped together as the cerebral peduncle of the midbrain (See Figs. 8.98 and 8.99) appear as separate frontopontine (F), corticospinal (pyramidal, P) and parieto-temporopontine (PT) tracts that course individually through the basis pontis.

7 Rubrospinal tract
8 Reticular formation
10 Spinothalamic tract
14 Tectospinal tract
17 Medial longitudinal fasciculus
20 Pontine nuclei (pontine counterpart of medullary arcuate nuclei)
20′ Lateral tegmental extension of pontine nuclei
21 Medial lemniscus
22 Ventral trigeminothalamic tract
23 Superior cerebellar peduncle (partially resected laterally)
24 Central tegmental tract
38 Middle cerebellar peduncle
41 Ventral pontine decussation
42 Dorsal pontine decussation
43 Trigeminal nerve (CN V)
44 Mesencephalic tract and surrounding mesencephalic nucleus of CN V
46′ Intrapontine fascicles of the sensory root of CN V
47 Lateral lemniscus
52 Dorsal trigeminothalamic tract

Letter labels

4V Fourth ventricle
F Frontopontine tract
L Site of the locus ceruleus
P Pyramidal tract (containing corticospinal fibers)
PT Parieto-temporopontine tract

Arrowheads and arrows

Open arrowhead: Ventral nucleus of the lateral lemniscus (also 48 in other images)
Three white arrowheads: Pontocerebellar fibers crossing to the middle cerebellar peduncle (38)

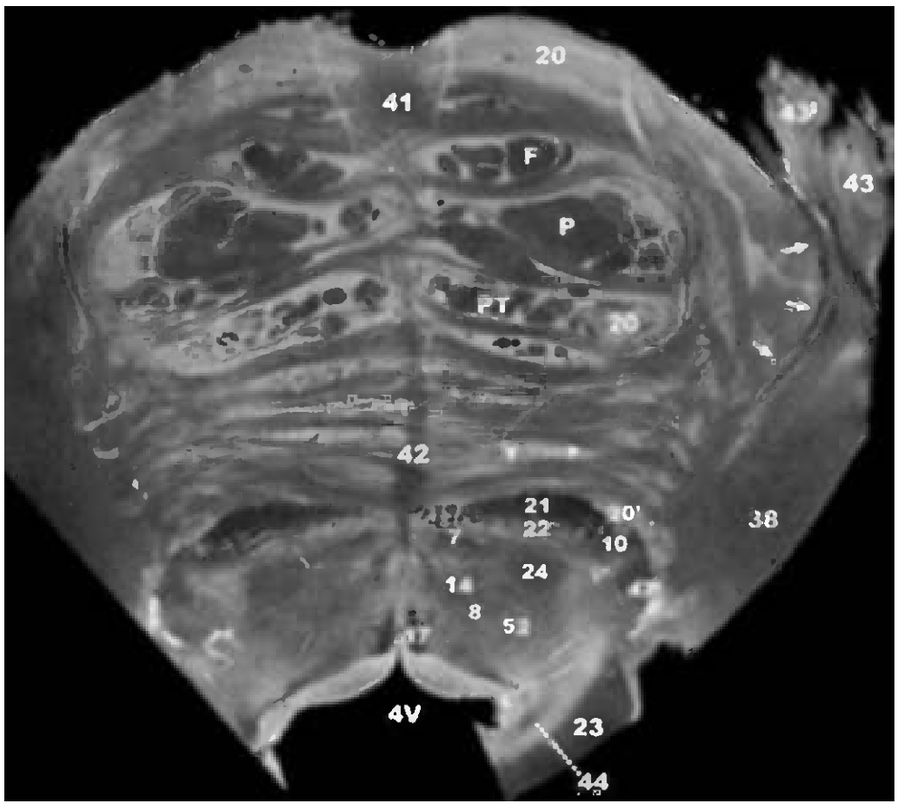

Fig. 8.42. High pons. Axial section.

In this section, trigeminal fibers (white arrows) coursing through the middle cerebellar peduncle pass superomedial (43′) to the main group of trigeminal fibers (43), indicating that they represent the mesencephalic sensory and motor fibers (portio minor) of the trigeminal nerve. The medial lemniscus (21), spinothalamic tract (10), rubrospinal tract (7) and lateral lemniscus (47) begin to form paired crescents of white matter, with their tips directed posteriorly toward the superior cerebellar peduncles. Over the following rostral sections, the tips of these crescents will slide dorsally, superficial to the superior cerebellar peduncles. The medial longitudinal fasciculus (17), tectospinal tract (14), and central tegmental tract (24) continue to ascend as well developed fiber bundles within the pontine tegmentum.

7 Rubrospinal tract
8 Reticular formation
10 Spinothalamic tract
14 Tectospinal tract
17 Medial longitudinal fasciculus
20 Pontine nuclei (pontine counterpart of medullary arcuate nuclei)
20′ Lateral tegmental extension of pontine nuclei
21 Medial lemniscus
22 Ventral trigeminothalamic tract
23 Superior cerebellar peduncle (trimmed laterally)
24 Central tegmental tract
38 Middle cerebellar peduncle
41 Ventral pontine decussation
42 Dorsal pontine decussation
43 Trigeminal nerve, sensory root (CN V)
43′ Trigeminal nerve, motor root (CN V)
44 Mesencephalic tract and surrounding mesencephalic nucleus of CN V
52 Dorsal trigeminothalamic tract

Letter labels

4V Fourth ventricle
F Frontopontine tract
L Site of the locus ceruleus
P Pyramidal tract containing corticospinal fibers
PT Parieto-temporopontine tract

Arrowheads and arrows

Open arrowhead: Ventral nucleus of the lateral lemniscus (also 48 in other images)
Two white arrowheads: Pontocerebellar fibers arising in the contralateral pontine nuclei and passing to the middle cerebellar peduncle (38)
Three white arrows: Intrapontine fascicles of the motor root of CN V (43′)

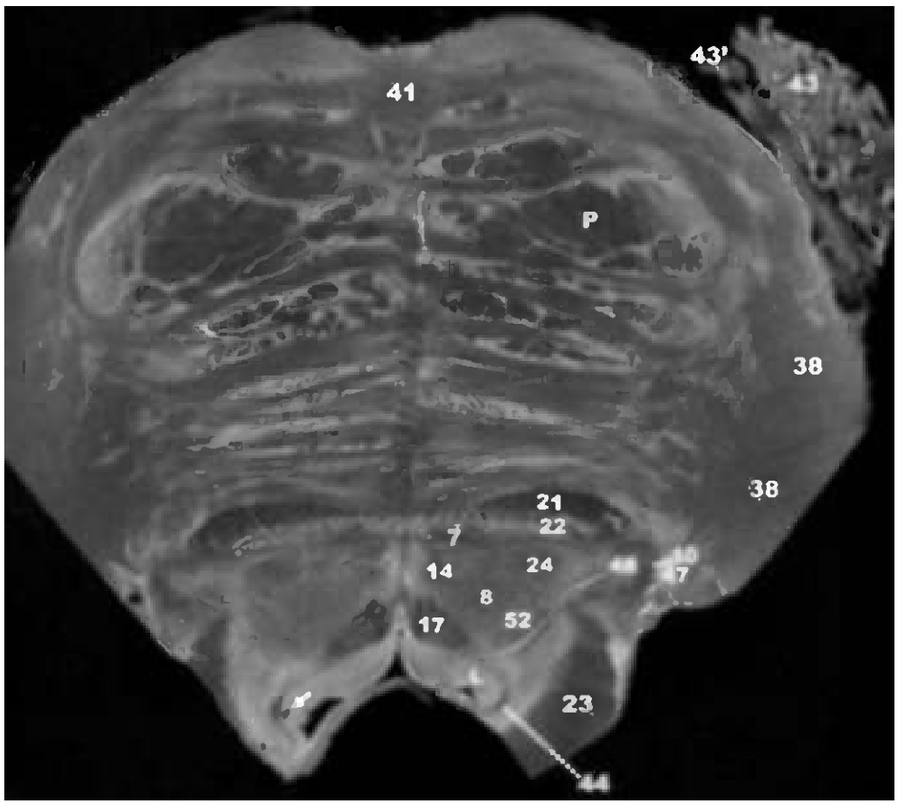

Fig. 8.43. Pontomedullary junction. Axial section.

The ventral nucleus (48) of the lateral lemniscus is an auditory relay nucleus that forms a well defined zone of gray matter along the medial aspect of the base of the lateral lemniscus (47). The mesencephalic nucleus (44) of the trigeminal nerve is thin column of neurons situated along the lateral border of the floor of the fourth ventricle and the periaqueductal gray matter in the high pons and midbrain. The peripheral processes of these mesencephalic trigeminal neurons descend in the midbrain and pons as the mesencephalic tract of the trigeminal nerve [467]. The mesencephalic trigeminal sensory fibers exit the pons with the trigeminal motor fibers and distribute to the muscles of mastication to provide pressure and kinesthetic data on bite. The central processes of the mesencephalic trigeminal neurons pass to the motor trigeminal nucleus and participate in reflex control of bite (See also Sect. IX, Cranial Nerves) [467]. Efferent fascicles (single white arrow) of the contralateral trochlear nucleus pass posteriorly within the periaqueductal gray matter toward their decussation in the inferior medullary velum.

7 Rubrospinal tract
8 Reticular formation
10 Spinothalamic tract
14 Tectospinal tract
17 Medial longitudinal fasciculus
21 Medial lemniscus
22 Ventral trigeminothalamic tract
23 Superior cerebellar peduncle (trimmed laterally)
24 Central tegmental tract
38 Middle cerebellar peduncle
41 Ventral pontine decussation
43 Trigeminal nerve, sensory root (CN V)
43' Trigeminal nerve, motor root (CN V)
44 Mesencephalic tract and surrounding mesencephalic nucleus of CN V
47 Lateral lemniscus
48 Ventral nucleus of the lateral lemniscus (also open arrowhead in other images)
52 Dorsal trigeminothalamic tract

Letter labels

L Site of locus ceruleus
P Pyramidal tract (containing corticospinal fibers)

Arrowheads and arrows

Single white arrow: Trochlear nerve fascicle

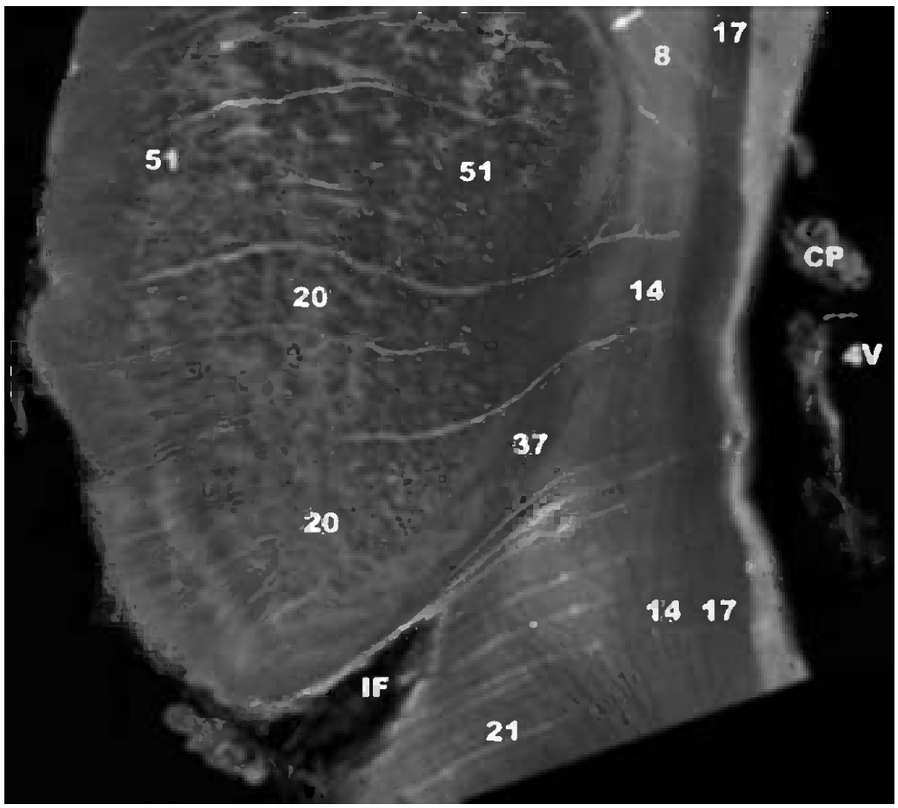

B 2. Sagittal pontomedullary junction

Sagittal sections displayed from midline to lateral (Figs. 8.44–8.51)

Fig. 8.44. Pontomedullary junction. Mid-sagittal section.

As in the medulla, the medial longitudinal fasciculus (17), tectospinal tract (14) and medial lemniscus (21) form a vertically oriented, paramedian column of fibers in which the "individual tracts" have a general location but no precise separation from each other. The trapezoid body lies caudally, along the junction of the basis pontis with the pontine tegmentum, approximately in line with the pontine portion of the medial lemniscus. Inferiorly, paramedian penetrating vessels enter the pontomedullary junction at the inferior foramen cecum (IF) and ascend into the low pontine tegmentum. Further superiorly at the midpons, the paramedian perforating vessels extend directly into the midpontine tegmentum. The cut cross sections of the pontocerebellar fibers (51) form an array of "dots", that surround the pontine nuclei (20).

8 Reticular formation
14 Tectospinal tract
17 Medial longitudinal fasciculus
20 Pontine nuclei
21 Medial lemniscus
37 Trapezoid body
51 Cut cross-sections of the pontocerebellar fibers

Letter labels
4V Fourth ventricle
CP Choroid plexus
IF Inferior foramen cecum (deepest midline portion of the pontomedullary sulcus)

Arrowheads and arrows
Single white arrow: Corticobulbar fibers

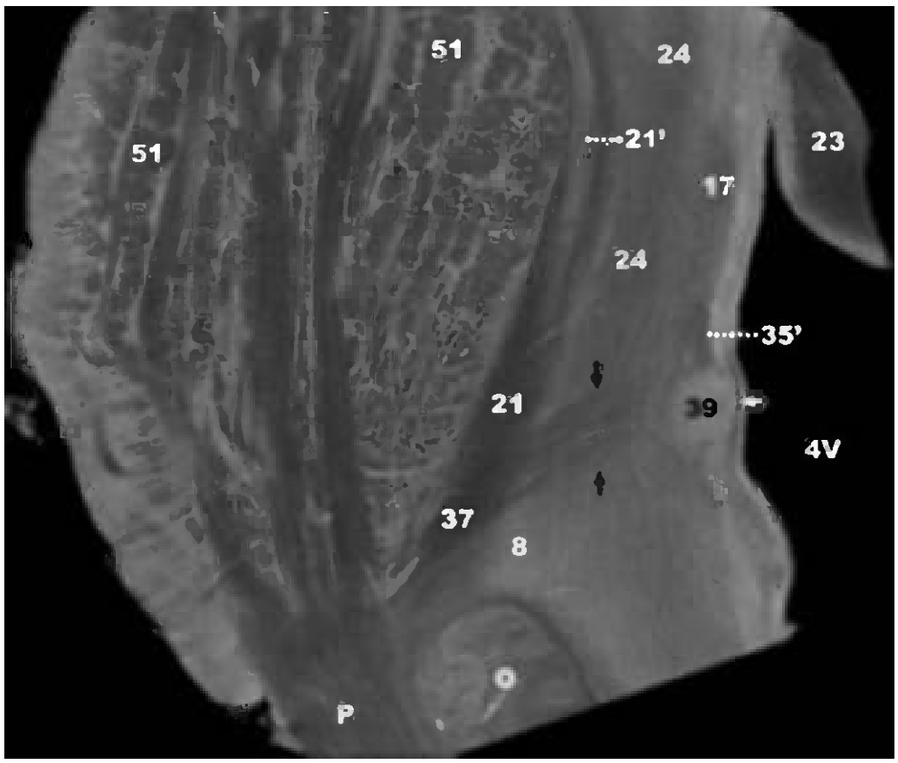

Fig. 8.45 Pontomedullary junction. Medial sagittal section.

The individual pontocerebellar fibers (51) are grouped into fascicles, which form a prominent mosaic pattern with the gray pontine nuclei (unlabeled). The descending cortical fibers that are separated into discrete bundles in the pons re-aggregate at the pontomedullary junction to form the pyramid (P) of the medulla. The medial lemniscus becomes attenuated (21′) along its curvature through the pons, where it encompasses multiple medial nuclei. The central tegmental tract (24) forms a clearly defined bundle (24) between the medial longitudinal fasciculus dorsally (17) and the medial lemniscus (21) ventrally as it descends from the red nucleus (above the edge of the image) to the inferior olivary nucleus (O). The abducens nucleus (39), and the facial nerve fibers (35′) that arch over the rostral pole of the abducens nucleus, form the facial colliculus in the floor of the fourth ventricle medially. Individual abducens fibers (between black arrrows) course caudally and ventrally toward their exit at the pontomedullary junction. The dorsal longitudinal fasciculus (white arrow) courses longitudinally along the floor of the fourth ventricle (4V). The superior cerebellar peduncle (23) is seen superiorly.

8 Reticular formation
17 Medial longitudinal fasciculus
21 Medial lemniscus
21′ Rete of the medial lemniscus (where medial meniscal fibers have a reticular relationship with multiple medial nuclei)
23 Superior cerebellar peduncle
24 Central tegmental tract
35′ Genu of the facial nerve (CN VII) atop the abducens nucleus (CN VI) (39)
37 Trapezoid body
39 Abducens nucleus (CN VI)
51 Cut cross-sections of the pontocerebellar fibers

Letter labels

4V Fourth ventricle
O Inferior olivary nucleus
P Pyramid containing the corticospinal tract

Arrowheads and arrows

Single white arrow: Dorsal longitudinal fasciculus
Two black arrows: Descending intrapontine fascicles of the abducens nerve (CN VI)

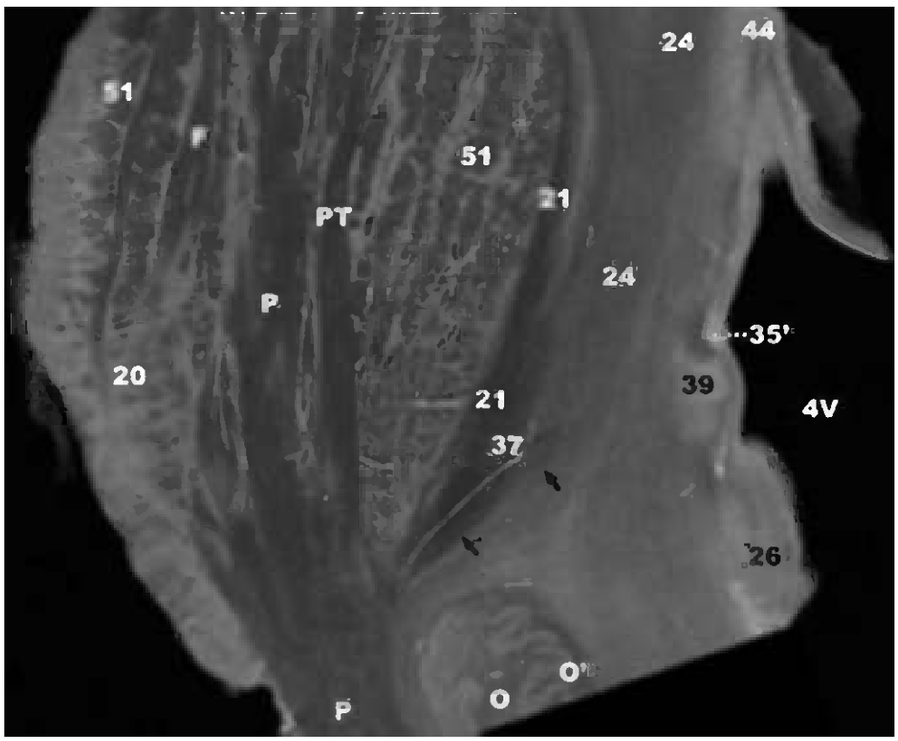

Fig. 8.46. Pontomedullary junction. Medial sagittal section.

This section displays a smaller cross section of the abducens nucleus, a more prominent and compact bundle of facial nerve fibers (35′), and more caudal portions of the descending abducens fibers (black arrows). Note the vessel that co-fasciculates with the abducens fibers. The medial vestibular nucleus (26) presents in the floor of the fourth ventricle (4V). The trajectory of the central tegmental tract (24) is directed toward the rostral pole of the inferior olivary nucleus (O) and its capsule (O′).

20 Pontine nuclei
21 Medial lemniscus
24 Central tegmental tract
26 Medial vestibular nucleus
35′ Genu of the facial nerve (CN VII)
37 Trapezoid body
39 Abducens nucleus (CN VI)
44 Mesencephalic nucleus and tract of the trigeminal nerve (CN V)
51 Cut cross-sections of the pontocerebellar fibers

Letter labels

4V Fourth ventricle
F Frontopontine tract
O Inferior olivary nucleus
O′ Amiculum (capsule of the inferior olivary nucleus)
P Pyramidal tracts leading to the pyramid
PT Temporoparietopontine tract

Arrowheads and arrows

Two black arrows: Descending intrapontine fascicles of the abducens nerve (CN VI) passing to the pontomedullary sulcus

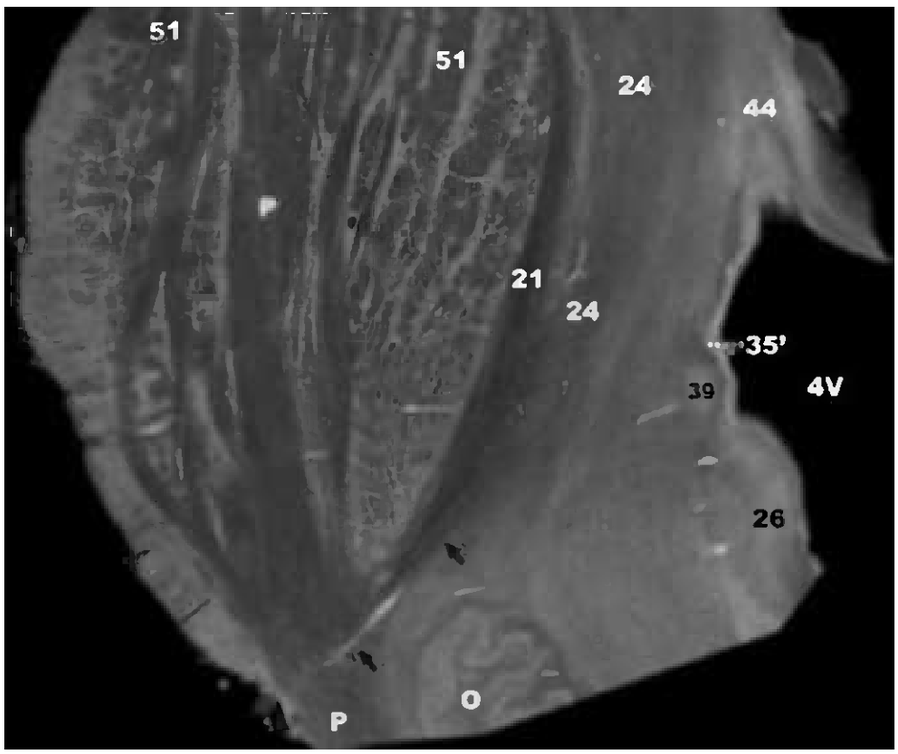

Fig. 8.47. Pontomedullary junction. Medial sagittal section.

The abducens fibers and accompanying vessel (black arrows) continue caudally to the pontomedullary sulcus. The mesencephalic nucleus of the trigeminal nerve forms a thin "angle" or caret at the rostrolateral aspect of the fourth ventricle, deep to the superior cerebellar peduncle (heavily trimmed) (See Figs. 8.65 and 8.68)

21 Medial lemniscus
24 Central tegmental tract
26 Medial vestibular nucleus
35′ Genu of the facial nerve (CN VII)
39 Abducens nucleus (CN VI)
44 Mesencephalic nucleus and tract of CN V
51 Cut cross-sections of the pontocerebellar fibers

Letter labels

4V Fourth ventricle
O Inferior olivary nucleus
P Pyramidal tracts leading to the pyramid

Arrowheads and arrows

Two black arrows: Descending intrapontine fascicles of the abducens nerve (CN VI) passing to the pontomedullary sulcus

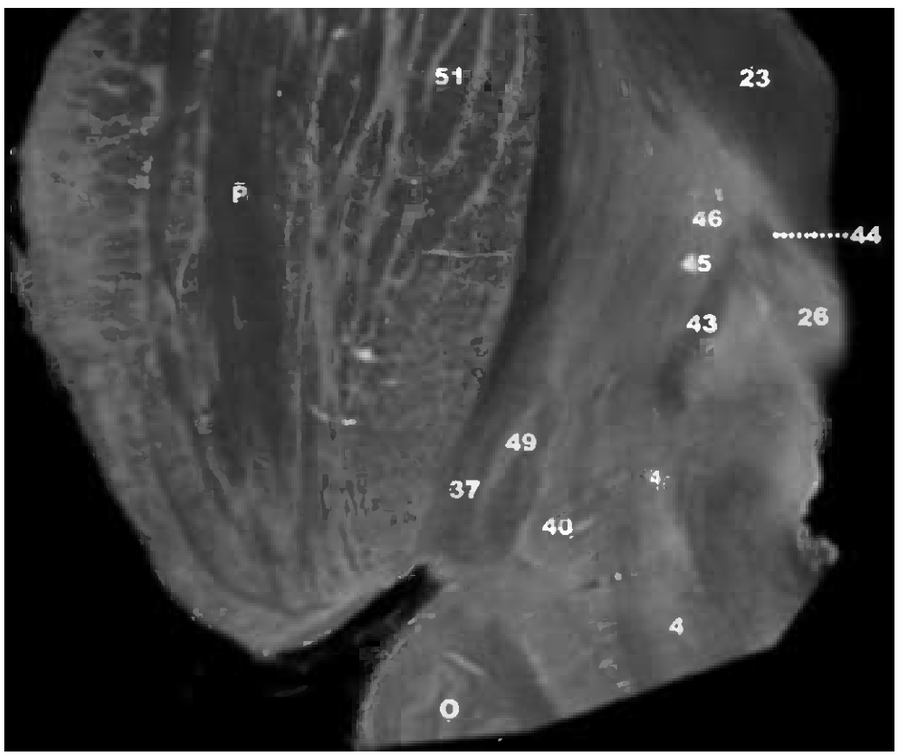

Fig. 8.48. Pontomedullary junction. Medial sagittal section.

The spinal nucleus (4), mesencephalic nucleus (44), motor nucleus (45) and principal sensory nucleus (46) of the trigeminal system converge toward the edge of fourth ventricle, rostral to the vestibular nuclei (26) and inferomedial to the superior cerebellar peduncle (23). Intrapontine fibers (43) of the trigeminal nerve course between the nuclei. Many auditory fibers synapse at the supra-olivary nuclear complex (49) before joining the lateral lemnisci.

4 Spinal trigeminal nucleus
23 Superior cerebellar peduncle
26 Medial vestibular nucleus
37 Trapezoid body
40 Facial nucleus (CN VII)
43 Intrapontine fascicles of the trigeminal nerve (CN V)
45 Motor nucleus of CN V
46 Principal sensory nucleus of CN V
49 Supra-olivary complex
51 Cut cross-sections of the pontocerebellar fibers

Letter labels
O Inferior olivary nucleus
P Pyramidal tracts leading to the pyramid

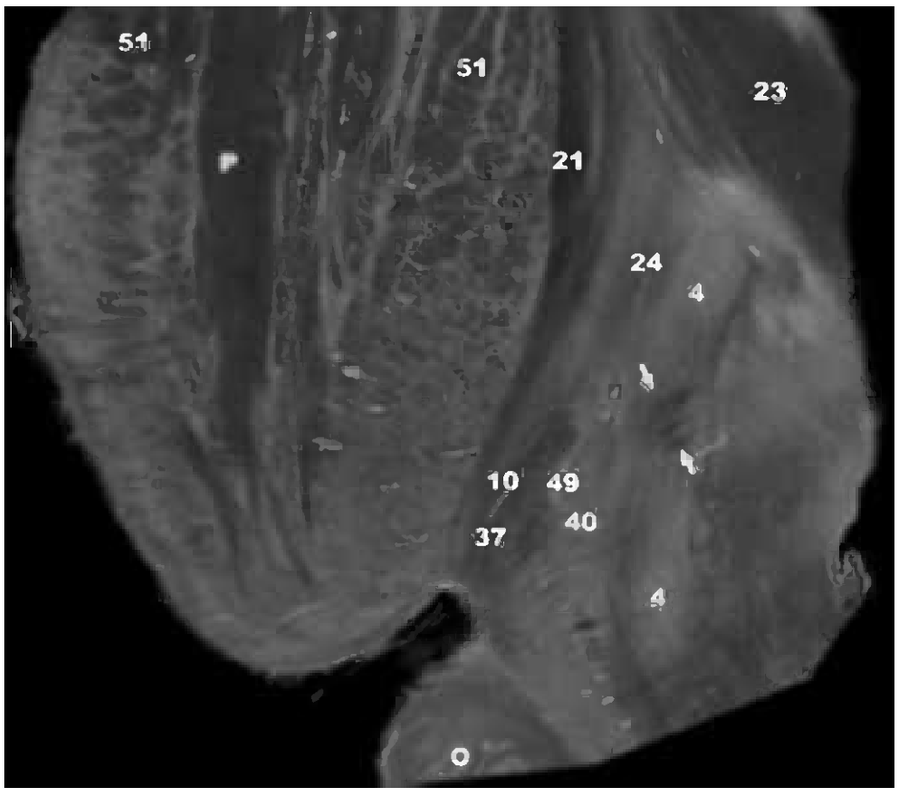

Fig. 8.49. Pontomedullary junction. Sagittal section.

The trapezoid body (37) and supra-olivary nuclear complex (49) of the auditory relay system lie rostral to the inferior olivary nucleus (O) and the facial nerve nucleus (40), in relation to the medial lemniscus (21). As seen here and the following sections (**Figs. 8.50 and 8.51**), the descending intrapontine fascicles of the facial nerve (between white arrows) course ventrally, caudally and laterally, pass lateral to the facial nerve nucleus, and emerge into the cerebellopontine angle just inferior to the middle cerebellar peduncle.

4 Spinal trigeminal nucleus
10 Spinothalamic tract
21 Medial lemniscus
23 Superior cerebellar peduncle
24 Central tegmental tract curving ventrally toward the inferior olivary nucleus (O)
37 Trapezoid body
40 Facial nucleus (CN VII)
49 Supra-olivary nuclear complex
51 Cut cross-sections of the pontocerebellar fibers

Letter labels
O Inferior olivary nucleus
P Pyramidal tracts leading to the pyramid

Arrowheads and arrows
Two white arrows: Descending intrapontine fascicles of the facial nerve (CN VII)

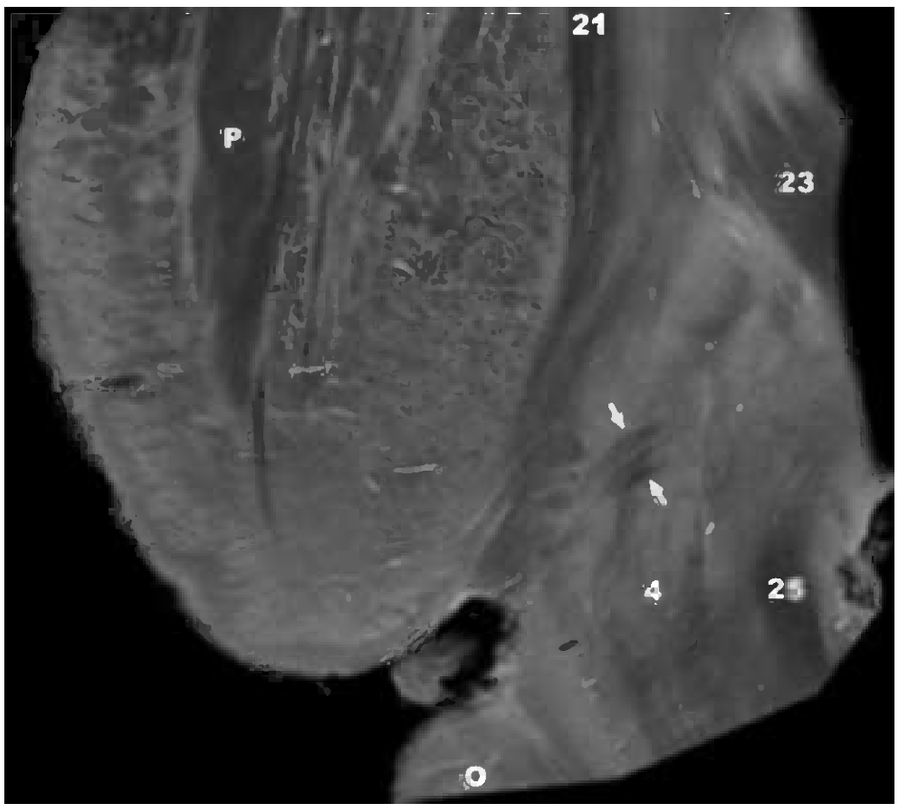

Fig. 8.50. Pontomedullary junction. Sagittal section.

The facial nerve fibers pass medial to the spinal trigeminal nucleus (4) and tract as they descend to their exit beneath the middle cerebellar peduncle. The medial lemniscus arches superiorly at the junction of the basis pontis and the pontine tegmentum. The inferior cerebellar peduncle (25) ascends toward the cerebellum dorsal to the spinal trigeminal nucleus (4) and tract.

4 Spinal trigeminal nucleus
21 Medial lemniscus
23 Superior cerebellar peduncle
25 Inferior cerebellar peduncle

Letter labels
O Inferior olivary nucleus
P Pyramidal tracts leading to the pyramid

Arrowheads and arrows
Two white arrows: Descending intrapontine fascicles of the facial nerve (CN VII)

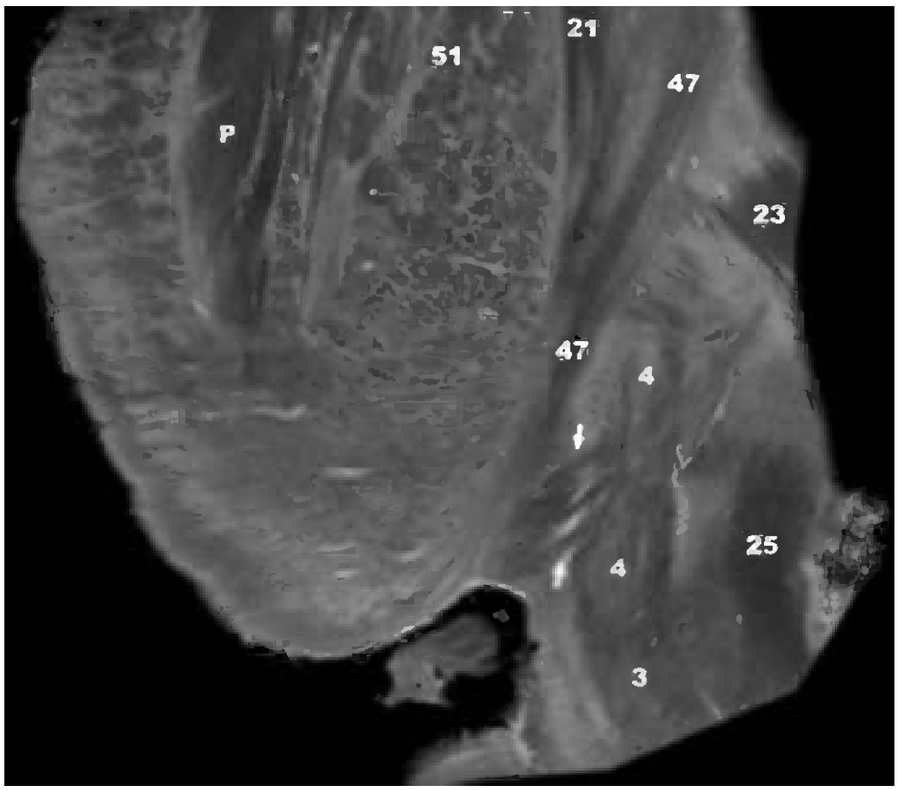

Fig. 8.51. Pontomedullary junction. Lateral sagittal section.

The spinal trigeminal tract (3) lies along the lateral border of the nucleus (4), so it is better shown in this lateral section. This section also shows the facial nerve fibers (white arrows) now passing ventral to the spinal trigeminal nucleus (4) and tract (3). The superior (23) and inferior (25) cerebellar peduncles begin to converge toward the cerebellar hemisphere. The lateral lemniscus (47) ascends toward the inferior colliculus dorsal lateral to the medial lemniscus (21).

3 Spinal trigeminal tract
4 Spinal trigeminal nucleus
21 Medial lemniscus
23 Superior cerebellar peduncle
25 Inferior cerebellar peduncle
47 Lateral lemniscus
51 Cut cross-sections of pontocerebellar fibers

Letter labels

P Pyramidal tracts leading to the pyramid

Arrowheads and arrows

Two white arrows: Descending intrapontine fascicles of the facial nerve (CN VII)

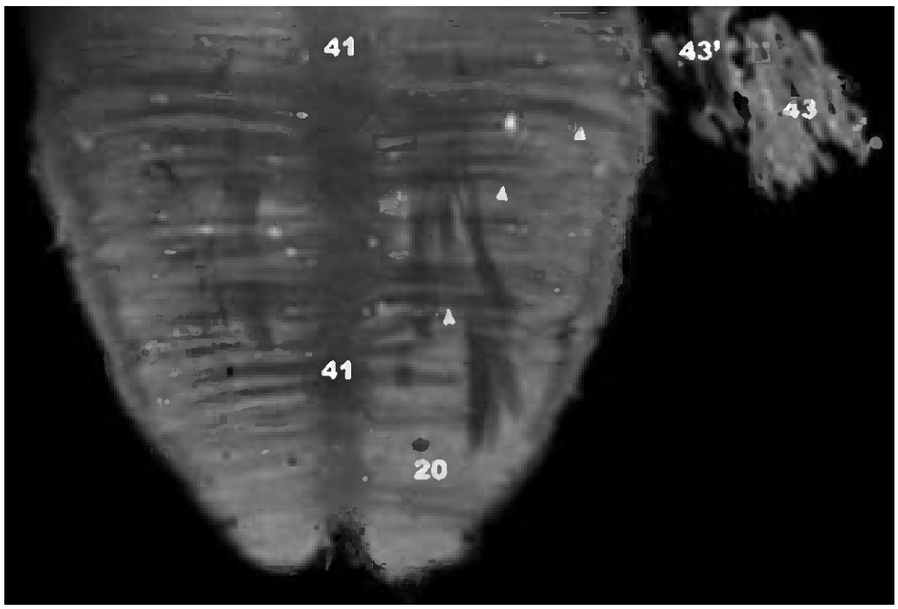

B 3. Coronal pontomedullary junction

Coronal sections displayed from ventral to dorsal (Figs. 8.52 to 8.65)

Fig. 8.52. Pontomedullary junction. Ventral coronal section. The pontocerebellar fibers (white arrowheads) arise from the pontine nuclei (20) on each side, cross the midline, and enter the contralateral middle cerebellar peduncles. 41 marks the ventral pontine decussation. The motor (43') and sensory (43) trigeminal nerves pass anteriorly along the lateral border of the pons, en route toward Meckel's cave.

20 Pontine nuclei
41 Ventral pontine decussation
43 Sensory root of the trigeminal nerve (CN V)
43' Motor root of the trigeminal nerve (CN V)

Arrowheads and arrows
White arrowheads: Pontocerebellar fibers crossing to the middle cerebellar peduncle

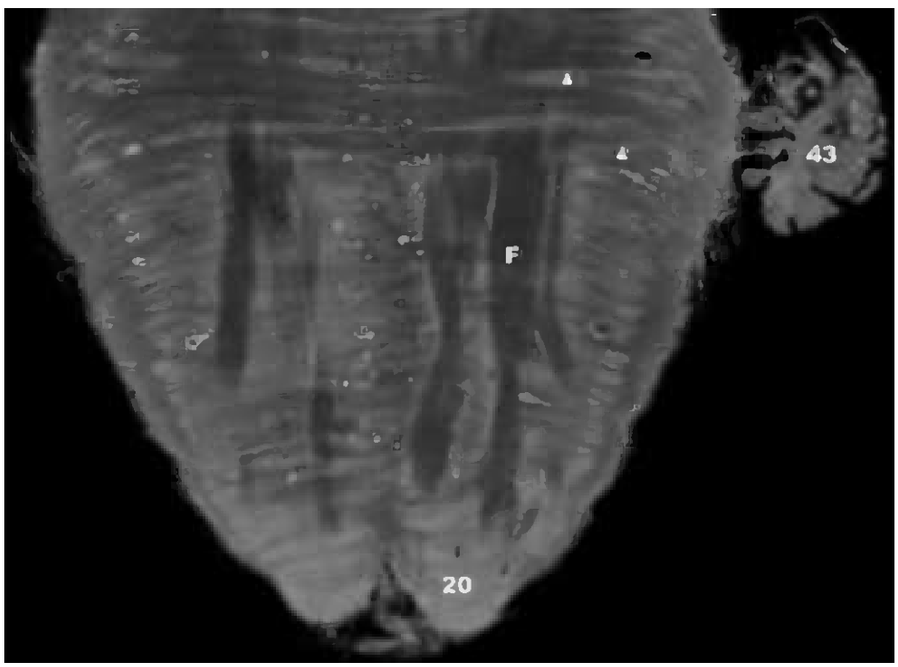

Fig. 8.53. Pontomedullary junction. Ventral coronal section.

The descending cortical tracts separate into individual fiber bundles as they traverse the pons. The most anterior of the major bundles is the frontopontine tract (F).

20 Pontine nuclei
43 Sensory root of the trigeminal nerve (CN V)

Letter labels
F Frontopontine tract

Arrowheads and arrows
White arrowheads: Pontocerebellar fibers crossing to the middle cerebellar peduncle

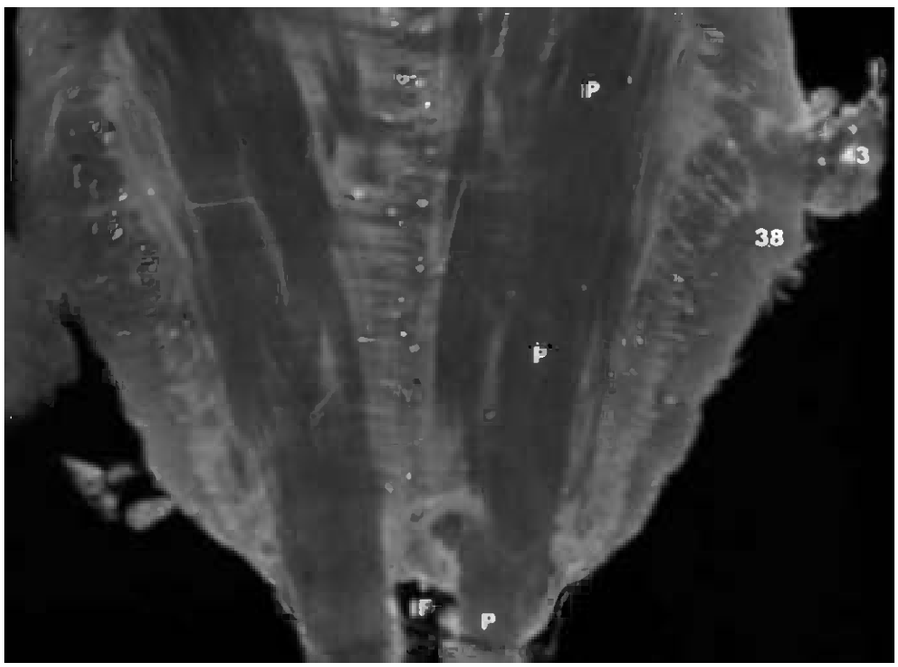

Fig. 8.54. Pontomedullary junction. Ventral coronal section.

The corticospinal (pyramidal) tract (P) lies posterior to the frontopontine tract and is the largest of the descending cortical tracts within the pons. The pontocerebellar fibers gather laterally to form the middle cerebellar peduncles (38). Distinct longitudinal lines of "dots" mark the vascular entry and exit zones for the anteromedial (paramedian) vessels and the anterolateral vessels which perforate the brain stem to supply its interior. The anteromedial (paramedian) vessels enter just off the median raphe, medial to the pyramidal tract (P). The anterolateral vessels enter lateral to the pyramidal tract. Because the pons widens in its midportion, the longitudinal vascular entry/exit zones are vertical at the midline but oblique laterally.

38 Middle cerebellar peduncle
43 Sensory root of the trigeminal nerve (CN V)

Letter labels

IF Foramen cecum (deepest midline portion of the pontomedullary sulcus)
P Pyramidal tract descending to form the pyramid along the ventral medulla

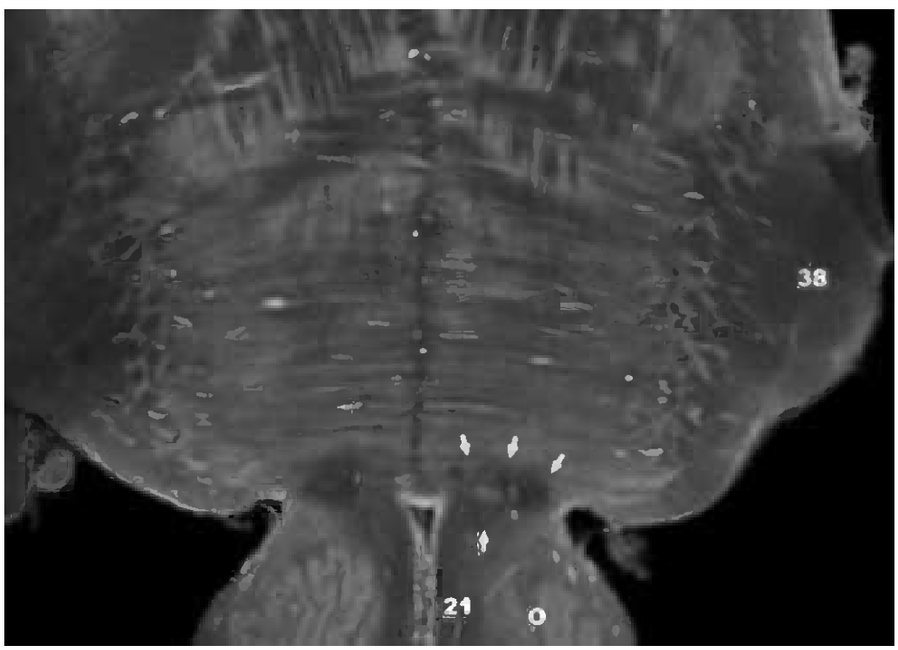

Fig. 8.55. Pontomedullary junction. Ventral coronal section.

The pontocerebellar fibers group together laterally to form the middle cerebellar peduncles (38). The individual fascicles of the abducens nerve (single vertical white arrow) pass immediately ventral to the medial lemniscus (three white arrows) and then emerge into the pontomedullary sulcus approximately 1-2 cm lateral to the midline (**See Figs. 8.44–8.47**). These abducens fibers can be traced dorsally to their origin at the abducens nucleus over the following coronal sections. The caudal portions of the medial lemenisci (21) align vertically, to each side of the midline, between the inferior olivary nuclei (O). More rostral portions of the medial lemnisci (three white arrows) curve laterally into a coronal array and pass further dorsally as they ascend through the pons. The anteromedial (paramedian) and anterolateral groups of perforating vessels again form longitudinal vascular entry/exit zones in both the medulla and the pons (**See Figs. 7.2 and 7.3**).

21 Medial lemniscus
38 Middle cerebellar peduncle

Letter labels
O Inferior olivary nucleus

Arrowheads and arrows
Single white arrow: Intrapontine fascicles of the abducens nerve (CN VI)
Three white arrows: Medial lemniscus curving from sagittal to coronal orientation

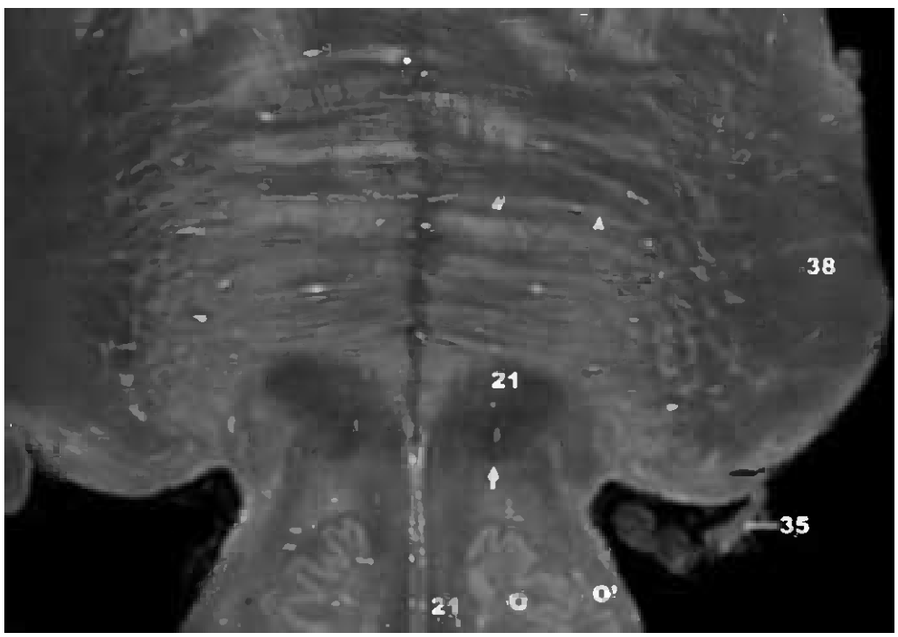

Fig. 8.56. Pontomedullary junction. Ventral coronal section.

The ascending fibers of the medial lemnisci (21) begin to arch upward, curve laterally and realign into the coronal plane as they ascend through the pons. The abducens fibers (white arrow) lie caudal to the medial lemnisci. The facial nerve exits the brain stem immediately caudal to the middle cerebellar peduncle (38). Over the subsequent sections, the facial and abducens fibers converge toward the abducens nucleus and the facial colliculus.

21 Medial lemniscus
35 Facial nerve (CN VII)
38 Middle cerebellar peduncle

Letter labels

O Inferior olivary nucleus
O′ Amiculum (capsule of the inferior olivary nucleus)

Arrowheads and arrows

Paired white arrowheads: Pontocerebellar fibers crossing to the middle cerebellar peduncle
Single white arrow: Intrapontine fascicles of the abducens nerve (CN VI)

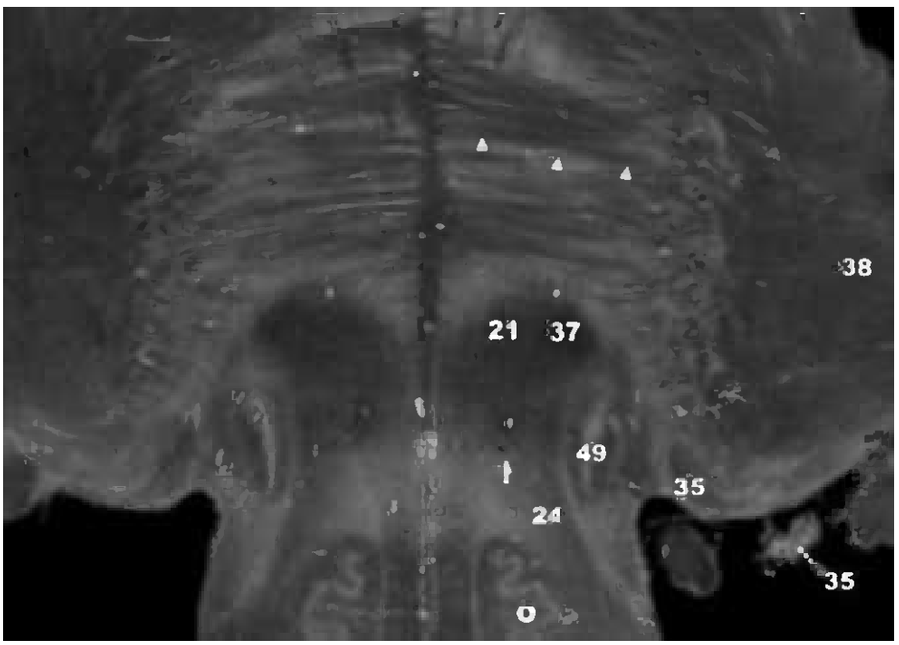

Fig. 8.57. Pontomedullary junction. Ventral coronal section.

The medial lemniscus (21) continues to ascend through the pons. The trapezoid body (37) lies near to the medial lemniscus (21) as the medial lemniscus curves from sagittal to coronal orientation. The supra-olivary nucleus (49) and the trapezoid body (37) form part of the auditory relay system that connects the cochlear nuclei with the inferior colliculi. The facial (35) and abducens fibers (white arrow) are well separated within the ventral brain stem. The central tegmental tract (24) approaches the superior pole of the inferior olivary nucleus (O).

21 Medial lemniscus
24 Central tegmental tract descending onto the inferior olivary nucleus (O)
35 Facial nerve (CN VII) (descending segment emerging into the cerebellopontine angle cistern)
37 Trapezoid body
38 Middle cerebellar peduncle
49 Supra-olivary nucleus

Letter labels
O Inferior olivary nucleus

Arrowheads and arrows
Three white arrowheads: Pontocerebellar fibers crossing to the middle cerebellar peduncle
Single white arrow: Intrapontine fascicles of the abducens nerve (CN VI)

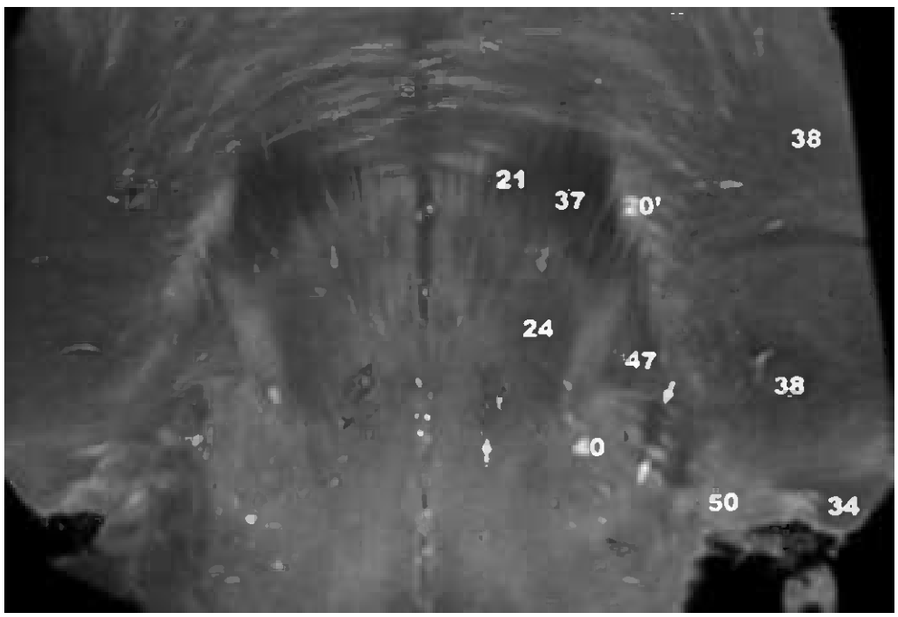

Fig. 8.58. Pontomedullary junction. Ventral coronal section.

The facial nucleus (40) lies caudal, ventral and lateral to the abducens nucleus (**See Figs. 8.62 and 9.5**). The descending intrapontine facial fibers (between white arrows) pass ventrally just lateral to the facial nucleus (40). The abducens fibers (white arrow) and facial fibers (between white arrows) now lie closer together (**See Fig. 9.5**). The medial lemniscus (21) and the lateral lemniscus (47) lie at the two extremes of an arc of fibers, which ascend through the pons into the midbrain (**See Fig. 8.72**, axial plane). The pontobulbar body (50) is a large mass of gray matter situated between the roots of the facial and vestibulocochlear nerves, ventral to the inferior cerebellar peduncle, at the junction of the pons with medulla [358]. Its cells appear to be similar to those of the pontine and external arcuate nuclei [358].

20′ Lateral tegmental process of pontine nuclei
21 Medial lemniscus
24 Central tegmental tract
34 Vestibulocochlear nerve (CN VIII)
37 Trapezoid body
38 Middle cerebellar peduncle
40 Facial nerve nucleus
47 Lateral lemniscus
50 Pontobulbar body (pontobulbar nucleus)

Arrowheads and arrows

Single white arrow: Intrapontine fascicles of the abducens nerve (CN VI)
Two white arrows: Intrapontine fascicles of the facial nerve (CN VII)

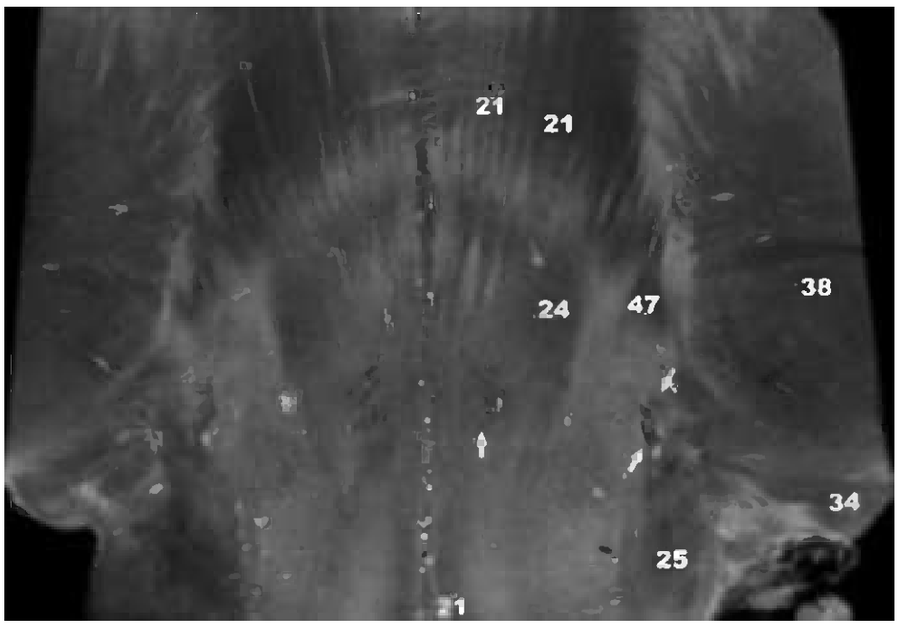

Fig. 8.59. Pontomedullary junction. Ventral coronal section.

The ascending lemniscal fibers form a corona extending from the medial lemniscus (21) rostromedially to the lateral lemniscus (47) caudolaterally. The central tegmental tract (24) passes nearly vertically, dorsal to this lemniscal arch, as it descends from the red nucleus to the inferior olivary nucleus. The fibers of the abducens nerve (single white arrow) and the descending portion of the facial nerve (between two white arrows) continue to converge dorsally. The inferior cerebellar peduncle (25) ascends along the lateral border of the medulla toward the middle cerebellar peduncle (38). The vestibulocochlear nerve (34) crosses the surface of the brain stem to enter the cerebellopontine angle immediately caudal to the middle cerebellar peduncle.

21 Medial lemniscus
24 Central tegmental tract
25 Inferior cerebellar peduncle
34 Vestibulocochlear nerve
38 Middle cerebellar peduncle
47 Lateral lemniscus

Arrowheads and arrows

Single white arrow: Intrapontine fascicles of the abducens nerve (CN VI)
Two white arrows: Intrapontine fascicles of the facial nerve (CN VII)

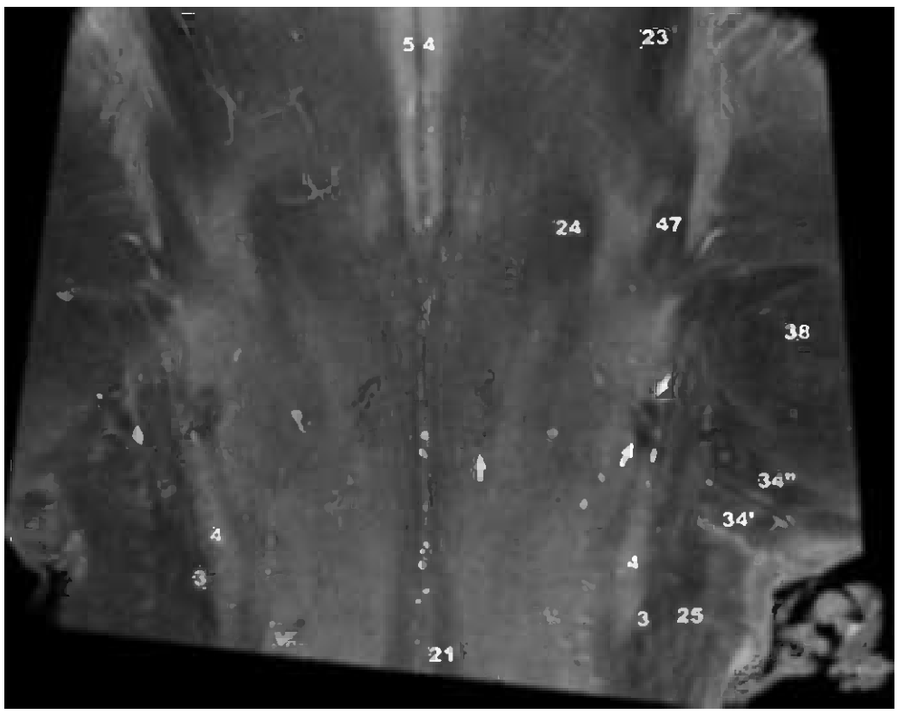

Fig. 8.60. Pontomedullary junction. Ventral coronal section.

The interrelationships among the fiber tracts are seen well in this and the following dorsal coronal sections. The inferior cerebellar peduncle (25) approaches the superior cerebellar peduncle (23) medial to the middle cerebellar peduncle (38). The spinal trigeminal tract (3) and nucleus (4) ascend just medial to the inferior cerebellar peduncle (25). The central tegmental tract (24), superior cerebellar peduncle (23), and lateral lemniscus (47) align vertically and nearly in parallel. The nucleus centralis superior (54) is a large nuclear region in the tegmentum of the pons and mesencephalon, which also aligns vertically, to each side of the median raphe. The serotonergic nuclei B6 and B8 are largely confined to the nucleus centralis superior (54) (**See Fig. 3.10**) [321]. The facial nerve fibers (between white arrows) pass medial to the trigeminal system (3,4). The vestibular (34′) and cochlear (34″) divisions of the vestibulocochlear nerve (CN VIII) angle transversely lateral to the trigeminal system.

3 Spinal trigeminal tract
4 Spinal trigeminal nucleus
21 Medial lemniscus
23 Superior cerebellar peduncle
24 Central tegmental tract
25 Inferior cerebellar peduncle
34′ Vestibular division of CN VIII
34″ Cochlear division of CN VIII
38 Middle cerebellar peduncle
47 Lateral lemniscus
54 Nucleus centralis superior (of Bechterew)

Arrowheads and arrows

Single white arrow: Intrapontine fascicles of the abducens nerve (CN VI)
Two white arrows: Intrapontine fascicles of the facial nerve (CN VII)

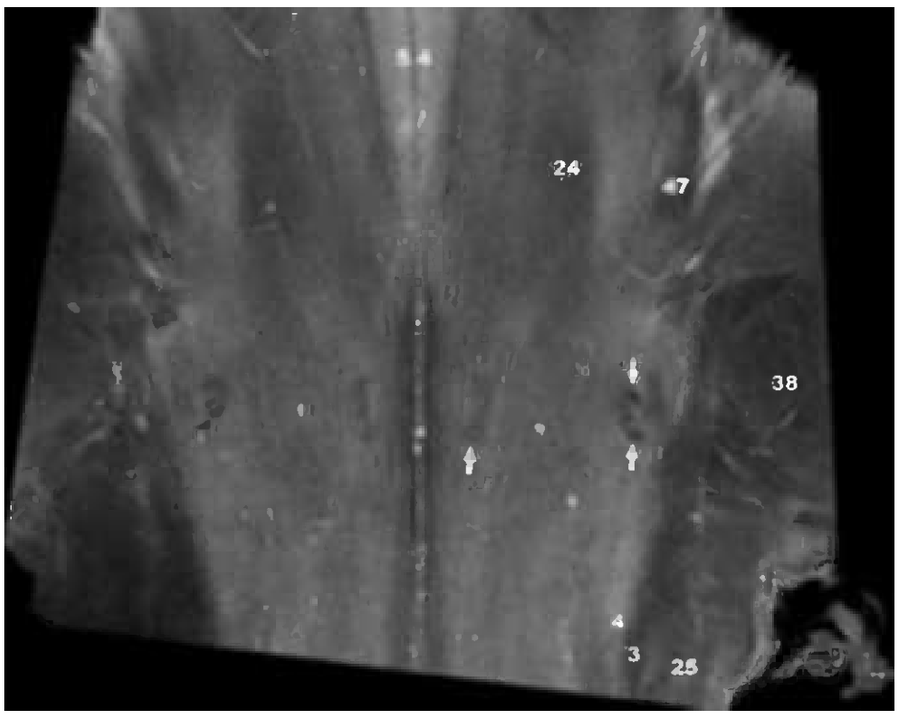

Fig. 8.61. Pontomedullary junction. Mid coronal section.

The abducens fibers (single white arrow) and facial fibers (between two white arrows) continue to converge toward the abducens nucleus. There is clear longitudinal orientation and parallelism of pontine structures, both superiorly (nucleus centralis superior (54), central tegmental tract (24), and lateral lemniscus (47)), and inferiorly (spinal trigeminal tract and nucleus (3,4) and inferior cerebellar peduncle (25)).

3 Spinal trigeminal tract
4 Spinal trigeminal nucleus
24 Central tegmental tract
25 Inferior cerebellar peduncle
38 Middle cerebellar peduncle
47 Lateral lemniscus
54 Nucleus centralis superior (of Bechterew)

Arrowheads and arrows

Single white arrow: Intrapontine fascicles of the abducens nerve (CN VI)
Two white arrows: Descending intrapontine fascicles of the facial nerve (CN VII)

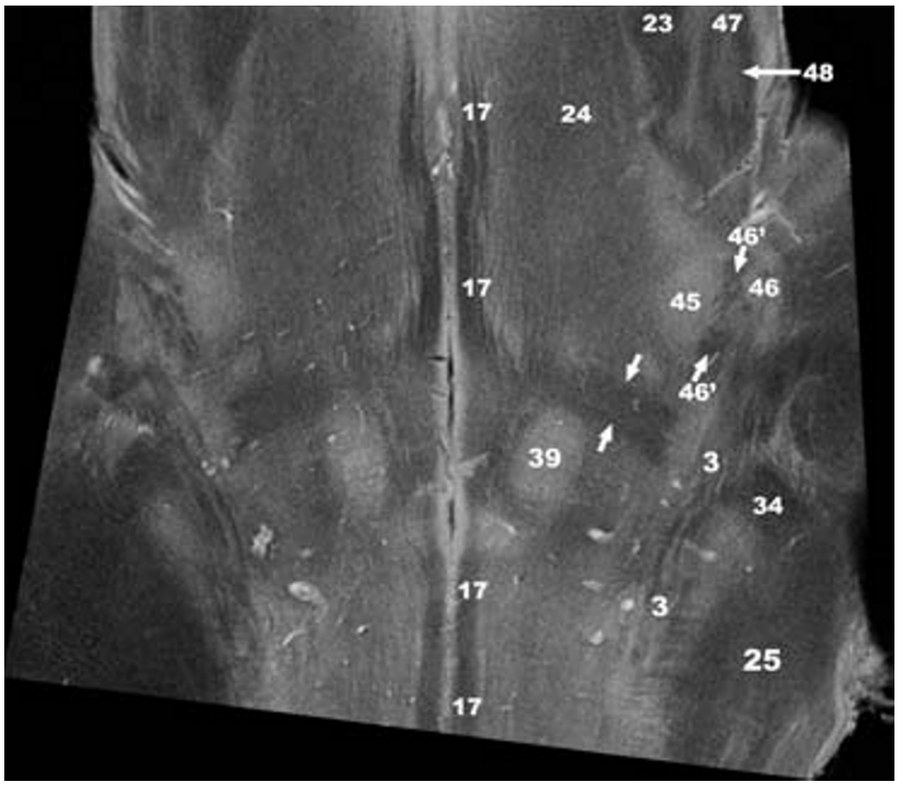

Fig. 8.62. Pontomedullary junction. Dorsal coronal section.

Coronal section along the floor of the fourth ventricle shows the abducens nucleus (39), the motor trigeminal nucleus (45), the principal sensory trigeminal nucleus (46), and the ventral nucleus of the lateral lemniscus (48). The fiber tracts align longitudinally, nearly in parallel. Superiorly, the medial longitudinal fasciculus (17), central tegmental tract (24), superior cerebellar peduncle (23) and lateral lemniscus (47) align vertically with the midline. Inferiorly, the medial longitudinal fasciculus (17), spinal trigeminal system (3) and inferior cerebellar peduncle (25) align nearly vertically with the midline. The rostral end of the spinal trigeminal nucleus (pars oralis) merges with the principal sensory nucleus (46). Afferent trigeminal fibers (46') enter the pons through the sensory trigeminal nerve, which courses between the motor (45) and principal sensory (46) trigeminal nuclei. Many of these fibers divide into short ascending rami that pass to the principal sensory nucleus (46) and long descending rami that descend as the spinal trigeminal tract (3) to synapse in the surrounding spinal trigeminal nucleus [78]. Other entering sensory fibers ascend or descend without branching [78]. Although the facial fibers (between white arrows) and the vestibulocochlear fibers (34) appear to form one structure, in fact the two nerves pursue separate, roughly co-curvilinear, arching courses medial to (facial) and lateral to (vestibulocochlear) the trigeminal system.

3 Spinal trigeminal tract
17 Medial longitudinal fasciculus
23 Superior cerebellar peduncle
24 Central tegmental tract
25 Inferior cerebellar peduncle
34 Vestibulocochlear nerve (CN VIII)
45 Motor nucleus of the trigeminal nerve (CN V)
46 Sensory nucleus of the trigeminal nerve (CN V)
46' Intrapontine fascicles of the trigeminal nerve (CN V) (between arrows)
47 Lateral lemniscus
48 Ventral nucleus of the lateral lemniscus

Arrowheads and arrows

Two white arrows: Descending fascicles of the facial nerve (CN VII)

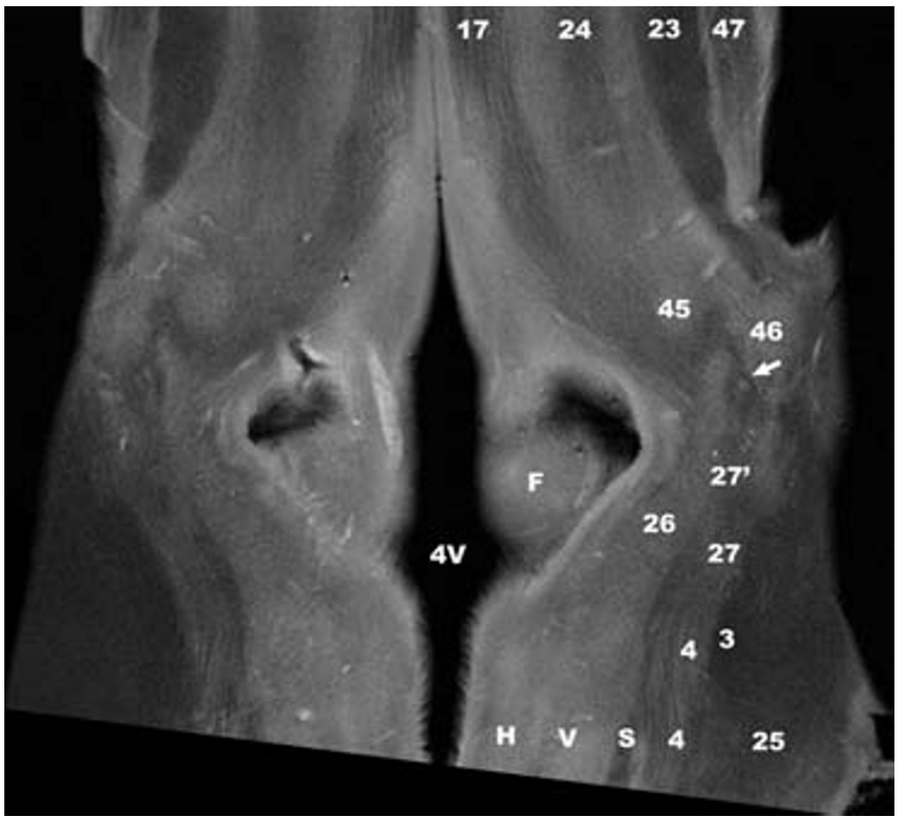

Fig. 8.63. Pontomedullary junction. Dorsal coronal section.

Coronal section directly through the facial colliculus (F) displays the rhomboid shape of the floor of the fourth ventricle and the parallelism of the dorsal fiber tracts and nuclei. Superiorly, the medial longitudinal fasciculus (17), the central tegmental tract (24), superior cerebellar peduncle (23), and lateral lemniscus (47) align with each other and deflect laterally to conform to the shape of the upper fourth ventricle. Inferiorly, the hypoglossal nucleus (H), dorsal vagal nucleus (V), solitary nucleus and tract (S), spinal trigeminal nucleus (4) and tract (3) and inferior cerebellar peduncle (25) show similar parallel alignment. The vestibular nuclei (26, 27) lie at the lateral angle of the fourth ventricle. The motor nucleus (45) of the trigeminal nerve creates the superior (trigeminal) fovea in the floor of the fourth ventricle (**See Figs. 2.4 and 2.6**)

3 Spinal trigeminal tract (CN V)
4 Spinal trrigeminal nucleus (CN V)
17 Medial longitudinal fasciculus
23 Superior cerebellar peduncle
24 Central tegmental tract (including portions of fasciculus tegmentalis dorsolateralis)
25 Inferior cerebellar peduncle
26 Medial vestibular nucleus
27 Inferior vestibular nucleus
27′ Descending fascicles of the vestibular nerve (CN VIII)
45 Motor nucleus of the trigeminal nerve (CN V)
46 Sensory nucleus of the trigeminal nerve (CN V)
47 Lateral lemniscus

Letter labels
4V Fourth ventricle
F Facial colliculus
H Hypoglossal nucleus
V Dorsal nucleus of the vagus
S Solitary tract (dark) with surrounding solitary nucleus (light gray)

Arrowheads and arrows
Single white arrow: Fascicles of the trigeminal nerve (CN V)

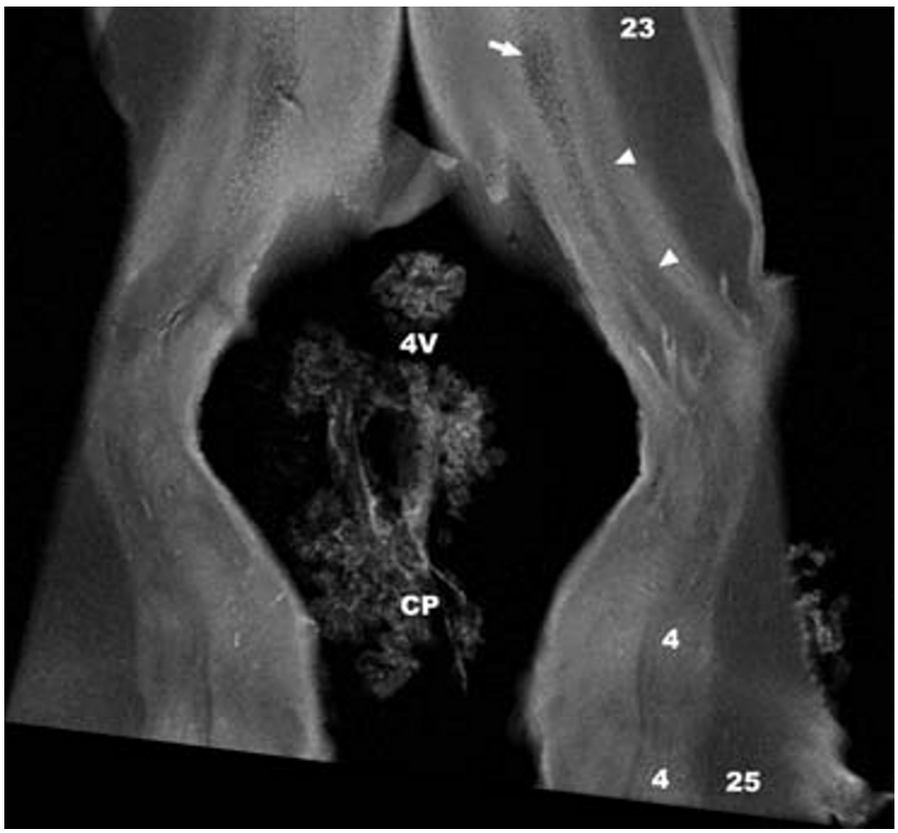

Fig. 8.64. Pontomedullary junction. Dorsal coronal section.

Coronal section through the side walls of the fourth ventricle, dorsal to the floor, displays the parallel array of the superior cerebellar peduncle (23), mesencephalic nucleus and tract (white arrowheads) of the trigeminal system, and the locus ceruleus (white arrow) superiorly, and similar parallelism of the spinal trigeminal nucleus (4) and inferior cerebellar peduncle (25) inferiorly. The stippling seen in the locus ceruleus is also present in the substantia nigra and may reflect the deposits of neuromelanin (**See Figs. 10.1–10.3**)

4 Spinal trigeminal tract (CN V)
23 Superior cerebellar peduncle
25 Inferior cerebellar peduncle

Letter labels
4V Fourth ventricle
CP Choroid plexus

Arrowheads and arrows
Two white arrowheads: Mesencephalic tract of the trigeminal nerve (CN V)
Single white arrow: Locus ceruleus

Fig. 8.65. Pontomedullary junction. Dorsal coronal section.

The mesencephalic tract (white arrowheads) of the trigeminal nerve forms a thin, well defined stripe of white matter (white arrowheads) just deep to the superior cerebellar peduncle (23). This tract is composed of the peripheral processes of the primary sensory neurons that reside in the surrounding mesencephalic trigeminal nucleus. The sensory mesencephalic processes are largely distributed with the motor trigeminal nerve. (**See Fig. 8.68**)

23 Superior cerebellar peduncle

Letter labels

4V Fourth ventricle
CP Choroid plexus

Arrowheads and arrows

Two white arrowheads: Mesencephalic tract of the trigeminal nerve (CN V)

C. Pontomesencephalic junction (Figs. 8.66–8.97).

C 1. Axial Pontomesencephalic Junction

Axial sections displayed from caudal to cranial (Figs. 8.66 to 8.76)

These cartoons (A–B) display the anatomic region imaged in **Figs. 8.66–8.97**.

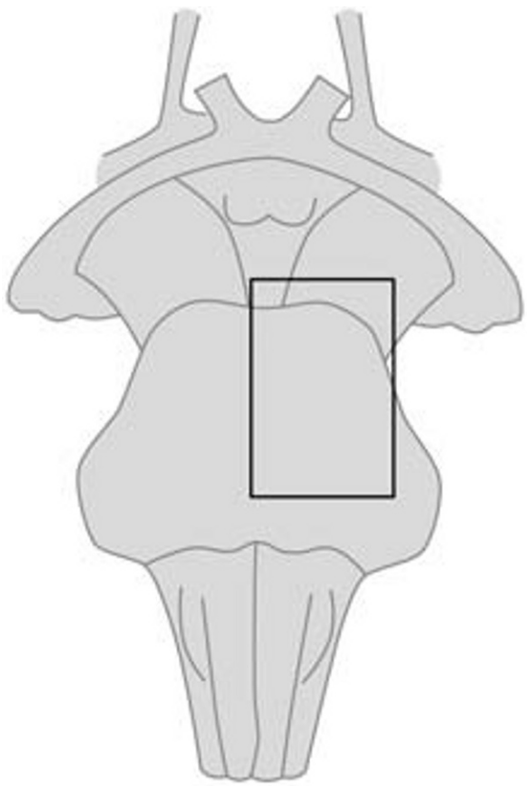

A

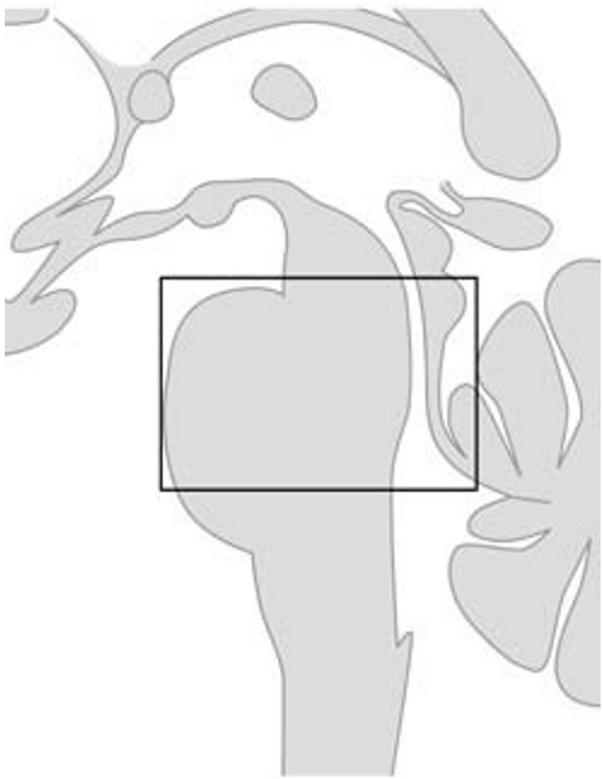

B

Fig. 8.66. Pontomesencephalic junction. Axial section.

The rubrospinal tract (7) and spinothalamic (10) tract lie near to each other at this level, but the anterior spinocerebellar tract (6) has now separated from them and passed dorsal to the superior cerebellar peduncle (23), en route to the cerebellum. The anterior spinocerebellar fibers end in the anterior lobe of the cerebellum, and in the pyramis and gracile lobule of the posterior lobe of the cerebellum [322]. The unlabeled cleft between the anterior spinocerebellar tract (6) and the middle cerebellar peduncle (38) is the ambient cistern. The intrapontine fascicles of the trigeminal nerve (43) pass lateral to the lateral lemniscus (47) at this level. The ascending ventral (22) and dorsal (52) trigeminothalamic tracts and the descending central tegmental tract (24) extend longitudinally through the tegmentum. The area acclinus (Ac) is a zone within the dorsomedial tegmentum. It extends the length of the stem from medulla nearly to the diencephalon, and lies just ventral to the hypoglossal nucleus, the dorsal vagal nucleus and the medial longitudinal fasciculus (17). The dorsal longitudinal fasciculus (white arrow), seen prominently in the medulla (See Fig. 8.9), appears here as a thin stripe of white matter within the gray matter at the high fourth ventricle – periaqueductal region. The lingula of the vermis (Li) is directly continuous with the superior medullary velum (white arrowheads). No fissure or cistern lies between them.

6 Ventral (anterior) spinocerebellar tract arching over the superior cerebellar peduncle (23) to reach the cerebellum "retrograde"
7 Rubrospinal tract
8 Reticular formation
10 Spinothalamic tract
14 Tectospinal tract
17 Medial longitudinal fasciculus
20 Pontine nuclei
22 Ventral trigeminothalamic tract
21 Medial lemniscus
23 Superior cerebellar peduncle
24 Central tegmental tract
37 Trapezoid body and trapezoid tracts
38 Middle cerebellar peduncle
42 Dorsal pontine decussation for the traversing pontocerebellar fibers
43 Intrapontine fascicles of the trigeminal nerve (CN V)
47 Lateral lemniscus
51 Pontocerebellar fibers
52 Dorsal trigeminothalamic tract

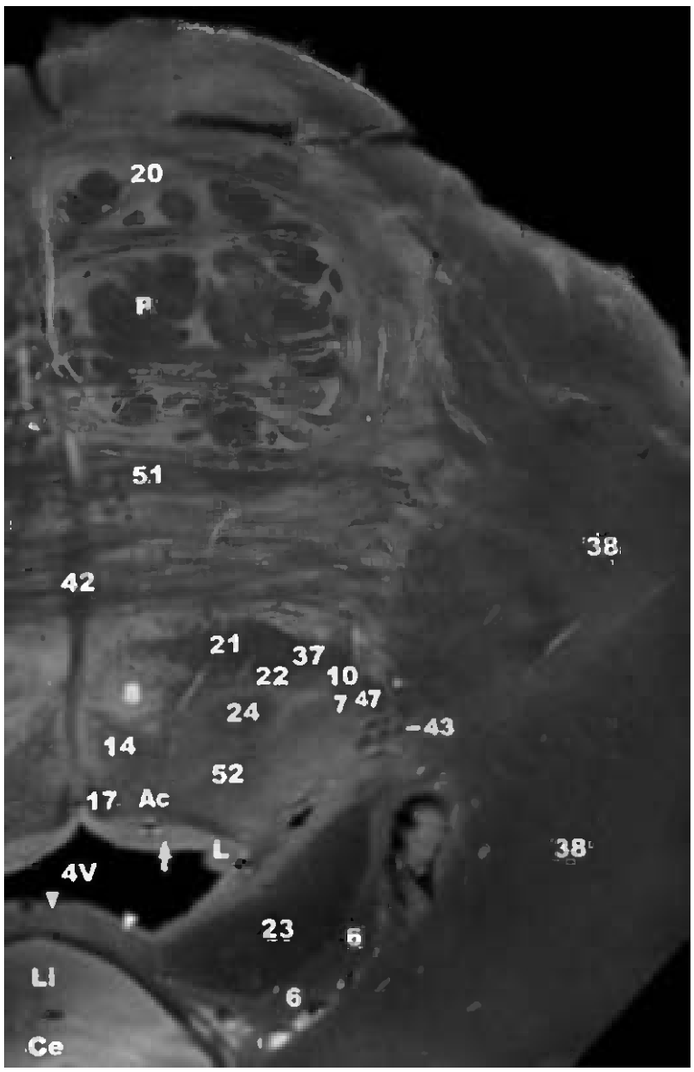

Letter labels

4V Fourth ventricle
Ac Area acclinus
Ce Central lobule of vermis
L Site of the locus ceruleus (See Fig. 10.1)
Li Lingula of the vermis applied to the superior medullary velum (white)
P Pyramidal tracts leading to the pyramid

Arrowheads and arrows

Paired white arrowheads: Superior medullary velum of the fourth ventricle (4V)
Single white arrow: Dorsal longitudinal fasciculus
Single black arrow: Mesencephalic nucleus and root of CN V

Fig. 8.67. Pontomesencephalic junction. Axial section.

The lateral lemniscus (47) lies at the lateral edge of the coronal lemniscal arc (21, 21, 47). Over the following sections, the lateral lemniscus will turn dorsally, superficial to the superior cerebellar peduncle (23), and enter the inferior colliculus. The rubrospinal tract (7) is beginning to transition medially toward the midline. The rubrospinal tract arises from the medial aspect of the contralateral red nucleus, crosses the midline in the ventral tegmental decussation, and then descends laterally through the contralateral pons and medulla. The tegmento-olivary tract (53) lies dorsolateral to the central tegmental tract (24). It arises from nuclear formations of the brain stem and carries thalamo-olivary and rubro-olivary fibers. The locus ceruleus (L) is a compact column of pigmented, norepinephrine-producing cells situated at the ventral lateral border of the periaqueductal gray matter, just ventral and medial to the mesencephalic root and nucleus of the trigeminal nerve (black arrow). It extends longitudinally from the level of the principal sensory nucleus of the trigeminal nerve in the upper pons to the level of the trochlear nucleus in the midbrain [78, 322]. The noradrenergic fibers of the locus ceruleus are distributed bilaterally to all levels of the brain along two major ascending pathways: a large dorsal adrenergic bundle and a smaller periventricular pathway (See Fig. 3.9) [322]. Additional pathways extend to the brain stem, cerebellum and spinal cord [322].

7 Rubrospinal tract
8 Reticular formation
10 Spinothalamic tract
14 Tectospinal tract
17 Medial longitudinal fasciculus
20 Pontine nuclei
21 Medial lemniscus
22 Ventral trigeminothalamic tract
23 Superior cerebellar peduncle
24 Central tegmental tract
38 Middle cerebellar peduncle
42 Dorsal pontine decussation of pontocerebellar fibers
47 Lateral lemniscus
51 Pontocerebellar fibers
52 Dorsal trigeminothalamic tract
53 Tegmento-olivary tract

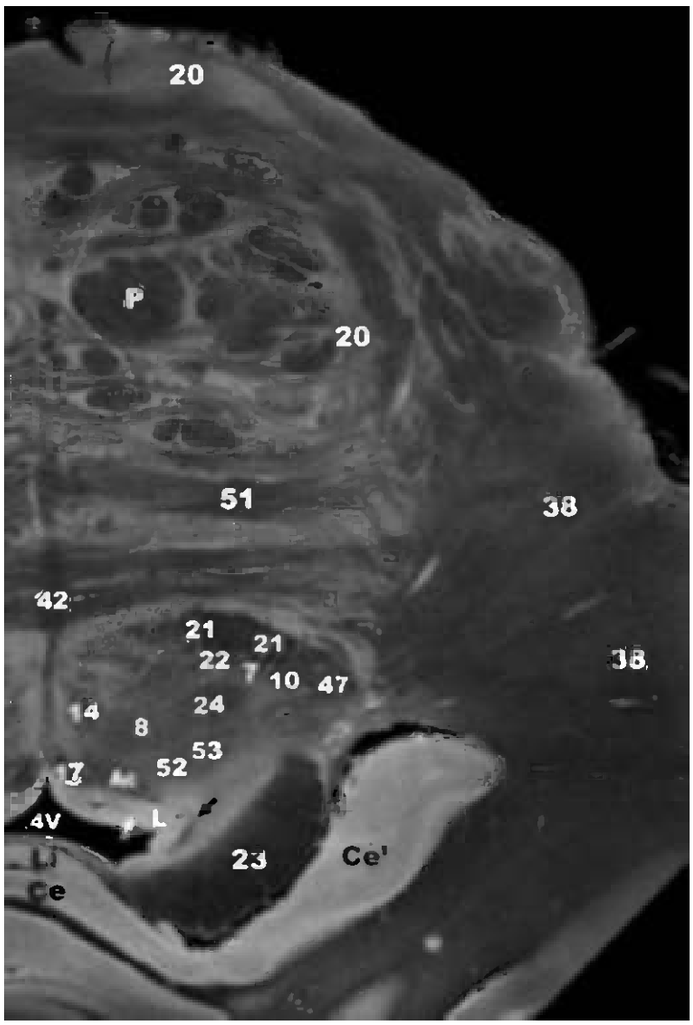

Letter labels

4V Fourth ventricle
Ac Area acclinus (dorsomedial tegmental zone)
Ce Central lobule of vermis
Ce' Wing of the central lobule of vermis (hemispheric analogue of Ce)
L Site of the locus ceruleus
Li Lingula of the vermis applied to the superior medullary velum
P Pyramidal tracts leading to the pyramid

Arrowheads and arrows

Single white arrow: Dorsal longitudinal fasciculus
Single black arrow: Mesencephalic nucleus and tract of CN V

Fig. 8.68. Pontomesencephalic junction. Axial section.

The basis pontis displays the pontine nuclei (20), the descending cortical tracts (P), and the pontocerebellar fibers (51), which gather to form the middle cerebellar peduncles (38). The pontine tegmentum demonstrates the longitudinal fiber tracts, including the medial longitudinal fasciculus (17), tectospinal tract (14), tegmento-olivary tract (53), central tegmental tract (24), ventral trigeminothalamic tract (22), dorsal trigeminothalamic tract (52), and mesencephalic trigeminal tract (black arrow). The medial lemniscus (21), spintothalamic tract (10) and lateral lemniscus (47) form the broad arc of fibers at the ventral margin of the tegmentum.

7 Rubrospinal tract
10 Spinothalamic tract
14 Tectospinal tract
17 Medial longitudinal fasciculus
20 Pontine nuclei
21 Medial lemniscus
22 Ventral trigeminothalamic tract
23 Superior cerebellar peduncle
24 Central tegmental tract
38 Middle cerebellar peduncle
47 Lateral lemniscus surrounding the nucleus of the lateral lemniscus (open arrowhead)
51 Pontocerebellar fibers
52 Dorsal trigeminothalamic tract
53 Tegmento-olivary tract

Letter labels

4V Fourth ventricle
Ac Area acclinus (dorsomedial tegmental zone)
Ce Central lobule of vermis
Ce' Wing of the central lobule of vermis (hemispheric analogue of Ce)
L Site of the locus ceruleus
Li Lingula of the vermis applied to the superior medullary velum
P Pyramidal tracts leading to the pyramid

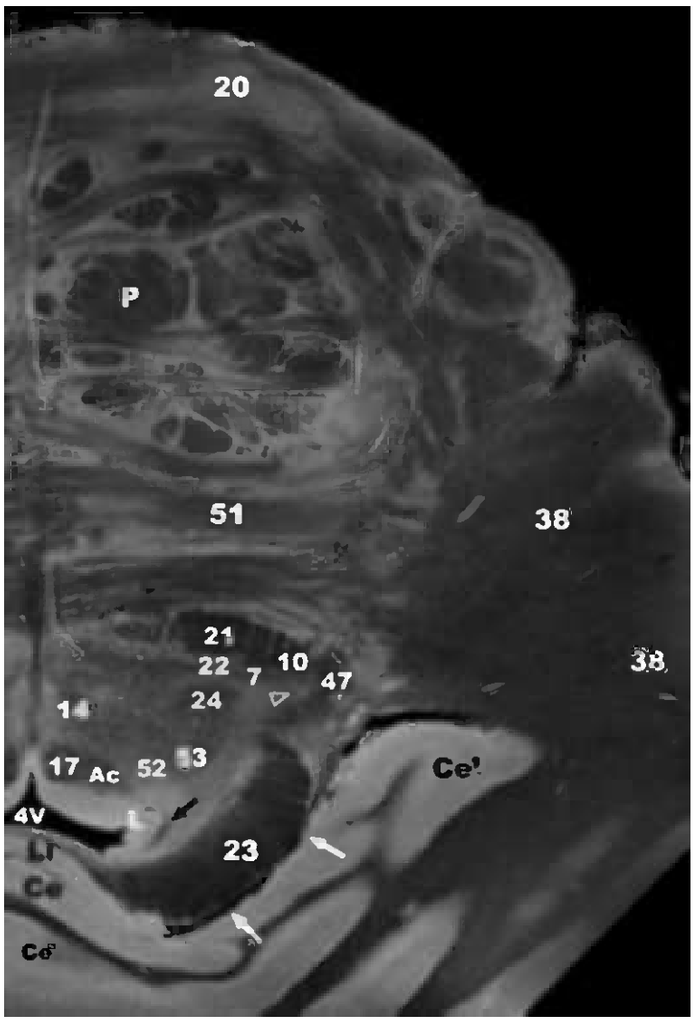

Arrowheads and arrows

Open arrowhead: Ventral nucleus of the lateral lemniscus (also 48 in other images)
Single black arrow: Mesencephalic nucleus and tract of CN V
Paired white arrows: Ambient cistern between the superior cerebellar peduncle (23) and the wing of the central lobule (Ce')

Fig. 8.69. Pontomesencephalic junction. Axial section.

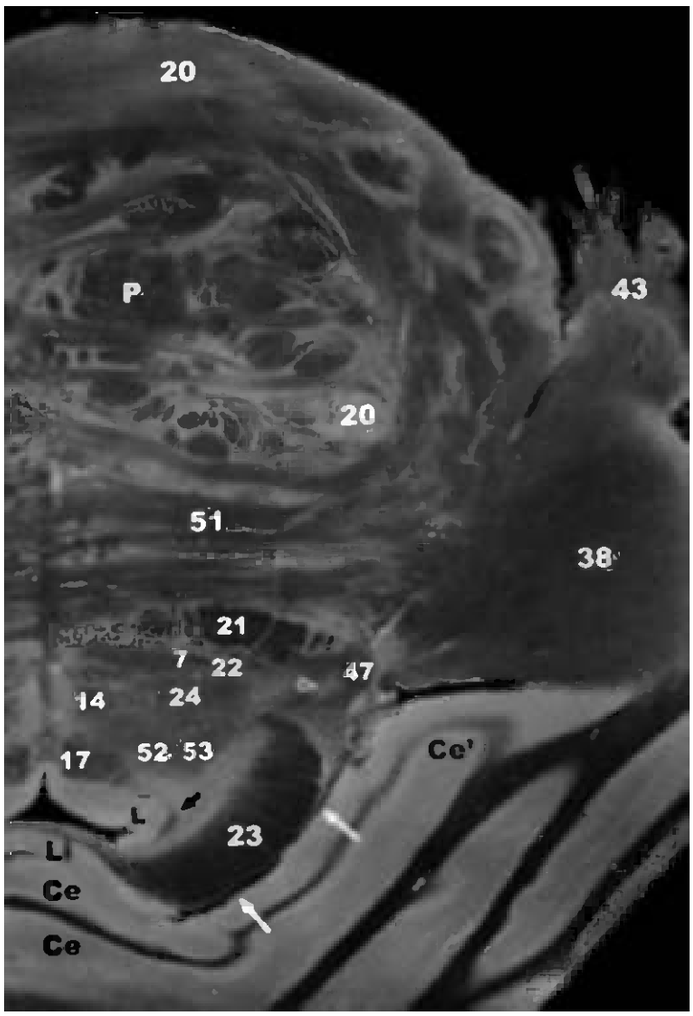

At this level, the lateral lemniscus (47) lies at the lateral aspect of the pons in approximately the same coronal plane as the medial lemniscus (21). The ventral nucleus of the lateral lemniscus (open arrowhead) lies along its base medially. The ventral nucleus is an important relay between the cochlear nuclei and the central nucleus of the inferior colliculus [322a]. The rubrospinal tract (7) continues to transition medially toward its origin from the contralateral red nucleus. The fibers of the sensory root (43) of the trigeminal nerve enter the lateral aspect of the pons and traverse the middle cerebellar peduncle.

7 Rubrospinal tract
14 Tectospinal tract
17 Medial longitudinal fasciculus
20 Pontine nuclei
21 Medial lemniscus
22 Ventral trigeminothalamic tract
23 Superior cerebellar peduncle
24 Central tegmental tract
38 Middle cerebellar peduncle
43 Trigeminal nerve (CN V)
47 Lateral lemniscus partially surrounding the ventral nucleus (open arrowhead) of the lateral lemniscus
51 Pontocerebellar fibers
52 Dorsal trigeminothalamic tract
53 Tegmento-olivary tract

Letter labels

Ce Central lobule of vermis
Ce′ Wing of the central lobule of vermis (hemispheric analogue of Ce)
L Site of the locus ceruleus
Li Lingula of the vermis applied to the superior medullary velum
P Pyramidal tracts leading to the pyramid

Arrowheads and arrows

Open arrowhead: Ventral nucleus of the lateral lemniscus (also 48 in other sections)
Paired white arrows: Ambient cistern
Single black arrow: Mesencephalic nucleus and tract of CN V

Fig. 8.70. Pontomesencephalic junction. Axial section.

The rubrospinal tract (7) now lies just dorsal to the medial edge of the medial lemniscus (21) (**See Figs 8.68 and 8.69**). The spinothalamic tract (10) lies dorsal to the lateral edge of the medial lemniscus. The ventral nucleus (single white arrow) of the lateral lemniscus lies at the base of the lateral lemniscus medially. The nucleus centralis superior (54) forms a large expanse of gray matter symmetrically situated on both sides of the median raphe. It contains the B6 and B8 serotoninergic raphe nuclei. The predorsal longitudinal fasciculus (double black arrows) is composed predominantly of the tectospinal fibers (14), plus efferent fibers from the superior and inferior colliculi. These pass through the nucleus centralis superior (54) to supply bulbar nuclei, the cervical spinal cord and the thoracic cord [352]. The parabrachial area is a horseshoe-shaped band of gray matter composed of the medial parabrachial nucleus (x), Kölliker-Fuse nucleus (y), and lateral parabrachial nucleus (z). These partially circumscribe the superior cerebellar peduncle (brachium conjunctivum) (23) (**See Figs. 2.16, 2.17 and 3.13**). The medial parabrachial nucleus (x) is a relay nucleus in the gustatory system. It receives input from the cephalic gustatory portion of the solitary nucleus and sends output to the ventral posteromedial nucleus of the thalamus [322]. The Kölliker-Fuse nucleus (y) is the functionally-defined pneumotaxic center (**See Fig. 3.6**). It receives input from the caudal "cardio-respiratory" portion of the solitary nucleus and sends outputs both caudally (to the lower medulla oblongata and spinal cord) and cranially (to the lateral hypothalamus and amygdala) [322]. The lateral parabrachial nucleus (z) receives input from the caudal solitary tract. It has major output to the medial hypothalamus and lesser output to the lateral hypothalamus and many of the same nuclei as the medial parabrachial nucleus [322]. (**See Fig. 3.13**)

7 Rubrospinal tract
17 Medial longitudinal fasciculus
20 Pontine nuclei
21 Medial lemniscus
22 Ventral trigeminothalamic tract
23 Superior cerebellar peduncle
24 Central tegmental tract
38 Middle cerebellar peduncle
43 Trigeminal nerve (CN V)
47 Lateral lemniscus partially surrounding the ventral nucleus (white arrow) of the lateral lemniscus
51 Pontocerebellar fibers
52 Dorsal trigeminothalamic tract
54 Nucleus centralis superior (of Bechterew)

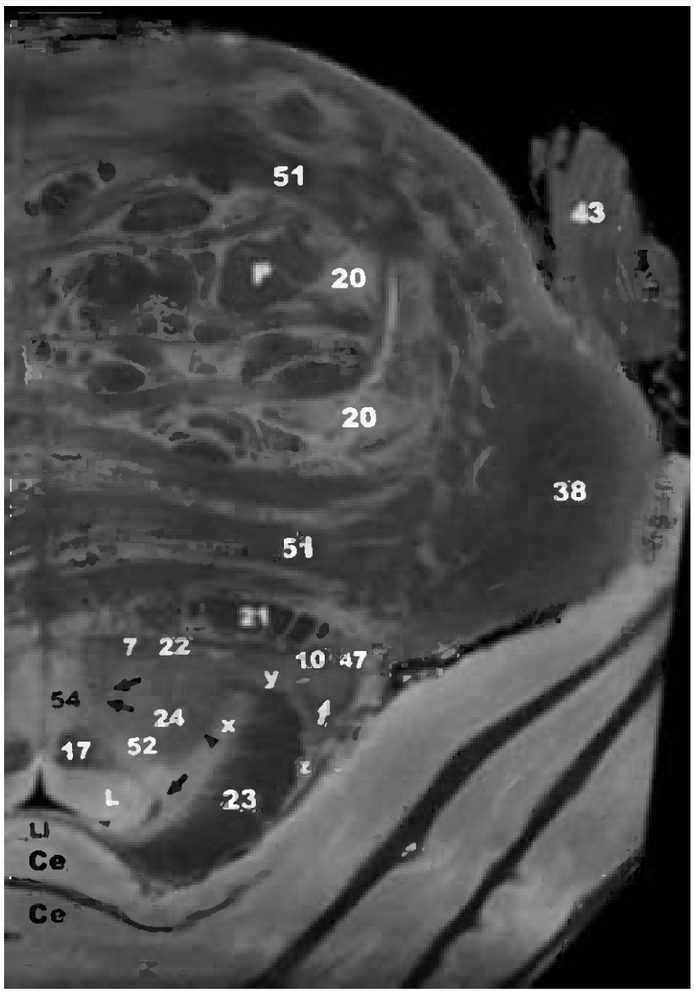

Letter labels

x Medial parabrachial nucleus
y Kölliker-Fuse nucleus
z Lateral parabrachial nucleus
Ce Central lobule of vermis
L Site of the locus ceruleus
Li Lingula of the vermis applied to the superior medullary velum
P Pyramidal tracts

Arrowheads and arrows

Single black arrowhead: Tegmento-olivary tract (also 53 on other images)
Single white arrow: Ventral nucleus of the lateral lemniscus (also 48, also open arrowhead)
Single black arrow: Mesencephalic nucleus and tract of CN V
Paired black arrows: Predorsal longitudinal fasciculus (fasciculus predorsalis)

Fig. 8.71. Pontomesencephalic junction. Axial section.

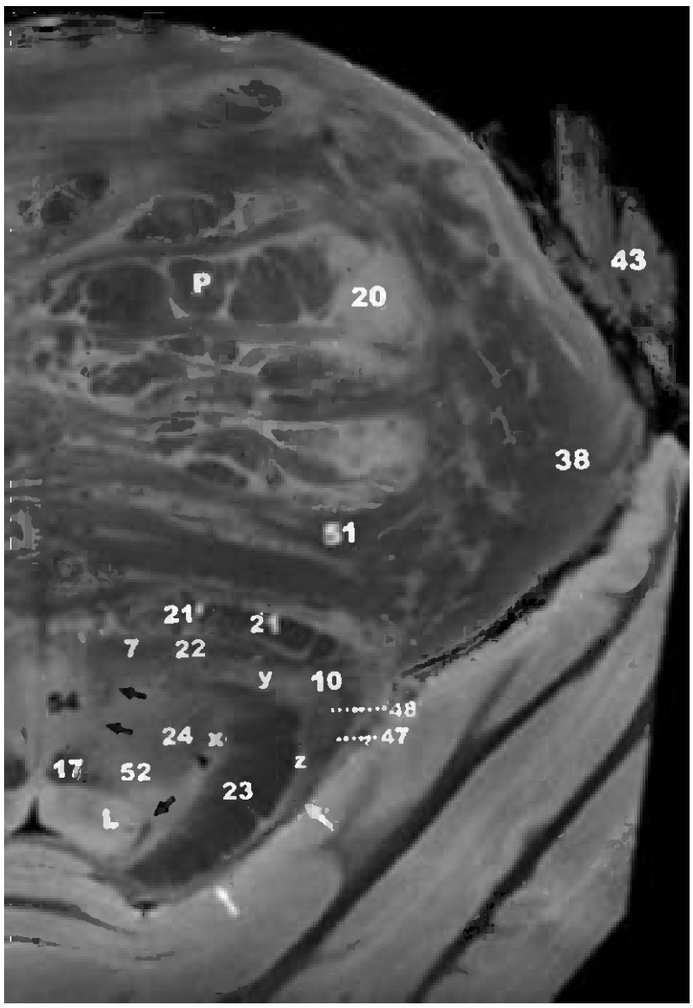

The lateral lemniscus (47) now curves dorsally, superficial to the superior cerebellar peduncle (23). The medial border of the superior cerebellar peduncle remains sharply defined and is partially circumscribed by the medial parabrachial nucleus (x), Kölliker-Fuse nucleus (y) and lateral parabrachial nucleus (z). The dorsal trigeminothalamic tract (52) lies close to the mesencephalic tract (black arrow) of the trigeminal nerve.

7 Rubrospinal tract
10 Spinothalamic tract
17 Medial longitudinal fasciculus
20 Pontine nuclei
21 Medial lemniscus
22 Ventral trigeminothalamic tract
23 Superior cerebellar peduncle
24 Central tegmental tract
38 Middle cerebellar peduncle
43 Trigeminal nerve
47 Lateral lemniscus
48 Ventral nucleus of the lateral lemniscus
51 Pontocerebellar fibers
52 Dorsal trigeminothalamic tract
54 Nucleus centralis superior (of Bechterew)

Letter labels

x Medial parabrachial nucleus
y Kölliker-Fuse nucleus
z Lateral parabrachial nucleus
L Site of the locus ceruleus
P Pyramidal tracts leading to the pyramid

Arrowheads and arrows

Single black arrowhead: Tegmento-olivary tract (also 53)
Single black arrow: Mesencephalic nucleus and tract of CN V
Paired white arrows: Ambient cistern
Paired black arrows: Predorsal longitudinal fasciculus (fasciculus predorsalis)

Fig. 8.72. Pontomesencephalic junction. Axial section.

The rubrospinal (7) and spinothalamic (10) tracts are widely separated. The lateral lemniscus (47) extends far dorsally as a crescent of white matter notched medially by the ventral nucleus (48) of the lateral lemniscus. The medial border of the superior cerebellar peduncle (23) has now become blurred as its fibers begin to arch medially toward their decussation. The medial lemniscus (21) is thinned medially at the rete (21′) where it encompasses medial nuclei (**See Fig. 8.45**, sagittal section). Within the periaqueductal gray matter, the fascicles of the trochlear nerve (white arrowhead) pass posteriorly to decussate (white arrow) in the superior medullary velum of the fourth ventricle. The predorsal longitudinal fasciculus (paired black arrows) passes through the nucleus centralis superior, dividing it into medial (54′) and lateral (54″) portions. The locus ceruleus (L) lies within and along the border of the periaqueductal gray matter. The mesencephalic nucleus and tract (single black arrow) of the trigeminal nerve lie at and just lateral to the border of the periaqueductal gray matter, near to the dorsal trigeminothalamic tract (52).

7 Rubrospinal tract
10 Spinothalamic tract
17 Medial longitudinal fasciculus
20 Pontine nuclei
21 Medial lemniscus
21′ Rete of the medial lemniscus
22 Ventral trigeminothalamic tract
23 Superior cerebellar peduncle
24 Central tegmental tract
47 Lateral lemniscus notched medially by the ventral nucleus of the lateral lemniscus (48)
48 Ventral nucleus of the lateral lemniscus
51 Pontocerebellar fibers
52 Dorsal trigeminothalamic tract
54′ Nucleus centralis superioris medialis
54″ Nucleus centralis superioris lateralis

Letter labels

L Site of the locus ceruleus
P Pyramidal tracts leading to the pyramid

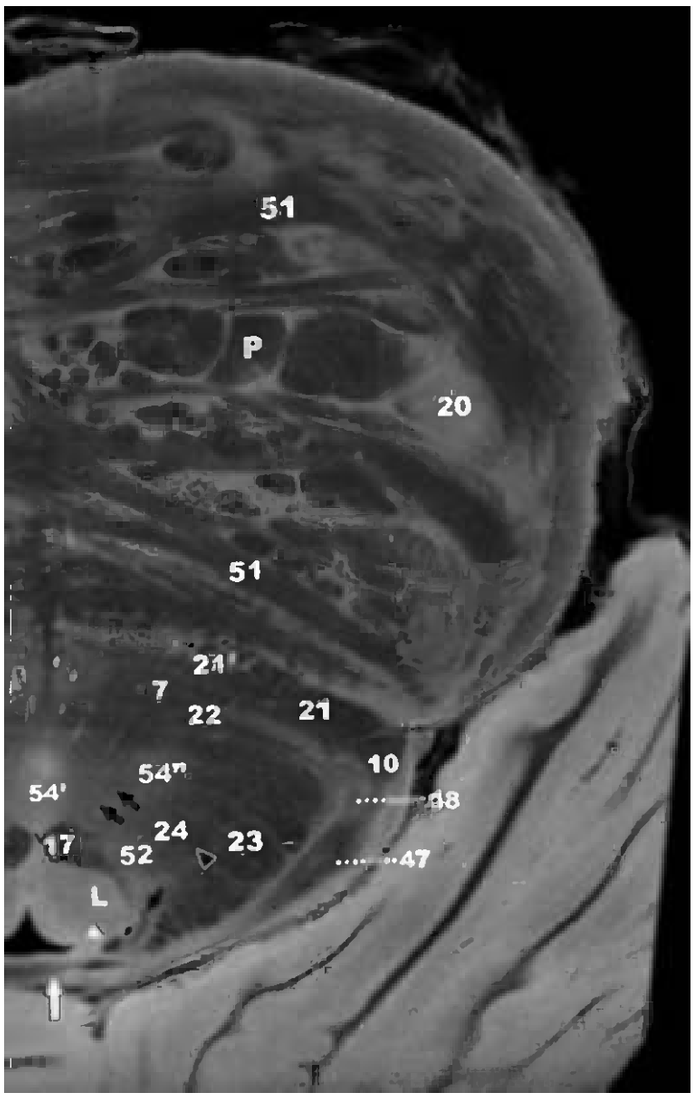

Arrowheads and arrows

Single white arrowhead: Undecussated fascicles from the ipsilateral trochlear nucleus moving postero-inferiorly toward the decussation
Single black arrowhead: Tegmento-olivary tract (also 53)
Single white arrow: Decussation of the troclear fascicles in the superior medullary velum
Single black arrow: Mesencephalic nucleus and tract of CN V
Paired black arrows: Predorsal longitudinal fasciculus (fasciculus predorsalis) [358]

Fig. 8.73. Pontomesencephalic junction. Axial section.

The spinothalamic tract (10) moves further dorsally. The dorsal nucleus (47′) of the lateral lemniscus (47) forms a prominent ovoid within the lemniscus. The dorsal nucleus is an important relay between the superior olives and both inferior colliculi [322a]. The trochlear nerve fibers that arose in the contralateral trochlear nucleus and that decussated in the superior medullary velum, now emerge (white arrow) from the brain stem just caudal to the inferior colliculus (See next two sections 8.74 and 8.75). The medial border of the superior cerebellar peduncle (23) has blurred more completely. At this level, the nucleus centralis superior is separated into medial (54′) and lateral (54″) subnuclei.

7 Rubrospinal tract
10 Spinothalamic tract
17 Medial longitudinal fasciculus
20 Pontine nuclei
21 Medial lemniscus
23 Superior cerebellar peduncle
24 Central tegmental tract
47 Lateral lemniscus surrounding the dorsal nucleus (47′) of the lateral lemniscus
47′ Dorsal nucleus of the lateral lemniscus
51 Pontocerebellar fibers
54′ Nucleus centralis superioris medialis
54″ Nucleus centralis superioris lateralis
55 Predorsal longitudinal fasciculus

Letter labels

L Site of the locus ceruleus
P Pyramidal tracts leading to the pyramid

Arrowheads and arrows

Single white arrowhead: Undecussated fascicles from the ipsilateral trochlear nucleus moving postero-inferiorly toward the decussation

Single white arrow: Decussated fascicles of the troclear nerve emerging from the low midbrain just inferior to the inferior colliculus on the contralateral side.

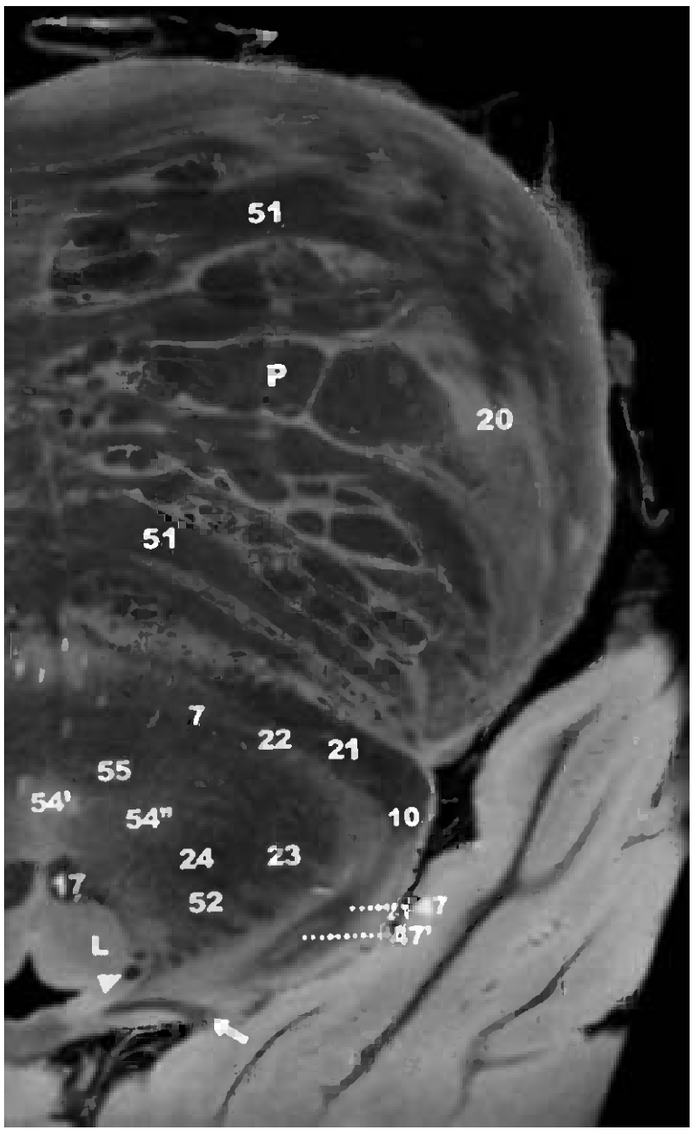

Fig. 8.74. Pontomesencephalic junction. Axial section.

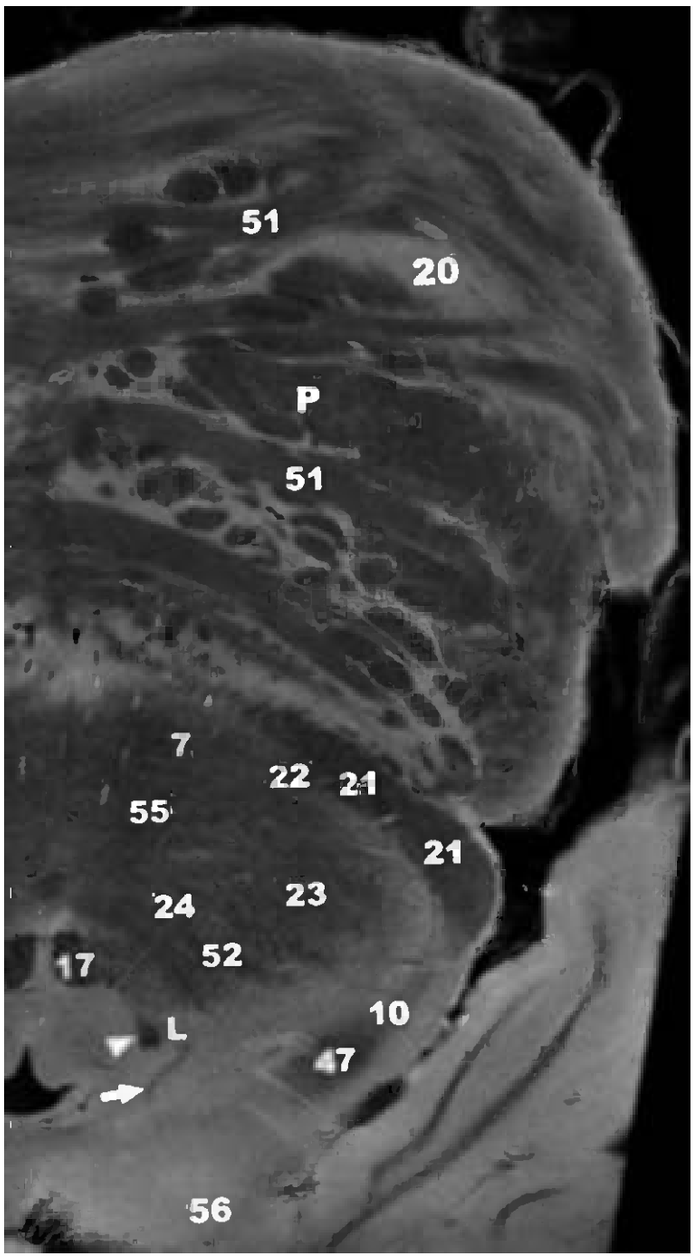

The lower border of the inferior colliculus (56) marks the transition from the pons to the midbrain dorsally. The lateral lemniscus (47) approaches the inferior pole of the inferior colliculus (56). The spinothalamic tract (10) has moved dorsally with the lateral lemniscus, and is further separated from the rubrospinal tract (7). The superior cerebellar peduncle (23) has shifted medially and its medial border has become completely blurred. The trochlear nerve fibers (single white arrowhead) descend through the periaqueductal gray matter from their origin at the trochlear nuclei to their decussation in the superior medullary velum, so sequential rostral sections display progressively more ventral (proximal) portions of the nerve. The mesencephalic tract and nucleus of the trigeminal nerve (single white arrow) lie lateral to the trochlear nerve fibers, and form a thin arc of low signal at and just lateral to the border of the periaqueductal gray matter.

7 Rubrospinal tract
10 Spinothalamic tract
17 Medial longitudinal fasciculus
20 Pontine nuclei
21 Medial lemniscus
22 Ventral trigeminothalamic tract
23 Superior cerebellar peduncle
24 Central tegmental tract
47 Lateral lemniscus
51 Pontocerebellar fibers
53 Tegmento-olivary tract
55 Predorsal longitudinal fasciculus
56 Inferior colliculus

Letter labels

L Site of the locus ceruleus
P Pyramidal tracts leading to the pyramid

Arrowheads and arrows

Single white arrowhead: Undecussated fascicles from the ipsilateral trochlear nucleus moving postero-inferiorly toward the decussation

Single white arrow: Mesencephalic nucleus and tract of CN V

Fig. 8.75. Pontomesencephalic junction. Axial section.

The dorsal edge of the cerebral peduncle (60) just enters the section, marking the transition to the midbrain laterally. The superior cerebellar peduncle (23) has shifted far medially toward its decussation. The lateral lemniscus joins the inferior colliculus (56), which is outlined by its medial and lateral medullary laminae (black arrowheads). Most lateral lemniscal fibers end directly within the central nucleus of the inferior colliculus [78]. The area parabigemina posterior (57) lies immediately medial to the junction of the lateral lemniscus with the medial medullary lamina. The tectopontine tract (dual white arrows) lies lateral to the lateral lemniscus. It transmits visual information to the pontine nuclei for relay, via pontocerebellar fibers, to the central portion of the vermis (declive, folium, tuber) (the visual projection area of the cerebellum) [322]. The sagulum (191) is the superficial layer of gray matter lateral to the lateral lemniscus. It contains the tectopontine tract (dual white arrows) and the corpus parabigeminum, an oval field with a structure similar to the inferior colliculus [358]. The pedunculopontine nucleus (58) lies within the lateral reticular formation of the tegmentum. It receives input from the medial nucleus of the globus pallidus and pars reticulata of substantia nigra, and projects mainly to the pars compacta of substantia nigra [78].

7 Rubrospinal tract
10 Spinothalamic tract
17 Medial longitudinal fasciculus
20 Pontine nuclei
21 Medial lemniscus
22 Ventral trigeminothalamic tract
23 Superior cerebellar peduncle
24 Central tegmental tract
47′ Dorsal nucleus of the lateral lemniscus
51 Pontocerebellar fibers
52 Dorsal trigeminothalamic tract
53 Tegmento-olivary tract
54′ Nucleus centralis superioris medialis
55 Predorsal longitudinal fasciculus
56 Inferior colliculus
57 Area parabigemina posterior
58 Pedunculopontine nucleus of the tegmentum
60 Cerebral peduncle
191 Sagulum

Letter labels
L Site of the locus ceruleus
P Pyramidal tracts leading to the pyramid

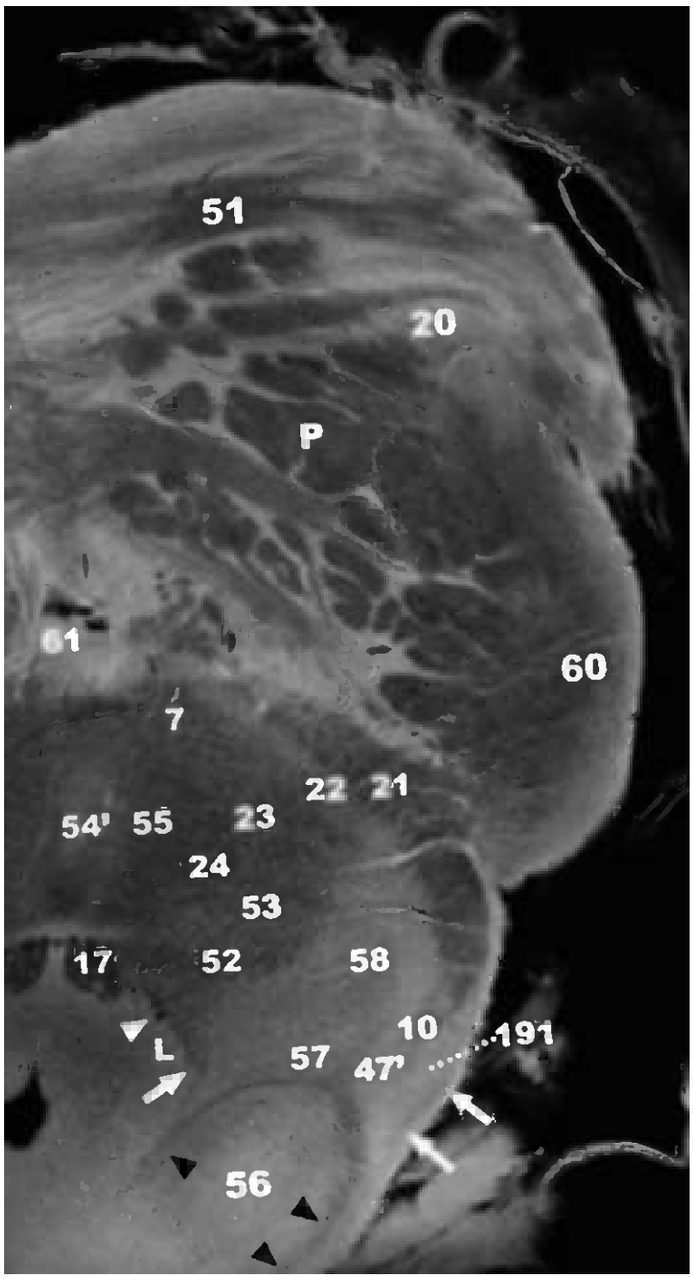

Arrowheads and arrows

Single white arrowhead:	Undecussated fascicles from the ipsilateral trochlear nucleus moving postero-inferiorly toward its decussation
Single black arrowhead:	Medial medullary lamina of the inferior colliculus (56)
Paired black arrowheads:	Lateral medullary lamina of the inferior colliculus (56)
Single white arrow:	Mesencephalic nucleus and tract of CN V
Paired white arrows:	Tectopontine tract

Fig. 8.76. Pontomesencephalic junction. Axial section.

The interpeduncular fossa (IP) marks the pontomesencephalic junction ventrally. The interpeduncular nucleus (61) forms a layer of gray matter that outlines the interpeduncular fossa. The rubrospinal tract (7) arises cephalically from the medial aspect of the red nucleus on each side (See Figs. 8.99 and 8.100), and immediately crosses the midline (7′) through the ventral tegmental decussation. On the contralateral side, the rubrospinal tract passes dorsally, laterally and caudally into the spinal cord, where it lies in the lateral funiculus, partially intermingled with fibers of the lateral corticospinal tract. In its descent, the rubrospinal tract first approximates iteslf to the spinothalamic tract (See Fig. 8.68), then the anterior spinocerebellar tract (See Fig. 8.13), and then the lateral corticospinal tract [78]. Dorsally, the trochlear nucleus (59) appears at the ventral edge of the periaqueductal gray matter, and is partially encompassed by the fibers of the medial longitudinal fasciculus (17) ventral to it. Laterally, the cerebral peduncle is better developed (60). The tectopontine tract (paired white arrows) courses along the lateral aspect of the the inferior colliculus within the sagulum (191). The inferior pole of the medial geniculate body (104) is just seen at the lateral mesencephalic sulcus immediately posterior to the cerebral peduncle (60).

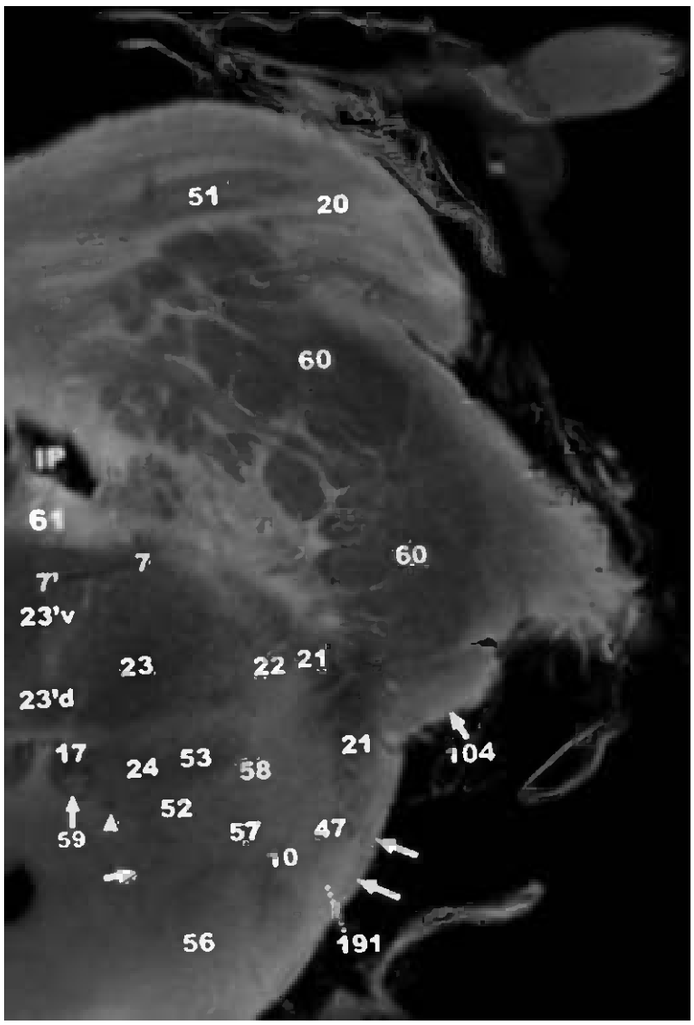

7 Rubrospinal tract
7′ Ventral tegmental decussation (including rubrospinal fibers)
10 Spinothalamic tract
17 Medial longitudinal fasciculus
20 Pontine nuclei
21 Medial lemniscus
22 Ventral trigeminothalamic tract
23 Superior cerebellar peduncle
23′ Decussation of superior cerebellar peduncle, dorsal (23′d) and ventral (23′v) portions
24 Central tegmental tract
47 Lateral lemniscus
51 Pontocerebellar fibers
53 Tegmento-olivary tract
55 Predorsal longitudinal fasciculus
56 Inferior colliculus
57 Area parabigemina posterior
58 Pedunculopontine nucleus of the tegmentum
59 Trochlear nucleus (CN IV), inferior pole
60 Cerebral peduncle
104 Medial geniculate body (caudal pole)

Letter labels
IP Interpeduncular fossa

Arrowheads and arrows
Single white arrowhead: Undecussated fascicles from the ipsilateral trochlear nucleus moving postero-inferiorly toward the decussation
Single white arrow: Mesencephalic nucleus and tract of CN V
White arrow 59: Inferior pole of the trochlear nucleus (CN IV)
Dual white arrows: Tectopontine tract

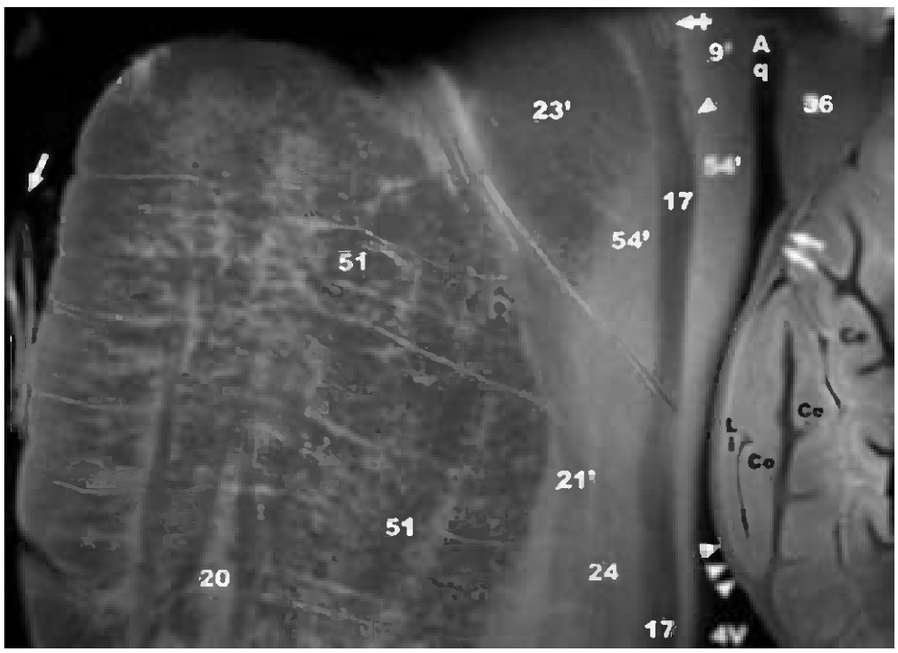

C 2. Sagittal Pontomesencephalic Junction

Sagittal sections displayed from midline to lateral (Figs. 8.77– 8.87)

Fig. 8.77. Pontomesencephalic junction. Paramedian sagittal section.

The cerebral aqueduct (Aq) extends caudally into the fourth ventricle (4V). Dorsally, the superior medullary velum (three white arrowheads) contains the decussating portions of the trochlear nerve fibers (paired white arrows). The lingula (Li) of the vermis attaches directly to the dorsal surface of the superior medullary velum. The precentral cerebellar fissure (unlabelled) separates the lingula (Li) from the central lobule (Ce) of the vermis. Ventrally, the medial longitudinal fasciculus (17) ascends through the tegmentum of the pons into the midbrain, where it passes through the medial portion (54′) of the nucleus centralis superior. The medial longitudinal fasciculus (17) passes immediately ventral to the trochlear nucleus (single white arrowhead) and the oculomotor nucleus (crossed white arrow), partially enclosing their ventral aspects. The decussation of the superior cerebellar peduncle (23′) forms a prominent lens-shape of low signal in the center of the midbrain.

9′ Periaqueductal gray matter
17 Medial longitudinal fasciculus
20 Pontine nuclei
21′ Rete of the medial lemniscus
24 Central tegmental tract
23′ Decussation of the superior cerebellar peduncle
51 Pontocerebellar fibers
54′ Nucleus centralis superior medialis
56 Inferior colliculus

Letter labels

4V Fourth ventricle
Aq Cerebral aqueduct (of Sylvius)
Ce Central lobule of vermis
Li Lingula of vermis

Arrowheads and arrows

Single white arrowhead: Nucleus of the trochlear nerve (CN IV)
Triple white arrowheads: Superior medullary velum
Single white arrow: Basilar artery
Single crossed arrow: Most inferomedial portion of the oculomotor nucleus (CN III)
Dual white arrows: Decussation of the trochlear nerves (CN IV) in the superior medullary velum

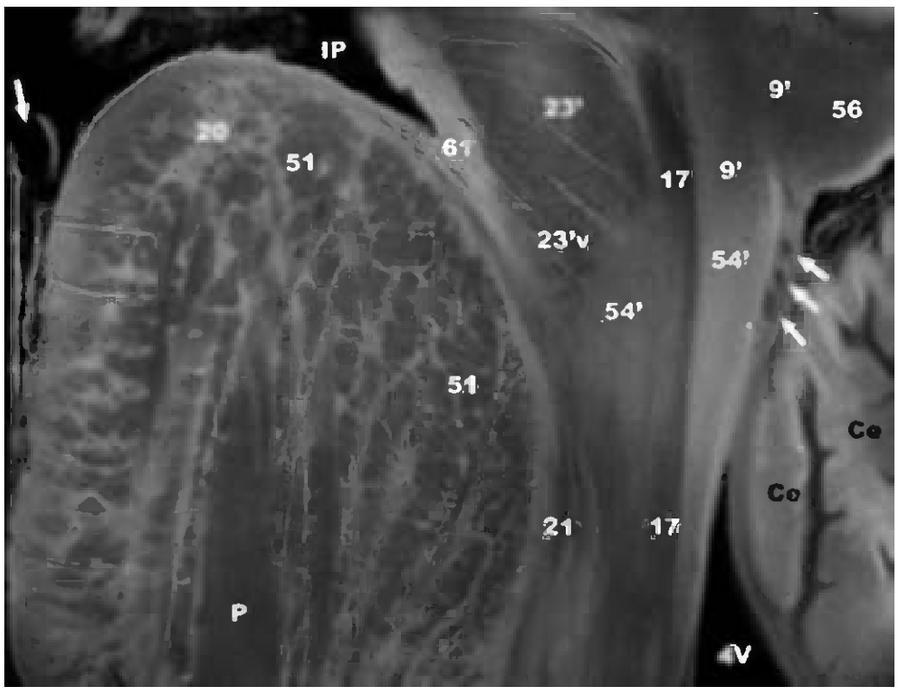

Fig. 8.78. Pontomesencephalic junction. Sagittal section. Individual fascicles (triple white arrows) of both trochlear nerves decussate in the superior medullary velum, just caudal to the lower margin of the inferior colliculus (56). The nucleus centralis superior forms the prominent mass of gray matter dorsal and ventral to the medial longitudinal fasciculus (17) at the pontomesencephalic junction. The periaqueductal gray matter (9′) surrounds the aqueduct. The medial lemniscus (21) arches superiorly along the posterior margin of the basis pontis, dorsal to the pontocerebellar fibers (51) and pontine nuclei (20). The interpeduncular nucleus (61) outlines the interpeduncular fossa (IP).

9′ Periaqueductal gray matter
17 Medial longitudinal fasciculus
20 Pontine nuclei
23′ Decussation of the superior cerebellar peduncle
23′v Ventral portion of (23′), which crosses more caudally
51 Pontocerebellar fibers
54′ Nucleus centralis superior medialis
56 Inferior colliculus
61 Interpeduncular nucleus

Letter labels

4V Fourth ventricle
Ce Central lobule of vermis
IP Interpeduncular fossa
P Corticospinal tract

Arrowheads and arrows

Single white arrow: Basilar artery
Triple white arrows: Decussating fibers of the trochlear nerves, one side composed of a single (lowest) fascicle, the other of two fascicles (middle and highest)

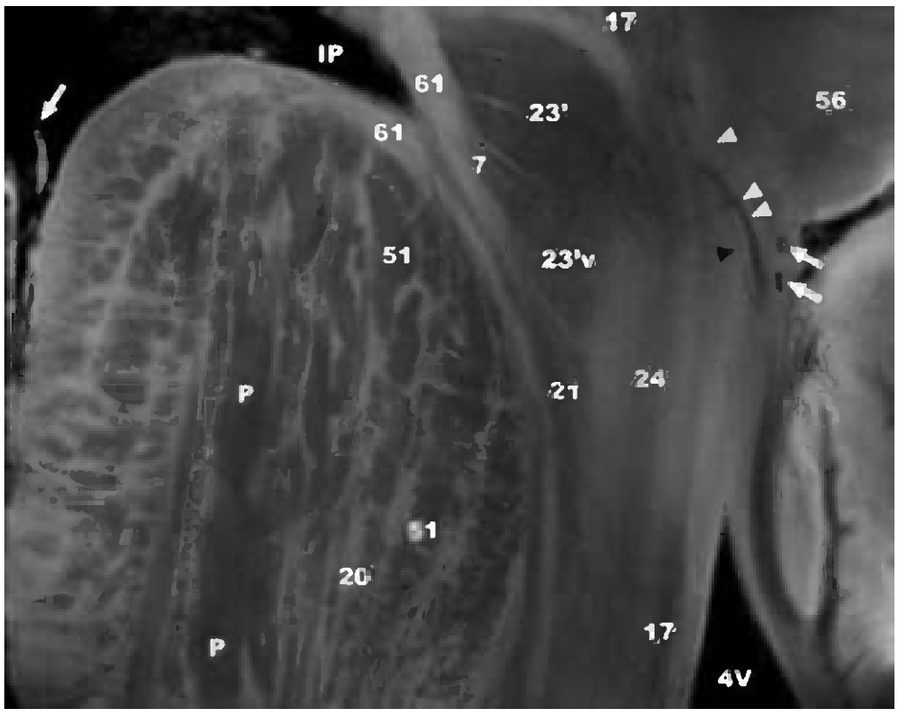

Fig. 8.79. Pontomesencephalic junction. Sagittal section.

The pontine nuclei (20), pontocerebellar fibers (51), and descending corticospinal (pyramidal) tracts (P) occupy the basis pontis. The medial lemniscus (21), central tegmental tract (24), and medial longitudinal fasciculus (17) extend longitudinally through the tegmentum of the pons and mesencephalon. At the pontomesencephalic junction, the rubrospinal tract (7) lies in medial position, ventral to the decussation (23') of the susperior cerebellar peduncle. Fibers of the superior cerebellar peduncle cross the midline both ventrally (23'v) and dorsally (See 23'd in **Fig. 8.80**).

17 Medial longitudinal fasciculus
20 Pontine nuclei
21 Medial lemniscus
23' Decussation of the superior cerebellar peduncle
23'v Ventral portion of (23'), which crosses more caudally
24 Central tegmental tract
51 Pontocerebellar fibers
56 Inferior colliculus
61 Interpeduncular nucleus

Letter labels
4V Fourth ventricle
IP Interpeduncular fossa
P Descending corticospinal fibers

Arrowheads and arrows
Single white arrowhead: Nucleus of the trochlear nerve (CN IV)
Single black arrowhead: Small fascicle of the trochlear nerve travelling independently
Dual white arrowheads: Large fascicles of the ipsilateral trochlear nerve moving posteroinferiorly
Single white arrow: Basilar artery
Paired white arrows: Paired nearly equal fascicles of the contralateral trochlear nerve decussating in the superior medullary velum

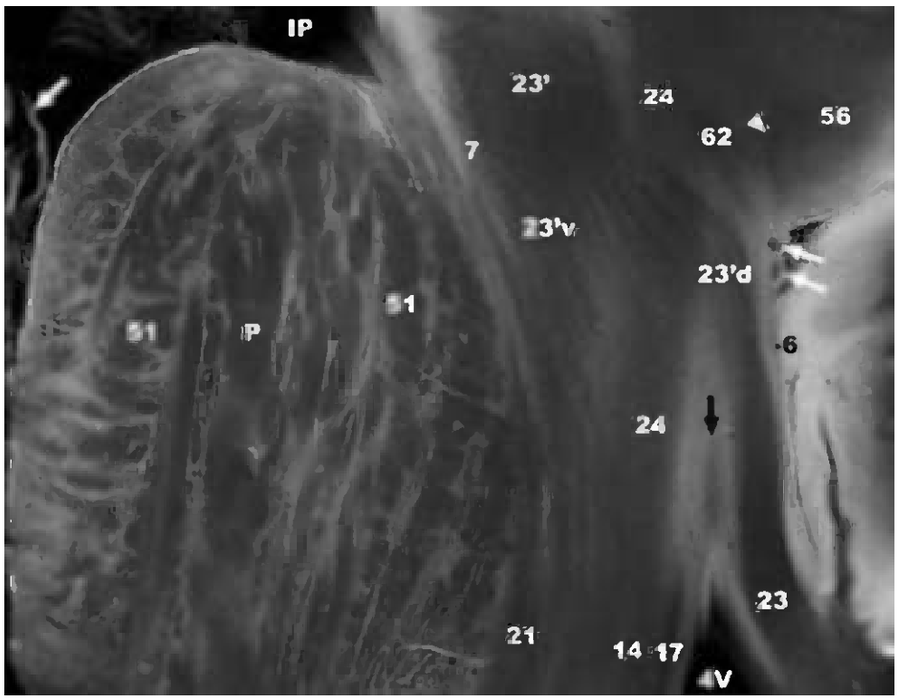

Fig. 8.80. Pontomesencephalic junction. Sagittal section.

The dorsal (23'd) and ventral (23'v) streams of decussating superior cerebellar peduncular fibers converge superiorly. The rostral end of the anterior spinocerebellar tract (6) forms a thin lamina, which arches over the superior cerebellar peduncle to enter the cerebellum "retrograde". The central tegmental tract (24) descends from the red nucleus as a robust bundle visualized both rostral and caudal to the superior cerebellar peduncle. The dorsolateral tegmental fasciculus (62) courses in the pons and midbrain in the dorsal portion of the central tegmental tract. It may arise from fibers surrounding the red nucleus [358]. In sagittal sections, the mesencephalic nucleus and tract of the trigeminal nerve form an "angle" or caret that mimics the shape of the fourth ventricle caudal to it and the arched shape of the junction of the superior cerebellar peduncle (23'd) with the central tegmental tract (24) rostral to it.

6 Ventral (anterior) spinocerebellar tract arching over the superior cerebellar peduncle
7 Rubrospinal tract
14 Tectospinal tract (part of predorsal longitudinal fasciculus (62))
17 Medial longitudinal fasciculus
21 Medial lemniscus
23 Superior cerebellar peduncle
23' Decussation of the superior cerebellar peduncle
23'd Dorsal portion of the superior cerebellar peduncle arriving at 23'
23'v Ventral portion of the superior cerebellar peduncle arriving at 23'
24 Central tegmental tract
51 Pontocerebellar fibers
56 Inferior colliculus
62 Dorsolateral tegmental fasciculus

Letter labels

4V Fourth ventricle
IP Interpeduncular fossa
P Descending corticospinal fibers

Arrowheads and arrows

Single white arrowhead: Medial medullary lamina of the inferior colliculus (56)
Single white arrow: Basilar artery
Single black arrow: Mesencephalic nucleus and tract of CN V
Paired white arrows: Paired nearly equal fascicles of the contralateral trochlear nerve decussating in the superior medullary velum

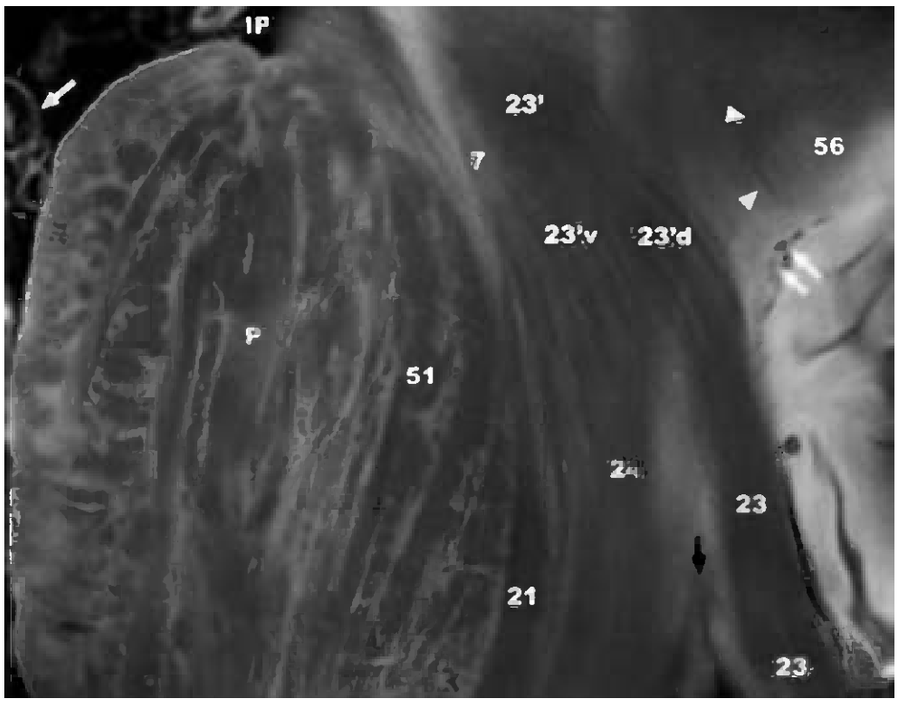

Fig. 8.81. Pontomesencephalic junction. Sagittal section.

The capsule of the inferior colliculus (white arrowheads) becomes more prominent in this section. The trochlear nerves (white arrows) just reach the surface of the brain stem caudal to the inferior colliculus (56).

6 Ventral (anterior) spinocerebellar tract arching over the superior cerebellar peduncle
7 Rubrospinal tract
21 Medial lemniscus
23 Superior cerebellar peduncle
23' Decussation of the superior cerebellar peduncle
23'd Dorsal portion of 23'
23'v Ventral portion of 23'
24 Central tegmental tract
51 Pontocerebellar fibers
56 Inferior colliculus

Letter labels
IP Interpeduncular fossa
P Descending corticospinal fibers

Arrowheads and arrows
Paired white arrowheads: Medial medullary lamina of the inferior colliculus (56)
Single white arrow: Basilar artery
Single black arrow: Mesencephalic nucleus and tract of CN V
Paired white arrows: Trochlear nerves emerging into the perimesencephalic cistern

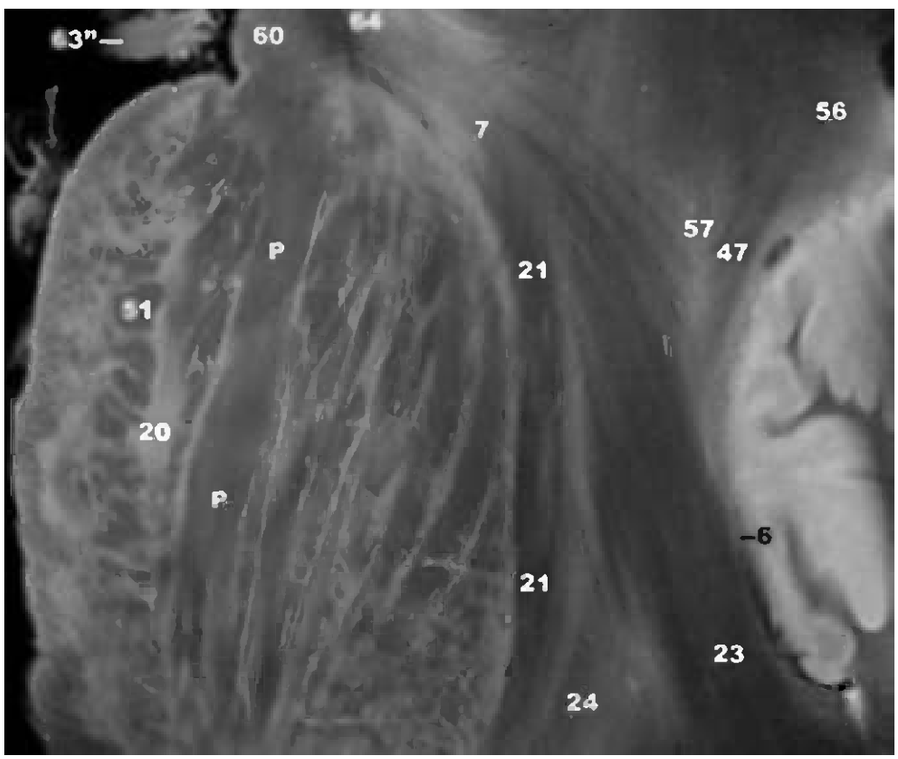

Fig. 8.82. Pontomesencephalic junction. Sagittal section.

The lateral lemniscus (47) ascends obliquely to reach the inferior colliculus (56). The anterior spinocerebellar tract (6) recurves over the upper border of the superior cerebellar peduncle (23). The medial lemniscus (21) arches upward at the interface of the basis pontis and pontine tegmentum. It shows thinning at the rete (between the two 21s) as it ascends to the thalamus (See Fig. 8.71).

6 Ventral (anterior) spinocerebellar tract arching over the superior cerebellar peduncle
7 Rubrospinal tract
20 Pontine nuclei
21 Medial lemniscus
23 Superior cerebellar peduncle
24 Central tegmental tract
47 Lateral lemniscus
51 Pontocerebellar fibers
56 Inferior colliculus
57 Area parabigemina posterior
60 Cerebral peduncle
63″ Oculomotor nerve (CN III) in the interpeduncular fossa
64 Substantia nigra

Letter labels
P Descending corticospinal fibers

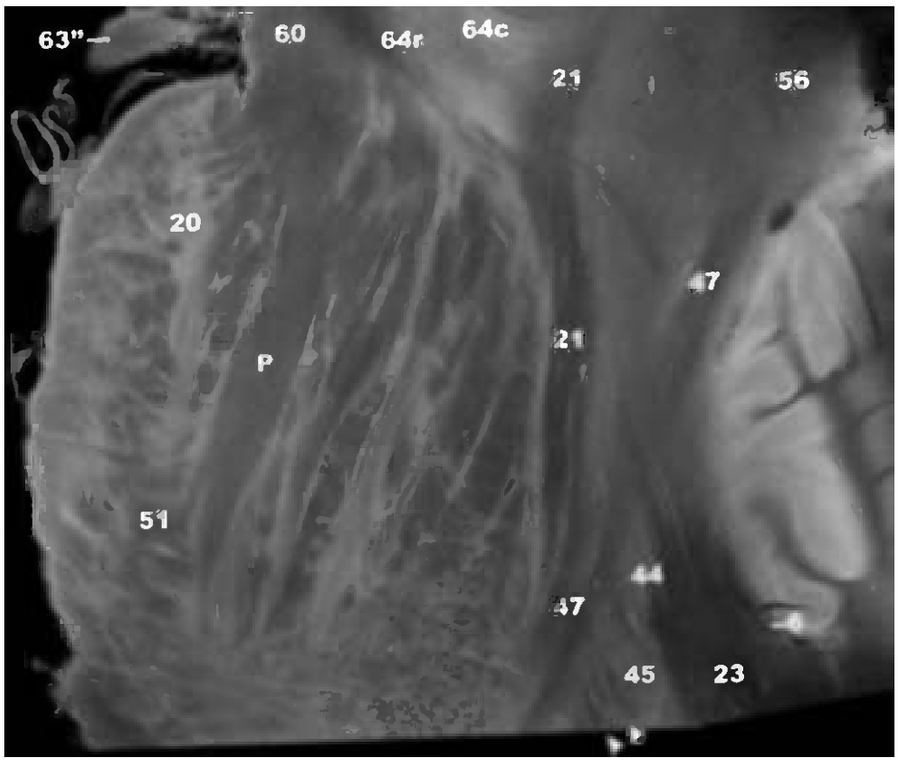

Fig. 8.83. Pontomesencephalic junction. Sagittal section.

The medial lemniscus (21) recurves dorsally as it ascends from the upper pons into the midbrain. The lateral lemniscus (47) follows the oblique contour of the lateral surface of the upper pons as it ascends to the inferior colliculus (56). The cerebral peduncle (60), oculomotor nerve (63″) and substantia nigra (64) partes reticulata (r) and compacta (c) are just visualized at the upper margin of the image. At the lower margin the mesencephalic trigeminal tract and nucleus (44) approach the motor nucleus (45) of the trigeminal nerve.

6 Ventral (anterior) spinocerebellar tract arching over the superior cerebellar peduncle
20 Pontine nuclei
21 Medial lemniscus
23 Superior cerebellar peduncle
44 Mesencephalic tract and surrounding mesencephalic nucleus of CN V
45 Motor nucleus of CN V
47 Lateral lemniscus
51 Pontocerebellar fibers
56 Inferior colliculus
60 Cerebral peduncle
63″ Oculomotor nerve (CN III) in the interpeduncular fossa
64c Substantia nigra, pars compacta
64r Substantia nigra, pars reticulata

Letter labels
P Descending corticospinal fibers

Arrowheads and arrows
Paired white arrowheads: (at bottom of image) Fascicles of the trigeminal nerve, likely motor fibers

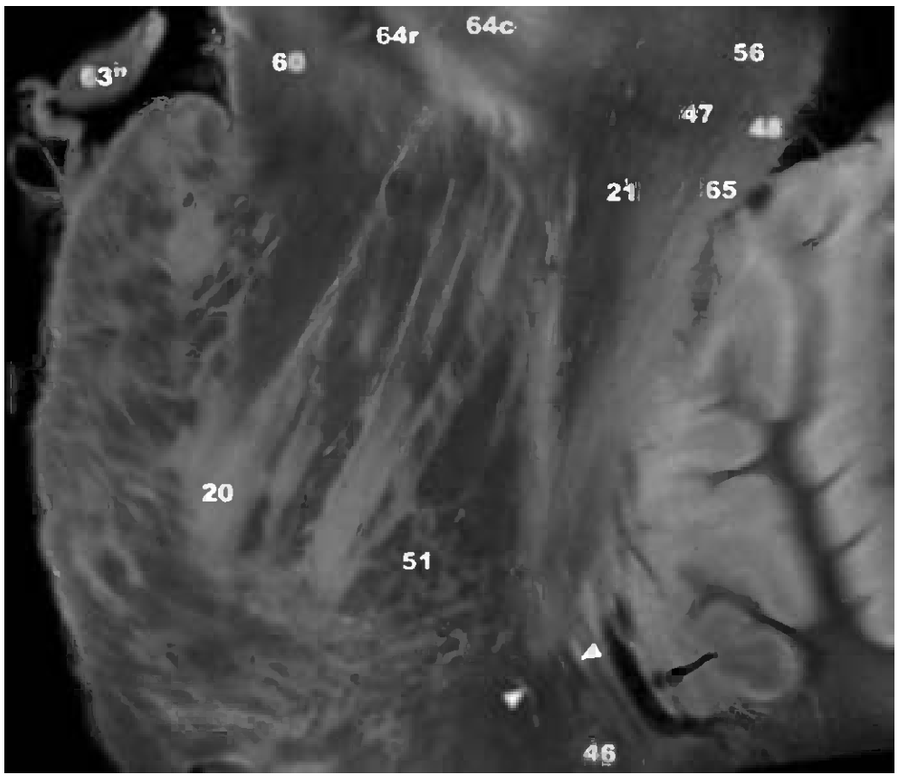

Fig. 8.84 Pontomesencephalic junction. Sagittal section.

The principal sensory trigeminal nucleus (46), the motor nucleus of the trigeminal nerve (45 in the prior image), and the trigeminal nerve fascicles (white arroweads) form the trigeminal area at the lateral aspect of the brain stem. The stragulum (65) is a layer of gray matter situated external to the superior cerebellar peduncle. It contains remnants of the inferior cerebellar peduncle and anterior spinocerebellar tract.

20 Pontine nuclei
21 Medial lemniscus
46 Principal sensory nucleus of the trigeminal nerve (CN V)
47 Lateral lemniscus
48 Nucleus of the lateral lemniscus
51 Pontocerebellar fibers
56 Inferior colliculus
60 Cerebral peduncle
63″ Oculomotor nerve (CN III) in the interpeduncular fossa
64c Substantia nigra, pars compacta
64r Substantia nigra, pars reticulata
65 Stragulum

Arrowheads and arrows
Paired white arrowheads: Fascicles of the trigeminal nerve, likely motor fibers

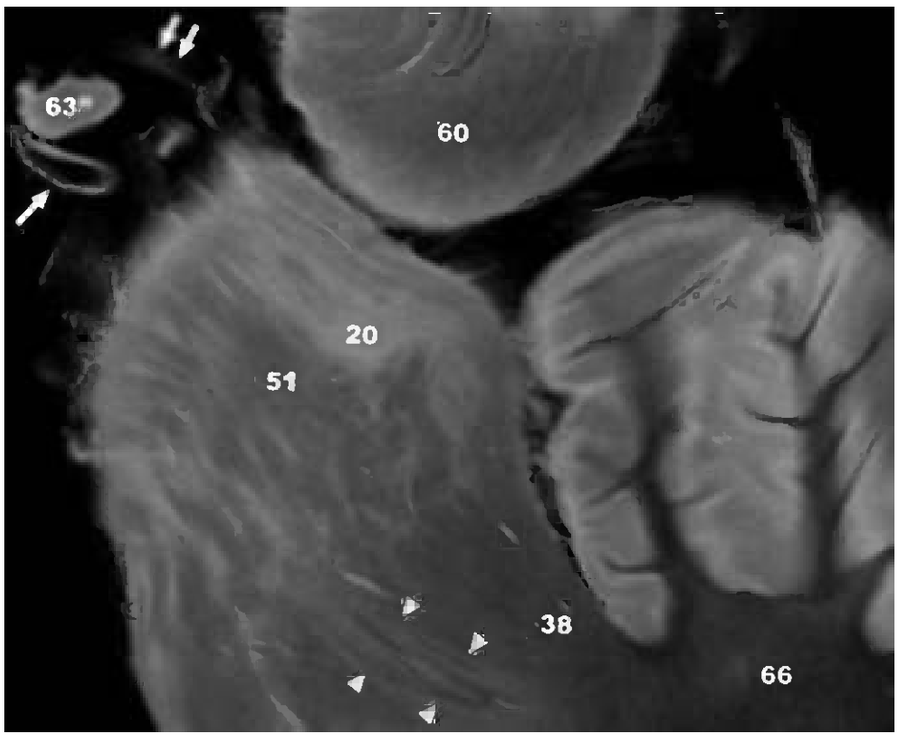

Fig. 8.85. Pontomesencephalic junction. Sagittal section.

The trigeminal fibers (between white arrowheads) traverse the middle cerebellar peduncle (38) as they pass from the trigeminal ganglion (semilunar ganglion) situated outside the brain stem to the trigeminal nuclei situated within the brain stem. The cisternal segment of the oculomotor nerve (63″) passes between the posterior cerebral artery (paired white arrows) superiorly and the superior cerebellar artery (single white arrrow) inferiorly.

20 Pontine nuclei
38 Middle cerebellar peduncle
51 Pontocerebellar fibers
60 Cerebral peduncle
63″ Oculomotor nerve (CN III) passing between the superior cerebellar artery below and the posterior cerebral artery above

Arrowheads and arrows

Paired white arrowheads: The course of the sensory fibers of the trigeminal nerve (CN V) through the middle cerebellar peduncle
Single white arrow: Superior cerebellar artery
Paired white arrows: Posterior cerebral artery

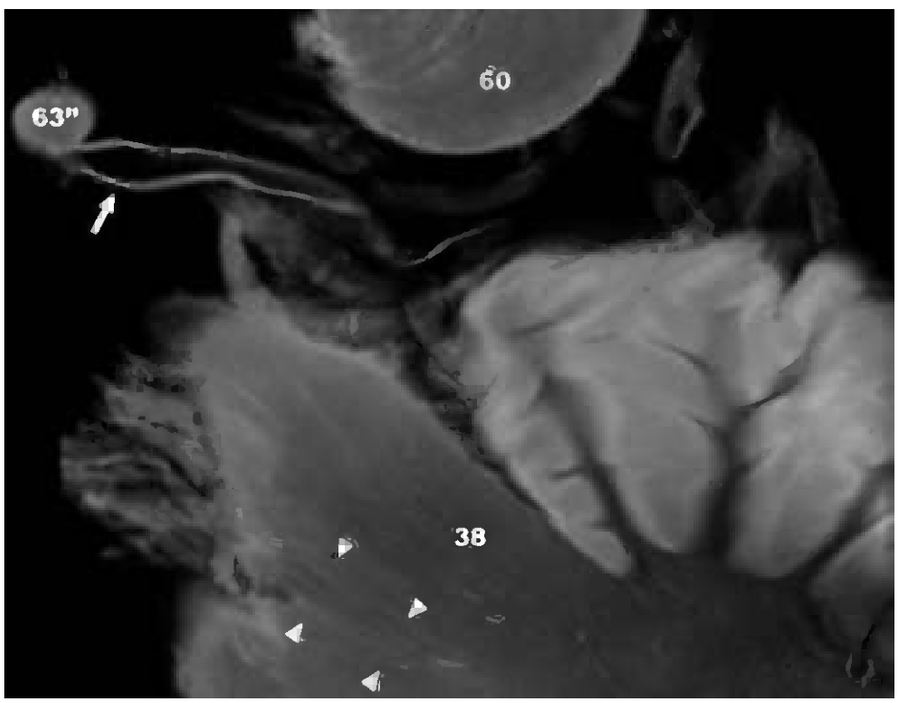

Fig. 8.86. Pontomesencephalic junction. Sagittal section.

Far lateral sections display the emergence of the trigeminal fibers (between white arrowheads) from the brain stem.

38 Middle cerebellar peduncle
60 Cerebral peduncle
63″ Oculomotor nerve (CN III) passing above the superior cerebellar artery

Arrowheads and arrows
Paired white arrowheads: The course of the sensory fibers of the trigeminal nerve (CN V) through the middle cerebellar peduncle
Single white arrow: Superior cerebellar artery

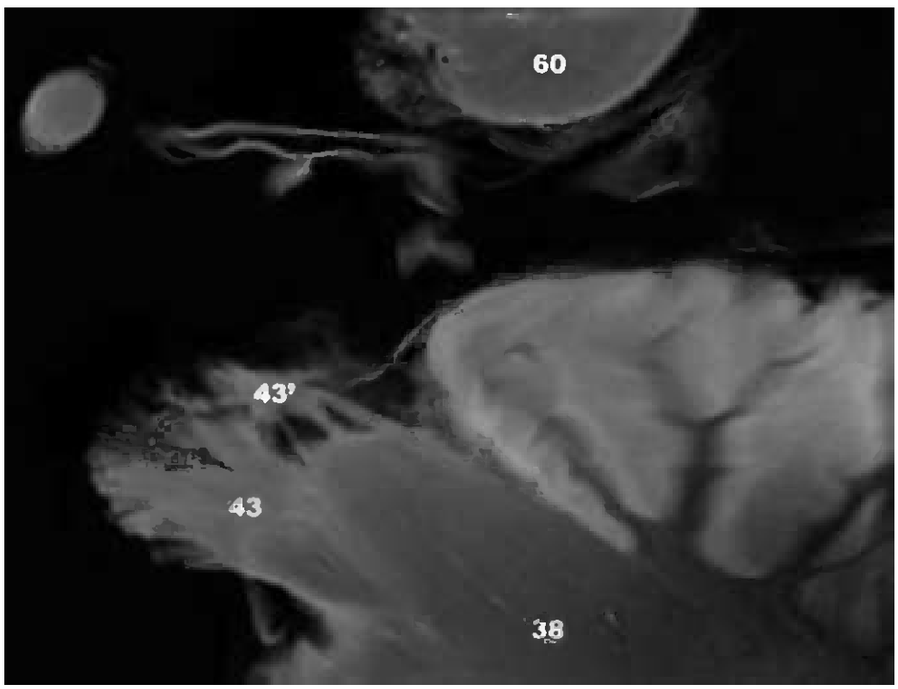

Fig. 8.87. Pontomesencephalic junction. Sagittal section.

The motor root (43') of the trigeminal nerve emerges from the brain stem superomedial to the sensory root (43). The motor root forms part of the *portio minor* while the sensory root forms part of the *portio major* of the trigeminal system.

38 Middle cerebellar peduncle
43 Sensory root of the trigeminal nerve (CN V)
43' Motor root of the trigeminal nerve (CN V)
60 Cerebral peduncle

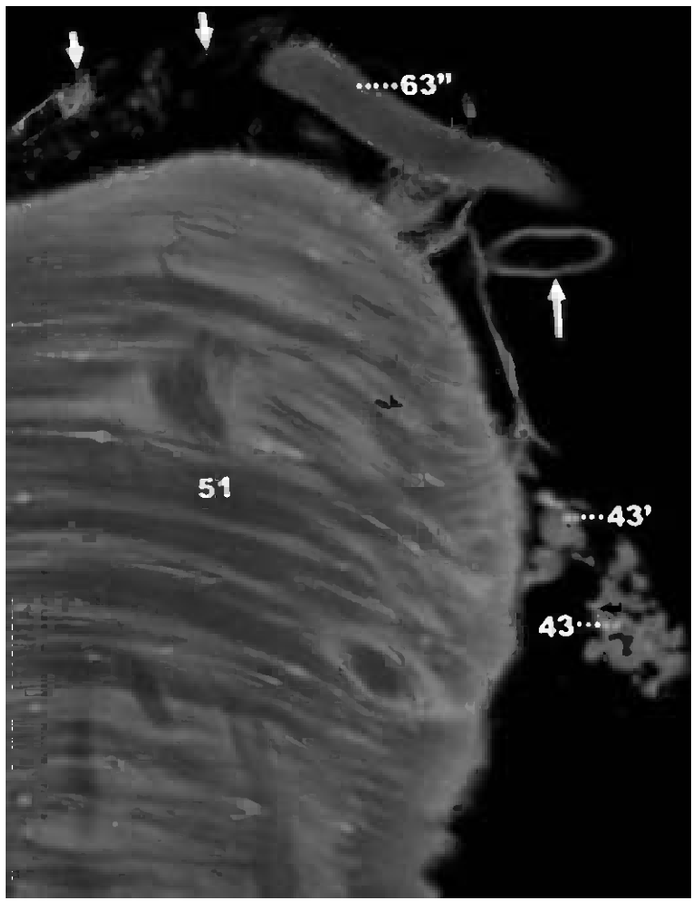

C 3. Coronal Pontomesencephalic Junction

Coronal sections displayed from ventral to dorsal (Figs. 8.88–8.97)

Fig. 8.88. Pontomesencephalic junction. Ventral coronal section.

The pontocerebellar fibers (51) that arise in the pontine nuclei of one side cross the midline, traverse the basis pontis to enter the opposite middle cerebellar peduncle, and then continue into the contralateral cerebellar hemisphere. The small motor root of the trigeminal nerve (43′) arises superomedial to the larger sensory root (43).

43 Sensory root of the trigeminal nerve (CN V)
43′ Motor root of the trigeminal nerve (CN V)
51 Pontocerebellar fibers
63″ Cisternal portion of the oculomotor nerve (CN III)

Arrowheads and arrows
Single white arrow: Superior cerebellar artery
Paired white arrows: Posterior cerebral artery

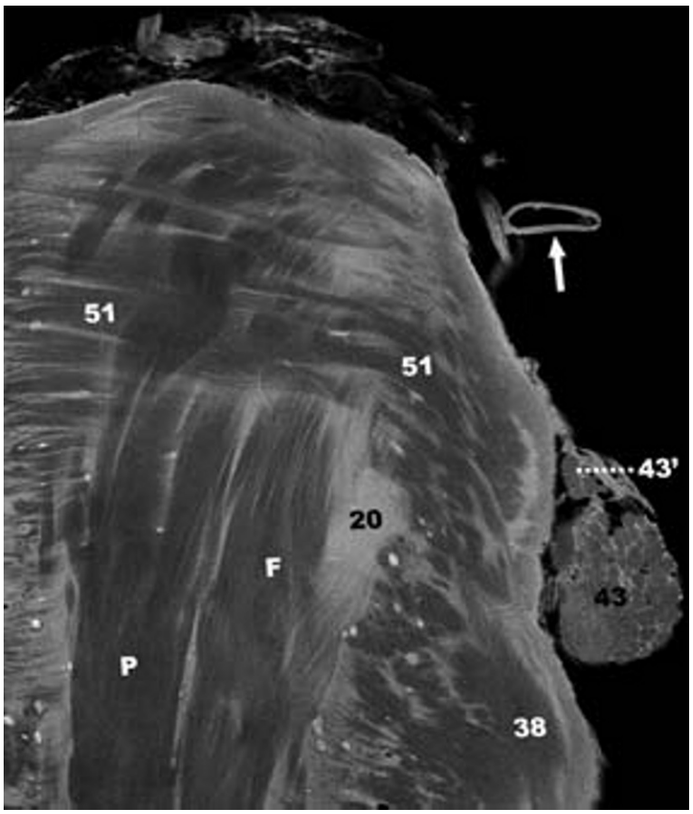

Fig. 8.89. Pontomesencephalic junction. Ventral coronal section.

The frontopontine (F) and corticospinal (pyramidal) (P) fibers descend through the basis pontis and appear interleaved with the pontine nuclei (20) and crossing pontocerebellar fibers (51). Because the basis pontis has a rounded shape, coronal images section through a deeper portion of the pons medially and a more superficial portion laterally.

20 Pontine nuclei
38 Middle cerebellar peduncle (most ventral portion)
43 Sensory root of the trigeminal nerve (CN V)
43′ Motor root of the trigeminal nerve (CN V)
51 Pontocerebellar fibers

Letter labels
F Frontopontine tracts
P Pyramidal tracts (corticospinal fibers)

Arrowheads and arrows
Single white arrow: Superior cerebellar artery

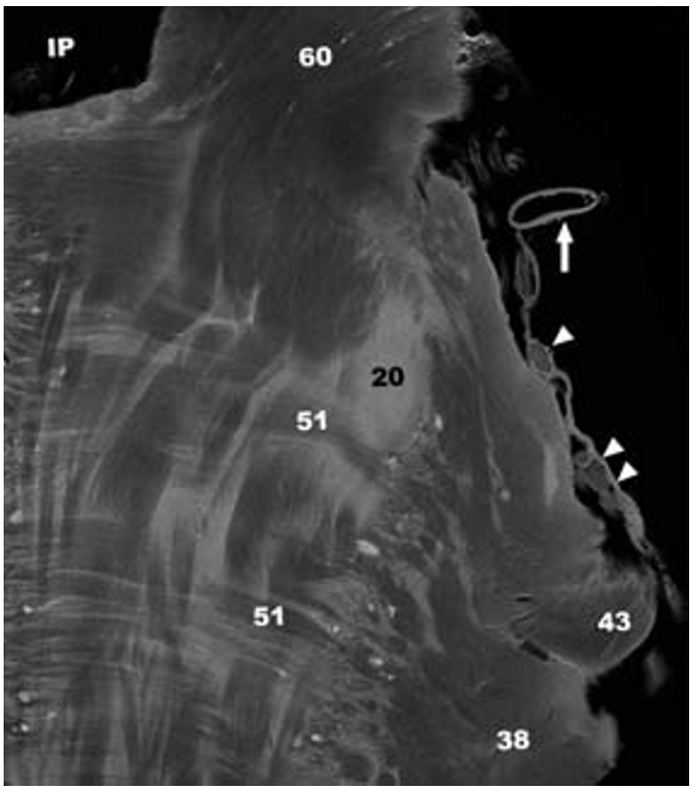

Fig. 8.90. Pontomesencephalic junction. Ventral coronal section.

The interpeduncular fossa (IP) and cerebral peduncle (60) identify the midbrain and mark the transition from pons to midbrain. The trochlear nerve (single white arrowhead) and trigeminal nerve fibers (dual white arrowheads) curve around the brain stem as they course ventrally toward their exit.

20 Pontine nuclei
38 Middle cerebellar peduncle (most ventral portion)
43 Sensory root of the trigeminal nerve (CN V)
51 Pontocerebellar fibers
60 Cerebral peduncle

Letter labels
IP Interpeduncular fossa

Arrowheads and arrows
Single white arrowhead: Cisternal portion of the trochlear nerve (CN IV)
Paired white arrowheads: Fascicles of the trigeminal nerve root (CN V)
Single white arrow: Superior cerebellar artery

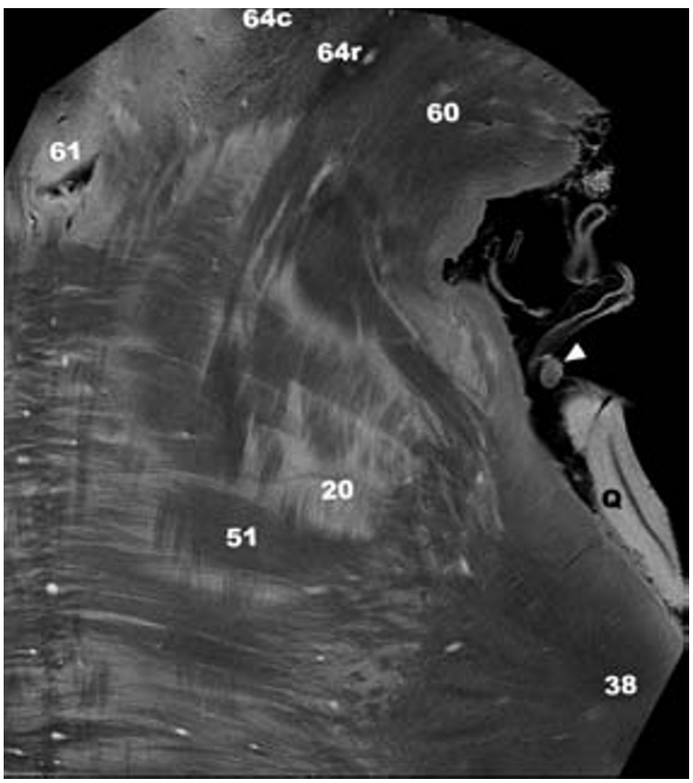

Fig. 8.91. Pontomesencephalic junction. Middle coronal section.

Further posterior, coronal sections display deeper structures of the midbrain including the substantia nigra (64), partes compacta (c) and reticulata (r), and the interpeduncular nucleus (61). The quadrangular lobule (Q) of the cerebellum overhangs the brachium pontis.

20 Pontine nuclei
38 Middle cerebellar peduncle (most ventral portion)
51 Pontocerebellar fibers
60 Cerebral peduncle
61 Interpeduncular nucleus surrounding the deepest portion of the interpeduncular fossa (foramen cecum)
64c Substantia nigra, pars compacta
64r Substantia nigra, pars reticulata

Letter labels
Q Quadrangular lip of the anterior lobe of cerebellum

Arrowheads and arrows
Single white arrowhead: Cisternal portion of the trochlear nerve (CN IV)

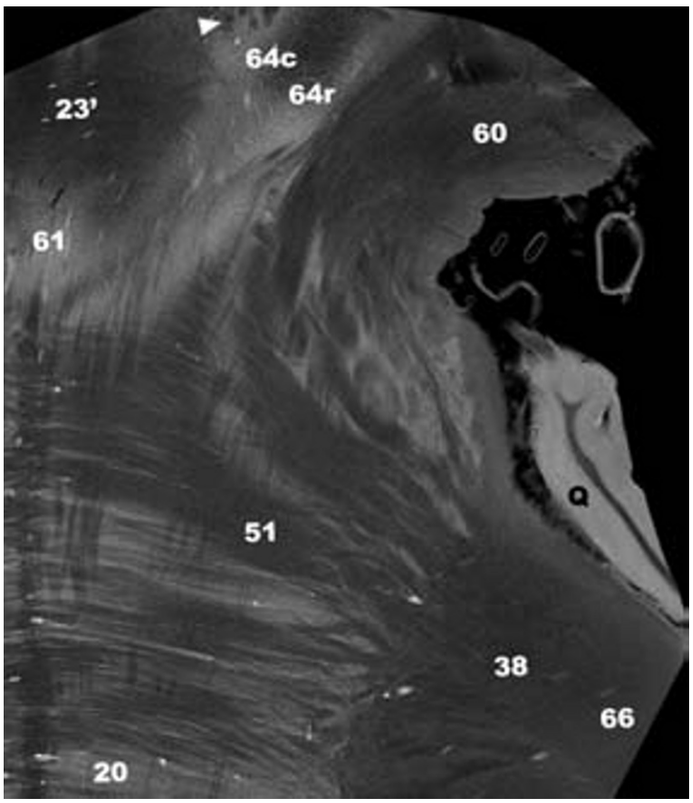

Fig. 8.92. Pontomesencephalic junction. Middle coronal section.

Fascicles of the oculomotor nerve (white arrowhead) emerge from the medial aspect of the cerebral peduncle into the interpeduncular fossa rostral to the decussation (23′) of the superior cerebellar peduncles.

20 Pontine nuclei
23′ Decussation of the superior cerebellar peduncle
38 Middle cerebellar peduncle (most ventral portion)
51 Pontocerebellar fibers
60 Cerebral peduncle
61 Interpeduncular nucleus surrounding the deepest portion of the interpeduncular fossa (foramen cecum)
64c Substantia nigra, pars compacta
64r Substantia nigra, pars reticulata
66 Corpus medullare of the cerebellar hemisphere

Letter labels
Q Quadrangular lip of the anterior lobe of cerebellum

Arrowheads and arrows
Single white arrowhead: Fascicles of the oculomotor nerve root (CN III)

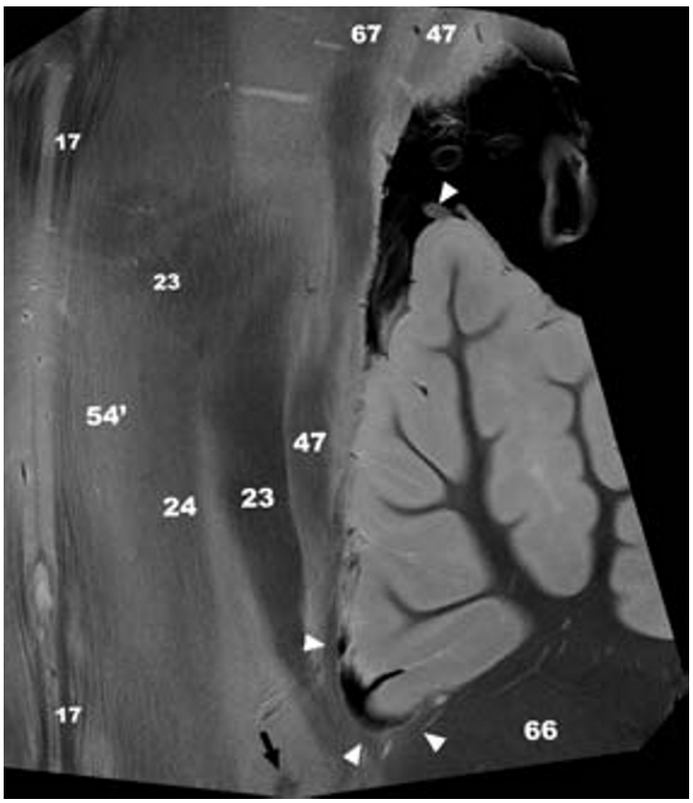

Fig. 8.93. Pontomedullary junction. Middle coronal section.

The medial longitudinal fasciculus (17), central tegmental tract (24), superior cerebellar peduncle (23), and lateral lemniscus (47) form parallel longitudinal columns. Rostrally, the superior cerebellar peduncle curves medially toward its decussation. The anterior spinocerebellar tract (three white arrowheads) becomes a thin layer of fibers that curve over the superior cerebellar peduncle to pass "retrograde" into the anterior and posterior lobes of the cerebellum [322]. The brachium of the inferior colliculus (67) ascends toward the medial geniculate body.

17 Medial longitudinal fasciculus
23 Superior cerebellar peduncle (the cephalic portion appears striated as it curves medially toward its decussation)
24 Central tegmental tract
47 Lateral lemniscus
54′ Nucleus centralis superior medialis
66 Corpus medullare of the cerebellar hemisphere
67 Brachium of the inferior colliculus

Arrowheads and arrows

Single white arrowhead: Cisternal portion of the trochlear nerve (CN IV). (These fibers arose solely within the contralateral trochlear nucleus.)
Three white arrowheads: The ventral (anterior) spinocerebellar tract at this level forms a thin lamina that curves around the superior border of the superior cerebellar peduncle to enter the cerebellum retrograde.
Single black arrow: Fascicles of the trigeminal nerve

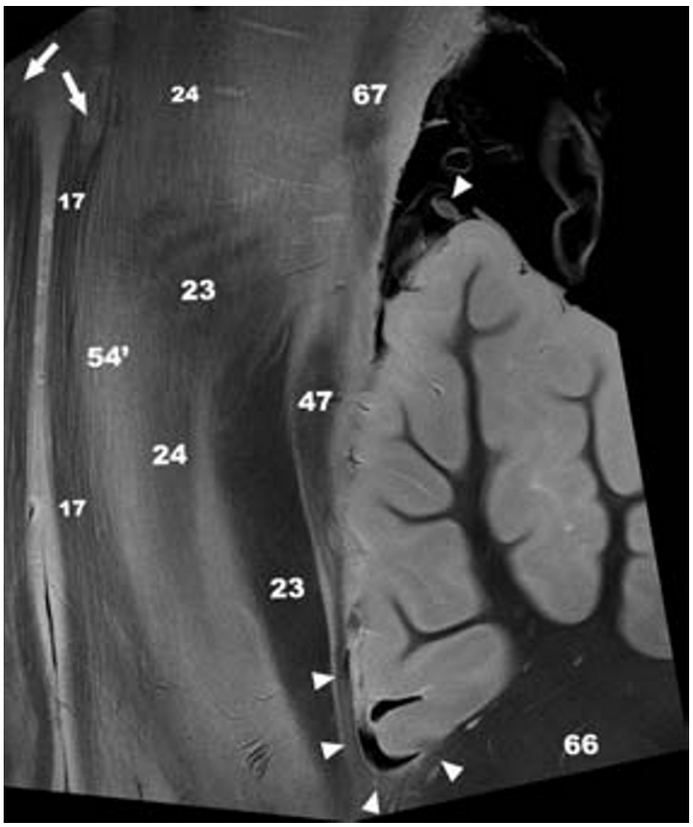

Fig. 8.94. Pontomesencephalic junction. Middle coronal section

The medial longitudinal fasciculus (17) of each side ascends to envelop the ventral border of the trochlear nucleus (paired white arrows). The nucleus centralis superioris (54′) lies lateral to the medial longitudinal fasciculus. The anterior spinocerebellar tract (white arrowheads) and lateral lemniscus (47) lie superficial to the lateral surface of the superior cerebellar peduncle (23). The cisternal segment of the trochlear nerve (single white arrowhead) courses around the brain stem.

17 Medial longitudinal fasciculus partially enclosing the trochlear nucleus (arrow), then continuing superiorly and ventrally toward the oculomotor nuclei (not seen)

23 Superior cerebellar peduncle
24 Central tegmental tract
47 Lateral lemniscus
54′ Nucleus centralis superior medialis
66 Corpus medullare of the cerebellar hemisphere
67 Brachium of the inferior colliculus

Arrowheads and arrows

Single white arrowhead: Cisternal portion of the trochlear nerve (CN IV)
Four white arrowheads: Ventral (anterior) spinocerebellar tract arching over the superior cerebellar peduncle
Paired white arrows: Left and right trochlear nerve nuclei

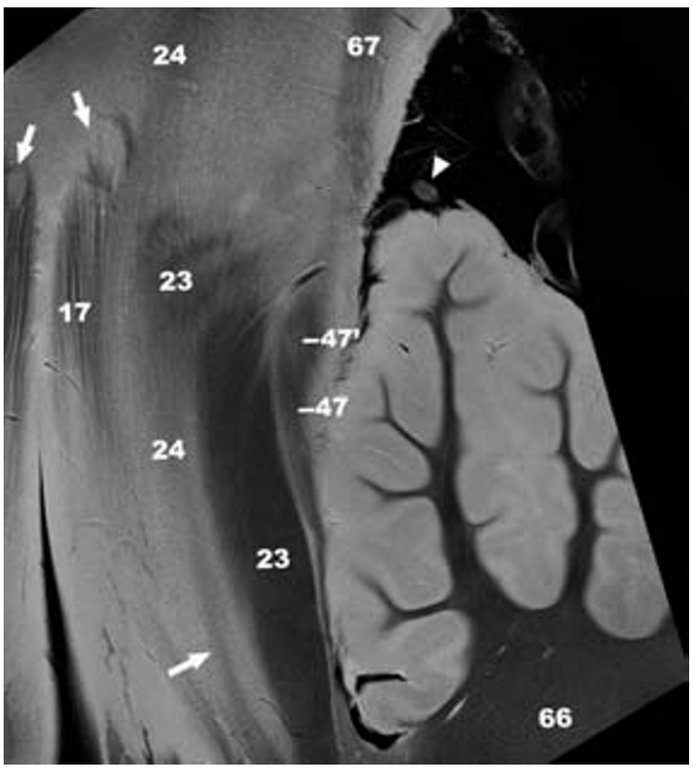

Fig. 8.95. Pontomesencephalic junction. Dorsal coronal section.

Superficial to the superior cerebellar peduncle (23), the lateral lemniscus (47) ascends to the inferior colliculus (not seen in this section). The brachium of the inferior colliculus (67) conveys auditory information further cranially from the inferior colliculus to the medial geniculate body. Deep to the superior cerebellar peduncle (23), the mesencephalic nucleus and tract (single white arrow) ascend into the midbrain. The central tegmental tract (24) descends past the decussation of the superior cerebellar peduncle (23) from the red nucleus rostrally to the inferior olivary nucleus caudally.

17 Medial longitudinal fasciculus partially enclosing the trochlear nucleus (arrows) superiorly
23 Superior cerebellar peduncle
24 Central tegmental tract
47 Lateral lemniscus
47′ Dorsal nucleus of the lateral lemniscus
66 Corpus medullare of the cerebellar hemisphere
67 Brachium of the inferior colliculus

Arrowheads and arrows

Single white arrowhead:	Cisternal portion of the trochlear nerve (CN IV)
Single white arrow:	Mesencephalic nucleus and tract of the trigeminal nerve (CN V)
Paired white arrows:	The two trochlear nerve nuclei partially enclosed by the medial longitudinal fasciculus (17)

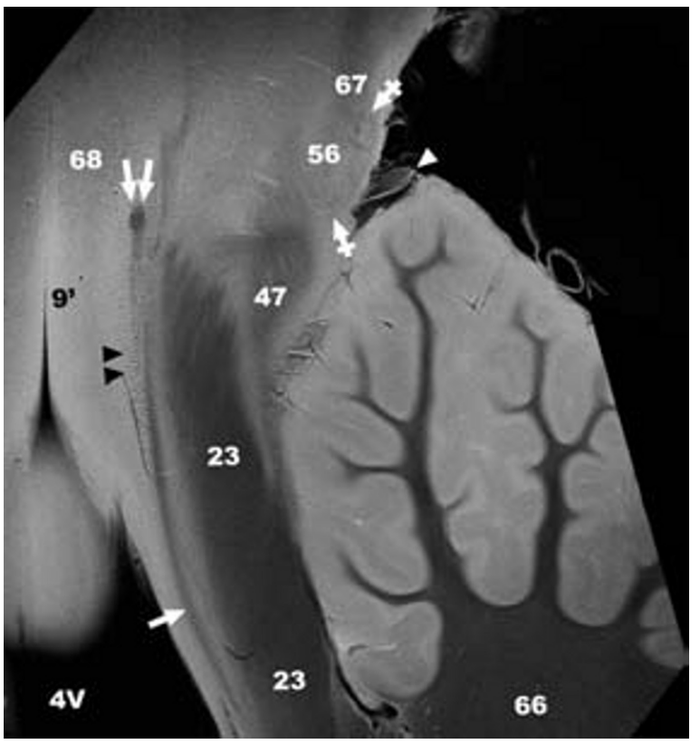

Fig. 8.96. Pontomesencephalic junction. Dorsal coronal section.

The inferior colliculus (56) is interposed between the lateral lemniscus (47) and the brachium (67) of the inferior colliculus. The mesencephalic nucleus and tract (single white arrow) of the trigeminal nerve form a thin well-defined stripe deep to the superior cerebellar peduncle (23). The locus ceruleus (paired black arrowheads) appears as a stippled band aligned with and just deep to the mesencephalic tract. The dorsal longitudal fasciculus (68) forms a thin faint band of fibers within the periaqueductal gray matter (9′). The superior medullary velum indents the midline portion of the fourth ventricle (4V).

9′ Periaqueductal gray matter
23 Superior cerebellar peduncle
47 Lateral lemniscus
56 Inferior colliculus
66 Corpus medullare of the cerebellar hemisphere
67 Brachium of the inferior colliculus
68 Dorsal longitudinal fasciculus

Letter labels
4V Fourth ventricle

Arrowheads and arrows

Single white arrowhead:	Cisternal segment of the trochlear nerve
Paired black arrowheads:	Locus ceruleus
Single white arrow:	Mesencephalic nucleus and tract of the trigeminal nerve (CN V)
Two white arrows:	Fascicle emerging from the ipsilateral trochlear nucleus and coursing postero-inferomedially toward the decussation in the superior medullary velum
Paired white crossed arrows:	Medullary lamina of the inferior colliculus

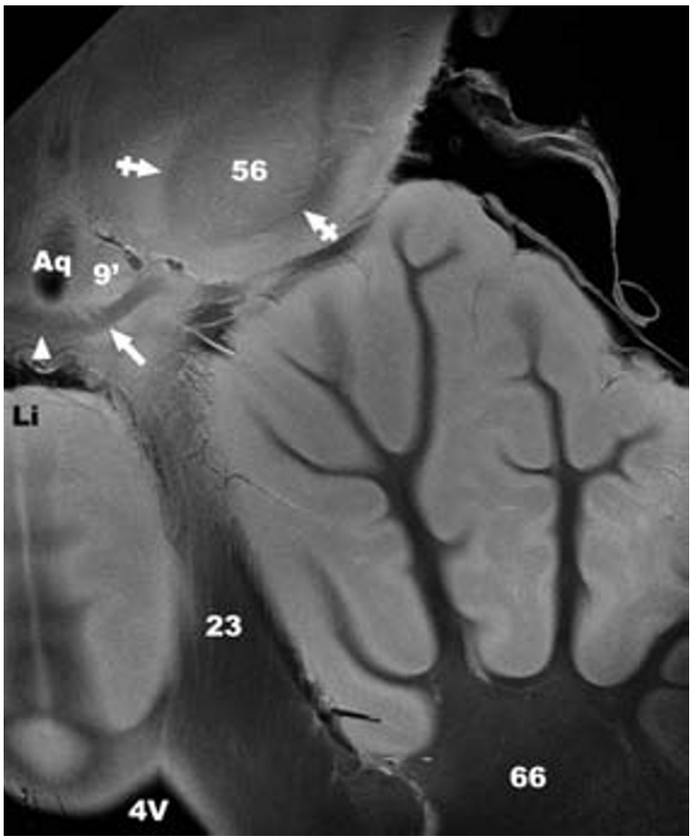

Fig. 8.97. Pontomesencephalic junction. Dorsal coronal section.

The trochlear nerve fascicles (white arrow) of both sides decussate (white arrowhead) in the superior medullary velum, just caudal to the inferior colliculi (56). The lingula of the vermis (Li) lies just superfical to the superior medullary velum, and contributes to the depression of the roof seen in the prior figure. The inferior colliculus (56) is readily identified by its well-defined capsule (crossed arrows).

9' Periaqueductal gray matter
23 Superior cerebellar peduncle
56 Inferior colliculus
66 Corpus medullare of the cerebellar hemisphere

Letter labels
4V Fourth ventricle
Aq Cerebral aqueduct (of Sylvius)
Li Lingula

Arrowheads and arrows
Single white arrowhead: Decussation of the trochlear nerves
Single white arrow: Fascicles of the trochlear nerve
Paired white crossed arrows: Medullary laminae of the inferior colliculus

D. Mesencephalic-diencephalic junction (Figs. 8.98–8.120)

D 1. Axial Mesencephalic-Diencephalic Junction

Axial sections displayed from caudal to cranial (Figs. 8.98–8.100)

See also **Figs. 2.21C and 2.22C** for more superior axial sections through the diencephalon.

These cartoons (A–B) display the anatomic region imaged in **Figs. 8.98–8.120**.

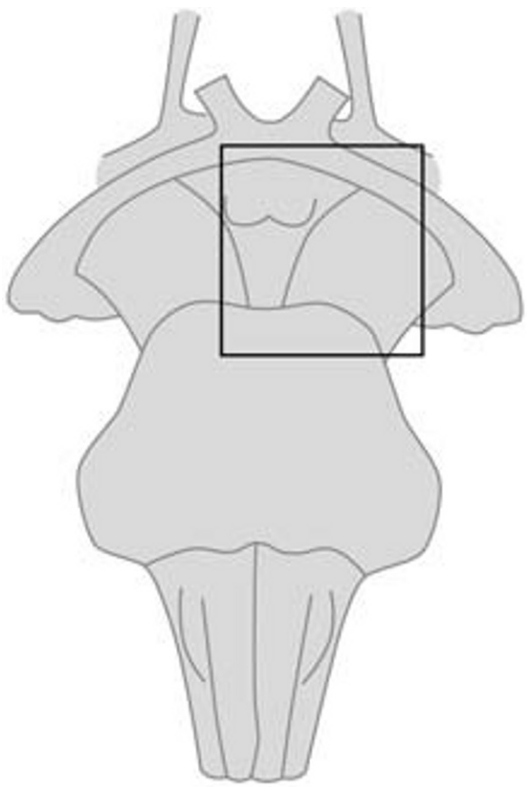

A

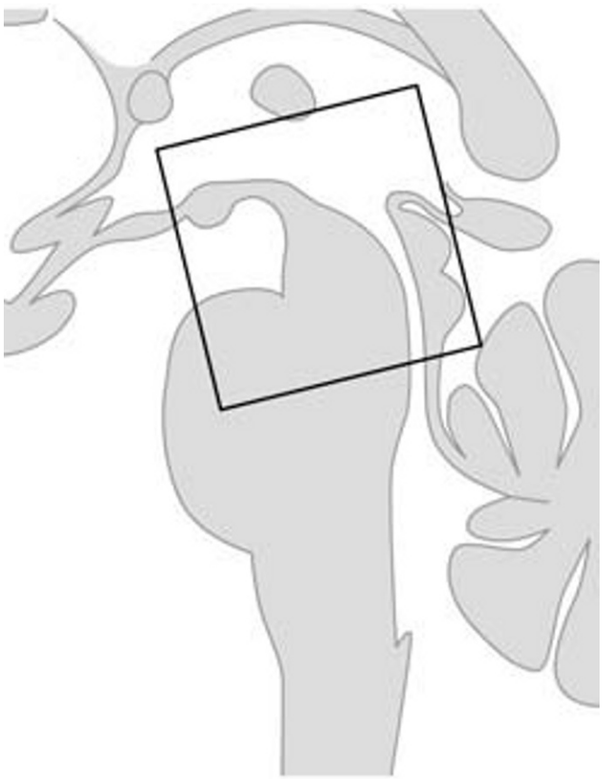

B

Fig. 8.98. Mesencephalic-diencephalic junction. Axial section through the inferior colliculus.

The inferior colliculus (56) gives rise to the brachium of the inferior colliculus (67), which extends to the medial geniculate body (See Fig. 8.99). Marginal fibers (paired black arrowheads) delimit the periaqueductal gray matter (9′) from the surrounding tegmentum. The decussation of the inferior colliculus (single black arrowhead) thickens the fiber bundle at the dorsal edge of the periaqueductal gray matter (9′) (See Figs. 8.101 and 8.120). The paired trochlear nuclei (two black arrows) and medial longitudinal fasciculi (17) lie at the ventral edge of the periaqueductal gray matter at this level. The superior cerebellar peduncle decussates ventral to the medial longitudinal fasciculus (17). The descending rubrospinal fibers decussate (7′) in the ventral tegmental decussation (also 7′) just dorsal to the interpeduncular nucleus (61) and then diverge inferolaterally as the descending rubrospinal tracts (7) on the contralateral side [78, 358]. The frontopontine tract (F), corticospinal tract (CS), and parietotemporopontine tract (PT) descend through the cerebral peduncle to each side of the interpeduncular fossa (IP). The partes reticulata (r) and compacta (c) of the substantia nigra (64) layer just deep to the cerebral peduncle. The stippling seen in the substantia nigra is also seen in the locus ceruleus (See Figs. 8.64, 8.96 and 10.1–10.3) and may result from the neuromelanin.

7 Rubrospinal tract
7′ Ventral tegmental dedcussation
9′ Periaqueductal gray matter
10 Spinothalamic tract
17 Medial longitudinal fasciculus
21 Medial lemniscus
22 Ventral central trigeminothalamic tract
23 Superior cerebellar peduncle
23′d Decussation of 23 (dorsal portion)
23′v Decussation of 23 (ventral portion)
24 Central tegmental tract
52 Dorsal trigeminothalamic tract
53 Tegmento-olivary tract
56 Inferior colliculus
61 Interpeduncular nucleus
64c Pars compacta of substantia nigra
64r Pars reticulata of substantia nigra
67 Brachium of the inferior colliculus
110 Nucleus lateralis mesencephali [358]
191 Sagulum

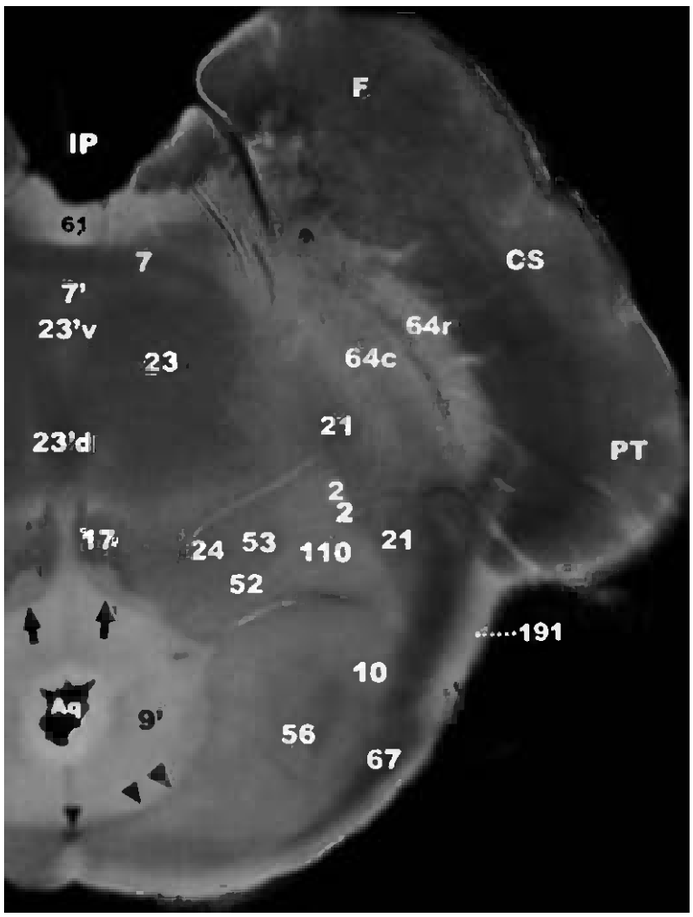

Letter labels

Aq Cerebral aqueduct (of Sylvius)
CS Corticospinal tract
F Frontopontine tract
IP Interpeduncular fossa
PT Parietotemporopontine tract

Arrowheads and arrows

Single black arrowhead: Decussation of the inferior colliculus
Paired black arrowheads: Marginal fibers of the periaqueductal gray matter
Paired black arrows: Nuclei of the trochlear nerve (CN IV)

Fig. 8.99. Mesencephalic-diencephalic junction. Axial section through the superior colliculus.

At this level, the oculomotor nuclei (paired black arrows) lie at the ventral edge of the periaqueductal gray matter (9′). The parasympathetic subnuclei of Edinger-Westphal lie dorsomedially, and provide presynaptic innervation to the ciliary ganglion for the ciliary and pupillary constrictors [467]. The dorsal longitudinal fasciculi manifest as faint crescents of white matter dorsal to these nuclei, within the ventral periaqueductal gray matter (9′). The medial longitudinal fasciculi (17) lie ventrolateral to the oculomotor nuclei. The oculomotor fibers curve gracefully as they pass ventrally through, and medial to, the red nuclei (95) and interpeduncular nucleus (unlabeled) to reach (white arrows) the medial aspect of the cerebral peduncle at the interpeduncular fossa (IP). The brachium of the inferior colliculus (67) reaches to the medial aspect (hilum) of the medial geniculate body (104). The central tegmental tract (24) lies near to its origin in the red nucleus (95). The rubrospinal fibers (7) arise from the medial aspect of the red nuclei. Prerubral radiations (cerebellorubrothalamic tracts, 96) partially circumscribe the red nucleus. The ascending ventral trigeminothalamic tract (22) along the dorsal border of the medial lemniscus (21) converges towrd the ascending dorsal trigeminothalamic tract (52), which lies dorsolateral to the red nucleus (95). The superior colliculus (69) shows distinct lamination, with alternating layers of gray matter (G1-G3) and white matter (S1-S3).

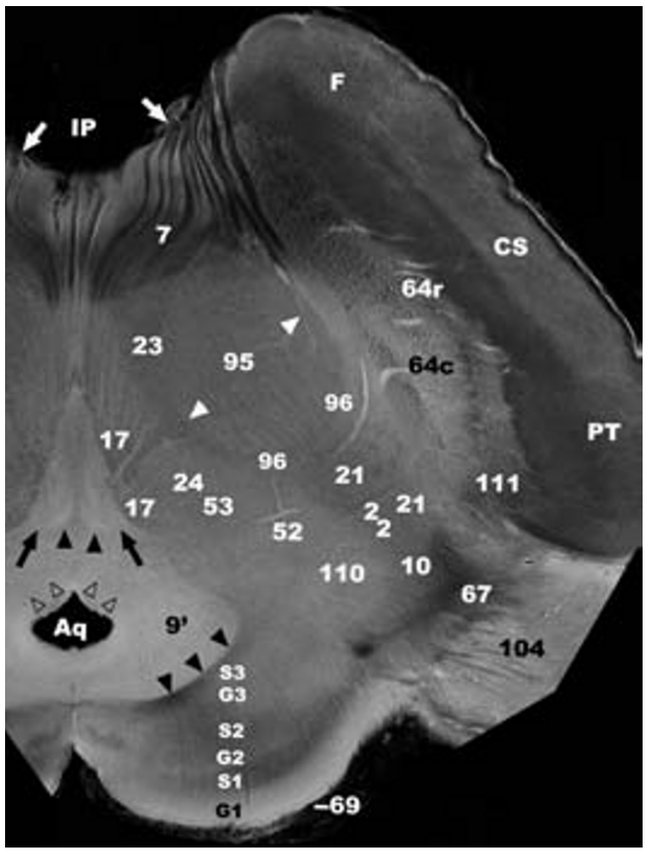

7 Rubrospinal fibers arising from the medial red nucleus
9′ Periaqueductal gray matter
10 Spinothalamic tract
17 Medial longitudinal fasciculus
21 Medial lemniscus
22 Ventral trigeminothalamic tract
23 Superior cerebellar peduncle
24 Central tegmental tract
52 Dorsal trigeminothalamic tract [106]
53 Tegmento-olivary tract
64c Pars compacta of substantia nigra
64r Pars reticulata of substantia nigra
67 Brachium of the inferior colliculus
69 Superior colliculus
95 Red nucleus within its capsule (white arrowheads)
96 Prerubral radiations (cerebellorubrothalamic tract)
104 Medial geniculate body (trimmed laterally)
110 Nucleus lateralis mesencephali [358]
111 Pallidonigral and corticonigral tracts

Letter labels

Aq Cerebral aqueduct (of Sylvius)
CS Corticospinal tract
G1 Stratum griseum primum (superficiale). The faint thin black line at the superficial margin of G1 may be the stratum zonale.
G2 Stratum griseum secundum (medium)
G3 Stratum griseum tertium (profundum)
F Frontopontine tract
IP Interpeduncular fossa
PT Parietotemporopontine tract
S1 Stratum opticum of the superior colliculus
S2 Stratum lemnisci of the superior colliculus
S3 Stratum profundum of the superior colliculus.

Arrowheads and arrows

Paired white arrowheads: Capsule of the red nucleus (95)
Hollow arrowheads: Dorsal longitudinal fasciculus in the ventral periaqueductal gray matter
Paired black arrowheads: Nucleus of Edinger-Westphal (parasympathetic) of each side
Triple black arrowheads: Marginal fibers of the periaqueductal gray matter
Paired white arrows: Fascicles of the oculomotor nerves (CN III) emerging into the interpeduncular fossa (IP). Note their curved path through the midbrain
Paired black arrows: Oculomotor nuclei (CN III) of both sides

Fig. 8.100. Mesencephalic-diencephalic junction. Rostral axial section through the subthalamic nucleus and posterior commissure.

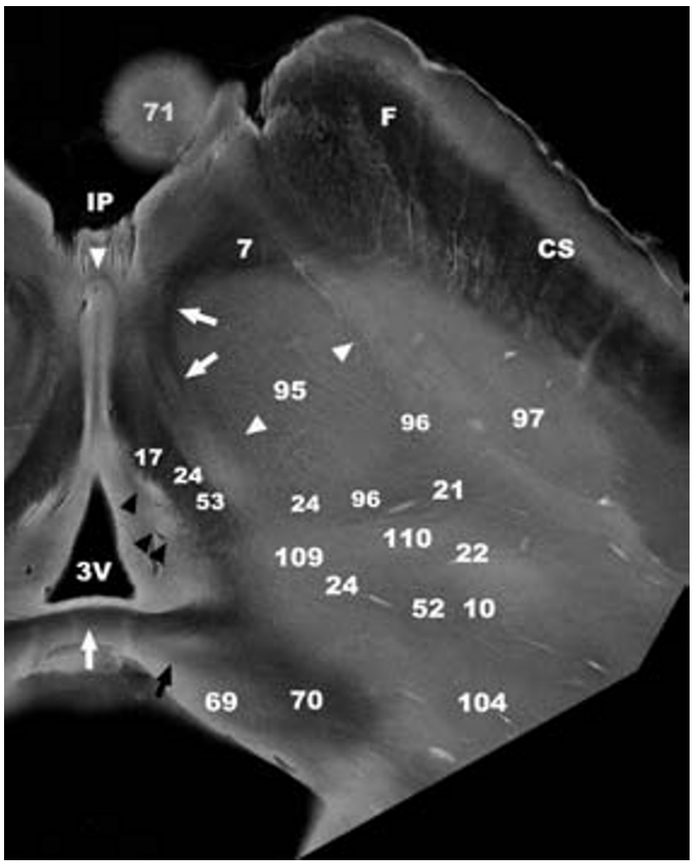

The posterior commissure (single white arrow) forms a prominent tract at the dorsal aspect of the third ventricle. The interstitial nucleus of Cajal (single black arrowhead) and the nucleus of Darkschewitsch (paired black arrowheads) are accessory oculomotor nuclei seen in the paramedian gray matter in relation to the medial longitudinal fasciculus (17) [78]. The interstitial nucleus of Cajal (single black arrowhead) lies in and lateral to the fibers of the medial longitudinal fasciculus [78]. It sends fibers to both trochlear nuclei, to much of the contralateral oculomotor nucleus (via the posterior commissure), and to the ipsilateral medial vestibular nucleus and spinal cord [78]. It is the vertical gaze center for conjugated vertical eye movements and maintains eye position following saccades involving vertical and rotational eye movements [322a]. The nucleus of Darkschewitsch (paired black arrowheads) lies in the subependymal gray matter of the wall of the third ventricle, lateral to the nucleus of Edinger-Westphal. Its fibers make up a large part of the posterior commissure and extend to the medial longitudinal fasciculi bilaterally [358]. Riley considers the nucleus of Darkschewitsch to be synonymous with the nucleus of the posterior commissure [358]. However, Carpenter and Sutin define the nuclei of the posterior commissure as a group of cells that collectively surround the posterior commissure rostrally, laterally and ventrally, and distinguish these from the accessory oculomotor nucleus of Darkschewitsch [78]. The habenulo-interpeduncular tract, and the nucleus contained within it, form a "triplet" signal (paired white arrows) as they curve along the medial border of the red nucleus (95). The superior colliculus (69) gives rise to the decussation of the superior colliculus (black arrow) medially and the brachium of the superior colliculus (70) laterally. The subthalamic nucleus (97) appears as a distinct lens of gray matter just deep to the substantia nigra and cerebral peduncle.

7 Rubrospinal tract
10 Spinothalamic tract
17 Medial longitudinal fasciculus
21 Medial lemniscus
22 Ventral trigeminothalamic tract
24 Central tegmental tract (components) [106]
52 Dorsal trigeminothalamic tract
53 Tegmento-olivary tract
69 Superior colliculus
70 Brachium of the superior colliculus
71 Mammillary body
95 Red nucleus within its capsule (white arrowheads)
96 Prerubral radiations (cerebellorubrothalamic tract)
97 Subthalamic nucleus
104 Medial geniculate body
109 Nucleus medialis mesencephali
110 Nucleus lateralis mesencephali [358]

Letter labels

3V Third ventricle
CS Corticospinal tract
F Frontopontine tract
IP Interpeduncular fossa

Arrowheads and arrows

Single white arrowhead: Ventral tegmental decussation
Single black arrowhead: Interstitial nucleus of Cajal
Paired white arrowheads: Capsule of the red nucleus (95)
Paired black arrowheads: Nucleus of Darkschewitsch
Single white arrow: Posterior commissure (with commissure of the superior colliculus along its dorsal border)
Single black arrow: Commissural fibers of the superior colliculus (69)
Paired white arrows: Habenulo-interpeduncular tract (fasciculus retroflexus)

Additional more cephalic axial sections are displayed in **Figs. 2.20–2.22**.

D 2. Sagittal Mesencephalic-Diencephalic Junction

Sagittal sections displayed from the midline to lateral (Figs. 8.101–8.108)

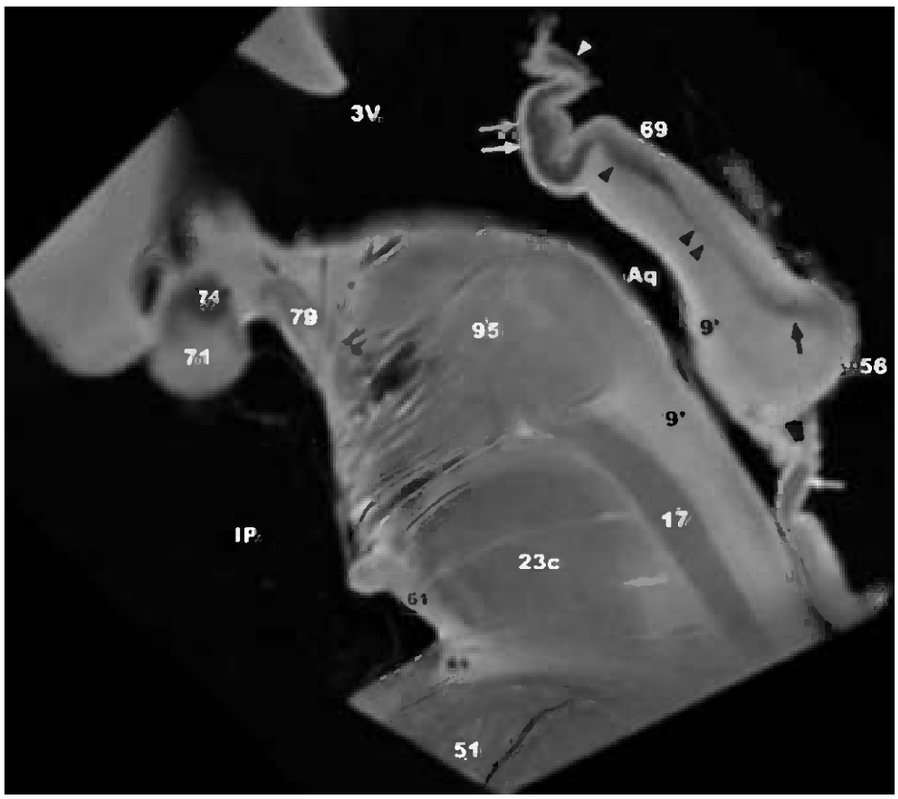

Fig. 8.101. Mesencephalic-diencephalic junction. Midline sagittal section.

Dorsally, the tectum shows a prominent dark band (the commissural layer) formed by the commissure of the superior colliculus (single black arrowhead), marginal fibers of the periaqueductal gray matter (paired black arrowheads) and the commissure of the inferior colliculus (single black arrow). The habenular commissure (single white arrowhead) and posterior commissure (double white arrows) align with the commissural layer of the tectum. The decussation (single white arrow) of the trochlear nerves is seen in the superior medullary velum of the fourth ventricle. Ventrally, the medial longitudinal fasciculus (17) ascends into the midbrain just dorsal to the crossed fibers of the superior cerebellar peduncle (23c). Rostral to the medial longitudinal fasciculus (17) the red nucleus (95) is traversed by the oculomotor fibers. The multiple parallel striations ventral to the red nucleus represent both oculomotor fibers and perforating vessels of the anteromedial group. The interpeduncular nucleus (61) delineates the interpeduncular fossa (IP). Rostrally, the mammillary body (71) gives rise to the principal mammillary fasciculus (74) and a group of fibers (79) interconnecting the tegmentum with the hypothalamus.

9′ Periaqueductal gray matter
17 Medial longitudinal fasciculus
23c Cruciate portion of the superior cerebellar peduncle (post decussation fiber mass) [358]
51 Pontocerebellar fibers
56 Inferior colliculus
61 Interpeduncular nucleus
69 Superior colliculus
71 Mammillary body
74 Principal mammillary fasciculus
79 Hypothalamo-tegmental fibers, supramammillary commissure and peduncle of the mammillary body
95 Red nucleus

Letter labels

3V Third ventricle
Aq Cerebral aqueduct (of Sylvius)
IP Interpeduncular fossa

Arrowheads and arrows

Single white arrowhead: Habenular commissure
Single black arrowhead: Decussation of the superior colliculus
Paired black arrowheads: Marginal fibers of the periaqueductal gray matter, separating the periaqueductal gray matter from the tegmentum of the midbrain. They include portions of the mesencephalic root of the trigeminal nerve (CN V)
Single white arrow: Decussation of the trochlear nerve fascicles
Single black arrow: Decussation of the inferior colliculus
Paired white arrows: Posterior commissure

Fig. 8.102. Mesencephalic-diencephalic junction. Paramedian sagittal section.

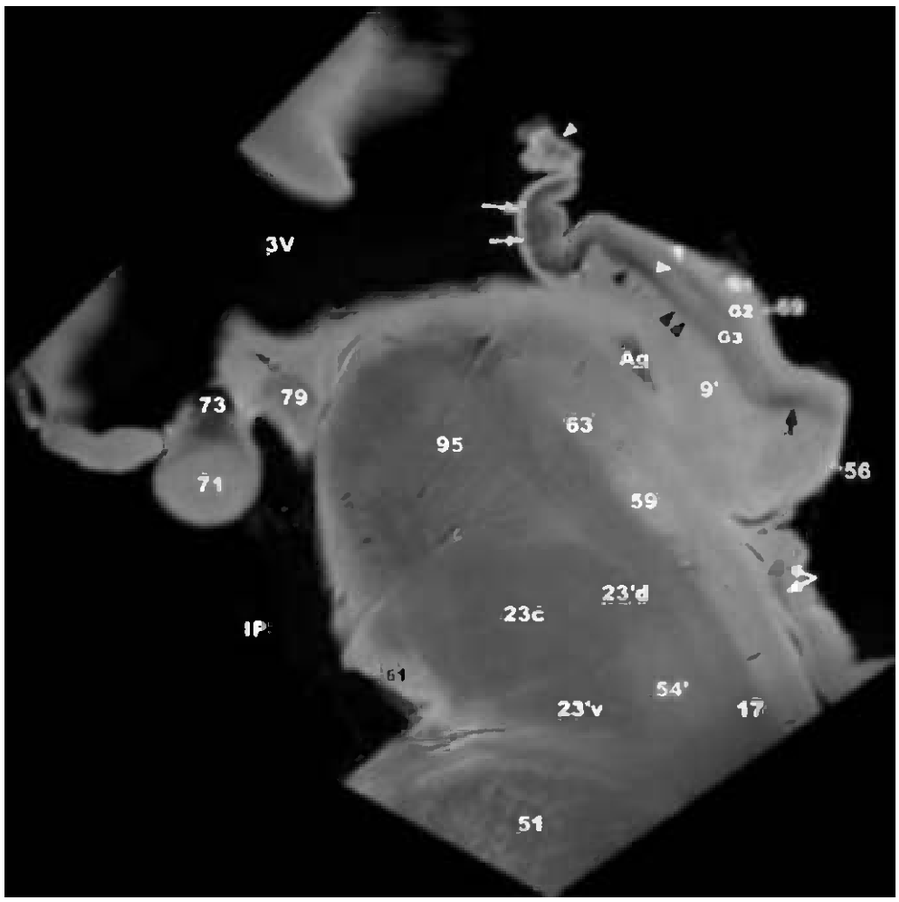

Just to each side of midline, the medial longitudinal longitudinal fasciculus (17) ascends along the ventral aspects of the trochlear nucleus (59) and the oculomotor nucleus (63). The superior cerebellar peduncle shows separate dorsal (23'd) and ventral (23'v) bundles of decussating fibers.

9' Periaqueductal gray matter
17 Medial longitudinal fasciculus
23c Cruciate portion of the superior cerebellar peduncle (post decussation fiber mass) [358]
23'd Decussation of the superior cerebellar peduncle (dorsal portion)
23'v Decussation of the superior cerebellar peduncle (ventral portion)
51 Pontocerebellar fibers
54' Nucleus centralis superior medialis
56 Inferior colliculus
59 Nucleus of the trochlear nerve (CN IV)
61 Interpeduncular nucleus
63 Nucleus of the oculomotor nerve (CN III)
69 Superior colliculus
71 Mammillary body
73 Principal mammillary fasciculus
79 Hypothalamo-tegmental fibers and peduncle of the mammillary body
95 Red nucleus

Letter labels

3V Third ventricle
Aq Cerebral aqueduct (of Sylvius)
G1 Stratum griseum primum (superficiale). The faint thin black line at the superfical margin of G1 may be the stratum zonale.
G2 Stratum griseum secundum (medium)
G3 Stratum griseum tertium (profundum)
IP Interpeduncular fossa

Arrowheads and arrows

Single white arrowhead: Habenular commissure
Paired white arrowheads: Stratum lemnisci of the quadrigeminal plate
Single black arrowhead: Decussation of the superior colliculus
Paired black arrowheads: Marginal fibers of the periaqueductal gray matter, including the stratum profundum of the white matter of the superior colliculus
Single black arrow: Decussation of the inferior colliculus
Branched white arrow: Decussating trochlear nerve fascicles
Paired white arrows: Posterior commissure

Fig. 8.103. Mesencephalic-diencephalic junction. Parasagittal section.

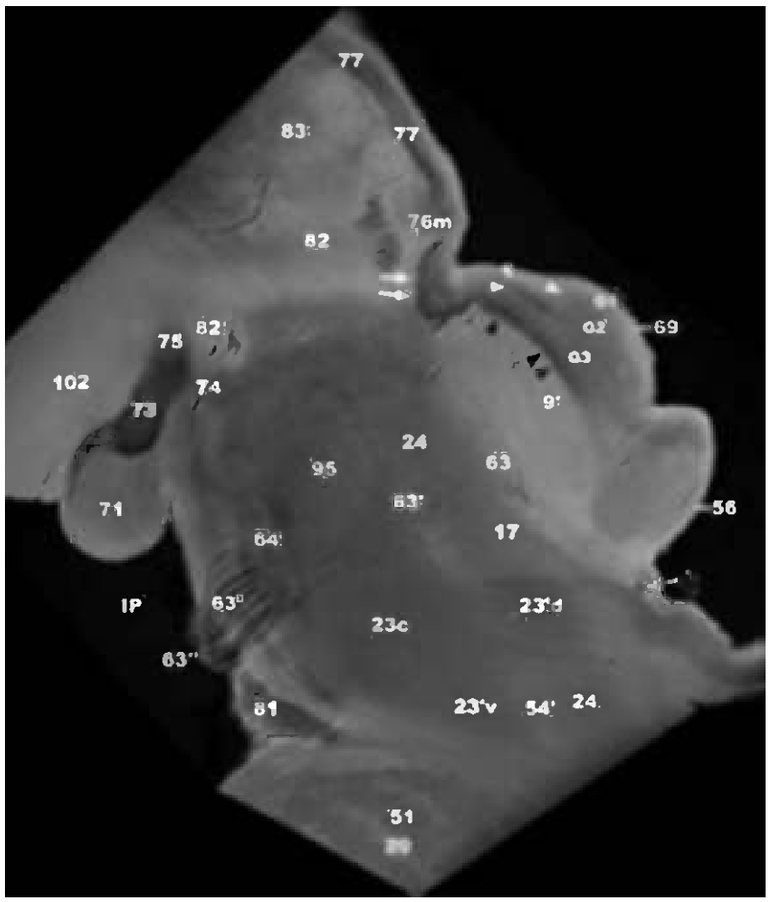

The stria medullaris thalami (77) courses over the dorsomedial nucleus of the thalamus (83) to reach the habenular nuclei (here the medial habenular nucleus, 76m). The principal mammillary fasciculus (73) ascends from the mammillary body (71) and divides into the mammillothalamic tract (75) directed toward the anterior nuclei of the thalamus, and the mammillotegmental tract (74) directed toward the dorsal and ventral tegmental nuclei of the midbrain. The course of the oculomotor fibers from the nucleus (63), through the parenchyma of the midbrain (63′) to the interpeduncular fossa (63″) is shown in segments, because the sinuous course of the oculomotor fibers arches into and out of any single sagittal section. The medialmost portion of the cerebral peduncle contains corticobulbar fibers (81).

9′ Periaqueductal gray matter
17 Medial longitudinal fasciculus
20 Pontine nuclei
23c Cruciate portion of the superior cerebellar peduncle
23′d Decussation of the superior cerebellar peduncle (dorsal portion)
23′v Decussation of the superior cerebellar peduncle (ventral portion)
24 Central tegmental tract
51 Pontocerebellar fibers
54′ Nucleus centralis superior medialis
56 Inferior colliculus
63 Oculomotor nucleus
63′ Intramesencephalic fibers of the oculomotor nerve
63″ Fibers of the oculomotor nerve emerging into the interpeduncular fossa (IP)
64 Substantia nigra
69 Superior colliculus
71 Mammillary body
73 Principal mammillary fasciculus
74 Mammillotegmental tract
75 Mammillothalamic fasciculus
76m Medial habenular nucleus
77 Stria medullaris thalami interconnecting septal and habenular nuclei (76m)
81 Corticobulbar fibers in the medial cerebral peduncle
82 Nuclei mediani thalami (group of nuclei including the more medial portions of the nucleus medialis thalami, the nucleus centri mediani thalami, and the subependymal collections of thalamic nuclei) [358]
83 Nucleus dorsomedialis thalami
95 Red nucleus
102 Hypothalamus

Letter labels

G1 Stratum griseum primum (superficiale). The faint thin black line at the superfical margin of G1 may be the stratum zonale.
G2 Stratum griseum secundum (medium)
G3 Stratum griseum tertium (profundum)
IP Interpeduncular fossa

Arrowheads and arrows

Single white arrowhead: Stratum opticum of the superior colliculus
Paired white arrowheads: Stratum lemnisci of the superior colliculus
Single black arrowhead: Decussation of the superior colliculus
Paired black arrowheads: Marginal fibers of the periaqueductal gray matter, including the stratum profundum of the white matter of the superior colliculus
Single white arrow: Trochlear nerve fascicles passing medially to their decussation
Paired white arrows: Posterior commissure

Fig. 8.104. Mesencephalic-diencephalic junction. Parasagittal section.

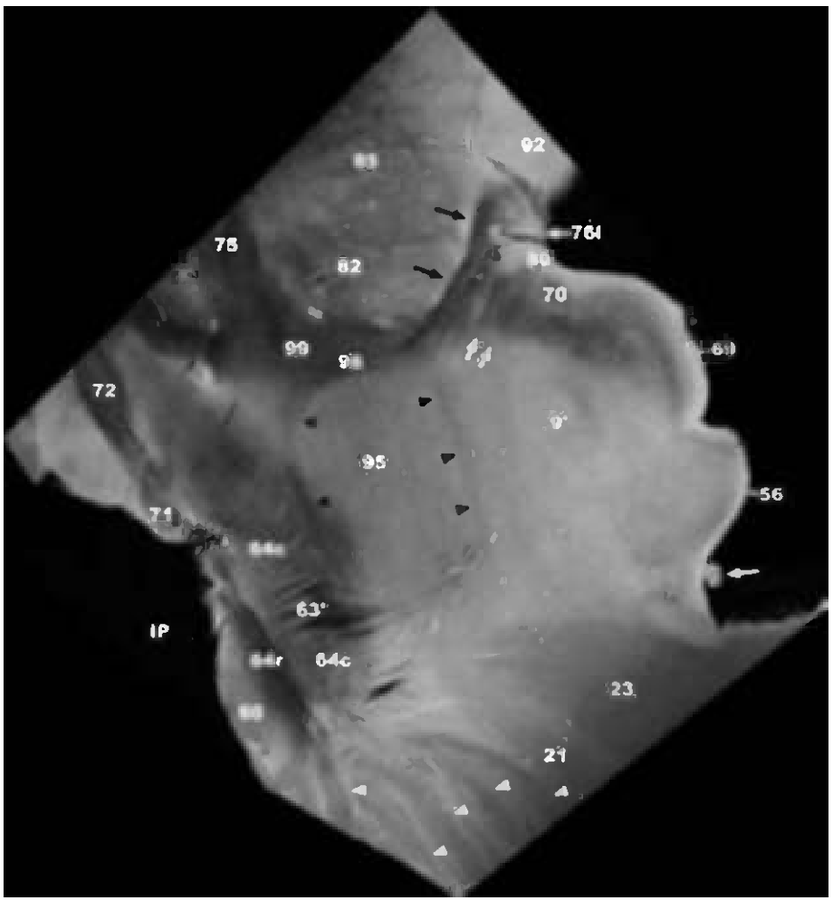

The medial and lateral habenular nuclei (here the lateral habenular nucleus, 76l) give rise to the habenulo-interpeduncular tract (fasciculus retroflexus) (paired black arrows). This angles obliquely along the medial aspect of the rostral portion of the red nucleus (95) and then recurves, ventral and inferior to the red nucleus, to reach the ventral interpeduncular nucleus and midline reticular nuclei [78]. Fibers from the medial habenular nucleus end solely in the interpeduncular nucleus [322]. Efferents of the interpeduncular nucleus project massively to the nucleus centralis superior (See **Figs. 8.61** and **8.78**) and the dorsal raphe nuclei [322]. Fibers from the lateral habenular nucleus descend through the habenulo-interpeduncular tract, bypass the interpeduncular nucleus, and terminate widely in the pars compacta of substantia nigra, ventral periaqueductal gray matter, nucleus centralis superior, and dorsal raphe nuclei [322]. The lateral end of the posterior commissure (paired white arrows) extends into this section inferior to the habenular nuclei. Fibers from the globose, emboliform and dentate nuclei of the cerebellum ascend via the superior cerebellar peduncle (23) to terminate in the red nucleus (95). The prerubral radiations (cerebellothalamic tract) (96) include fibers from these nuclei that bypass the red nucleus to synapse in the thalamus (intermediate ventral, anterior ventral, and intralaminar nuclei) [294]. The anterior column of the fornix (72) curves ventrally to reach the mammillary body (71). The upper end of the mammillothalamic tract (75) continues toward the anterior nucleus of the thalamus. The thin trochlear nerve (white arrow) is cut in cross section as it curves around the midbrain.

9′ Periaqueductal gray matter
21 Medial lemniscus
23 Superior cerebellar peduncle
56 Inferior colliculus
60 Cerebral peduncle
63′ Intramesencephalic fibers of the oculomotor nerve
64c Pars compacta of substantia nigra
64r Pars reticulata of substantia nigra
69 Superior colliculus
70 Brachium of the superior colliculus
71 Mammillary body (capsule)
72 Fornix (anterior column)
75 Mammillothalamic tract
76l Lateral habenular nucleus
80 Pretectal area
82 Nuclei mediani thalami
85 Nucleus medialis thalami, pars ventromedianis
92 Pulvinar
95 Red nucleus
96 Prerubral radiations (cerebellorubrothalamic tract)
99 Fields of Forel (group label for fields H, H1 and H2)

Letter labels

IP Interpeduncular fossa

Arrowheads and arrows

Multiple white arrowheads: Descending cortical fibers
Multiple black arrowheads: Capsule of the red nucleus
Single white arrow: Trochlear nerve (cisternal segment)
Paired white arrows: Posterior commissure (lateral portion)
Paired black arrows: Habenulo-interpeduncular tract (fasciculus retroflexus)

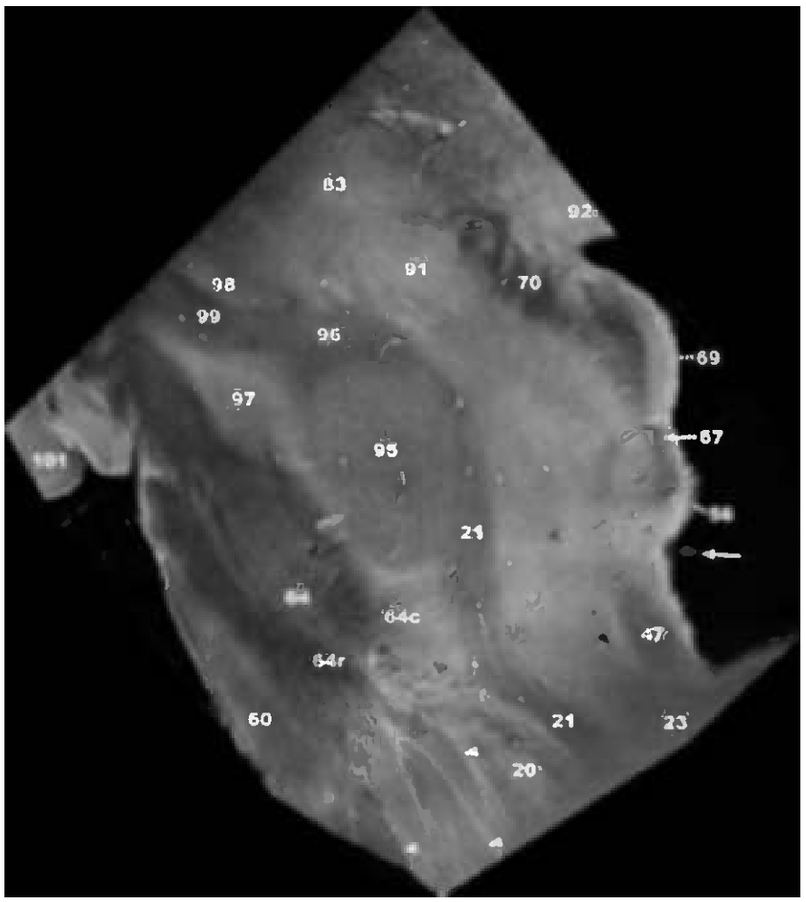

Fig. 8.105. Mesencephalic-diencephalic junction. Sagittal section.

The inferior colliculus (56) gives rise to the brachium (67) of the inferior colliculus. The superior colliculus (69) gives rise to the brachium (70) of the superior colliculus. The medial lemniscus (21) ascends through the midbrain around the red nucleus, to reach the ventral posterolateral nucleus of the thalamus. The centromedian nucleus (91) of the thalamus lies rostral to the red nucleus. The cerebral peduncle (60), substantia nigra (64), subthalamic nucleus (97), Forel fields (99), and zona incerta (98) form a series of strata from superficial ventral to deep dorsal position.

21 Medial lemniscus
23 Superior cerebellar peduncle
47 Lateral lemniscus
56 Inferior colliculus
60 Cerebral peduncle
64 Substantia nigra
64c Pars compacta of substantia nigra
64r Pars reticulata of substantia nigra
67 Brachium of the inferior colliculus
69 Superior colliculus
70 Brachium of the superior colliculus
83 Nucleus dorsomedialis thalami
91 Centromedian nucleus of the thalamus
92 Pulvinar of the thalamus
95 Red nucleus
96 Prerubral tract (cerebellorubrothalamic tract)
97 Subthalamic nucleus
98 Zona incerta
99 Fields of Forel (group label for fields H, H1 and H2)
101 Optic tract

Arrowheads and arrows

Multiple white arrowheads: Descending cortical fibers
Single white arrow: Trochlear nerve (cisternal segment)

Fig. 8.106. Mesencephalic-diencephalic junction. Sagittal section.

The auditory pathway can be traced through the lateral lemniscus (47), inferior colliculus (see prior sections), brachium (67) of the inferior colliculus, and medial geniculate body (104). The brachium (70) of the superior colliculus arches over the medial geniculate body to reach the medial aspect of the lateral geniculate body (**See Figs. 8.141–8.147**). The optic tract (101) curves along the surface of the cerebral peduncle to reach the anterior pole of the lateral geniculate body (**See Figs. 8.141–8.147**). The rostral end of the medial lemniscus (21) and the rostral end of the spinothalamic tract (10) converge, as both approach the ventral posterolateral nucleus of the thalamus. Rostrolateral to the lens-shaped subthalamic nucleus (97), the zona incerta (98) lies between the thalamic fasciculus (Forel field H1) and the lenticular fasciculus (Forel field H2). The zona incerta is regarded as a rostral extension of the brain stem reticular formation. It receives input from a wide range of structures, including the medial prefrontal, cingulate and somatosensory cortices, the amygdala, the substantia innominata, the hypothalamus and the brain stem [322]. It sends fibers to the thalamus, hypothalamus, multiple midbrain nuclei, the inferior olivary nucleus and the spinal cord [322].

10 Spinothalamic tract
21 Medial lemniscus
47 Lateral lemniscus
60 Cerebral peduncle
64 Substantia nigra
64c Pars compacta of substantia nigra
64r Pars reticulata of substantia nigra
67 Brachium of the inferior colliculus
70 Brachium of the superior colliculus
80 Pretectal area
91 Centromedian nucleus of the thalamus
93m Ventral posteromedial nucleus of the thalamus
96 Prerubral radiations
97 Subthalamic nucleus
98 Zona incerta
101 Optic tract
104 Medial geniculate body

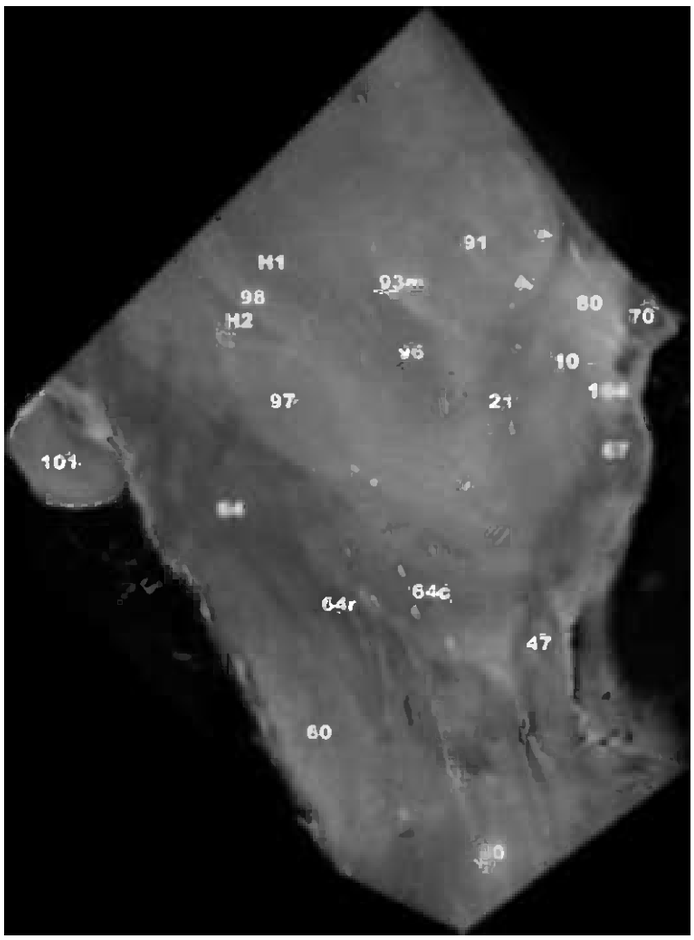

Letter labels
H1 Forel field H1 (thalamic fasciculus)
H2 Forel field H2 (lenticular fasciculus)

Arrowheads and arrows
Paired white arrowheads: Capsule of the nuclei centri mediani thalami

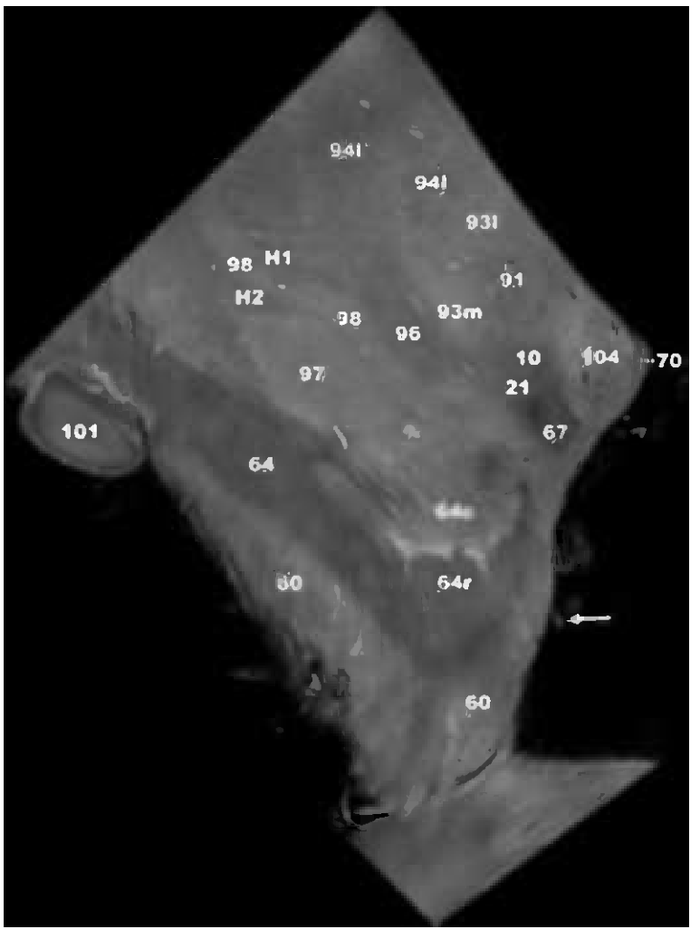

Fig. 8.107. Mesencephalic-diencephalic junction. Sagittal section.

The cerebral peduncle (60), substantia nigra (64) and subthalamic nucleus (97) form broad arches of tissue in lateral sections. The medial lemniscus (21) and spinothalamic tract (10) are now approximated. The zona incerta (two 98s) displays its characteristic serpentine configuration (See Fig. 8.108). The approximate locations of multiple thalamic nuclei are noted.

10 Spinothalamic tract (nearing the ventral posteromedial nucleus of the thalamus (93m))
21 Medial lemniscus (nearing the ventral posterolateral nucleus of the thalamus (93l))
60 Cerebral peduncle
64 Substantia nigra
64c Substantia nigra, pars compacta
64r Substantia nigra, pars reticulata
67 Brachium of the inferior colliculus
70 Brachium of the superior colliculus (crossing over the medial geniculate body (104))
91 Centromedian nucleus of the thalamus
93m Ventral posteromedial nucleus of the thalamus
93l Ventral posterolateral nucleus of the thalamus
94i Ventral intermediate nucleus of the thalamus
94l Ventral lateral nucleus of the thalamus
96 Prerubral radiations (cerebellorubrothalamic tract)
97 Subthalamic nucleus
98 Zona incerta
101 Optic tract
104 Medial geniculate body

Letter labels
H1 Forel field H1 (thalamic fasciculus)
H2 Forel field H2 (lenticular fasciculus)

Arrowheads and arrows
Single white arrow: Trochlear nerve (cisternal segment)

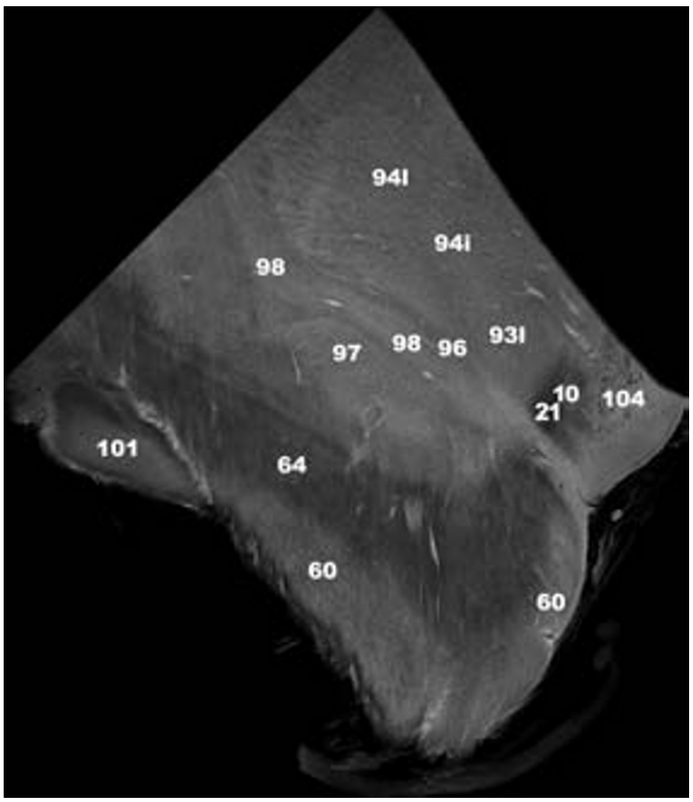

Fig. 8.108. Mesencephalic-diencephalic junction. Sagittal section.

The medial lemniscus (21) and spinothalamic tract (10) reach the ventral posterolateral nucleus of the thalamus (93l). A phylogenetically older portion, the paleospinothalamic tract, extends to the intralaminar nuclei of the thalamus [164, 322a]. The serpentine zona incerta (two 98s) extends from the top edge of the specimen to the level of the substantia nigra (64).

10 Spinothalamic tract
21 Medial lemniscus
60 Cerebral peduncle
64 Substantia nigra
93l Ventral posterolateral nucleus of the thalamus
94i Ventral intermediate nucleus of the thalamus
94l Ventral lateral nucleus of the thalamus
96 Prerubral radiations (cerebellorubrothalamic tract)
97 Subthalamic nucleus
98 Zona incerta
101 Optic tract
104 Medial geniculate body

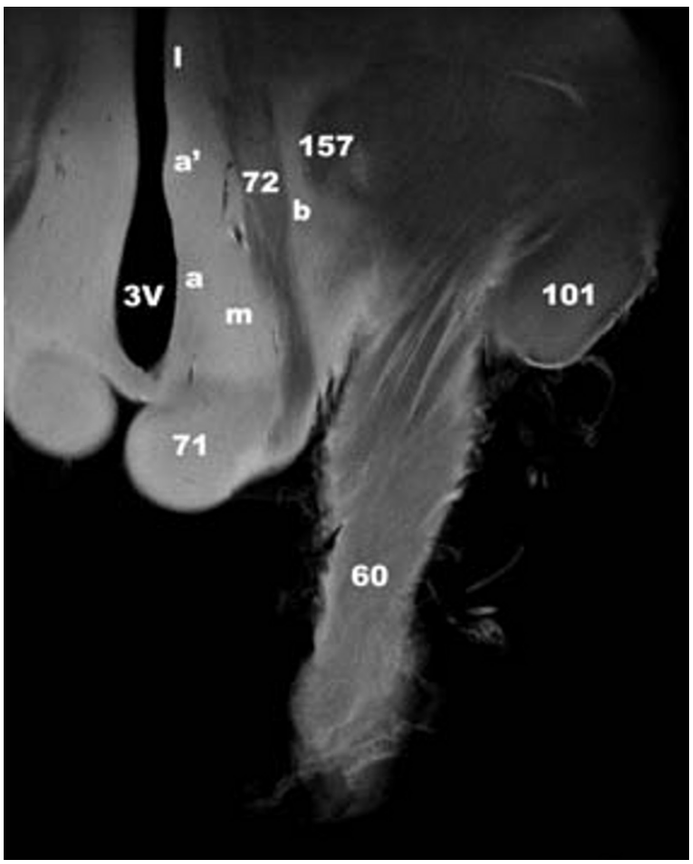

D 3. Coronal mesencephalic-diencephalic junction

Coronal sections displayed from ventral to dorsal (Figs. 8.109–8.120)

Fig. 8.109. Mesencephalic-diencephalic junction. Ventral coronal section.

The anterior column of the fornix (72) descends to the anterolateral aspect of the mammillary body (71). The hypothalamus lies to each side of the third ventricle (3V), inferior to the hypothalamic sulcus. The hypothalamic nuclei are divided into medial and lateral groups by an imaginary sagittal plane through the anterior column of the fornix [78].

60 Cerebral peduncle
71 Mammillary body
72 Fornix (anterior column)
101 Optic tract
157 Ansa lenticularis

Letter labels

3V Third ventricle
a Ventromedial nucleus of the hypothalamus
a' Dorsomedial nucleus of the hypothalamus
b Lateral area of the hypothalamus
l Paraventricular nucleus of the hypothalamus
m Posterior area of the hypothalamus

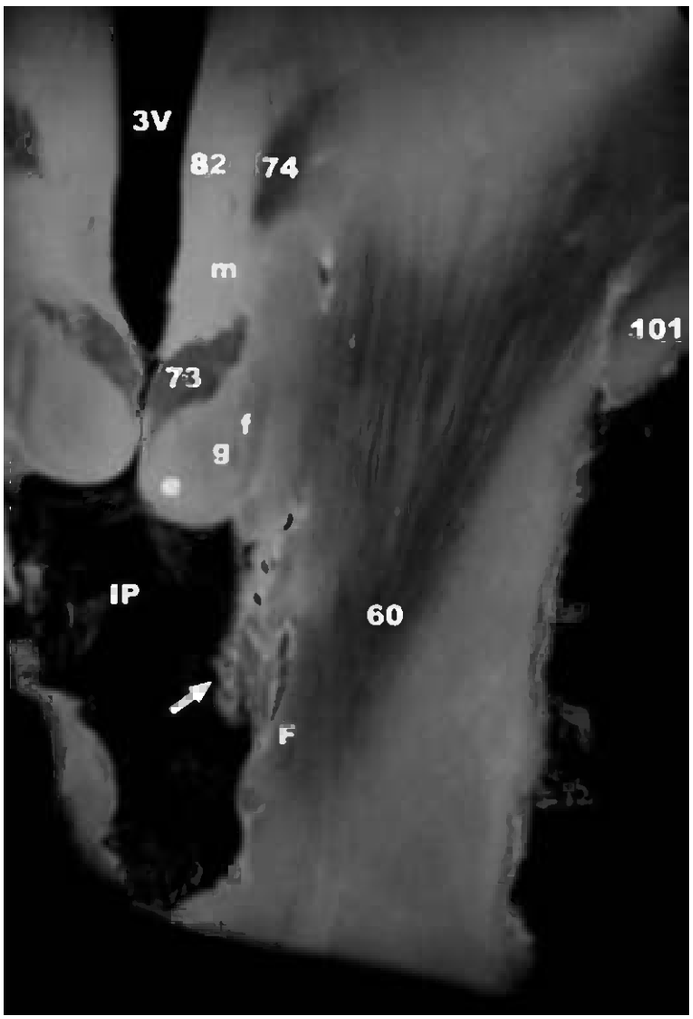

Fig. 8.110. Mesencephalic-diencephalic junction. Ventral coronal section.

The mammillary body displays a capsule (unlabeled) and three main nuclei: medial (e), lateral (f) and intercalated (g) nuclei. These three nuclei (predominantly the medial nucleus) contribute to the efferent principal mammillary fasciculus (73). This fasciculus arises from the posteromedial aspect of the mammillary body, ascends a short distance, and then divides into the mammillothalamic tract to the anterior thalamic nuclei (See Fig. 8.137) and the mammillotegmental tract (74) to the midbrain tegmentum. The term nuclei mediani thalami designates a group of the more medial portions of the nucleus medialis thalami and nucleus centri mediani thalami plus other subependymal collections of nuclei [358]. The oculomotor fibers (white arrow) emerge into the interpeduncular fossa (IP) along the medial wall of the cerebral peduncle (60). The optic tract (101) encircles the lateral edge of the cerebral peduncle en route to the lateral geniculate body.

60 Cerebral peduncle
73 Principal mammillary fasciculus
74 Mammillotegmental tract
82 Nuclei mediani thalami
101 Optic tract

Letter labels

3V Third ventricle
e Medial nucleus of the mammillary body
f Lateral nucleus of the mammillary body
g Intercalated nucleus of the mammillary body
m Posterior area of the hypothalamus
F Frontopontine tract
IP Interpeduncular fossa

Arrowheads and arrows

Single white arrow: Emerging fascicles of the oculomotor nerve (CN III)

Fig. 8.111. Mesencephalic-diencephalic junction. Mid-ventral coronal section.

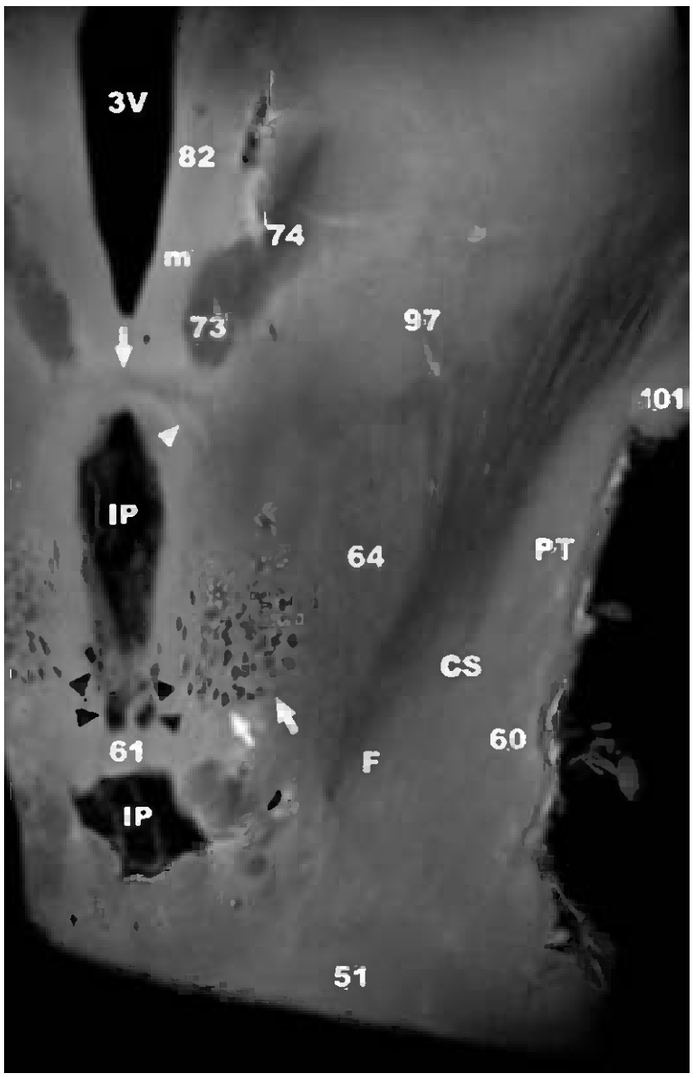

The third ventricle (3V) and interpeduncular fossa (IP) define the midline. The principal mammillary fasciculus (73) gives rise to the mammillotegmental tract (74). Together with these structures, the oculomotor fibers (dual white arrows) and the thalamoperforating vessels (black arrowheads) form a "dotted" array that resemble a cat's face with "whiskers." The supramammillary commissure (posterior hypothalamic decussation) (single white arrow) is a slender fiber bundle, which lies dorsal to the mammillary bodies. It connects the mammillary body, subthalamic nucleus (97) and globus pallidus with the contralateral red nucleus and tegmental area [358]. It also connects the mammillary body with the habenulo-interpeduncular fasciculus and interconnects the medial geniculate bodies (**See Figs 8.112** and **8.138–8.140**) [358]. The mammillary peduncle (white arrowhead) arises in the tegmental nuclei of the midbrain and ascends lateral to the interpeduncular nucleus, through the rootlets of the oculomotor nerves, to reach the lateral mammillary nucleus [78].

51 Pontocerebellar fibers
60 Cerebral peduncle
61 Interpeduncular nucleus
64 Substantia nigra
73 Principal mammillary fasciculus
74 Mammillotegmental tract
82 Nuclei mediani thalami
97 Subthalamic nucleus
101 Optic tract (lateral portion resected)

Letter labels

3V Third ventricle
m Posterior area of the hypothalamus
F Frontopontine tract of cerebral peduncle
CS Corticospinal tract of cerebral peduncle
IP Interpeduncular fossa
PT Parietotemporopontine tract of cereberal peduncle

Arrowheads and arrows

Single white arrowhead: Peduncle of the mammillary bodies
Multiple black arrowheads: Posterior thalamoperforating vessels
Single white arrow: Supramammillary commissure (posterior hypothalamic decussation)
Paired white arrows**:** Intramesencephalic fascicles of the oculomotor nerve (CN III)

Fig. 8.112. Mesencephalic-diencephalic junction. Mid coronal section.

The pontocerebellar fibers (51), interpeduncular nucleus (61), and superior cerebellar peduncle (23c, 23′) form a narrow "U" under the third ventricle (3V). The oculomotor fibers (white arrows) and thalamoperforating vessels (black arrowheads) penetrate through these structures. The stria medullaris thalami (77) arches posteriorly along the medial border of the thalamus to the habenular nuclei. From there, the habenulo-interpeduncular tract (white arrowhead) descends along the medial margin of the red nucleus (95) to reach the interpeduncular nucleus, nucleus centralis superior (See Fig. 8.15), and other raphe nuclei of the midbrain (See Figs. 8.103 and 8.104). Medial to the red nucleus, this tract contains the nucleus of the habenulo-interpeduncular tract, and displays a characteristic "triplet" signal (white arrowheads) of paired dark fibers flanking the high-signal central nucleus. The fields of Forel (H1, H2), the zona incerta (98), and the subthalamic nucleus (97) lie superolateral to the red nucleus (95).

23c Cruciate portion superior cerebellar peduncle [358]
23′ Decussation of the superior cerebellar peduncle
38 Middle cerebellar peduncle
51 Pontocerebellar fibers
60 Cerebral peduncle
61 Interpeduncular nucleus
64 Substantia nigra
74 Mammillotegmental tract
77 Stria medullaris thalami
82 Nuclei mediani thalami
83 Nucleus dorsomedialis thalami
86 Nucleus lateralis thalami
95 Red nucleus
97 Subthalamic nucleus
98 Zona incerta
108 Frontal radiations of the red nucleus

Letter labels

3V Third ventricle
CS Corticospinal tract
F Frontopontine tract
H1 Forel field H1 (thalamic fasciculus)
H2 Forel field H2 (lenticular fasciculus)
PT Parietotemporopontine tract

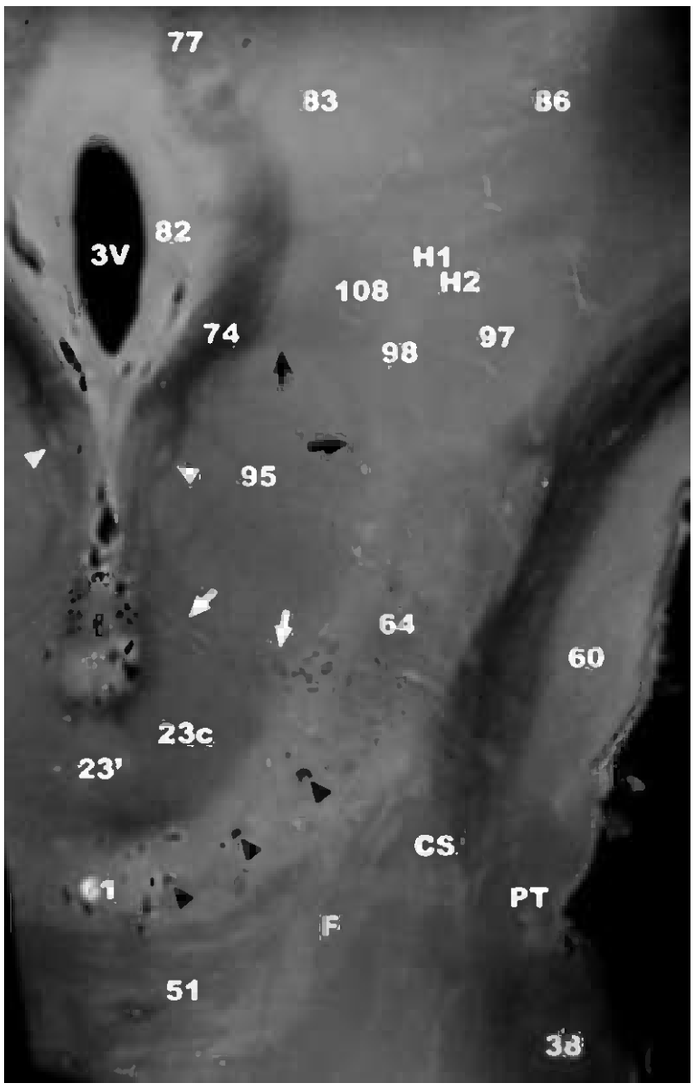

Arrowheads and arrows

Paired white arrowheads:	Habenulo-interpeduncular tracts (fasciculi retroflexus)
Multiple black arrowheads:	Posterior thalamoperforating and other mesencephalic perforating vessels
Paired white arrows:	Intramesencephalic oculomotor fibers (CN III)
Paired black arrows:	Capsule of the red nucleus

Fig. 8.113. Mesencephalic-diencephalic junction. Dorsal coronal section.

The medial lemniscus (21) ascends toward the thalamus. The fascicles of the medial longitudinal fasciculi (17) enclose the paired paramedian oculomotor nuclei (paired black arrows) and the nuclei of Edinger-Westphal (black arrowheads). The nuclei of Edinger-Westphal supply preganglionic parasympathetic fibers to the ciliary ganglion for ciliary and pupillary constriction. The ventral tegmental nuclei (white arrowheads) lie just caudal to these structures, and are one target of the mammillotegmental tract (**See Figs. 8.103, 8.110 and 8.112**).

17 Medial longitudinal fasciculus
21 Medial lemniscus
23 Superior cerebellar peduncle
23' Decussation of the superior cerebellar peduncle
24 Central tegmental tract
38 Middle cerebellar peduncle
51 Pontocerebellar fibers
60 Cerebral peduncle
64 Substantia nigra
82 Nuclei mediani thalami
83 Nucleus dorsomedialis thalami
86 Nucleus lateralis thalami
94l Ventral lateral nucleus of the thalamus

Letter labels
3V Third ventricle

Arrowheads and arrows
Paired white arrowheads: Ventral tegmental nuclei
Paired black arrowheads: Nuclei of Edinger-Westphal
Single white arrow: Intramesencephalic fibers of CN III
Single black arrow: Habenulo-interpeduncular tract (fasciculus retroflexus)
Paired black arrows: Oculomotor nuclei

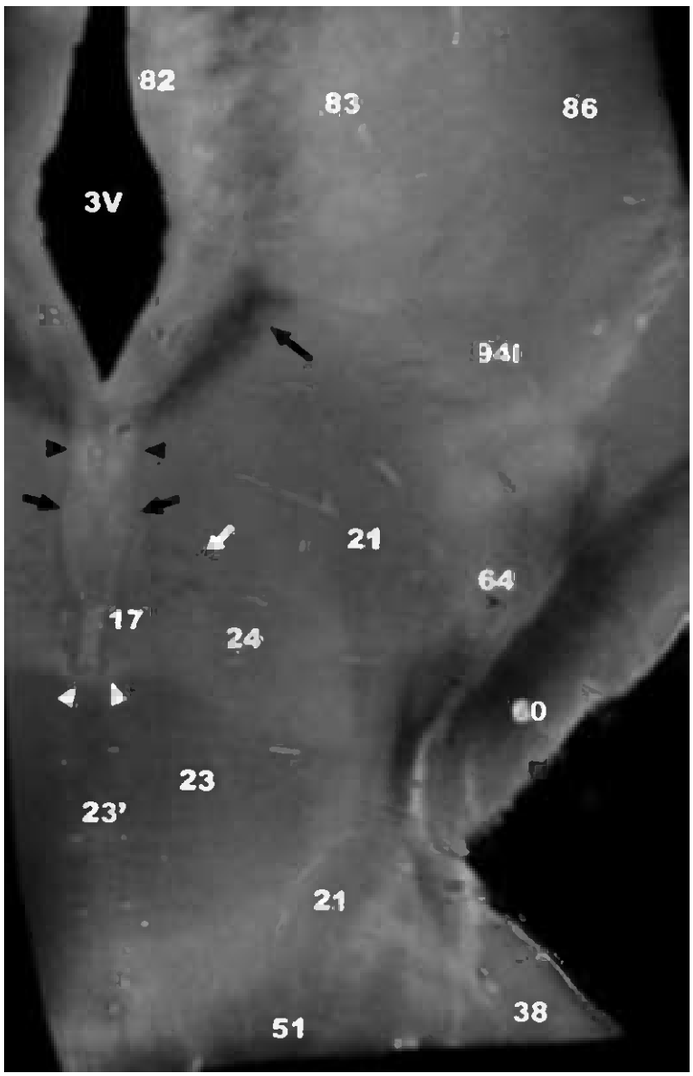

Fig. 8.114. Mesencephalic-diencephalic junction. Dorsal coronal section.

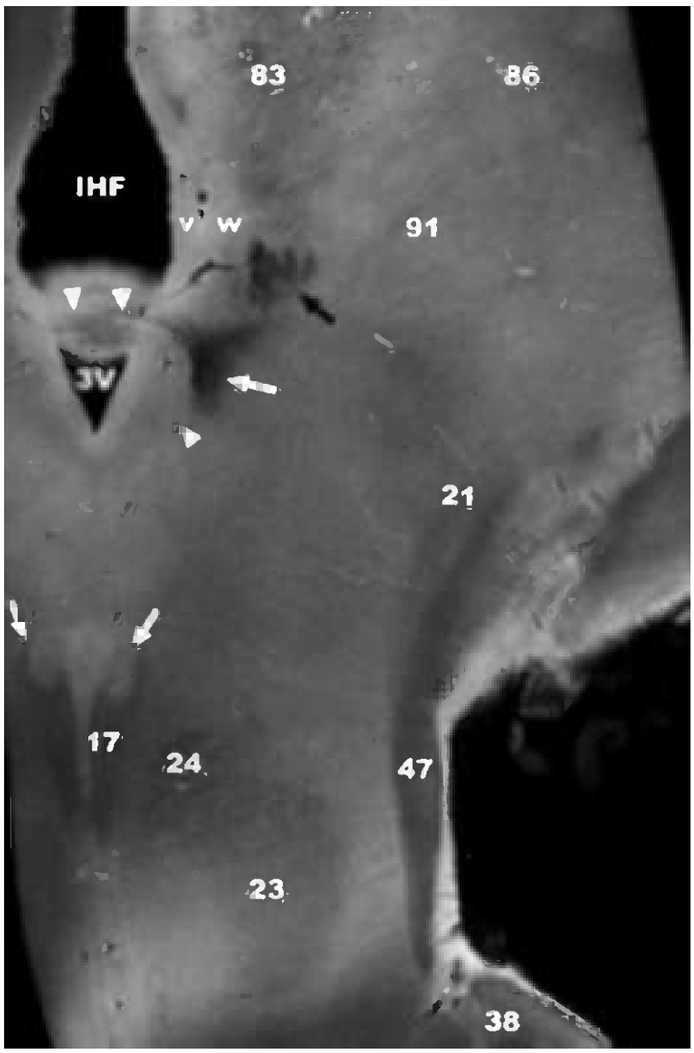

Further caudally, the medial longitudinal fasciculi (17) enclose the ventral aspects of the trochlear nerve nuclei (white arrows). The medial (v) and lateral (w) habenular nuclei give rise to the habenulo-interpeduncular tract (single black arrow) The anterior edge of the posterior commissure (dual white arrowheads) crosses the midline above the visualized portion of the third ventricle (3V) (See also next Fig. 8.115). The nucleus of Darkschewitsch (single white arrowhead) lies in the subependymal gray matter of the third ventricle inferomedial to the lateral edge of the posterior commissure. Its fibers give rise to the medial tegmental tract, which descends through the medial longitudinal fasciculus (17) to the medial accessory olive [322a]. The broad unlabeled area rostral, lateral and ventral to the lateral end of the posterior commissure may be designated the (composite) nuclei of the posterior commissure [78] **(**although Riley considers the nucleus of Darkschewitsch to be the nucleus of the posterior commissure [358]). The lateral lemniscus (47) ascends along the lateral edge of the midbrain carrying auditory information toward the inferior colliculus

17 Medial longitudinal fasciculus
21 Medial lemniscus
23 Superior cerebellar peduncle
24 Central tegmental tract
38 Middle cerebellar peduncle
47 Lateral lemniscus
83 Nucleus dorsomedialis thalami
86 Nucleus lateralis thalami
91 Centromedian nucleus

Letter labels

3V Third ventricle
v Medial habenular nucleus
w Lateral habenular nucleus
IHF Interhemispheric fissure

Arrowheads and arrows

Single white arrowhead: Nucleus of Darkschewitsch
Paired white arrowheads: Posterior commissure (anteriormost portion)
Single white arrow: Fascicles of the posterior commissure
Single black arrow: Habenulo-interpeduncular tract (fasciculus retroflexus)
Paired white arrows: Nuclei of the trochlear nerves (CN IV) partially enclosed by the medial longitudinal fasciculi (17)

Fig. 8.115. Mesencephalic-diencephalic junction. Dorsal coronal section.

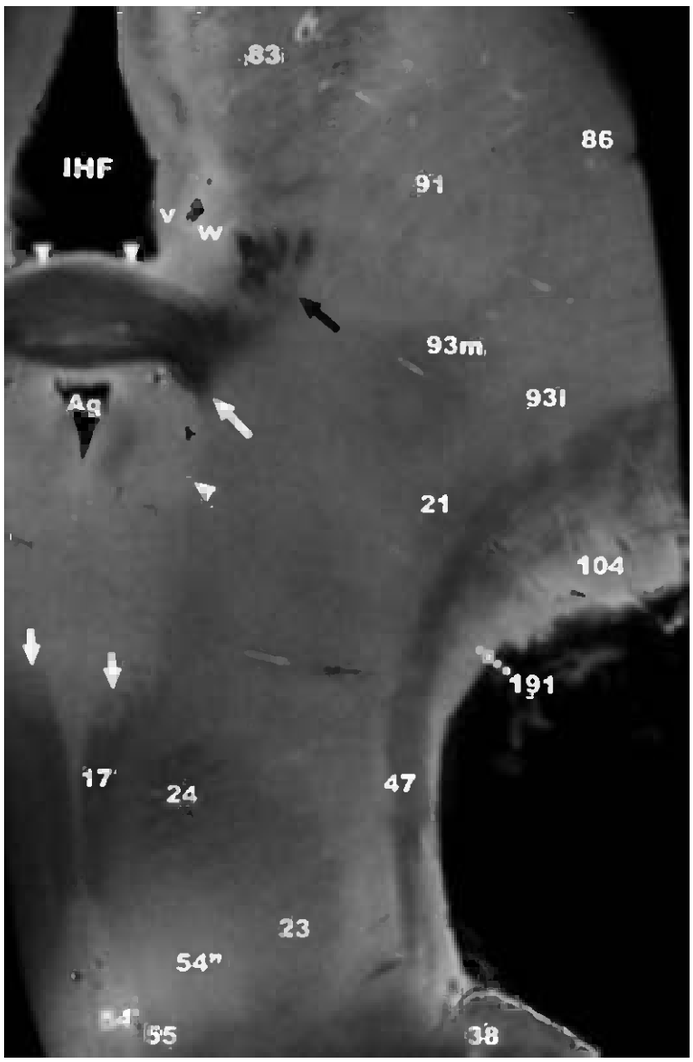

The posterior commissure (paired white arrowheads) forms the roof of the aqueduct of Sylvius rostrally. The medial (v) and lateral (w) habenular nuclei give rise to the habenulo-interpeduncular tract (black arrow) that will descend to the interpeduncular nucleus. Medial habenular fibers relay within the interpeduncular nucleus to reach the nucleus centralis superior (54′, 54″), while lateral habenular fibers may reach this nucleus directly [322]. The medial lemniscus approaches the inferior aspect of the ventral posterolateral nucleus of the thalamus (93l). The ventral posteromedial nucleus (93m) lies just medially.

17 Medial longitudinal fasciculus
23 Superior cerebellar peduncle
24 Central tegmental tract
38 Middle cerebellar peduncle
47 Lateral lemniscus
54′ Nucleus centralis superior medialis (Synonym: Superior nucleus of the raphe)
54″ Nucleus centralis superior lateralis
55 Predorsal longitudinal fasciculus (containing the tectospinal tract)
83 Nucleus dorsomedialis thalami
86 Nucleus lateralis thalami (partially resected)
91 Centromedian nucleus of the thalamus
93m Ventral posteromedial nucleus of the thalamus
93l Ventral posterolateral nucleus of the thalamus
104 Medial geniculate body (partially resected)
191 Sagulum, containing the corpus parabigeminum

Letter labels

v Medial habenular nucleus
w Lateral habenular nucleus
Aq Cerebral aqueduct (of Sylvius)
IHF Interhemispheric fissure

Arrowheads and arrows

Single white arrowhead: Nucleus of Darkschewitsch
Paired white arrowheads: Posterior commissure
Single white arrow: Fascicles of the posterior commissure
Single black arrow: Habenulo-interpeduncular tract (fasciculus retroflexus)
Paired white arrows: Nuclei of the trochlear nerves (CN IV) related to the medial longitudinal fasciculi (17)

Fig. 8.116. Mesencephalic-diencephalic junction. Dorsal coronal section.

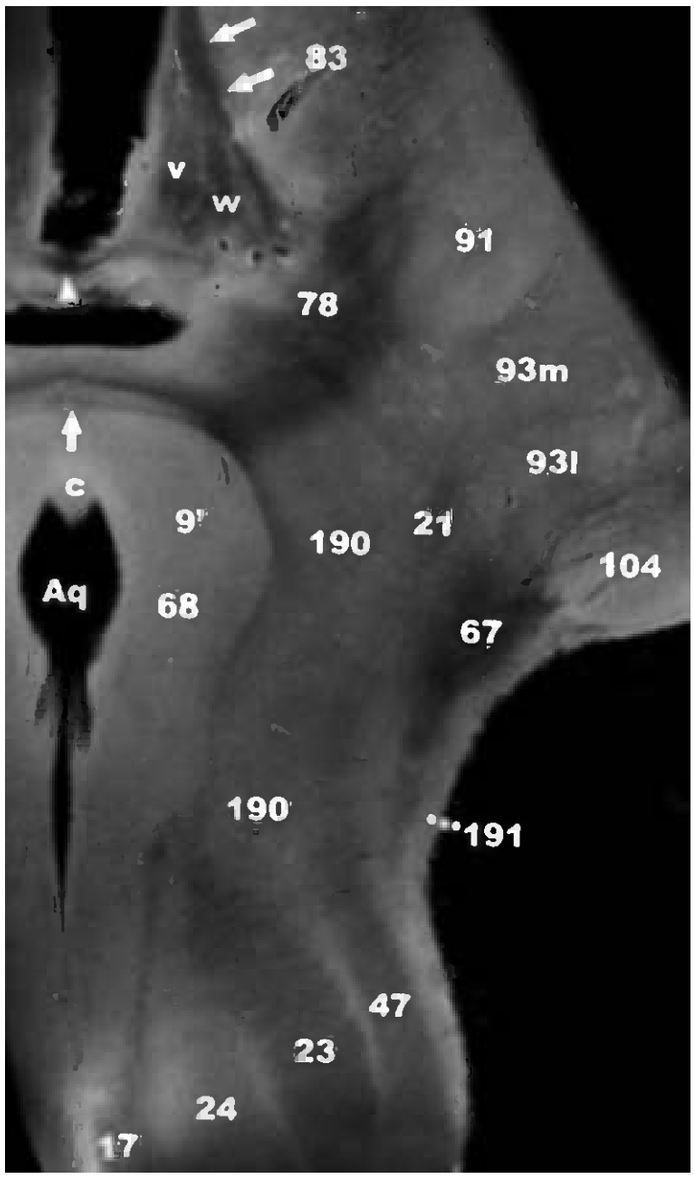

The stria medullaris thalami is a mixed afferent-efferent fiber bundle that interconnects the habenular nuclei with the septal region and basal structures including the area olfactoria and possibly the nucleus basalis [358]. Strial fibers cross the midline through the habenular commissure (single white arrowhead) bilaterally to reach the contralateral habenular nuclei, medial longitudinal fasciculi and superior colliculi [358]. The posterior commissure (See prior **Fig. 8.15**) transitions (single white arrow) into the commissure of the superior colliculus and the marginal fibers of the periaqueductal gray matter (9′). The subcommissural organ (c) is a specialized area of ciliated columnar ependymal cells that indents the dorsal surface of the aqueduct just at this transition point [78, 358]. The subcommissural organ belongs to the group of chemosensitive circumventricular organs, that have no blood-brain barrier. These organs may integrate signals from the cerebrospinal fluid, plasma concentrations of metabolites, and afferent impulses from distant parts of the central nervous system to help regulate body homeostasis, including fluid volume and salt/water balance [78, 322]. The dorsal longitudinal fasciculus (68) appears as a faint band within the periaqueductal gray matter (9′). Superolaterally, the dorsomedial nucleus (83), centromedian nucleus (91), ventral posteromedial nucleus (93m), ventral posterolateral nucleus (93l) and medial geniculate body (104) form a "stack" of gray nuclei. Inferiorly, the lateral lemniscus (47), superior cerebellar peduncle (23), central tegmental tract (24) and medial longitudinal fasciculus (17) form co-curvilinear fiber columns. The brachium of the inferior colliculus (67) carries auditory information onward from the inferior colliculus to the medial geniculate body (104).

9′ Periaqueductal gray matter
17 Medial longitudinal fasciculus
21 Medial lemniscus
23 Superior cerebellar peduncle
24 Central tegmental tract
47 Lateral lemniscus
67 Brachium of the inferior colliculus
68 Dorsal longitudinal fasciculus
78 Habenulo-interpeduncular tract (fasciculus retroflexus)
83 Nucleus dorsomedialis thalami
91 Centromedian nucleus
93m Ventral posteromedial nucleus of the thalamus
93l Ventral posterolateral nucleus of the thalamus
104 Medial geniculate body (resected laterally)
190 Lateral mesencephalic nucleus
191 Sagulum, containing the corpus parabigeminum

Letter labels

c Subcommissural organ
v Medial habenular nucleus
w Lateral habenular nucleus
x Dorsal longitudinal fasciculus within the periaqueductal gray matter.
Aq Cerebral aqueduct (of Sylvius)

Arrowheads and arrows

Single white arrowhead: Habenular commissure
Single white arrow: Transition between the posterior commissure and the commissure of the superior colliculus, plus the marginal fibers of the periaqueductal gray matter
Paired white arrows: Stria medullaris thalami

Fig. 8.117. Mesencephalic-diencephalic junction. Dorsal coronal section.

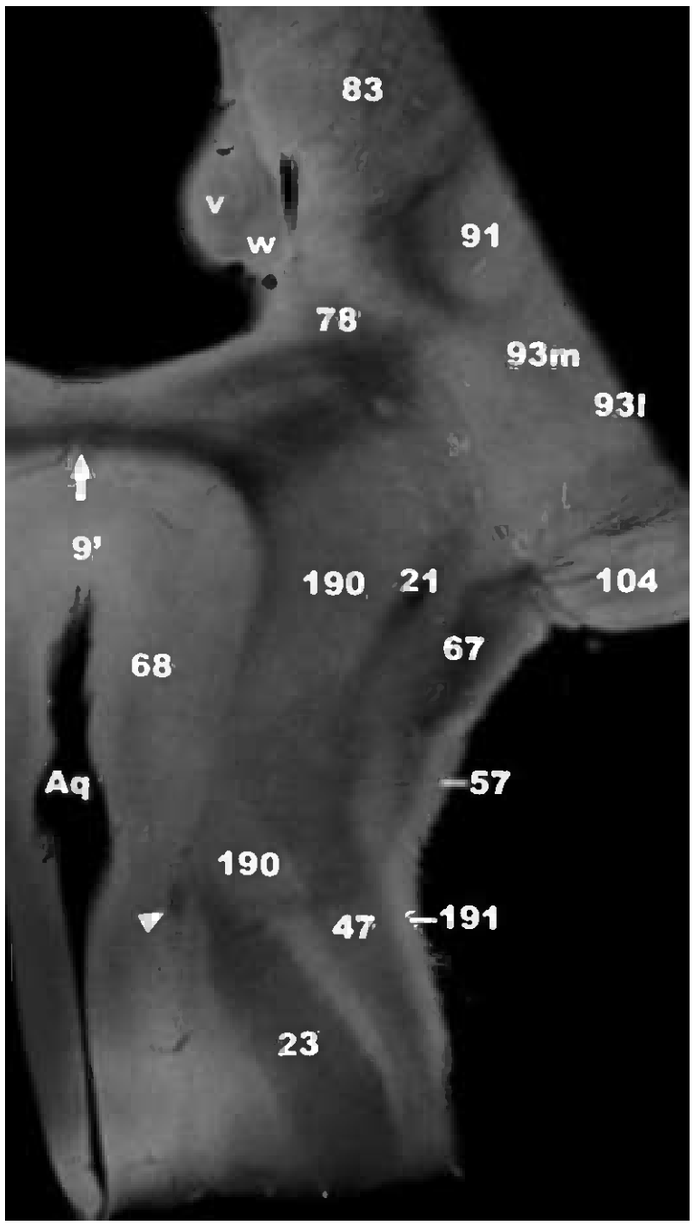

The upper contours of the medial (v) and lateral (w) habenular nuclei now project into the cistern of the velum interpositum superior to the third ventricle. The commissure of the superior colliculi (white arrow) is well formed. Fascicles of the ipsilateral trochlear nerve (white arrowhead) course dorsally from the nucleus (See Fig. 8.114) through the periaqueductal gray matter (9′) to the decussation in the superior medullary velum (See Fig. 8.120). The sagulum (191) is a cell-poor layer of superficial gray matter situated ventrolateral to the inferior colliculus. It corresponds to the region of the corpus parabigeminum and contains the tectopontine tract (See Fig. 8.75) [358].

9′ Periaqueductal gray matter
21 Medial lemniscus
23 Superior cerebellar peduncle
47 Lateral lemniscus
57 Area parabigeminum posterior
67 Brachium of the inferior colliculus
68 Dorsal longitudinal fasciculus within the periaqueductal gray matter
78 Habenulo-interpeduncular tract (fasciculus retroflexus)
83 Nucleus dorsomedialis thalami
91 Centromedian nucleus
93m Ventral posteromedial nucleus of the thalamus
93l Ventral posterolateral nucleus of the thalamus
104 Medial geniculate body (resected laterally)
190 Lateral mesencephalic nucleus
191 Sagulum (containing the corpus parabigeminum)

Letter labels

v Medial habenular nucleus
w Lateral habenular nucleus
Aq Cerebral aqueduct (of Sylvius)

Arrowheads and arrows

Single white arrowhead: Intramesencephalic fascicles of the trochlear nerve (CN IV)
Single white arrow: Marginal fibers of the periaqueductal gray matter plus commissural fibers of the superior colliculus

Fig. 8.118. Mesencephalic-diencephalic junction. Dorsal coronal section.

The lateral lemniscus (47) ascends along the lateral border of the upper pons and midbrain to the inferior colliculus (56). The brachium (67) of the inferior colliculus (56) ascends toward the medial geniculate body (104). The brachium (70) of the superior colliculus (69) passes laterally over the superior pole of the medial geniculate body (104) (en route to the lateral geniculate body). The commissure (single white arrow) of the superior colliculus lies in the midline superiorly. Intramesencephalic fascicles of the trochlear nerve (white arrowhead) continue posteriorly. The mesencephalic nucleus and tract of the trigeminal nerve (black arrowheads) form a thin stripe medial to the superior cerebellar peduncle (23) (See Fig. 8.96).

23 Superior cerebellar peduncle
47 Lateral lemniscus
56 Inferior colliculus
57 Area parabigeminum
67 Brachium of the inferior colliculus
69 Superior colliculus
70 Brachium of the superior colliculus
104 Medial geniculate body (resected laterally)
190 Lateral mesencephalic nucleus
191 Sagulum (corresponding to the corpus parabigeminum)

Arrowheads and arrows

Single white arrowhead: Intramesencephalic fascicles of the trochlear nerve (CN IV)
Paired black arrowheads: Mesencephalic nucleus and tract of the trigeminal nerve (CN V)
Single white arrow: Commissure of the superior colliculus

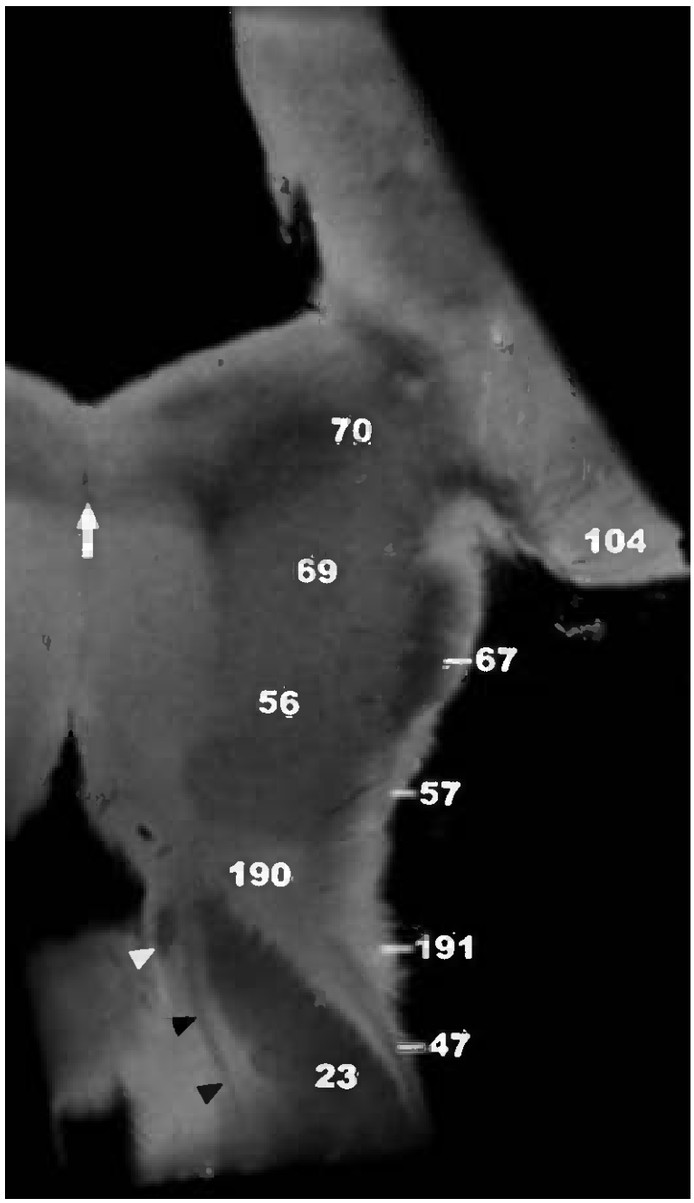

Fig. 8.119. Mesencephalic-diencephalic junction. Dorsal coronal section.

The fascicles of the trochlear nerve decussate **(**single white arrow**)** in the superior medullary velum, emerge into the quadrigeminal plate cistern just caudal to the inferior colliculus (56), and then recurve ventrally (paired white arrows) below the inferior colliculus (56) to pass to their exit from the skull. The tectopontine tract (single white arrowhead) relays visual information via the pontine nuclei and pontocerebellar fibers to the central portion of the vermis (declive, folium, tuber) [322]. This region is the visual projection area of the cerebellum [322].

23 Superior cerebellar peduncle
56 Inferior colliculus
67 Brachium of the inferior colliculus
69 Superior colliculus
70 Brachium of the superior colliculus

Arrowheads and arrows

Single white arrowhead: Tectopontine tract
Paired white arrowheads: Capsule of the inferior colliculus
Paired black arrowheads: Capsule of the superior colliculus
Single white arrow: Trochlear nerve fibers decussating in the superior medullary velum of the fourth ventricle
Paired white arrows: Trochlear nerve emerging into the quadrigeminal plate cistern

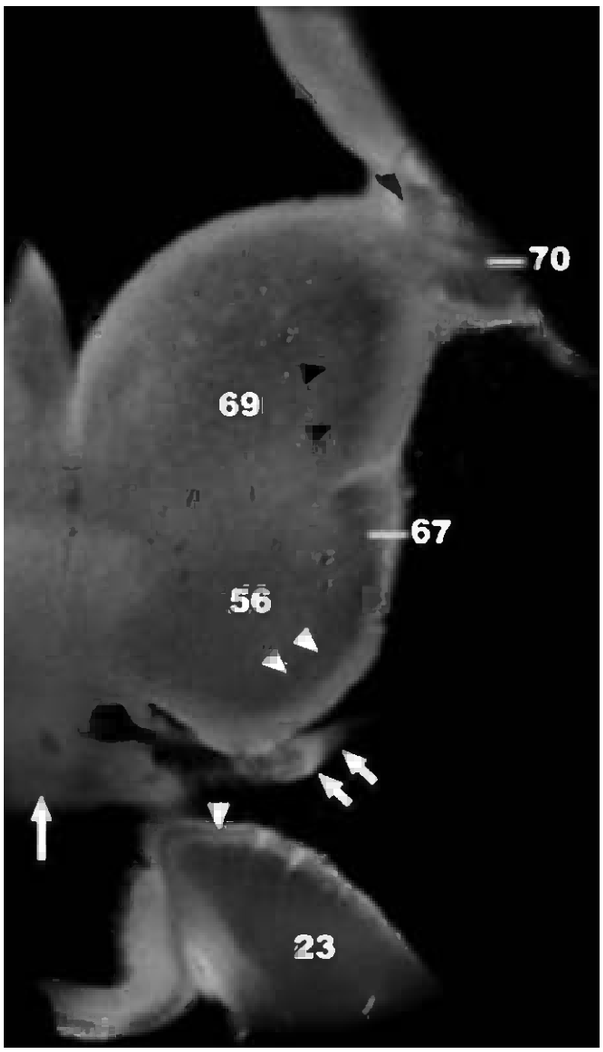

Fig. 8.120. Mesencephalic-diencephalic junction. Dorsal coronal section

The band of fibers (single white arrow) crossing the midline between the superior (69) and inferior (56) colliculi is the decussation of the inferior colliculus.

23 Superior cerebellar peduncle
56 Inferior colliculus
69 Superior colliculus

Arrowheads and arrows
Paired white arrowheads: Capsule of the inferior colliculus
Single white arrow: Decussation of the inferior colliculus

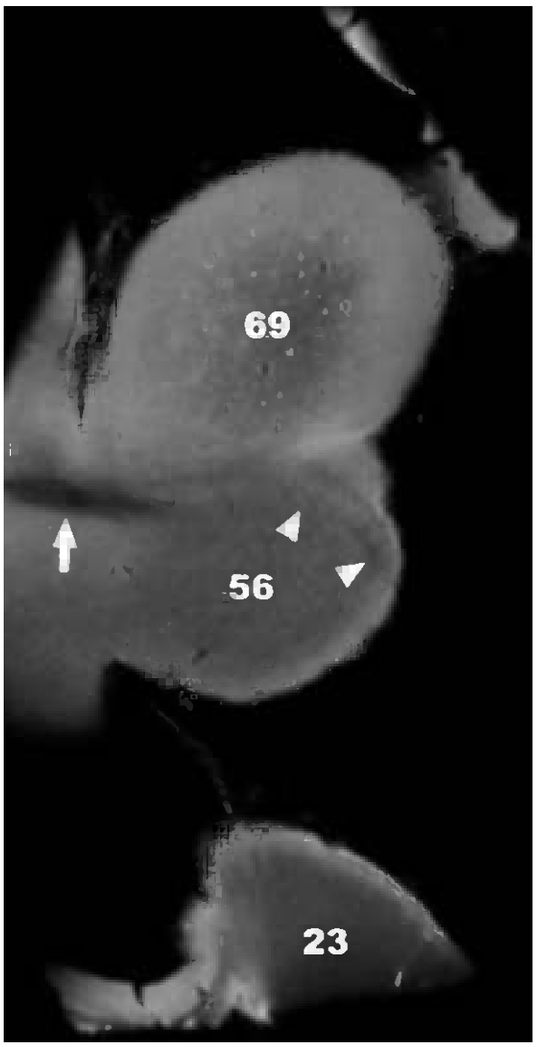

E. Hypothalamus-Epithalamus (Figs. 8.121–8.137)

E 1. Axial hypothalamus-epithalamus

Axial sections displayed from caudal to cranial (Figs. 8.121–8.127)

These cartoons (A–B) display the anatomic region imaged in **Figs. 8.121–8.137**.

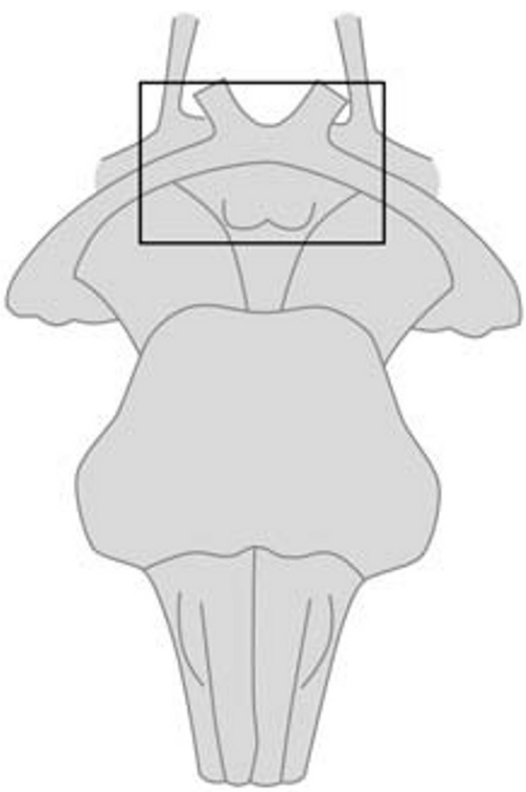

A

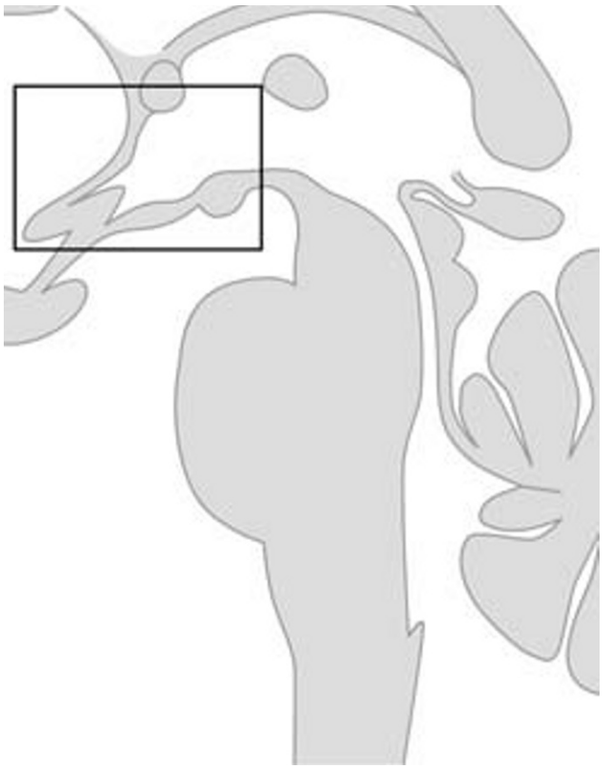

B

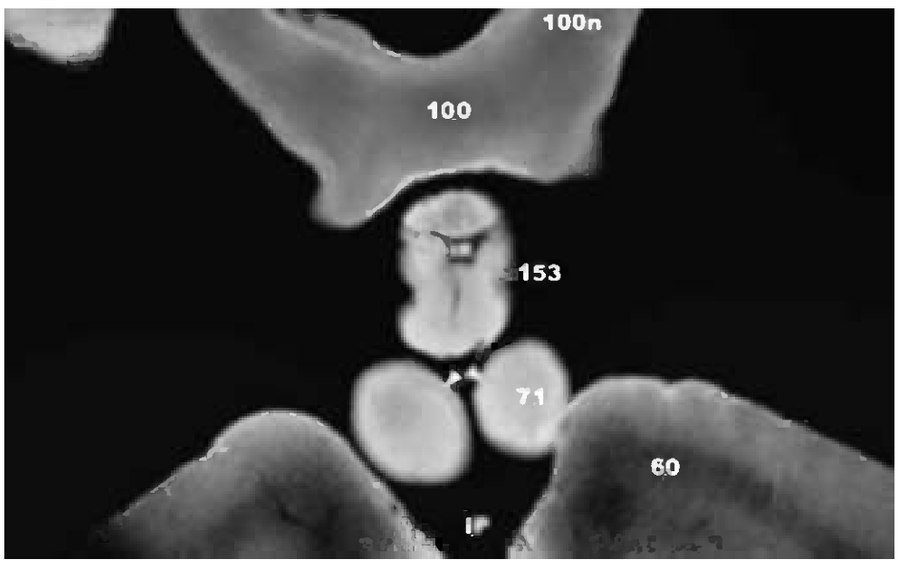

Fig. 8.121. Hypothalamus-epithalamus. Caudal axial section.

The intracranial segments of the optic nerves (100n) converge to form the optic chiasm (100). The hypothalamus surrounds the infundibular recess (IR) of the third ventricle. The mammillary bodies (71) project inferiorly into the suprasellar cistern and interpeduncular fossa.

60 Cerebral peduncle
71 Mammillary body
100 Optic chiasm
100n Optic nerve (intracranial pre-chiasmal segement)
153 Tuber cinereum

Letter labels
IP Interpeduncular fossa
IR Infundibular recess of the third ventricle

Arowheads and arrows
White arrowheads: Capsule of the mammillary bodies

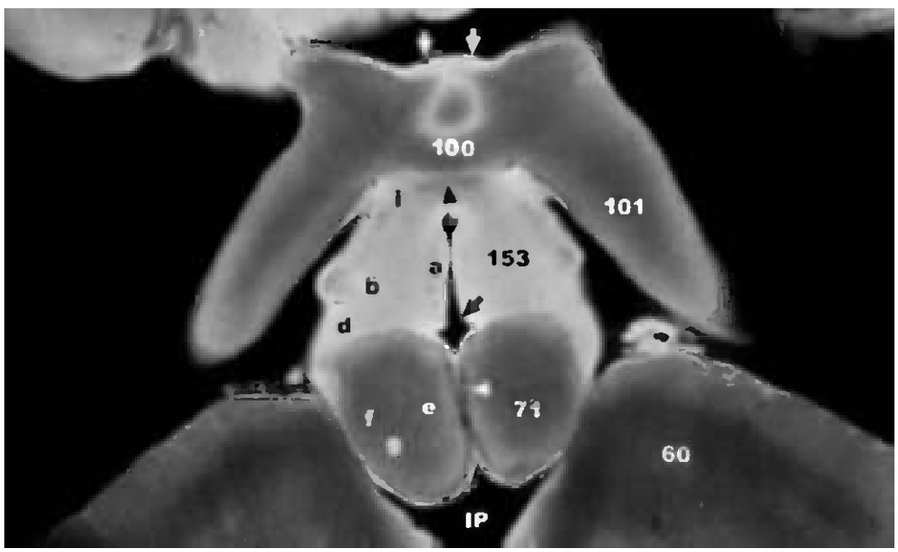

Fig. 8.122. Hypothalamus-epithalamus. Caudal axial section.

The optic tracts (101) diverge from the chiasm (100) and begin to pass posteriorly along the superficial surface of the cerebral peduncles (60) toward the lateral geniculate bodies. The dorsal supra-optic commissure (of Meynert) (black arrowhead) crosses the midline just posterosuperior to the chiasm and extends far laterally (**See Figs. 8.123 and 8.124**). The hypothalamus lies to each side of the inferior third ventricle (arrow) and extends from the region of the optic chiasm anteriorly to the posterior border of the mammillary bodies posteriorly. It contains multiple individual nuclei, which are subdivided into medial and lateral groups by a sagittal plane through the anterior column of the fornix (**See Figs. 8.123 and 8.124**). The mammillary bodies are delimited by an external capsule (white arrowhead) and contain a predominent medial nucleus (e) plus smaller lateral (f) and intermediate (g) mammillary nuclei.

60 Cerebral peduncle
71 Mammillary body
100 Optic chiasm
101 Optic tract
153 Tuber cinereum

Letter labels

a Ventromedial nucleus of the hypothalamus
b Lateral area of the hypothalamus
d Lateral nuclei of the tuber cinereum
e Medial nucleus of the mammillary body
f Lateral nucleus of the mammillary body
g Intercalated nucleus of the mammillary body
i Supra-optic nucleus
IP Interpeduncular fossa

Arrowheads and arrows

Single white arrowhead: Capsule of the mammillary body
Single black arrowhead: Dorsal supra-optic commissure (of Meynert) (See following figures)
Single black arrow: Third ventricle leading to the infundibular recess
Paired white arrows: Lamina supra-optica

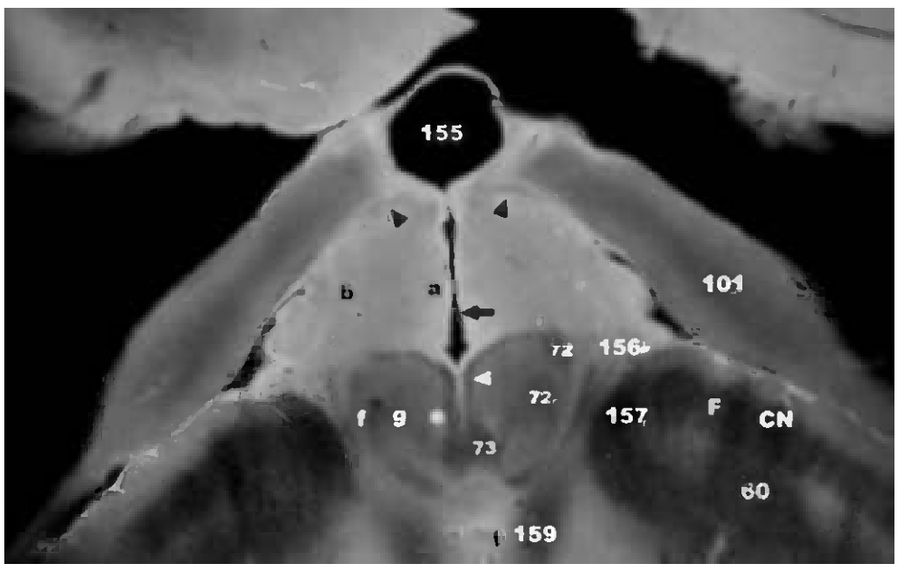

Fig. 8.123. Hypothalamus-epithalamus. Caudal axial section.

The anterior column of the fornix extends inferiorly to converge upon the anterolateral aspect of the mammillary body. The principal mammillary fasciculus (73) ascends through the hypothalamus into the thalamus from the posteromedial aspect of the mammillary body. The dorsal supra-optic decussation (black arrowheads) begins to pass laterally, just internal to the diverging optic tracts (101). Lateral to the mammillary bodies, the ansa lenticularis (157) and its nucleus (156) pass around the antero-inferomedial end of the cerebral peduncle (60). Posterior to the mammillary bodies, the area densa (159) is composed of multiple fibers of uncertain nature, situated ventral and medial to the red nucleus [358].

60 Cerebral peduncle
72 Fornix (anterior column)
73 Principal mammillary fasciculus
101 Optic tract
155 Supra-optic recess of the third ventricle
156 Nucleus of the ansa lenticularis
157 Ansa lenticularis
159 Area densa

Letter labels

a Ventromedial nucleus of the hypothalamus
b Lateral area of the hypothalamus
e Medial nucleus of the mammillary body
f Lateral nucleus of the mammillary body
g Intercalated nucleus of the mammillary body
F Frontopontine tract
CN Corticonuclear tract

Arrowheads and arrows

Single white arrowhead: Capsule of the mammillary body
Paired black arrowheads: Dorsal supra-optic commissure to each side of midline
Single black arrow: Third ventricle leading to the infundibular recess

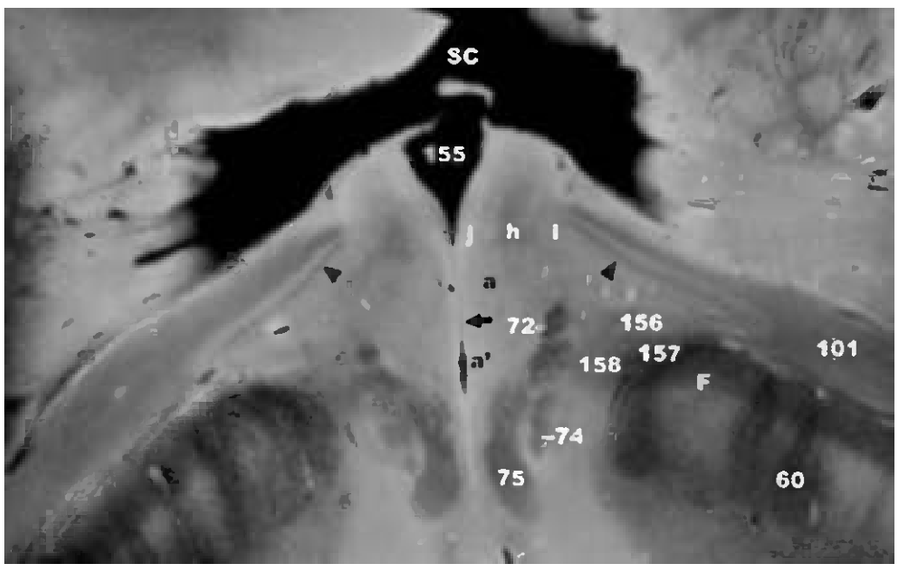

Fig. 8.124. Hypothalamus-epithalamus. Caudal axial section.

The individual fascicles of the anterior column of the fornix (72) pass inferiorly toward the anterolateral aspect of the mammillary body (See Fig. 8.123). The principal mammillary fasciculus, seen at the posteromedial aspect of the mammillary body on prior Fig. 8.123, now divides into the mammillotegmental tract (74) and the mammillothalamic fasciculus (75). The dorsal supra-optic commissure (of Meynert) (black arrowheads) extends far laterally deep to the optic tracts (101). The nucleus basalis of Meynert is a long, overwhelmingly cholinergic nucleus (> 90% of cells) that has medial and lateral components. The medial component is the nucleus of the ansa lenticularis (156) situated ventromedial to the medial edge of the posterior limb of the internal capsule, and interspersed along the fibers of the ansa lenticularis. The lateral component lies in the substantia innominata inferior to the globus pallidus, and is designated the nucleus of the dorsal supra-optic commissure (of Meynert). The ansa lenticularis (157), its nucleus (156) and the ansa peduncularis (158) circumscribe the anterior medial edge of the cerebral peduncle (60). The ansa lenticularis carries fibers from the globus pallidus around the cerebral peduncle and through Forel field H1 (thalamic fasciculus) to reach the *ipsilateral* ventral thalamic nuclei. Its fibers reach the *contralateral* thalamus via the supramammillary commissure (See Fig. 8.111) [358]. The ansa lenticularis also conveys pallidal fibers to the subthalamic nucleus via Forel field H2 (lenticular fasciculus) [358]. The ansa peduncularis (158) carries fibers from both the ansa lenticularis and the inferior thalamic peduncle, and interconnects the globus pallidus and medial thalamus with the orbital gyri.

60 Cerebral peduncle
72 Fornix (anterior column)
74 Mammillotegmental fasciculus
75 Mammillothalamic fasciculus
101 Optic tract
15 Supra-optic recess of the third ventricle
156 Nucleus of the ansa lenticularis
157 Ansa lenticularis
158 Ansa peduncularis

Letter labels
a Ventromedial nucleus of the hypothalamus
a' Dorsomedial nucleus of the hypothalamus
h Paraventriculo-hypophyseal tract [358]
i Supra-optic nucleus
j Pre-optic area
F Frontopontine tract
SC Suprasellar cistern

Arrowheads and arrows
Paired black arrowheads: Dorsal supra-optic commissure
Single black arrow: Third ventricle

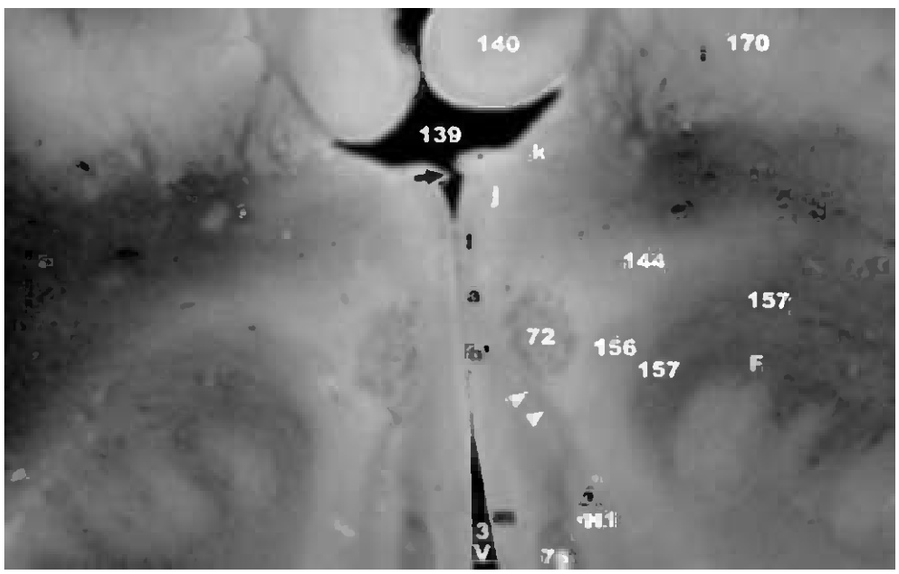

Fig. 8.125. Hypothalamus-epithalamus. Mid axial section.

The ansa lenticularis (157) and its nucleus (156) arch around the medial end of the cerebral peduncle. The area olfactoria (144) lies anteromedial to these. The anterior columns of the fornix (72) lie anterolateral to the mammillothalamic tracts (75) and the H1 fields of Forel (thalamic fasciculus). The pallidohypothalamic tract (dual white arrowheads) links the hypothalamus with the globus pallidus via the subthalamic nucleus [358]. The fasciculus olfactorius (k) approaches the area olfactoria (144).

72 Fornix (anterior column)
75 Mammillothalamic fasciculus
139 Cistern of the lamina terminalis
140 Gyrus rectus
144 Area olfactoria
156 Nucleus of the ansa lenticularis
157 Ansa lenticularis
170 Caudate nucleus (head)

Letter labels

3V Third ventricle
a Ventromedial nucleus of the hypothalamus
a' Dorsomedial nucleus of the hypothalamus
j Pre-optic area
k Fasciculus olfactorius
l Paraventricular nucleus of the thalamus
m Posterior hypothalamic area
F Frontopontine tract
H1 Forel field H1 (thalamic fasciculus)

Arrowheads and arrows

Paired white arrowheads: Pallidohypothalamic tract [358]
Single black arrow: Lamina terminalis (torn)

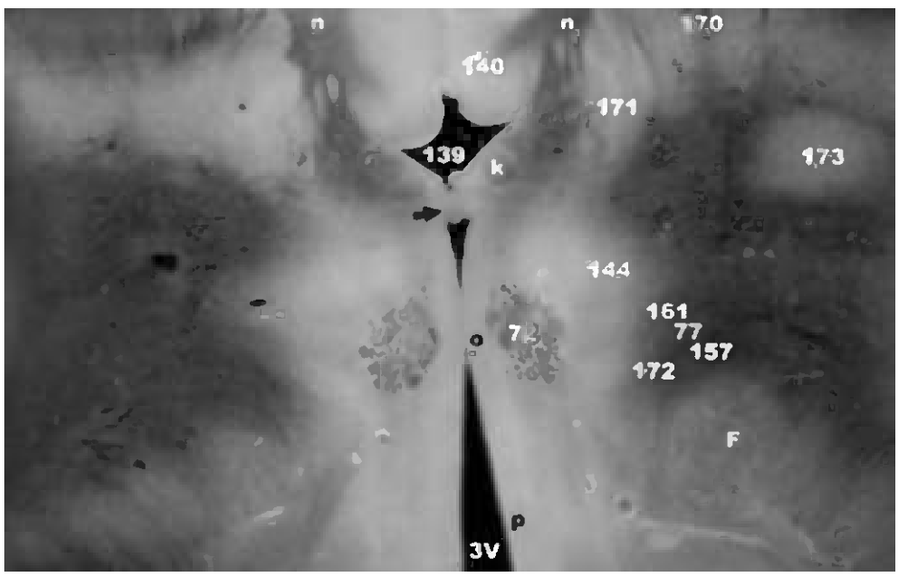

Fig. 8.126. Hypothalamus-epithalamus. Mid axial section.

The area olfactoria (144) lies in the medial portion of the anterior perforated substance and is a center for integrating olfactory information [358]. It is related to the stria medullaris thalami (77), stria semicircularis (161), ventral thalamic peduncle (172), and the fasciculus olfactorius (k). The area olfactoria gives rise to or transmits the olfactory radiations to the subthalamic nuclei and the tegmental area. The nucleus accumbens septi (171) is an antero-inferomedial expansion of the head (170) of the caudate nucleus, which extends under the lateral ventricle to the medial or septal wall of the cerebral hemisphere [322a].

72 Fornix (anterior column)
77 Stria medullaris thalami
139 Cistern of the lamina terminalis
140 Gyrus rectus
144 Area olfactoria
157 Ansa lenticularis
161 Stria semicircularis
170 Caudate nucleus (head)
171 Nucleus accumbens septi
172 Ventral thalamic peduncle
173 Anterior commissure
174 Cingulate gyrus

Letter labels
3V Third ventricle
k Fasciculus olfactorius
n Radiations of the corpus callosum
o Dorsomedian hypothalamic nucleus
p Nuclei mediani thalami
F Frontopontine tract

Arrowheads and arrows
Single black arrow: Lamina terminalis

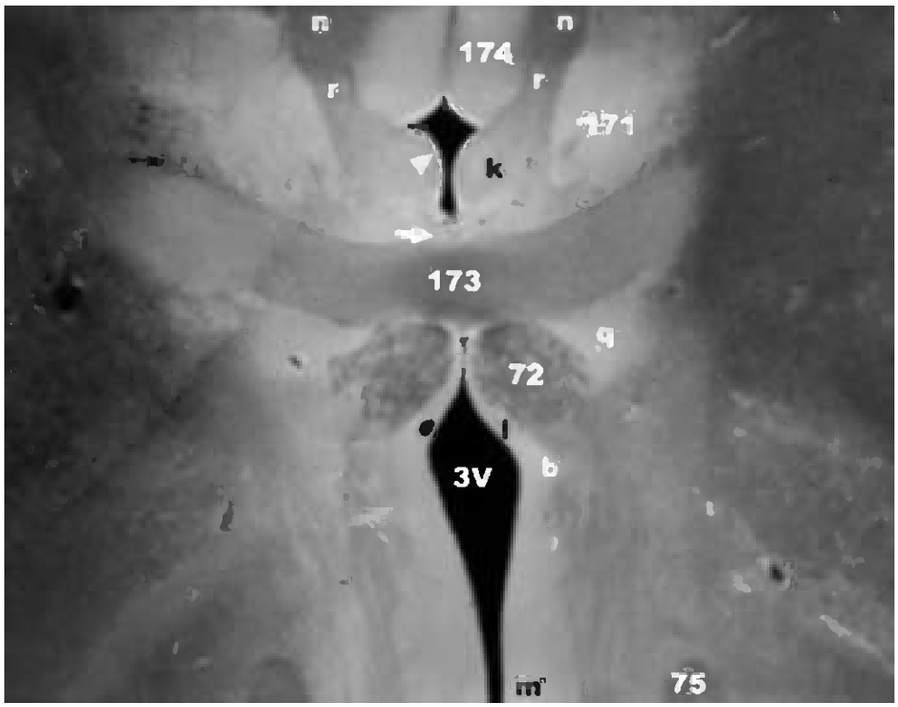

Fig. 8.127. Hypothalamus-epithalamus. Mid axial section.

The anterior commissure (173) forms a compact fiber bundle that crosses the midline in the anterior wall of the third ventricle (3V) at the transition between the lamina terminalis inferiorly and the rostrum of corpus callosum superiorly. As the anterior fornix arches forward and then curves downward toward the anterior commissure, its fascicles divide into a diffuse spread of precommissural fibers to the septal region and the compact paired retrocommissural columns of the fornix (72). The subcallosal gyrus (paraterminal gyrus) is the rostral continuation of the vestigal supracallosal gyrus. This curves forward around and then under the genu, becomes tighly applied to the anterior surface of the rostrum and lamina terminalis (white arrow), and displaces the cingulate gyrus (174) forward, away from the rostrum. The fasciculus olfactorius (k) courses within the subcallosal gyrus. The medial and lateral longitudinal striae, which can be seen separately above the body of corpus callosum, merge together into one layer (white arrowhead) along the subcallosal gyrus. The cingulum (r) courses within the core of the cingulate gyrus as a long rhinencephalic association bundle. The anterior portion of the cingulum bundle connects the anterior perforated substance with the frontal lobe.

72 Fornix (anterior column)
75 Mammillothalamic fasciculus
171 Nucleus accumbens septi
173 Anterior commissure
174 Cingulate gyrus

Letter labels

3V Third ventricle
b Lateral area of the hypothalamus
k Fasciculus olfactorius within the subcallosal gyrus
l Paraventricular nucleus of the hypothalamus
m Posterior area of the hypothalamus
n Radiations of the corpus callosum
q Lateral pre-optic nucleus
r Cingulum bundle
F Frontopontine tract

Arrowheads and arrows

White arrowhead: Stria longitudinalis
White arrow**:** Lamina terminalis

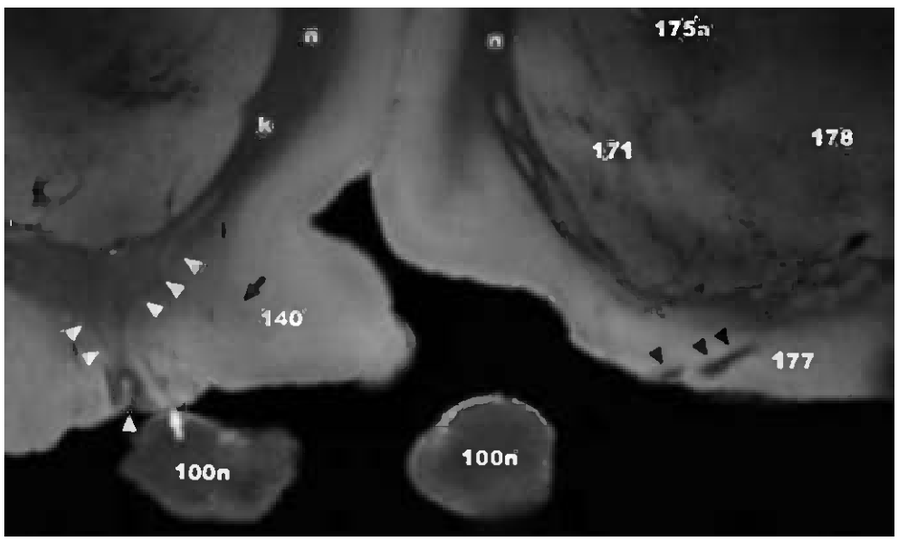

E 2. Coronal Hypothalamus-Epithalamus

Coronal sections displayed from ventral to dorsal (Figs. 8.128–8.137)

Note: The sagittal plane has already been displayed in Sect. D 2. (Figs. 8.101–8.108)

Fig. 8.128. Hypothalamus-epithalamus. Anterior coronal section. The plane of section is slighly asymmetrical.

Superior to the prechiasmal segments of the optic nerves (100n), the gyrus rectus (140) forms the inferomedial border of the frontal lobe. The olfactory tracts (anterior to this plane) pass posteriorly to reach the olfactory trigone (single white arrowhead), from which arise the deep olfactory radiations (dual white arrowheads) and the medial olfactory radiations (triple white arrowheads). The fasciculus olfactorius (k) ascends within the radiations of the rostrum of the corpus callosum. The medial olfactory stria (single black arrowhead) and lateral olfactory stria (dual black arrowheads) are seen within the substantia innominata (177). Deep to these tracts, the putamen (178) becomes continuous with the nucleus accumbens septi (171) antero-inferomedial to the anterior limb of the internal capsule (175a).

100n Optic nerve (prechiasmal segment)
140 Gyrus rectus
171 Nucleus accumbens septi
175a Internal capsule (anterior limb)
177 Substantia innominata
178 Putamen

Letter labels

k Fasciculus olfactorius (within the radiations of the corpus callosum)
n Radiations of the corpus callosum

Arrowheads and arrows

Single white arrowhead: Olfactory trigone
Single black arrowhead: Medial olfactory stria
Paired white arrowheads: Deep olfactory radiations
Paired black arrowheads: Lateral olfactory stria
Triple white arrowheads: Medial olfactory radiations
Single white arrow: Olfactory tuberculum
Single black arrow: Radiations of the gyrus rectus

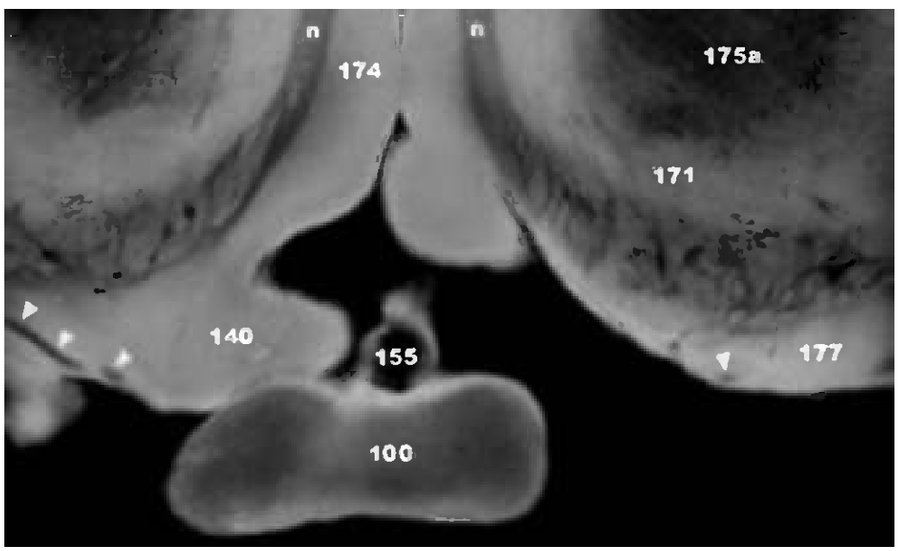

Fig. 8.129. Hypothalamus-epithalamus. More posterior coronal section.

The optic nerves have converged to form the optic chiasm (100). The supra-optic recess (155) of the third ventricle lies above. The medial (single white arrowhead) and lateral (dual white arrowheads) olfactory striae pass through the substantia innominata (177).

100 Optic chiasm
140 Gyrus rectus
155 Supra-optic recess of the third ventricle
171 Nucleus accumbens septi
174 Cingulate gyrus
175a Internal capsule (anterior limb)
177 Substantia innominata

Letter labels
n Radiations of the corpus callosum

Arrowheads and arrows
Single white arrowhead: Medial olfactory stria
Paired white arrowheads: Lateral olfactory stria

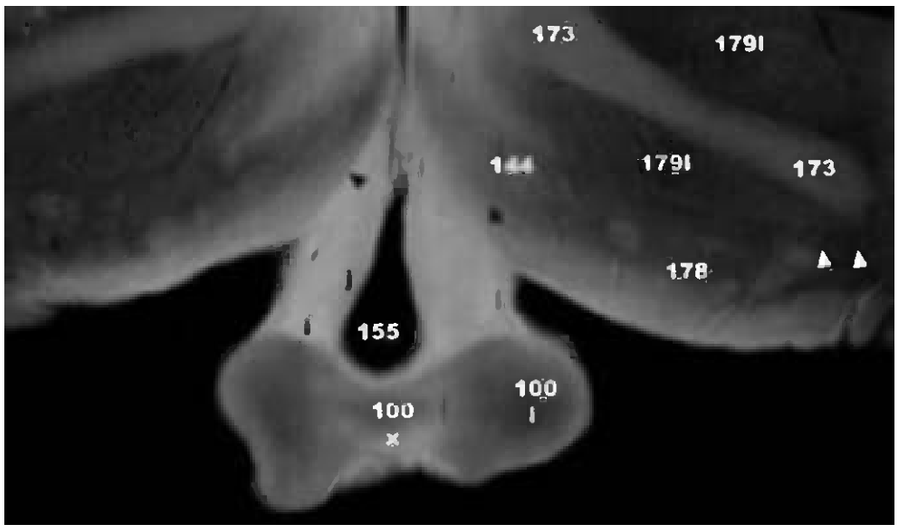

Fig. 8.130. Hypothalamus-epithalamus. Coronal section.

Optic nerve fibers that decussate (100x) lie centrally within the chiasm, while those that continue ipsilaterally (100i) are positioned to their own side of the chiasm. The fasciculus olfactorius (k) and the medial olfactory stria (black arrowhead) ascend medially in relation to the olfactory area (144). The deep olfactory radiations extend laterally (dual white arrowheads). The anterior commissure (173) crosses directly through the bottom of the lateral nucleus of the globus pallidus (179l). The approximate positions of the individual hypothalamic nuclei are indicated.

144 Area olfactoria
100x Medial optic chiasm containing decussating fibers
100i Lateral optic chiasm containing nondecussating fibers
155 Supra-optic recess of the third ventricle
173 Anterior commissure
178 Substantia innominata
179l Globus pallidus (lateral nucleus, external nucleus)

Letter labels
i Supra-optic nucleus
j Pre-optic area
k Fasciculus olfactorius

Arrowheads and arrows
Single black arrowhead: Medial olfactory stria
Paired white arrowheads: Deep olfactory radiations

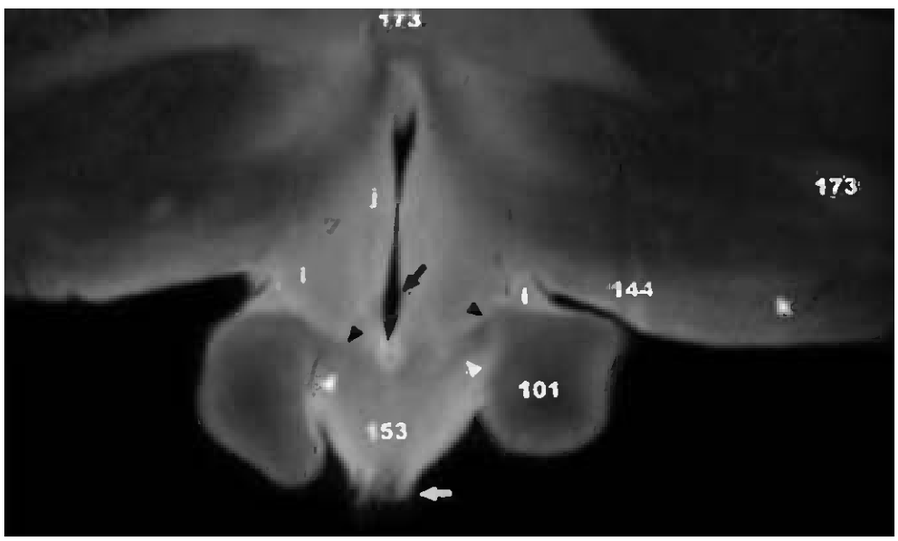

Fig. 8.131. Hypothalamus-epithalamus. Coronal section.

The optic tracts (101) diverge laterally to each side of the tuber cinereum (153). The dorsal supra-optic commissure (of Meynert) (black arrowheads) and the ventral supra-optic commissure (of Gudden) (white arrowheads) cross the midline medial to the supra-optic nucleus (i).

101 Optic tract
144 Area olfactoria
153 Tuber cinereum
173 Anterior commissure

Letter labels

i Supra-optic nucleus
j Pre-optic area
k Fasciculus olfactorius

Arrowheads and arrows

Paired white arrowheads: Ventral supra-optic commissure
Paired black arrowheads: Dorsal supra-optic commissure
Single white arrow: Infundibulum (avulsed at attachment)
Single black arrow: Infundibular recess of the third ventricle

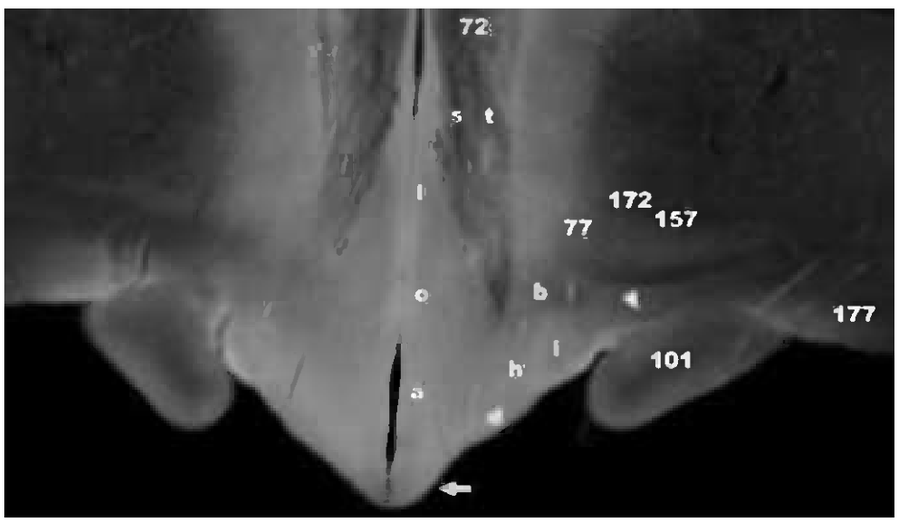

Fig. 8.132. Hypothalamus-epithalamus. Coronal section.

Within the anterior column of the fornix (72), individual fascicles from the alveus of the hippocampal formation (s) lie medial to those from the fimbria of the hippocampal formation (t). The supra-optic commissures continue laterally (white arrowhead). The stria medullaris thalami (77), ansa lenticularis (157) and the ventral thalamic peduncle (172) lie in close proximity at the antero-inferomedial edge of the lenticular nucleus. (See Figs. 8.123–8.126).

72 Fornix (anterior column)
77 Stria medullaris thalami
101 Optic tract
157 Ansa lenticularis
172 Ventral thalamic peduncle
177 Substantia innominata

Letter labels

a Ventromedial nucleus of the hypothalamus
b Lateral area of the hypothalamus
d Lateral nuclei of the tuber cinereum
h Paraventriculo-hypophyseal tract [358]
i Supra-optic nucleus
l Paraventricular nucleus of the hypothalamus
o Dorsomedian nucleus of the hypothalamus
s Alveus
t Fimbria

Arrowheads and arrows

Single white arrowhead: Dorsal and ventral supra-optic commissures
Single white arrow: Infundibulum

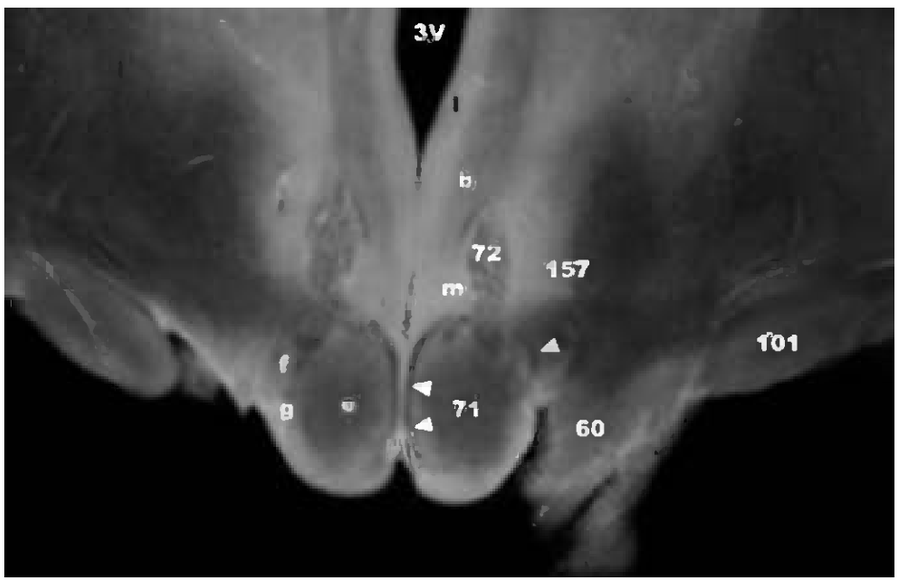

Fig. 8.133. Hypothalamus-epithalamus. Dorsal coronal section.

The anterior columns of the fornices (72) descend behind the anterior commissure (retrocommissural fornix) to the anterolateral aspects of the mammillary bodies (71). The peduncle (single white arrowhead) of the mammillary body courses anteroposteriorly along the ventral surface of the midbrain to convey fibers from the dorsal tegmental nucleus to the mammillary body [322]. The capsule of the mammillary body appears thicker (dual white arrowheads) where the principal mammillary fasciculus will arise (See Fig. 8.123). The optic tract (101) courses posteriorly under and around the cerebral peduncle (60).

60 Cerebral peduncle
71 Mammillary body
72 Fornix (anterior column)
101 Optic tract
157 Ansa lenticularis

Letter labels
3V Third ventricle
b Lateral area of the hypothalamus
e Medial nucleus of the mammillary body
f Lateral nucleus of the mammillary body
g Intercalated nucleus of the mammillary body
l Paraventricular nucleus of the hypothalamus
m Posterior area of the hypothalamus

Arrowheads and arrows
Single white arrowhead: Peduncle of the mammillary body
Paired white arrowheads: Capsule of the mammillary body

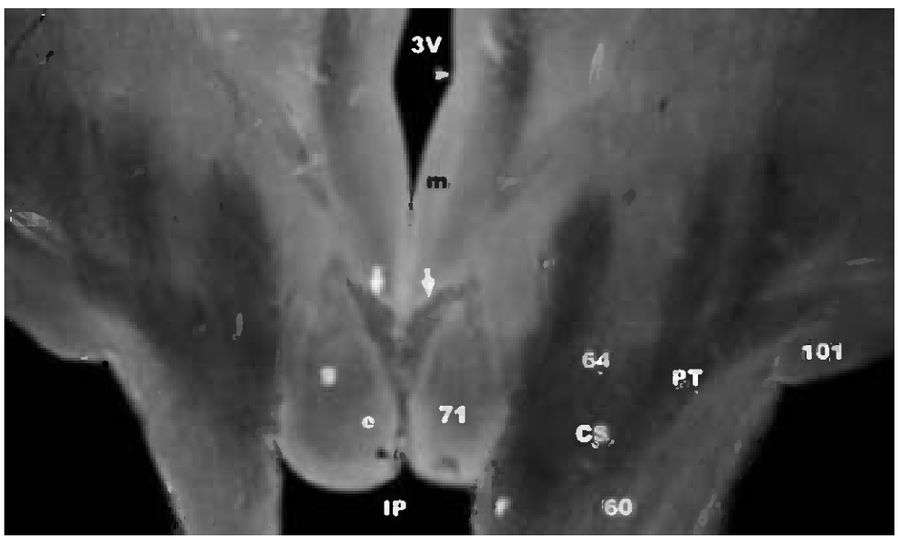

Fig. 8.134. Hypothalamus-epithalamus. Dorsal coronal section.

The principal mammillary fasciculus (white arrows) arises from the medial aspect of the mammillary bodies (71). The sulcus limitans (hypothalamic sulcus) (white arrowhead) marks the interface between the thalamus dorsally and the hypothalamus ventrally. From anteromedial to posterolateral, the cerebral peduncle (60) contains fibers of the frontopontine tract (F), corticospinal tract (pyramidal tract) (CS), and parietotemporal pontine tract (PT).

60 Cerebral peduncle
64 Substantia nigra
71 Mammillary body
101 Optic tract

Letter labels

3V Third ventricle
e Medial nucleus of the mammillary body
g Intercalated nucleus of the mammillary body
m Posterior area of the hypothalamus
CS Corticospinal tract
F Frontopontine tract
IP Interpeduncular fossa
PT Parietotemporopontine tract

Arrowheads and arrows

Single white arrowhead: Sulcus limitans (hypothalamic sulcus) of the third ventricle
Single black arrowhead: Capsule of the mammillary body
Paired white arrows: Principal mammillary fasciculi of each side

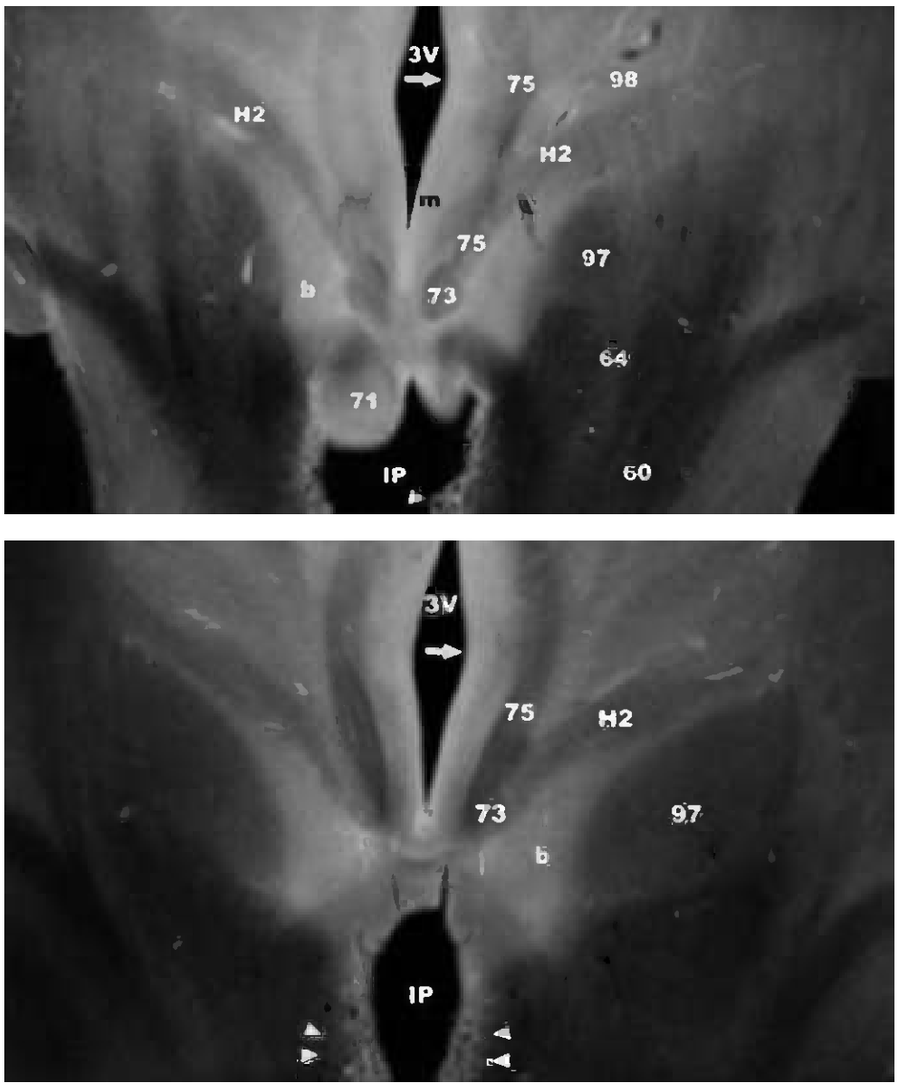

Figs. 8.135 and 8.136. Hypothalamus-epithalamus. Dorsal coronal section.

The principal mammillary fasciculus (73) ascends from the mammillary body (71) and divides into the mammillothalamic tract (75) to the anterior thalamic nuclei and the mammillotegmental tract to the midbrain tegmentum. Deep to the cerebral peduncle (60) lie the substantia nigra (64) and subthalamic nucleus (97). Forel field H2 (lenticular fasciculus) is interposed between the subthalamic nucleus (97) and the zona incerta (98).

60 Cerebral peduncle
64 Substantia nigra
71 Mammillary body
73 Principal mammillary fasciculus
75 Mammillothalamic tract
97 Subthalamic nucleus
98 Zona incerta

Letter labels

3V Third ventricle
b Lateral area of the hypothalamus (containing the medial forebrain bundle)
m Posterior area of the hypothalamus
H2 Forel field H2 (lenticular fasciculus)
IP Interpeduncular fossa

Arrowheads and arrows

White arrowheads: Fibers of the oculomotor nerve (CN III) exiting (Fig. 8.135) and within (Fig. 8.136) the cerebral peduncles
White arrows: Sulcus limitans (hypothalamic sulcus) of the third ventricle

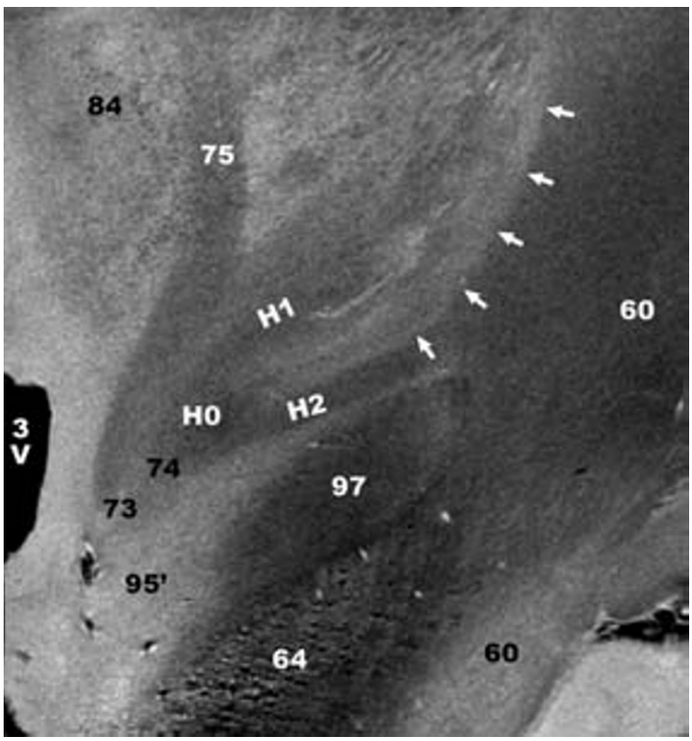

Fig. 8.137. Hypothalamus-epithalamus. Single dorsal coronal section from a different specimen. Subthalamic nucleus, Forel fields. Zona incerta.

At the rostral pole of the red nucleus (capsule: 95'), the posterior border of the substantia nigra (64) marks the widest width of the lens-shaped subthalamic nucleus (97). The zona incerta (white arrows) has a narrow, serpentine shape. Fibers traversing Forel field H2 (lenticular fasciculus) curve around the medial edge of the zona incerta into Forel field H (H0) and then enter Forel field H1 (thalamic fasciculus) to reach the ventral anterior and ventral lateral nuclei of the thalamus. The division of the principal mammillary fasciculus (73) into the mammillothalamic tract (75) and the mammillotegmental tract (74) plus the arching contours of the Forel fields produce a characteristic staghorn configuration that identifies all of the structures.

60 Cerebral peduncle
64 Substantia nigra
73 Principal mammillary tract
74 Mammillotegmental fasciculus
75 Mammillothalamic tract
84 Nucleus medialis thalami, pars dorsolateralis
95' Capsule of the red nucleus
97 Subthalamic nucleus

Letter labels
3V Third ventricle
H0 Forel field H (area tegmentalis H)
H1 Forel field H1 (thalamic fasciculus)
H2 Forel field H2 (lenticular fasciculus)

Arrowheads and arrows
Multiple white arrows: Zona incerta

F. Epithalamus: Habenulo-interpeduncular-tract (fasciculus retroflexus)

Axial, sagittal and coronal sections (Figs. 8.138 to 8.140)

The epithalamus is composed of the pineal gland, the striae medullares thalami and epithelial roof of the third ventricle, the habenular trigones, the habenular commissure, and the habenulo-interpeduncular tract (fasciculus retroflexus). The habenular trigones are formed by smaller medial and larger lateral habenular nuclei. The medial and lateral habenular nuclei appear to be independent, mutually-isolated, processing systems [322]. The medial system receives information from the medial septal nuclei, and through these nuclei, from the hippocampus. Medial habenular efferents traverse the habenulo-interpeduncular tract to end exclusively in the interpeduncular nucleus. From there, a "massive" outflow reaches the nucleus centralis superior, and the dorsal raphe nuclei [322]. The lateral habenular system receives information from the nuclei of the diagonal band of Broca at the posterior edge of the anterior perforated substance, from the lateral preoptic area, the substantia nigra, and the medial nucleus of the globus pallidus [322]. Lateral habenular efferents traverse the habenulo-interpeduncular tract, but bypass the interpeduncular nucleus, to end in multiple mesencephalic centers includng substantia nigra pars compacta, ventral periaqueductal gray matter, the nucleus centralis superior, the dorsal raphe and the reticular formation of the midbrain [322].

These cartoons (A–B) display the anatomic region imaged in **Figs. 8.138–8.140**.

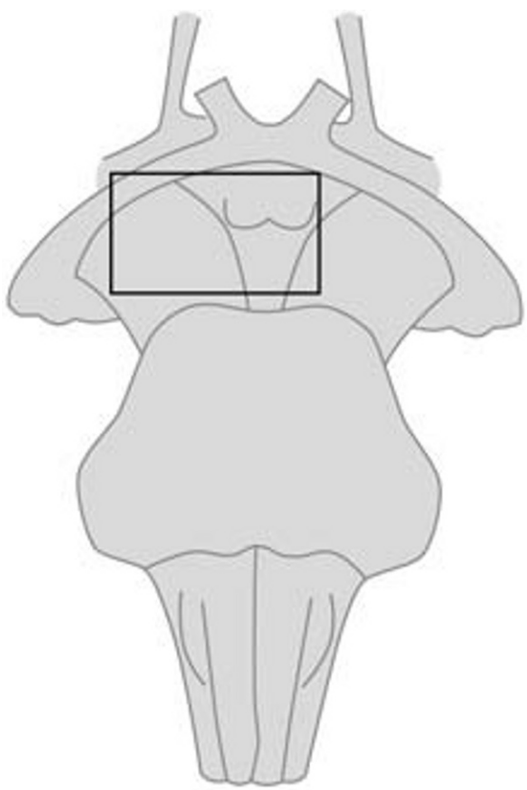

A

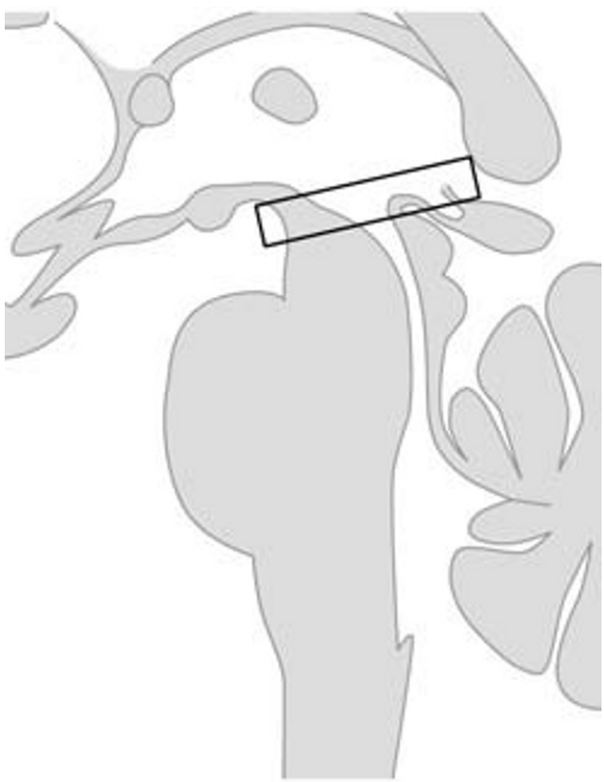

B

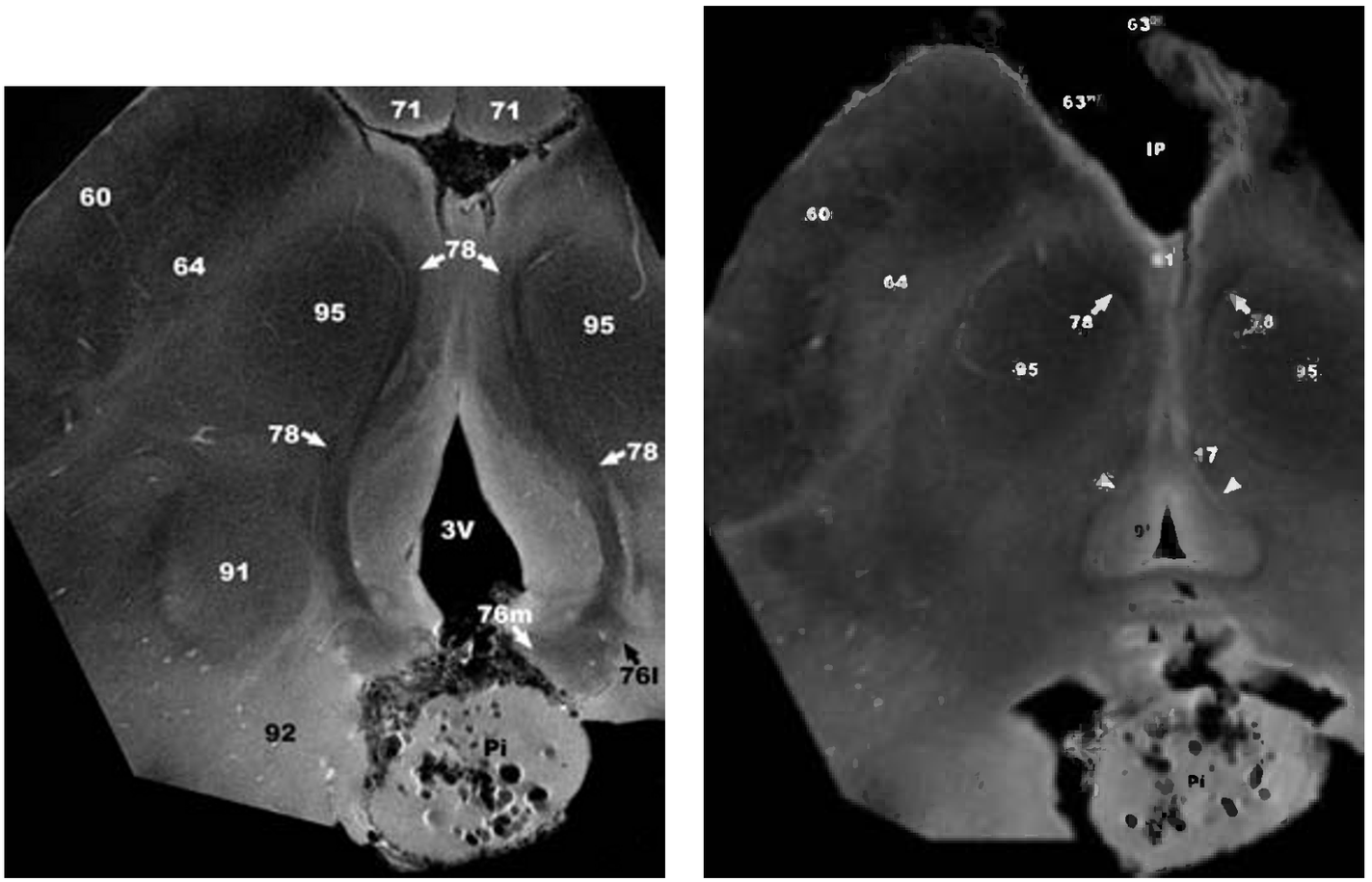

A B

Fig. 8.138 (A–B). Habenulo-interpeduncular tract. Axial sections displayed from caudal (A) to cranial (B).

The paired habenulo-interpeduncular tracts (78) assume a lyre shape as they descend from the habenular nuclei (76m, 76l), arch laterally around the periaqueductal gray matter, approach but remain medial to the centromedial nuclei (91) of the thalami, and then curve medially along the rostromedial border of the red nuclei (95) [322]. Near the rostral pole of the red nucleus, they recurve ventrally and posteriorly to enter the interpeduncular nucleus (61). The nucleus of the habenulo-interpeduncular tract is contained within the tract, medial to the red nucleus, producing a characteristic "triplet" signature of high signal central gray matter and flanking low signal white matter fascicles [358]. Calcifications cause multiple low signal foci within the pineal gland (Pi).

9′ Periaqueductal gray matter
17 Medial longitudinal fasciculus
60 Cerebral peduncle
61 Interpeduncular nucleus
63" Oculomotor nerve
64 Substantia nigra
71 Mammillary body
76m Medial habenular nucleus (also v)
76l Lateral habenular nucleus (also w)
78 Habenulo-interpeduncular tract (fasciculus retroflexus)
91 Centromedian nucleus
92 Pulvinar
95 Red nucleus

Letter labels

3V Third ventricle
IP Interpeduncular fossa
Pi Pineal gland

Arrowheads and arrows

Paired white arrowheads: Nuclei of Darkschewitsch [358]
Paired black arrowheads: Habenular commissure
Single black arrow: Posterior commissure

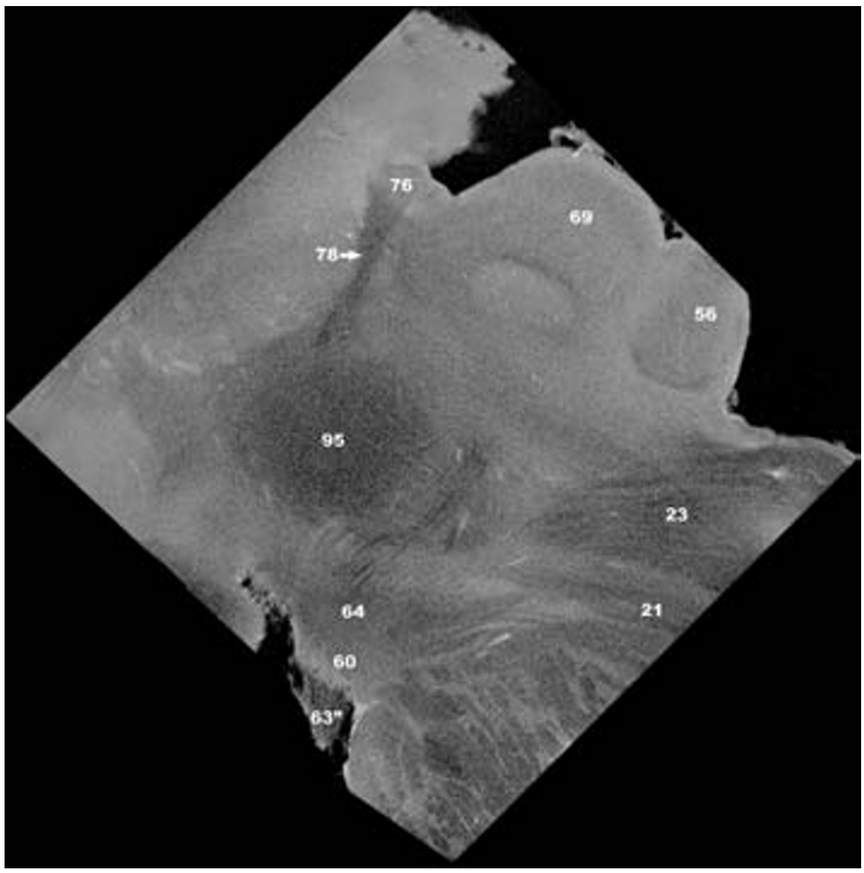

A

Fig. 8.139 (A–C). Habenulo-interpeduncular tract. Sagittal sections displayed from medial (A) to lateral (C).

From the habenular nuclei (76), the habenulo-interpeduncular tract (fasciculus retroflexus) (78) angles antero-inferiorly, courses along the medial border of the rostral end of the red nucleus, (95) and then recurves postero-inferiorly, beneath the red nucleus to reach the interpeduncular nucleus (61). Medial to the red nucleus, this tract contains the nucleus of the habenulo-interpeduncular tract, and displays the characteristic "triplet" signature.

9′ Periaqueductal gray matter
17 Medial longitudinal fasciculus
21 Medial lemniscus
23 Superior cerebellar peduncle
23′ Decussation of the superior cerebellar peduncle
51 Pontocerebellar fibers, seen longitudinally or in cut cross-section
56 Inferior colliculus
60 Cerebral peduncle
61 Interpeduncular nucleus
63 Oculomotor nucleus (CN III)
63′ Intramesencephalic oculomotor fibers
63″ Oculomotor nerve
64 Substantia nigra
69 Superior colliculus
71 Mammillary body
72 Anterior column of the fornix
76 Habenular nuclei
78 Habenulo-interpeduncular tract (fasciculus retroflexus)
95 Red nucleus

Letter labels

IP Interpeduncular fossa
Pi Pineal gland

Arrowheads and arrows

Single white arrowhead: Trochlear fascicles passing caudally to their decussation
Single white arrow: Posterior commissure

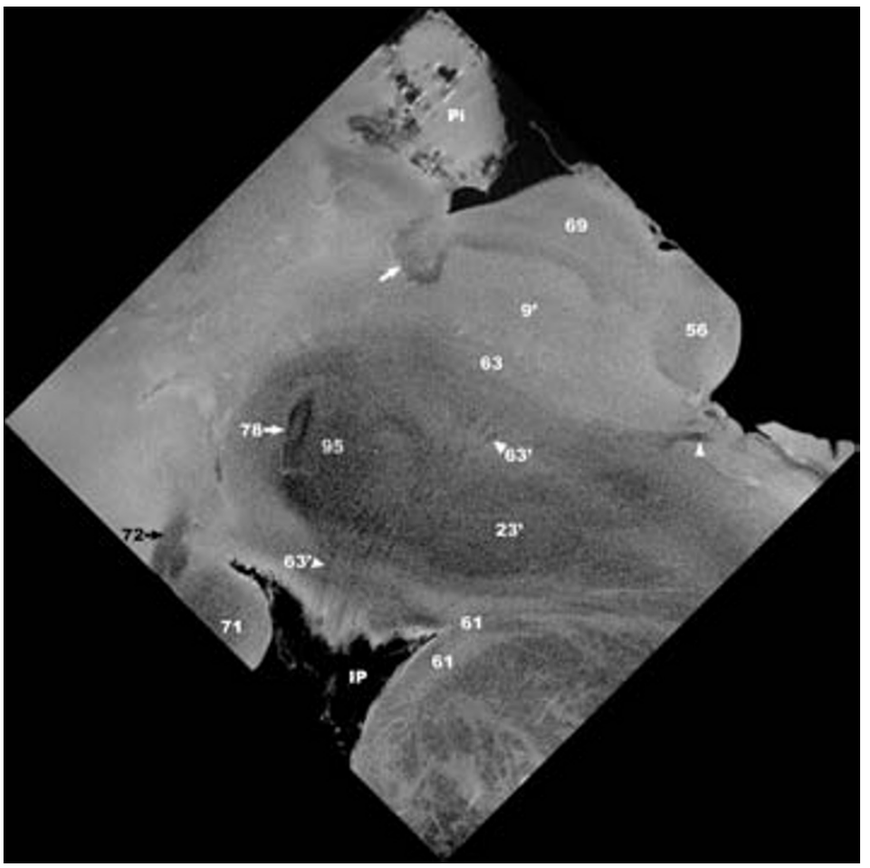
Pi
69
9'
56
63
78
95
63'
72
23'
63'
71
61
IP
61

B

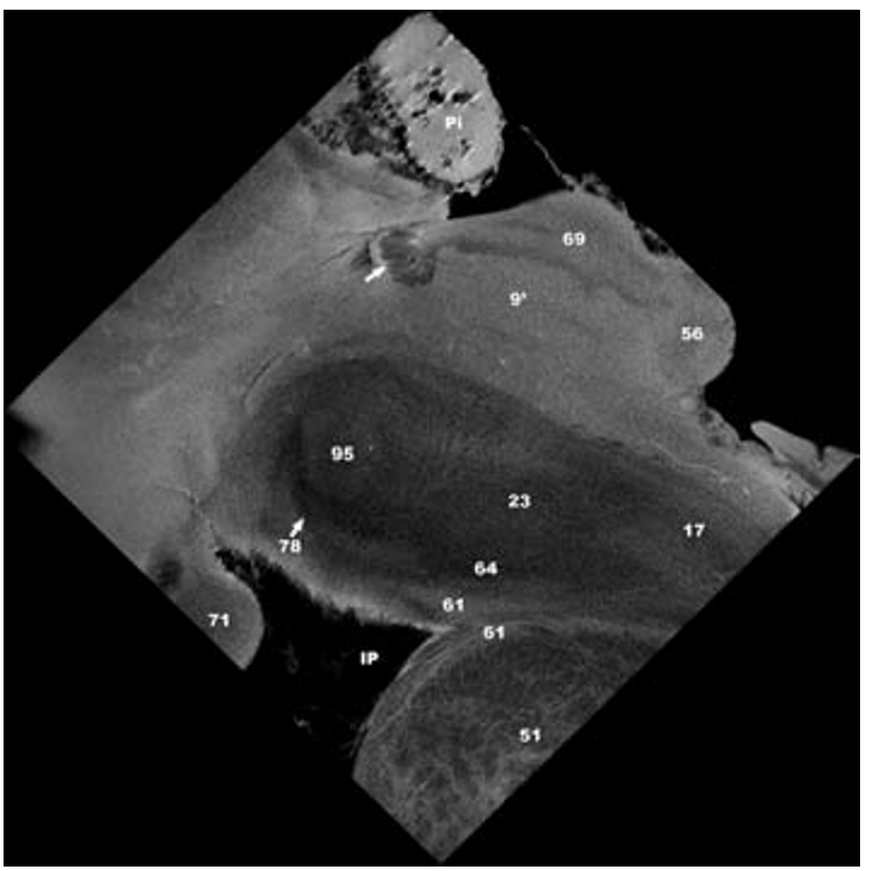
Pi
69
9'
56
95
23
17
78
64
61
71
61
IP
51

C

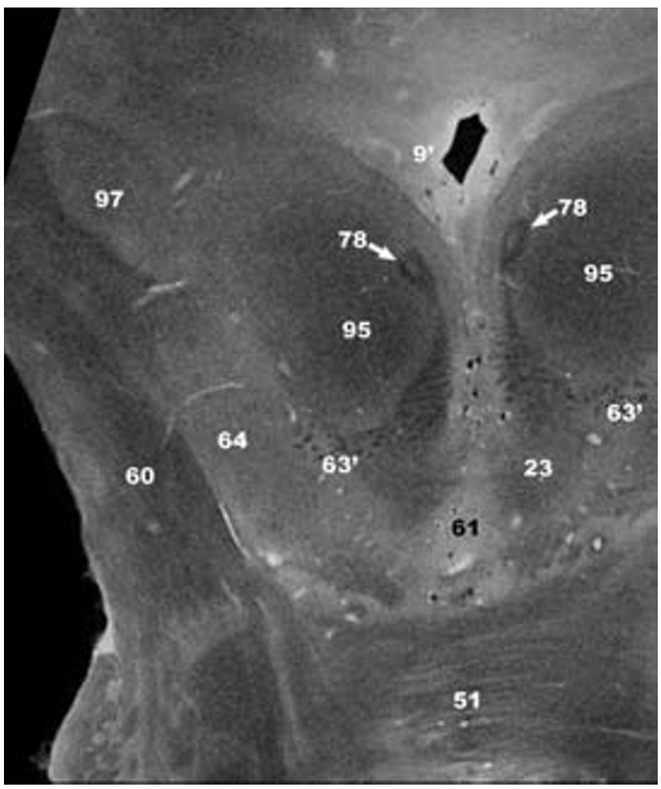

A

Fig. 8.140 (A–C). Habenulo-interpeduncular tract. Coronal sections displayed from anterior (A) to posterior (C).

The relationship of the habenulo-interpeduncular tract (78) to the medial aspect of the red nucleus (95) and the "triplet" configuration of the tract are well displayed in the coronal plane.

9′ Periaqueductal gray matter
17 Medial longitudinal fasciculus
23 Superior cerebellar peduncle
23′ Decussation of the superior cerebellar peduncle
38 Middle cerebellar peduncle (brachium pontis)
51 Pontocerebellar fibers, seen longitudinally
60 Cerebral peduncle
61 Interpeduncular nucleus
63′ Intramesencephalic oculomotor fibers
64 Substantia nigra
78 Habenulo-interpeduncular tract
95 Red nucleus
97 Subthalamic nucleus
98 Zona incerta

Letter labels
3V Third ventricle

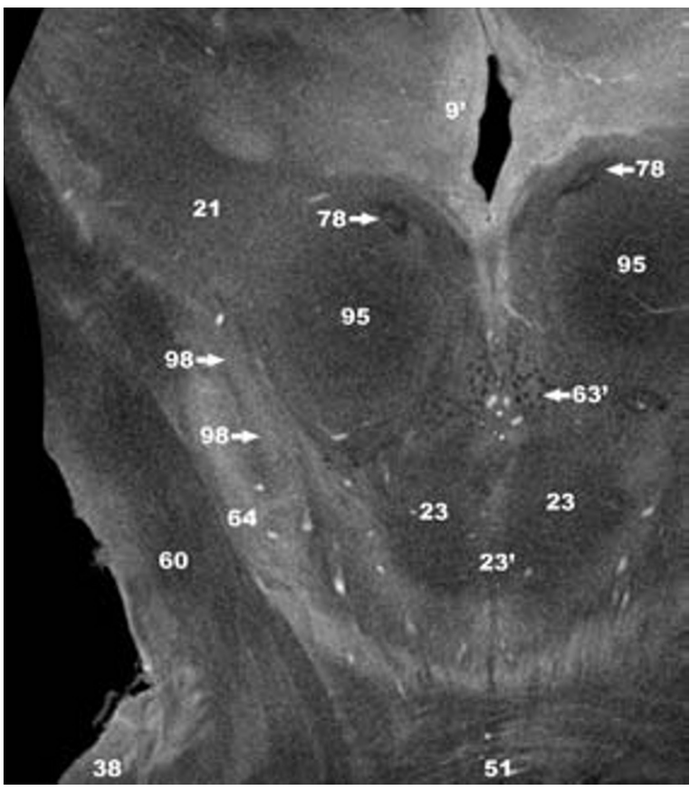

B

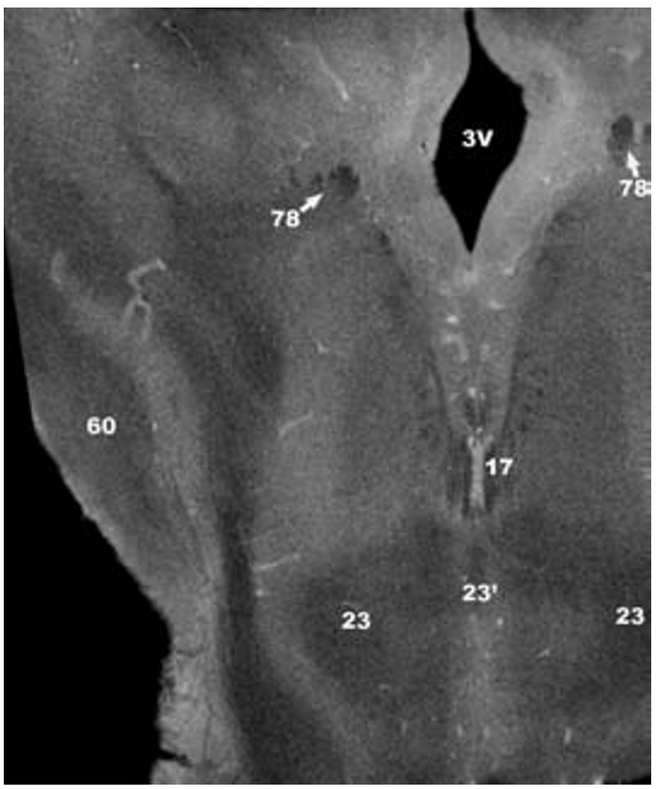

C

G. Metathalamus (medial and lateral geniculate bodies)

Gross anatomy and sections in the axial and coronal planes (Figs. 8.141–8.147)

The metathalamus is composed of the medial and lateral geniculate bodies. These lie inferolateral to the pulvinar of the thalamus, along the lateral aspect of the midbrain (medial geniculate body) or lateral to the midbrain (lateral geniculate body).

These cartoon (A–B) display the anatomic region imaged in Figs. 8.141–8.147.

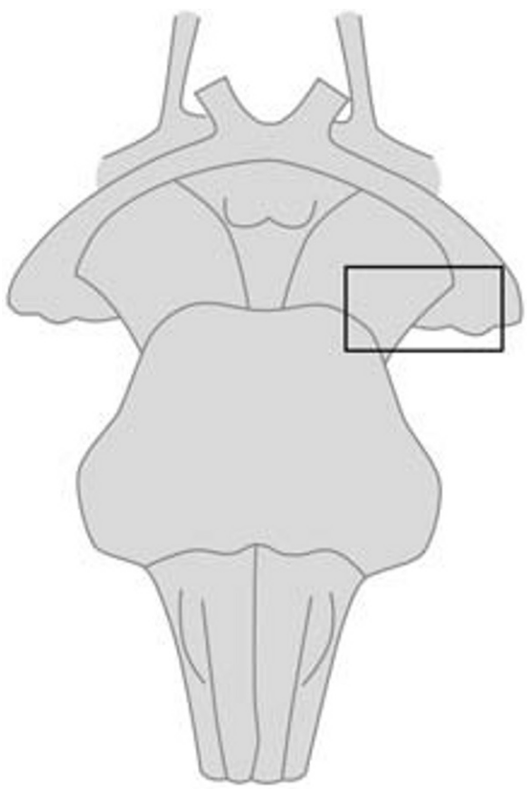

A

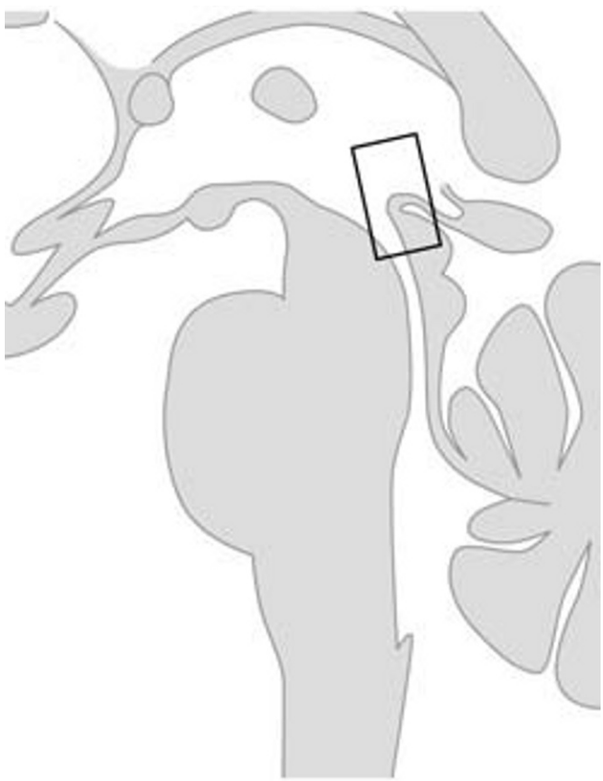

B

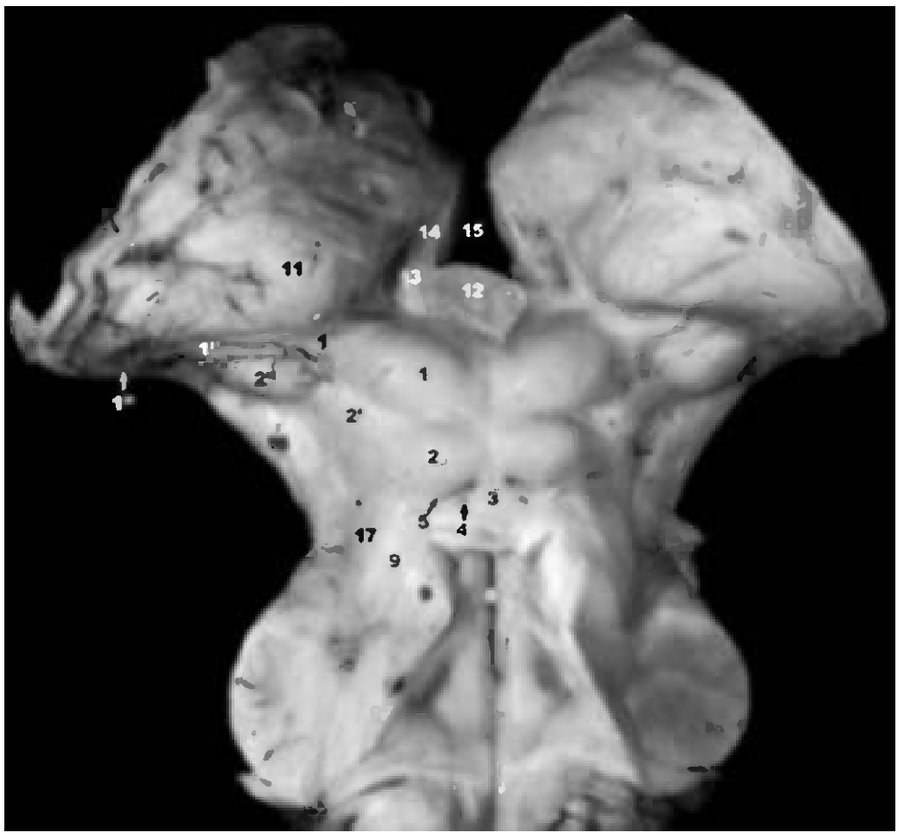

A

Fig. 8.141 (A–B). Metathalamus. Gross anatomic preparations.

Dorsal **(A)** and dorsal oblique **(B)** views of the thalami, midbrain and pons. Resection of overlying portions of the cerebrum, the cerebellum and the vascular network reveals the relationships among the quadrigeminal plate and the medial and lateral geniculate bodies.

1 Vision-related fibers from the superior colliculus (1) form the brachium of the superior colliculus (1′) that arches over the medial geniculate body (2″) to reach the lateral geniculate body (1″)
2 Auditory fibers from the inferior colliculus (2) form the brachium of the inferior colliculus (2′) that extends to the medial geniculate body (2″)
3 The midline frenulum veli (3) anchors the superior medullary velum (7)
4 Deep veins emerge onto the dorsal surface of the midbrain at the infracollicular recess (4)
5 At 5, the trochlear nerves that decussated in the superior medullary velum (7) emerge from the dorsal surface of the midbrain to enter the quadrigeminal plate cistern
8 Median sulcus of the floor of the fourth ventricle
9 Superior cerebellar peduncle
11 The pulvinar (11) overhangs the lateral (1″) and medial (2″) geniculate bodies
12 Pineal gland
13 The habenular trigone (13) is formed by the medial and lateral habenular nuclei
14 Paired striae medullares thalami (14) extend ventrodorsally along the lateral margins of the roof of the third ventricle (15), where the roof inserts into the medial wall of the thalamus. They interconnect the habenular nuclei with the septal and basal regions.
16 Exposed posterior margin of the cerebral peduncle
17 Lateral lemniscus, carrying auditory fibers to the medial geniculate body (2)

B

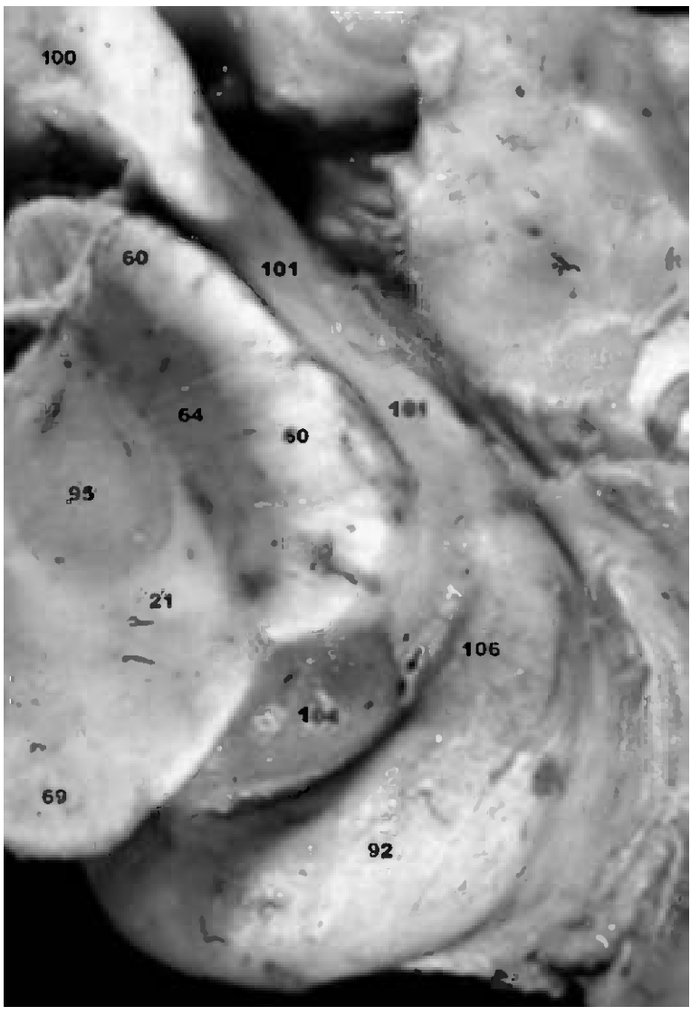

Fig. 8.142. Gross anatomic preparation of the left midbrain and metathalamus.

View from inferior after resection of all overlying tissue. The medial geniculate body (104) lies immediately posterior to the cerebral peduncle (60), within the lateral mesencephalic sulcus. It is separated from the lateral geniculate body (106) by the intergeniculate sulcus and vein (small black arrow). From the optic chiasm (100), the optic tract (101) extends posteriorly to envelop and pass into the lateral geniculate body (106). The pulvinar (92) lies posterosuperior to and overhangs the geniculate bodies.

21 Medial lemniscus
60 Cerebral peduncle
64 Substantia nigra
69 Superior colliculus
95 Red nucleus
100 Optic chiasm
101 Optic tract
104 Medial geniculate body
106 Lateral geniculate body. The lateral portion of the lateral geniculate body curves downward and extends further inferiorly than the medial portion.

Fig. 8.143. Medial and lateral geniculate bodies. Coronal section, with midline to the reader's left. Intravascular India ink injection. Bar: 0.8 mm.

The intergeniculate sulcus and vein (4) separate the medial (1) from the lateral (2) geniculate body. The medial geniculate nucleus shows a gently convex inferior border and more nearly homogeneous texture. The lateral geniculate body shows a pronounced inferior prolongation of its lateral portion and a highly laminated internal structure composed of two magnocellular laminae (a,b) ventrally and four parvocellular laminae (c,d,e,f) dorsally. The optic tracts convey fibers from the ipsilateral eye to layers b, c and e, and fibers from the contralateral eye to layers a, d and f [322]. Each eye projects fibers to one magnocellular layer and two parvocellular layers, and each layer has a complete representation of the contralateral visual hemifield [322]. There is great visuotopic organization of the lateral geniculate body.

1 Medial geniculate body
2 Lateral geniculate body. Fibers from the optic tract extend around and through the individual layers of gray matter:
a.–b.: Magnocellular layers,
c.–f.: Parvocellular layers.
Optic fibers from the ipsilateral retina synapse in layers b, c and e, while optic fibers from the contralateral retina synapse in layers a, d and f.
3 Thalamogeniculate vessels
4 Prominent intergeniculate vein, which emerges at the surface just between the medial and lateral geniculate bodies

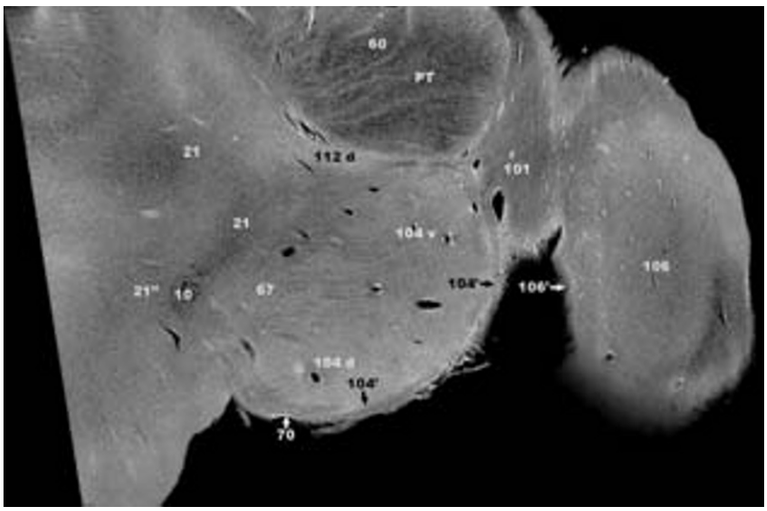

A

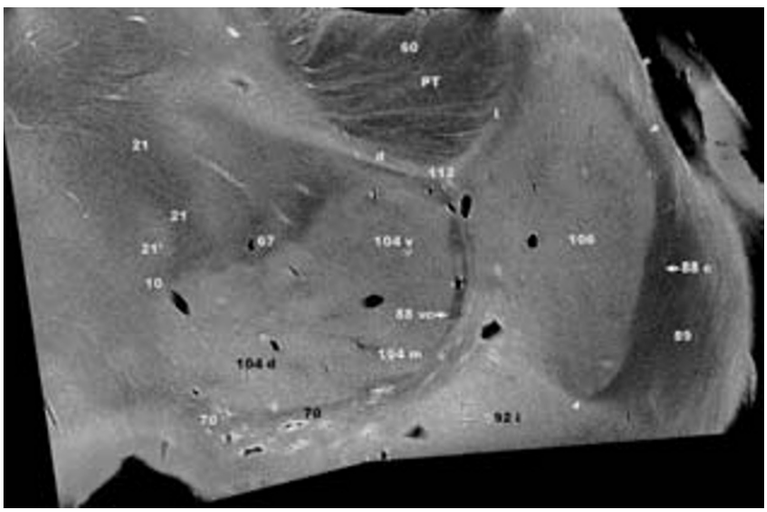

B

Fig. 8.144 (A–D). Metathalamus. Axial MR Microscopy at 9.4 T, displayed from caudal (A) to cranial (D).

The medial geniculate body (104) attaches to the lateral margin of the midbrain through a medially-directed hilus and is encapsulated (104′) laterally. The brachium of the inferior colliculus (67) enters the medial geniculate body through the hilus. The medial lemniscus (21) and the spinothalamic tract (10) ascend into the thalamus medial to the medial geniculate body. The peripeduncular nucleus (112) is a caudal prolongation of the zona incerta. This nucleus delimits the posterior margin of the cerebral peduncle (60) and separates the peduncle from the medial geniculate body (104). The medial geniculate body contains ventral, dorsal and marginal subnuclei [358]. Of these, the ventral nucleus shows a laminar structure that may facilitate frequency discrimination (tonotopy), with high frequencies represented medially and low frequencies laterally [358].

The lateral geniculate body (106) lies posterolateral to the medial geniculate body and cerebral peduncle. The medial portion of the lateral geniculate body lies at approximately the same level as the medial geniculate body. The lateral portion shows a prominent process that hooks inferiorly. The intergeniculate sulcus and vein separate the medial and lateral geniculate bodies. The intergeniculate nucleus of the thalamus (92i) is interposed between the posterior ends of the medial and lateral geniculate bodies. The peduncle of the superior colliculus (70) crosses over the medial geniculate body to reach the lateral geniculate nucleus. The lateral geniculate body shows a strong laminar structure (See next **Figs. 8.145–8.147**). The area triangularis of Wernicke (89) lies dorsolateral to the lateral geniculate body and contains fibers of the optic (geniculocalcarine) radiations, the acoustic (geniculotemporal) radiations, the temporal and occipital contingents of the parietotemporopontine tract, and fibers passing to and from the pulvinar [358].

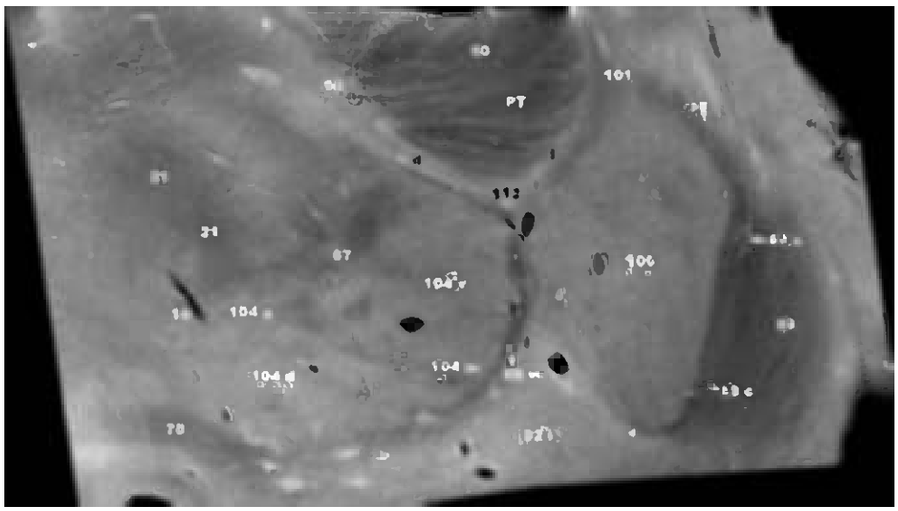

C

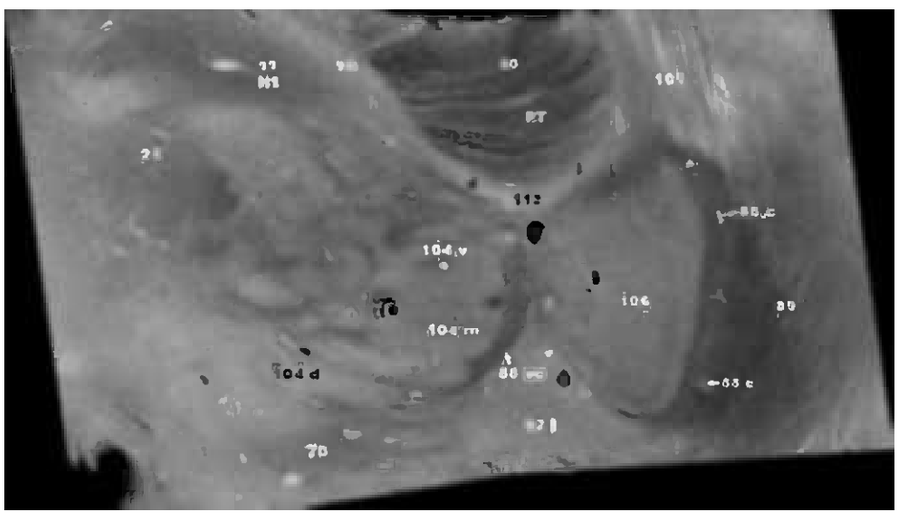

D

10 Spinothalamic tract
21 Medial lemniscus
21″ Nucleus of the medial lemniscus
60 Cerebral peduncle
67 Brachium of the inferior colliculus
70 Brachium of the superior colliculus
88c Caudal thalamic peduncle
88vc Ventrocaudal thalamic peduncle
89 Area triangularis of Wernicke
92i Nucleus pulvinaris inferior thalami
98 Zona incerta
99 Fields of Forel
101 Optic tract
104 Medial geniculate body
104′ Capsule of the medial geniculate body
104d Dorsal nucleus of the medial geniculate body
104m Marginal nucleus of the medial geniculate body
104v Ventral nucleus of the medial geniculate body
106 Lateral geniculate body
106′ Capsule of the lateral geniculate body
112 Peripeduncular nucleus, with dorsal (d) and lateral (l) divisions

Letter labels

H1 Forel field H1 (also 99, which is used generically for any Forel fields)
PT Parieto-temporopontine tract within the cerebral peduncle (60)

Arrowheads and arrows

White arrowheads: Capsule of the lateral geniculate body

Fig. 8.145 (A–C). Metathalamus. Coronal MR Microscopy at 9.4 T, displayed from anterior pole **(A)** to mid-body **(C).** Figure 8.146 displays the posterior half of these structures.

The optic tract (101) carries the visual information posteriorly, around the cerebral peduncle (60) to the lateral geniculate body (106), where it distributes to the magnocellular and parvocellular layers for the ipsilateral and contralateral eyes. The intergeniculate sulcus and vein (white arrow) separate the medial from the lateral geniculate bodies. The optic (geniculocalcarine) radiations (107) extend outward from the posterosuperolateral aspect of the lateral geniculate body. These fibers traverse the retrolenticular portion of the internal capsule (175r) and then arch around the lateral ventricle [322]. Those fibers arising from the lateral portion of the lateral geniculate body and ending inferior to the calcarine sulcus first sweep ventrally and laterally, over the temporal horn and into the temporal lobe as Meyer's loop before turning posteriorly to the calcarine cortex

21 Medial lemniscus
60 Cerebral peduncle
64 Substantia nigra
67 Brachium of the inferior colliculus
78 Habenulo-interpeduncular tract (fasciculus retroflexus)
85 Nucleus medialis thalami, pars ventromedianis
86′ Thalamoparietal fibers
87 Nucleus reticularis thalami (within lateral (external) medullary lamina of the thalamus)
88c Caudal thalamic peduncle
91 Centromedian nucleus of the thalamus
93m Ventral posteromedial nucleus of the thalamus
94l Ventral lateral nucleus of the thalamus
95 Red nucleus
98 Zona incerta
101 Optic tract
104 Medial geniculate body
104′ Capsule of the medial geniculate body
105 Auditory radiations (geniculotemporal radiations)
106 Lateral geniculate body
106′ Capsule of the lateral geniculate body
107 Optic radiations (geniculocalcarine radiations)
113 Pregeniculate nucleus
161 Stria semicircularis
175p Internal capsule, posterior limb
175r Retrolenticular portion of the internal capsule
175s Sublenticular portion of the internal capsule
178 Putamen
178′ Caudato-lenticular bridges of gray matter
179 Globus pallidus (lateral nucleus, external nucleus)
179′ Lateral (external) medullary lamina of the lenticular nucleus

Arrowheads and arrows

White arrow: Intergeniculate vein exiting at the intergeniculate groove

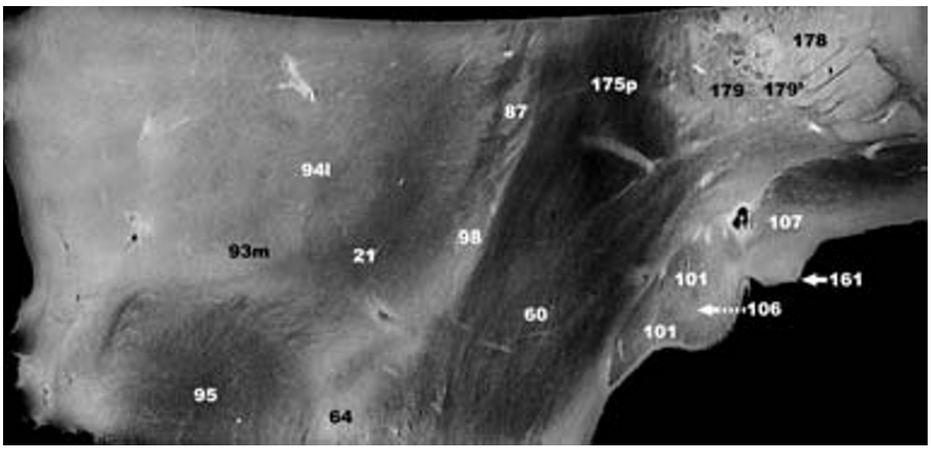
178
175p
179
179'
87
94l
107
98
93m
21
101
161
106
60
101
95
64

A

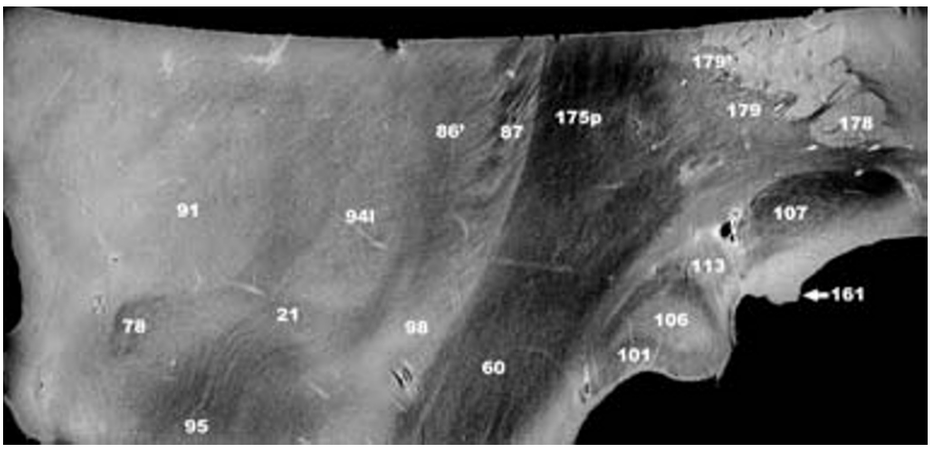
179'
86'
87
175p
179
178
91
94l
107
113
161
78
21
98
106
60
101
95

B

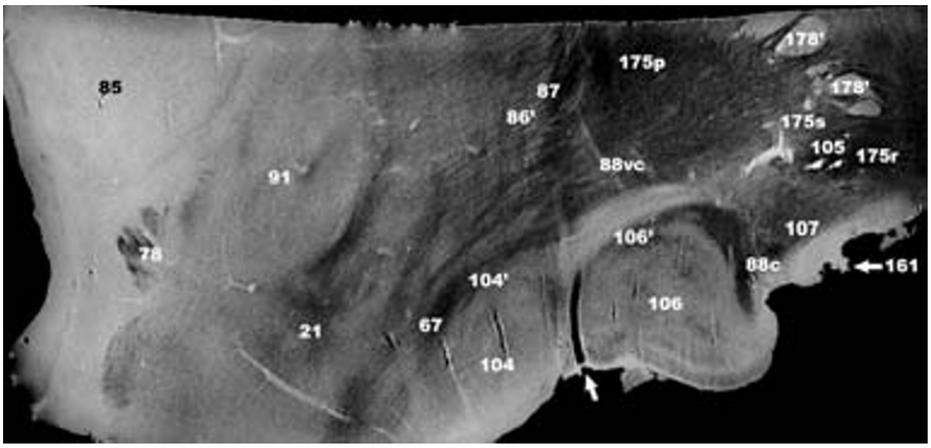
178'
175p
85
87
178'
86'
175s
105
175r
88vc
91
106'
107
78
88c
161
104'
106
21
67
104

C

Fig. 8.146. Metathalamus. Coronal MR Microscopy at 9.4 T, displayed from mid body **(A)** to posterior pole **(C).** Figure 8.145 displays the anterior half of these structures.

The pretectal area (80) lies just rostral to the superior colliculus at the level of the posterior commissure. Multiple nuclei in this region participate in the visual system. This region is believed to be the principal midbrain center for the pupillary light reflex [78]. The carrefour sensitif (Car S) (sensory crossroads) is a portion of the internal capsule in which the dorsal, caudal, and caudoventral thalamic peduncles converge as they convey somesthetic, visual and auditory stimuli to their primary cortical centers.

9′ Periaqueductal gray matter
21 Medial lemniscus
57 Area parabigemina posterior
67 Brachium of the inferior colliculus
69 Superior colliculus
70 Brachium of the superior colliculus
76l Lateral habenular nucleus (also w)
76m Medial habenular nucleus (also v)
77 Stria medullaris thalami
78 Habenulo-interpeduncular tract (fasciculus retroflexus)
80 Pretectal area
85 Nucleus medialis thalami, pars ventromedianis
86 Nucleus lateralis thalami
86′ Thalamoparietal fibers
87 Nucleus reticularis thalami (within lateral (external) medullary lamina of the thalamus)
88c Caudal thalamic peduncle
88vc Ventrocaudal thalamic peduncle
89 Area triangularis of Wernicke
91 Centromedian nucleus of the thalamus
92i Nucleus pulvinaris inferior thalami
92l Nucleus pulvinaris lateralis thalami
93m Ventral posteromedial nucleus of the thalamus
93l Ventral posterolateral nucleus of the thalamus
104 Medial geniculate body
105 Auditory radiations (geniculotemporal radiations)
106 Lateral geniculate body
107 Optic radiations (geniculocalcarine radiations)
112 Peripeduncular nucleus (with dorsal (d) and lateral (l) divisions)
175p Internal capsule, posterior limb
175r Retrolenticular portion of the internal capsule
175s Sublenticular portion of the internal capsule

Letter labels

Car S Carrefour sensitif

Arrowheads and arrows

Single white arrowhead: Capsule of the medial geniculate body
Dual white arrowheads: Capsule of the lateral geniculate body
Multiple black arrowheads: Internal medullary lamina of the thalamus
Single white arrow: Posterior commissure
Single black arrow: Habenular commissure

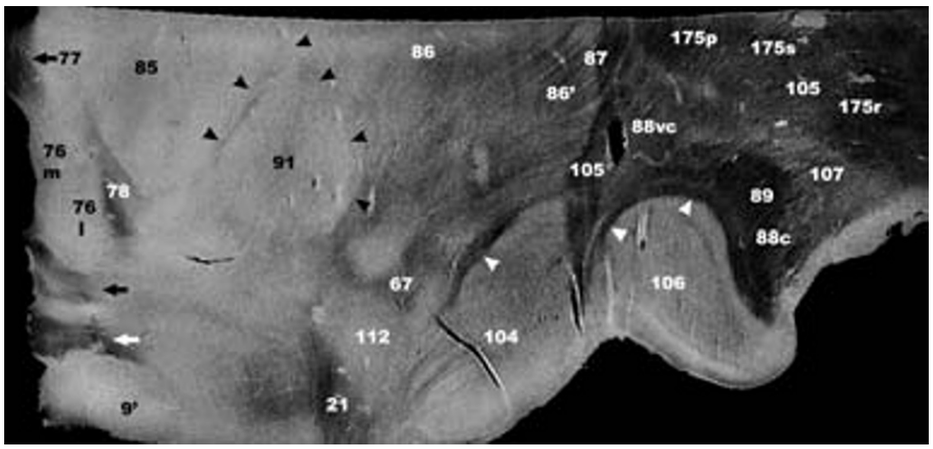
77
85
86
87
175p
175s
86'
105
175r
88vc
76
m
91
105
107
78
89
76
l
88c
67
106
112
104
9'
21

A

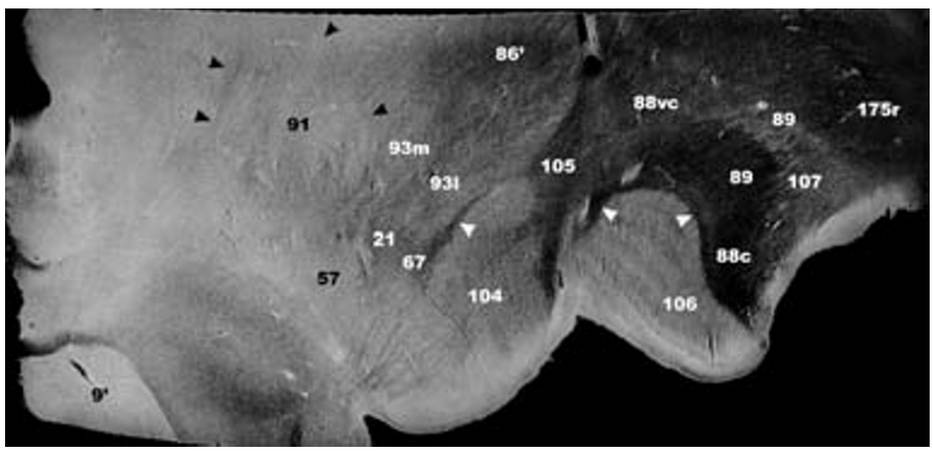
86'
88vc
89
175r
91
93m
105
93l
89
107
21
67
88c
57
104
106
9'

B

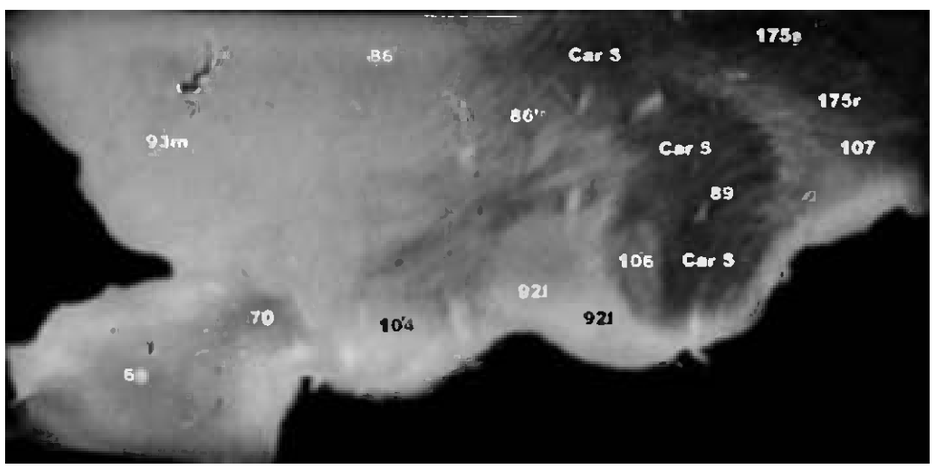
175p
86
Car 3
175r
86'
93m
Car 3
107
89
106
Car 3
92l
70
104
92l
6

C

Fig. 8.147 (A–B). Metathalamus. Anatomic – MR Correlation
A. Oblique MR Microscopy at 9.4 T.
B. Oblique histological section of the same tissue with Nissl stain (for neurons).

The lateral geniculate body lies lateral to the medial geniculate body (104), medial to the triangular area of Wernicke (89), posterior to the cerebral peduncle (60) and interpeduncular nucleus (112), and anterior to the pulvinar (92i). The magnocellular layers (1,2) of the lateral geniculate nucleus lie ventrally, and the parvocellular layers (3,4,5,6) dorsally. The optic tract penetrates into the lateral geniculate body, carrying fibers from the ipsilateral eye to layers 2,3,5, and fibers from the contralateral eye to layers 1,4,6. The cells of parvocellular layers 3-6 project to the calcarine cortex via the geniculocalcarine radiations [78].

60 Cerebral peduncle
67 Brachium of the inferior colliculus
88vc Ventrocaudal thalamic peduncle
89 Area triangularis of Wernicke
92i Nucleus pulvinaris inferior thalami
104v Ventral nucleus of the medial geniculate body
106 Lateral geniculate body, composed of 6 layers:
Magnocellular layers: 1–2 , and
Parvocellular layers: 3–6
112 Peripeduncular nucleus (with dorsal (d) and lateral (l) divisions)

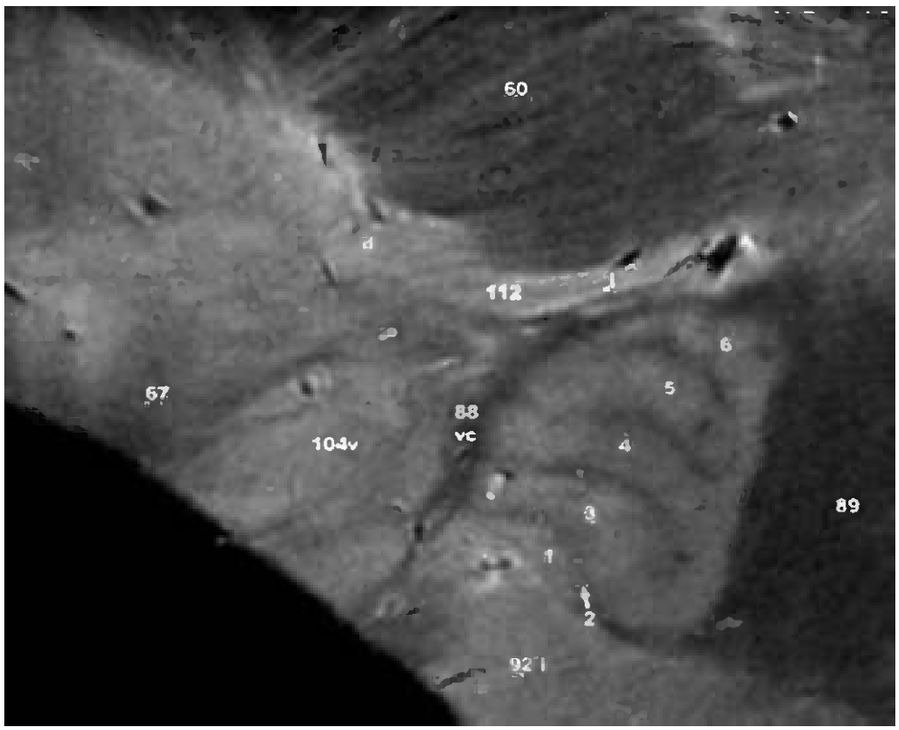

A

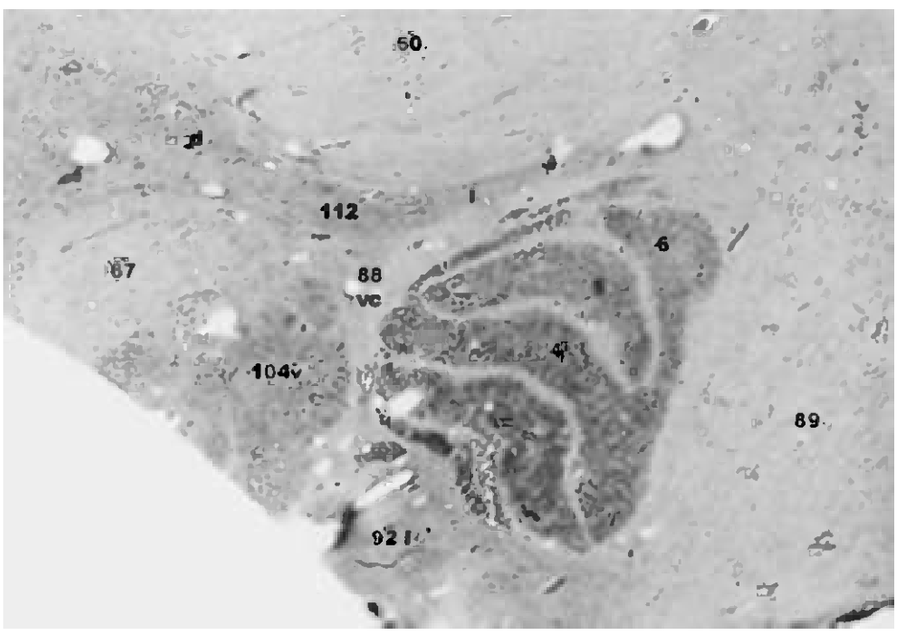

B

Table 9.1. The cranial nerves: Type and function*

C.N. No.	Name	Nerve Type	Function
I.	**Olfactory**	**SVA**	Olfactory sensation from primary sensory neurons in the olfactory mucosa, with secondary relay via the olfactory bulb and tract
II.	**Optic**	**SSA**	Visual sensation from primary sensory neurons in the retina, with secondary relay via the optic nerve
III.	**Oculomotor**	**GSE**	Motor from the oculomotor nucleus to the medial rectus, superior rectus, inferior rectus, inferior oblique, and levator palpebrae superioris
		GVE	Parasympathetic motor supply from the nucleus of Edinger-Westphal to the ciliary ganglion for the ciliary and pupillary constrictors
IV.	**Trochlear**	**GSE**	Motor from the trochlear nucleus to the contralateral superior oblique
V.	**Trigeminal Motor Root**	**SVE**	Motor from the masticator nucleus to the muscles of mastication (masseter, temporalis, medial pterygoid, lateral pterygoid, tensor veli palatini) and to the tensor tympani, mylohyoid, and anterior belly of the digastric muscle
	Trigeminal Sensory Root	**GSA**	Sensory from (i) the mesencephalic nucleus to proprioceptive muscle spindles within the masticator muscles for muscle stretch, and (ii) the semilunar (Gasserian) ganglion to (a) mechanoreceptors for tactile discrimination (relayed secondarily via the principal sensory nucleus), (b) nociceptors, thermoreceptors, and light touch receptors (relayed secondarily via the spinal trigeminal nucleus) These GSA fibers extend to the surface of the scalp, face and neck; mucous membranes of the paranasal, nasal and oral cavities including tongue and teeth; meninges of the anterior and middle fossae; and the external surface of the tympanic membrane
VI.	**Abducens**	**GSE**	Motor from the abducens nucleus to the lateral rectus
VII.	**Facial Nerve**	**SVE**	Motor from the facial nucleus to the stapedius, stylohyoid, posterior belly of the digastric, the muscles of facial expression, the buccinator, platysma, and occipitalis
	Nervus intermedius	**GVE**	Parasympathetic motor supply from the superior salivatory nucleus to the (i) pterygopalatine ganglion for the lacrimal, nasal and palatine glands (ii) submandibular and sublingual ganglia for the submandibular and sublingual glands
		GSA	General sensation from the geniculate ganglion to the concha of the external ear, a small area of skin behind the external ear, and possibly supplemental to CN V3, for supply to the external acoustic meatus and the external surface of the tympanic membrane
		SVA	Taste sensation from the geniculate ganglion to the anterior 2/3 of the tongue and the hard and soft palates
VIII.	**Vestibulo-cochlear** **Vestibular division**	**SSA**	Vestibular sensation from the vestibular ganglion (of Scarpa)
	Cochlear division	**SSA**	Auditory sensation from the cochlear ganglion (spiral ganglion of Corti)
IX.	**Glossopharyngeal**	**SVE**	Motor from the nucleus ambiguus to the striated stylopharyngeus
		GVE	Parasympathetic motor supply from the inferior salivatory nucleus (via complex course) to the otic ganglion for the parotid gland
		GSA	General sensation from the superior and inferior glossopharyngeal ganglia to the posterior 1/3 of the tongue, skin of the external ear and the internal surface of the tympanic membrane
		SVA	Taste sensation from the inferior glossopharyngeal (petrosal) ganglion to the posterior 1/3 of the tongue
X.	**Vagus**	**SVE**	Motor from the nucleus ambiguus to the striated muscle of the pharynx and larynx, except the stylopharyngeus (supplied by CN IX) and the tensor veli palatini (supplied by CN V3). Motor function to the palatoglossus of the tongue.
		GVE	Parasympathetic motor fibers from the dorsal motor nucleus of the vagus and the dorsal gray matter of the lower medulla to terminal ganglia near to the smooth muscles and glands of the pharynx, larynx, thoracic and abdominal viscera as far caudally as the splenic flexure
		GSA	General sensation from the superior (jugular) ganglion of the vagus to a small area in and around the external ear
		GVA	Visceral sensation from the inferior (nodose) ganglion of the vagus to the pharynx, larynx and viscera, stretch receptors in the aortic arch and chemoreceptors in the aortic bodies
		SVA	Taste sensation from the inferior (nodose) ganglion of the vagus to the epiglotits
XI.	**Accessory**	**SVE**	Motor function from the lateral motor column of cervical cord segments C2-C5 and from the nucleus ambiguus to the sternocleidomastoid and trapezius
XII.	**Hypoglossal**	**GSE**	Motor from the hypoglossal nucleus to the intrinsic and extrinsic muscles of the tongue, except the palatoglossus (supplied by CN X)

*Based in part on Table 1: *The Cranial Nerves and Their Function* [467, Wilson, p. viii])

SECTION IX

CRANIAL NERVES: INTRA-AXIAL AND CISTERNAL SEGMENTS

Classically, twelve cranial nerves (CN) are described: CN I to CN XII (Table 9.1) [78, 164, 249, 250, 260, 467, 487, 488]. Of these, CN III-XII have myelin sheaths derived from Schwann cells and are true nerves. The olfactory nerve (CN I) and the optic nerve (CN II) have myelin sheaths derived from oligodendroglia, and, therefore constitute intrinsic tracts of the brain, not nerves. None-the-less, the twelve "nerves" will be considered together in this section, and will be presented from caudal to cranial, the same order used in the other sections of this text.

Cranial nerves are classified as motor, sensory, or mixed motor-sensory nerves. They are then subclassified by the specific motor and sensory information conducted.

GSE: Motor fibers to the musculature of the body derived from the myotomes are designated general somatic efferent (GSE) motor fibers [322, 467].

GVE: Motor fibers to the smooth muscles of the internal organs, to the cardiac muscle, and to the glands are designated general visceral efferent (GVE) motor fibers [322, 467].

SVE: Motor fibers to the musculature derived from the mesenchyme of the visceral, branchial arches are designated special visceral efferent (SVE) branchial motor fibers [322, 467].

GSA: Sensory fibers from the skin, skeletal muscles, joints and ligaments are designated general somatic afferent (GSA) sensory fibers [322, 467].

GVA: Sensory fibers from central receptors in the visceral organs and blood vessels are designated general visceral afferent (GVA) sensory fibers [322, 467].

SSA: Sensory fibers from receptors in the retina, cochlea and vestibular apparatus are designated special somatic afferent (SSA) sensory fibers [322, 467].

SVA: Sensory fibers from receptors in the visceral sense organs such as taste and smell are designated special visceral afferent (SVA) sensory fibers [322, 467].

The purely motor cranial nerves are CN III, IV and VI (for the extra-ocular muscles), XI (for the sternocleidomastoid and trapezius muscles) and XII (for the tongue). The purely sensory cranial nerves are CN I (olfaction), II (vision) and VIII (vestibular function and audition). Cranial nerves V, VII, IX and X are mixed motor-sensory nerves (Table 9.1). The *visceral* afferent fibers of cranial nerves VII, IX and X form the compact solitary tract, travel within the tract, and synapse within the solitary nucleus that surrounds the tract [78]. These include both the general *visceral* afferent fibers **(GVA)** and the special *visceral* afferent fibers **(SVA)** of CN VII, IX and X. General *somatic* afferent (**GSA)** fibers of cranial nerves V, VII, IX and X form the spinal trigeminal tract, travel within it, and synapse in the spinal trigeminal nucleus immediately medial to it [78].

Root entry/exit zones

The portions of the cranial nerves that traverse the *surface* of the brain stem to enter/exit the brain stem are designated the root entry/exit zones. In all cranial nerves, these short zones are myelinated by central myelin derived from oligodendroglia. The lengths of these root entry/exit zones are measured from the surface of the brain stem to the point of transition where the short zone of central myelin gives way to the major portion of the nerve myelinated by peripheral myelin. This length is different for each nerve and shows a range of variation for each specific nerve. Because the root entry/exit zones of central myelin are peculiarly vulnerable to compression by vascular loops, leading to clinical syndromes [322, 467], the lengths of the central root entry/exit zones are tabulated for each cranial nerve (Table 9.2). For the "brain tracts" called cranial nerves I and II, the length of the central segment is taken to be the full length of the cranial nerve.

Table 9.2. Lengths of the root entry and exit zones of the cranial nerves

The root entry/exit zone of a cranial nerve is taken to be the portion of the cisternal segment of the nerve that is covered with central myelin derived from oligodendroglia (ODG). This length is different for each cranial nerve [251a, 396a, 427a, 427b]. For the brain tracts called "cranial nerves I and II", the length is taken to be the complete length of the "cranial nerve".

Specific Cranial Nerve	Mean length (mm) of the root entry/ root exit zone	Range (mm) of the root entry/ root exit zone	References
CN I – Olfactory Nerve			
Olfactory Bulb	**10.0**	**6.0 – 15.0**	Lang 1982 [251a]
Olfactory Tract	**25.0**	**14.0 – 35.0**	Lang 1982 [251a]
CN II – Optic Nerve			
Intracranial	**12.11**	**7.0 – 16.0**	Lang 1982 [251a]
Intracanalicular	**4.8**	**3.0 – 9.3**	Lang 1982 [251a]
Intra-orbital	**28.0**		Lang 1982 [251a]
CN III – Oculomotor Nerve	**1.88**	**1.0 – 4.0**	Lang 1982 [251a]
	0.6		Tarlov 1937 [427a,b]
	1.2		Skinner 1931 [396a]
CN IV – Trochlear Nerve	**0.3**	**0.0 – 1.0**	Lang 1982 [251a]
CN V – Trigeminal Nerve			
Motor Root	**0.67**	**0.0 – 1.5**	Lang 1982 [251a]
	0.5		Tarlov 1937 [427a,b]
Sensory Root	**3.57**	**2.0 – 6.0**	Lang 1982 [251a]
	2.2		Tarlov 1937 [427a,b]
	3.0		Skinner 1931 [396a]
CN VI – Abducens Nerve	**0.3**	**0.1 – 1.0**	Lang 1982 [251a]
	0.5		Tarlov 1937 [427a,b]
			Skinner 1931 [396a]
CN VII – Facial Nerve	**2.05**	**0.5 – 4.0**	Lang 1982 [251a]
	2.0		Tarlov 1937 [427a,b]
	2.5		Skinner 1931 [396a]
CN VIII – Vestibulocochlear Nerve	**10.0**	**6.0 – 15.0**	Lang 1982 [251a]
		8.2 – 9.0	Skinner 1931 [396a]
Vestibular Nerve	**8.0**	**5.0 – 11.5**	Tarlov 1937 [427a,b]
Cochlear Nerve	**8.3**	**5.0 – 11.5**	Tarlov 1937 [427a,b]
CN IX – Glossopharyngeal Nerve			
Motor Root (medial)		**< 0.1**	Tarlov 1937 [427a,b]
Sensory Root (lateral)	**1.1**		Tarlov 1937 [427a,b]
CN X – Vagus Nerve			
Motor Root (medial)	**0.1**		Tarlov 1937 [427a,b]
Sensory Root (lateral)	**1.3**	**Up to 2**	Tarlov 1937 [427a,b]
CN XI – Accessory Nerve		**< 0.1**	Lang 1982 [251a]
CN XII – Hypoglossal Nerve		**< 0.1**	Lang 1982 [251a]

[251a] Lang J (1982) Anatomy, length and blood vessel relations of "central" and "peripheral" paths of intracisternal cranial nerves. Zentralbl Neurochir. 43: 217-258.

[427a] Tarlov IM (1937) Structure of the nerve root. I. Nature of the junction between the central and the peripheral nervous system. Arch Neurol Psychiatry 37: 555-583.

[427b] Tarlov IM (1937) Structure of the nerve root. II. Differentiation of sensory from motor roots; observations on identification of function in roots of mixed cranial nerves. Arch Neurol Psychiatry. 37: 1338-1355.

[396a] Skinner HA (1931) Some histological features of the cranial nerves. Arch Neurol Psychiatry 25: 356-72.

The Hypoglossal Nerve: CN XII.

GSE of CN XII: General somatic efferent fibers for the striated muscle of the tongue arise from the hypoglossal nucleus at the hypoglossal trigone of the medullary portion of the floor of the fourth ventricle (**Fig. 2.3**). Multiple hypoglossal fascicles emerge from the ventral aspect of the nucleus, curve ventrally through the reticular nuclei of the medulla, pass between the medial accessory olivary and the inferior olivary nuclei, dip toward the hilum of the inferior olivary nucleus, and then emerge as a row of 12-16 rootlets immediately ventral to the olive in the pre-olivary sulcus. The hypoglossal nerve is the only cranial nerve to emerge in the pre-olivary sulcus. [260]. It does not decussate.

The cisternal segment of the hypoglossal nerve begins at the pre-olivary sulcus, where the multiple hypoglossal fibers merge into three to six nerve bundles. These course anterolaterally through the premedullary cistern between the vertebral artery anteriorly and the posterior inferior cerebellar artery (PICA) posteriorly and then condense into one, two, rarely three, major hypoglossal trunks. These penetrate the dura mater separately, forming one, two or three sleeves of cerebrospinal fluid (CSF) that mark their entrance into a single or duplicated hypoglossal canal [479, 481 483, 487, 488]. The hypoglossal nucleus innervates all of the intrinsic and extrinsic muscles of the tongue, except the palatoglossus (supplied by CN X) and provides motor control to the tongue [467].

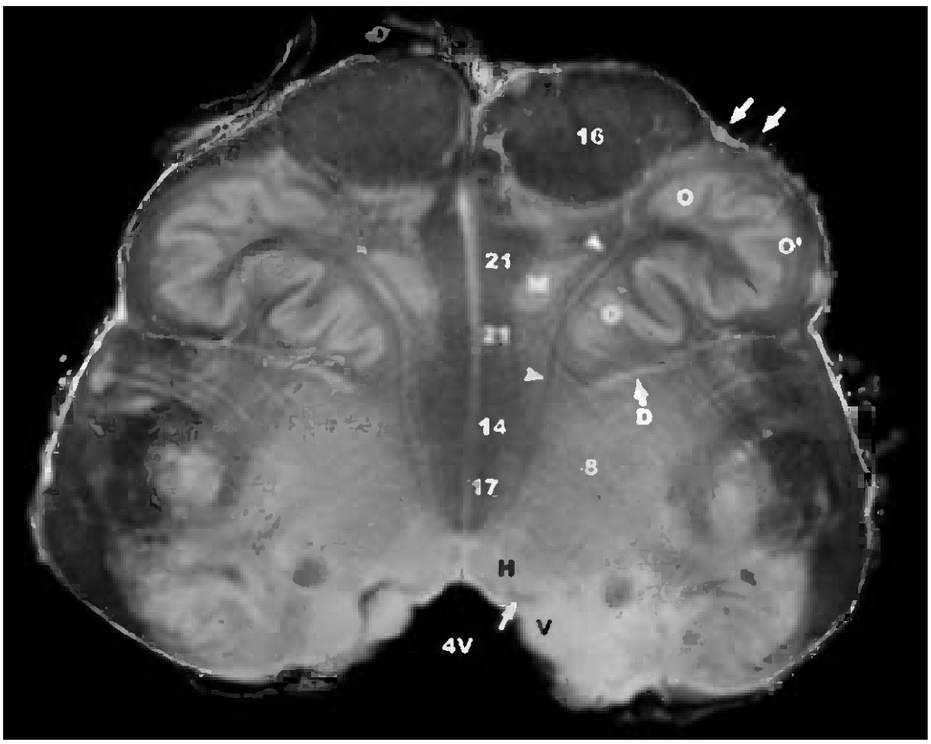

A

Fig. 9.1 (A–D). Cranial nerve XII: The hypoglossal nucleus, roots and nerve.
(A–D). MR Microscopy displays the nucleus and intramedullary fibers of the hypoglossal nerve in the axial **(A),** sagittal (**B)** and coronal **(C–D)** planes.

1 Nucleus gracilis
1′ Fasciculus gracilis approaching the caudal pole of the nucleus gracilis
2 Nucleus cuneatus
2′ Fasciculus cuneatus
8 Extensive reticular formation (light gray)
14 Tectospinal tract
16 Pyramid containing the corticospinal tract
16′ Anterior corticospinal tract
17 Medial longitudinal fasciculus
18 Decussation of the internal arcuate fibers
21 Medial lemniscus

Letter labels
4V Fourth ventricle
H Hypoglossal nucleus (CN XII)
D Dorsal accessory olivary nucleus
M Medial accessory olivary nucleus
O Inferior olivary nucleus
O′ Amiculum (capsule of the inferior olivary nucleus)
O″ Hilum of the inferior olivary nucleus
V Dorsal motor nucleus of the vagus (CN X) with the dorsal longitudinal fasciculus (white arrow) immediately dorsal to it.

Arrowheads and arrows
Between arrowheads: Intramedullary fibers of the hypoglossal nerve passing lateral to and through the medial accessory olivary nucleus
Single white arrow: Dorsal longitudinal fasciculus related to the vagal nucleus (V)
Double white arrows: Pre-olivary sulcus, where the hypoglossal fibers emerge from the medulla to enter the perimedullary cistern

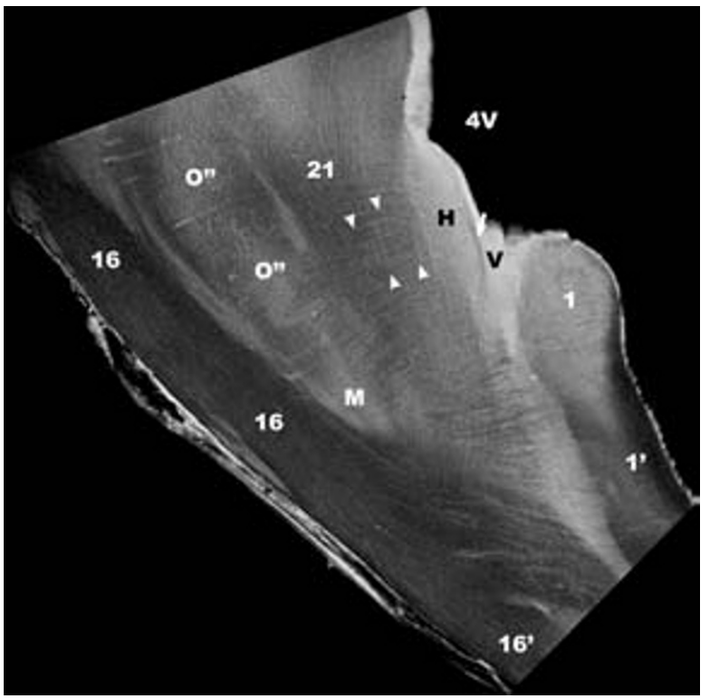

B

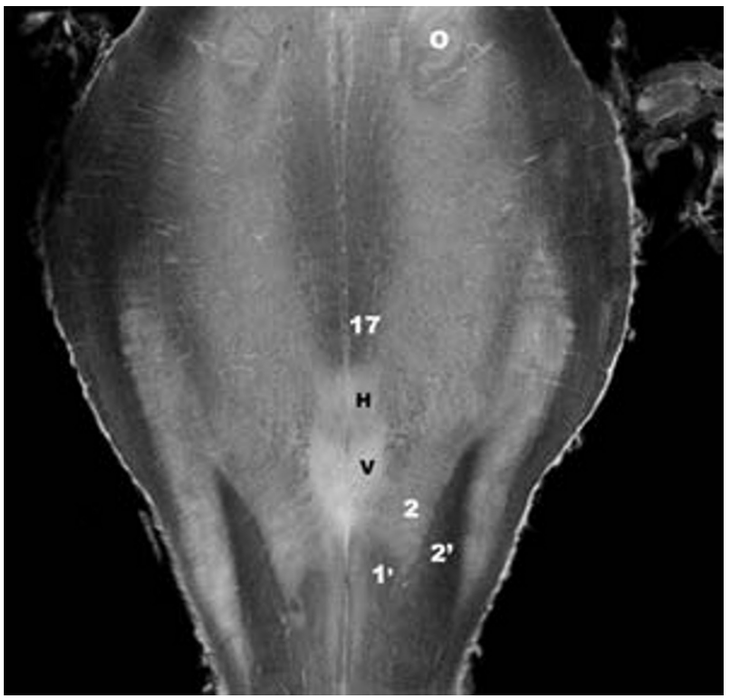

C

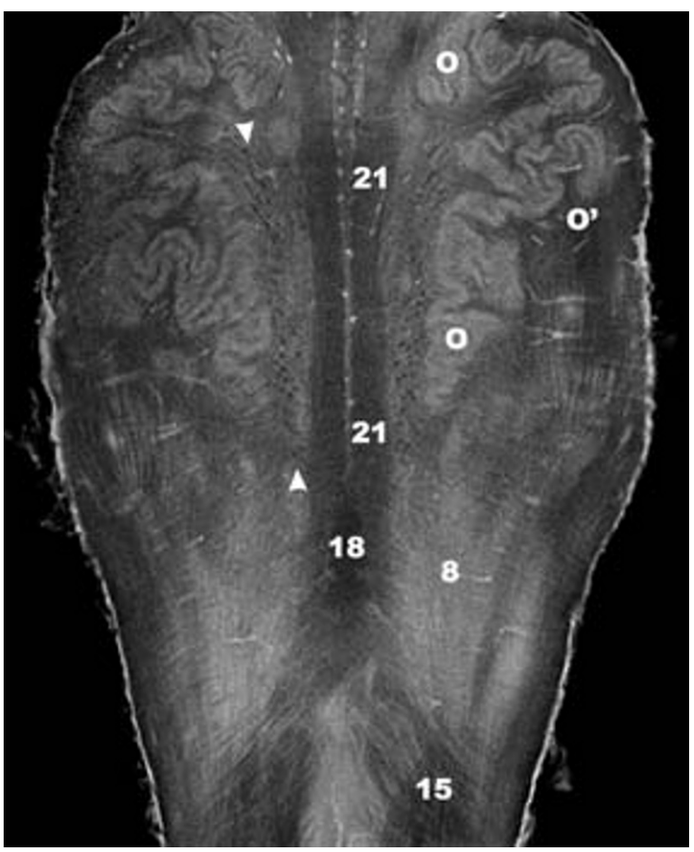

D

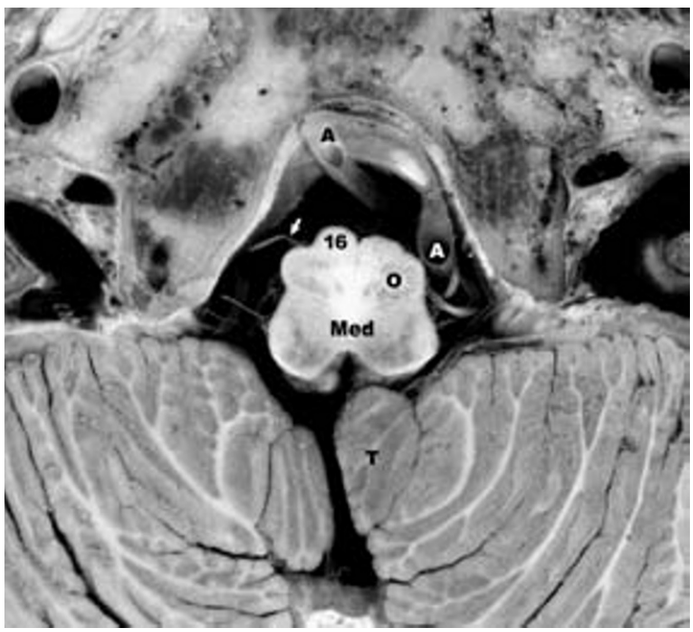

A

C

Fig. 9.2 (A–D). Cranial nerve XII: The hypoglossal nucleus, roots and nerve.
A–B. Anatomic sections through the medulla in the axial **(A)** and coronal **(B)** planes.
See also: **Figs. 11.5 D and 11.42 B**
C–D. MR Cisternography in the axial (**C**) and coronal (**D**) planes.

16 Pyramid containing the corticospinal tract

Letter labels

A	Vertebral artery
HC	Hypoglossal canal
JT	Jugular tubercle
Med	Medulla
O	Inferior olivary nucleus
OC	Occipital condyle
Pons	Pons
T	Tonsil

Arrowheads and arrows

Single arrows (white or black):	Cisternal segments of the hypoglossal nerves emerging from the medulla at the pre-olivary sulcus
Crossed white arrow:	Sleeve of cerebrospinal fluid surrounding the penetrating hypoglossal trunk

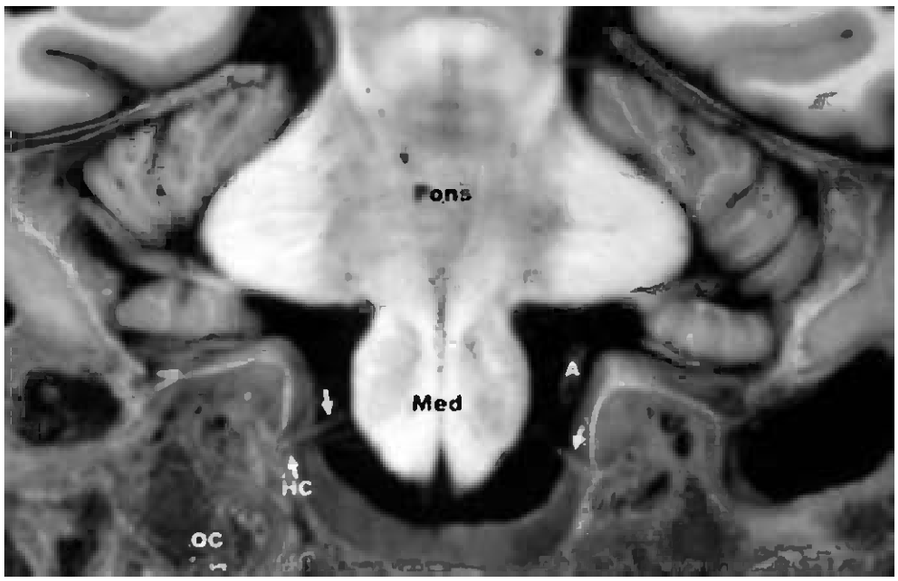

B

D

The Accesssory, Vagal and Glossopharyngeal Nerves: CN XI, X and IX

Overview: Motor fibers of cranial nerves IX, X and XI arise from the nucleus ambiguus in the dorsolateral medulla, from the dorsal motor nucleus of the vagus in the vagal trigone of the dorsomedial medulla, from the parasympathetic inferior salivatory nucleus in the dorsomedial medulla, and from the lateral motor column of the upper cervical spinal cord (**Fig. 2.3**). Sensory fibers of the glossopharyngeal and vagal nerves arise within and below the jugular fossa from the inferior and superior ganglia of each of these nerves [52, 78, 260, 467, 487, 488] (See **Fig. 2.3**, diagram of the locations of the motor and sensory nuclei of the brain stem). The fibers of the glossopharyngeal, vagus and spinal accessory nerves do not decussate.

Ten to 20 rootlets of the glossopharyngeal nerve (CN IX) exit the brain stem along the upper one-third of the postolivary sulcus, between the olive and the inferior cerebellar peduncle, just cephalic to the rootlets of the vagus nerve (CN X). The glossopharyngeal fibers condense into a single nerve bundle that traverses the cerebellopontine angle cistern, and enters the jugular foramen through the glossopharyngeal meatus. Within the jugular fossa the glossopharyngeal fibers lie anterior to the vagus and accessory nerves, and are separated from them by a fibrous septum.

Variable numbers (4–18) of delicate rootlets of the vagus nerve (CN X) exit the brain stem at the postolivary sulcus just caudal to the glossopharyngeal rootlets and pass across the cerebellopontine cistern [260, 467]. The vagal rootlets typically merge into two (upper and lower) nerve roor bundles that enter the jugular foramen via the vagal meatus, inferior to the glossopharyngeal meatus. Within the jugular foramen, the vagus lies posterior to the glossopharyngeal nerve, and is separated from it by a fibrous septum [260].

The accessory nerve (CN XI) may be considered to have both a *medullary* and a *spinal* origin [260] or to have solely a *spinal* origin (in which case the medullary fibers are assigned to the vagus (CN X) [467]. In either case, 6–16 rootlets of the *cranial* portion of the accessory nerve arise in the postolivary sulcus of the medulla and and condense into 4–5 nerve root bundles. Six to seven rootlets of the *spinal* accessory nerve emerge from the posterolateral sulcus of the spinal cord just anterior to the dorsal sensory nerve roots. The spinal rootlets unite into a single trunk that ascends through the spinal canal posterior to the denticulate ligament, enters the skull via foramen magnum posterior to the vertebral artery, and joins the caudal end of the cranial trunk of the accessory nerve. The combined craniospinal trunk enters the jugular fossa through the vagal meatus with the vagus but separates from the vagus within the jugular fossa [260].

More specifically:

CN IX. Glossopharyngeal nerve

SVE of CN IX: Special visceral efferent fibers for the branchial muscles arise in the rostral nucleus ambiguus in the dorsolateral medulla [78, 260]. These fascicles first curve dorsomedially and inferiorly toward the floor of the fourth ventricle. Within the reticular substance, they then turn sharply ventrolaterally, pass across the spinal trigeminal nucleus and tract, and emerge from the medulla along the postolivary sulcus. The SVE fibers pass along the glossopharyngeal nerve to supply the stylopharyngeus, part of the superior pharyngeal constrictor, and the styloglossus [78, 467]. The styloglossus raises the pharynx during swallowing and speech [467].

GVE of CN IX: General visceral efferent parasympathetic motor fibers for the parotid gland arise in the inferior salivatory nucleus of the upper medulla oblongata. The preganglionic parasympathetic fibers pass ventrolaterally with the other glossopharyngeal fibers to exit the skull at the jugular foramen. They then follow a complex course. The fibers first pass via the tympanic nerve to the middle ear, form a plexus on the inner aspect of the tympanic membrane, emerge from the plexus as the lesser petrosal nerve, re-enter the skull via the lesser petrosal hiatus, re-exit the skull via foramen ovale, and synapse in the otic ganglion immediately inferior to foramen ovale. Postganglionic parasympathetic secretomotor fibers of the otic ganglion travel with the auriculotemporal nerve (branch of CN V3) to the parotid gland [78, 467]. Stimulation of the nerve causes salivation.

GVA of CN IX: General visceral afferent fibers from the mucous membranes of the posterior third of the tongue, the tonsil, the posterior wall of the upper pharynx, and the Eustachian tube arise from the inferior glossopharyngeal ganglion (petrosal ganglion) in the jugular fossa [59, 60, 78, 81]. The peripheral processes of these neurons course with the glossopharyngeal nerve. The central processes enter the postolivary sulcus of the medulla, ascend within the solitary tract, and synapse in the rostral solitary nucleus [78]. These nerves provide tactile, temperature and pain sensation to the areas innervated.

GVA neurons of the inferior glossopharyngeal (petrosal) ganglion also send peripheral processes via the carotid nerve to chemoreceptors for oxygen tension in the carotid body and to baroreceptors for arterial pressure in the carotid bulb [456]. The central processes for these neurons enter the posterolateral sulcus, traverse the solitary tract and synapse in the solitary nucleus [78]. Secondary fibers from the solitary nucleus extend to the reticular formation, the dorsal motor nucleus of the vagus, and the hypothalamus for control of respiration, blood pressure and cardiac output [78, 467].

GSA of CN IX: General somatic afferent fibers from skin within the external ear, the inner surface of the tympanic membrane, the posterior one-third of the tongue, and the upper pharynx arise from the small (inconstant) superior glossopharyngeal ganglion (no synonym) or from the larger inferior glossopharyngeal (petrosal) ganglion within the jugular fossa [467]. The peripheral processes of these neurons course in the glossopharyngeal nerve. The central processes enter the postolivary sulcus of the medulla, descend within the spinal trigeminal tract, and synapse within the caudal spinal trigeminal nucleus [467]. Secondary fibers then cross the midline in the medulla and ascend in the rostral portion of the medial lemniscus (trigeminal

lemniscus) to the contralateral ventral posterior nucleus of the thalamus [78, 260, 467]. These fibers provide pain and temperature sensation to the areas innervated.

SVA of CN IX: Special visceral afferent fibers for taste from the posterior third of the tongue arise within the inferior glossopharyngeal (petrosal) ganglion in the jugular fossa. The peripheral processes of these neurons course through the lingual branch of the glossopharyngeal nerve to reach the posterior tongue. The central processes enter the postolivary sulcus of the medulla, ascend within the solitary tract, and synapse in the rostral portion of the solitary nucleus (designated the gustatory nucleus). Secondary fibers then ascend within the central tegmental tract(s) to the ventral posterior nuclei of the thalami. It is unclear whether these fibers distribute solely to the contralateral thalamus, or bilaterally [467].

CN X. Vagus nerve

SVE of CN X: Special visceral efferent fibers of the vagus arise from the nucleus ambiguus in the dorsal lateral portion of the medulla. These fascicles first curve dorsomedially and inferiorly, away from the nucleus ambiguus and toward the floor of the fourth ventricle. Within the reticular substance, they then turn sharply ventrolaterally, pass across the spinal trigeminal nucleus and tract, and emerge from the medulla along the postolivary sulcus. They exit the skull through the jugular fossa with the vagus nerve and then branch off as the pharyngeal, superior laryngeal, and recurrent laryngeal nerves to supply the muscles of the tongue (palatoglossus only), soft palate, pharynx and larynx (except the stylopharyngeus (CN IX) and the tensor veli palatini (CN V3)) [78, 467]. These fibers provide motor control to the pharynx and larynx.

GVE of CN X: General visceral efferent parasympathetic motor fibers for the smooth muscles and glands of the viscera arise within the dorsal motor nucleus of the vagus in the floor of the fourth ventricle and in the dorsal central gray matter of the closed portion of the medulla [80, 295, 467]. Preganglionic vagal fibers cross the spinal trigeminal tract and nucleus and the restiform body, emerge from the lateral surface of the medulla at the postolivary sulcus, and join the branchial motor rootlets. The preganglionic fibers distribute widely to parasympathetic terminal ganglia located in or near the organs of the head, neck, thorax and abdomen. The terminal ganglia send short postganglionic fibers directly to the non-striated muscle of viscera of the thorax (esophagus, heart, bronchi and lungs) and the abdomen (stomach, liver, pancreas, spleen, small intestine and proximal colon as far as the splenic flexure) [467, 489]. Stimulation of these fibers slows the heart rate, constricts the glands of the bronchial musosa, promotes peristalsis in the gastro-intestinal tract, relaxes the pyloric and ileocolic sphincters, and increases secretion of gastric and pancreatic juices [488].

GSA of CN X: General somatic afferent fibers of the vagus for the external ear originate from the superior (jugular) ganglion of the vagus high within the jugular foramen. The peripheral processes of these neurons pass along the auricular branch of the vagus to the skin of the external auditory canal and a portion of the auricle. The central processes of these neurons ascend through the jugular foramen, enter the postolivary sulcus of the medulla, descend within the spinal trigeminal tract, and synapse in the spinal trigeminal nucleus. Secondary fibers then cross the midline to ascend within the contralateral ventral trigeminothalamic tract to the ventral posterior nucleus of the thalamus. The GSA fibers carry pain and temperature sensation from the skin of the external ear and the external surface of the tympanic membrane.

GVA of CN X: General visceral afferent fibers for the viscera may arise in the inferior (nodose or plexiform) ganglion of the vagus [260, 467]. The peripheral processes of these neurons descend into the neck within the vagus nerve and then extend widely to the pharynx, larynx, cardiovascular, tracheobronchial and pulmonary systems, plus the meninges of the posterior cranial fossa. The central processes of the inferior ganglion ascend through the jugular fossa, enter the medulla, and then descend in the solitary tract to synapse in the caudal solitary nucleus [467]. From there, information is conveyed to the reticular formation and hypothalamus bilaterally for reflex control of cardiovascular, respiratory and gastro-intestinal functions [467]. Connections to the dorsal motor nucleus of the vagus empower parasympathetic control of those reflexes [467].

SVA of CN X: Special visceral afferent fibers for taste from the epiglottis arise in the inferior (nodose) ganglion of the vagus. Peripheral fibers pass along the superior laryngeal nerve to the epiglottis. Central fibers of these neurons enter the solitary tract and traverse it to synapse in the rostral portion of the solitary nucleus (gustatory nucleus). From there, secondary fibers ascend ipsilaterally within the central tegmental tract to the ventral posteromedial nucleus of the thalamus.

CN XI. Acessory nerve

SVE of CN XI: Special visceral efferent fibers for the branchial muscles pass posterolaterally through the white matter of the spinal cord to emerge as 6-7 rootlets at the posterolateral sulcus, just anterior to the dorsal sensory nerve roots. The *spinal rootlets* form a single vertical trunk that ascends through foramen magnum to join the medullary (cranial) root of the accessory nerve. The fascicles of the *medullary root* arise in the nucleus ambiguus and pass ventrolaterally to emerge as 6–16 rootlets in the postolivary sulcus of the medulla. These condense into 4-5 nerve root bundles that join the ascending spinal root of the accessory nerve and pass with CN X into the jugular fossa through the vagal meatus [260]. The cranial fibers blend into the vagus at the level of the superior vagal ganglion. The spinal fibers descend through the neck to provide motor control of the sternocleidomastoid and trapezius muscles.

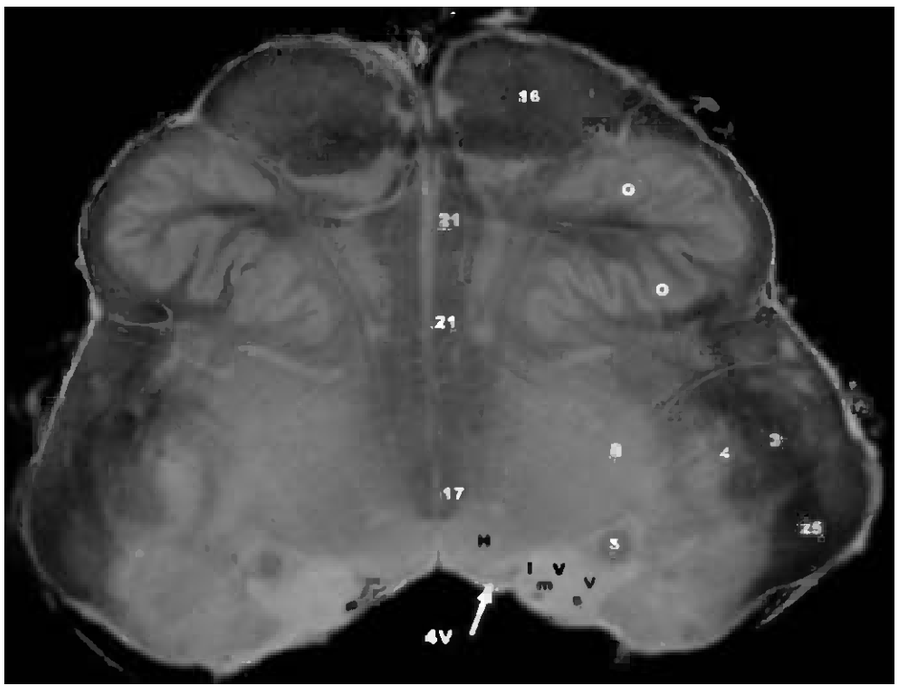

A

Fig. 9.3 (A–E). Cranial nerves IX, X and XI: The nucleus ambiguus. The accessory, vagal and glossopharyngeal roots and nerves

A–E. MR Microscopy displays the nuclei and intramedullary fibers of the glossopharyngeal and vagal nerves in the axial **(A–C),** sagittal **(D)** and coronal **(E)** planes.

1 Nucleus gracilis
1′ Fasciculus gracilis approaching the caudal pole of the nucleus gracilis
2 Nucleus cuneatus
2″ Accessory (lateral) nucleus cuneatus
3 Spinal trigeminal tract
4 Spinal trigeminal nucleus
8 Extensive reticular formation (light gray)
16 Pyramid containing the corticospinal tract
16′ Anterior corticospinal tract
17 Medial longitudinal fasciculus
21 Medial lemniscus
25 Inferior cerebellar peduncle (restiform body)
31 Glossopharyngeal nerve (CN IX)

Letter labels

4V Fourth ventricle
H Hypoglossal nucleus
I Intercalated nucleus
O Inferior olivary nucleus
S Solitary tract surrounded by the solitary nucleus (light gray)
V Nucleus of the Vagus
Vm Dorsal *motor* nucleus of the Vagus, situated ventromedial to the
Vs Dorsal *sensory* nucleus of the Vagus

Arrowheads and arrows

Arrowheads: Solitary tract
Single white arrow: Dorsal longitudinal fasciculus descending from the hypothalamus to the nucleus of the vagus
Paired white arrows: Intramedullary fibers of the glossopharyngeal nerve (CN IX). Note the proximity of the vagal and solitary nuclei to this nerve

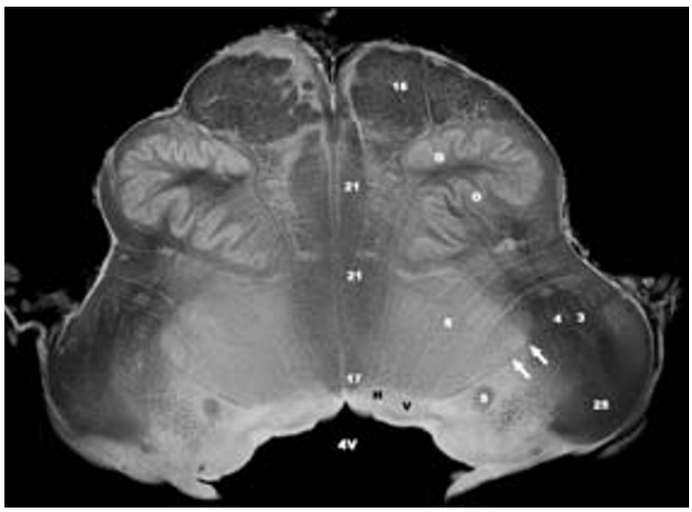
16
21
O
21
S
4
3
17
H
V
5
25
4V

B

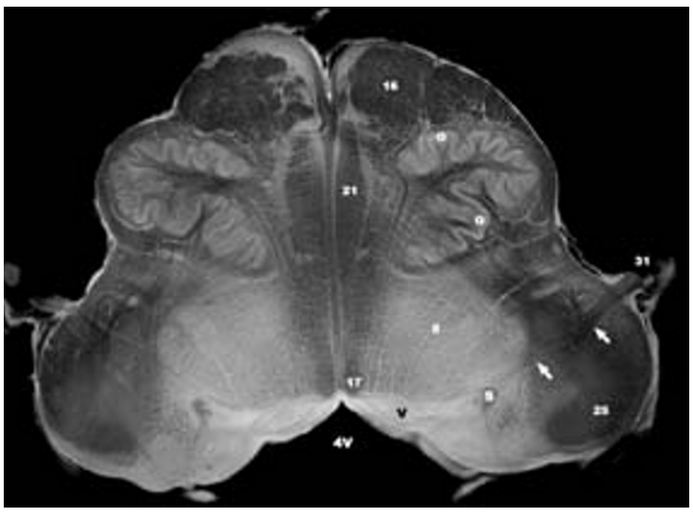
16
21
O
31
S
17
V
5
25
4V

C

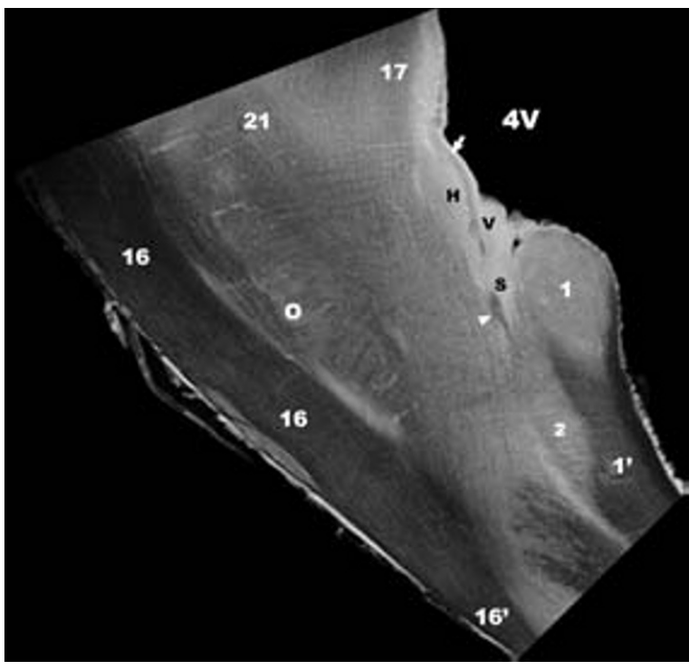
17
21
4V
H
V
16
S
1
O
16
2
1'
16'

D


4V
25
S
2"
H
V
S
2
2
3
4
4

E

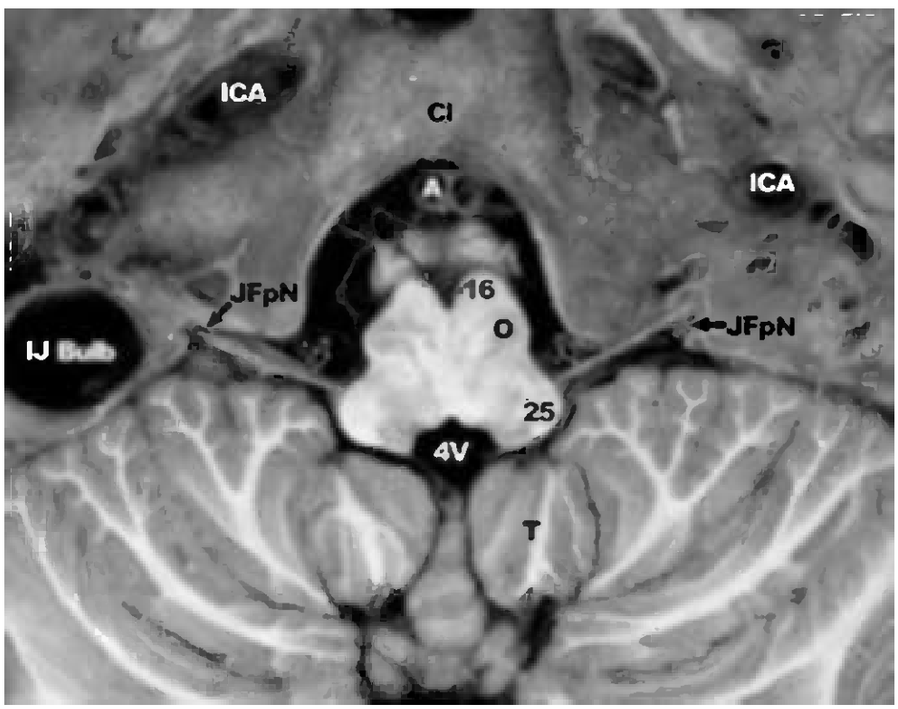

A

Fig. 9.4 (A–I). Cranial nerves IX, X and XI: The nucleus ambiguus. The accessory, vagal and glossopharyngeal roots.
A–B. Anatomic sections through the medulla in the axial **(A)** and coronal **(B)** planes. See also: **Figs. 11.7 D and 11.43 C**.
C. Axial plane through the glossopharyngeal nerve (CN IX)
D. Axial plane through the vagus nerve (CN X)
E. Oblique coronal plane through CN IX, CN X and the cranial portion of CN XI (asterisks).
F. Oblique coronal plane through spinal CN XI
G–H. Oblique sagittal planes through spinal CN XI
I. Axial plane just superior to foramen magnum for spinal CN XI

16 Pyramid containing the corticospinal tract
21 Medial lemniscus
23 Superior cerebellar peduncle
24 Central tegmental tract
25 Inferior cerebellar peduncle (restiform body)
31 Glossopharyngeal nerve (CN IX)
31′ Vagal nerve (CN X)
38 Middle cerebellar peduncle (brachium pontis)
237′ Flocculus

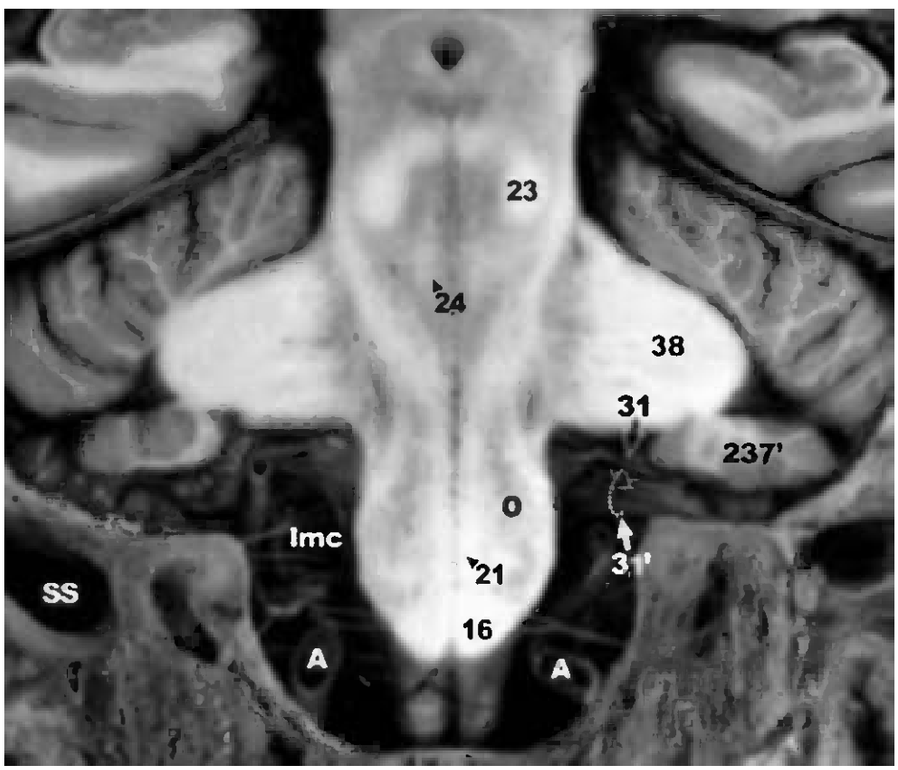

B

Letter labels

CN XI	cranial roots
4V	Fourth ventricle
lmc	Lateral medullary cistern
A	Vertebral artery
Cl	Clivus
ICA	Internal carotid artery
IJ Bulb	Internal jugular bulb
JFpN	Jugular fossa, pars nervosa
Med	Medulla
O	Inferior olivary nucleus
Pons	Pons
SS	Sigmoid sinus
T	Tonsil

Arrowheads, arrows and asterisks

Outlined white arrowheads:	Cisternal segments of cranial nerve XI (spinal root) (**Figs. 9.4 F–I**)
Black arrows:	Cisternal segments of cranial nerves IX (**Fig. 9.4C**) and X (**Fig. 9.4D**)
White arrow:	Cisternal segment of cranial nerve IX (**Fig. 9.4E**)
Outlined white arrows:	Choroid plexus in the cerebello-pontomedullary cistern (**Fig. 9.4C**)
Outlined black arrows:	Cisternal segments of the vagus nerve (CN X) (**Figs. 9.4A and 9.4E**)
Asterisks:	Cisternal segments of the medullary roots of CN XI (**Fig. 9.4E**)

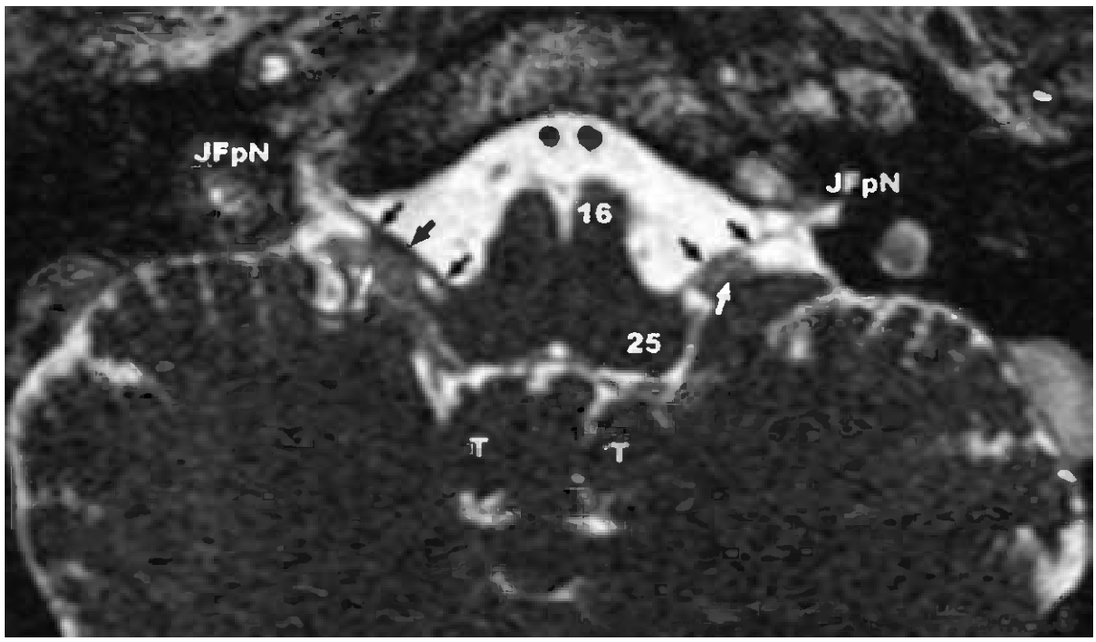
JFpN
JFpN
16
25
T
T

C


A
A
JFpN
JFpN
16
O
237'
237'
25
T
T

D

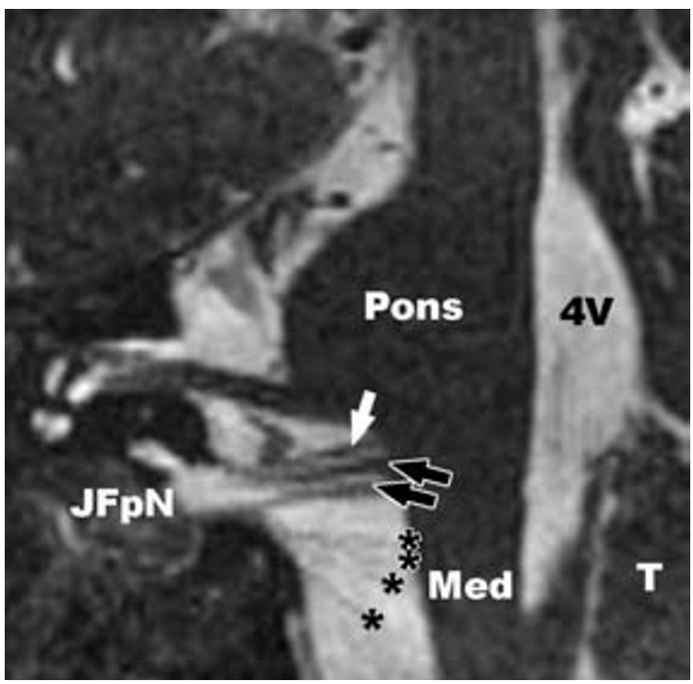
Pons
4V
JFpN
Med
T

E

F

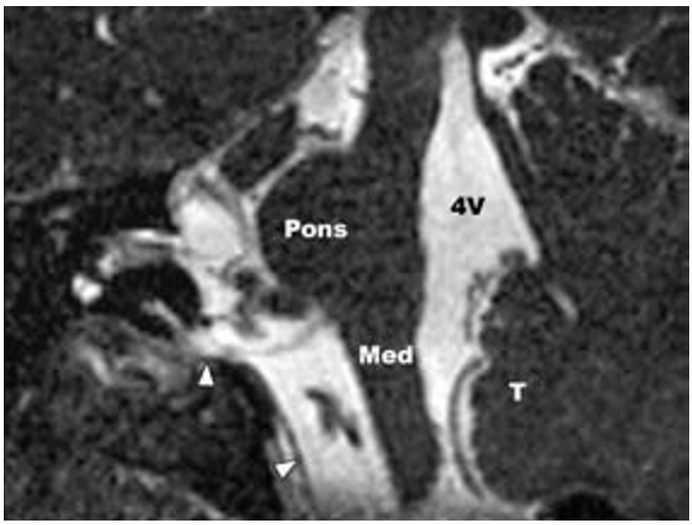

G

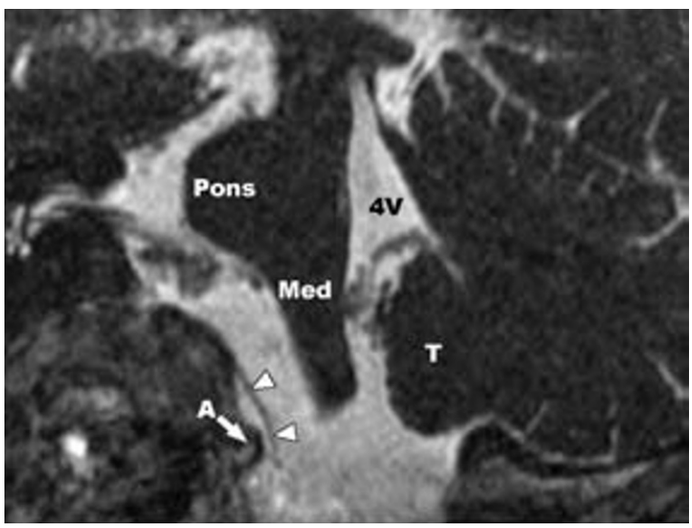

H

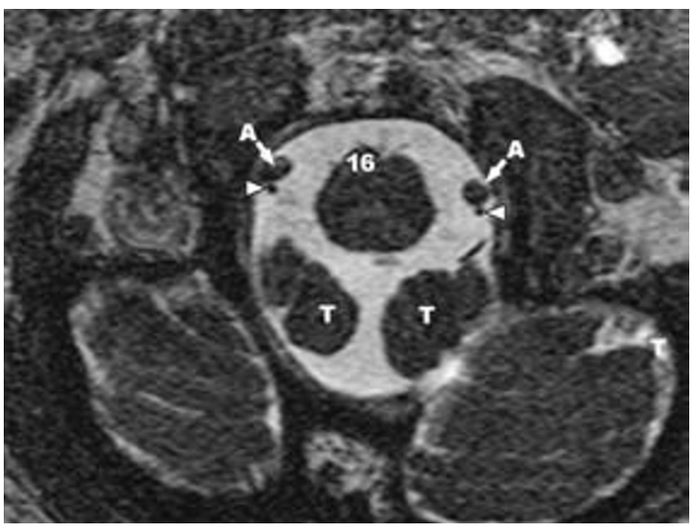

I

The Facial and Vestibulocochlear Nerves: CN VII and VIII

CN VII. The facial nerve and nervus intermedius

Cranial nerve seven contains two distinct roots: a motor root to the muscles of the face and scalp designated the facial nerve, and a mixed sensory-motor root to the salivary glands of the head and neck and to the taste receptors of the tongue, designated the nervus intermedius [78, 140, 260, 467, 483, 487, 488]. The fibers of the facial nerve and nervus intermedius do not decussate.

Facial nerve

SVE of CN VII: Special visceral efferent motor fibers of the facial nerve for branchial muscles arise from the facial nucleus in the pontine tegmentum as a diffuse spread of fibers. These fibers pass dorsomedially toward the floor of the fourth ventricle, converge at the medial aspect of the abducens nucleus, and then form a compact fiber bundle that arcs over the superior pole of the abducens nucleus, from medial to lateral, to create the facial colliculus. The facial fibers then continue laterally as a compact fiber bundle that recurves ventrolaterally, passes between the ipsilateral facial nucleus (medially) and the spinal trigeminal nucleus and tract (laterally), and emerges from the brain stem at the lateral aspect of the pontomedullary junction, just inferior to the brachium pontis. The facial fibers then traverse the cerebellopontine cistern and the internal auditory meatus with the vestibulocochlear fibers, pass through the facial canal (of Fallopius) in the petrous temporal bone, exit the skull through the stylomastoid foramen, and pass through the parotid gland to provide motor control for the muscles of the face and scalp, including the platysma, buccinator, stapedius, stylohyoid, and posterior belly of the digastric and occipitalis. [488].

Nervus intermedius

GVE of CN VII (Nervus intermedius): General visceral efferent parasympathetic motor fibers of the facial nerve arise within the superior salivatory nuclei in the pontine portion of the floor of the fourth ventricle. These fibers course with the nervus intermedius, cross the cerebellopontine angle cistern, and enter the internal auditory meatus, adjacent to, but separate from, the branchial motor portion of the facial nerve [467]. The intermediate fibers enter the facial nerve canal, pass through the geniculate ganglion, and then divide into peripheral branches. Those preganglionic parasympathetic GVE fibers that join the greater petrosal nerve pass to the pterygoid nerve, synapse within the pterygopalatine ganglion, and provide secretomotor innervation to the lacrimal and nasal glands [230]. The preganglionic parasympathetic GVE fibers that join the chorda tympani pass to the lingual nerve, synapse within the submandibular and sublingual ganglia, and provide secretomotor innervation to the submandibular and sublingual glands [230].

GSA of CN VII (Nervus intermedius): A small component of general sensory afferent fibers arises from neurons within the geniculate ganglion of the facial nerve. The peripheral processes of these neurons pass via the auricular branch of the vagus to the concha of the external ear, a small area of skin behind the ear, and may supplement fibers of the mandibular division of the trigeminal nerve (CN V3) for sensation from the external auditory meatus and the external surface of the tympanic membrane [467]. The central processes of the geniculate neurons traverse the nervus intermedius to reach the brain stem, descend within the spinal trigeminal tract, and synapse in the spinal trigeminal nucleus in the upper medulla [467]. Secondary fibers pass via the ventral trigeminothalamic tract to the contralateral ventral posteromedial nucleus of the thalamus.

SVA of CN VII (Nervus intermedius): Special sensory taste fibers of the nervus intermedius also arise in the geniculate ganglion. The peripheral processes of these neurons traverse the chorda tympani to reach taste receptors in the the anterior two-thirds of the tongue, the hard palate and the soft palate. The central processes of these neurons traverse the nervus intermedius to the brain stem, ascend within the solitary tract, and synapse in the rostral portion of the solitary nucleus (gustatory nucleus). Secondary fibers from the solitary nucleus ascend to higher centers via the central tegmental tract. [467].

CN VIII. The vestibulocochlear nerve

Cranial nerve VIII (the vestibulocochlear nerve) also contains two distinct divisions. The special sensory root carrying vestibular data is designated the vestibular division. The special sensory root carrying auditory data is designated the auditory division [78, 140, 260, 467, 483, 487, 488]. The fibers of the vestibulocochlear nerve do not decussate.

Vestibular division.

SSA of CN VIII: Special somatic afferent fibers for vestibular sensation arise from neurons within the vestibular ganglion (of Scarpa) located in the posterior portion of the internal auditory canal [230]. Peripheral processes of these neurons receive data from hair cells of the saccule, utricle and semicircular canals of the membranous labyrinth of the inner ear. The central processes of these neurons pass to the brain stem with the cochlear and facial nerves to synapse in the medial, inferior and superior (but not lateral) vestibular nuclei at the lateral angles of the floor of the fourth ventricle [78, 157, 175, 260, 322a, 367, 467]. The central fibers entering the vestibular complex bifurcate into ascending bundles to the superior vestibular nucleus and descending bundles to the inferior and medial vestibular nuclei [322a]. The entering vestibular fibers are organized from lateral to medial, with fibers from the saccule most lateral, followed by fibers from the utricle, anterior semicircular, horizontal semicircular and posterior semicircular canals situated progressively further medial within the vestibular nuclei [322a]. The lateral vestibular nucleus receives no direct vestibular input [322a]. It

is innervated instead by Purkinje cells and is best regarded as a cerebellar nucleus [322a]. Central processes of the vestibular ganglion also proceed directly through the juxtarestiform body to the cortex of the nodulus, ventral uvula, tonsil, lingula and depths of the deep fissures to mediate cerebellar response to vestibular data [164].

From the vestibular nuclei, secondary fibers pass to the cerebellum and to lower motor neurons in the brain stem and spinal cord for maintenance of balance. The lateral vestibular nuclei (of Deiter) give rise to the uncrossed lateral vestibulospinal tracts [467]. Fibers within these tracts extend the length of the spinal cord and synapse on interneurons that facilitate contraction of antigravity (extensor) muscles [488]. The medial vestibular nuclei (with some fibers from the spinal trigeminal nuclei) give rise to the medial vestibulospinal tracts. These tracts descend through the cervical spinal cord bilaterally within the descending portion of the medial longitudinal fasciculi, and also synapse on interneurons that facilitate contraction of antigravity (extensor) muscles [467, 488]. The medial and inferior vestibular nuclei interconnect with the cerebellum via the vestibulocerebellar tracts to coordinate balance during movement. All of the vestibular nuclei extend fibers to the oculomotor, trochlear and abducens nuclei via the medial longitudinal fasciculus (MLF) to maintain visual fixation during body movement.

Cochlear division

SSA of CN VIII: Special sensory nerve fibers carrying auditory data arise in the cochlear ganglion (spiral ganglion of Corti) situated around the modiolus of the cochlea. Very short peripheral processes of cochlear ganglion neurons synapse with the sensory hair cells along the basilar membrane of the cochlea [467]. Central processes of cochlear ganglion neurons traverse the internal auditory meatus and cerebellopontine angle to enter the brain stem just caudal to the middle cerebellar peduncle. The central processes enter the ventral cochlear nucleus, bifurcate there into ascending and descending processes, and then distribute tonotopically, so high frequency fibers from the basal turn of the cochlea reach the dorsal cochlear nucleus and low frequency fibers from the apical spiral ganglion reach the ventral cochlear nucleus [164, 322a]. The dorsal nucleus bulges into the lateral portion of the floor of the fourth ventricle as the acoustic tubercle. The ventral nucleus lies on the anterolateral face of the inferior cerebellar peduncle [260].

Secondary postsynaptic fibers pass from the cochlear nuclei to both lateral lemnisci, ipsilateral (20%) and contralateral (~80%) to the cochlea of origin [320]. These fibers help form the large, transversely oriented fiber bundle called the trapezoid body. Secondary fibers emerging from the cochlear nuclei follow three pathways to the lateral lemnisci and inferior colliculi [164]. (i) The dorsal cochlear nucleus gives rise to the dorsal acoustic stria. This passes dorsal to the inferior cerebellar peduncle, crosses the midline ventral to the medial longitudinal fasciculus (MLF), joins the trapezoid body on the far side of midline, and enters the contralateral lateral lemniscus. The dorsal acoustic stria contributes to the transverse striae medullares in the floor of the fourth ventricle [322a]. (ii) The ventral cochlear nucleus gives rise to the intermediate acoustic stria, which passes across the spinal trigeminal tract, joins the ipislateral trapezoid body on the near side of midline, and continues across the midline into the contralateral lateral lemniscus. (iii) The ventral cochlear nucleus also gives rise to the large ventral acoustic stria, which courses ventral to the inferior cerebellar peduncle and ventral to the spinal trigeminal tract to join the ipsilateral trapezoid body. The fibers of the ventral acoustic striae terminate in the paired trapezoid nuclei and the paired superior olivary nuclei, which are embedded within the trapezoid body [164]. Fibers from these nuclei then ascend within both lateral lemnisci to both inferior colliculi. The superior olivary nuclei contribute to the spatial localiztion of sound. The medial superior olives encode interaural time differences (which are maximal at low frequencies), while the lateral superior olives encode interaural level differences (which are maximal at high frequencies) [322a].

The brachia of the inferior colliculi convey fibers to the ipsilateral medial geniculate bodies, from which the geniculotemporal radiations carry the auditory data to the transverse temporal gyri of Heschl (primary auditory cortex) [322a]. The auditory system displays multiple commisures that interconnect the auditory centers at multiple levels, but the predominant pathway is primarily a crossed excitatory pathway from the organ of Corti to the contralateral auditory cortex [322a].

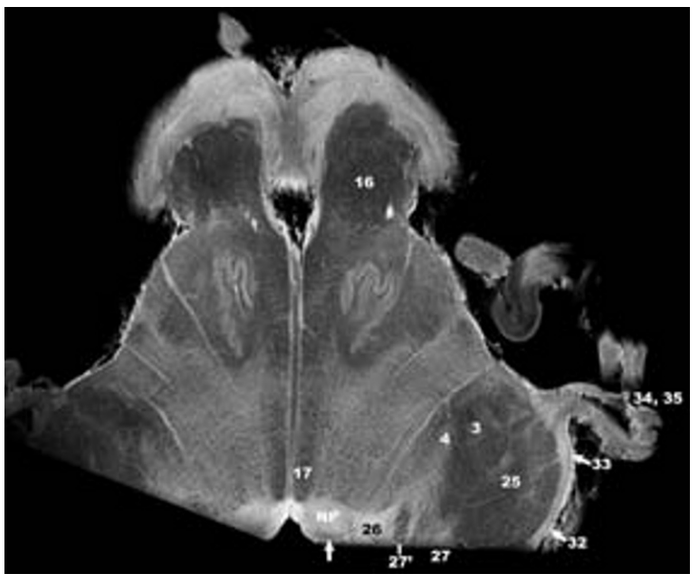

A

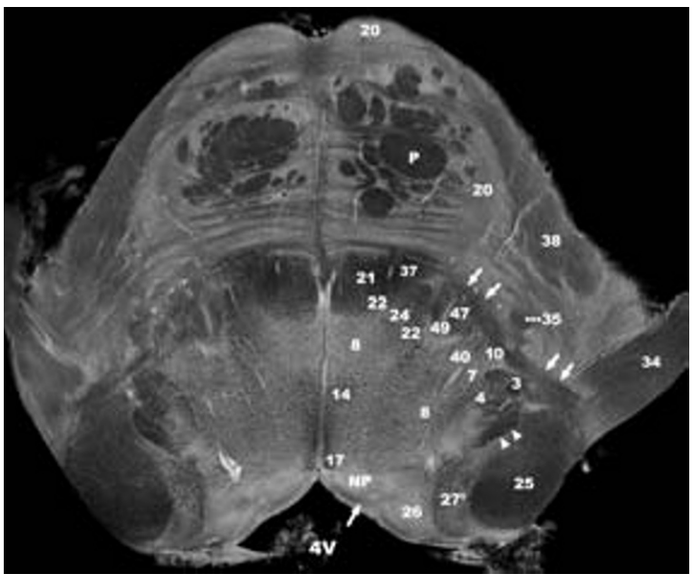

B

Fig. 9.5 (A–E). Cranial nerves VII-VIII: The facial and vestibulocochlear nuclei, roots and nerves.
MR Microscopy displays the nuclei and intramedullary fibers of the facial and vestibulocochlear nerves in the axial **(A–C),** and coronal **(D–E)** planes (two specimens).

3 Spinal trigeminal tract
4 Spinal trigeminal nucleus
7 Rubrospinal tract
8 Extensive reticular formation (light gray)
10 Spinothalamic tract
14 Tectospinal tract (with tectobulbar fibers, this forms part of the predorsal longitudinal fasciculus (55) [358]
16 Pyramid containing the corticospinal tract
16″ Descending corticospinal tract
17 Medial longitudinal fasciculus
20 Pontine nuclei
21 Medial lemniscus
22 Ventral trigeminothalamic tract
23 Superior cerebellar peduncle
24 Central tegmental tract
25 Inferior cerebellar peduncle (restiform body)
26 Medial vestibular nucleus
27 Inferior vestibular nucleus
27′ Descending root of the vestibular nerve (primary sensory neurons of the vestibular nerve extending caudally to synapse in the inferior vestibular nucleus)
28 Superior vestibular nucleus
29 Lateral vestibular nucleus
32 Dorsal cochlear nucleus
33 Ventral cochlear nucleus
34 Vestibulocochlear nerve (CN VIII)
35 Facial nerve (CN VII)
35″ Facial colliculus where the facial nerve (35) crosses dorsal and superior to the abducens nucleus (39)
37 Trapezoid body (auditory fibers)
38 Middle cerebellar peduncle (brachium pontis)
39 Abducens nucleus (CN VI)
40 Facial nerve nucleus (CN VII)
47 Lateral lemniscus
48 Ventral nucleus of the lateral lemniscus
49 Supra-olivary nucleus complex (superior olivary nucleus and trapezoid nucleus)

Letter labels
4V Fourth ventricle
NP Nucleus prepositus hypoglossi
P Corticospinal (pyramidal) tract

C

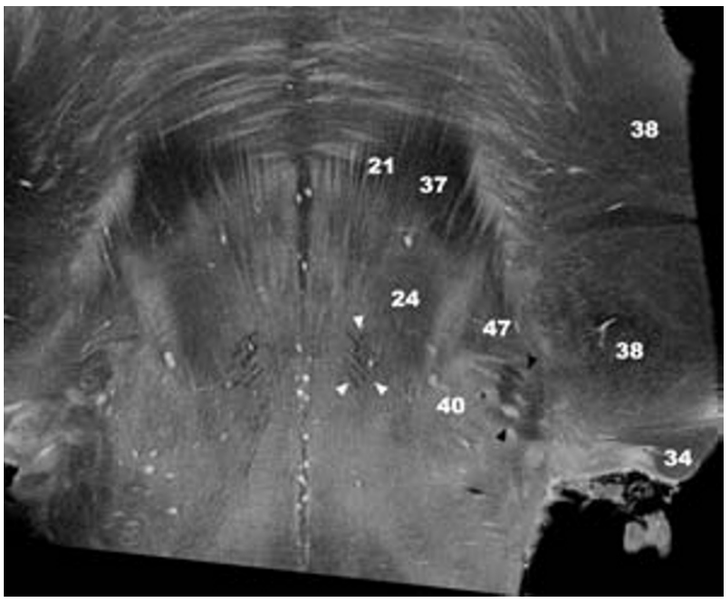

D

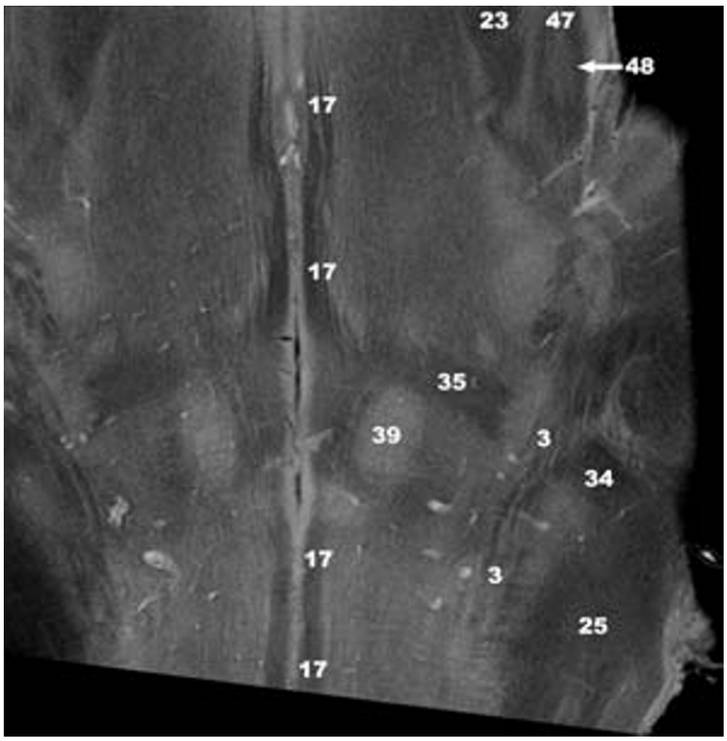

E

Arrowheads and arrows

Single black arrowhead (Fig. 9.5C):	Genu of the facial nerve as it curves over the abducens nucleus on each side
Single pair of white arrowheads (Fig. 9.5B):	Afferent vestibular fibers descending to the inferior vestibular nucleus (27′), passing lateral to the spinal trigeminal tract and nucleus (3, 4)
Single pair of black arrowheads (Fig. 9.5C, D):	Descending segment of the facial nerve, passing medial to the spinal trigeminal tract and nucleus (3, 4) and then laterally to emerge inferior to the middle cerebellar peduncle (38)
Multiple white arrowheads (Fig. 9.5C, D):	Fascicles of the abducens nerve
Single white arrow (Fig. 9.5A, B):	Dorsal longitudinal fasciculus
Two pairs of white arrows (Fig. 9.5B):	Trapezoid tract and body (crossing auditory fibers)

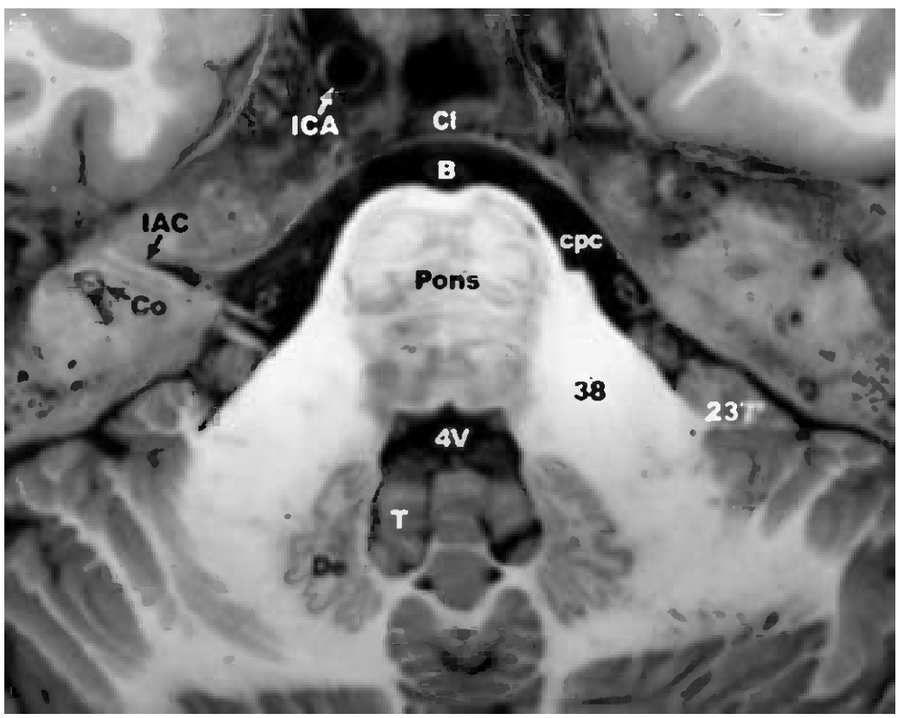

A

Fig. 9.6 (A–G). Cranial nerves VII-VIII: The facial and vestibulocochlear nuclei, roots and nerves.

A–B. Anatomic sections through the medulla in the axial **(A)** and coronal **(B)** planes. See also **Figs. 11.12 D, 11.41 B and 11.60D**.

C–H. MR Cisternography of the vestibulocochlear nerve (CN VIII) and the facial nerve (CN VII) in the axial **(C–D),** oblique sagittal **(E–F),** and coronal **(G–H)** planes.

16 Pyramid containing the corticospinal tract
23′ Decussation of the superior cerebellar peduncle
34 Vestibulocochlear nerve (CN VIII)
35 Facial nerve (CN VII)
38 Middle cerebellar peduncle (brachium pontis)
51 Pontocerebellar fibers
237′ Flocculus

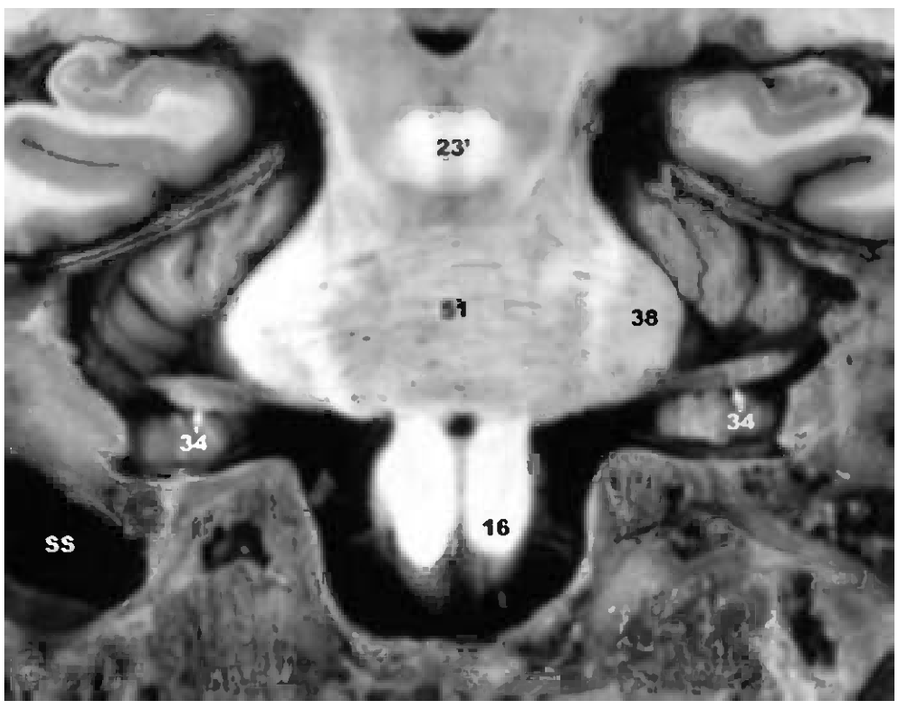

B

Letter labels

4V	Fourth ventricle
cpc	Cerebellopontine angle cistern
A	Vertebral artery (also V)
B	Basilar artery
Cl	Clivus
Co	Cochlea of the inner ear
De	Dentate nucleus
IAC	Internal auditory canal
ICA	Internal carotid artery
JT	Jugular tubercle
Med	Medulla
OC	Occipital condyle
Pons	Pons
SS	Sigmoid sinus
T	Tonsil
V	Vertebral arteries (Also A)
Ve	Vestibule

Arrowheads and arrows

Single arrows: Cisternal segments of cranial nerves VII and VIII

Crossed arrows: Cisternal segments of the abducens nerve (CN VI)

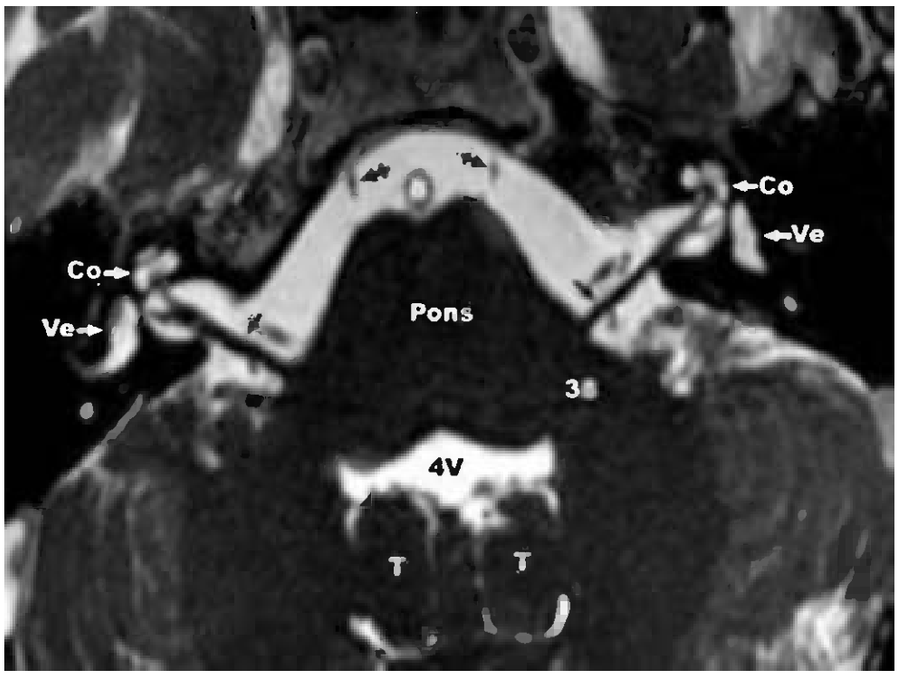

C

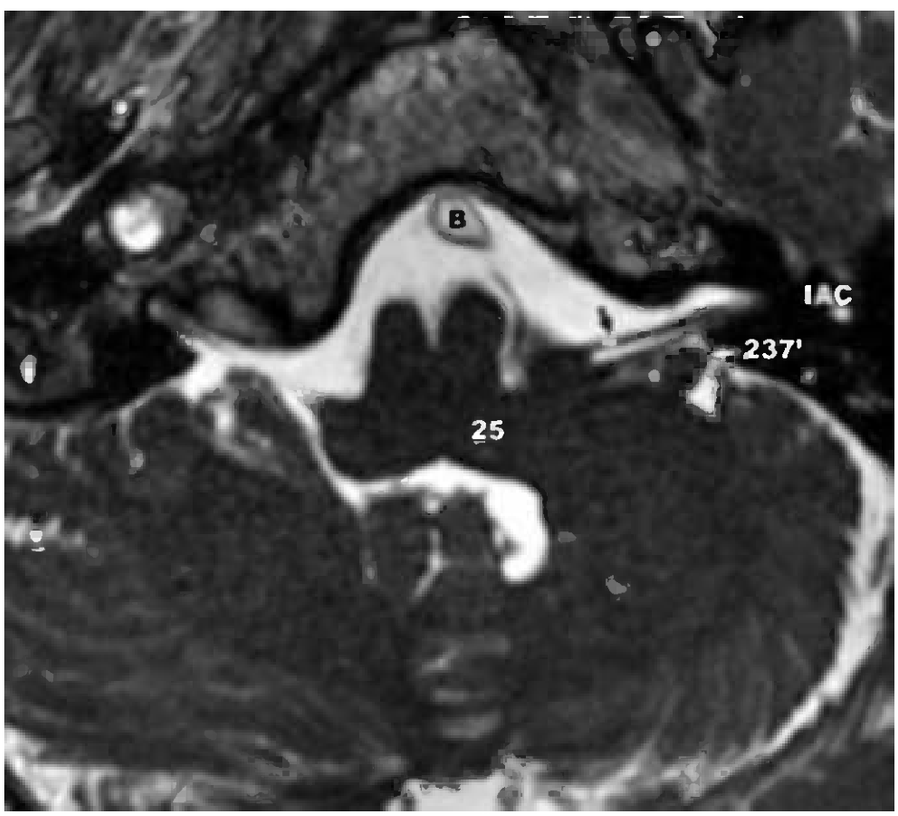

D

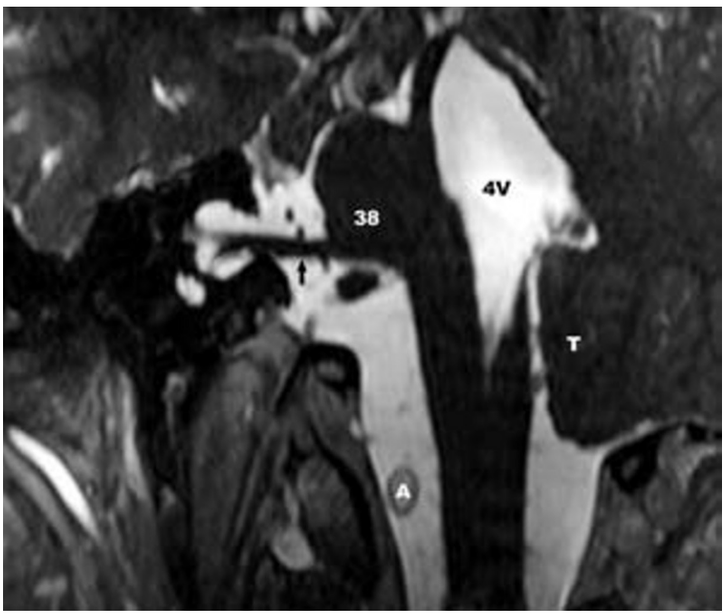

E

F

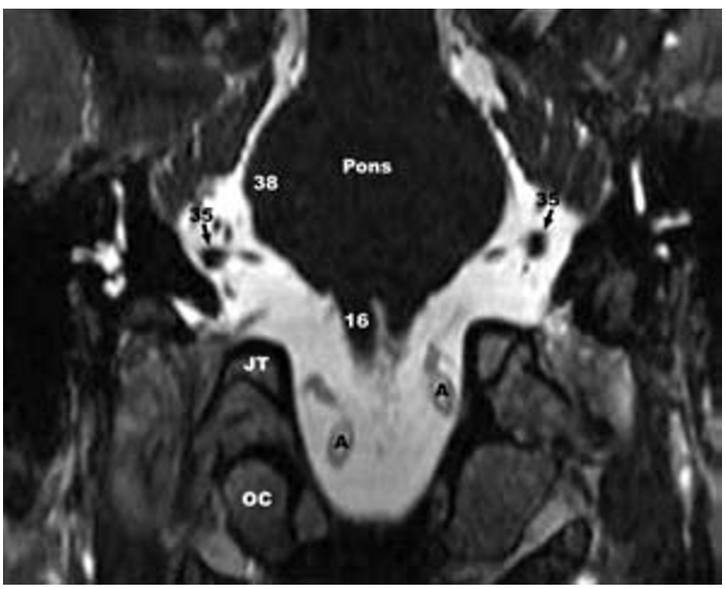

G

The abducens nerve: CN VI

The abducens nucleus lies in the dorsomedial pontine tegmentum at the floor of the fourth ventricle, immediately ventral to the facial colliculus [78, 260, 467, 478, 483, 487, 488].

GSE of CN VI: The motor fibers of the abducens nerve for striated muscle arise as a diffuse spread of fibers from the medial aspect of the abducens nucleus (**Fig. 9.7**). Fifteen to twenty fascicles of the nerve pass ventrally, laterally and caudally, through the reticular formation, the medial lemniscus, the pontocerebellar fibers, the pontine nuclei and the descending corticospinal tracts, toward the pontomedullary sulcus. The abducens rootlets typically coalesce to emerge from the brain stem as a compact bundle precisely at the pontomedullary sulcus immediately superior to the medullary pyramids, approximately 1–2 cm off midline. On occasion 1–3 of the rootlets, or all of the rootlets, may emerge rostral to the pontomedullary sulcus instead. The abducens fibers do not decussate.

From their exit point, the abducens rootlets recurve superiorly, anteriorly and slightly laterally, and course upward within the prepontine cistern toward the dura overlying the dorsal surface of the upper clivus (**Fig. 9.8**). The abducens nerve pierces the inner leaf of the clival dura, usually via a single ostium (93–95%) that contains one (45–94%) or two nerve trunks (55%). Less frequently, there are duplicate dural foramina, with each ostium containing a single trunk (5–13.5%). A sleeve of arachnoid and cerebrospinal fluid accompanies the nerve as it enters the dura. Sequentially, the abducens nerve traverses a venous confluence located between the dural leaves, crosses over the petrous apex, enters a fibro-osseous conduit (Dorello's canal), and then enters the postero-inferior aspect of the cavernous sinus. Within the cavernous sinus, the abducens nerve passes anteriorly along the lateral surface of the internal carotid artery, and exits the skull via the superior orbital fissure within the annulus of Zinn (the common tendinous ring of the extra-ocular muscles) [467]. It supplies the lateral rectus muscle ipsilateral to the abducens nucleus.

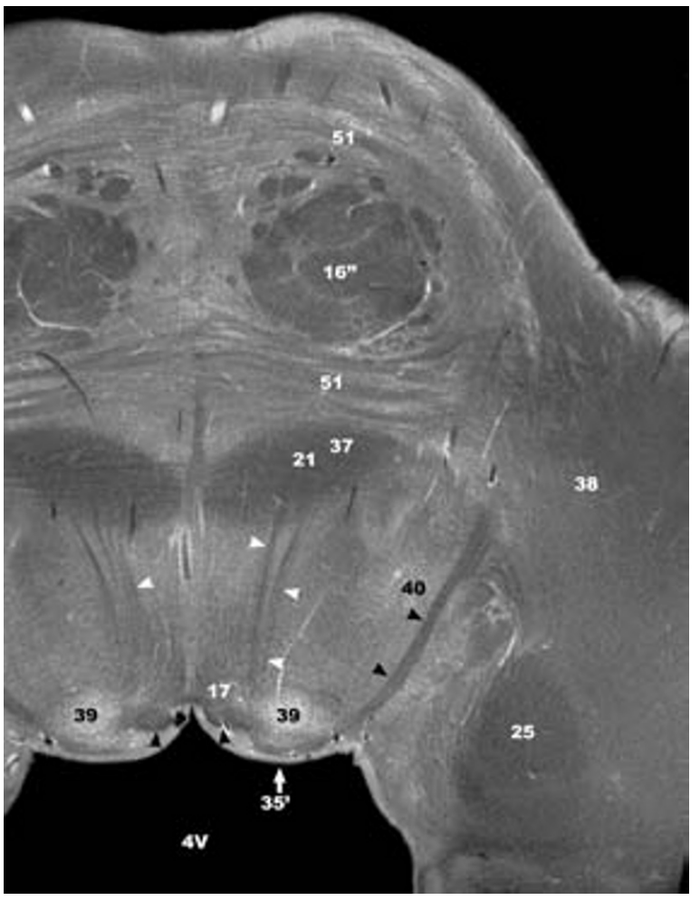

A

Fig. 9.7 (A–E). Cranial nerve VI: The abducens nerve (with some features of cranial nerves VII and VIII).
MR Microscopy displays the nuclei and intramedullary fibers of the abducens nerve in the axial **(A),** sagittal **(B–C)** and coronal **(D–E)** planes (with some features of the facial and vestibulocochlear nerves).

16″ Descending corticospinal tract
17 Medial longitudinal fasciculus
21 Medial lemniscus
23 Superior cerebellar peduncle
24 Central tegmental tract
25 Inferior cerebellar peduncle (restiform body)
26 Medial vestibular nucleus
34 Vestibulocochlear nerve (CN VIII)
35 Facial nerve (CN VII)
35′ Genu of the facial nerve as it curves over the abducens nucleus (39)
37 Trapezoid body (auditory fibers)
38 Middle cerebellar peduncle (brachium pontis)
39 Abducens nucleus (CN VI)
40 Facial nerve nucleus (CN VII)
51 Pontocerebellar fibers, seen longitudinally or in cross-section

Letter labels
4V Fourth ventricle
O Inferior olivary nucleus
P Pyramid

Arrowheads and arrows
Single black arrowhead: Genu of the facial nerve as it curves over the abducens nucleus
Paired black arrowheads: Descending segment of the facial nerve
Paired or multiple white arrowheads: Intra-axial fascicles of the abducens nerve (CN VI). Note the accompanying vessel.
Single white arrow**:** Dorsal longitudinal fasciculus

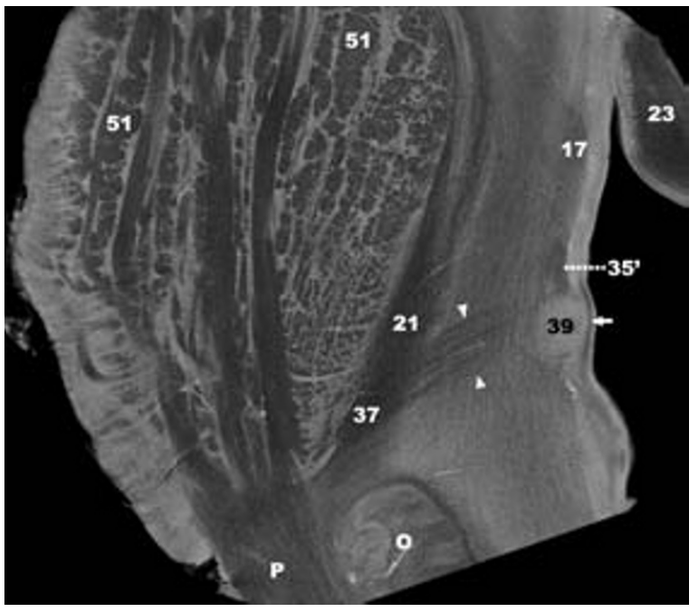
51
51
23
17
35'
21
39
37
O
P

B

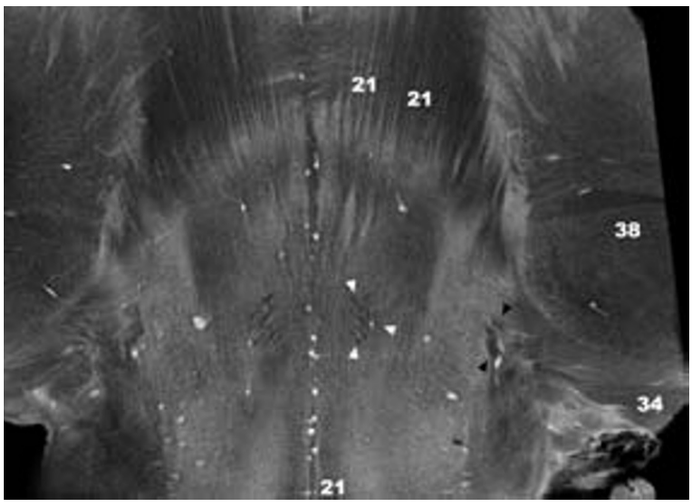
21
21
38
34
21

D

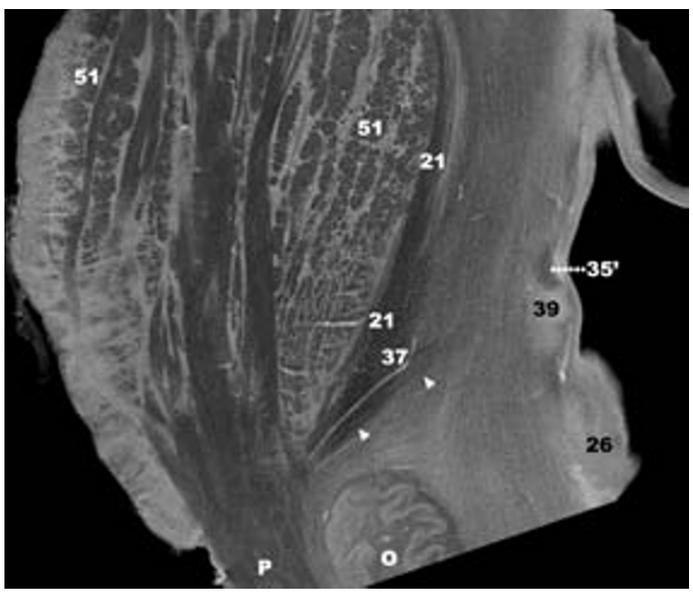
51
51
21
35'
39
21
37
26
P
O

C


23
17
24
17
35
39
34
17
25
17

E

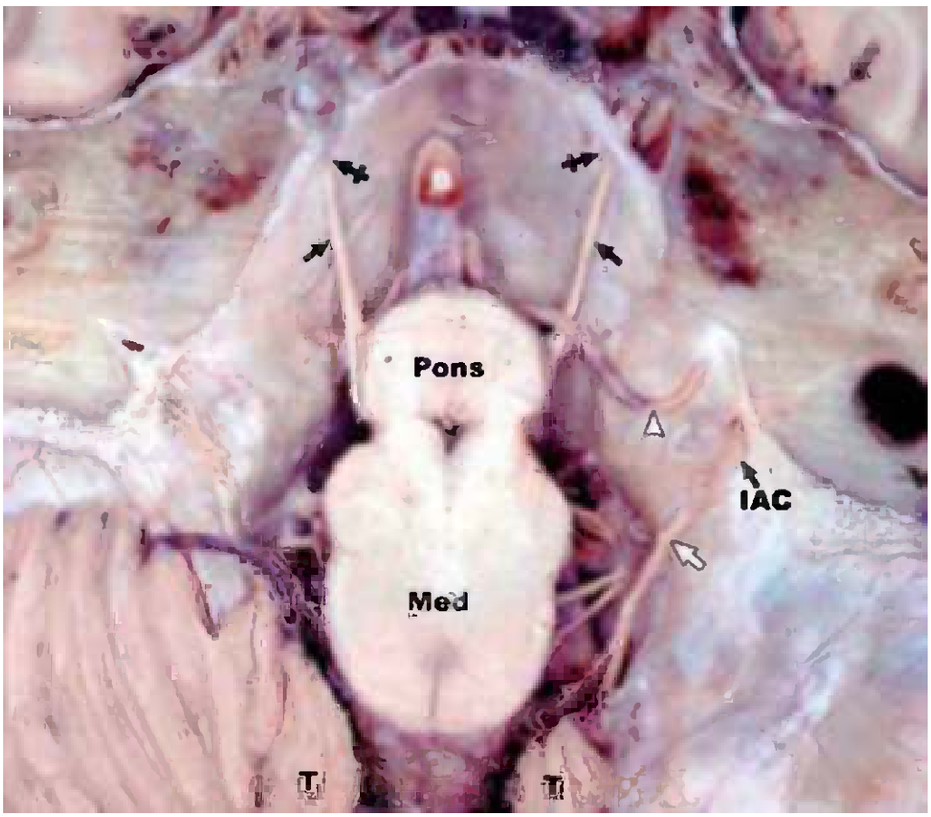

A

Fig. 9.8. Cranial nerve VI: The abducens nerve (with some features of cranial nerves VII and VIII).
A–D. Gross anatomic – MR cisternographic correlation.
A. Axial gross anatomic section of the brain stem *in situ*.
B. Corresponding axial 3T MR cisternogram in a volunteer
C. Sagittal gross anatomic section of the brain stem *in situ*
D. Corresponding sagittal 3T MR cisternogram in a volunteer

Letter labels

4V	Fourth ventricle
A	Vertebral artery
B	Basilar artery
Cl	Clivus
IAC	Internal auditory canal
Med	Medulla
Pons	Pons
T	Tonsil

Arrowheads and arrows

Single arrowheads:	Anterior inferior cerebellar artery (AICA)
Single white arrow:	Ascending cisternal segment of CN XI (Accessory nerve)
Single black arrows:	Cisternal segments of CN VI (abducens nerve)
Crossed black arrows:	Arachnoid sleeve and cerebrospinal fluid accompanying the abducens nerve as it pierces the dura of the clivus.

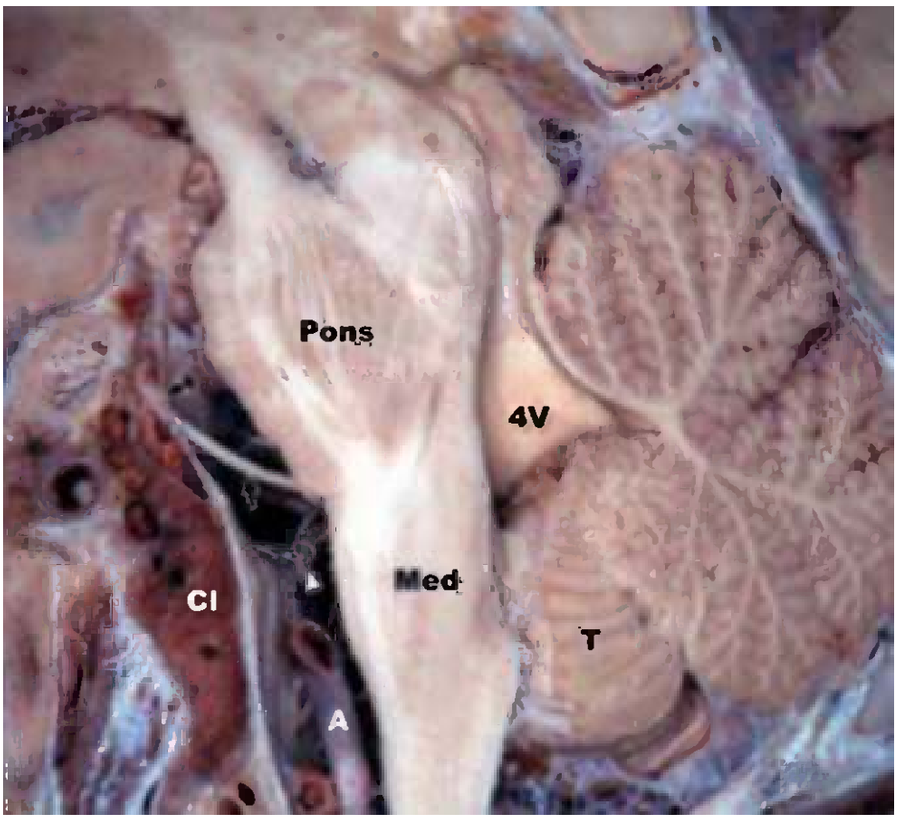

C

B

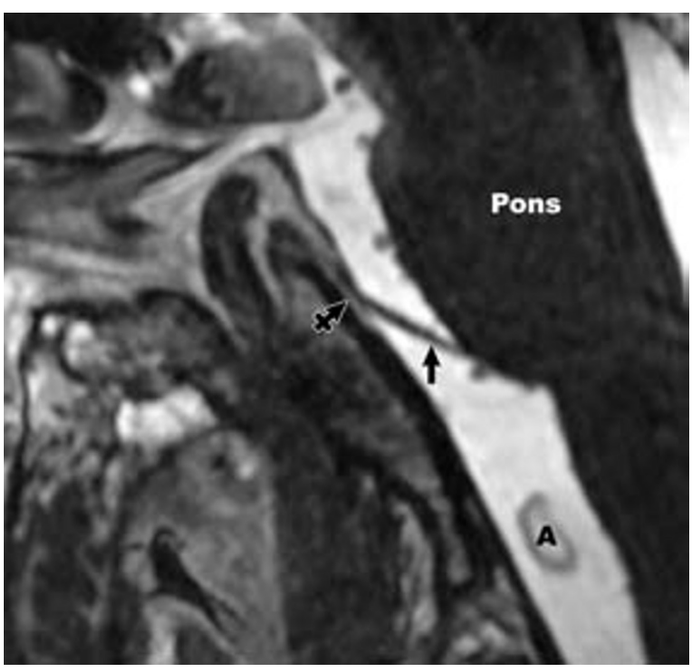

D

The trigeminal nerve. CN V.

The trigeminal nerve is a mixed motor and sensory nerve [78, 103, 260, 467, 482, 484, 488].

SVE of CN V: Motor fibers of the trigeminal nerve for branchial muscles arise from the branchial motor nucleus (masticator nucleus) of the trigeminal nerve. The trigeminal motor nucleus lies in the lateral portion of the upper pons, just medial to the entry point of the trigeminal fibers, medial to the principal sensory nucleus, and immediately caudal to the inferior end of the mesencephalic nucleus and tract of the trigeminal system. The motor nucleus is the most cranial of all branchial motor nuclei [467].

Typically, the motor trigeminal fibers form one or more small motor roots that emerge from the pons anterosuperomedial to the entry point of the large sensory root. The thin motor root initially lies superomedial to the larger sensory root, but it comes to lie inferior to the sensory root as the two course anteriorly. The motor and sensory roots pass anteriorly through the high cerebellopontine angle cistern, between the middle cerebellar peduncle and the petrous bone, cross over the petrous apex at the trigeminal impression, and pass beneath the petroclinoid ligament to enter Meckel's cave. Within Meckel's cave, the motor roots pass inferior to the sensory plexus and then curve inferiorly to merge with the sensory fibers of the mandibular (V3) division of the trigeminal nerve within foramen ovale. The fibers of the motor root course peripherally with the sensory mandibular fibers to provide motor control for the masseter, temporalis, medial pterygoid, and lateral pterygoid muscles (of mastication) plus the tensor tympani, tensor veli palatini, mylohyoid and the anterior belly of the digastric muscle [488].

GSA of CN V: The general somatic afferent nerves of the trigeminal system arise from neurons in two distinct locations:

(i). The mesencephalic nucleus of the trigeminal system. The primary neurons that provide proprioceptive fibers to the muscle spindles of the face and head reside in the long thin mesencephalic nucleus of the trigeminal nerve in the midbrain and upper pons. Superiorly, the mesencephalic nucleus lies just lateral to the lateral margin of the periaqueductal gray matter, deep to the superior cerebellar peduncle. Inferiorly, the mesencephalic column descends into the upper pons along the sloping lateral wall of the upper fourth ventricle to reach the motor (masticator) nucleus of the trigeminal nerve. The peripheral processes of the mesencephalic nucleus descend into the upper pons as the mesencephalic tract of the trigeminal nerve. These peripheral fibers distribute predominantly with the motor fibers of the masticator nucleus to provide proprioception from the muscles of mastication. The central processes of the mesencephalic neurons project mainly to the motor nucleus of CN V for reflex control of bite [78]. The neurons of the mesencephalic nucleus are the only primary unipolar sensory neurons to reside within the central nervous system, rather than within external ganglia [488].

(ii). The spinal trigeminal and principal sensory nuclei of the trigeminal system. The primary neurons for all other afferent fibers of the trigeminal system reside outside the brain stem within the semilunar (trigeminal, Gasserian) ganglion at the anteroinferior aspect of Meckel's cave. The peripheral processes of these primary semilunar ganglion neurons exit the skull through the superior orbital fissure (ophthalmic division V1), the foramen rotundum (maxillary division V2), and the foramen ovale (mandibular division V3) of the trigeminal nerve for distribution to wide areas of the face, head and meninges. The central processes of the semilunar neurons condense into the sensory trigeminal root that enters the lateral tegmentum of the high pons and distributes to the principal sensory nucleus and the spinal trigeminal nucleus of the trigeminal nerve.

Principal sensory nucleus. The principal sensory nucleus is a large group of secondary neurons situated within the lateral pons just lateral to the entry point of the trigeminal nerve and just rostral to the upper end of the spinal trigeminal nucleus. Mechanoreceptors for tactile discrimination, joint position sense, and pressure sensation distribute to and terminate somatotopically in the principal sensory nucleus of the trigeminal nerve [78]. Fibers of the ophthalmic division (V1) terminate within the ventral portion of the nucleus. Fibers of the maxillary division (V2) terminate in intermediate position, and fibers of the mandibular division (V3) terminate dorsally [78]. Second order fibers from the ventral portion of the principal sensory nucleus cross the midline to join the ventral trigeminothalamic tract, while fibers from the dorsomedial portion of the principal sensory nucleus ascend uncrossed to form the dorsal trigeminothalamic tract. Both tracts enter the ventral posteromedial nuclei of the two thalami [78, 322a].

Spinal trigeminal nucleus. The spinal trigeminal nucleus is a large column of secondary neurons, which extends from the central gray matter (substantia gelatinosa) of the spinal cord inferiorly to the inferior aspect of the principal sensory nucleus in the pons [467]. Central processes of semilunar sensory neurons that convey pain, temperature and light touch enter the pons with the main sensory root, turn inferiorly, and descend somatotopically as the spinal trigeminal tract along the lateral border of the spinal trigeminal nucleus. As in the principal sensory nucleus, the sensory fibers from V1, V2 and V3 descend through the tract in anterior, intermediate and posterior position, respectively [78]. The descending fibers exit the spinal trigeminal tract to synapse somatotopically within specified portions of the contiguous spinal trigeminal nucleus.

The caudal portion of the spinal trigeminal nucleus lies at the surface of the low medulla, just anterolateral to the fasciculus and nucleus cuneatus. Cephalically, the nucleus becomes buried deep to the posterior spinocerebellar tract and the restiform body. In the pons, the spinal trigeminal nucleus and tract curve slightly lateral, pass lateral to the facial nucleus, and merge into the principal sensory nucleus of CN V. Secondary fibers arising from the upper and mid thirds of the spinal trigeminal nucleus project ventromedially into the reticular formation, cross the median raphe, and ascend as the ventral trigeminothalamic tract to terminate in the ventral posteromedial nucleus of the thalamus. Fibers from the lower third cross the midline to the contralateral dorsal trigeminothalamic tract and ascend with the spinothalamic tract in the anterolateral fasciculus to terminate in the intralaminar, posterior ventromedial and medial dorsal nuclei of the thalamus [322a].

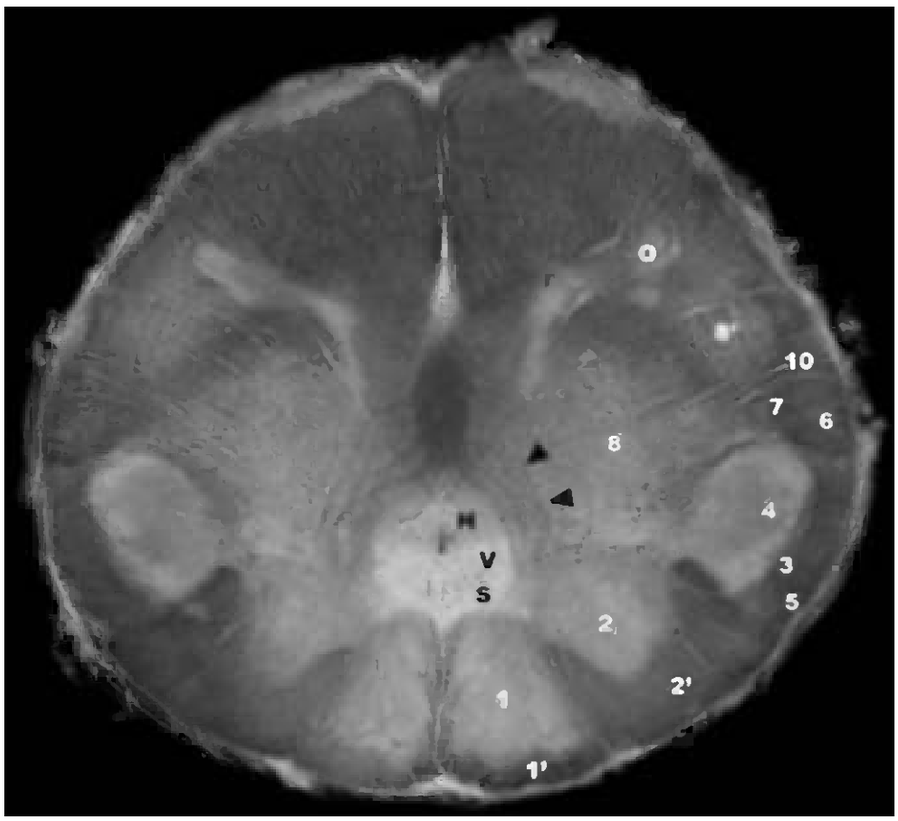

A

Fig. 9.9 (A–C). Cranial nerve V: The spinal trigeminal nuclei and tracts.
MR Microscopy displays the nuclei and intramedullary fibers of the spinal root of the trigeminal nerve in the axial **(A),** coronal **(B)** and sagittal **(C)** planes.

1 Nucleus gracilis
1′ Fasciculus gracilis approaching the caudal pole of the nucleus gracilis
2 Nucleus cuneatus
2′ Fasciculus cuneatus
2″ Accessory (lateral) nucleus cuneatus
3 Spinal trigeminal tract
4 Spinal trigeminal nucleus
5 Posterior (dorsal) spinocerebellar tract
6 Anterior (ventral) spinocerebellar tract
7 Rubrospinal tract
8 Extensive reticular formation (light gray)
8′ Lateral reticular nucleus
10 Spinothalamic tract
36 Tracts of the ventrolateral columns of the spinal cord

Letter labels
4V Fourth ventricle
H Hypoglossal nucleus
O Inferior olivary nucleus
S Solitary nucleus
V Dorsal vagal nucleus

Arrowheads and arrows
Black arrowheads: Internal arcuate fibers

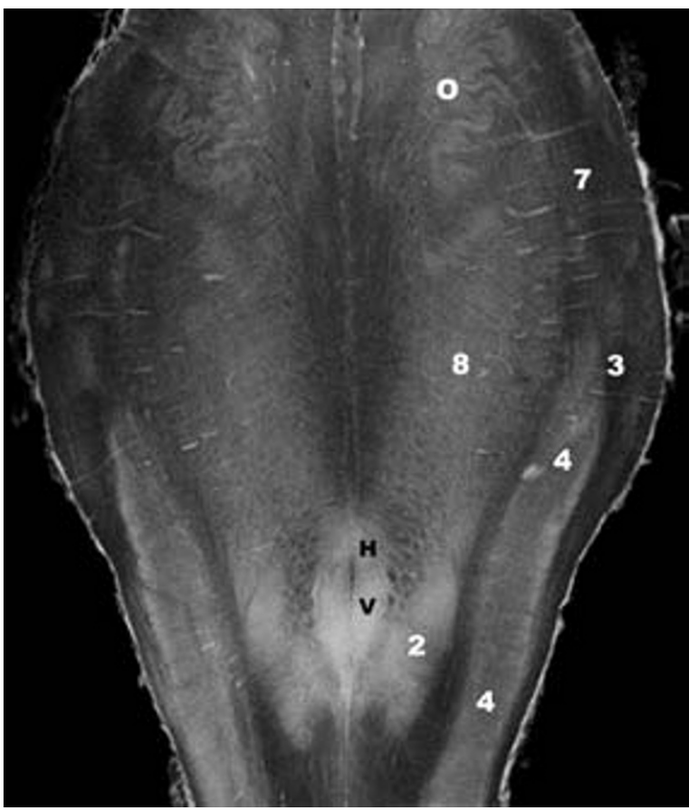

B

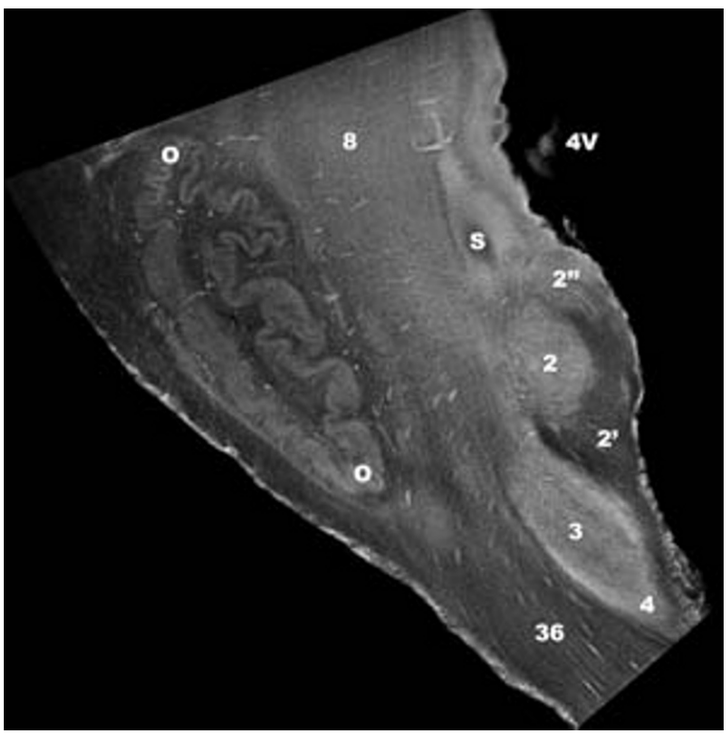

C

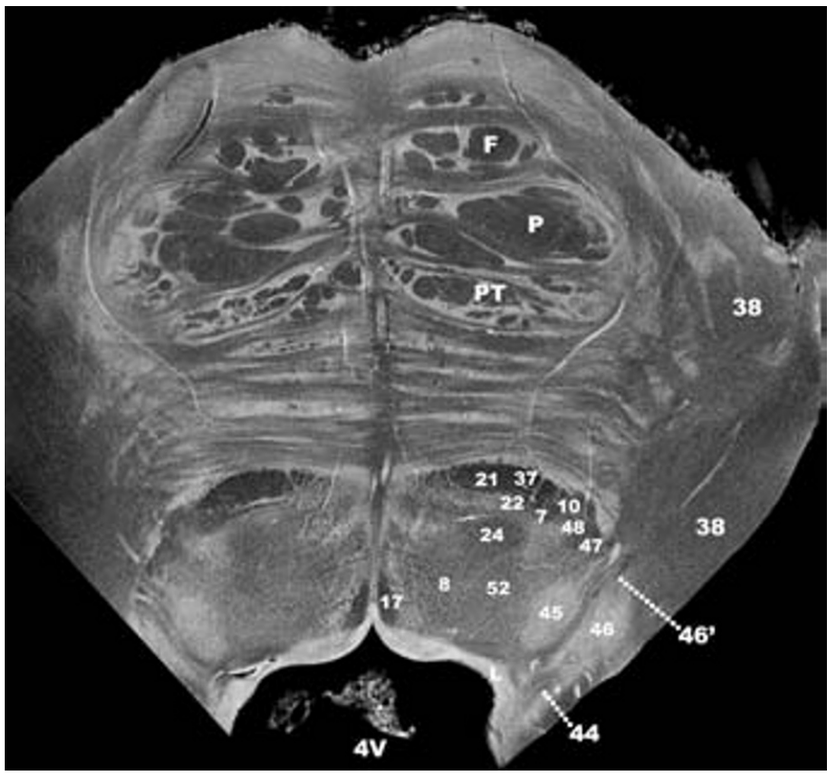

A

Fig. 9.10 (A–D). Cranial nerve V: The principal sensory and motor nuclei and roots.
MR Microscopy displays the nuclei and intramedullary fibers of the motor and principal sensory roots of the trigeminal nerve in the axial (**A–B**), coronal (**C**), and sagittal (**D**) planes.

3 Spinal trigeminal tract
4 Spinal trigeminal nucleus
7 Rubrospinal tract
8 Extensive reticular formation (light gray)
10 Spinothalamic tract
14 Tectospinal tract
17 Medial longitudinal fasciculus
21 Medial lemniscus
22 Ventral trigeminothalamic tract
23 Superior cerebellar peduncle
24 Central tegmental tract
25 Inferior cerebellar peduncle (restiform body)
26 Medial vestibular nucleus
34 Vestibulocochlear nerve (CN VIII)
37 Trapezoid body (auditory fibers)
38 Middle cerebellar peduncle (brachium pontis)
39 Abducens nucleus (CN VI)
43 Trigeminal nerve (CN V)
43′ Motor root of the trigeminal nerve (CN V)
44 Mesencephalic tract and surrounding mesencephalic nucleus of CN V
45 Motor nucleus of CN V
46 Principal sensory nucleus of CN V
46′ Intrapontine fascicles of the sensory root of CN V
47 Lateral lemniscus
48 Ventral nucleus of the lateral lemniscus
52 Dorsal trigeminothalamic tract

Letter labels
4V Fourth ventricle
F Frontopontine tract
L Site of the locus ceruleus
O Inferior olivary nucleus
P Corticospinal tracts descending through the pons
PT Temporoparietopontine fibers

Arrowheads and arrows
Paired white arrows: Descending root of the facial nerve (CN VII)
Multiple white arrows: Fascicles of the trigeminal nerve coursing through the middle cerebellar peduncle to exit the pons as the motor root of the trigeminal nerve (CN V)

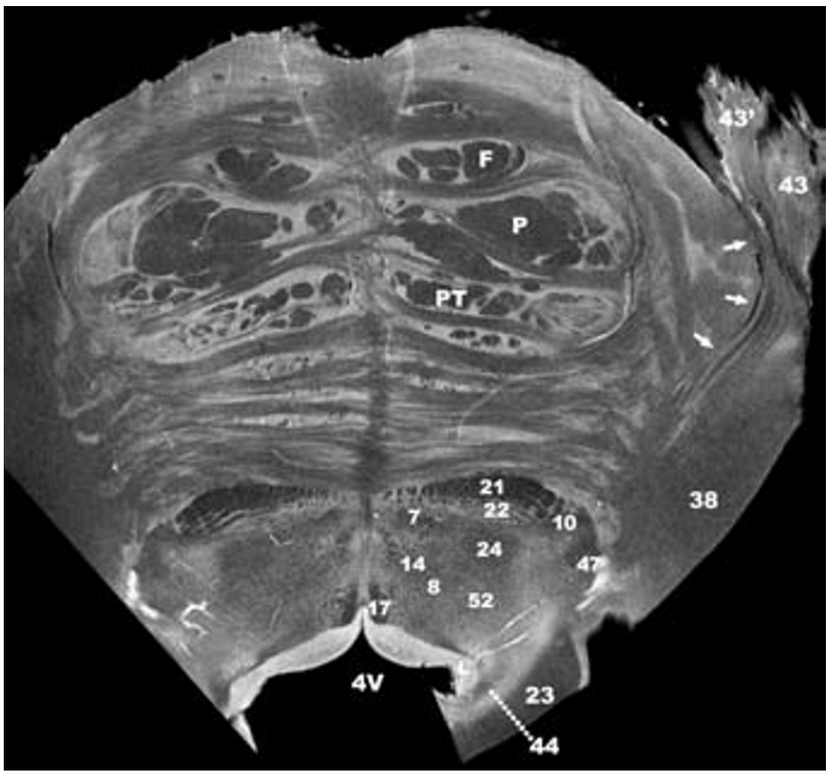
43'
43
F
P
PT
21
22
7
10
38
24
14
47
8
52
17
4V
23
44

B

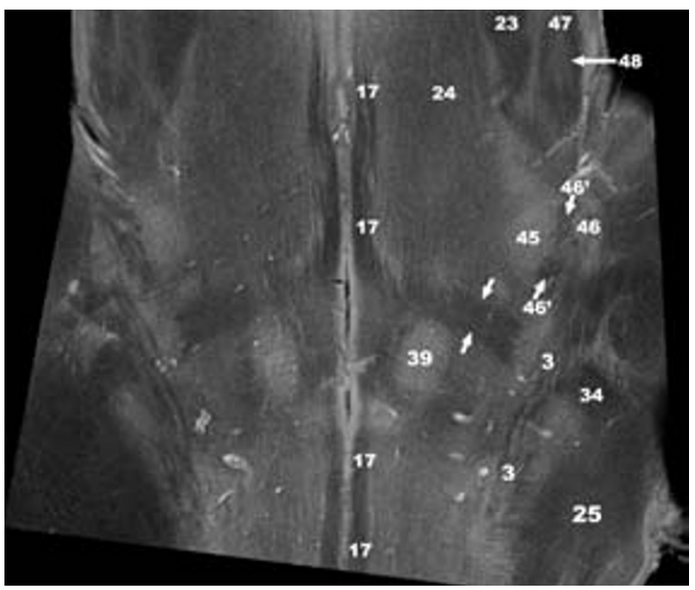
23
47
48
17
24
46'
17
45
46
46'
39
3
34
17
3
25
17

C

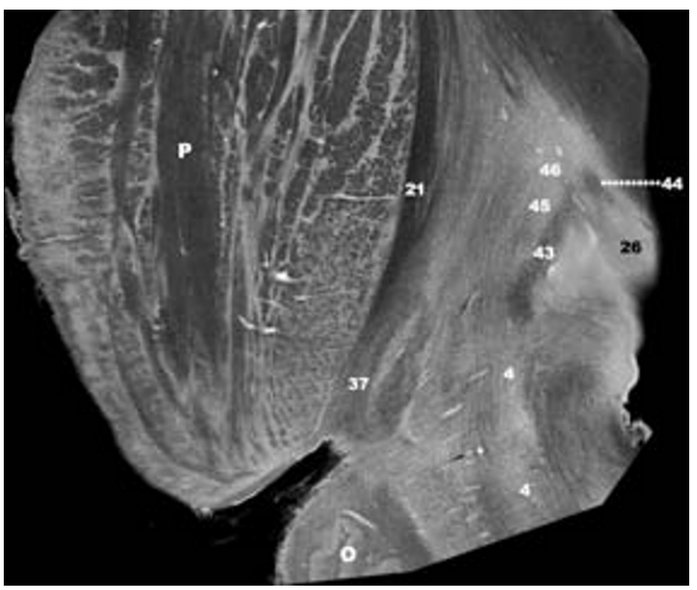
P
21
46
44
45
43
26
37
4
4
O

D

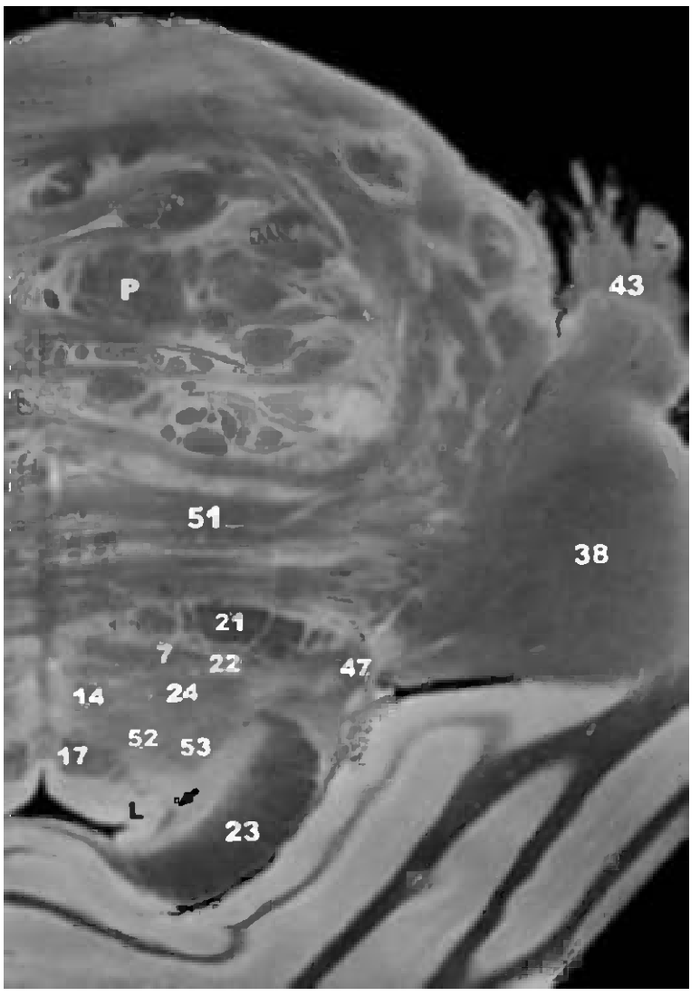

A

Fig. 9.11 (A–C). Cranial nerve V: The principal sensory and motor nuclei and roots.
MR Microscopy displays the intramedullary fibers of the mesencephalic root of the trigeminal nerve in the axial **(A)**, coronal **(B)**, and sagittal **(C)** planes. The actual mesencephalic nucleus is too small to recognize by this technique.

7 Rubrospinal tract
14 Tectospinal tract
17 Medial longitudinal fasciculus
21 Medial lemniscus
22 Ventral trigeminothalamic tract
23 Superior cerebellar peduncle
23′ Decussation of the superior cerebellar peduncle
23′d Dorsal portion of decussation of the superior cerebellar peduncle
23′v Ventral portion of decussation of the superior cerebellar peduncle
24 Central tegmental tract
38 Middle cerebellar peduncle (brachium pontis)
43 Trigeminal nerve (CN V)
47 Lateral lemniscus
52 Dorsal trigeminothalamic tract
53 Tegmento-olivary tract
56 Inferior colliculus

Letter labels
L Site of the locus ceruleus
P Corticospinal tracts descending through the pons

Arrowheads and arrows
Single black arrow: Mesencephalic tract of the trigeminal nerve (CN V)

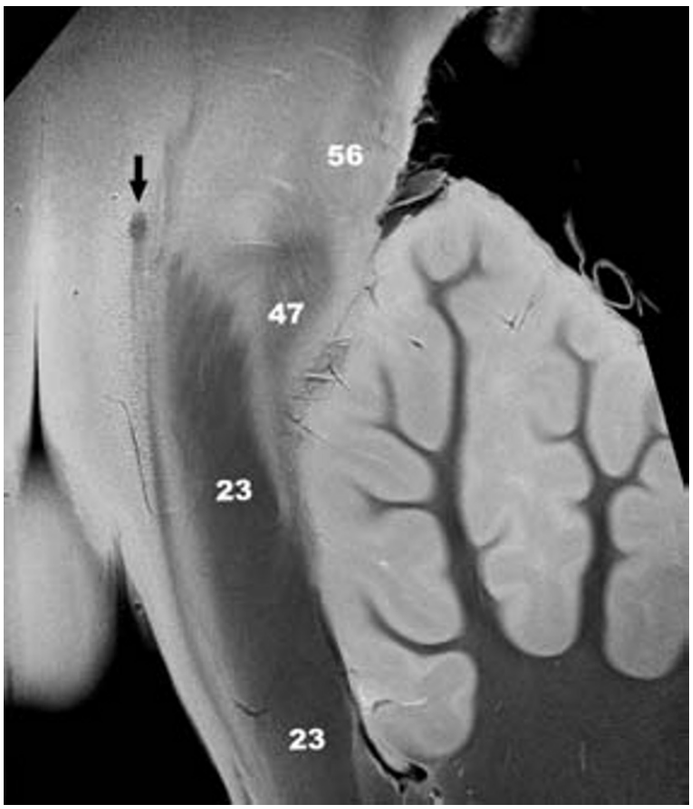

B

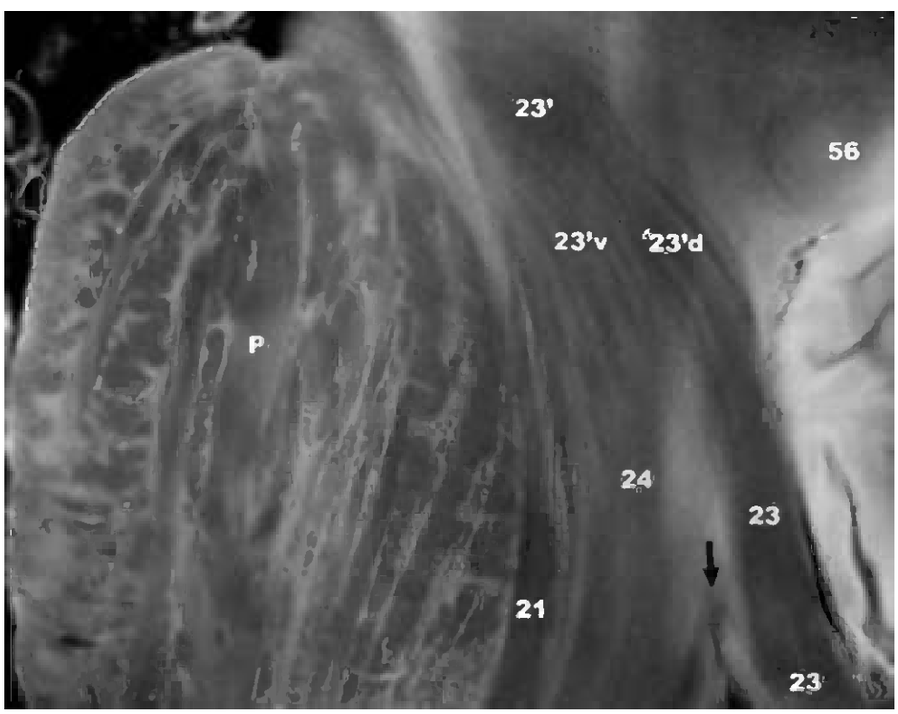

C

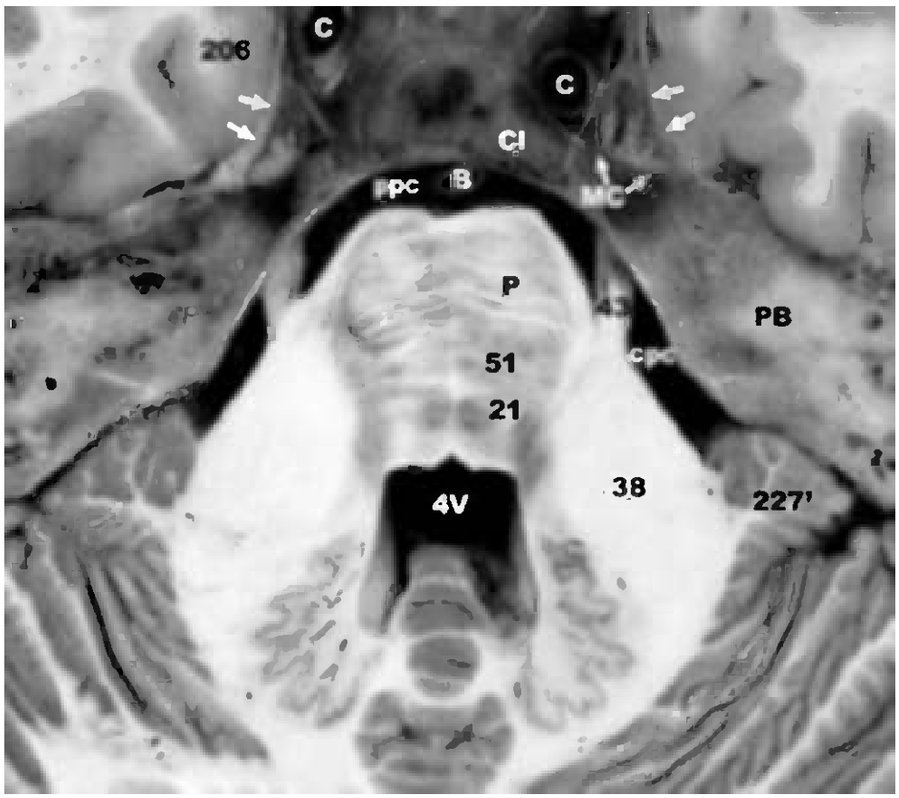

A

Fig. 9.12 (A–D). Cranial nerve V: Gross anatomic sections in the axial **(A–B),** coronal **(C)** and sagittal **(D)** planes. See also Figs.11.14 D, 11.16 D, 11.30, and 11.62.

21 Medial lemniscus
38 Middle cerebellar peduncle (brachium pontis)
43 Trigeminal nerve (CN V)
51 Pontocerebellar fibers
100 Optic chiasm
176 Anterior perforated substance
206 Parahippocampal gyrus
207 Uncus
208 Amygdala
227′ Simple lobule (posterior quadrangular lobule)

Letter labels

3V Third ventricle
4V Fourth ventricle
ppc Prepontine cistern
cpc Cerebellopontine angle cistern
B Basilar artery
C Internal carotid artery within the cavernous sinus
Cl Clivus
MC Meckel's (trigeminal) cave
P Corticospinal tracts descending through the pons
PB Petrous bone
Sph Sphenoid sinus

Arrowheads and arrows

Two white arrowheads: Trigeminal (semilunar, Gasserian) ganglion within Meckel's cave (MC)
Three white arrowheads: Tentorium
White arrows: Lateral wall of Meckel's (trigeminal) cave

B

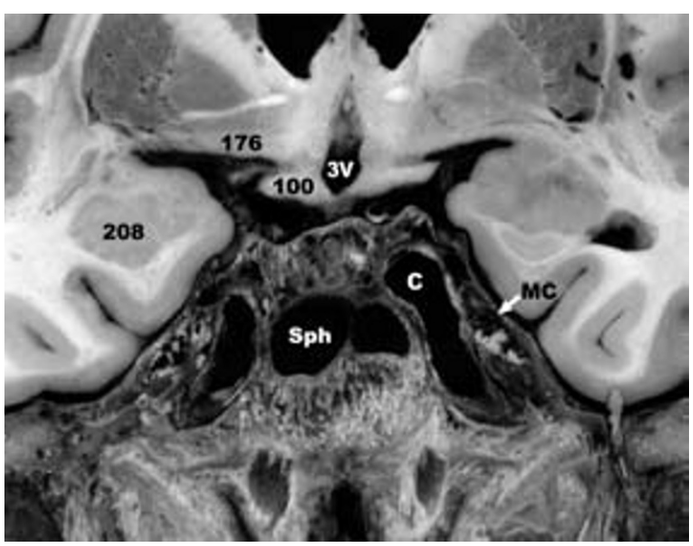

C

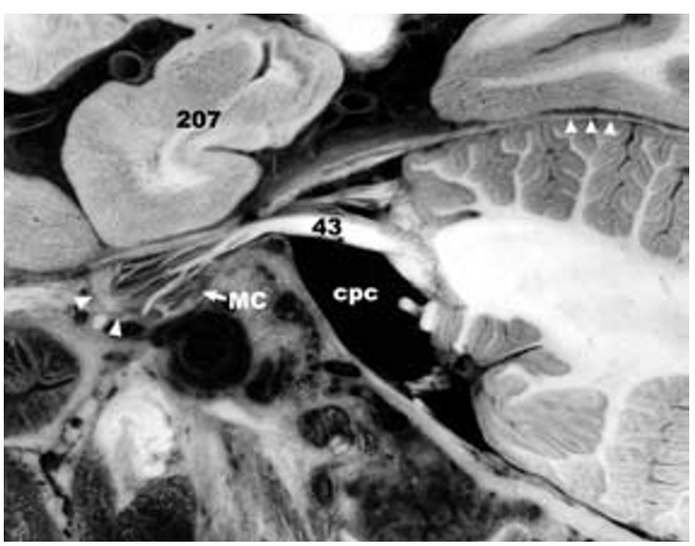

D

A

Fig. 9.13 (A–C). Cranial nerve V: MR Cisternography of the trigeminal nerve in the axial (A), coronal (B) and oblique sagittal (C) planes

38 Middle cerebellar peduncle (brachium pontis)
227' Simple lobule (posterior quadrangular lobule)

Letter labels
4V Fourth ventricle
A Vertebral artery
B Basilar artery
C Internal carotid artery
IAC Internal auditory canal
Pons Pons

Arrowheads and arrows
Multiple white arrowheads: Trigeminal (semilunar, Gasserian) ganglion (CN V)
White arrows: Lateral walls of Meckel's (trigeminal) cave
Black arrows: Trigeminal nerves (CN V), cisternal segments

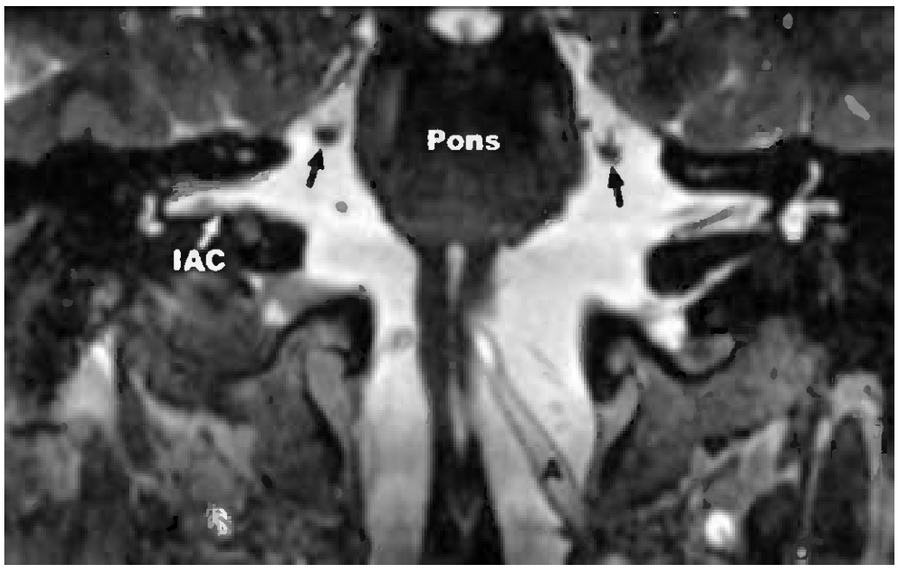

B

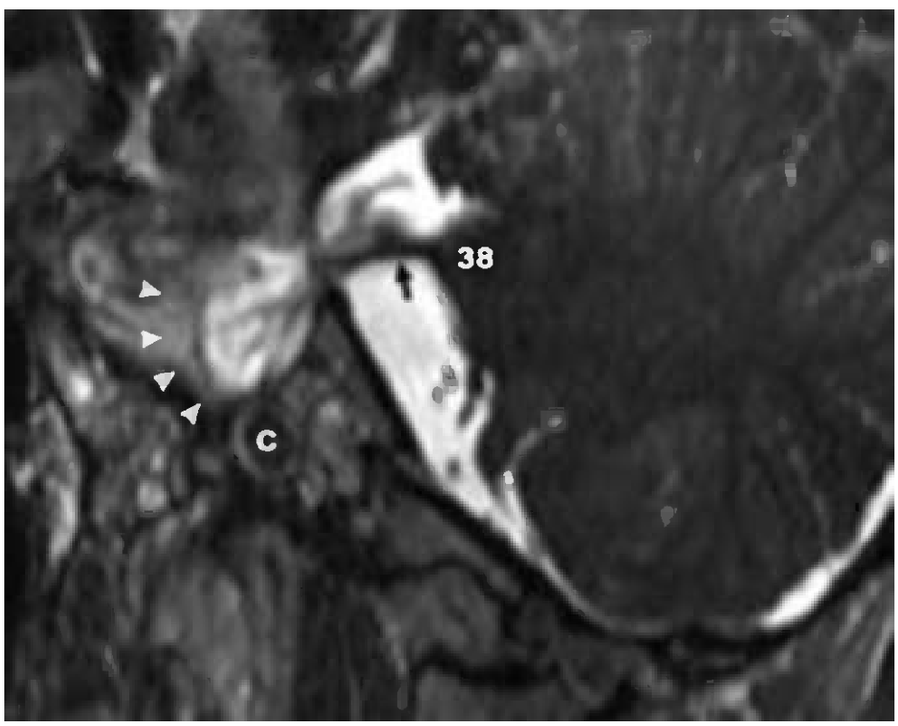

C

The trochlear nerve. CN IV.

GSE of CN IV: Motor fibers of the trochlear nerve for striated muscle arise from the trochlear nuclei at the ventral aspect of the periaqueductal gray matter in the caudal midbrain (inferior collicular level). The motor fascicles pass dorsally and laterally within the lateral periaqueductal gray matter, and then recurve dorsally and medially to decussate in the superior medullary velum of the fourth ventricle. The crossed fibers then emerge into the quadrigeminal cistern on the contralateral side, just inferior to the inferior colliculi and just lateral to the frenulum veli. See [78, 260 336, 467, 479, 480, 487, 488].

At the point of exit, a variable number of rootlets, usually two, unite to form the nerve trunk. The cisternal segment of the trochlear nerve extends from the level of the inferior colliculus to the rostrolateral free edge of the tentorium. The short initial portion of the cisternal segment lies within the quadrigeminal plate cistern. The longer distal portion runs through the caudal portion of the ambient cistern. In 35% the trochlear nerve first passes laterally from the inferior colliculus to the free edge of the tentorium in a nearly coronal plane and then passes anteriorly in a sagittal plane. In approximately 60% the trochlear nerve pursues an oblique anterolateral course, advancing in both directions simultaneously. The cisternal segment of the trochlear nerve parallels the courses of the superior cerebellar artery, the posterior cerebral artery, and the basal vein of Rosenthal. It extends anteriorly between the posterior cerebral artery (superiorly) and the superior cerebellar artery (inferiorly), lateral to the oculomotor nerve (CN III). Within the quadrigeminal plate cistern, twigs from the medial branch of the superior cerebellar artery usually surround the nerve. The cisternal segment terminates at the rostrolateral margin of the tentorium, where the nerve pierces the dura.

The trochlear fibers course anteriorly within the lateral dural wall of the cavernous sinus, between the fibers of CN III (superiorly) and the ophthalmic division of CN V (inferiorly). The trochlear nerve exits the skull through the superior orbital fissure, superior to the annulus of Zinn (the common tendinous ring of the extra-ocular muscles). The trochlear nerve is the thinnest cranial nerve, the only cranial nerve to exit on the dorsal side of the brain stem, and the only cranial nerve to decussate completely [467].

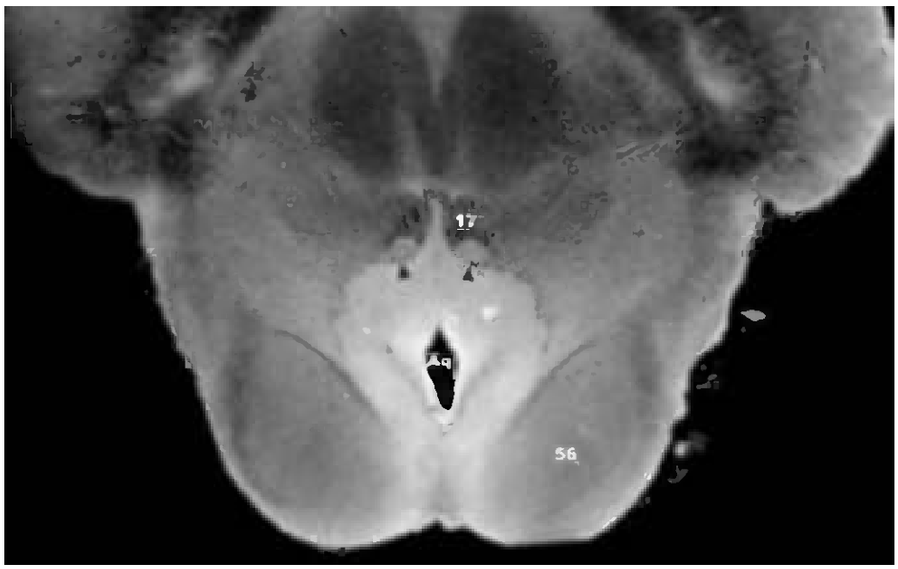

A

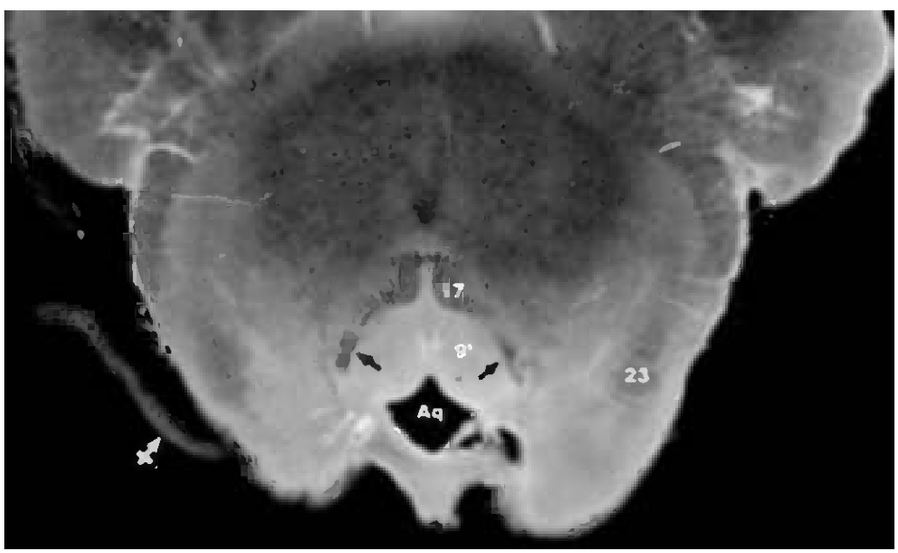

B

Fig. 9.14 (A–H). Cranial nerve IV: The trochlear nuclei, tracts, roots and nerves.

A–H. MR Microscopy displays the nuclei and intramedullary fibers of the trochlear nerves

A–D. Axial sections displayed from cranial to caudal.

E. Paramedian sagittal section through the trochlear nucleus and medial longitudinal fasciculus (MLF)

F–H. Sagittal sections shown from one side **(F)** through the midline **(G)** to the other **(H).**

9′ Periaqueductal gray matter
17 Medial longitudinal fasciculus
23 Superior cerebellar peduncle
23′ Decussation of the superior cerebellar peduncle
47 Lateral lemniscus
56 Inferior colliculus
69 Superior colliculus
76 Habenular nuclei

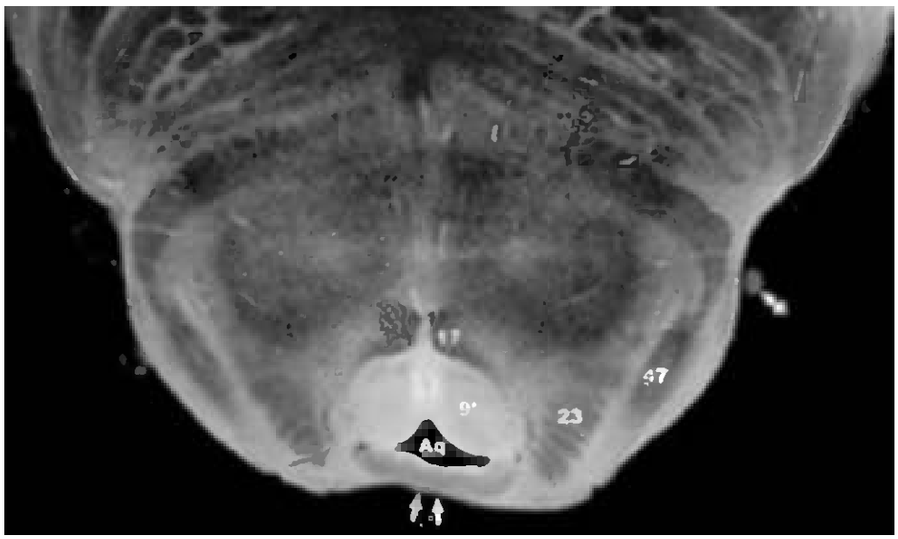

C

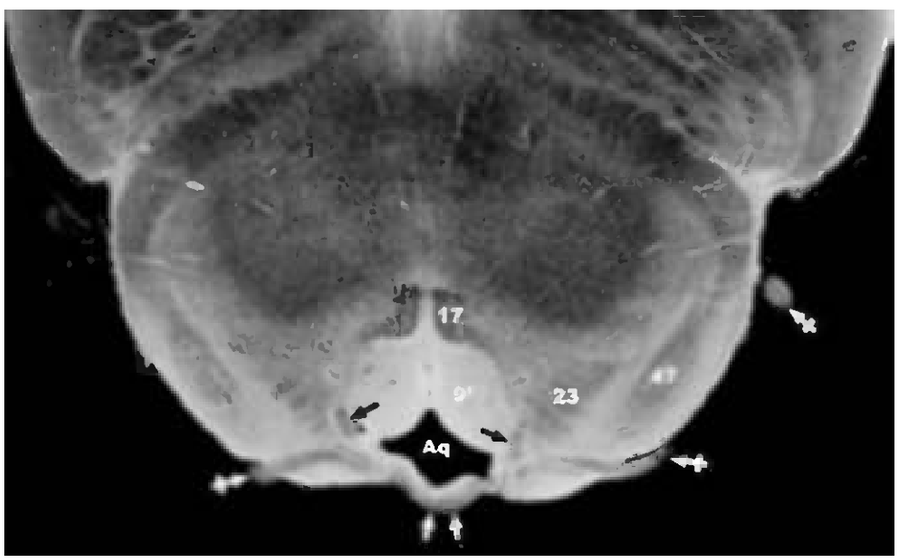

D

Letter labels

Aq	Cerebral aqueduct (of Sylvius)
Pi	Pineal gland
PC	Posterior commissure

Arrowheads and arrows

Single black arrowheads:	Nuclei of the trochlear nerve (CN IV)
Multiple white arrowheads:	Intra-axial fascicles of the oculomotor nerve (CN III)
Straight black arrows:	Intra-axial fascicles of the trochlear nerve (CN IV)
Crossed white arrows:	Cisternal segments of the trochlear nerve (CN IV)
Paired white arrows:	Decussation of the trochlear nerves (CN IV) in the superior medullary velum of the fourth ventricle

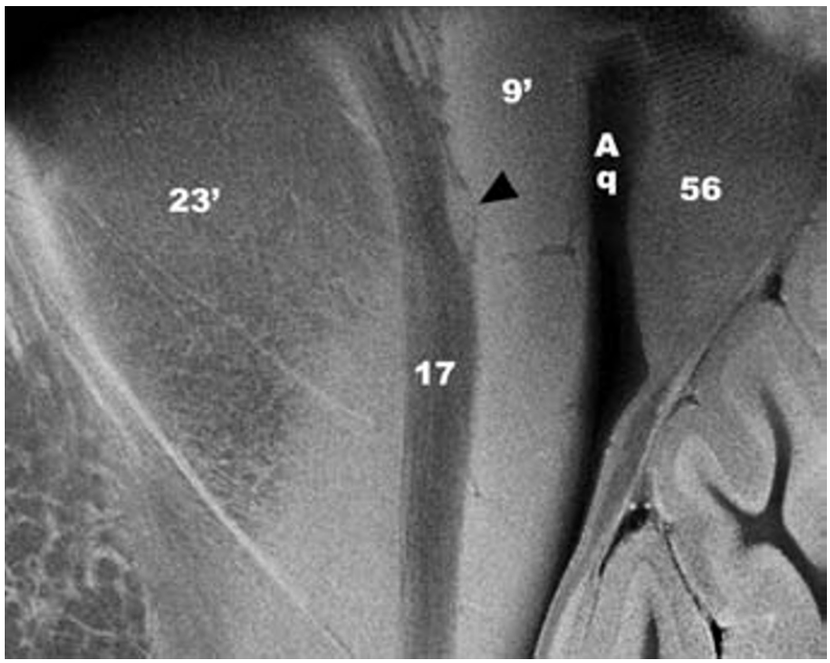

E

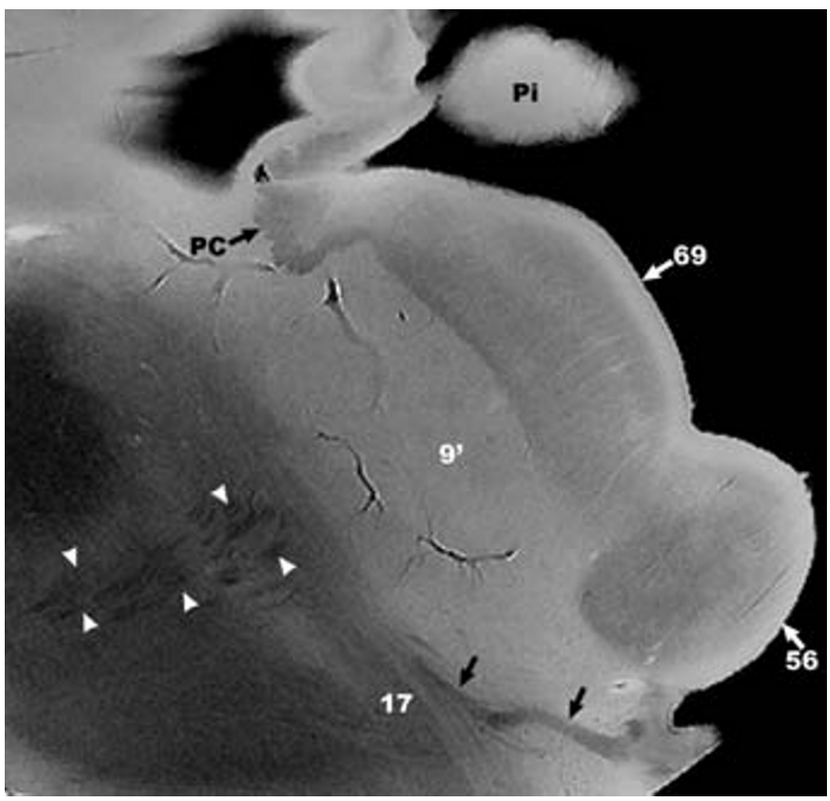

F

G

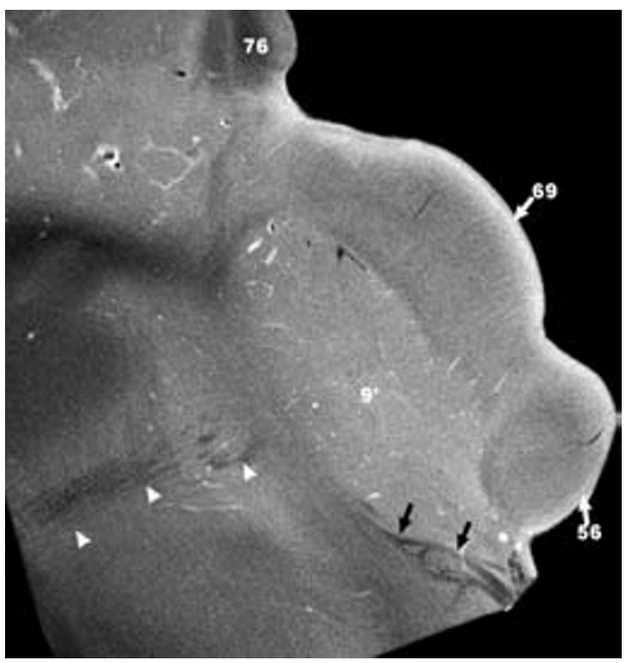

H

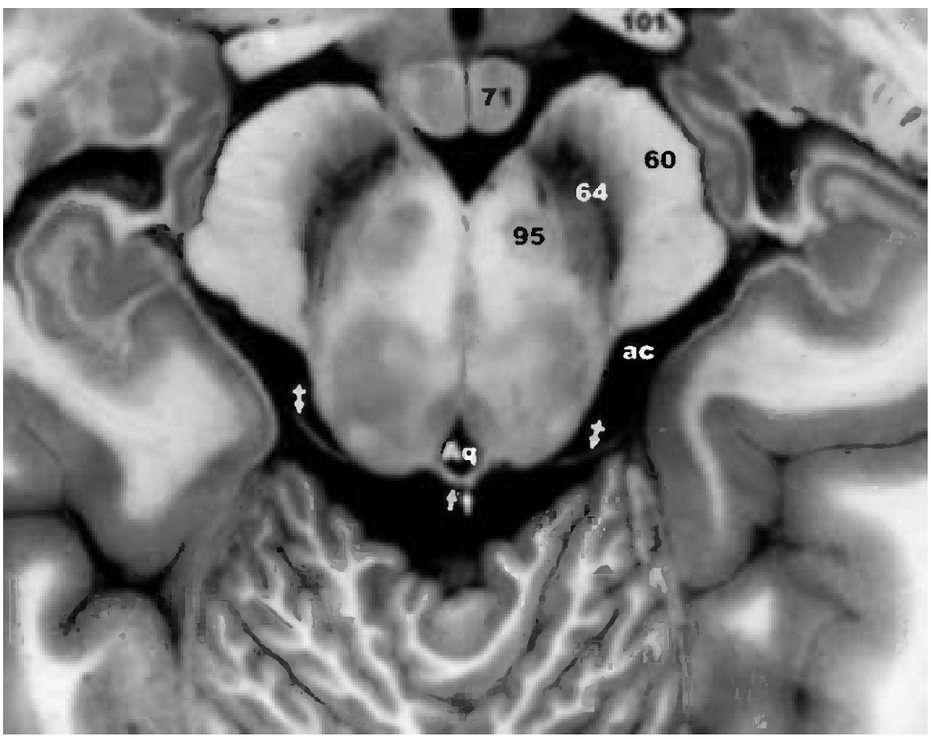

A

Fig. 9.15 (A–D). Cranial nerve IV: The trochlear nuclei, tracts, roots and nerves.
A. Anatomic axial section through the mesencephalon.
See also Fig. 11.24 C
B–D. MR cisternography in the axial **(B),** coronal **(C)** and sagittal **(D)** planes

23 Superior cerebellar peduncle
38 Middle cerebellar peduncle (brachium conjunctivum)
56 Inferior colliculus
60 Cerebral peduncle
64 Substantia nigra
71 Mammillary body
95 Red nucleus
101 Optic tract

Letter labels
4V Fourth ventricle
ac Ambient cistern
Aq Cerebral aqueduct (of Sylvius)
B Basilar artery

Arrowheads and arrows
Crossed arrows: Cisternal segments of the trochlear nerve (CN IV)
Paired white arrows: Decussation of the trochlear fascicles in the superior medullary velum of the fourth ventricle

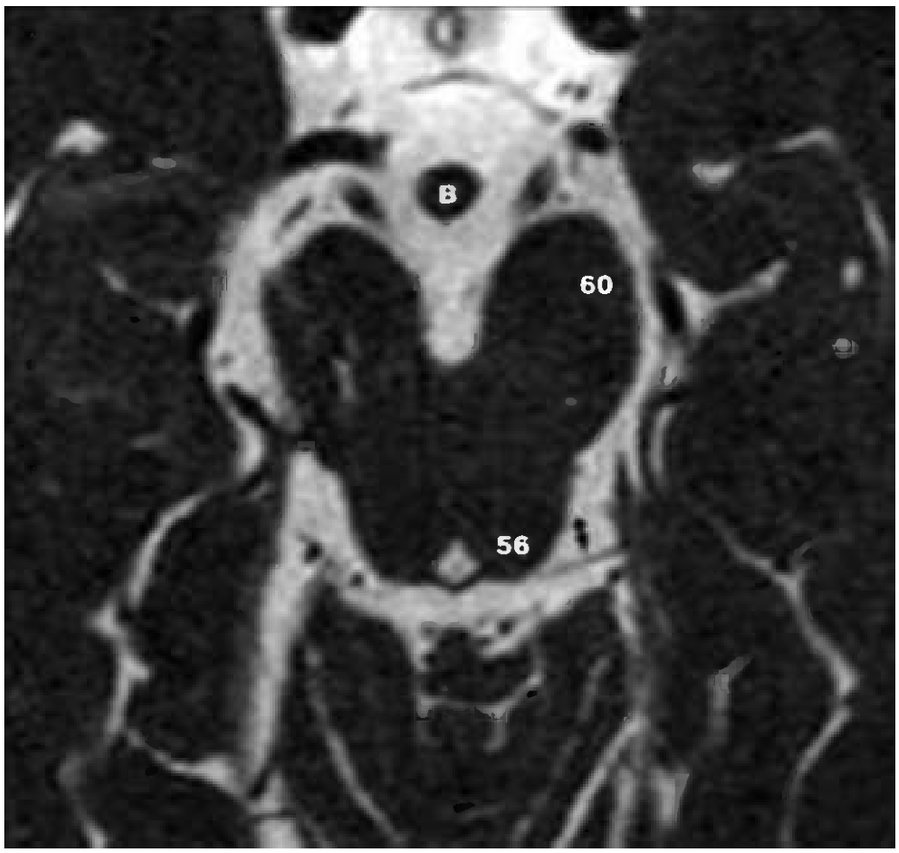

B

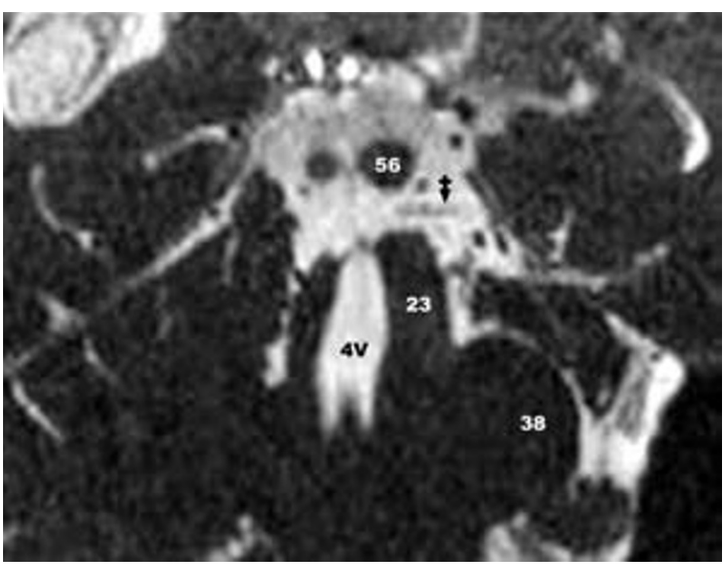

C

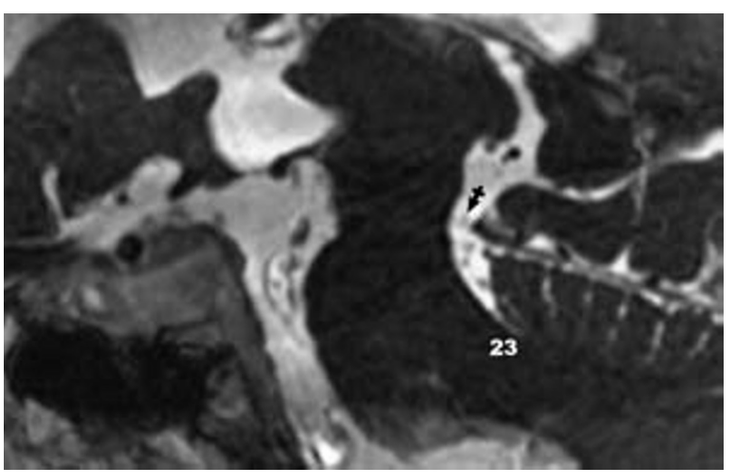

D

The oculomotor nerve. CN III.

GSE of CN III: Motor fibers of the oculomotor nerve for striated muscle arise from the oculomotor nucleus situated at the ventral aspect of the periaqueductal gray matter of the upper midbrain (superior collicular level). The medial longitudinal fasiculi lie immediately ventrolateral to the oculomotor nuclei. Within the oculomotor nuclei, lateral subnuclei supply, from dorsal to ventral, the ipsilateral inferior rectus, the inferior oblique, and the medial rectus muscle [43, 78, 260, 467, 487, 488]. Medial subnuclei supply the contralateral superior rectus. Central subnuclei at the caudal end of the oculomotor complex supply the levator palpebrae superioris bilaterally [467]. From the nucleus, the oculomotor fibers curve smoothly ventrally, first medially then laterally then medially again, through and medial to the red nuclei and the medial cerebral peduncles, to emerge into the interpeduncular fossa. Of all oculomotor subnuclei, only the subnucleus for the superior oblique muscle innervates the contralateral side. The other oculomotor fibers do not decussate.

GVE of CN III: Parasympathetic motor fibers to the viscera (pupillary and ciliary constrictors) arise from the nucleus of Edinger-Westphal situated dorsal to the anterior portion of the oculomotor nuclei. These parasympathetic fibers course with the oculomotor fibers to form the oculomotor nerve. The combined nerve then passes ventrolaterally through the interpeduncular fossa, travels between the posterior cerebral artery (superiorly) and the superior cerebellar artery (inferiorly), medial to the trochlear (IV) nerve, and pierces the dura to run in the lateral dural wall of the cavernous sinus, just superior to the trochlear nerve. The oculomotor fibers exit the skull through the superior orbital fissure within the annulus of Zinn (the common tendinous ring of the extra-ocular muscles) [467].

Structures that pass through the annulus of Zinn in the orbit are the superior and inferior divisions of the oculomotor nerve, nasociliary branch of the ophthalmic (V1) division of the trigeminal nerve, and the abducens nerve. Structures that pass outside the annulus of Zinn, near the roof of the orbit, are the lacrimal and frontal branches of the ophthalmic (V1) division of the trigeminal nerve, and the trochlear nerve.

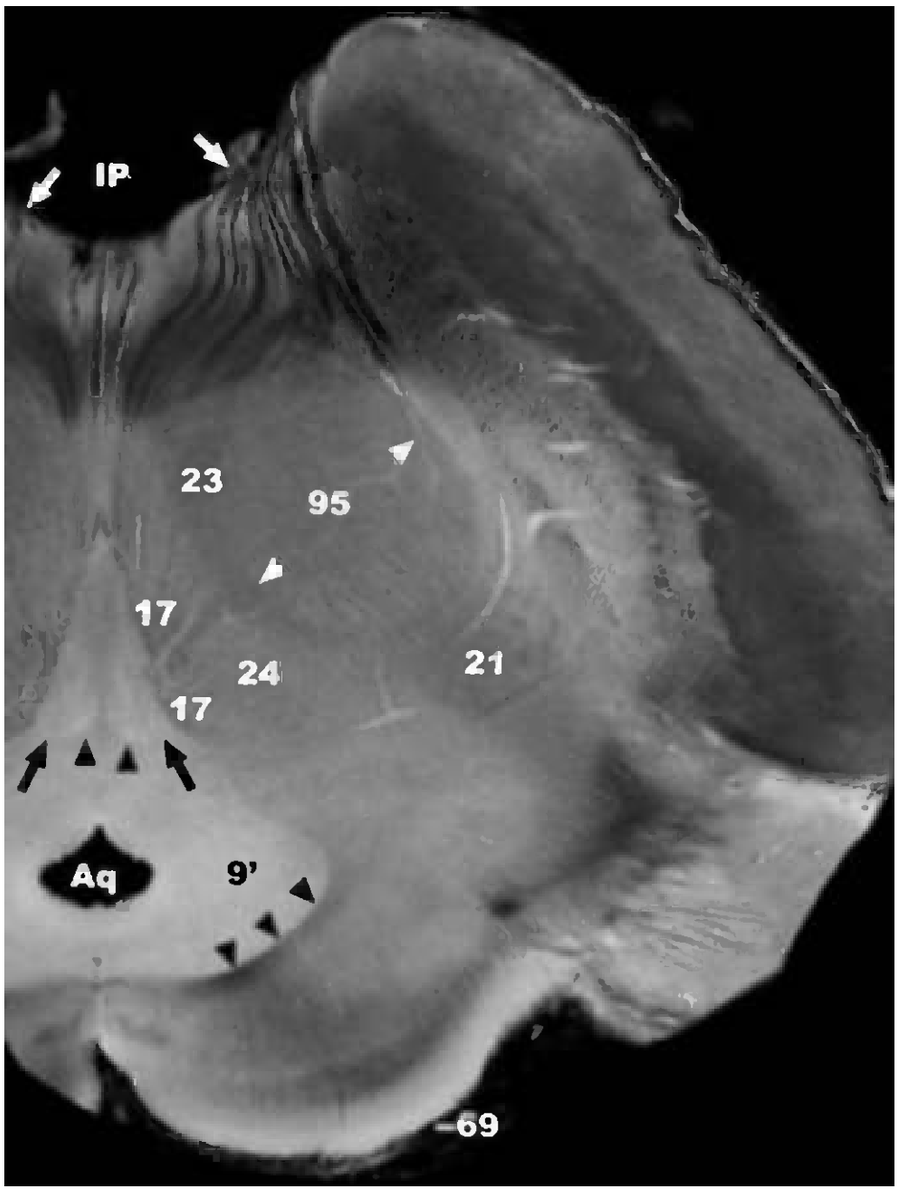

A

Fig. 9.16 (A–C). Cranial nerve III: The oculomotor nuclei, roots and nerves.
MR Microscopy displays the nuclei and intramedullary fibers of the oculomotor nerve in the axial **(A)** and sagittal **(B–C)** planes.

9′ Periaqueductal gray matter
17 Medial longitudinal fasciculus
20 Pontine nuclei
21 Medial lemniscus
23 Superior cerebellar peduncle
23c Cruciate portion of superior cerebellar peduncle
23′d Dorsal portion of decussation of the superior cerebellar peduncle
23′v Ventral portion of decussation of the superior cerebellar peduncle
24 Central tegmental tract
51 Pontocerebellar fibers
54′ Nucleus centralis superioris medialis (superior nucleus of the raphe)
56 Inferior colliculus
59 Nucleus of the trochlear nerve (CN IV)

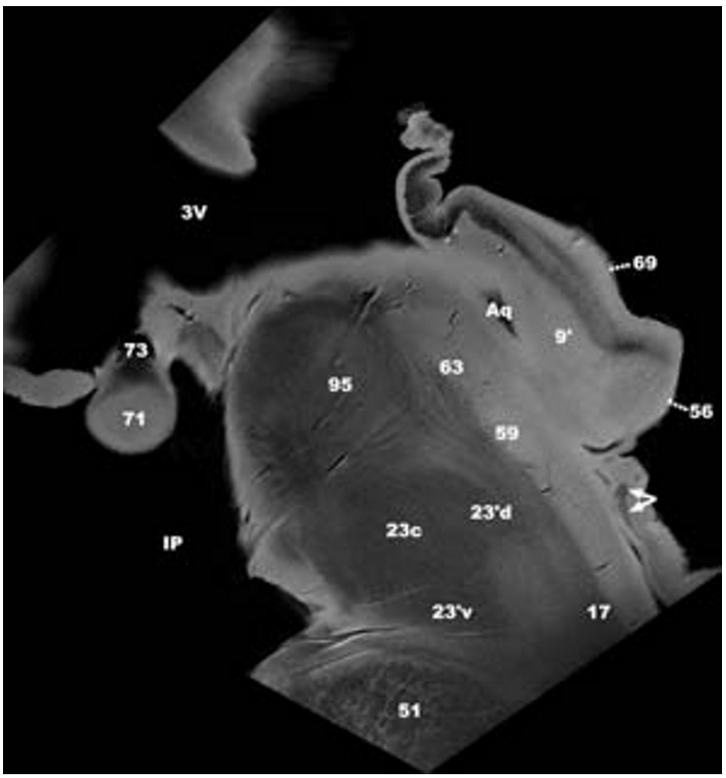

B

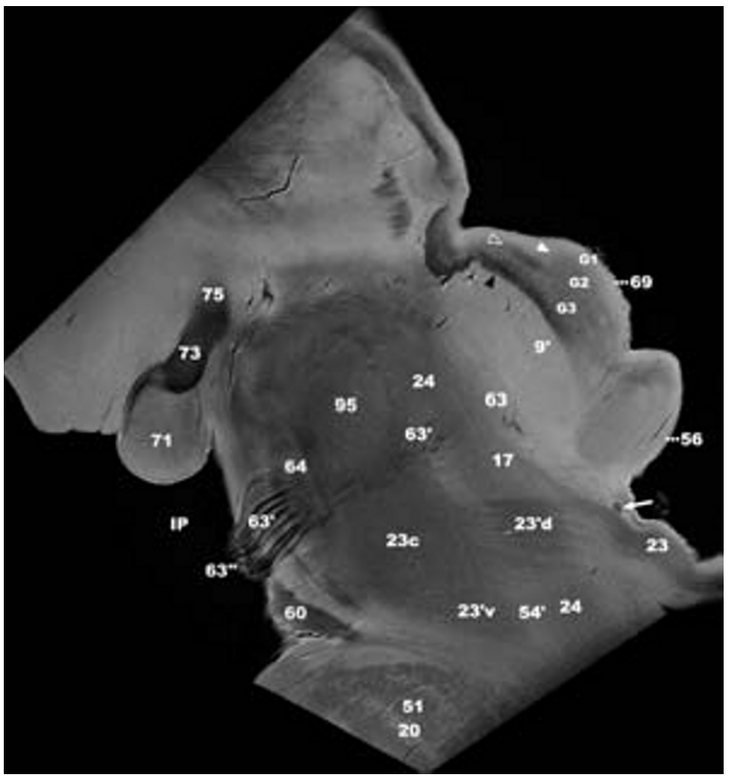

C

60 Cerebral peduncle
63 Oculomotor nucleus (CN III)
63′ Intramesencephalic fibers of the oculomotor nerve
63″ Fibers of the oculomotor nerve emerging into the interpeduncular fossa (IP)
64 Substantia nigra
69 Superior colliculus
71 Mammillary body
73 Principal mammillary fasciculus
95 Red nucleus within its capsule (white arrowheads)

Letter labels

3V Third ventricle
Aq Cerebral aqueduct (of Sylvius)
G1 Stratum griseum primum (superficiale). The faint thin black line at the superficial margin of G1 may be the stratum zonale.
G2 Stratum griseum secundum (medium)
G3 Stratum griseum tertium (profundum)
IP Interpeduncular fossa

Arrowheads and arrows

Single white arrowhead: Stratum opticum of the superior colliculus immediately dorsal to the dark horizontal band of the stratum lemniscale
Single open arrrowhead: Stratum lemniscale
Single black arrowhead: Decussation of superior colliculus
Paired white arrowheads: Capsule of the red nucleus (95)
Paired black arrowheads: Nuclei of Edinger-Westphal (parasympathetic)
Triple black arrowheads: Marginal fibers of the periaqueductal gray matter
Single white arrow: Fascicles of the trochlear nerve
Paired white arrows: Fascicles of the oculomotor nerves (CN III)
Two-headed white arrow: Trochlear nerve fascicles extending to their decussation
Paired black arrows: Oculomotor nuclei (CN III) of the two sides

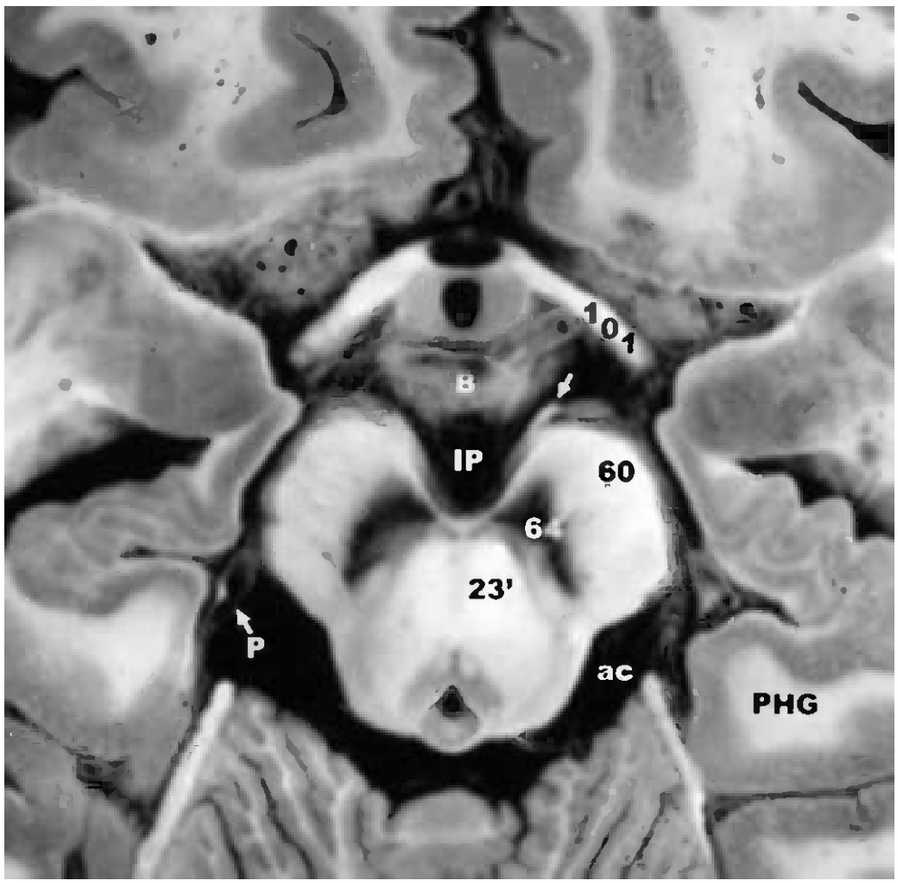

A

Fig. 9.17 (A–E). Cranial nerve III: The oculomotor nuclei, roots and nerves.

A–B. Anatomic sections through the mesencephalon and the oculomotor nerve in the axial plane **(A)** and the sagittal plane **(B).** See also **Figs.11.22 D and 11.67 D.**

C–E. 3T MR Cisternography of the oculomotor nerve in the axial (**C**), coronal (**D**) and oblique sagittal **(E)** planes.

16″ Corticospinal fibers descending through the pons toward the pyramid
21 Medial lemniscus
23 Superior cerebellar peduncle
23′ Decussation of the superior cerebellar peduncle
51 Pontocerebellar fibers
56 Inferior colliculus
60 Cerebral peduncle
63″ Oculomotor nerve (cisternal segment) (also single arrows)
64 Substantia nigra
69 Superior colliculus
71 Mammillary body
83 Nucleus dorsomedialis thalami
91 Centromedian nucleus of the thalamus
92 Pulvinar
95 Red nucleus within its capsule (white arrowheads)
101 Optic tract
173 Anterior commissure
223′ Ala of the central lobule of vermis
225′ Anterior quadrangular lobule
253 Splenium

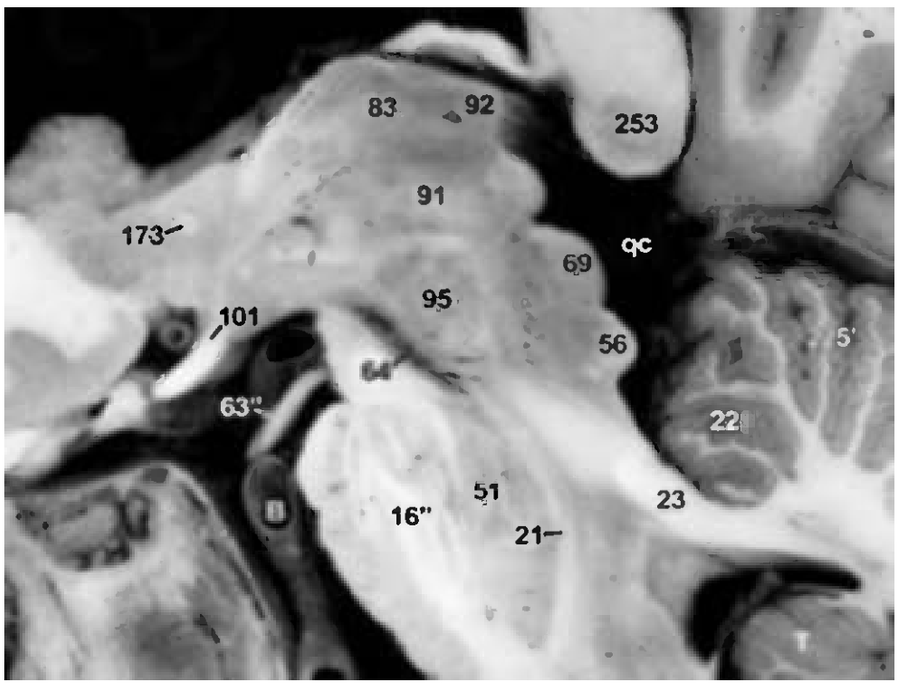

B

Letter labels

3V	Third ventricle
ac	Ambient cistern
qc	Quadrigeminal plate cistern
B	Basilar artery
IP	Interpeduncular cistern
P	Posterior cerebral artery (cisternal segnment)
PHG	Parahippocampal gyrus
Pons	Pons
S	Superior cerebellar artery
T	Tonsil
Un	Uncus

Arrowheads and arrows

Black and white arrows: Cisternal segments of the oculomotor nuclei (CN III) (Also 63″)

C

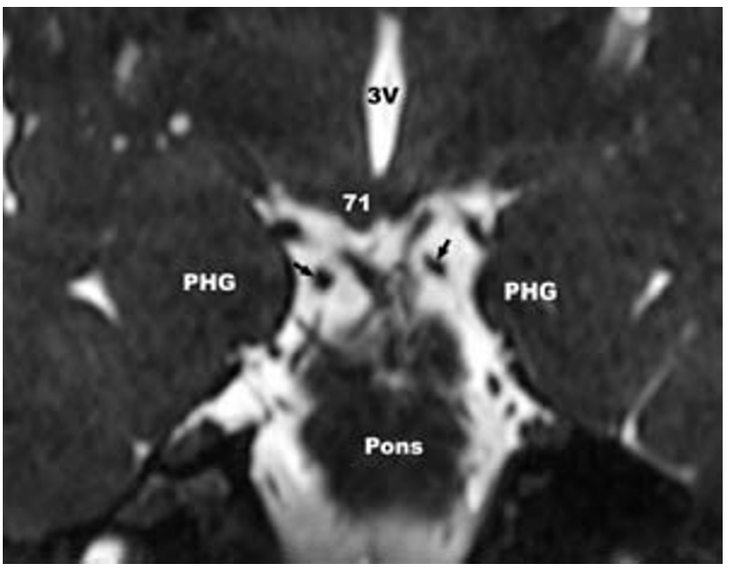

D

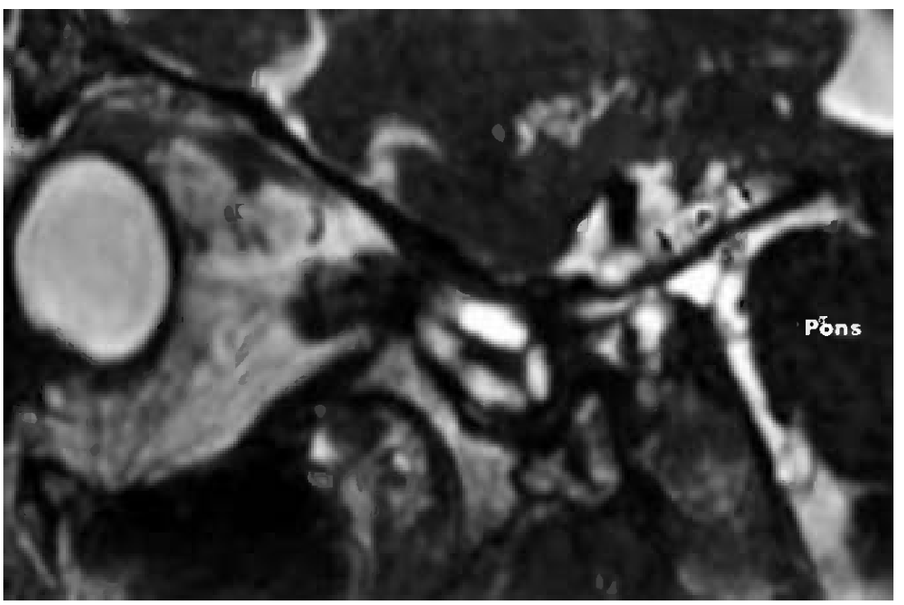

B

The brain tracts: The olfactory and optic "nerves". CN I and II

CN I. The primary sensory neurons of the olfactory nerve lie within the olfactory mucosa of the nasal fossa, medial to the superior nasal concha and just inferior to the cribriform plate of the ethmoid bone. The peripheral processes of these neurons are sensory receptors for odorants of specific shapes. The central processes of these neurons collect into approximately 12-20 bundles that traverse the cribriform plate to synapse with secondary neurons, such as mitral cells and tufted cells, in the olfactory bulb.

SVA of CN I: Secondary fibers carrying special sensory data on olfaction pass posteriorly from the olfactory bulb through the olfactory tract to a group of basal olfactory nuclei collectively designated the basal olfactory area. The basal olfactory nuclei include the anterior olfactory nucleus, the olfactory tubercle, the prepyriform cortex, and the cortical nucleus of the amygdala. The anterior olfactory nucleus is formed by a dispersed group of cells within the posterior portion of the olfactory bulb, the olfactory tract and the proximal olfactory trigone. The olfactory tubercle (in man) is a thin sheet of gray matter in the region of the anterior perforated substance. The prepyriform cortex is composed of (i) the gray matter overlying the lateral olfactory stria (also called the lateral olfactory gyrus) and (ii) superficial gray matter extending medially from the limen insulae to the anteromedial surface of the temporal lobe. The superficial cortical nucleus of the amygdala lies just posterior to the prepyriform cortex. Although the posterior end of the olfactory tract trifurcates into the medial, intermediate and lateral olfactory striae, according to Nieuwenhuys no secondary olfactory fibers enter the medial olfactory stria [322]. Instead, the secondary olfactory data pass via the intermediate stria to the olfactory tubercle and via the lateral olfactory stria to the other basal olfactory nuclei [322].

CN II. The retina has three zones: outer, intermediate and inner. The primary visual neurons are bipolar cells that lie within the intermediate zone of the retina. Photoreceptor cells (rods and cones) in the outer (superficial) zone of the retina, superficial to the bipolar cells, pass visual sensory data to the bipolar cells. Short axons of the bipolar cells pass to the inner zone of the retina and terminate there on large ganglion cells. Unmyelinated axons of the ganglion cells pass to the optic disc at the posterior pole of the globe, perforate the sclera, become myelinated posterior to the sclera, and then constitute the "optic nerve". The optic nerve traverses the orbit.

Secondary fibers carrying special sensory data on vision (SSA) pass posteromedially, exit the ocular globe at the nerve head (papilla), and continue posteriorly as the intra-orbital, intracanalicular and intracranial segments of the optic nerves. The paired intracranial segments of the optic nerves interweave at the optic chiasm, such that nasal fibers of each globe cross the midline to the opposite optic tracts, while temporal fibers continue on into the ipsilateral optic tracts without decussating. A small number of crossing fibers extend anteriorly into the posterior end of the contralateral optic nerve (von Willebrand's knee) before recurving posteriorly into the optic chiasm and tract. The optic tracts also contain macular fibers from both ocular globes. The fibers in the optic tracts course posteriorly, curve around the cerebral peduncles, and enter the lateral geniculate bodies. There, decussated nasal fibers pass to geniculate layers 1,4 and 6, while undecussated temporal fibers pass to geniculate layers 2, 3 and 5. From the lateral geniculate bodies, the geniculocalcarine (optic) radiations carry data to the calcarine cortex. A limited number of fibers leave the optic tract, bypass the geniculate bodies, and pass directly to the pretectal area. These fibers travel through the brachium of the superior colliculus to the pretectal area, and partially cross the midline via the posterior commissure to reach the central oculomotor nucleus bilaterally. Connections to the parasympathetic fibers via the Edinger-Westphal nucleus then complete the pupillary light reflex [467].

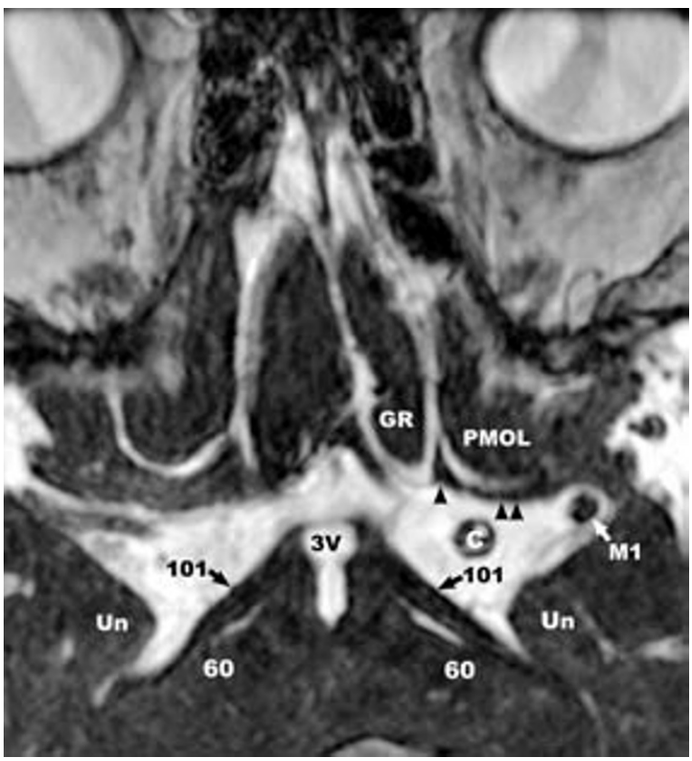

A

Fig. 9.18. (A–E). The olfactory nerve and optic nerves (CN I and II).
A–D, MR Cisternography of CN I and II in the axial (**A–B**), coronal (**C**) and oblique sagittal (**D–E**) planes.

See also: MR Microscopy **Figs. 7.123–7.126 and 7.130–7.134**, and Anatomic head sections **Figs. 11.17–11.26**, **Figs. 11.30–11.41, and Figs. 11.69–11.70D.**

60 Cerebral peduncle
71 Mammillary body
101 Optic tract
139 Cistern of the lamina terminalis

Letter labels

I Cranial nerve I (Olfactory nerve), labeled on the olfactory bulb
II Cranial nerve II (Optic nerve), labeled on the optic chiasm
3V Third ventricle (labeled within the supra-optic recess (so) in A.)
so Supra-optic recess of the third ventricle (3V)
C Internal carotid artery, supraclinoid segment
GR Gyrus rectus
M1 Horizontal segment of the middle cerebral artery
PMOL Posteromedial orbital lobule, a prominence formed by the confluence of the medial orbital gyrus with the posterior orbital gyrus
Un Uncus

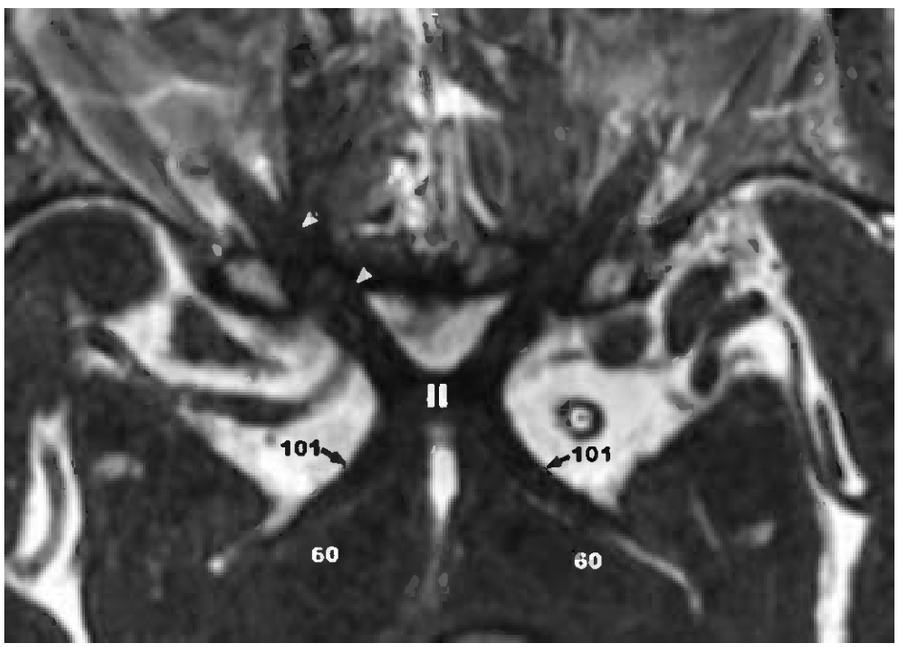

B

Arrowheads and arrows

Multiple white arrowheads: The intraorbital optic nerve (most anterior of the three arrowheads) passes posteriorly through the optic canal (posterior two arrowheads) to become the cisternal segment of the optic nerve, which then merges into the chiasm (II)

Single black arrowhead: Bifurcation of the olfactory tract into medial and lateral stria

Paired black arrowheads: Lateral olfactory stria

Single black arrow: Hypophyseal stalk

White arrows bilaterally: Lateral walls of Meckel's caves, filled with cerebrospinal fluid and the fascicles of the trigeminal nerve

Five white arrows: Oblique sagittal view of the optic nerve: orbital segment (anterior two arrows), intracanalicular segment (middle two arrows) and intracranial segment (single posterior arrow) (**Fig. 9.18E**)

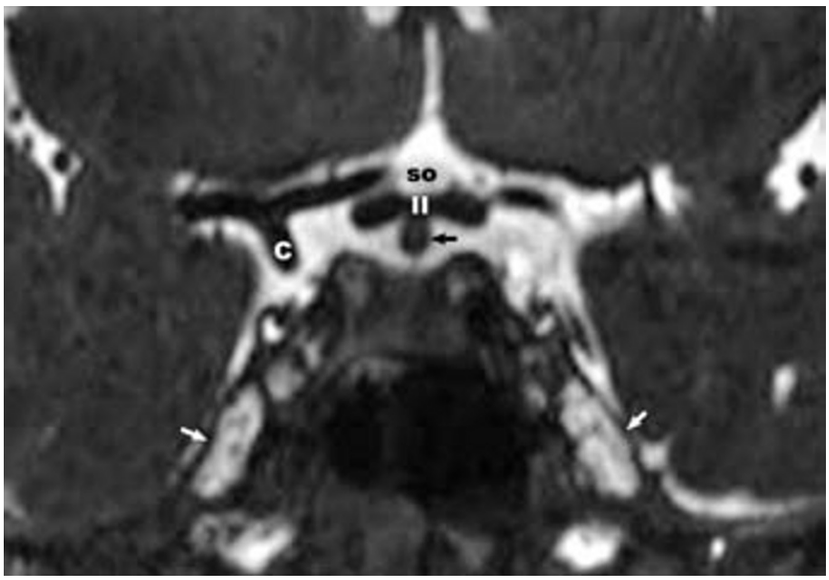

C

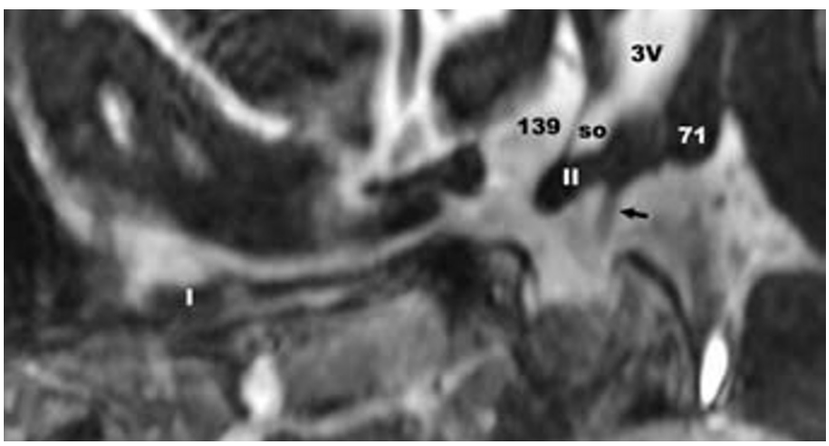

D

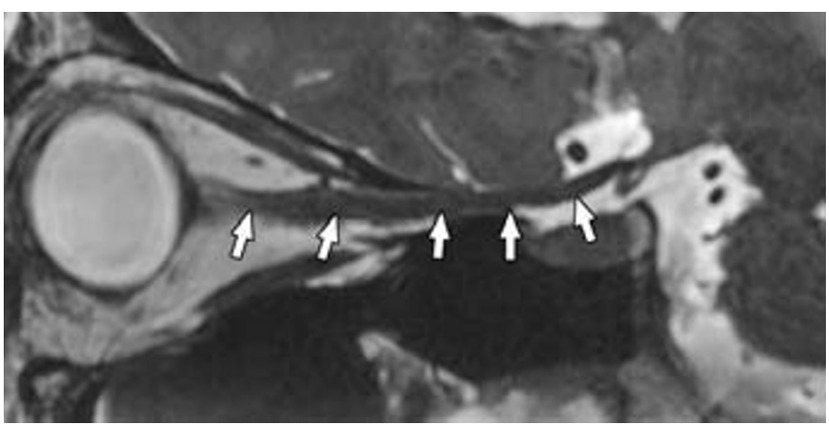

E

SECTION X (A–D)

ADVANCED STRUCTURAL MRI

Technological advances now permit display of anatomic structures and relationships not demonstrable before. These include imaging of neuromelanin, imaging of brain iron, noncontrast angiography of the veins of the parenchyma, and diffusion tensor mapping of fiber tract orientation and trajectory.

A. Imaging Neuromelanin (Figs. 10.1–10.3.)

Eri Shibata and Makoto Sasaki

Neuromelanin forms as a byproduct of the synthesis of monoamine neurotransmitters such as noradrenalin and dopamine. The distribution of neuromelanin, therefore, conforms to the distribution of dopaminergic neurons within the substantia nigra (pars compacta) of the midbrain and the noradrenergic neurons within the locus ceruleus of the pontomesencephalic junction. Neuromelanin appears dark (black) on gross anatomic specimens. On T1-weighted MRI, neuromelanin can become paramagnetic when associated with metals such as copper or iron. Highly paramagnetic substances shorten T1 recovery time, yielding bright white signal [373, 394].

Technique: Neuromelanin is displayed well by MR imaging at 3 Tesla using a T1-weighted fast spin echo pulse sequence: Repetition time: 600 ms, Echo time: 14 ms, Echo train length: 2, Field of view; 220 mm, Matrix size: 512 x 320, Slice thickness: 2.5 mm, Interslice gap: 1 mm , and Number of averages: 8 for an acquisition time of 12 minutes [373, 394]. The resultant in-plane resolution is 0.31 x 0.36 mm. These images demonstrate the locus ceruleus and substantia nigra pars compacta.

Locus ceruleus

The position and contour of the locus ceruleus are marked by the dark coloration of neuromelanin in the gross images and the bright signal intensity on the T1-weighted MRI.

A

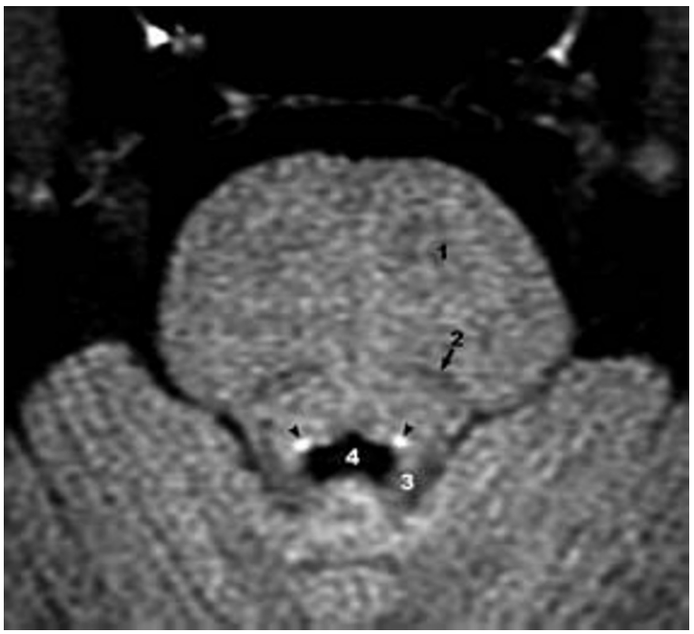

D

Fig. 10.1 (A–F). Locus ceruleus. High pons and pontomesencephalic junction.
A–C. Gross anatomic specimens in axial **(A),** coronal **(B)** and sagittal **(C)** planes.
D–F. Corresponding 3T T1-weighted MRI in axial **(D),** coronal **(E)** and sagittal **(F)** planes.
See also **Figs. 11.19D** (axial), **11.44D** (coronal) and **11.69A** (sagittal) sections.

1 Pons
2 Medial lemniscus
3 Superior cerebellar peduncle and its decussation
4 Fourth ventricle
5 Superior colliculus
6 Inferior colliculus
7 Cerebral aqueduct (of Sylvius)
8 Abducens nucleus (CN VI)
9 Red nucleus
10 Periaqueductal gray matter
11 Central tegmental tract

Arrowheads and arrows
arrowheads: Locus ceruleus
arrow: Substantia nigra, pars compacta

B

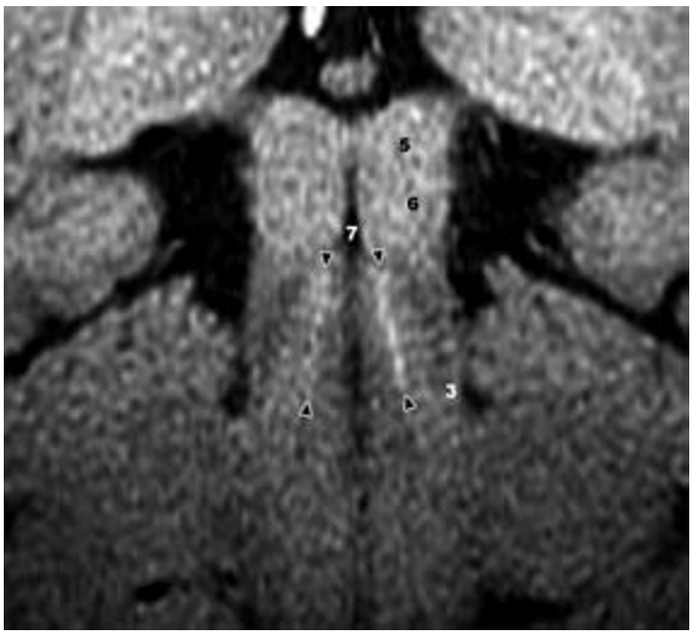

E

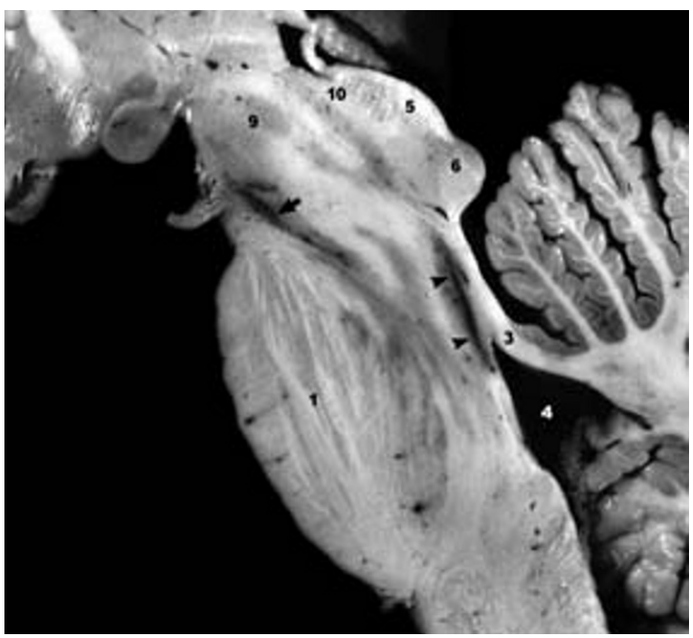

C

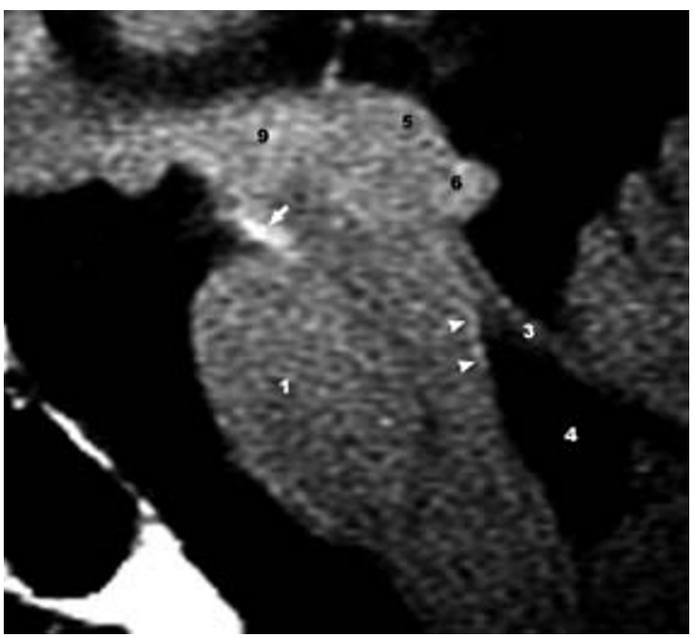

F

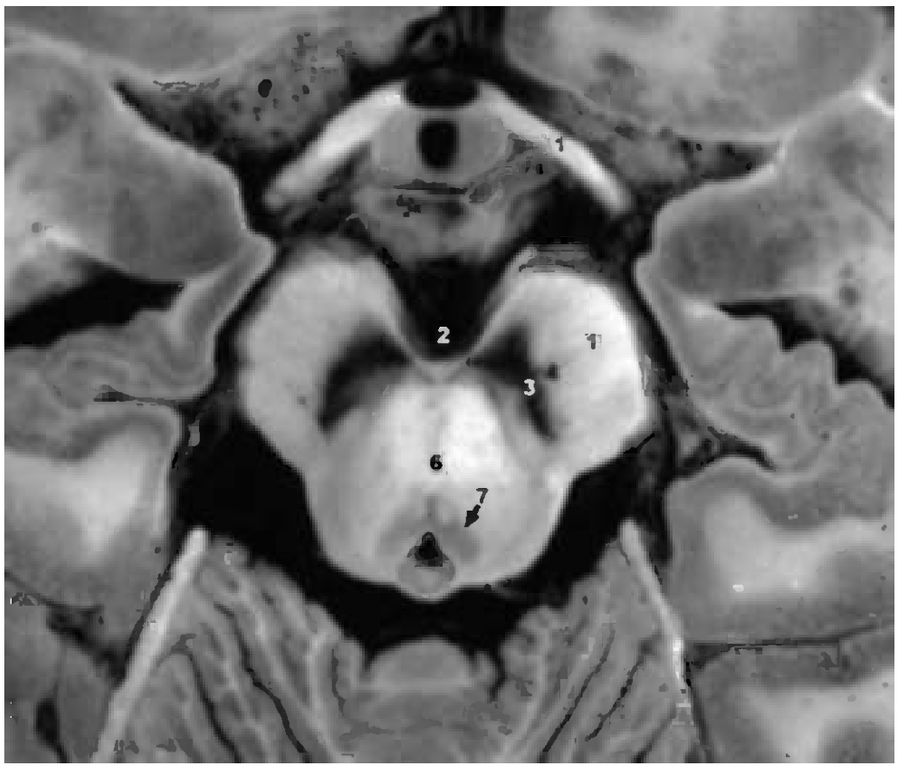

A

Fig. 10.2 (A–D). Substantia nigra, pars compacta. Mesencephalon. Axial sections.

A–B. Gross anatomic axial sections at more caudal **(A)** and cranial **(B)** levels.
C–D. Corresponding 3T T1-weighted images. See also **Figs. 11.22D and 11.24C**.
The position and configuration of the substantia nigra pars compacta are marked by the dark coloration of neuromelanin in the gross images and the bright signal intensity on the T1-weighted MRI.

1 Crus cerebri
2 Interpeduncular fossa
3 Substantia nigra, pars compacta
4 Substantia nigra, pars reticulata
6 Decussation of the superior cerebellar peduncle
7 Periqueductal gray matter
8 Cerebral aqueduct (of Sylvius)
9 Red nucleus
10 Mammillary bodies
11 Optic tracts

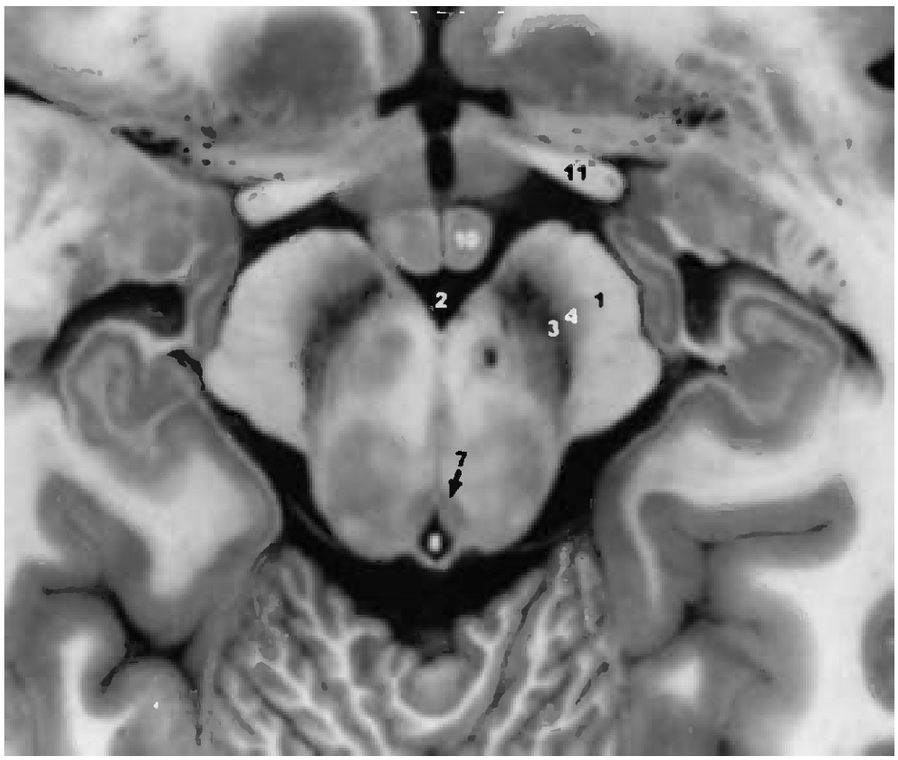

B

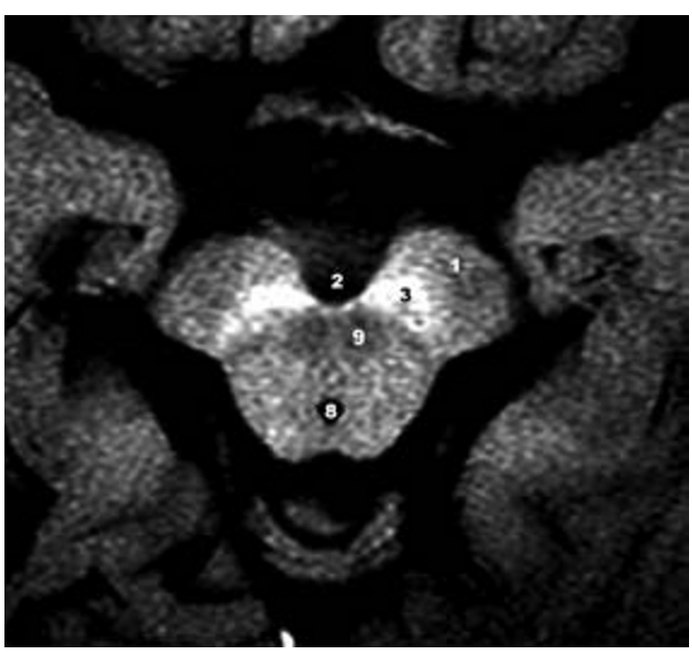

C

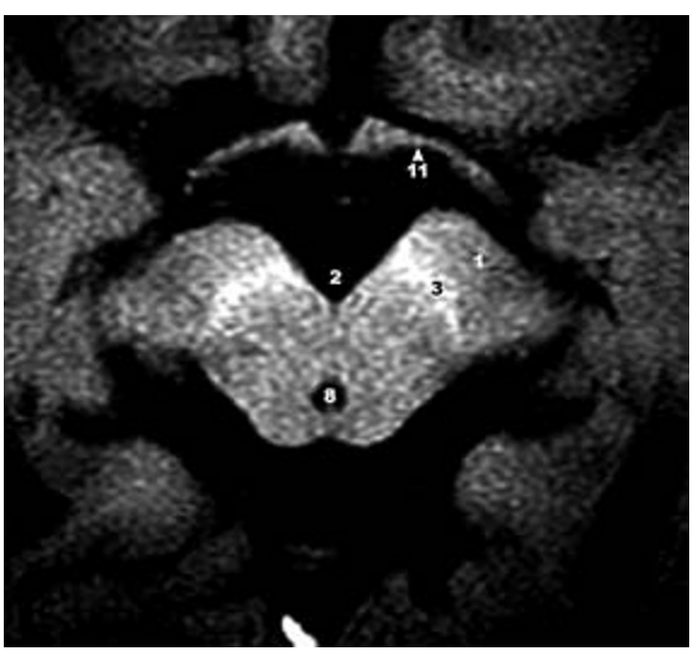

D

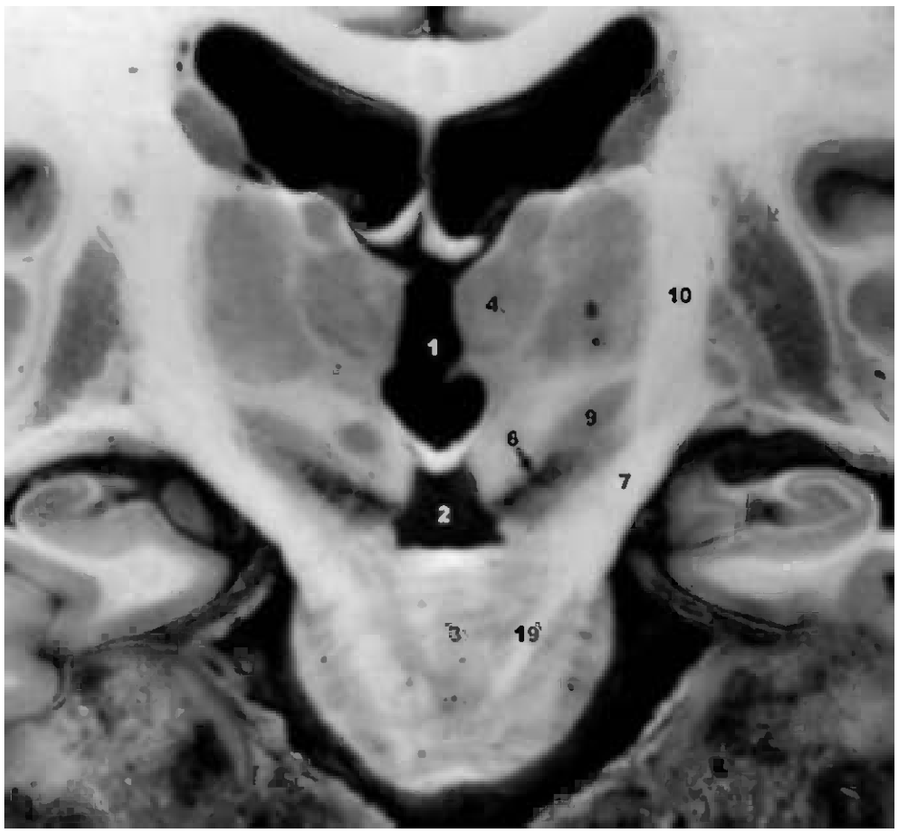

A

Fig. 10.3 (A–D). Substantia nigra, pars compacta. Mesencephalon.

A–B. Gross anatomic specimens in the coronal **(A)** and sagittal **(B)** planes.
C–D. Corresponding 3T T1-weighted MRI.
See also **Figs. 11.38C** (coronal) and **11.67D** (sagittal) sections

The position and contour of the substantia nigra are marked by the dark coloration of neuromelanin in the gross images and the bright signal intensity on the T1-weighted MRI.

1 Third ventricle
2 Interpeduncular fossa
3 Pons, basilar portion, pontine nuclei
4 Dorsomedial thalamic nuclei
5 Red nucleus
6 Substantia nigra, pars compacta
7 Crus cerebri and corticospinal tract
8 Ventral lateral thalamic nucleus
9 Subthalamic nucleus
10 Internal capsule, posterior limb
11 Pulvinar
12 Superior colliculus
13 Inferior colliculus
14 Superior cerebellar peduncle
15 Medial lemniscus
16 Optic chiasm
17 Oculomotor nerve (CN III)
19 Pons, basilar portion, corticospinal tract

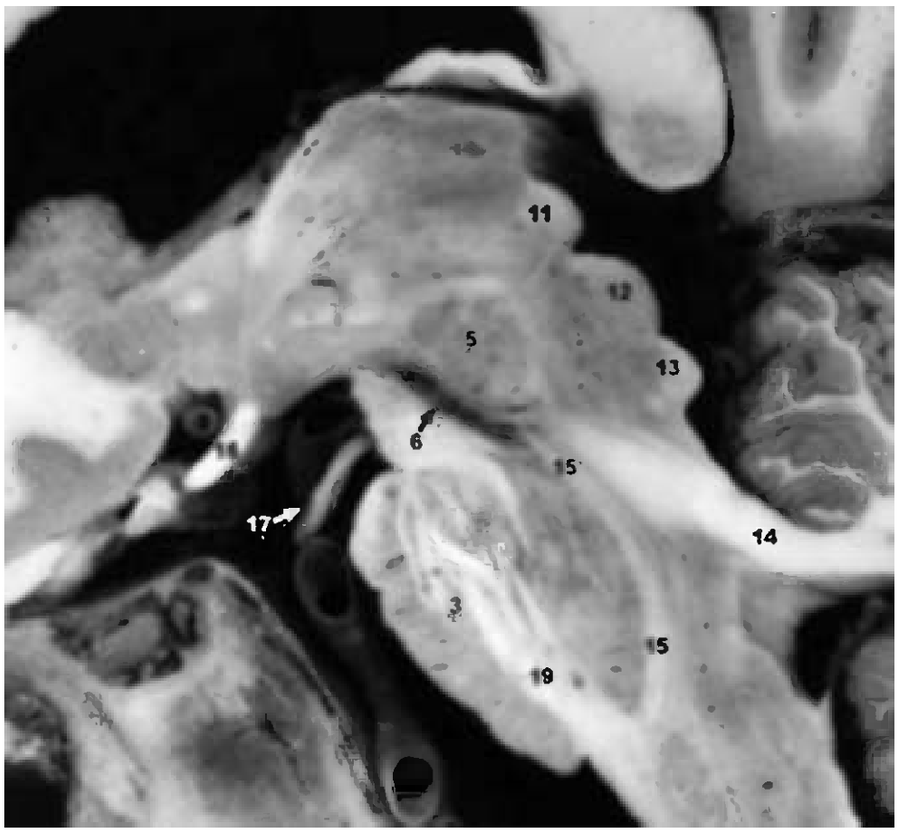

B

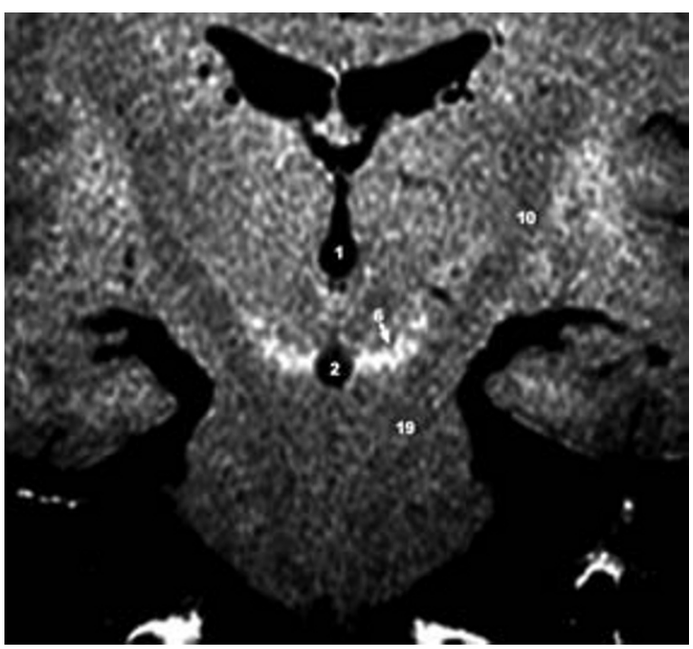

C

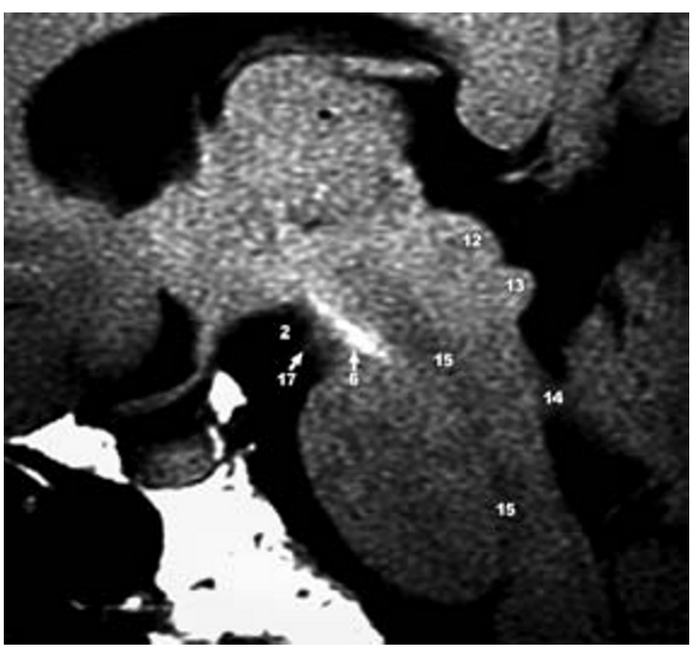

D

B. Susceptibility Weighted Imaging (SWI) (Figs. 10.4–10.14)

E. Mark Haacke and Elena Manova

The term susceptibility signifies the tendency for a substance to become magnetic when placed within a static magnetic field. Different brain tissues exhibit differing degrees of susceptibility. Ferric iron deposited in the basal ganglia and the desaturated hemoglobin (deoxyhemoglobin) within venous blood both show paramagnetic susceptibility. This means that they cause the local magnetic field in the vicinity of this tissue to be larger than the surrounding field [57, 58, 112, 115, 180, 189, 380]. Non-heme-related ferritin associated with blood vessels of the gray matter and white matter similarly shows paramagnetic susceptibility [222, 374, 402].

When placed within the magnetic field of the scanner, these naturally-occurring substances become magnetic, cause local inhomogeneities in the magnetic field, and modify the precise gradation of the magnetic field by which the position, intensity and phase of the MR signal are determined for each voxel. The signal from these substances becomes exaggerated by virtue of their magnetic susceptibility, so these substances become detectable by MRI. This effect is greater in gray matter than white matter, because gray matter has a higher capillary density [94–96, 97, 116, 264]. The effect is also greater at high magnetic fields, so susceptiblity changes become increasingly evident on high-field MR systems. [49, 64, 83, 104, 136, 137, 325, 380]

Susceptibility-weighted imaging (SWI) is an MR technique that exploits tissue differences in magnetic susceptibility to enhance the difference between adjacent tissues and thereby produce images of the tissue. The resultant images display a "pseudo-susceptibility map" of a section of the brain. This map depicts variations in the degree of iron deposition within the brain and the venous anatomy of the brain.

Technically, susceptibility weighted images may be presented in at least four different ways:

1. Use the original magnitude image without any processing.
2. "High-pass filter" the original phase image to create an SWI high-pass filtered image [177]. These images are labeled *"single slice high-pass filtered phase images"*.
3. Take the high-pass filtered phase image and modify the phase at each pixel as follows: Map all pixels with a phase from -180^{o} to 0^{o} into a number between zero and unity and all phases greater than zero to unity. These modified data are referred to as the phase mask. The original magnitude image is then multiplied by the phase mask to the fourth power (or the eighth power). This new image is referred to as the SWI magnitude image [355] and is labeled "SWI magnitude image (multiplied by the phase mask to the 4th/8th power)" (e.g., SWI x phase mask 4).
4. A series of these images can be further processed by taking the minimum intensity pixels in each of, for example, five slices (that is, the section of interest plus two sections above and two sections below that section). Projecting the minimum intensities of all those images onto the slice of interest creates a minimum-intensity pixel projection across those 5 slices. These images are labeled "five-slice minimum intensity projection SWI image". Such images are most useful for highlighting the continuity of the veins about the slice of interest.

At present, the high pass filtered phase images do not completely remove all aliasing, so there are signal drop out artifacts near air/tissue interfaces. Sometimes these artifacts are clearly recognizable, for example at the superior petrosal sinus (SPS) in **Fig. 10.9**. At other times, the artifacts influence the image in less easily appreciable ways.

Technique: The images shown here were obtained with a 3-dimensional flow-compensated gradient recalled echo (GRE) sequence using the following pulse sequence parameters: repetition time (TR): 29 ms; echo time (TE): 15 ms; flip angle: 12^{o}; field of view: 256 mm x 256 mm; matrix size: 512 x 512; and slice thickness: 2.0 mm; for an acquisition time of 12.5 minutes. The resultant voxel size is 0.5 mm x 0.5 mm (in-plane) x 2 mm (thickness).

The susceptibility images were correlated with 3 Tesla anatomic images of a whole, formalin-fixed cadaver brain [101, 188, 200, 203, 205, 206–208, 209, 225, 239, 309–313, 360]. The venous system was identified in accord with prior angiographic experience and references [54, 75, 76, 165, 166, 178, 185, 203–210, 225, 231, 239, 241, 242, 318, 319, 362, 363, 369, 403, 417, 418, 422, 436, 451, 452, 468–472].

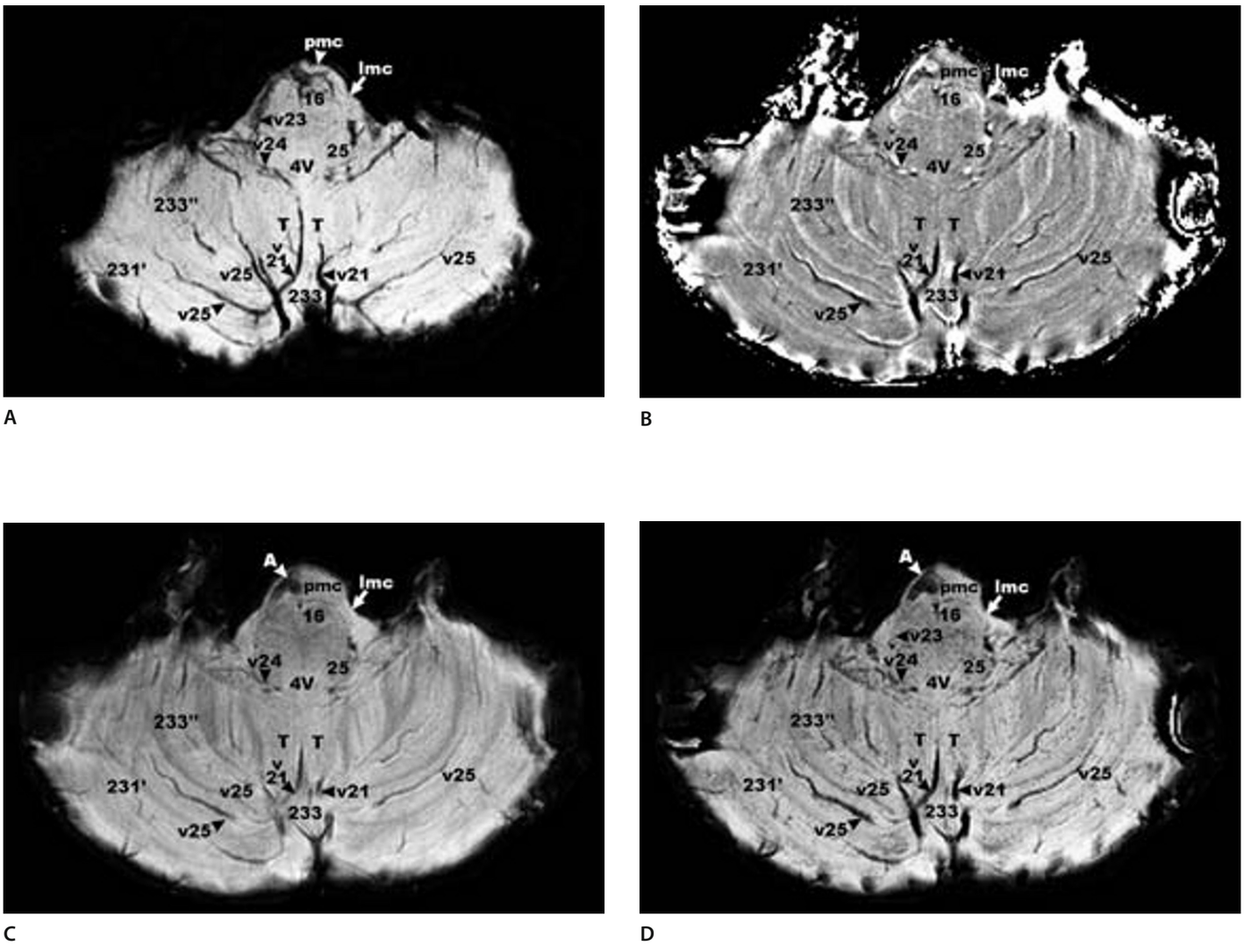

Fig. 10.4 (A–D). Low medulla and low cerebellum. Axial SWI.
A. Minimum intensity pixel projection from 5 sequential SWI images
B. Single slice high-pass filtered phase image
C. Single slice original magnitude image
D. SWI magnitude image (phase mask[8])

16 Pyramid containing the corticospinal tract
25 Inferior cerebellar peduncle (restiform body)
231′ Inferior semilunar lobule (Crus II)
233 Pyramis of the vermis (pyramid of the vermis)
233″ Biventral lobule

Letter labels
4V Fourth ventricle
lmc Lateral medullary cistern
pmc Premedullary cistern
A Vertebral artery
T Tonsil

Veins
v21 Inferior vermian vein
v23 Lateral medullary vein
v24 Vein of the inferior cerebellar peduncle
v25 Inferior hemispheric vein (of cerebellum)

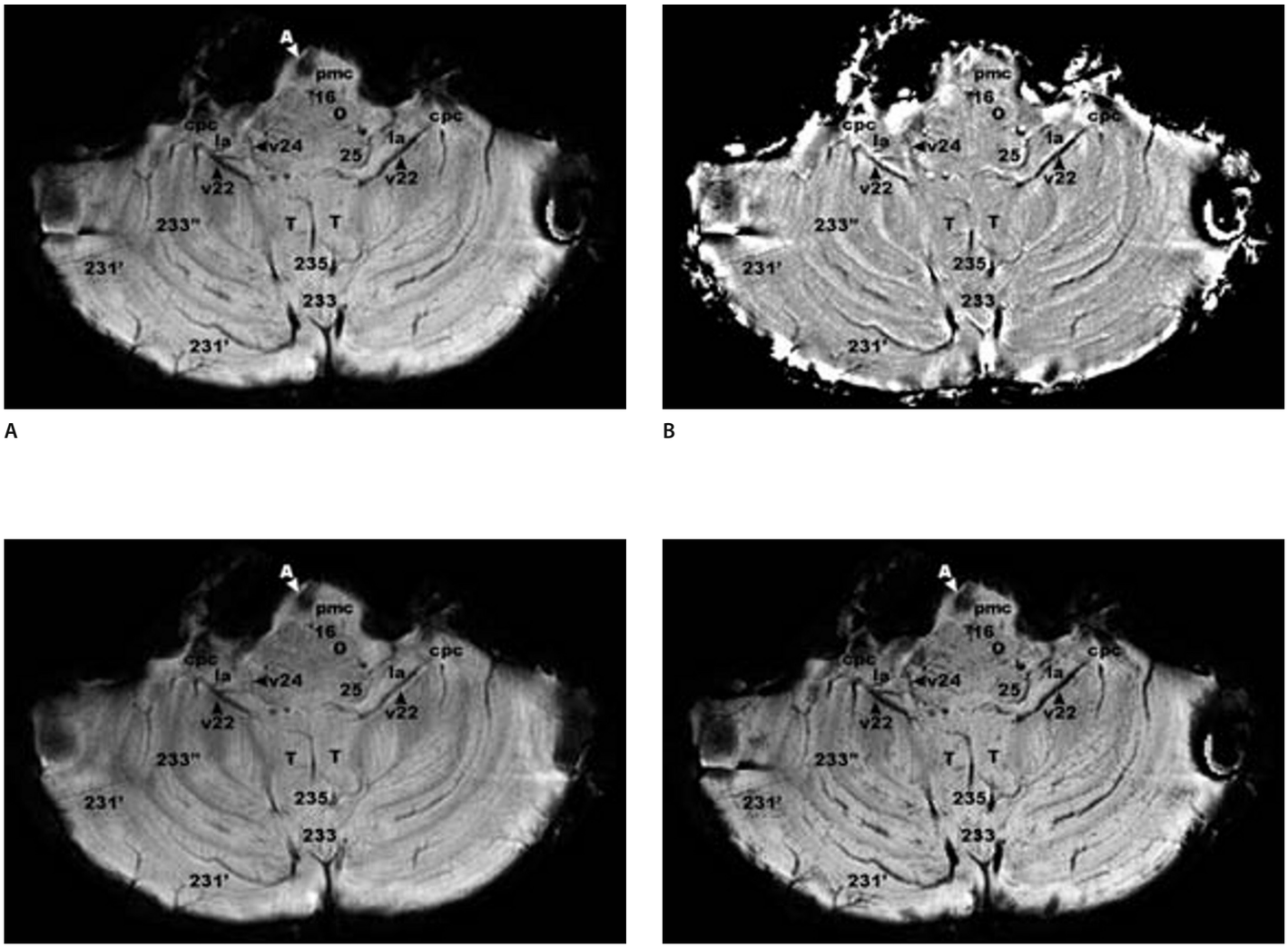

Fig. 10.5 (A–D). Mid medulla and low cerebellum. Axial SWI.
A. Single slice original magnitude image
B. Single slice high-pass filtered phase image
C. SWI magnitude image (phase mask[4])
D. SWI magnitude image (phase mask[8])

16 Pyramid containing the corticospinal tract
25 Inferior cerebellar peduncle (restiform body)
231′ Inferior semilunar lobule (Crus II)
233 Pyramis of the vermis (pyramid of the vermis)
233″ Biventral lobule
235 Uvula of the vermis

Letter labels
cpc Cerebellopontine angle cistern
la Lateral aperture of the fourth venticle (foramen of Luschka)
pmc Premedullary cistern
A Vertebral artery
O Inferior olivary nucleus
T Tonsil

Veins
v22 Vein of the lateral recess
v24 Vein of the inferior cerebellar peduncle

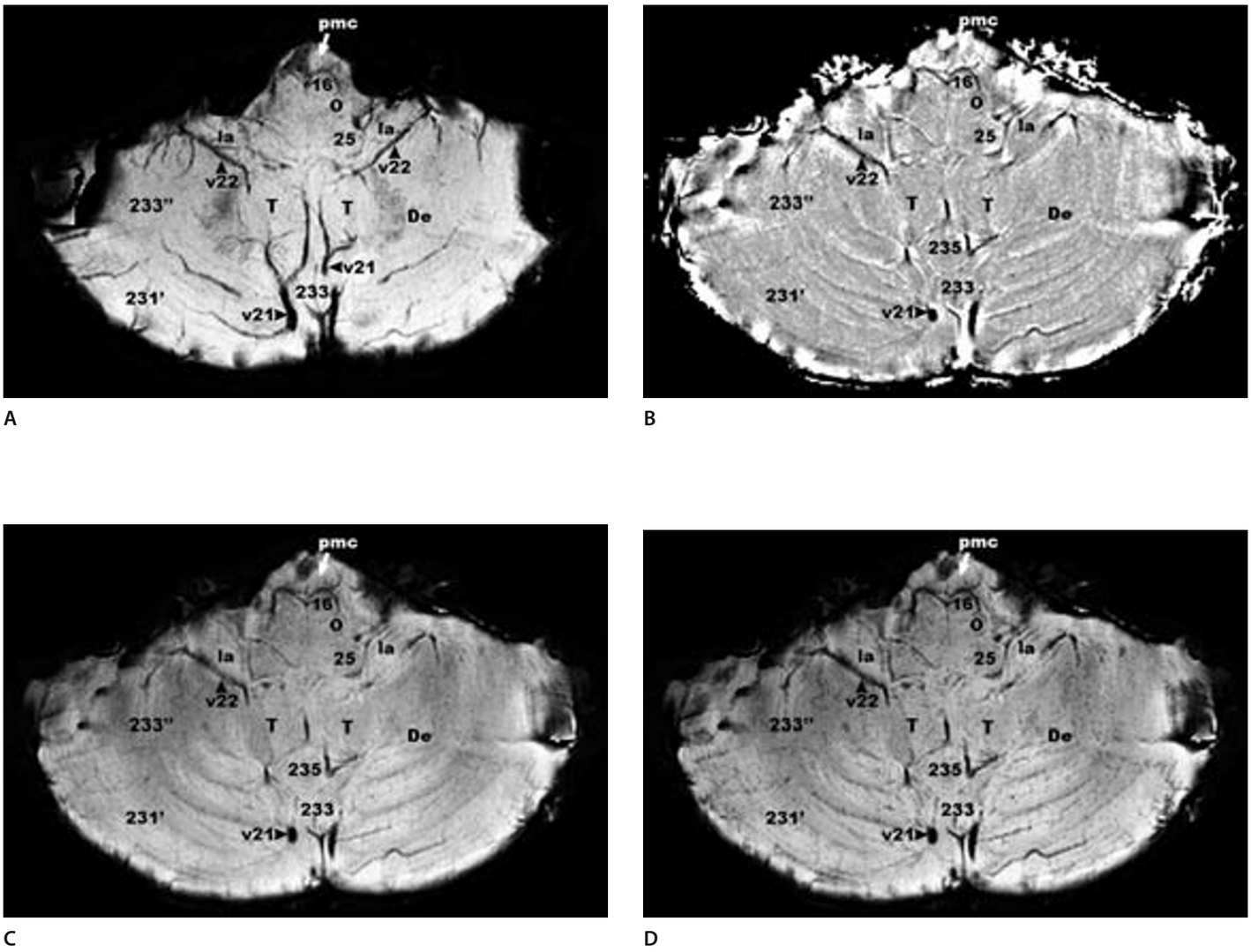

Fig. 10.6 (A–D). **High medulla and low-mid cerebellum. Axial SWI.**
A. Minimum intensity pixel projection from 5 sequential SWI
B. Single slice high-pass filtered phase image
C. SWI magnitude image (phase mask[4])
D. SWI magnitude image (phase mask[8])

16 Pyramid containing the corticospinal tract
25 Inferior cerebellar peduncle (restiform body)
231′ Inferior semilunar lobule (Crus II)
233 Pyramis of the vermis (pyramid of the vermis)
233″ Biventral lobule
235 Uvula of the vermis

Letter labels
la Lateral aperture of the fourth ventricle (foramen of Luschka)
pmc Premedullary cistern
De Dentate nucleus
O Inferior olivary nucleus
T Tonsil

Veins
v21 Inferior vermian vein
v22 Vein of the lateral recess

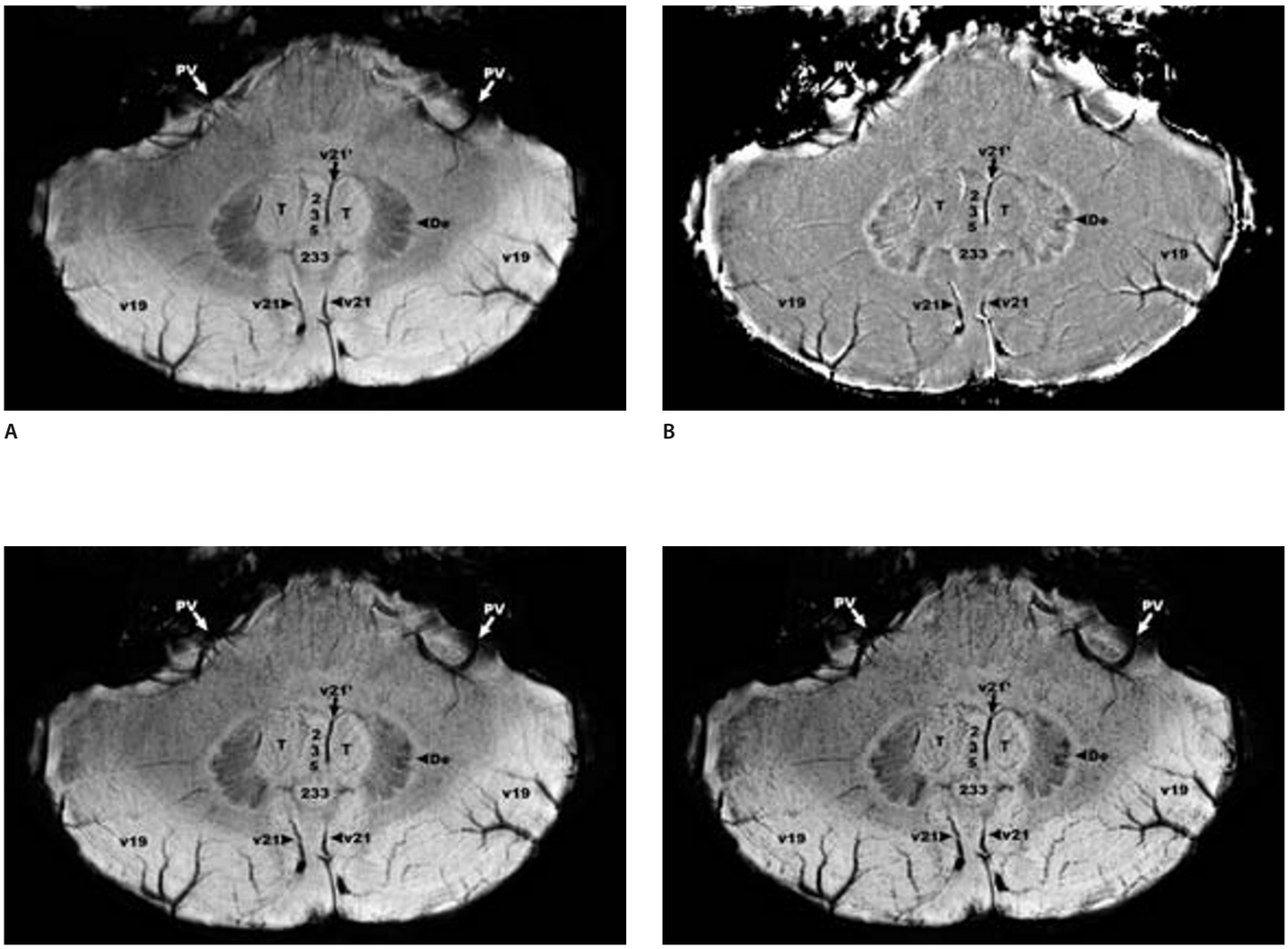

Fig. 10.7 (A–D). **Pons and mid cerebellum. Axial SWI.**
A. Single slice original magnitude image
B. Single slice high-pass filtered phase image
C. SWI magnitude image (phase mask[4])
D. SWI magnitude image (phase mask[8])

233 Pyramis of the vermis (pyramid of the vermis)
235 Uvula of the vermis

Letter labels
De Dentate nucleus
PV Petrosal vein
T Tonsil

Veins
v19 Cerebellar hemispheric veins draining to the transverse sinuses
v21 Inferior vermian vein
v21′ Superior retrotonsillar tributary of the inferior vermian vein

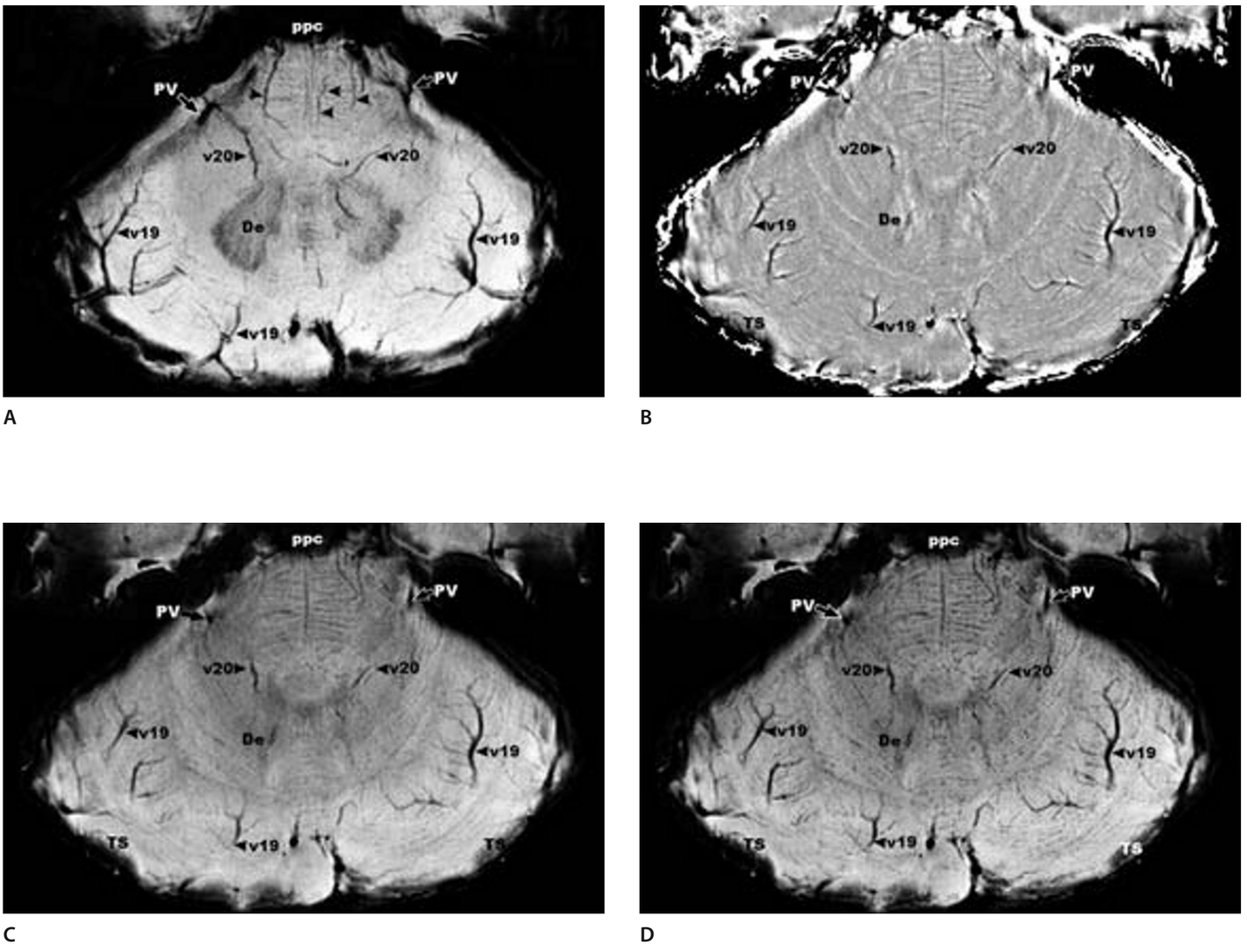

Fig. 10.8 (A–D). Pons and mid-upper cerebellum. Axial SWI.
A. Minimum intensity pixel projection from 5 sequential SWI
B. Single slice high-pass filtered phase image
C. SWI magnitude image (phase mask[4])
D. SWI magnitude image (phase mask[8])

Letter labels
ppc Prepontine cistern
De Dentate nucleus
PV Petrosal vein
TS Transverse sinus

Veins
v19 Cerebellar hemispheric veins draining to the transverse sinuses
v20 Anterolateral marginal vein (along the anterior cerebellar margin at the ambient cistern)

Arrowheads and arrows
Medial arrowheads in **A**: Anteromedial pontine veins
Lateral arrowheads in **A**: Anterolateral pontine veins
The dark lines crossing the pons transversely in (**B)–(D)** may represent, in part, transverse tributaries of the anteromedial and anterolateral pontine veins.

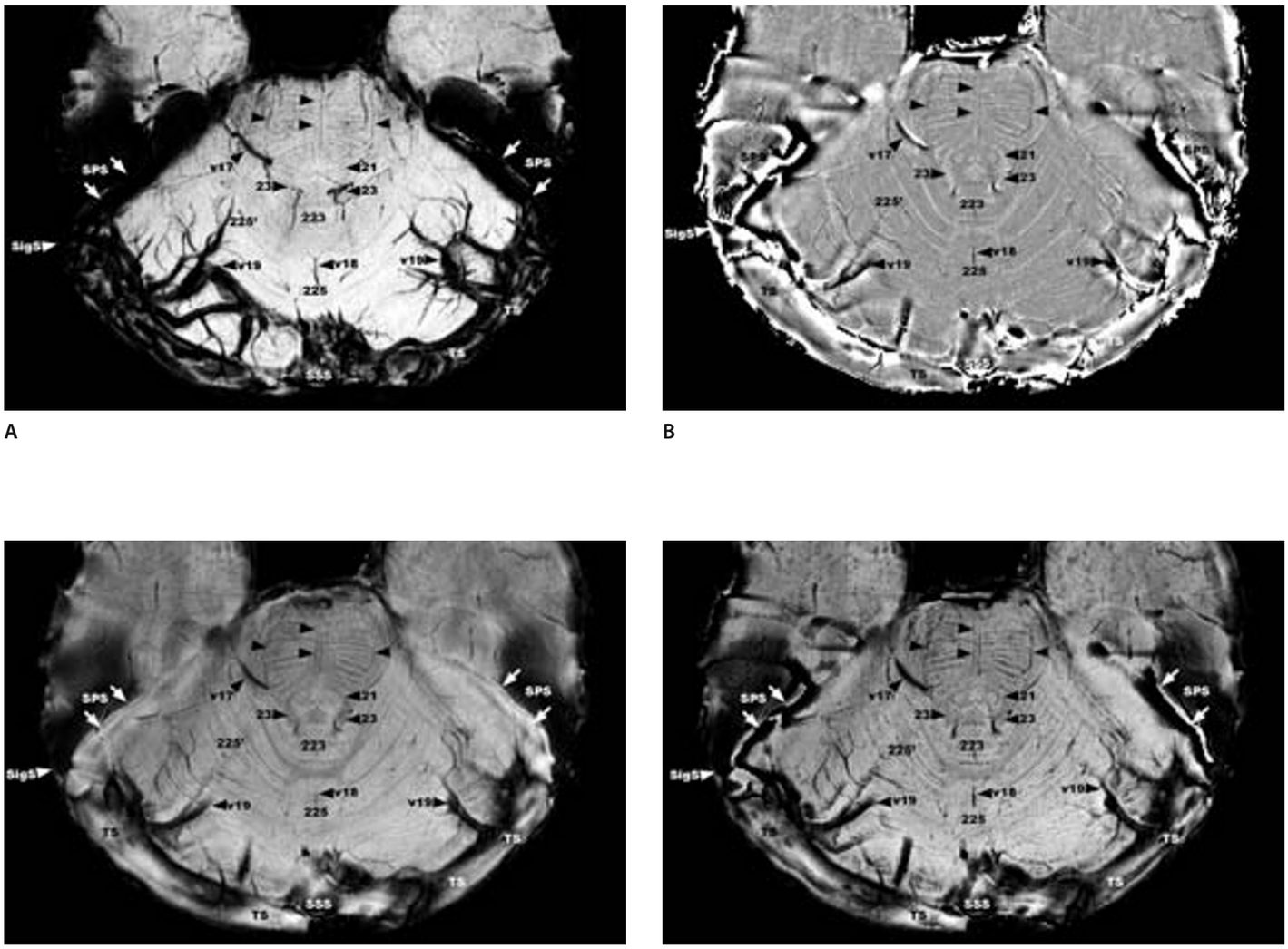

Fig. 10.9 (A–D). High pons and high cerebellum. Axial SWI.
A. Minimum intensity pixel projection from 5 sequential SWI
B. Single slice high-pass filtered phase image
C. SWI magnitude image (phase mask[4])
D. SWI magnitude image (phase mask[8])

21 Medial lemniscus
23 Superior cerebellar peduncle
223 Central lobule of vermis
225 Culmen of vermis
225′ Quandrangular lobule (anterior quadrangular lobule)

Letter labels
SigS Sigmoid sinus
SPS Superior petrosal sinus (with aliasing artifact)
SSS Superior sagittal sinus
TS Transverse sinus

Veins
v17 Lateral mesencephalic vein
v18 Preculminate vein
v19 Cerebellar hemispheric veins draining to the transverse sinus (TS)

Arrowheads and arrows
Medial arrowheads: Anteromedial pontine veins
Lateral arrowheads: Anterolateral pontine veins

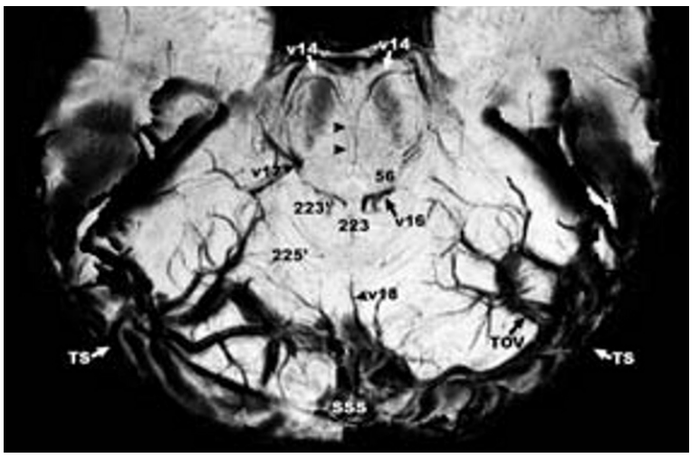

A

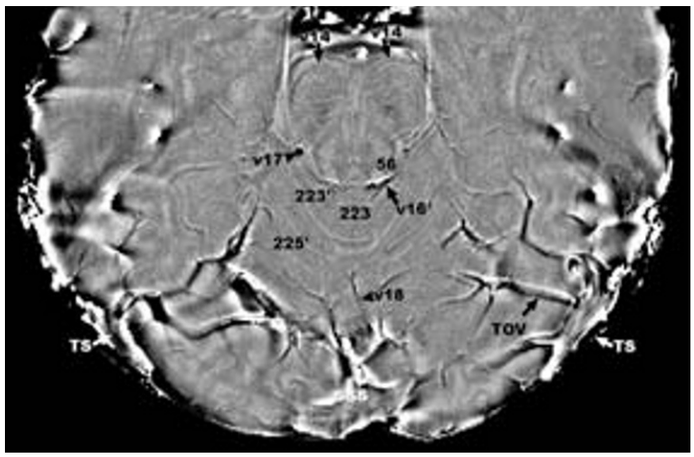

B

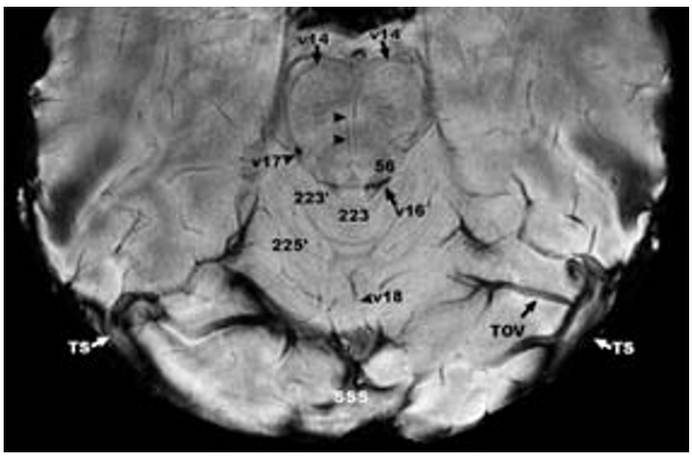

C

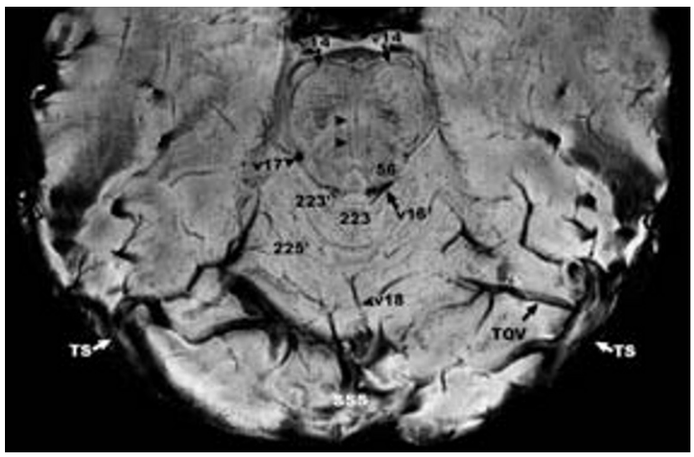

D

Fig. 10.10 (A–D). Pontomesencephalic junction and high cerebellum. Axial SWI.
A. Minimum intensity pixel projection from 5 sequential SWI
B. Single slice high-pass filtered phase image
C. SWI magnitude image (phase mask[4])
D. SWI magnitude image (phase mask[8])
In A., oblique dark bands overlying the anterior pons result from blooming of the susceptibilty in the substantia nigra (See next Fig. 10.11).

56 Inferior colliculus
223 Central lobule of vermis
223′ Wing of the central lobule
225′ Quandrangular lobule (anterior quadrangular lobule)

Letter labels
SSS Superior sagittal sinus
TOV Temporo-occipital veins
TS Transverse sinus

Veins:
v14 Peduncular vein (vein of the pontomesencephalic sulcus)
v16 Vein of the superior cerebellar peduncle
v17 Lateral mesencephalic vein
v18 Preculminate vein

Arrowheads and arrows
Medial arrowheads: Anteromedial pontine veins

Fig. 10.11 (A–D). Mesencephalon and apex of cerebellum. Axial SWI.

A. Minimum intensity pixel projection from 5 sequential SWI images

B. Single slice high-pass filtered phase image

C. SWI magnitude image (phase mask[4])

D. SWI magnitude image (phase mask[8])

9′ Periaqueductal gray matter
23′ Decussation of the superior cerebellar peduncle
56 Inferior colliculus
60 Cerebral peduncle
64 Substantia nigra
95 Red nucleus
207 Uncus
225 Culmen
225′ Quandrangular lobule (anterior quadrangular lobule)

Letter labels

BVR Basal vein of Rosenthal, composed of segments I, II and III.
Segment I (striate segment) arises along the anterior perforated substance by the union of the anterior cerebral, deep middle cerebral and inferior striate veins.
Segment II (peduncular segment) begins at the most medial point of the BVR anterior to the cerebral peduncle and courses posterosuperiorly to the level of the lateral mesencephalic vein.
Segment III (posterior mesencephalic segment) continues around the brain stem to unite with the vein of Galen)
IP Interpeduncular fossa
MCA Middle cerebral artery
SS Straight sinus
SSS Superior sagittal sinus
TS Transverse sinus

Veins:

v14 Peduncular vein (vein of the pontomesencephalic sulcus)
v15 Vein of the temporal horn
v16 Vein of the superior cerebellar peduncle

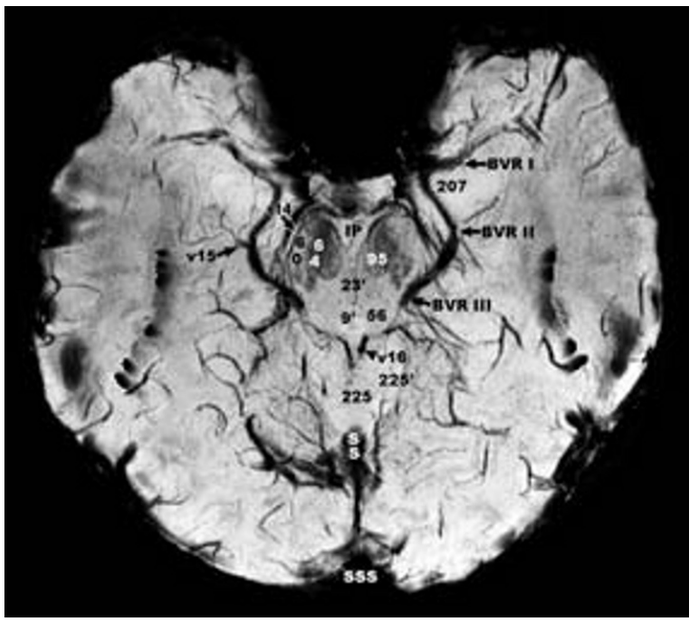
BVR I
207
BVR II
IP
v15
95
23'
BVR III
9' 56
v16
225'
225
SSS

A

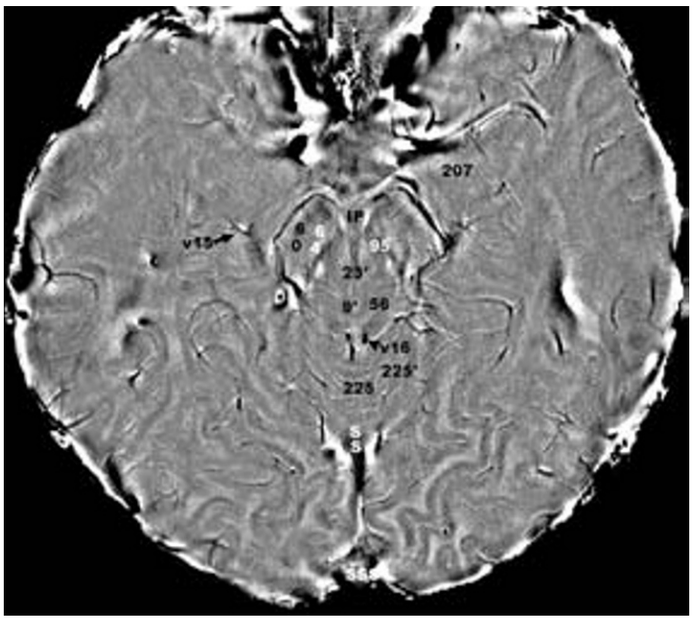
207
IP
v15
95
23'
9' 56
v16
225'
225
SSS

B

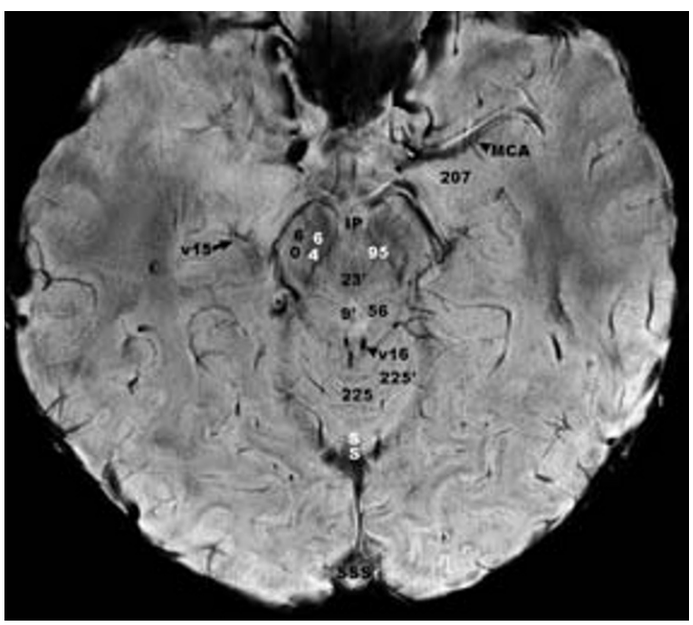
vMCA
207
IP
v15
95
23'
9' 56
v16
225'
225
SSS

C

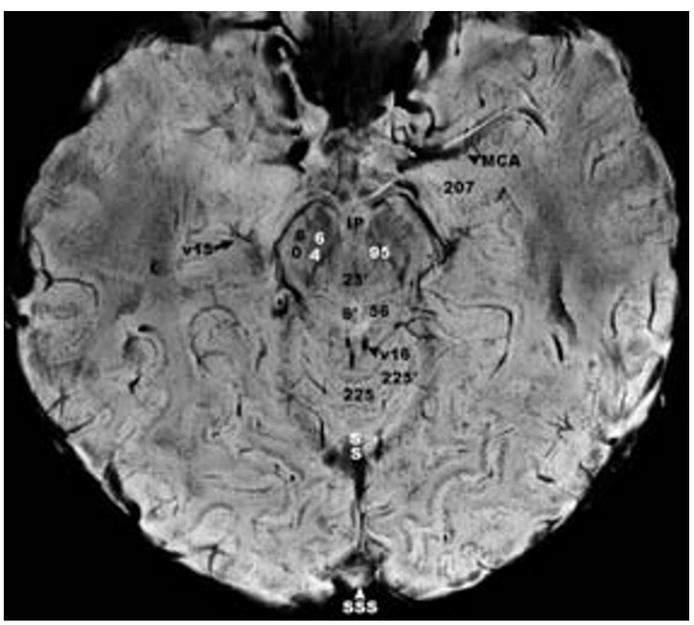
vMCA
207
IP
v15
95
23'
9' 56
v16
225'
225
SSS

D

Fig. 10.12 (A–D). Mesencephalon and apex of cerebellum. Axial plane SWI.

A. Minimum intensity pixel projection from 5 sequential SWI images
B. Single slice high-pass filtered phase image
C. SWI magnitude image (phase mask[4])
D. SWI magnitude image (phase mask[8])

9′ Periaqueductal gray matter
60 Cerebral peduncle
64 Substantia nigra
69 Superior colliculus
71 Mammillary bodies and capsules
72 Fornix (anterior columns)
95 Red nucleus
101 Optic tract
225 Culmen

Letter labels
3V Third ventricle
ACV Anterior cerebral vein
BVR Basal vein of Rosenthal (Segments I, II and III).
Segment I (striate segment) arises along the anterior perforated substance by the union of the anterior cerebral, deep middle cerebral and inferior striate veins.
Segment II (peduncular segment) begins at the most medial point of the BVR anterior to the cerebral peduncle and courses posterosuperiorly to the level of the lateral mesencephalic vein.
Segment III (posterior mesencephalic segment) continues around the brain stem to unite with the vein of Galen

DMCV Deep middle cerebral vein draining to the basal vein of Rosenthal
In Insula
ISV Inferior striate veins
SS Straight sinus
SSS Superior sagittal sinus

Veins
v8 Stem of the inferior ventricular vein
v9 Precentral cerebellar vein, and its brachial tributaries outlining the brachia conjunctiva (superior cerebellar peduncles)
v11 Multiple, approximately parallel, veins crossing through the cerebral peduncle at right angles to the surface of the peduncle. These are part of the anterolateral group of mesencephalic veins.
v12 Vein of the orbital surface of frontal lobe
v16 Vein of the superior cerebellar peduncle


v12
ISV
ACV
In
BVR I
DMCV
v8
BVR II
95
BVR III
v9
225
SS
SSS

A

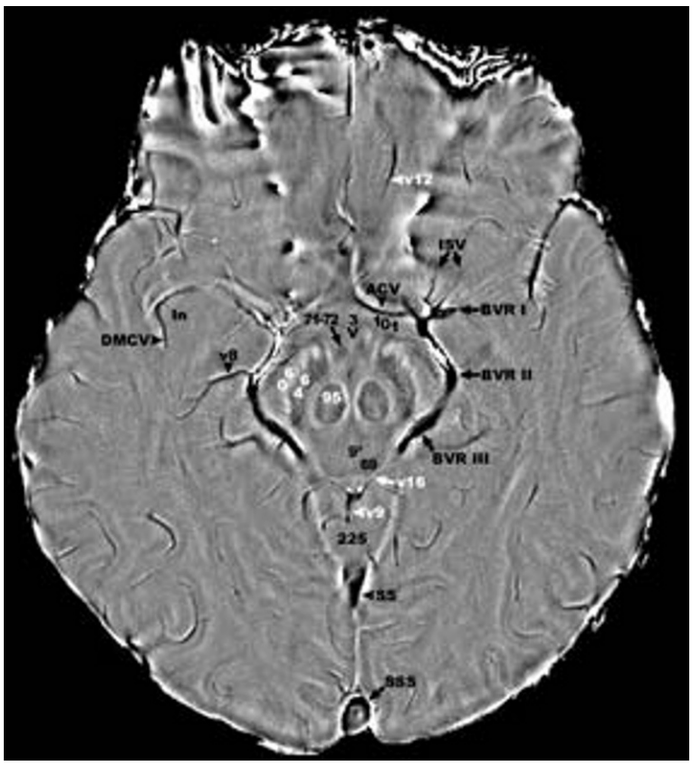
v12
ISV
ACV
In
BVR I
DMCV
v8
BVR II
95
BVR III
v16
v9
225
SS
SSS

B

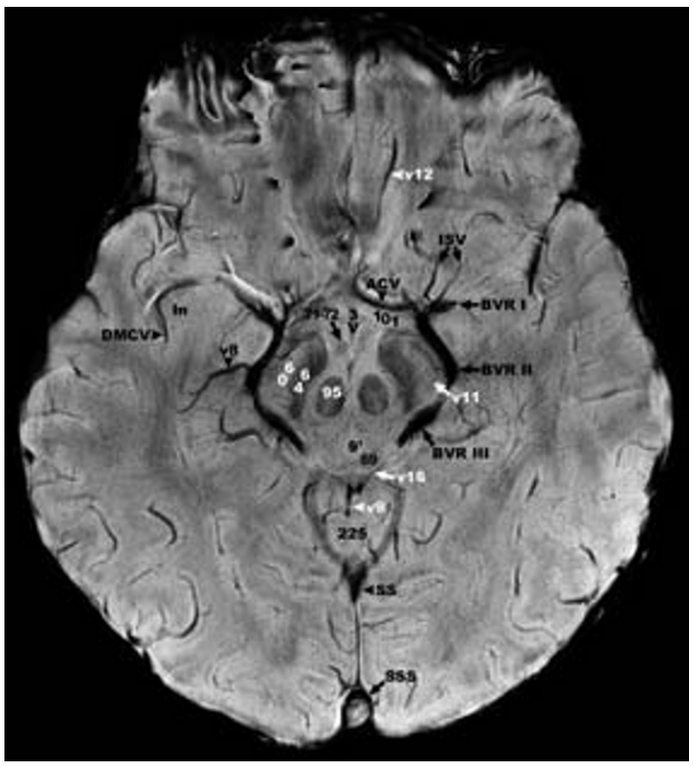
v12
ISV
ACV
In
BVR I
DMCV
v8
BVR II
95
v11
BVR III
v16
v9
225
SS
SSS

C

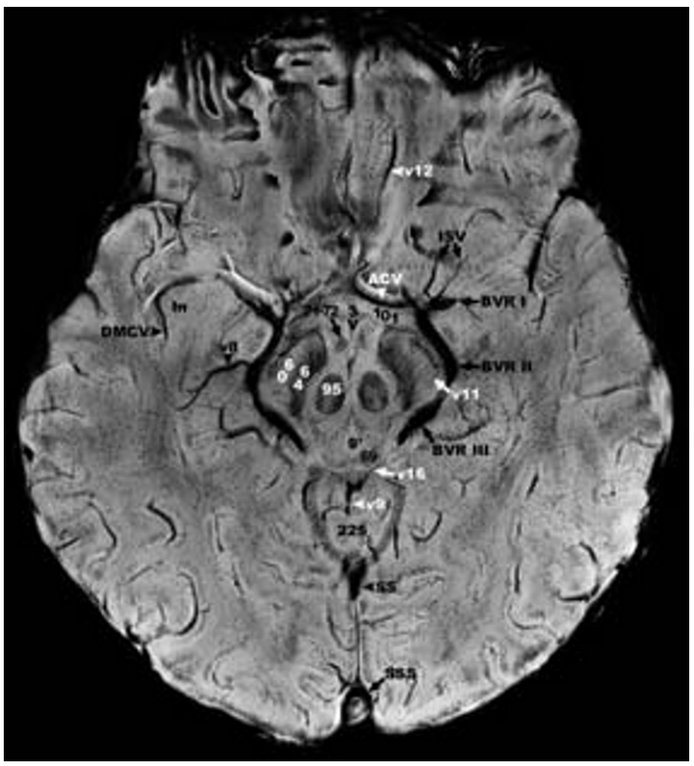
v12
ISV
ACV
In
BVR I
DMCV
v8
BVR II
95
v11
BVR III
v16
v9
225
SS
SSS

D

Fig. 10.13 (A–D). Low basal ganglia and capsules. Axial SWI.
A. Minimum intensity pixel projection from 5 sequential SWI images (slightly different level from B.-D.)
B. Single slice high-pass filtered phase image
C. SWI magnitude image (phase mask[4])
D. SWI magnitude image (phase mask[8])

The third ventricle is not labeled to avoid obscuration of other landmarks.

92 Pulvinar
97 Subthalamic nucleus
170 Caudate nucleus (head)
178 Putamen
175p Internal capsule (posterior limb)
175r Internal capsule (retrolenticular portion)
179 Globus pallidus (lateral (l), and medial (m) segments)
210 Hippocampal formation
251 Corpus callosum (genu)

Letter labels
l Lateral nucleus of the globus pallidus
m Medial nucleus of the globus pallidus
BVR Basal vein of Rosenthal (Segment *III*).
FO Frontal operculum
In Insula (Island of Reil)
ICV Internal cerebral vein with additional pineal veins in close proximity
Pi Pineal gland
SS Straight sinus
SSS Superior sagittal sinus
TO Temporal operculum

Veins
v13 Medial atrial vein

Arrowheads and arrows
Black arrowhead: Superior pole of the red nucleus just showing within this section.


FO
In
TO
251
170
178
97
175r
ICV
BVR
92
210
v13
SS
SSS

A

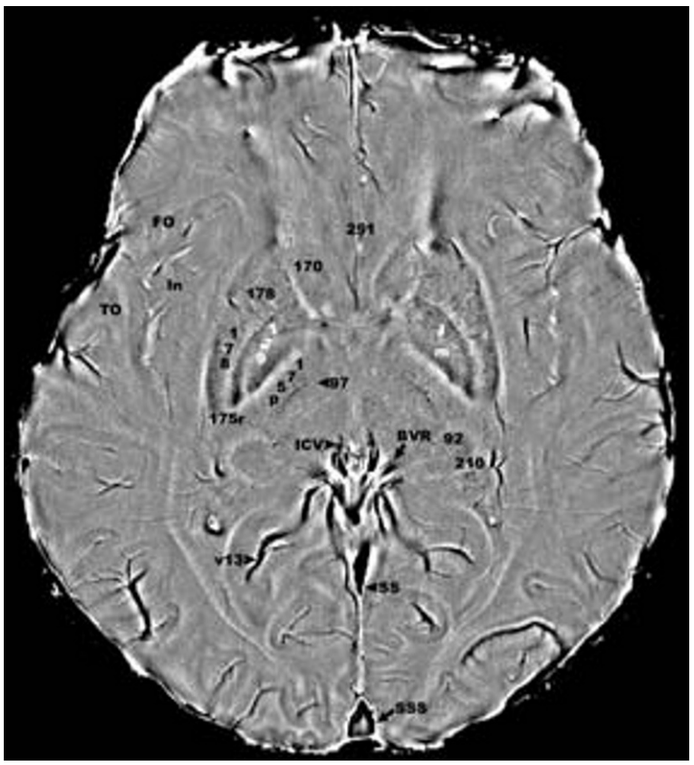
FO
In
TO
291
170
178
97
175r
ICV
BVR
92
210
v13
SS
SSS

B

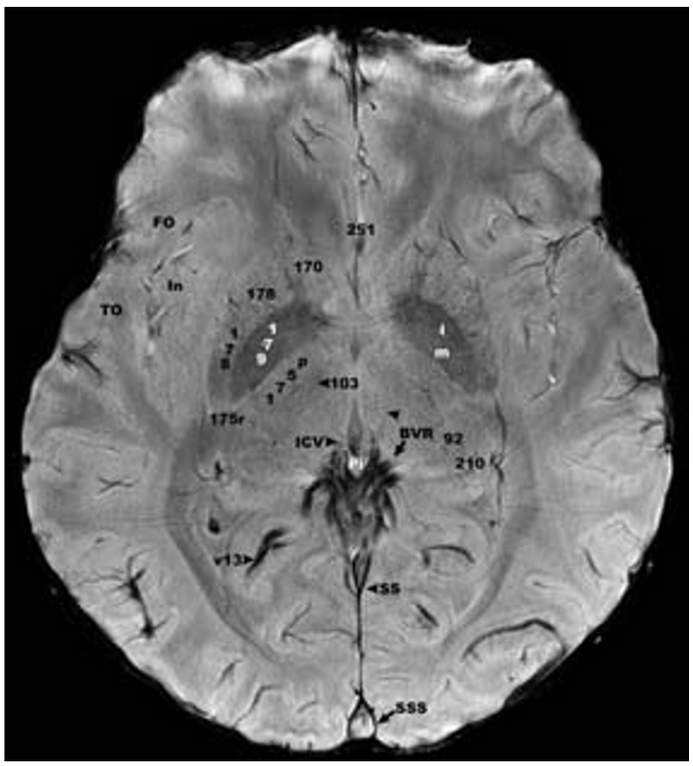
FO
In
TO
251
170
178
103
175r
ICV
BVR
92
210
v13
SS
SSS

C

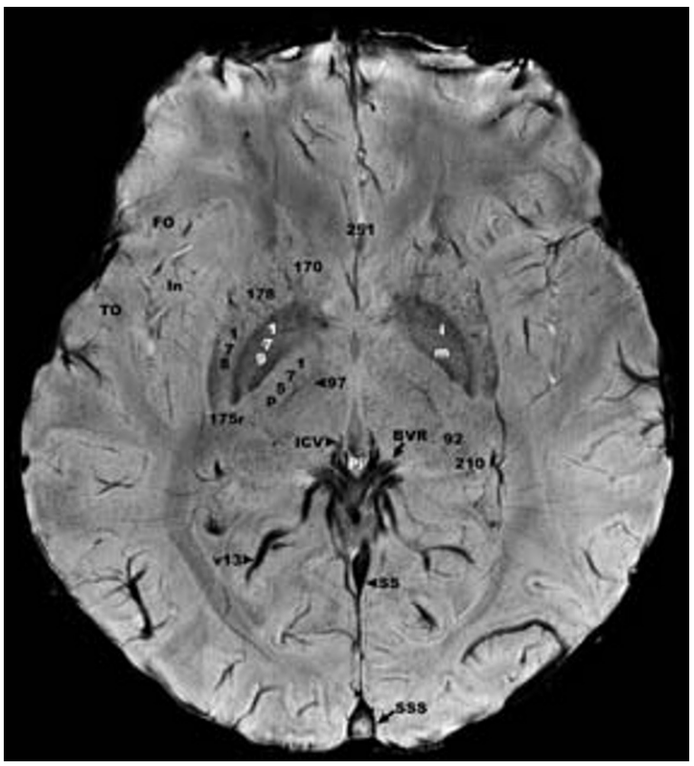
FO
In
TO
291
170
178
97
175r
ICV
BVR
92
210
v13
SS
SSS

D

Fig. 10.14 (A–D). High basal ganglia and capsules. Axial SWI.
A. Minimum intensity pixel projection from 5 sequential SWI
B. Single slice high-pass filtered phase image
C. SWI magnitude image (phase mask[4])
D. SWI magnitude image (phase mask[8])

72 Fornix (anterior columns)
170 Caudate nucleus (head)
178 Putamen
175p Internal capsule (posterior limb)
179 Globus pallidus (lateral (l) and medial (m) segments)
251 Corpus callosum (genu)
253 Corpus callosum (splenium)
254 Forceps major

Letter labels
FO Frontal operculum
In Insula (Island of Reil)
ICV Paired internal cerebral veins
SM Superficial middle cerebral vein draining the insula and overlying opercula
SS Straight sinus
SSS Superior sagittal sinus
TO Temporal operculum
TSV Thalamostriate vein

Veins
v1 Septal vein, with deep medullary tributaries (on right)
v2 Anterior inferior group of caudate veins
v3 Anterior caudate vein
v4 Longitudinal caudate vein
v5 Superior thalamic vein
v6 Vein of the occipital horn

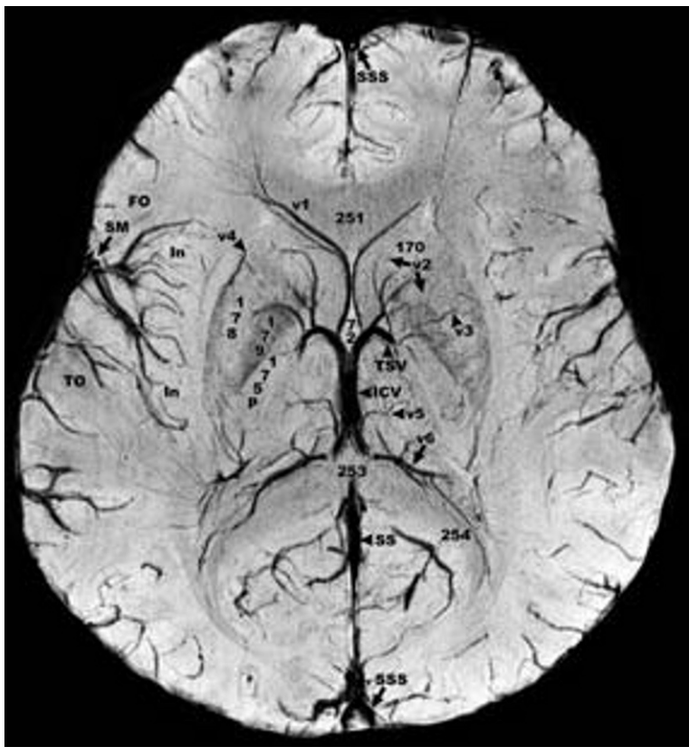
SSS
FO
SM
In
v4
v1
251
170
v2
v3
TSV
ICV
v5
v6
TO
In
253
SS
254
SSS

A

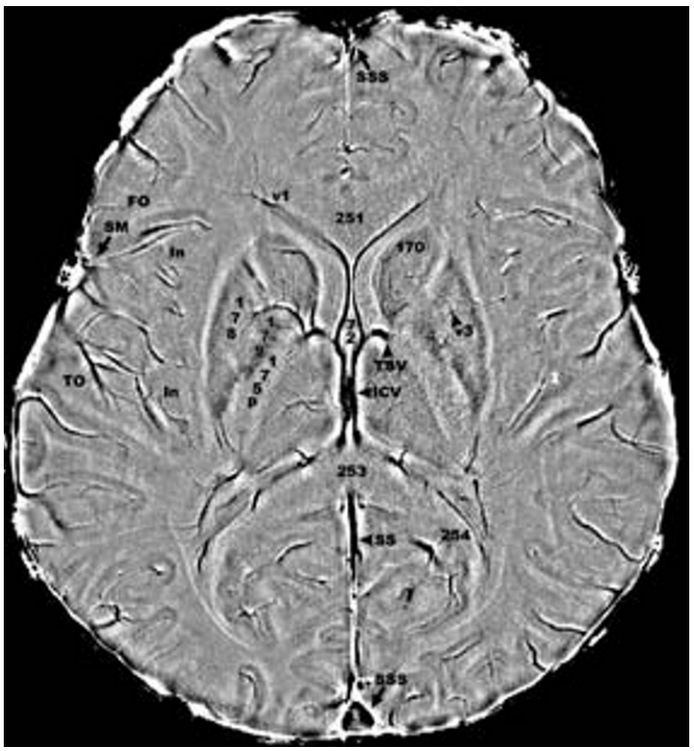
SSS
FO
SM
In
v1
251
170
v3
TSV
ICV
TO
In
253
SS
254
SSS

B

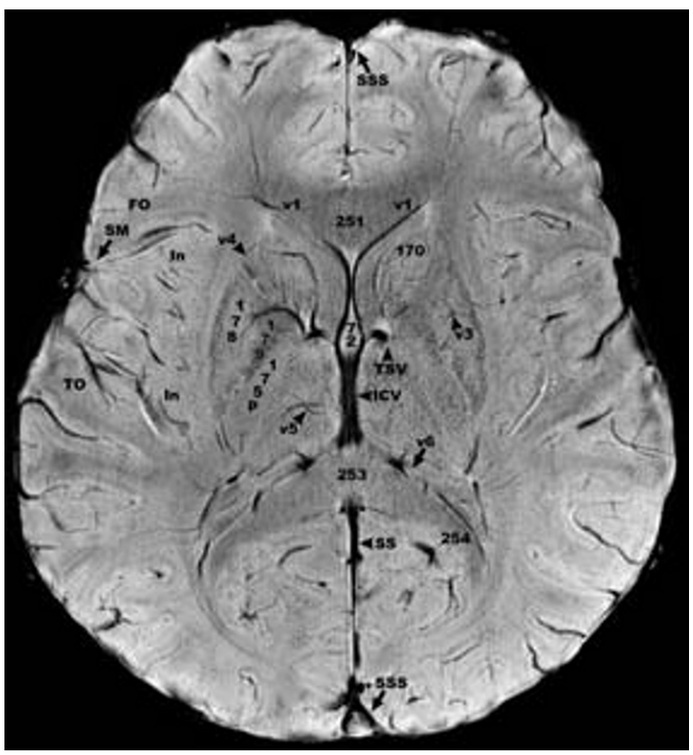
SSS
FO
SM
In
v4
v1
v1
251
170
v3
TSV
ICV
v5
v6
TO
In
253
SS
254
SSS

C

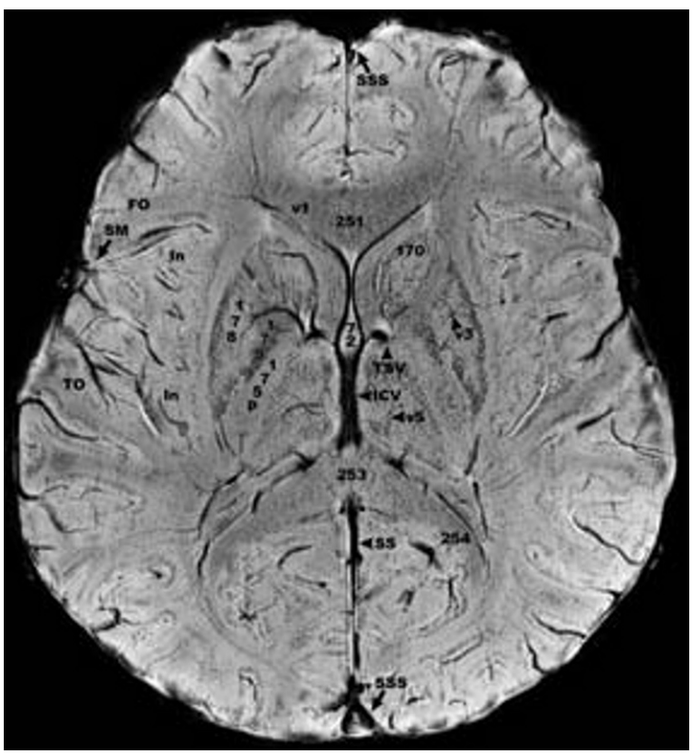
SSS
FO
SM
In
v1
251
170
v3
TSV
ICV
v5
TO
In
253
SS
254
SSS

D

C. Diffusion Tensor Imaging (DTI) *in vivo:* Anatomic-DTI correlation at 3T (Figs. 10.15–10.37)

Spyros S. Kollias, Meng Law, Yvonne Lui, Thomas P. Naidich, and Bradley N. Delman

Water molecules undergo random Brownian motion and spread outward from a center over time (i.e. diffuse). In a *homogeneous* liquid, the water molecules diffuse equally in all directions. Equal diffusion is termed *isotropic.* If the environment around the water molecules is *inhomogeneous,* the water molecules may diffuse more in one direction than another. Unequal diffusion is termed *anisotropic.* Within the white matter of the brain, axonal proteins, axonal membranes, and myelin sheaths introduce barriers to free diffusion of water, so the water molecules diffuse preferentially along the axons. Within the white matter, therefore, the diffusion of water is characteristically anisotropic. Greater numbers of axons and tighter packing of axons cause greater anisotropy [28, 34, 63, 146, 177a, 192, 217, 223, 230, 275, 276, 293, 296–299, 301–303, 306, 316, 317, 345, 371, 407, 431, 447, 453, 459]. MR imaging can detect anisotropy, quantify it, and display both the degree and the preferred direction of diffusion. Uni-dimensional measures of the "quantity" of diffusion are termed scalars. Commonly used scalars include *fractional anisotropy* (FA) and *mean diffusivity* (MD). The scalar factors may be color coded to show the direction of preferential diffusion (by color) as well as the degree of anisotropy (by intensity of color). For measures of fractional anisotropy, the scalars and colors are determined for every volume element (voxel) of the image, and displayed as a color-coded map of the fractional anisotropy at every point within that section of the brain.

Multi-dimensional measures of the *quantity-plus-direction* of diffusion are termed tensors. Tensors specify both quantitative and directional information simultaneously and are typically displayed as diffusion tensor matrices. Tensors are conceptualized as *ellipsoids* of differing lengths, widths and orientation. Mathematically, the ellipsoids are characterized by the length and orientation of the long axis of the ellipsoid (major eigenvector) and the two short axes of the ellipsoid (minor eigenvectors). The diffusion tensor matrices may be color coded, so the color gives the direction of the major eigenvector. Within each voxel, a single ellipsoid gives the summated average of the intensity and direction of diffusion for all of the tissue within that voxel. This is presumed to reflect the average orientation of the axons and fiber tracts that traverse that voxel. Determining and displaying the major eigenvectors for each voxel of the image provides a diffusion tensor map of all structures within that section of the brain. The tensor data may also be grouped together by the orientations of neighboring major eigenvectors to show sets of voxels in which the orientations are nearly parallel and remain parallel over lengths through the brain. Maps of coherent (parallel or co-curvilinear) eigenvector orientations appear to track the courses of fiber bundles and are designated diffusion tensor tractography.

FA color map: By convention, specific colors are assigned to indicate the preferred direction of diffusion *within each voxel* (color coded sphere). Blue signifies preferential diffusion in the superior-inferior (SI) orientation. Green signifies preferential diffusion in the anteroposterior (AP) direction. Red signifies preferential diffusion in the transverse (latero-lateral, LL) direction. Diffusion within tracts coursing at oblique angles is represented by a weighted-mix of colors. For instance, a tract coursing at 45° to the rostral-caudal (blue) and to anteroposterior (green) orientations would be coded with an equal mix of blue and green coloration, so it would appear cyan (blue + green).

Eigenvector maps (Whisker plots): In addition to color maps, color-coded *whisker plots* can also be generated to display the diffusion tensor data within each voxel of the image. In these plots, the net diffusion within each voxel is represented by a single bar. The orientation of the bar indicates the net preferred direction of diffusion *within that voxel.* The size of the bar indicates the average magnitude of diffusion along that preferred direction. For ease of interpretation, the whisker plots are coded according to the same color convention, so the color of each bar indicates the preferred direction of diffusion for all structures within that voxel.

Fiber tractography: Fiber tracts coursing from voxel to voxel tend to follow parallel or gently curving paths, so the orientations of their major eigenvectors tend to be nearly parallel or co-curviliear in adjacent voxels. Computer algorithms can now calculate the relative parallelism and coherence of major eigenvectors in neighboring voxels. By setting specific thresholds for coherence, these algorithms can "string together" adjacent voxels to display trajectories that are believed to represent the actual courses of fiber tracts within the brain. These tractograms are coded by the same color convention used for the FA color maps and whisker plots.

Specific parameters used for Diffusion Tensor Imaging *in vivo* at 3 Tesla

Data acquisition: For data acquisition, a 3 T whole body MR system (Philips Achieva, Best, the Netherlands), equipped with 80mT/m/ms gradient coils and an 8-element receive head coil array (MRI Devices Corp., Waukesha, USA) was used. For the axial DTI scans, a diffusion-weighted single-shot spin-echo echoplanar imaging (EPI) sequence was applied with the following parameters: Field of view: 170x170 mm^2; In-plane matrix: 96 x 96 reconstructed to 128 x 128; Slices selected: 30 contiguous slices each 2.0 mm thick, TR: 3000 ms, TE: 46 ms, Number of signal averages: 3, 60% partial k-space acquisition. Diffusion weighting with a maximal b-factor of 1000 s/mm^2 was carried out along 15 icosahedral directions [34] complemented by one scan with b = 0. Scan time and susceptibility artifacts were reduced and image quality improved by the use of parallel imaging with an acceleration (Sensitivity encoding) factor of 2 [28, 217].

DTI data analysis: Retrospective interscan motion correction and a reduction of eddy current-induced image warping were achieved using a correlation-based 3D-affine registration algorithm [317]. The independent elements of the diffusion tensors and their corresponding eigenvalues/eigenvectors (and subsequently the fiber tracks) were computed using an in-house dedicated software package developed in C++. The fiber trajectories were reconstructed using standard line propagation based on the "fiber assignment by continuous tracking" (FACT) algorithm [299]. The seed areas were placed in specific white matter areas of the brainstem and the cerebellum depending on the white matter tracts or fasciculi that needed to be reconstructed. From each voxel trajectories were launched in both directions. The algorithm terminated when a certain lower limit FA value (threshold = 0.2) was reached. To reconstruct tracts of interest, we used a multiple-region-of-interest approach, which exploits existing anatomical knowledge of track trajectories. The major fibers are identified on standard color-coded DTI maps.

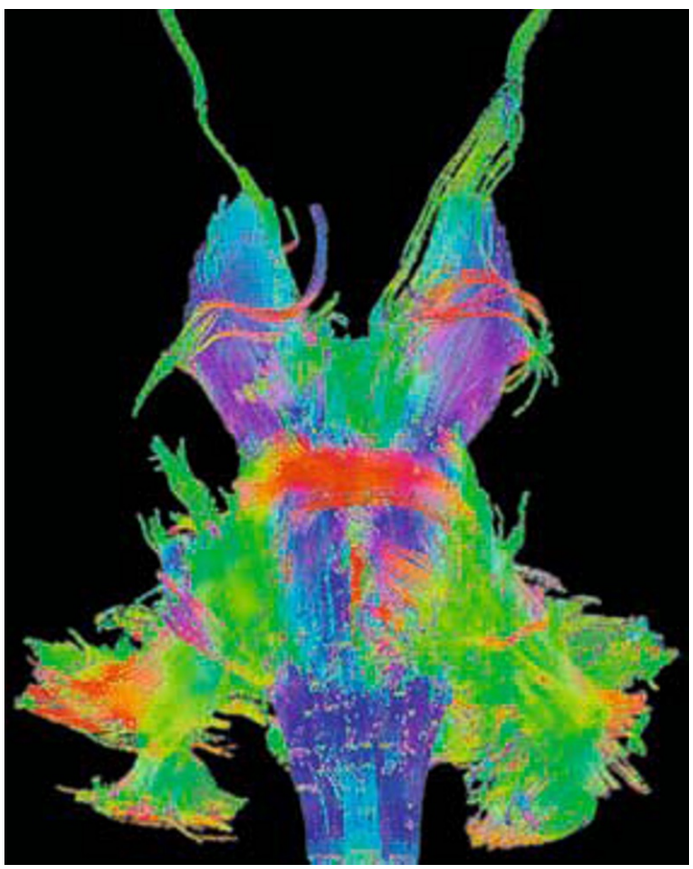

A

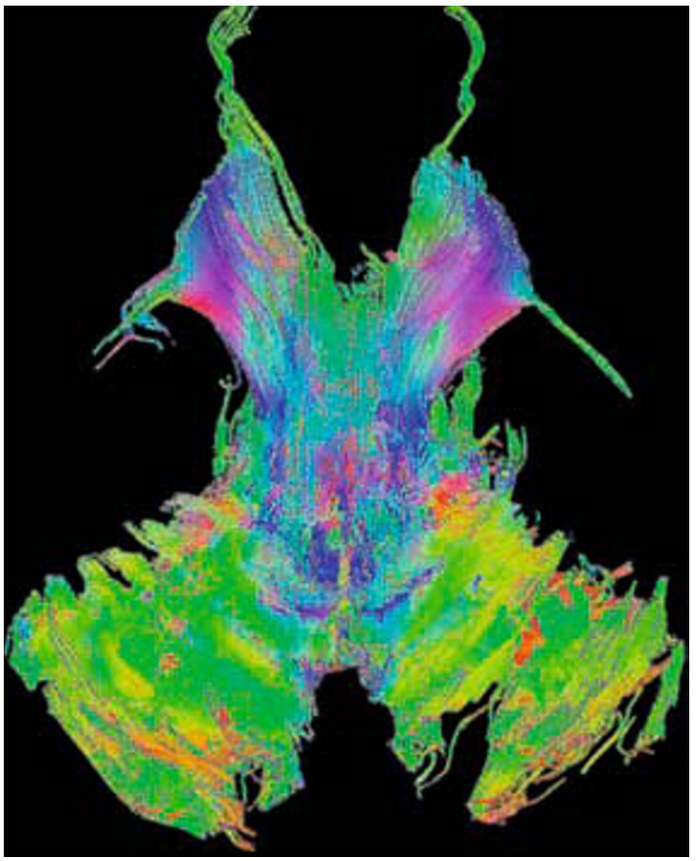

D

Fig. 10.15 (A–F). Multidirectional diffusion tensor images (DTI) of the brain stem and cerebellum, displayed as tractograms.

A. Anterior view. **B.** Far lateral view. **C.** Parasagittal lateral view. **D.** Posterosuperior view. **E.** Direct posterior view. **F.** Postero-inferior view.

By convention, the directional orientation of the fibers is coded Red for latero-lateral, Green for anterior-posterior, and Blue for cranial-caudal. In all of the following anatomic MRI and DTI, the numbering sequence used will be the standard system that was used for Sect. VIII, MR microscopy, supplemented as needed with additional labels of structures peculiar to a specific image.

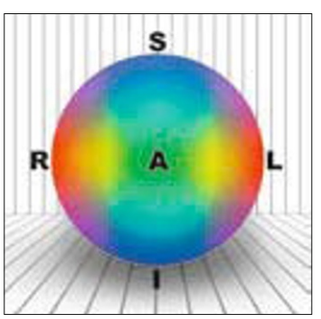

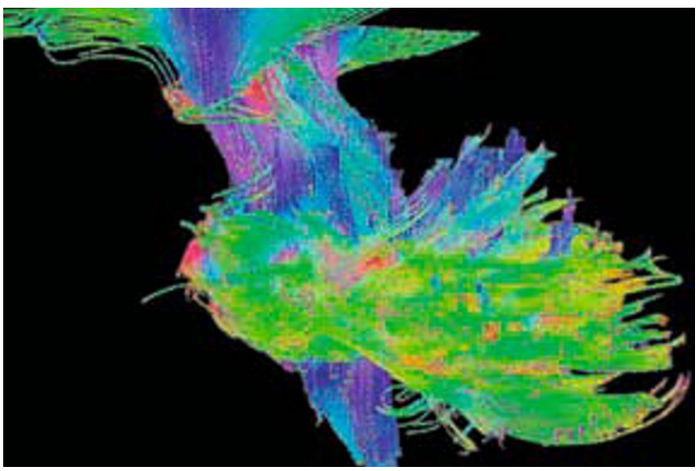

B

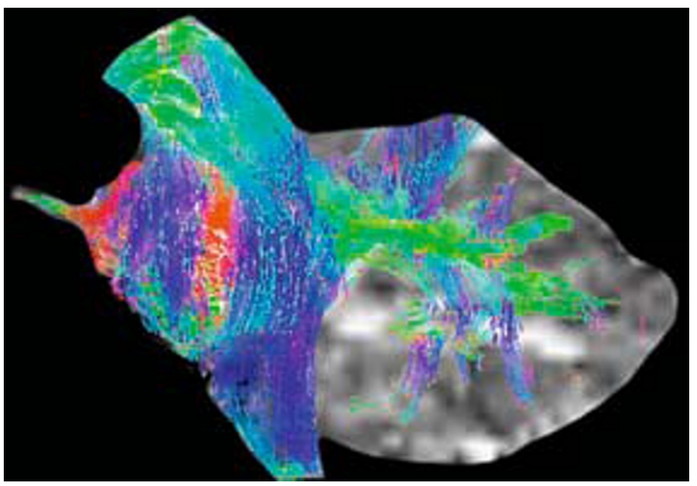

C

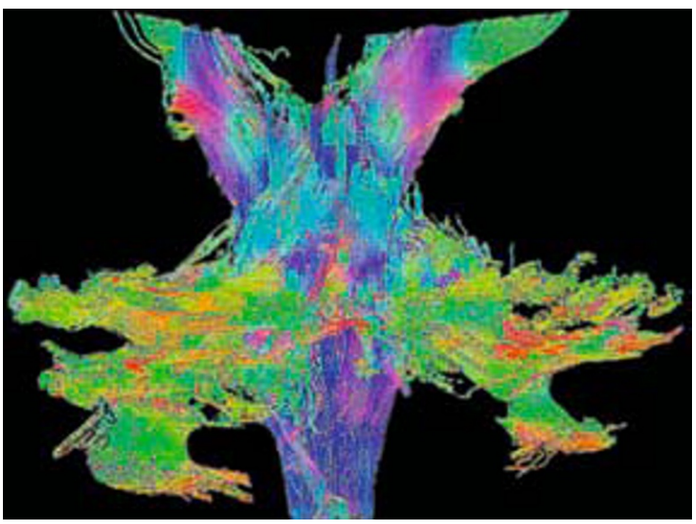

E

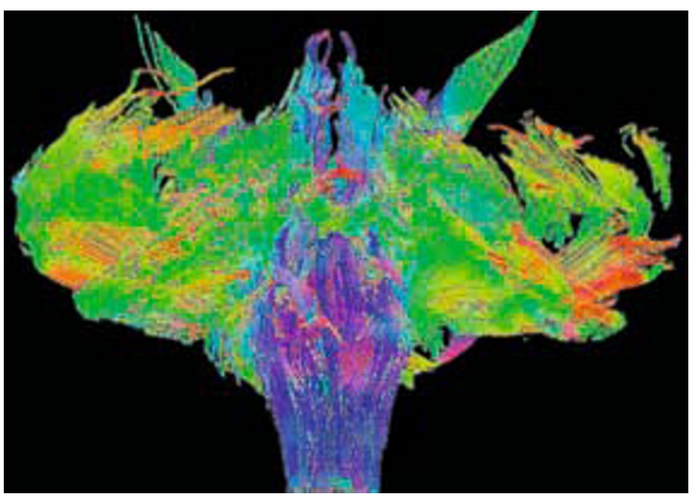

F

Axial Anatomic-DTI Correlations

Figures 10.16–10.24 correlate 3 Tesla axial diffusion tensor images (DTI) of a living human volunteer with 3T anatomic MR images of a formalin-fixed human brain specimen. All axial images are presented in sequence at selected levels from caudal toward cranial position. The anatomic and DTI images selected have been grouped into broad anatomic regions to permit correlation despite slight slice-slice variation due to differences in scan angle and normal anatomic variation. The imaging features shown by diffusion tensor imaging were correlated with known anatomical structures [92, 101, 102, 106, 107, 124, 148, 218, 292, 294, 309, 310, 311, 312, 332, 335, 342, 343, 358, 360, 370, 416, 423].

Fig.10.16 (A–D).
The medulla and low cerebellum. Axial plane.
A–B. **3 Tesla axial MRI** of a formalin-fixed human brain specimen, displayed from caudal **(A)** to cranial **(B)**
C–D. **Diffusion tensor imaging** displayed as a color map **(C)** and whisker plot **(D)**

1 Nucleus gracilis
2 Nucleus cuneatus
8 Extensive reticular formation
14 Tectospinal tract
16 Pyramid containing the corticospinal tract
17 Medial longitudinal fasciculus
21 Medial lemniscus
25 Inferior cerebellar peduncle (restiform body)
231′ Inferior semilunar lobule
233′ Gracile lobule
233 Pyramis of the vermis
233″ Biventral lobule
235 Uvula
235′ Tonsil of the cerebellum

Letter labels
O Inferior olivary nucleus
P Pyramid of the medulla
T Tonsil
U Uvula

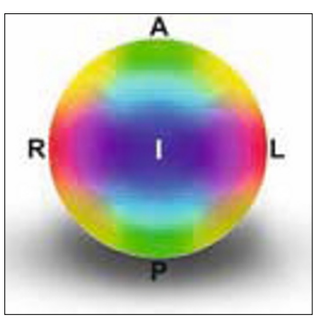


16
O
-21
-14
8
-17
-25
2
1
235'
235'
233"
233"
233'
233
231'

A


16
O
-21
-14
-17
-25
233"
233"
233'
235'
235'
235
233
231'
231'

B

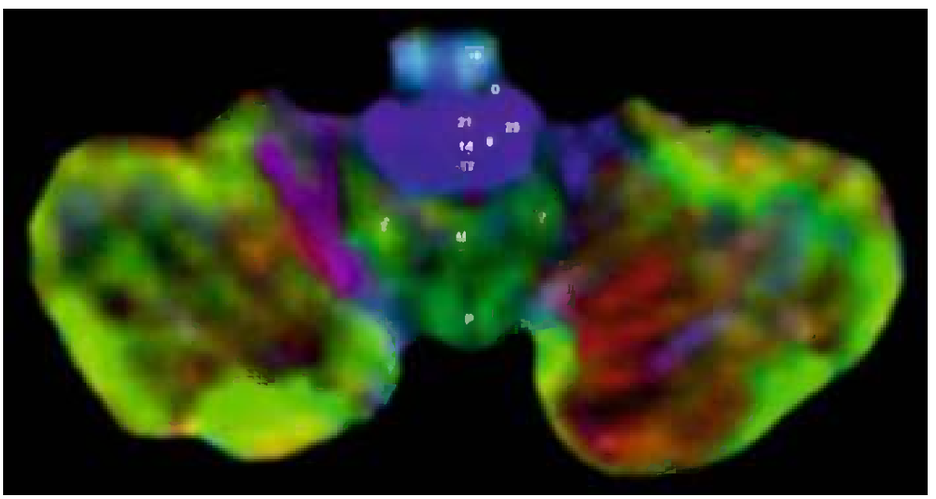

C

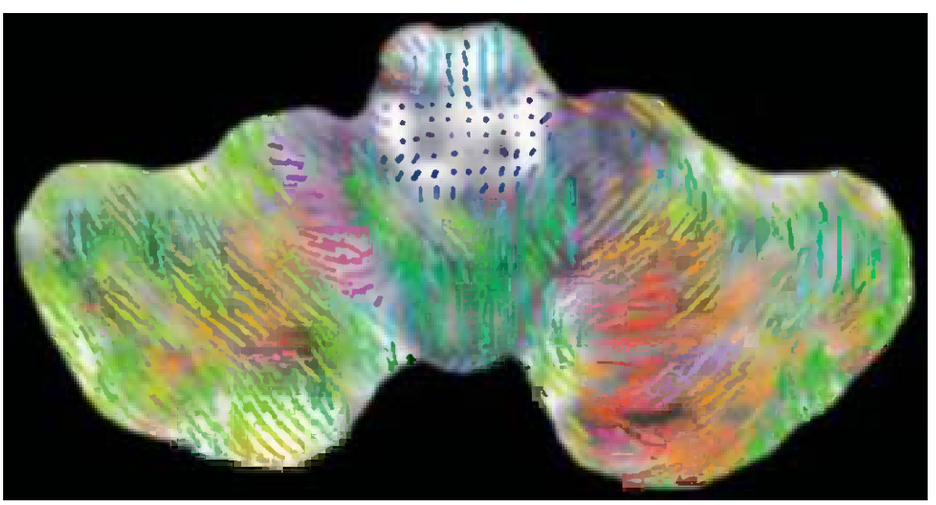

D

Fig. 10.17 (A–D). The lower pons and mid cerebellum. Axial plane.
A–D. 3 Tesla axial MRI of a formalin-fixed human brain specimen, displayed from caudal **(A)** to cranial **(D).**

14 Tectospinal tract
16 Pyramid containing the corticospinal tract
17 Medial longitudinal fasciculus
20 Pontine nuclei
21 Medial lemniscus
23 Superior cerebellar peduncle
24 Central tegmental tract
25 Inferior cerebellar peduncle (restiform body)
26 Medial vestibular nucleus
35 Facial nerve (CN VII)
38 Middle cerebellar peduncle (brachium pontis)
39 Abducens nucleus (CN VI)
41 Ventral pontine decussation
42 Dorsal pontine decussation
43 Trigeminal nerve (CN V)
51 Pontocerebellar fibers
66 Corpus medullare (central white matter of the cerebellar hemisphere)
227 Declive
227′ Simple lobule (posterior quadrangular lobule)
229 Folium of the vermis
229′ Superior semilunar lobule
231 Tuber of the vermis
231′ Inferior semilunar lobule
233 Pyramis of the vermis
233′ Gracile lobule
233″ Biventral lobule
235 Uvula of the vermis
235′ Tonsil of the cerebellum
237 Nodulus of the vermis
237′ Flocculus

Letter labels
4V Fourth ventricle
CN VII, VIII Cranial nerves VII (facial nerve) and VIII (vestibulocochlear nerve)
De Dentate nucleus

Arrowheads and arrows
Paired white arrows: Pontomedullary sulci

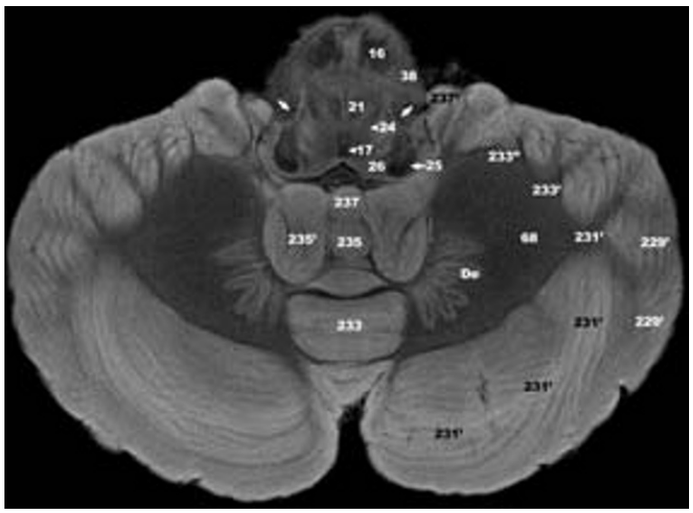
16
38
21
237
<24
<17
26
<25
233'
233'
237
235'
235
68
231'
229'
De
233
231'
229'
231'
231'

A

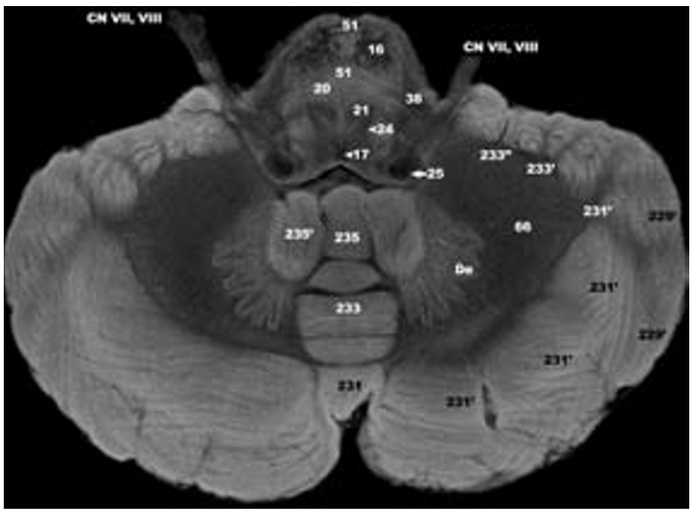
CN VII, VIII
51
16
CN VII, VIII
51
20
38
21
<24
<17
233'
<25
233'
231'
229'
66
235'
235
De
231'
233
229'
231'
231
231'

B

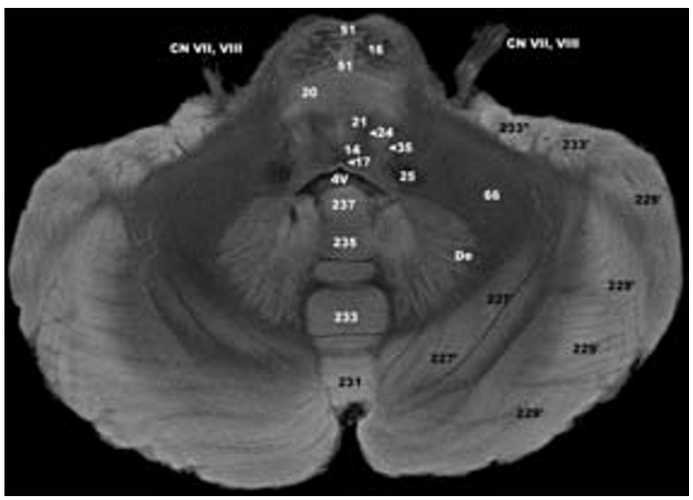
CN VII, VIII
51
16
CN VII, VIII
51
20
21
<24
<35
14
<17
4V
25
233'
233'
66
229'
237
235
De
229'
227'
233
229'
227'
231
229'

C

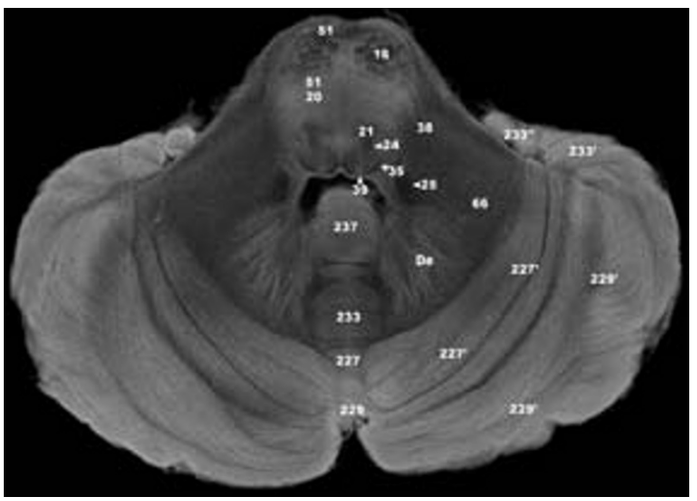
51
16
51
20
21
38
<24
233'
233'
<35
<28
33
66
237
De
227'
229'
233
227'
227'
229'
229'

D

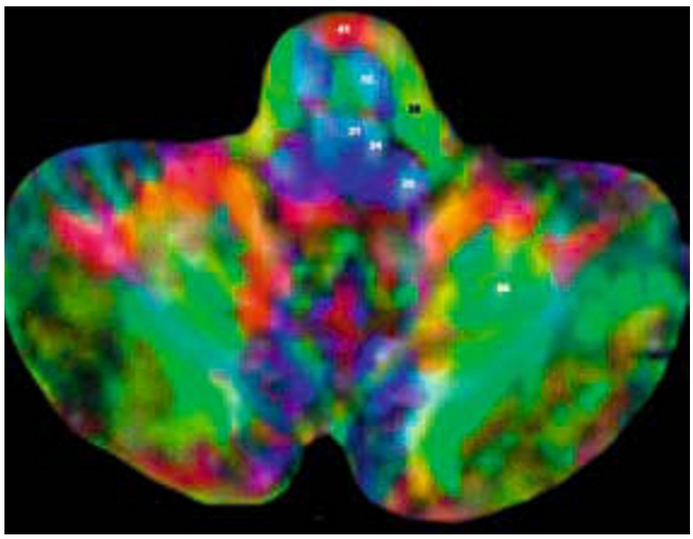

A

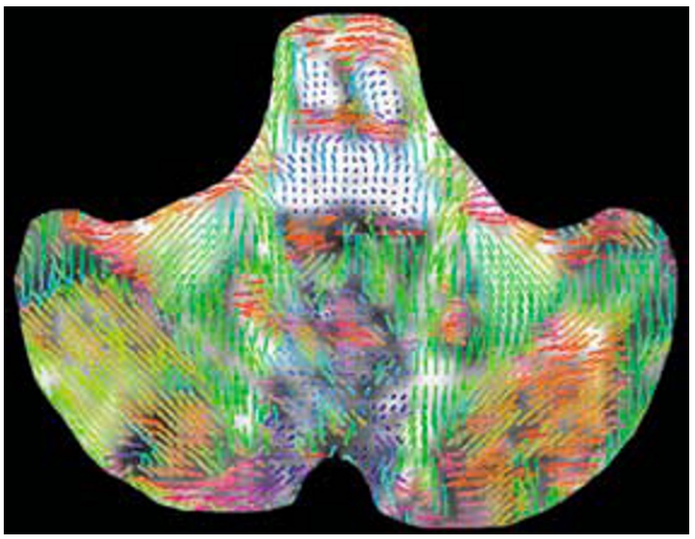

D

Fig. 10.18 (A–F). The lower pons and mid cerebellum. Axial plane.
Diffusion tensor imaging at three selected axial planes, displayed from caudal to cranial as
(A–C). Color maps
(D–F). corresponding whisker plots.

14 Tectospinal tract
16 Pyramid containing the corticospinal tract
17 Medial longitudinal fasciculus
21 Medial lemniscus
23 Superior cerebellar peduncle
24 Central tegmental tract
25 Inferior cerebellar peduncle (restiform body)
38 Middle cerebellar peduncle (brachium pontis)
41 Ventral pontine decussation
42 Dorsal pontine decussation
43 Trigeminal nerve (CN V)
66 Corpus medullare (central white matter of the cerebellar hemisphere)

Letter labels
4V Fourth ventricle
De Dentate nucleus

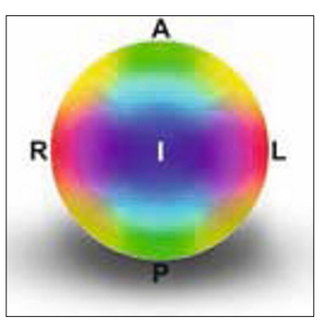

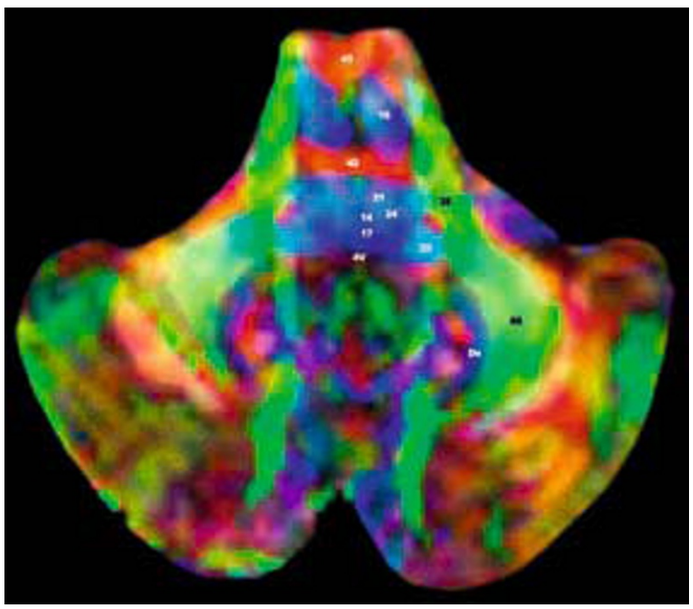

B

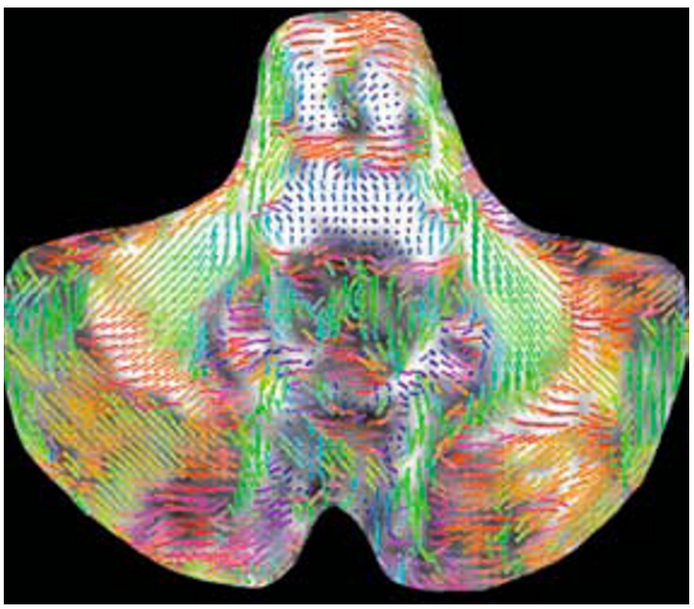

E

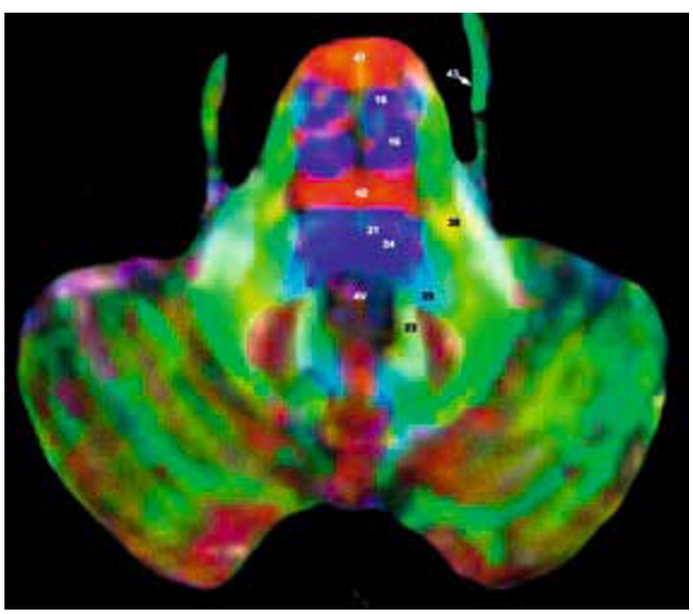

C

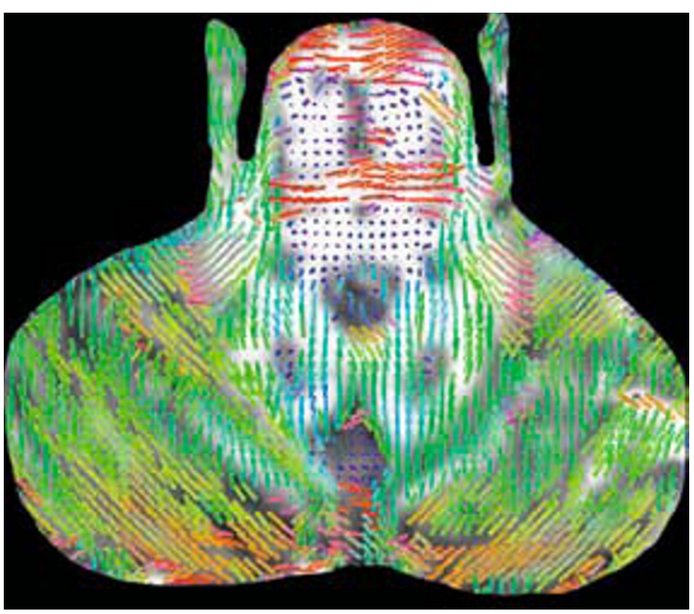

F

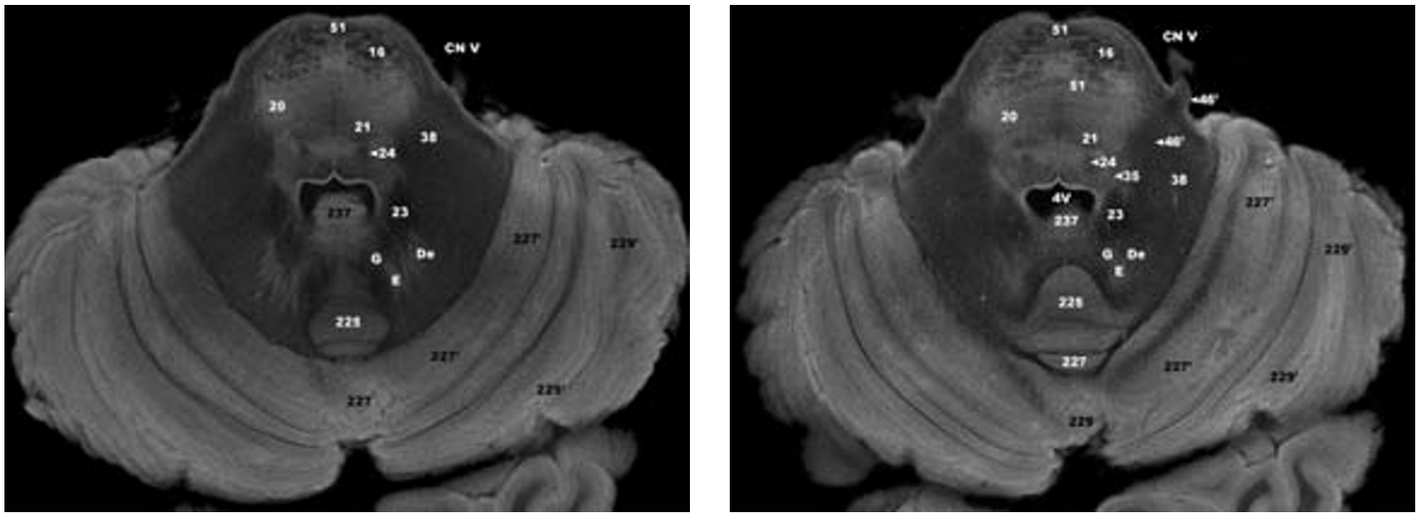

Fig. 10.19 (A–D) High pons and upper cerebellum. Axial plane.
A–D. 3 Tesla axial MRI of a formalin-fixed human brain specimen, displayed from caudal **(A)** to cranial **(D).**

16 Pyramid containing the corticospinal tract
20 Pontine nuclei
21 Medial lemniscus
23 Superior cerebellar peduncle
23′ Decussation of the superior cerebellar peduncle
24 Central tegmental tract
38 Middle cerebellar peduncle (brachium pontis)
46′ Intrapontine fascicles of the sensory root of CN V
47 Lateral lemniscus
51 Pontocerebellar fibers
223 Central lobule of vermis
223′ Wings of the central lobule
225 Culmen of the vermis
225′ Quandrangular lobule (anterior quadrangular lobule)
227 Declive of the vermis
227′ Simple lobule (posterior quadrangular lobule)
229 Folium of the vermis
229′ Superior semilunar lobule
237 Nodulus of the vermis

Letter labels
4V Fourth ventricle
CN V Cranial nerve V (trigeminal nerve)
De Dentate nucleus
E Emboliform nucleus
G Globose nucleus

Arrowheads and arrows
Single white arrowhead: Medial longitudinal fasciculus (also 17 in other images)

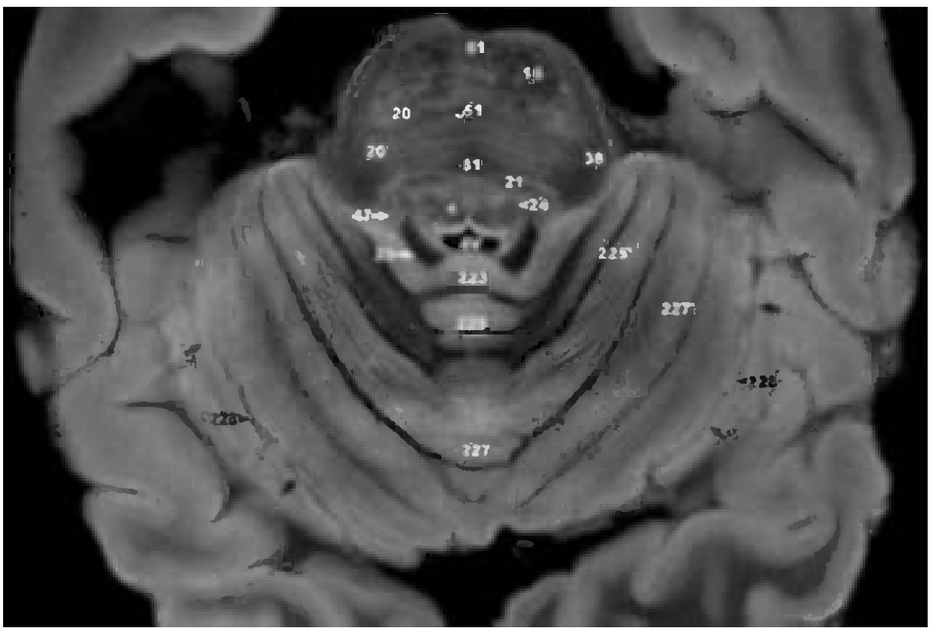

C

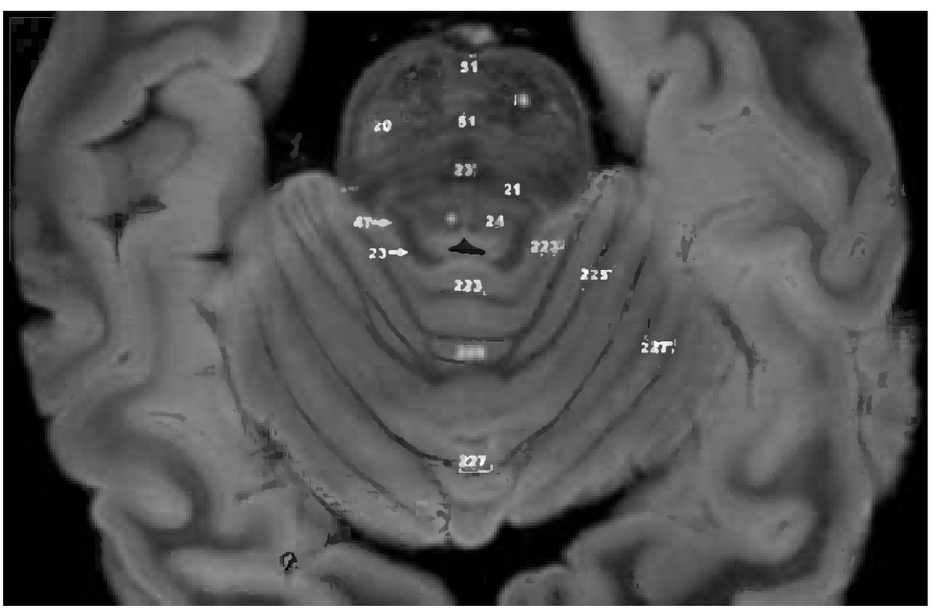

D

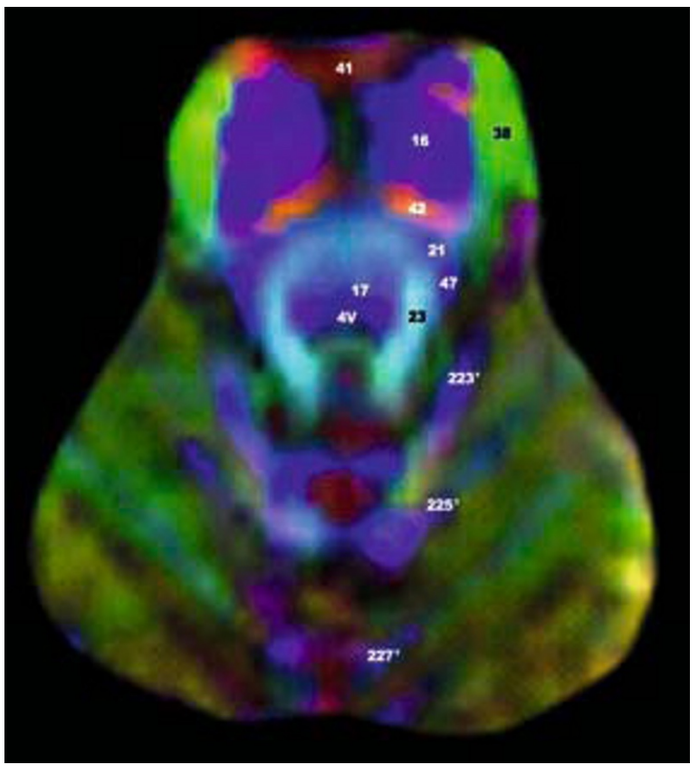

A

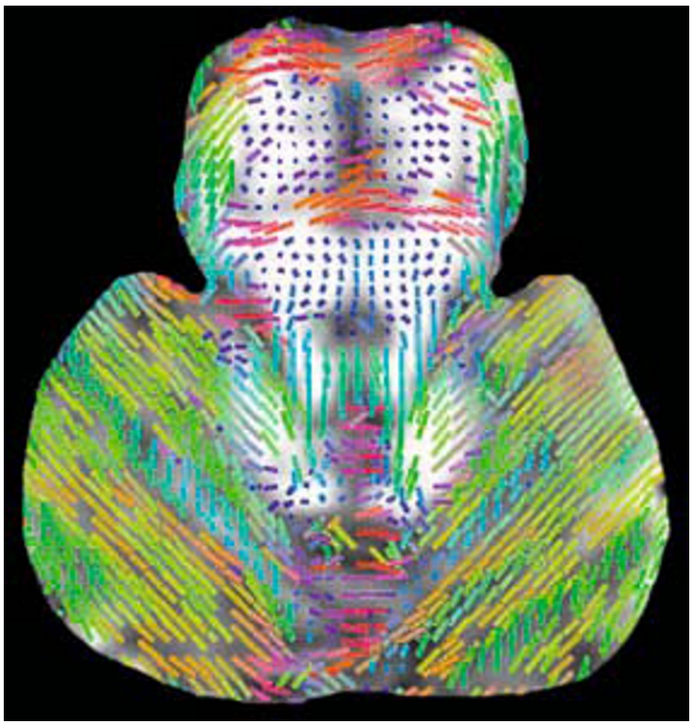

C

Fig. 10.20 (A–D) High pons and upper cerebellum. Axial plane.
Diffusion tensor imaging at two selected axial planes, displayed from caudal to cranial as
(A–B). Color maps
(C–D). Corresponding whisker plots

16 Corticospinal tract
17 Medial longitudinal fasciculus
21 Medial lemniscus
23 Superior cerebellar peduncle
23′ Decussation of the superior cerebellar peduncle
38 Middle cerebellar peduncle (brachium pontis)
41 Ventral pontine decussation
42 Dorsal pontine decussation
47 Lateral lemniscus
51 Pontocerebellar fibers
223′ Wing of central lobule
225′ Quadrangular lobule (anterior quadrangular lobule)
227′ Simple lobule (posterior quadrangular lobule)

Letter labels
4V Fourth ventricle
IP Interpeduncular fossa

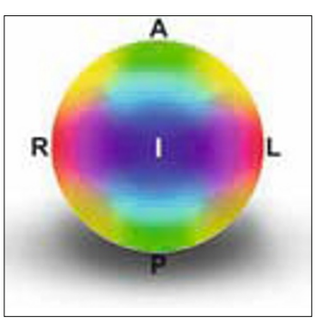

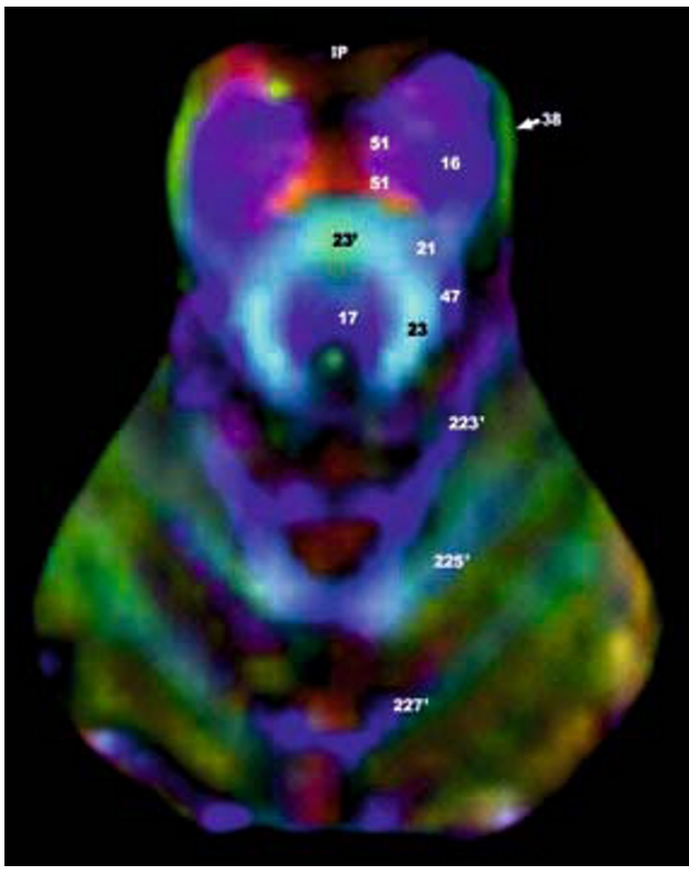

B

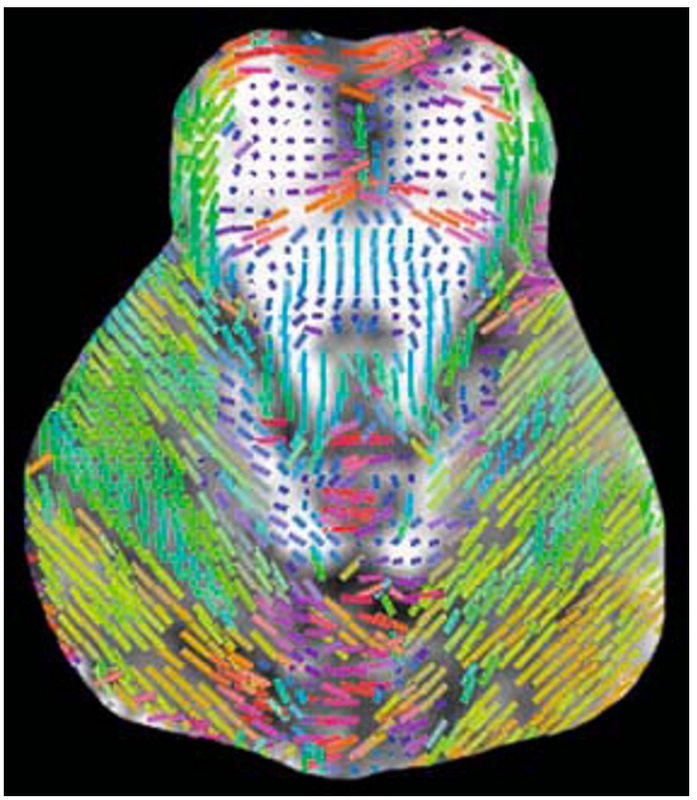

D

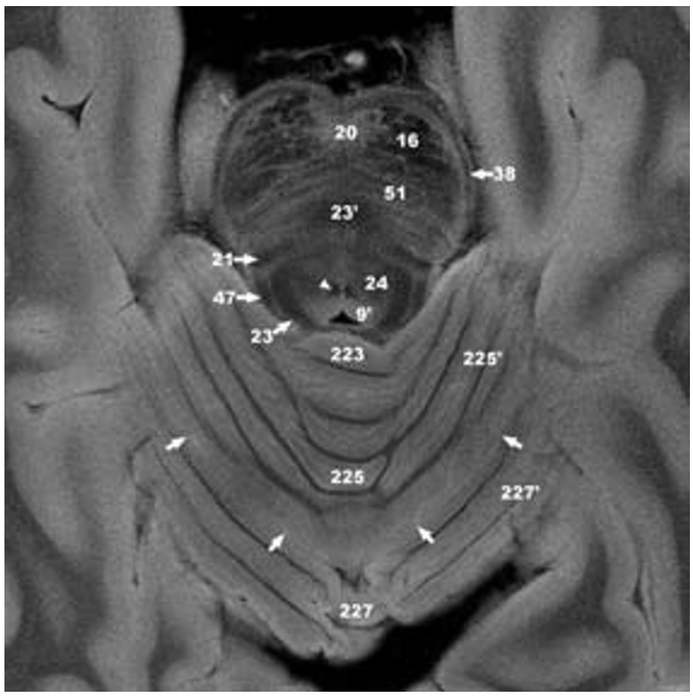

A

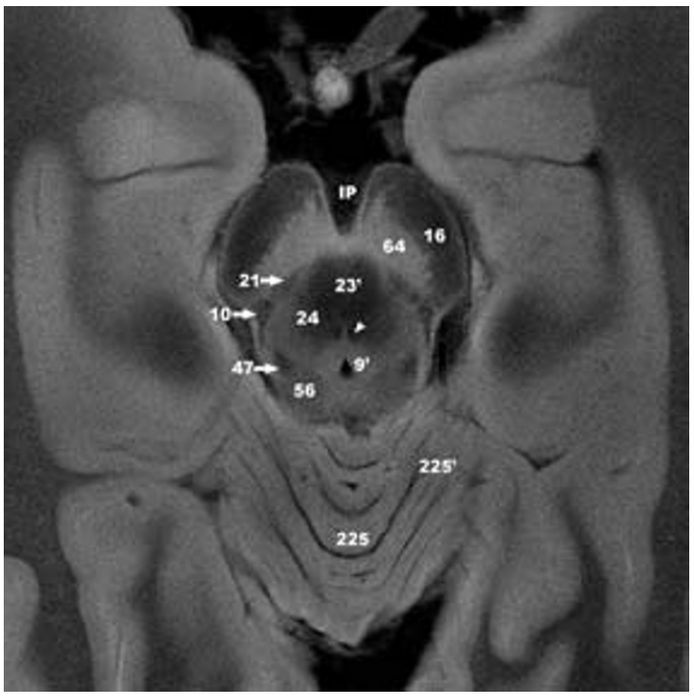

B

Fig. 10.21 (A–D) Midbrain. Axial plane.
A.-D. 3 Tesla axial MRI of a formalin-fixed human brain specimen, displayed from caudal **(A)** to cranial **(D).**

9′ Periaqueductal gray matter
10 Spinothalamic tract
16 Pyramid containing the corticospinal tract
20 Pontine nuclei
21 Medial lemniscus
23 Superior cerebellar peduncle
23′ Decussation of the superior cerebellar peduncle
24 Central tegmental tract
38 Middle cerebellar peduncle (brachium pontis)
47 Lateral lemniscus
51 Pontocerebellar fibers
56 Inferior colliculus
64 Substantia nigra
67 Brachium of the inferior colliculus
95 Red nucleus
100 Optic chiasm
223 Central lobule of vermis
225 Culmen of the vermis
225′ Quandrangular lobule (anterior quadrangular lobule)
227 Declive of the vermis
227′ Simple lobule (posterior quadrangular lobule)

Letter labels
CN II Cranial nerve II (optic nerve) (also 100)
CS Corticospinal fibers in the cerebral peduncle
F Frontopontine fibers in the cerebral peduncle
IP Interpeduncular fossa
PT Temporoparieto-occipital fibers in the cerebral peduncle

Arrowheads and arrows
Single white arrowheads: Medial longitudinal fasciculus (also 17)
White arrows: Primary (anterior superior) fissure between the anterior and posterior lobes of the cerebellum
Crossed white arrows: Pallidopeduncular tract (synonyms: pallidonigral tract and striato-peduncular tract)

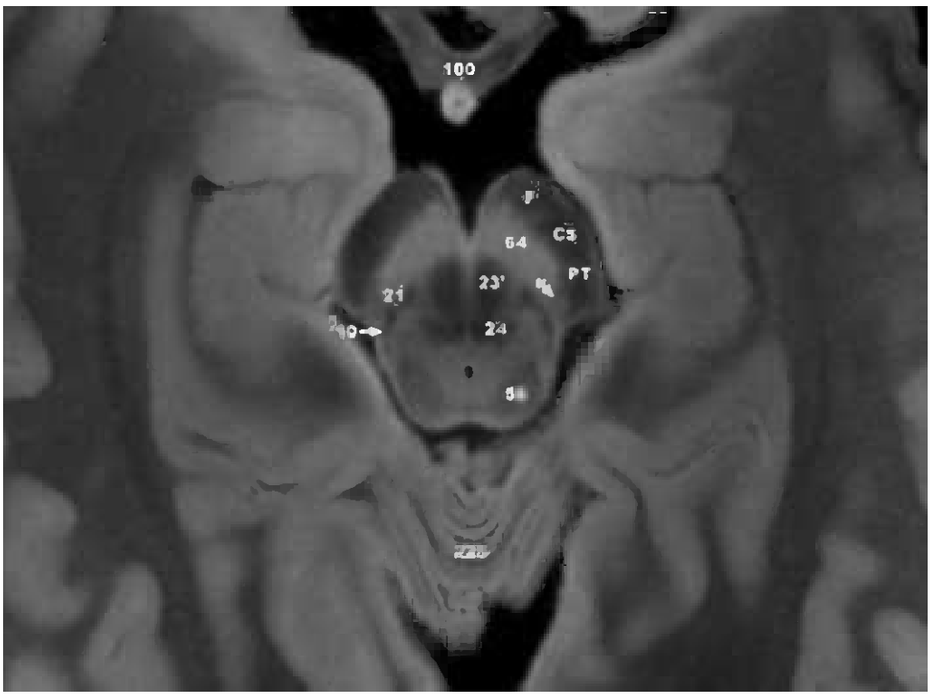

C

D

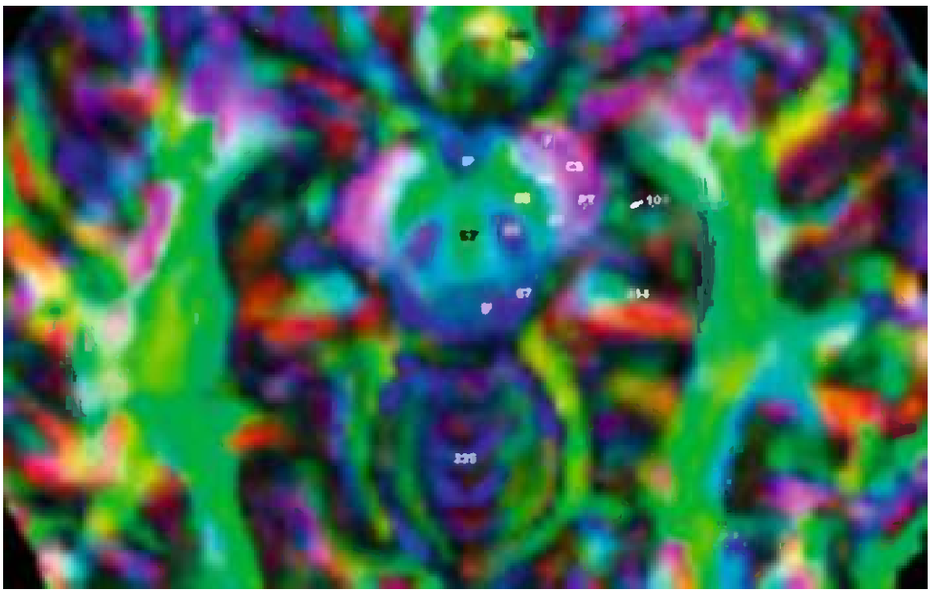

A

Fig. 10.22 (A–B). **Midbrain. Axial plane.**
Diffusion tensor imaging at the midbrain, displayed as a color map **(A)** and the corresponding whisker plot **(B).**

9′ Periaqueductal gray matter
21 Medial lemniscus
23 Superior cerebellar peduncle
63′ Intramesencephalic oculomotor fibers (CN III)
64 Substantia nigra
67 Brachium of the inferior colliculus
95 Red nucleus
101 Optic tract
140 Gyrus rectus
210 Hippocampal formation
225 Culmen of the vermis

Letter labels
CS Corticospinal fibers in the cerebral peduncle
F Frontopontine fibers in the cerebral peduncle
IP Interpeduncular fossa
PT Temporoparieto-occipital fibers in the cerebral peduncle

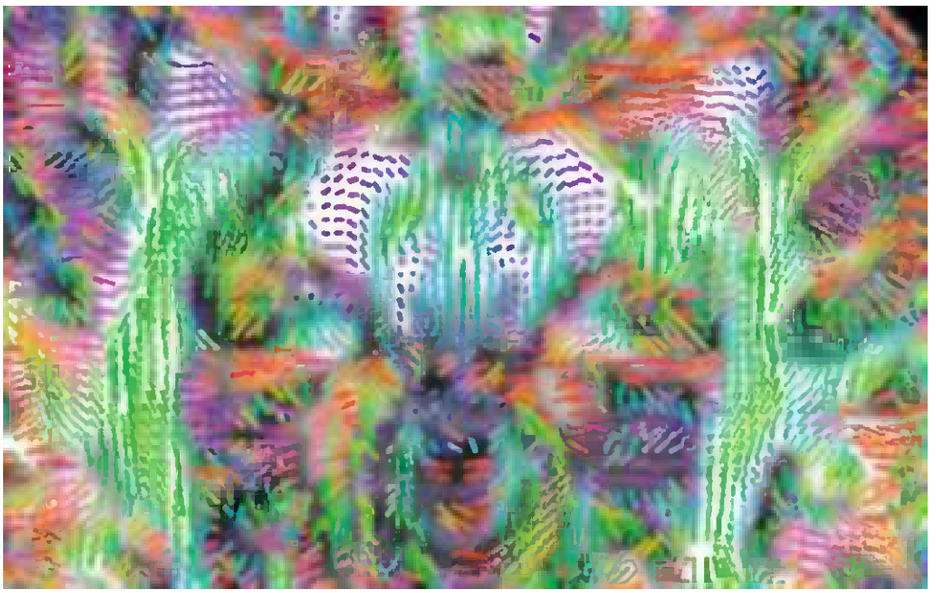

B

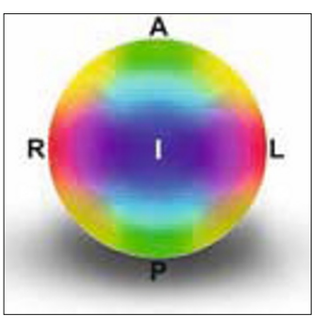

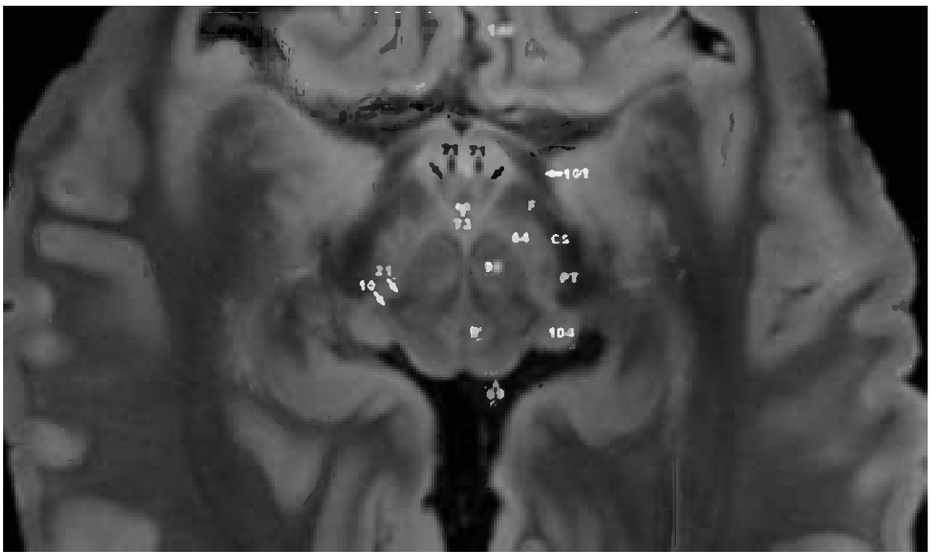

A

Fig. 10.23 (A–B). Diencephalon and basal ganglia. Axial plane.
A–B. 3 Tesla axial MRI of a formalin-fixed human brain specimen, displayed from caudal **(A)** to cranial **(B).**

9′ Periaqueductal gray matter
10 Spinothalamic tract
21 Medial lemniscus
64 Substantia nigra
69 Superior colliculus
71 Mammillary body
73 Principal mammillary fasciculus
75 Mammillothalamic fasciculus
77 Stria medullaris thalami
92 Pulvinar
95 Red nucleus
101 Optic tract
104 Medial geniculate body
170 Caudate nucleus (head)
173 Anterior commissure
175g Internal capsule (genu)
175p Internal capsule (posterior limb)
175r Internal capsule (retrolenticular portion)
178 Putamen
179l Globus pallidus (lateral nucleus, external nucleus)
179m Globus pallidus (medial nucleus, internal nucleus)
182 External and extreme capsules enclosing a portion of the claustrum
253 Corpus callosum, splenium
254 Forceps major

Letter labels
CS Corticospinal fibers in the cerebral peduncle
F Frontopontine fibers in the cerebral peduncle
PT Temporoparieto-occipital fibers in the cerebral peduncle

Arrowheads and arrows
Black arrows: Fornices (anterior columns) reaching mammillary bodies

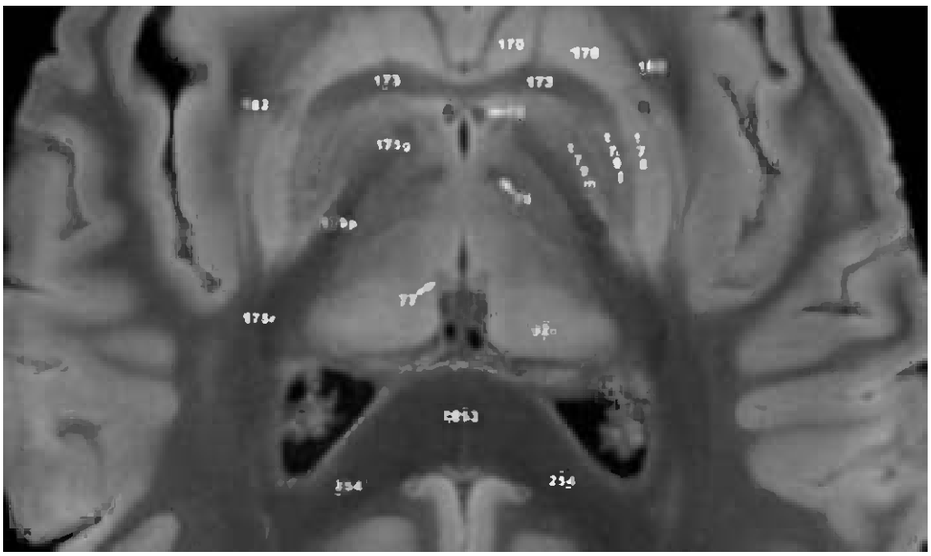

B

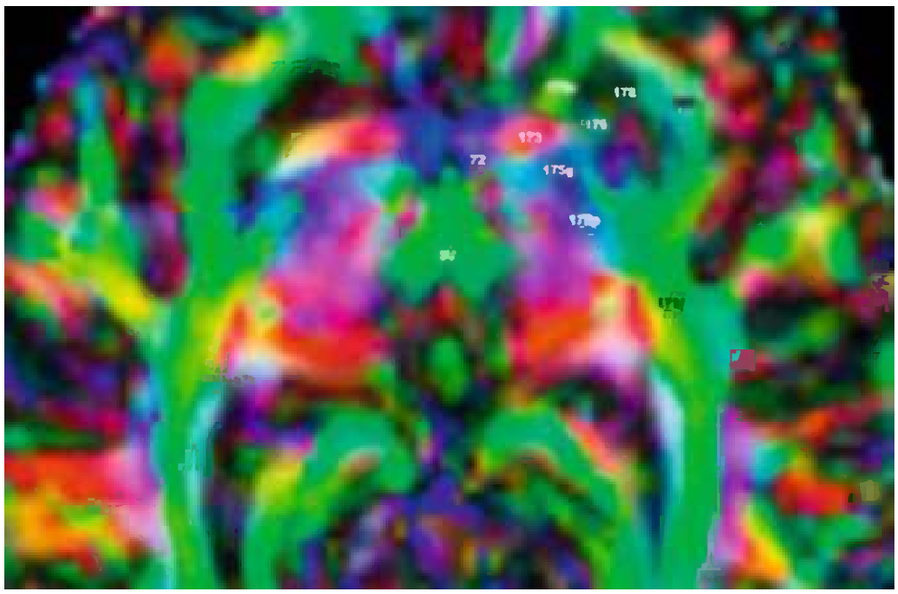

A

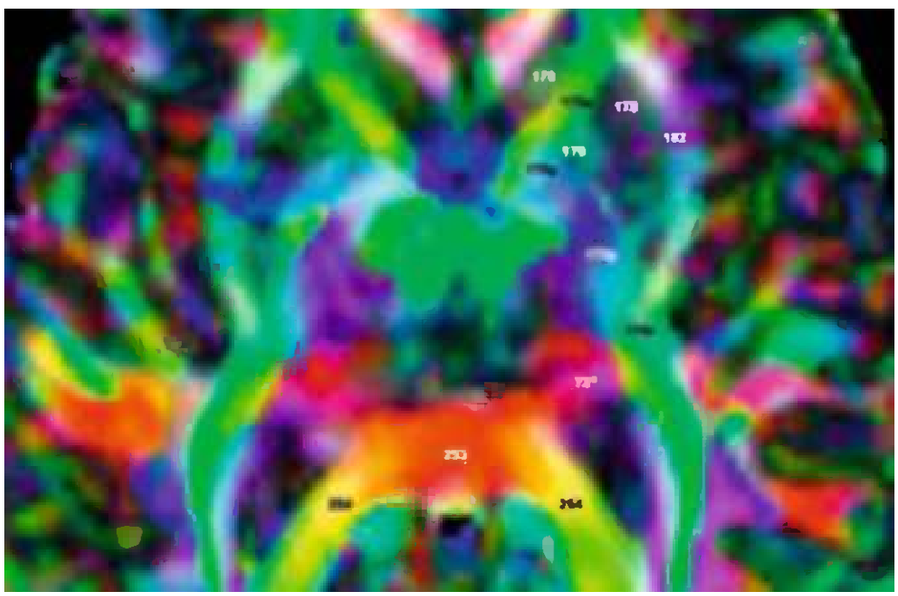

B

Fig. 10.24 (A–D). Diencephalon and basal ganglia. Axial. Diffusion tensor imaging at two levels, displayed as
(A–B). Color maps
(C–D). Corresponding whisker plots

72 Fornix (anterior column)
72″ Brachium of the superior colliculus (?)
170 Caudate nucleus (head)
173 Anterior commissure
175a Internal capsule (anterior limb)
175g Internal capsule (genu)
175p Internal capsule (posterior limb)
175r Internal capsule (retrolenticular portion)
178 Putamen
179 Globus pallidus
182 External and extreme capsules enclosing a portion of the claustrum
253 Corpus callosum, splenium
254 Forceps major

Letter labels
3V Third ventricle

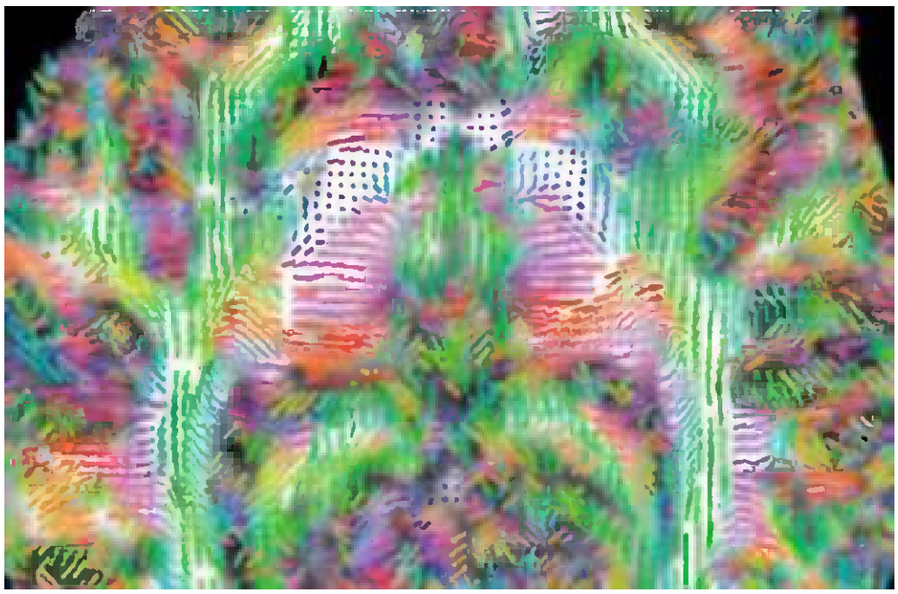

C

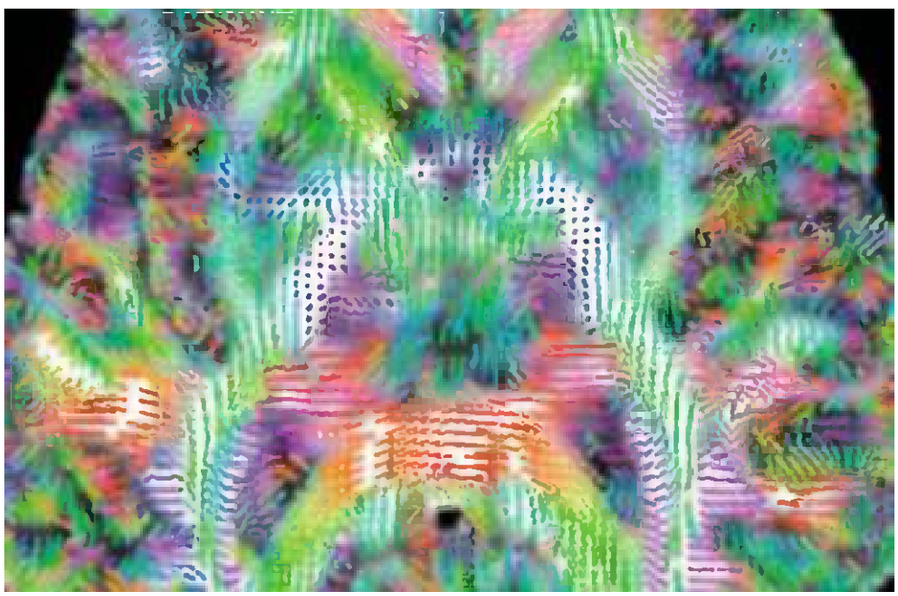

D

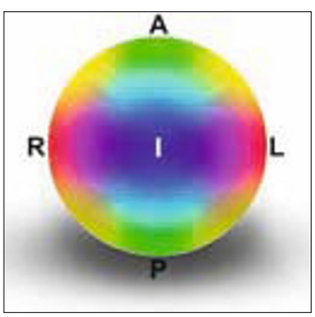

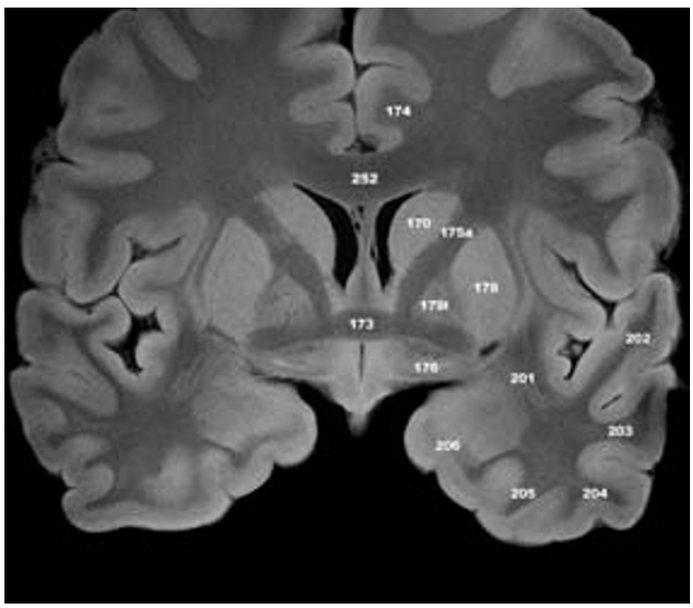

A

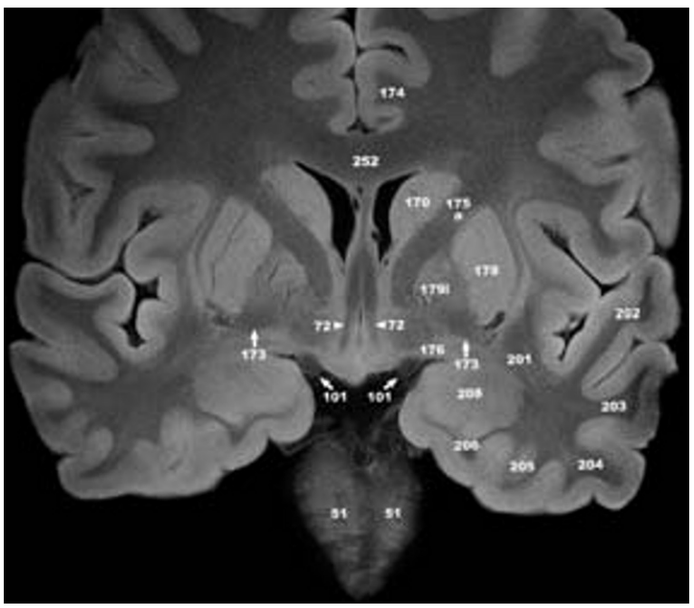

B

Coronal DTI correlations

Figures 10.25–10.33 correlate 3 Tesla coronal diffusion tensor images (DTI) of a living human volunteer with 3T MR images of a formalin-fixed human brain specimen. All the coronal images are presented in sequence at selected levels from anterior toward posterior position. The anatomic and DTI images selected have been grouped into broad regions to permit correlation despite slight slice-slice variation due to normal anatomic variation and to differences in scan angle.

Fig. 10.25 (A–D). The basal ganglia and and diencephalon. Anatomic-DTI Correlation. 3 Tesla coronal MRI of a formalin-fixed human brain specimen, displayed from anterior **(A)** to posterior **(D).**

16″ Corticospinal fibers descending through the pons toward the pyramid
51 Pontocerebellar fibers, seen longitudinally or in cut cross-section
60 Cerebral peduncle
71 Mammillary body
72 Fornix (anterior column)
101 Optic tract
157 Ansa lenticularis
158 Ansa peduncularis
170 Caudate nucleus (head)
173 Anterior commissure
174 Cingulate gyrus
175a Anterior limb of the internal capule
175g Genu of the internal capsule
176 Anterior perforated substance
178 Putamen
179l Lateral (external) nucleus of the globus pallidus
179m Medial (internal) nucleus of the globus pallidus
179′ Lateral (external) medullary lamina of the lenticular nucleus
201 Temporal stem (narrow attachment of the temporal lobe to the central brain)
202 Superior temporal gyrus
203 Middle temporal gyrus
204 Inferior temporal gyrus
205 Lateral occipito-temporal gyrus (fusiform gyrus)
206 Parahippocampal gyrus (also PHG)
208 Amygdala
210 Hippocampal formation
252 Corpus callosum, body

Arrowheads and arrows
Two black arrows: Mammillary bodies (capsules)

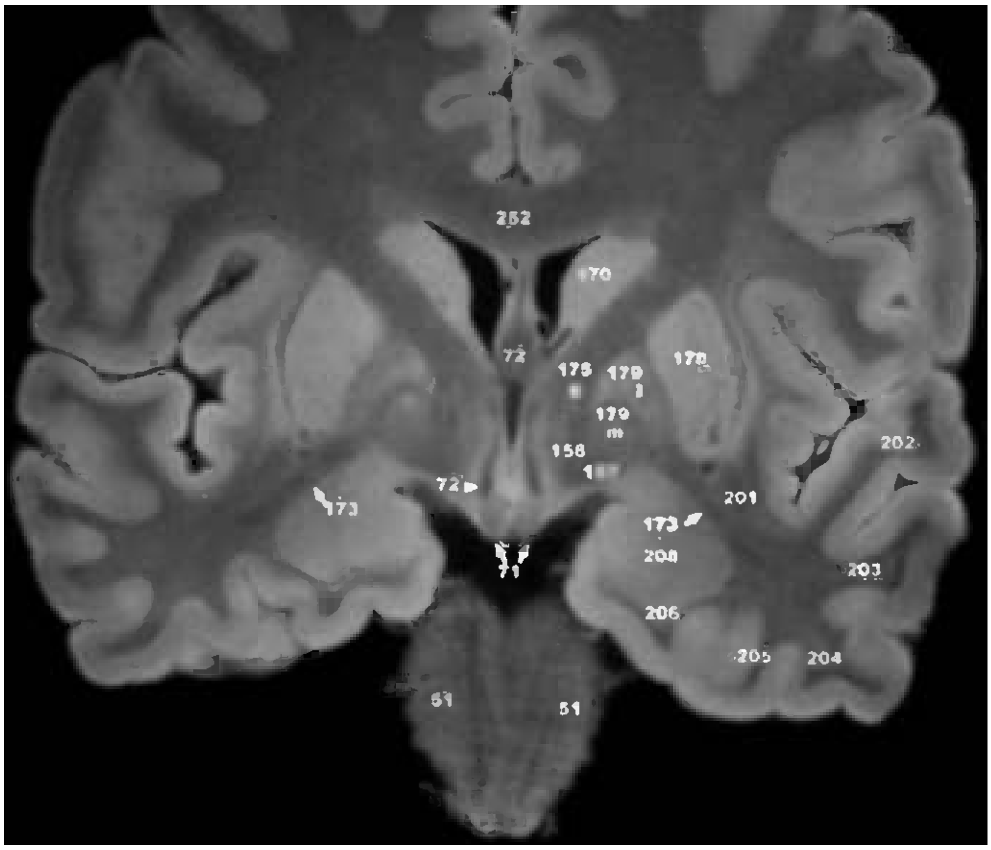

252
170
72
175
179
178
179
m
158
72
173
173
201
202
208
203
206
205
204
51
51

C

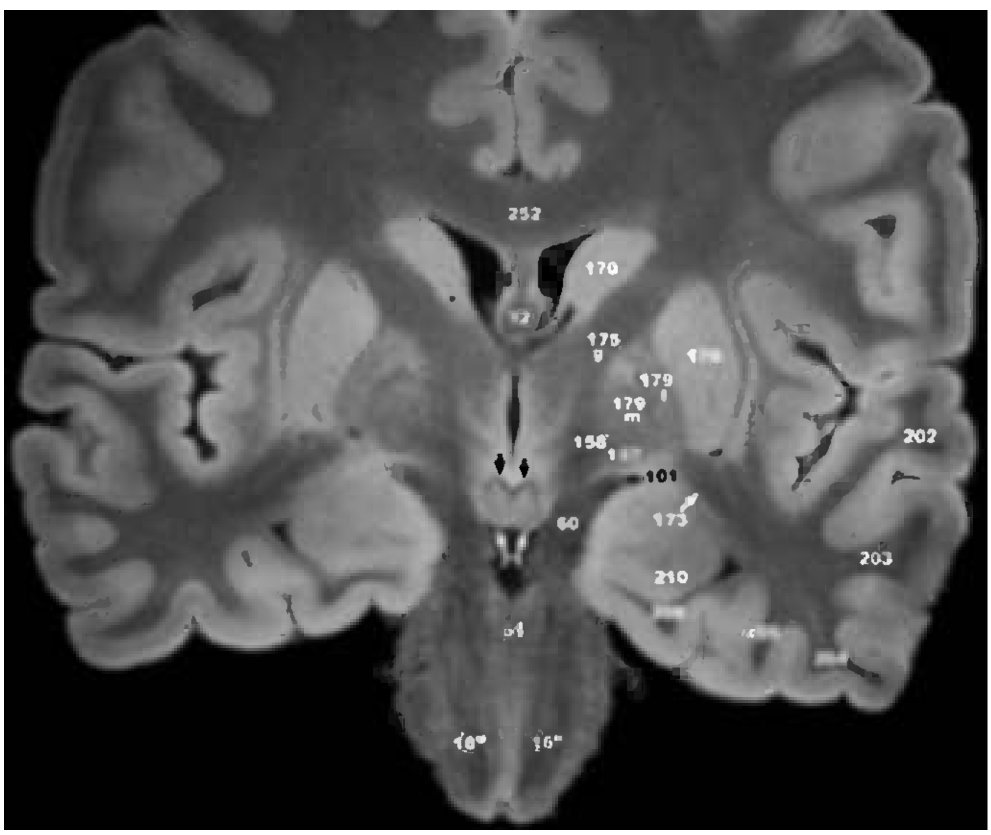

252
170
175
179
179
m
158
101
173
60
202
203
210

D

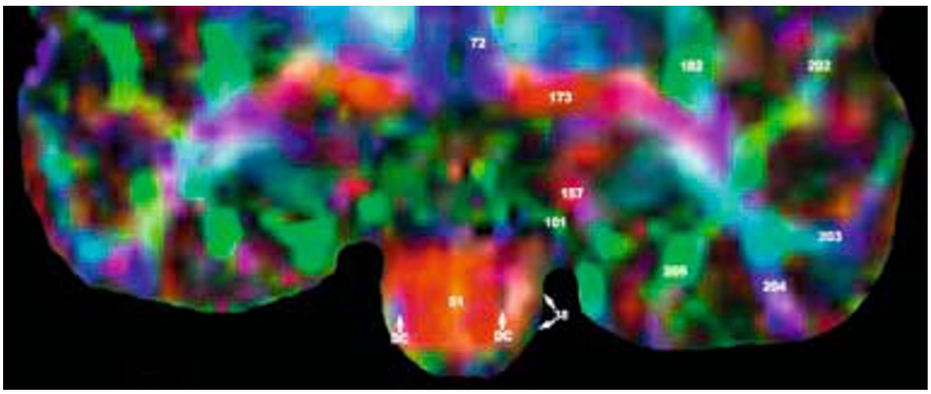

A

Fig. 10.26 (A–C). The basal ganglia and and diencephalon. Anatomic-DTI Correlation. Diffusion tensor imaging displayed as a color map **(A),** whisker plot **(B)** and tractogram **(C).**

38 Middle cerebellar peduncle (brachium pontis)
51 Pontocerebellar fibers, seen longitudinally or in cut cross-section
72 Fornix (anterior column)
101 Optic tract
157 Ansa lenticularis
173 Anterior commissure
182 Extreme capsule, claustrum and external capsule
202 Superior temporal gyrus
203 Middle temporal gyrus
204 Inferior temporal gyrus
205 Lateral occipito-temporal gyrus (fusiform gyrus)

Letter labels
DC Descending columns

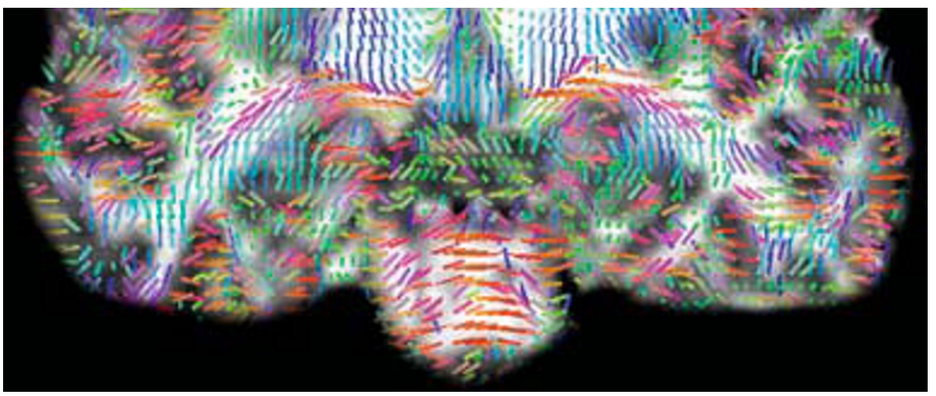

B

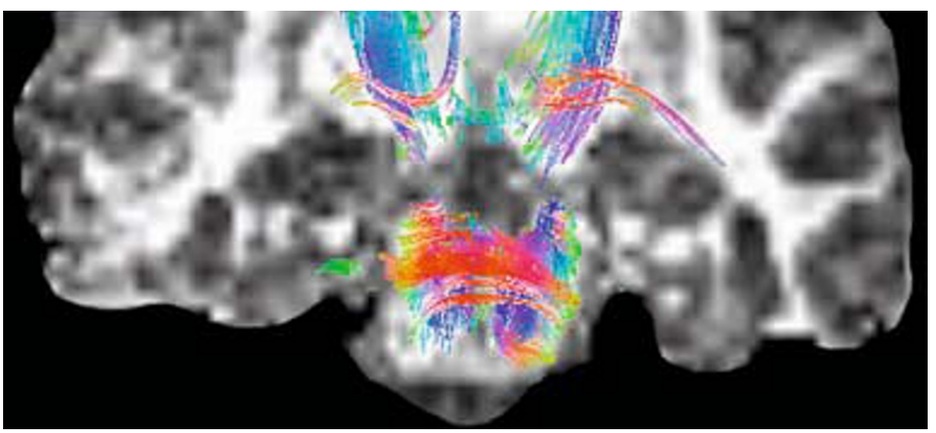

C

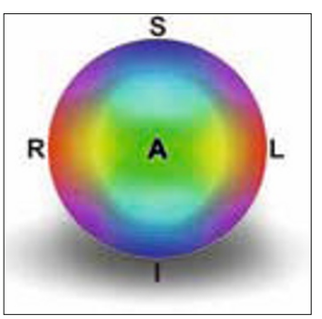

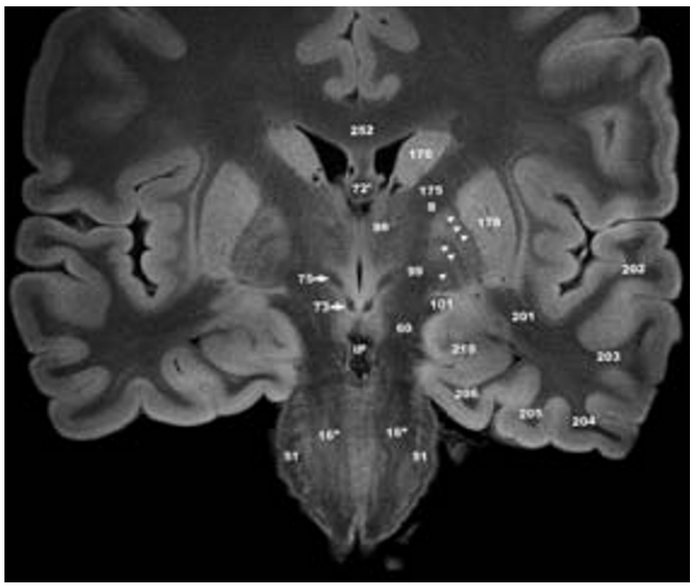

A

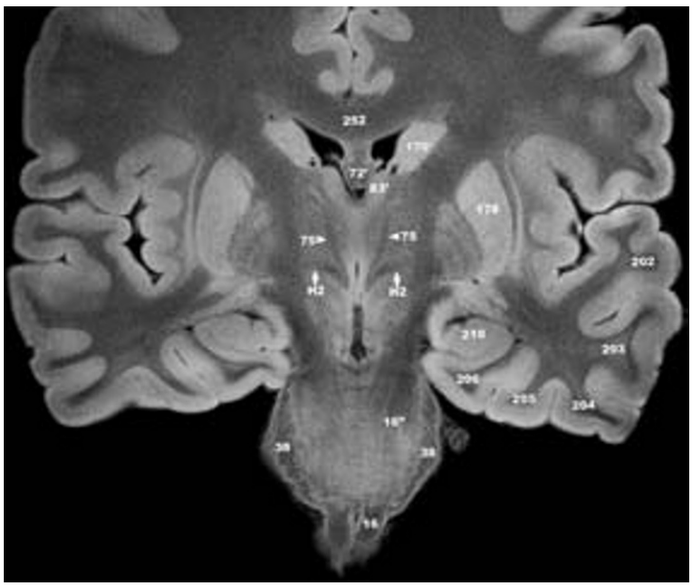

B

Fig. 10.27 (A–D). The diencephalon and anterior brain stem. Anatomic-DTI Correlation. 3 Tesla coronal MRI of a formalin-fixed human brain specimen, displayed from anterior **(A)** to posterior **(D).**

16 Pyramid containing the corticospinal tract
16″ Corticospinal fibers descending through the pons toward the pyramid
20 Pontine nuclei
21 Medial lemniscus
21+ Area tegmentalis containing the medial lemniscus, frontal radiations of the red nucleus, rubrothalamic tract and other structures
23′ Decussation of the superior cerebellar peduncle
24 Central tegmental tract
38 Middle cerebellar peduncle (brachium pontis)
51 Pontocerebellar fibers, seen longitudinally or in cut cross-section
60 Cerebral peduncle
64 Substantia nigra
72′ Fornix (body)
73 Principal mammillary fasciculus
75 Mammillothalamic fasciculus (also white arrows)
83′ Anteroventral nucleus of the thalamus
86 Nucleus lateralis thalami
95 Red nucleus
97 Subthalamic nucleus
99 Fields of Forel (H, H1 (thalamic fasciculus), and H2 (lenticular fasciculus))
101 Optic tract
170 Caudate nucleus (head)
170′ Caudate (body)
175 Internal capsule
175g Genu of the internal capsule
175p Posterior limb of the internal capsule
178 Putamen
201 Temporal stem (narrow attachment of the temporal lobe to the central brain)
202 Superior temporal gyrus
203 Middle temporal gyrus
204 Inferior temporal gyrus
205 Lateral occipito-temporal gyrus (fusiform gyrus)
206 Parahippocampal gyrus (also PHG)
210 Hippocampal formation
211 Transverse temporal gyrus (of Heschl)
227′ Simple lobule (posterior quadrangular lobule)
233″ Biventral lobule
237′ Flocculus
252 Corpus callosum, body

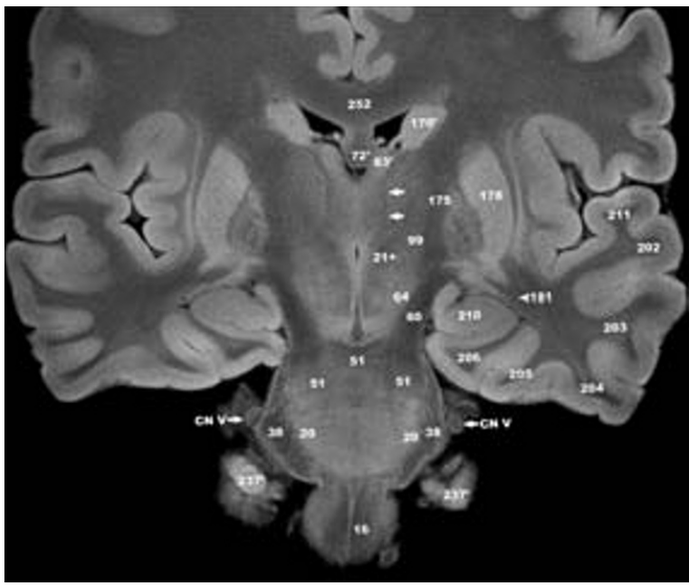

C

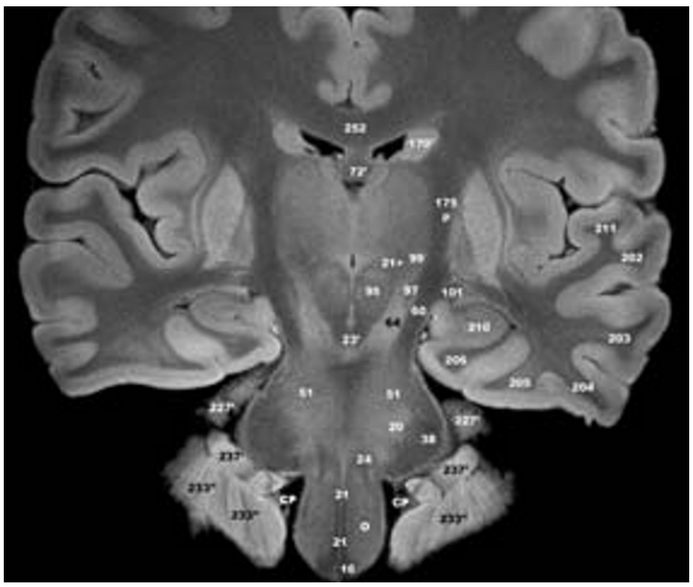

D

Letter labels

CN V	Cranial nerve V (trigeminal nerve)
CP	Choroid plexus at the lateral aperture of the foutth ventricle
H2	Forel field H2 (lenticular fasciculus) (also 99 – used generically for any of these fields)
IP	Interpeduncular fossa
O	Inferior olivary nucleus

Arrowheads and arrows

Single white arrowhead:	Intermediate medullary lamina within the medial nucleus of the globus pallidus
Two white arrowheads:	Internal medullary lamina of the lenticular nucleus between the medial and lateral nuclei of the globus pallidus
Three white arrowheads:	Lateral medullary lamina between the lateral nucleus of the globus pallidus and the putamen
White arrows:	Mammillothalamic fasciculus (also 75)

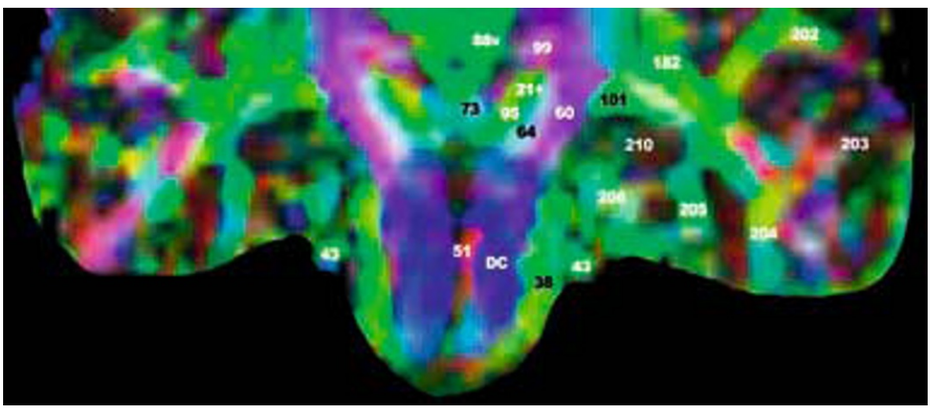

A

Fig. 10.28 (A–C). The diencephalon and anterior brain stem. Anatomic-DTI Correlation.
Diffusion tensor imaging displayed as a color map **(A),** whisker plot **(B)** and tractogram **(C).**

21+ Area tegmentalis containing the medial lemniscus, frontal radiations of the red nucleus, rubrothalamic tract and other structures
38 Middle cerebellar peduncle (brachium pontis)
43 Trigeminal nerve (CN V)
51 Pontocerebellar fibers, seen longitudinally or in cut cross-section
60 Cerebral peduncle
64 Substantia nigra
73 Principal mammillary fasciculus
88v Ventral thalamic peduncle
95 Red nucleus
99 Fields of Forel (H, H1 (thalamic fasciculus), and H2 (lenticular fasciculus))
101 Optic tract
182 Extreme capsule, claustrum and external capsule
202 Superior temporal gyrus
203 Middle temporal gyrus
204 Inferior temporal gyrus
205 Lateral occipito-temporal gyrus (fusiform gyrus)
206 Parahippocampal gyrus (also PHG)
210 Hippocampal formation

Letter labels
DC Descending columns

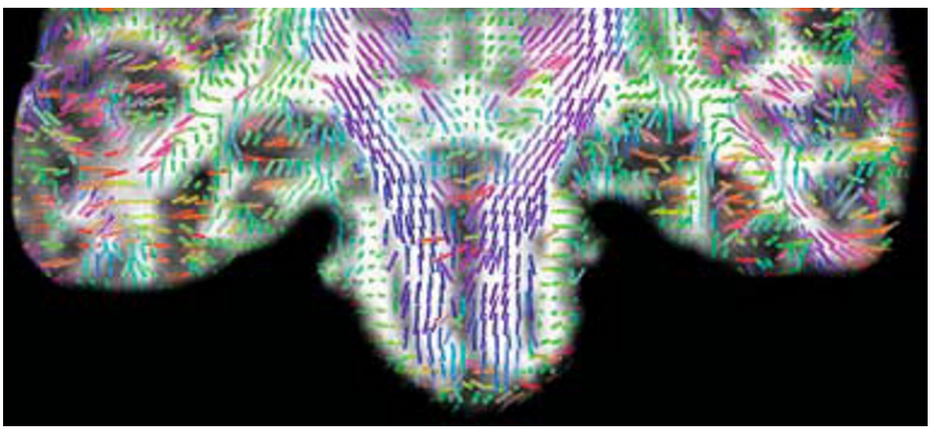

B

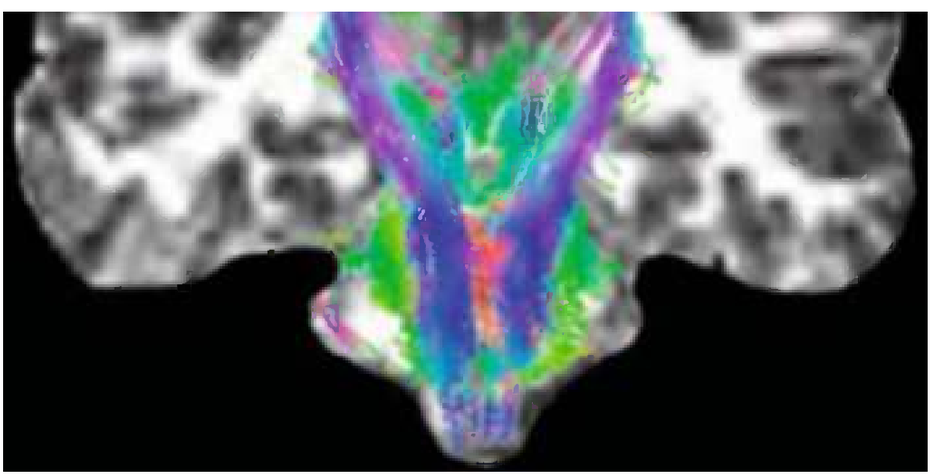

C

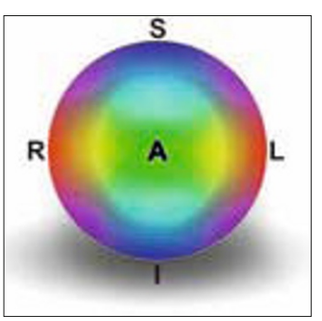

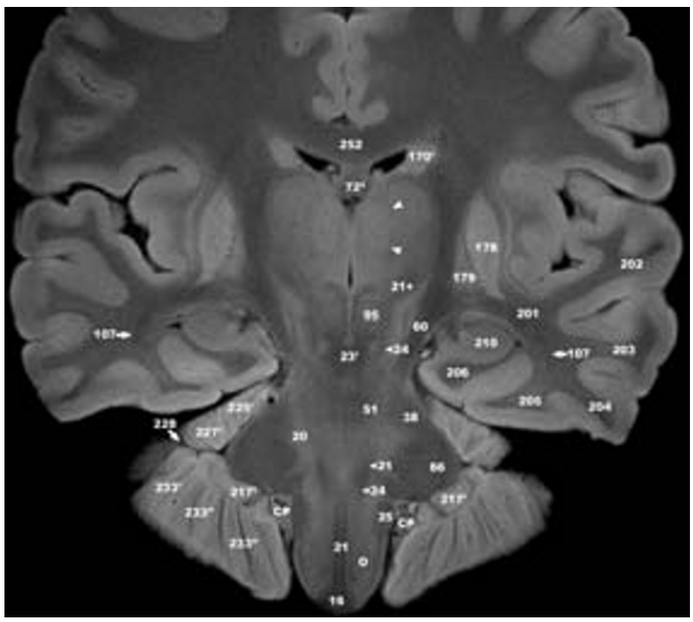

A

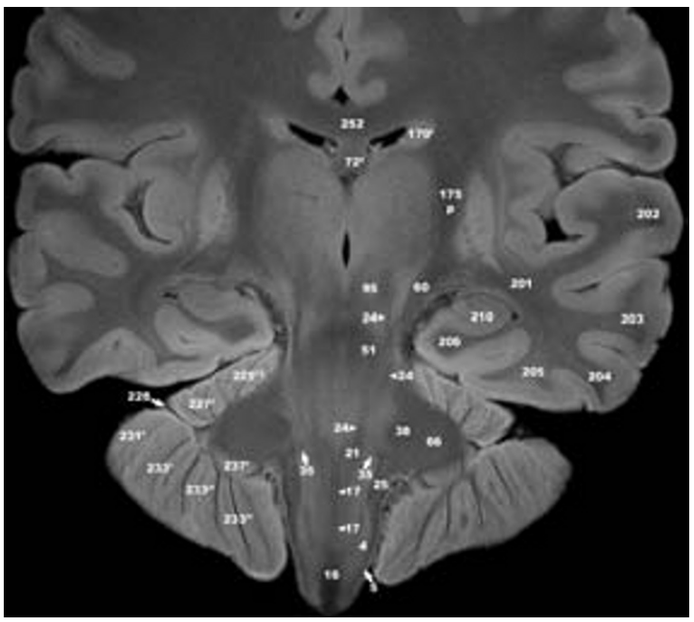

B

Fig. 10.29 (A–D). The posterior brain stem and anterior cerebellum. Anatomic-DTI Correlation. 3 Tesla coronal MRI of a formalin-fixed human brain specimen, displayed from anterior **(A)** to posterior **(D).**

1′ Fasciculus gracilis
2′ Fasciculus cuneatus
3 Spinal trigeminal tract
4 Spinal trigeminal nucleus
5 Posterior (dorsal) spinocerebellar tract
9′ Periaqueductal gray matter
10 Spinothalamic tract
16 Pyramid containing the corticospinal tract
17 Medial longitudinal fasciculus
20 Pontine nuclei
21 Medial lemniscus
21+ Area tegmentalis containing the medial lemniscus, frontal radiations of the red nucleus, rubrothalamic tract and other structures
23 Superior cerebellar peduncle
23′ Decussation of the superior cerebellar peduncle
24 Central tegmental tract
25 Inferior cerebellar peduncle (restiform body)
35 Facial nerve (CN VII)
38 Middle cerebellar peduncle (brachium pontis)
39 Abducens nucleus
47 Lateral lemniscus
51 Pontocerebellar fibers, seen longitudinally or in cut cross-section
60 Cerebral peduncle
66 Corpus medullare (central white matter of the cerebellar hemisphere)
67 Brachium of the inferior colliculus
69′ Commissure of the superior colliculus
70 Brachium of the superior colliculus
72′ Fornix (body)
76 Habenular nuclei
77 Stria medullaris thalami
78 Habenulo-interpeduncular tract (fasciculus retroflexus)
87 Nucleus reticularis thalami (within the lateral (external) medullary lamina of the thalamus)
95 Red nucleus
104 Medial geniculate body
106 Lateral geniculate body
107 Optic radiations (geniculocalcarine radiations)
170′ Caudate (body)

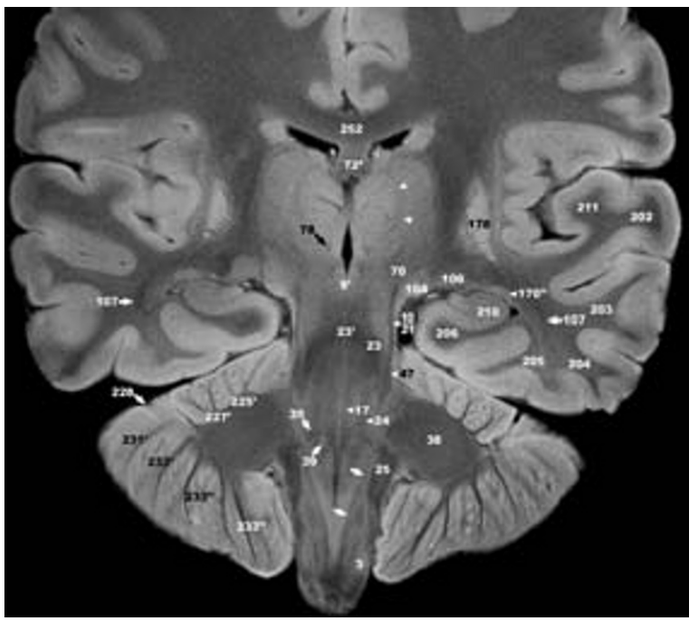

C

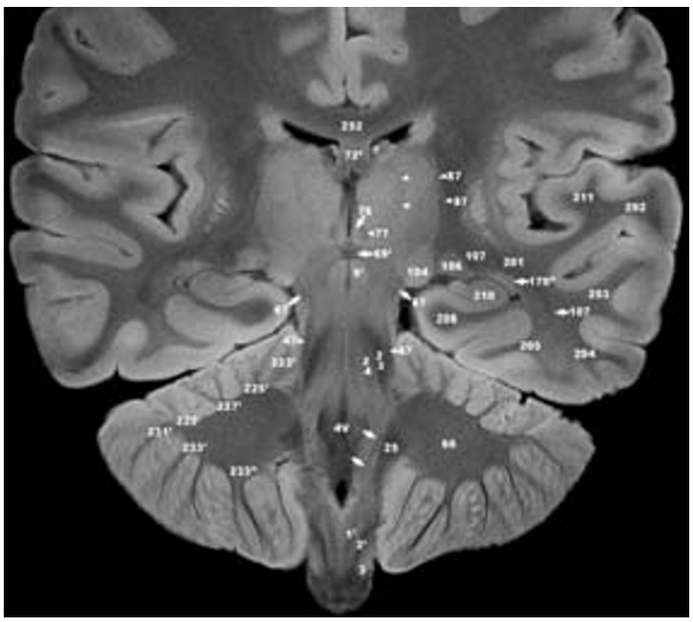

D

170″ Caudate (tail)
175p Posterior limb of the internal capsule
178 Putamen
179 Globus pallidus
201 Temporal stem (narrow attachment of the temporal lobe to the central brain)
202 Superior temporal gyrus
203 Middle temporal gyrus
204 Inferior temporal gyrus
205 Lateral occipito-temporal gyrus (fusiform gyrus)
206 Parahippocampal gyrus (also PHG)
210 Hippocampal formation
211 Transverse temporal gyrus (of Heschl)
223′ Wings of the central lobule
225′ Quandrangular lobule (anterior quadrangular lobule)
227′ Simple lobule (posterior quadrangular lobule)
228 Posterior superior fissure (post clival fissure)
231′ Inferior semilunar lobule
233′ Gracile lobule
233″ Biventral lobule
237′ Flocculus
252 Corpus callosum, body

Letter labels

4V Fourth ventricle
CP Choroid plexus at the lateral aperture of the fourth ventricle
O Inferior olivary nucleus

Arrowheads and arrows

Two white arrowheads: Internal medullary lamina of the thalamus
Two white arrows: Solitary tract

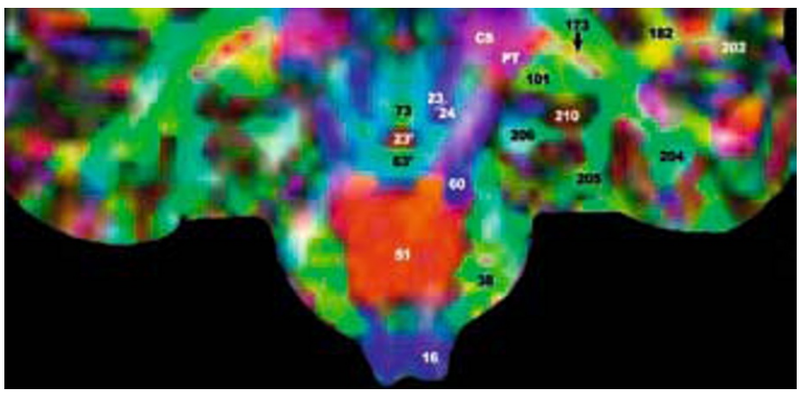

A

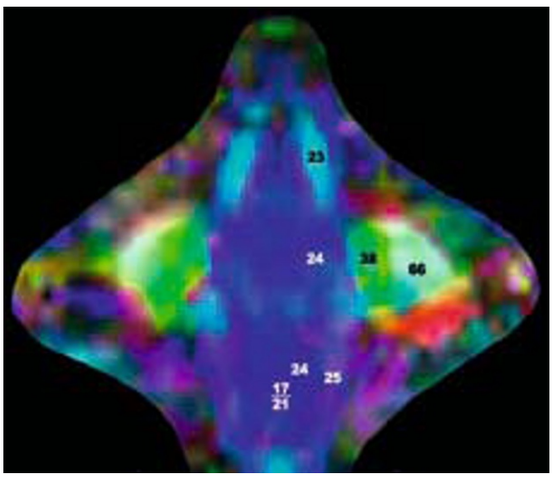

B

Fig. 10.30 (A–F). The posterior brain stem and anterior cerebellum. Anatomic-DTI Correlation.
Diffusion tensor imaging displayed as
A–B. Color maps
C–D. Whisker plots, and
E–F. Tractograms

16 Pyramid containing the corticospinal tract
17 Medial longitudinal fasciculus
21 Medial lemniscus
23 Superior cerebellar peduncle
23′ Decussation of the superior cerebellar peduncle
24 Central tegmental tract
25 Inferior cerebellar peduncle (restiform body)
38 Middle cerebellar peduncle (brachium pontis)
51 Pontocerebellar fibers, seen longitudinally or in cut cross-section
60 Cerebral peduncle
63′ Intramesencephalic oculomotor fibers (CN III)
66 Corpus medullare (central white matter of the cerebellar hemisphere)
73 Principal mammillary fasciculus
101 Optic tract
173 Anterior commissure
182 Extreme capsule, claustrum and external capsule
202 Superior temporal gyrus
204 Inferior temporal gyrus
205 Lateral occipito-temporal gyrus (fusiform gyrus)
206 Parahippocampal gyrus (also PHG)
210 Hippocampal formation

Letter labels
CS Corticospinal tract
PT Parietotemporopontine tract

C

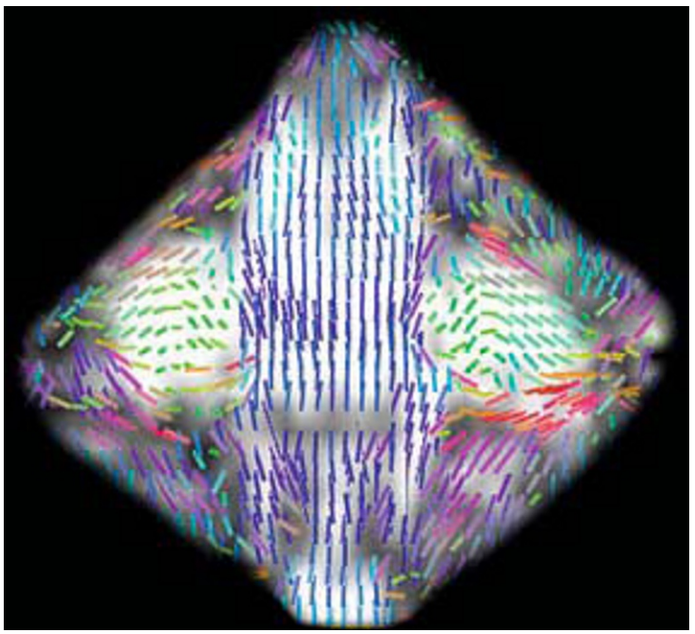

D

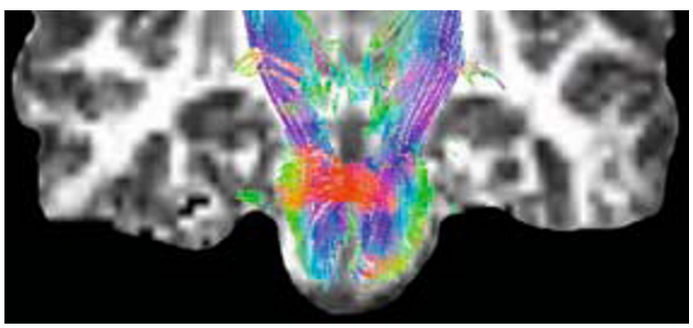

E

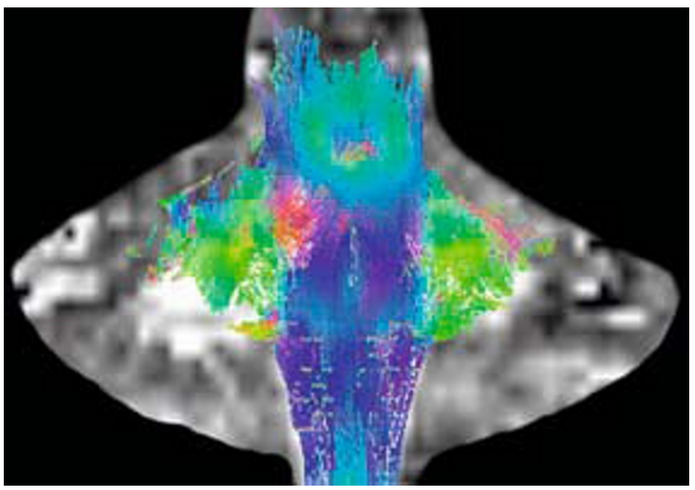

F

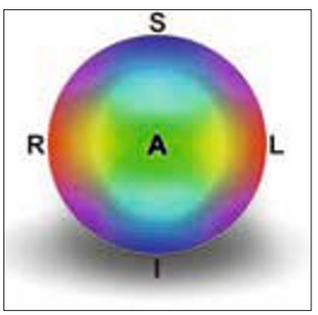

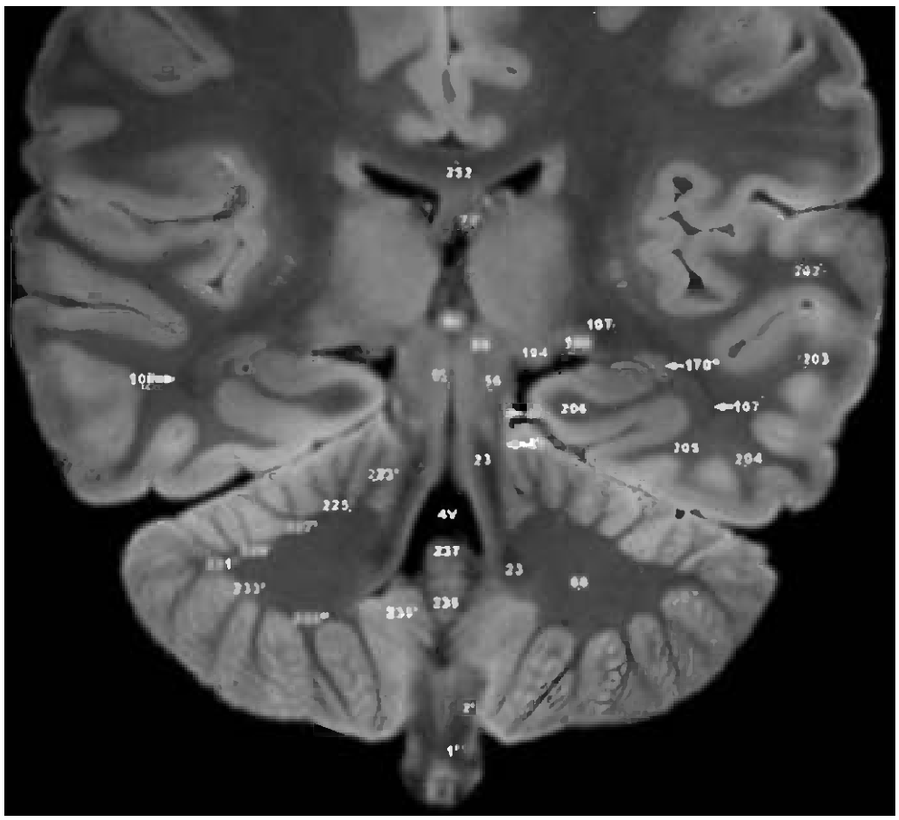

A

Fig. 10.31 (A–C). The mid-cerebellum. Anatomic-DTI Correlation. 3 Tesla coronal MRI of a formalin-fixed human brain specimen, displayed from anterior **(A)** to posterior **(C).**

1′ Fasciculus gracilis
2′ Fasciculus cuneatus
9′ Periaqueductal gray matter
23 Superior cerebellar peduncle
47 Lateral lemniscus
56 Inferior colliculus
66 Corpus medullare (central white matter of the cerebellar hemisphere)
69 Superior colliculus
72′ Fornix (body)
104 Medial geniculate body
106 Lateral geniculate body
107 Optic radiations (geniculocalcarine radiations)
170″ Caudate (tail)
202 Superior temporal gyrus
203 Middle temporal gyrus
204 Inferior temporal gyrus
205 Lateral occipito-temporal gyrus (fusiform gyrus)
206 Parahippocampal gyrus (also PHG)
223 Central lobule of vermis
223′ Wings of the central lobule
225′ Quandrangular lobule (anterior quadrangular lobule)
227′ Simple lobule (posterior quadrangular lobule)
229′ Superior semilunar lobule
231′ Inferior semilunar lobule of the vermis
233′ Gracile lobule
233″ Biventral lobule
235 Uvula of the vermis (Also U)
235′ Tonsil of the cerebellum (Also T)
237 Nodulus of the vermis
252 Corpus callosum, body

Letter labels
4V Fourth ventricle
De Dentate nucleus
De′ Hilum of dentate nucleus
Pi Pineal gland
VG Vein of Galen

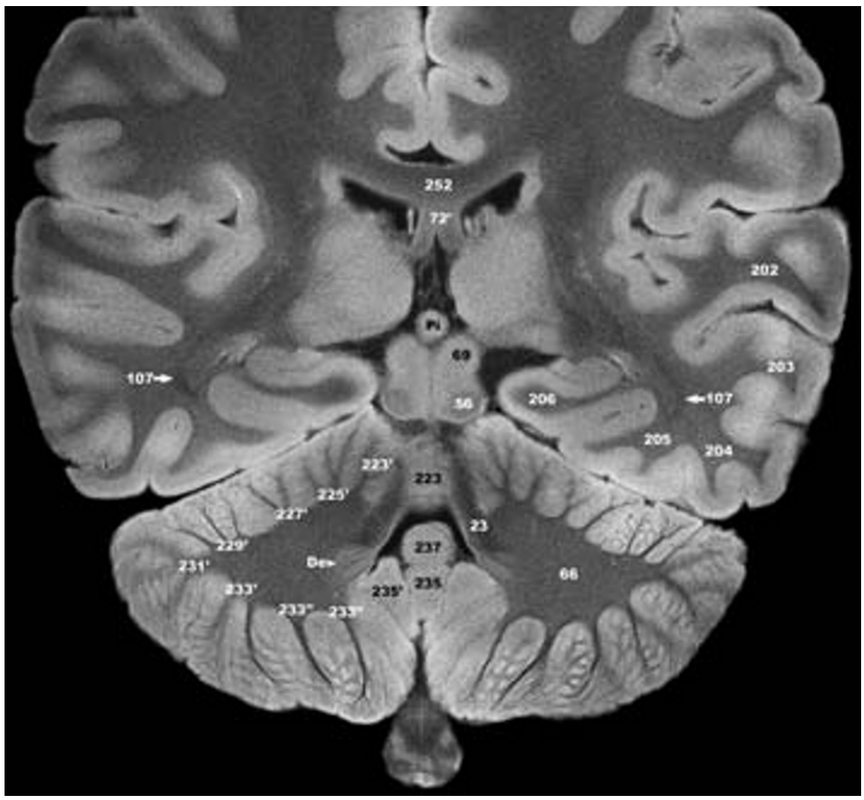
252
72'
202
Pi
69
107
203
56
206
107
205
204
223'
223
225'
227'
23
229'
237
231'
Dev
66
233'
235'
235
233"
233"

B

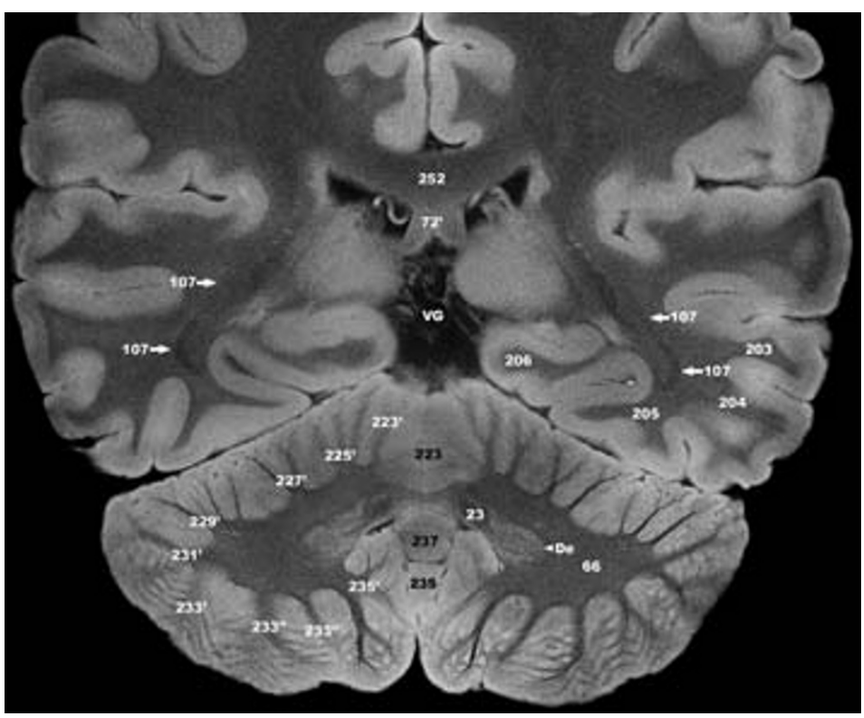
252
72'
107
VG
107
107
203
206
107
205
204
223'
225'
223
227'
23
229'
237
231'
De
66
235'
235
233'
233"
233"

C

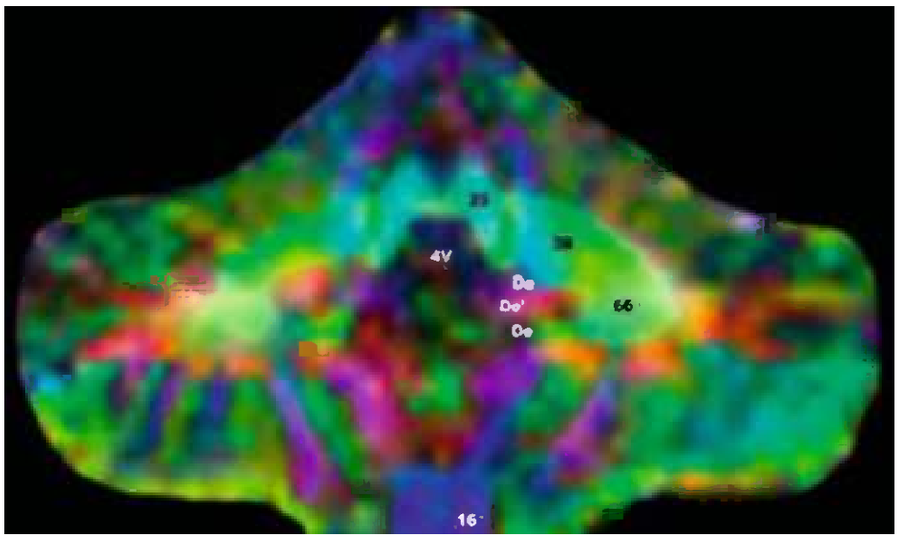

A

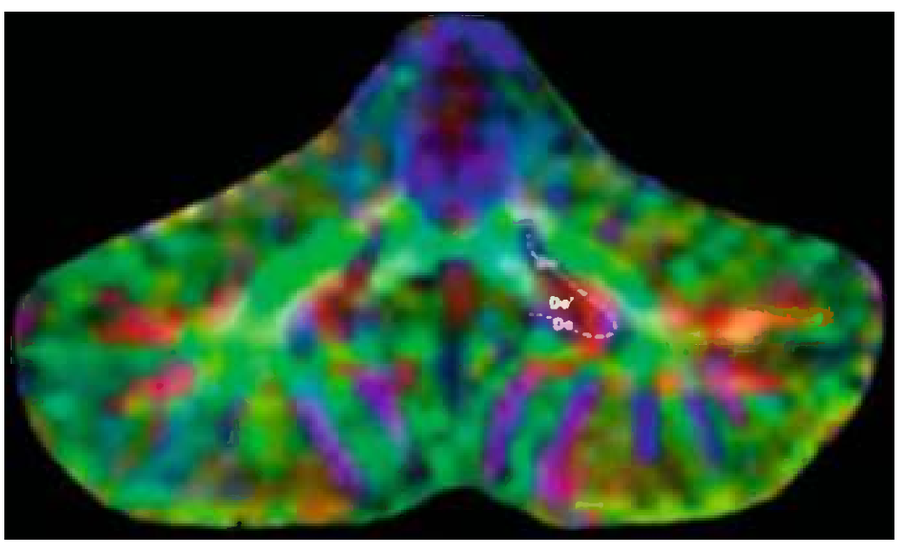

B

Fig. 10.32 (A–F). The mid-cerebellum. Anatomic-DTI Correlation. Diffusion tensor imaging displayed as
A–B. Color maps
C–D. Whisker plots
E–F. Tractograms

16 Pyramid containing the corticospinal tract
23 Superior cerebellar peduncle
38 Middle cerebellar peduncle (brachium pontis)
66 Corpus medullare (central white matter of the cerebellar hemisphere)

Letter labels
4V Fourth ventricle
De Dentate nucleus and hilum (De')

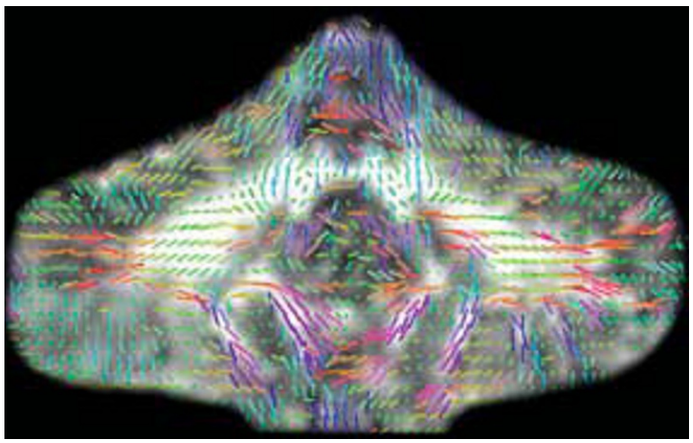

C

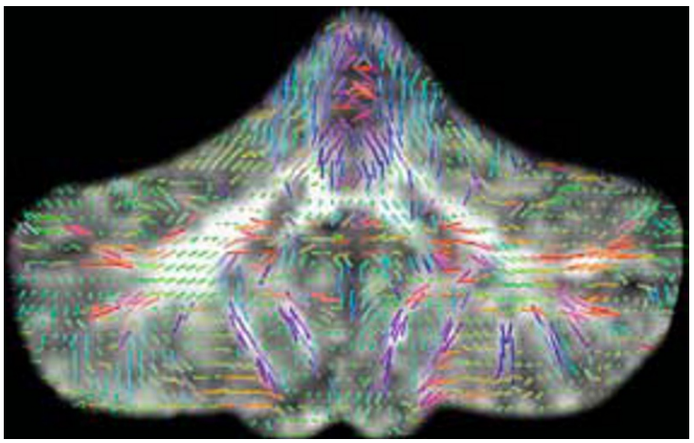

D

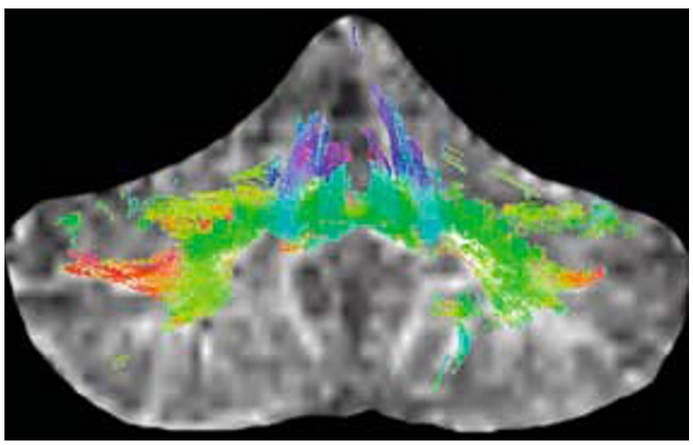

E

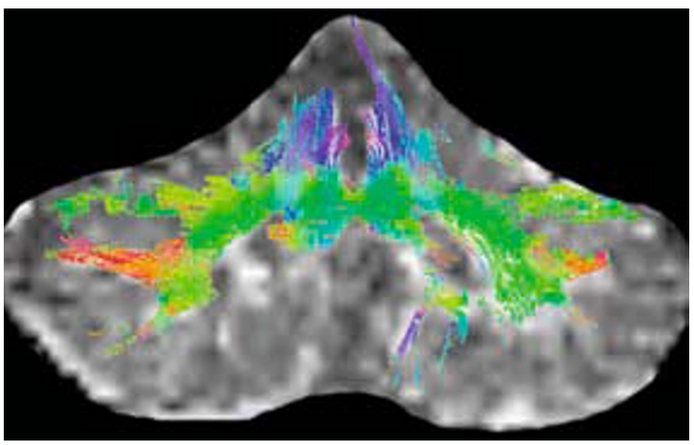

F

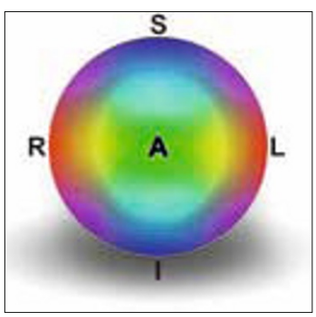

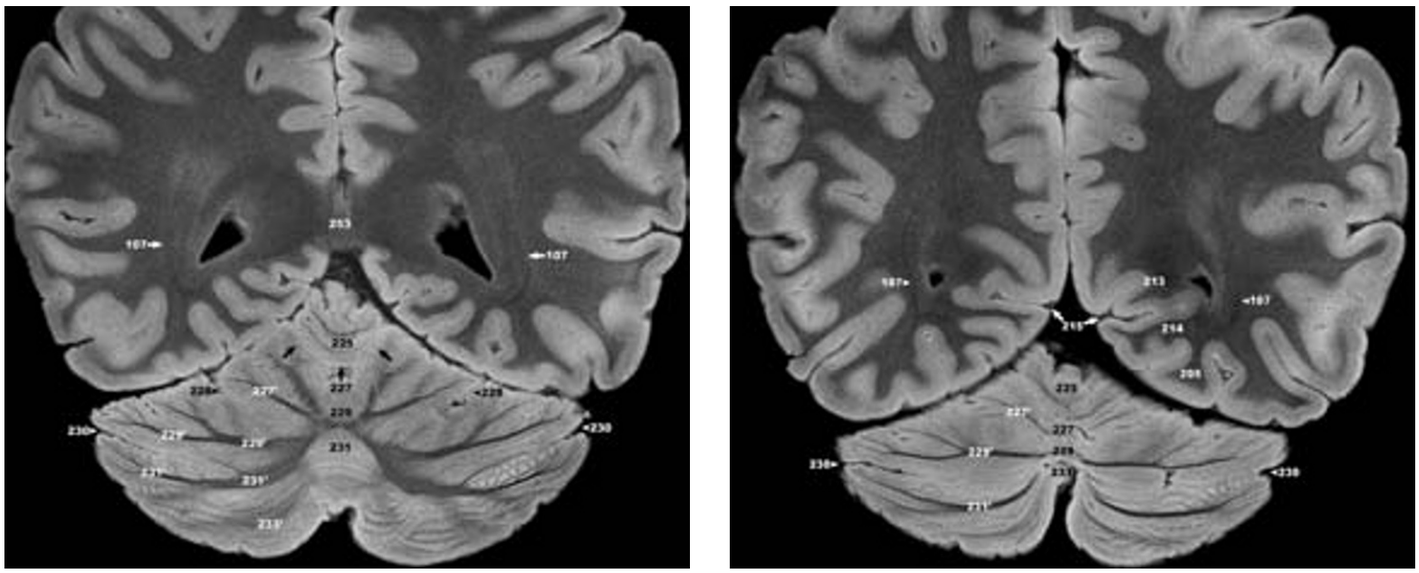

A B

Fig. 10.33 (A–E). The posterior cerebellum. Anatomic-DTI Correlation.
A–B. 3 Tesla coronal MRI of a formalin-fixed human brain specimen, displayed from anterior **(A)** to posterior **(B).**
C–E. Diffusion tensor imaging displayed as a color map **(C),** whisker plot **(D)** and tractogram **(E).**

107 Optic radiations (geniculocalcarine radiations)
205 Lateral occipito-temporal gyrus (fusiform gyrus)
213 Cuneus
214 Lingual gyrus
215 Calcarine sulcus
225 Culmen
227 Declive of the vermis
227′ Simple lobule (posterior quadrangular lobule)
228 Posterior superior fissure (post clival fisssure)
229 Folium of the vermis
229′ Superior semilunar lobule
230 Great horizontal fissure
231 Tuber of the vermis
231′ Inferior semilunar lobule of the vermis
233′ Gracile lobule
253 Corpus callosum, splenium

Arrowheads and arrows
Black arrows: Primary fissure between the anterior and posterior lobes

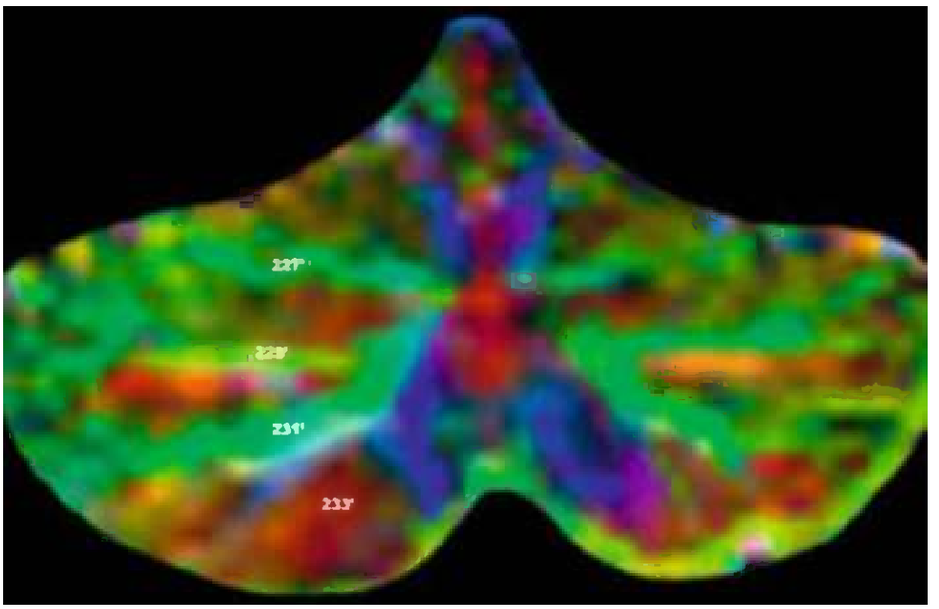

C

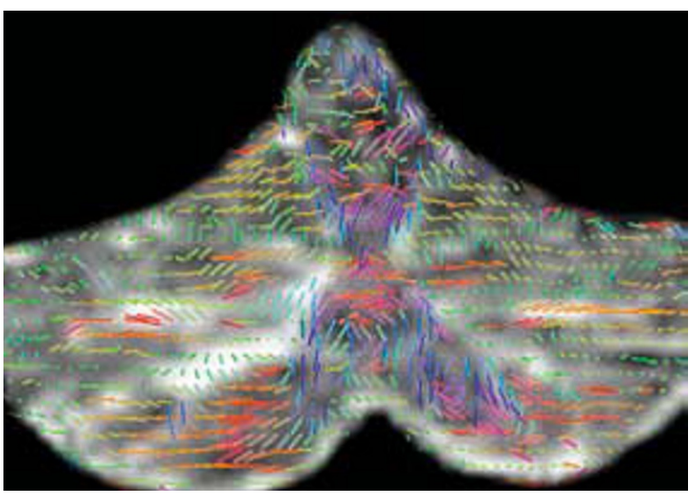

D

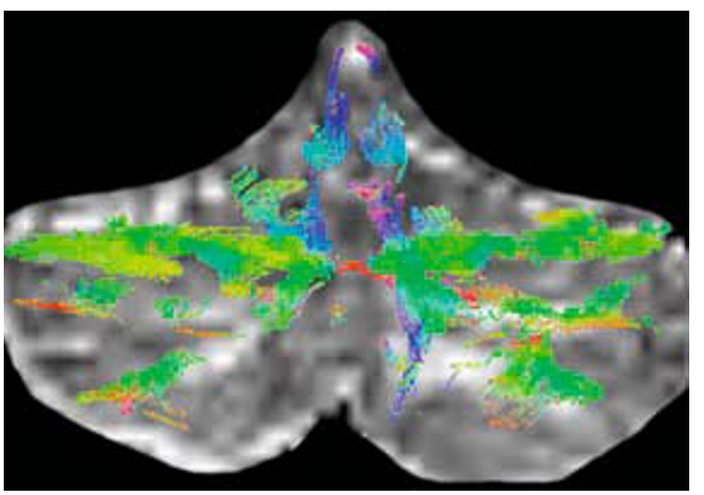

E

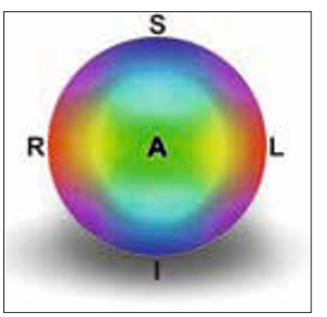

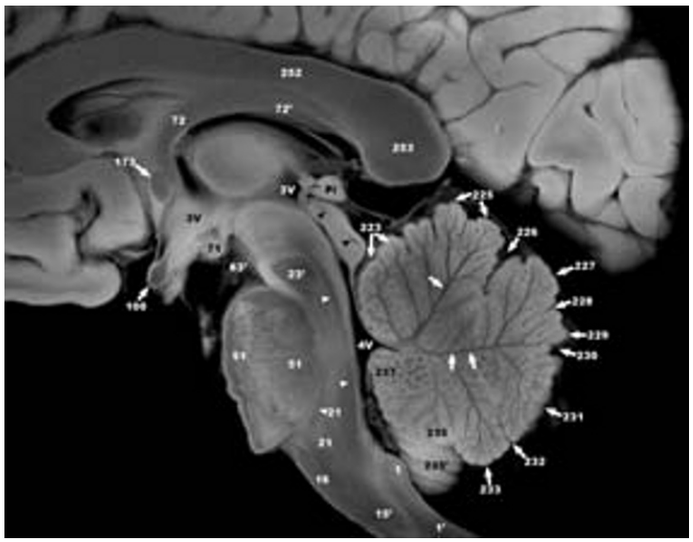

A

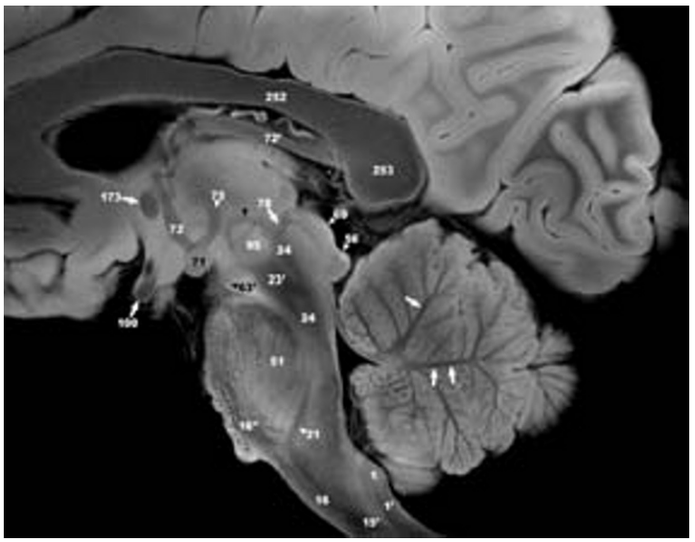

B

Sagittal Anatomic DTI Correlations

Figures 10.34–10.37 display sagittal diffusion tensor images in selected planes, displayed from midline to lateral. The anatomic and DTI images selected have been grouped into broad anatomic regions to permit correlation despite slight slice-slice variation due to differences in scan angle and normal anatomic variation.

Fig. 10.34 (A–D). Mid-sagittal and parasagittal sections through the brain stem and cerebellum. Anatomic-DTI Correlation.
A–B. 3 Tesla sagittal MRI of a formalin-fixed human brain specimen in the midline **(A)** and a parasagittal plane **(B).**
C–D. Diffusion tensor imaging in comparable planes displayed as a color map **(C)** and whisker plot **(D).**

1 Nucleus gracilis
1′ Fasciculus gracilis
15′ Decussation of the corticospinal tracts
16 Pyramid containing the corticospinal tract
16′ Anterior corticospinal tract
16″ Corticospinal fibers descending through the pons toward the pyramid
17 Medial longitudinal fasciculus (along dashed white line)
21 Medial lemniscus
23 Superior cerebellar peduncle
23′ Decussation of the superior cerebellar peduncle
24 Central tegmental tract
51 Pontocerebellar fibers
56 Inferior colliculus
63′ Intramesencephalic oculomotor fibers (CN III)
63″ Oculomotor nerve (CN III)
69 Superior colliculus
69′ Commissure of the superior colliculus
71 Mammillary body
72 Fornix (anterior column) (along dashed white line)
72′ Fornix (body) (along dashed white line)
73 Principal mammillary fasciculus
75 Mammillothalamic fasciculus
78 Habenulo-interpeduncular tract (fasciculus retroflexus)
95 Red nucleus
100 Optic chiasm
173 Anterior commissure (midline portion)
174 Cingulate gyrus changing color as it curves around the corpus callosum
223 Central lobule of vermis
225 Culmen of the vermis
226 Primary fissure (anterior superior fissure) separating anterior from posterior lobes
227 Declive of the vermis

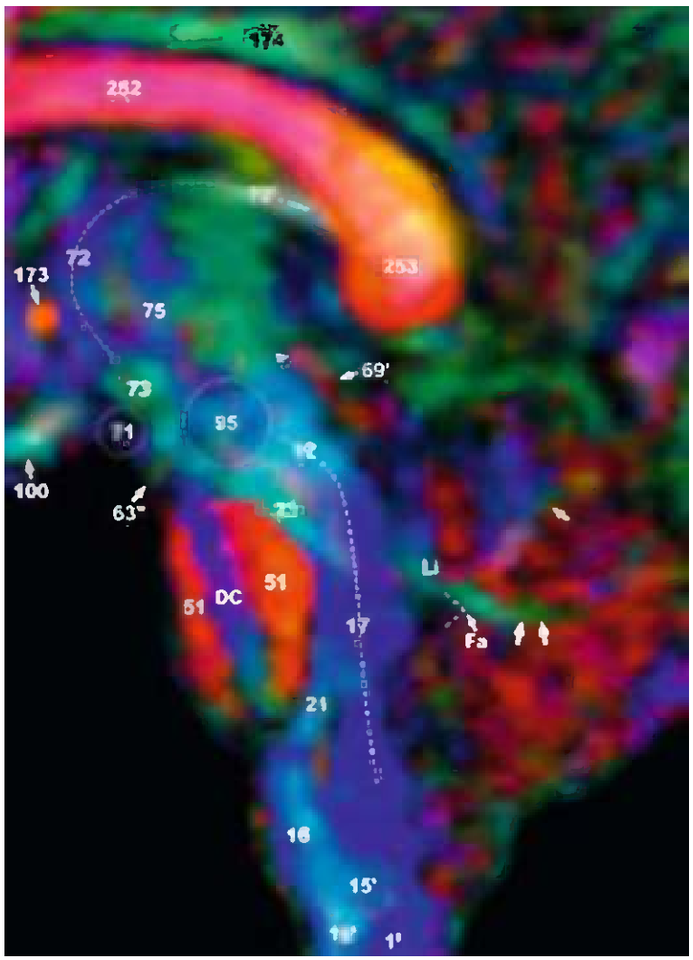

C

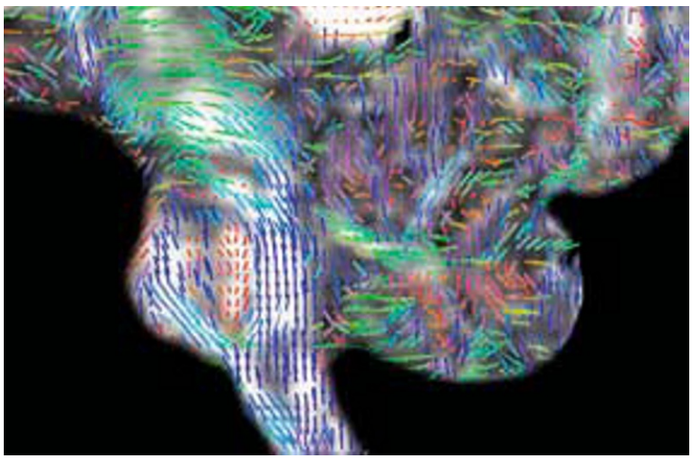

D

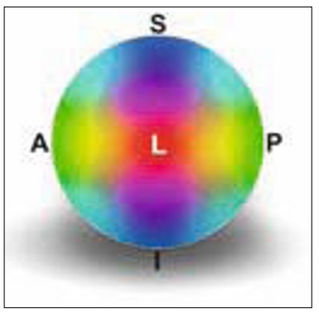

228 Posterior superior fissure (post clival fisssure)
229 Folium of the vermis
230 Great horizontal fissure
231 Tuber of the vermis
232 Prepyramidal fissure
233 Pyramis of the vermis
235 Uvula of the vermis (Also U)
235′ Tonsil of the cerebellum (Also T)
237 Nodulus of the vermis
252 Corpus callosum, body
253 Corpus callosum, splenium

Letter labels

3V Third ventricle
4V Fourth ventricle
DC Descending columns
Fa Fastigial recess of the fourth ventricle (dashed white outline)
Li Lingula of the vermis
Pi Pineal gland

Arrowheads and arrows

Single white arrowhead: Posterior commissure
Single black arrowhead: Capsule of the red nucleus
Dual spaced white arrowheads: Medial longitudinal fasciculus (also 17)
Dual black arrowheads: Commissural lamina of the tectal plate
Single white arrow: Apical arm of the arbor vitae directed into the culmen
Dual white arrows: Central arm of the arbor vitae directed toward the folium (229)

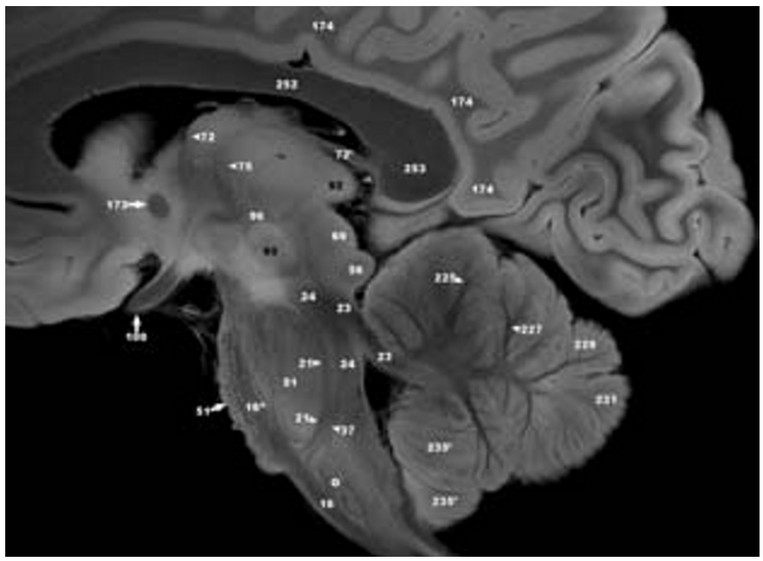

A

Fig. 10.35 (A–D). Parasagittal sections through the mid-lateral brain stem and cerebellum. Anatomic-DTI Correlation.
A–B. 3 Tesla parasagittal MRI of a formalin-fixed human brain specimen displayed from medial **(A)** toward lateral **(B).**
C–D. Diffusion tensor imaging in a comparable plane displayed as a color map **(C)** and whisker plot **(D).**

1′ Fasciculus gracilis
3 Spinal trigeminal tract
15 Lateral corticospinal tract converging superiorly to the decussation of the pyramids
16 Pyramid containing the corticospinal tract
16″ Corticospinal fibers descending through the pons toward the pyramid
17 Medial longitudinal fasciculus (along dashed white line)
21 Medial lemniscus
23 Superior cerebellar peduncle (along dashed white line)
24 Central tegmental tract
25 Inferior cerebellar peduncle (restiform body)
37 Trapezoid body (auditory fibers)
38 Middle cerebellar peduncle (brachium pontis)
47 Lateral lemniscus
51 Pontocerebellar fibers
56 Inferior colliculus
60 Cerebral peduncle
63″ Oculomotor nerve (CN III)
64 Sustantia nigra
69 Superior colliculus
69′ Commissure of the superior colliculus
71 Mammillary body
72 Fornix (anterior column) (along dashed white line)
72′ Fornix (body) (along dashed white line)
75 Mammillothalamic fasciculus
92 Pulvinar
95 Red nucleus
96 Prerubral radiations (Cerebellorubrothalamic tract)
100 Optic chiasm
100n Prechiasmal optic nerve
101 Optic tract
173 Anterior commissure (midline portion)
174 Cingulate gyrus changing color as it curves around the corpus callosum
225 Culmen of the vermis
227 Declive of the vermis
229 Folium of the vermis
230 Great horizontal fissure
231 Tuber of the vermis
233 Pyramis of the vermis
235 Uvula of the vermis (Also U)
235′ Tonsil of the cerebellum (Also T)
252 Corpus callosum, body
253 Corpus callosum, splenium

Letter labels
DC Descending columns
IP Interpeduncular fossa
O Inferior olivary nucleus

Arrowheads and arrows
Single white arrowhead: Posterior commissure
Single white arrow: Apical arm of the arbor vitae directed into the culmen
Dual white arrows: Central arm of the arbor vitae directed toward the folium (229)

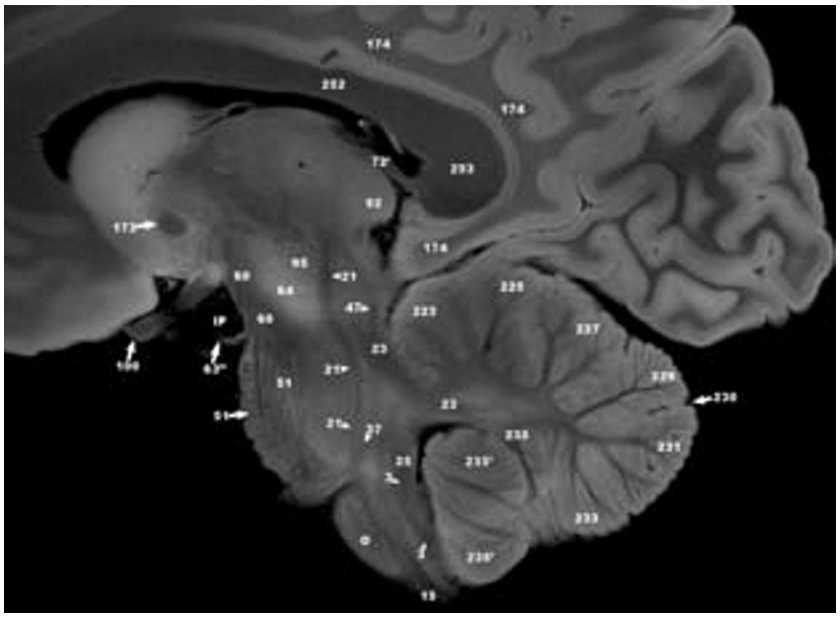

B

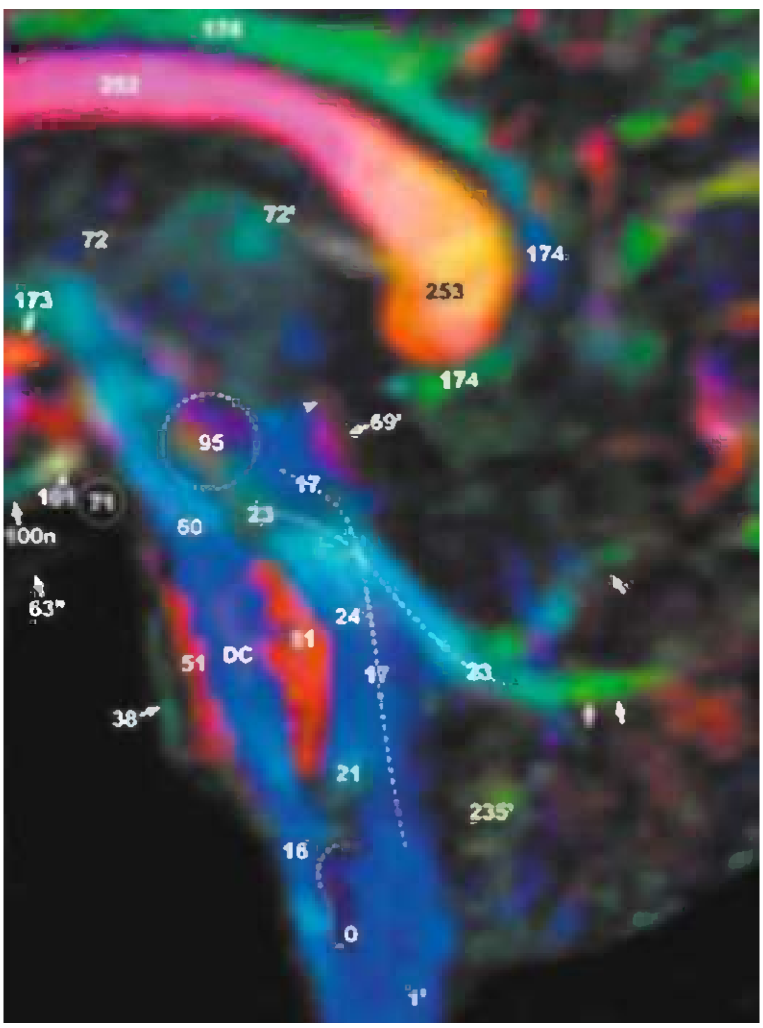
72'
72
173
174
253
174
69'
95
17
60
23
100n
63"
24
51
DC
17
23
38
21
235'
16
0
1'

C

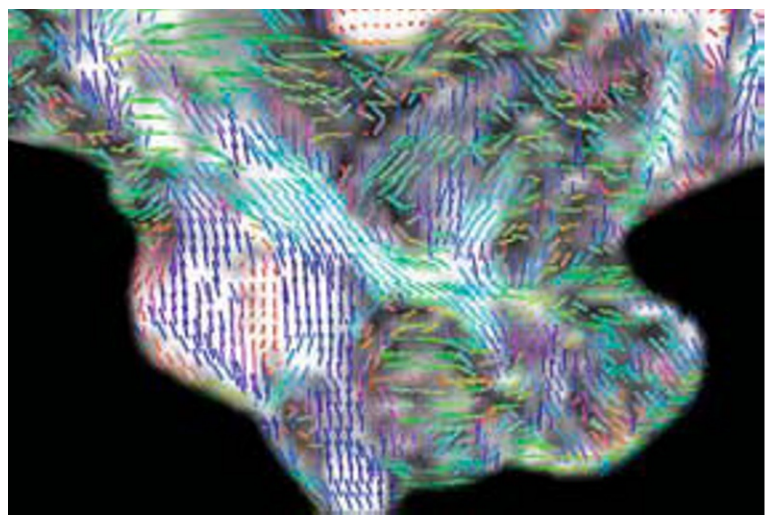

D

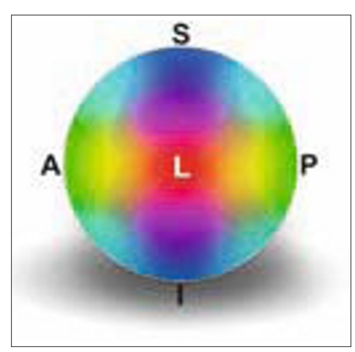
S
A
L
P
I

Fig. 10.36 (A–D). Parasagittal sections through the mid-lateral brain stem and cerebellum. Anatomic-DTI Correlation. A–B. 3 Tesla parasagittal MRI of a formalin-fixed human brain specimen displayed from medial **(A)** toward lateral **(B).** **C–E. Diffusion tensor imaging** in comparable planes displayed as a color maps **(C–D)** and a whisker plot **(E).**

10 Spinothalamic tract
16 Pyramid containing the corticospinal tract
16″ Corticospinal fibers descending through the pons toward the pyramid
21 Medial lemniscus
23 Superior cerebellar peduncle
24 Central tegmental tract
25 Inferior cerebellar peduncle (restiform body)
37 Trapezoid body
38 Middle cerebellar peduncle (brachium pontis)
51 Pontocerebellar fibers
56 Inferior colliculus
60 Cerebral peduncle
64 Substantia nigra
66 Corpus medullare (central white matter of the cerebellar hemisphere)
67 Brachium of the inferior colliculus
69 Superior colliculus
70 Brachium of the superior colliculus
72 Fornix (anterior column)
72′ Fornix (body)
75 Mammillothalamic fasciculus
86 Nucleus lateralis thalami
86p Nucleus lateralis posterior thalami
88d Dorsal thalamic peduncle
92 Pulvinar
92m Nucleus pulvinaris medialis thalami
93l Ventral posterolateral nucleus of the thalamus
93m Ventral posteromedial nucleus of the thalamus
94l Ventral lateral nucleus of the thalamus
95 Red nucleus
96 Prerubral radiations (Cerebellorubrothalamic tract)
97 Subthalamic nucleus
99 Fields of Forel (H, H1 (thalamic fasciculus), and H2 (lenticular fasciculus))
100 Optic chiasm
101 Optic tract
104 Medial geniculate body
140′ Medial orbital gyrus
144 Area olfactoria
157 Ansa lenticularis
170 Caudate nucleus (head)
171 Nucleus accumbens septi
173 Anterior commissure (midline portion)
174 Cingulate gyrus changing color as it curves around the corpus callosum
175a Anterior limb of the internal capsule
175g Genu of the internal capsule
178 Putamen
179l Globus pallidus (lateral nucleus, external nucleus)
179m Globus pallidus (medial nucleus, internal nucleus)
207 Uncus
225 Culmen
225′ Quandrangular lobule (anterior quadrangular lobule)
227 Declive
227′ Simple lobule (posterior quadrangular lobule)
229 Folium
229′ Superior semilunar lobule
230 Great horizontal fissure
231 Tuber
231′ Inferior semilunar lobule
233′ Gracile lobule
233″ Biventral lobule
235′ Tonsil of the cerebellum (Also T)
252 Corpus callosum, body
253 Corpus callosum, splenium

Letter labels

k Fasciculus olfactorius
n Radiations of the corpus callosum
nr Radiations of the rostrum of the corpus callosum
De Dentate nucleus
DC Descending cortical tracts
O Inferior olivary nucleus

Arrowheads and arrows

Paired white arrowheads: Arms of the arbor vitae

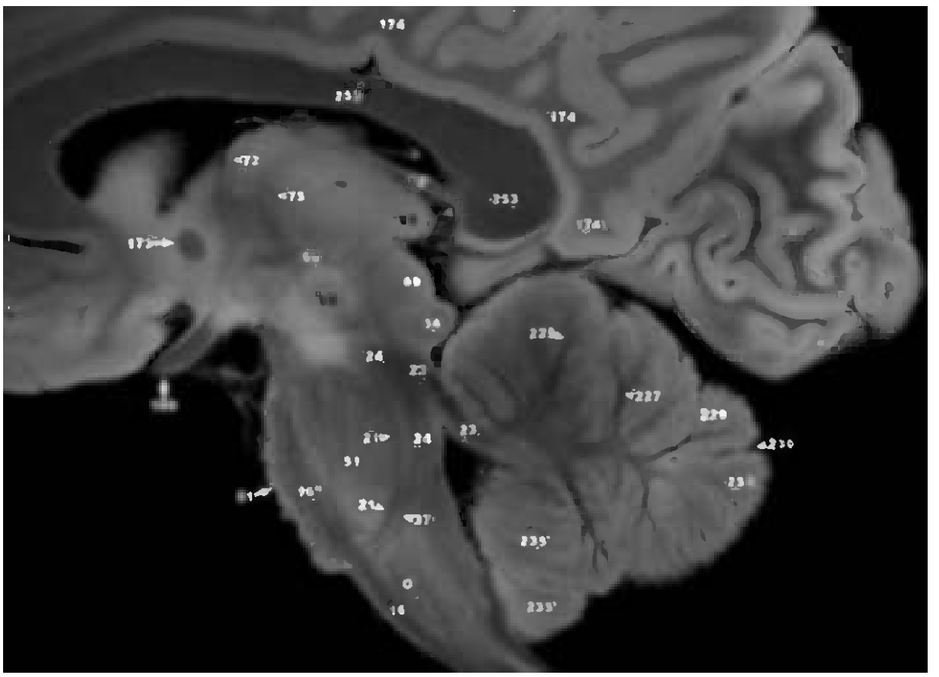

A

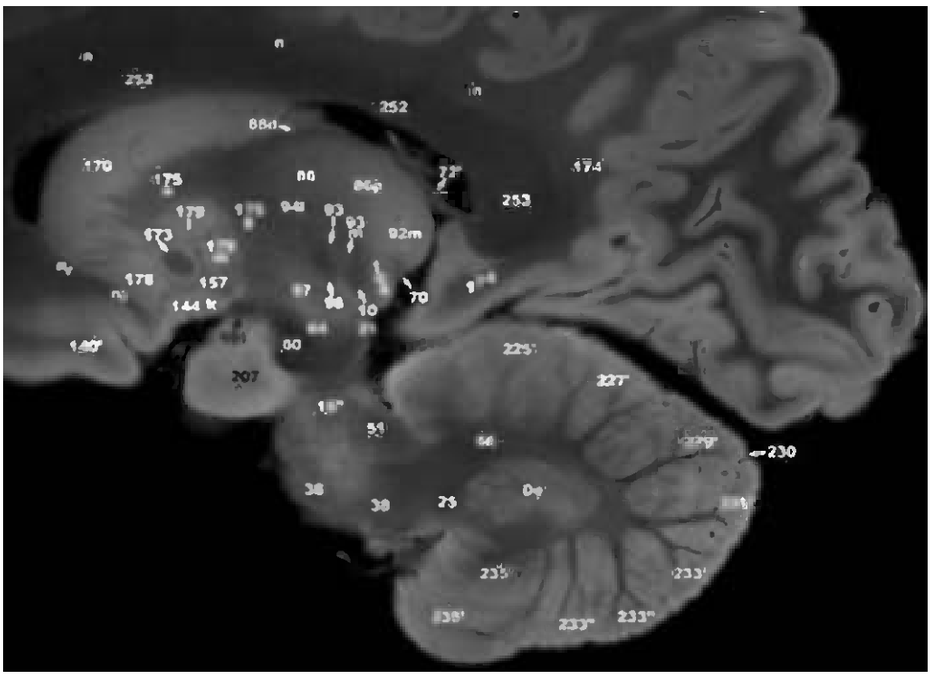

B

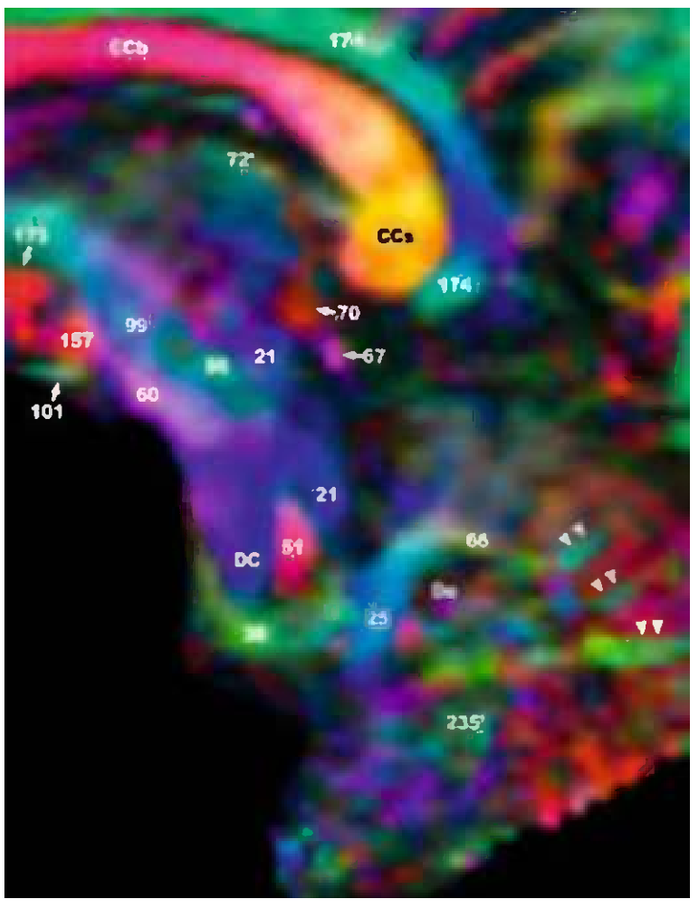
Cb
72
CCs
174
70
99
157
21
67
101
60
21
DC
51
66
25
235

C

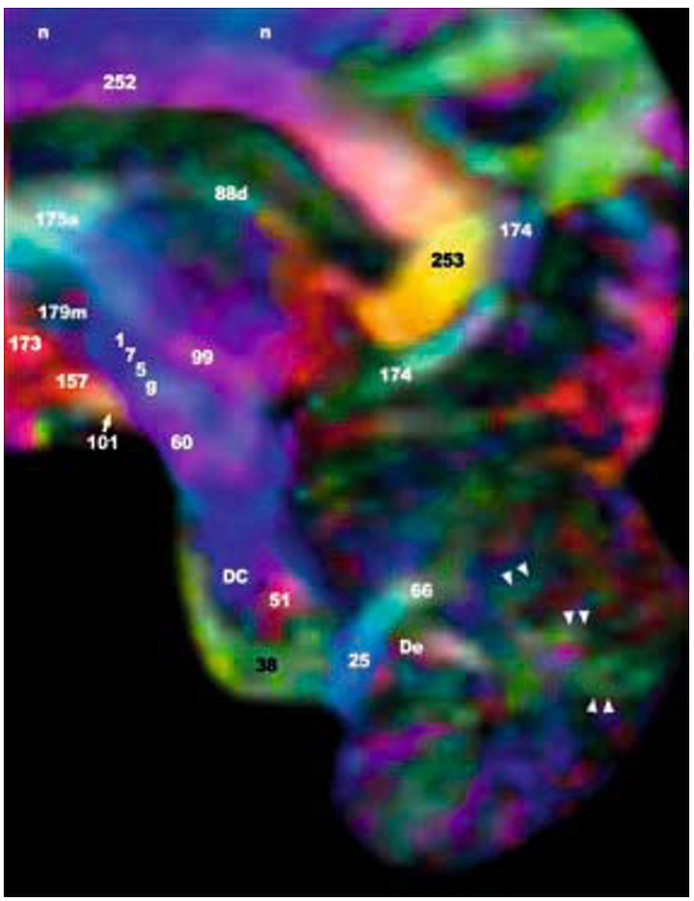
n
n
252
88d
175a
174
253
179m
173
1
7
5
g
99
157
174
101
60
DC
51
66
38
25
De

D

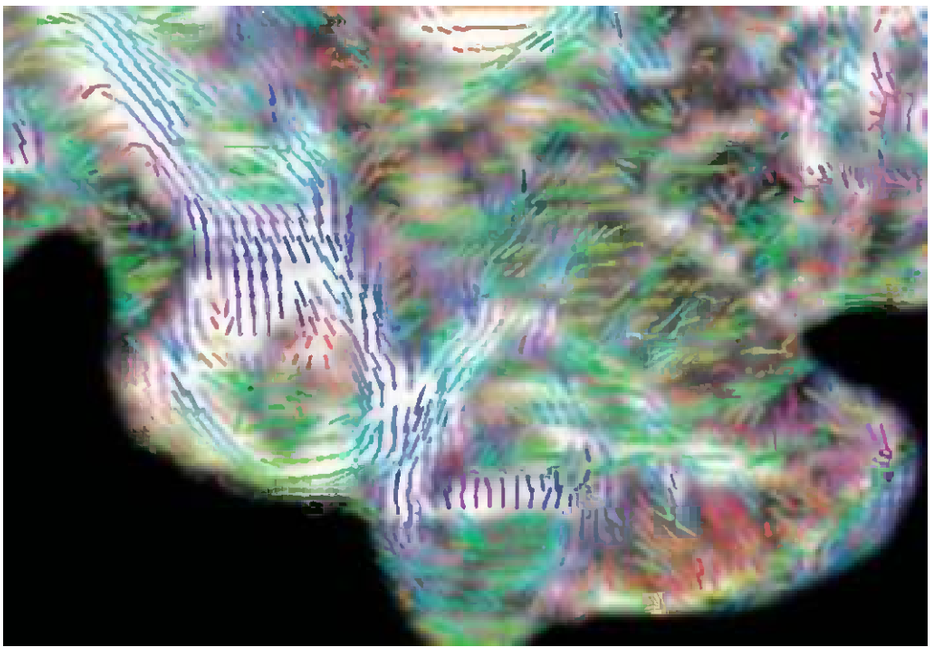

E

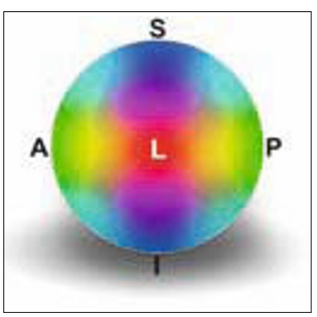

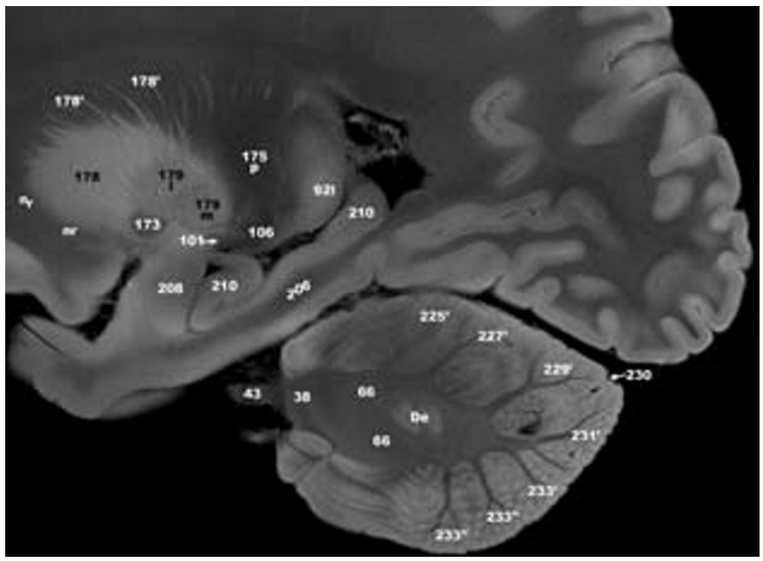

A

Fig. 10.37 (A–F). Lateral sagittal sections through the lateral brain stem and cerebellum. Anatomic-DTI Correlation.
A-B. 3 Tesla parasagittal MRI of a formalin-fixed human brain specimen displayed from medial **(A)** toward lateral **(B).**
C–F. Diffusion tensor imaging in comparable planes displayed as color maps **(C–D)** and whisker plots **(E–F).**

38 Middle cerebellar peduncle (brachium pontis)
43 Trigeminal nerve (CN V)
66 Corpus medullare (central white matter of the cerebellar hemisphere)
88c Caudal thalamic peduncle
92 Pulvinar
92l Nucleus pulvinaris lateralis thalami
101 Optic tract
105 Auditory radiations (geniculotemporal radiations
106 Lateral geniculate body
107 Optic radiations (geniculocalcarine radiations)
170″ Caudate (tail)
173 Anterior commissure (midline portion)
175p Posterior limb of the internal capsule
175r Retrolenticular portion of the internal capsule
178 Putamen
178′ Caudato-lenticular bridges of gray matter
179l Globus pallidus (lateral nucleus, external nucleus)
179m Globus pallidus (medial nucleus, internal nucleus)
192 Superior longitudinal fasciculus
206 Parahippocampal gyrus (also PHG)
208 Amygdala
210 Hippocampal formation
225′ Quandrangular lobule (anterior quadrangular lobule)
227′ Simple lobule (posterior quadrangular lobule)
228 Posterior superior fissure
229′ Superior semilunar lobule
230 Great horizontal fissure
231′ Inferior semilunar lobule
233′ Gracile lobule
233″ Biventral lobule
253 Corpus callosum, splenium

Letter lables
nr Radiations of the rostrum of the corpus callosum
De Dentate nucleus
In Insula

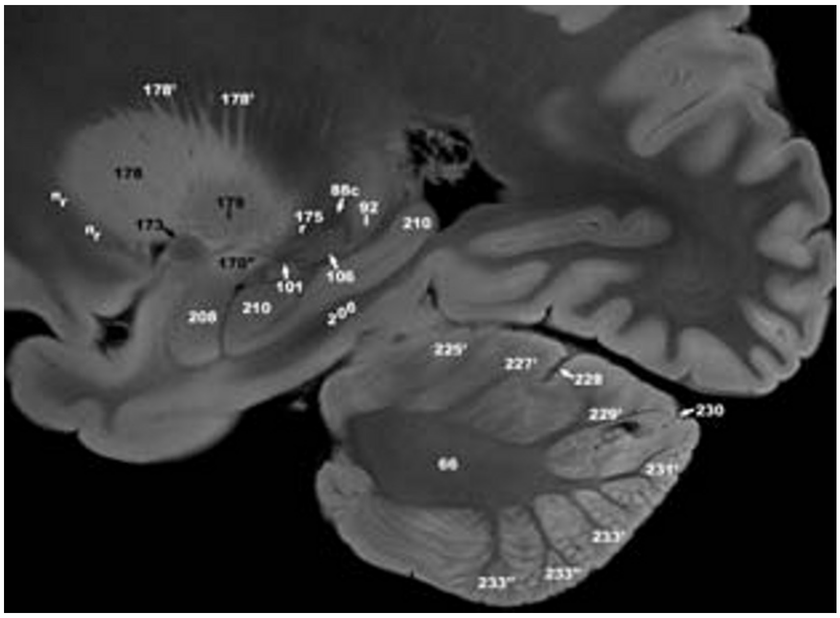
175
88c
92
210
101
106
210
225'
227'
228
229'
230
66
231'
233'

B

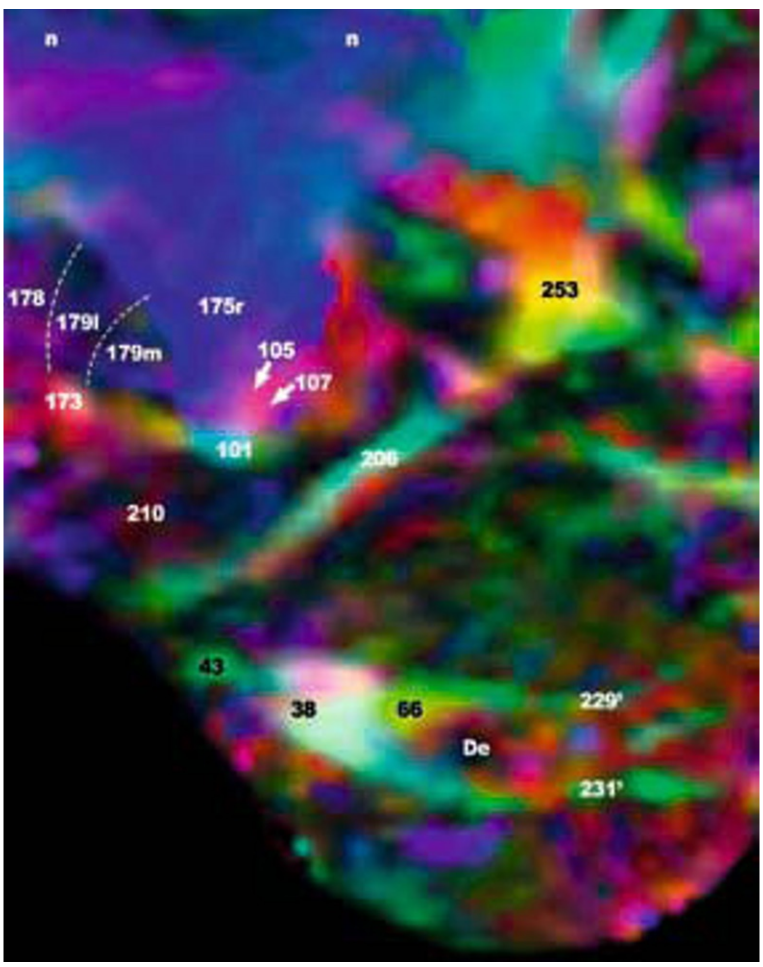
n
n
253
178
179l
175r
179m
105
107
173
101
206
210
43
38
66
229'
De
231'

C

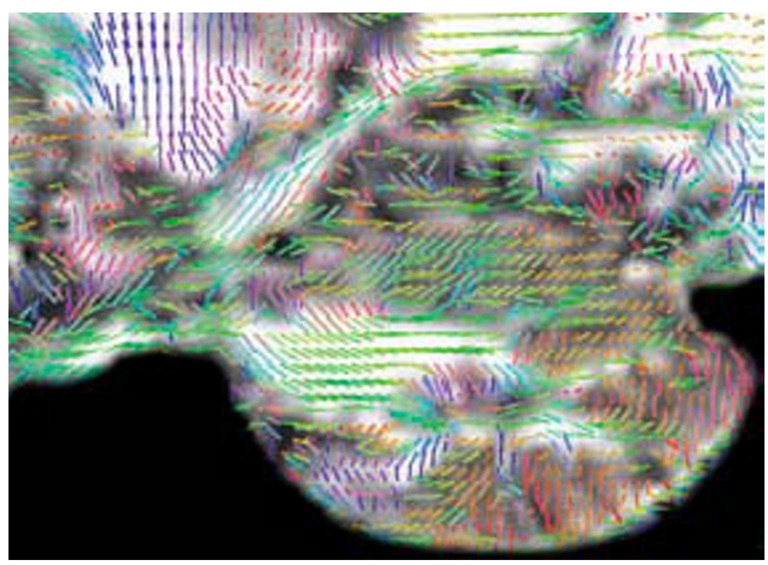

E

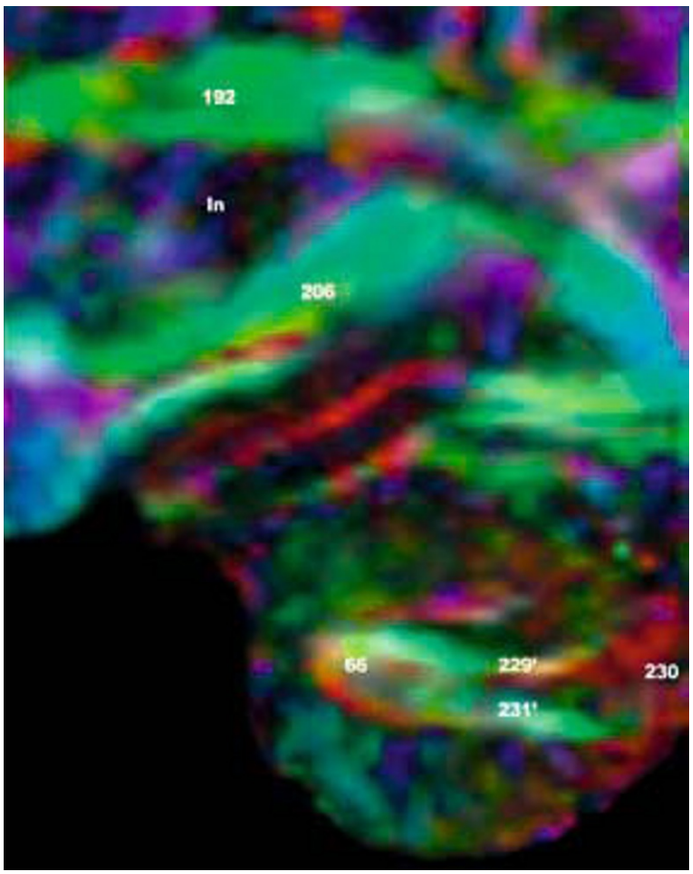

D

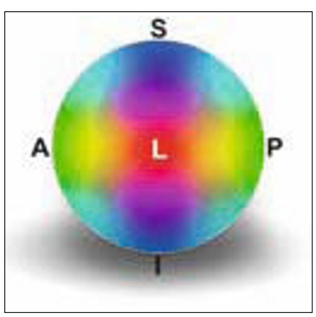

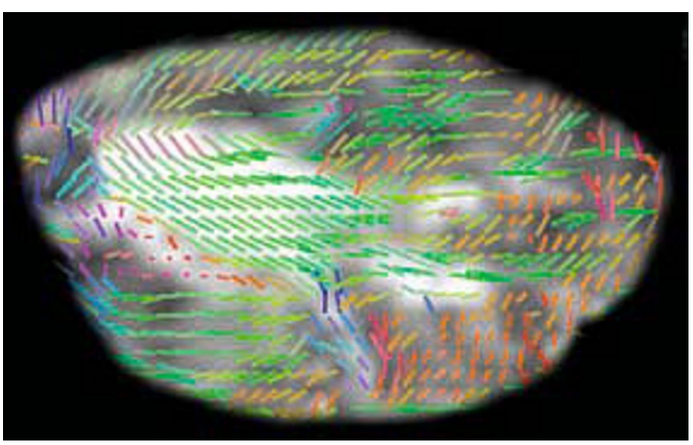

F

D. Diffusion Tensor Imaging of Fixed Brain Tissue at 9.4 Tesla (Figs. 10.38–10.41)

Bradley N. Delman, Cheuk Y. Tang, and Thomas P. Naidich

Diffusion tensor images were obtained from formalin-fixed cadaver tissue, utilizing a 9.4 Tesla superconducting Magnex magnet (Bruker Analytik, Rheinstetten, Germany) with an 89 mm vertical bore, a 30 mm bird cage coil, and a pulsed gradient spin echo sequence: B-value: 1600s/mm^2, repetition time (TR): 12,000 msec, echo time (TE): 25.7 msec, slice thickness: 1 mm, field of view: 30 mm, data matrix: 128 x 128, diffusion directions: 6, and averages: 8. The total scan time for 24 slices was approximately 24 hours. Data were imported into DtiStudio v2.4 (S. Mori, Ph. D. and H. Jiang, Ph. D., Johns Hopkins University) and directionally encoded color maps were generated for each slice. Color maps were superimposed on the corresponding anatomic images of the same specimens (i) to aid in identification of nuclei which have low anisotropy and are poorly represented on color maps, and (ii) to lend higher resolution to the images overall.

As with the standard diffusion tensor imaging, the colors used signify standard directions. Blue signifies preferential diffusion in the superior-inferior (SI) orientation. Green signifies preferential diffusion in the anteroposterior (AP) direction. Red signifies preferential diffusion in the transverse (latero-lateral, LL) direction. Diffusion within tracts coursing at oblique angles is represented by a weighted mix of colors. For example, fibers coursing obliquely between AP and SI (e.g., anterosuperior to posteroinferior, or posterosuperior to anteroinferior) would be represented by cyan, the combination of blue and green. Fibers running obliquely between LL and AP would appear yellow (red plus green), and fibers running obliquely between SI and LL would appear magenta (red plus blue). Those voxels which contain crossing fibers may appear dark or colorless on color maps, since in those areas the dominant fiber trajectory could not be calculated.

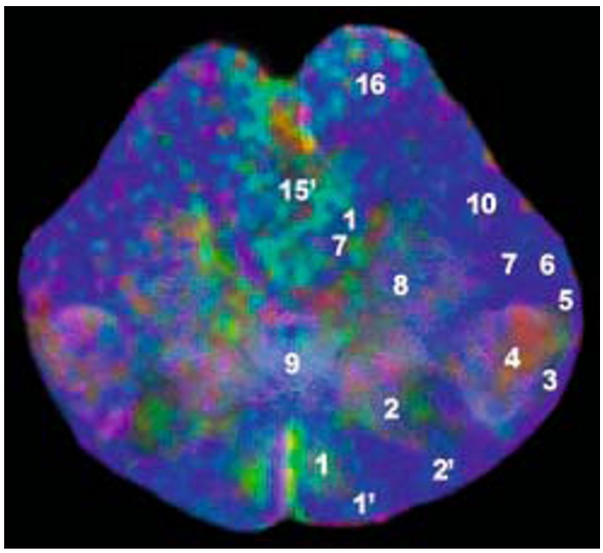

A

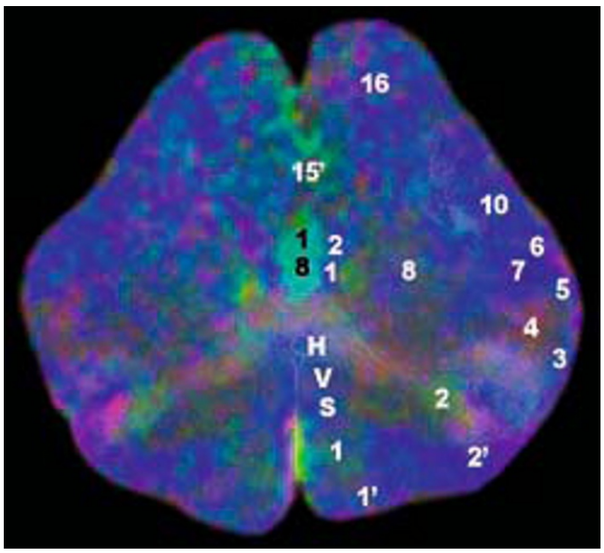

B

Fig. 10.38 (A–I). Axial diffusion tensor images of the medulla. Post mortem specimen.
Images displayed from caudal to rostral. See also **Figs. 8.2– 8.13** and **8.34–8.35**.

A–B. Cervico-medullary junction. The predominant blue color signifies that most fiber tracts ascend or descend through the medulla longitudinally. The ascending fasciculi gracilis (1′) and cuneatus (2′) reach the nuclei gracilis (1) and cuneatus (2) and synapse within them. The secondary internal arcuate fibers arise from these nuclei, pass ventrally around the central gray matter (9), and cross the midline in the great sensory decussation (18) just ventral to the central gray matter to form the medial lemnisci. The majority of descending corticospinal fibers decussate at this level (15′) and then pass postero-inferolaterally to the posterior aspects of the lateral columns of the spinal cord.
The anterior spinocerebellar tract (6) and spinothalamic tract (10) ascend within the anterolateral fasciculus at the anterolateral aspect of the brain stem. The rubrospinal tract (7) is juxtaposed medially. The fibers of the posterior spinocerebellar tract (5) ascend just posterior to the anterior spinocerebellar tract, but then curve dorsally toward the inferior cerebellar peduncle. The spinal trigeminal nuclei (4) appear reddish. The spinal trigeminal tracts (3) that descend along their lateral aspects are blue. Most nuclei and the 'butterfly' of central gray matter appear as stippled mixes of colors, perhaps because the entering and emerging fibers course in different directions. The hypoglossal nucleus (H), dorsal motor nucleus of the vagus (V) and solitary nucleus (S) lie just dorsal to the central portion of the butterfly.

C–D. Low medulla. The pyramids of medulla (16) course nearly vertically (blue). The decussating internal arcuate fibers (18) pass ventrally (green), so fibers from more caudal portions of the body lie ventral to fibers from more cranial portions. This establishes the ventral dorsal somatotomy of the fibers within the ascending medial lemnisci (21). Secondary fibers from the spinal trigeminal nucleus also cross the midline to lie just lateral to the contralateral medial lemniscus (21), where they form the ventral trigeminothalamic tracts on each side. The solitary tract (S) begins to move laterally. The lower poles of the inferior olivary nuclei (O) just come into view (see following figures). The dorsal longitudinal fasciculus (white arrow) courses just dorsal to the hypoglossal nucleus (H) en route toward the dorsal vagal (V) and solitary (S) nuclei.

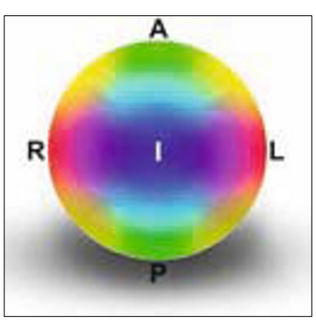

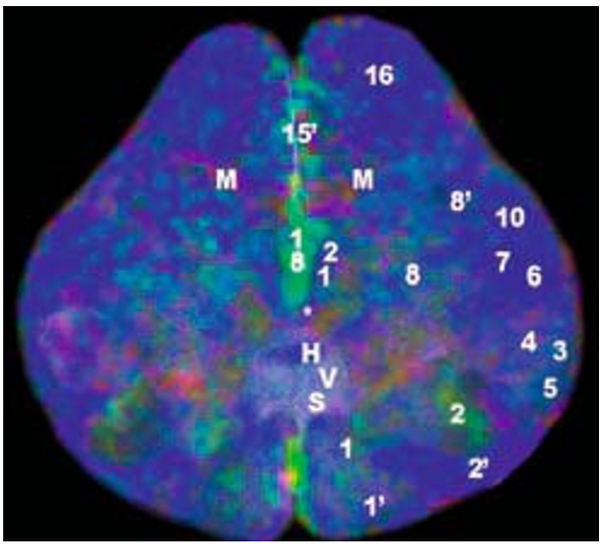

C

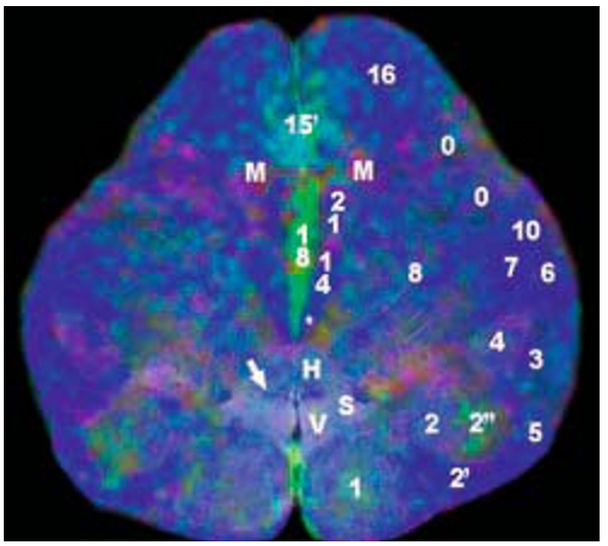

D

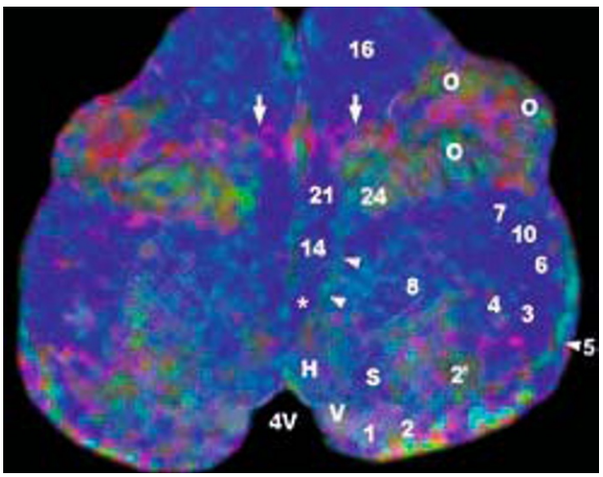

E

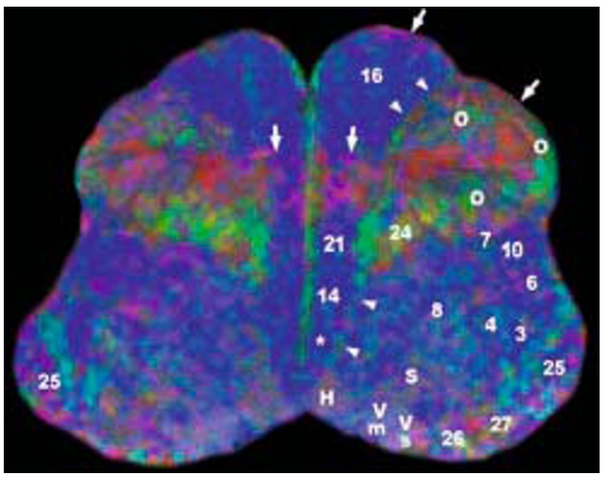

F

E–F. Low-Mid medulla. Deep blue coloration indicates vertical longitudinal courses for the ventral pyramids (16); the anterolateral fasciculi (6, 10) and juxtaposed rubrospinal tract (7); and the medial fiber column formed by the medial longitudinal fasciculi (asterisk), tectospinal tracts (14) and medial lemnisci (21). The olivocerebellar fibers (line of white arrows in G.) form a dominant transverse fiber system (red) that crosses the midline ventrally and then curves dorsally through the contralateral olive and reticular substance toward the inferior cerebellar peduncle (25). The posterior spinocerebellar fibers (5) pass posteriorly along the periphery of the brain stem toward the inferior cerebellar peduncle (25), forming a green border along the dorsal margin of the medulla. The accessory cuneate nuclei (2') give rise to the cuneocerebellar tract that enters the inferior cerebellar peduncle. The hypoglossal nuclei (H), dorsal motor vagal nucleus (Vm), and vestibular nuclei (26, 27) show mixed stippled coloration. The ventrally-directed intra-axial hypoglossal nerve fibers (white arrowheads) and glossopharyngeal nerve fibers show strong green coloration. The structures of the median raphe form a well-defined green band. The central tegmental tract (24) descends inferiorly and ventrally to enclose the dorsolateral aspect of the inferior olivary nucleus, forming the mixed yellow coloration. The arcuate nuclei interspersed among the pyramidal fibers (16) give rise to the external arcuate fibers that course circumferentially along the ventral lateral aspect of the medulla (two ventral white arrows).

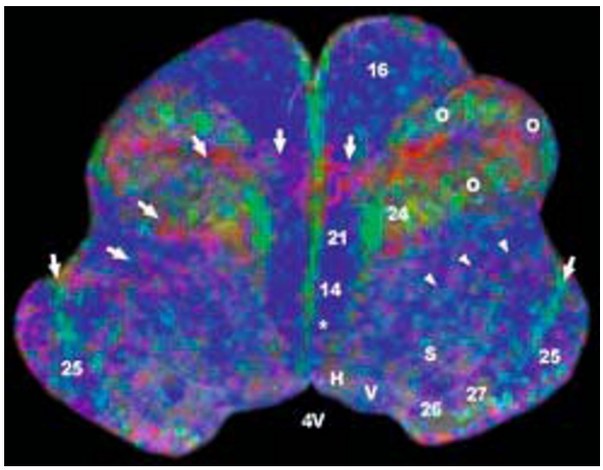

G

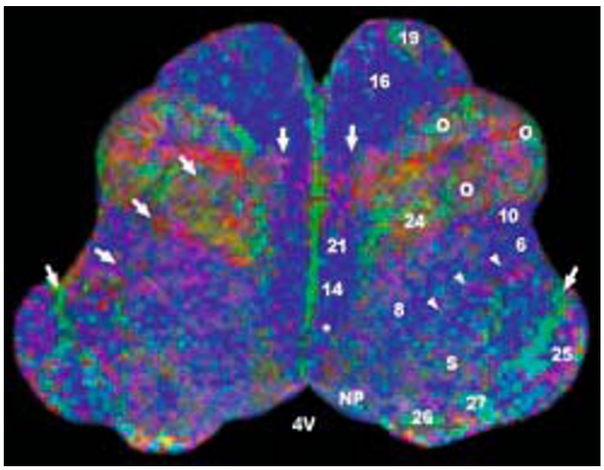

H

G–H. Mid medulla. The inferior cerebellar peduncles (25) expand the contour of the medulla dorsolaterally. These images emphasize the orientations and contours of the pyramid (16) ventrally, the bulge of the olive (O) ventrolaterally, the anterolateral fasciculus (6,10) just behind the olive, and the medial column of longitudinal fibers (asterisk, 14, 21). They also show the broad swath of fibers (three white arrowheads) that appear to arise from the nucleus ambiguus, and the strong dorsoinferolateral directionality of the descending vestibular fibers (single white arrow). At this level (and as far superiorly as the abducens nucleus), the nucleus prepositus hypoglossi (NP) occupies the position that is occupied by the hypoglossal nucleus more caudally. At the mid-high medulla, the nuclei and fibers of the median raphe form a narrow sagittal band with distinct green coloration.

1 Nucleus gracilis
1′ Fasciculus gracilis
2 Nucleus cuneatus
2′ Fasciculus cuneatus
2″ Accessory (lateral) nucleus cuneatus
3 Spinal trigeminal tract
4 Spinal trigeminal nucleus
5 Posterior (dorsal) spinocerebellar tract
6 Anterior (ventral) spinocerebellar tract
7 Rubrospinal tract
8 Extensive reticular formation (light gray)
8′ Lateral reticular nucleus
9 Central gray matter around central canal of spinal cord
10 Spinothalamic tract
14 Tectospinal tract
15′ Decussation of the corticospinal tracts
16 Pyramid containing the corticospinal tract
17 Medial longitudinal fasciculus (also asterisk)
18 Decussation of the internal arcuate fibers
21 Medial lemniscus
24 Central tegmental tract
25 Inferior cerebellar peduncle (restiform body)
26 Medial vestibular nucleus
27 Inferior vestibular nucleus

Letter labels

* Medial longitudinal fasciculus (also labeled 17 in other images)
4V Fourth ventricle
H Hypoglossal nucleus (CN XII)
M Medial accessory olivary nucleus
NP Nucleus prepositus hypoglossi
O Inferior olivary nucleus
S Solitary nucleus and tract
V Nucleus of the vagus (CN X)
Vm Dorsal motor nucleus of the vagus (CN X)
Vs Dorsal sensory nucleus of the vagus (CN X)

Arrowheads and arrows

These are specified for each image in the caption for that image.

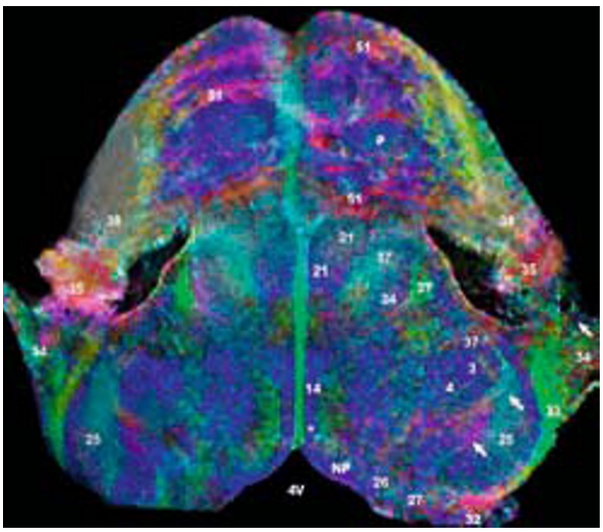

Fig. 10.38 I. Axial diffusion image of the ponstomedullary junction. Post mortem specimen.
See also **Figs. 8.34–8.35**.

I. Pontomedullary junction. The well developed inferior cerebellar peduncles (25) show a predominant anterosuperior course (cyan). The dorsal cochlear nucleus (32) forms the distinct auditory tubercle on the surface of the inferior cerebellar peduncle. The ventral cochlear nucleus (33) lies anteriorly. It gives rise to the ventral acoustic stria, which passes to the trapezoid body (37). The vestibulocochlear nerve (34) and the facial nerve (35) pass dorsolaterally as they enter/exit the brain stem just caudal to the middle cerebellar peduncle (38). The descending vestibular fibers (three white arrows) pass to the vestibular nuclei (26, 27). The ascending (blue) medial lemnisci (21) curve over ventrolaterally as they reposition from their sagittal orientation within the medulla to their coronal orientation in the pons. The sinuous structure arching through the right inferior cerebellar peduncle likely represents a penetrating vein (**See Fig. 9.10A**).

3 Spinal trigeminal nucleus (CN V)
4 Spinal trigeminal tract (CN V)
14 Tectospinal tract
21 Medial lemniscus
24 Central tegmental tract
25 Inferior cerebellar peduncle
26 Medial vestibular nucleus
27 Inferior vestibular nucleus
32 Dorsal cochlear nucleus
33 Ventral cochlear nucleus
34 Vestibulocochlear nerve (CN VIII)
35 Facial nerve (CN VII)
37 Ventral acoustic stria and trapezoid body
38 Middle cerebellar peduncle
51 Pontocerebellar fibers

Letter labels
* Medial longitudinal fasciculus
4V Fourth ventricle
NP Nucleus prepositus
P Pyramidal tract

Arrowheads and arrows
White arrows: Descending vestibular fibers

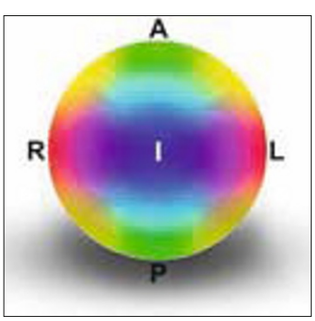

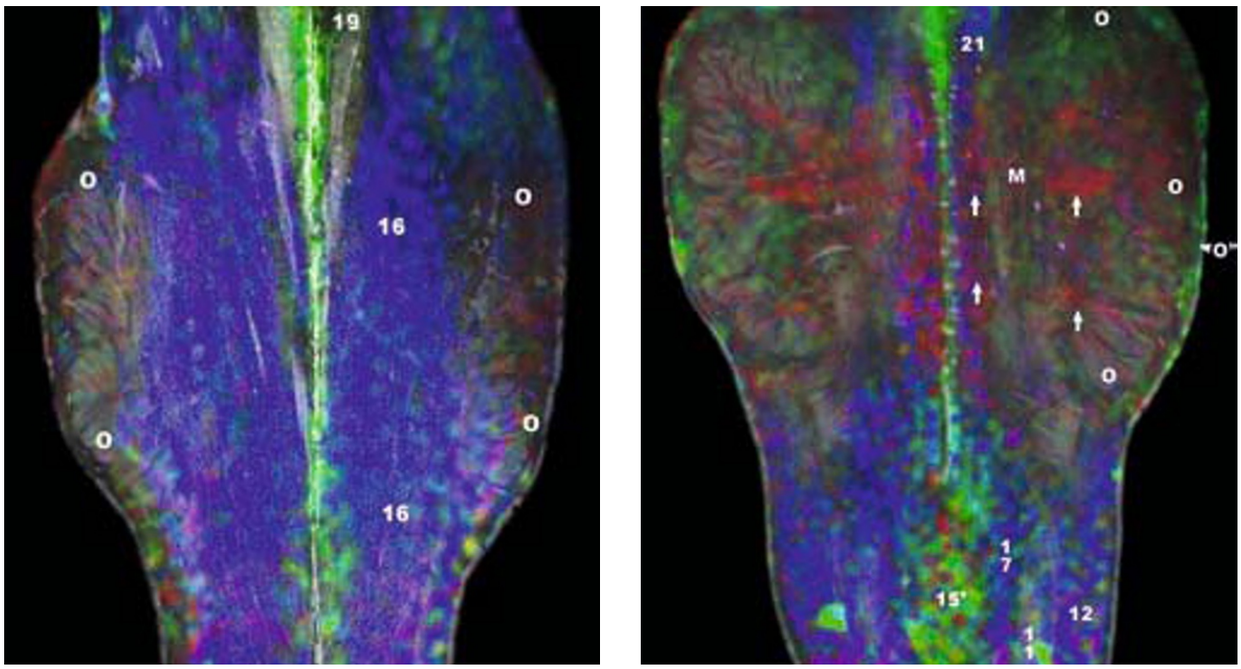

Fig. 10.39 (A–F). Coronal diffusion tensor images of the medulla. Post mortem specimen. Images displayed from ventral to dorsal. See also Figs. 8.24–8.33.

A–C. Ventral medulla. The corticospinal fibers descend (blue) within the pyramids (16), decussate (15′) (oblique fiber bands of mixed-color) at the cervicomedullary junction, and then pass postero-inferolaterally (15) (mixed green, blue and red) toward the posterior aspect of the lateral columns of the spinal cord. The medial lemnisci (21), the lateral spinovestibular tracts (12), and the caudal portions of the medial longitudinal fasciculi (17) form prominent longitudinal fiber bundles (blue) dorsal to the pyramids. The inferior olivary nuclei (O) and the medial accessory olivary nuclei (M) show the mixed coloration of gray matter. The amiculum (O′) encapsulates the lateral border of the inferior olivary nucleus, so it appears green at the midpoint of its curved course. The olivocerebellar fibers (white arrows) emerge from the medially-situated hila of the inferior olivary nuclei and course transversely (red) toward the contralateral inferior cerebellar peduncles. The central tegmental tracts (24) descend from the ipsilateral red nuclei of the midbrain to the inferior olivary nuclei. The arcuate nuclei (19) of the medulla appear as masses of mixed gray matter coloration interspersed within and alongside the fascicles of the pyramids.

D–F. Dorsal medulla. The fasciculus gracilis (1′) and fasciculus cuneatus (2′) ascend (blue) to synapse within the corresponding nuclei gracilis (1) and cuneatus (2) (mixed color of gray matter). The internal arcuate fibers (white arrowheads) arise from these nuclei, arch ventrally (green) around the central gray matter, turn medially (red) to cross the midline in the ventral half of the medulla, and then ascend (blue) as the crossed fibers of the medial lemnisci (21) to the contralateral thalami. General *somatic* afferent (**GSA)** fibers of cranial nerves V, VII, IX and X form the spinal trigeminal tracts (3), which descend (blue) along the lateral borders of the prominent spinal trigeminal nuclei (mixed coloration of gray matter) (4). The fibers of the spinal trigeminal tracts synapse within the spinal trigeminal nuclei. General *visceral* afferent **(GVA)** and special *visceral* afferent **(SVA)** fibers of cranial nerves VII, IX and X form the solitary tracts (S) and course longitudinally (blue) within it, both superiorly and inferiorly, to synapse in the surrounding cylindrical solitary nuclei (mixed coloration of gray matter). The extensive reticular formation of the medulla (8), the hypoglossal nuclei (H), and the dorsal motor nuclei of the vagus (V) show the expected mixed coloration of gray matter.

1 Nucleus gracilis
1′ Fasciculus gracilis
2 Nucleus cuneatus
2′ Fasciculus cuneatus
3 Spinal trigeminal tract
4 Spinal trigeminal nucleus
7 Rubrospinal tract
8 Extensive reticular formation (light gray)
11 Ventral horn
14 Tectospinal tract
15 Lateral corticospina tract
17 Medial longitudinal fasciculus (also asterisk)
21 Medial lemniscus
24 Central tegmental tract
25 Inferior cerebellar peduncle (restiform body)

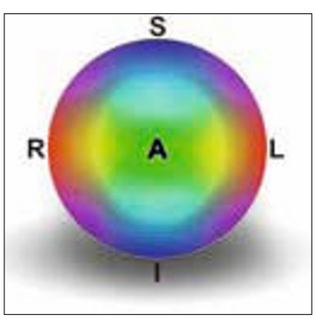

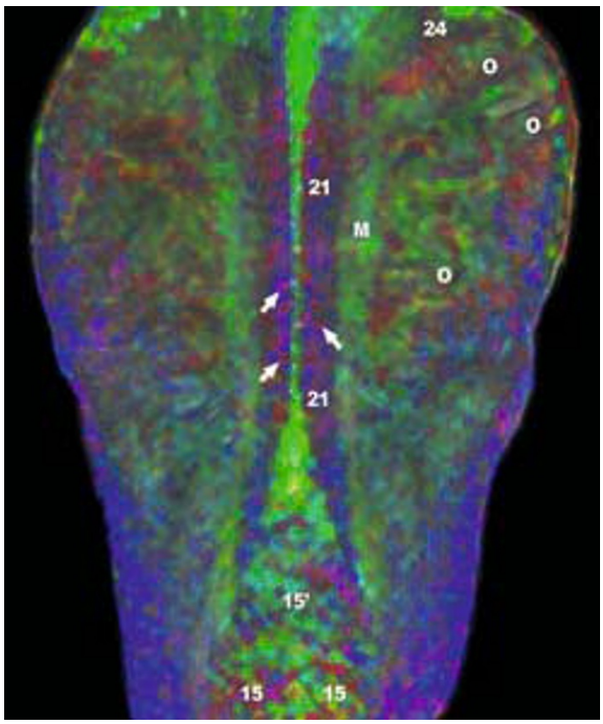

C

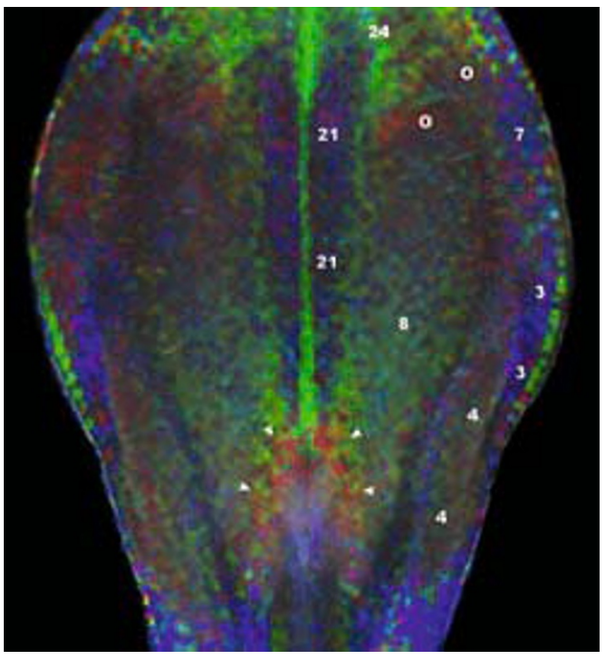

D

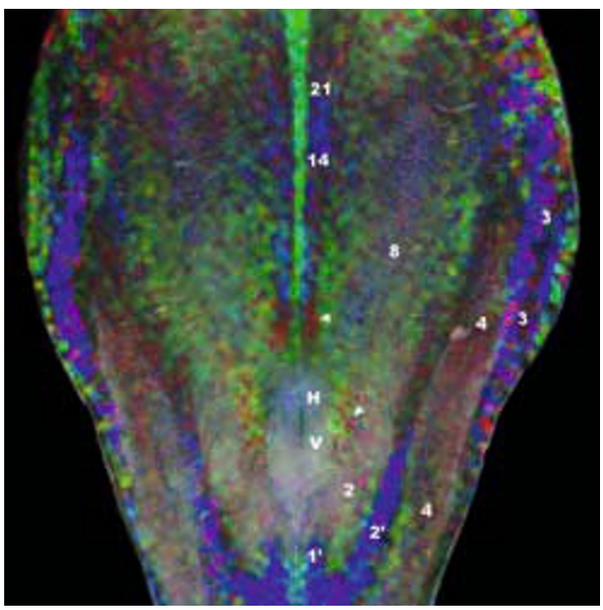

E

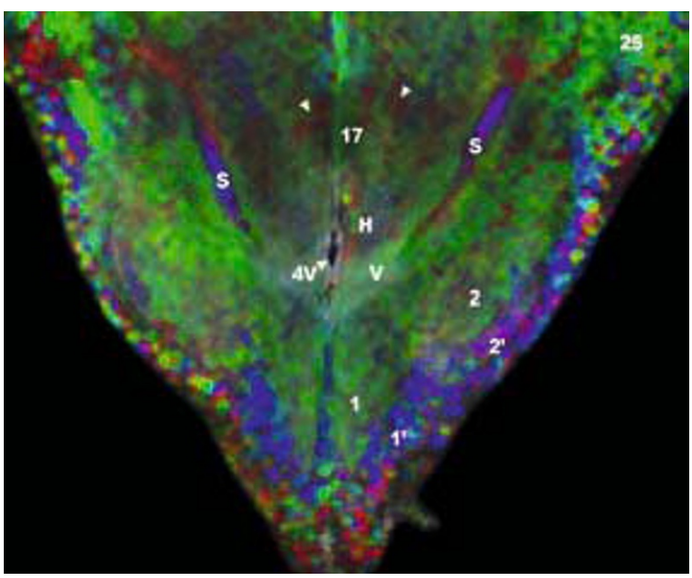

F

Letter labels

4V Fourth ventricle
H Hypoglossal nucleus
M Medial accessory olivary nucleus
O Inferior olivary nucleus
O′ Amiculum (capsule) of the inferior olivary nucleus
S Solitary tract surrounded by the solitary nucleus
V Dorsal motor nucleus of the vagus

Arrowheads and arrows

White arrowheads: Internal arcuate fibers
White arrows: Olivocerebellar fibers

Fig. 10.40 (A–D). Axial diffusion tensor images of the pons. Post mortem specimen.
Images displayed from caudal to rostral.
See also **Figs. 8.36–8.43**.

A–B. Low-mid pons. The transverse pontocerebellar fibers (51) form dominant red bands as they cross the basis pontis, but turn green as they curve dorsally and merge into the oblique predominantly sagittal (green) fibers of the middle cerebellar peduncles (38). The corticospinal tracts (P) form dominant blue bundles as they descend through the mid basis pontis. The ascending medial lemnisci (21), ascending spinothalamic tracts (10) and descending rubrospinal fibers (7) form an arc of blue that abuts the pontocerebellar fibers (51) and delimits the ventral border of the pontine tegmentum. The medial longitudinal fasciculi (*) and central tegemental tracts (24) course longitudinally (blue) within the tegmentum. The abducens (39) and facial (40) nuclei form stippled zones of mixed coloration. The intrapontine fascicles of the abducens nerve (single arrowheads) are a somewhat dispersed group of fibers that course ventrally in the medial tegmentum, so their green coloration is partially obscured. The intrapontine fascicles of the facial nerve arise from the facial nucleus (40), pass dorsomedially as a diffuse spread of fibers (not resolved), and arch dorsal to the abducens nucleus (39) to form the facial colliculus in the floor of the fourth ventricle (4V). The facial fibers then turn laterally (red) as a now-compact fiber bundle (paired white arrowheads in C.) and descend ventrolaterally (green) (paired white arrowheads in B.) to course just lateral to the facial nucleus (40) from which they emerged and just medial to the spinal trigeminal nucleus (4) and tract (3). Bilateral white arrows in B. indicate fibers of the trigeminal nerve.

C–D. Upper pons. The striking coloration of the basis pontis results from the strong directionality of the fiber tracts that traverse it. The pontocerebellar fibers (51) change course from transverse (red) to dorsal (green) as they join the middle cerebellar peduncles (38). The descending corticospinal (P) and corticobulbar fibers form well defined blue bands interspersed among the red pontocerebellar fibers. The midline is sharply delineated by sagittally oriented (green) fibers within the median raphe. The basis pontis (ventrally) is delimited from the pontine tegmentum (dorsally) by the sharp interface between the red transverse pontocerebellar fibers (51) and the arch of blue longitudinal fibers formed by the medial lemniscus (21), the lateral lemniscus (47), the rubrospinal tract (7) and the spinothalamic tract (10). The superior cerebellar peduncles form dorsolateral arcs of cyan as they course anterosuperiorly. The cisternal segments of the sensory (43) and motor (43′) roots of the trigeminal nerve course obliquely (blue and green) along the lateral aspect of the pons.

3 Spinal trigeminal tract
4 Spinal trigeminal nucleus
6 Anterior (ventral) spinocerebellar tract
7 Rubrospinal tract
10 Spinothalamic tract
14 Tectospinal tract
21 Medial lemniscus
23 Superior cerebellar peduncle
24 Central tegmental tract
25 Inferior cerebellar peduncle (restiform body)
38 Middle cerebellar peduncle
39 Abducens nucleus
40 Facial nucleus
43 Sensory root of the trigeminal nerve (cisternal segment)
43′ Motor root of the trigeminal nerve (cisternal segment)
44 Mesencephalic nucleus and tract of the trigeminal nerve
45 Motor nucleus of the trigeminal nerve (masticator nucleus)
46 Principal sensory nucleus of the trigeminal nerve
47 Lateral lemniscus
47′ Dorsal nucleus of the lateral lemniscus.
51 Pontocerebellar fibers

Letter labels

* Medial longitudinal fasciculus (labeled 17 in other images)
4V Fourth ventricle
F Frontopontine tract
P Corticospinal (pyramidal) tract
PT Parieto-temporopontine tract

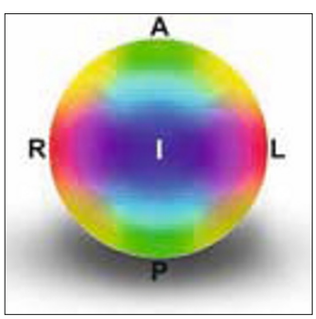

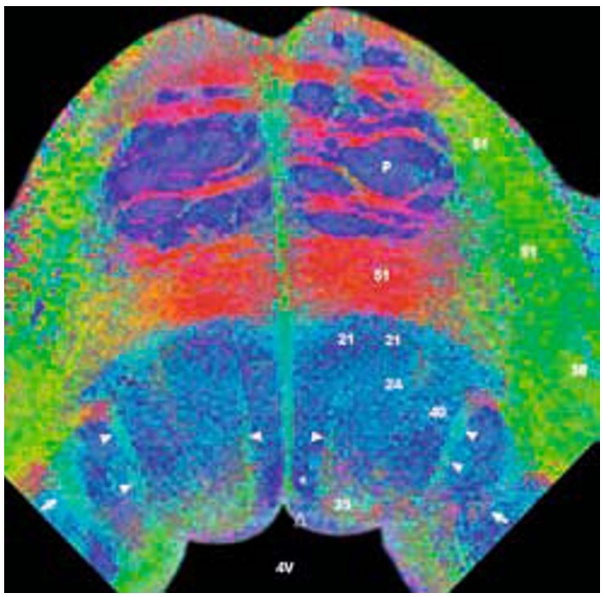

A

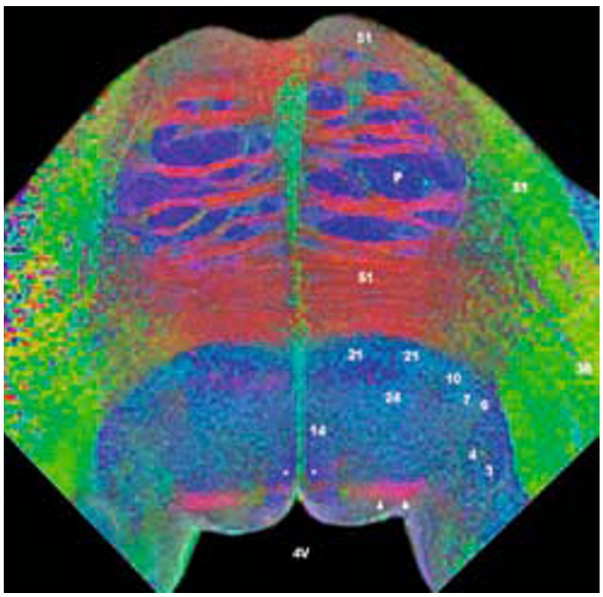

B

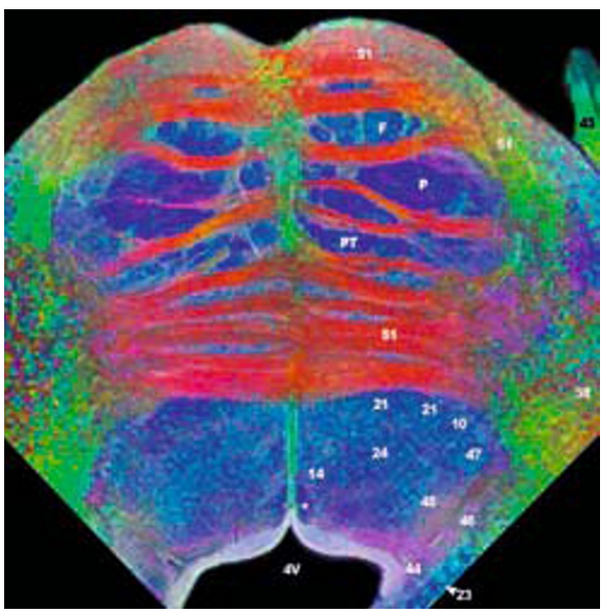

C

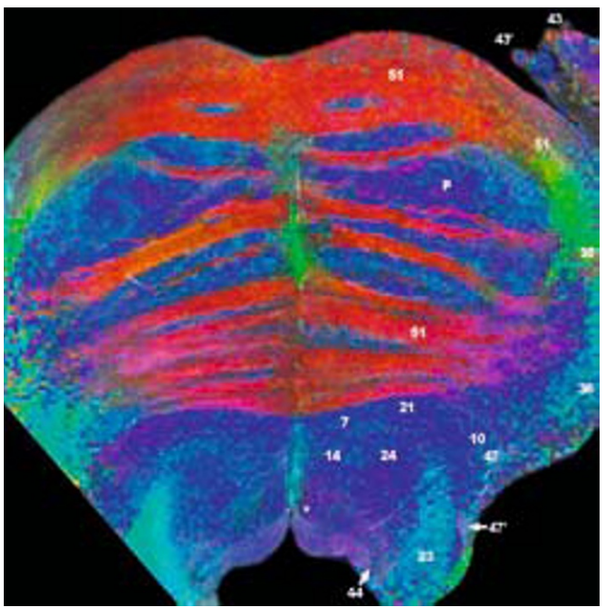

D

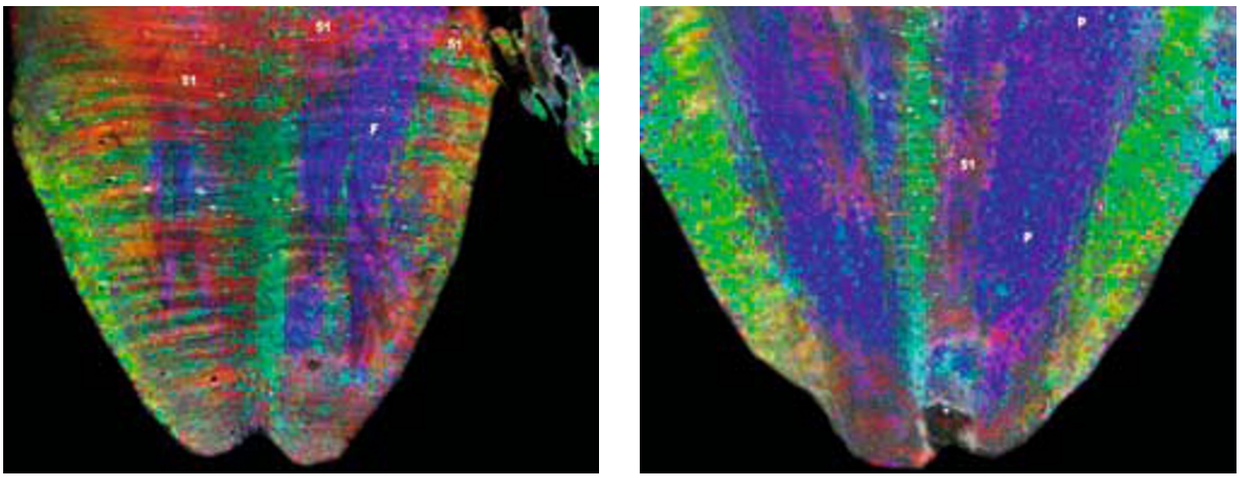

A B

Fig. 10.41 (A–H). Coronal diffusion tensor image of the pons. Post mortem specimen. Images displayed from ventral to dorsal. See also **Figs. 8.52–8.65**.

A–D. Ventral-Mid pons. The red transverse pontocerebellar fibers (51) curve dorsally (green) to join the middle cerebellar peduncles (38). They form prominent sheets of transverse fibers ventral (A) and dorsal (D) to the descending (blue) frontopontine (F) and corticospinal (P) tracts (B and C). The cisternal segment of the trigeminal nerve (CN V) (43) courses sagittally just lateral to the pons. The fascicles of the abducens nerve (CN VI) (single white arrowhead) appear cyan as they course ventrocaudally toward the pontomedullary sulcus. The facial nerve (CN VII) (35) emerges into the cerebellopontine angle cistern just caudal to the middle cerebellar peduncle. This section of the cut nerve is curled, so it appears multicolored. The pontomedullary junction appears as a narrow waist between the laterally bulging middle cerebellar peduncles (38) rostrally and the laterally bulging inferior olivary nuclei (O) caudally.

E–F. Mid-pons. The ascending fibers of the medial (21) and lateral (47) lemnisci and the (predominantly) descending fibers of the central tegmental tract (24) appear blue as they course through the mid-pons. The fibers of the inferior cerebellar peduncle (25) approach the cerebellum posterosuperiorly (cyan), while the fibers of the middle cerebellar peduncle (38) run dorsally and laterally (mixed green and red) into the cerebellum. The inferior olivary nucleus (O), the supra-olivary complex (49) and the pontobulbar body (50) show the mixed stippled coloration of nuclear groups. The facial nerves (35) form well-defined red bands as they pass laterally just beneath the middle cerebellar peduncles, and then become multicolored as the cut ends curl under the peduncle.

G–H. Dorsal pons The dominant blue coloration results from the longitudinal courses of the medial longitudinal fasciculi (17) and inferior cerebellar peduncles (25) caudally and from the medial longitudinal fasciculi (17), central tegmental tracts (24) and lateral lemnisci (47) cranially. The ventrally coursing intrapontine abducens fibers (single white arrowheads) and descending intrapontine segments of the facial nerves (single white arrows) create four short lines of green within the blue dorsal tegmentum (C). The transversely coursing genu and proximal descending segment of the facial nerve (between white arrows) appear red (G). The motor (45), principal sensory (46), and spinal nuclei (4) of the trigeminal nerve and the nucleus centralis superior (54) within the median raphe appear as zones of stippled mixed coloration. The intrapontine fascicles (46′) of the trigeminal nerve appear green as they course ventrodorsally in G. The prominent red band (paired white arrows in H) crossing the middle cerebellar peduncle is probably formed by fibers of the trigeminal nerve.

3 Spinal trigeminal tract
4 Spinal trigeminal nucleus
17 Medial longitudinal fasciculus
21 Medial lemniscus
23 Superior cerebellar peduncle
24 Central tegmental tract
25 Inferior cerebellar peduncle (restiform body)
34 Vestibulocochlear nerve (CN VIII)
35 Facial nerve (CN VII)
37 Ventral acoustic stria and trapezoid body
38 Middle cerebellar peduncle
39 Nucleus of the abducens nerve
45 Motor nucleus of the trigeminal nerve (masticator nucleus)
46 Principal sensory nucleus of the trigeminal nerve
46′ Intrapontine fascicles of the trigeminal nerve
47 Lateral lemniscus
49 Supra-olivary nuclear complex
50 Pontobulbar body
51 Pontocerebellar fibers
54 Nucleus centralis superior

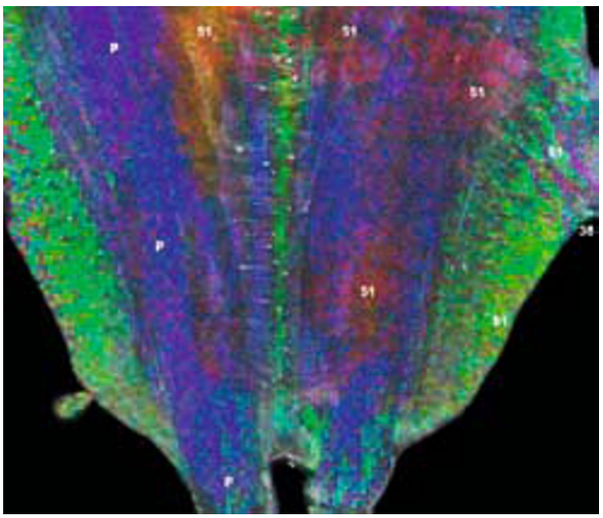

C

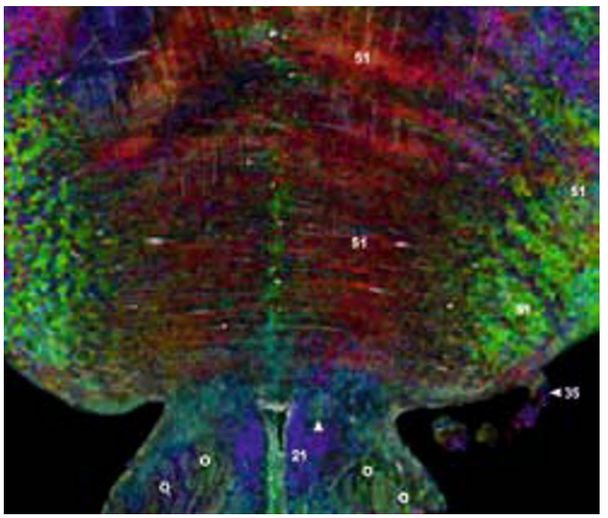

D

Letter labels

F Frontpontine fibers
O Inferior olivary nucleus
P Corticospinal (pyramidal) tract

Arrowheads and arrows

Single white arrowhead: Intrapontine fascicles of the abducens nerve (CN VI)
Single white arrows: Intrapontine fascicles of the facial nerve (CN VII)
Dual white arrows: Fascicles of the trigeminal nerve (CN V) traversing the middle cerebellar peduncle
Between white arrows: Genu of the facial nerve over the abducens nucleus (39) forming the facial colliculus (in H)

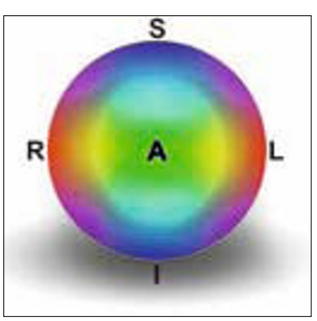

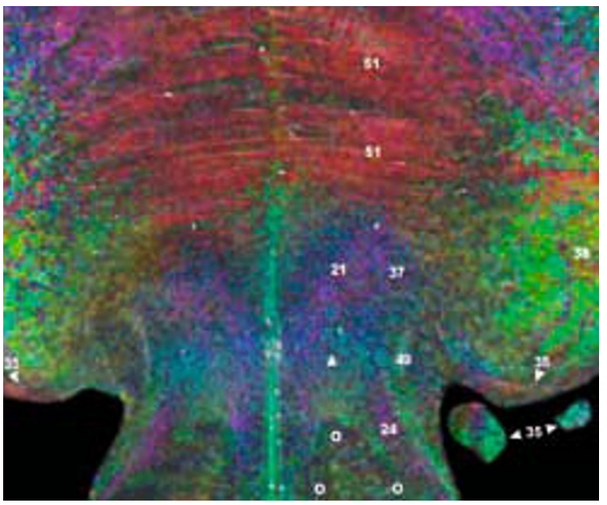
51
51
21
37
38
35
49
35
24
35

E

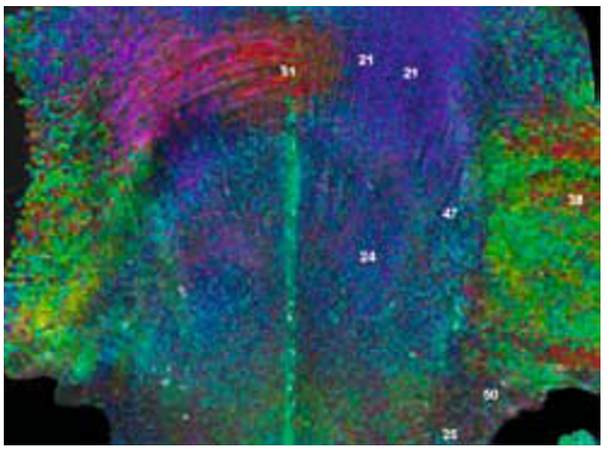
31
21
21
47
38
24
50
25

F

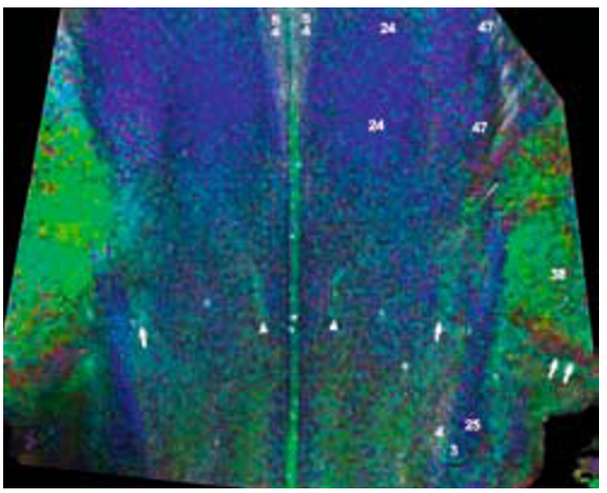
24
47
24
47
38
25
3

G

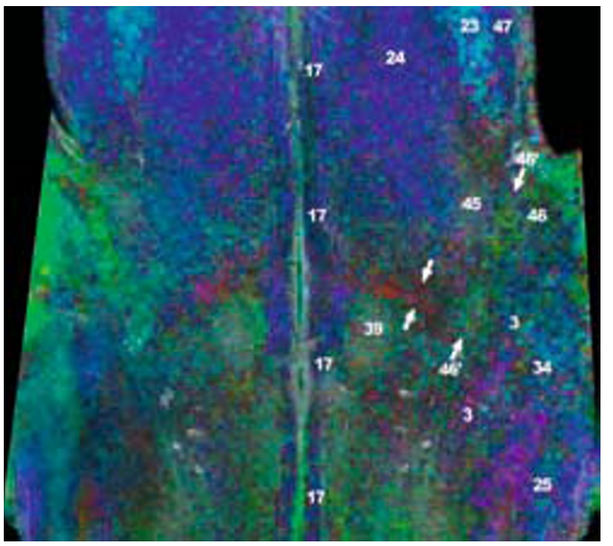
23
47
17
24
46
45
46
17
38
3
17
46
34
3
17
25

H

SECTION XI

GROSS SECTIONAL ANATOMY AND 3T MRI CORRELATIONS IN AXIAL, CORONAL AND SAGITTAL PLANES

Axial, coronal, and sagittal serial sections of the brain stem and cerebellum will be successively studied.

Additional information is available in numerous other works about gross morphology, sectional anatomy and MRI [4, 11, 14, 15, 22, 23, 30, 39, 56. 68, 71, 79, 90, 92, 110, 122, 123, 125, 126, 134, 147, 148, 167, 181, 193, 194, 240, 291, 310, 322, 343, 348, 358, 360, 370, 372, 377, 396, 400, 401, 402, 431, 440, 441, 442].

Axial (horizontal) sections in the intercommissural plane extending from the mid anterior commissure to the mid posterior commissure. (Figs. 11.1–11.29)

In the following figures, the anatomic specimen of the brain stem, cerebellum, and diencephalon is progressively reduced by 2 mm thick sections to show each new level in relation to the remaining portion of the specimen. Each figure consists of the inferior view of the remaining axial surface, with oblique views demonstrating the level of the section. Corresponding sections of the head are provided for nearly all levels to demonstrate the relationship of the brain to the skull and adjoining structures. At each level, both T1- and T2-weighted 3 Tesla MR images are provided for comparison. On each pair of facing pages all of the structures are labelled coherently, using the single key provided. However, the specific key does change from page to page.

The 3 Tesla *in vivo* T1- and T2-weighted images were obtained at the MGH/ MIT/ HMS Athinoula A. Martinos Center for Functional and Structural Biomedical Imaging, Charlestown, MA, USA on a commercially available Siemens Magnetom TIM Trio (VB13A) [Siemens, Erlangen, Germany] using a 32-channel custom-built head coil courtesy of Graham C. Wiggins, Ph. D. and Larry L. Wald, Ph. D..

The specific pulse sequences used to obtain the clinical images illustrated are given below:

T1-weighted Images: Three-dimensional TFL (MPRAGE) (Magnetization-prepared acquisition by gradient (recalled) echo):
Repetition time: 2250 ms; Echo time: 5.7 ms; Inversion time: 900 ms; Flip angle: 9 degrees; Matrix: 512 x 416 pixels; Field of view: 200 x 162 mm; Slice thickness 4 mm; Interslice gap: 0 mm; 48 slices, 1 average.

T2-weighted Images: Two-dimensional turbo spin echo sequence with:
Repetition time: 6550 ms; Echo time: 139 ms; Echo train length: 19; Matrix: 512 x 416 pixels, Field of view: 220 x 178 mm; Slice thickness 2 mm; Interslice gap: 0 mm; 49 slices; 1 average.

MR Cisternograms: Three-dimensional CISS (Constructive Interference in Steady State) sequence with a quadrature head coil using:
Repetition time: 12.25 ms; Echo time: 5.9 ms; Flip angle: 70 degrees; Matrix: 512 x 512 pixels; 196 phase encoding steps; Field of view: 180 mm; Slice thickness: 0.66 mm; 1 average.

For each section, the cartoon indicates the section level (light line) with respect to Schaltenbrand's intercommissural plane (bold line).

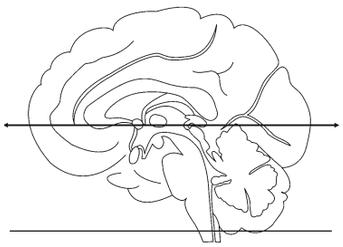

Fig. 11.1 (A–C). Axial (horizontal) section.
Cervicomedullary junction
A. Inferior view after removal of the cerebral hemispheres. Bar: 10 mm.
B. Anterior oblique view. **C.** Posterior oblique view.

See **Fig. 2.7** for more information about the structures demonstrated at this level.

1 Decussation of pyramids (corticospinal tract)
2 Nucleus supraspinalis (first cervical nerve)
3 Spinal trigeminal nucleus (pars caudalis)
4 Cuneate fasciculus
5 Gracile fasciculus
6 Pyramid of medulla (including the corticospinal tract)
7 Inferior olive
8 Tonsil
9 Postpyramidal (secondary) fissure
10 Biventral lobule
11 Prepyramidal fissure
12 Gracile lobule
13 Inferior semilunar lobule
14 Great horizontal fissure
15 Pyramid of vermis

A

B

C

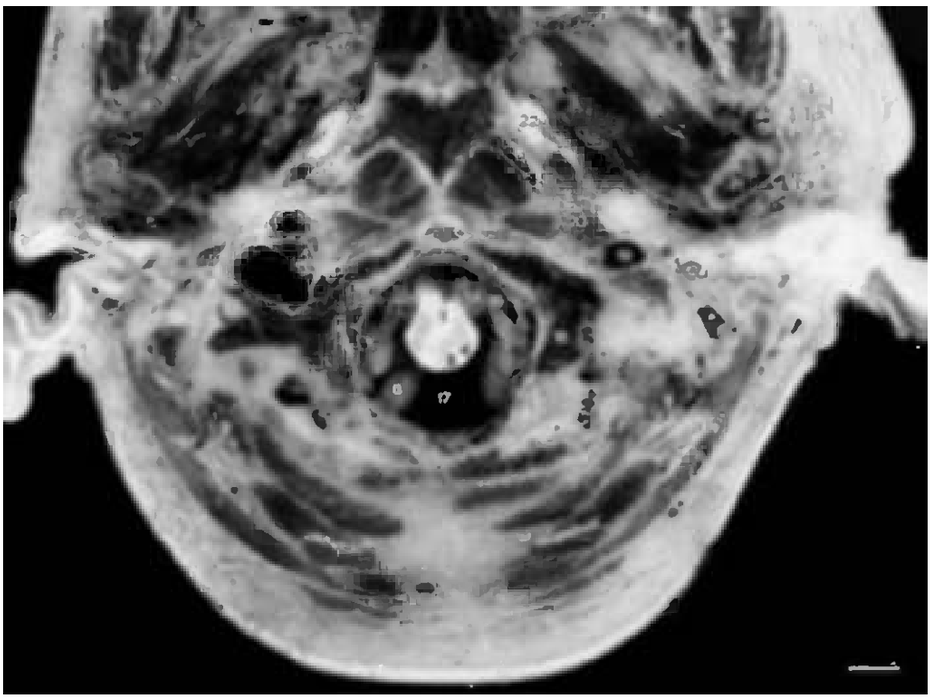

D

Fig. 11.1 (D–F).
D. Axial section of the head. Inferior view. Bar: 10 mm.
E–F. 3 Tesla MRI. E. T1-weighted MRI. **F.** T2-weighted MRI.

1 Decussation of pyramids (corticospinal tract)
4 Cuneate fasciculus
5 Gracile fasciculus
8 Tonsil
16 Paired vertebral arteries
16′ Paired posterior inferior cerebellar arteries
17 Foramen magnum and cerebellomedullary cistern
18 Occipital bone, lateral portion
19 Internal jugular vein
20 Internal carotid artery
21 Mandibular condyle
22 Eustachian tube

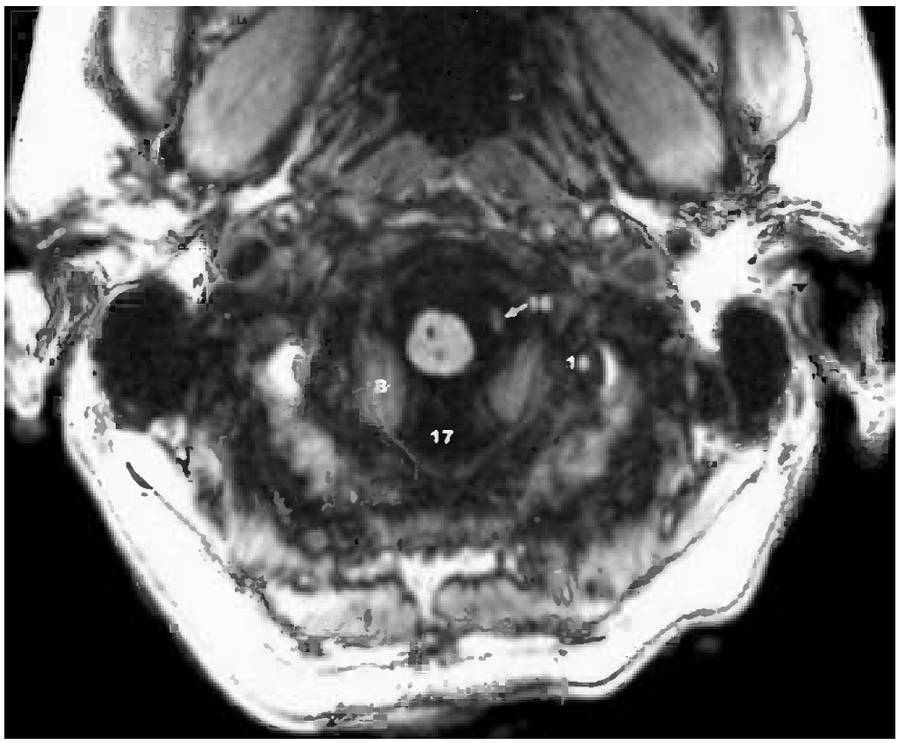

E

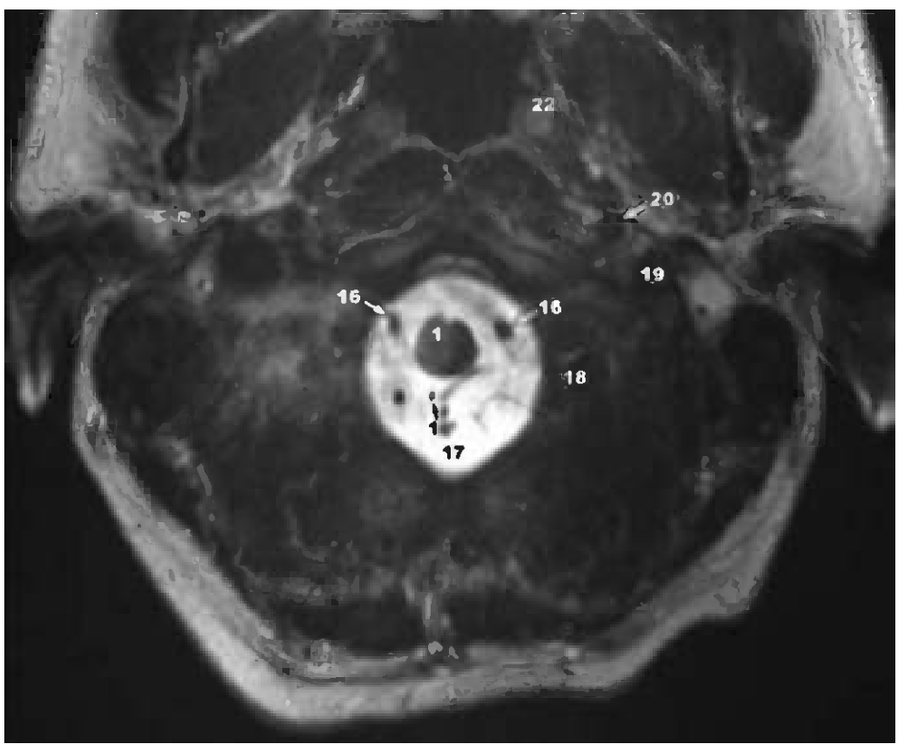

F

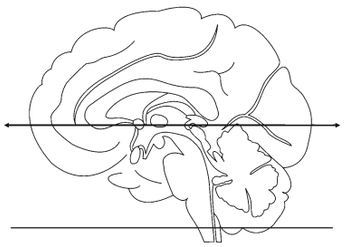

Fig. 11.2 (A–C). Axial (horizontal) section.
Medulla
A. Inferior view after removal of the cerebral hemispheres. Bar: 10 mm.
B. Anterior oblique view. **C.** Posterior oblique view.

1 Corticospinal tract
2 Lemniscal decussation (great sensory decussation)
3 Spinal trigeminal nucleus (pars caudalis) (CN V)
4 Cuneate fasciculus
5 Gracile fasciculus
6 Nucleus of the solitary tract
7 Hypoglossal nucleus (CN XII)
8 Pyramid of the medulla (including the corticospinal tract)
9 Inferior olive
10 Tonsil
11 Postpyramidal (secondary) fissure
12 Biventral lobule
13 Prepyramidal fissure
14 Gracile lobule
15 Inferior semilunar lobule
16 Great horizontal fissure
17 Pyramid of the vermis

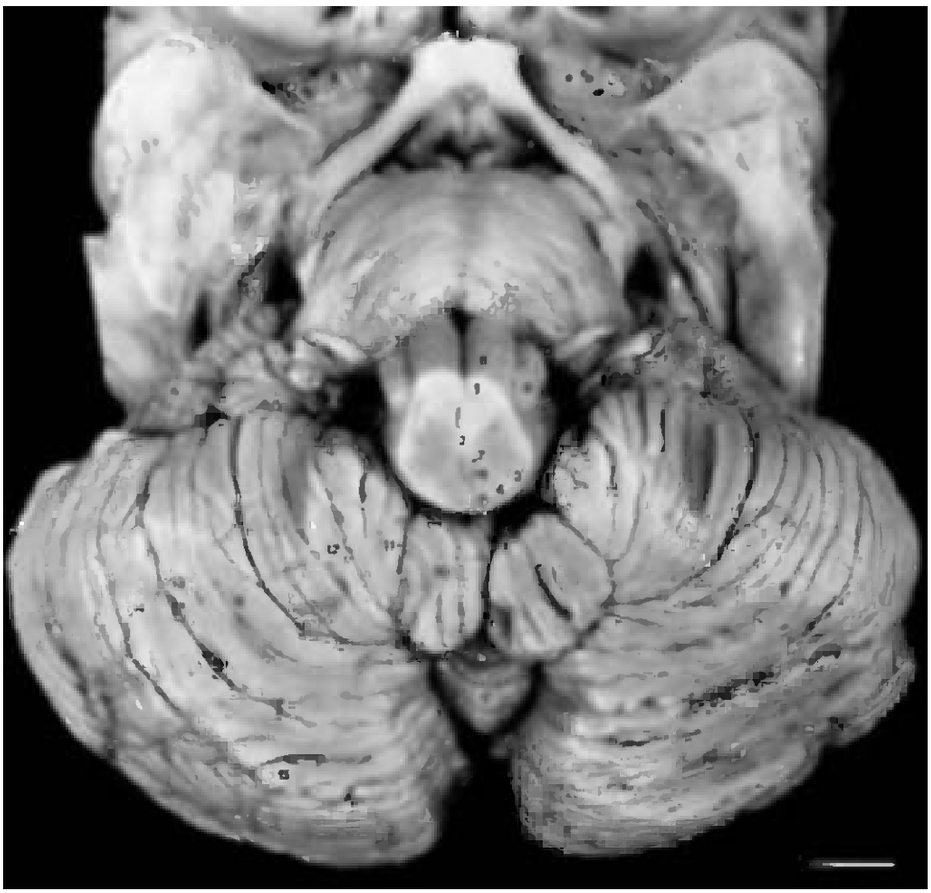

A

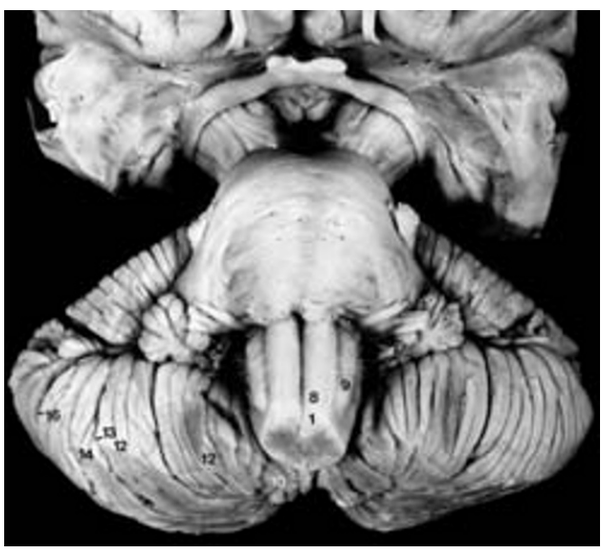

B

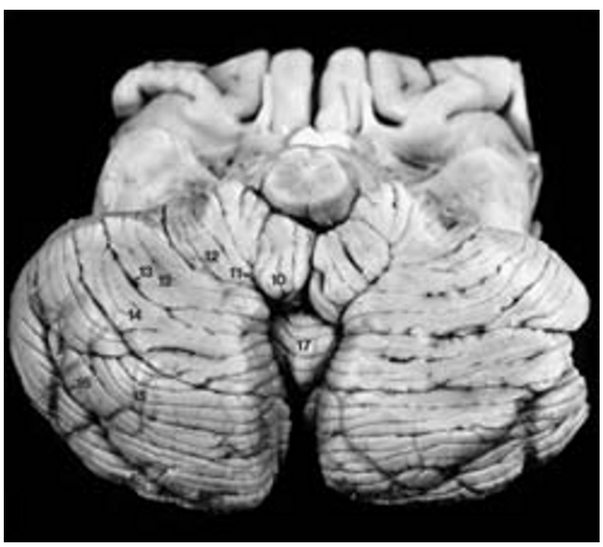

C

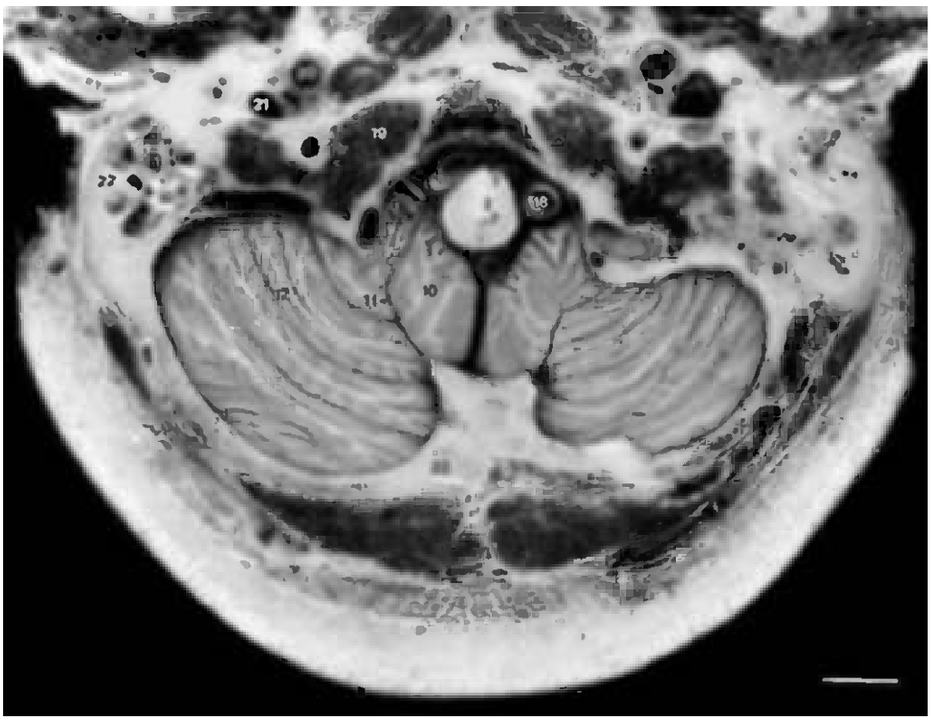

D

Fig. 11.2 (D–F).
D. Axial section of the head. Inferior view. Bar: 10 mm.
E–F. 3 Tesla MRI. E. T1-weighted MRI**. F.** T2-weighted MRI.

1 Corticospinal tract
2 Lemniscal decussation (great sensory decussation)
7 Hypoglossal nucleus (CN XII)
10 Tonsil
11 Postpyramidal (secondary) fissure
12 Biventral lobule
18 Vertebral artery
18′ Posterior inferior cerebellar artery
19 Occipital bone, lateral portion
19′ Occipital bone, basal portion
20 Internal carotid artery
21 Internal jugular vein
22 Mastoid process
23 Occipital bone, squama

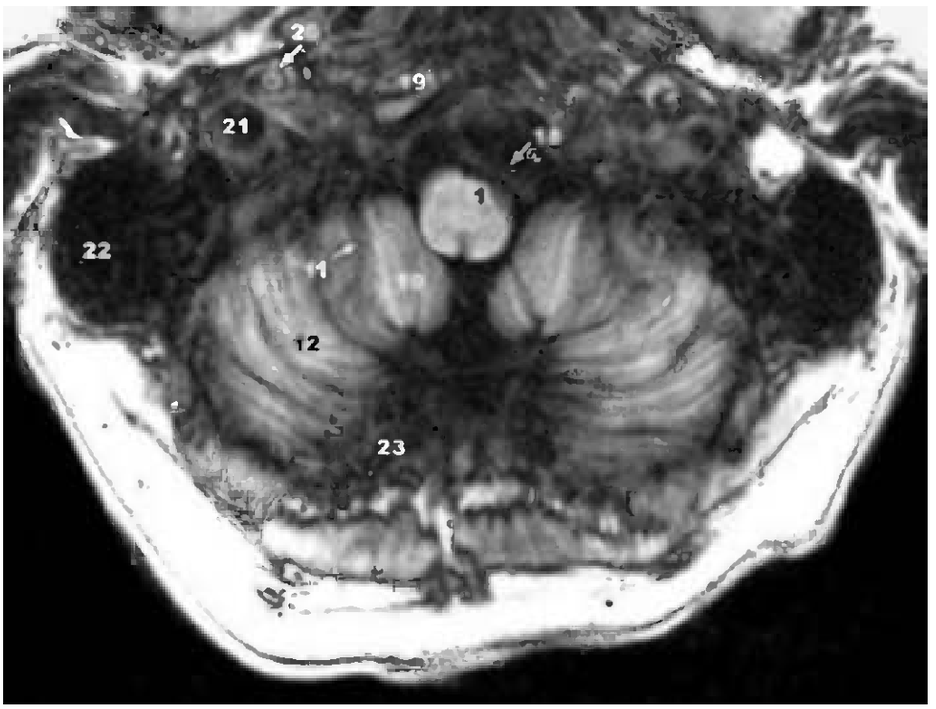

E

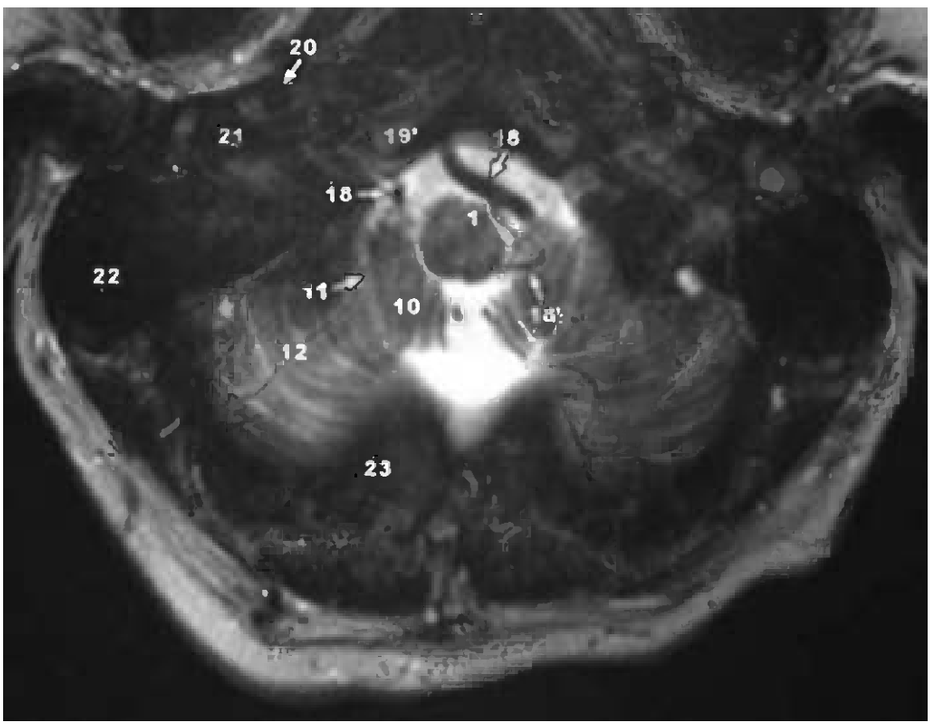

F

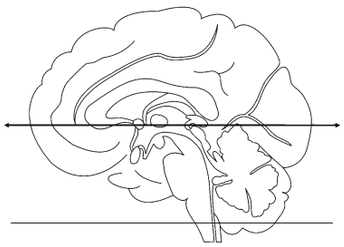

Fig. 11.3 (A–C). Axial (horizontal) section.
Medulla

A. Inferior view after removal of the cerebral hemispheres. Bar: 10 mm.
B. Anterior oblique view. **C.** Posterior oblique view.

See Fig. 2.8 for more information about the structures demonstrated at this level and Fig. 7.4 for the vascular territories.

1 Pyramid of the medulla (including corticospinal tract)
2 Medial lemniscus
3 Inferior olive
4 Spinal trigeminal tract and nucleus (pars caudalis) (CN V)
5 Cuneate nucleus (medial cuneate nucleus)
6 Gracile nucleus
7 Nucleus of the solitary tract
8 Hypoglossal nucleus (CN XII)
9 Tonsil
10 Postpyramidal (secondary) fissure
11 Biventral lobule
11′ Intrabiventral fissure
12 Prepyramidal fissure
13 Gracile lobule
14 Great horizontal fissure
15 Inferior semilunar lobule
16 Pyramid of vermis

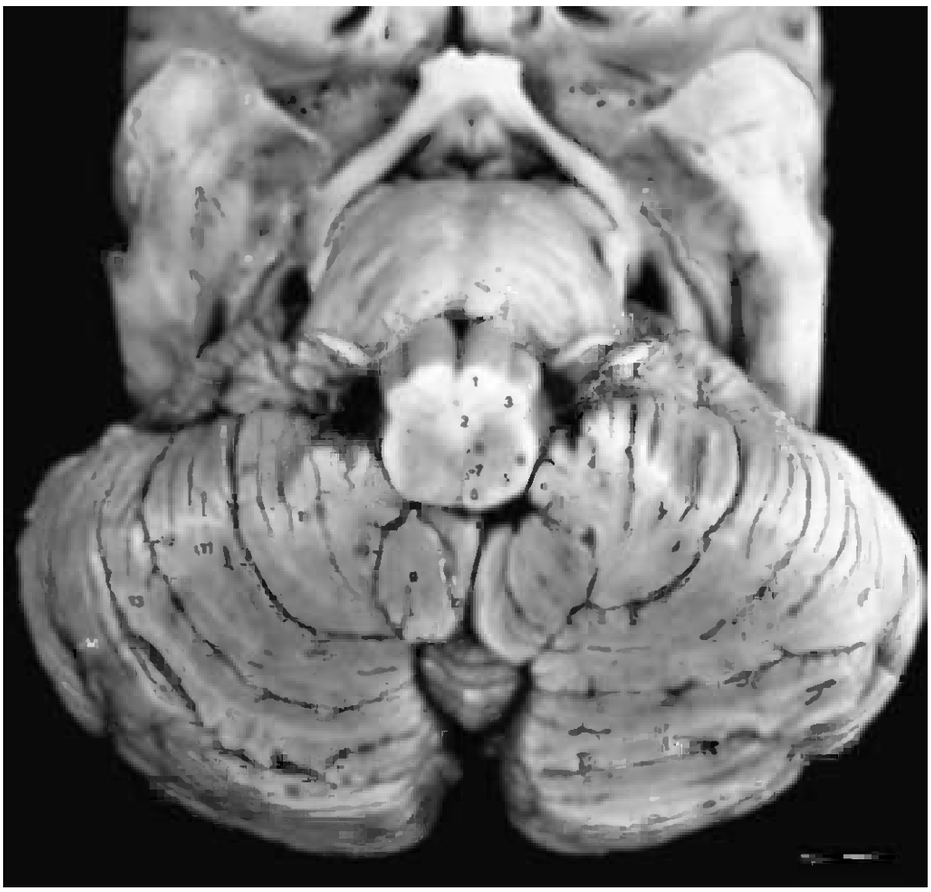

A

B

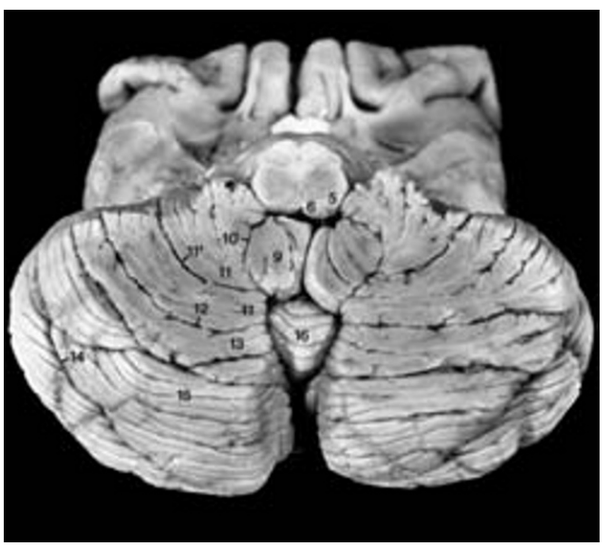

C

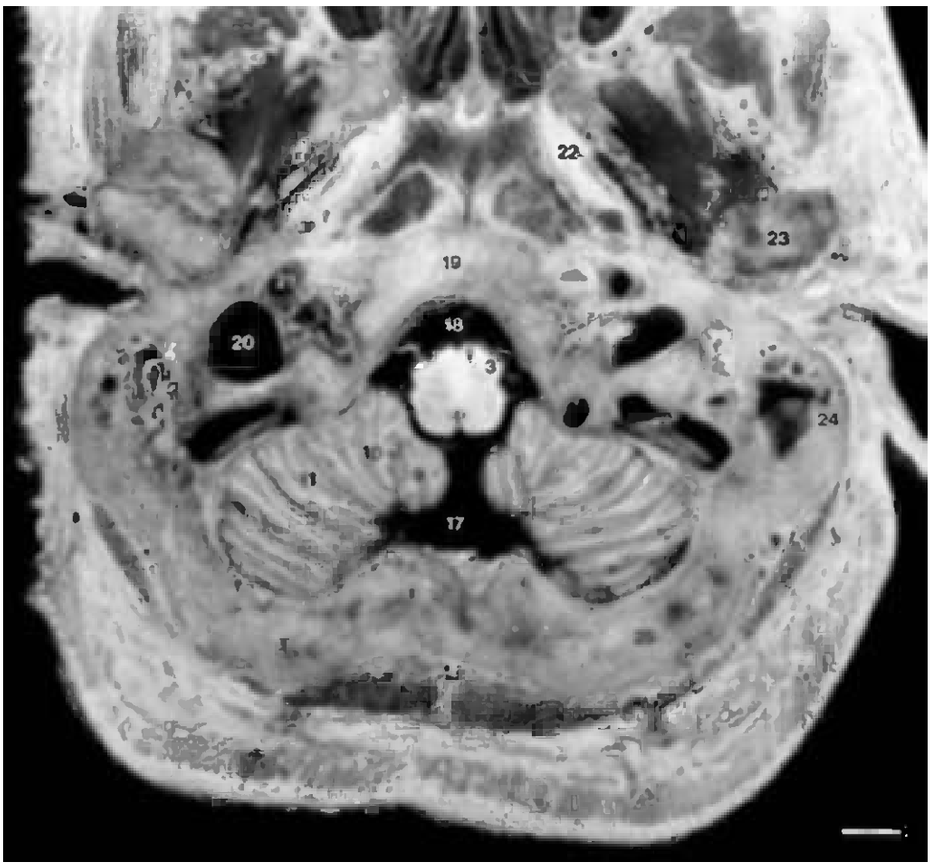

D

Fig. 11.3 (D–F).
D. Axial section of the head. Inferior view. Bar: 10 mm.
E–F. 3 Tesla MRI. **E.** T1-weighted MRI. **F.** T2-weighted MRI.

1 Pyramid of the medulla (including corticospinal tract)
3 Inferior olive
9 Tonsil
10 Postpyramidal (secondary) fissure
11 Biventral lobule
17 Cerebellomedullary cistern (cisterna magna)
18 Premedullary cistern
18′ Posterior inferior cerebellar artery
18″ Vertebro-basilar artery
19 Occipital bone, basilar portion
20 Internal jugular vein
21 Internal carotid artery
22 Eustachian tube
23 Mandibular condyle
24 Mastoid process
25 Occipital bone, squama

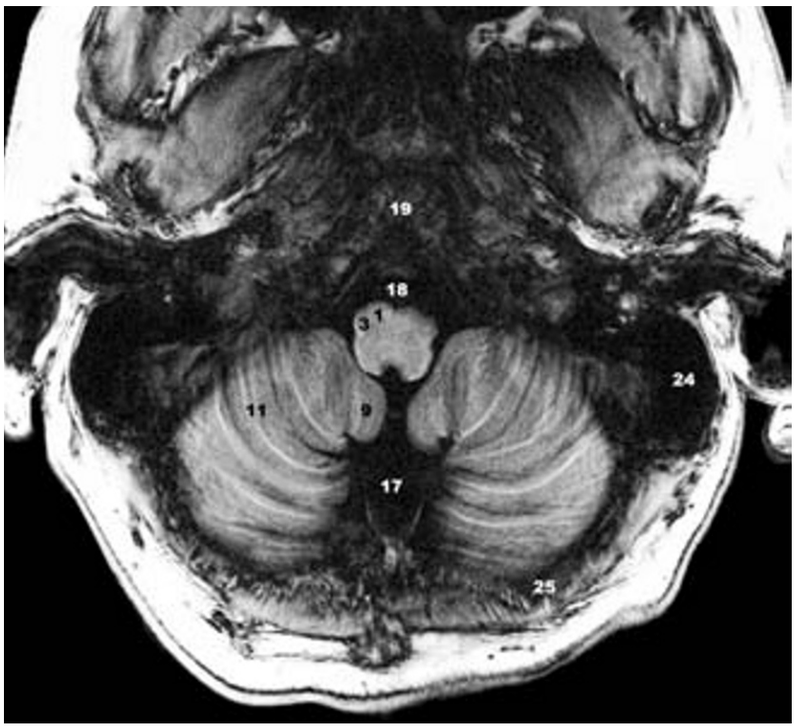

E

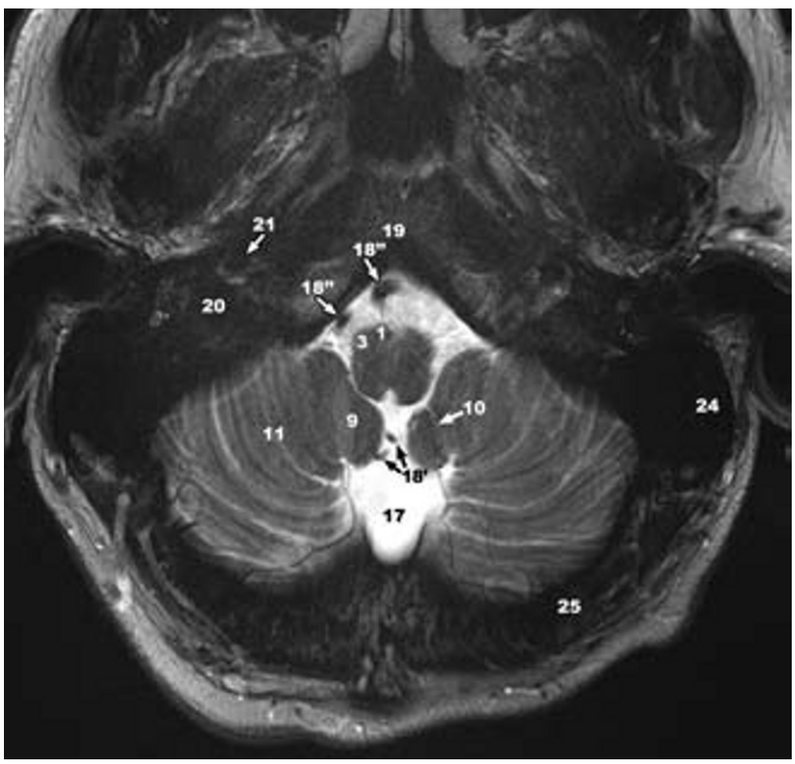

F

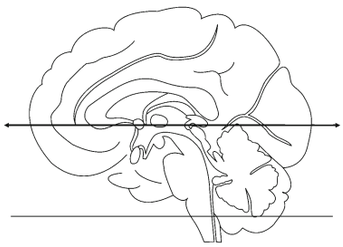

Fig. 11.4 (A–E). Axial (horizontal) section.
Medulla
A. Inferior view after removal of the cerebral hemispheres. Bar: 10 mm.
B. Anterior oblique view. **C.** Posterior oblique view.
D and E. 3 Tesla MRI. **D.** T1-weighted MRI. **E.** T2-weighted MRI.

1 Pyramid of the medulla (including the corticospinal tract)
2 Medial lemniscus
3 Inferior olive, formed by the inferior olivary nucleus
4 Spinothalamic tract
5 Spinal trigeminal tract and nucleus (pars caudalis) (CN V)
6 Cuneate nucleus (medial cuneate nucleus)
7 Gracile nucleus
8 Nucleus of the solitary tract
9 Hypoglossal nucleus (CN XII)
10 Tonsil
11 Postpyramidal (secondary) fissure
12 Biventral lobule
13 Prepyramidal fissure
14 Gracile lobule
15 Inferior semilunar lobule
16 Great horizontal fissure
17 Pyramid of vermis
18 Premedullary cistern
18′ Vertebral artery
19 Occipital bone, basilar portion
20 Occipital bone, squama

B

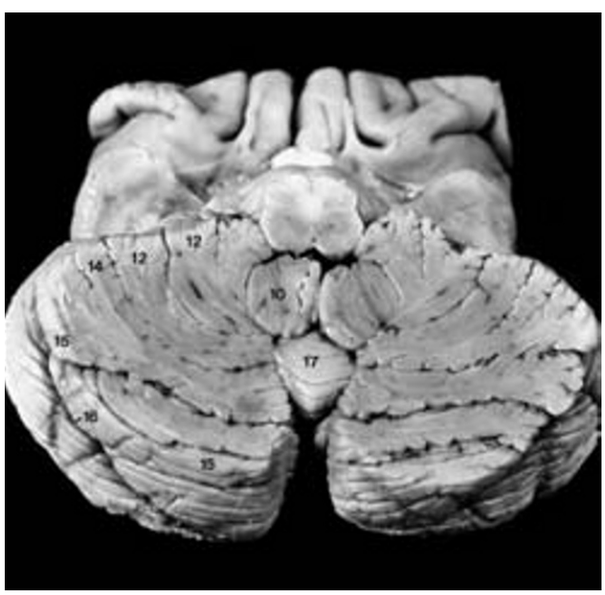

C

A

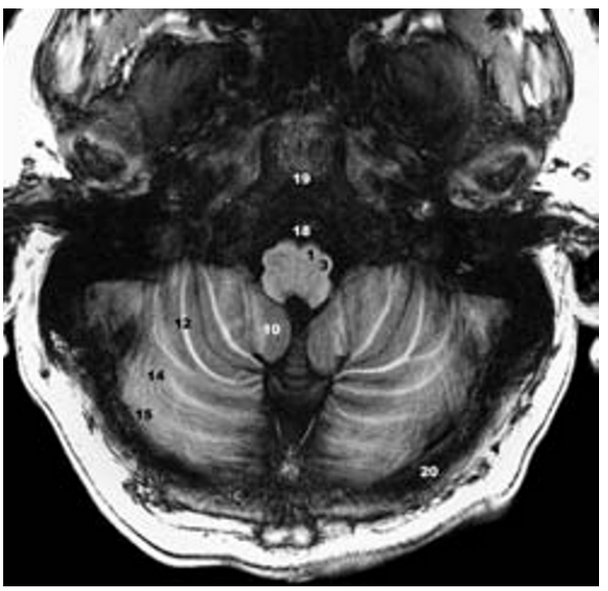

D

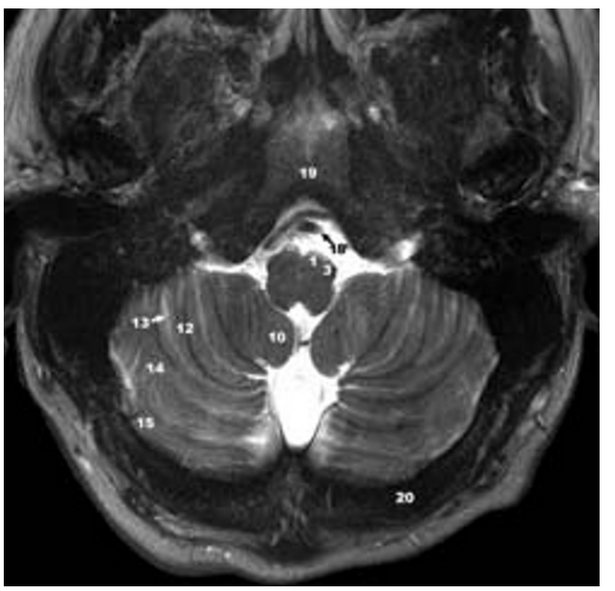

E

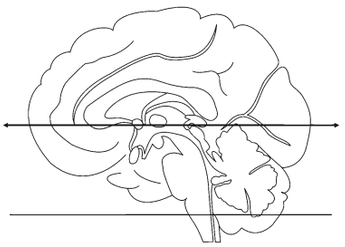

Fig. 11.5 (A–C). Axial (horizontal) section.
Medulla

A. Inferior view after removal of the cerebral hemispheres. Bar: 10 mm.

B. Anterior oblique view. **C.** Posterior oblique view.

See Fig. 2.9 for more information about the structures demonstrated at this level and Fig. 7.6 for the vascular territories.

1 Pyramid of medulla (including the corticospinal tract)
2 Medial lemniscus
3 Inferior olive, formed by the inferior olivary nucleus
4 Spinothalamic tract
5 Spinal trigeminal tract and nucleus (pars caudalis) (CN V)
6 Inferior cerebellar peduncle (restiform body)
7 Cuneate nucleus (medial cuneate nucleus)
8 Gracile nucleus
9 Nucleus of the solitary tract
10 Hypoglossal nucleus (CN XII)
11 Tonsil
12 Postpyramidal (secondary) fissure
13 Biventral lobule
14 Prepyramidal fissure
15 Gracile lobule
16 Inferior semilunar lobule
17 Great horizontal fissure
18 Pyramid of vermis

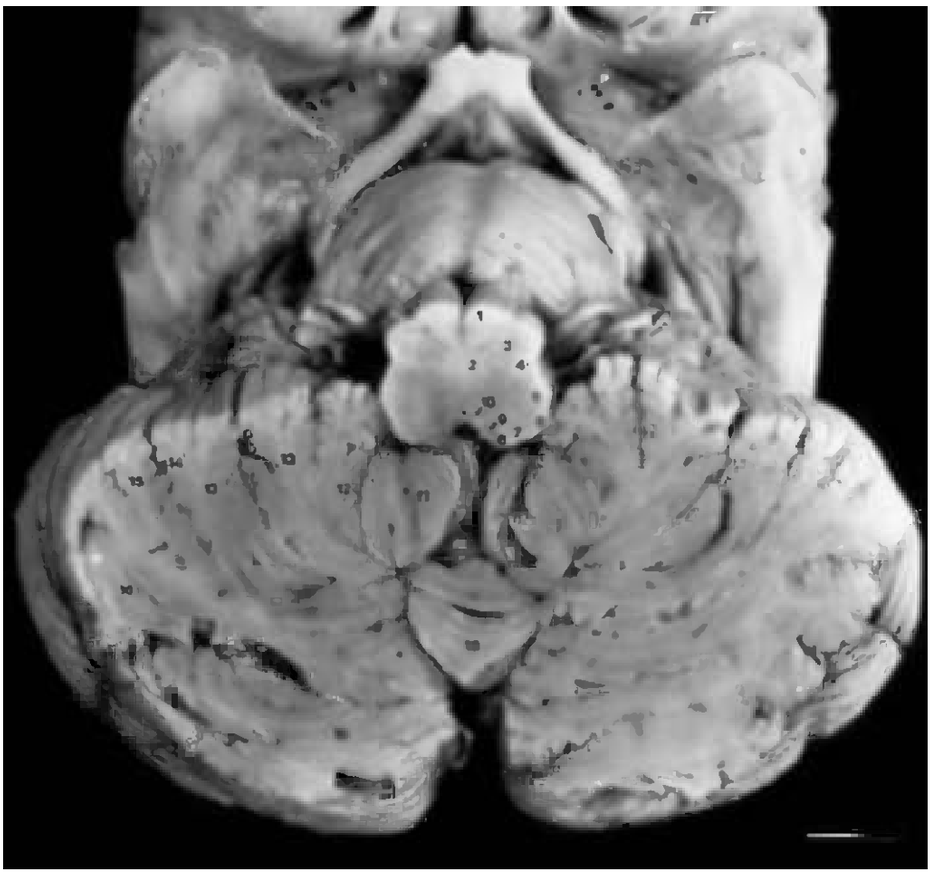

A

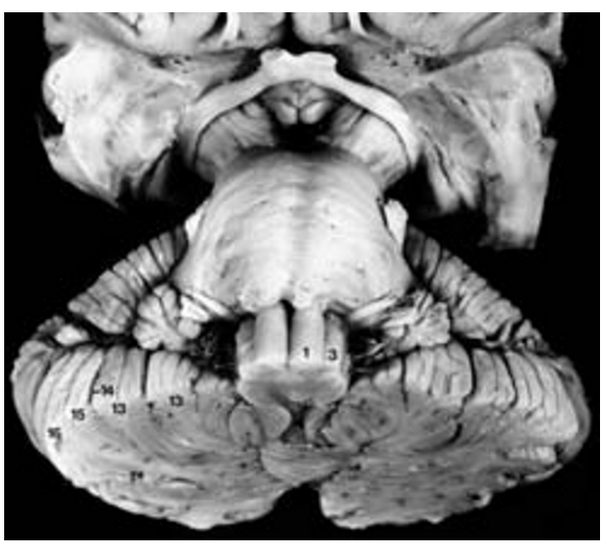

B

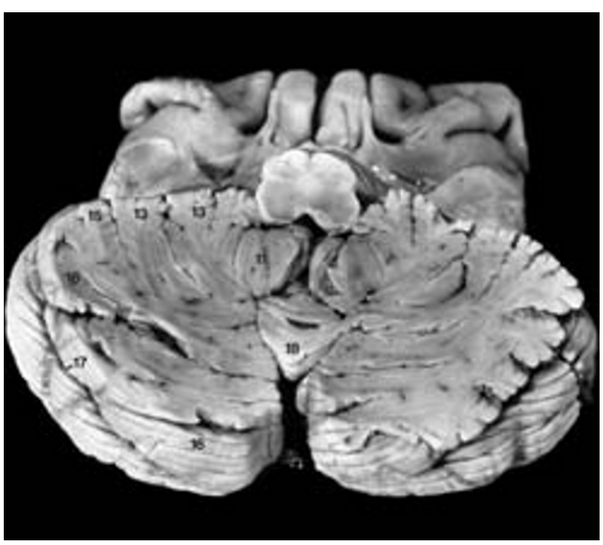

C

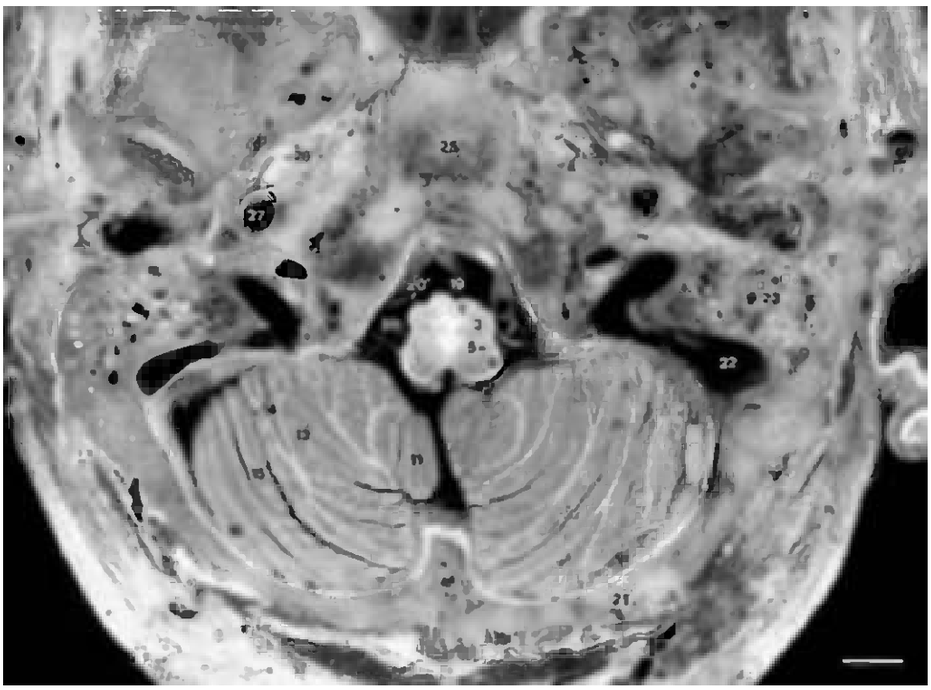

D

Fig. 11.5 (D–F).
D. Axial section of the head. Superior view. Bar: 10 mm.
E.-F. 3T MR Cisternograms.

1 Pyramid of medulla (including the corticospinal tract)
3 Inferior olivary nucleus
5 Spinal trigeminal tract and nucleus (pars caudalis) (CN V)
6 Inferior cerebellar peduncle (restiform body)
11 Tonsil
12 Postpyramidal (secondary) fissure
13 Biventral lobule
13′ Intrabiventral fissure
14 Prepyramidal fissure
15 Gracile lobule
15′ Ansoparamedian fissure
16 Inferior semilunar lobule
19 Premedullary cistern and vertebral arteries
20 Lateromedullary cistern
20′ Hypoglossal nerve (CN XII)
21 Occipital bone, squama
22 Sigmoid sinus
22′ Internal jugular vein (jugular bulb)
23 Mastoid process
24 Mandibular condyle
25 Occipital bone, basilar portion
26 Eustachian tube
27 Internal carotid artery

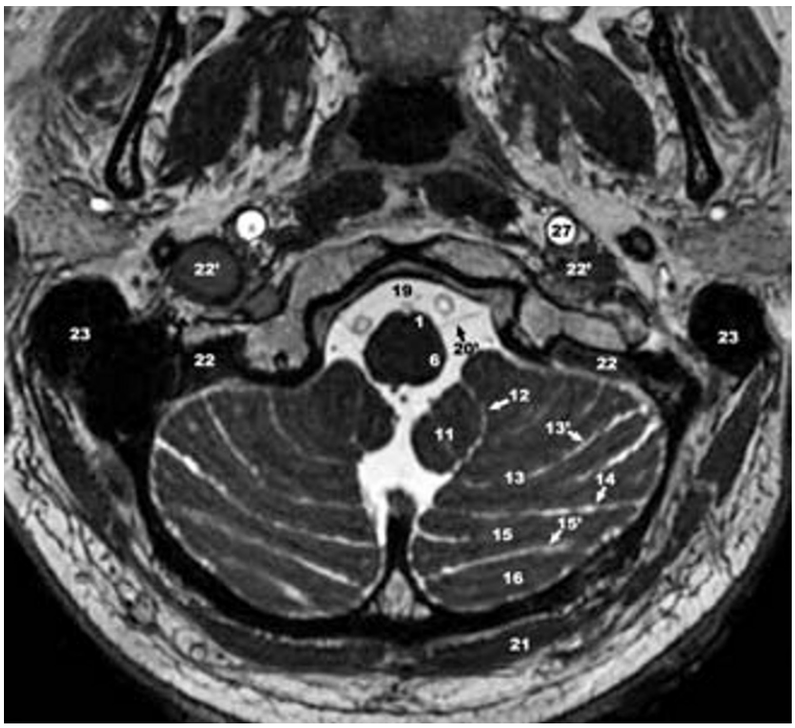
27
22'
22'
19
1
23
22
6
20'
22
23
12
13'
11
13
14
15
15'
16
21

E

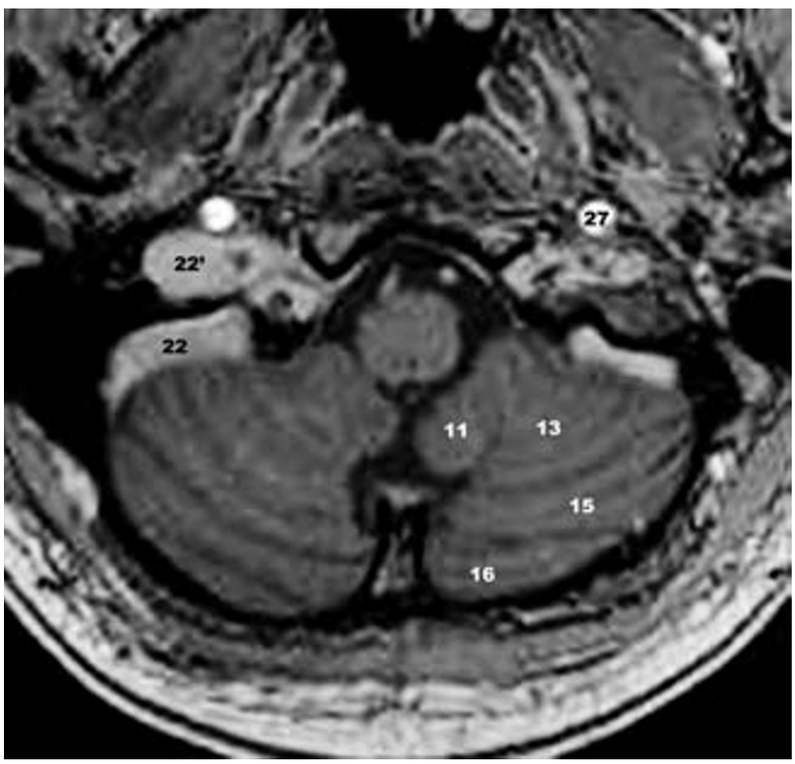
27
22'
22
11
13
15
16

F

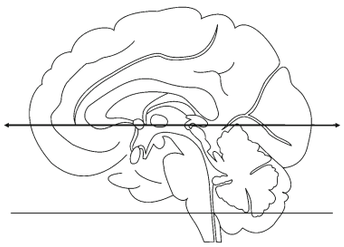

Fig. 11.6 (A–C). Axial (horizontal) section.
Medulla
A. Inferior view after removal of the cerebral hemispheres. Bar: 10 mm.
B. Anterior oblique view. **C.** Posterior oblique view.

1 Pyramid of the medulla (including the corticospinal tract)
2 Medial lemniscus
3 Inferior olive, formed by the inferior olivary nucleus
4 Spinothalamic tract
5 Spinal trigeminal tract and nucleus (pars caudalis) (CN V)
6 Inferior cerebellar peduncle (restiform body)
7 Medial vestibular nucleus (CN VIII)
8 Nucleus of the solitary tract
9 Hypoglossal nucleus (CN XII)
9′ Hypoglossal nerve (CN XII)
10 Accessory nerve (CN XI)
11 Vagus nerve (CN X)
12 Glossopharyngeal nerve (CN IX)
13 Vestibulocochlear nerve (CN VIII)
14 Facial nerve (CN VII)
15 Abducens nerve (CN VI)
16 Tonsil
17 Postpyramidal (secondary) fissure
18 Biventral lobule
19 Prepyramidal fissure
20 Gracile lobule
21 Inferior semilunar lobule
22 Great horizontal fissure
23 Superior semilunar lobule
24 Pyramid of the vermis
25 Uvula
26 Fourth ventricle (very near to the median aperture (foramen of Magendie))
27 Choroid plexi and lateral aperture of the fourth ventricle (foramen of Luschka)

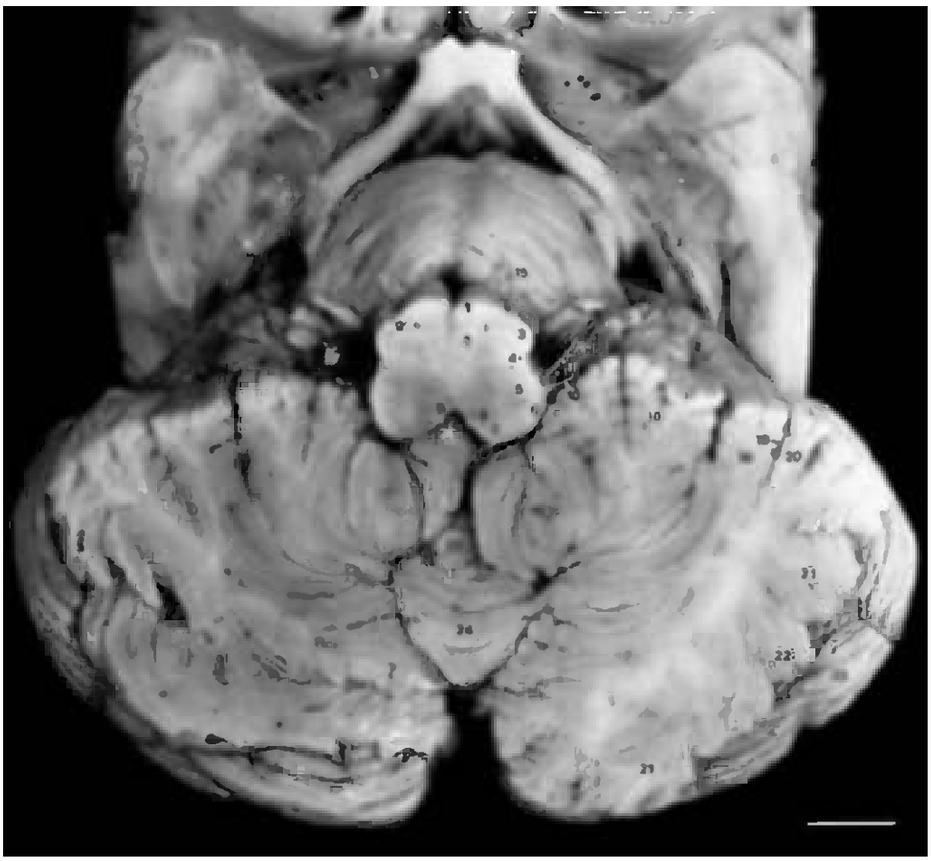

A

B

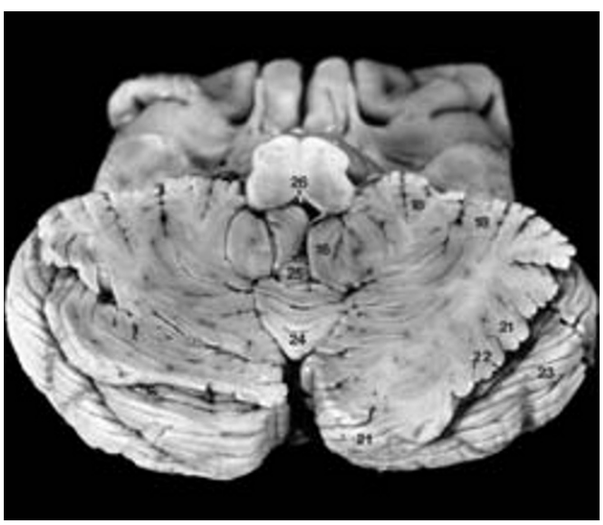

C

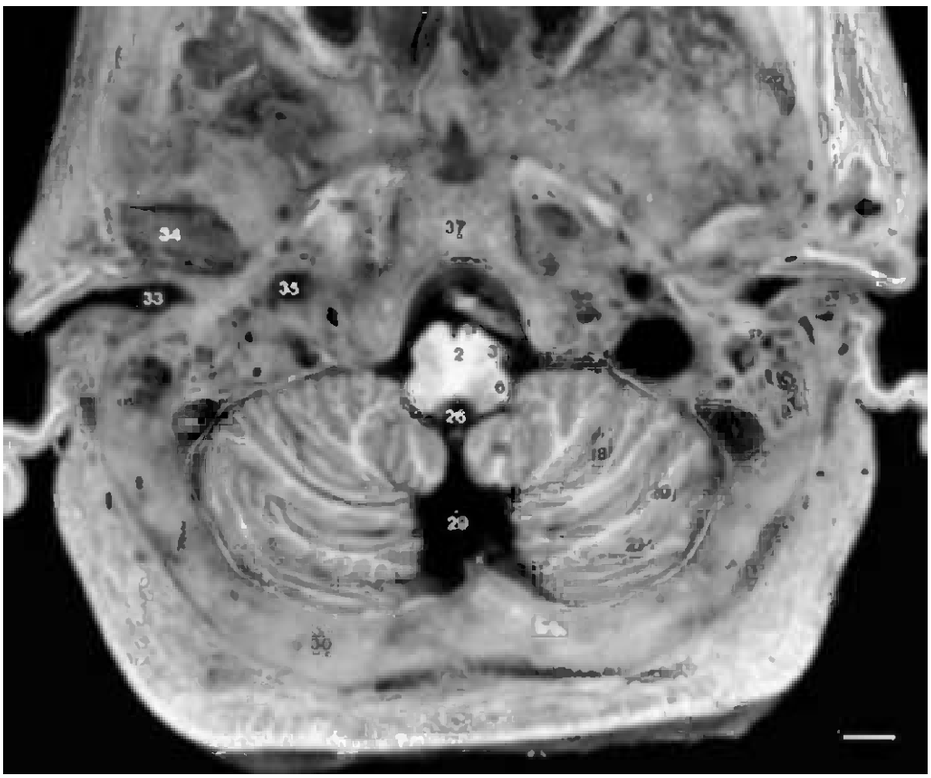

D

Fig. 11.6 (D–F).
D. Axial section of the head. Superior view. Bar: 10 mm.
E–F. 3 Tesla MRI. E. T1-weighted MRI. **F.** T2-weighted MRI.

1 Pyramid of the medulla (including the corticospinal tract)
2 Medial lemniscus
3 Inferior olive, formed by the inferior olivary nucleus
6 Inferior cerebellar peduncle (restiform body)
16 Tonsil
18 Biventral lobule
20 Gracile lobule
21 Inferior semilunar lobule
24 Pyramid of the vermis
25 Uvula
26 Inferior fourth ventricle
28 Premedullary cistern
28′ Vertebral artery
29 Cerebellomedullary cistern (cisterna magna)
30 Occipital bone, squama
31 Sigmoid sinus
32 Mastoid process
33 External acoustic meatus
34 Mandibular condyle
35 Internal carotid artery
36 Eustachian tube
37 Occipital bone, basilar portion

IX–XI Cranial nerves IX–XI

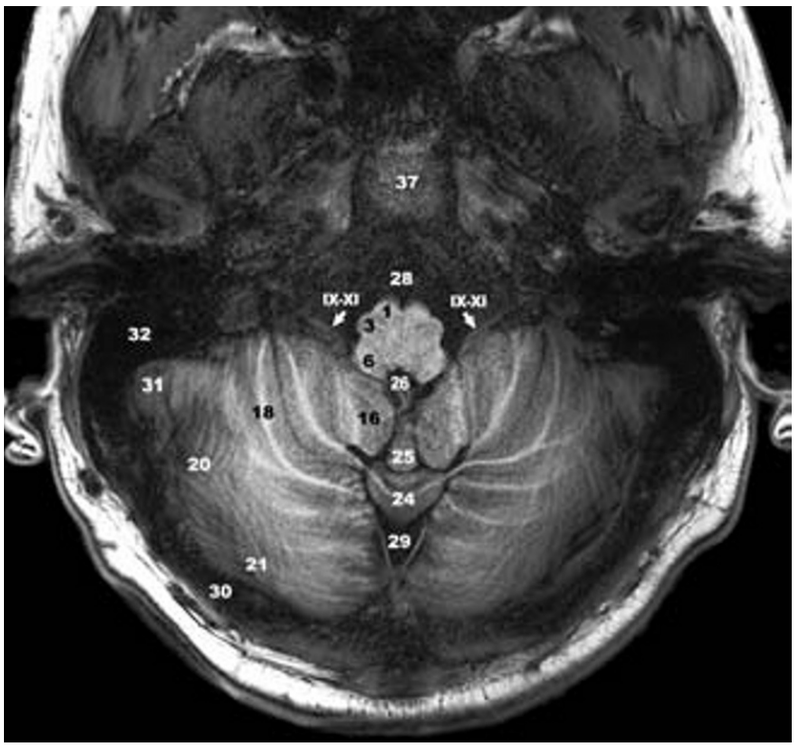
37
28
IX-XI
1
IX-XI
3
32
6
31
26
18
16
20
25
24
29
21
30

E

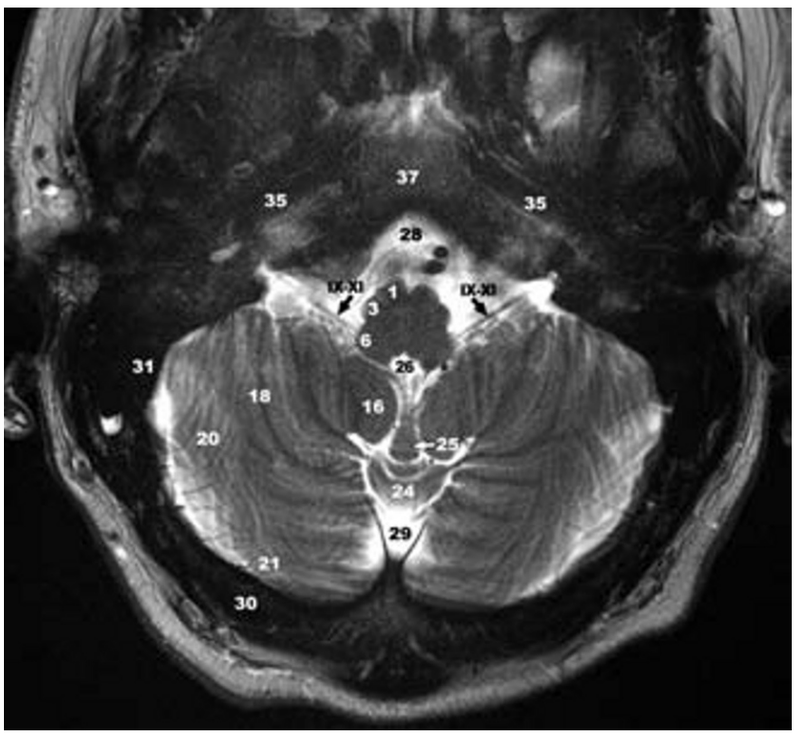
37
35
35
28
IX-XI
1
IX-XI
3
6
31
26
18
16
20
25
24
29
21
30

F

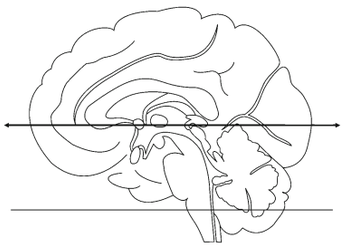

Fig. 11.7 (A–C). Axial (horizontal) section.
Medulla

A. Inferior view after removal of the cerebral hemispheres. Bar: 10 mm.

B. Anterior oblique view. **C.** Posterior oblique view.

See **Fig. 2.10** for more information about the structures demonstrated at this level and **Fig. 7.8** for the vascular territories.

1 Pyramid of medulla (including the corticospinal tract)
2 Medial lemniscus
3 Inferior olive, formed by the inferior olivary nucleus
4 Spinothalamic tract
5 Spinal trigeminal nucleus (pars interpolaris) (CN V)
6 Inferior cerebellar peduncle (restiform body)
7 Medial vestibular nucleus (CN VIII)
8 Nucleus of the solitary tract
9 Hypoglossal nucleus (CN XII)
10 Choroid plexus and lateral aperture of the fourth ventricle (foramen of Luschka)
11 Vagus nerve (CN X)
12 Vestibulocochlear nerve (CN VIII)
13 Facial nerve (CN VII)
14 Abducens nerve (CN VI)
15 Pons, basilar portion
16 Tonsil
17 Postpyramidal (secondary) fissure
18 Biventral lobule
19 Flocculus
20 Prepyramidal fissure
21 Gracile lobule
22 Inferior semilunar lobule
23 Great horizontal fissure
24 Superior semilunar lobule
25 Pyramid of the vermis
26 Uvula
27 Inferior fourth ventricle

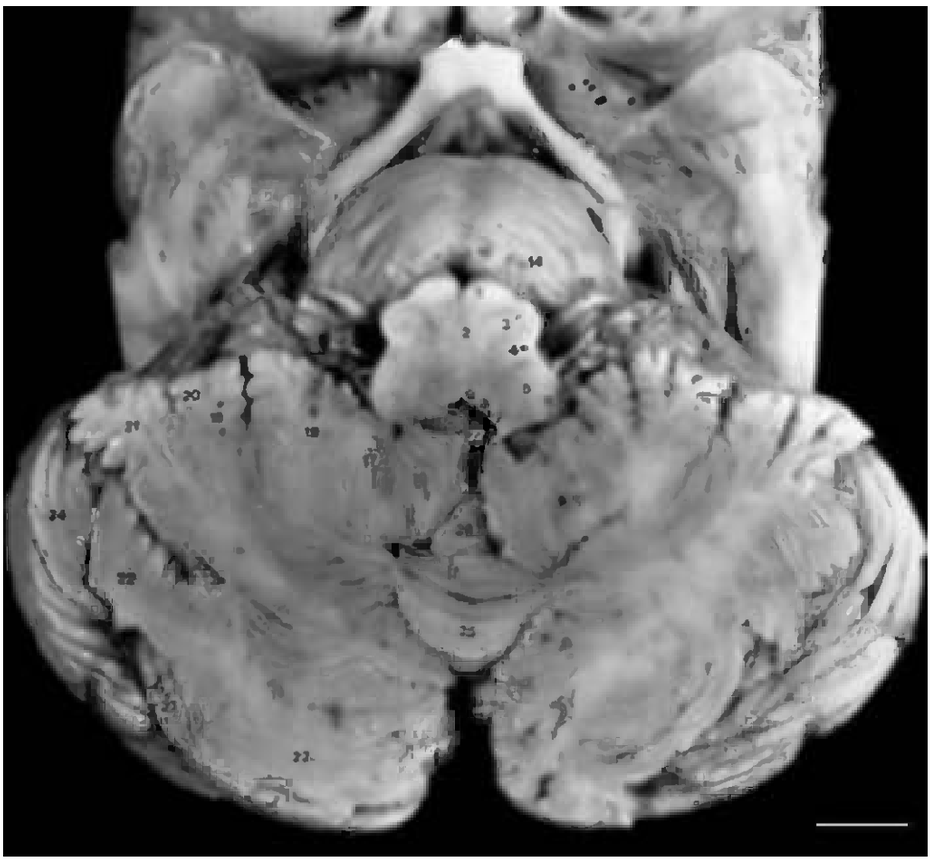

A

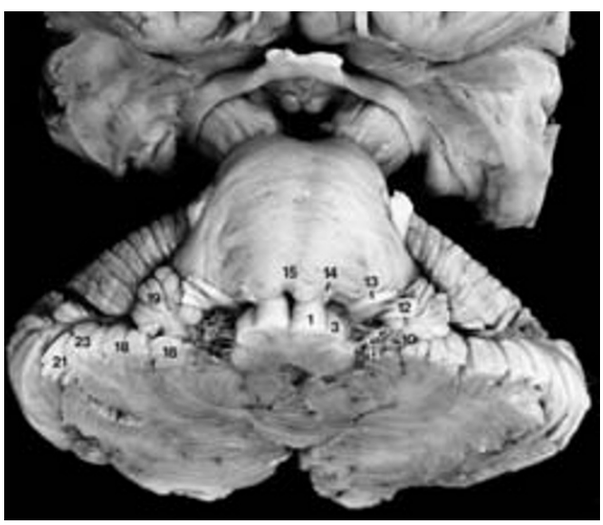

B

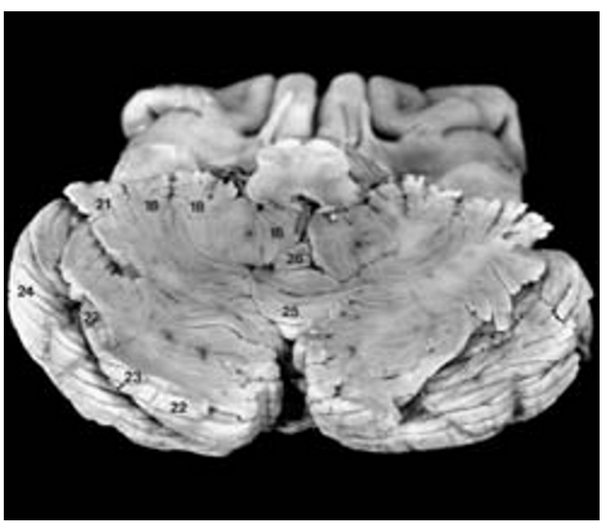

C

D

Fig. 11.7 (D–E).
D. Axial section of the head, inferior view. Bar: 10 mm.
E. 3 Tesla MR Cisternogram.

1 Pyramid of medulla (including the corticospinal tract)
2 Medial lemniscus
3 Inferior olivary nucleus
6 Inferior cerebellar peduncle (restiform body)
11 Vagus nerve (CN X) (arrows)
15 Pons, basilar portion
16 Tonsil
18 Biventral lobule
19 Flocculus
22 Inferior semilunar lobule
25 Pyramid of the vermis
26 Uvula
27 Inferior fourth ventricle
27′ Tela choroidea inferior
28 Occipital bone, squama
29 Sigmoid sinus
29′ Internal jugular vein (jugular bulb)
30 Mastoid air cells
31 External acoustic meatus
32 Internal carotid artery
33 Mandibular condyle
34 Eustachian tube
35 Occipital bone, basilar portion
36 Vertebro-basilar arterial junction

Arrows: Cranial nerves X exiting into the jugular foramen

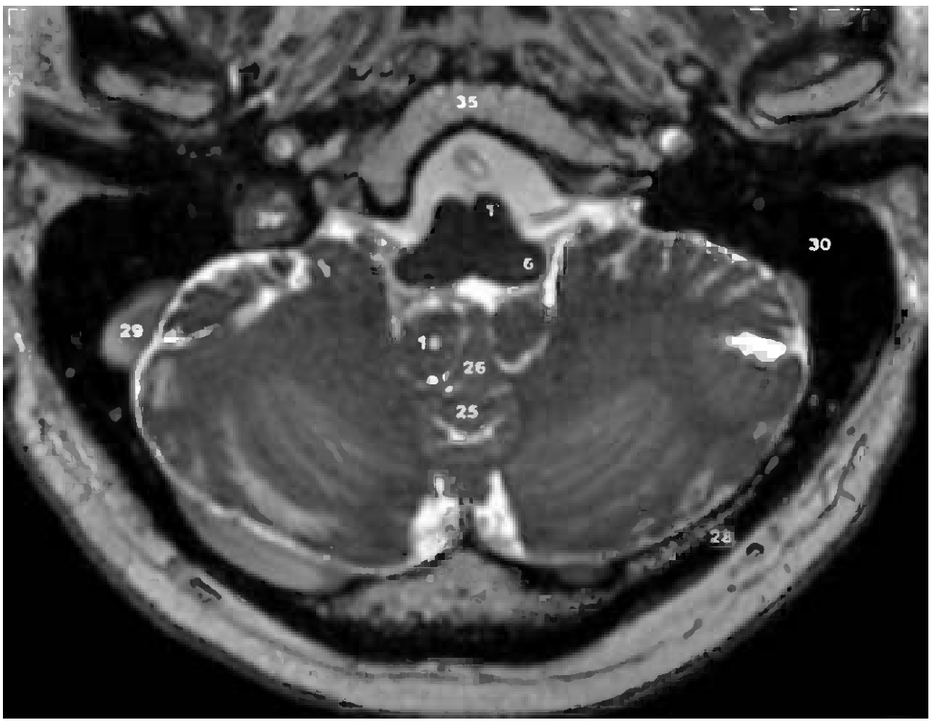

E

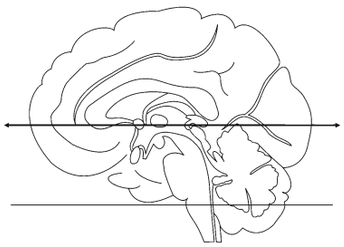

Fig. 11.8 (A–C). Axial (horizontal) section.
Medulla
A. Inferior view after removal of the cerebral hemispheres. Bar: 10 mm.
B. Anterior oblique view. **C.** Posterior oblique view.

See **Fig. 2.10** for more information about the structures demonstrated at this level and **Fig. 7.8** for the vascular territories.

1 Pyramid of the medulla and corticospinal tract
2 Medial lemniscus
3 Inferior olive, formed by the inferior olivary nucleus
4 Spinothalamic tract
5 Spinal trigeminal nucleus (pars interpolaris) (CN V)
6 Inferior cerebellar peduncle (restiform body)
7 Dorsal cochlear nucleus (CN VIII)
8 Medial vestibular nucleus (CN VIII)
9 Dorsal motor nucleus of the vagus (CN X)
10 Hypoglossal nucleus (CN XII)
11 Choroid plexus and lateral aperture of the fourth ventricle (foramen of Luschka)
12 Glossopharyngeal nerve (CN IX)
13 Vestibulocochlear nerve (CN VIII)
14 Facial nerve (CN VII)
15 Abducens nerve (CN VI)
16 Pons, basilar portion
17 Tonsil
18 Biventral lobule
19 Flocculus
20 Prepyramidal fissure
21 Gracile lobule
22 Inferior semilunar lobule
23 Great horizontal fissure
24 Superior semilunar lobule
25 Pyramid of vermis
26 Postpyramidal (secondary) fissure
27 Uvula
28 Inferior fourth ventricle

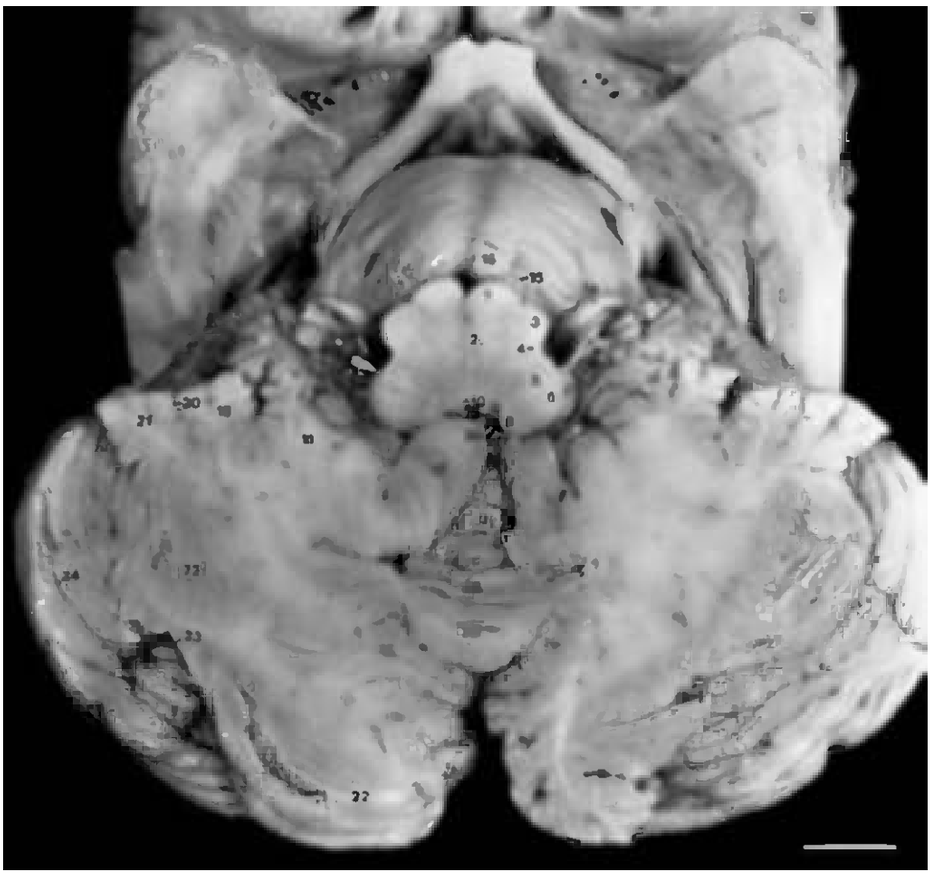

A

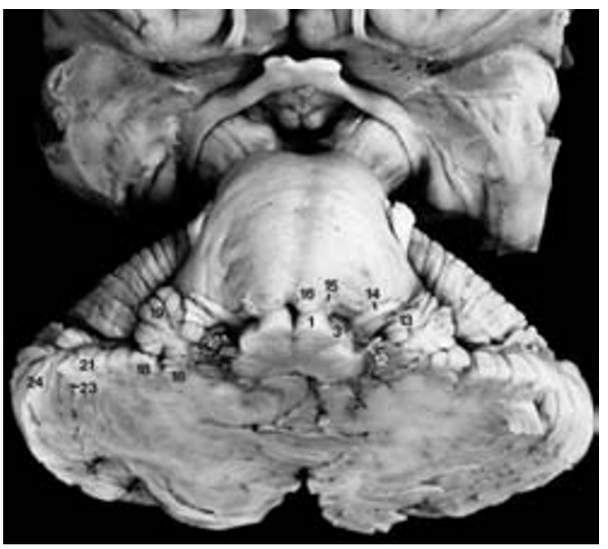

B

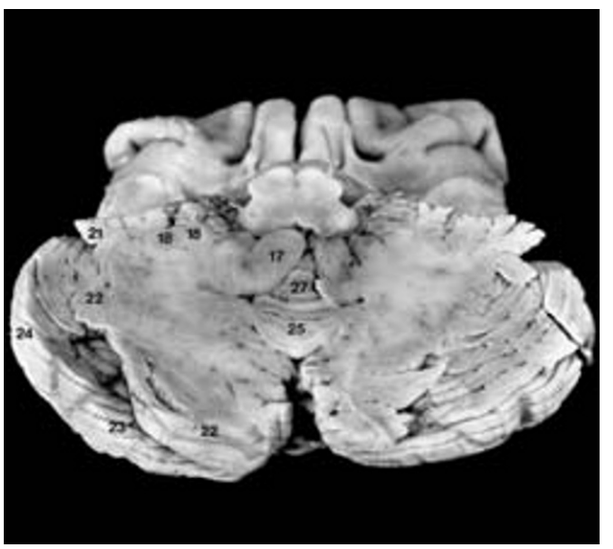

C

D

Fig. 11.8 (D–F).
D. Axial section of the head. Inferior view. Bar: 10 mm.
E–F. 3 Tesla MRI. E. T1-weighted MRI. **F.** T2-weighted MRI.

1 Pyramid of the medulla and corticospinal tract
2 Medial lemniscus
3 Inferior olivary nucleus
6 Inferior cerebellar peduncle (restiform body)
12 Glossopharyngeal nerve (CN IX)
16 Pons, basilar portion
17 Tonsil
18 Biventral lobule
19 Flocculus
21 Gracile lobule
22 Inferior semilunar lobule
23 Great horizontal fissure
24 Superior semilunar lobule
25 Pyramid of vermis
27 Uvula
28 Fourth ventricle
29 Occipital bone, squama
30 Sigmoid sinus
31 Mastoid air cells
32 Internal carotid artery
33 Mandibular condyle
34 Eustachian tube
35 Occipital bone, basilar portion
36 Vomer

Arrowhead: Anterior inferior cerebellar artery (AICA)

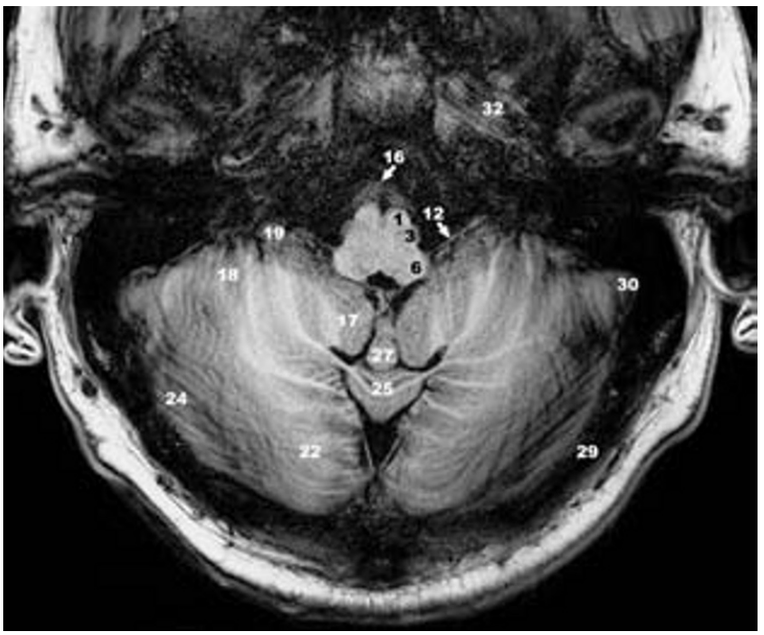
32
16
1
12
3
19
6
18
30
17
27
25
24
22
29

E

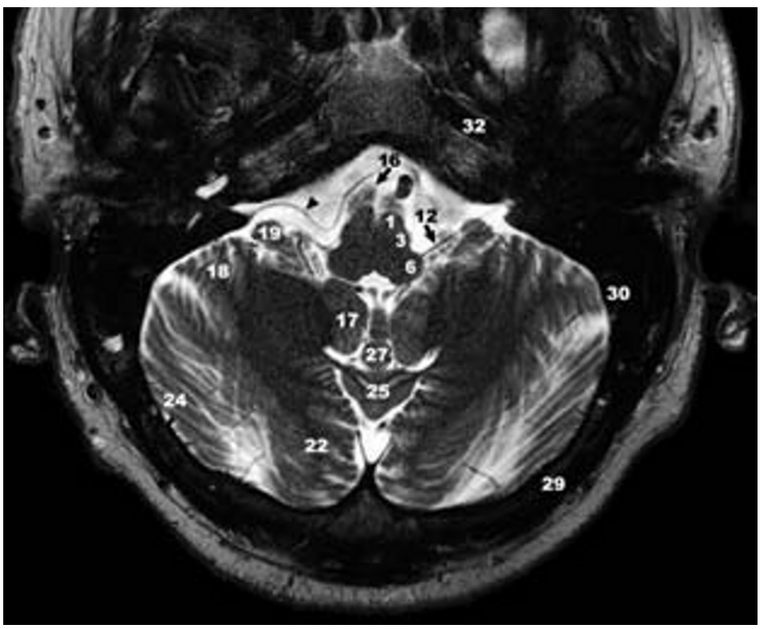
32
16
1
12
3
19
6
18
30
17
27
25
24
22
29

F

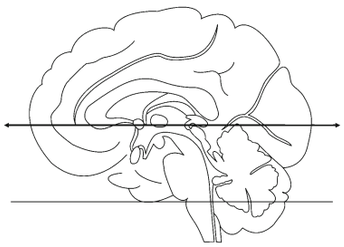

Fig. 11.9 (A–C). Axial (horizontal) section.
Pontomedullary junction
A. Inferior view after removal of the cerebral hemispheres. Bar: 10 mm.
B. Anterior oblique view. **C.** Posterior oblique view.

See **Fig. 2.11** for more information about the structures demonstrated at this level.

1 Pons, basilar portion
2 Pyramid of the medulla (including the corticospinal tract)
3 Medial lemniscus
4 Inferior olivary nucleus (superior pole)
5 Spinothalamic tract
6 Spinal trigeminal nucleus (pars oralis) (CN V)
7 Inferior cerebellar peduncle (restiform body)
7′ Pontomedullary sulcus
8 Ventral cochlear nucleus (CN VIII)
9 Medial vestibular nucleus (CN VIII)
10 Nucleus prepositus hypoglossi
11 Vestibulocochlear nerve (CN VIII)
12 Nervus intermedius (CN VII)
13 Facial nerve (CN VII)
14 Abducens nerve (CN VI)
15 Flocculus
16 Inferior semilunar lobule
17 Great horizontal fissure
18 Superior semilunar lobule
19 Tuber of vermis
20 Prepyramidal fissure
21 Pyramid of vermis
22 Postpyramidal fissure
23 Uvula
24 Tonsil
25 Inferior fourth ventricle
26 Lateral recess of the fourth ventricle
27 Posterior superior fissure
28 Simple lobule
29 Declive
30 Anterior superior (primary) fissure

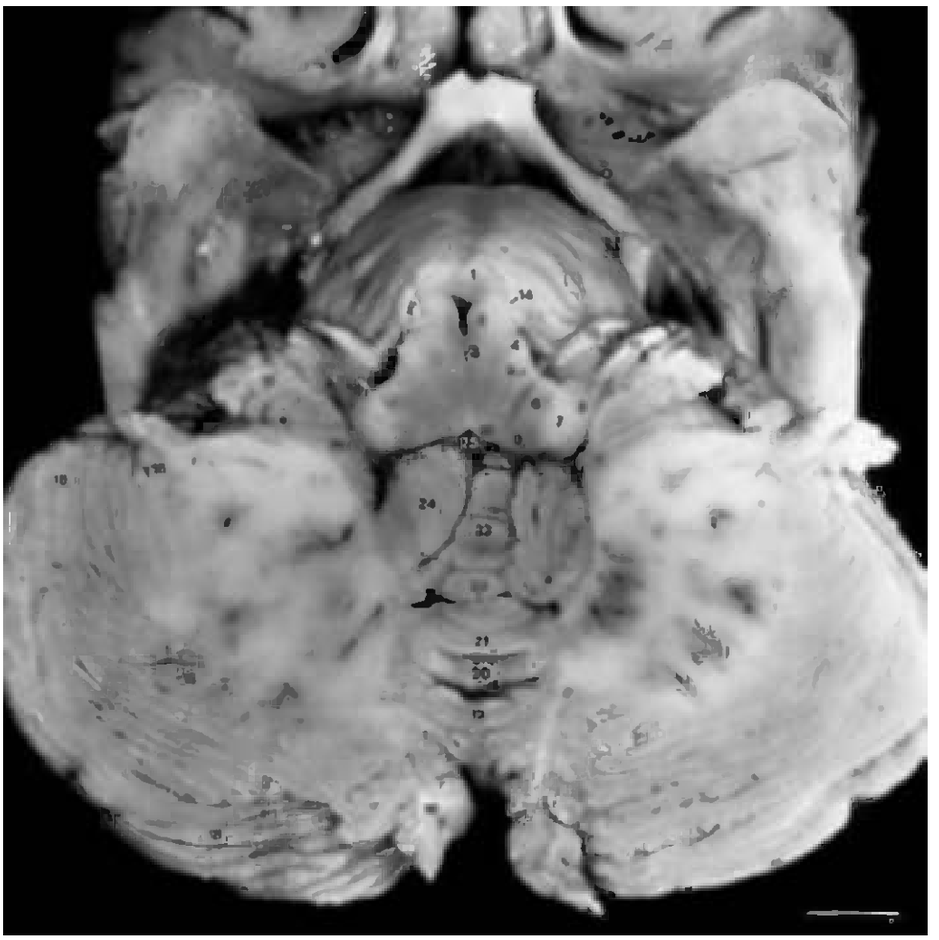

A

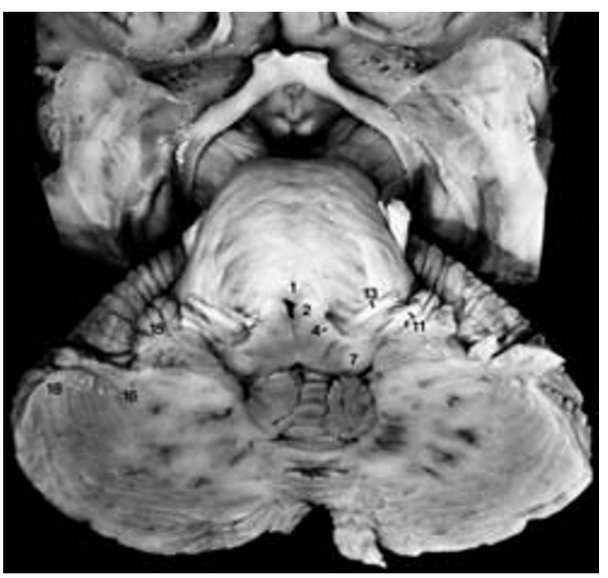

B

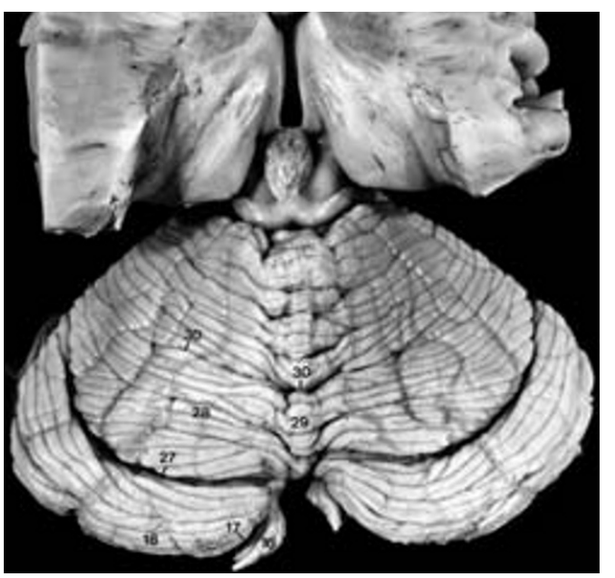

C

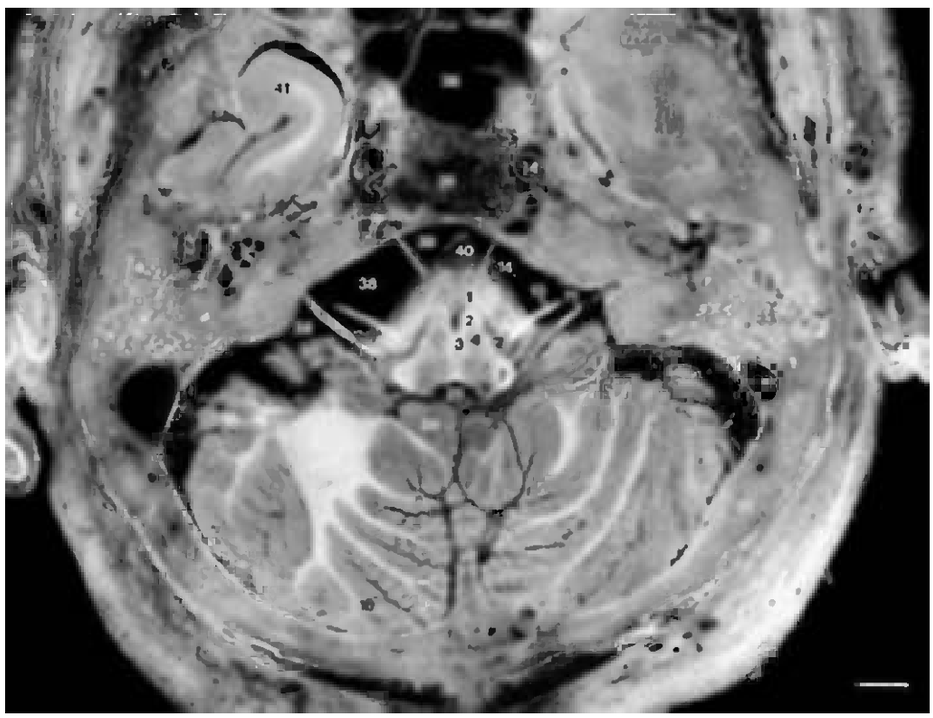

D

Fig. 11.9 (D–E).
D. Axial section of the head. Inferior view. Bar: 10 mm.
E. 3 Tesla MR Cisternogram.

1 Pons, basilar portion
2 Pyramid of the medulla (including the corticospinal tract)
3 Medial lemniscus
4 Inferior olivary nucleus (superior portion)
7 Inferior cerebellar peduncle (restiform body)
7′ Pontomedullary sulcus
9 Medial vestibular nucleus (CN VIII)
11 Vestibulocochlear nerve (CN VIII)
13 Facial nerve (CN VII)
14 Abducens nerve (CN VI)
14′ Dorello's canal (for CN VI)
15 Flocculus
16 Inferior semilunar lobule
18 Superior semilunar lobule
19 Tuber
21 Pyramid
23 Uvula
24 Tonsil
25 Inferior fourth ventricle
26 Posterolateral (secondary) fissure
27 Biventral lobule
27′ Intrabiventral fissure
28 Prepyramidal fissure (prebiventral fissure)
29 Gracile lobule
31 Occipital bone, squama
32 Sigmoid sinus
33 Mastoid air cells
34 Internal carotid artery

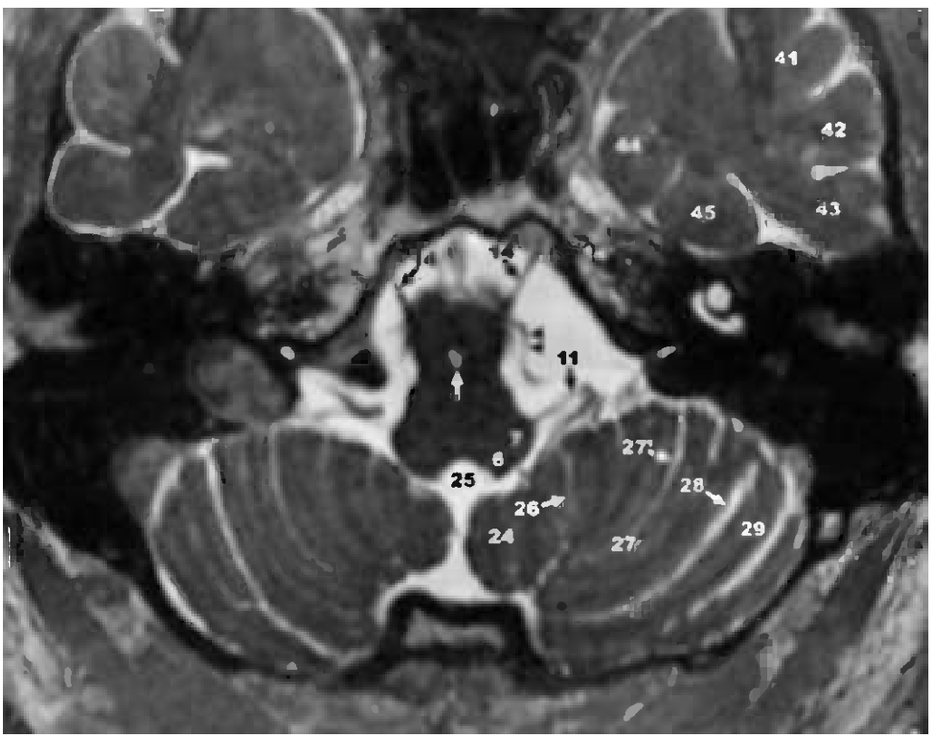

E

35 Clivus (the clivus is composed of the basiocciput and the basisphenoid bones)
36 Sphenoid sinus
38 Cerebellopontine angle and cistern
39 Prepontine cistern
40 Basilar artery
41 Superior temporal gyrus
42 Middle temporal gyrus
43 Inferior temporal gyrus
44 Parahippocampal gyrus
45 Fusiform gyrus

Paired black arrowheads: Anterior inferior cerebellar artery (AICA)
White arrow: Foramen cecum

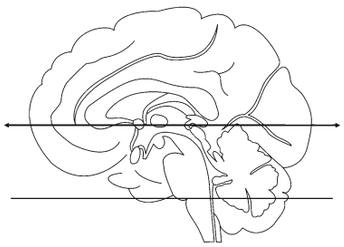

Fig. 11.10 (A–C). Axial (horizontal) section. Pontomedullary junction

A. Inferior view after removal of the cerebral hemispheres. Bar: 10 mm.

B. Anterior oblique view. **C.** Superior view.

See **Fig. 2.12** for more information about the structures demonstrated at this level and **Fig. 7.10** for the vascular territories.

1 Pons, basilar portion, pontocerebellar fibers
2 Pons, basilar portion, corticospinal tract
3 Pontomedullary sulcus
4 Medial lemniscus
5 Spinothalamic tract
6 Facial nucleus (CN VII)
7 Spinal trigeminal nucleus (pars oralis) (CN V)
8 Inferior cerebellar peduncle (restiform body)
9 Ventral cochlear nucleus (CN VIII)
10 Vestibular nuclei (CN VIII)
11 Nucleus prepositus hypoglossi
12 Facial nerve (CN VII)
13 Vestibulocochlear nerve (CN VIII)
14 Flocculus
15 Middle cerebellar peduncle (brachium pontis)
16 Dentate nucleus (inferior pole)
17 Superior semilunar lobule
18 Great horizontal fissure
19 Inferior semilunar lobule
20 Tuber of vermis
21 Prepyramidal fissure
22 Pyramid of vermis
23 Uvula
24 Tonsil
25 Mid fourth ventricle
26 Postclival superior fissure
27 Simple lobule
28 Declive
29 Anterior superior (primary) fissure

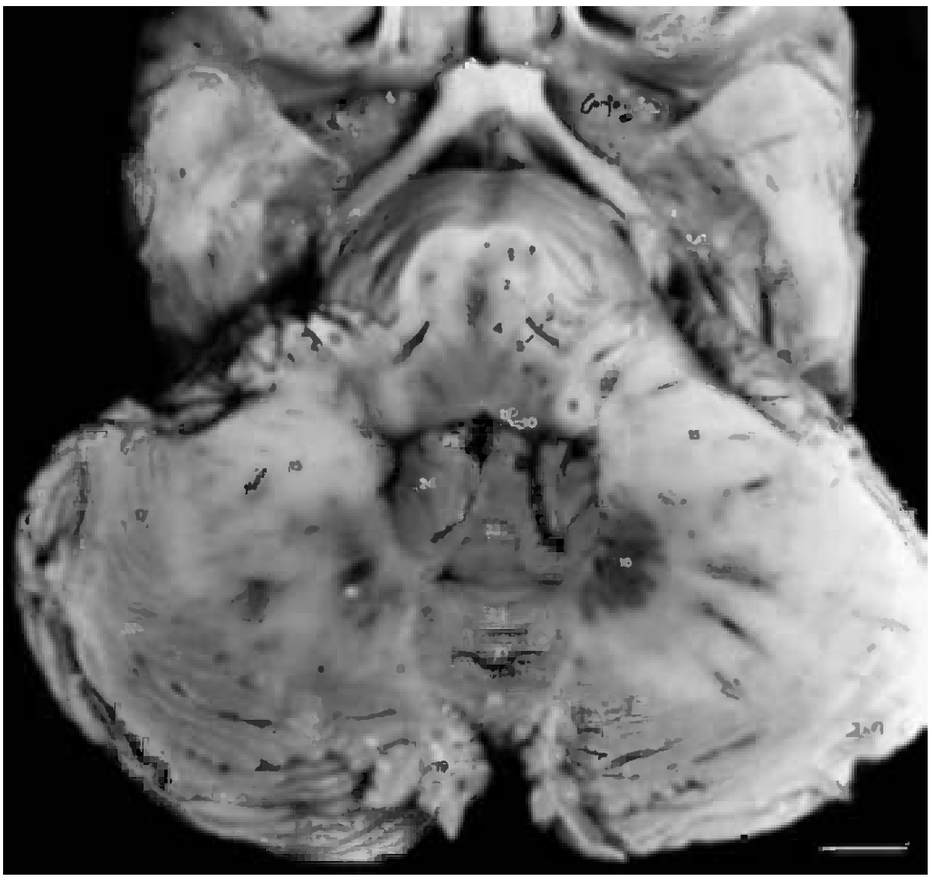

A

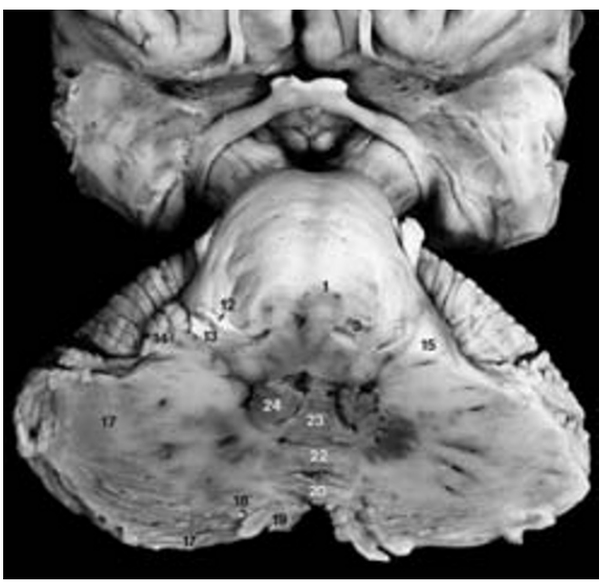

B

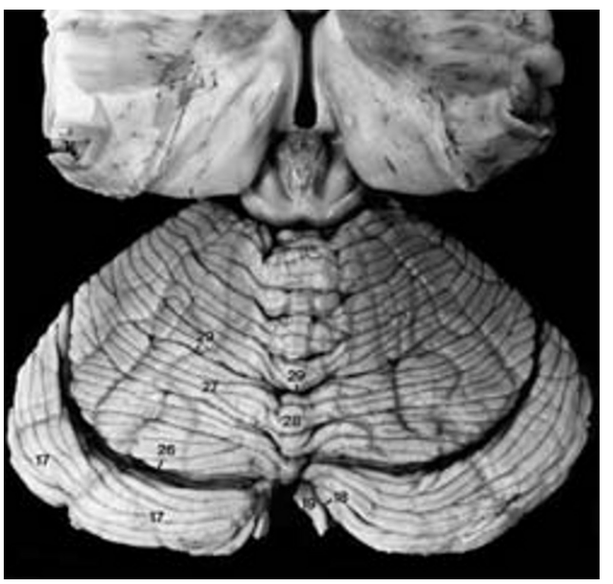

C

D

Fig. 11.10 (D–F).
D. Axial section of the head. Inferior view. Bar: 10 mm.
E–F. 3 Tesla MRI. E. T1-weighted MRI. **F.** T2-weighted MRI.

1 Pyramid of medulla
2 Pons, basilar portion, corticospinal tract
3 Pontomedullary sulcus
4 Medial lemniscus
8 Inferior cerebellar peduncle (restiform body)
14 Flocculus
17 Superior semilunar lobule
22 Pyramid of vermis
23 Uvula
24 Tonsil
25 Fourth ventricle
30 Occipital bone, squama
31 Sigmoid sinus
32 Mastoid air cells
33 Temporal bone, petrous portion
34 Internal carotid artery
35 Sphenoid sinus
35′ Occipital bone bone, basal portion
36 Inferior temporal gyrus
37 Superior temporal gyrus
38 Basilar artery
39 Abducens nerve (CN VI)

Single arrows: Vestibulocochlear nerves (CN VIII)

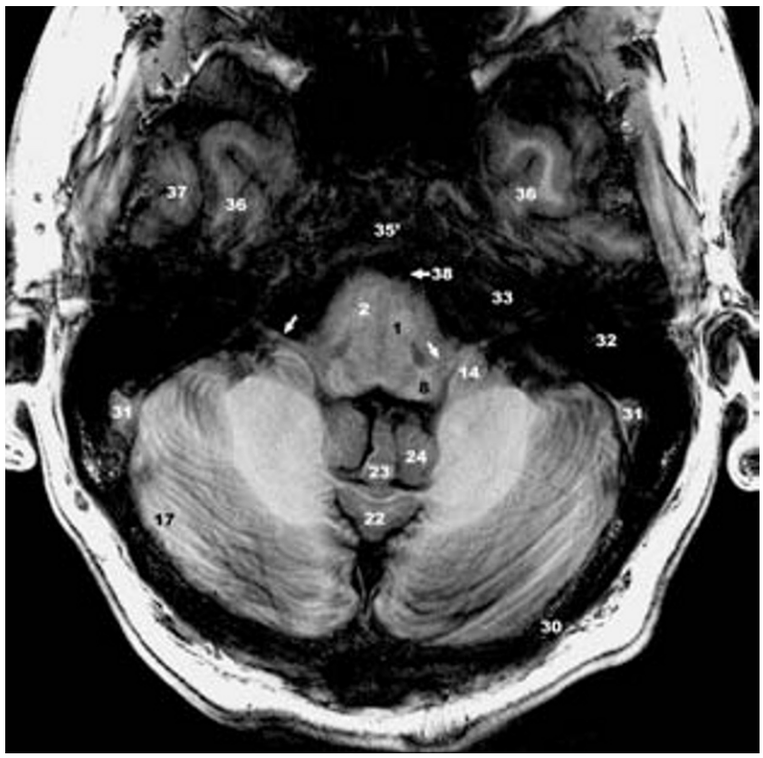
37
36
36
35'
38
33
2
1
32
14
8
31
31
24
23
17
22
30

E

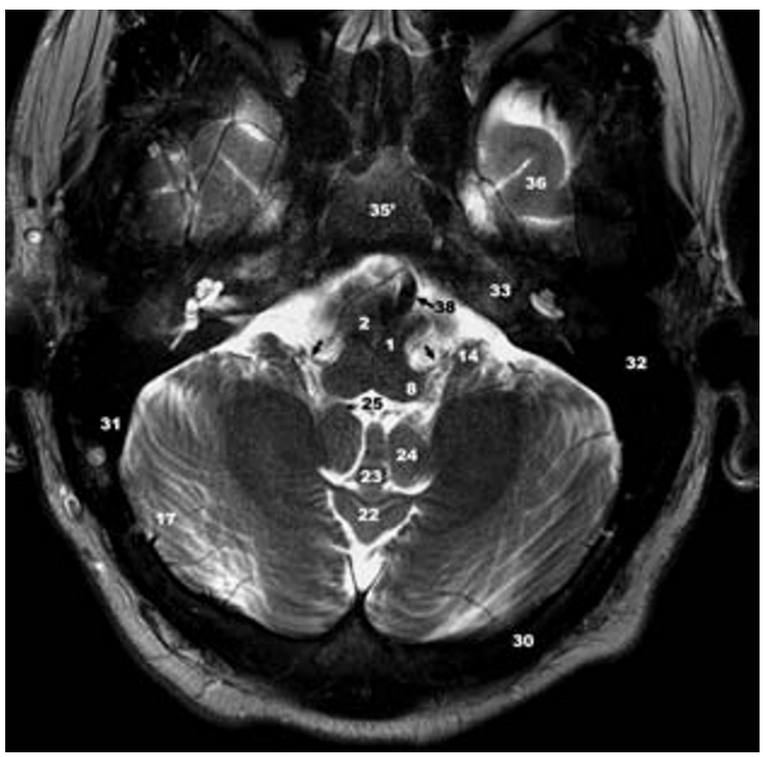
36
35'
33
38
2
1
14
32
8
25
31
24
23
17
22
30

F

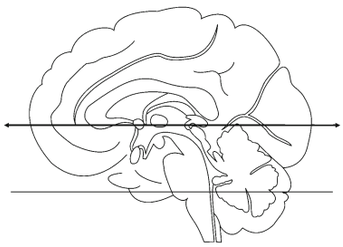

Fig. 11.11 (A–C). Axial (horizontal) section.
Pons
A. Inferior view after removal of the cerebral hemispheres. Bar: 10 mm.
B. Anterior oblique view. **C.** Superior view.

1 Pons, basilar portion, pontine nuclei
2 Pons, basilar portion, corticospinal tract
3 Pons, basilar portion, pontocerebellar fibers
4 Pontomedullary sulcus
5 Medial lemniscus
6 Spinothalamic tract
7 Facial nucleus
8 Spinal trigeminal nucleus (pars oralis) (CN V)
9 Ventral cochlear nucleus (CN VIII)
10 Inferior cerebellar peduncle (restiform body)
11 Vestibular nuclei (CN VIII)
12 Nucleus prepositus hypoglossi
13 Facial nerve (CN VII)
14 Vestibulocochlear nerve (CN VIII)
15 Middle cerebellar peduncle (brachium pontis)
16 Flocculus
17 Anterior superior (primary) fissure
18 Simple lobule
18′ Declive
19 Posterior superior fissure
20 Superior semilunar lobule
21 Inferior semilunar lobule
22 Tuber
23 Prepyramidal fissure
24 Pyramid
25 Dentate nucleus
26 Postpyramidal (secondary) fissure
27 Uvula
28 Tonsil
29 Fourth ventricle

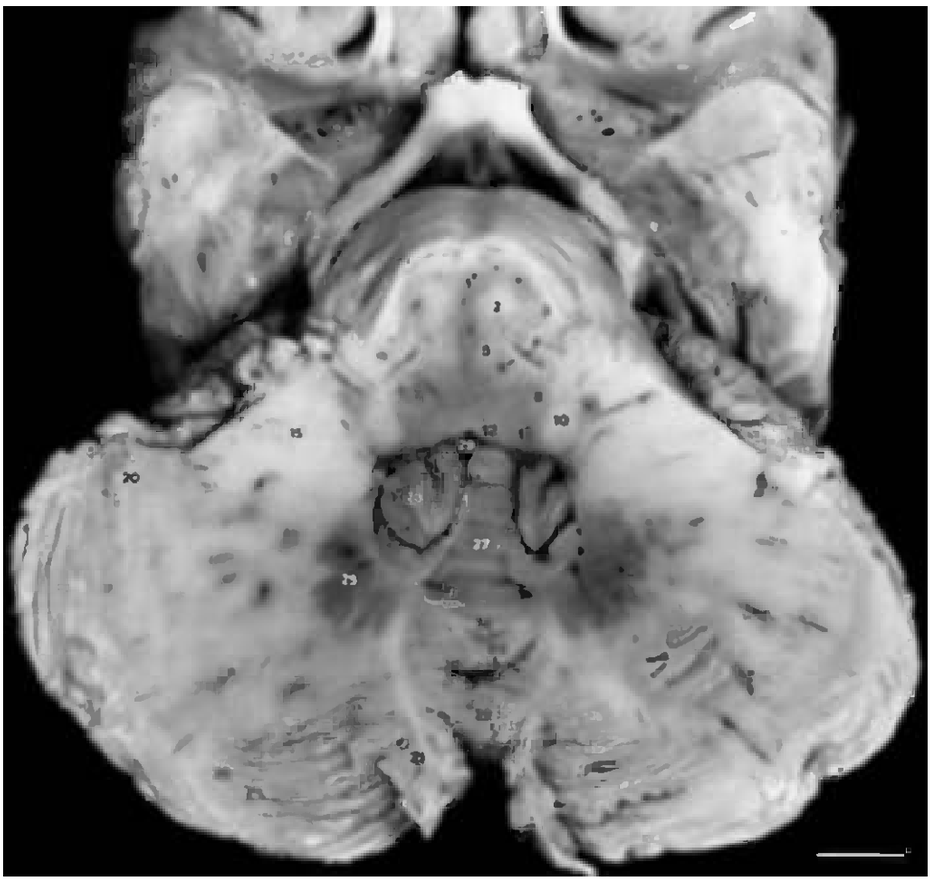

A

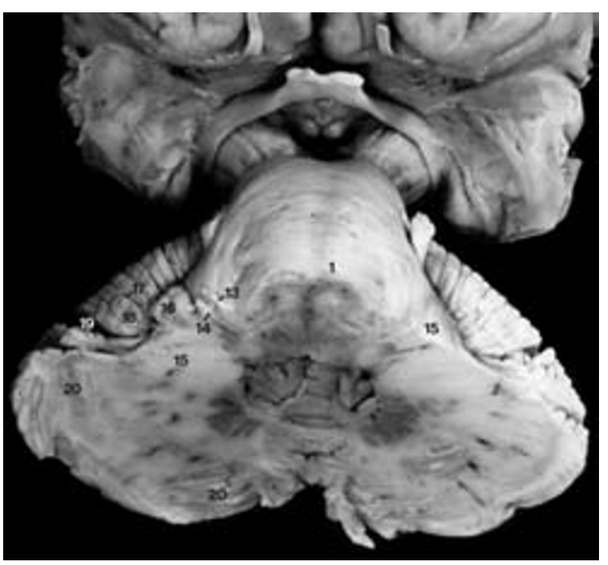

B

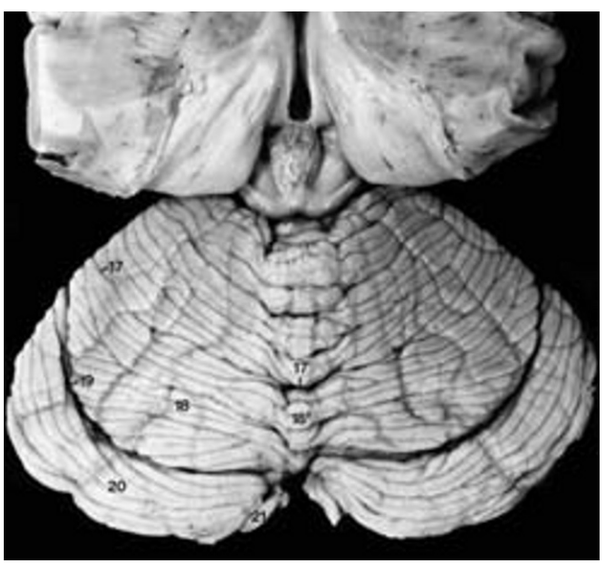

C

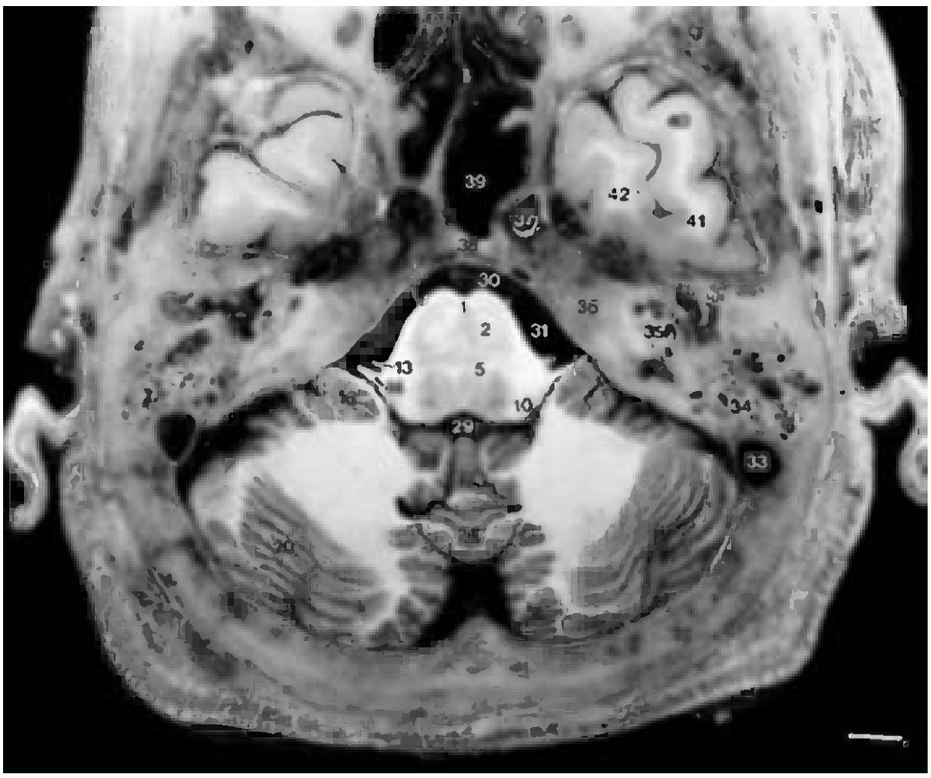

D

Fig. 11.11 (D–F).
D. Axial section of the head. Superior view. Bar: 10 mm.
E–F. 3 Tesla MRI. E. T1-weighted MRI. **F.** T2-weighted MRI.

1 Pons, basilar portion, pontine nuclei
2 Pons, basilar portion, corticospinal tract
4 Pontomedullary sulcus
5 Medial lemniscus
10 Inferior cerebellar peduncle (restiform body)
13 Facial nerve (arrowhead) (CN VII)
14 Vestibulocochlear nerve (arrow) (CN VIII)
14′ Internal acoustic meatus
16 Flocculus
20 Superior semilunar lobule
24 Pyramid
27 Uvula
28 Tonsil
29 Fourth ventricle leading laterally to the lateral recesses
30 Prepontine cistern and basilar artery (note abducens fibers crossing anterolaterally through the cistern)
31 Cerebellopontine angle and cistern
32 Occipital bone, squama
33 Sigmoid sinus
34 Mastoid air cells
35 Internal ear
36 Temporal bone, petrous portion
37 Internal carotid artery
37′ Meckel's cave
38 Clivus
39 Sphenoid sinus
40 Superior temporal gyrus
41 Middle temporal gyrus
42 Inferior temporal gyrus

Arrowhead: Facial nerve (CN VII)
Single arrow: Vestibulocochlear nerve (CN VIII)

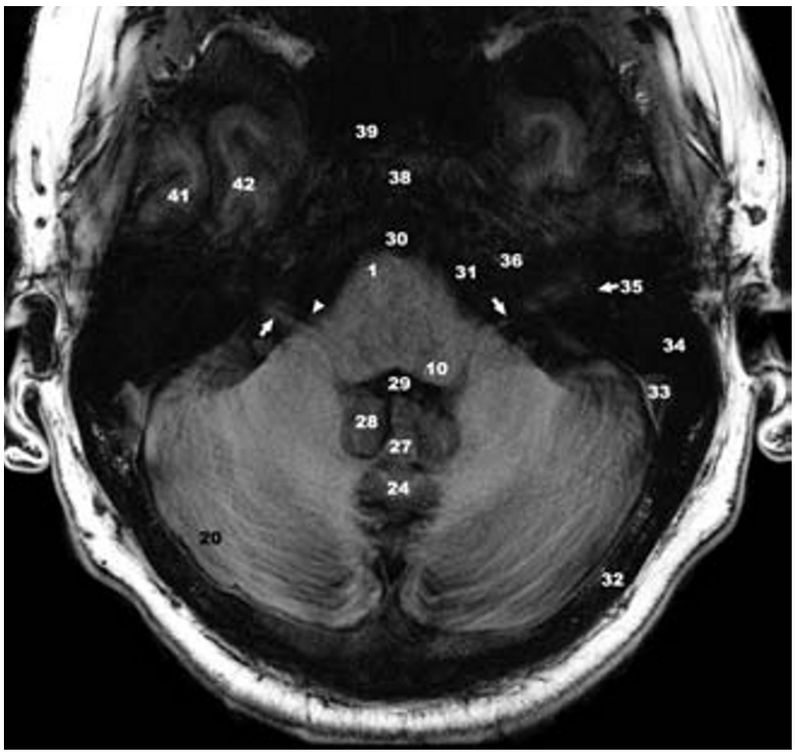
39
38
41
42
30
1
31
36
35
34
10
29
33
28
27
24
20
32

E

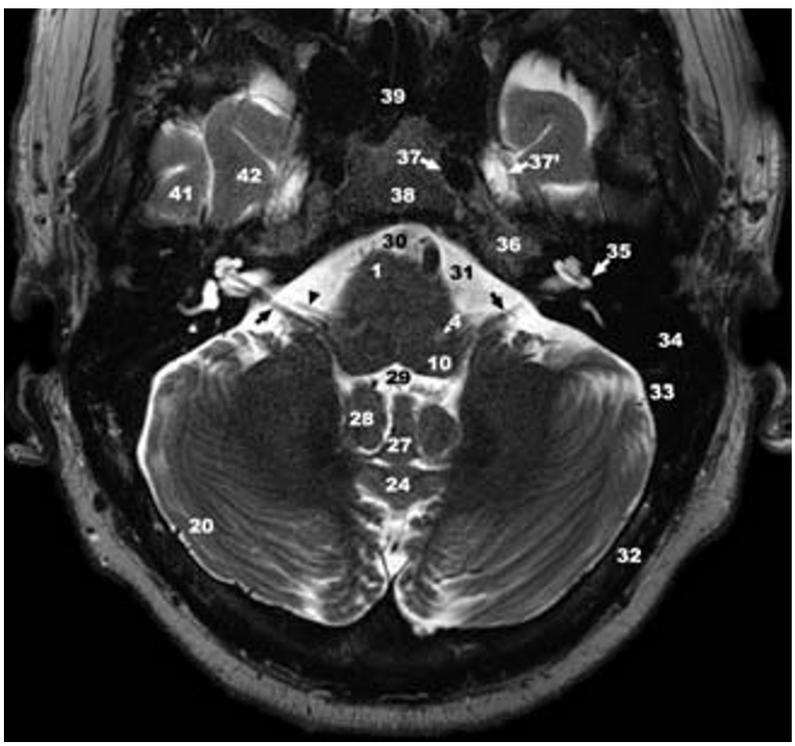
39
37
37'
41
42
38
30
36
35
1
31
34
10
29
33
28
27
24
20
32

F

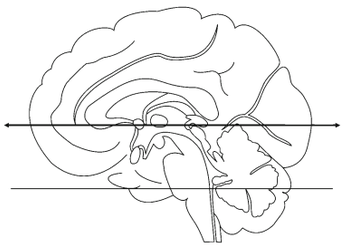

Fig. 11.12 (A–C). Axial (horizontal) section.
Pons
A. Inferior view after removal of the cerebral hemispheres. Bar: 10 mm.
B. Anterior oblique view. **C**. Superior view.

See **Fig. 2.13** for more information about the structures demonstrated at this level.

1 Pons, basilar portion, corticospinal tract
2 Pons, basilar portion, pontine nuclei
3 Medial lemniscus
4 Trapezoid body
5 Superior olivary nucleus
6 Facial nucleus (CN VII)
7 Spinal trigeminal nucleus (pars oralis) (CN V)
8 Abducens nucleus (inferior pole) (CN VI)
9 Vestibular nuclei (CN VIII)
10 Inferior cerebellar peduncle (restiform body)
11 Middle cerebellar peduncle (brachium pontis)
12 Quadrangular lobule
12′ Culmen
13 Anterior superior (primary) fissure
14 Simple lobule
14′ Declive
15 Posterior superior fissure
16 Superior semilunar lobule
17 Inferior semilunar lobule
18 Great horizontal fissure
19 Tuber
20 Folium
21 Prepyramidal fissure
22 Pyramid
23 Uvula
24 Tonsil
25 Dentate nucleus
26 Fourth ventricle

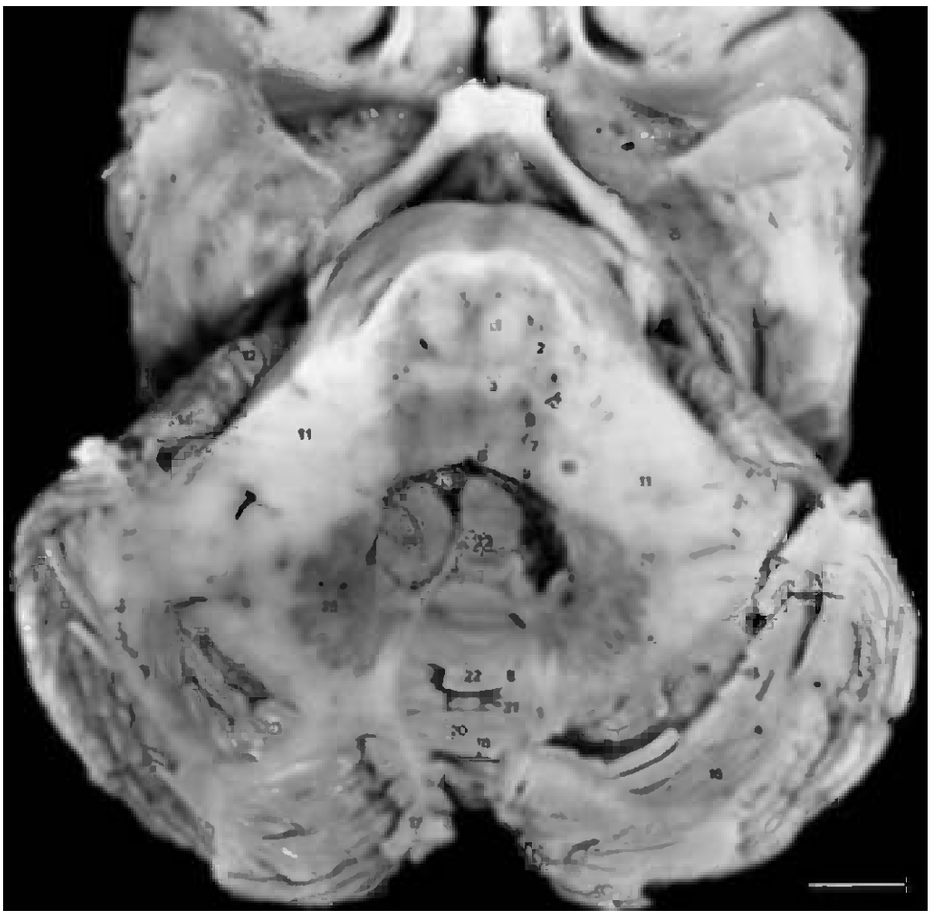

A

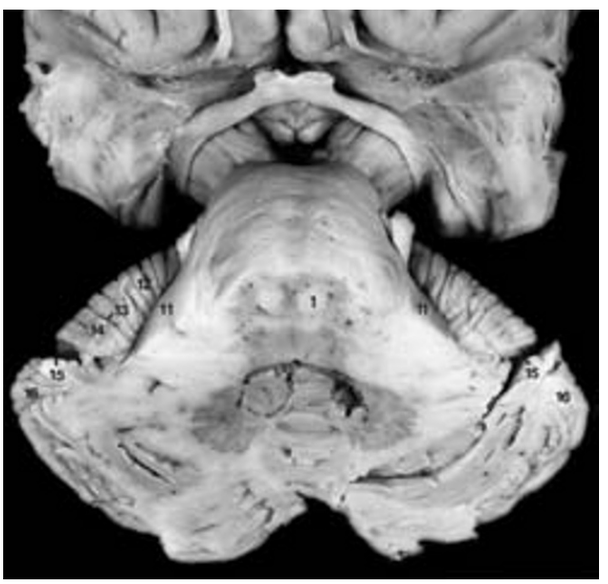

B

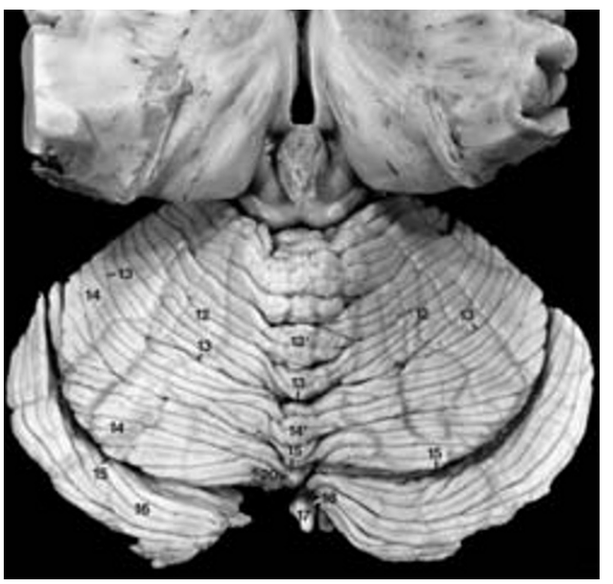

C

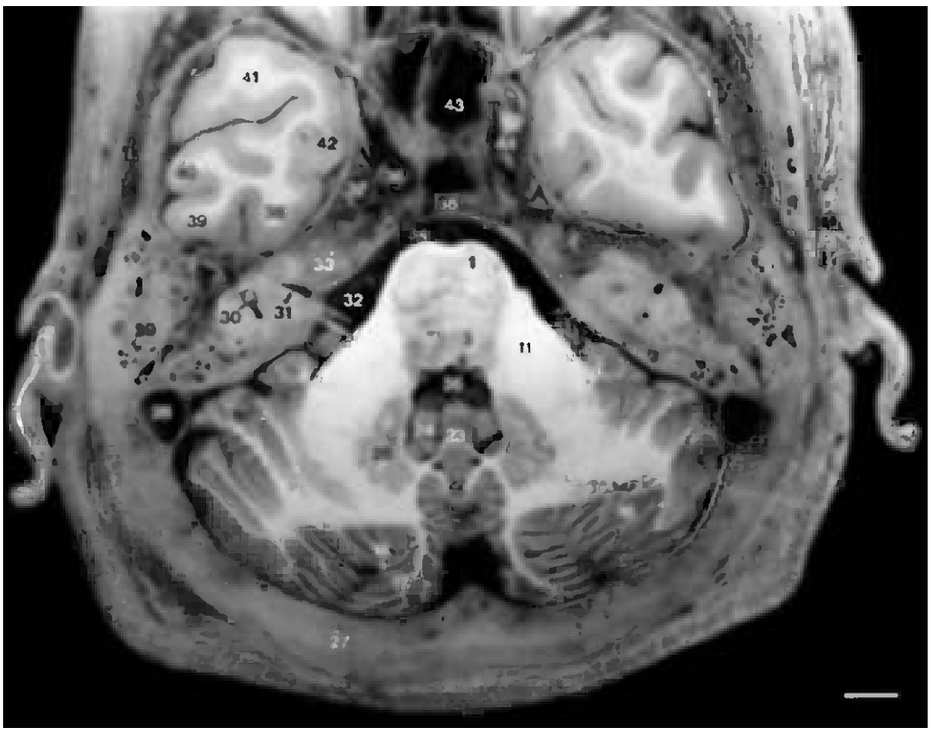

D

Fig. 11.12 (D–F).
D. Axial section of the head. Superior view. Bar: 10 mm.
E–F. 3 Tesla MRI. E. T1-weighted MRI. **F.** T2-weighted MRI.

1 Pons, basilar portion, corticospinal tract
3 Medial lemniscus
8 Abducens nucleus (inferior pole) (CN VI)
10 Inferior cerebellar peduncle (restiform body)
11 Middle cerebellar peduncle (brachium pontis)
16 Superior semilunar lobule
17 Inferior semilunar lobule
18 Great horizontal fissure
19 Tuber
20 Folium
22 Pyramid
23 Uvula
24 Tonsil
25 Dentate nucleus
26 Fourth ventricle
27 Occipital bone, squama
28 Sigmoid sinus
29 Mastoid air cells
30 Internal ear
31 Internal acoustic meatus, containing the facial nerve (CN VII) and the vestibular (black arrowhead) and cochlear (black arrow) divisions of the vestibulocochlear nerve (CN VIII)
32 Cerebellopontine angle and cistern
33 Temporal bone, petrous portion
34 Prepontine cistern
35 Clivus
36 Internal carotid artery in the cavernous sinus (44)
37 Meckel's cave
38 Fusiform gyrus
39 Inferior temporal gyrus
40 Middle temporal gyrus
41 Superior temporal gyrus
42 Parahippocampal gyrus
43 Sphenoid sinus
44 Cavernous sinus containing the internal carotid artery (36)

Black arrowhead: Vestibular nerve (CN VIII)
Black arrow: Cochlear nerve (CN VIII)

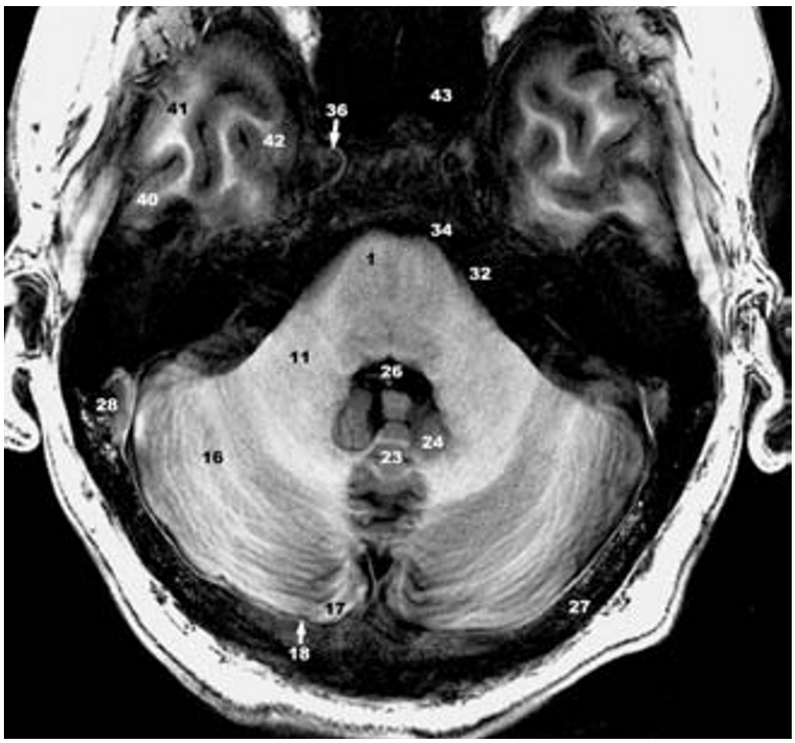
41
36
43
42
40
34
1
32
11
26
28
24
16
23
17
27
18

E

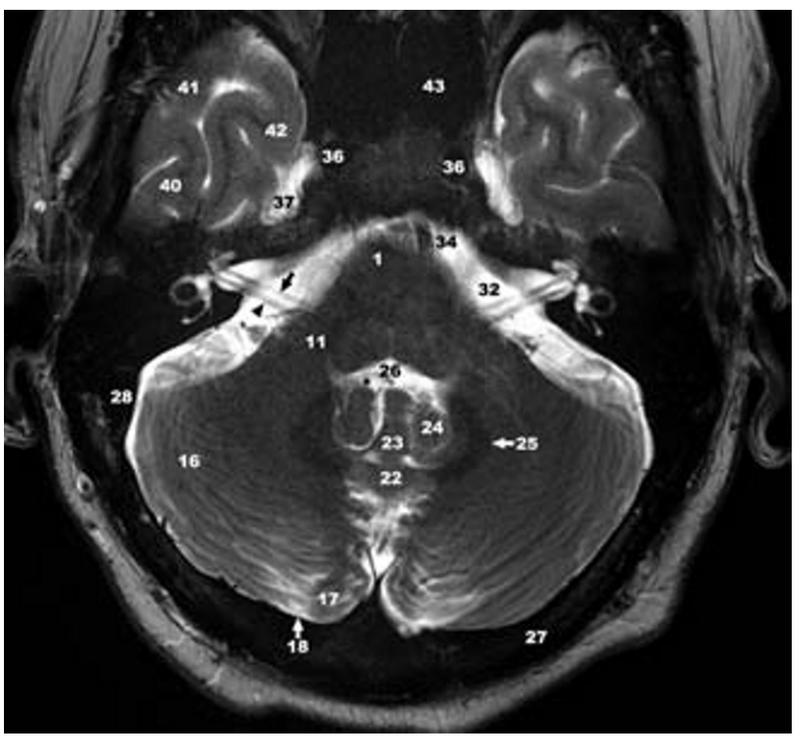
41
43
42
36
36
40
37
34
1
32
11
26
28
24
25
23
16
22
17
18
27

F

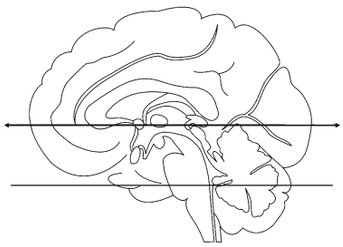

Fig. 11.13 (A–E). Axial (horizontal) section.
Pons
A. Inferior view after removal of the cerebral hemispheres. Bar: 10 mm.
B. Anterior oblique view. **C.** Superior view.
D and E. 3 Tesla MRI. D. T1-weighted MRI. **E.** T2-weighted MRI.

See **Fig. 2.14** for more information about the structures demonstrated at this level, and **Fig. 7.13** for the vascular territories.

1 Pons, basilar portion
2 Corticospinal tract
3 Pontine nuclei
4 Pontocerebellar fibers
5 Medial lemniscus
6 Spinothalamic tract
7 Superior olivary nucleus
8 Facial nucleus (CN VII)
9 Fibers of facial nerve (CN VII)
10 Spinal trigeminal nucleus (pars oralis)
11 Inferior cerebellar peduncle (restiform body)
12 Vestibular nuclei (CN VIII)
13 Abducens nucleus (CN VI). The facial nerve fibers cross over the abducens nuclei on each side, creating the facial colliculi (arrowheads).
14 Fibers of abducens nerve
15 Middle cerebellar peduncle (brachium pontis)
15′ Trigeminal nerve
16 Quadrangular lobule
16′ Culmen
17 Anterior superior (primary) fissure
18 Simple lobule
18′ Declive
19 Posterior superior fissure
20 Superior semilunar lobule
21 Uvula
22 Dentate nucleus
23 Tonsil
24 Posterolateral fissure
25 Nodulus
26 Fourth ventricle
27 Pyramid
28 Basilar artery
29 Superior temporal gyrus
30 Parahippocampal gyrus

Arrowheads: Facial colliculi (See 13 above)

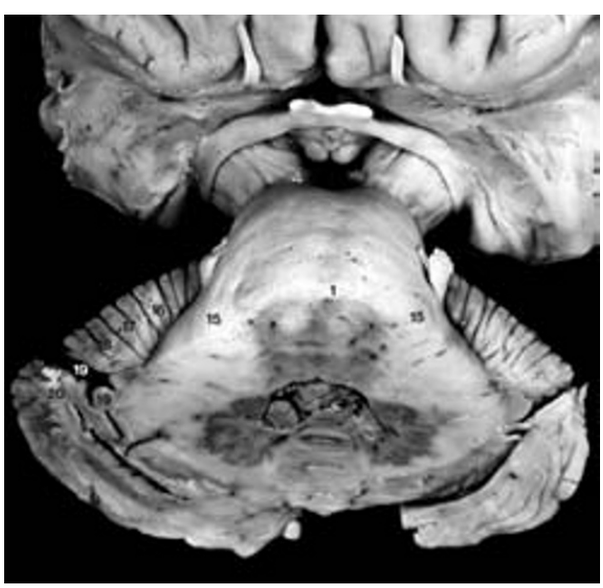

B

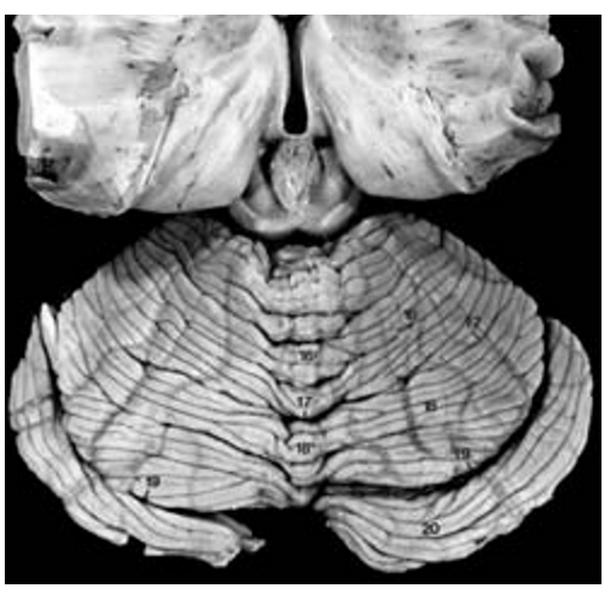

C

A

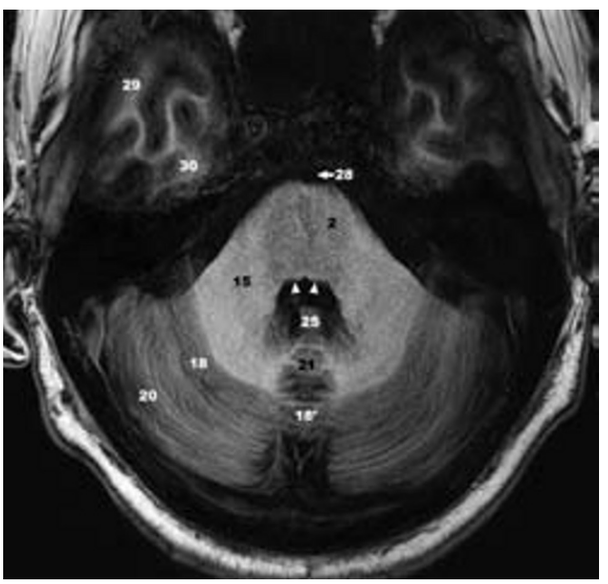

D

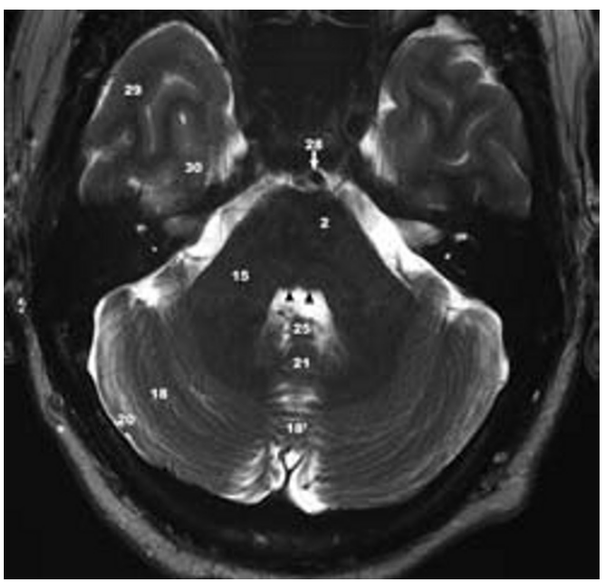

E

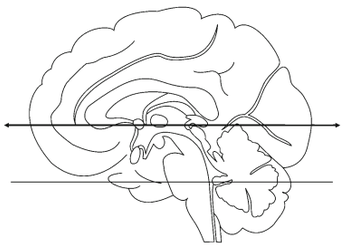

Fig. 11.14 (A–C). Axial (horizontal) section.
Pons
A. Inferior view after removal of the cerebral hemispheres. Bar: 10 mm.
B. Anterior oblique view. **C.** Superior view.

See **Fig. 4.13A** for a comparable post mortem 3T MR image.

1 Pons, basilar portion
2 Corticospinal tract
3 Pontine nuclei
4 Pontocerebellar fibers
5 Medial lemniscus
6 Superior olivary nucleus
7 Spinal trigeminal nucleus (pars oralis) (CN V)
8 Superior vestibular nucleus (CN VII)
9 Fibers of facial nerve (facial colliculus) (CN VII)
10 Middle cerebellar peduncle (brachium pontis)
11 Trigeminal nerve (CN V)
12 Quadrangular lobule
12′ Culmen
13 Anterior superior (primary) fissure
14 Simple lobule
15 Declive
16 Uvula
17 Nodulus
18 Dentate nucleus

A

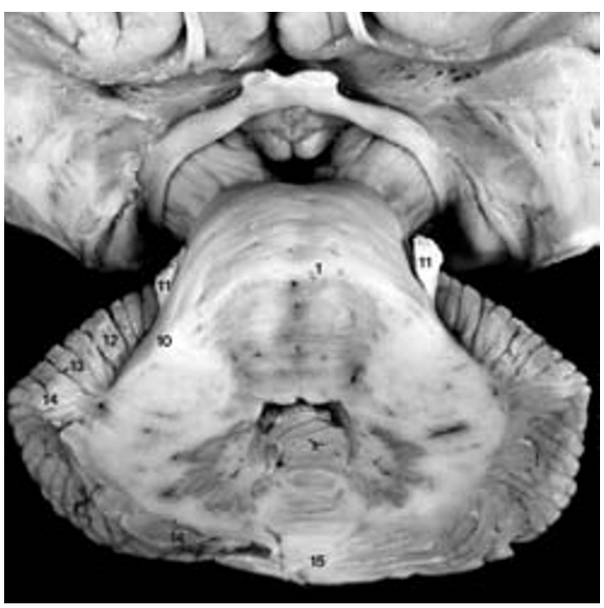

B

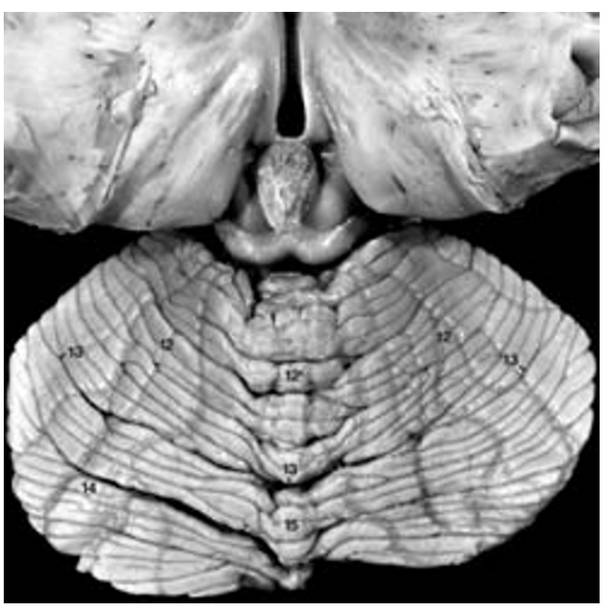

C

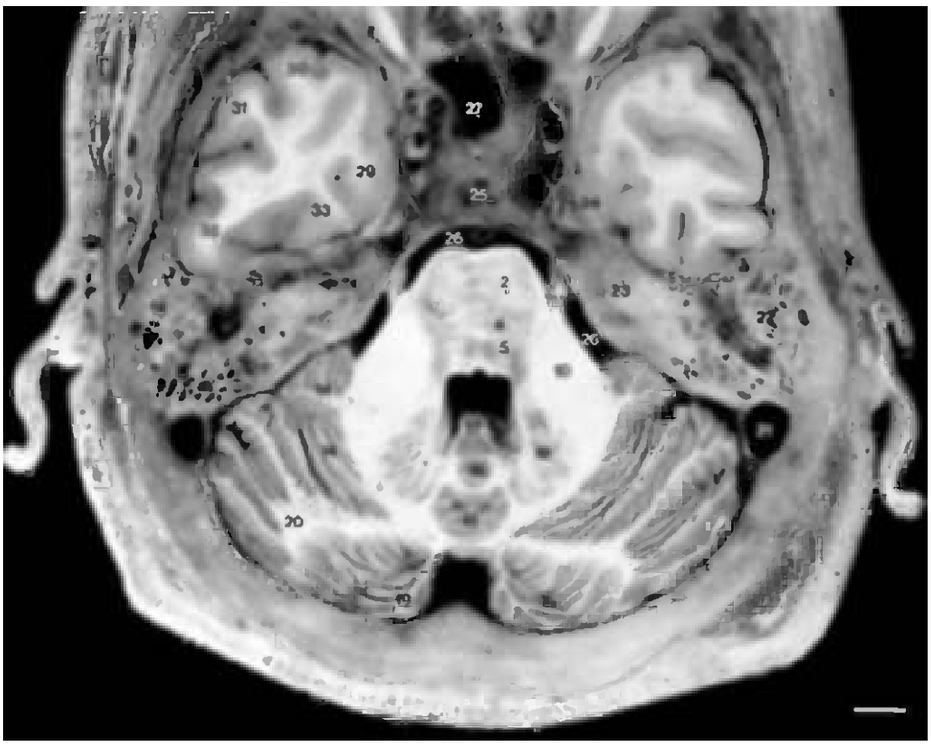

D

Fig. 11.14 (D–E).
D. Axial section of the head. Inferior view. Bar: 10 mm.
E. 3 Tesla MR cisternogram. See Fig. 4.13A for a comparable post mortem 3T MR image.

2 Corticospinal tract
4 Pontocerebellar fibers
5 Medial lemniscus
10 Middle cerebellar peduncle (brachium pontis)
11 Trigeminal nerve (CN V)
14 Simple lobule
15 Declive
16 Uvula
17 Nodulus
18 Dentate nucleus
19 Inferior semilunar lobule
20 Superior semilunar lobule
21 Sigmoid sinus
22 Mastoid air cells
23 Temporal bone, petrous portion
24 Meckel's cave
25 Clivus
26 Prepontine cistern and basilar artery
26′ Cerebellopontine angle cistern
27 Sphenoid sinus
28 Cavernous sinus and internal carotid artery
29 Parahippocampal gyrus
30 Superior temporal gyrus
31 Middle temporal gyrus
32 Inferior temporal gyrus
33 Fusiform gyrus

E

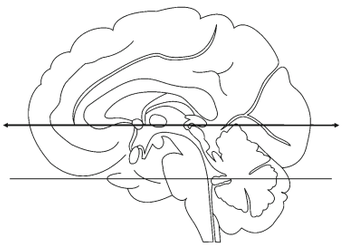

Fig. 11.15 (A–E). Axial (horizontal) section.
Pons
A. Inferior view after removal of the cerebral hemispheres. Bar: 10 mm.
B. Anterior oblique view. **C.** Superior view.
D and E. 3 Tesla MRI. **D.** T1-weighted MRI. **E**. T2-weighted MRI.

1 Pons, basilar portion
2 Corticospinal tract
3 Pontocerebellar fibers
4 Pontine nuclei
5 Medial lemniscus
6 Superior olivary nucleus
7 Lateral lemniscus
8 Principal sensory trigeminal nucleus (CN V)
9 Superior vestibular nucleus (CN VIII)
10 Genu of facial nerve (facial colliculus) (CN VII)
11 Trigeminal nerve (CN V)
11′ Meckel's cave
12 Middle cerebellar peduncle (brachium pontis)
13 Quadrangular lobule
14 Anterior superior (primary) fissure
15 Simple lobule
16 Declive
17 Culmen
18 Nodulus
19 Dentate nucleus
20 Emboliform nucleus
21 Fourth ventricle
24 Superior temporal gyrus
25 Parahippocampal gyrus
26 Middle temporal gyrus

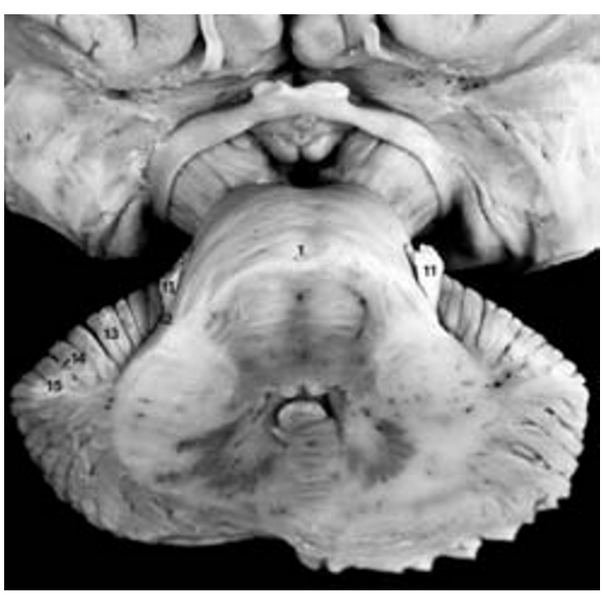

B

C

A

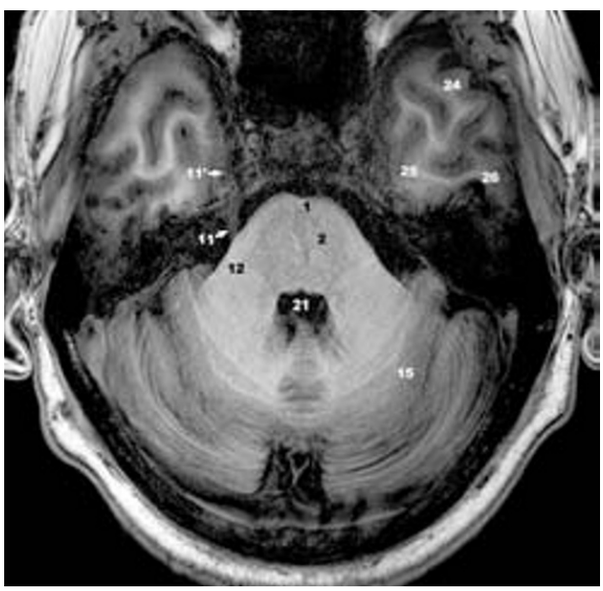

D

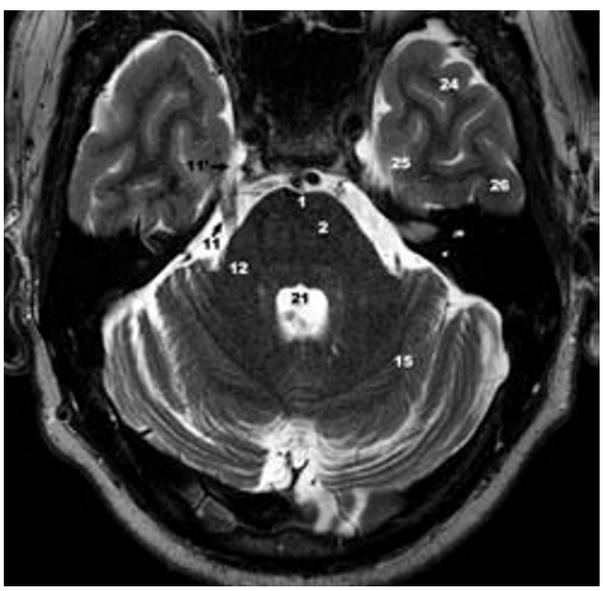

E

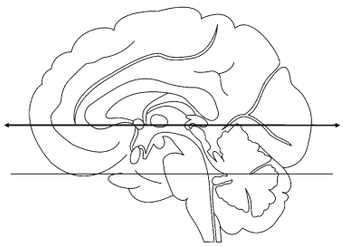

Fig. 11.16 (A–C). Axial (horizontal) section.
Pons
A. Inferior view after removal of the cerebral hemispheres. Bar: 10 mm.
B. Anterior oblique view. **C.** Superior view.

See **Fig. 2.15** for more information about the structures demonstrated at this level and **Fig. 7.15** for the vascular territories.

1 Pons, basilar portion
2 Corticospinal tract
3 Pontocerebellar fibers
4 Nucleus reticularis tegmenti pontis
5 Medial lemniscus
6 Trigeminal nerve (CN V)
6′ Fibers of trigeminal nerve (CN V)
7 Principal sensory trigeminal nucleus (CN V)
8 Motor trigeminal nucleus (CN V)
9 Superior cerebellar peduncle (brachium conjunctivum)
10 Middle cerebellar peduncle (brachium pontis)
11 Quadrangular lobule
12 Anterior superior (primary) fissure
13 Simple lobule
14 Declive
15 Culmen
16 Dentate nucleus
17 Emboliform nucleus
18 Globose nucleus
19 Fastigial nucleus

A

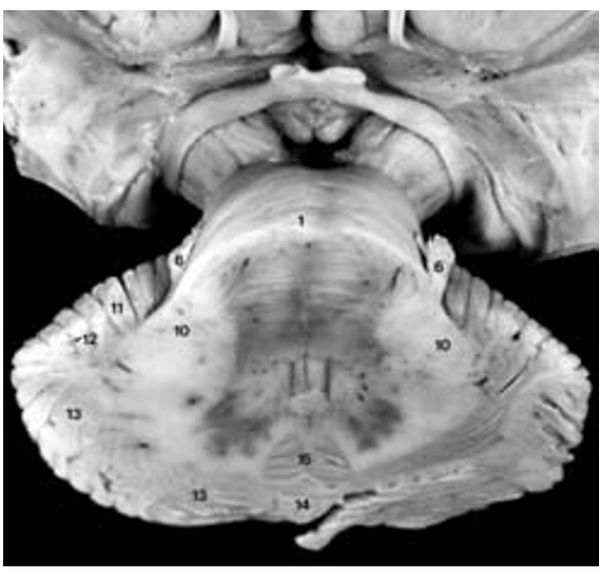

B

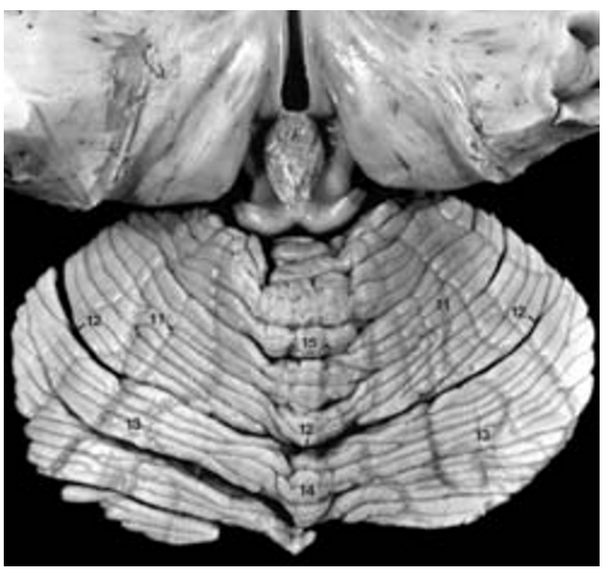

C

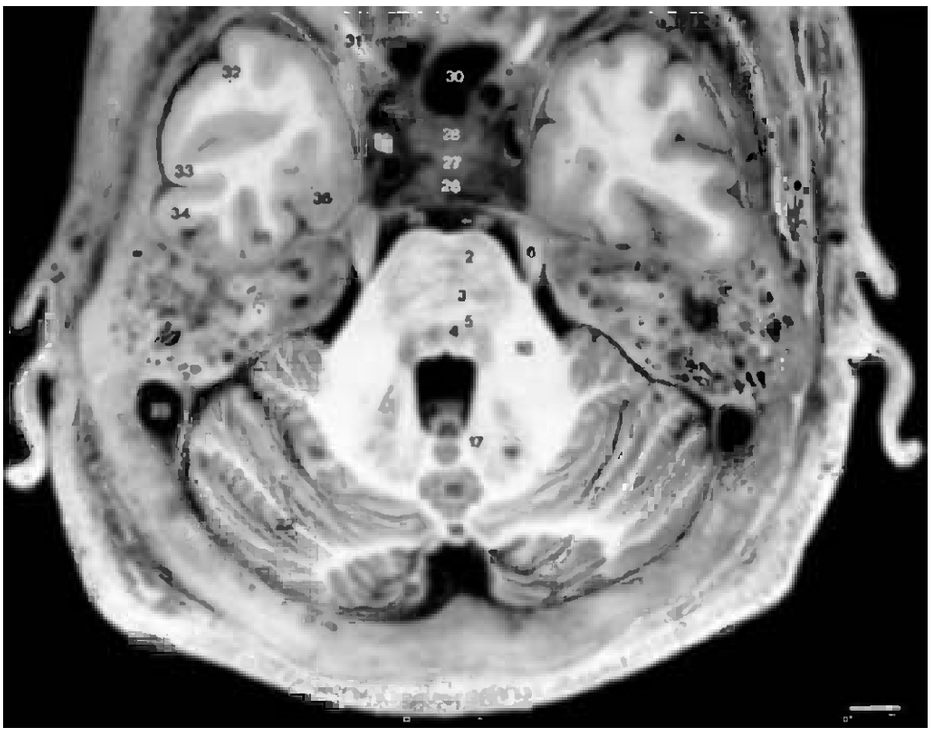

D

Fig. 11.16 (D–F).
D. Axial section of the head. Superior view. Bar: 10 mm.
E–F. 3 Tesla MRI. E. T1-weighted MRI. **F.** T2-weighted MRI.

2 Corticospinal tract
3 Pontocerebellar fibers
4 Nucleus reticularis tegmenti pontis
5 Medial lemniscus
6 Trigeminal nerve (CN V)
10 Middle cerebellar peduncle (brachium pontis)
13 Simple lobule
14 Declive
15 Culmen
16 Dentate nucleus
17 Emboliform nucleus
20 Nodulus
21 Inferior semilunar lobule
22 Superior semilunar lobule
23 Sigmoid sinus
24 Mastoid air cells
25 Prepontine cistern
25′ Basilar artery
26 Dorsum sellae
27 Hypophysis: posterior lobe (Neurohypophysis)
28 Hypophysis: anterior lobe (Adenohypophysis)
29 Cavernous sinus and internal carotid artery
30 Sphenoid sinus
31 Optic nerve (CN II)
32 Superior temporal gyrus
33 Middle temporal gyrus
34 Inferior temporal gyrus
35 Fusiform gyrus
36 Parahippocampal gyrus

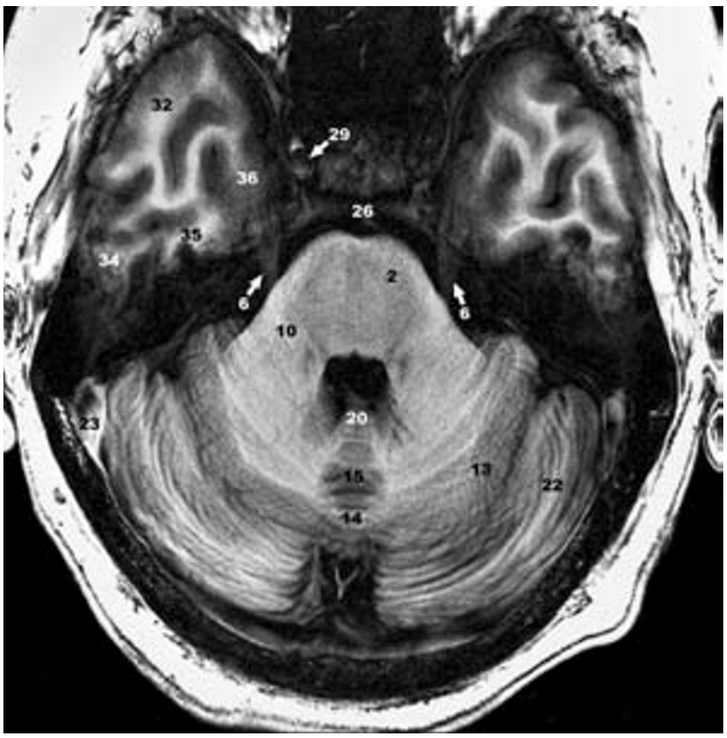
32
29
36
26
35
34
6
2
6
10
23
20
15
13
22
14

E

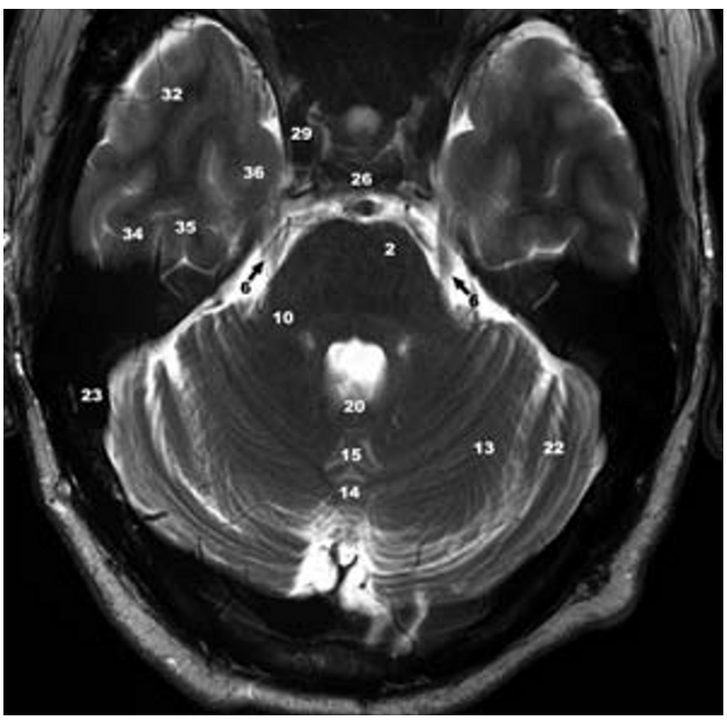
32
29
36
26
34
35
2
6
6
10
23
20
15
13
22
14

F

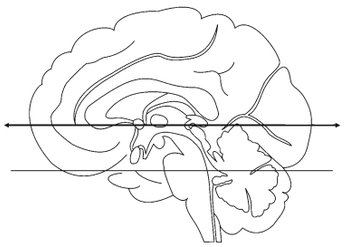

Fig. 11.17 (A–C). Axial (horizontal) section.
Pons
A. Inferior view after removal of the cerebral hemispheres. Bar: 10 mm.
B. Anterior oblique view. **C**. Superior view.

See **Fig. 2.15** for more information about the structures demonstrated at this level.

1 Pons, basilar portion
2 Corticospinal tract
3 Pontocerebellar fibers
4 Medial lemniscus
5 Principal sensory trigeminal nucleus (CN V)
6 Middle cerebellar peduncle (brachium pontis)
7 Medial longitudinal fasciculus
8 Nucleus reticularis tegmenti pontis
9 Superior cerebellar peduncle (brachium conjunctivum)
10 Parabrachial recess (between brachium pontis and brachium conjunctivum)
11 Trigeminal nerve (CN V)
12 Quadrangular lobule
13 Anterior superior (primary) fissure
14 Simple lobule
15 Declive
16 Culmen
17 Dentate nucleus
18 Emboliform nucleus
19 Globose nucleus
20 Fastigial nucleus
21 Fourth ventricle

A

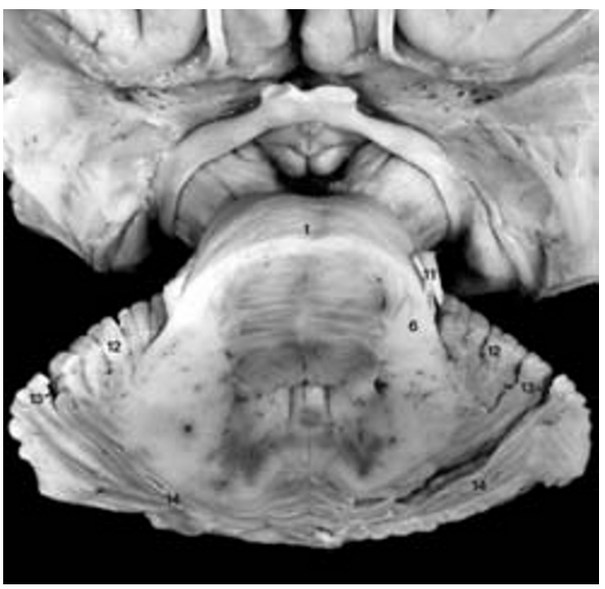

B

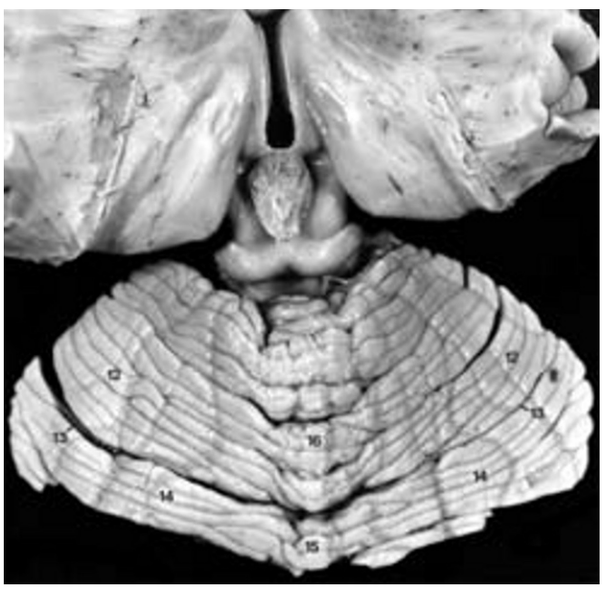

C

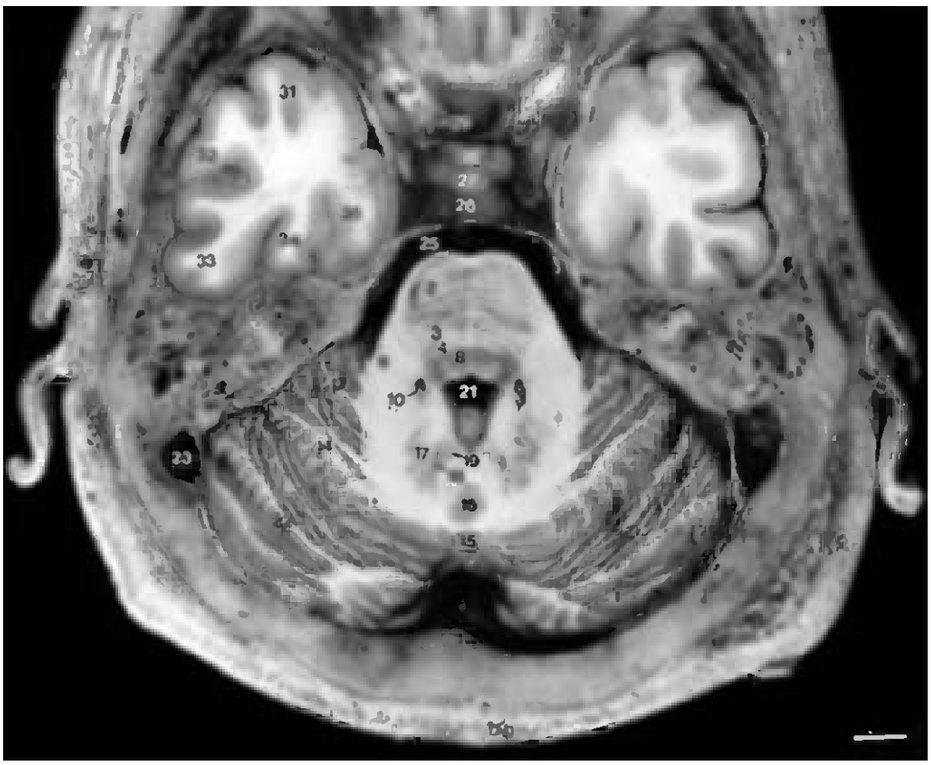

D

Fig. 11.17 (D–F).
D. Axial section of the head. Inferior view. Bar: 10 mm.
E–F. 3 Tesla MRI. E. T1-weighted MRI. **F.** T2-weighted MRI.

2 Corticospinal tract
3 Pontocerebellar fibers
4 Medial lemniscus
6 Middle cerebellar peduncle (brachium pontis)
8 Nucleus reticularis tegmenti pontis
10 Parabrachial recess (between brachium pontis and brachium conjunctivum)
12 Quadrangular lobule
14 Simple lobule
15 Declive
16 Culmen
17 Dentate nucleus
18 Emboliform nucleus
19 Globose nucleus
21 Fourth ventricle
22 Superior semilunar lobule
23 Sigmoid sinus
24 Mastoid air cells
25 Prepontine cistern
26 Dorsum sellae
27 Hypophysis: posterior lobe (Neurohypophysis)
28 Hypophysis: anterior lobe (Adenohypophysis)
29 Internal carotid artery within the cavernous sinus
30 Optic nerve (CN II)
31 Superior temporal gyrus
32 Middle temporal gyrus
33 Inferior temporal gyrus
34 Fusiform gyrus
35 Parahippocampal gyrus

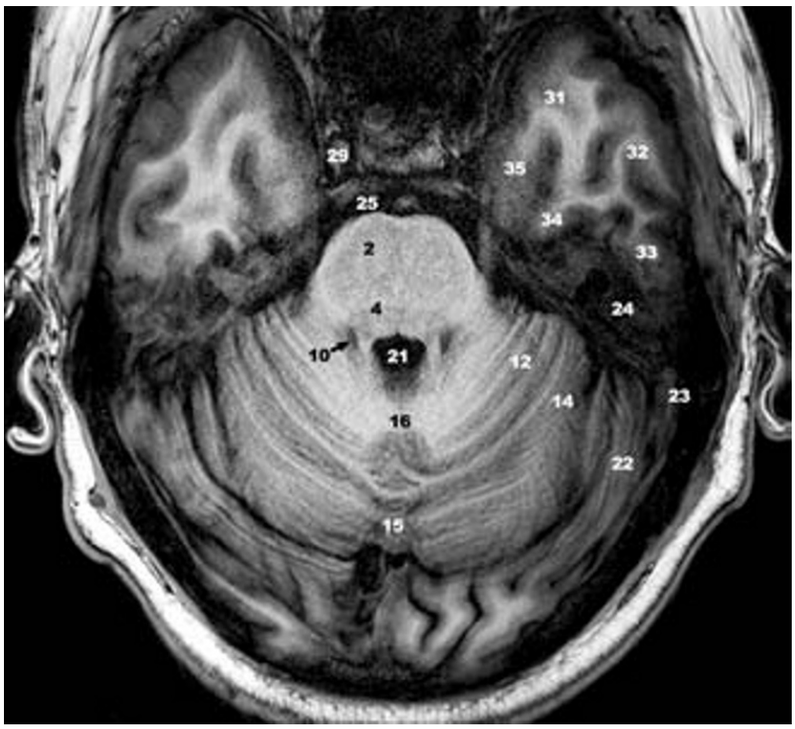
31
29
35
32
25
34
2
33
4
24
10
21
12
14
23
16
22
15

E

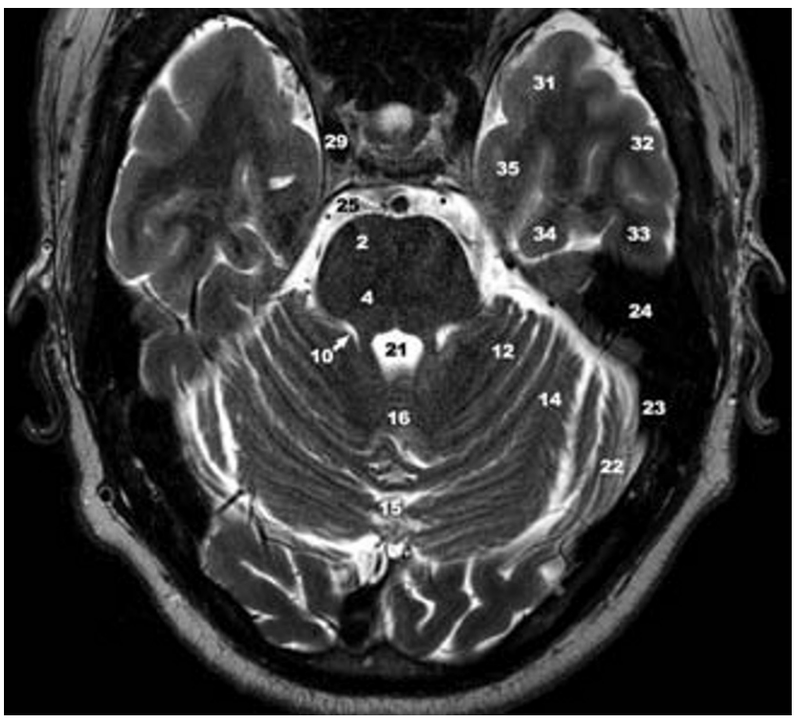
31
29
32
35
25
2
34
33
4
24
10
21
12
14
23
16
22
15

F

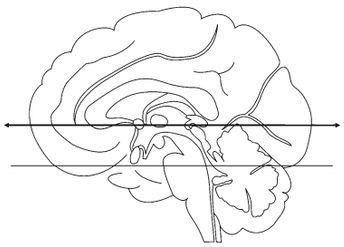

Fig. 11.18 (A–C). Axial (horizontal) section.
Pons
A. Inferior view after removal of the cerebral hemispheres. Bar: 10 mm.
B. Anterior oblique view. **C.** Superior view.

1 Pons, basilar portion
2 Corticospinal tract
3 Pontocerebellar fibers
4 Medial lemniscus
5 Trigeminal nerve (CN V)
6 Middle cerebellar peduncle (brachium pontis)
7 Superior cerebellar peduncle (brachium conjunctivum)
8 Parabrachial recess
9 Medial parabrachial nucleus
10 Nucleus ceruleus
11 Medial longitudinal fasciculus
12 Nucleus reticularis tegmenti pontis
13 Quadrangular lobule
14 Culmen
15 Anterior superior (primary) fissure
16 Simple lobule
17 Declive
18 Dentate nucleus
19 Emboliform nucleus
20 Fourth ventricle
38 Hypophyseal stalk

A

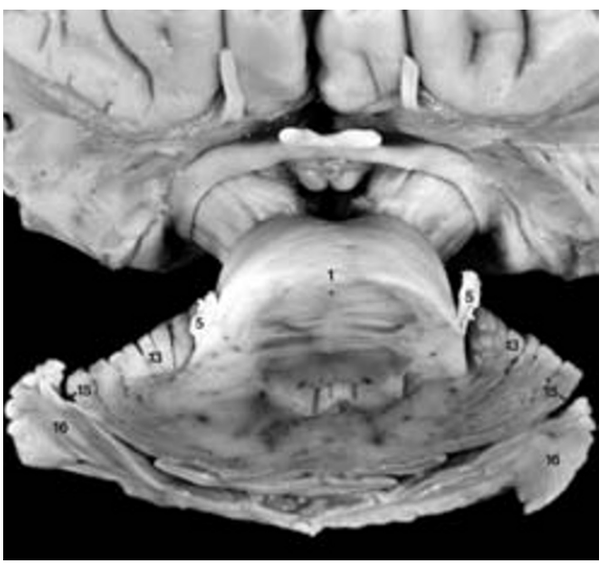

B

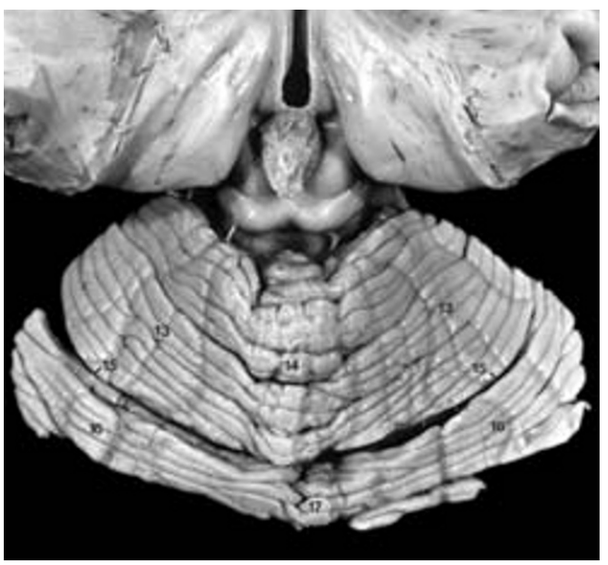

C

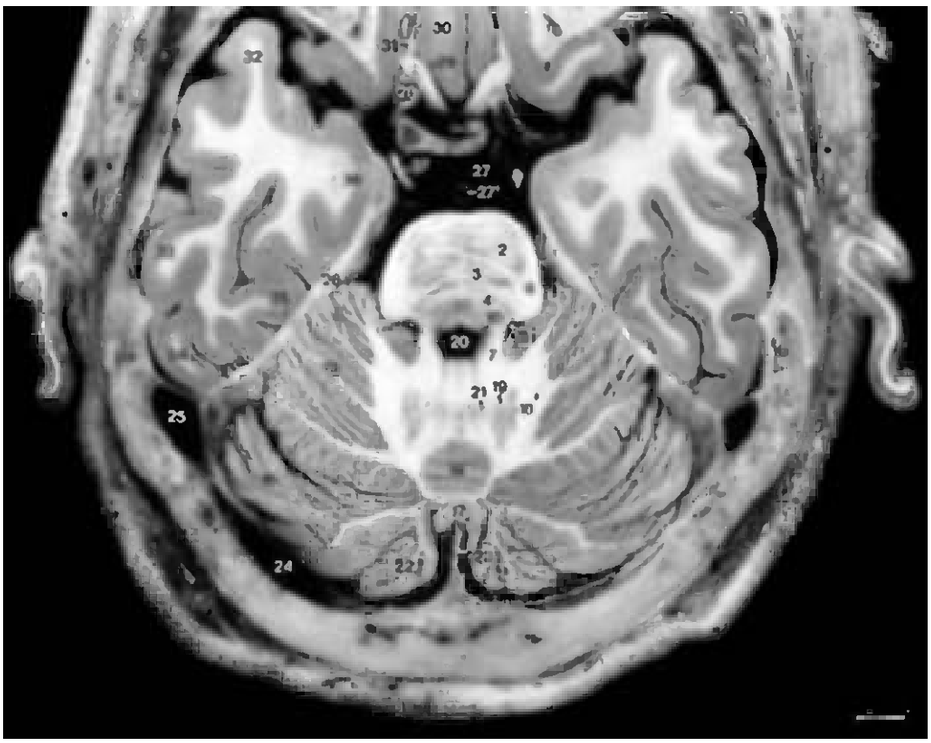

D

Fig. 11.18 (D–F).
D. Axial section of the head. Inferior view. Bar: 10 mm.
E–F. 3 Tesla MRI. E. T1-weighted MRI. **F.** T2-weighted MRI.

2 Corticospinal tract
3 Pontocerebellar fibers
4 Medial lemniscus
6 Middle cerebellar peduncle (brachium pontis)
7 Superior cerebellar peduncle (brachium conjunctivum)
8 Parabrachial recess
10 Nucleus ceruleus
13 Quadrangular lobule
14 Culmen
16 Simple lobule
17 Declive
18 Dentate nucleus
19 Emboliform nucleus
20 Fourth ventricle
21 Globose nucleus
22 Superior semilunar lobule
23 Falx cerebelli
24 Transverse sinus
25 Sigmoid sinus
26 Tentorium cerebelli
27 Prepontine cistern
27′ Basilar artery
28 Internal carotid artery
29 Optic nerve (CN II)
30 Gyrus rectus
31 Olfactory tract
32 Superior temporal gyrus
33 Middle temporal gyrus
34 Inferior temporal gyrus
35 Fusiform gyrus
36 Parahippocampal gyrus
37 Oculomotor nerve (CN III)
38 Hypophyseal stalk

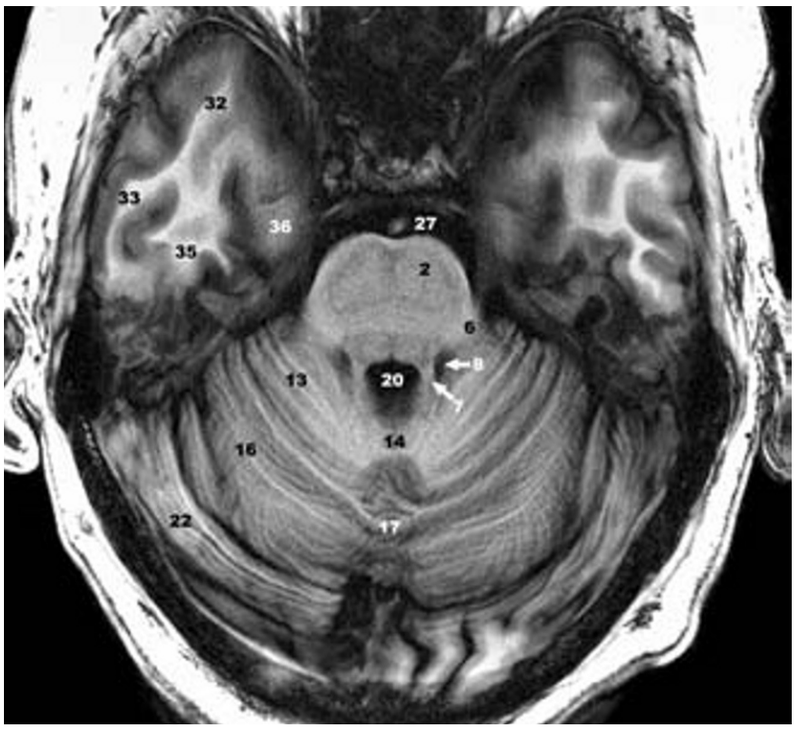
32
33
36
27
35
2
6
8
13
20
7
16
14
22
17

E

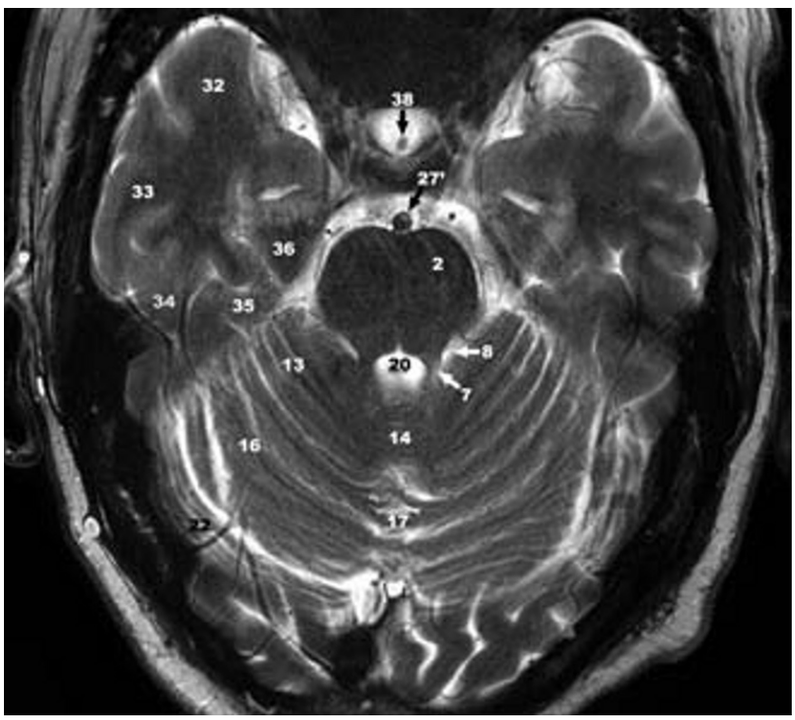
32
38
27'
33
36
2
34
35
8
13
20
7
16
14
22
17

F

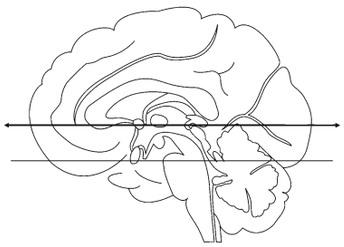

Fig. 11.19 (A–C). Axial (horizontal) section.
Pons
A. Inferior view after removal of the cerebral hemispheres. Bar: 10 mm.
B. Anterior oblique view. **C.** Superior view.

See **Fig. 2.16** for more information about the structures demonstrated at this level, and **Fig. 7.17** for vascular territories.

1 Pons, basilar portion
2 Corticospinal tract
3 Pontocerebellar fibers
4 Medial lemniscus
5 Middle cerebellar peduncle (brachium pontis)
6 Superior cerebellar peduncle (brachium conjunctivum)
7 Parabrachial recess
8 Lateral lemniscus
9 Mesencephalic trigeminal tract (CN V)
10 Nucleus ceruleus
11 Medial longitudinal fasciculus
12 Nucleus reticularis centralis superior
13 Nucleus reticularis tegmenti pontis
14 Quadrangular lobule
15 Culmen
16 Dentate nucleus (superior pole)
17 Fourth ventricle
18 Crus cerebri
19 Hypophyseal stalk
20 Optic chiasm (CN II)
21 Optic tract (CN II)
22 Lateral geniculate body
23 Anterior perforated substance
24 Olfactory tract (CN I)

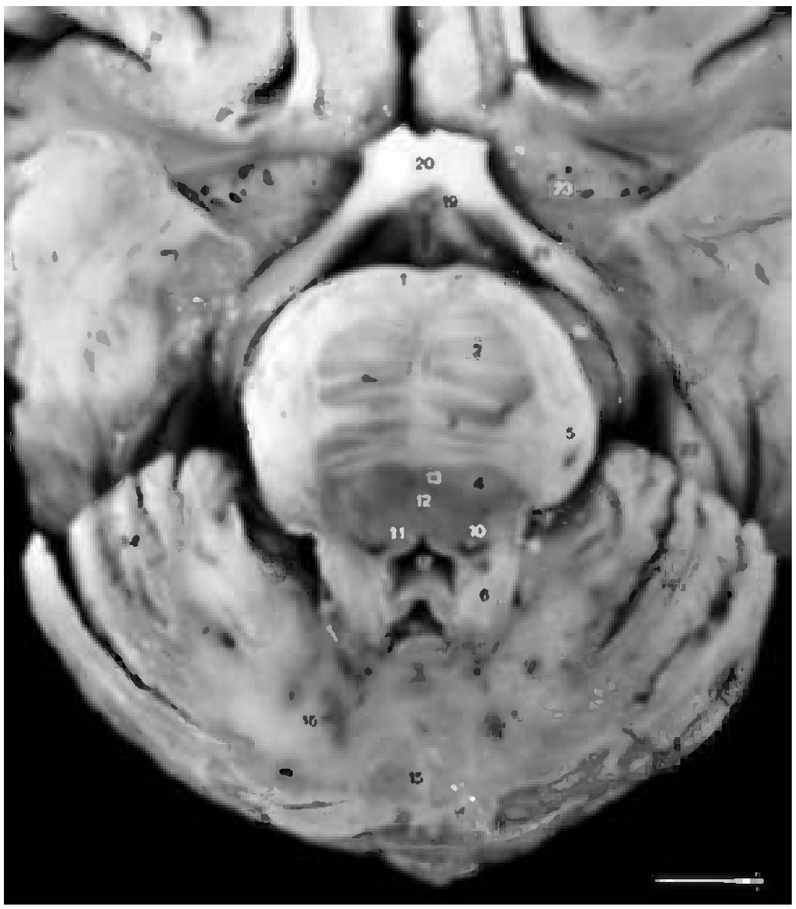

A

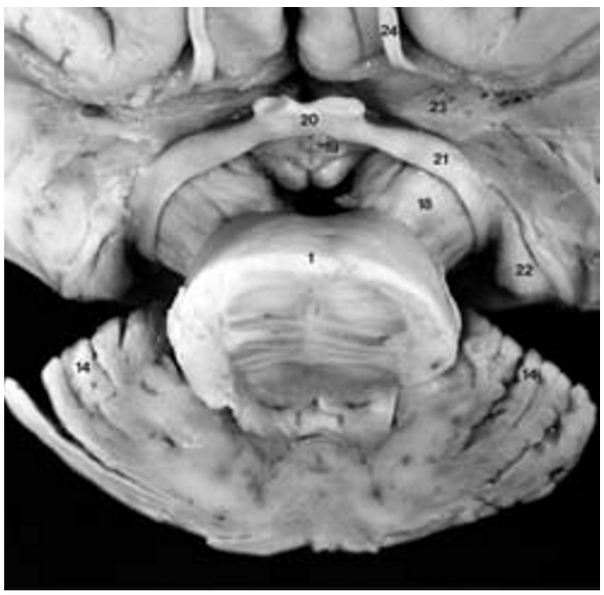

B

C

D

Fig. 11.19 (D–F).
D. Axial section of the head. Inferior view. Bar: 10 mm.
E–F. 3 Tesla MRI. E. T1-weighted MRI. **F.** T2-weighted MRI.

2 Corticospinal tact
3 Pontocerebellar fibers
4 Medial lemniscus
6 Superior cerebellar peduncle (brachium conjunctivum)
7 Parabrachial recess
10 Nucleus ceruleus
14 Quadrangular lobule
15 Culmen
17 Fourth ventricle
25 Simple lobule
26 Confluens sinuum (torcular Herophili)
27 Transverse sinus
28 Sigmoid sinus
29 Tentorium cerebelli
30 Prepontine cistern
30′ Basilar artery
31 Dorsum sellae
32 Oculomotor nerve (CN III)
33 Internal carotid artery
34 Hypophyseal stalk (arrow)
35 Optic nerve (CN II)
36 Gyrus rectus
37 Olfactory tract (CN I)
38 Medial orbital gyrus
39 Superior temporal gyrus
40 Middle temporal gyrus
41 Inferior temporal gyrus
42 Fusiform gyrus
43 Parahippocampal gyrus
44 Hippocampus, head
45 Amygdala

Arrow: Hypophyseal stalk

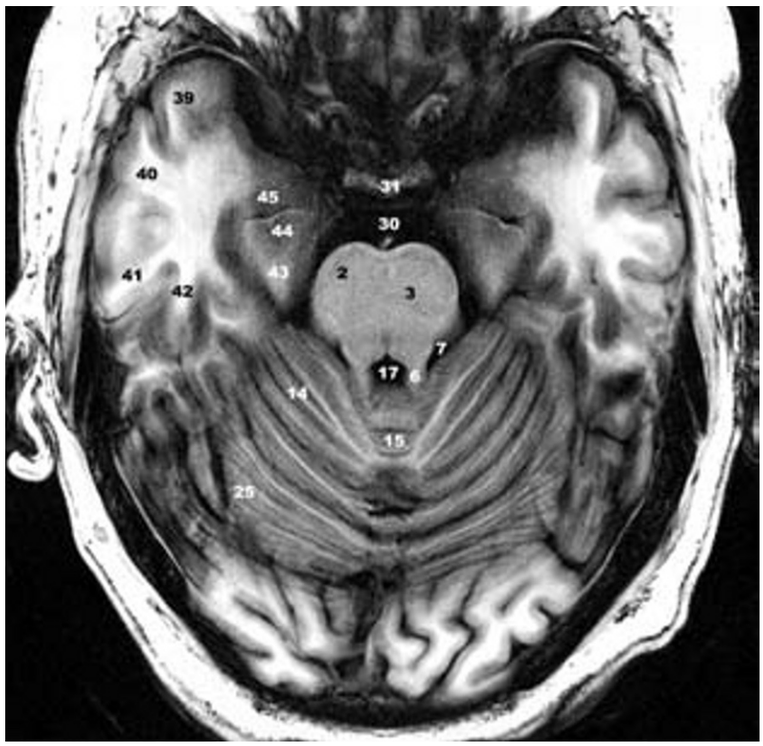
39
40
45
31
44
30
41
43
2
42
3
7
17
6
14
15
25

E

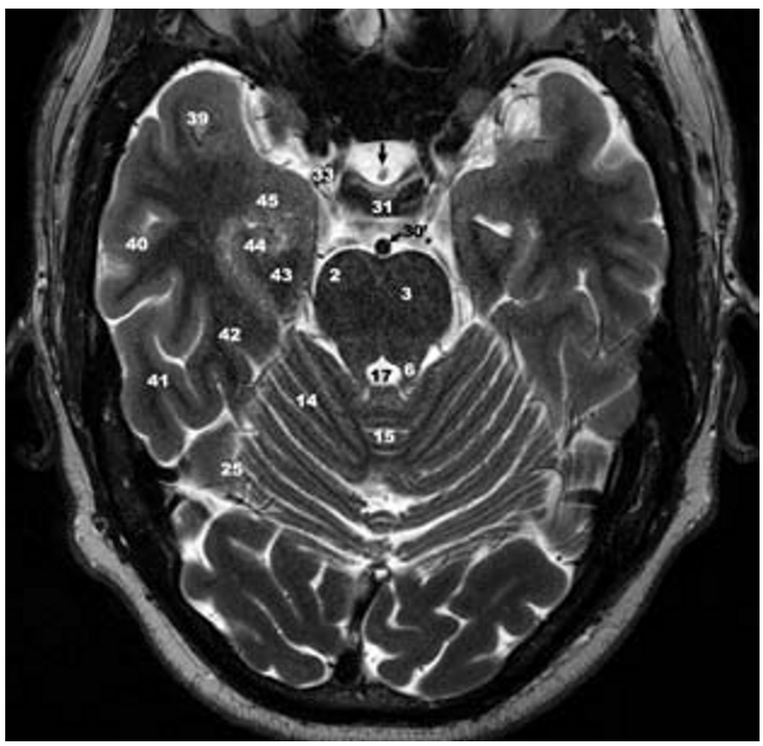
39
33
45
31
40
44
30
43
2
3
42
17
6
41
14
15
25

F

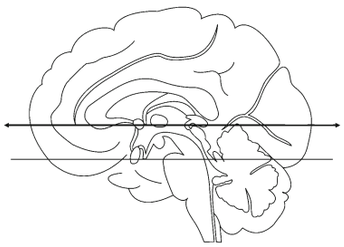

Fig. 11.20 (A–C). Axial (horizontal) section.
Pons
A. Inferior view after removal of the cerebral hemispheres. Bar: 10 mm.
B. Posterior oblique view after removal of the cerebellum.
C. Superior view.

See **Fig. 2.17** for more information about the structures demonstrated at this level, and **Fig. 7.19** for vascular territories.

1 Corticospinal tract
2 Crus cerebri
3 Pontocerebellar fibers
4 Medial lemniscus
5 Lateral lemniscus
6 Superior cerebellar peduncle
7 Nucleus ceruleus
8 Mesencephalic trigeminal tract (CN V)
9 Medial parabrachial nucleus
10 Nucleus reticularis centralis superior
11 Nucleus reticularis tegmenti pontis
12 Superior medullary velum
13 Frenulum veli
14 Inferior colliculus
14′ Brachium of the inferior colliculus
15 Superior colliculus
16 Quadrangular lobule
17 Culmen
18 Central lobule
19 Ala of the central lobule
20 Lateral geniculate body
20′ Medial geniculate body
21 Optic tract (CN II)
22 Hypophyseal stalk
23 Optic chiasm (CN II)
24 Anterior perforated substance
25 Olfactory tract (CN I)
25′ Lateral olfactory stria
25″ Medial olfactory stria
26 Pineal gland
27 Stria medullaris thalami
28 Pulvinar

A

B

C

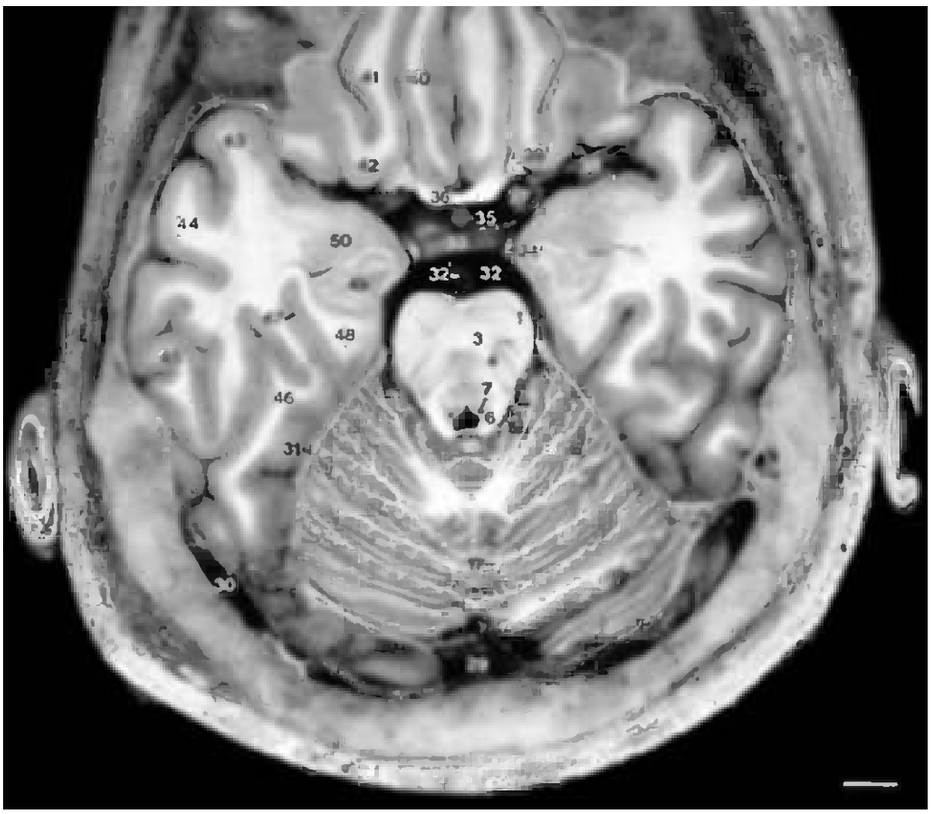

D

Fig. 11.20 (D–F).
D. Axial section of the head. Superior view. Bar: 10 mm.
E–F. 3 Tesla MRI. E. T1-weighted MRI. **F.** T2-weighted MRI.

1 Corticospinal tract
3 Pontocerebellar fibers
4 Medial lemniscus
6 Superior cerebellar peduncle
7 Nucleus ceruleus
16 Quadrangular lobule
17 Culmen
18 Central lobule
19 Ala of the central lobule
29 Confluens sinuum (torcular Herophili)
30 Transverse sinus
31 Tentorium cerebelli
32 Prepontine cistern
32′ Basilar artery
33 Dorsum sellae
34 Oculomotor nerve (CN III)
35 Hypophyseal stalk
36 Optic chiasm (CN II)
36′ Prechiasmal optic nerve (CN II)
37 Internal carotid artery
38 Middle cerebral artery and basal part of the lateral fissure
39 Olfactory tract
40 Gyrus rectus
41 Medial orbital gyrus
42 Posterior orbital gyrus
43 Superior temporal gyrus
44 Middle temporal gyrus
45 Inferior temporal gyrus
46 Fusiform gyrus
47 Collateral sulcus
48 Parahippocampal gyrus
49 Hippocampus (head)
50 Amygdala
51 Posterior cerebral artery
52 Trochlear nerve (CN IV)

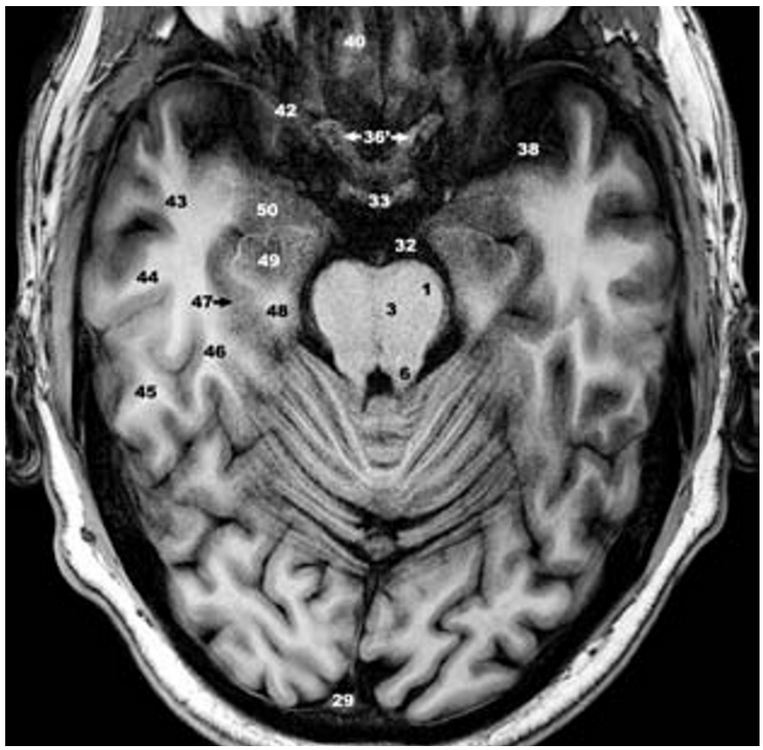
40
42
36'
38
43
50
33
32
49
44
47
48
1
3
46
6
45
29

E

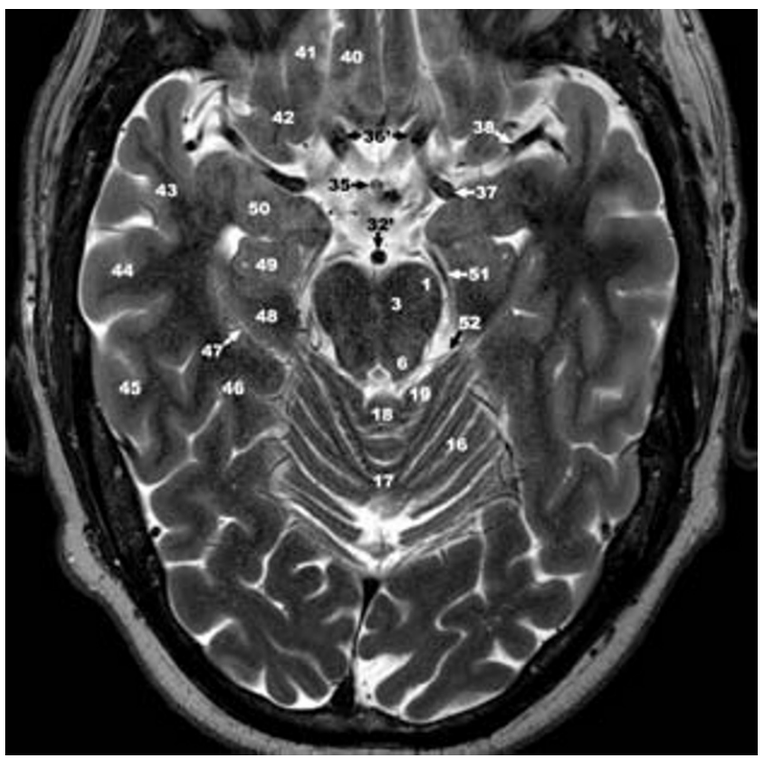
41
40
42
36'
38
43
35
37
50
32'
49
44
1
51
3
48
52
47
6
45
46
19
18
16
17

F

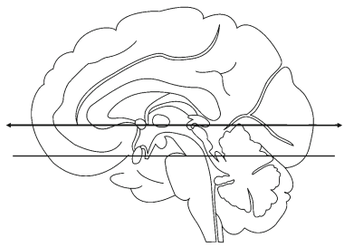

Fig. 11-21 (A–E.). Axial (horizontal) section. Pontomesencephalic junction
A. Inferior view after removal of the cerebral hemispheres. Bar: 10 mm.
B. Anterior oblique view after removal of the cerebellum.
C. Posterior oblique view.
D– E. 3 Tesla MRI. **D.** T1-weighted MRI. **E.** T2-weighted MRI.

1 Pons
2 Crus cerebri
3 Superior cerebellar peduncle (brachium conjunctivum)
4 Medial lemniscus
5 Lateral lemniscus
6 Nucleus ceruleus
7 Superior medullary velum
8 Frenulum veli
9 Trochlear nerve (CN IV)
10 Inferior colliculus
11 Superior colliculus
12 Central lobule
13 Ala of the central lobule
14 Quadrangular lobule
15 Culmen
16 Lateral geniculate body
17 Medial geniculate body
18 Optic tract
19 Optic chiasm
19′ Prechiasmal optic nerve
20 Hypophyseal stalk (small arrow)
21 Mammillary body
22 Anterior perforated substance
23 Lateral olfactory stria
24 Pulvinar
26 Interpeduncular fossa
33 Gyrus rectus
34 Medial orbital gyrus
35 Superior temporal gyrus
36 Superior temporal sulcus (parallel sulcus)
37 Middle temporal gyrus
38 Inferior temporal gyrus
39 Temporo-occipital incisure
40 Middle occipital gyrus
41 Fusiform gyrus
42 Collateral sulcus
43 Parahippocampal gyrus
44 Hippocampus, head
45 Temporal horn of the lateral ventricle
46 Amygdala

Small vertical arrow: Hypophyseal stalk

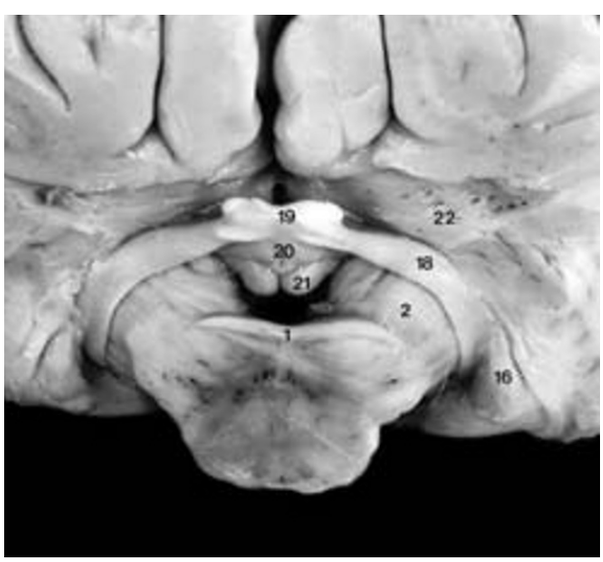

B

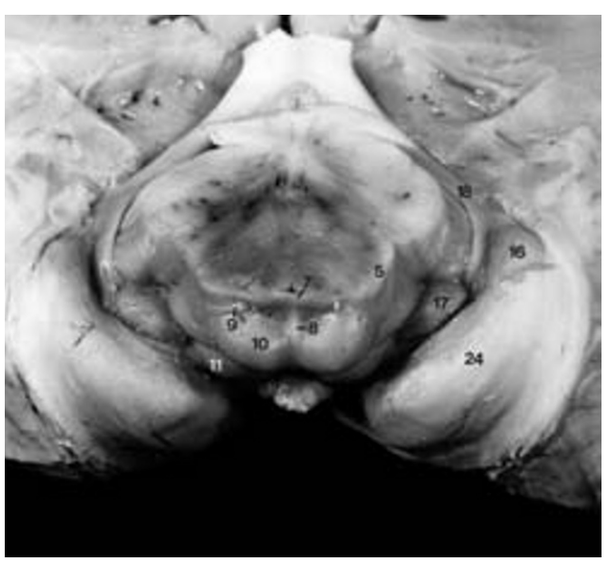

C


1
18
2
3
4
6
24
7
13
12
14
15

A

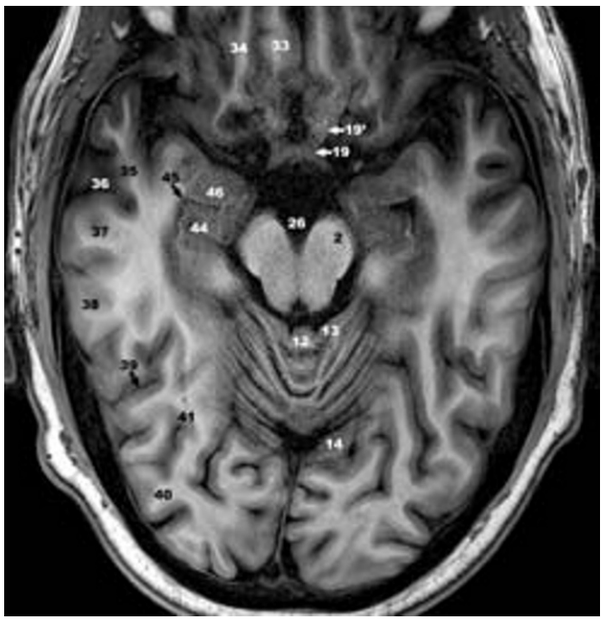
34
33
19'
19
35
36
45
46
37
44
26
2
38
12
13
39
41
14
40

D

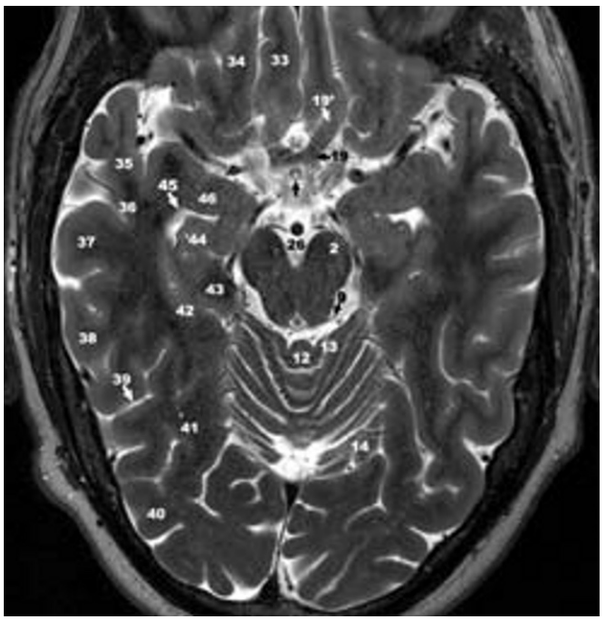
34
33
19'
19
35
36
45
46
37
44
26
2
43
42
38
12
13
39
41
14
40

E

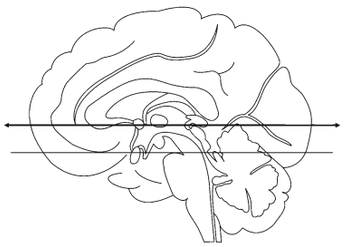

Fig. 11.22 (A–C). Axial (horizontal) section. Mesencephalon

A. Inferior view after removal of the cerebral hemispheres. Bar: 10 mm.

B. Anterior oblique view after removal of the cerebellum.

C. Posterior oblique view.

1 Crus cerebri
2 Oculomotor nerve (CN III)
3 Interpeduncular (intercrural) fossa (interpeduncular cistern)
4 Substantia nigra (pars compacta)
5 Decussation of the superior cerebellar peduncles (brachium conjunctivum)
6 Medial lemniscus
7 Lateral lemniscus
8 Dorsal nucleus of raphe
9 Trochlear nerve nucleus (CN IV)
10 Cerebral aqueduct
11 Inferior colliculus
12 Superior colliculus
13 Mesencephalon, lateral surface
14 Central lobule
15 Ala of central lobule
16 Culmen
17 Quadrangular lobule
18 Medial geniculate body
19 Lateral geniculate body
20 Optic tract (CN II)
21 Optic chiasm (CN II)
22 Tuber cinereum
23 Mammillary body
24 Anterior perforated substance
25 Pulvinar
26 Pineal gland


21
24
22
20
3
1
4
8
18
9
7
1
25
11
14
17
16

A

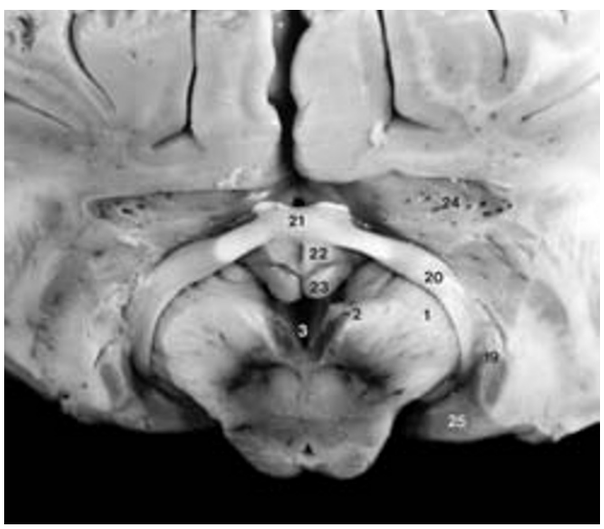
21
24
22
20
23
2
1
3
19
25
4

B

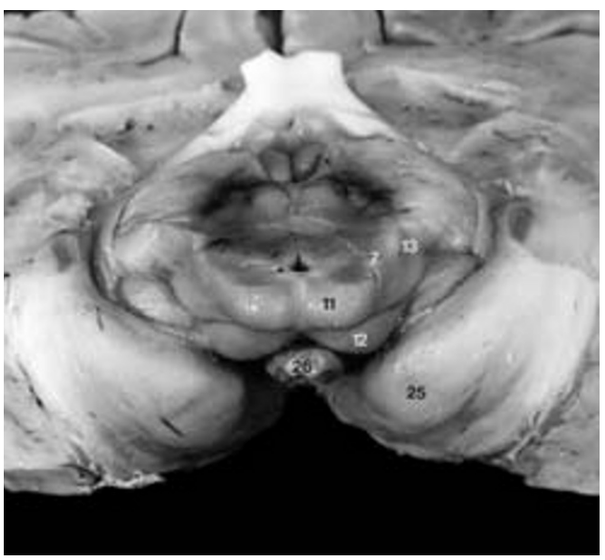
13
11
12
26
25

C

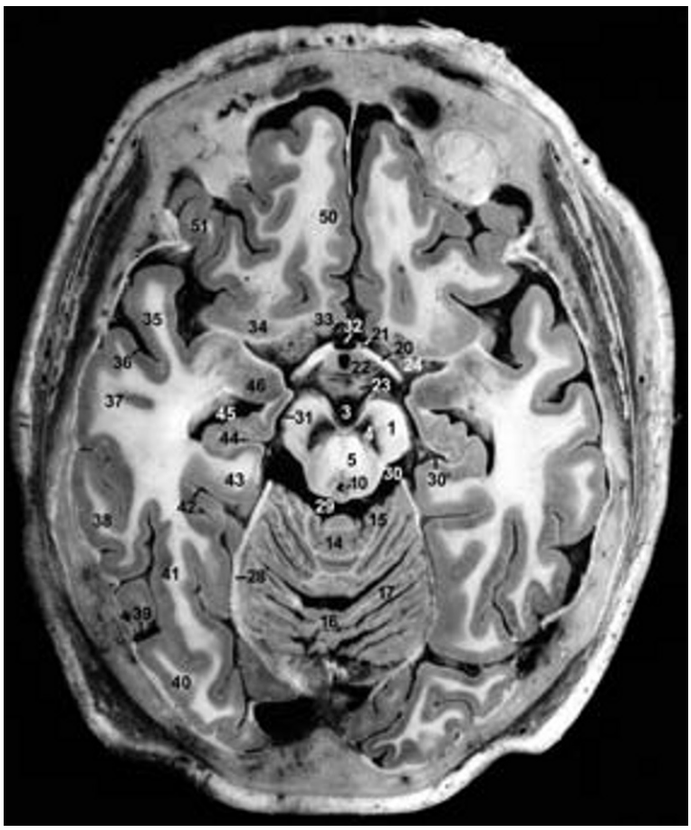

D

Fig. 11.22 (D–F).
D. Axial section of the head. Inferior view. Bar: 10 mm.
E–F. 3 Tesla MRI. E. T1-weighted MRI. **F.** T2-weighted MRI.

1 Crus cerebri
3 Interpeduncular (intercrural) fossa (interpeduncular cistern)
4 Substantia nigra (pars compacta)
5 Decussation of the superior cerebellar peduncles (brachium conjunctivum)
10 Cerebral aqueduct (of Sylvius) (arrow)
14 Central lobule
15 Ala of central lobule
16 Culmen
17 Quadrangular lobule
20 Optic tract (CN II)
21 Optic chiasm (CN II)
22 Tuber cinereum
23 Mammillary body (covered by the origin of the posterior cerebral arteries)
24 Anterior perforated substance
27 Confluens sinuum (torcular Herophili)
28 Tentorium cerebelli
29 Quadrigeminal cistern
30 Ambient cistern
30′ Wing of ambient cistern
31 Crural cistern
32 Suprachiasmatic (supra-optic) recess and lamina terminalis
33 Subcallosal gyrus
34 Posterior orbital gyrus
35 Superior temporal gyrus
36 Superior temporal sulcus (parallel sulcus)
37 Middle temporal gyrus
38 Inferior temporal gyrus
39 Temporo-occipital incisure
40 Middle occipital gyrus
41 Fusiform gyrus
42 Collateral sulcus
43 Parahippocampal gyrus
44 Hippocampus, head
45 Temporal horn of the lateral ventricle
46 Amygdala
47 Anterior cerebral artery
48 Middle cerebral artery
49 Basilar artery

Arrow: Cerebral aqueduct (of Sylvius)

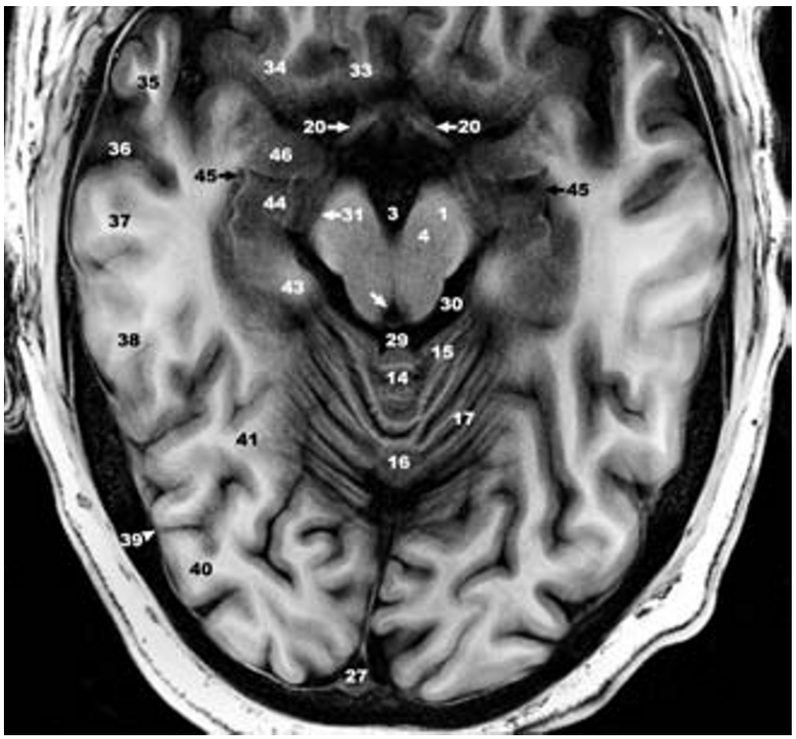
35
34
33
20
20
36
46
45
45
44
31
3
1
4
37
43
30
38
29
15
14
17
41
16
39
40
27

E

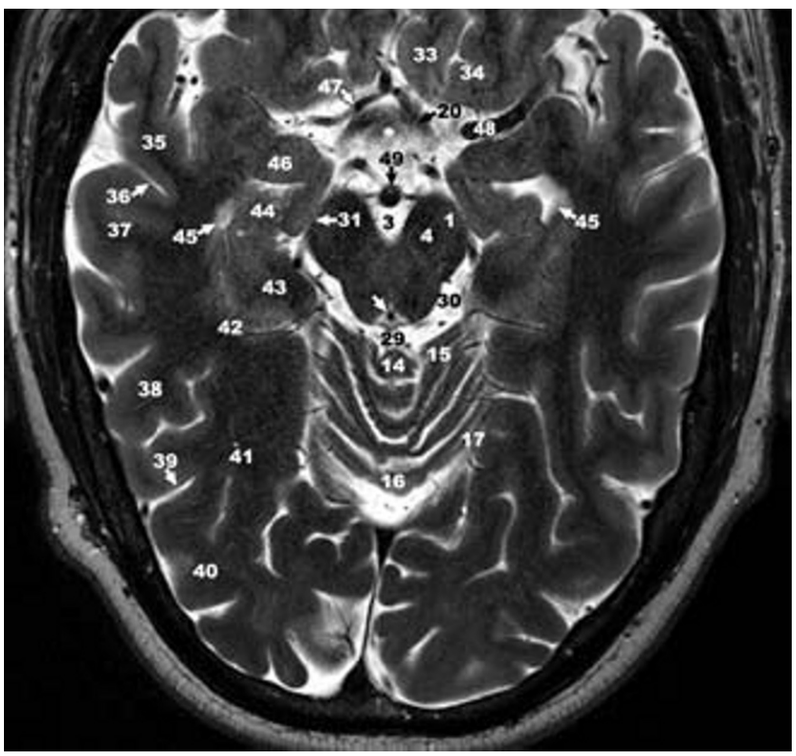
33
34
47
20
48
35
46
49
36
44
31
3
1
45
37
45
4
43
30
42
29
14
15
38
17
39
41
16
40

F

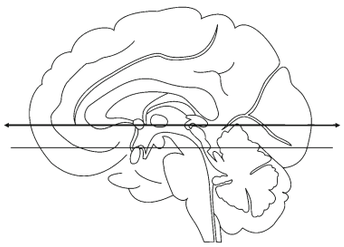

Fig. 11.23 (A–B). Axial (horizontal) section.
Mesencephalon
A. Inferior view after removal of the cerebral hemispheres and cerebellum. Bar: 10 mm.
B. Superior view.

See **Fig. 2.18** for more information about the structures demonstrated at this level and **Fig. 7.21** for the vascular territories.

1 Crus cerebri
2 Substantia nigra (pars compacta)
3 Superior cerebellar peduncle (brachium conjunctivum)
4 Interpeduncular nucleus
5 Oculomotor nerve (CN III)
6 Interpeduncular (intercrural) fossa
7 Medial lemniscus
8 Lateral lemniscus
9 Trochlear nerve nucleus (CN IV)
10 Dorsal nucleus of raphe
11 Cerebral aqueduct (of Sylvius)
12 Inferior colliculus
13 Superior colliculus
14 Medial geniculate body
15 Lateral geniculate body
16 Optic tract (CN II)
17 Optic chiasm (CN II)
18 Tuber cinereum
19 Mammillary body
20 Anterior perforated substance
21 Pulvinar
22 Pineal gland
23 Stria medullaris thalami
24 Anterior columns of the fornix
25 Third ventricle

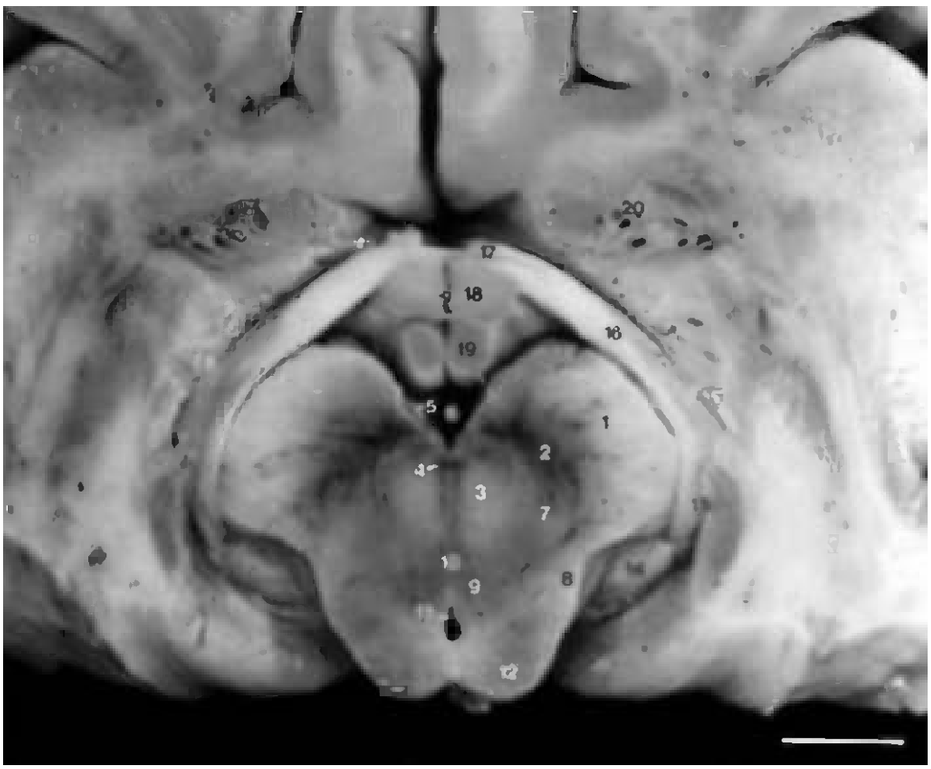

A

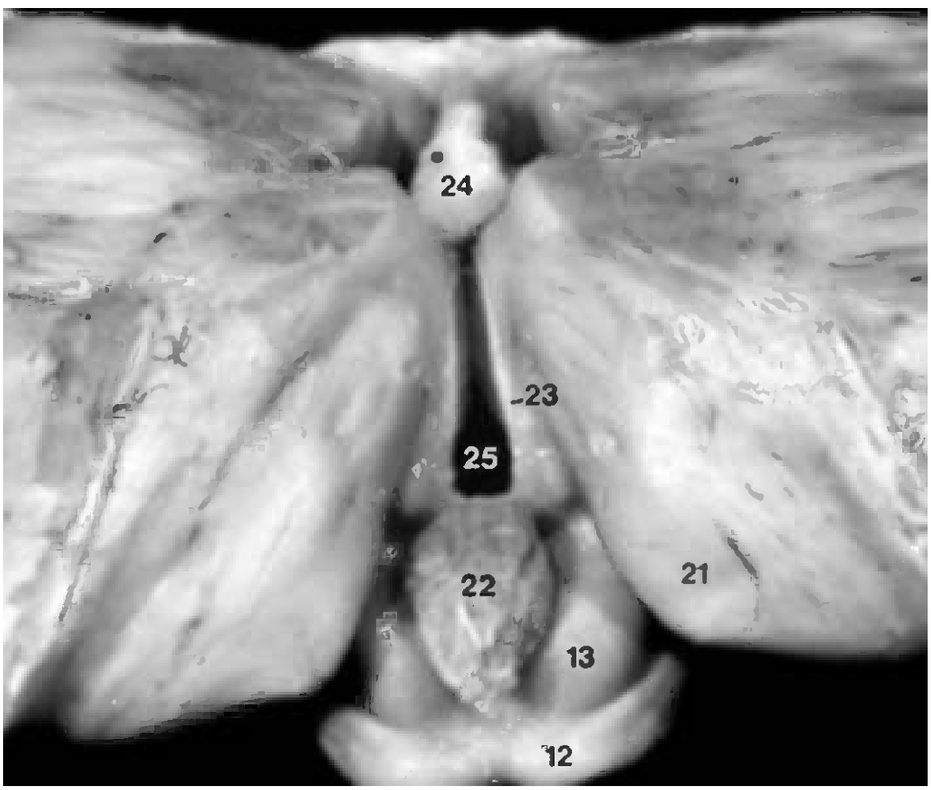

B

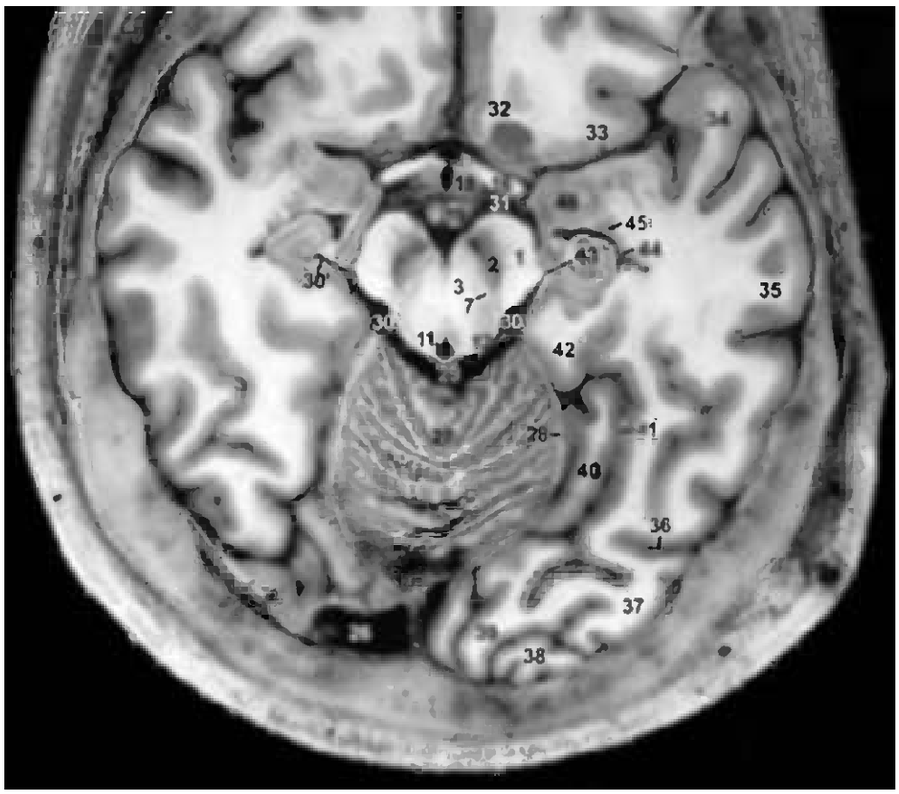

C

Fig. 11.23 (C–E).
C. Axial section of the head. Inferior view. Bar: 10 mm.
D–E. 3 Tesla MRI. D. T1-weighted MRI. **E.** T2-weighted MRI.

1 Crus cerebri
2 Substantia nigra (pars compacta)
3 Superior cerebellar peduncle (brachium conjunctivum)
7 Medial lemniscus
11 Cerebral aqueduct (of Sylvius)
12 Inferior colliculus
16 Optic tract
18 Tuber cinereum
19 Mammillary body
26 Superior sagittal sinus
27 Culmen
28 Tentorium cerebelli
29 Quadrigeminal cistern
30 Ambient cistern
30′ Wing of ambient cistern
31 Chiasmatic cistern
32 Subcallosal gyrus
33 Lateral fissure, basal portion
34 Superior temporal gyrus
35 Middle temporal gyrus
36 Anterior occipital sulcus
37 Middle occipital gyrus
38 Gyrus descendens
39 Cuneus
40 Lingual gyrus
41 Collateral sulcus
42 Parahippocampal gyrus
43 Hippocampus, head
44 Temporal horn of the lateral ventricle
45 Caudate nucleus, tail
46 Amygdala
47 Anterior cerebral artery (two sites)
48 Interpeduncular (intercrural) cistern
49 Gyrus rectus
50 Medial orbital gyrus
51 Posterior orbital gyrus
54 Basal vein, ventral segment (for more about the basal vein, see [208, 469])
55 Basilar artery bifurcation


50
51
49
32
34
16
18
31
46
48
2
1
43
35
30
42
41
29
27
40
41
36
37
39

D

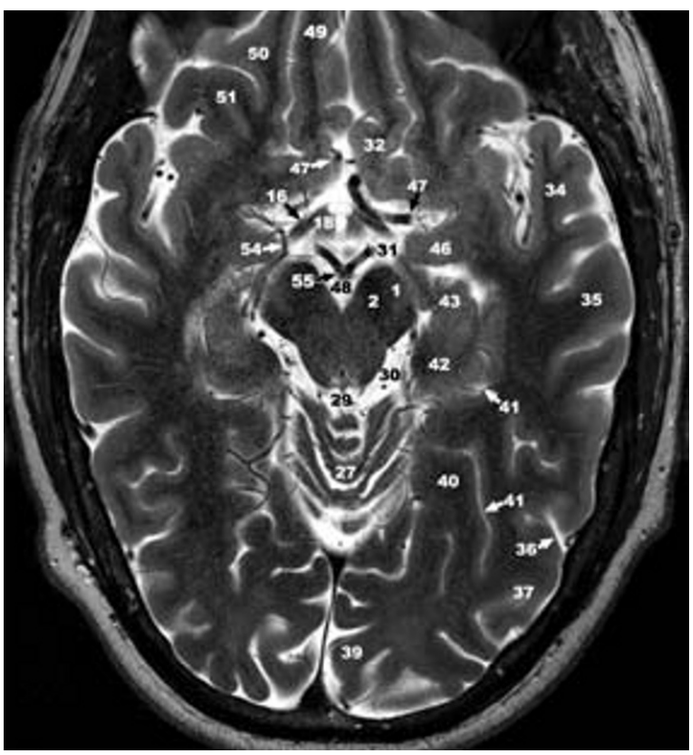
49
50
51
32
47
47
34
16
18
54
31
46
55
48
2
1
43
35
30
42
29
41
27
40
41
36
37
39

E

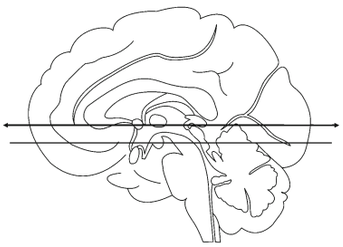

Fig. 11.24 (A–B). Axial (horizontal) section.
Mesencephalon
A. Inferior view after removal of the cerebral hemispheres and cerebellum. Bar: 10 mm.
B. Superior view.

See **Fig. 2.19** for more information about the structures demonstrated at this level.

1 Crus cerebri
2 Substantia nigra, pars reticulata
3 Substantia nigra, pars compacta
4 Interpeduncular (intercrural) fossa
5 Red nucleus
6 Superior cerebellar peduncle (brachium conjunctivum)
7 Medial lemniscus
8 Lateral lemniscus
9 Oculomotor nucleus (CN III)
10 Cerebral aqueduct (of Sylvius)
11 Periaqueductal gray matter
12 Intercollicular nucleus (at the junction between superior and inferior colliculi)
13 Superior colliculus
14 Pretectal area
15 Medial geniculate body
16 Lateral geniculate body
17 Optic tract (CN II)
18 Hypothalamus
19 Mammillary body
20 Third ventricle
21 Anterior perforated substance
22 Pulvinar
23 Pineal gland
24 Habenular trigone
25 Stria medullaris thalami
26 Third ventricle
27 Anterior columns of the fornix

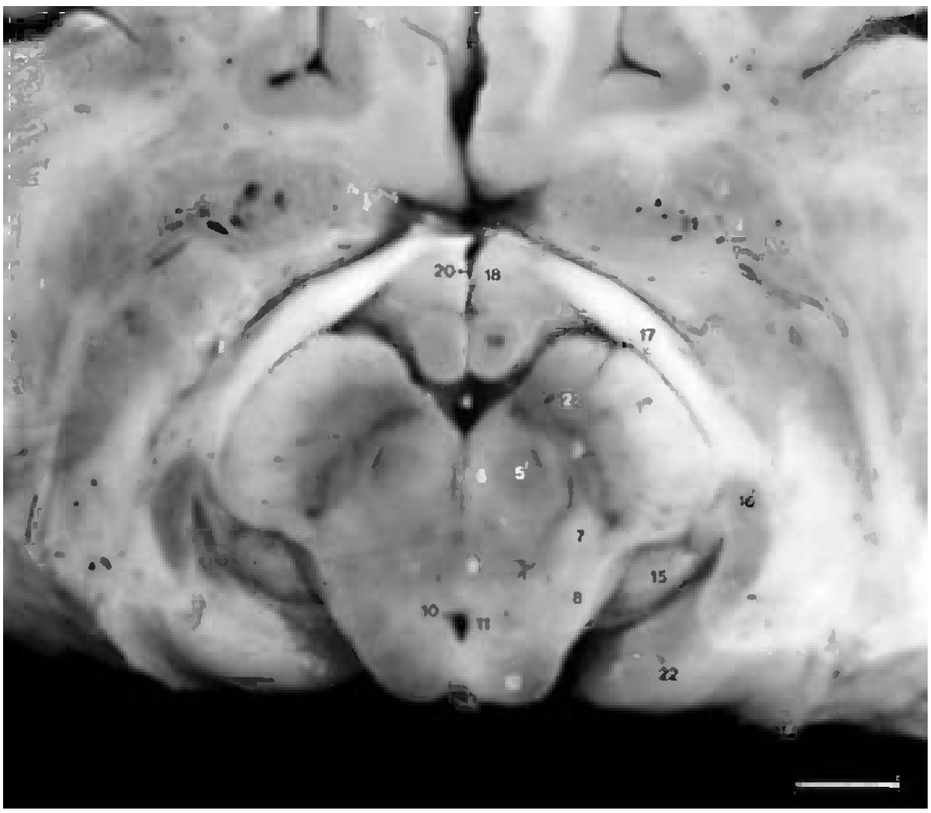

A

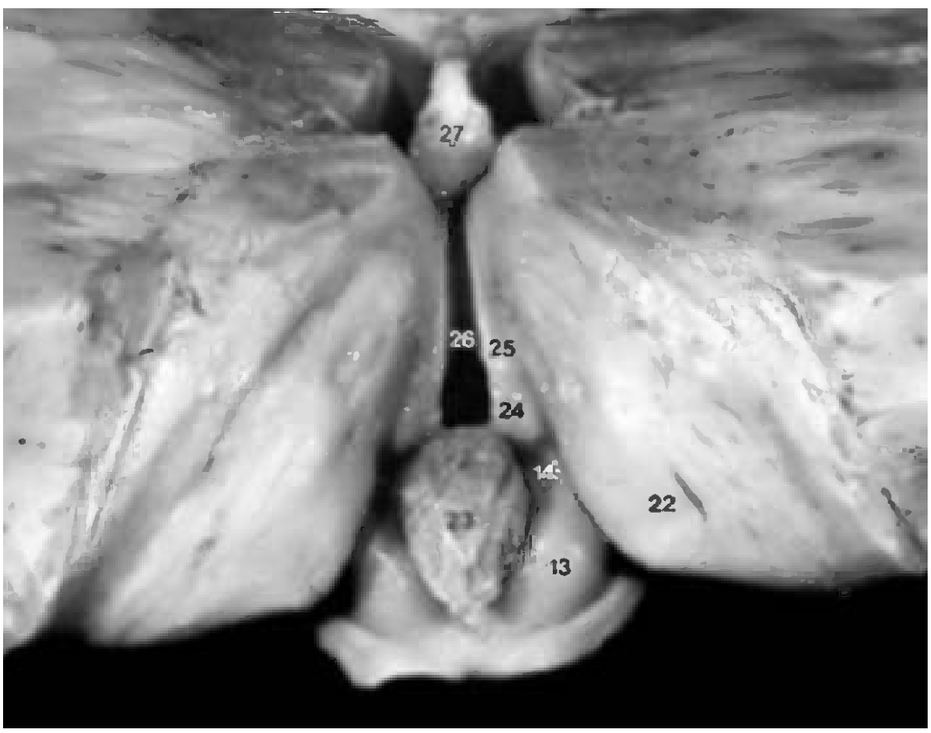

B

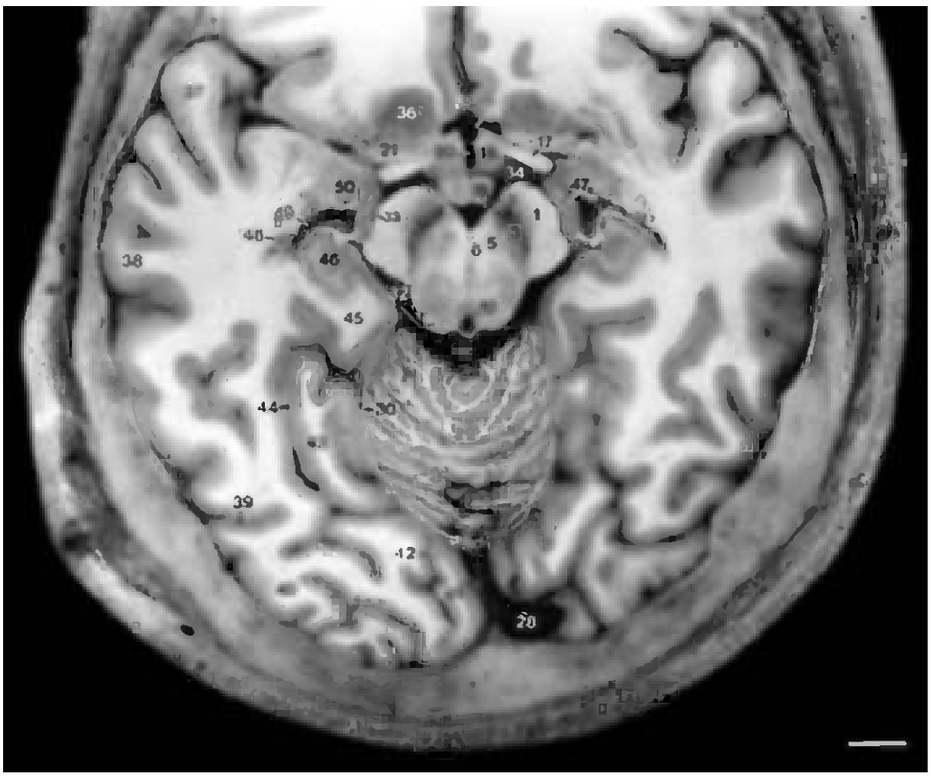

C

Fig. 11.24 (C–E).
C. Axial section of the head. Superior view. Bar: 10 mm.
D–E. 3 Tesla MRI. D. T1-weighted MRI. **E.** T2-weighted MRI.

1 Crus cerebri
2 Substantia nigra, pars reticulata
3 Substantia nigra, pars compacta
4 Interpeduncular (intercrural) fossa
5 Red nucleus
6 Superior cerebellar peduncle (brachium conjunctivum)
10 Cerebral aqueduct
17 Optic tract (CN II)
18 Hypothalamus
19 Mammillary body
21 Anterior perforated substance
28 Superior sagittal sinus
29 Culmen
30 Tentorium cerebelli
31 Quadrigeminal cistern
32 Ambient cistern (containing CN IV)
33 Crural cistern
34 Chiasmatic cistern
35 Cistern of the lamina terminalis
35′ Lamina terminalis
36 Nucleus accumbens septi
37 Superior temporal gyrus
38 Middle temporal gyrus
39 Anterior occipital sulcus
40 Middle occipital gyrus
41 Cuneus
42 Calcarine sulcus
43 Lingual gyrus
44 Collateral sulcus
45 Parahippocampal gyrus
46 Hippocampus, body
47 Hippocampus, head, uncal portion
48 Caudate nucleus (tail)
49 Temporal horn of the lateral ventricle
50 Amygdala
51 Gyrus rectus
52 Medial orbital gyrus
53 Posterior orbital gyrus
54 Lateral orbital gyrus


54
52
53
51
37
18
17
33
4
1
3
5
46
10
49
45
12
32
38
31
29
44
43
39
40
41
39
37
28

D

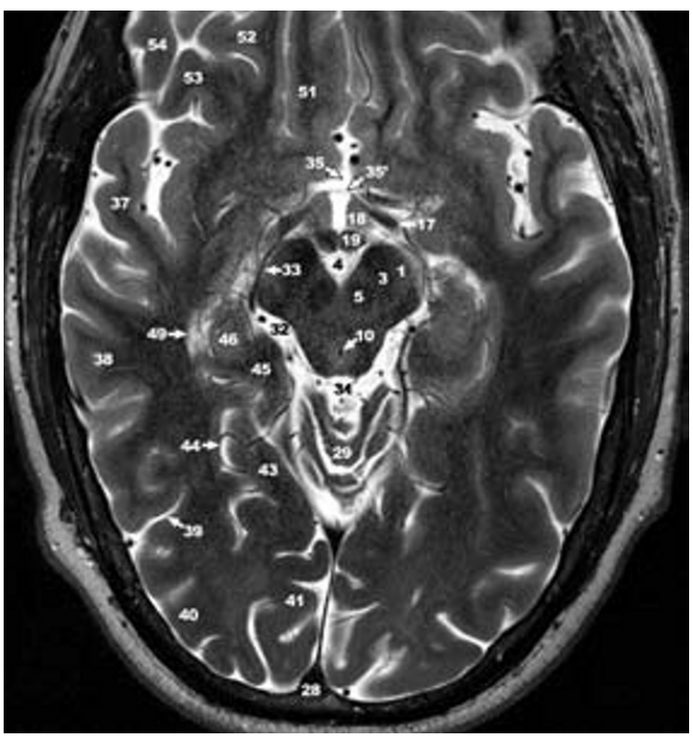
54
52
53
51
35
35'
37
18
17
19
33
4
3
1
5
49
46
32
10
38
45
34
44
29
43
39
41
40
28

E

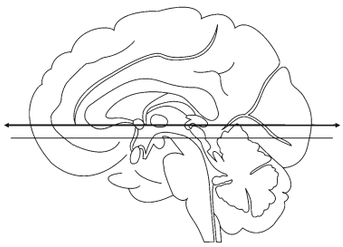

Fig. 11.25 (A–B). Axial (horizontal) section.
Mesencephalon
A. Inferior view after removal of the cerebral hemispheres and cerebellum. Bar: 10 mm.
B. Superior view.

See Fig. 2.20 for more information about the structures demonstrated at this level and Fig. 7.23 for the vascular territories.

1 Crus cerebri
2 Substantia nigra, pars reticulata
2′ Pars reticulata, extension into the ventral portion of the crus cerebri
3 Substantia nigra, pars compacta
4 Interpeduncular (intercrural) fossa
5 Red nucleus
6 Medial lemniscus
7 Lateral lemniscus
8 Oculomotor nucleus (CN III)
9 Cerebral aqueduct (of Sylvius)
10 Periaqueductal gray matter
11 Superior colliculus
12 Pretectal area
13 Medial geniculate body
14 Lateral geniculate body
15 Optic tract (CN II)
16 Hypothalamus
17 Mammillary body
18 Third ventricle
19 Lamina terminalis
20 Anterior perforated substance and striate vessels
21 Anterior commissure
22 Pulvinar
23 Pineal gland
24 Habenular trigone
25 Stria medullaris thalami
26 Third ventricle
27 Anterior thalamic nucleus
28 Anterior columns of the fornix
29 Caudate nucleus

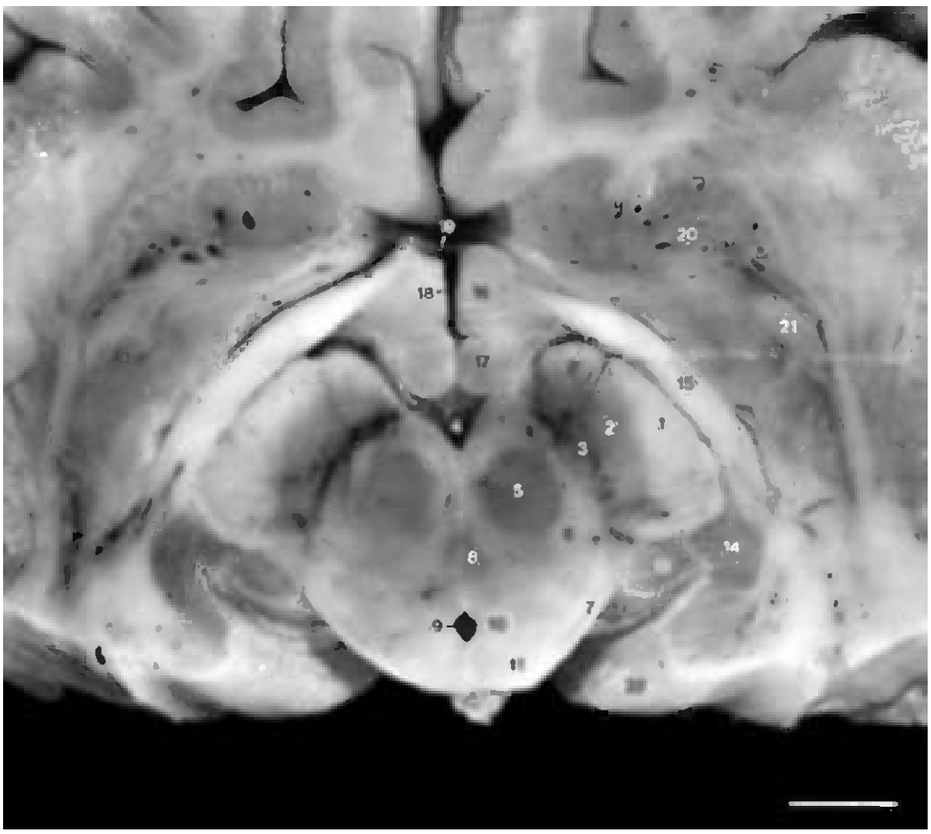

A

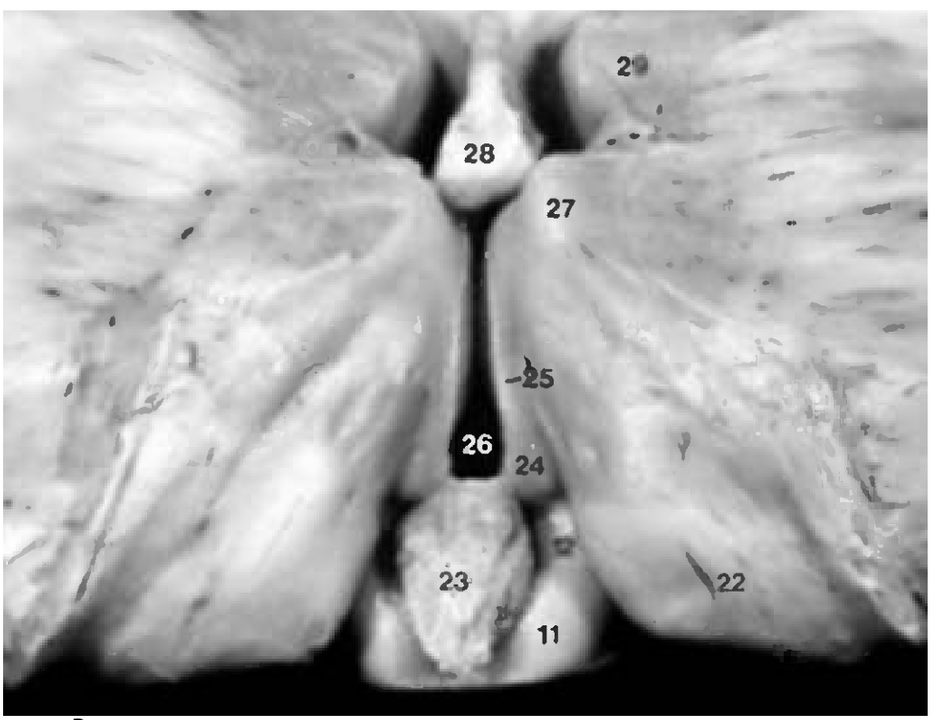

B

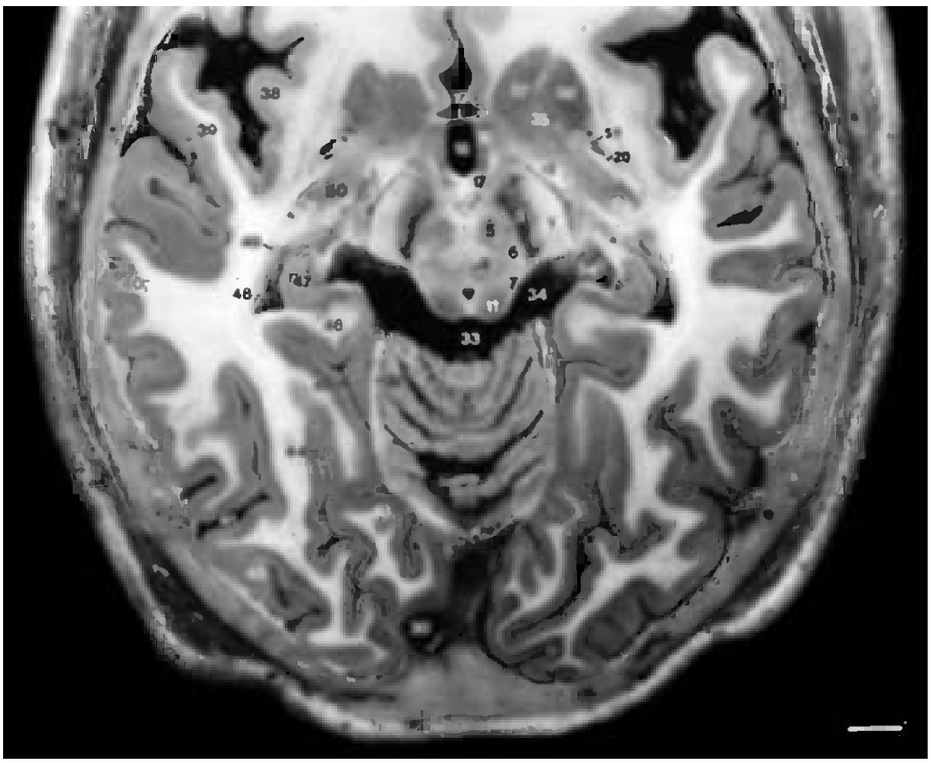

C

Fig. 11.25 (C–E).
C. Axial section of the head. Inferior view. Bar: 10 mm.
D–E. 3 Tesla MRI. **D.** T1-weighted MRI. **E.** T2-weighted MRI.

1 Crus cerebri
2′ Pars reticulata, extension into the ventral portion of the crus cerebri
3 Substantia nigra, pars compacta
5 Red nucleus
6 Medial lemniscus
7 Lateral lemniscus
8 Oculomotor nucleus (CN III)
11 Superior colliculus
15 Optic tract (CN II)
16 Hypothalamus
17 Mammillary body
18 Third ventricle
19 Lamina terminalis
19′ Anterior cerebral artery
20 Anterior commissure
30 Superior sagittal sinus
31 Culmen
32 Tentorium cerebelli
33 Quadrigeminal cistern
34 Ambient cistern
34′ Wing of the ambient cistern
35 Nucleus accumbens septi
36 Putamen
37 Caudate nucleus (head)
38 Insula
39 Superior temporal gyrus
40 Middle temporal gyrus
41 Anterior occipital sulcus
42 Middle occipital gyrus
43 Lingual gyrus
44 Collateral sulcus
45 Lingual sulcus (anterior calcarine sulcus)
46 Parahippocampal gyrus
47 Hippocampus, body
48 Temporal horn of the lateral ventricle
49 Caudate nucleus, tail
50 Amygdala
51 Perivascular (Virchow-Robin) spaces surrounding the penetrating vessels anterior and posterior to the anterior commissure (20)

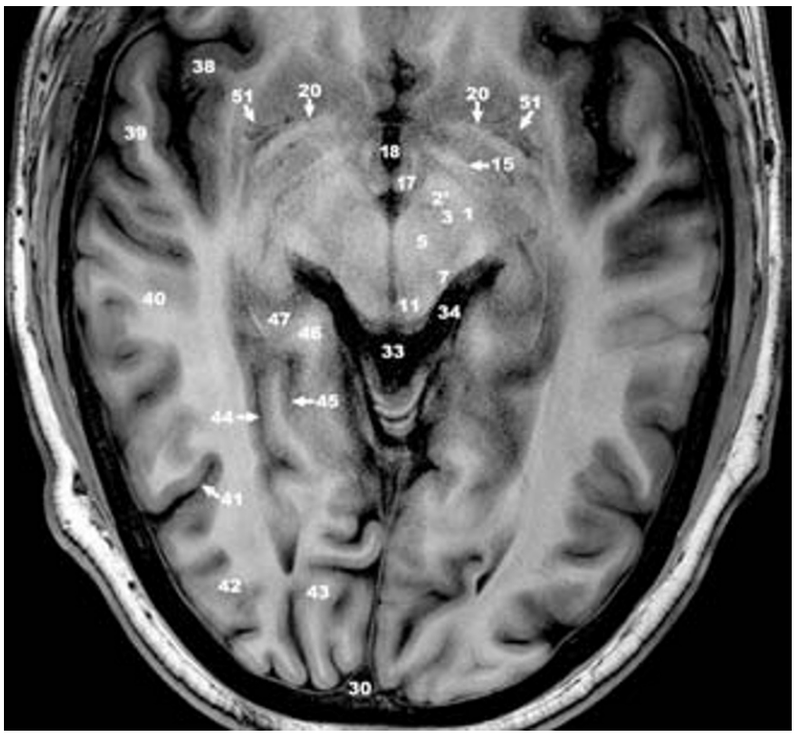
38
51
20
20
51
39
18
15
17
2'
3
1
5
7
40
11
34
47
46
33
45
44
41
42
43
30

D

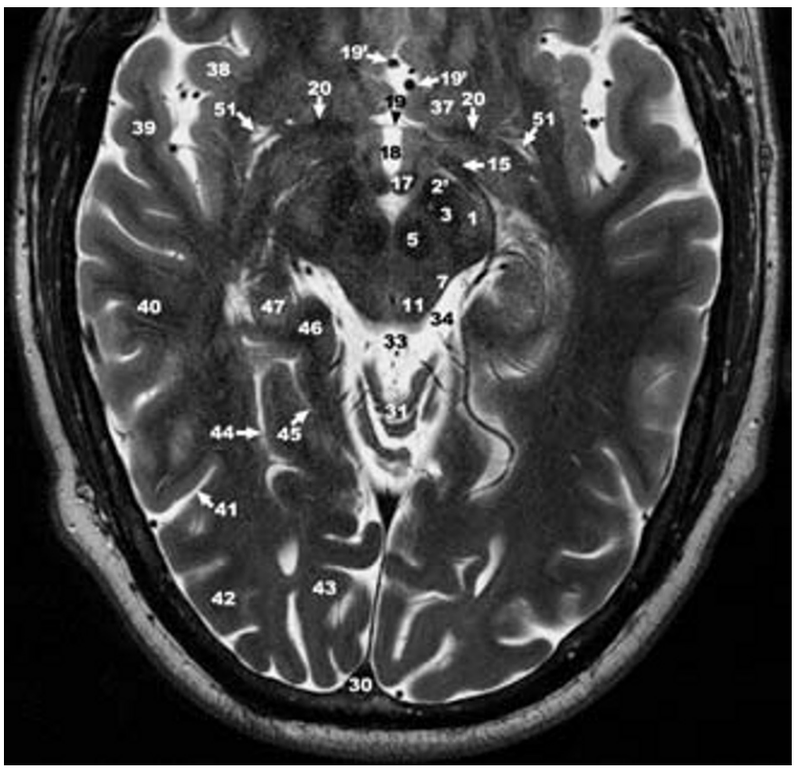
19'
19'
38
20
19
37
20
51
51
39
18
15
17
2'
3
1
5
7
40
47
11
34
46
33
31
44
45
41
42
43
30

E

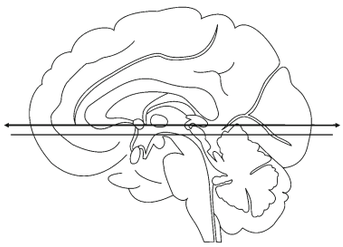

Fig. 11.26 (A–B). Axial (horizontal) section. Mesencephalon

A. Inferior view after removal of the cerebral hemispheres and cerebellum. Bar: 10 mm.

B. Superior view.

1 Crus cerebri
2 Substantia nigra, pars reticulata
2′ Pars reticulata, extension into the ventral portion of the crus cerebri
3 Thalamoperforating blood vessels
4 Habenulo-interpeduncular tract
5 Red nucleus
6 Medial lemniscus
7 Nigrostriate fibers
8 Brachium of the superior colliculus
9 Pretectal area
10 Oculomotor nucleus (CN III)
11 Cerebral aqueduct (of Sylvius)
12 Periaqueductal gray matter
13 Superior colliculus
14 Medial geniculate body
15 Lateral geniculate body
16 Pulvinar
17 Putamen
18 Lateral (external) pallidum
19 Striate blood vessels
20 Anterior commissure
21 Caudate nucleus (head)
22 Lamina terminalis
23 Third ventricle
24 Anterior column of fornix
25 Mammillothalamic tract
26 Pineal gland
27 Habenular trigone
28 Stria medullaris thalami
29 Anterior thalamic nucleus
30 Anterior columns of fornix

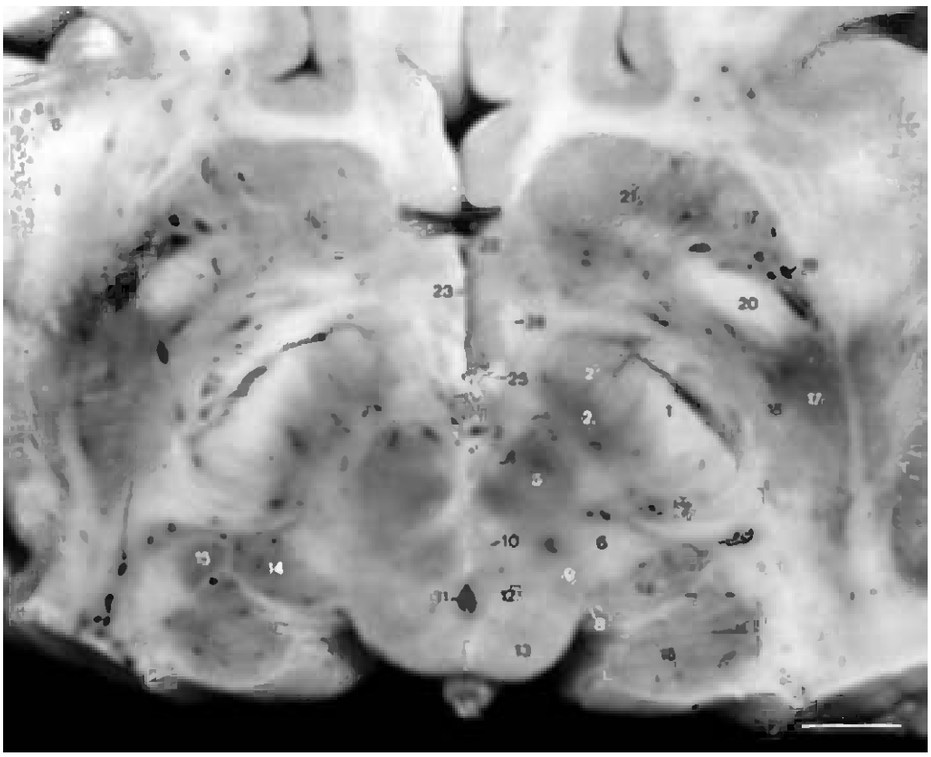

A

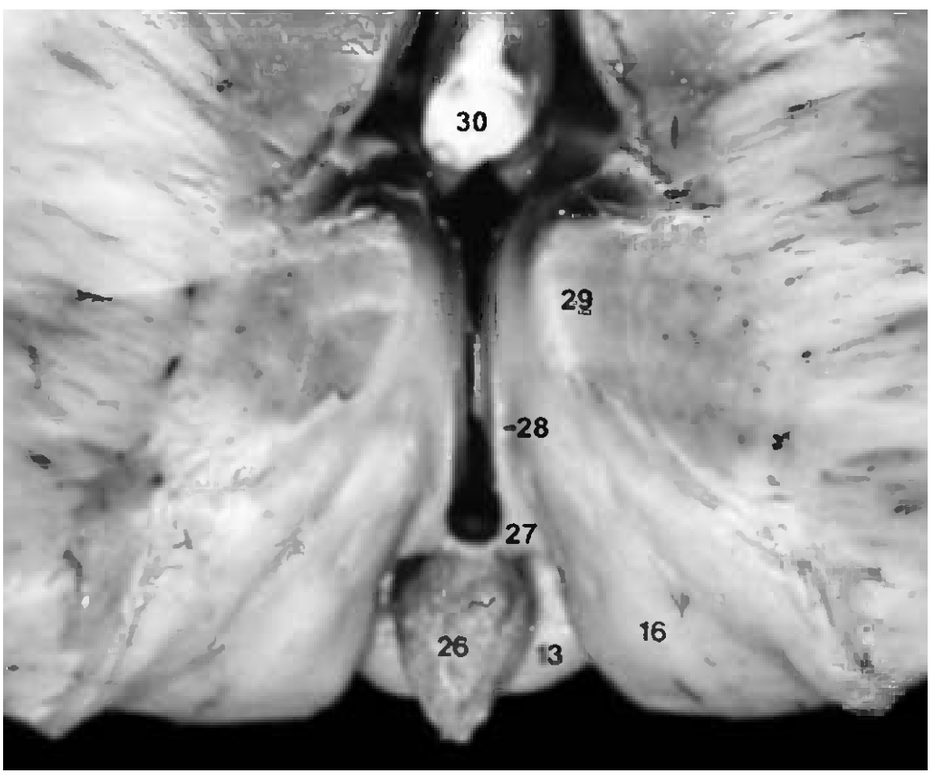

B

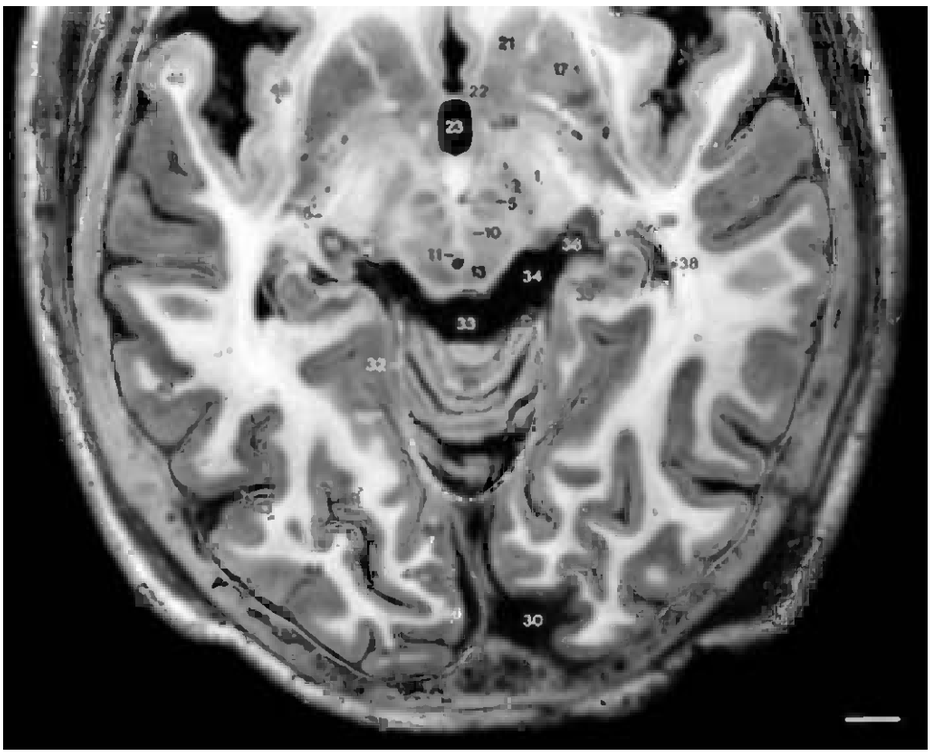

C

Fig. 11.26 (C–E).
C. Axial section of the head. Superior view. Bar: 10 mm.
D–E. 3 Tesla MRI. D. T1-weighted MRI. **E.** T2-weighted MRI.

1 Crus cerebri
2 Substantia nigra, pars reticulata
4 Habenulo-interpeduncular tract
5 Red nucleus
10 Oculomotor nucleus
11 Cerebral aqueduct (of Sylvius)
13 Superior colliculus
14 Medial geniculate body
15 Lateral geniculate body
15′ Optic tract (CN II)
17 Putamen
20 Anterior commissure, lateral portion
21 Caudate nucleus (head)
22 Lamina terminalis
23 Third ventricle
24 Anterior columns of the fornices (arrows)
30 Superior sagittal sinus
31 Culmen
32 Tentorium cerebelli
33 Quadrigeminal cistern
34 Ambient cistern
35 Parahippocampal gyrus and subiculum
36 Wing of the ambient cistern (transverse fissure lateral portion)
37 Hippocampus, body
38 Temporal horn of the lateral ventricle
39 Caudate nucleus, tail
40 Insula
41 Superior temporal gyrus
42 Middle temporal gyrus
43 Anterior occipital sulcus
44 Middle occipital gyrus
45 Gyrus descendens
46 Cuneus
47 Calcarine sulcus
48 Lingual gyrus
49 Collateral sulcus
50 Lingual (anterior calcarine) sulcus
52 Anterior cerebral artery
53 Perivascular (Virchow-Robin) spaces

Arrows: Anterior columns of the fornices

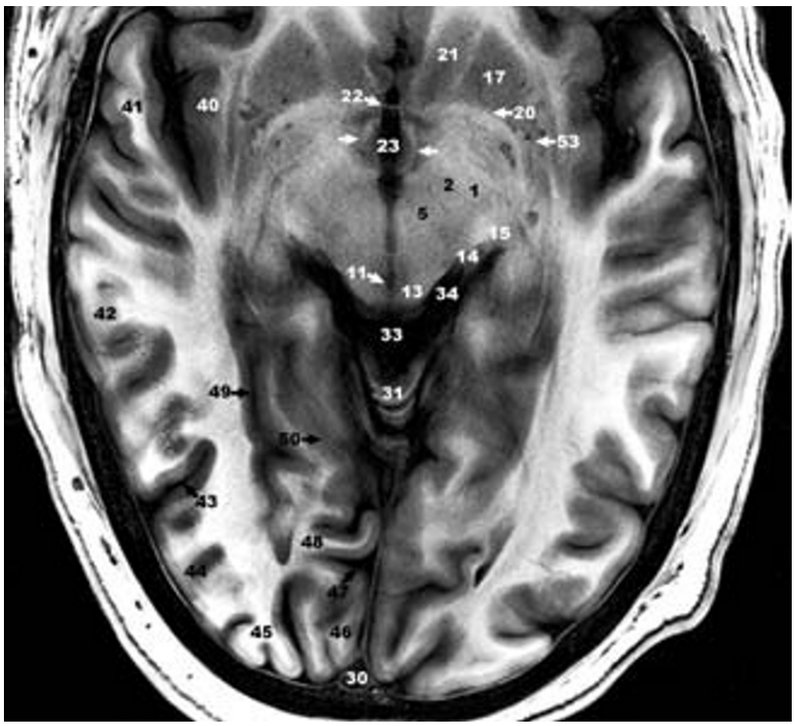
21
17
41
40
22
20
23
53
2
1
5
15
14
11
13
34
42
33
49
31
50
43
48
44
47
45
46
30

D

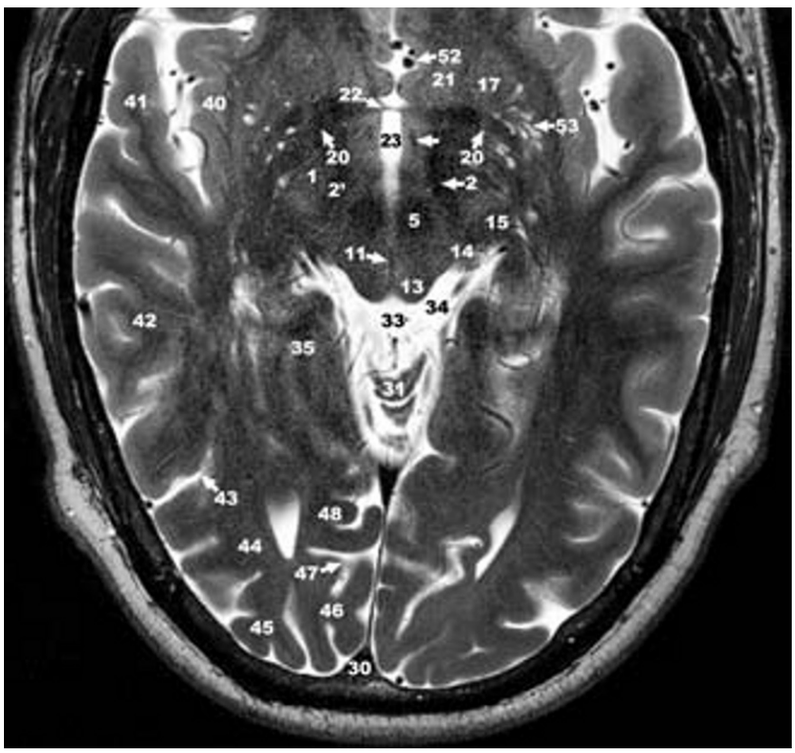
52
21
17
41
40
22
53
23
20
20
1
2'
2
5
15
11
14
13
34
42
33
35
31
43
48
44
47
46
45
30

E

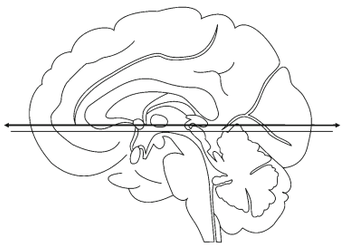

Fig. 11.27 (A). Axial (horizontal) section. Diencephalo-mesencephalic junction

A. Inferior view after removal of the cerebral hemispheres and cerebellum. Bar: 10 mm.

See **Fig. 2.21** for more information about the structures demonstrated at this level.

1 Crus cerebri (cerebral peduncle)
2 Subthalamic nucleus
3 Medial lemniscus
4 Red nucleus
5 Habenulo-interpeduncular tract
6 Cerebral aqueduct (of Sylvius)
7 Superior colliculus
8 Pineal gland
9 Brachium of the superior colliculus
10 Pretectal area
11 Pulvinar
12 Medial geniculate body
13 Nigrostriate fibers
14 Putamen
15 Lateral (external) pallidum
16 Medial (internal) pallidum
17 Striate blood vessels
18 Anterior commissure
19 Caudate nucleus, head
20 Anterior column of the fornix
21 Hypothalamus
22 Third ventricle
23 Mammillothalamic tract
24 Thalamoperforating blood vessels

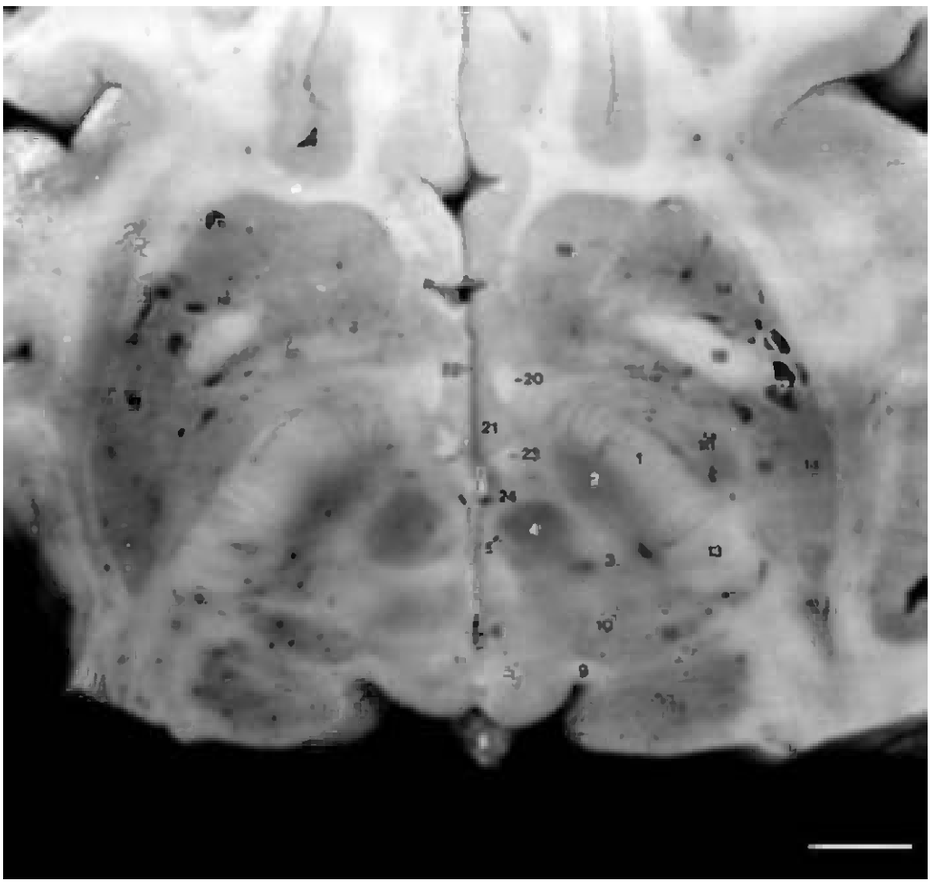

A

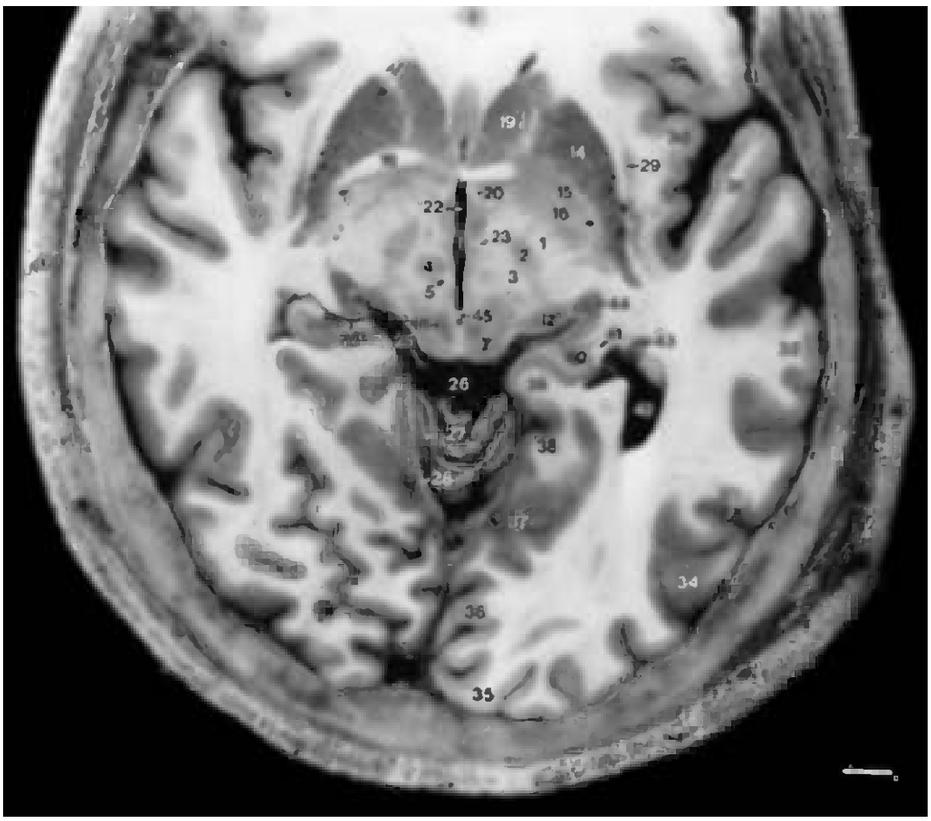

B

Fig. 11.27 (B–D).
B. Axial section of the head. Superior view. Bar: 10 mm.
C–D. 3 Tesla MRI. C. T1-weighted MRI. **D.** T2-weighted MRI.

1 Crus cerebri
2 Subthalamic nucleus
3 Medial lemniscus
4 Red nucleus
5 Habenulo-interpeduncular tract
7 Superior colliculus
12 Medial geniculate body
14 Putamen
15 Lateral (external) pallidum
16 Medial (internal) pallidum
18 Anterior commissure
19 Caudate nucleus, head
20 Anterior column of fornix
21 Lamina terminalis
22 Third ventricle
23 Mammillothalamic tract
25 Ambient cistern
25′ Wing of ambient cistern
26 Quadrigeminal cistern
27 Culmen
28 Tentorium cerebelli
29 Claustrum
30 Insula
31 Superior temporal gyrus
31′ Transverse temporal gyrus (of Heschl)
32 Middle temporal gyrus
33 Anterior occipital sulcus
34 Middle occipital gyrus
35 Gyrus descendens
36 Cuneus
37 Calcarine sulcus
38 Anterior calcarine sulcus
39 Isthmus of the cingulate gyrus
40 Hippocampus (tail)
41 Crus fornicis
42 Atrium of the lateral ventricle
43 Caudate nucleus (tail)
44 Lateral geniculate body
45 Posterior commissure
46 Periaqueductal gray matter

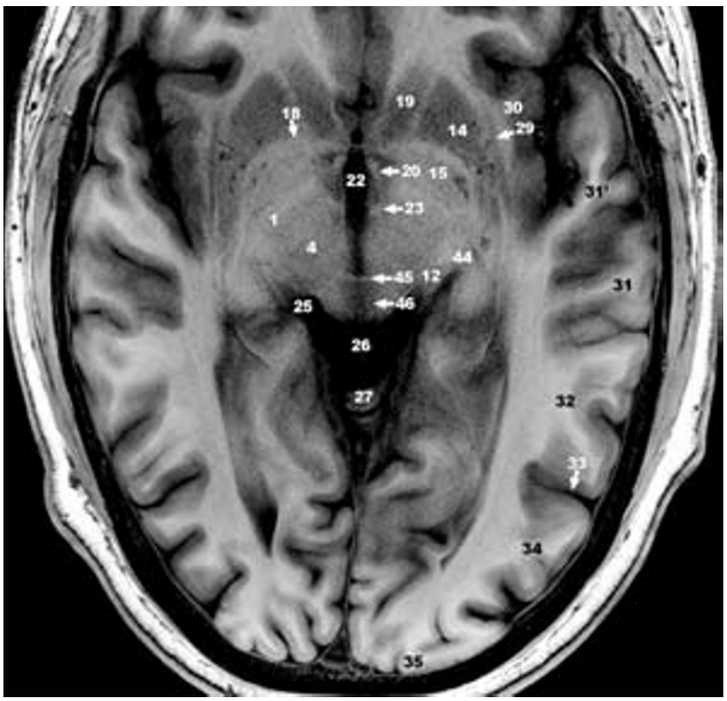
18
19
30
14
29
22
20
15
31'
23
1
4
44
45
12
31
25
46
26
27
32
33
34
35

C

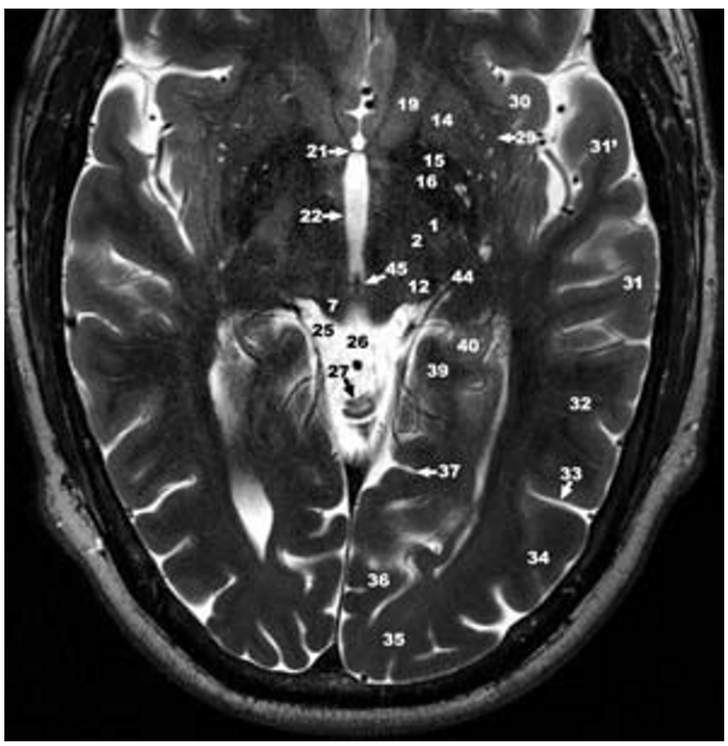
19
30
14
29
21
15
31'
16
22
1
2
45
12
44
31
7
25
26
40
27
39
32
37
33
34
36
35

D

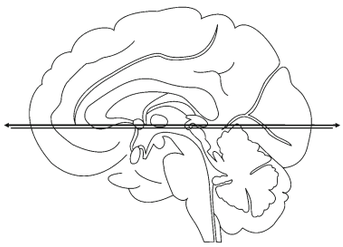

Fig. 11.28 (A–B). Axial (horizontal) section. Diencephalo-mesencephalic junction

A. Inferior view after removal of the cerebral hemispheres. Bar: 10 mm.

B. Superior view

1 Anterior commissure, lateral portions
2 Anterior columns of the fornix
3 Hypothalamus
4 Third ventricle
5 Mammillothalamic tract
6 Red nucleus, superior pole
7 Habenulo-intepeduncular tract
8 Posterior commissure, midline portion
9 Superior colliculus
10 Pineal gland
11 Brachium of the superior colliculus
12 Pulvinar
13 Petectal area
14 Medial geniculate body
15 Medial lemniscus
16 Subthalamic nucleus
17 Internal capsule, posterior limb
17′ Intenal capsule, genu
17″ Internal capsule, anterior limb
18 Medial (internal) pallidum
19 Lateral (external) pallidum
20 Putamen
21 Claustrum
22 Caudate nucleus (head)
23 Stria medullaris thalami
24 Anterior thalamic nucleus

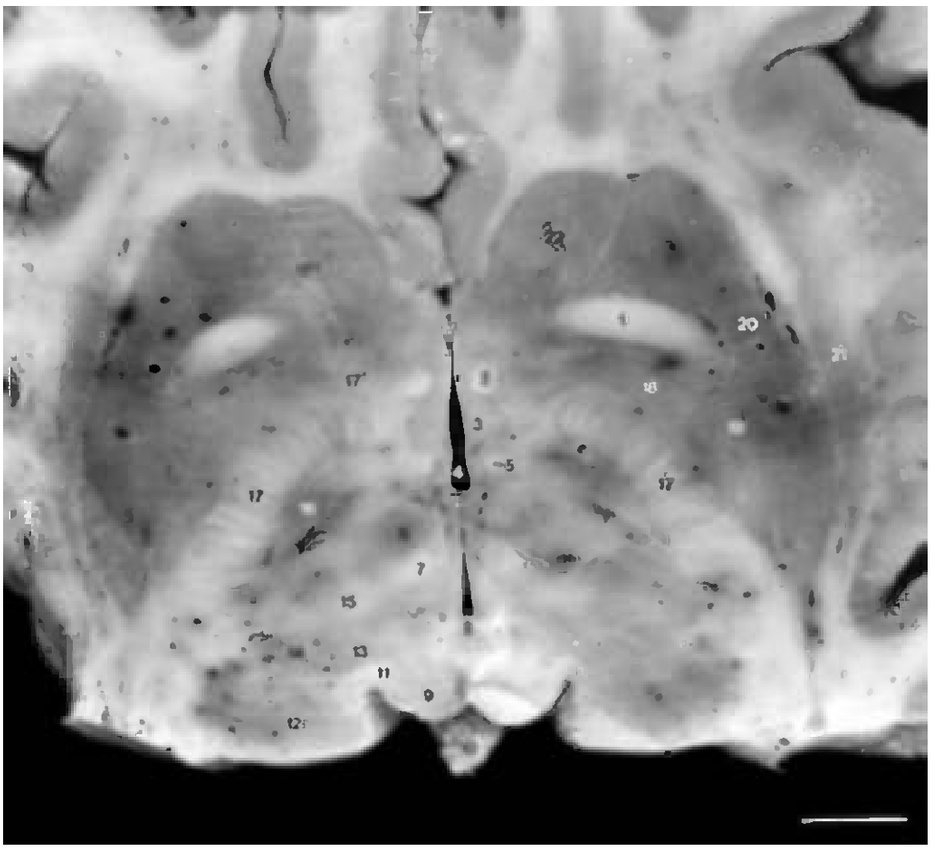

A

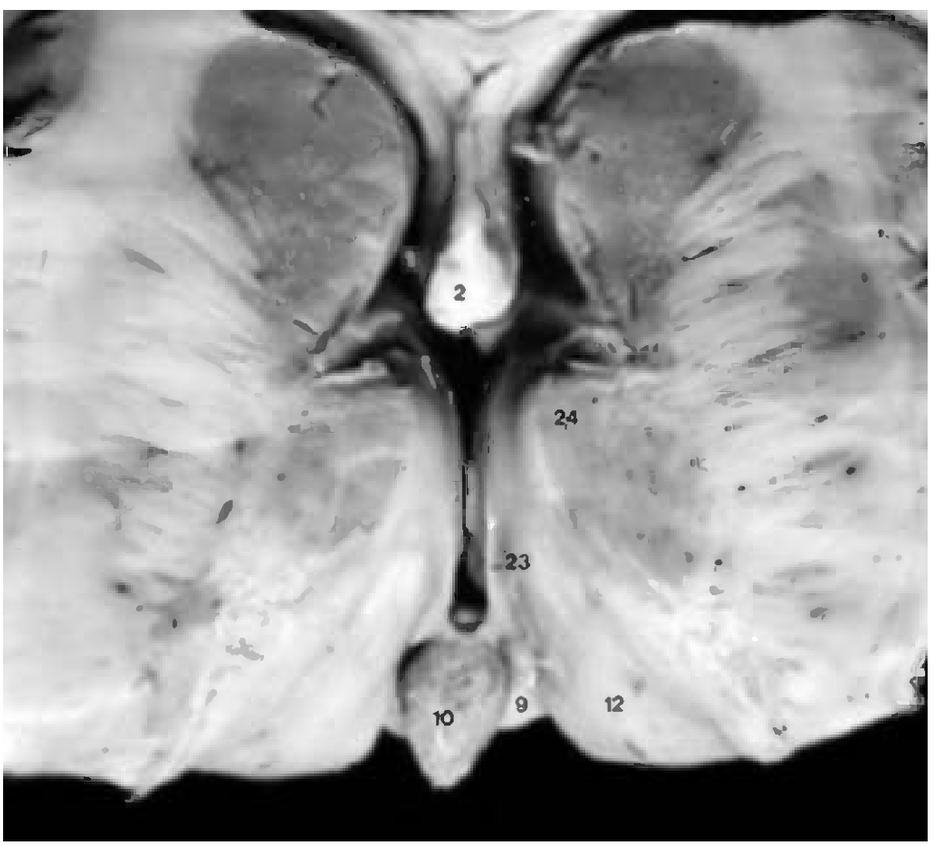

B

C

Fig. 11.28 (C–E).
Axial (horizontal) section.
C. Axial section of the head. Superior view.
D–E. 3 Tesla MRI. D. T1-weighted MRI. **E.** T2-weighted MRI.

1 Anterior commissure, midline portion (vertical arrow)
3 Hypothalamus
4 Third ventricle
5 Mammillothalamic tract
8 Posterior commissure (midline portion)
8′ Posterior commissure (lateral portion)
10 Pineal gland
12 Pulvinar
13 Petectal area
17 Internal capsule, posterior limb
17′ Intemal capsule, genu
17″ Internal capsule, anterior limb
18 Medial (internal) pallidum
19 Lateral (external) pallidum
20 Putamen
21 Claustrum
22 Caudate nucleus (head)
25 Insula
26 Lateral (Sylvian) fissure
27 Superior temporal gyrus
28 Middle temporal gyrus
29 Middle occipital gyrus
30 Superior occipital gyrus
31 Calcarine sulcus
32 Isthmus of the cingulate gyrus
33 Hippocampus, tail
34 Occipital horn of the lateral ventricle
35 Quadrigeminal cistern

Single vertical arrow: Anterior commissure, midline portion
Paired arrows: Anterior columns of the fornices

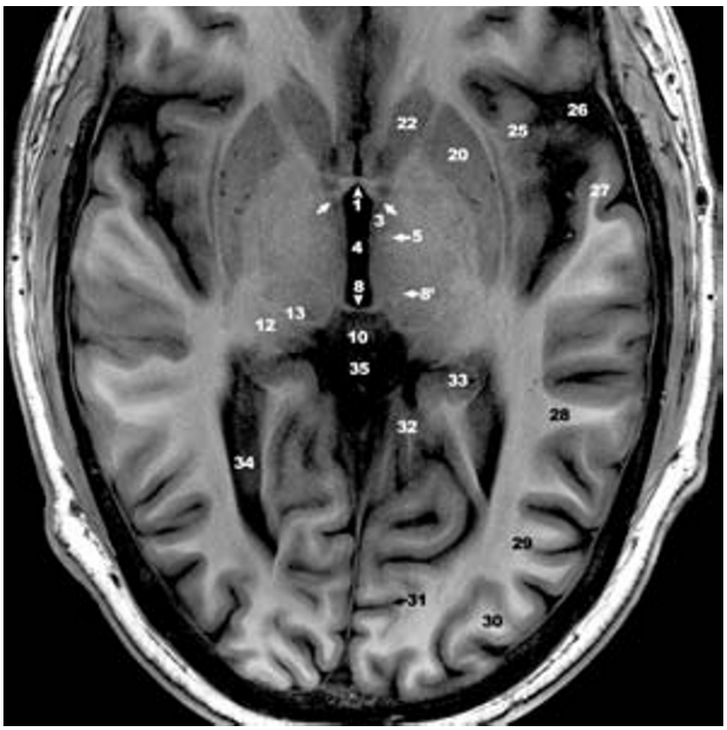
22
26
25
20
27
1
3
5
4
8
8'
12
13
10
35
33
28
32'
34
29
31
30

D

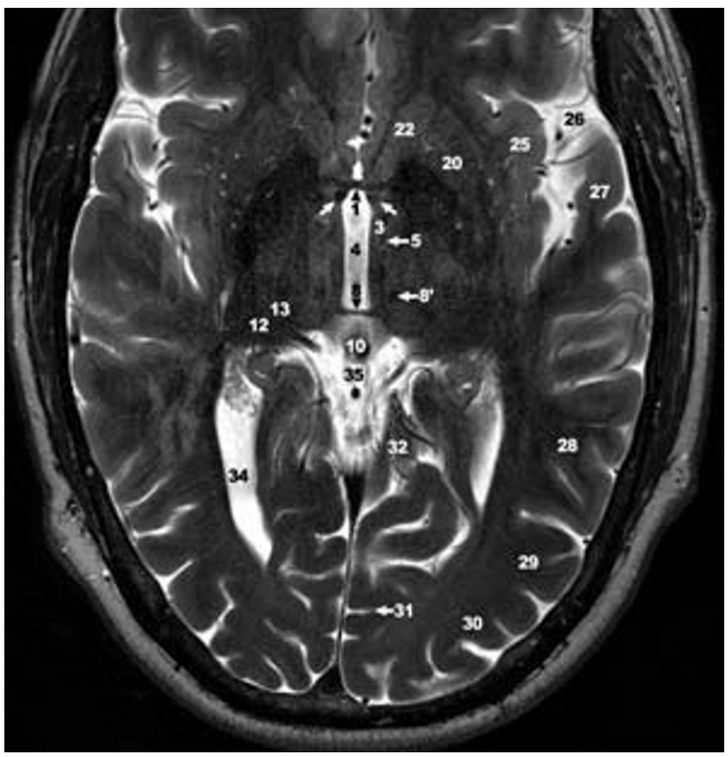
22
26
25
20
27
1
3
5
4
8'
13
12
10
35
32
28
34
29
31
30

E

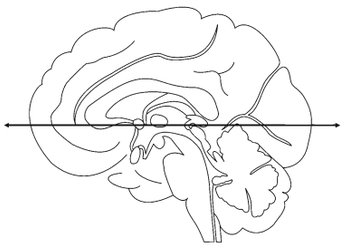

Fig. 11.29 (A–B). Axial (horizontal) section. Intercommissural plane

A. Inferior view after removal of the cerebral hemispheres and cerebellum. Bar: 10 mm.

B. Superior view.

See **Fig. 2.22** for more information about the structures concerned with this section level.

1 Anterior commissure
2 Anterior column of fornix
3 Hypothalamus
4 Mammillothalamic tract
5 Third ventricle
6 Posterior commissure
7 Pineal gland
8 Superior colliculus
9 Pretectal area
10 Pulvinar
11 Habenulo-interpeduncular tract
12 Centromedian thalamic nucleus
13 Ventral posteromedial thalamic nucleus
14 Ventral posterolateral thalamic nucleus
15 Internal capsule, posterior limb
15′ Internal capsule, genu
15″ Internal capsule, anterior limb
16 Subthalamic nucleus
17 Medial (internal) pallidum
18 Lateral (external) pallidum
19 Putamen
20 Claustrum
21 Caudate nucleus (head)
22 Anterior thalamic nucleus
23 Stria medullaris thalami
24 Anterior columns of the fornices
25 Third ventricle

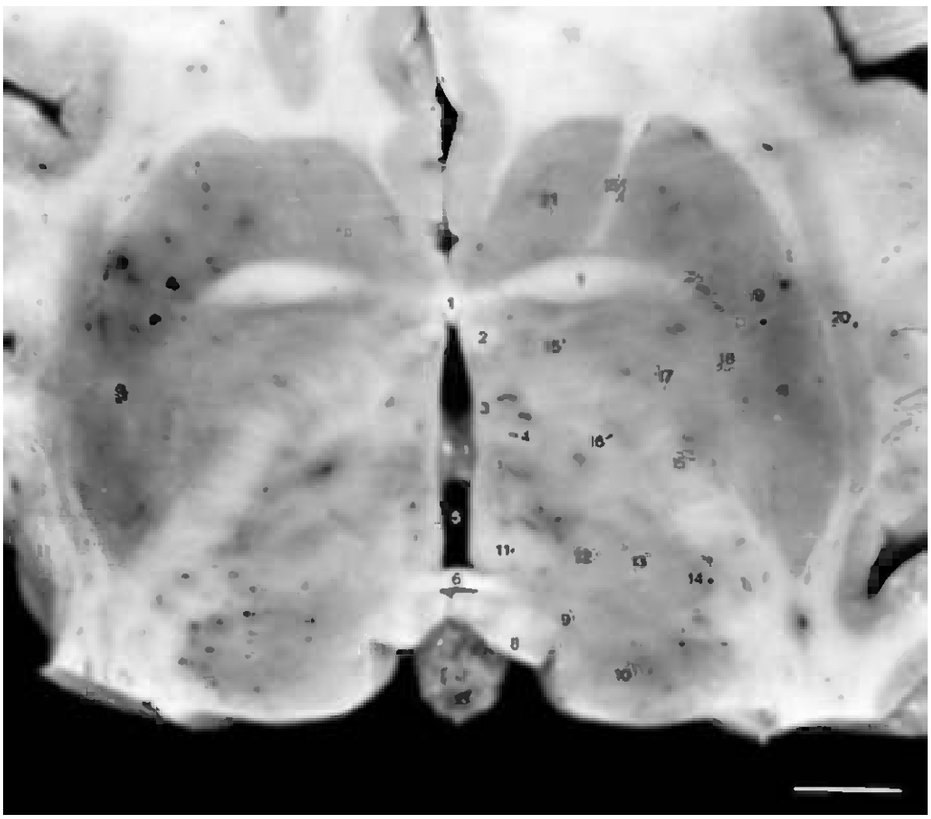

A

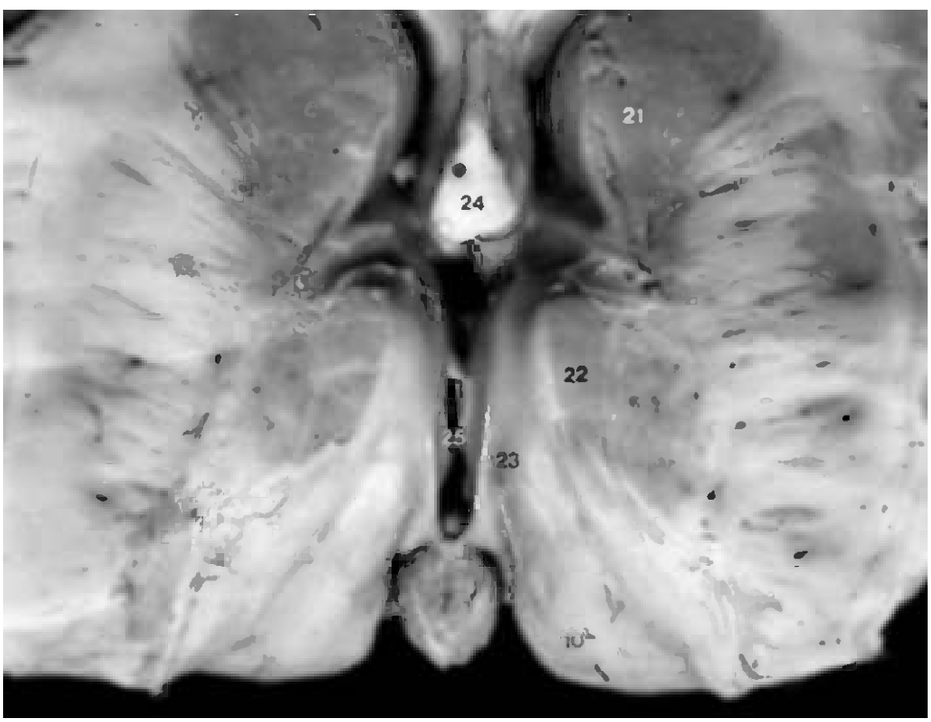

B

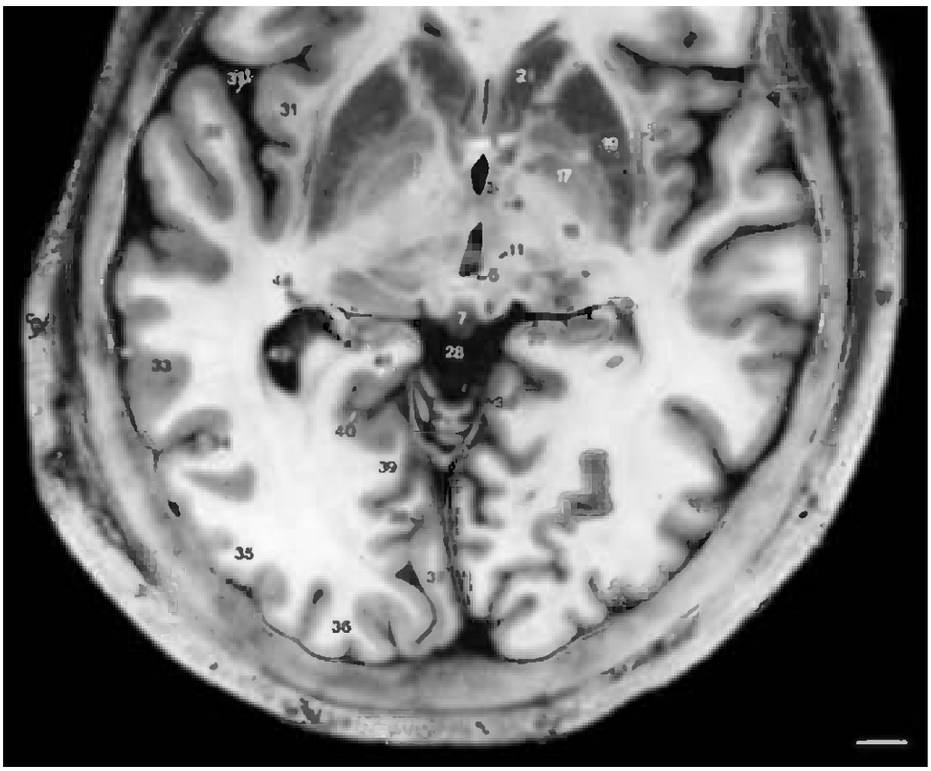

C

Fig. 11.29 (C–E).
C. Axial section of the head. Superior view. Bar: 10 mm.
D–E. 3 Tesla MRI D. T1-weighted MRI. **E.** T2-weighted MRI.

2 Anterior columns of the fornices
3 Hypothalamus
4 Mammillothalamic tract
5 Third ventricle
6 Posterior commissure
7 Pineal gland
8 Superior colliculus
10 Pulvinar
11 Habenulo-interpeduncular tract
15 Internal capsule, posterior limb
15′ Internal capsule, genu
15″ Internal capsule, anterior limb
17 Medial (internal) pallidum
18 Lateral (external) pallidum
19 Putamen
20 Claustrum
21 Caudate nucleus (head)
26 Medial geniculate body
27 Wing of the ambient cistern
28 Quadrigeminal cistern
29 Culmen
30 Tentorium cerebelli
31 Insula
31′ Lateral (Sylvian) fissure
32 Superior temporal gyrus
33 Middle temporal gyrus
34 Anterior occipital sulcus
35 Middle occipital gyrus
36 Gyrus descendens
37 Cuneus
38 Calcarine sulcus
39 Lingual gyrus
40 Lingual (anterior calcarine) sulcus
41 Isthmus of the cingulate gyrus
42 Hippocampus, tail
43 Atrium of the lateral ventricle
44 Caudate nucleus, tail

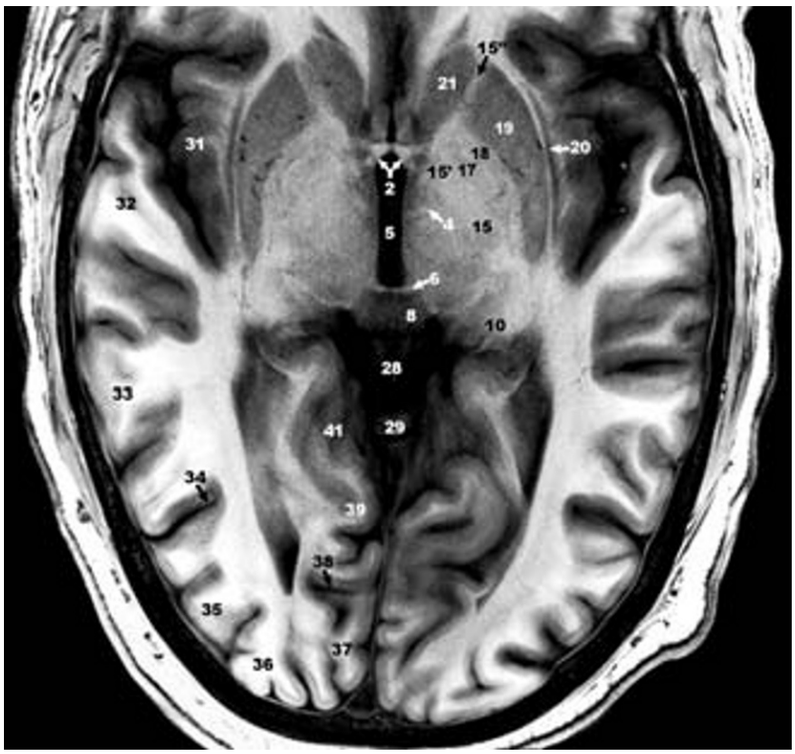
15"
21
19
31
20
18
2
15' 17
32
4
15
5
6
8
10
28
33
41
29
34
39
38
35
37
36

D

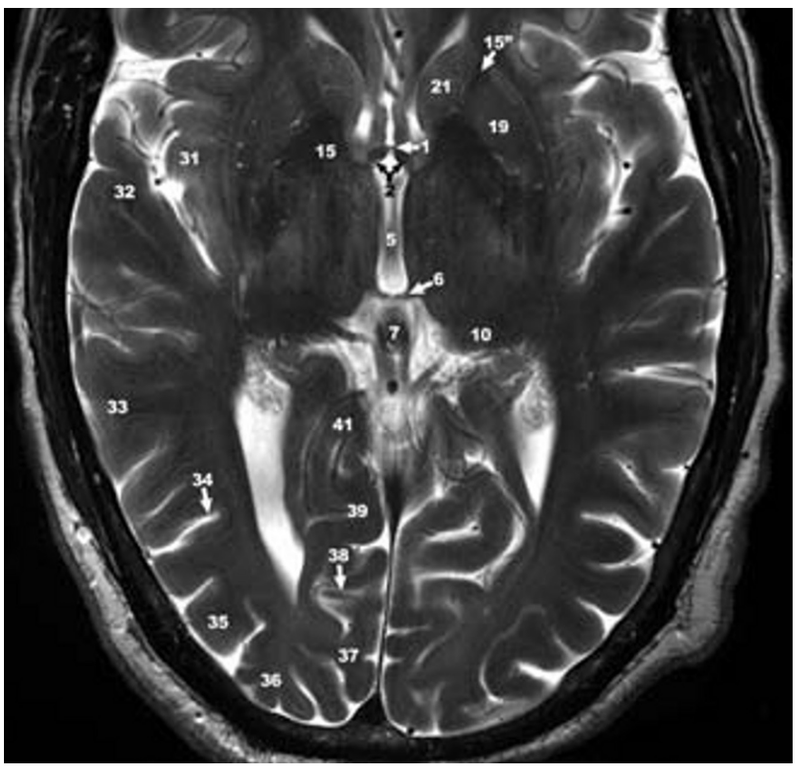
15"
21
19
31
15
1
32
2
5
6
7
10
33
41
34
39
38
35
37
36

E

Coronal (frontal) sections perpendicular to the intercommissural plane extending from the mid anterior commissure to the mid posterior commissure (Figs. 11.30–11.55)

In the following figures, the anatomic specimen of the brain stem, cerebellum, and diencephalon is progressively reduced by 2 mm thick sections for **Figs. 11.30–11.48**, then by 4 mm thick sections for **Figs. 11.49–11.55** to show each new level in relation to the remaining portion of the specimen. The coronal sections are particularly useful for the study of diencephalic structures and the diencephalomesencephalic junction. They also provide precise images of the cerebellar cortical anatomy.

Each figure consists of the posterior view of the remaining coronal surface, with oblique views demonstrating the level of the section. Corresponding sections of the head are provided for most levels to demonstrate the relationship of the brain to the skull and adjoining structures. At each level, both T1- and T2-weighted 3 Tesla MR images are provided for comparison. On each pair of facing pages all of the structures are labelled coherently, using the single key provided. However, the specific key changes from page to page.

For each section the cartoon indicates the section level (light vertical line) perpendicular to the intercommissural plane of Schaltenbrand (bold horizontal line).

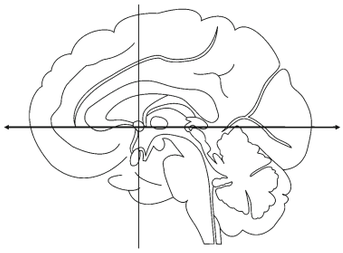

Fig. 11.30 (A–B). Coronal (frontal) section.
A. Frontal view after removal of the cerebral hemispheres. Bar: 10 mm.
B. Inferior oblique view.

1 Caudate nucleus
2 Internal capsule, anterior limb
3 Putamen
3′ Claustrum
4 Lateral pallidum
5 Anterior commissure
6 Anterior perforated substance
7 Septal nuclei
8 Anterior column of fornix
9 Pre-optic area
10 Supra-optic nucleus
11 Third ventricle
12 Optic chiasm (CN II)
13 Optic tract (CN II)
14 Lateral geniculate body
15 Hypophyseal stalk
16 Mammillary body
17 Crus cerebri
18 Oculomotor nerve (CN III)
19 Pons, basilar portion
20 Medulla, pyramid

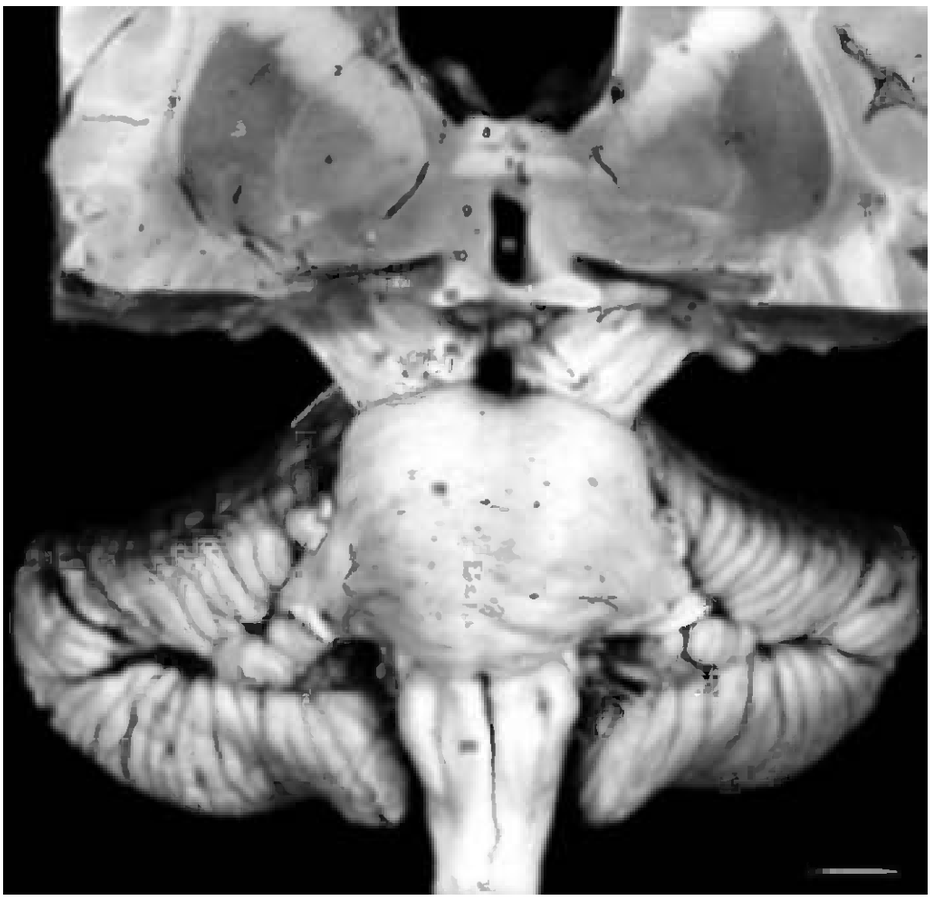

A

B

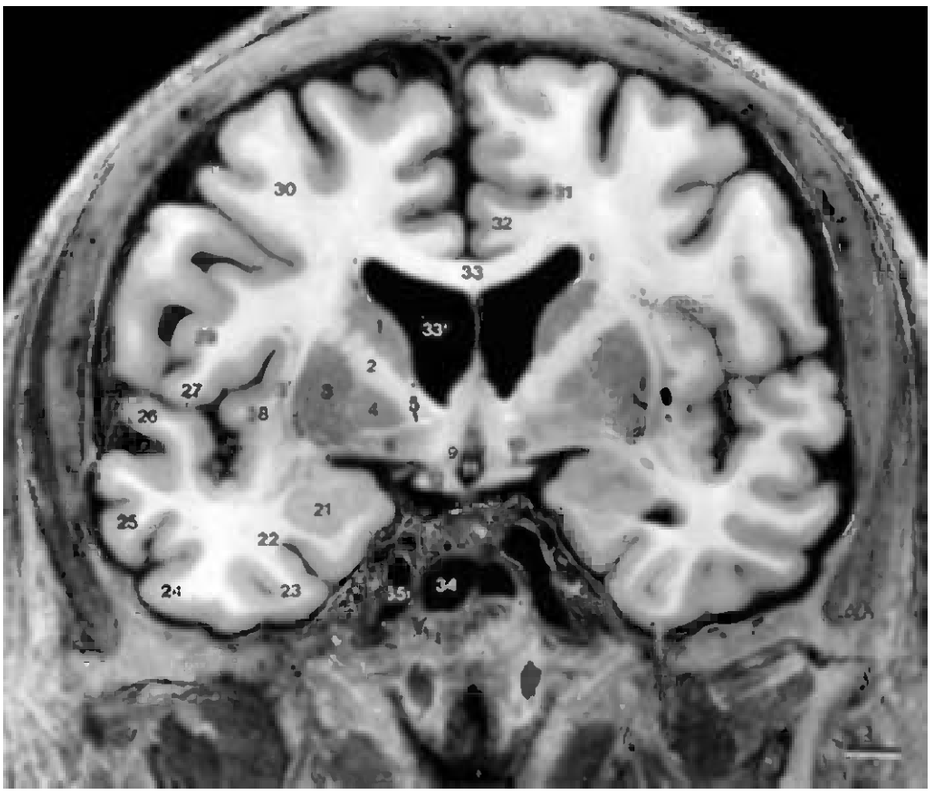

C

Fig. 11.30 (C–E).
C. Coronal section of the head. Posterior view. Bar: 10 mm.
D–E. 3 Tesla MRI. D. T1-weighted MRI. **E.** T2-weighted MRI.

1 Caudate nucleus
2 Internal capsule, anterior limb
3 Putamen
3′ Claustrum
4 Lateral pallidum
5 Anterior commissure (paramedian portion)
The true midline portion lies further posteriorly.
6 Anterior perforated substance
9 Pre-optic area
10 Supra-optic nucleus
11 Third ventricle
12 Optic chiasm (CN II)
12′ Hypophyseal stalk
21 Amygdala
22 Collateral sulcus
23 Fusiform gyrus
24 Inferior temporal gyrus
25 Middle temporal gyrus
26 Superior temporal gyrus
27 Lateral fissure (Sylvian fissure)
28 Insula
29 Precentral gyrus
30 Middle frontal gyrus
30′ Superior frontal gyrus
31 Cingulate sulcus
32 Cingulate gyrus
33 Corpus callosum
33′ Frontal horn of the lateral ventricle
34 Sphenoid sinus
35 Internal carotid artery

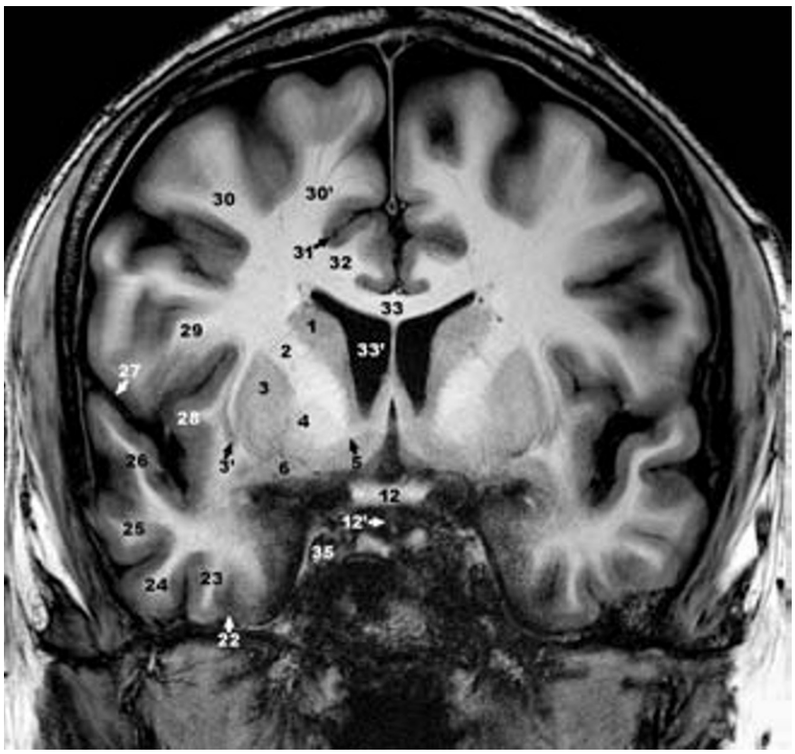
30
30'
31
32
33
29
1
33'
2
27
3
28
4
26
3'
6
5
12
12'
25
35
24
23
22

D

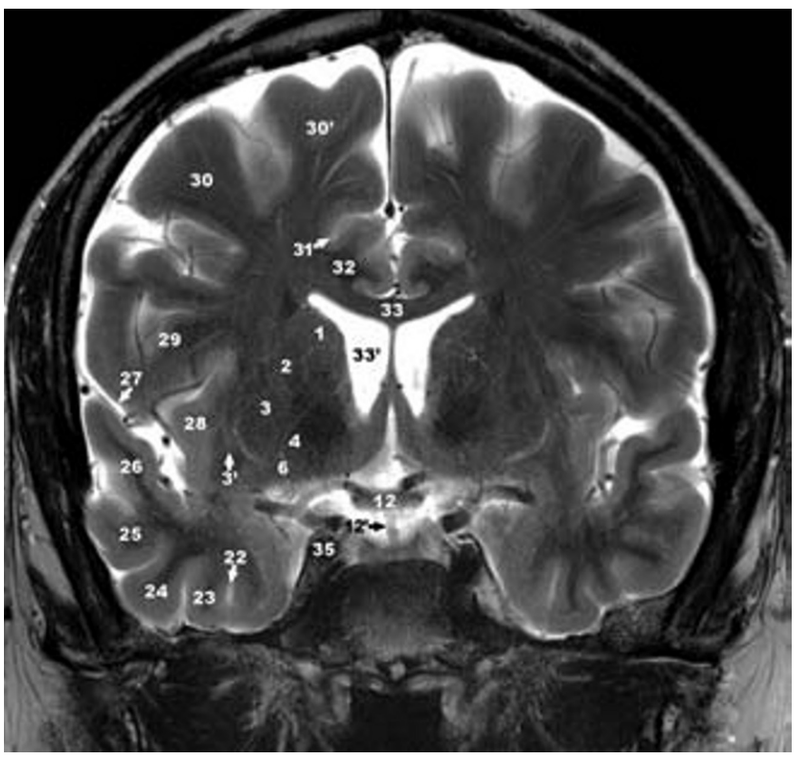
30'
30
31
32
33
29
1
33'
2
27
3
28
4
26
3'
6
12
12'
25
22
35
24
23

E

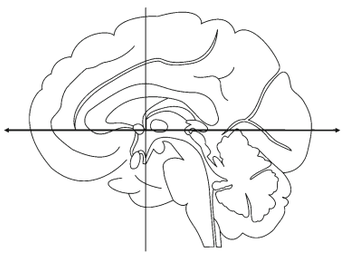

Fig. 11.31 (A–B). Coronal (frontal) section.
A. Frontal view after removal of the cerebral hemispheres. Bar: 10 mm.
B. Inferior oblique view.

1 Caudate nucleus
2 Internal capsule, anterior limb
3 Claustrum
4 Putamen
5 Lateral pallidum
6 Medial pallidum
7 Stria terminalis
8 Column of fornix
8′ Third ventricle
9 Paraventricular hypothalamic nucleus
10 Lateral hypothalamus
11 Tuber cinereum
12 Hypophyseal stalk
13 Optic tract (CN II)
14 Supra-optic hypothalamic nucleus
15 Anterior perforated substance
16 Anterior commissure (lateral portion)
17 Striate blood vessels
18 Mammillary body
19 Lateral geniculate body
20 Crus cerebri
21 Oculomotor nerve (CN III)
22 Pons, basilar portion
23 Medulla, pyramid

A

B

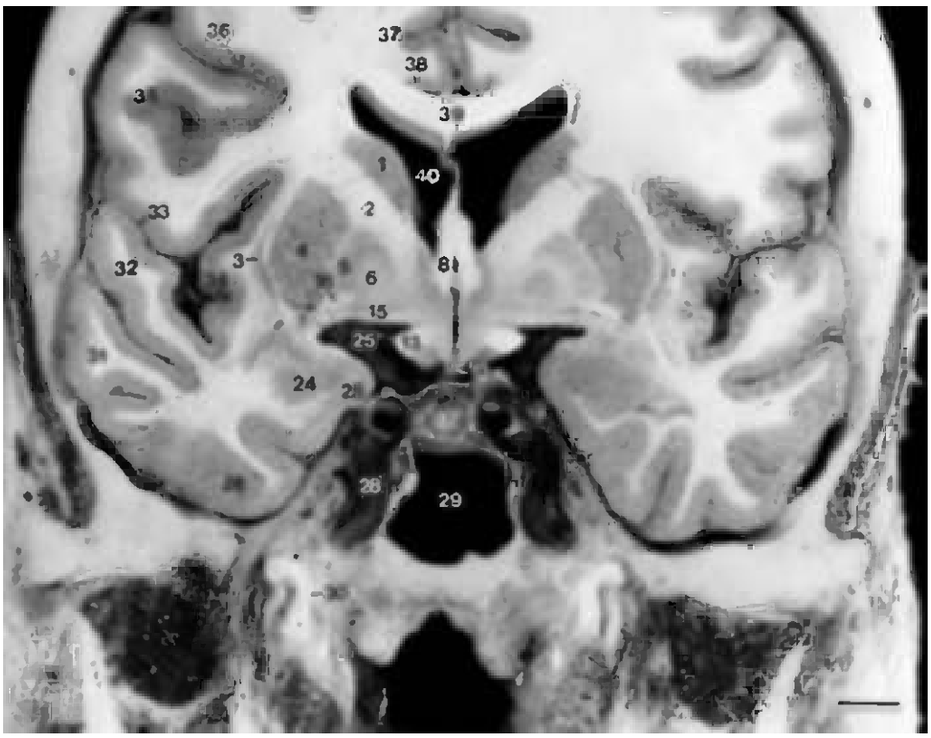

C

Fig. 11.31 (C–E).
C. Coronal section of the head. Posterior view. Bar: 10 mm.
D–E. 3 Tesla MRI. D. T1-weighted MRI. **E.** T2-weighted MRI.

1 Caudate nucleus
2 Internal capsule, anterior limb
3 Claustrum
4 Putamen
5 Lateral pallidum
6 Medial pallidum
8 Anterior column of fornix
12 Hypophyseal stalk
13 Optic tract
15 Anterior perforated substance
16 Anterior commissure (C.: lateral portion. D-E.: midline portion in the anterior wall of the third ventricle)
24 Amygdala
25 Gyrus ambiens (of temporal lobe)
25′ Chiasmatic cistern
26 Fusiform gyrus
27 Hypophysis
28 Internal carotid artery and cavernous sinus
29 Sphenoid sinus
30 Eustachian tube
31 Middle temporal gyrus
31′ Inferior temporal gyrus
32 Superior temporal gyrus
33 Lateral fissure (Sylvian fissure)
34 Insula
35 Precentral gyrus
36 Middle frontal gyrus
37 Cingulate sulcus
38 Cingulate gyrus
39 Corpus callosum
40 Frontal horn of the lateral ventricle

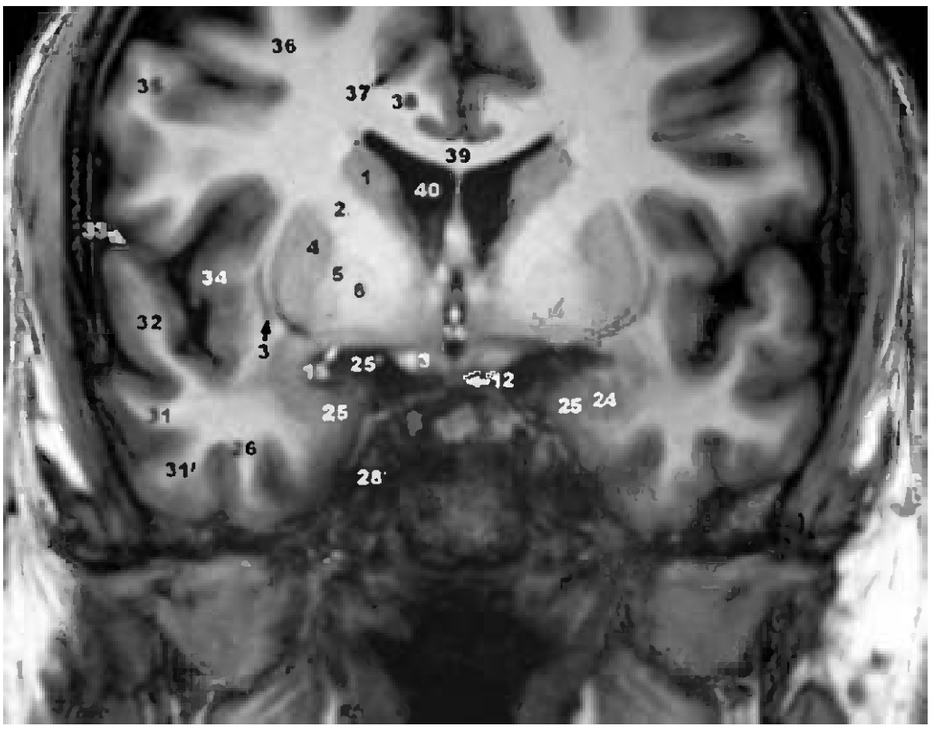
36
37
38
39
1
40
2
4
5
6
34
32
3
25
12
25
24
31
26
31'
28

D

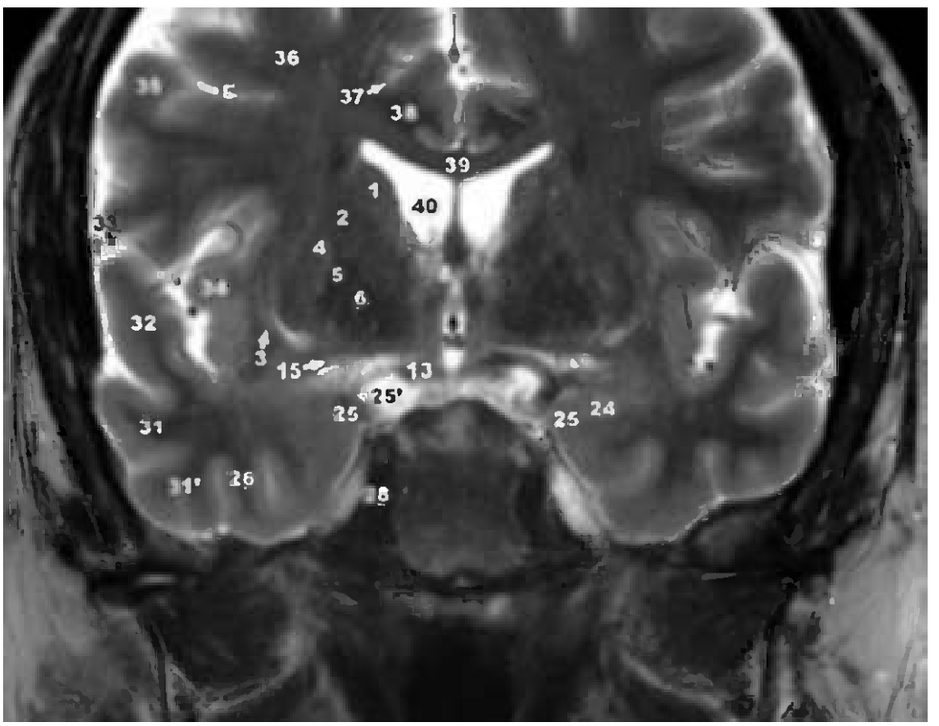
36
37
38
39
1
40
2
4
5
6
32
3
15
13
25'
25
25
24
31
31'
26
28

E

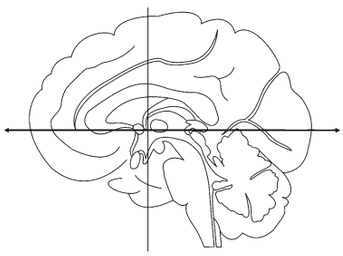

Fig. 11.32 (A–B). Coronal (frontal) section.
A. Frontal view after removal of the cerebral hemispheres. Bar: 10 mm.
B. Inferior oblique view.

1 Caudate nucleus
2 Internal capsule, genu
3 Claustrum
4 Putamen
5 Lateral pallidum
6 Medial pallidum
7 Anterior thalamic nucleus
8 Ventral anterior thalamic nucleus
9 Interthalamic adhesion (massa intermedia)
10 Third ventricle
11 Anterior column of fornix
12 Ventromedial and dorsomedial hypothalamic nuclei
13 Posterior tuber
14 Lateral tuber
15 Ansa lenticularis
16 Optic tract (CN II)
17 Anterior perforated substance
18 Anterior commissure (lateral portion)
19 Striate blood vessels
20 Mammillary body
21 Lateral geniculate body
22 Crus cerebri
23 Oculomotor nerve (CN III)
24 Pons, basilar portion
25 Medulla, pyramid

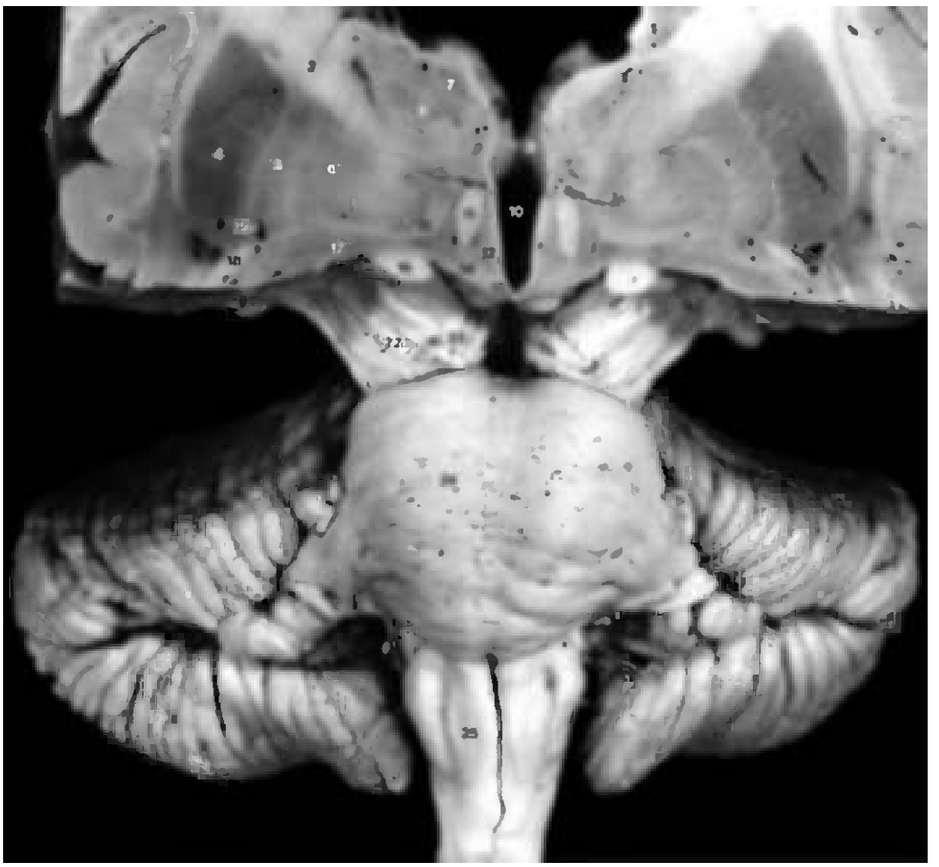

A

B

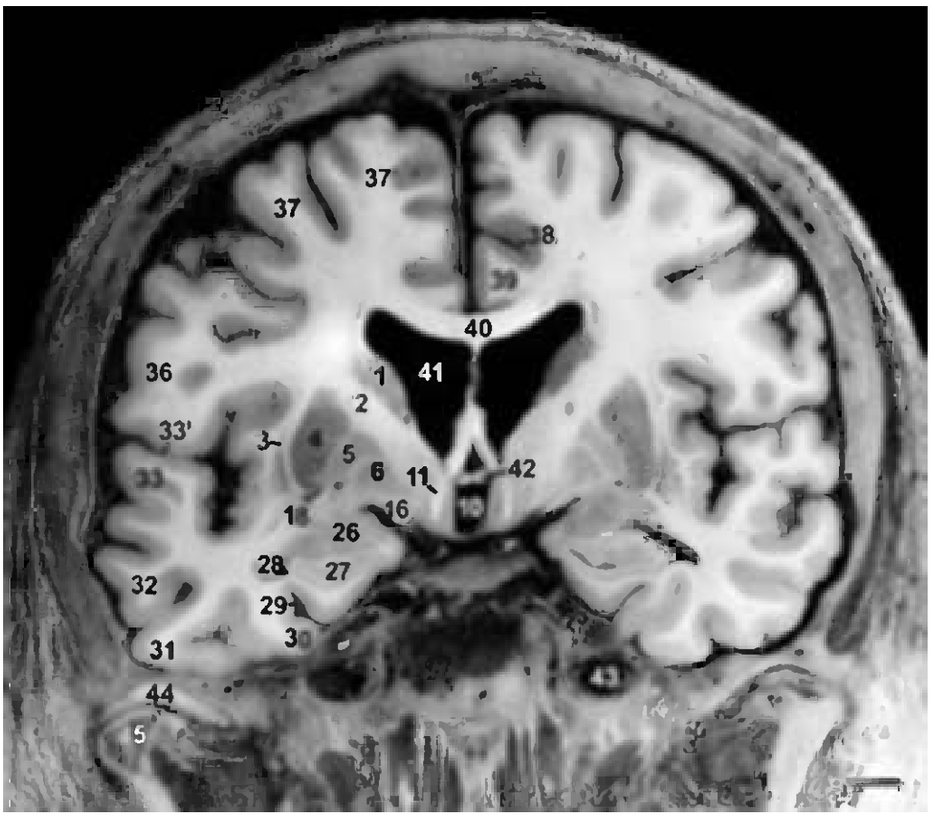

C

Fig. 11.32 (C–E).
C. Coronal section of the head. Posterior view. Bar: 10 mm.
D.–E. 3 Tesla MRI. D. T1-weighted MRI. **E**. T2-weighted MRI.

1 Caudate nucleus
2 Internal capsule, genu
3 Claustrum
4 Putamen
5 Lateral pallidum
6 Medial pallidum
10 Third ventricle
11 Anterior column of fornix
16 Optic tract
18 Anterior commissure (lateral portion approaching the temporal stem)
25 Meckel's cave
26 Amygdala
27 Hippocampus, head
28 Temporal horn of lateral ventricle
29 Collateral sulcus
30 Fusiform gyrus
31 Inferior temporal gyrus
32 Middle temporal gyrus
33 Superior temporal gyrus
33′ Lateral fissure (Sylvian fissure)
34 Temporal stem
35 Insula
36 Precentral gyrus
37 Middle frontal gyrus
37′ Superior frontal gyrus
38 Cingulate sulcus
39 Cingulate gyrus
40 Corpus callosum
41 Frontal horn of lateral ventricle
42 Anterior commissure (midline portion in the anterior wall of the third ventricle)
43 Internal carotid artery
44 Articular disc of the temporomandibular joint
45 Mandibular condyle

Arrows: Thalamostriate veins

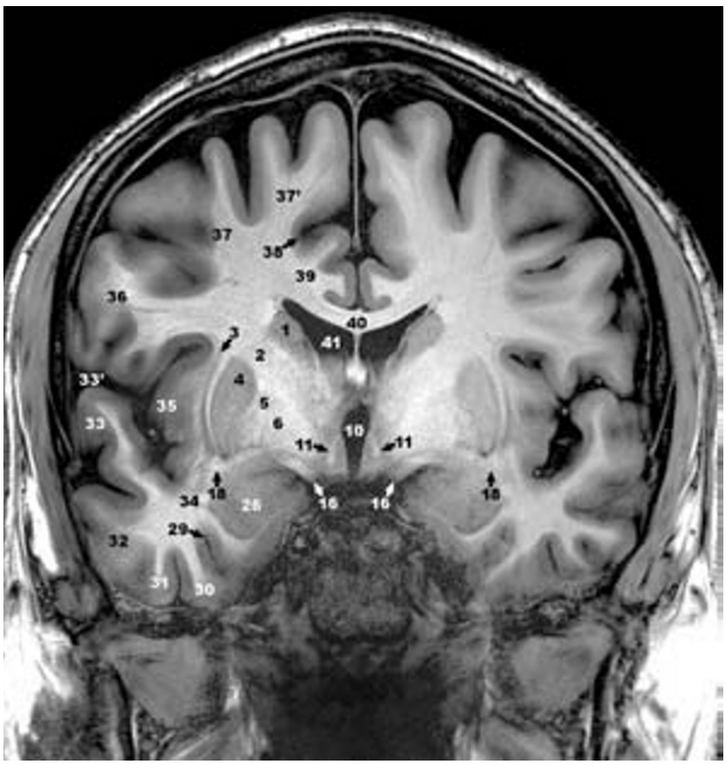
37'
37
38
39
36
40
1
41
2
33'
4
35
5
33
6
10
11
11
18
34
28
16
16
18
29
32
31
30

D


37
37'
38
39
36
40
1
41
2
33'
4
35
5
33
6
10
11
34
28
32
29
31
30
25

E

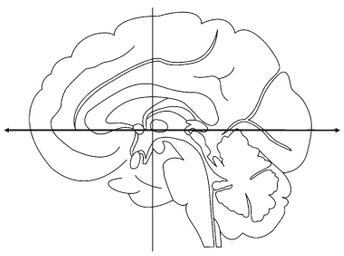

Fig. 11.33 (A–B). Coronal (frontal) section.
A. Frontal view after removal of the cerebral hemispheres. Bar: 10 mm.
B. Inferior oblique view.

1 Caudate nucleus
2 Internal capsule, posterior limb
3 Claustrum
4 Putamen
5 Lateral pallidum
6 Medial pallidum
7 Ventral lateral thalamic nucleus
8 Anterior thalamic nucleus
9 Dorsomedial thalamic nucleus
10 Interthalamic adhesion (massa intermedia) composed of gray matter
11 Third ventricle
12 Hypothalamus
13 Anterior column of fornix
14 Mammillary body
15 Optic tract (CN II)
16 Substantia innominata
17 Anterior commissure
18 Lateral geniculate body
19 Crus cerebri
20 Oculomotor nerve (CN III)
21 Pons, basilar portion
22 Medulla, pyramid

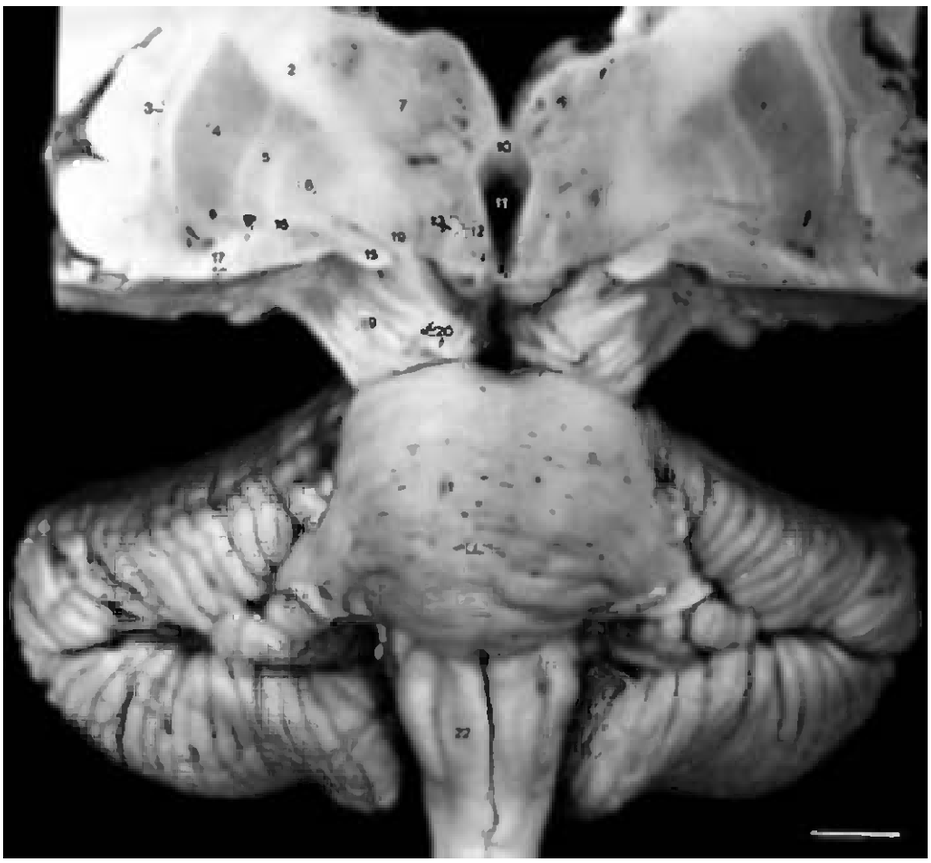

A

B

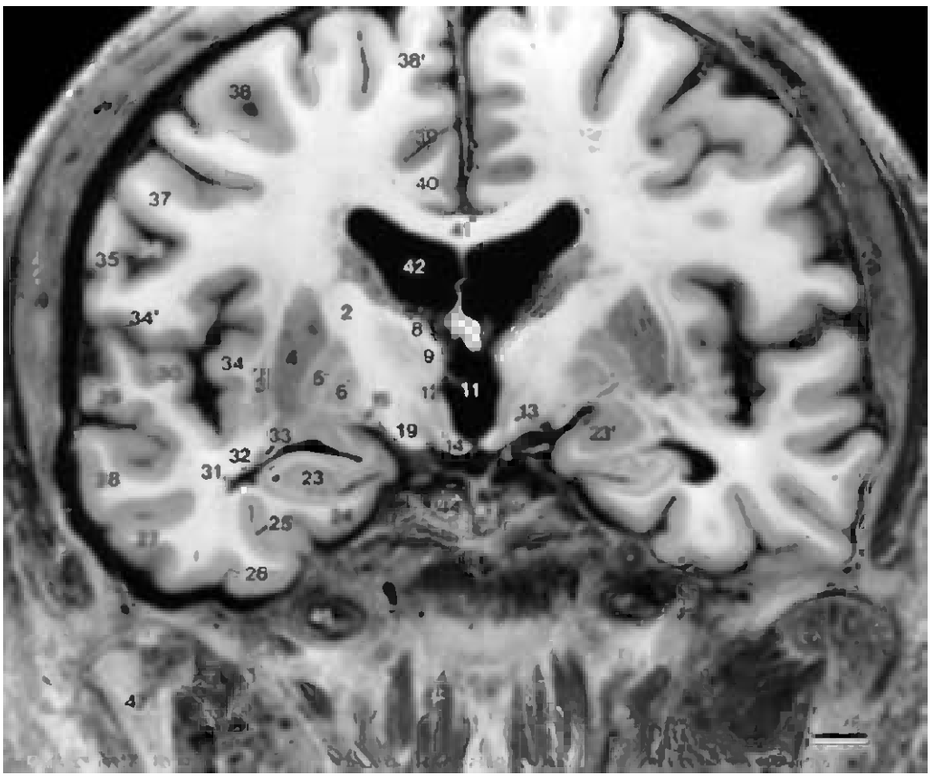

C

Fig. 11.33 (C–E).
C. Coronal section of the head. Anterior view. Bar: 10 mm.
D–E. 3 Tesla MRI. D. T1-weighted MRI. **E.** T2-weighted MRI.

1 Caudate nucleus
2 Internal capsule, posterior limb
3 Claustrum
4 Putamen
5 Lateral pallidum
6 Medial pallidum
8 Anterior thalamic nucleus
9 Dorsomedial thalamic nucleus
11 Third ventricle
12 Hypothalamus
13 Anterior column of fornix
14 Mammillary body
15 Optic tract (CN II)
19 Crus cerebri
22 Meckel's cave
23 Hippocampus, head
23′ Amygdala
24 Entorhinal area
25 Collateral sulcus
26 Fusiform gyrus
27 Inferior temporal gyrus
28 Middle temporal gyrus
29 Superior temporal gyrus
29′ Superior temporal sulcus (parallel sulcus)
30 Transverse temporal gyrus (of Heschl)
31 Temporal horn of lateral ventricle
32 Temporal stem
33 Caudate nucleus, tail
34 Insula
34′ Lateral fissure (Sylvian fissure)
35 Postcentral gyrus
36 Central fissure (central sulcus)
37 Precentral gyrus
38 Middle frontal gyrus
38′ Superior frontal gyrus
39 Cingulate sulcus
40 Cingulate gyrus
41 Corpus callosum
42 Frontal horn of lateral ventricle
42′ Body of lateral ventricle
43 Basilar artery
44 Pons
45 Internal carotid artery
46 Articular disc of the temporomandibular joint
47 Mandibular condyle

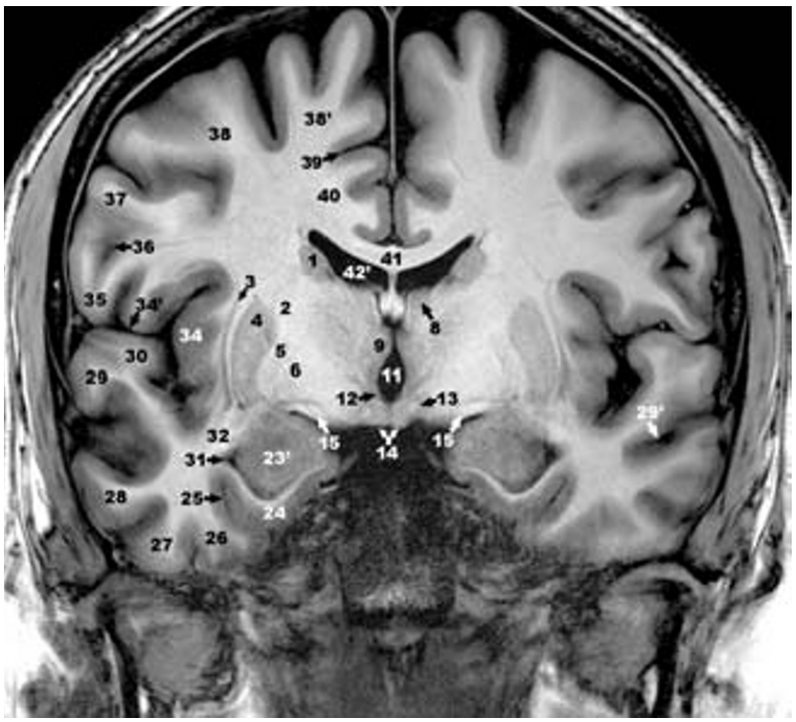
38
38'
39
40
37
36
1
41
42'
3
35
34'
2
4
34
8
30
5
9
29
6
11
12
13
29'
32
15
14
15
31
23'
28
25
24
27
26

D

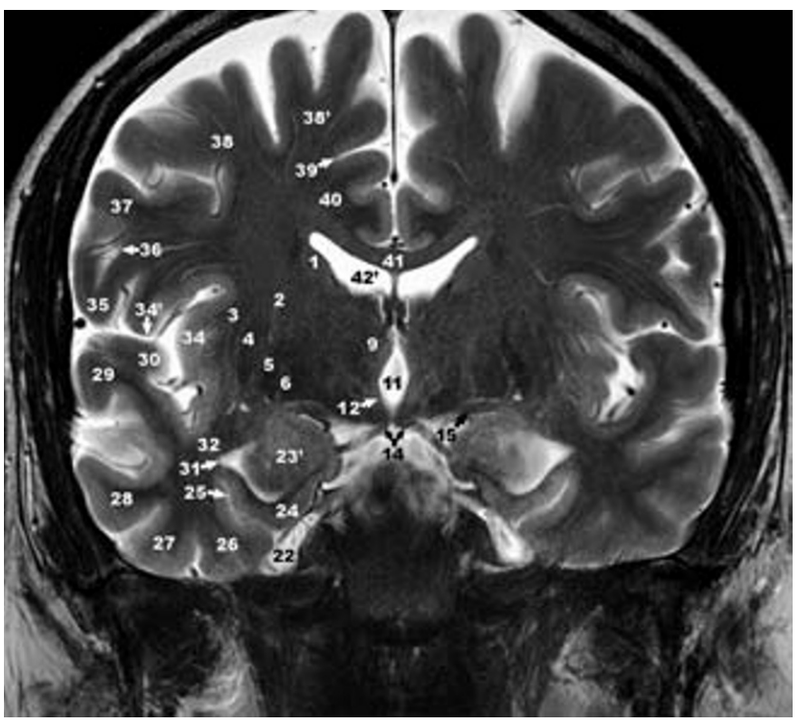
38'
38
39
40
37
36
1
41
42'
35
34'
2
3
34
4
9
30
5
29
6
11
12
15
32
14
23'
31
25
28
24
27
26
22

E

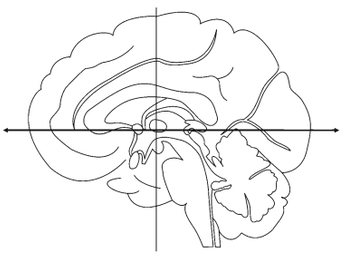

Fig. 11.34 (A–B). Coronal (frontal) section.
A. Frontal view after removal of the cerebral hemispheres. Bar: 10 mm.
B. Inferior oblique view.

1 Caudate nucleus
2 Internal capsule, posterior limb
3 Claustrum
4 Putamen
5 Lateral pallidum
6 Medial pallidum
7 Ventral lateral thalamic nucleus
8 Anterior thalamic nucleus
9 Dorsomedial thalamic nucleus
10 Interthalamic adhesion (massa intermedia)
11 Third ventricle
12 Mammillothalamic tract
13 Mammillary body
14 Lenticular fasciculus (H2 field of Forel)
15 Subthalamic nucleus
16 Optic tract (CN II)
17 Substantia innominata
18 Lateral geniculate body
19 Substantia nigra
20 Crus cerebri
21 Oculomotor nerve (CN III)
22 Interpeduncular (intercrural) fossa
23 Pons, basilar portion
24 Medulla, pyramid

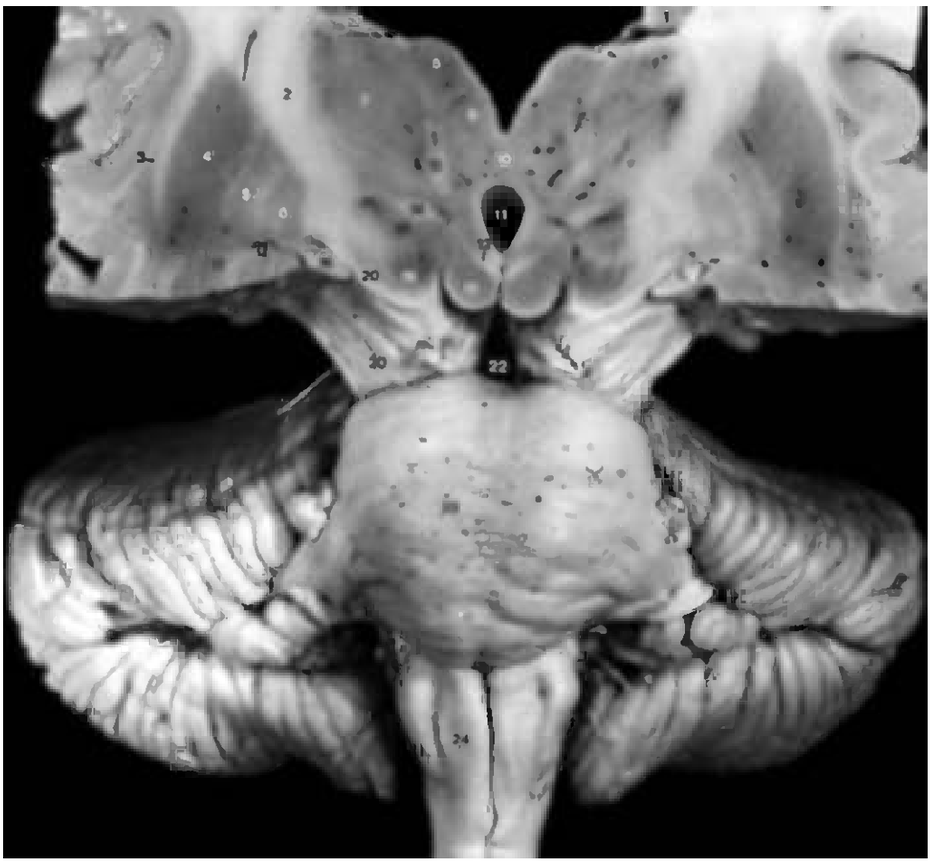

A

B

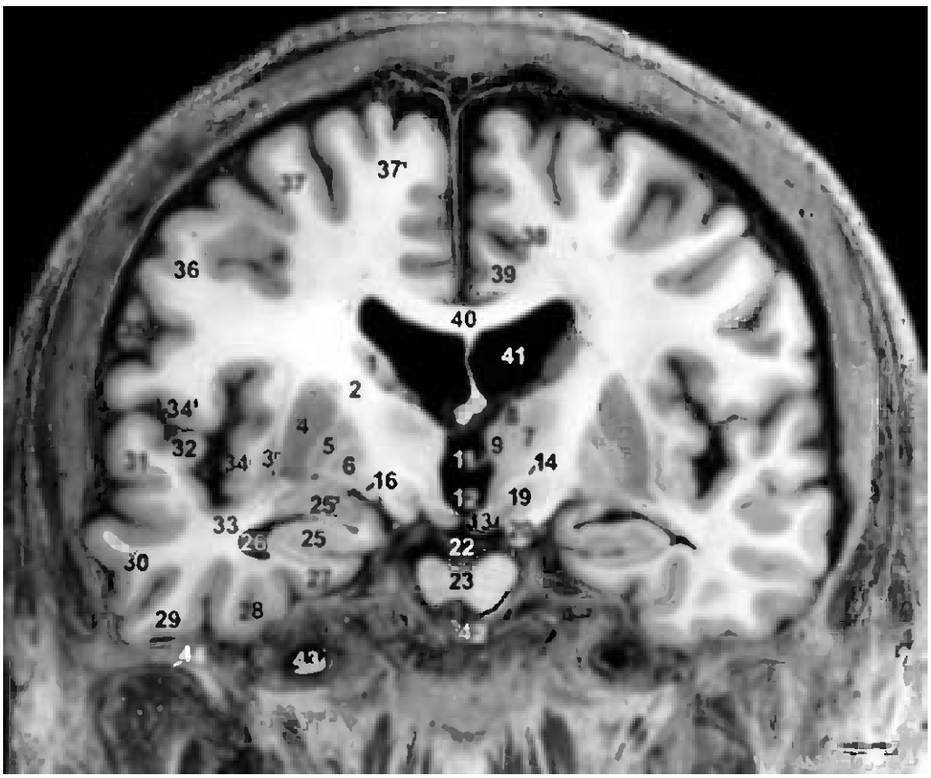

C

Fig. 11.34 (C–E).
C. Coronal section of the head. Posterior view. Bar: 10 mm.
D–E. 3 Tesla MRI. D. T1-weighted MRI. **E.** T2-weighted MRI.

1 Caudate nucleus
2 Internal capsule, posterior limb
3 Claustrum
4 Putamen
5 Lateral pallidum
6 Medial pallidum
7 Ventral lateral thalamic nucleus
8 Anterior thalamic nucleus
9 Dorsomedial thalamic nucleus
11 Third ventricle
12 Mammillothalamic tract
13 Mammillary body
14 Lenticular fasciculus (H2 field of Forel)
16 Optic tract (CN II)
19 Substantia nigra
20 Crus cerebri
21 Meckel's cave containing trigeminal nerve fibers (CN V)
22 Interpeduncular (intercrural) fossa
23 Pons, basilar portion
25 Hippocampus, head
25′ Amygdala
26 Temporal horn of lateral ventricle
27 Entorhinal area
28 Fusiform gyrus
29 Inferior temporal gyrus
30 Middle temporal gyrus
31 Superior temporal gyrus
32 Transverse temporal gyrus (of Heschl)
33 Temporal stem
34 Insula
34′ Lateral fissure (Sylvian fissure)
35 Postcentral gyrus
36 Precentral gyrus
37 Middle frontal gyrus
37′ Superior frontal gyrus
38 Cingulate sulcus
39 Cingulate gyrus
40 Corpus callosum
41 Lateral ventricle
42 Basilar artery
43 Internal carotid artery
44 Temporomandibular joint

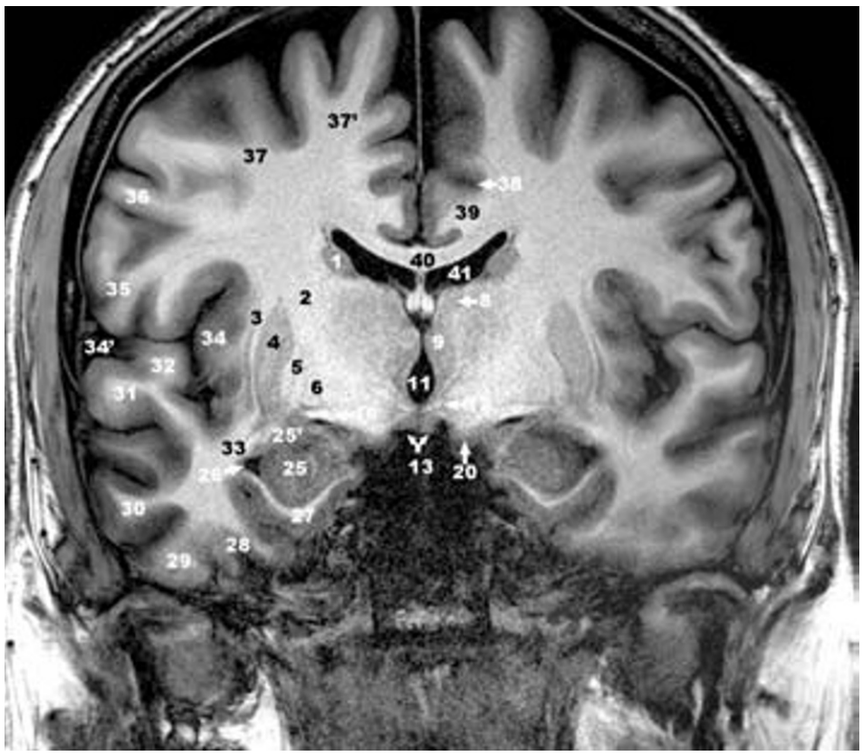
37'
37
36
38
39
1
40
41
35
2
3
34
4
34'
32
5
9
31
6
11
33
25'
Y
13
20
26
25
30
27
28
29

D

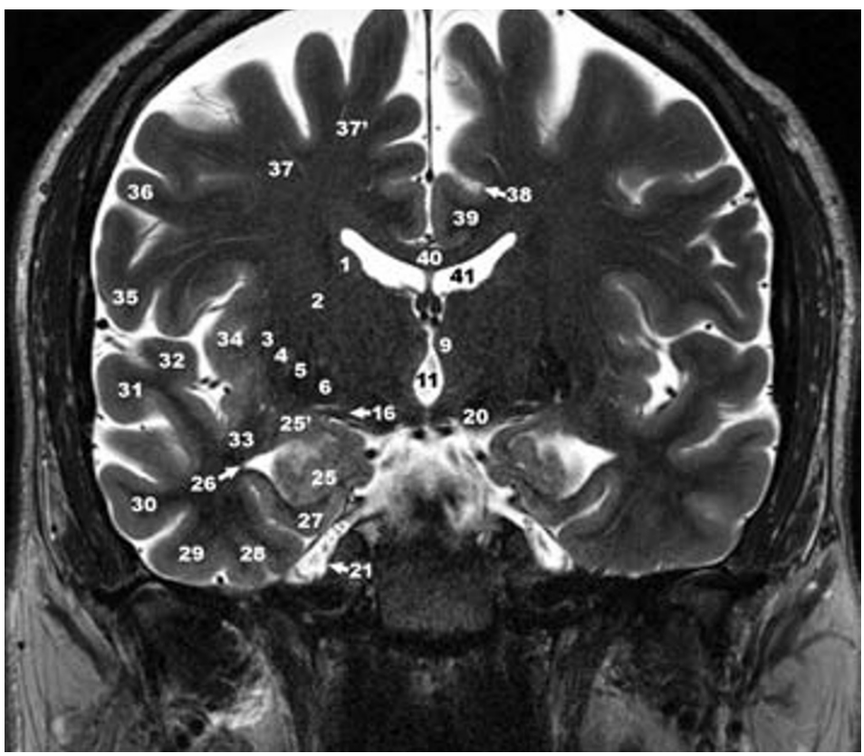
37'
37
36
38
39
1
40
41
35
2
34
3
4
5
9
32
6
11
31
25'
16
20
33
26
25
30
27
29
28
21

E

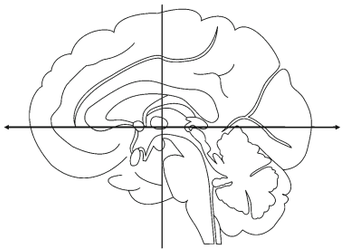

Fig. 11.35 (A–B). Coronal (frontal) section.
A. Frontal view after removal of the cerebral hemispheres. Bar: 10 mm.
B. Inferior oblique view.

1 Caudate nucleus
2 Internal capsule, posterior limb
3 Claustrum
4 Putamen
5 Lateral pallidum
6 Medial pallidum
7 Ventral lateral thalamic nucleus
8 Anterior thalamic nucleus
9 Dorsomedial thalamic nucleus
10 Mammillothalamic tract
11 Lenticular fasciculus (H2 Field of Forel)
12 Zona incerta
12′ Thalamic fasciculus (H1 Field of Forel)
13 Subthalamic nucleus
13′ Mammillary body
14 Optic tract (CN II)
15 Lateral geniculate body
16 Substantia nigra
17 Crus cerebri
18 Oculomotor nerve (CN III)
19 Interpeduncular (intercrural) fossa
20 Pons, basilar portion
21 Medulla, pyramid

A

B

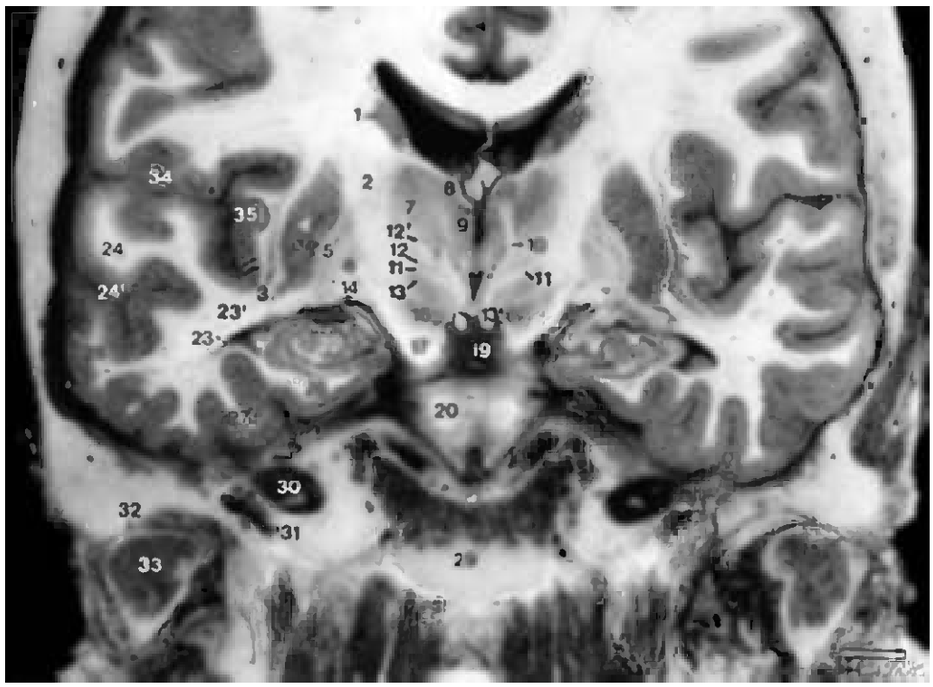

C

Fig. 11.35 (C–E).
C. Coronal section of the head. Anterior view. Bar: 10 mm.
D–E. 3 Tesla MRI. D. T1-weighted MRI. **E.** T2-weighted MRI.

1 Caudate nucleus
2 Internal capsule, posterior limb
3 Claustrum
4 Putamen
5 Lateral pallidum
6 Medial pallidum
7 Ventral lateral thalamic nucleus
8 Anterior thalamic nucleus
9 Dorsomedial thalamic nucleus
10 Mammillothalamic tract
11 Lenticular fasciculus (H2 field of Forel)
12 Zona incerta
12′ Thalamic fasciculus (H1 field of Forel)
13 Subthalamic nucleus
13′ Mammillary body
14 Optic tract (CN II)
16 Substantia nigra
17 Crus cerebri
19 Interpeduncular (intercrural) fossa
20 Pons, basilar portion
20′ Basilar artery
22 Hippocampus, head
23 Temporal horn of lateral ventricle
23′ Temporal stem
24 Superior temporal gyrus
24′ Superior temporal sulcus (parallel sulcus)
25 Middle temporal gyrus
26 Inferior temporal gyrus
27 Fusiform gyrus
27′ Collateral sulcus
28 Parahippocampal gyrus
29 Occipital bone, basilar portion
30 Internal carotid artery
31 Eustachian tube
32 Temporomandibular joint
33 Mandibular condyle
34 Lateral fissure (Sylvian fissure)
35 Insula

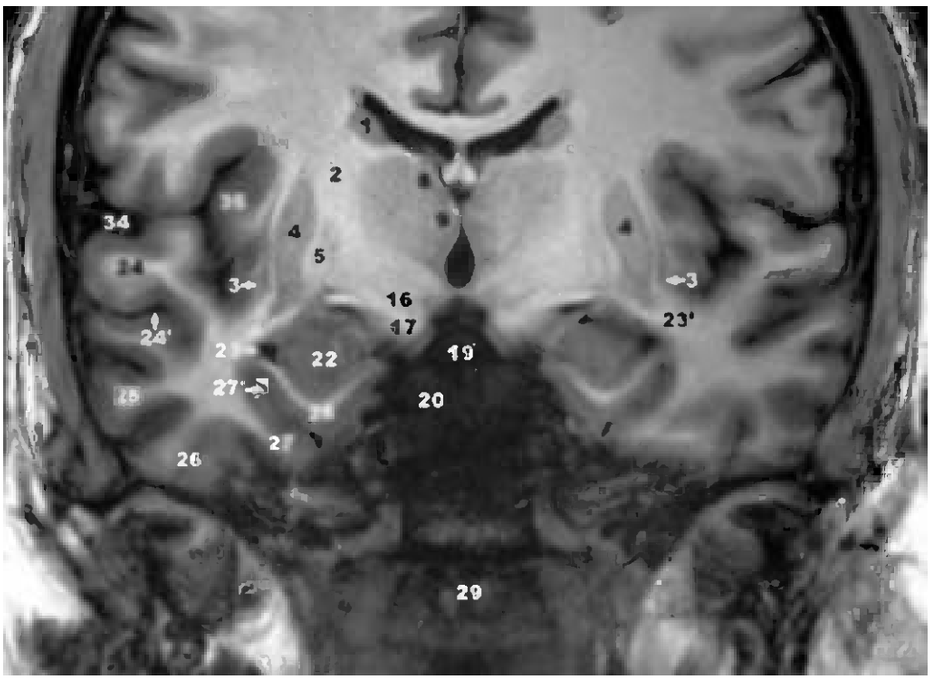
2
34
4
5
3
3
16
17
23'
24'
22
19
27'
20
26
29

D

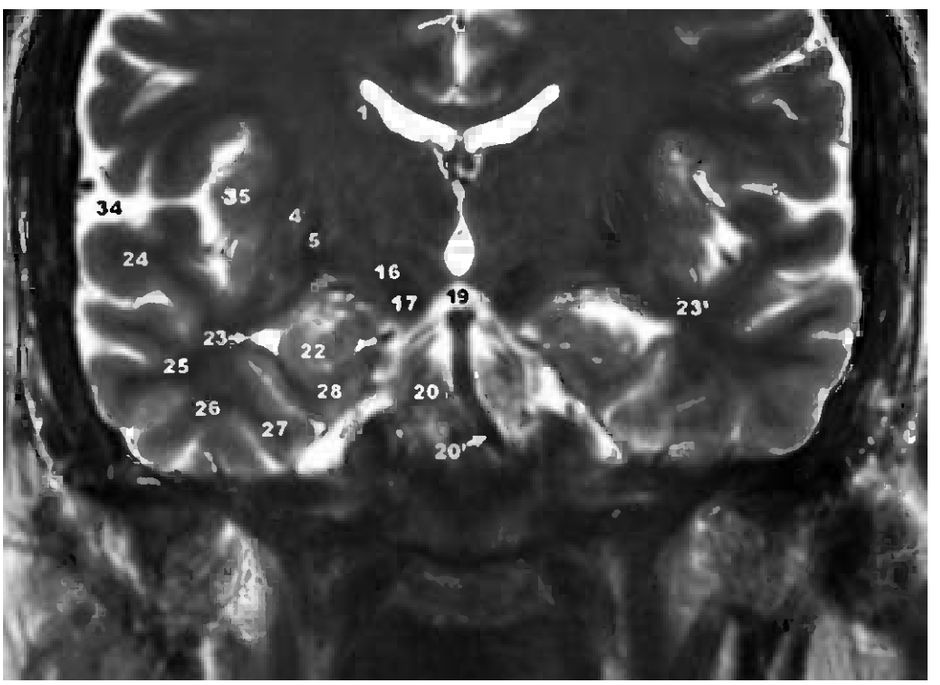
1
34
35
4
5
24
16
17
19
23'
23
22
25
28
20
26
27
20'

E

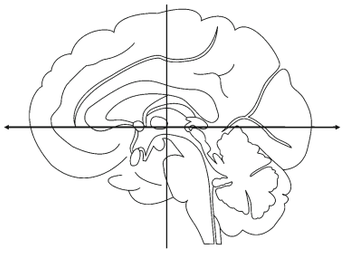

Fig. 11.36 (A–B). Coronal (frontal) section.
A. Frontal view after removal of the cerebral hemispheres. Bar: 10 mm.
B. Inferior oblique view.

1 Caudate nucleus
2 Claustrum
3 Putamen
4 Lateral pallidum
5 Medial pallidum
6 Internal capsule, posterior limb
7 Ventral lateral thalamic nucleus
8 Anterior thalamic nucleus
8′ Mammillothalamic tract
9 Dorsomedial thalamic nucleus
10 Interthalamic adhesion
11 Zona incerta
11′ Thalamic fasciculus (H1 field of Forel)
12 Subthalamic nucleus
13 Optic tract
14 Striate blood vessels
15 Lateral geniculate body
16 Substantia nigra
17 Crus cerebri
18 Oculomotor nerve (CN III)
19 Interpeduncular (intercrural) fossa
20 Pons, basilar portion, pontocerebellar fibers
21 Trigeminal nerve, motor root (CN V)
22 Trigeminal nerve, sensory root (CN V)
23 Medulla, pyramid

A

B

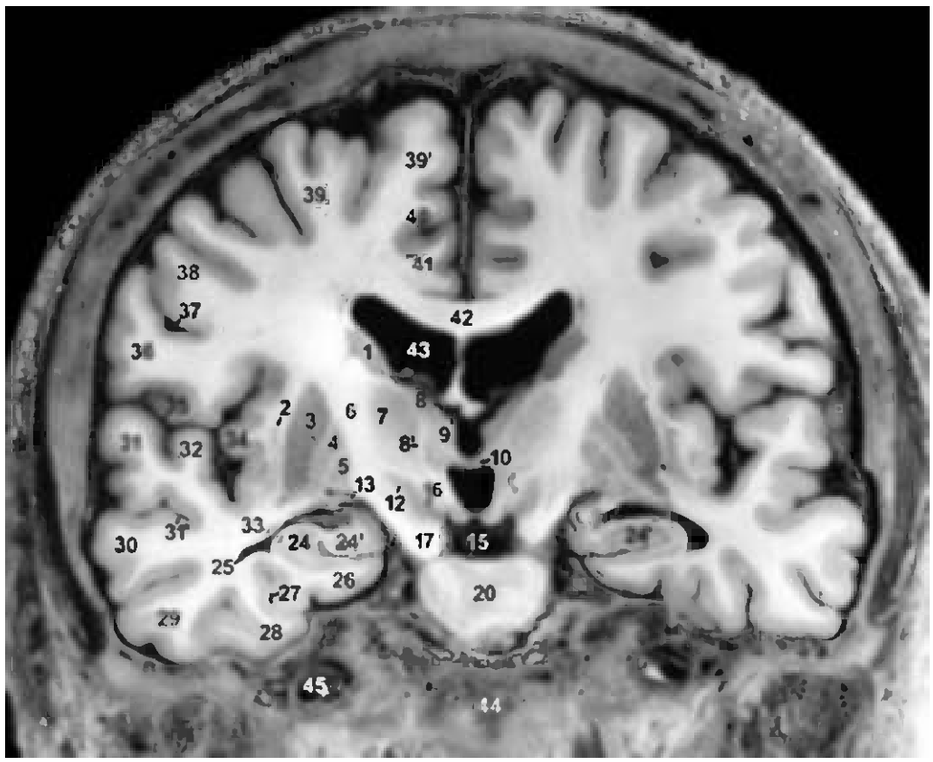

C

Fig. 11.36 (C–E).
C. Coronal section of the head. Anterior view. Bar: 10 mm.
D–E. 3 Tesla MRI. D. T1-weighted MRI. **E.** T2-weighted MRI.

1 Caudate nucleus
2 Claustrum
3 Putamen
4 Lateral pallidum
5 Medial pallidum
6 Internal capsule, posterior limb
7 Ventral lateral thalamic nucleus
8 Anterior thalamic nucleus
8′ Mammillothalamic tract
9 Dorsomedial thalamic nucleus
10 Interthalamic adhesion (massa intermedia)
12 Subthalamic nucleus
13 Optic tract (CN II)
15 Vessels within the interpeduncular fossa (19)
16 Substantia nigra
17 Crus cerebri
19 Interpeduncular (intercrural) fossa
20 Pons, basilar portion, pontocerebellar fibers
24 Hippocampus (body)
24′ Hippocampus (head)
25 Temporal horn of lateral ventricle
26 Entorhinal area
27 Collateral sulcus
28 Fusiform gyrus
29 Inferior temporal gyrus
30 Middle temporal gyrus
31 Superior temporal gyrus
31′ Superior temporal sulcus (parallel sulcus)
32 Transverse temporal gyrus (of Heschl)
33 Temporal stem
34 Insula
35 Lateral fissure
36 Postcentral gyrus
37 Central sulcus
38 Precentral gyrus
39 Middle frontal gyrus
39′ Superior frontal gyrus
40 Cingulate sulcus
41 Cingulate gyrus
42 Corpus callosum
43 Lateral ventricle
44 Sphenoid, basilar portion
45 Internal carotid artery
46 Basilar artery

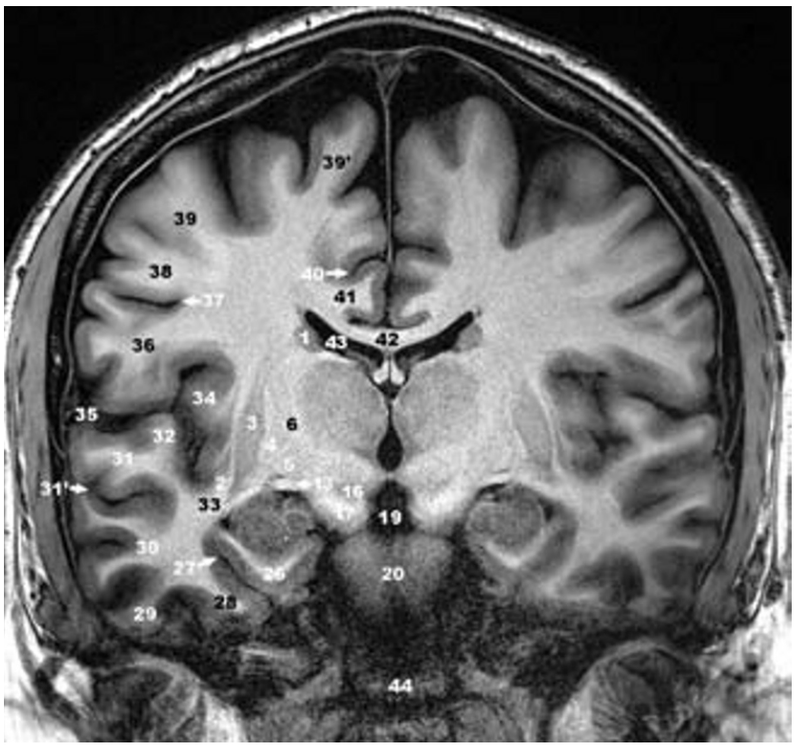
39'
39
38
40
41
37
1
43
42
36
34
35
3
6
32
4
31
31'
33
19
30
27
26
20
29
25
44

D

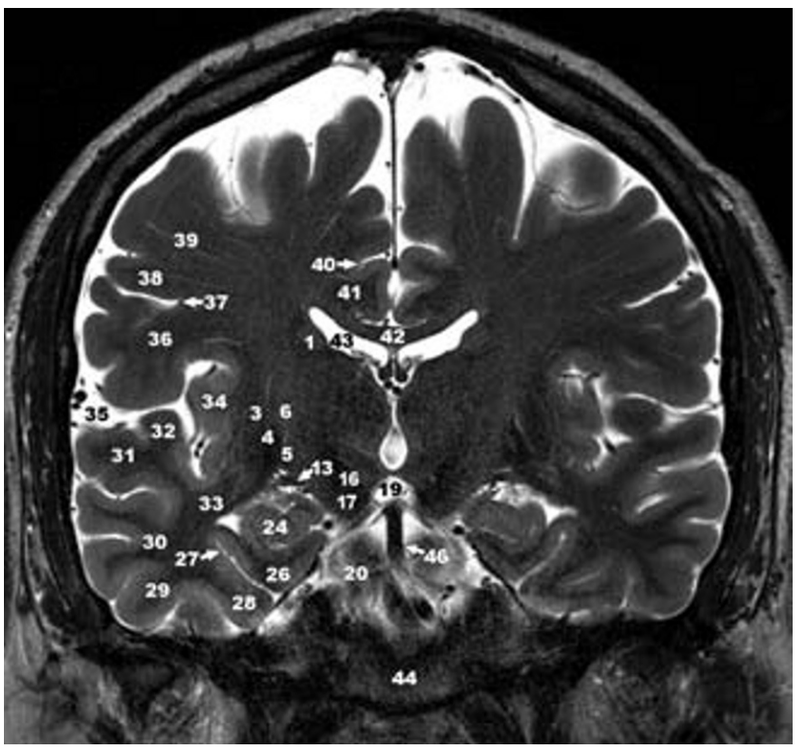
39
40
38
41
37
1
43
42
36
34
35
3
6
32
4
31
5
13
16
19
33
17
24
30
27
46
26
20
29
25
44

E

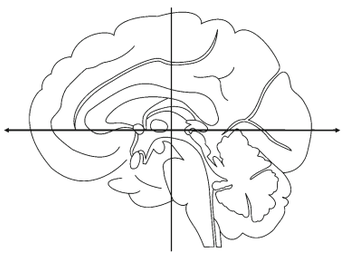

Fig. 11.37 (A–B). Coronal (frontal) section.
A. Frontal view after removal of the cerebral hemispheres. Bar: 10 mm.
B. Inferior oblique view.

1 Caudate nucleus
2 Internal capsule, posterior limb
3 Claustrum
4 Putamen
5 Lateral pallidum
6 Ventral lateral thalamic nucleus
6′ Anterior thalamic nucleus
7 Dorsomedial thalamic nucleus
8 Zona incerta
9 Prerubral area (H field of Forel)

The fields of Forel are composed of three narrow laminae:
Field H (Fig. 11.37) is situated in the prerubral area, rostral to the anterior pole of the red nucleus. It contains the ansa lenticularis arising from the ventral surface of the pallidum; (See also **Figs. 8.136 and 8.137**)

Field H2 (Fig. 11.34) is situated between the subthalamic nucleus and the zona incerta. It contains the lenticular fasciculus arising from the dorsal surface of the pallidum;
Field H1 (Fig. 11.35 and 11.36) is situated between the zona incerta and the thalamus. It contains the thalamic fasciculus, which includes the ansa lenticularis, lenticular fasciculus and cerebellothalamic fibers, en route to the thalamus.

10 Subthalamic nucleus
11 Optic tract (CN II)
12 Lateral geniculate body
13 Substantia nigra
14 Crus cerebri
15 Interpeduncular (intercrural fossa)
16 Corticospinal tract
17 Pons, basilar portion, pontocerebellar fibers
18 Trigeminal nerve, motor root (CN V)
19 Trigeminal nerve, sensory root (CN V)
20 Pons, lateral aspect (brachium pontis)
21 Medulla, pyramid

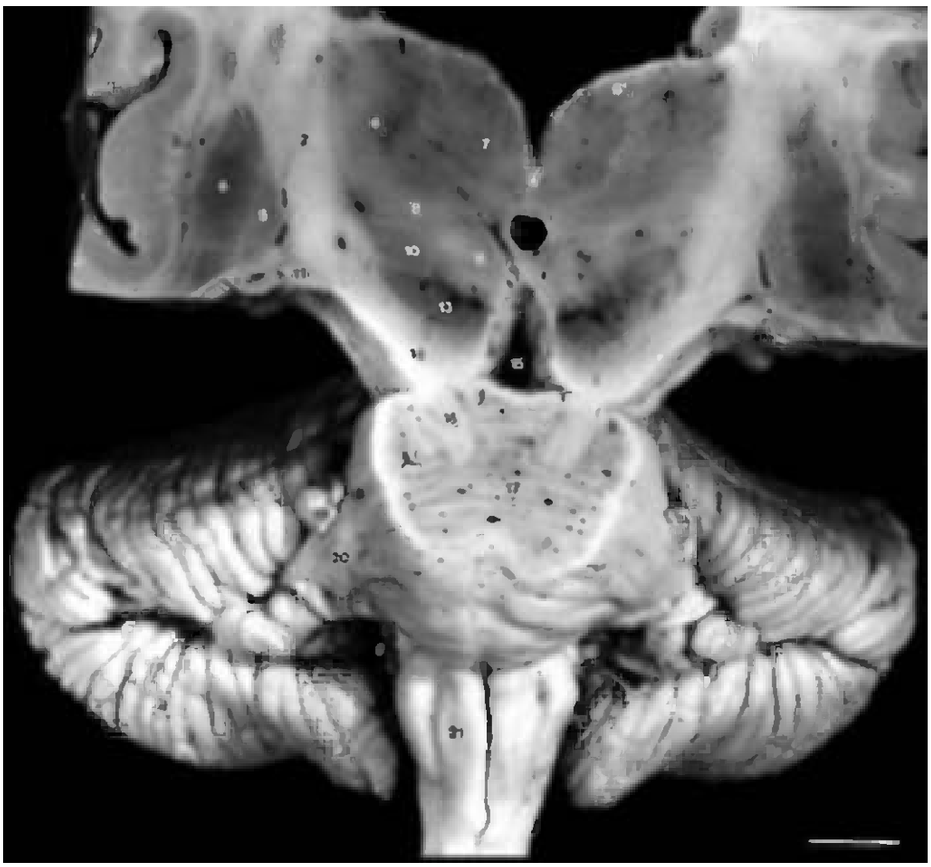

A

B

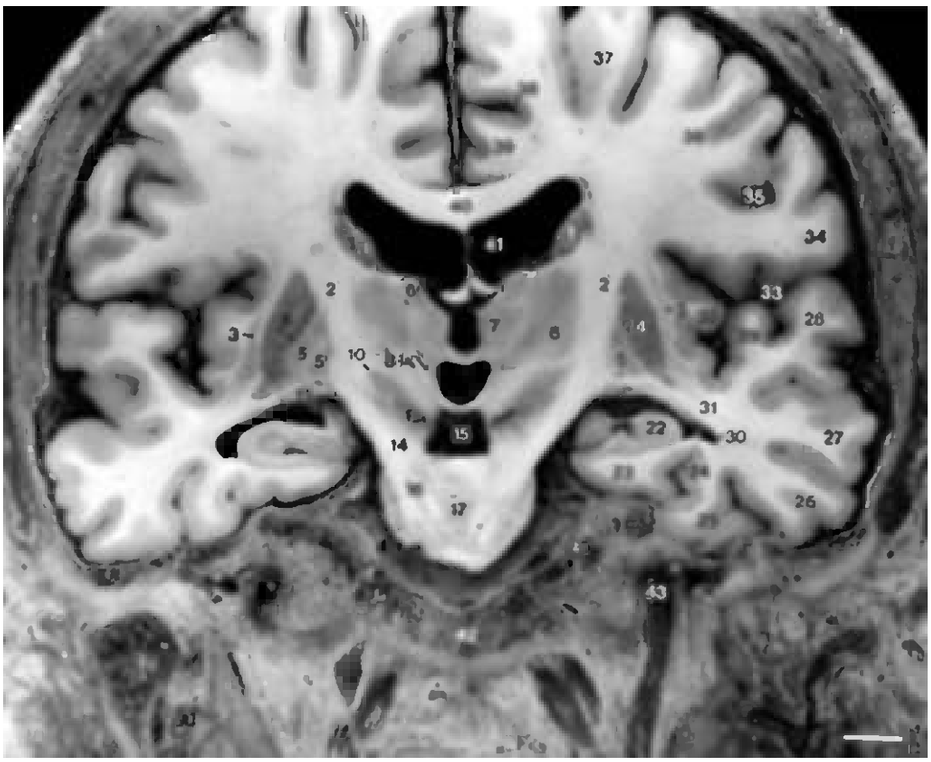

C

Fig. 11.37 (C–E).
C. Coronal section of the head. Posterior view. Bar: 10 mm.
D–E. 3 Tesla MRI. D. T1-weighted MRI. **E.** T2-weighted MRI.

1 Caudate nucleus
2 Internal capsule, posterior limb
3 Claustrum
4 Putamen
5 Lateral pallidum
5′ Medial pallidum
6 Ventral lateral thalamic nucleus
6′ Anterior thalamic nucleus
7 Dorsomedial thalamic nucleus
8 Zona incerta
10 Subthalamic nucleus
11 Optic tract
13 Substantia nigra
14 Crus cerebri
15 Interpeduncular (intercrural) fossa
16 Corticospinal tract
17 Pons, basilar portion, pontocerebellar fibers
22 Hippocampus (body)
23 Parahippocampal gyrus
24 Collateral sulcus
25 Fusiform gyrus
26 Inferior temporal gyrus
27 Middle temporal gyrus
28 Superior temporal gyrus
29 Transverse temporal gyrus (of Heschl)
30 Temporal horn of lateral ventricle
31 Temporal stem
32 Insula
33 Lateral fissure (Sylvian fissure)
34 Postcentral gyrus
35 Central sulcus
36 Precentral gyrus
37 Middle frontal gyrus
38 Cingulate sulcus
39 Cingulate gyrus
40 Corpus callosum
41 Lateral ventricle (body)
42 Occipital bone, basilar portion
43 Internal carotid artery

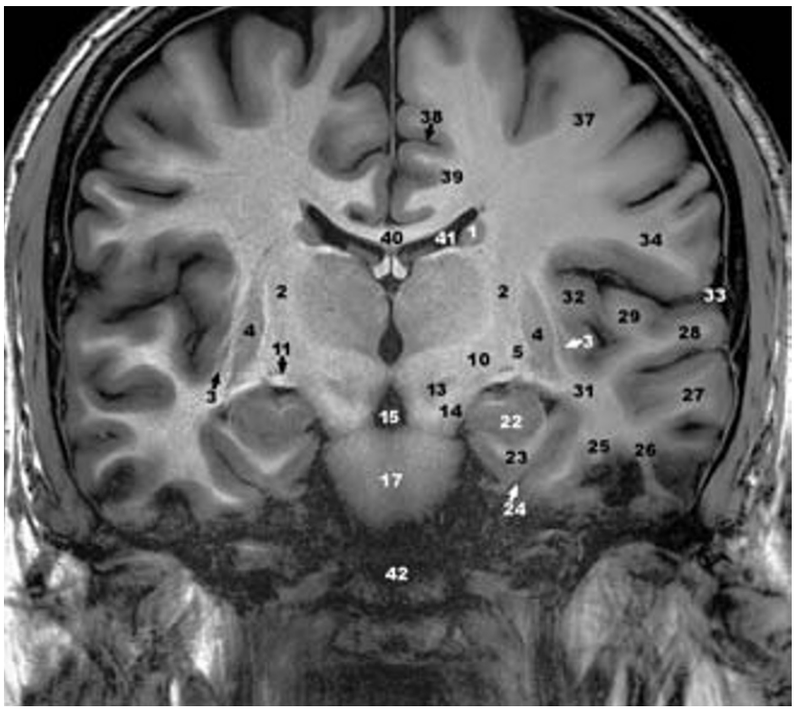
38
37
39
40
41
1
34
2
2
32
33
29
4
28
11
4
3
10
5
13
31
27
3
15
14
22
25
26
23
17
24
42

D

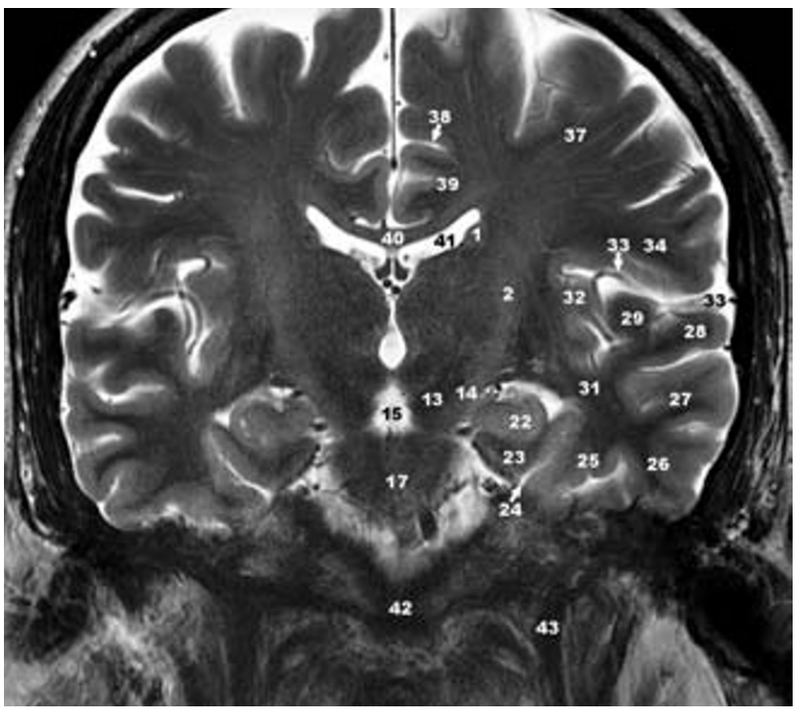
38
37
39
40
41
1
33
34
2
32
33
29
28
31
15
13
14
27
22
23
25
26
17
24
42
43

E

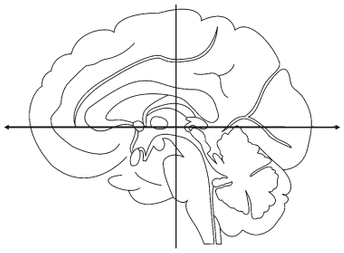

Fig. 11.38 (A–B). Coronal (frontal) section.
A. Frontal view after removal of the cerebral hemispheres. Bar: 10 mm.
B. Inferior oblique view

1 Insula
2 Claustrum
3 Putamen
4 Lateral pallidum
5 Internal capsule, posterior limb
6 Ventral lateral thalamic nucleus
7 Lateral dorsal thalamic nucleus
8 Stria medullaris thalami
9 Dorsomedial thalamic nucleus
9′ Internal medullary lamina
10 Zona incerta
11 Subthalamic nucleus
12 Optic tract (CN II)
13 Lateral geniculate body
14 Red nucleus (anterior pole)
15 Substantia nigra
16 Interpeduncular (intercrural) fossa
17 Crus cerebri and corticospinal tract
18 Pons, basilar portion, pontine nuclei
19 Corticospinal tract
20 Pontocerebellar fibers
21 Trigeminal nerve, motor root (CN V)
22 Trigeminal nerve, sensory root (CN V)
23 Pons, lateral aspect (brachium pontis)
24 Medulla, pyramid

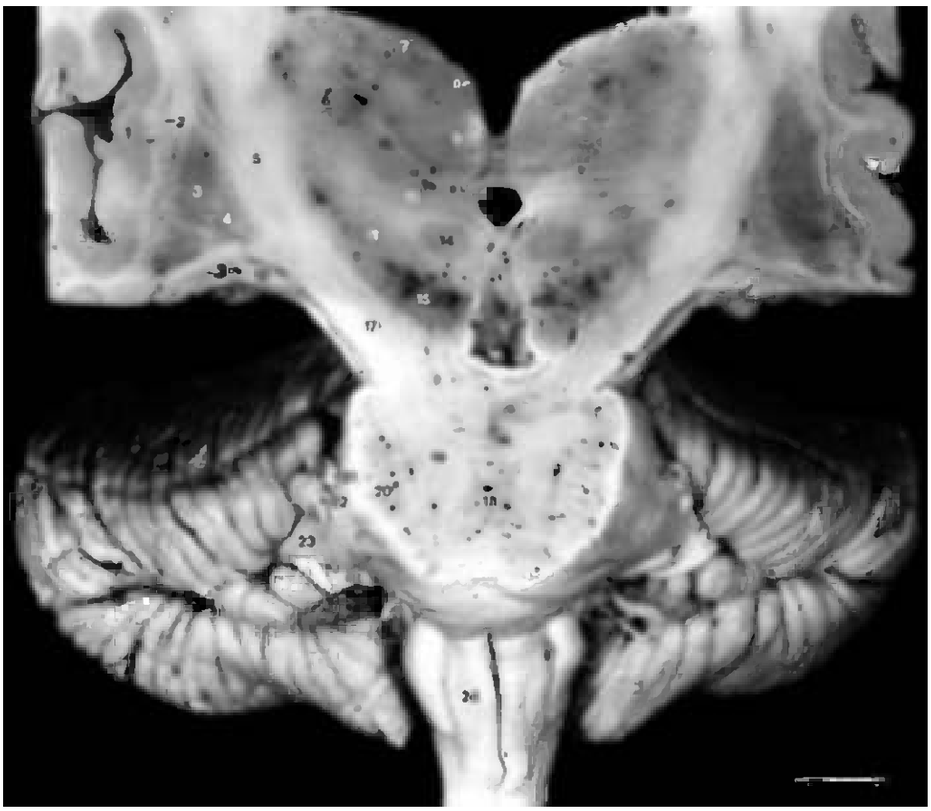

A

B

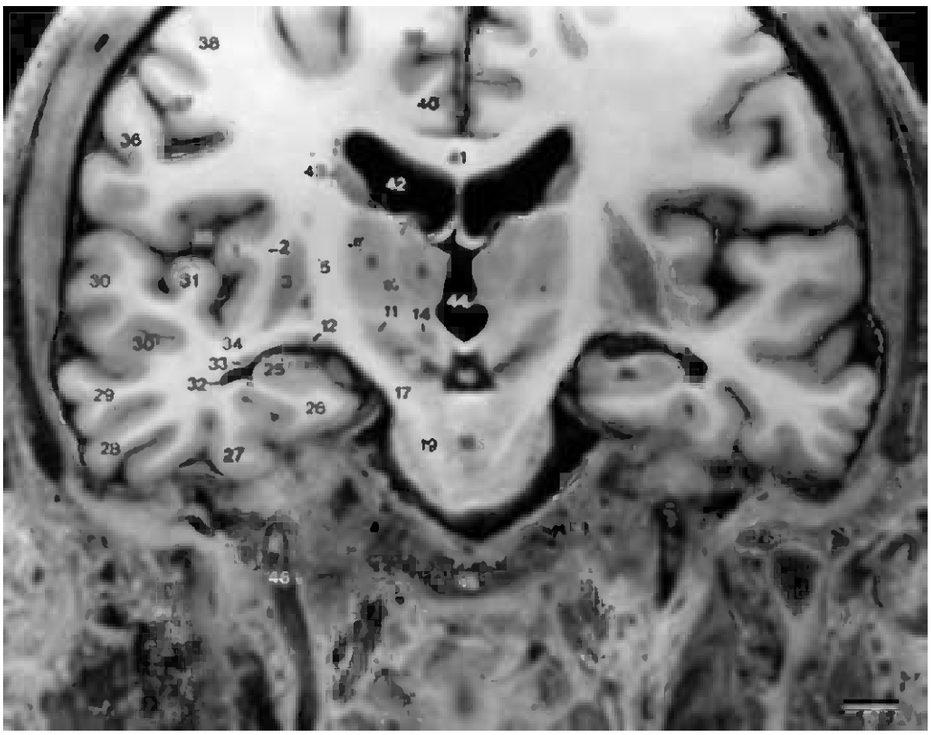

C

Fig. 11.38 (C–E).
C. Coronal section of the head. Anterior view. Bar: 10 mm.
D–E. 3 Tesla MRI. D. T1-weighted MRI. **E.** T2-weighted MRI.

1 Insula
2 Claustrum
3 Putamen
4 Lateral pallidum
5 Internal capsule, posterior limb
6 Ventral lateral thalamic nucleus
6′ External medullary lamina
7′ Anterior thalamic nucleus (the boundaries between the lateral dorsal and anterior thalamic nuclei are not clearly defined)
9 Dorsomedial thalamic nucleus
9′ Internal medullary lamina
11 Subthalamic nucleus
12 Optic tract (CN II)
14 Red nucleus (anterior pole)
15 Substantia nigra
16 Interpeduncular (intercrural) fossa (arrow)
17 Crus cerebri and corticospinal tract
18 Pons, basilar portion, pontine nuclei
19 Corticospinal tract
20 Trigeminal nerve (cisternal segments) (CN V)
25 Hippocampus (body)
26 Parahippocampal gyrus
27 Fusiform gyrus
28 Inferior temporal gyrus
29 Middle temporal gyrus
30 Superior temporal gyrus
30′ Superior temporal sulcus (parallel sulcus)
31 Transverse temporal gyrus (of Heschl)
32 Temporal horn of the lateral ventricle
33 Caudate nucleus (tail)
34 Temporal stem
35 Lateral fissure (Sylvian fissure)
36 Postcentral gyrus
37 Central sulcus
38 Precentral gyrus
39 Cingulate sulcus
40 Cingulate gyrus
41 Corpus callosum
42 Lateral ventricle
43 Caudate nucleus
44 Third ventricle
45 Occipital bone, basilar portion
46 Internal carotid artery

Arrow: Interpeduncular fossa (also 16)

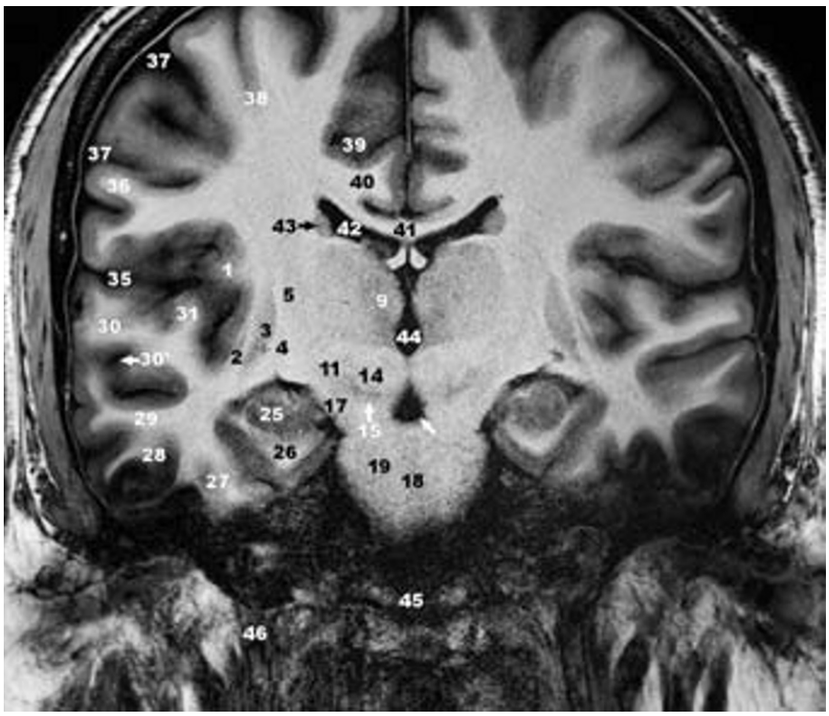
37
38
39
37
36
40
43
42
41
35
1
5
9
31
30
3
44
30'
2
4
11
14
17
29
25
15
28
26
19
27
18
45
46

D

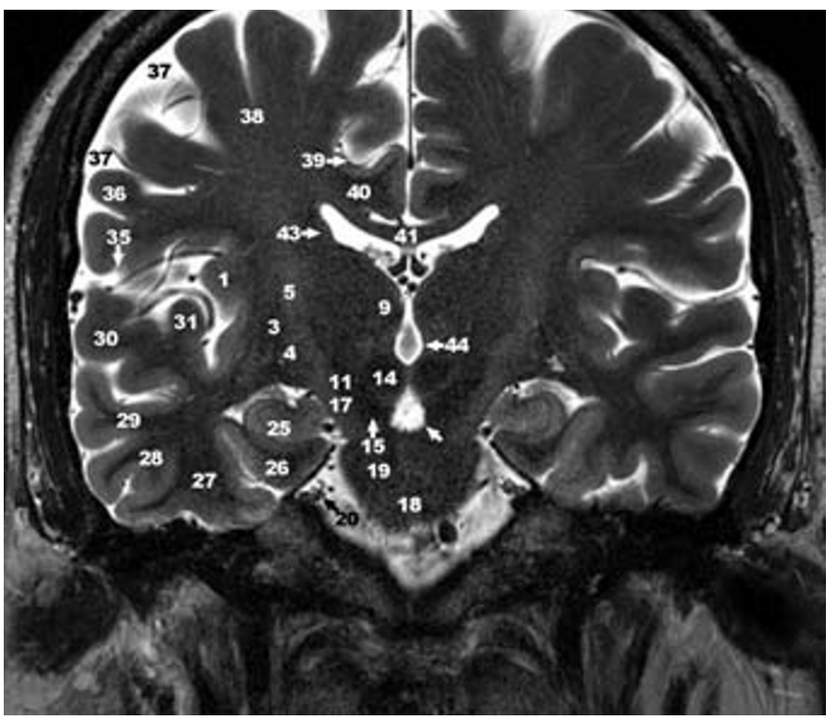
37
38
39
37
36
40
35
43
41
1
5
9
31
30
3
44
4
11
14
17
29
25
15
28
26
19
27
18
20

E

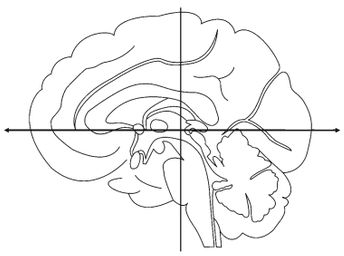

Fig. 11.39 (A–B). Coronal (frontal) section.
A. Frontal view after removal of the cerebral hemispheres. Bar: 10 mm.
B. Inferior oblique view.

1 Caudate nucleus
2 Putamen
3 Internal capsule, posterior limb, corticospinal tract
4 Lateral posterior thalamic nucleus
5 Lateral dorsal thalamic nucleus
6 Stria medullaris thalami
7 Dorsomedial thalamic nucleus
8 Centromedian thalamic nucleus
9 Ventral posteromedial thalamic nucleus
10 Ventral posterolateral thalamic nucleus
11 Medial lemniscus
12 Optic tract (CN II)
13 Lateral geniculate body
14 Red nucleus
15 Substantia nigra
16 Crus cerebri and corticospinal tract
17 Pontocerebellar fibers
18 Pontine nuclei
19 Corticospinal tract
20 Middle cerebellar peduncle (brachium pontis)
21 Trigeminal nerve (CN V)
22 Vestibulocochlear nerve (CN VIII)
23 Facial nerve (CN VII)
24 Medulla, pyramid (corticospinal tract)
25 Inferior olive
26 Quadrangular lobule
27 Anterior superior (primary) fissure
28 Simple lobule
29 Posterior superior fissure
30 Superior semilunar lobule
31 Great horizontal fissure
32 Inferior semilunar lobule
33 Prepyramidal fissure
34 Biventral lobule
35 Flocculus
36 Choroid plexus and lateral aperture of the fourth ventricle (foramen of Luschka)

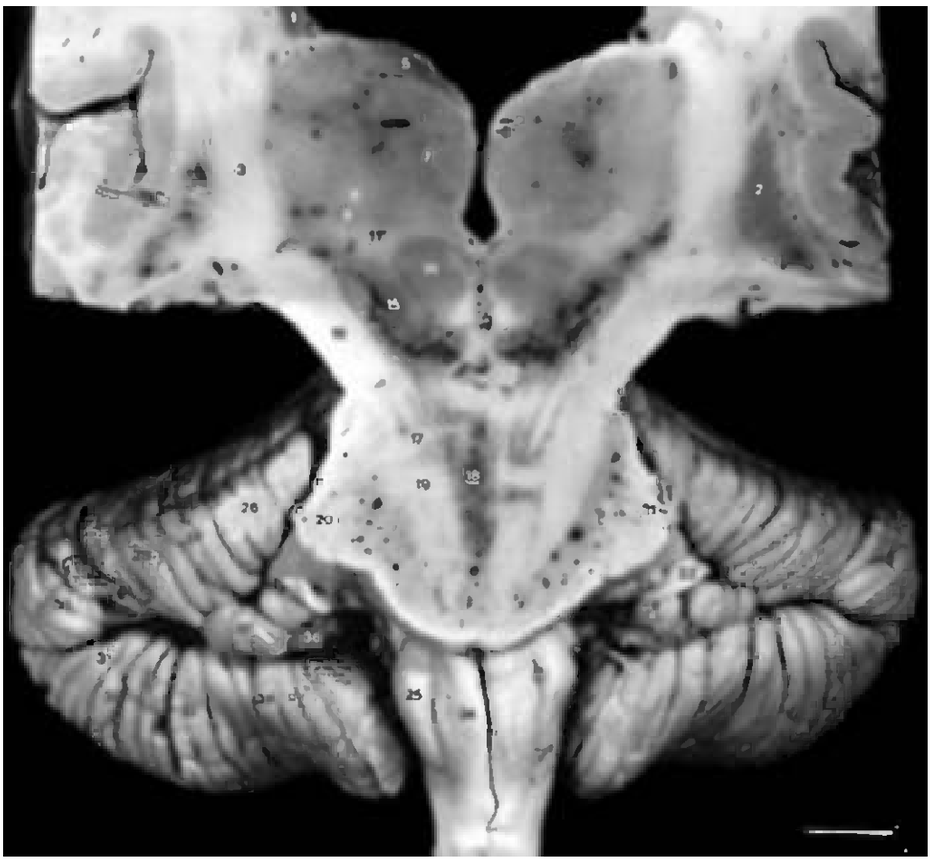

A

B

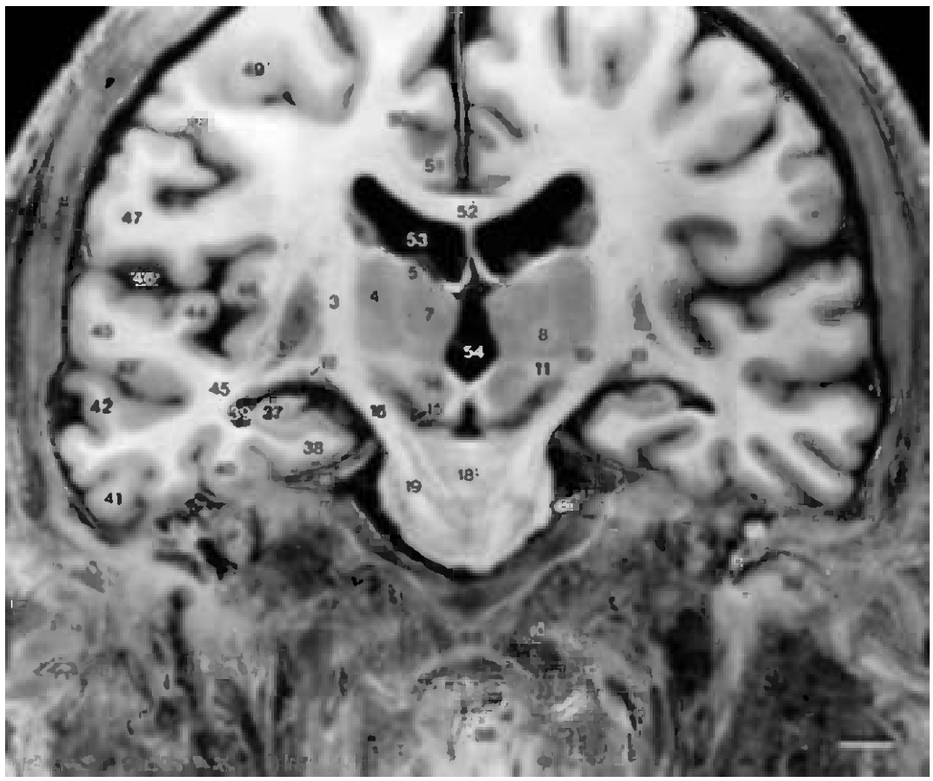

C

Fig. 11.39 (C–E).
C. Coronal section of the head. Posterior view. Bar: 10 mm.
D–E. 3 Tesla MRI. D. T1-weighted MRI. **E.** T2-weighted MRI.

1 Caudate nucleus
2 Putamen
3 Internal capsule, posterior limb, corticospinal tract
4 Lateral posterior thalamic nucleus
5 Lateral dorsal thalamic nucleus
7 Dorsomedial thalamic nucleus
8 Centromedian thalamic nucleus
10 Ventral posterolateral thalamic nucleus
11 Medial lemniscus
12 Optic tract
13 Lateral geniculate body
14 Red nucleus
15 Substantia nigra
16 Crus cerebri and corticospinal tract
18 Pontine nuclei
19 Corticospinal tract
21 Trigeminal nerve (CN V)
37 Hippocampus (body)
38 Parahippocampal gyrus
39 Temporal horn of lateral ventricle
40 Fusiform gyrus
41 Inferior temporal gyrus
42 Middle temporal gyrus
43 Superior temporal gyrus
43′ Parallel sulcus
44 Transverse temporal gyrus (of Heschl)
45 Temporal stem
46 Insula
46′ Lateral fissure (Sylvian fissure)
47 Postcentral gyrus
48 Central sulcus
49 Precentral gyrus
50 Cingulate sulcus
51 Cingulate gyrus
52 Corpus callosum
53 Lateral ventricle (body)
54 Third ventricle
55 Occipital bone, basilar portion
56 Dens of axis
57 Internal ear
57′ Cochlea
58 Middle ear
59 External acoustic meatus
60 Interpeduncular fossa

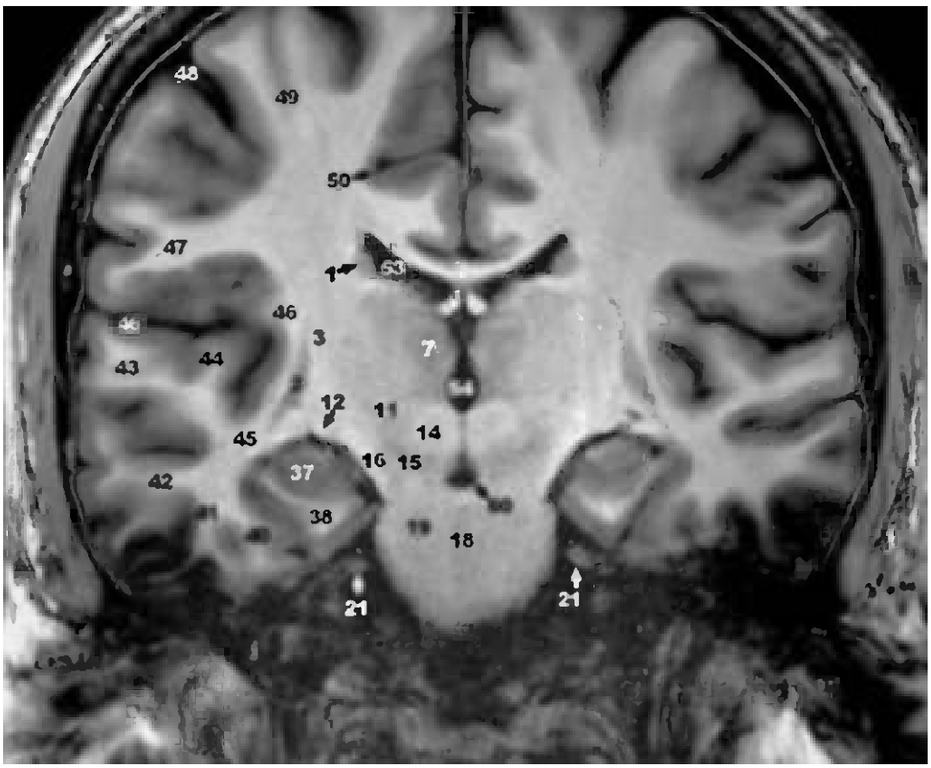
48
49
50
47
51
53
46
3
7
44
43
12
11
14
45
16
15
37
42
38
18
21
21

D

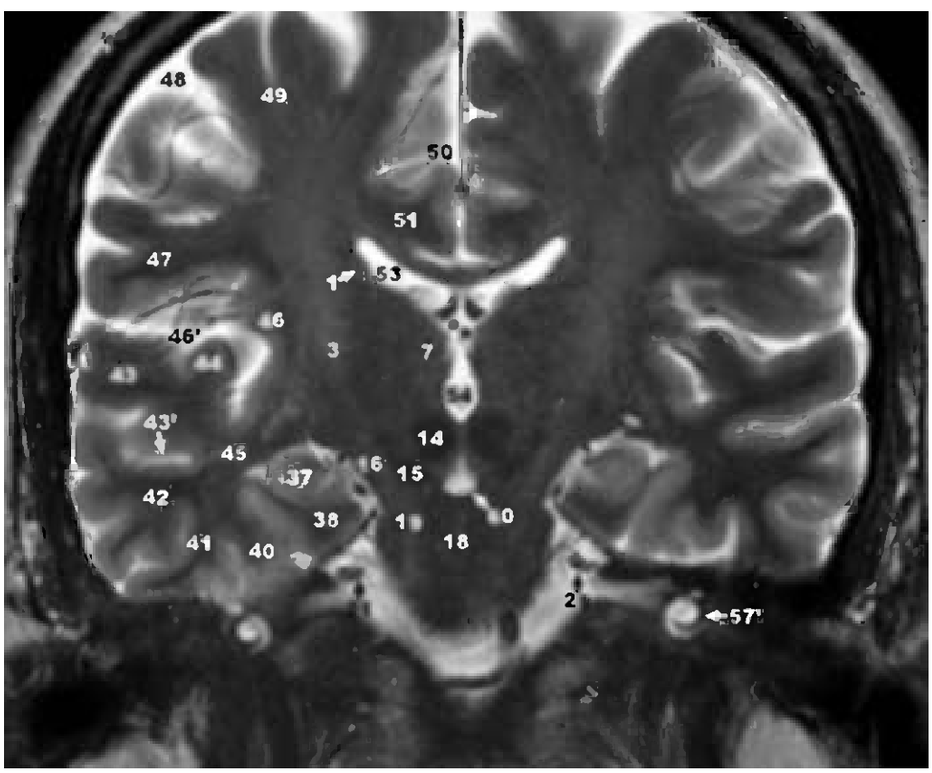
48
49
50
51
47
53
46'
3
7
43'
14
45
16
15
37
42
38
1
0
41
40
18
2
57

E

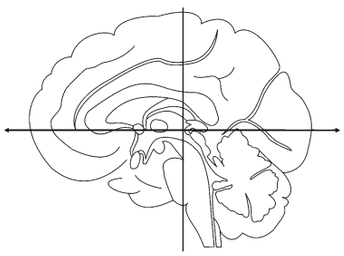

Fig. 11.40 (A–B). Coronal (frontal) section.
A. Frontal view after removal of the cerebral hemispheres. Bar: 10 mm.
B. Inferior oblique view

1 Caudate nucleus
2 Caudatolenticular bridges of gray matter (bridges of gray matter linking caudate nucleus with putamen)
3 Internal capsule, retrolenticular portion
4 Lateral posterior thalamic nucleus
5 Lateral dorsal thalamic nucleus
6 Stria medullaris thalami
7 Dorsomedial thalamic nucleus
8 Habenulo-interpeduncular tract
9 Centromedian thalamic nucleus
10 Ventral posteromedial thalamic nucleus
11 Ventral posterolateral thalamic nucleus
11′ Medial lemniscus
12 Lateral geniculate body
13 Medial geniculate body
14 Red nucleus (posterior pole)
15 Superior cerebellar peduncle (brachium conjunctivum)
16 Substantia nigra
17 Crus cerebri
18 Corticospinal tract
19 Pontine nuclei
20 Middle cerebellar peduncle (brachium pontis)
21 Trigeminal nerve (CN V)
22 Vestibulocochlear nerve (CN VIII)
23 Facial nerve (CN VII)
24 Medulla, pyramid
25 Inferior olive
26 Quadrangular lobule
27 Anterior superior (primary) fissure
28 Simple lobule
29 Posterior superior fissure
30 Superior semilunar lobule
31 Great horizontal fissure
32 Inferior semilunar lobule
33 Prepyramidal fissure
34 Biventral lobule
35 Flocculus
36 Choroid plexus and lateral aperture of the fourth ventricle (foramen of Luschka)

A

B

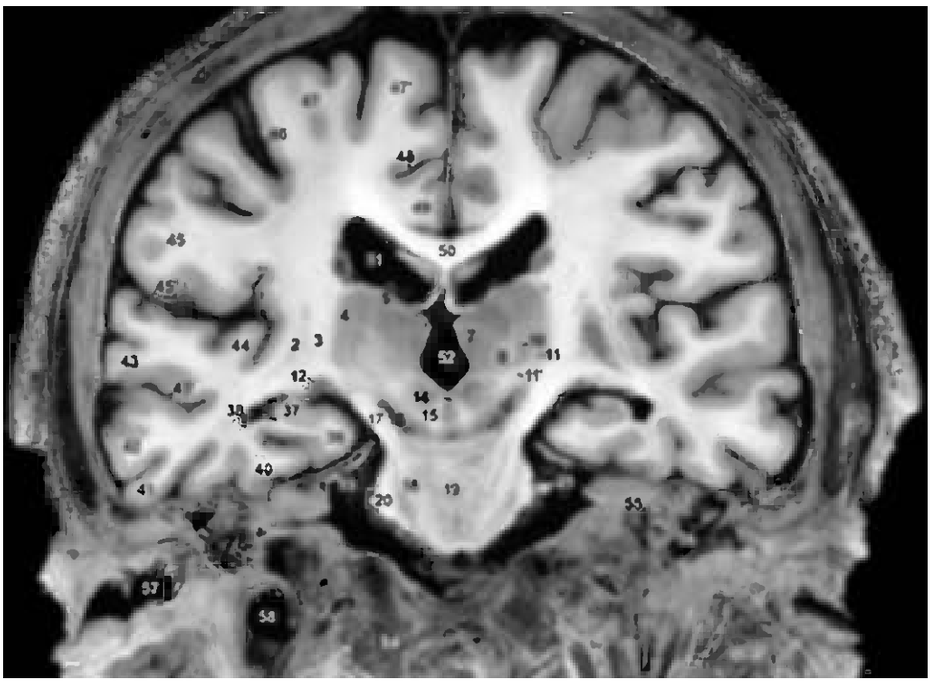

C

Fig. 11.40 (C–E).
C. Coronal section of the head. Anterior view. Bar: 10 mm.
D–E. 3 Tesla MRI. D. T1-weighted MRI. **E.** T2-weighted MRI

1 Caudate nucleus
2 Caudatolenticular bridges of gray matter (bridges of gray matter linking caudate nucleus with putamen)
3 Internal capsule, retrolenticular portion
4 Lateral posterior thalamic nucleus
5 Lateral dorsal thalamic nucleus
7 Dorsomedial thalamic nucleus
9 Centromedian thalamic nucleus
10 Ventral posteromedial thalamic nucleus
11 Ventral posterolateral thalamic nucleus
11′ Medial lemniscus
12 Lateral geniculate body
12′ Medial geniculate body
14 Red nucleus (posterior pole)
15 Superior cerebellar peduncle (brachium conjunctivum)
16 Substantia nigra
17 Crus cerebri
18 Corticospinal tract
19 Pontine nuclei
20 Middle cerebellar peduncle (brachium pontis)
21 Trigeminal nerve (CN V)
37 Hippocampus (body)
38 Temporal horn of the lateral ventricle
39 Parahippocampal gyrus
40 Fusiform gyrus
41 Inferior temporal gyrus
42 Middle temporal gyrus
43 Superior temporal gyrus
43′ Superior temporal sulcus (parallel sulcus)
44 Transverse temporal gyrus (of Heschl)
45 Postcentral gyrus
45′ Lateral fissure (Sylvian fissure)
46 Central sulcus
47 Precentral gyrus
47′ Superior frontal gyrus
48 Cingulate sulcus
49 Cingulate gyrus
50 Corpus callosum
51 Lateral ventricle
52 Third ventricle
53 Tentorium cerebelli
54 Occipital condyle
55 Internal ear
55′ Internal auditory meatus
56 Middle ear
57 External acoustic meatus
58 Internal jugular vein
59 Foramen cecum of the interpeduncular fossa (the deepest, most posterior portion)

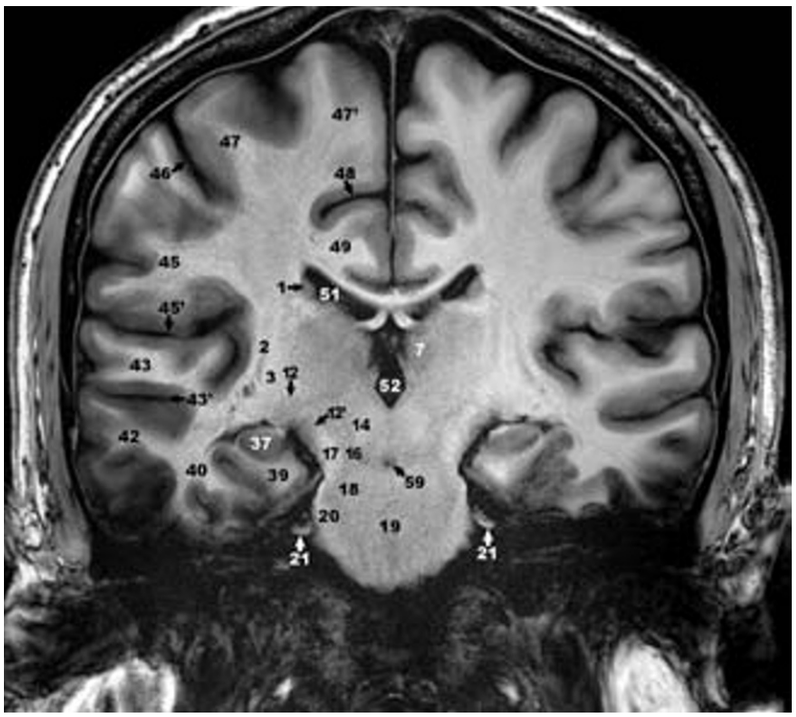
47'
47
46
48
49
45
1
51
45'
2
7
43
3
52
43'
42
37
14
17
16
40
39
59
18
20
19
21
21

D

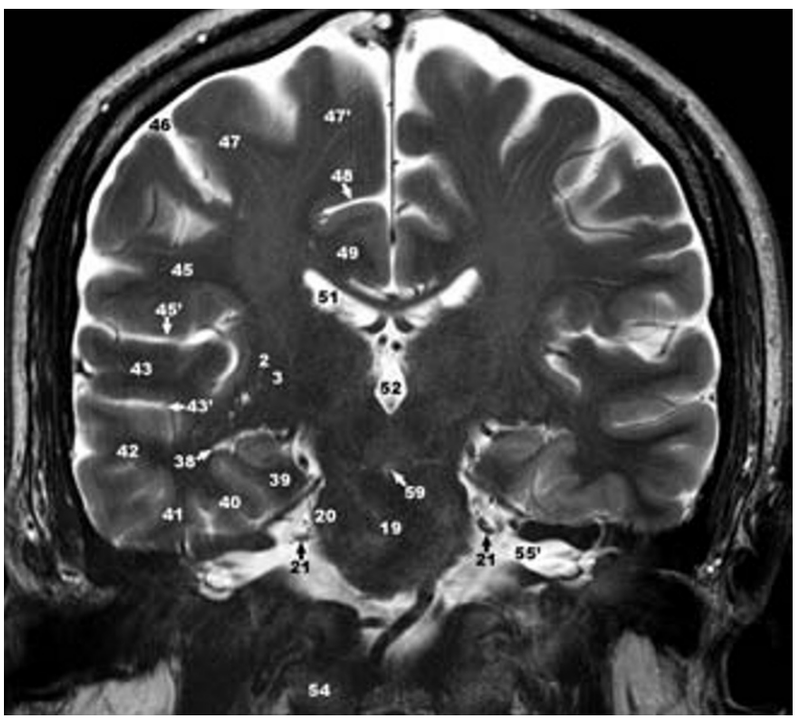
46
47
47'
48
49
45
51
45'
43
2
3
52
43'
42
38
39
59
40
41
20
19
21
21
55'
54

E

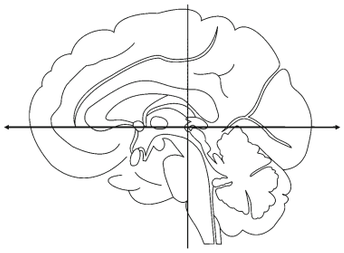

Fig. 11.41 A. Coronal (frontal) section.
A. Frontal view after removal of the cerebral hemispheres. Bar: 10 mm.

1 Caudate nucleus
2 Caudatolenticular bridges of gray matter
3 Internal capsule, retrolenticular portion
4 Lateral posterior thalamic nucleus
5 Lateral dorsal thalamic nucleus
6 Habenular nucleus
7 Posterior commissure
8 Habenulo-interpeduncular tract
9 Centromedian thalamic nucleus
10 Dorsomedial thalamic nucleus
11 Ventral posteromedial thalamic nucleus
12 Ventral posterolateral thalamic nucleus
13 Lateral geniculate body
14 Medial geniculate body
15 Medial lemniscus
16 Red nucleus (posterior pole)
17 Medial longitudinal fasciculus
18 Oculomotor nucleus (CN III)
19 Decussation of superior cerebellar peduncles
20 Crus cerebri
21 Substantia nigra
22 Pontocerebellar fibers and pontine nuclei
23 Middle cerebellar peduncle (brachium pontis)
24 Vestibulocochlear nerve (CN VIII)
25 Facial nerve (CN VII)
26 Medulla, pyramid (corticospinal tract)
27 Inferior olive
28 Quadrangular lobule
29 Anterior superior (primary) fissure
30 Simple lobule
31 Posterior superior fissure
32 Superior semilunar lobule
33 Great horizontal fissure
34 Inferior semilunar lobule
35 Prepyramidal fissure
36 Biventral lobule
37 Flocculus
38 Choroid plexus and lateral aperture of the fourth ventricle (foramen of Luschka)

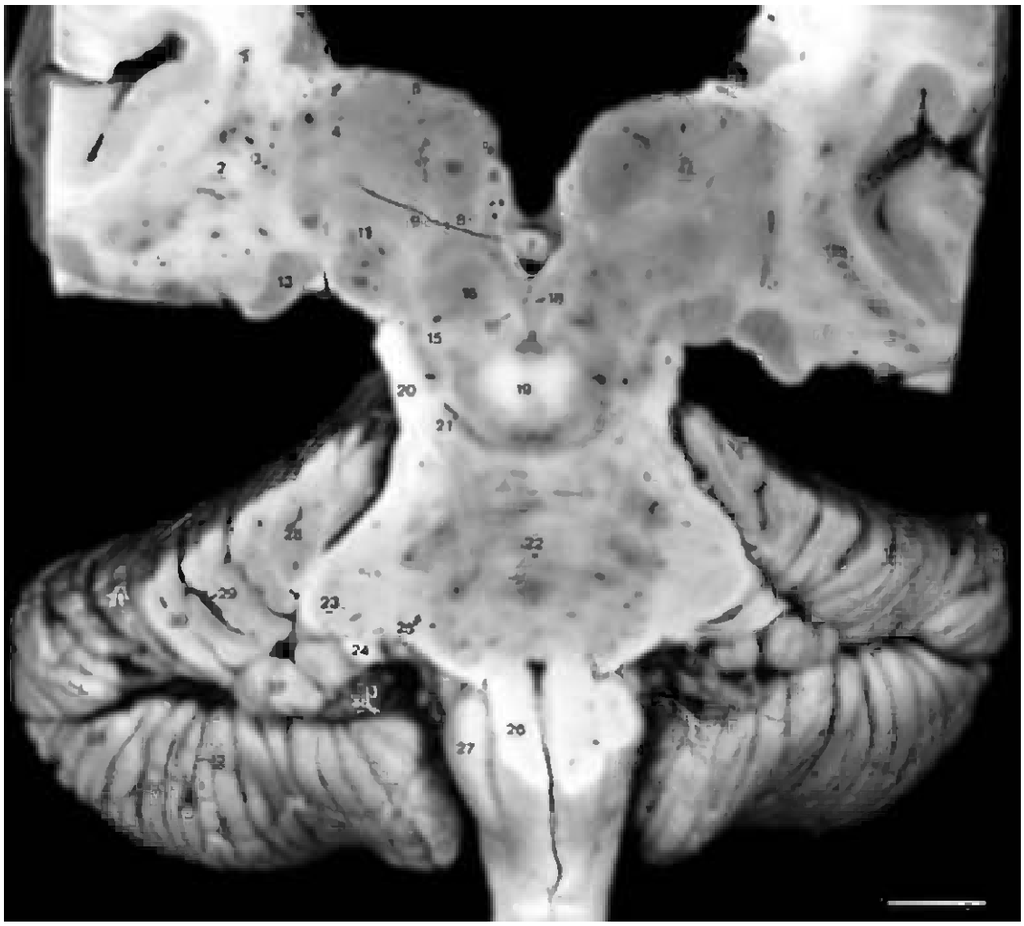

A

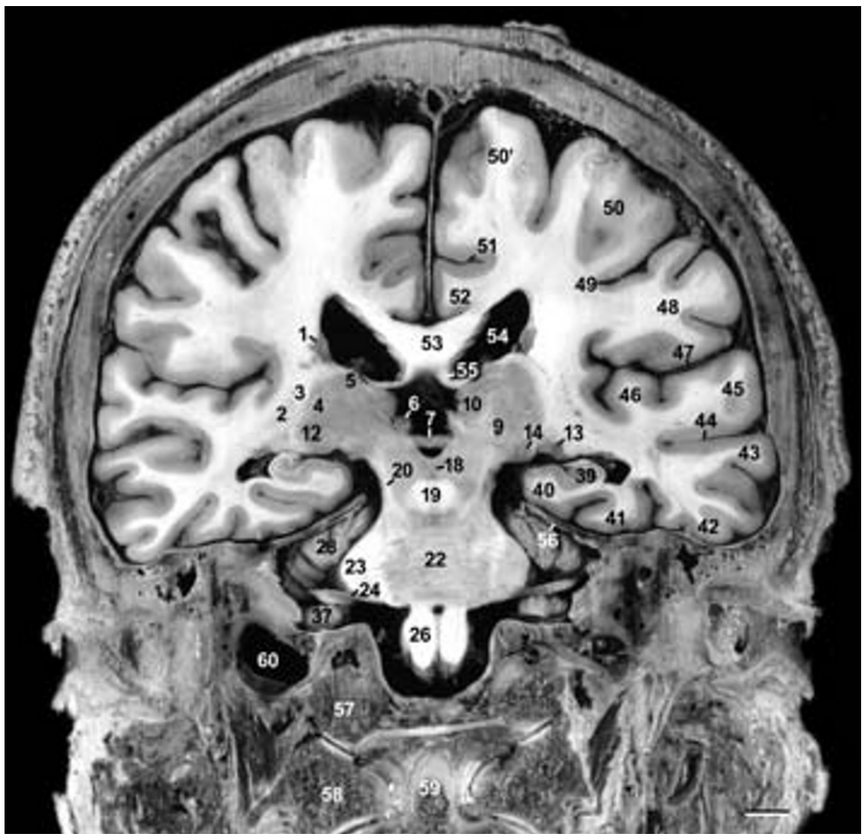

B

Fig. 11.41 (B–D).
B. Coronal section of the head. Anterior view. Bar: 10 mm.
C–D. 3 Tesla MRI. C. T1-weighted MRI. **D.** T2-weighted MRI.

1 Caudate nucleus
2 Caudatolenticular bridges of gray matter
3 Internal capsule, retrolenticular portion
4 Lateral posterior thalamic nucleus
5 Lateral dorsal thalamic nucleus
6 Habenular nucleus
7 Posterior commissure
9 Centromedian thalamic nucleus
10 Dorsomedial thalamic nucleus
12 Ventral posterolateral thalamic nucleus
13 Lateral geniculate body
14 Medial geniculate body
18 Oculomotor nucleus (CN III)
19 Decussation of superior cerebellar peduncles
20 Crus cerebri
22 Pontocerebellar fibers and pontine nuclei
23 Middle cerebellar peduncle (brachium pontis)
24 Vestibulocochlear nerve (CN VIII)
26 Medulla, pyramid (corticospinal tract)
28 Quadrangular lobule
37 Flocculus
39 Hippocampus, body
40 Parahippocampal gyrus
41 Fusiform gyrus
42 Inferior temporal gyrus
43 Middle temporal gyrus
44 Superior temporal sulcus (parallel sulcus)
45 Superior temporal gyrus
46 Transverse temporal gyrus (of Heschl)
47 Lateral fissure
48 Postcentral gyrus
49 Central sulcus
50 Precentral gyrus
50′ Superior frontal gyrus
51 Cingulate sulcus
52 Cingulate gyrus
53 Corpus callosum
54 Lateral ventricle
55 Fornix
56 Tentorium cerebelli
57 Occipital condyle
58 Atlas, lateral mass
59 Dens of axis
60 Sigmoid sinus

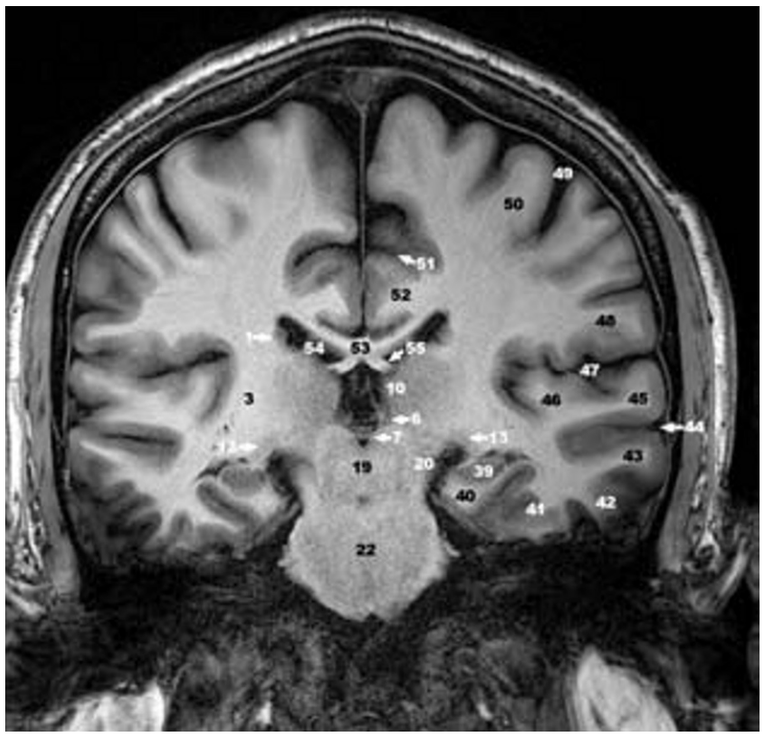
49
50
51
52
48
1
54
53
55
47
10
3
46
45
6
44
7
13
12
43
19
20
39
40
41
42
22

C

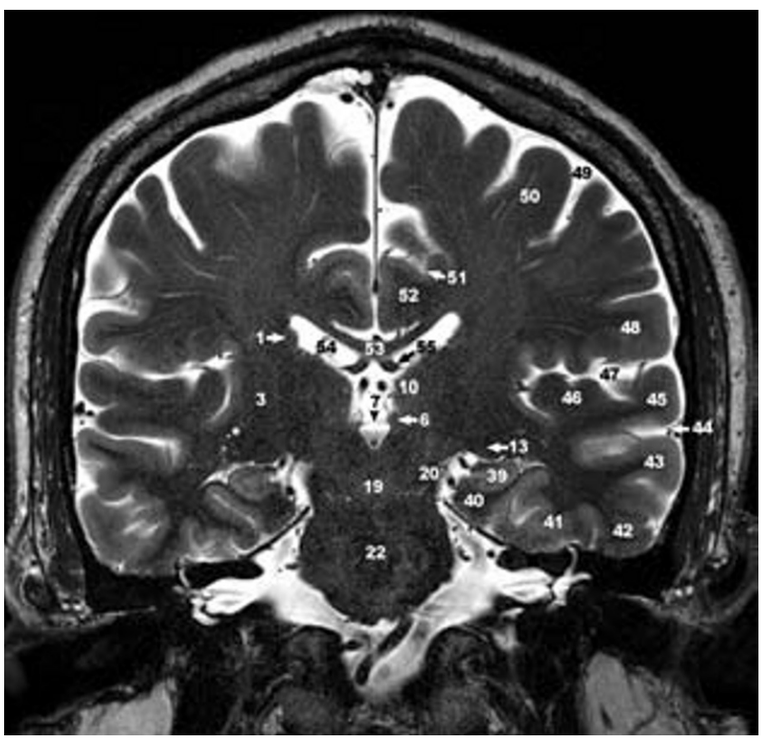
49
50
51
52
48
1
54
53
55
47
10
3
7
46
45
6
44
13
43
20
39
19
40
41
42
22

D

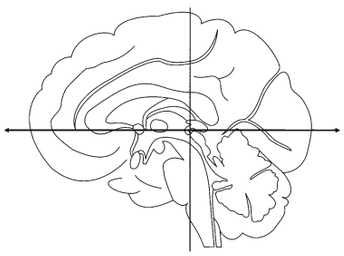

Fig. 11.42 A. Coronal (frontal) section.
A. Frontal view after removal of the cerebral hemispheres. Bar: 10 mm.

1 Caudate nucleus
2 Caudatolenticular bridges of gray matter
3 Stria terminalis
4 Pulvinar, medial nucleus
5 Pulvinar, lateral nucleus
6 Medial geniculate body
7 Brachium of the superior colliculus
8 Pretectal area
9 Superior colliculus
10 Posterior commissure
11 Cerebral aqueduct
12 Periaqueductal gray matter
13 Brachium of the inferior colliculus
14 Trochlear nerve nucleus (CN IV)
15 Dorsal nucleus of raphe
16 Medial longitudinal fasciculus
17 Lateral lemniscus
18 Superior cerebellar peduncle (brachium conjunctivum)
19 Nucleus reticularis centralis superior
20 Nucleus reticularis tegmenti pontis
21 Medial lemniscus
22 Pontine nuclei
23 Middle cerebellar peduncle (brachium pontis)
24 Nucleus raphe magnus
25 Inferior olivary nucleus
26 Corticospinal tract (pyramid of medulla)
27 Ala of the central lobule
28 Quadrangular lobule
29 Anterior superior (primary) fissure
30 Simple lobule
31 Posterior superior fissure
32 Superior semilunar lobule
33 Great horizontal fissure
34 Inferior semilunar lobule
35 Prepyramidal fissure
36 Biventral lobule
37 Flocculus
38 Lateral aperture of the fourth ventricle (foramen of Luschka)

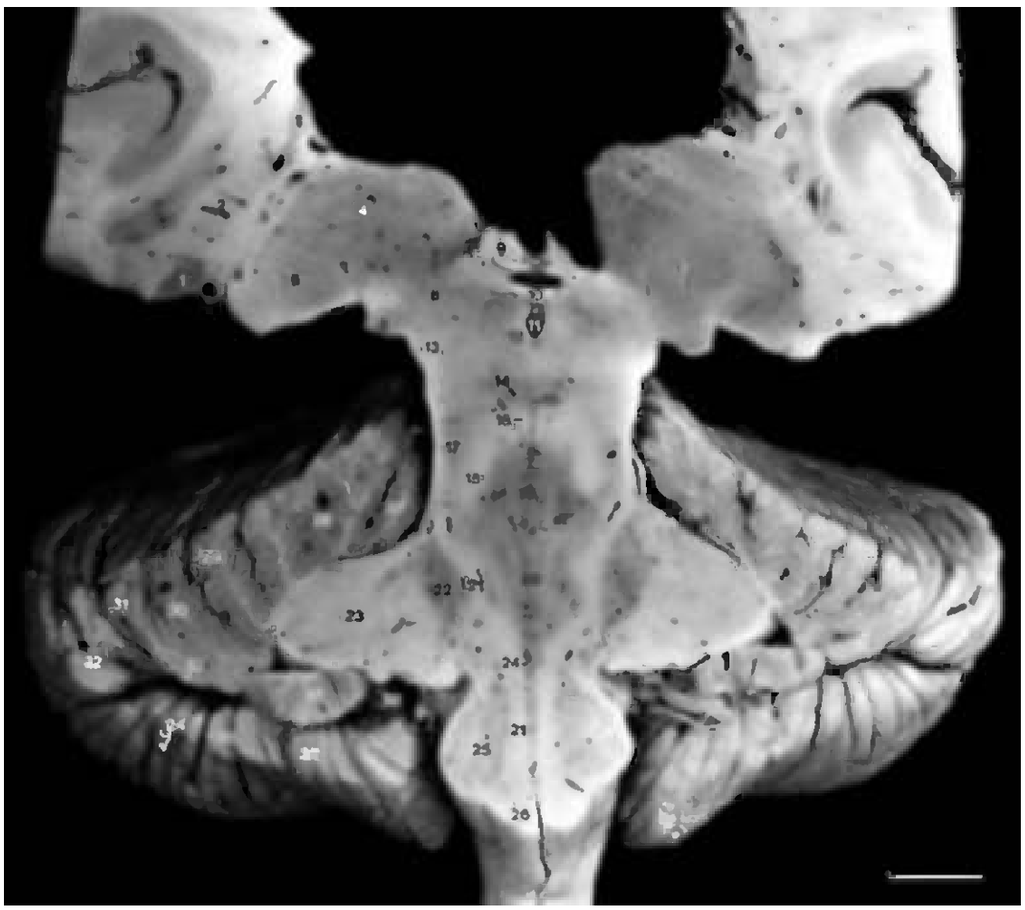

A

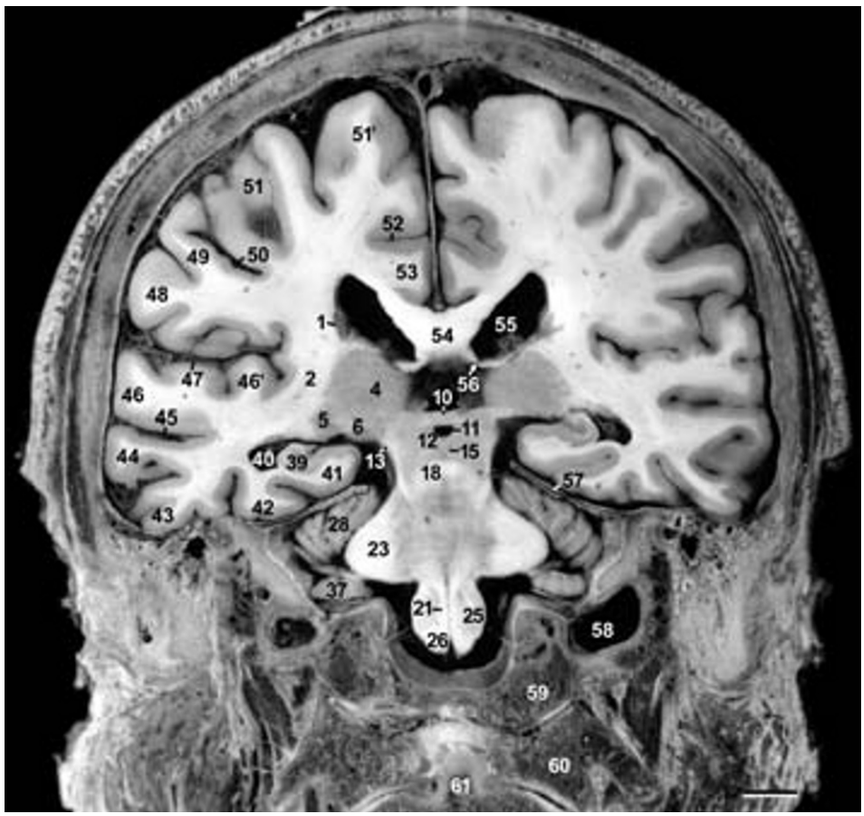

B

Fig. 11.42 (B–D).
B. Coronal section of the head. Posterior view. Bar: 10 mm.
C–D. 3 Tesla MRI. C. T1-weighted MRI. **D.** T2-weighted MRI.

1 Caudate nucleus
2 Caudatolenticular bridges of gray matter
4 Pulvinar, medial nucleus
5 Lateral geniculate body
6 Medial geniculate body
10 Posterior commissure
11 Cerebral aqueduct
12 Periaqueductal gray matter
13 Brachium of the inferior colliculus
15 Dorsal nucleus of raphe
18 Superior cerebellar peduncle (brachium conjunctivum)
21 Medial lemniscus
23 Middle cerebellar peduncle (brachium pontis)
25 Inferior olivary nucleus
26 Corticospinal tract (pyramid of medulla)
28 Quadrangular lobule
37 Flocculus
39 Hippocampus (body)
40 Temporal horn of the lateral ventricle
41 Parahippocampal gyrus
42 Fusiform gyrus
43 Inferior temporal gyrus
44 Middle temporal gyrus
45 Superior temporal sulcus (parallel sulcus)
46 Superior temporal gyrus
46′ Transverse temporal gyrus (of Heschl)
47 Lateral fissure (Sylvian fissure)
48 Supramarginal gyrus
49 Postcentral gyrus
50 Central sulcus
51 Precentral gyrus
51′ Superior frontal gyrus
52 Cingulate sulcus
53 Cingulate gyrus
54 Corpus callosum
55 Lateral ventricle
56 Fornix
57 Tentorium cerebelli
58 Sigmoid sinus
59 Occipital condyle
60 Atlas, lateral mass
61 Dens of axis
62 Internal cerebral veins

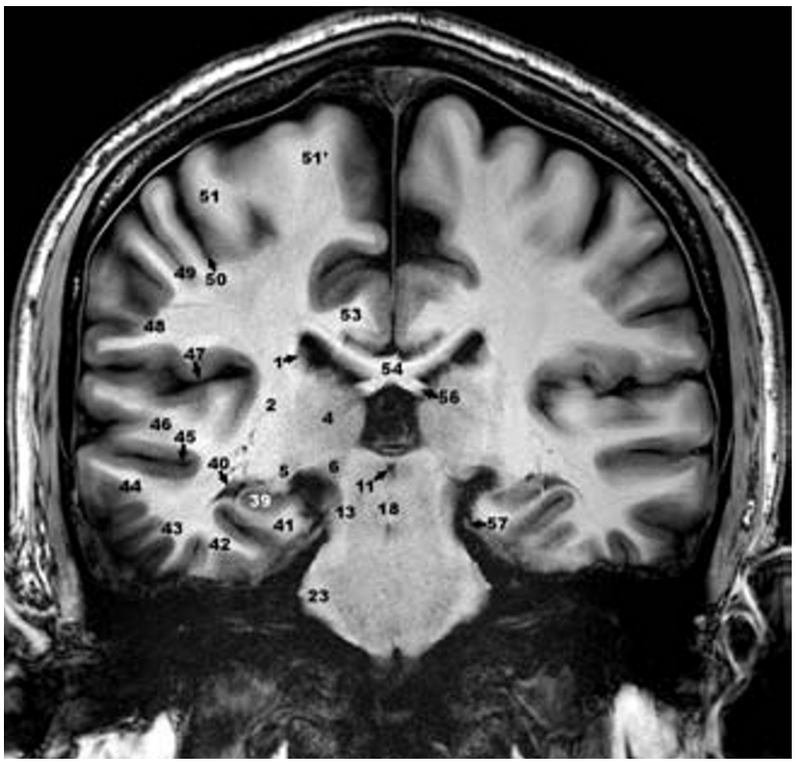
51'
51
49
50
48
53
47
1
54
56
2
4
46
45
40
5
6
11
44
39
13
18
43
41
57
42
23

C

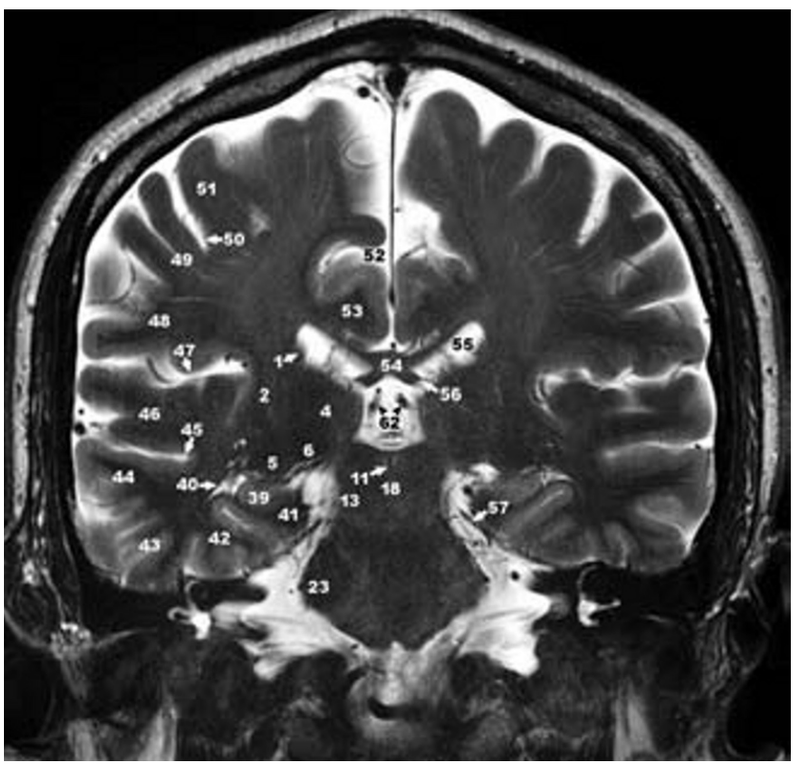
51
50
49
52
53
48
55
47
1
54
56
2
4
62
46
45
5
6
44
40
11
18
39
13
41
57
43
42
23

D

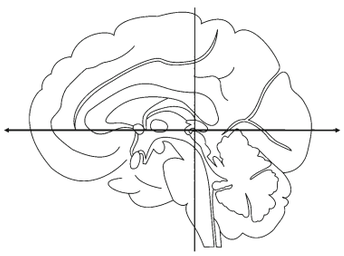

Fig. 11.43 (A–B). Coronal (frontal) section.
A. Frontal view after removal of the cerebral hemispheres. Bar: 10 mm.
B. Superior oblique view.

1 Brachium of the superior colliculus
2 Superior colliculus
3 Brachium of the inferior colliculus
4 Periaqueductal gray matter
5 Cerebral aqueduct
6 Lateral lemniscus
7 Superior cerebellar peduncle (brachium conjunctivum)
8 Medial longitudinal fasciculus
9 Central tegmental tract
10 Nucleus raphe magnus
11 Medial lemniscus
12 Superior olivary nucleus
13 Inferior olivary nucleus
14 Corticospinal tract (pyramid of medulla)
15 Ala of central lobule
16 Quadrangular lobule
16′ Culmen
17 Anterior superior (primary) fissure
18 Simple lobule
19 Posterior superior fissure
20 Superior semilunar lobule
21 Great horizontal fissure
22 Inferior semilunar lobule
23 Prepyramidal fissure
24 Biventral lobule
25 Flocculus
26 Lateral aperture of the fourth ventricle (foramen of Luschka)
27 Glossopharyngeal nerve (CN IX)
28 Vagus nerve (CN X)
29 Middle cerebellar peduncle (brachium pontis)

A

B

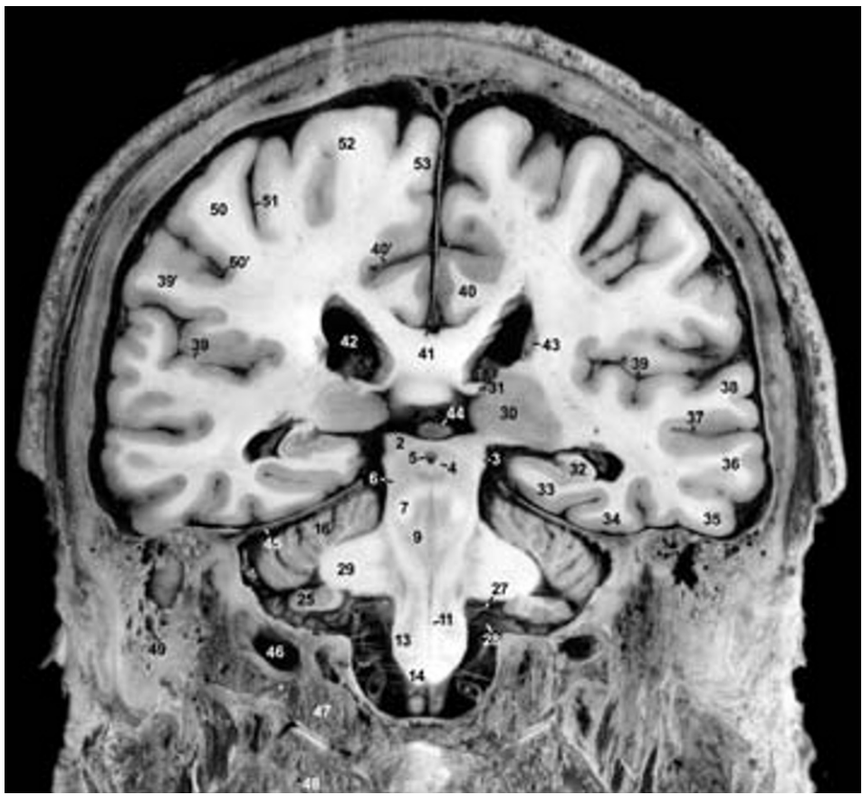

C

Fig. 11.43 (C–E).
C. Coronal section of the head. Anterior view. Bar: 10 mm.
D–E. 3 Tesla MRI. D. T1-weighted MRI. **E.** T2-weighted MRI.

2 Superior colliculus
3 Brachium of the inferior colliculus
4 Periaqueductal gray matter
5 Cerebral aqueduct
6 Lateral lemniscus
7 Superior cerebellar peduncle (brachium conjunctivum)
9 Central tegmental tract
11 Medial lemniscus
13 Inferior olivary nucleus
14 Corticospinal tract (pyramid of medulla)
16 Quadrangular lobule
25 Flocculus
27 Glossopharyngeal nerve (CN IX)
28 Vagus nerve (CN X)
29 Middle cerebellar peduncle (brachium pontis)
30 Pulvinar
31 Crus fornicis
32 Hippocampus (tail)
33 Parahippocampal gyrus
34 Fusiform gyrus
35 Inferior temporal gyrus
36 Middle temporal gyrus
37 Superior temporal sulcus (parallel sulcus)
38 Superior temporal gyrus
39 Lateral fissure (Sylvian fissure)
39′ Supramarginal gyrus
40 Cingulate gyrus
40′ Cingulate sulcus
41 Corpus callosum
42 Lateral ventricle (atrium)
43 Caudate nucleus
44 Pineal gland
44′ Internal cerebral veins
45 Tentorium cerebelli
46 Sigmoid sinus
47 Occipital condyle
48 Atlas, lateral mass
49 Mastoid process
50 Postcentral gyrus
50′ Postcentral sulcus
51 Central sulcus
52 Precentral gyrus
53 Superior frontal gyrus

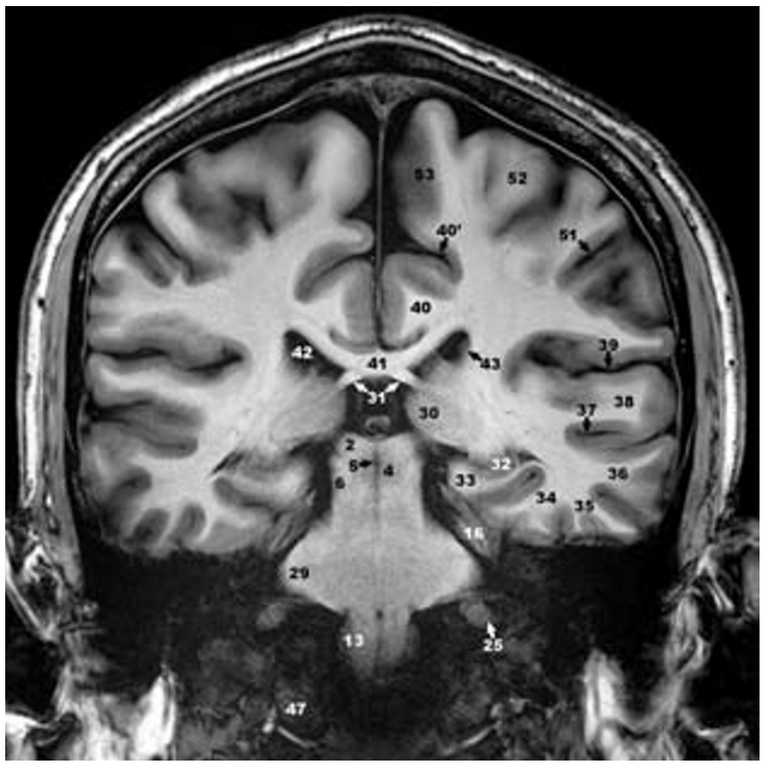
53
52
40'
51
40
39
42
41
43
31
30
37
38
2
5
4
32
33
36
34
35
6
16
29
13
25
47

D

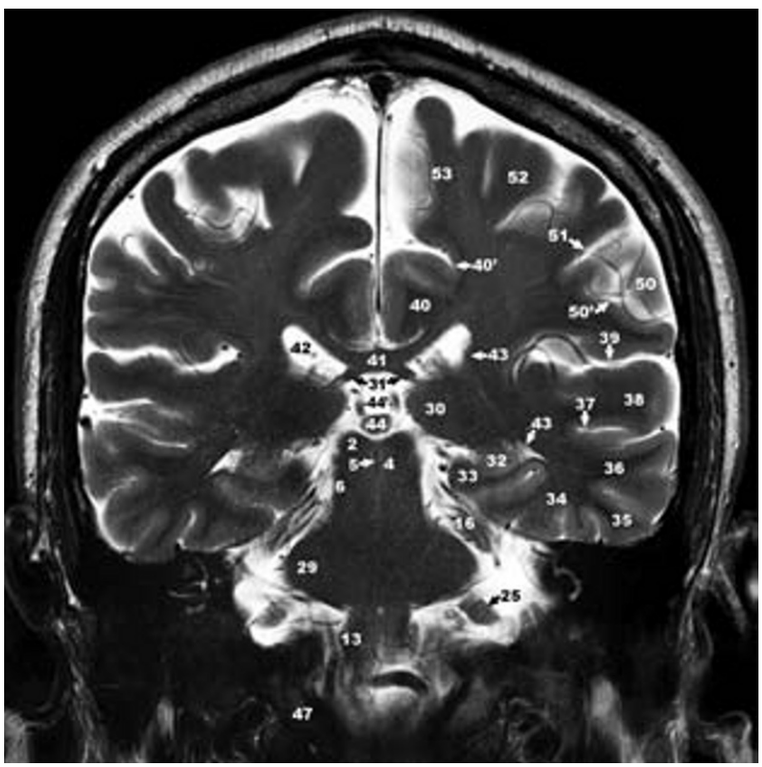
53
52
51
40'
50
40
50'
39
42
41
43
31
44'
44
30
37
38
43
2
5
4
32
33
36
34
6
16
35
29
25
13
47

E

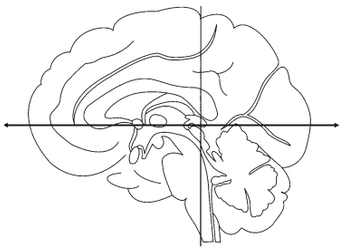

Fig. 11.44 (A–C). Coronal (frontal) section.
A. Frontal view after removal of the cerebral hemispheres. Bar: 10 mm.
B. Superior view. **C.** Inferior oblique view.

1 Superior colliculus
2 Inferior colliculus
3 Cerebral aqueduct
4 Superior cerebellar peduncle (brachium conjunctivum)
5 Nucleus ceruleus
6 Medial parabrachial nucleus
7 Medial longitudinal fasciculus
8 Nucleus reticularis pontis oralis
9 Nucleus reticularis pontis caudalis
10 Principal sensory trigeminal nucleus (CN V)
11 Spinal trigeminal tract
12 Middle cerebellar peduncle (brachium pontis)
12′ Parabrachial recess
13 Ventral cochlear nucleus (CN VIII)
14 Nucleus reticularis gigantocellularis
15 Medial lemniscus
16 Inferior olivary nucleus
17 Corticospinal tract (pyramid of the medulla)
18 Ala of central lobule
19 Quadrangular lobule
19′ Culmen
20 Anterior superior (primary) fissure
21 Simple lobule
22 Posterior superior fissure
23 Superior semilunar lobule
24 Great horizontal fissure
25 Inferior semilunar lobule
26 Gracile lobule
27 Prepyramidal fissure
28 Biventral lobule
29 Flocculus
30 Lateral aperture of the fourth ventricle (foramen of Luschka)
31 Vagus nerve

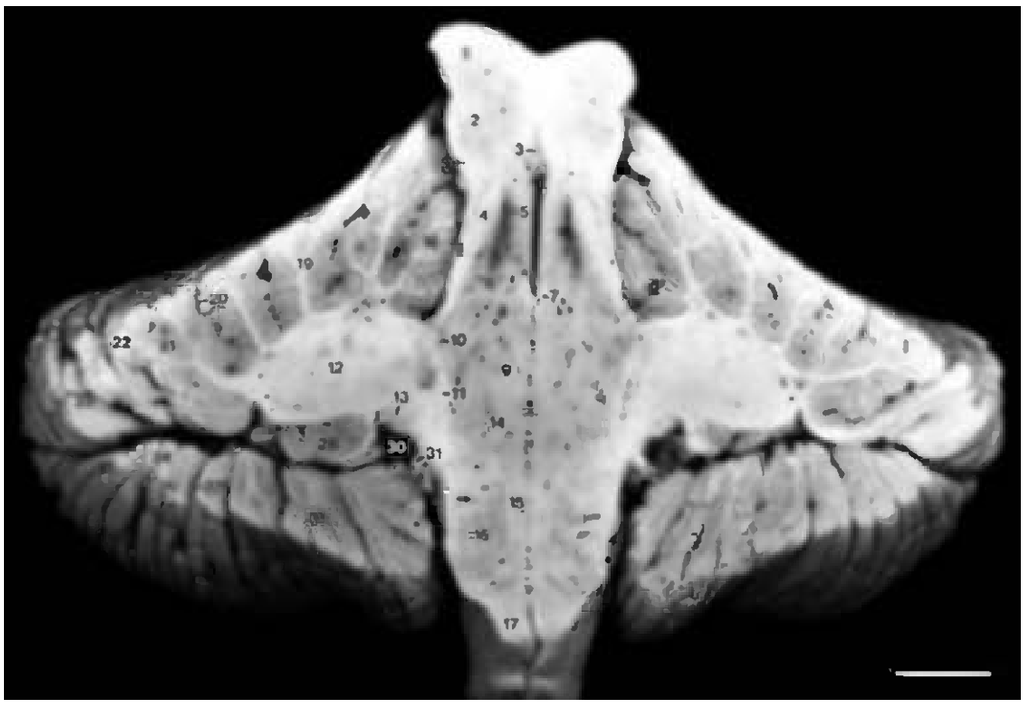
2
3
4
5
7
9
10
11
12
13
14
15
16
17
19
20
22
30
31

A

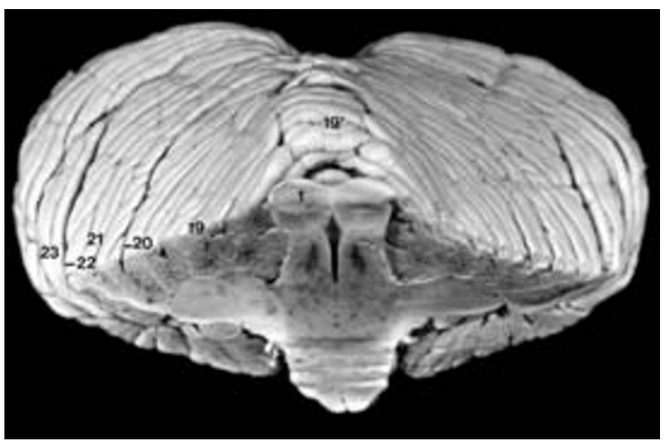
19
19
20
21
22
23

B


23
24
25
26
27
28
28
16
17

C

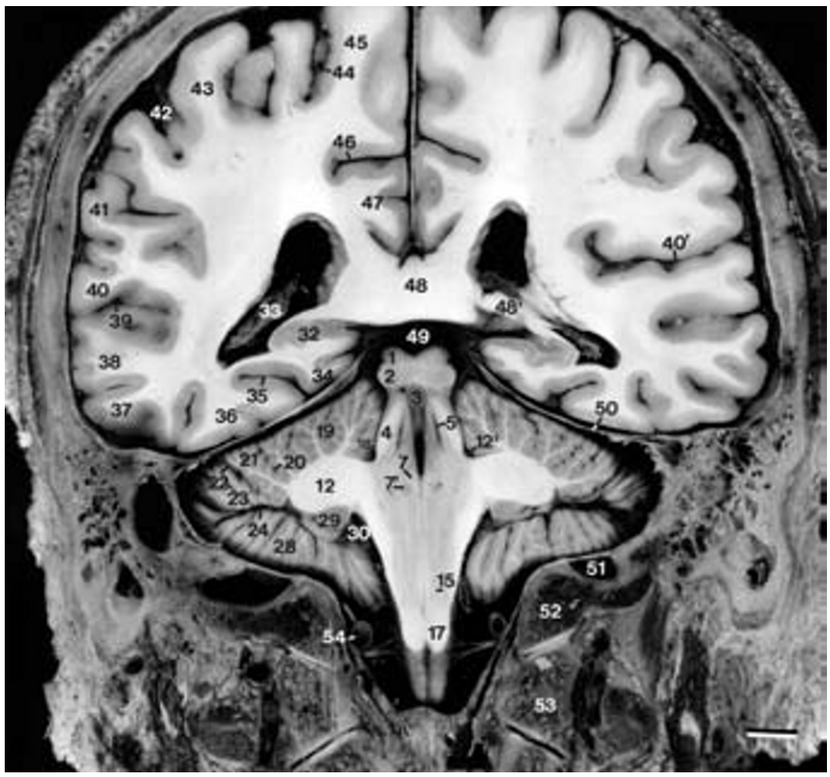

D

Fig. 11.44 (D–F).
D. Coronal section of the head. Anterior view. Bar: 10 mm.
E–F. 3 Tesla MRI. E. T1-weighted MRI. **F.** T2-weighted MRI.

1 Superior colliculus
2 Inferior colliculus
3 Cerebral aqueduct (of Sylvius)
4 Superior cerebellar peduncle (brachium conjunctivum)
5 Nucleus ceruleus (Locus ceruleus)
7 Medial longitudinal fasciculus
7′ Abducens nucleus (CN VI)
12 Middle cerebellar peduncle (brachium pontis)
12′ Parabrachial recess
15 Medial lemniscus
17 Corticospinal tract (pyramid of medulla)
18 Ala of central lobule
19 Quadrangular lobule
20 Anterior superior (primary) fissure
21 Simple lobule
22 Posterior superior fissure
23 Superior semilunar lobule
24 Great horizontal fissure
25 Inferior semilunar lobule
28 Biventral lobule
29 Flocculus
30 Lateral aperture of the fourth ventricle (foramen of Luschka)
32 Hippocampus (tail)
33 Atrium of the lateral ventricle
34 Parahippocampal gyrus
35 Collateral sulcus
36 Fusiform gyrus
37 Inferior temporal gyrus
38 Middle temporal gyrus
39 Superior temporal sulcus (parallel sulcus)
40 Superior temporal gyrus
40′ Lateral fissure (Sylvian fissure)
41 Supramarginal gyrus
42 Intraparietal sulcus
43 Postcentral gyrus
44 Central sulcus
45 Precentral gyrus
46 Cingulate sulcus
47 Cingulate gyrus
48 Splenium
48′ Crus fornicis
49 Quadrigeminal cistern
50 Tentorium cerebelli
51 Sigmoid sinus
52 Occipital condyle
53 Atlas, lateral mass
54 Vertebral artery on each side
55 Internal cerebral vein

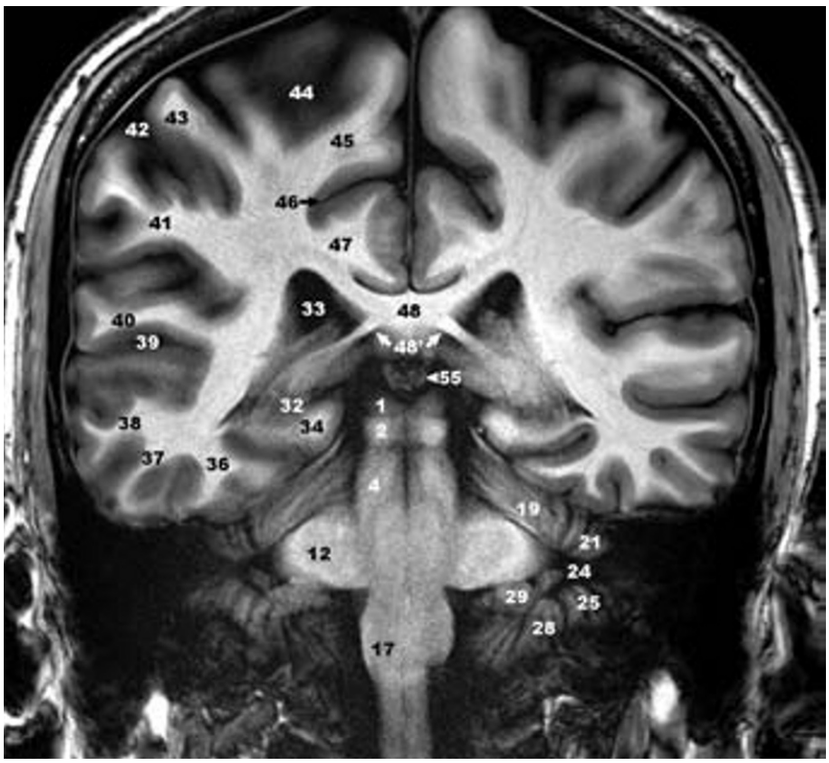
44
42
43
45
46
41
47
33
48
40
39
48'
55
32
1
38
34
2
37
36
4
19
21
12
24
29
25
28
17

E

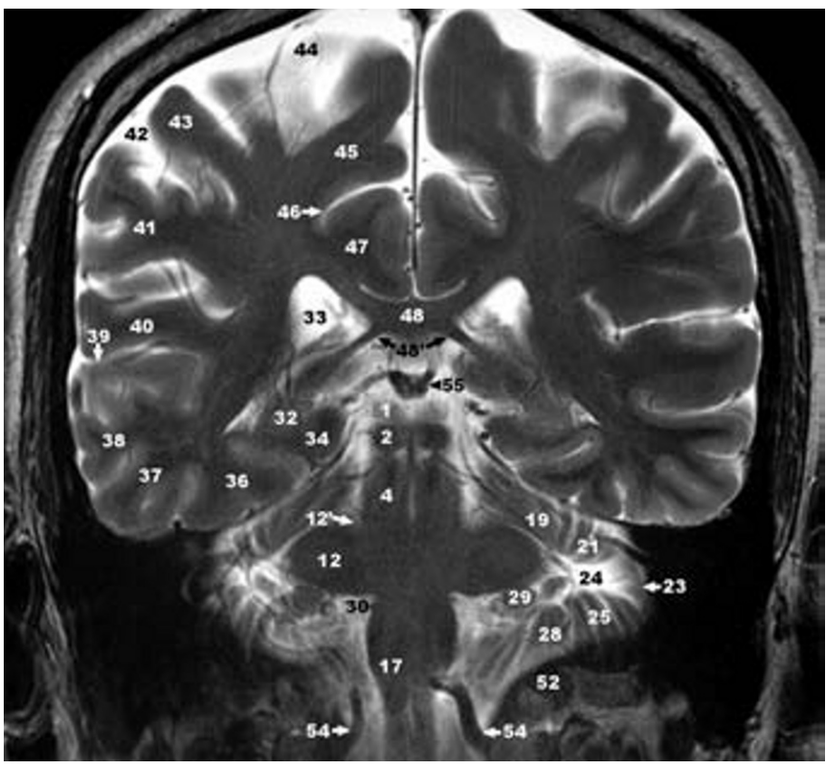
44
42
43
45
46
41
47
33
48
39
40
48'
55
1
32
38
34
2
37
36
4
12'
19
21
12
24
23
30
29
25
28
17
52
54
54

F

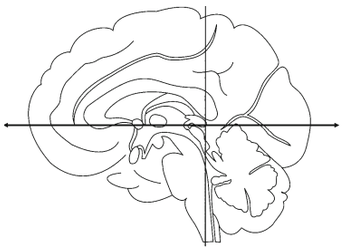

Fig. 11.45 (A–C). Coronal (frontal) section.
A. Frontal view after removal of the cerebral hemispheres. Bar: 10 mm.
B. Superior oblique view. **C.** Inferior oblique view.

1 Inferior colliculus
2 Frenulum veli
3 Superior medullary velum
4 Superior cerebellar peduncle (brachium conjunctivum)
5 Fourth ventricle
6 Medial parabrachial nucleus
7 Superior vestibular nucleus (CN VIII)
8 Middle cerebellar peduncle (brachium pontis)
8′ Parabrachial recess
9 Principal sensory trigeminal nucleus (CN V)
10 Nucleus reticularis pontis caudalis
11 Medial longitudinal fasciculus
12 Dorsal cochlear nucleus (acoustic tubercle) (CN VIII)
13 Inferior cerebellar peduncle (restiform body)
14 Nucleus reticularis gigantocellularis
15 Spinal trigeminal tract
16 Nucleus reticularis medullae oblongatae centralis
17 Decussation of corticospinal tract
18 Spinothalamic tract
19 Ala of central lobule
20 Quadrangular lobule
20′ Culmen
21 Anterior superior (primary) fissure
22 Simple lobule
23 Posterior superior fissure
24 Superior semilunar lobule
25 Great horizontal fissure
26 Inferior semilunar lobule
27 Gracile lobule
28 Prepyramidal fissure
29 Biventral lobule
30 Flocculus
31 Lateral aperture of the fourth ventricle (foramen of Luschka)

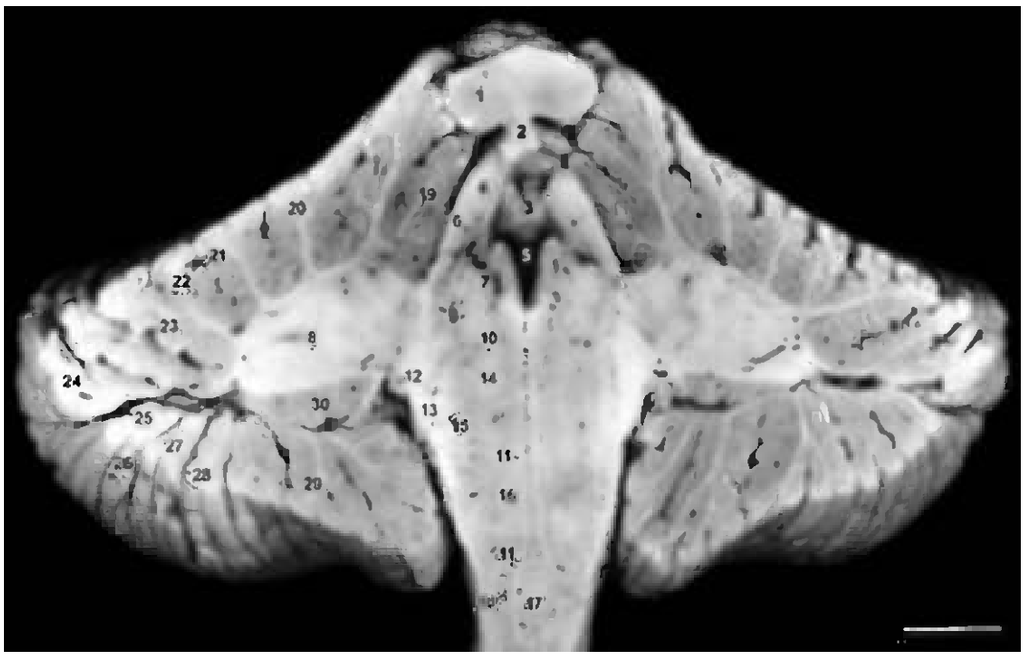
1
2
19
20
21
22
23
24
25
27
28
8
10
12
14
30
13
15
11
16
17

A

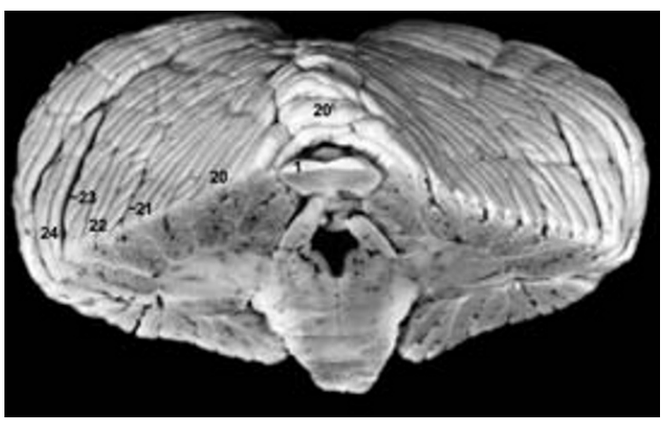
20
20
23
21
24
22

B

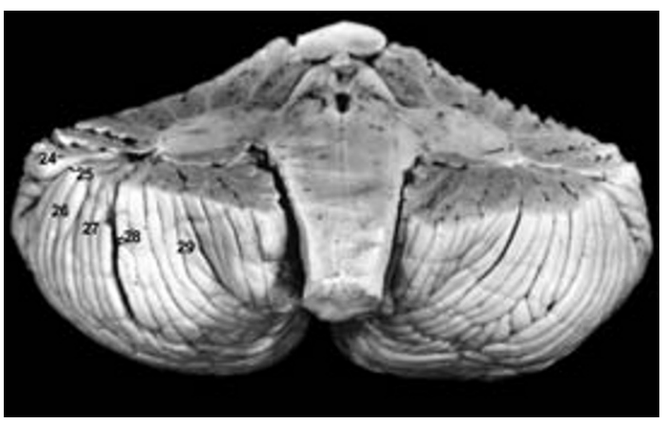
24
25
26
27
28
29

C

D

Fig. 11.45 (D–E). 3 Tesla MRI.
D. T1-weighted MRI. **E.** T2-weighted MRI

1 Inferior colliculus
4 Superior cerebellar peduncle (brachium conjunctivum)
5 Fourth ventricle
8 Middle cerebellar peduncle (brachium pontis)
8′ Parabrachial recess
13 Inferior cerebellar peduncle (restiform body)
19 Ala of central lobule
20 Quadrangular lobule
21 Anterior superior (primary) fissure
22 Simple lobule
25 Great horizontal fissure
26 Inferior semilunar lobule
27 Gracile lobule
28 Prepyramidal fissure
29 Biventral lobule
30 Flocculus
32 Splenium
33 Hippocampus, tail
34 Fusiform gyrus
35 Inferior temporal gyrus
36 Middle temporal gyrus
37 Superior temporal gyrus
37′ Superior temporal sulcus (parallel sulcus)
38 Supramarginal gyrus
39 Intraparietal sulcus
40 Postcentral gyrus
41 Precentral gyrus
42 Cingulate sulcus
43 Cingulate gyrus
44 Lateral ventricle, atrium
45 Internal cerebral vein


41
40
39
42
38
43
38'
44
32
37
37'
45
33
36
34
21
35
20
19
4
5
8'
22
8
25
30
26
27
13
29
28

E

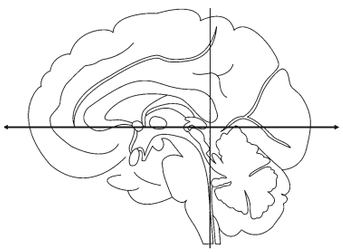

Fig. 11.46 (A–B). Coronal (frontal) section.
A. Frontal view after removal of the cerebral hemispheres. Bar: 10 mm.
B. Inferior oblique view.

1 Superior medullary velum
2 Superior cerebellar peduncle (brachium conjunctivum)
2′ Fourth ventricle
3 Middle cerebellar peduncle (brachium pontis)
4 Inferior cerebellar peduncle (restiform body)
5 Lateral vestibular nucleus (CN VIII)
6 Medial vestibular nucleus (CN VIII)
7 Abducens nucleus (CN VI)
8 Medial longitudinal fasciculus
9 Nucleus reticularis gigantocellularis
10 Spinal trigeminal tract (CN V)
11 Nucleus reticularis medullae oblongatae centralis
12 Nucleus reticularis lateralis (nucleus funiculi lateralis)
13 Spinothalamic tract
14 Hypoglossal nucleus (CN XII)
15 Ala of the central lobule
15′ Central lobule
16 Postcentral fissure
17 Quadrangular lobule
17′ Culmen
18 Anterior superior (primary) fissure
19 Simple lobule
20 Posterior superior fissure
21 Superior semilunar lobule
22 Great horizontal fissure
23 Inferior semilunar lobule
24 Gracile lobule
25 Prepyramidal fissure
26 Biventral lobule
27 Flocculus
28 Lateral recess of the fourth ventricle

A

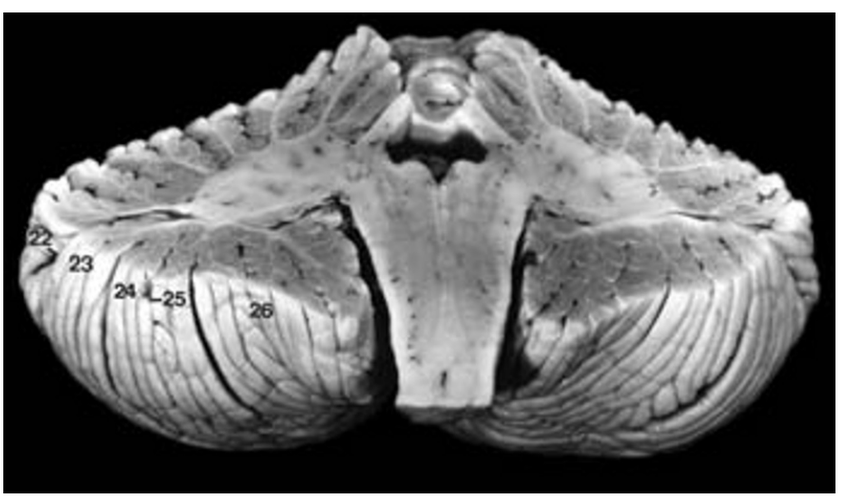

B

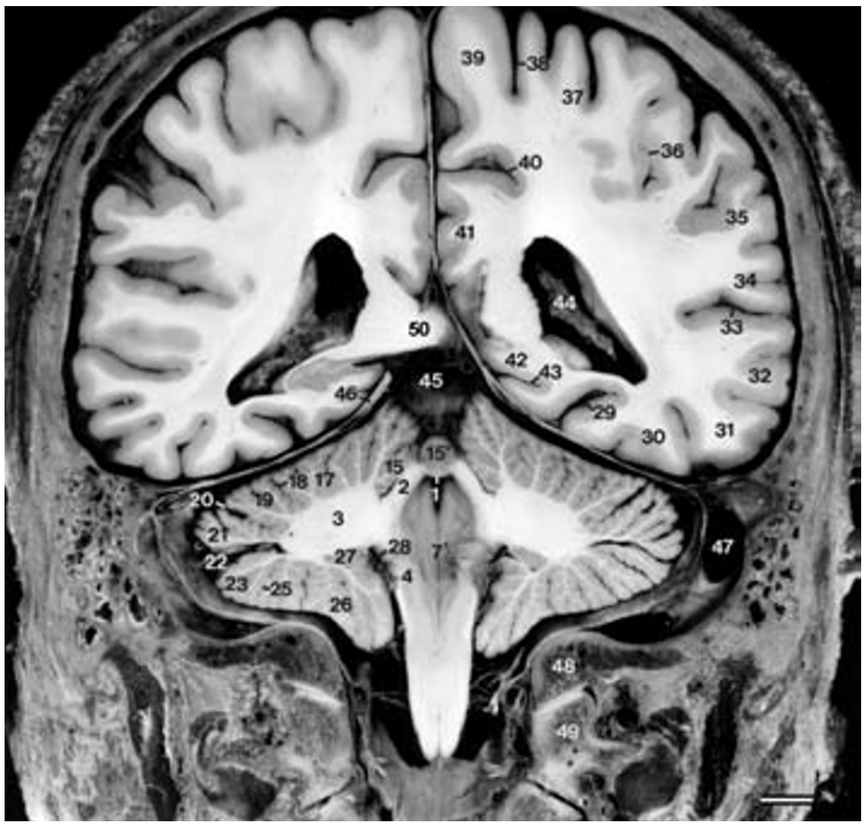

C

Fig. 11.46 (C–E).
C. Coronal section of the head. Posterior view. Bar: 10 mm.
D–E. 3 Tesla MRI. D. T1-weighted MRI. **E.** T2-weighted MRI.

1 Superior medullary velum
2 Superior cerebellar peduncle (brachium conjunctivum)
3 Middle cerebellar peduncle (brachium pontis)
4 Inferior cerebellar peduncle (restiform body)
7′ Floor of the fourth ventricle (rhomboid fossa)
15 Ala of the central lobule
15′ Central lobule
17 Quadrangular lobule
18 Anterior superior (primary) fissure
19 Simple lobule
20 Posterior superior fissure
21 Superior semilunar lobule
22 Great horizontal fissure
23 Inferior semilunar lobule
25 Prepyramidal fissure
26 Biventral lobule
27 Flocculus
28 Lateral recess of the fourth ventricle
29 Collateral sulcus
30 Fusiform gyrus
31 Inferior temporal gyrus
32 Middle temporal gyrus
33 Superior temporal sulcus (parallel sulcus)
34 Superior temporal gyrus
35 Supramarginal gyrus
36 Intraparietal sulcus
37 Postcentral gyrus
38 Central sulcus
39 Precentral gyrus
40 Cingulate sulcus
41 Cingulate gyrus
42 Isthmus of the cingulate gyrus
43 Anterior calcarine sulcus
44 Atrium
45 Quadrigeminal cistern
46 Tentorium cerebelli
47 Transverse sinus
48 Occipital condyle
49 Atlas, lateral mass
50 Splenium
51 Medial longitudinal striae (of Lancisi)

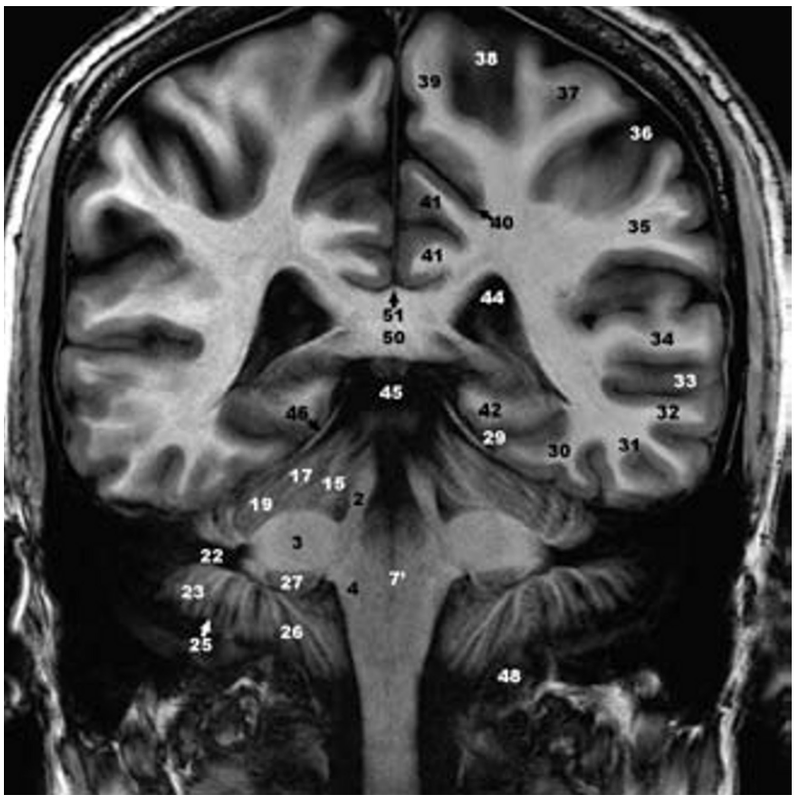
38
39
37
36
41
40
35
41
44
51
50
34
33
45
46
42
32
29
30
31
17
15
2
19
3
22
27
4
7'
23
25
26
48

D

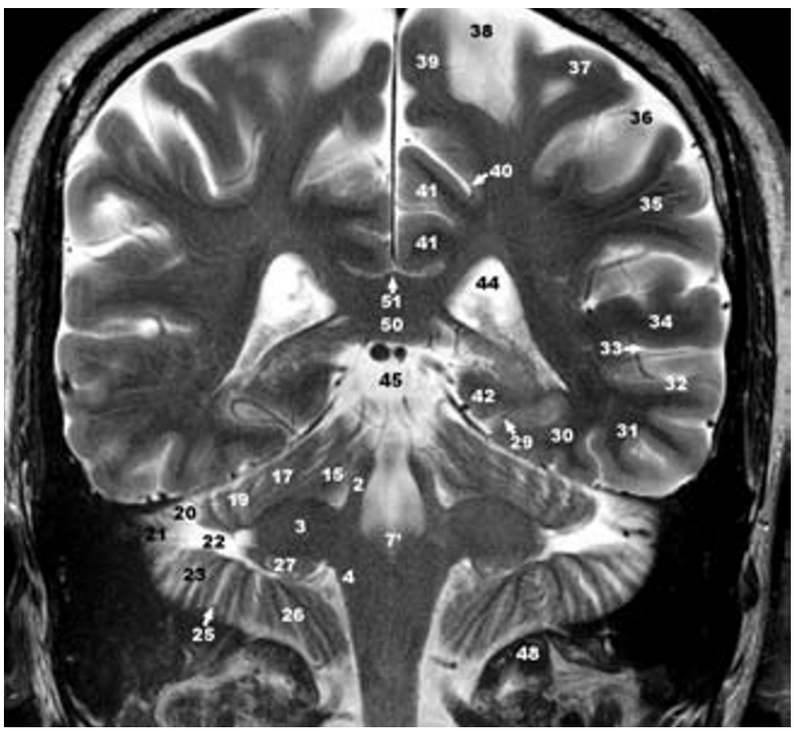
38
39
37
36
40
41
35
41
44
51
50
34
33
45
32
42
29
30
31
17
15
2
19
20
21
22
3
7'
27
4
23
25
26
48

E

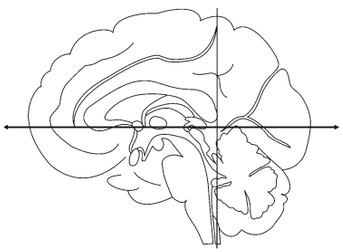

Fig. 11.47 (A–C). Coronal (frontal) section.
A. Frontal view after removal of the cerebral hemispheres. Bar: 10 mm.
B. Superior oblique view. **C.** Inferior oblique view.

1 Superior medullary velum
2 Superior cerebellar peduncle (brachium conjunctivum)
3 Middle cerebellar peduncle (brachium pontis)
4 Medial vestibular nucleus (CN VIII)
5 Vestibular descending root (CN VIII)
6 Inferior vestibular nucleus (CN VIII)
7 Inferior cerebellar peduncle (restiform body)
8 Dorsal motor nucleus of the vagus
9 Solitary tract surrounded by the nucleus of the solitary tract
10 Lateral cuneate nucleus
11 Hypoglossal nucleus (CN VII)
12 Nucleus reticularis medullae oblongatae centralis
13 Spinal tract and trigeminal nucleus (CN V)
14 Lingula
15 Ala of central lobule
15′ Central lobule
16 Postcentral fissure
17 Quadrangular lobule
17′ Culmen
18 Anterior superior (primary) fissure
19 Simple lobule
20 Posterior superior fissure
21 Superior semilunar lobule
22 Great horizontal fissure
23 Inferior semilunar lobule
24 Gracile lobule
25 Prepyramidal fissure
26 Biventral lobule
27 Brachium of the flocculus and inferior medullary velum
28 Lateral recess of the fourth ventricle
29 Ligula
30 Fourth ventricle
31 Nodulus

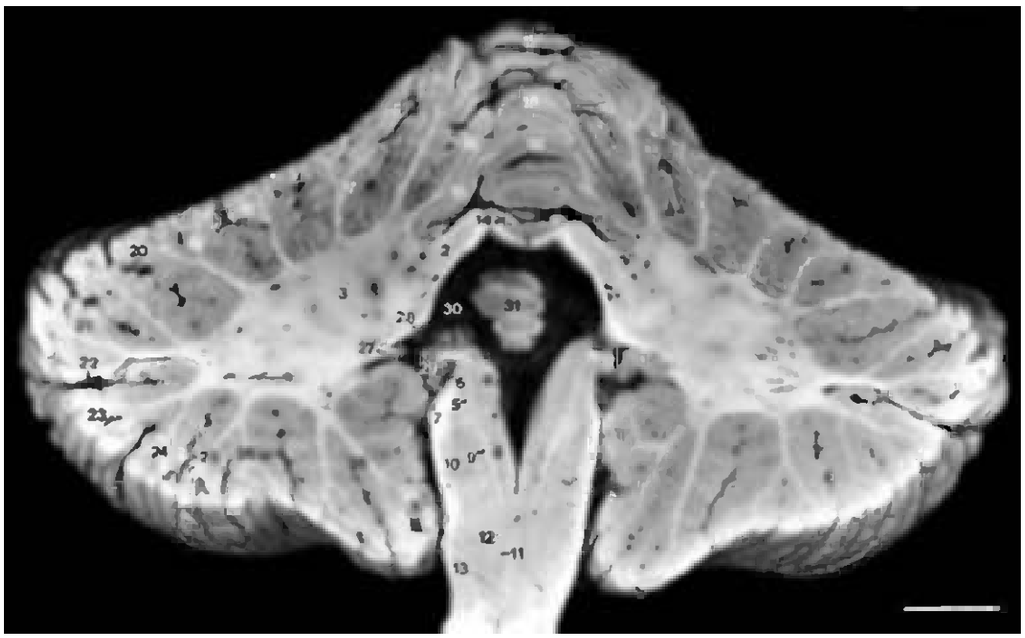

A

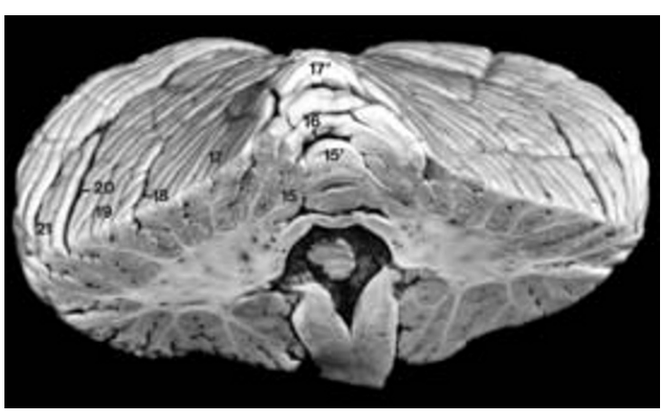

B

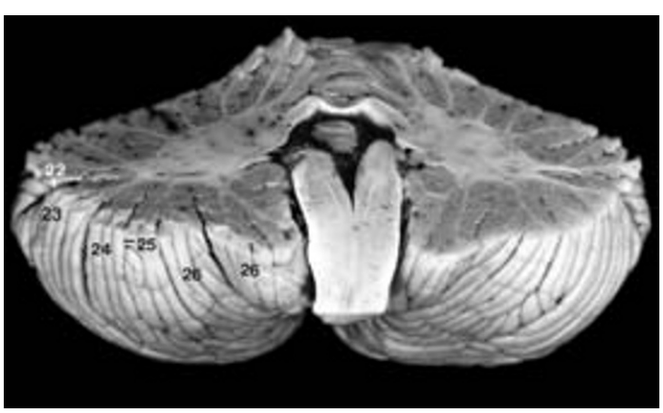

C

D

Fig. 11.47 (D–F).
D. Coronal section of the head. Anterior view. Bar: 10 mm.
E–F. 3 Tesla MRI. E. T1-weighted MRI. **F.** T2-weighted MRI.

1 Superior medullary velum
2 Superior cerebellar peduncle (brachium conjunctivum)
3 Middle cerebellar peduncle (brachium pontis)
15 Ala of central lobule
15′ Central lobule
17 Quadrangular lobule
18 Anterior superior (primary) fissure
19 Simple lobule
20 Posterior superior fissure
21 Superior semilunar lobule
22 Great horizontal fissure
23 Inferior semilunar lobule
25 Prepyramidal fissure
26 Biventral lobule
30 Fourth ventricle
31 Nodulus
32 Tonsil
33 Collateral sulcus
34 Fusiform gyrus
35 Inferior temporal gyrus
36 Middle temporal gyrus
37 Superior temporal sulcus (parallel sulcus)
38 Supramarginal gyrus
39 Intraparietal sulcus
39′ Precentral gyrus
40 Cingulate sulcus
40′ Postcentral gyrus
41 Cingulate gyrus
41′ Central sulcus
42 Anterior calcarine sulcus
43 Occipital horn of the lateral ventricle
44 Lingual gyrus
45 Tentorium cerebelli
46 Transverse sinus
47 Occipital condyle
48 Atlas, lateral mass
50 Posterior inferior cerebellar arteries (right (50R) and left (50L))

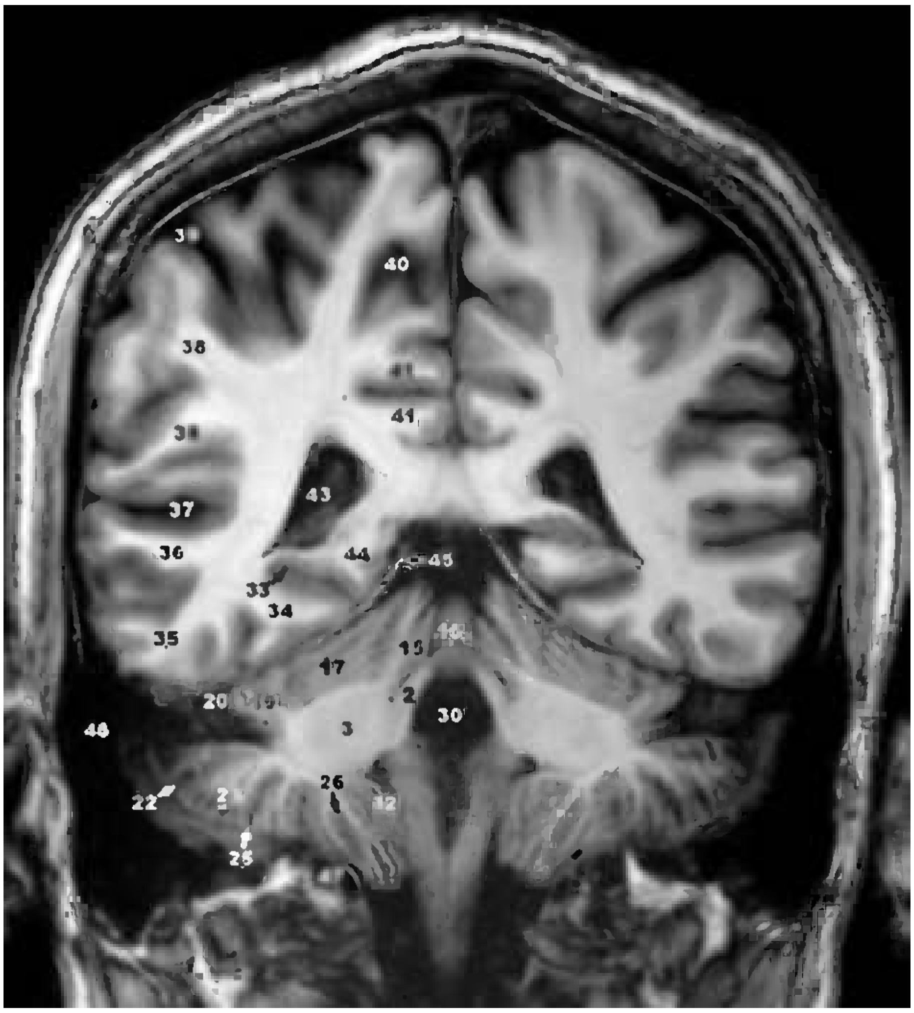

40
38
37
43
36
44
45
33
34
35
17
20
2
48
3
30'
26
22
32
25

E

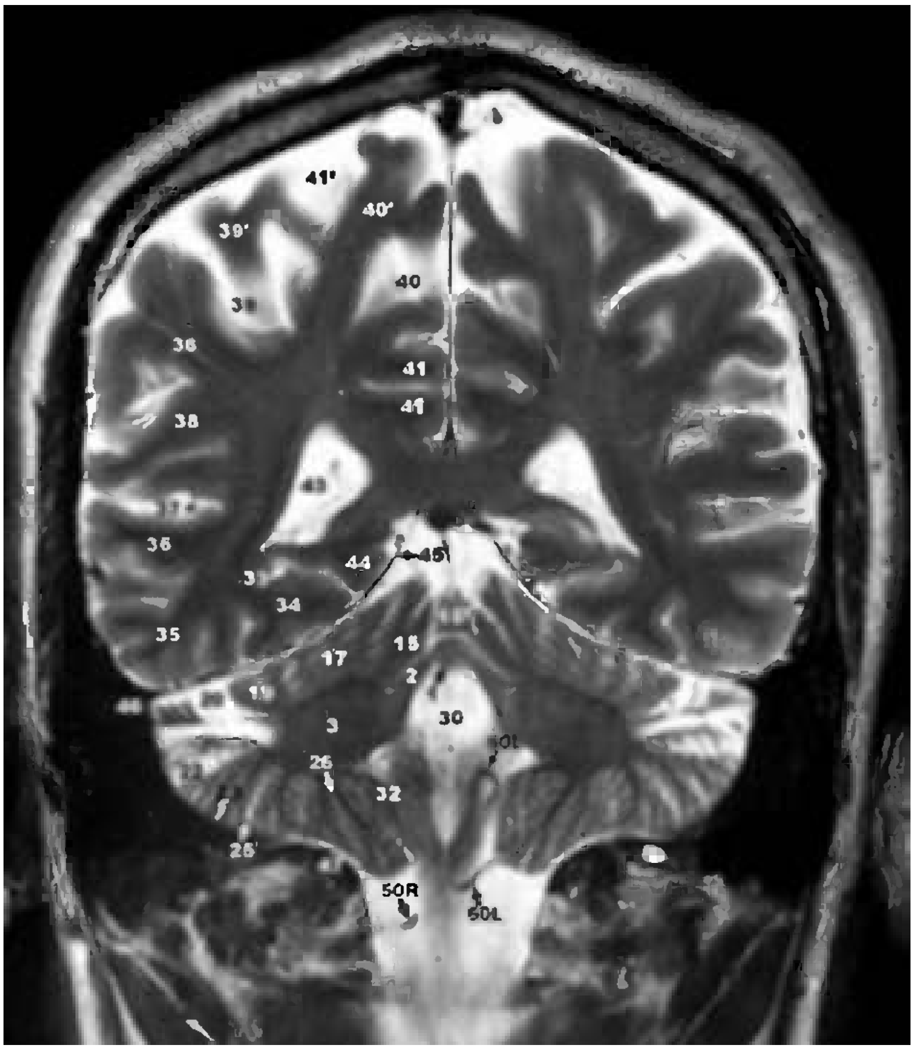

41'
40'
39'
40
36
41
41
38
36
44
45
34
35
17
18
2
3
30
26
32
25
50R
50L

F

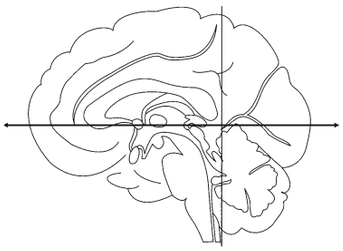

Fig. 11.48 (A–C). Coronal (frontal) section.
A. Frontal view after removal of the cerebral hemispheres. Bar: 10 mm.
B. Superior oblique view. **C.** Inferior oblique view.

1 Lingula
2 Superior cerebellar peduncle (brachium conjunctivum)
3 Dentate nucleus
4 Middle cerebellar peduncle (brachium pontis)
5 Ala of central lobule
5′ Central lobule
6 Postcentral fissure (preculminate fissure)
7 Quadrangular lobule
7′ Culmen
8 Anterior superior (primary) fissure
9 Simple lobule
10 Posterior superior fissure
11 Superior semilunar lobule
12 Great horizontal fissure
13 Inferior semilunar lobule
14 Gracile lobule
15 Prepyramidal fissure
16 Biventral lobule
17 Postpyramidal (secondary) fissure
18 Tonsil
19 Brachium of the flocculus
20 Nodulus
21 Posterolateral fissure
22 Uvula
23 Fourth ventricle and choroid plexi

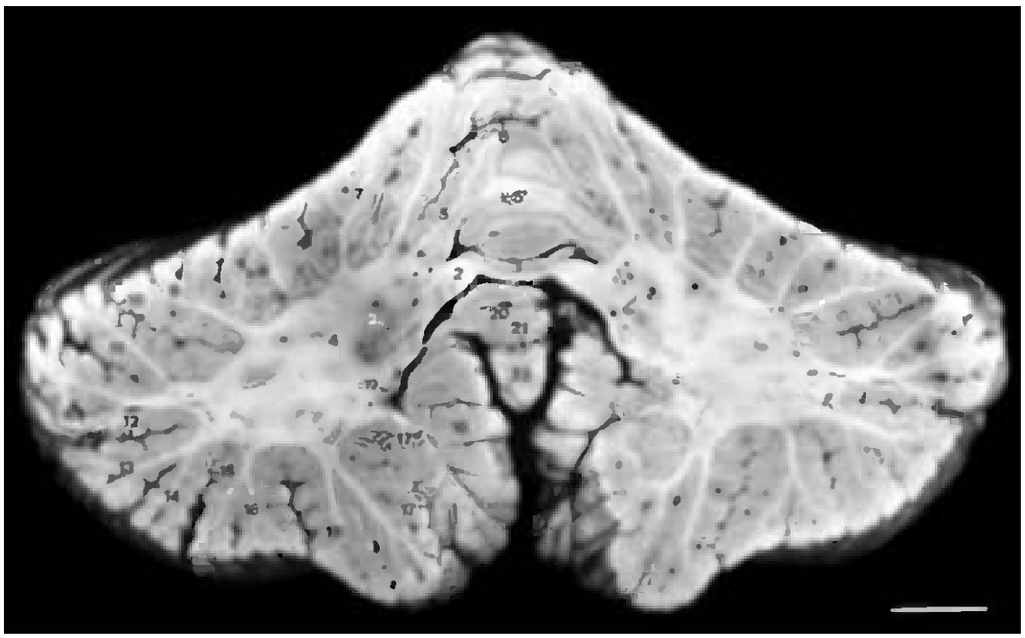

A

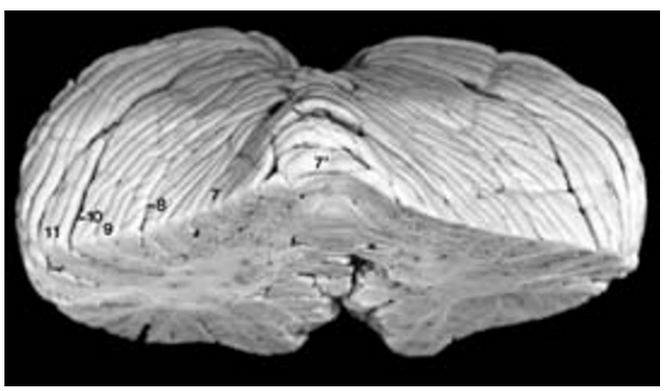

B

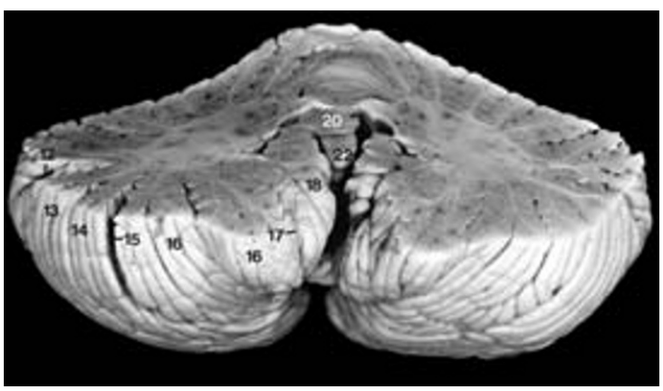

C

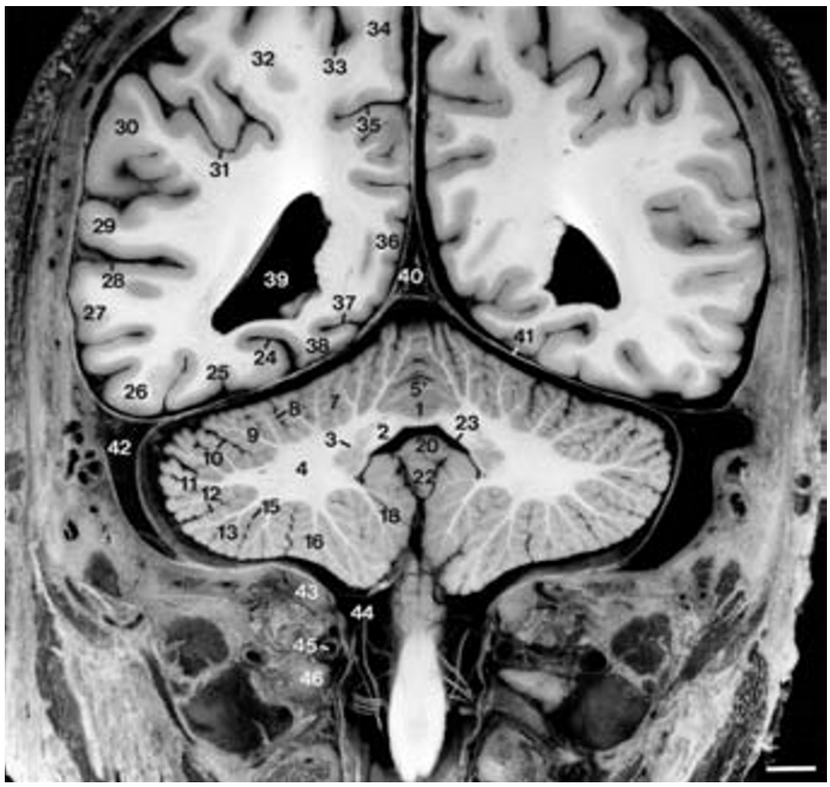

D

Fig. 11.48 (D–F).
D. Coronal section of the head. Posterior view. Bar: 10 mm.
E–F. 3 Tesla MRI. E. T1-weighted MRI. **F.** T2-weighted MRI.

1 Lingula
2 Superior cerebellar peduncle (brachium conjunctivum)
3 Dentate nucleus
4 Middle cerebellar peduncle (brachium pontis)
5′ Central lobule of vermis
7 Quadrangular lobule
8 Anterior superior (primary) fissure
9 Simple lobule
10 Posterior superior fissure
11 Superior semilunar lobule
12 Great horizontal fissure
13 Inferior semilunar lobule
15 Prepyramidal fissure
16 Biventral lobule
18 Tonsil
20 Nodulus
22 Uvula
23 Fourth ventricle and choroid plexus
24 Collateral sulcus
25 Fusiform gyrus
26 Inferior temporal gyrus
27 Middle temporal gyrus
28 Superior temporal sulcus (parallel sulcus)
29 Superior temporal gyrus
30 Angular gyrus
31 Intraparietal sulcus
32 Postcentral gyrus
33 Central sulcus
34 Precentral gyrus
35 Cingulate sulcus
36 Cingulate gyrus
37 Anterior calcarine sulcus
38 Lingual gyrus
39 Occipital horn of the lateral ventricle
40 Sinus rectus (straight sinus)
41 Tentorium cerebelli
42 Transverse sinus
43 Occipital bone, squama
44 Foramen magnum
45 Vertebral artery
46 Atlas
47 Cisterna magna and upper cervical spinal subarachnoid space

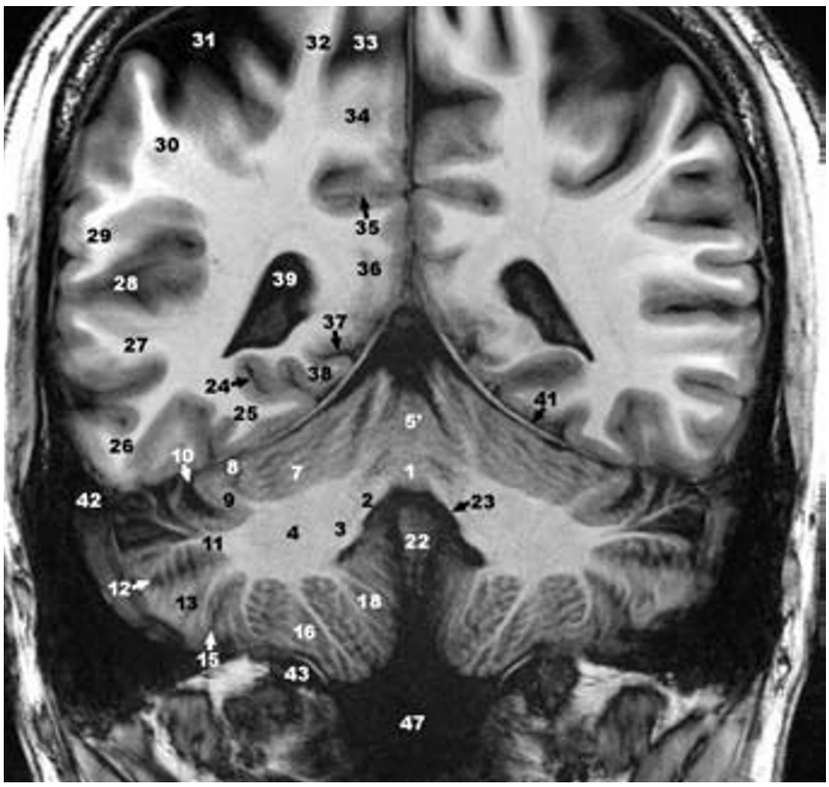
31
32
33
34
30
35
29
36
39
28
37
27
38
24
41
25
5'
26
10
8
7
1
42
9
2
23
4
3
22
11
12
13
18
16
15
43
47

E


31
32
33
34
30
35
29
36
39
28
37
27
24
38
26
25
5'
8
7
1
42
10
9
2
23
11
4
3
22
12
13
18
16
15
43
47

F

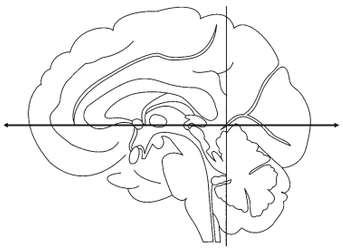

Fig. 11.49 (A–C). Coronal (frontal) section.
A. Frontal view after removal of the cerebral hemispheres. Bar: 10 mm.
B. Superior oblique view. **C.** Inferior oblique view.

1 Globose nucleus
2 Emboliform nucleus
3 Dentate nucleus
4 Quadrangular lobule
4′ Culmen
5 Anterior superior (primary) fissure
6 Simple lobule
6′ Declive
7 Posterior superior fissure
8 Superior semilunar lobule
9 Great horizontal fissure
10 Inferior semilunar lobule
11 Gracile lobule
12 Prepyramidal fissure
13 Biventral lobule
14 Postpyramidal (secondary) fissure
15 Tonsil
16 Nodulus
17 Posterolateral fissure
18 Uvula

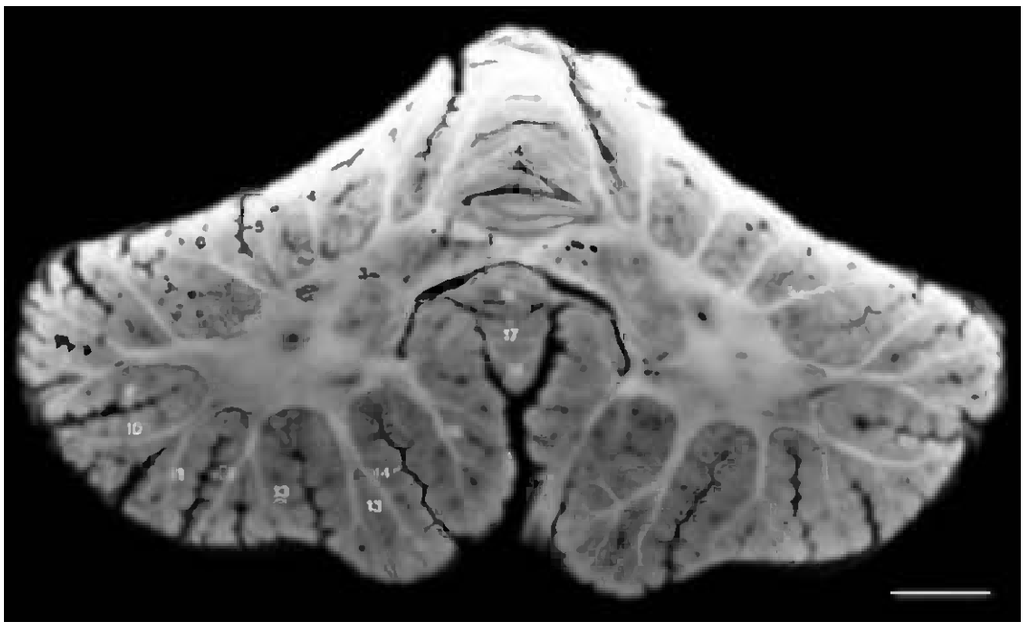

A

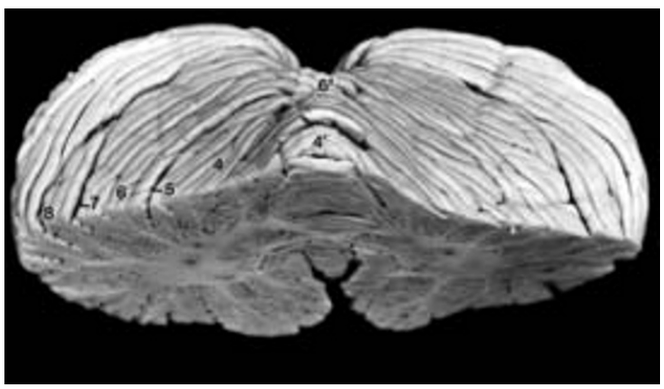

B

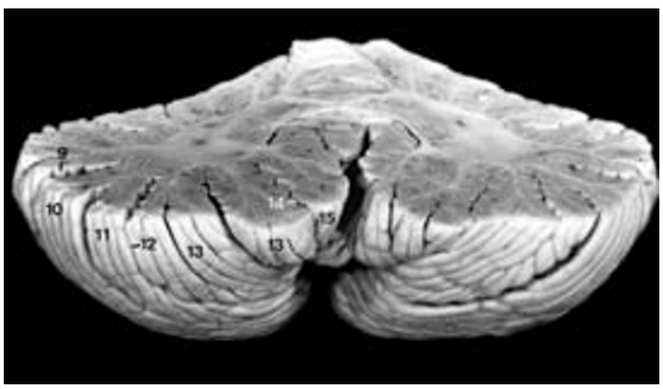

C

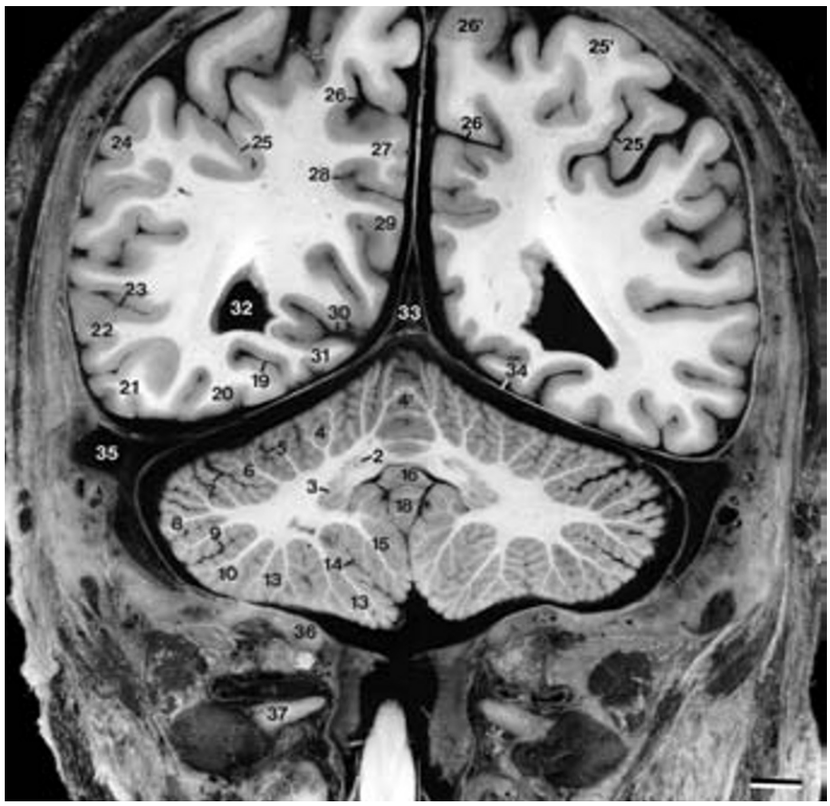

D

Fig. 11.49 (D–F).
D. Coronal section of the head. Anterior view. Bar: 10 mm.
E–F. 3 Tesla MRI. E. T1-weighted MRI. **F.** T2-weighted MRI.

2 Emboliform nucleus
3 Dentate nucleus
4 Quadrangular lobule
4′ Culmen
5 Anterior superior (primary) fissure
6 Simple lobule
7 Posterior superior fissure
8 Superior semilunar lobule
9 Great horizontal fissure
10 Inferior semilunar lobule
13 Biventral lobule
14 Postpyramidal (secondary) fissure
15 Tonsil
16 Nodulus
18 Uvula
19 Collateral sulcus
20 Fusiform gyrus
21 Inferior temporal gyrus
22 Middle temporal gyrus
23 Parallel sulcus
24 Angular gyrus
25 Intraparietal sulcus
25′ Postcentral gyrus
26 Cingulate sulcus
26′ Paracentral lobule
27 Precuneus
28 Subparietal sulcus
29 Cingulate gyrus
30 Anterior calcarine sulcus
31 Lingual gyrus
32 Occipital horn of the lateral ventricle
33 Sinus rectus (straight sinus)
34 Tentorium cerebelli
35 Transverse sinus
36 Occipital bone, squama
37 Atlas
38 Cisterna magna

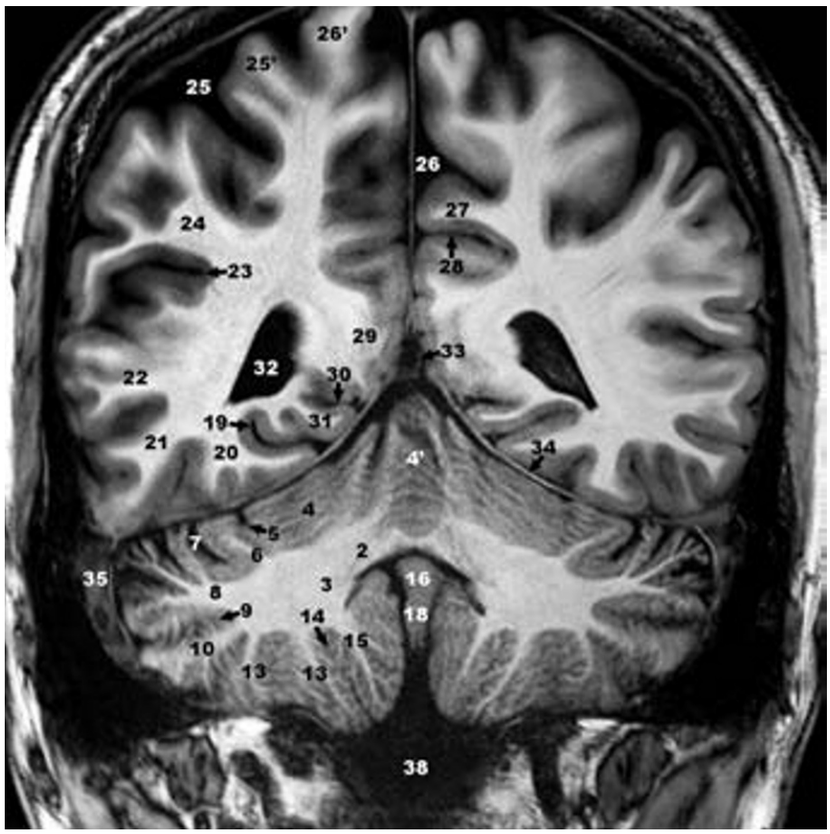
26'
25'
25
26
24
27
23
28
29
33
32
30
22
19
31
21
20
4'
34
4
5
7
6
2
35
8
3
16
9
14
18
15
10
13
13
38

E


26'
25'
25
26
24
27
28
29
33
32
30
22
31
21
20
19
4'
5
4
7
6
2
35
16
8
3
18
14
15
9
10
13
13
38

F

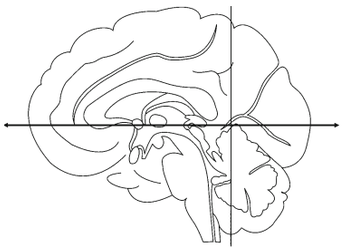

Fig. 11.50 (A–C). Coronal (frontal) section.
A. Frontal view after removal of the cerebral hemispheres. Bar: 10 mm.
B. Superior oblique view. **C.** Inferior oblique view.

1 Fastigial nucleus
2 Globose nucleus
3 Emboliform nucleus
4 Dentate nucleus
5 Quadrangular lobule
5′ Culmen
6 Anterior superior (primary) fissure
7 Simple lobule
7′ Declive
8 Posterior superior fissure
9 Superior semilunar lobule
10 Great horizontal fissure
11 Inferior semilunar lobule
12 Gracile lobule
13 Prepyramidal lobule
14 Biventral lobule
15 Postpyramidal (secondary) fissure
16 Tonsil
17 Nodulus
18 Uvula

A

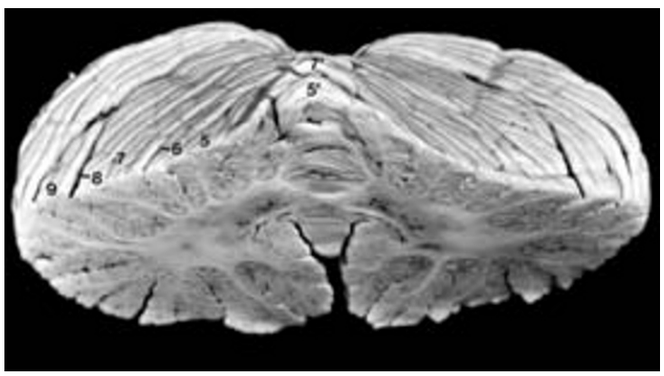

B

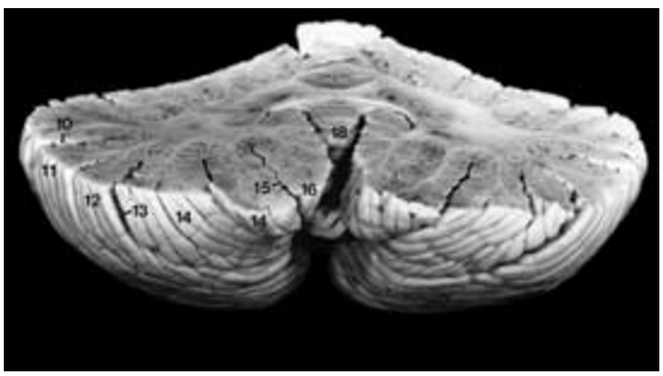

C

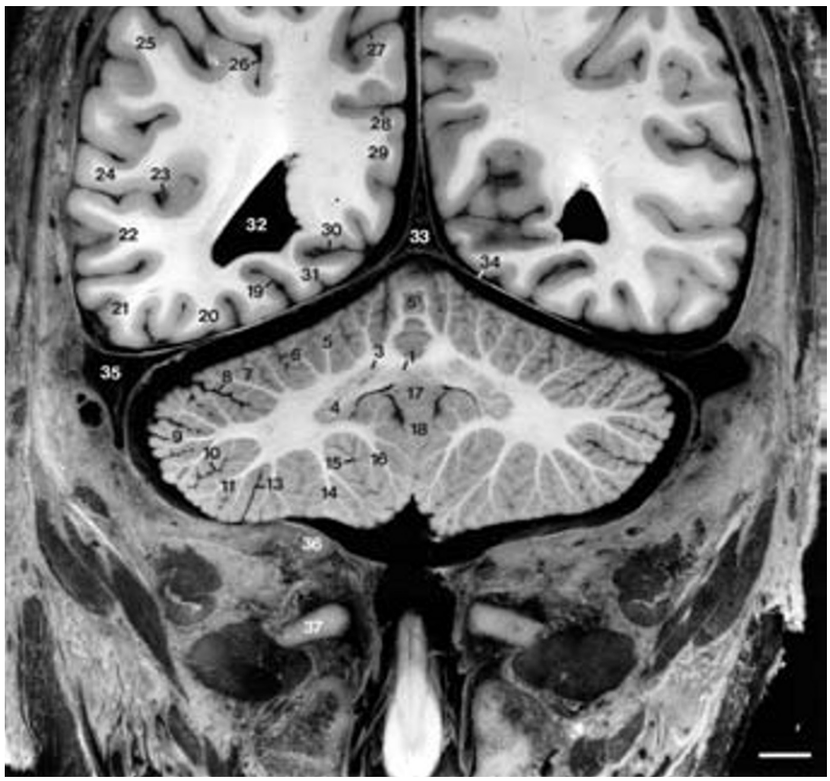

D

Fig. 11.50 (D–F).
D. Coronal section of the head. Posterior view. Bar: 10 mm.
E–F. 3 Tesla MRI. E. T1-weighted MRI. **F.** T2-weighted MRI.

1 Fastigial nucleus
3 Emboliform nucleus
4 Dentate nucleus
5 Quadrangular lobule
5′ Culmen
6 Anterior superior (primary) fissure
7 Simple lobule
8 Posterior superior fissure
9 Superior semilunar lobule
10 Great horizontal fissure
11 Inferior semilunar lobule
13 Prepyramidal fissure
14 Biventral lobule
15 Postpyramidal (secondary) fissure
16 Tonsil
17 Nodulus
18 Uvula
19 Collateral sulcus
20 Fusiform gyrus
21 Inferior temporal gyrus
22 Middle temporal gyrus
23 Parallel sulcus
24 Superior temporal gyrus
25 Angular gyrus
26 Intraparietal sulcus
27 Cingulate sulcus
28 Subparietal sulcus
29 Cingulate gyrus
30 Anterior calcarine sulcus
31 Lingual gyrus
32 Occipital horn of the lateral ventricle
33 Straight sinus
34 Tentorium cerebelli
35 Transverse sinus
36 Occipital bone, squama
37 Atlas
38 Cisterna magna

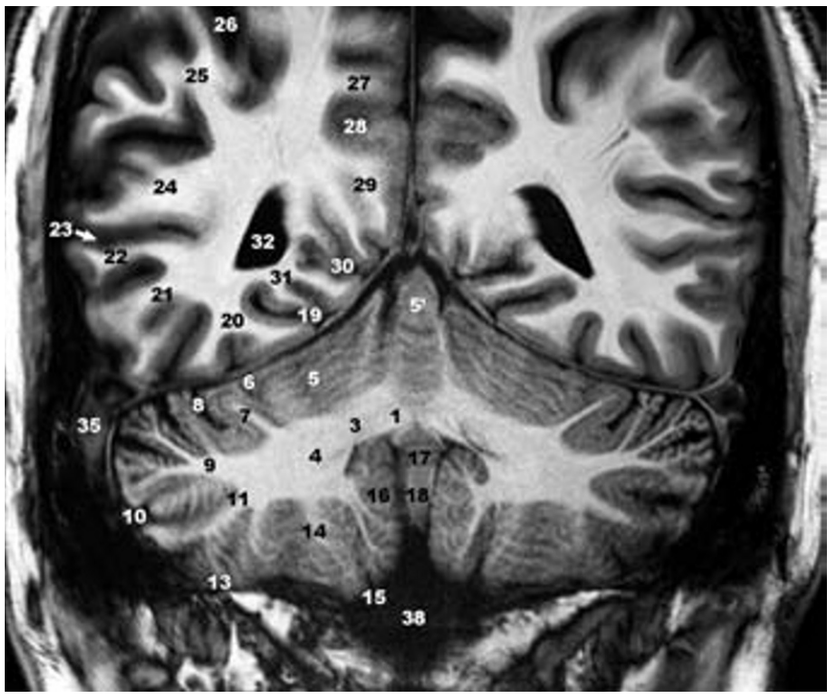
26
25
27
28
24
29
23
32
22
30
31
21
5'
20
19
6
5
8
7
3
1
35
4
17
9
16
18
11
10
14
13
15
38

E

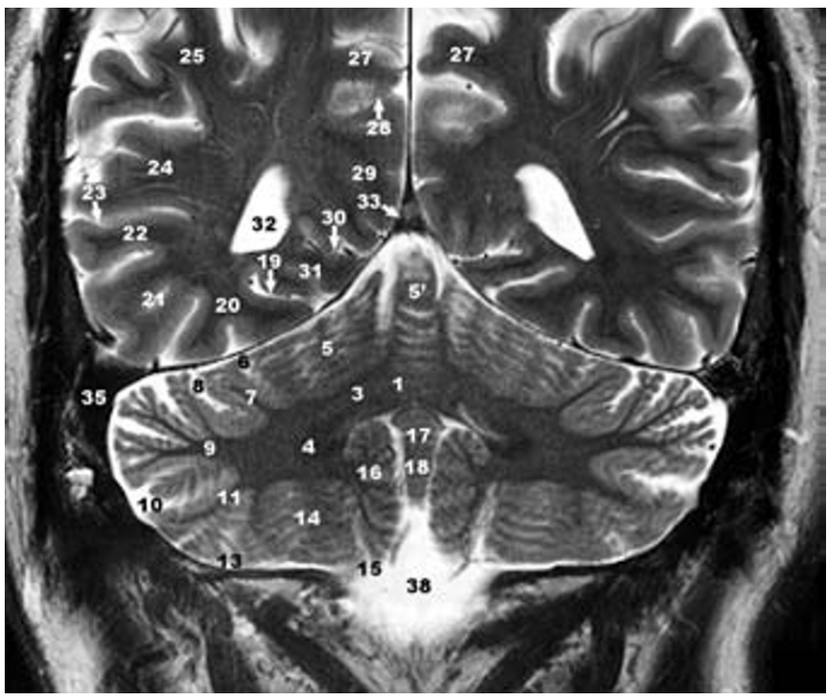
25
27
27
28
24
29
23
33
32
30
22
19
31
5'
21
20
5
8
8
7
3
1
35
17
9
4
16
18
10
11
14
13
15
38

F

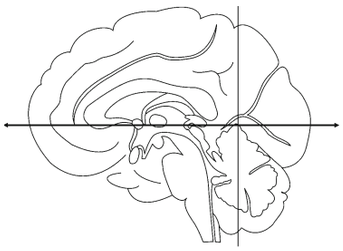

Fig. 11.51 (A–C). Coronal (frontal) section.
A. Frontal view after removal of the cerebral hemispheres. Bar: 10 mm.
B. Superior oblique view. **C.** Inferior oblique view.

1 Dentate nucleus
2 Quadrangular lobule
2′ Culmen
3 Anterior superior (primary) fissure
4 Simple lobule
5 Posterior superior fissure
6 Superior semilunar lobule
7 Great horizontal fissure
8 Inferior semilunar lobule
9 Gracile lobule
10 Prepyramidal fissure
11 Biventral lobule
12 Postpyramidal (secondary) fissure
13 Tonsil
14 Uvula
15 Pyramid of vermis

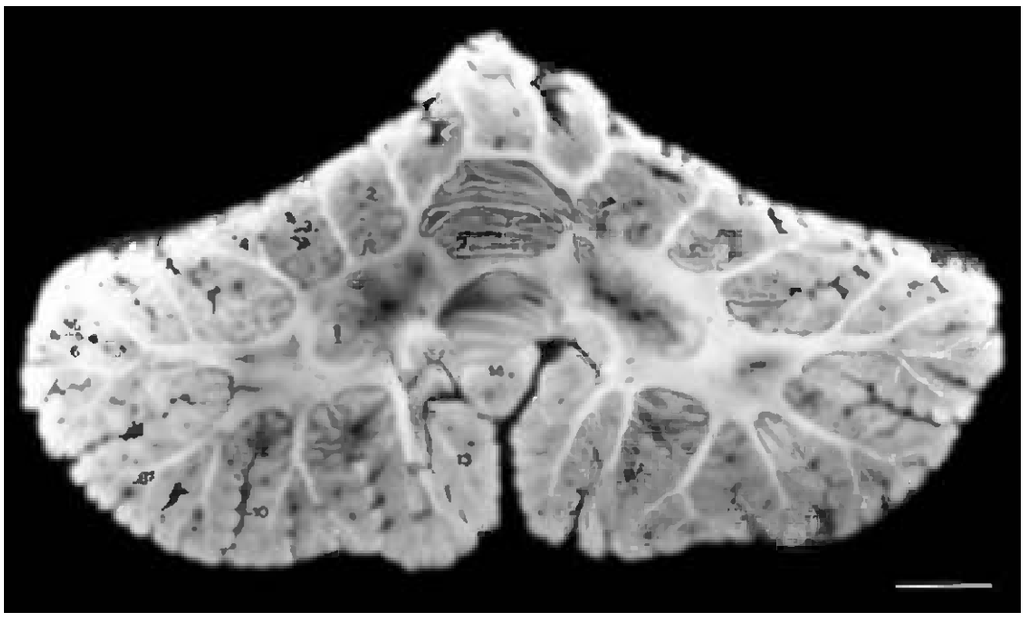

A

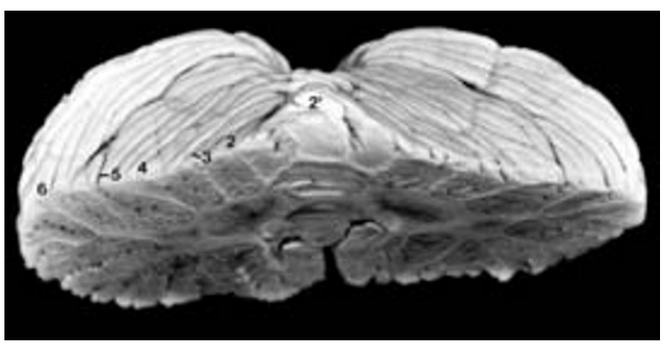

B

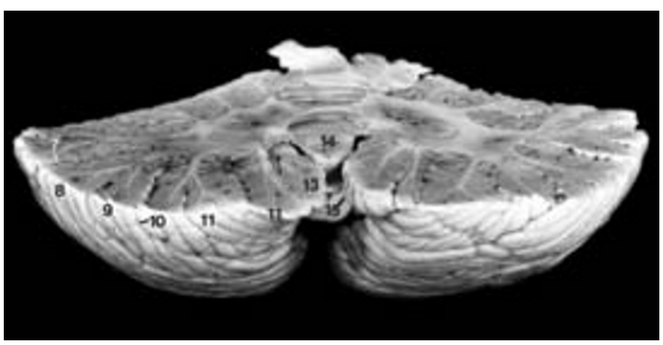

C

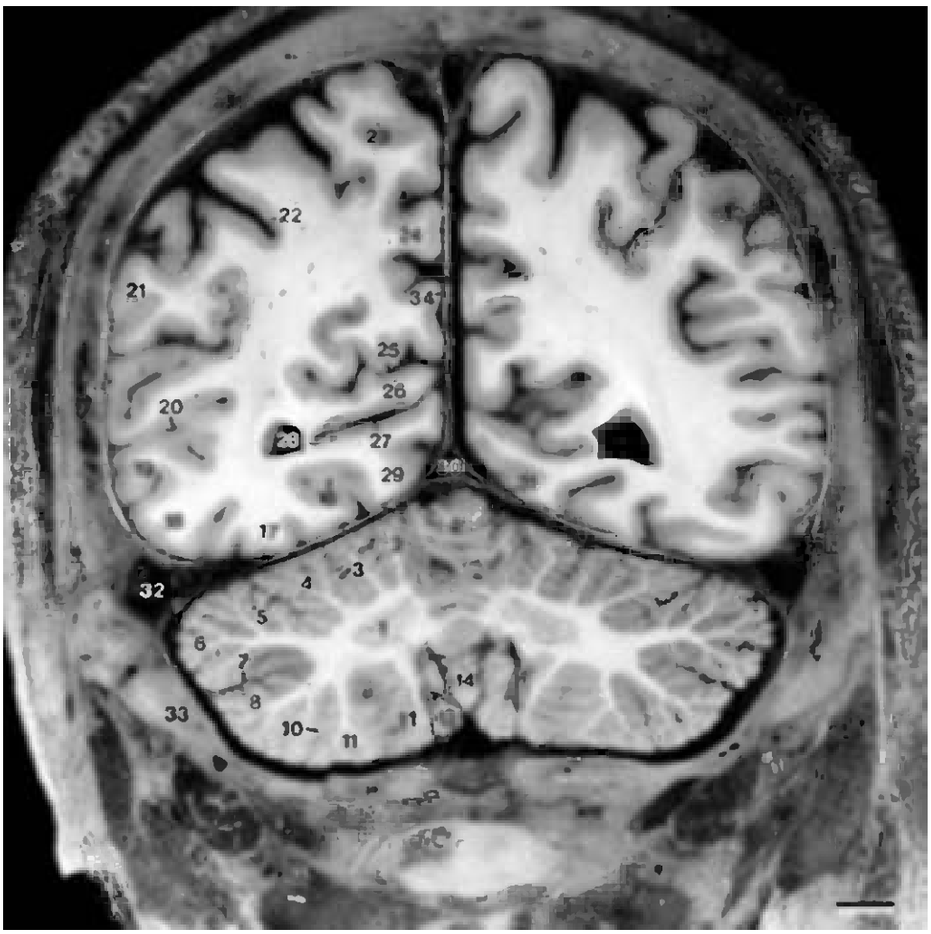

D

Fig. 11.51 (D–F).
D. Coronal section of the head. Anterior view. Bar: 10 mm.
E–F. 3 Tesla MRI. E. T1-weighted MRI. **F.** T2-weighted MRI.

1 Dentate nucleus
2 Quadrangular lobule
2 Culmen
3 Anterior superior (primary) fissure
4 Simple lobule
5 Posterior superior fissure
6 Superior semilunar lobule
7 Great horizontal fissure
8 Inferior semilunar lobule
10 Prepyramidal fissure
11 Biventral lobule
13 Tonsil
14 Uvula
16 Collateral sulcus
17 Fusiform gyrus
18 Inferior occipital gyrus
19 Middle occipital gyrus
20 Parallel sulcus
21 Angular gyrus
22 Intraparietal sulcus
23 Superior parietal lobule
24 Precuneus
25 Parieto-occipital fissure
26 Cuneus
27 Calcarine sulcus and striate cortex
28 Occipital horn of the lateral ventricle
29 Lingual gyrus
30 Straight sinus
31 Tentorium cerebelli
32 Transverse sinus
33 Occipital bone, squama
34 Falx cerebri
35 Cisterna magna

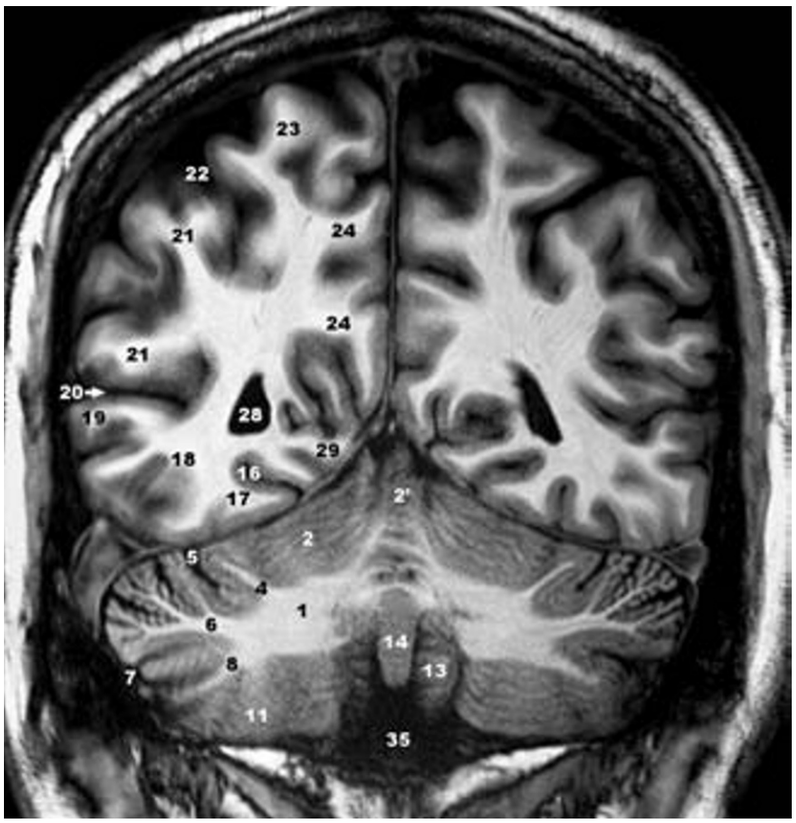
23
22
21
24
24
21
20
19
28
29
18
16
17
2'
2
5
4
1
6
14
8
13
7
11
35

E


23
22
24
21
24
21
30
20
19
28
26
18
16
29
17
2'
2
32
5
4
6
1
14
7
8
13
33
11
35

F

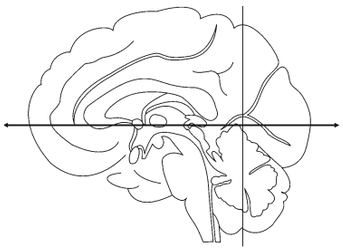

Fig. 11.52 (A–C).
Coronal (frontal) section.
A. Frontal view after removal of the cerebral hemispheres. Bar: 10 mm.
B. Superior oblique view. **C.** Inferior oblique view.

1 Dentate nucleus
2 Quadrangular lobule
2′ Culmen
3 Anterior superior (primary) fissure
4 Simple lobule
4′ Declive
5 Posterior superior fissure
6 Superior semilunar lobule
7 Great horizontal fissure
8 Inferior semilunar lobule
9 Gracile lobule
10 Prepyramidal fissure
11 Biventral lobule
12 Pyramid of vermis
13 Uvula

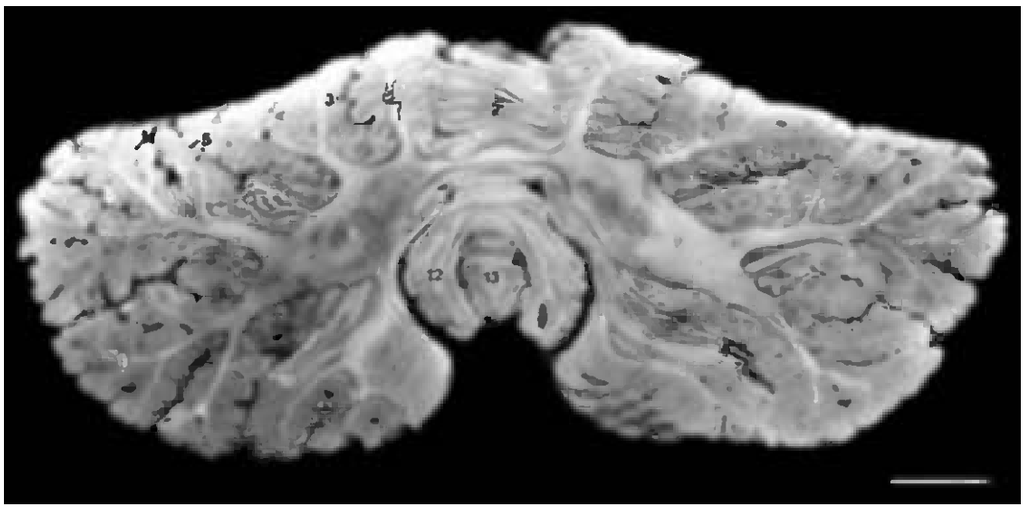

A

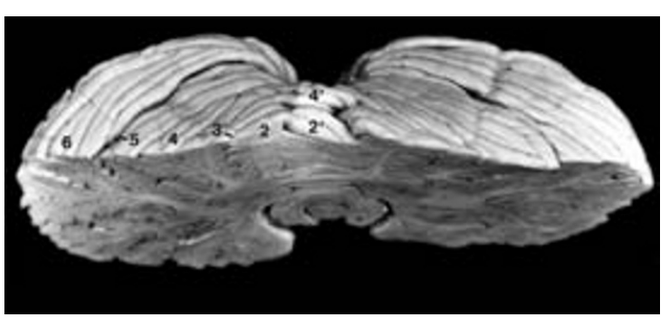

B

C

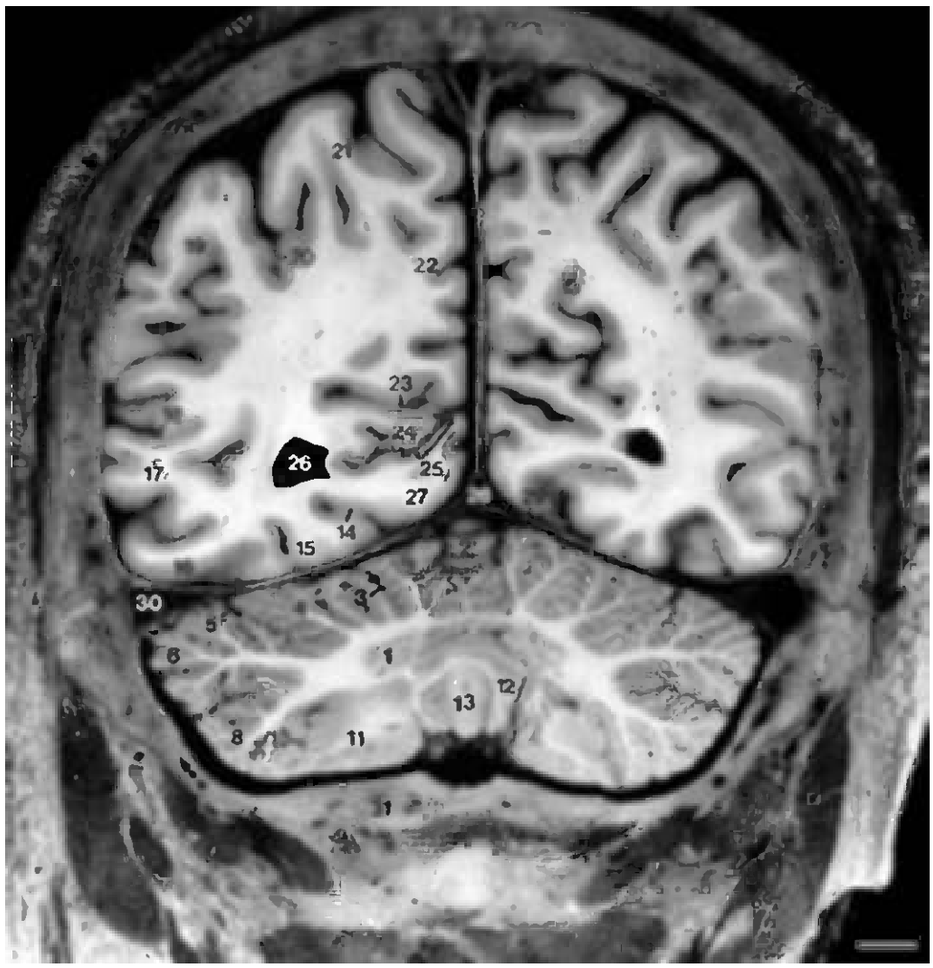

D

Fig. 11.52 (D–F). Coronal (frontal) section.
D. Coronal section of the head. Posterior view. Bar: 10 mm.
E–F. 3 Tesla MRI. E. T1-weighted MRI. **F.** T2-weighted MRI.

1 Dentate nucleus
2 Quadrangular lobule
2′ Culmen
3 Anterior superior (primary) fissure
4 Simple lobule
4′ Declive
5 Posterior superior fissure
6 Superior semilunar lobule
7 Great horizontal fissure
8 Inferior semilunar lobule
9 Gracile lobule
10 Prepyramidal fissure
11 Biventral lobule
12 Pyramid of vermis
13 Uvula
14 Collateral sulcus
15 Fusiform gyrus
16 Inferior occipital gyrus
17 Middle occipital gyrus
18 Lateral occipital sulcus
19 Angular gyrus
20 Intraparietal sulcus
21 Superior parietal lobule
22 Precuneus
23 Parieto-occipital fissure
24 Cuneus
25 Calcarine sulcus
26 Occipital horn of the lateral ventricle
27 Lingual gyrus
28 Straight sinus
29 Tentorium cerebelli
30 Transverse sinus
31 Occipital bone, squama

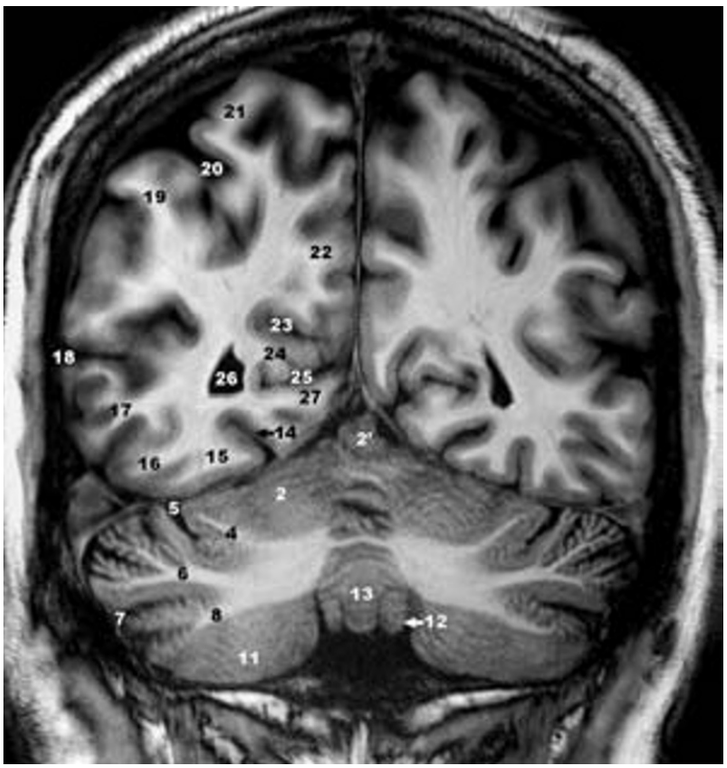
21
20
19
22
23
24
18
26
25
27
17
14
2'
16
15
2
5
4
6
13
7
8
12
11

E

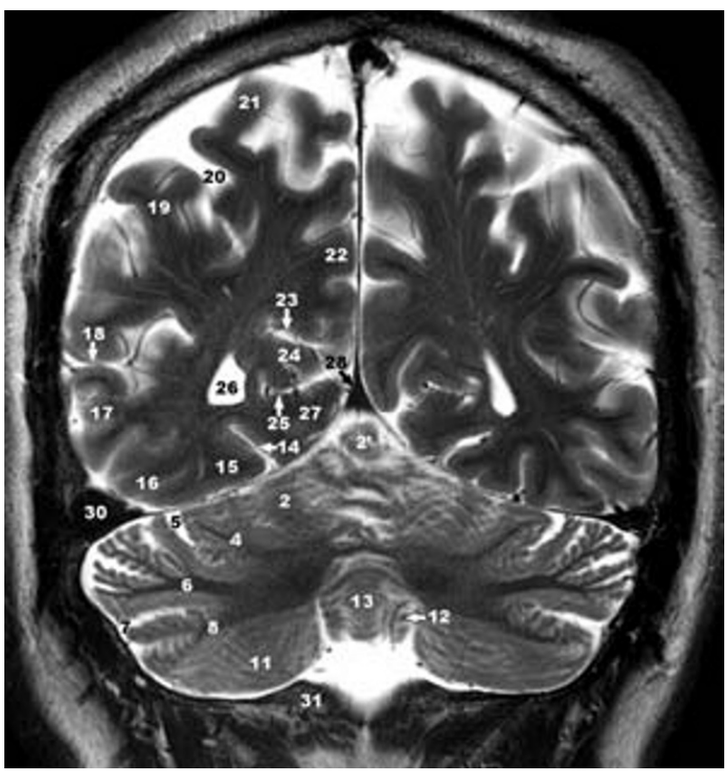
21
20
19
22
23
18
24
28
26
17
25
27
14
2'
15
16
2
30
5
4
6
13
12
7
8
11
31

F

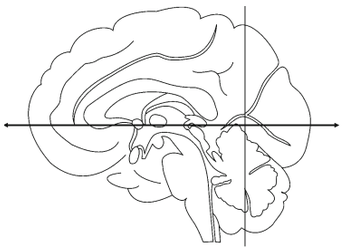

Fig. 11.53 (A–C). Coronal (frontal) section.
A. Frontal view after removal of the cerebral hemispheres. Bar: 10 mm.
B. Superior oblique view. **C.** Inferior oblique view.

1 Culmen
2 Anterior superior (primary) fissure
3 Simple lobule
3′ Declive
4 Posterior superior fissure
5 Superior semilunar lobule
6 Great horizontal fissure
7 Inferior semilunar lobule
8 Gracile lobule
9 Prepyramidal fissure
10 Biventral lobule
11 Pyramid of vermis
11′ Uvula
12 Dentate nucleus, superior pole

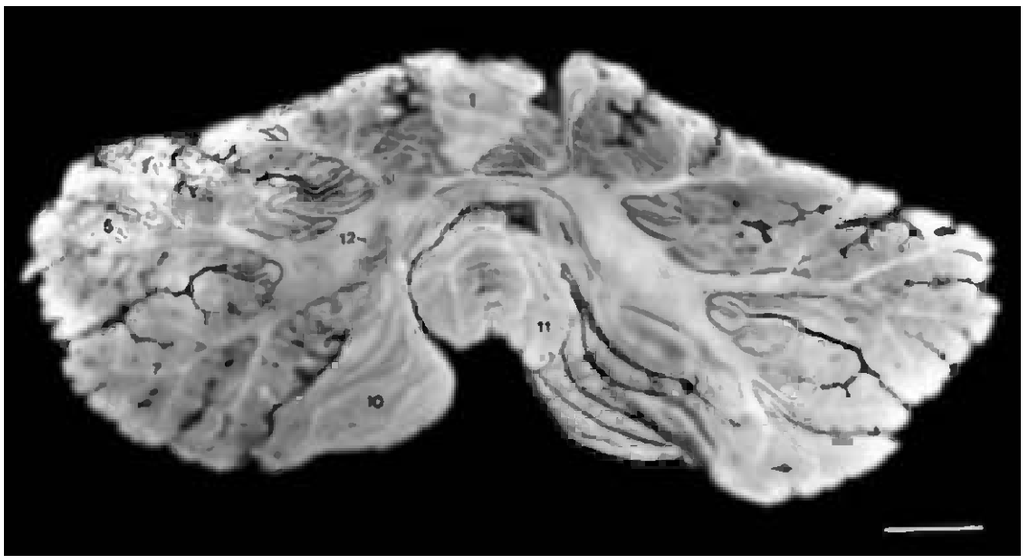

A

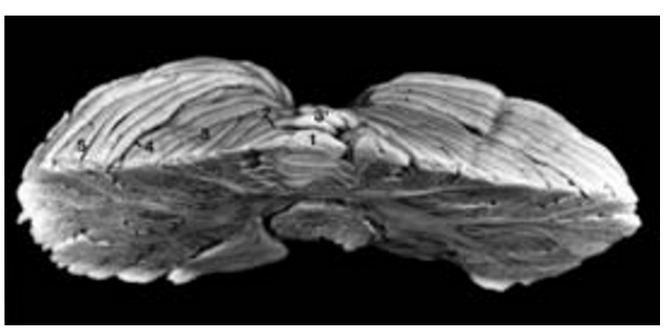

B

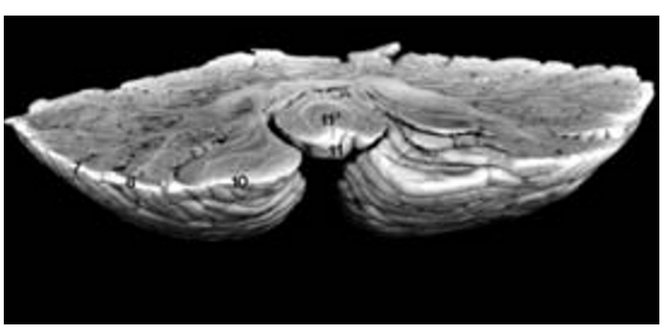

C

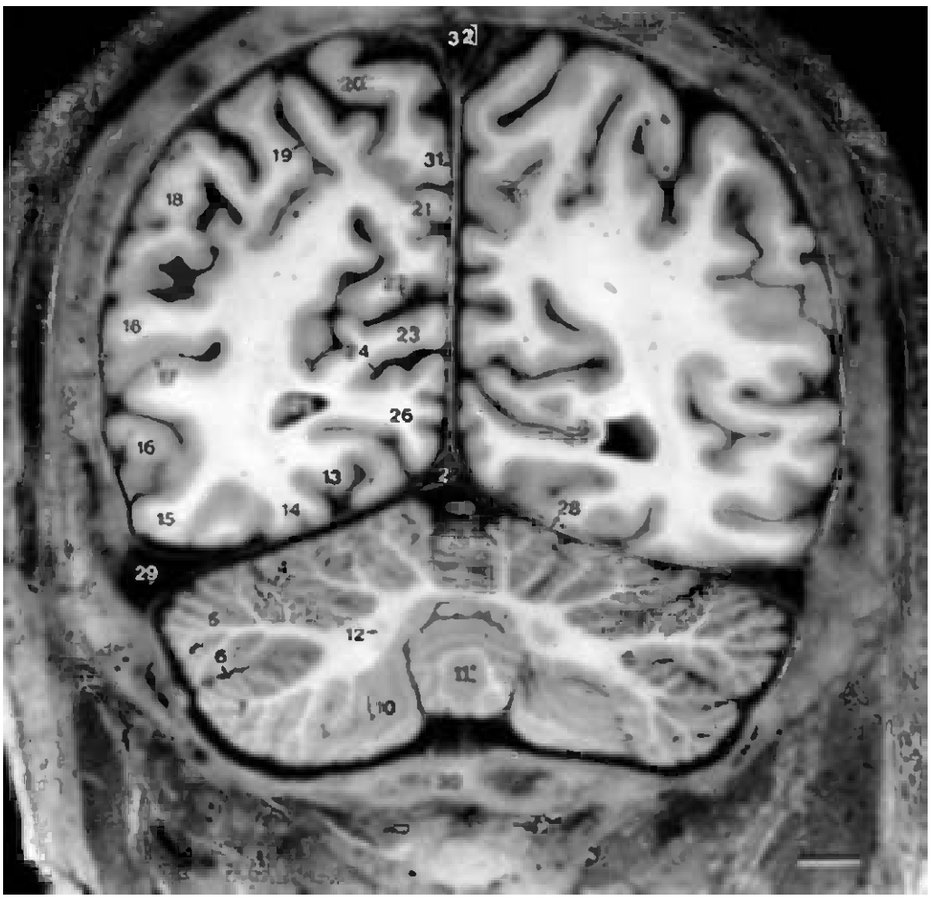

D

Fig. 11.53 (D–F). Coronal (frontal) section.
D. Coronal section of the head. Anterior view. Bar: 10 mm.
E–F. 3 Tesla MRI. E. T1-weighted MRI. **F.** T2-weighted MRI.

1 Culmen
2 Anterior superior (primary) fissure
3 Simple lobule
3′ Declive
4 Posterior superior fissure
5 Superior semilunar lobule
6 Great horizontal fissure
7 Inferior semilunar lobule
8 Gracile lobule
9 Prepyramidal fissure
10 Biventral lobule
11 Pyramid of vermis
11′ Uvula
12 Dentate nucleus, superior pole
13 Collateral sulcus
14 Fusiform gyrus
15 Inferior occipital gyrus
16 Middle occipital gyrus
17 Lateral occipital sulcus
18 Angular gyrus
19 Intraparietal sulcus
20 Superior parietal lobule
21 Precuneus
22 Parieto-occipital fissure
23 Cuneus
24 Calcarine sulcus and striate cortex
25 Occipital horn of the lateral ventricle
26 Lingual gyrus
27 Straight sinus
28 Tentorium cerebelli
29 Transverse sinus
30 Occipital bone, squama
31 Falx cerebri
32 Superior sagittal sinus

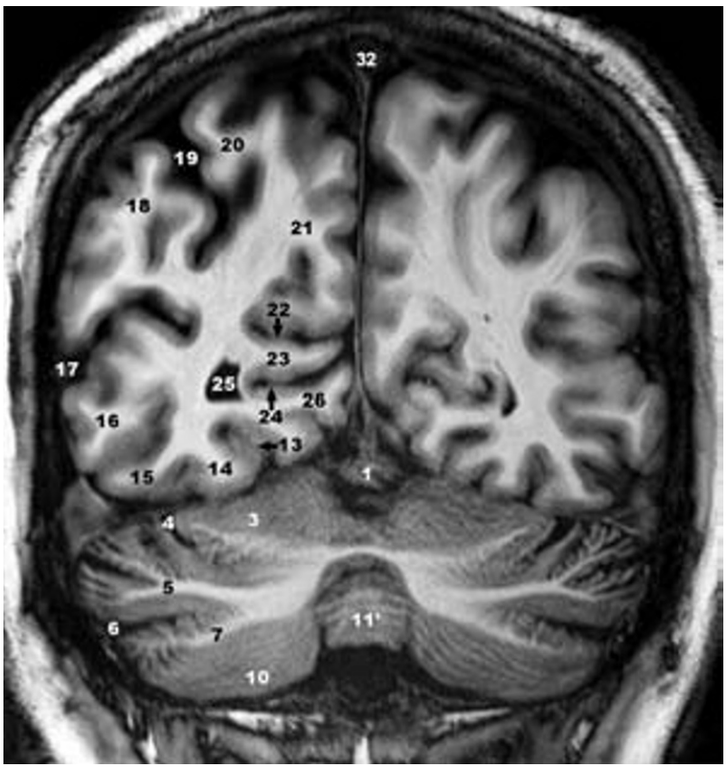
32
19
20
18
21
22
23
17
25
26
24
16
13
15
14
1
4
3
5
6
7
11'
10

E

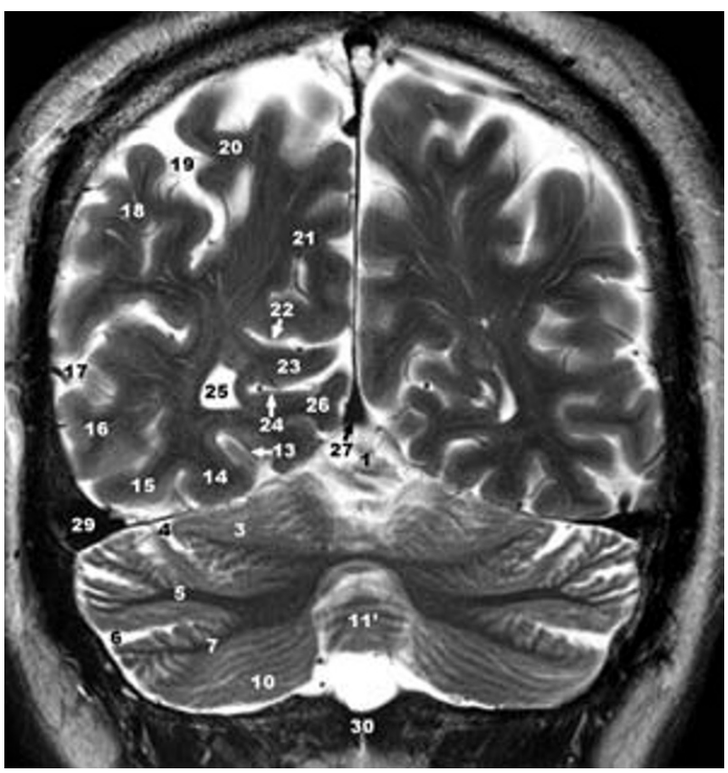
20
19
18
21
22
23
17
25
26
24
16
27
13
1
15
14
29
4
3
5
11'
6
7
10
30

F

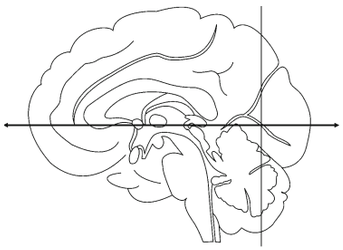

Fig. 11.54 (A–C). Coronal (frontal) section.
A. Frontal view after removal of the cerebral hemispheres. Bar: 10 mm.
B. Superior oblique view. **C.** Posterior oblique view.

1 Simple lobule
1′ Declive
2 Posterior superior fissure
3 Superior semilunar lobule
3′ Folium of vermis
4 Great horizontal fissure
5 Inferior semilunar lobule
5′ Tuber
6 Prepyramidal fissure
7 Pyramid

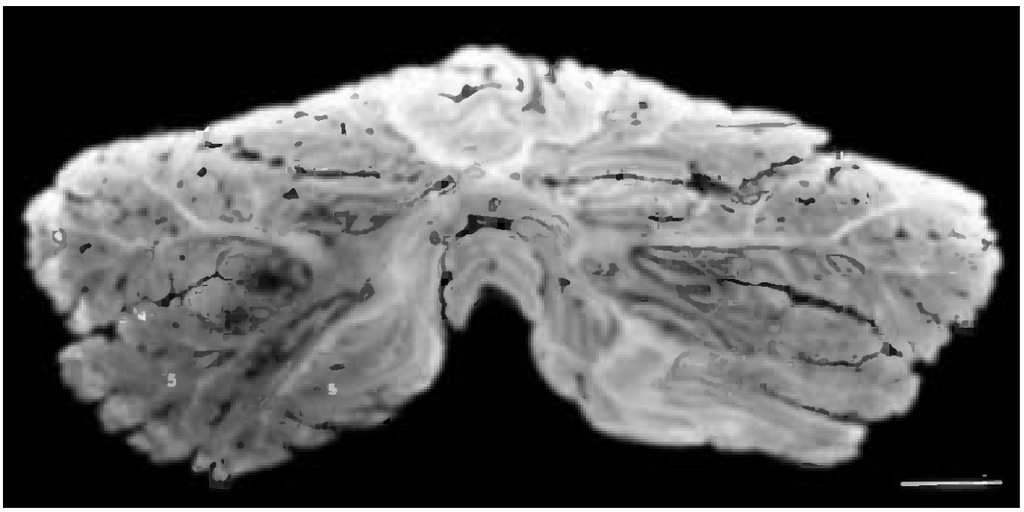

A

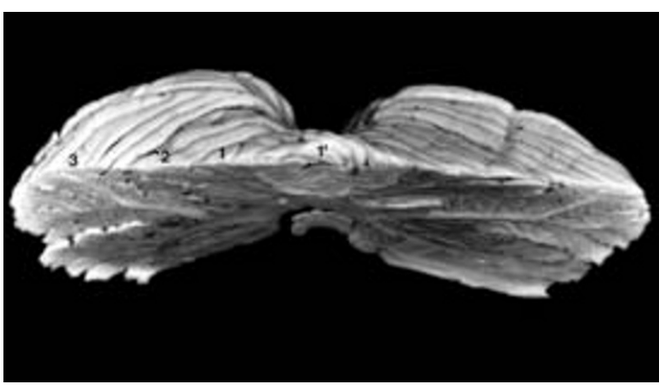

B

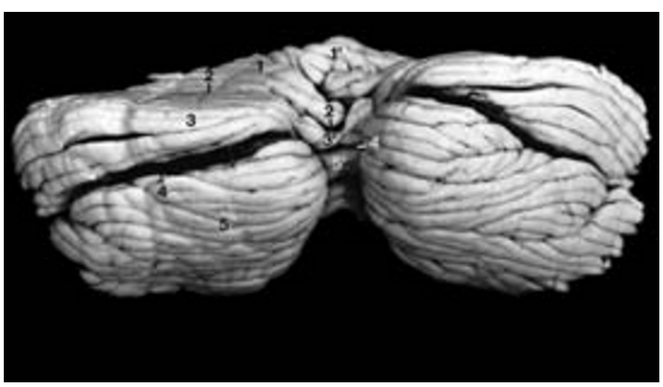

C

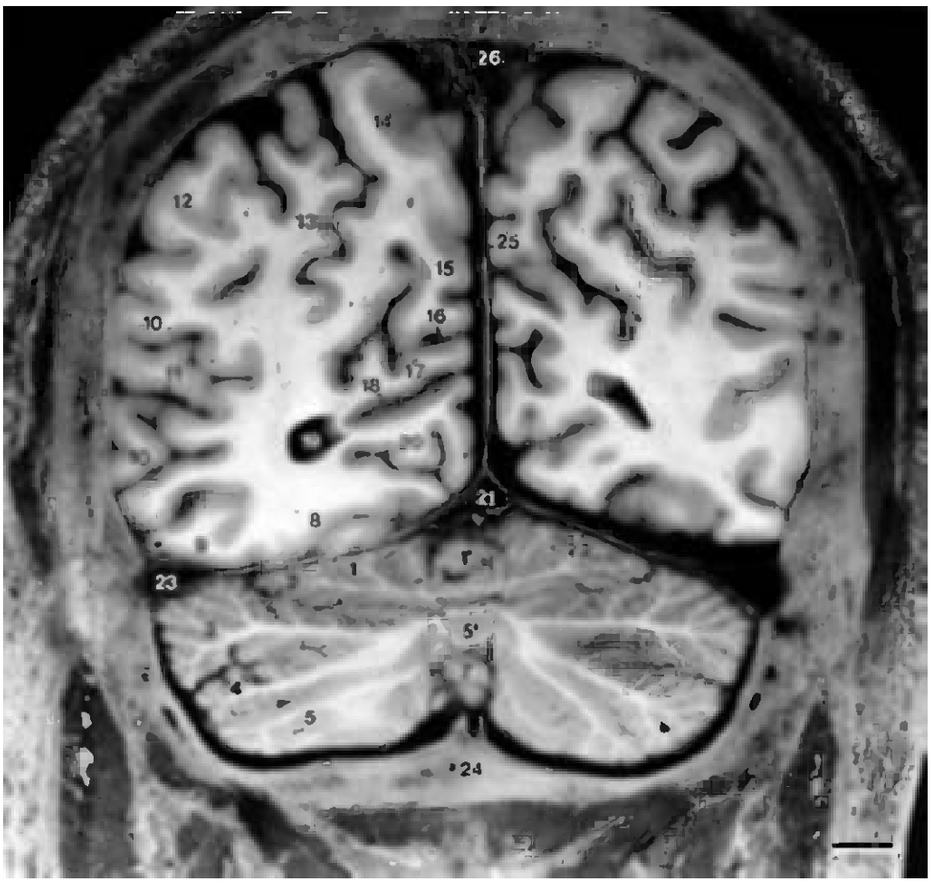

D

Fig. 11.54 (D–F). Coronal (frontal) section.
D. Coronal section of the head. Posterior view. Bar: 10 mm.
E–F. 3 Tesla MRI. E. T1-weighted MRI. **F.** T2-weighted MRI.

1 Simple lobule
1′ Declive
2 Posterior superior fissure
3 Superior semilunar lobule
3′ Folium of vermis
4 Great horizontal fissure
5 Inferior semilunar lobule
5′ Tuber
6 Prepyramidal fissure
7 Pyramid
8 Fourth occipital gyrus
9 Inferior occipital gyrus
10 Middle occipital gyrus
11 Lateral occipital sulcus
12 Angular gyrus
13 Intraparietal sulcus
14 Superior parietal lobule
15 Precuneus
16 Parieto-occipital fissure
17 Cuneus
18 Calcarine sulcus and striate cortex
19 Occipital horn of the lateral ventricle
20 Lingual gyrus
21 Straight sinus
22 Tentorium cerebelli
23 Transverse sinus
24 Occipital bone, squama
25 Falx cerebri
26 Superior sagittal sinus

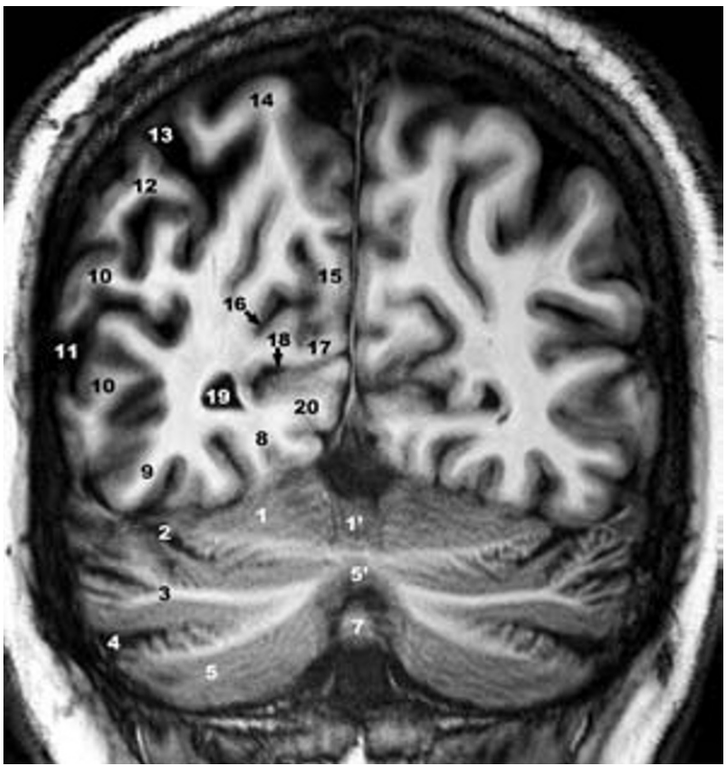
14
13
12
10
15
16
18
17
11
10
19
20
8
9
1
1'
2
5'
3
7
4
5

E

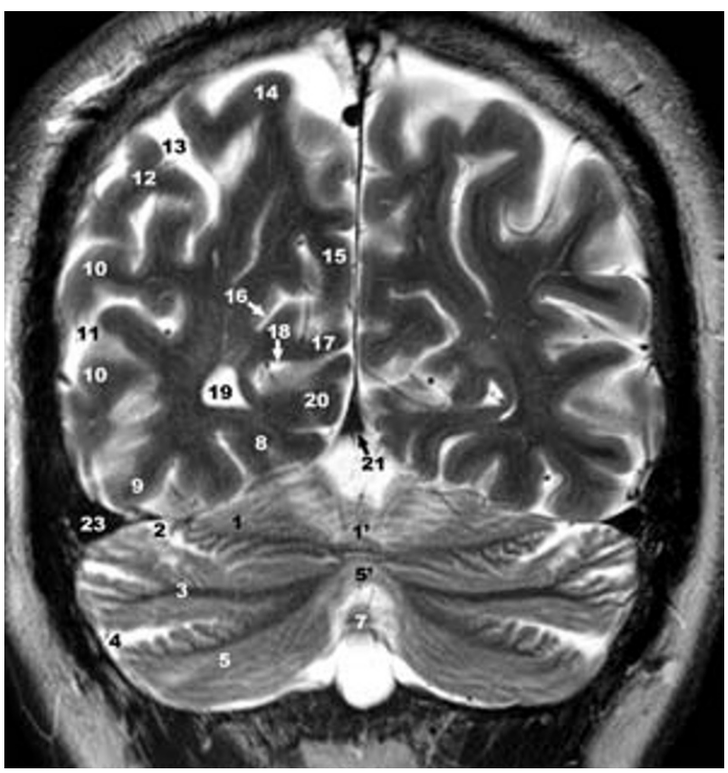
14
13
12
10
15
16
18
17
11
10
19
20
8
21
9
23
2
1
1'
5'
3
7
4
5

F

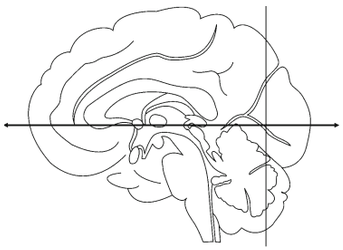

Fig. 11.55 (A–B). Coronal (frontal) section.
A. Frontal view after removal of the brain. Bar: 10 mm.,
B. Posterior oblique view.

1 Simple lobule
1′ Declive
2 Posterior superior fissure
3 Superior semilunar lobule
3′ Folium
4 Great horizontal fissure
5 Inferior semilunar lobule
5′ Tuber

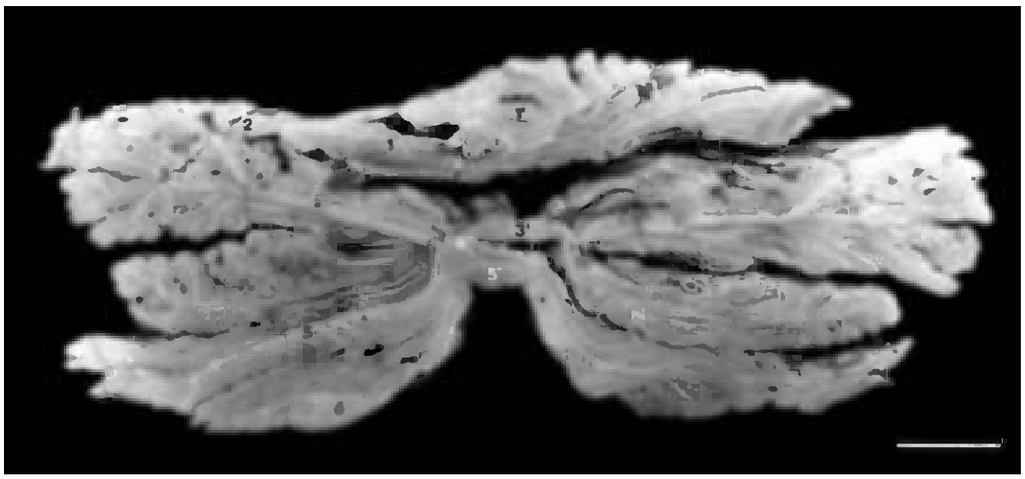

A

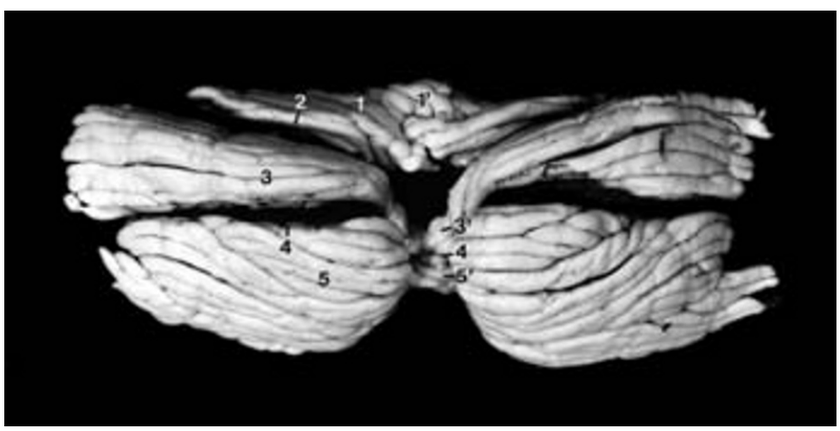

B

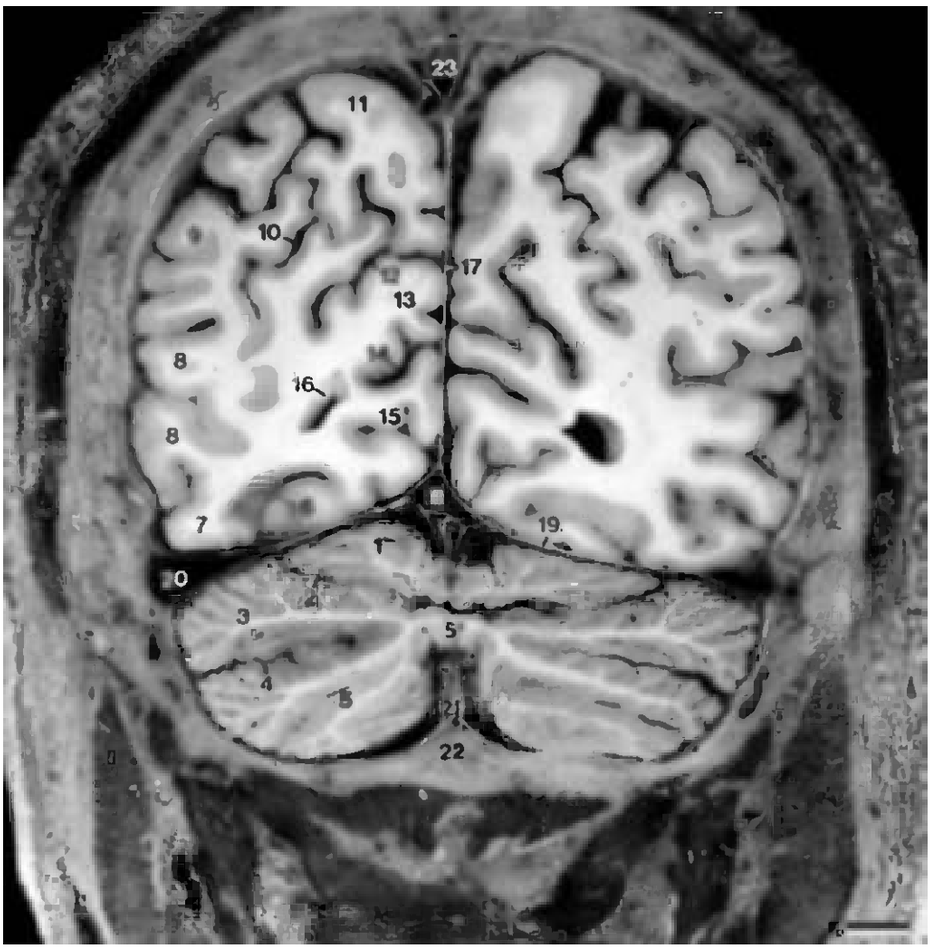

C

Fig. 11.55 (C–E). Coronal (frontal) section.
C. Coronal section of the head. Anterior view. Bar: 10 mm.
D–E. 3 Tesla MRI. D. T1-weighted MRI. **E.** T2-weighted MRI.

1 Simple lobule
1′ Declive
2 Posterior superior fissure
3 Superior semilunar lobule
3′ Folium
4 Great horizontal fissure
5 Inferior semilunar lobule
5′ Tuber
6 Fourth occipital gyrus
7 Inferior occipital gyrus
8 Middle occipital gyrus
9 Angular gyrus
10 Intraparietal sulcus
11 Superior parietal lobule
12 Parieto-occipital fissure
13 Cuneus
14 Calcarine sulcus
15 Lingual gyrus
16 Occipital horn of the lateral ventricle
17 Falx cerebri
18 Straight sinus
19 Tentorium cerebelli
20 Transverse sinus
21 Falx cerebelli
21′ Cisterna magna
22 Occipital bone, squama
23 Superior sagittal sinus

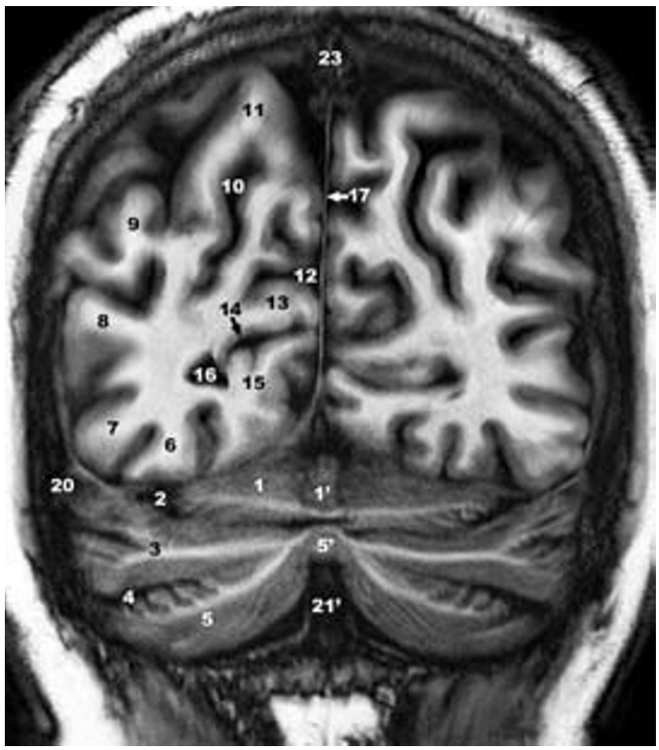
23
11
10
17
9
12
14
13
8
16
15
7
6
20
2
1
1'
3
5'
4
5
21'

D

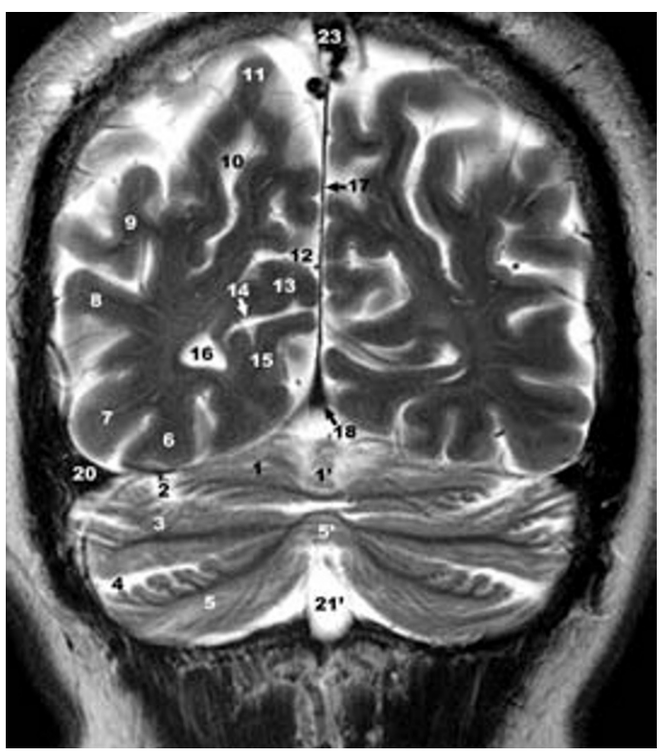
23
11
10
17
9
12
14
13
8
16
15
7
18
6
20
2
1
1'
3
5'
4
5
21'

E

Sagittal (lateral) sections parallel to the median plane (Figs. 11.56–11.70)

In the following figures, the anatomic specimen of the brain stem, cerebellum, and diencephalon is progressively reduced by 4 mm thick sections for **Figs. 11.56–11.67**, then by 1 mm thick sections for **Figs. 11.68–11.70** to show each new level in relation to the remaining portion of the specimen. The sagittal sections are most frequently used for the study of cerebellar fissures and lobules as well as for the diencephalomesencephalic junction. However, precise localization of deep brain stem structures may be difficult.

Each figure consists of the lateral view of the remaining sagittal surface, with oblique views demonstrating the level of the section. Corresponding sections of the head are provided for most levels to demonstrate the relationship of the brain to the skull and adjoining structures. At each level, both T1- and T2-weighted 3 Tesla MR images are provided for comparison. On each pair of facing pages all of the structures are labelled coherently, using the single key provided. However, the specific key changes from page to page.

For each section, the cartoon indicates the section level (light line).

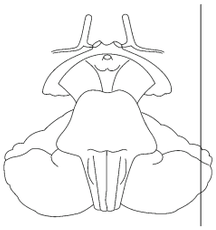

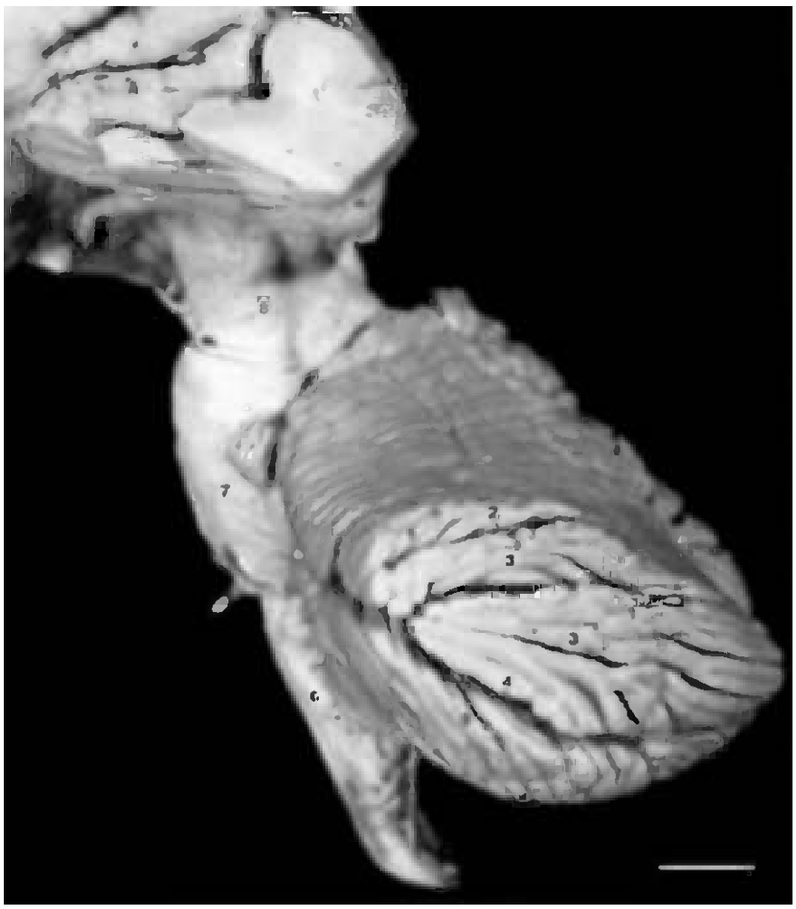

A

Fig. 11.56 (A–D). Sagittal (lateral) section.
A. Sagittal section after removal of the cerebral hemispheres. Bar: 10 mm.
B. Sagittal section of the head. Bar: 10 mm.
C–D. 3 Tesla MRI. **C.** T1-weighted MRI. **D.** T2-weighted MRI.

1 Simple lobule
2 Posterior superior fissure
3 Superior semilunar lobule
4 Great horizontal fissure
5 Inferior semilunar lobule
6 Medulla
7 Pons
8 Mesencephalon
9 Inferior temporal gyrus
10 Mastoid process
11 External acoustic meatus
12 Sigmoid sinus
13 Occipital bone, squama
14 Transverse sinus
15 Inferior occipital gyrus
16 Tentorium cerebelli
17 Superior temporal sulcus (parallel sulcus)
18 Superior temporal gyrus
18′ Transverse temporal gyrus (of Heschl)
19 Middle temporal gyrus

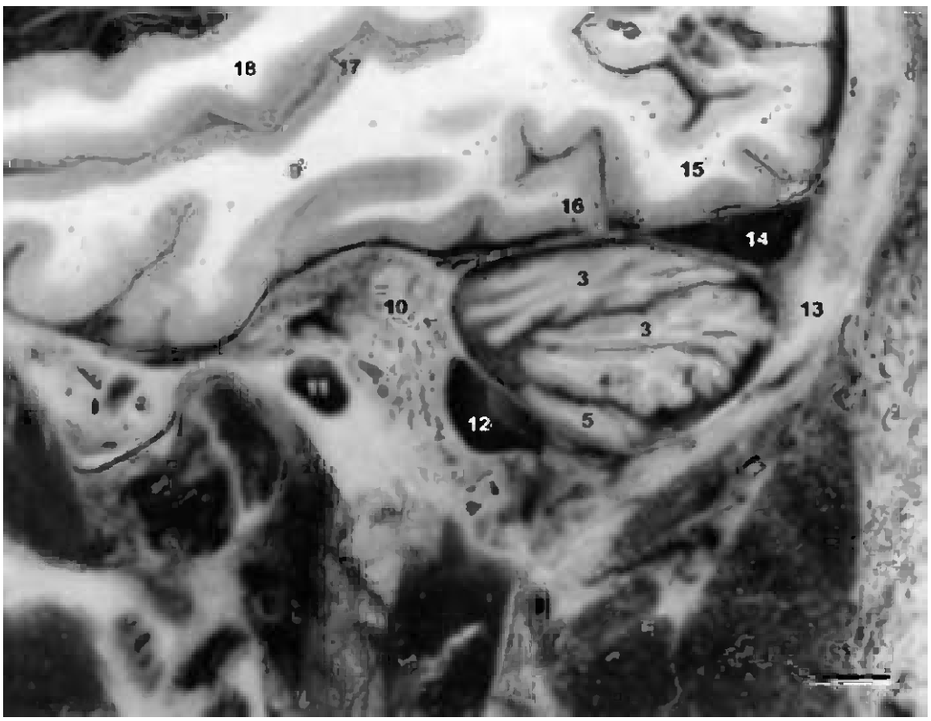
18
17
15
16
14
3
10
13
3
12
5

B

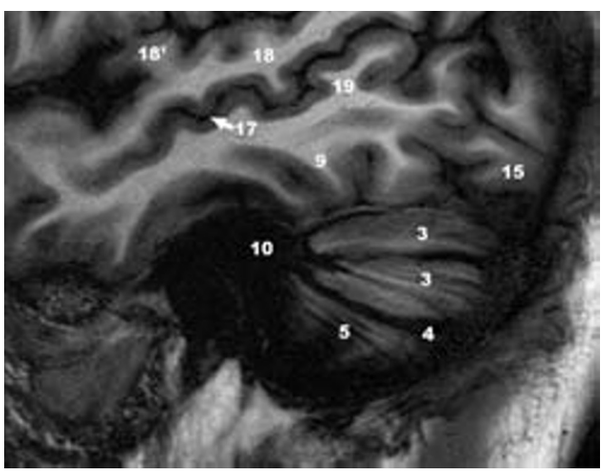
18'
18
19
17
9
15
10
3
3
5
4

C

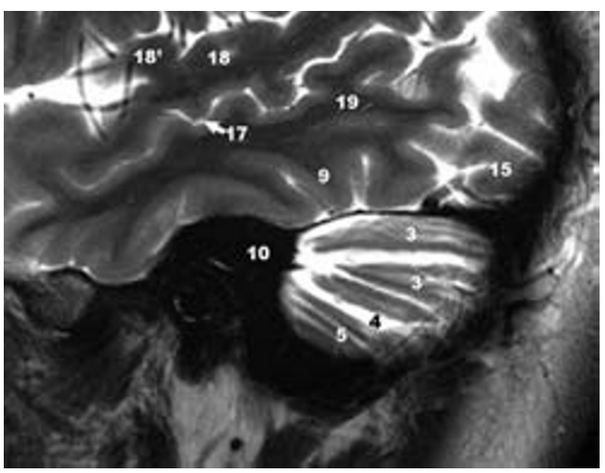
18'
18
19
17
9
15
10
3
3
5
4

D

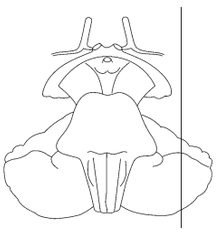

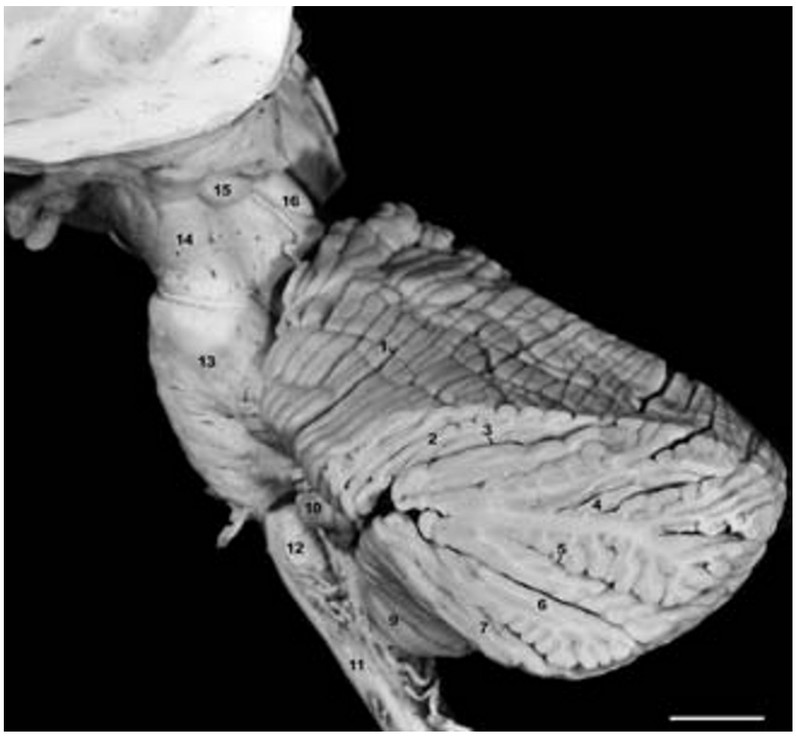

A

Fig. 11.57 (A–C). Sagittal (lateral) section.
A. Sagittal view after removal of the cerebral hemispheres. Bar: 10 mm.
B. Superior oblique view. **C.** Inferior oblique view.

1 Anterior superior (primary) fissure
2 Simple lobule
3 Posterior superior fissure
4 Superior semilunar lobule
5 Great horizontal fissure
6 Inferior semilunar lobule
7 Gracile lobule
8 Prepyramidal fissure
9 Biventral lobule
10 Flocculus
11 Medulla
12 Inferior olive
13 Pons
14 Crus cerebri
15 Medial geniculate body
16 Superior colliculus

B

C

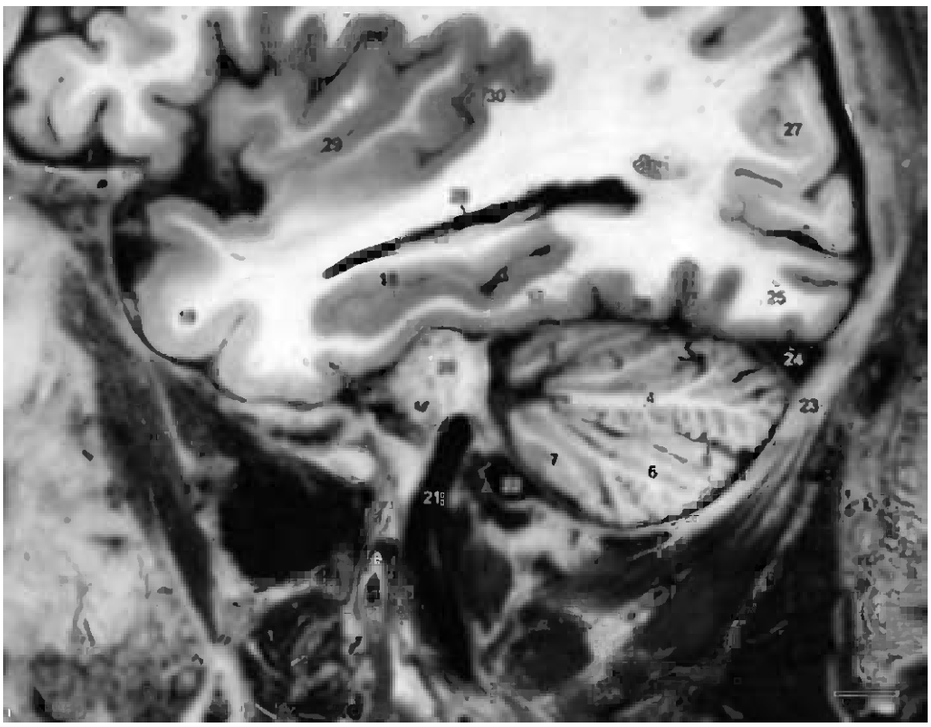

D

Fig. 11.57 (D–F).
D. Sagittal section of the head. Bar: 10 mm.
E–F. 3 Tesla MRI. E. T1-weighted MRI. **F.** T2-weighted MRI.

2 Simple lobule
3 Posterior superior fissure
4 Superior semilunar lobule
5 Great horizontal fissure
6 Inferior semilunar lobule
7 Gracile lobule
17 Fusiform gyrus
18 Collateral sulcus
19 Temporal pole
20 Temporal bone, petrous portion
21 Internal jugular vein
22 Sigmoid sinus
23 Occipital bone, squama
24 Transverse sinus
25 Inferior occipital gyrus
26 Tentorium cerebelli
27 Middle occipital gyrus
28 Temporal horn of the lateral ventricle
29 Central sulcus of the insula, dividing the insula into anterior (29′) and posterior (29″) lobules
29′ Anterior lobule of the insula
29″ Posterior lobule of the insula
30 Transverse temporal gyrus (of Heschl)

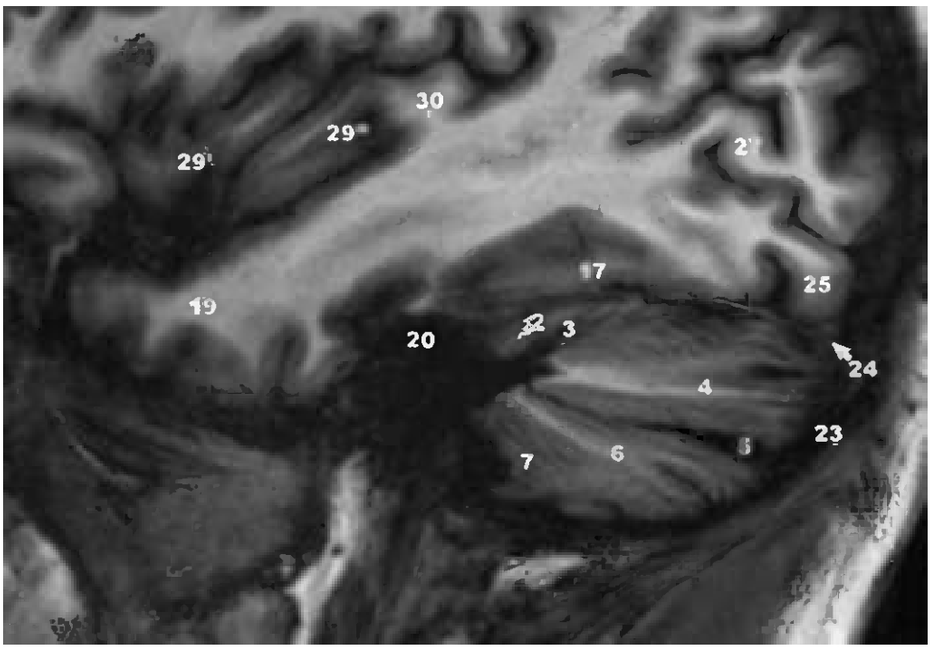
30
29
29'
27
17
25
19
20
3
24
4
23
7
6
5

E

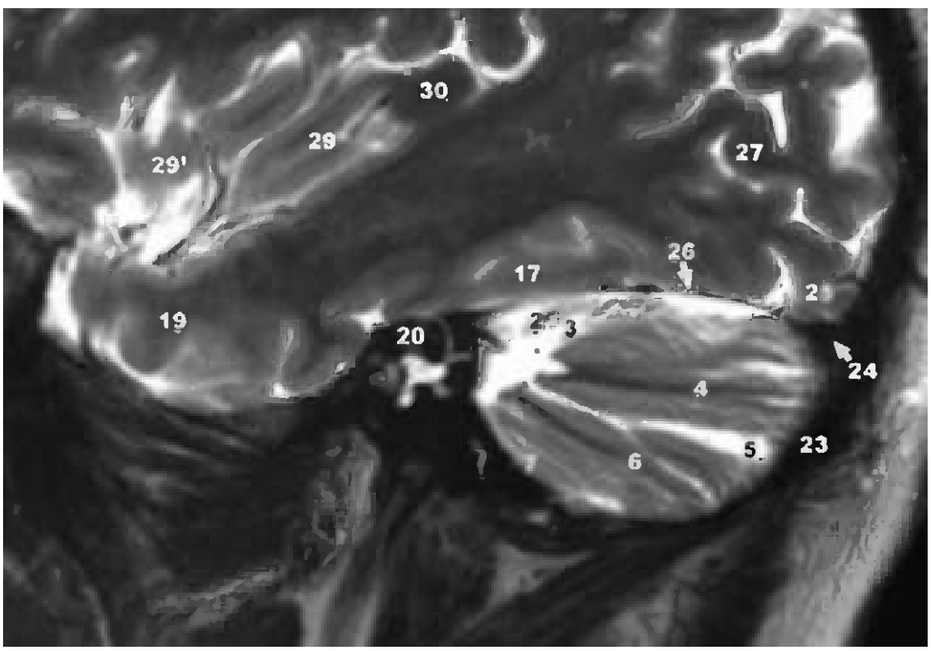
30
29
29'
27
26
17
2
19
20
3
24
4
23
6
5

F

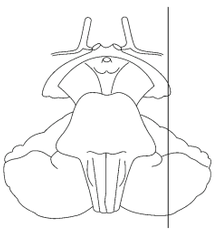

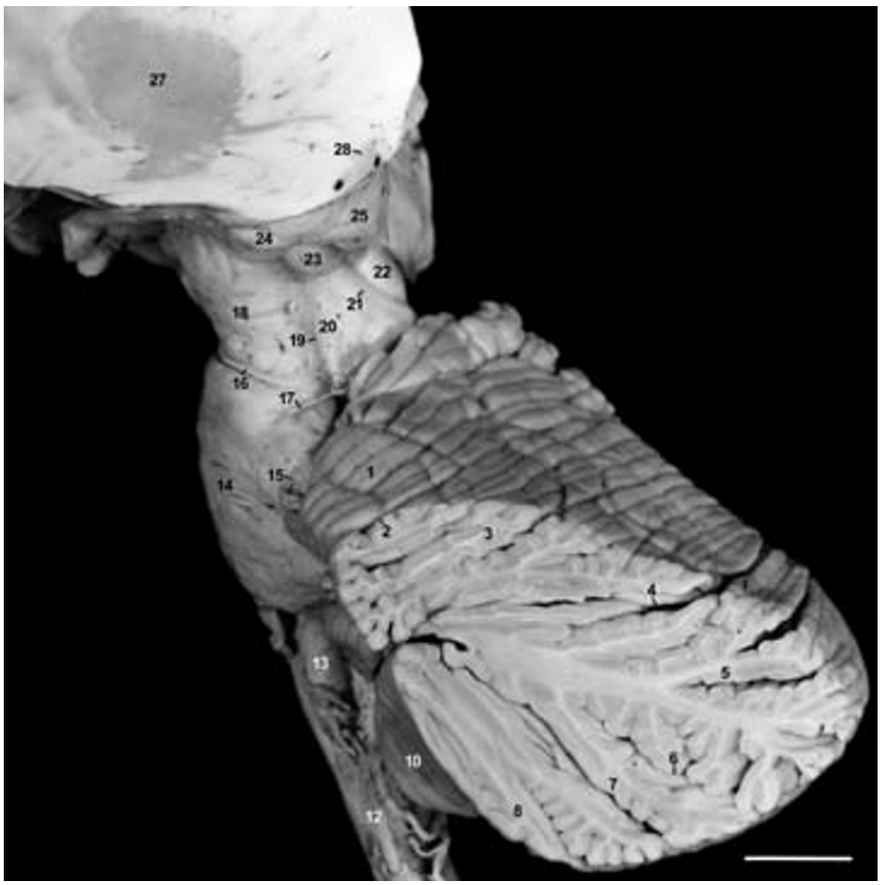

A

Fig. 11.58 (A–C). Sagittal (lateral) section.
A. Sagittal section after removal of the cerebral hemispheres. Bar: 10 mm.
B. Superior oblique view. **C.** Inferior oblique view.

1 Quadrangular lobule
2 Anterior superior (primary) fissure
3 Simple lobule
4 Posterior superior fissure
5 Superior semilunar lobule
6 Great horizontal fissure
7 Inferior semilunar lobule
8 Gracile lobule
9 Prepyramidal fissure
10 Biventral lobule
11 Flocculus
12 Medulla
13 Inferior olive
14 Pons
15 Trigeminal nerve (CN V)
16 Pontomesencephalic sulcus
17 Trochlear nerve (CN IV)
18 Crus cerebri
19 Lateral mesencephalic sulcus
20 Lateral aspect of mesencephalon
21 Brachium of the inferior colliculus
22 Superior colliculus
23 Medial geniculate body
24 Lateral geniculate body
25 Pulvinar
26 Pineal gland
27 Putamen
28 Caudate nucleus (tail)

B

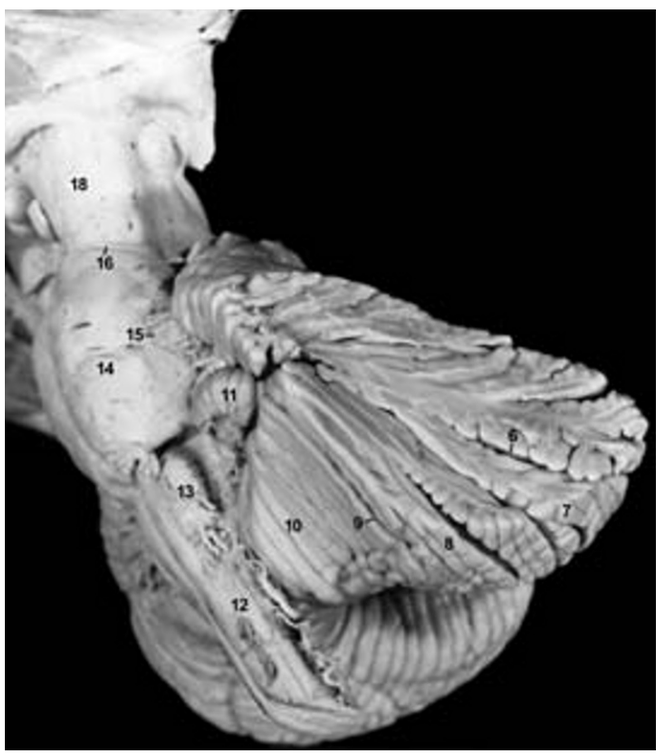

C

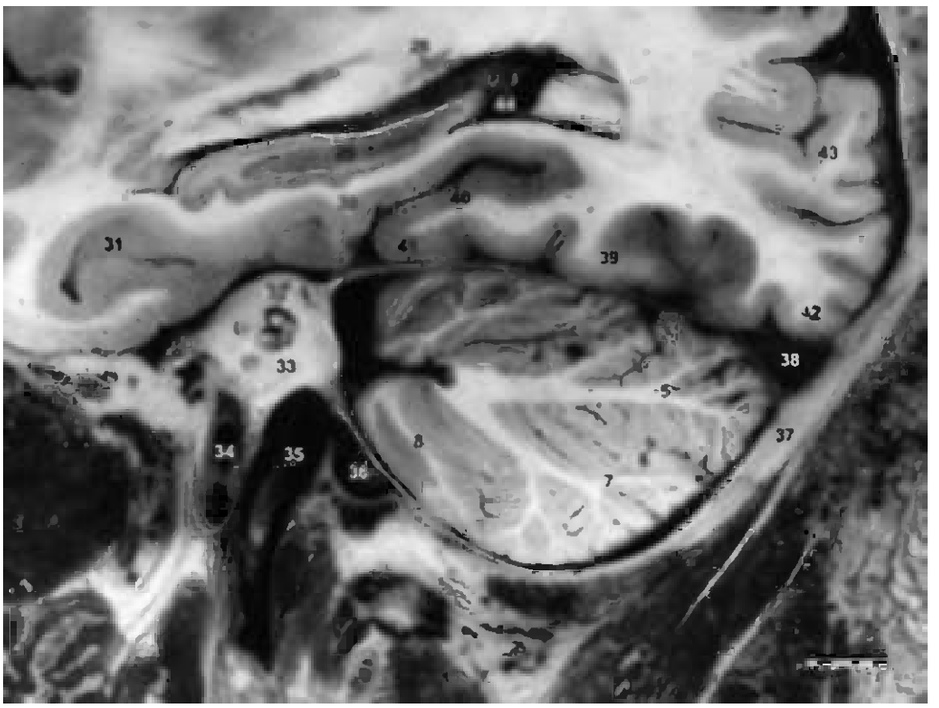

D

Fig. 11.58 (D–F).
D. Sagittal section of the head. Bar: 10 mm.
E–F. 3 Tesla MRI. **E.** T1-weighted MRI. **F.** T2-weighted MRI.

3 Simple lobule
4 Posterior superior fissure
5 Superior semilunar lobule
6 Great horizontal fissure
7 Inferior semilunar lobule
8 Gracile lobule
28 Caudate nucleus (tail)
29 Hippocampus
30 Parahippocampal gyrus
31 Temporal pole
32 Internal ear
33 Temporal bone, petrous portion
34 Internal carotid artery
35 Internal jugular vein
36 Sigmoid sinus
37 Occipital bone, squama
38 Transverse sinus
39 Fusiform gyrus
40 Collateral sulcus
41 Tentorium cerebelli
42 Inferior occipital gyrus
43 Middle occipital gyrus
44 Atrium of the lateral ventricle
45 Insula

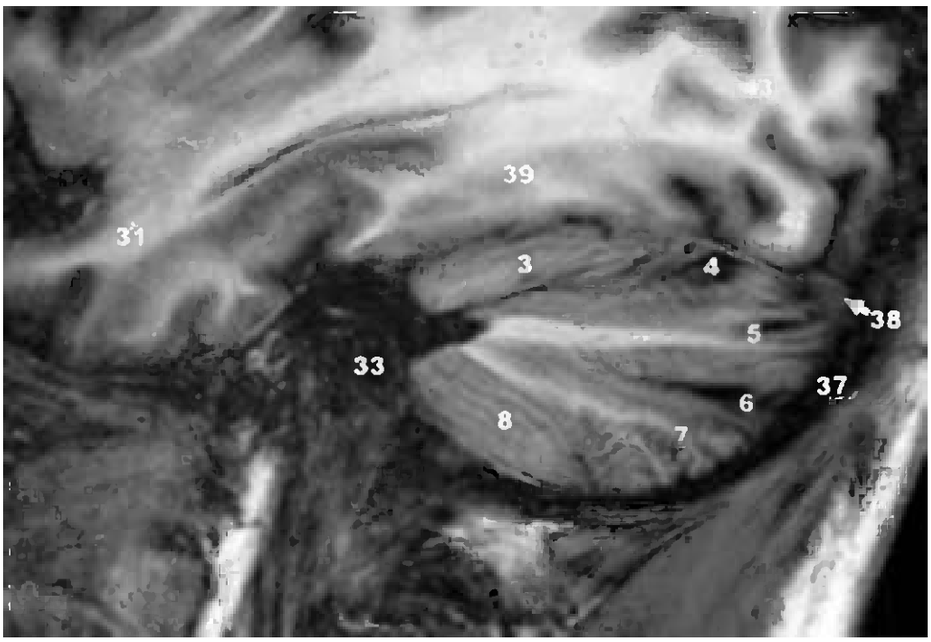

E

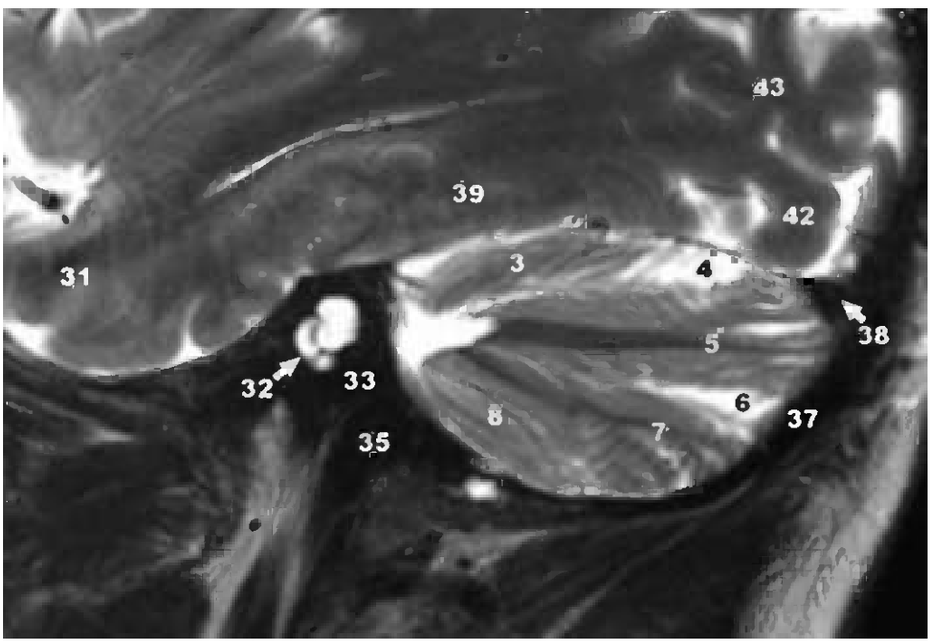

F

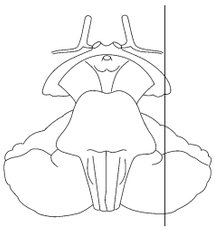

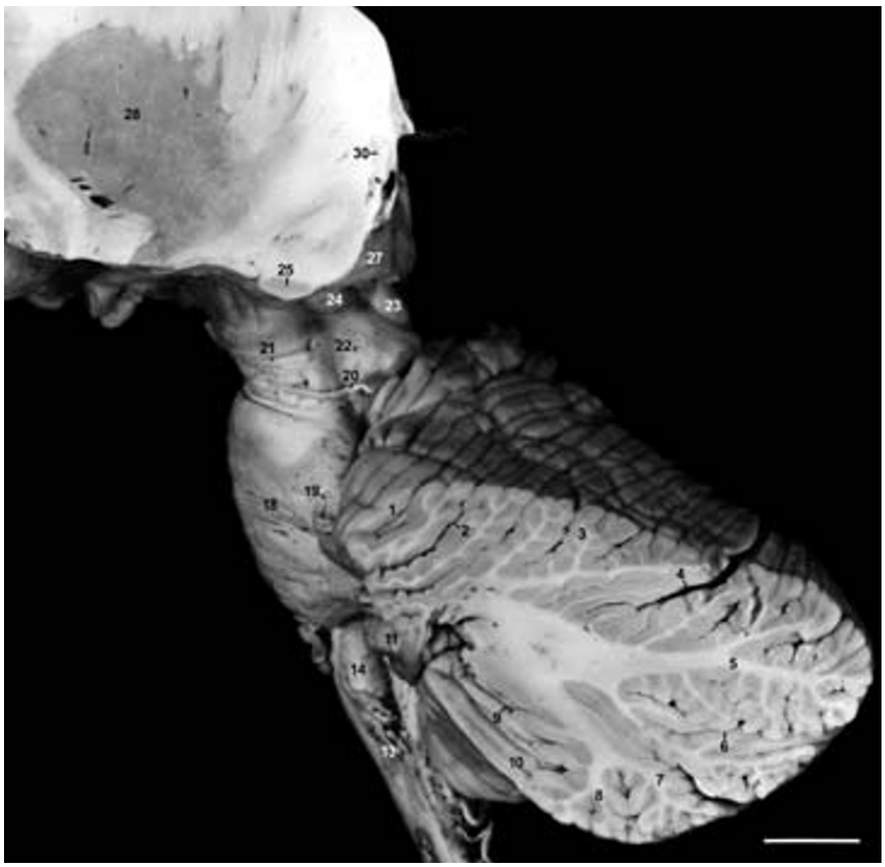

A

Fig. 11.59 (A–C). Sagittal (lateral) section.
A. Sagittal section after removal of the cerebral hemispheres. Bar: 10 mm.
B. Superior oblique view. **C.** Inferior oblique view.

1 Quadrangular lobule
2 Anterior superior (primary) fissure
3 Simple lobule
4 Posterior superior fissure
5 Superior semilunar lobule
6 Great horizontal fissure
7 Inferior semilunar lobule
8 Gracile lobule
9 Prepyramidal fissure
10 Biventral lobule
11 Flocculus
12 Choroid plexus (lateral aperture of the fourth ventricle) (foramen of Luschka)
13 Medulla
14 Inferior olive
15 Vagus nerve (CN X)
16 Vestibulocochlear nerve (CN VIII)
17 Facial nerve (CN VII)
18 Pons
19 Trigeminal nerve (CN V)
20 Trochlear nerve (CN IV)
21 Crus cerebri
22 Lateral aspect of mesencephalon
23 Superior colliculus
24 Medial geniculate body
25 Lateral geniculate body
26 Optic tract (CN II)
27 Pulvinar
28 Putamen
29 Pineal gland
30 Caudate nucleus

B

C

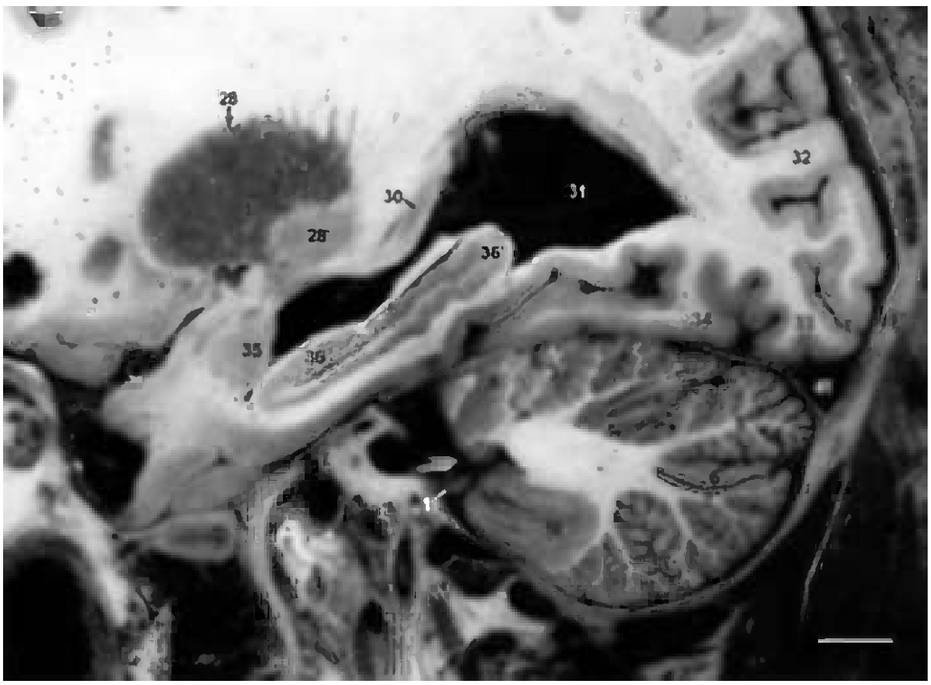

D

Fig. 11.59 (D–F).
D. Sagittal section of the head. Bar: 10mm.
E–F. 3 Tesla MRI. **E.** T1-weighted MRI. **F.** T2-weighted MRI.

1 Quadrangular lobule
3 Simple lobule
4 Posterior superior fissure
5 Superior semilunar lobule
6 Great horizontal fissure
7 Inferior semilunar lobule
8 Gracile lobule
10 Biventral lobule
11 Flocculus
28 Putamen
28′ Lateral (external) pallidum
30 Caudate nucleus
31 Atrium of the lateral ventricle
32 Middle occipital gyrus
32′ Lunate sulcus
33 Inferior occipital gyrus
34 Fusiform gyrus
35 Amygdala
36 Hippocampus, head
36′ Hippocampus, tail
37 Temporal stem
38 Internal auditory meatus
39 Temporal bone, petrous portion
40 Occipital bone, squama
41 Transverse sinus
42 Cistern of the cerebellopontine angle

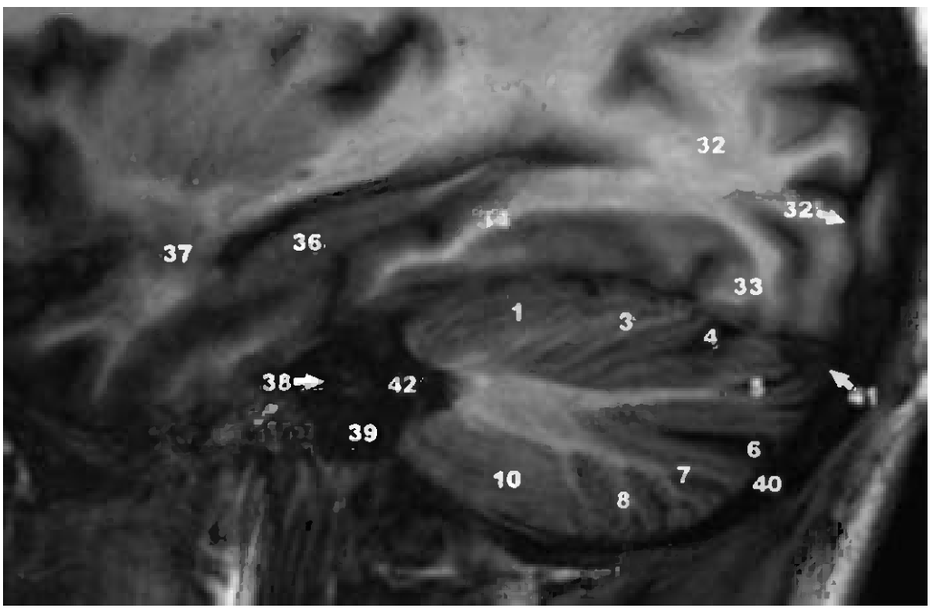
32
32
37
36
33
1
3
4
38
42
39
6
10
7
40
8

E

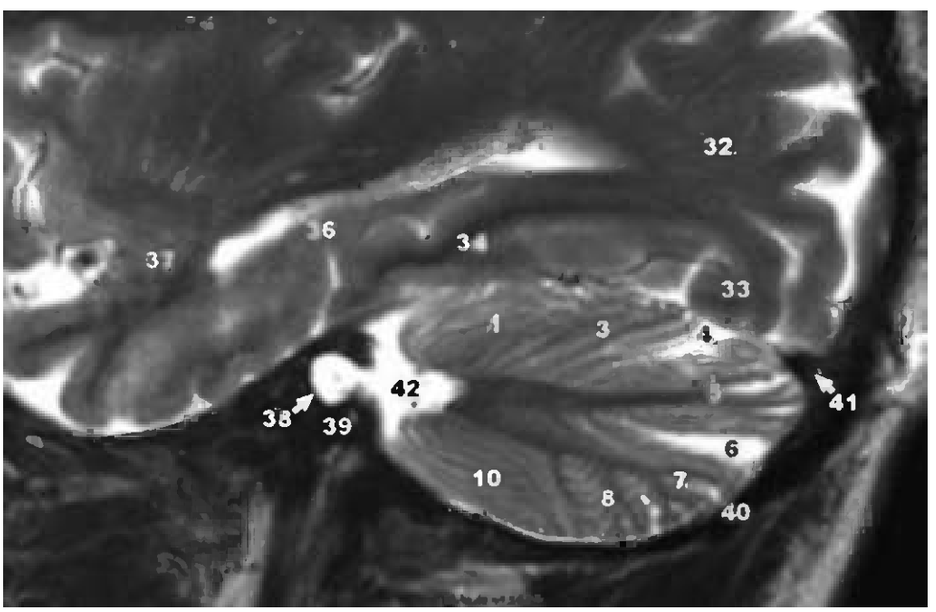
32
6
34
37
33
1
3
42
41
38
39
6
10
7
8
40

F

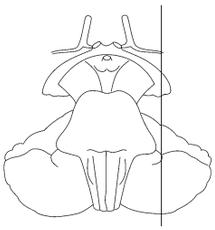

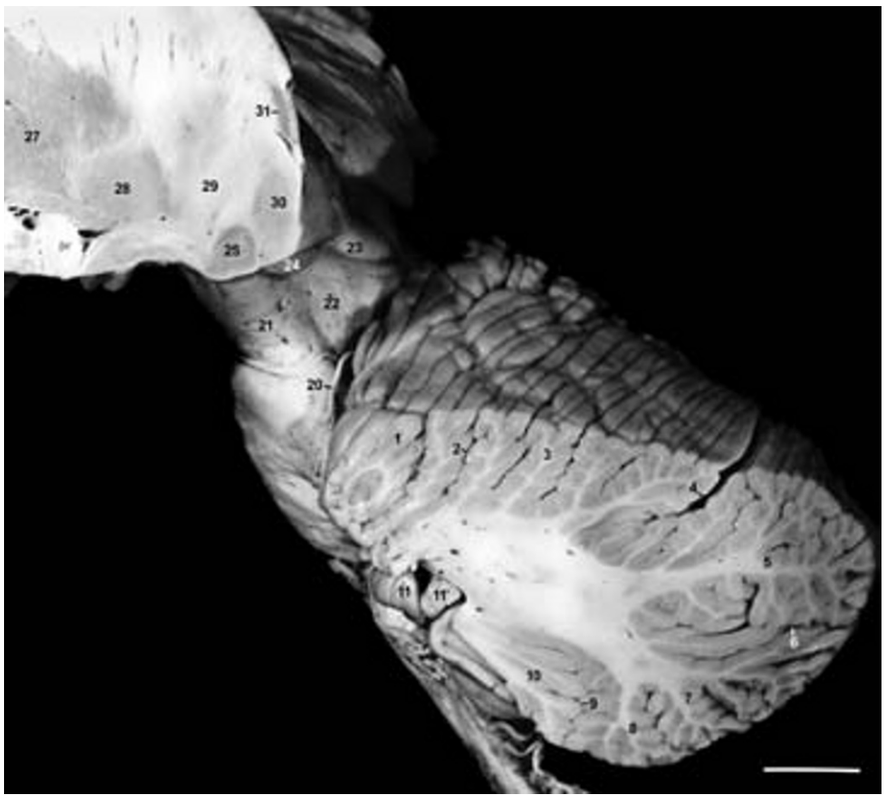

A

Fig. 11.60 (A–C). Sagittal (lateral) section.
A. Sagittal section after removal of the cerebral hemispheres. Bar: 10 mm.
B. Superior oblique view. **C.** Inferior oblique view.

1 Quadrangular lobule
2 Anterior superior (primary) fissure
3 Simple lobule
4 Posterior superior fissure
5 Superior semilunar lobule
6 Great horizontal fissure
7 Inferior semilunar lobule
8 Gracile lobule
9 Prepyramidal fissure
10 Biventral lobule
11 Flocculus
11′ Paraflocculus
12 Choroid plexus (lateral aperture of the fourth ventricle) (foramen of Luschka)
13 Medulla
14 Inferior olive
15 Vagus nerve (CN X)
16 Vestibulocochlear nerve (CN VIII)
17 Facial nerve (CN VII)
18 Pons
19 Trigeminal nerve (CN V)
20 Trochlear nerve (CN IV)
21 Crus cerebri
22 Lateral aspect of mesencephalon
23 Superior colliculus
24 Medial geniculate body
25 Lateral geniculate body
26 Optic tract (CN II)
27 Putamen
28 Lateral (external) pallidum
29 Internal capsule, posterior limb
30 Pulvinar
31 Caudate nucleus
32 Pineal gland

B

C

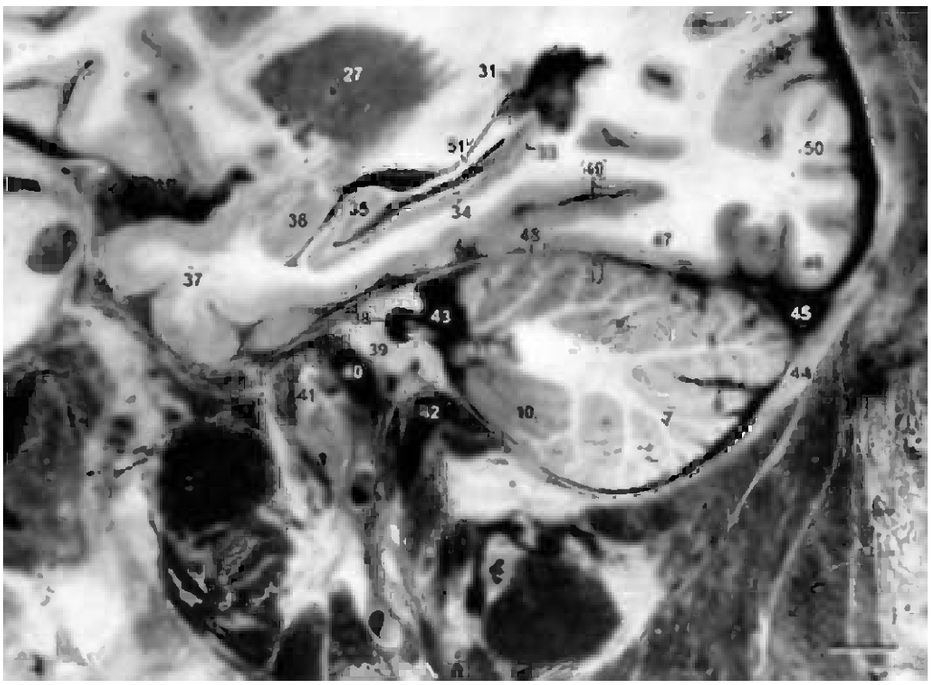

D

Fig. 11.60 (D–F).
D. Sagittal (lateral) section of the head. Bar: 10 mm.
E–F. 3 Tesla MRI. E. T1-weighted MRI. **F.** T2-weighted MRI.

1 Quadrangular lobule
3 Simple lobule
4 Posterior superior fissure
5 Superior semilunar lobule
6 Great horizontal fissure
7 Inferior semilunar lobule
10 Biventral lobule
11 Flocculus
27 Putamen
31 Caudate nucleus
33 Hippocampus, tail
34 Parahippocampal gyrus
35 Hippocampus, head
35′ Hippocampus
36 Amygdala
37 Temporal pole
38 Internal acoustic meatus
39 Temporal bone, petrous portion
40 Internal carotid artery
41 Eustachian tube
42 Jugular foramen
43 Cistern of the cerebellopontine angle
44 Occipital bone, squama
45 Transverse sinus
46 Inferior occipital gyrus
47 Lingual gyrus
48 Tentorium cerebelli
49 Collateral sulcus
50 Middle occipital gyrus
51 Fimbria
52 Lunate sulcus
53 Fusiform gyrus

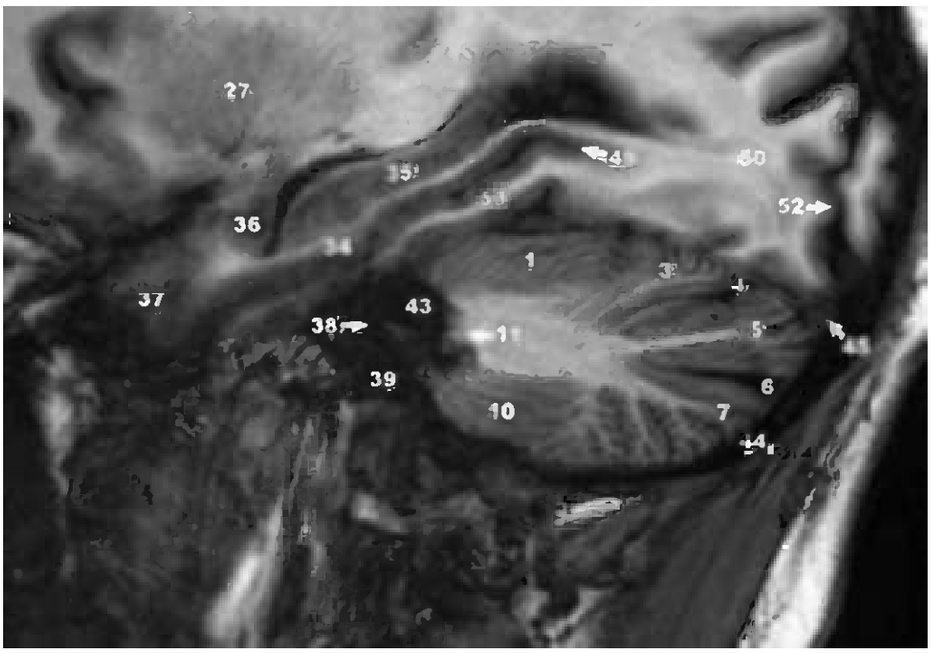

E

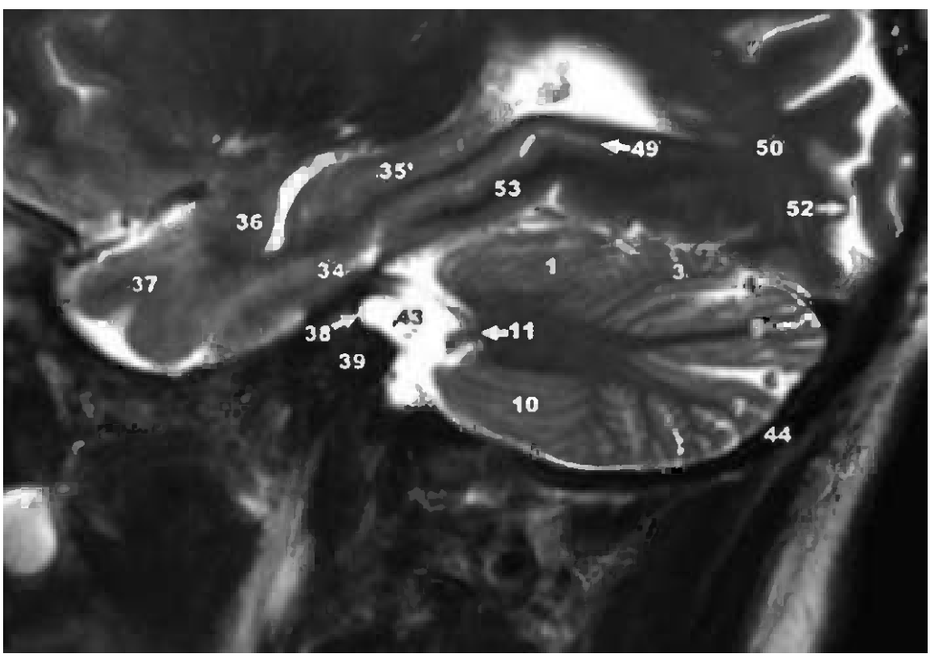

F

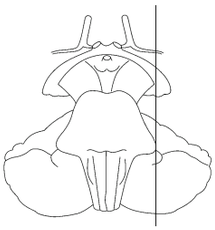

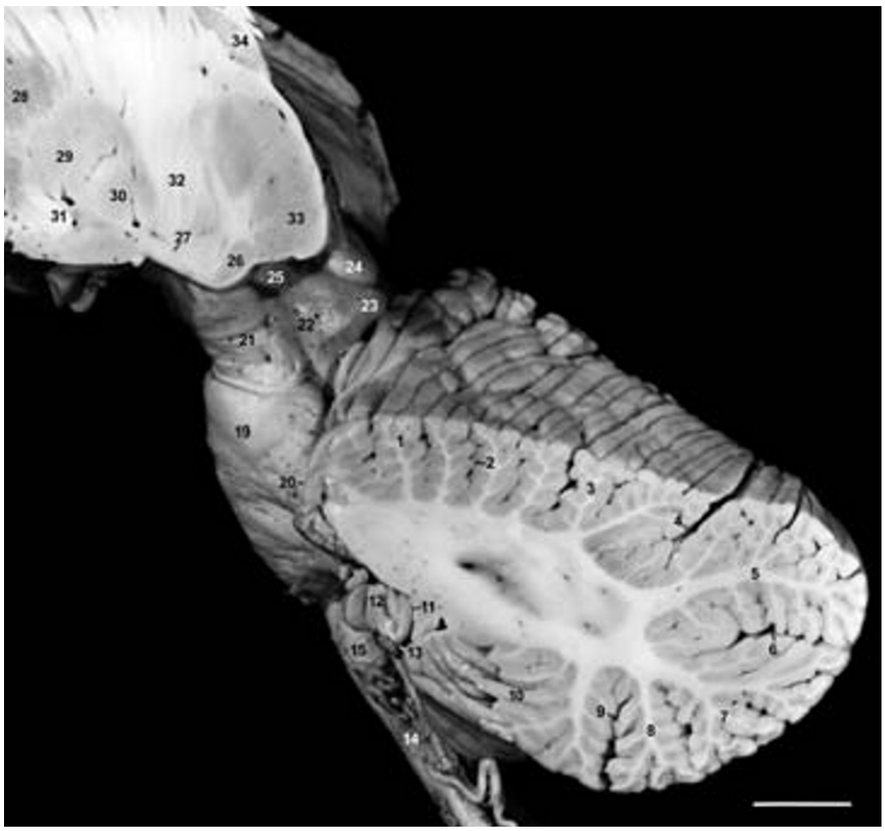

A

Fig. 11.61 (A–C). Sagittal (lateral) section.
A. Sagittal section after removal of the cerebral hemispheres. Bar: 10 mm.
B. Superior oblique view. **C.** Inferior oblique view.

1 Quadrangular lobule
2 Anterior superior (primary) fissure
3 Simple lobule
4 Posterior superior fissure
5 Superior semilunar lobule
6 Great horizontal fissure
7 Inferior semilunar lobule
8 Gracile lobule
9 Prepyramidal fissure
10 Biventral lobule
11 Posterolateral fissure
12 Flocculus
13 Choroid plexus (lateral aperture of the fourth ventricle) (foramen of Luschka)
14 Medulla
15 Inferior olive
16 Vagus nerve (CN X)
17 Vestibulocochlear nerve (CN VIII)
18 Facial nerve (CN VII)
19 Pons
20 Trigeminal nerve (CN V)
21 Crus cerebri
22 Lateral aspect of mesencephalon
23 Inferior colliculus
24 Superior colliculus
25 Medial geniculate body
26 Lateral geniculate body
27 Optic tract (CN II)
28 Putamen
29 Lateral (external) pallidum
30 Medial (internal) pallidum
31 Anterior commissure
32 Internal capsule, posterior limb
33 Pulvinar
34 Caudate nucleus
35 Pineal gland

B

C

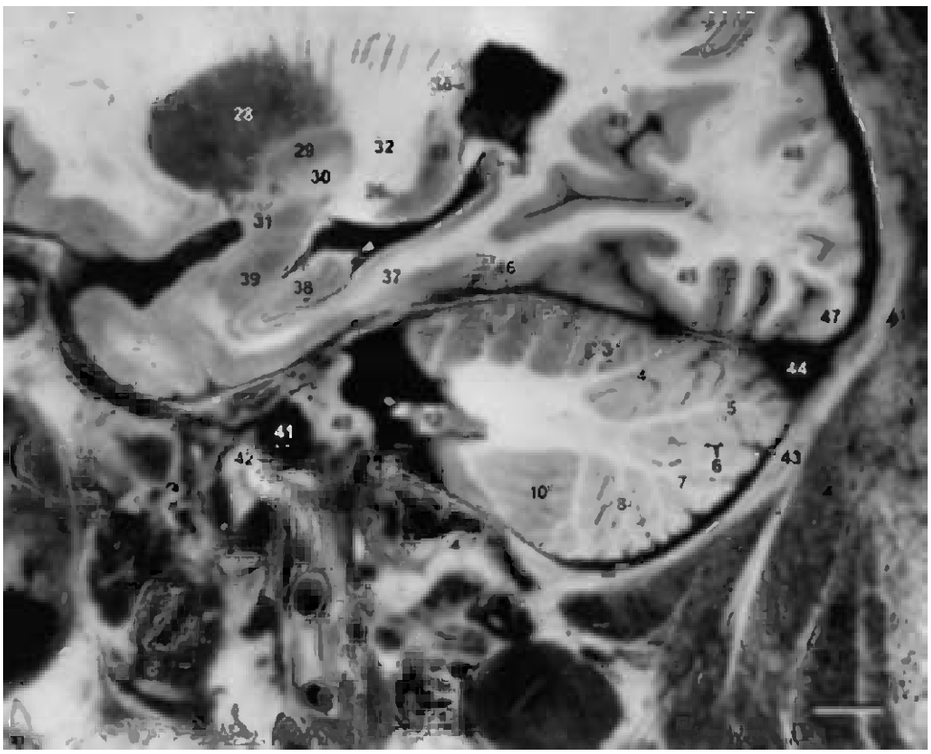

D

Fig. 11.61 (D–F).
D. Sagittal (lateral) section of the head. Bar: 10 mm.
E–F. 3 Tesla MRI. **E.** T1-weighted MRI. **F.** T2-weighted MRI.

1 Quadrangular lobule
3 Simple lobule
4 Posterior superior fissure
5 Superior semilunar lobule
6 Great horizontal fissure
7 Inferior semilunar lobule
8 Gracile lobule
10 Biventral lobule
12 Flocculus
26 Lateral geniculate body
28 Putamen
29 Lateral (external) pallidum
30 Medial (internal) pallidum
31 Anterior commissure
32 Internal capsule, posterior limb
33 Pulvinar
34 Caudate nucleus
36 Hippocampus, tail
37 Parahippocampal gyrus
38 Hippocampus, head (with fimbria (arrowheads))
39 Amygdala
40 Temporal bone, petrous portion
41 Internal carotid artery
42 Eustachian tube
43 Occipital bone, squama
44 Transverse sinus
45 Lingual gyrus
46 Tentorium cerebelli
47 Inferior occipital gyrus
48 Superior occipital gyrus
49 Parieto-occipital fissure
50 Collateral sulcus
51 Fusiform gyrus
52 Middle occipital gyrus
53 Lunate sulcus

Arrowheads: Fimbria of the hippocampal formation

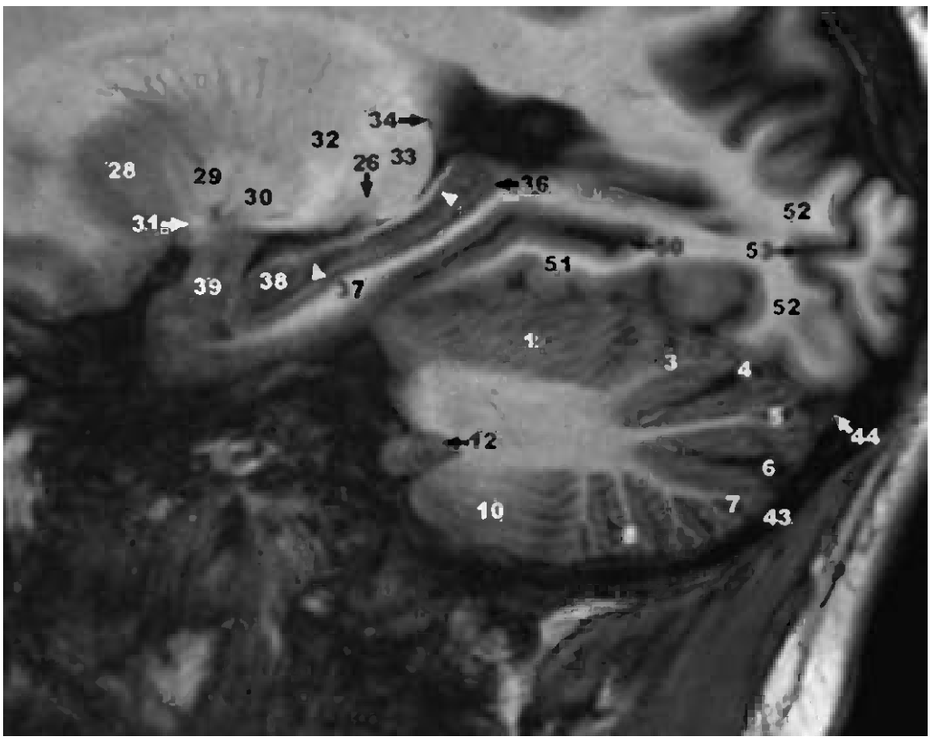
34
32
28
29
26
33
30
36
31
52
5
51
39
38
7
52
1
3
4
44
12
6
10
7
43

E

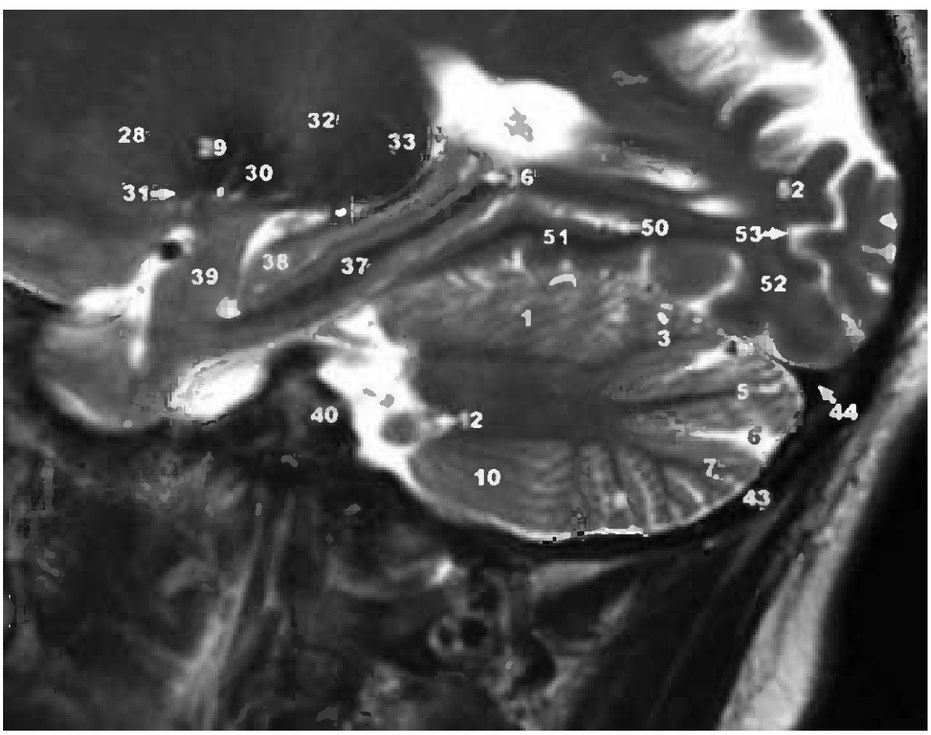
32
28
9
33
30
6
31
2
51
50
53
39
38
37
52
1
3
5
44
40
2
6
10
7
43

F

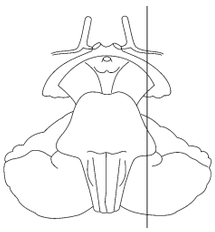

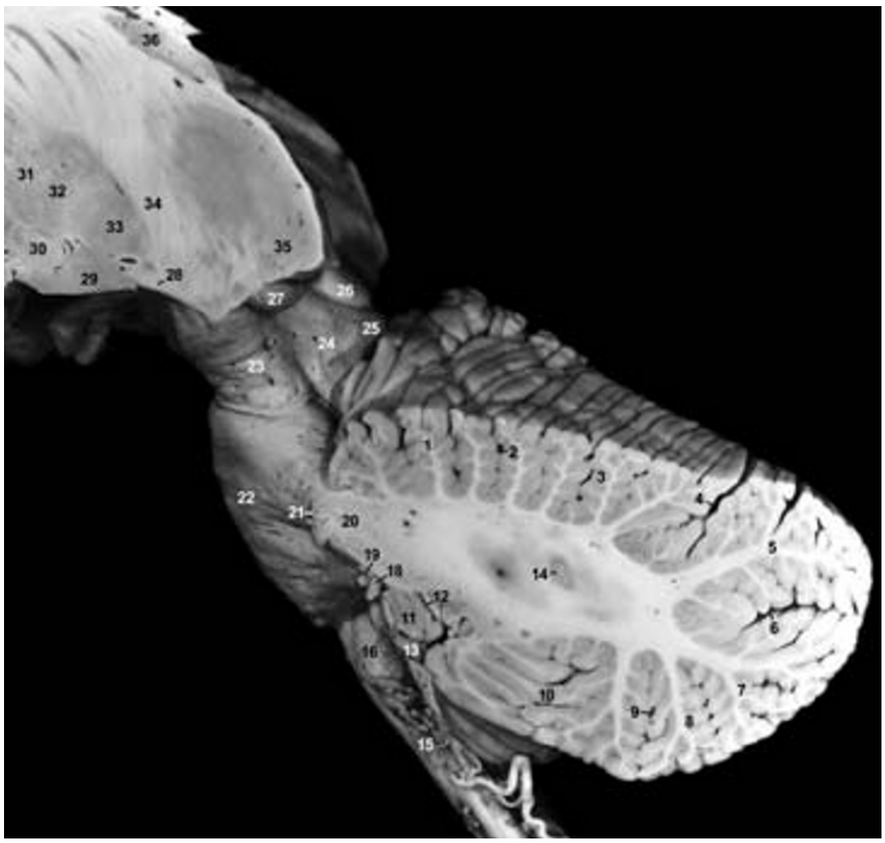

A

Fig. 11.62 (A–C). Sagittal (lateral) section.
A. Sagittal section after removal of the cerebral hemispheres. Bar: 10 mm.
B. Superior oblique view. **C.** Inferior oblique view.

1 Quadrangular lobule
2 Anterior superior (primary fissure)
3 Simple lobule
4 Posterior superior fissure
5 Superior semilunar lobule
6 Great horizontal fissure
7 Inferior semilunar lobule
8 Gracile lobule
9 Prepyramidal fissure
10 Biventral lobule
11 Flocculus
12 Posterolateral fissure
13 Choroid plexus (lateral aperture of the fourth ventricle) (foramen of Luschka)
14 Dentate nucleus
15 Medulla
16 Inferior olive
17 Vagus nerve (CN X)
18 Vestibulocochlear nerve (CN VIII)
19 Facial nerve (CN VII)
20 Middle cerebellar peduncle (brachium pontis)
21 Trigeminal nerve (CN V)
22 Pons
23 Crus cerebri
24 Mesencephalon, lateral aspect
25 Inferior colliculus
26 Superior colliculus
27 Medial geniculate body
28 Optic tract (CN II)
29 Anterior perforated substance
30 Anterior commissure
31 Putamen
32 Lateral (external) pallidum
33 Medial (internal) pallidum
34 Internal capsule, posterior limb
35 Pulvinar
36 Caudate nucleus
37 Pineal gland

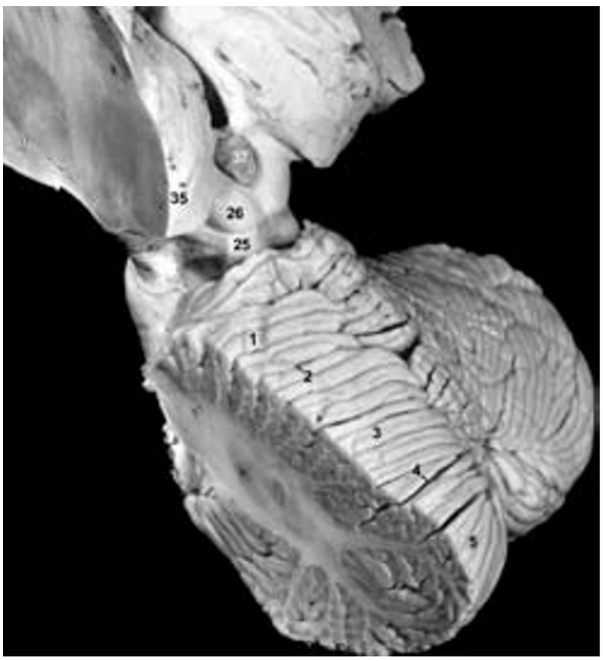

B

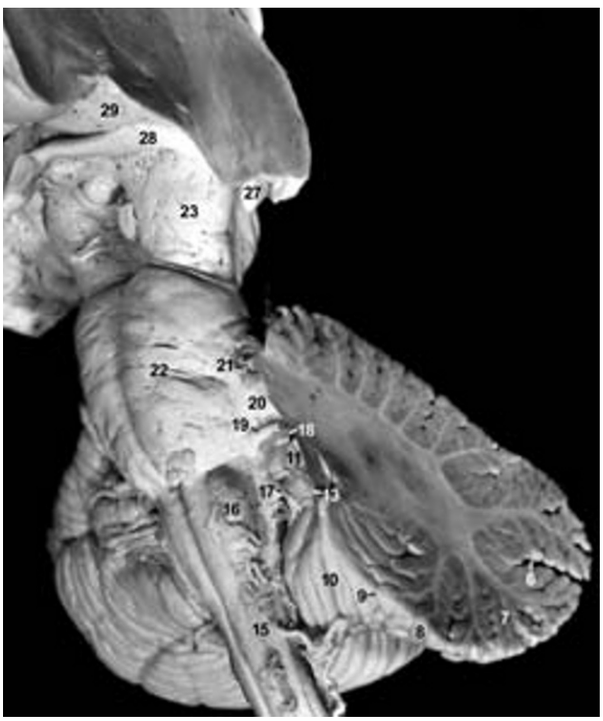

C

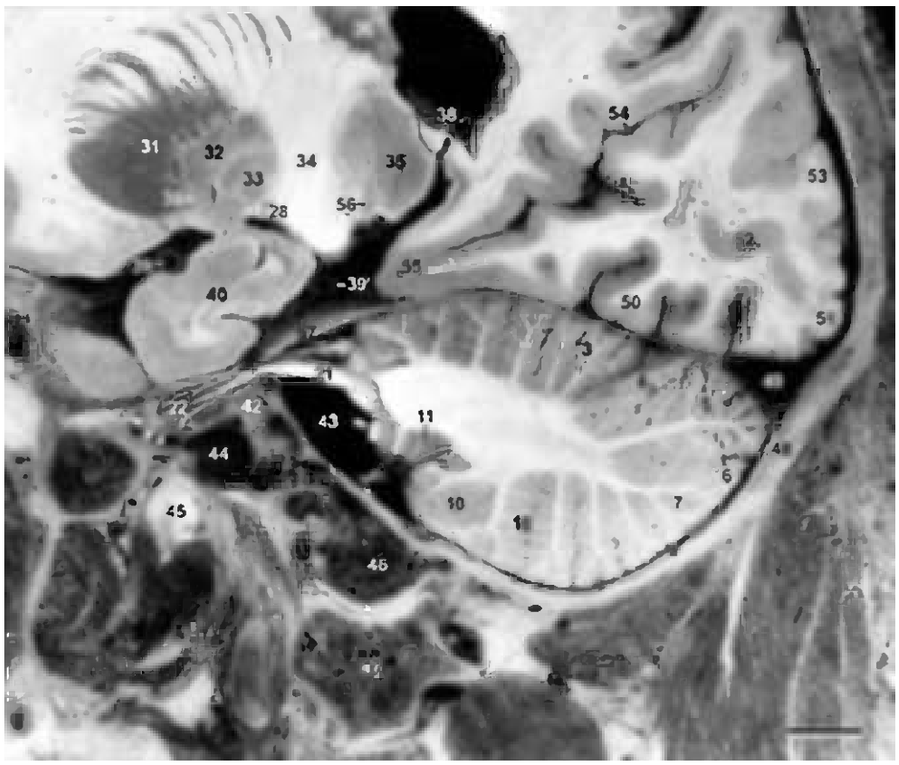

D

Fig. 11.62 (D–F).
D. Sagittal (lateral) section of the head. Bar: 10 mm.
E–F. 3 Tesla MRI. E. T1-weighted MRI. **F.** T2-weighted MRI.

1 Quadrangular lobule
3 Simple lobule
4 Posterior superior fissure
5 Superior semilunar lobule
6 Great horizontal fissure
7 Inferior semilunar lobule
10 Biventral lobule
11 Flocculus
20 Middle cerebellar peduncle (brachium pontis)
21 Trigeminal nerve (CN V)
22 Meckel's cave with the trigeminal (semilunar, Gasserian) ganglion at the antero-inferior aspect of Meckel's cave (arrowheads)
23 Amygdala
24 Hippocampus, head
25 Parahippocampal gyrus
26 Hippocampus, tail
28 Optic tract (CN II)
30 Anterior commissure
31 Putamen
32 Lateral (external) pallidum
33 Medial (internal) pallidum
34 Internal capsule, posterior limb
35 Pulvinar
36 Caudate nucleus
38 Crus fornicis
39 Middle cerebral artery within the lateral fissure (Sylvian fissure)
39′ Posterior cerebral artery
40 Uncus
42 Temporal bone, petrous portion
43 Cistern of the cerebellopontine angle
44 Internal carotid artery
45 Eustachian tube
46 Occipital condyle
47 Atlas, lateral mass
48 Occipital bone, squama
49 Transverse sinus
50 Lingual gyrus
50′ Collateral sulcus
50″ Fusiform gyrus
51 Gyrus descendens
52 Calcarine sulcus
53 Superior occipital gyrus
54 Parieto-occipital fissure
55 Isthmus of the cingulate gyrus
56 Lateral geniculate body
57 Tentorium cerebelli

Arrowheads: Trigeminal (semilunar, Gasserian) ganglion

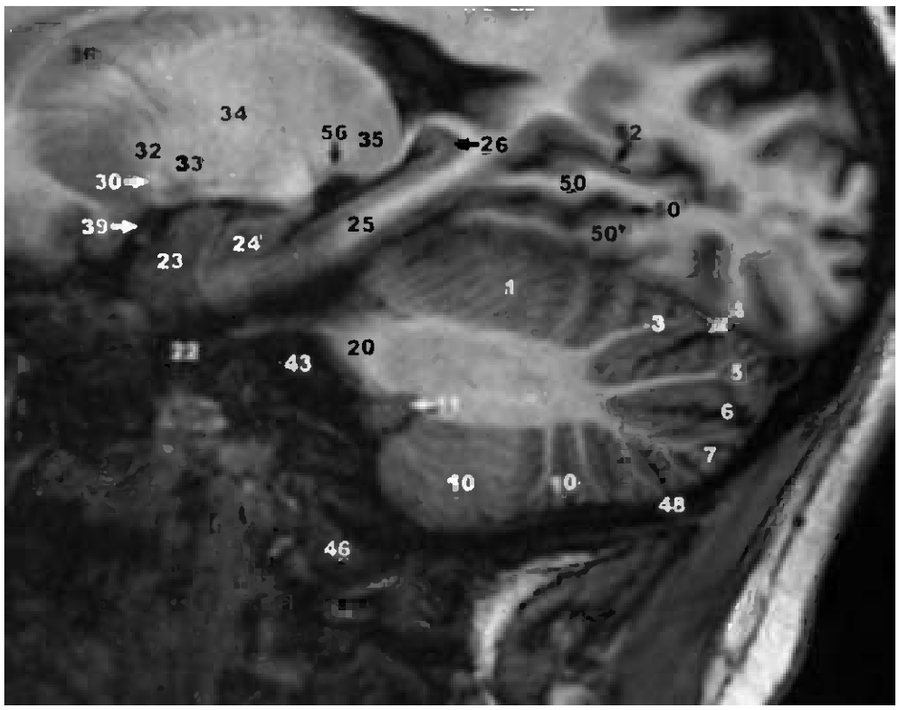
36
34
56
35
26
32
33
30
39
25
24
23
50
50'
1
3
20
43
11
5
6
7
10
10
48
46

E

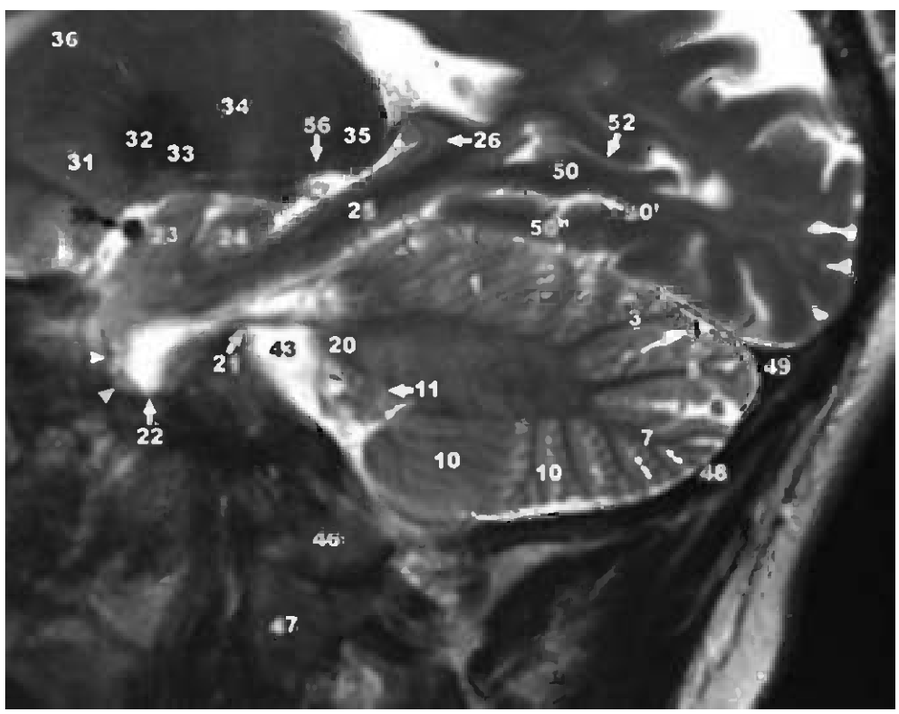
36
34
56
35
26
52
32
33
31
50
21
50'
3
43
20
2
49
11
22
7
10
10
48
46
47

F

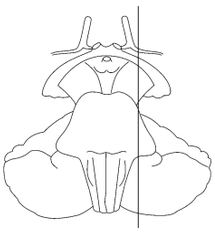

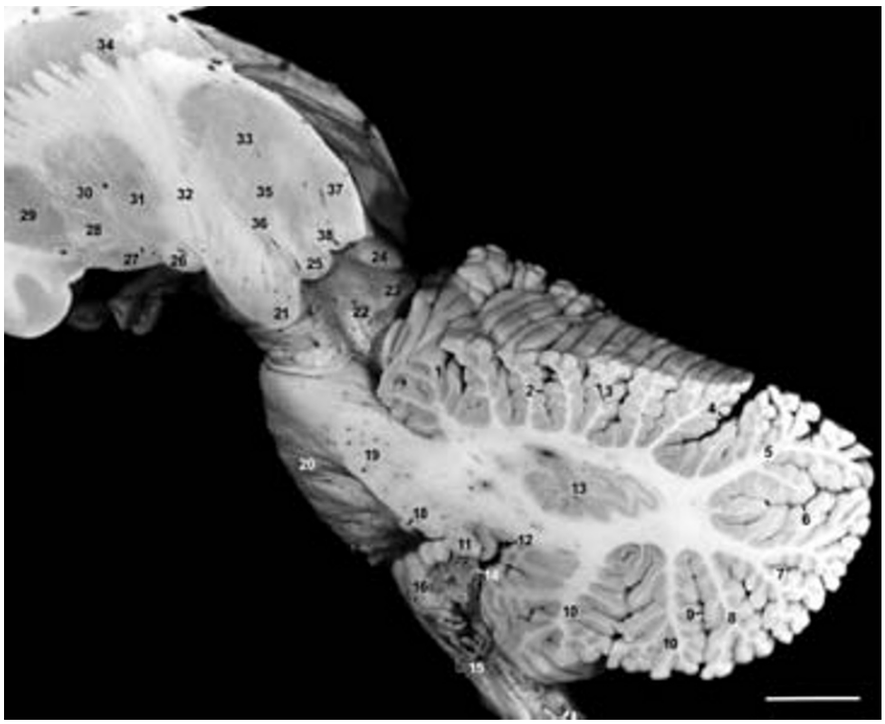

A

Fig. 11.63 (A–C). Sagittal (lateral) section.
A. Sagittal section after removal of the cerebral hemispheres. Bar: 10 mm.
B. Superior oblique view. **C.** Inferior oblique view.

1 Quadrangular lobule
2 Anterior superior (primary) fissure
3 Simple lobule
4 Posterior superior fissure
5 Superior semilunar lobule
6 Great horizontal fissure
7 Inferior semilunar lobule
8 Gracile lobule
9 Prepyramidal fissure
10 Biventral lobule
11 Flocculus
12 Posterolateral fissure
13 Dentate nucleus
14 Choroid plexus (lateral aperture of the fourth ventricle) (foramen of Luschka)
15 Medulla
16 Inferior olive
17 Vagus and glossopharyngeal nerves (CN X, IX)
18 Facial nerve (CN VII)
19 Middle cerebellar peduncle (brachium pontis)
20 Pons
21 Crus cerebri
22 Lateral aspect of mesencephalon
23 Inferior colliculus
24 Superior colliculus
25 Medial geniculate body
26 Optic tract (CN II)
27 Anterior perforated substance
28 Anterior commissure
29 Putamen
30 Lateral (external) pallidum
31 Medial (internal) pallidum
32 Internal capsule, posterior limb
33 Lateral posterior thalamic nucleus
34 Caudate nucleus
35 Ventral posterolateral thalamic nucleus
36 Ventral posteromedial thalamic nucleus
37 Pulvinar
38 Brachium of the superior colliculus
39 Pineal gland

B

C

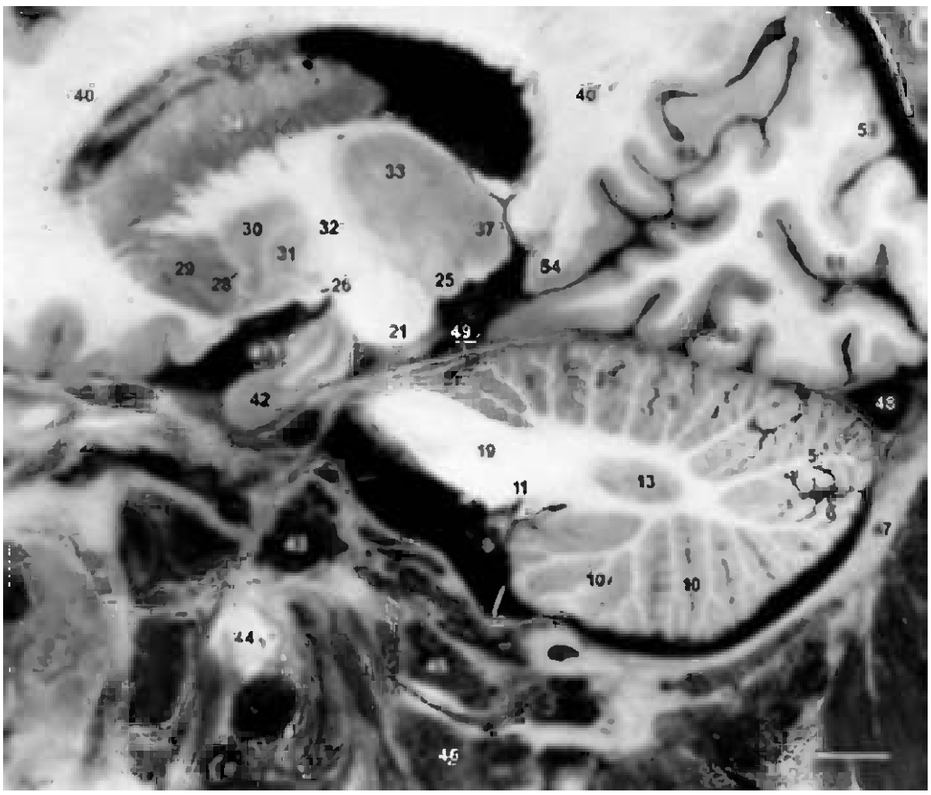

D

Fig. 11.63 (D–F).
D. Sagittal (lateral) section of the head. Bar: 10 mm.
E–F. 3 Tesla MRI. **E.** T1-weighted MRI. **F.** T2-weighted MRI.

1 Quadrangular lobule
2 Anterior superior (primary) fissure
3 Simple lobule
4 Posterior superior fissure
5 Superior semilunar lobule
6 Great horizontal fissure
7 Inferior semilunar lobule
10 Biventral lobule
11 Flocculus
13 Dentate nucleus
19 Middle cerebellar peduncle (brachium pontis)
21 Crus cerebri
25 Medial geniculate body
26 Optic tract (arrow)
28 Anterior commissure
29 Putamen
30 Lateral (external) pallidum
31 Medial (internal) pallidum
32 Internal capsule, posterior limb
33 Lateral posterior thalamic nucleus
34 Caudate nucleus
37 Pulvinar
40 Corpus callosum
41 Middle cerebral artery in the lateral fisssure (Sylvian fissure)
42 Uncus
43 Internal carotid artery
44 Eustachian tube
45 Occipital condyle
46 Atlas, lateral mass
47 Occipital bone, squama
48 Transverse sinus
49 Tentorium cerebelli
50 Lingual gyrus
51 Calcarine sulcus and striate cortex
52 Superior occipital gyrus
53 Parieto-occipital fissure
54 Isthmus of the cingulate gyrus

Arrow: Optic tract (also 26)

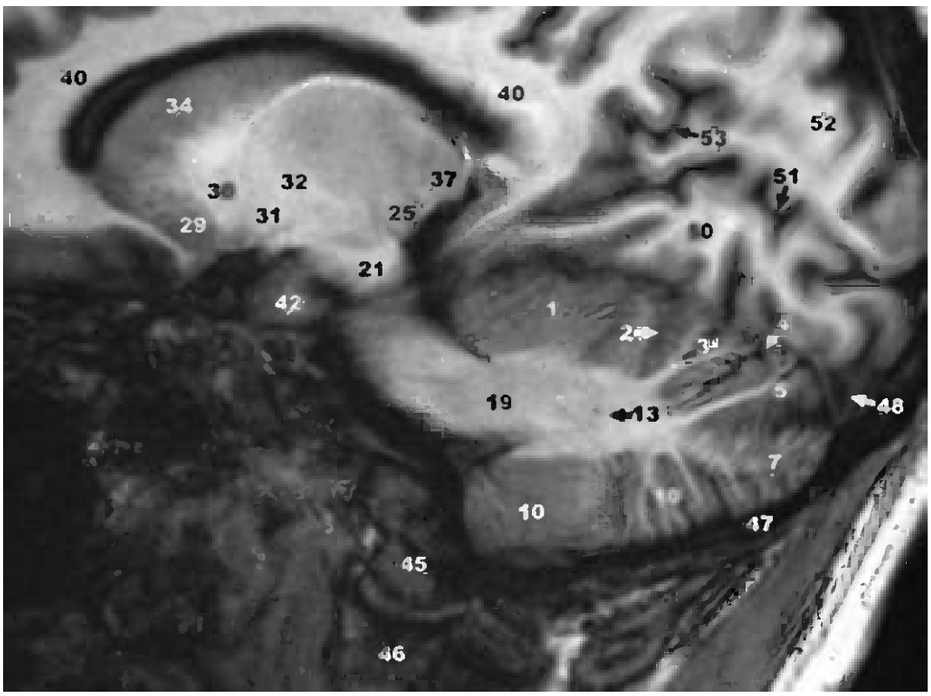
40
34
40
52
53
51
30
32
37
29
31
25
10
21
42
1
2
3
5
19
13
48
7
10
47
45
46

E

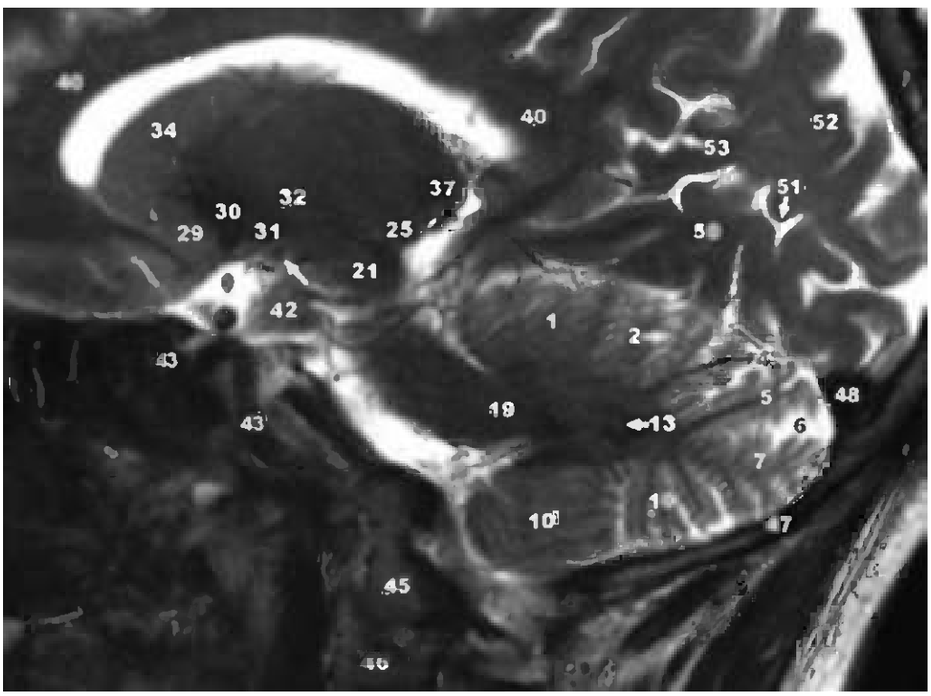
34
40
52
53
51
37
32
30
29
31
25
5
21
42
1
2
43
5
48
43
19
13
6
7
1
10
7
45
46

F

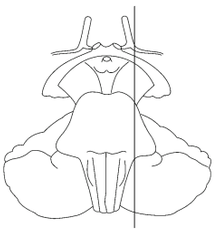

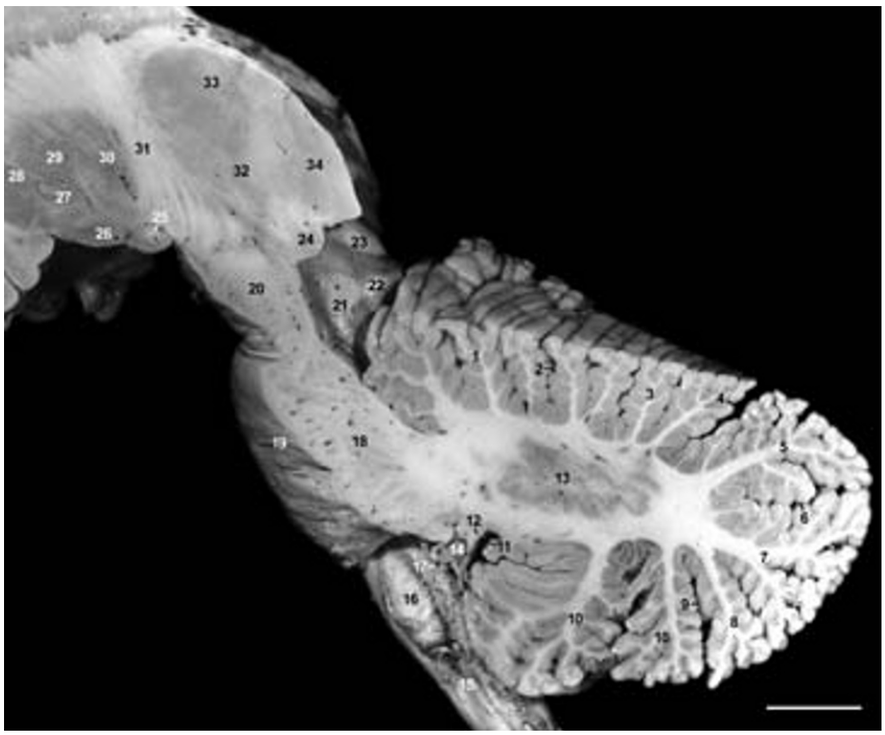

A

Fig. 11.64 (A–C). Sagittal (lateral) section.
A. Sagittal section after removal of the cerebral hemispheres. Bar: 10 mm.
B. Superior oblique view. **C.** Inferior oblique view.

1 Quadrangular lobule
2 Anterior superior (primary) fissure
3 Simple lobule
4 Posterior superior fissure
5 Superior semilunar lobule
6 Great horizontal fissure
7 Inferior semilunar lobule
8 Gracile lobule
9 Prepyramidal fissure
10 Biventral lobule
11 Posterolateral fissure
12 Brachium of the flocculus
13 Dentate nucleus
14 Choroid plexus (lateral aperture of the fourth ventricle) (foramen of Luschka)
15 Medulla
16 Inferior olive
17 Glossopharyngeal and vagus nerves (CN IX and X)
18 Middle cerebellar peduncle (brachium pontis)
19 Pons
20 Crus cerebri
21 Lateral aspect of mesencephalon
22 Inferior colliculus
23 Superior colliculus
24 Medial geniculate body
25 Optic tract (CN II)
26 Anterior perforated substance
27 Anterior commissure
28 Putamen
29 Lateral (external) pallidum
30 Medial (internal) pallidum
31 Internal capsule, genu
32 Ventral posterolateral thalamic nucleus
33 Lateral posterior thalamic nucleus
34 Pulvinar
35 Pineal gland

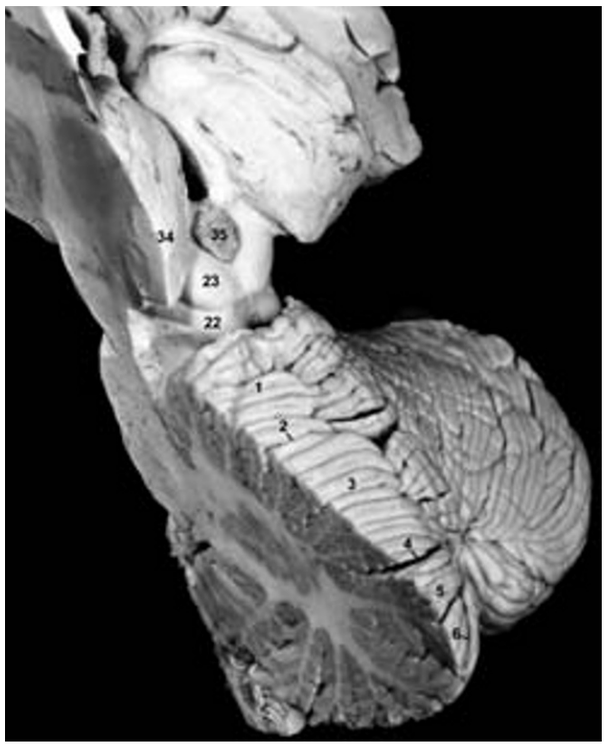

B

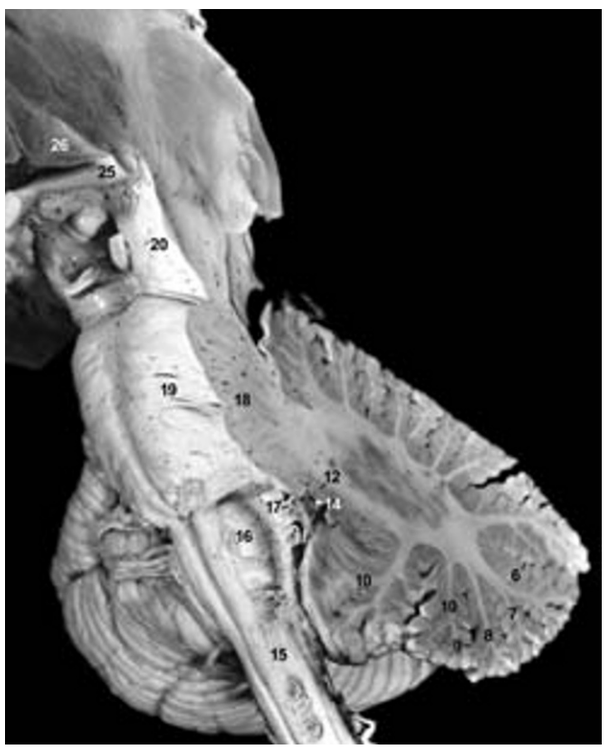

C

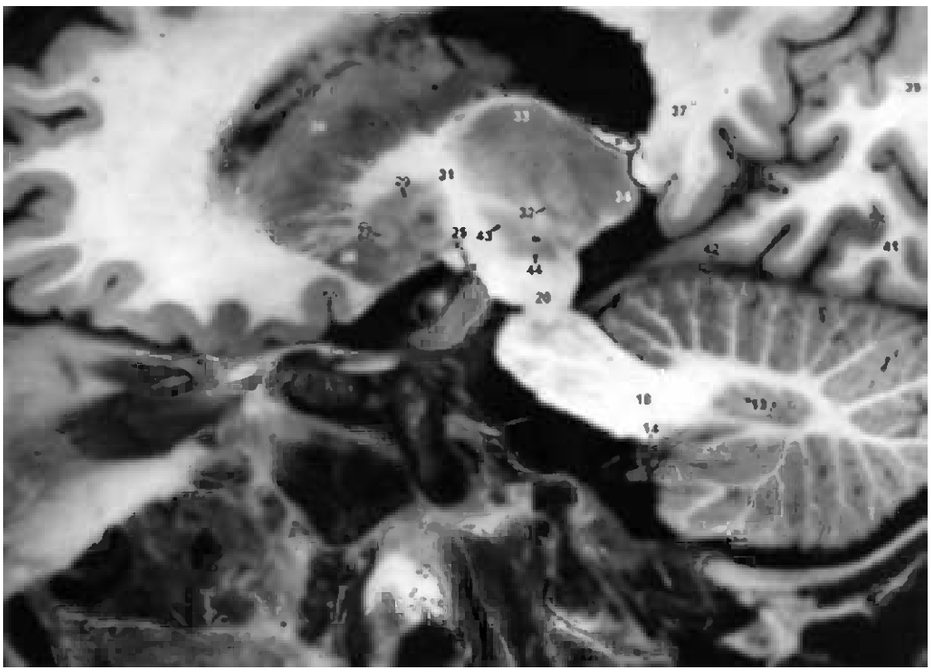

D

Fig. 11.64 (D–F).
D. Sagittal (lateral) section of the head.
E–F. 3 Tesla MRI. **E.** T1-weighted MRI. **F.** T2-weighted MRI.

1 Quadrangular lobule
2 Anterior superior (primary) fissure
3 Simple lobule
4 Posterior superior fissure
5 Superior semilunar lobule
6 Great horizontal fissure
7 Inferior semilunar lobule
10 Biventral lobule
13 Dentate nucleus
14 Choroid plexus (lateral aperture of the fourth ventricle) (foramen of Luschka)
18 Middle cerebellar peduncle (brachium pontis)
19 Pons
20 Crus cerebri
21′ Oculomotor nerve (CN III)
26 Anterior perforated substance
27 Anterior commissure
28 Putamen
29 Lateral (external) pallidum
30 Medial (internal) pallidum
31 Internal capsule, genu
32 Ventral posterolateral thalamic nucleus
33 Lateral posterior thalamic nucleus
34 Pulvinar
36 Caudate nucleus
37 Splenium
38 Parieto-occipital fissure
39 Cuneus
40 Calcarine sulcus
41 Lingual gyrus
42 Tentorium cerebelli
43 Subthalamic nucleus
44 Substantia nigra

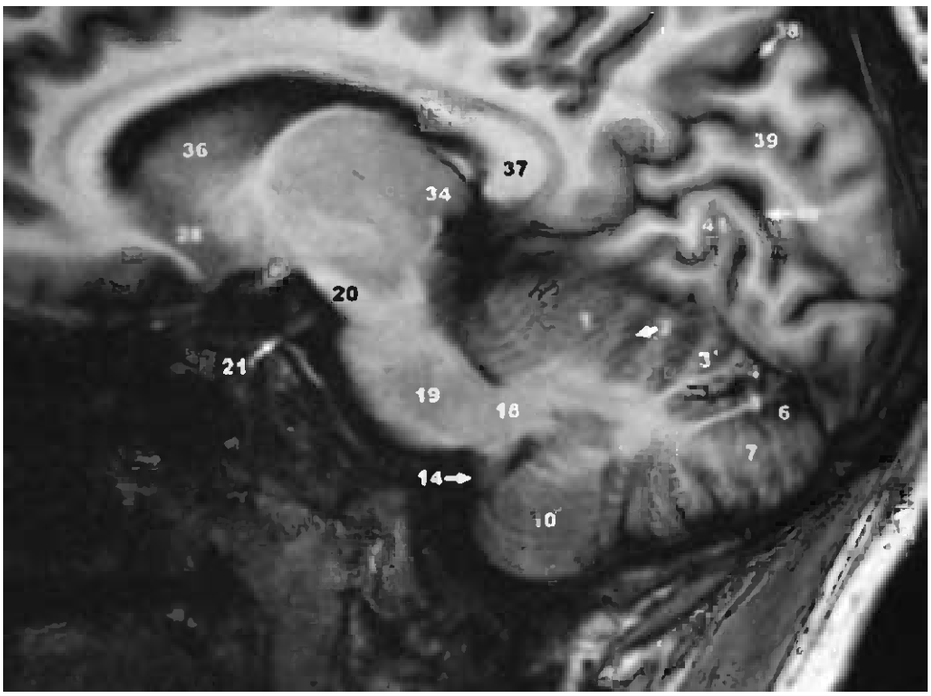

E

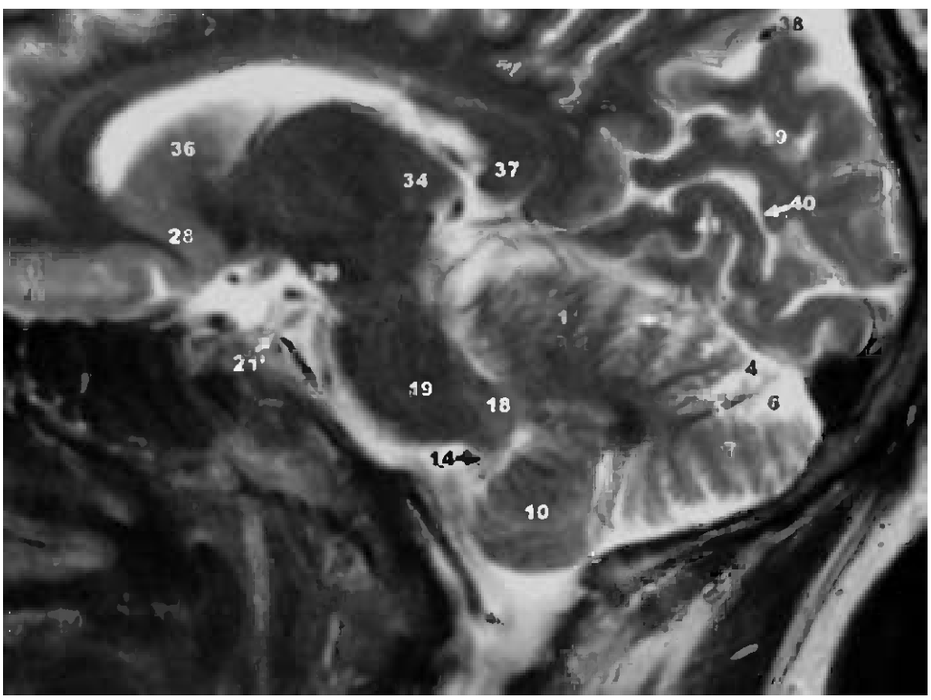

F

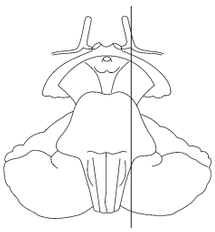

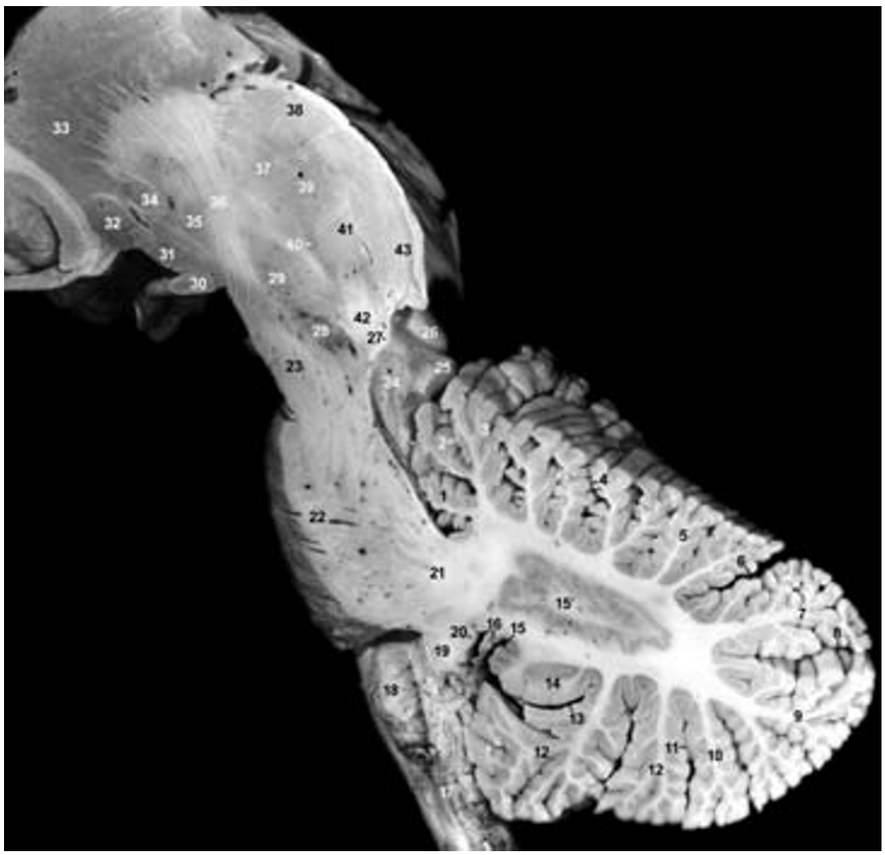

A

Fig. 11.65 (A–C). Sagittal (lateral) section.
A. Sagittal section after removal of the cerebral hemispheres. Bar: 10 mm.
B. Superior oblique view. **C.** Inferior oblique view.

1 Ala of central lobule
2 Postcentral fissure
3 Quadrangular lobule
4 Anterior superior (primary) fissure
5 Simple lobule
6 Posterior superior fissure
7 Superior semilunar lobule
8 Great horizontal fissure
9 Inferior semilunar lobule
10 Gracile lobule
11 Prepyramidal fissure
12 Biventral lobule
13 Postpyramidal (secondary) fissure
14 Tonsil
15 Posterolateral fissure
15′ Dentate nucleus
16 Brachium of the flocculus
17 Medulla
18 Inferior olive
19 Inferior cerebellar peduncle (restiform body)
20 Acoustic tubercle (dorsal cochlear nucleus)
21 Middle cerebellar peduncle (brachium pontis)
22 Pons, basilar portion
23 Crus cerebri
24 Mesencephalon, lateral aspect
25 Inferior colliculus
26 Superior colliculus
27 Brachium of the inferior colliculus
28 Substantia nigra
29 Subthalamic nucleus
30 Optic tract (CN II)
31 Anterior perforated substance
32 Nucleus accumbens septi
33 Caudate nucleus, head
34 Anterior commissure
35 Medial (internal) pallidum
36 Internal capsule (genu)
37 Ventral lateral thalamic nucleus
38 Lateral dorsal thalamic nucleus
39 Dorsomedial thalamic nucleus
40 Ventral posteromedial thalamic nucleus
41 Centromedian thalamic nucleus
42 Medial lemniscus
43 Pulvinar
44 Pineal gland

B

C

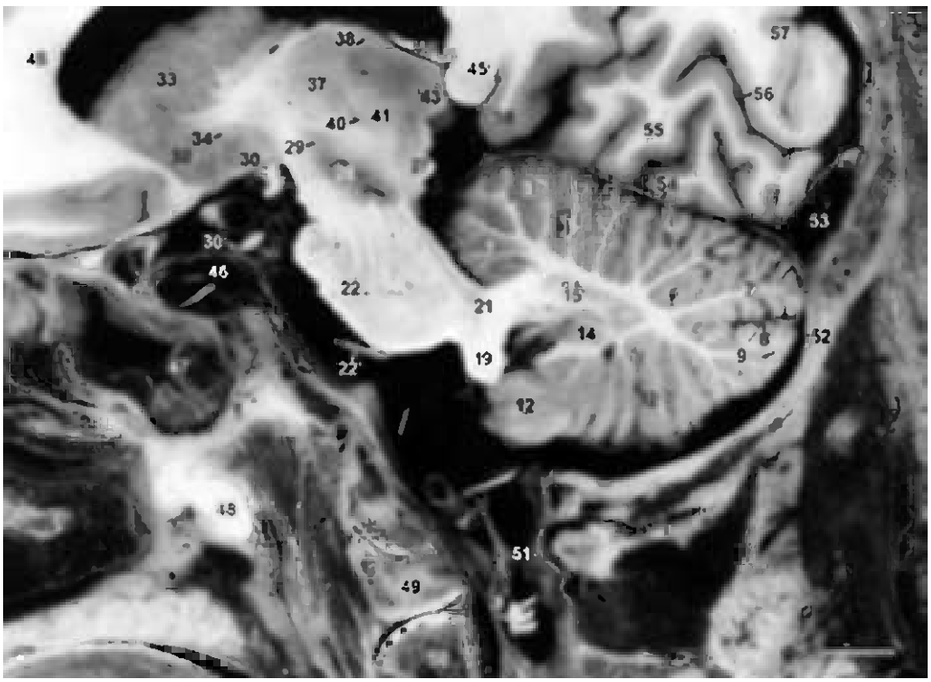

D

Fig. 11.65 (D–F).
D. Sagittal (lateral) section of the head. Bar: 10 mm.
E–F. 3 Tesla MRI. **E.** T1-weighted MRI. **F.** T2-weighted MRI.

1 Ala of central lobule
3 Quadrangular lobule
5 Simple lobule
6 Posterior superior fissure
7 Superior semilunar lobule
8 Great horizontal fissure
9 Inferior semilunar lobule
12 Biventral lobule
14 Tonsil
15′ Dentate nucleus
19 Inferior cerebellar peduncle (restiform body)
21 Middle cerebellar peduncle (brachium pontis)
22 Pons, basilar portion
22′ Abducens nerve (CN VI)
27 Brachium of the inferior colliculus
28 Substantia nigra
29 Subthalamic nucleus
30 Optic tract (CN II)
30′ Oculomotor nerve (CN III)
32 Nucleus accumbens septi
33 Caudate nucleus, head
34 Anterior commissure
37 Ventral lateral thalamic nucleus
38 Lateral dorsal thalamic nucleus
40 Ventral posteromedial thalamic nucleus
41 Centromedian thalamic nucleus
43 Pulvinar
45 Corpus callosum
45′ Crus fornicis
46 Cavernous sinus and internal carotid artery
47 Sphenoid sinus
48 Eustachian tube
49 Atlas, lateral mass
50 Axis
51 Foramen magnum
52 Occipital bone, squama
53 Transverse sinus
54 Tentorium cerebelli
55 Lingual gyrus
56 Calcarine sulcus and striate cortex
57 Cuneus
58 Isthmus of the cingulate gyrus

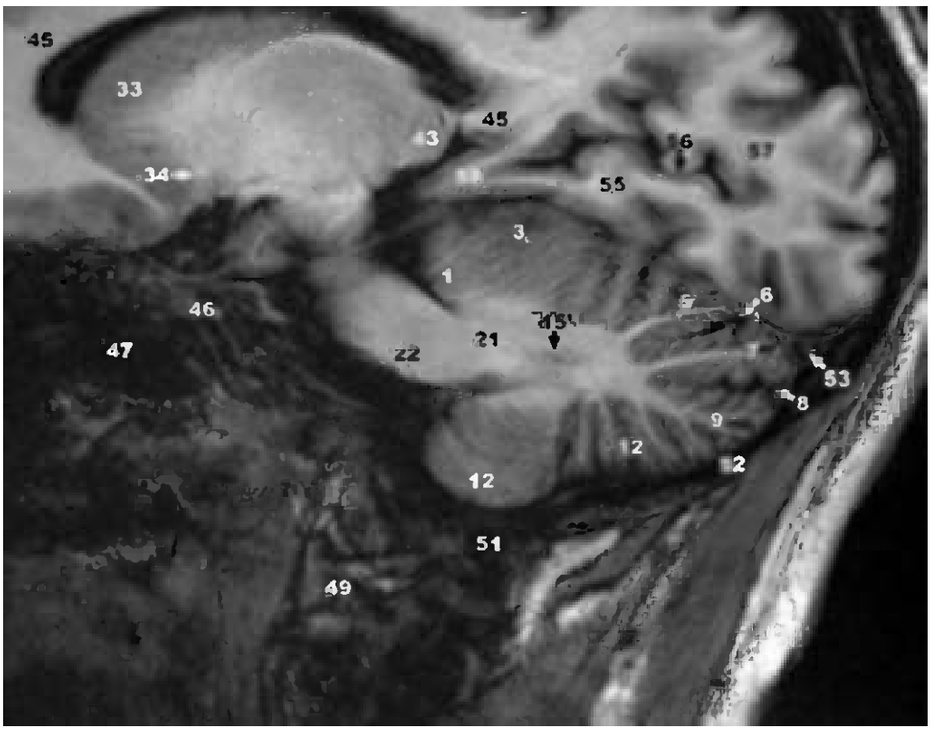
45
33
45
43
56
57
34
55
3
1
46
6
47
22
21
53
8
9
12
2
12
51
49

E

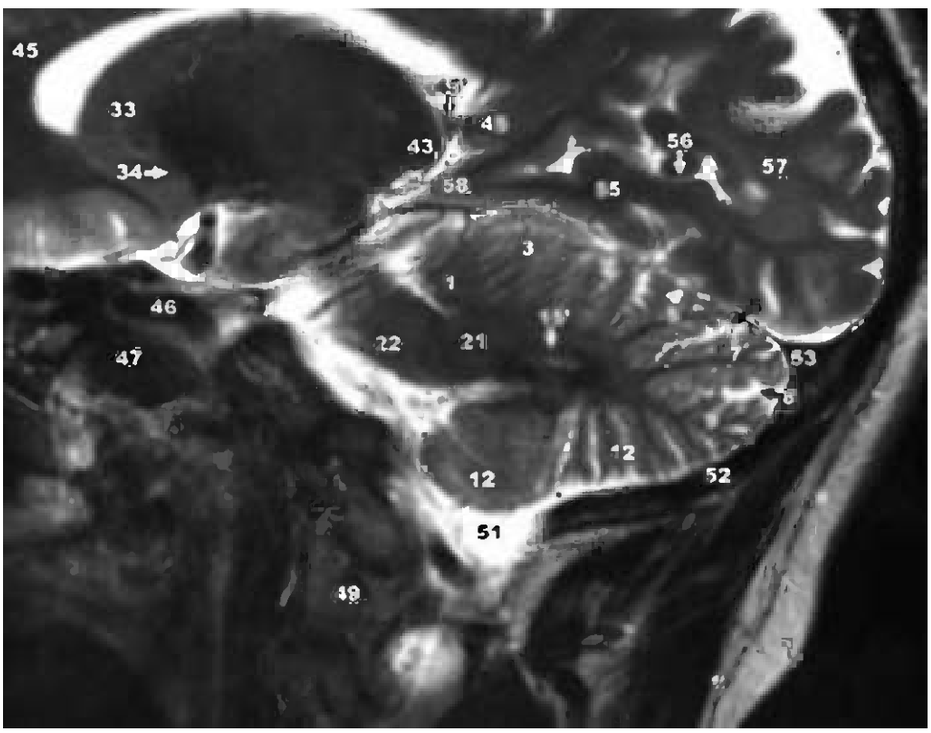
45
33
4
43
56
57
34
58
5
3
1
46
47
22
21
53
8
12
12
52
51
49

F

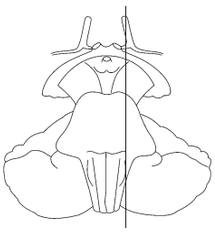

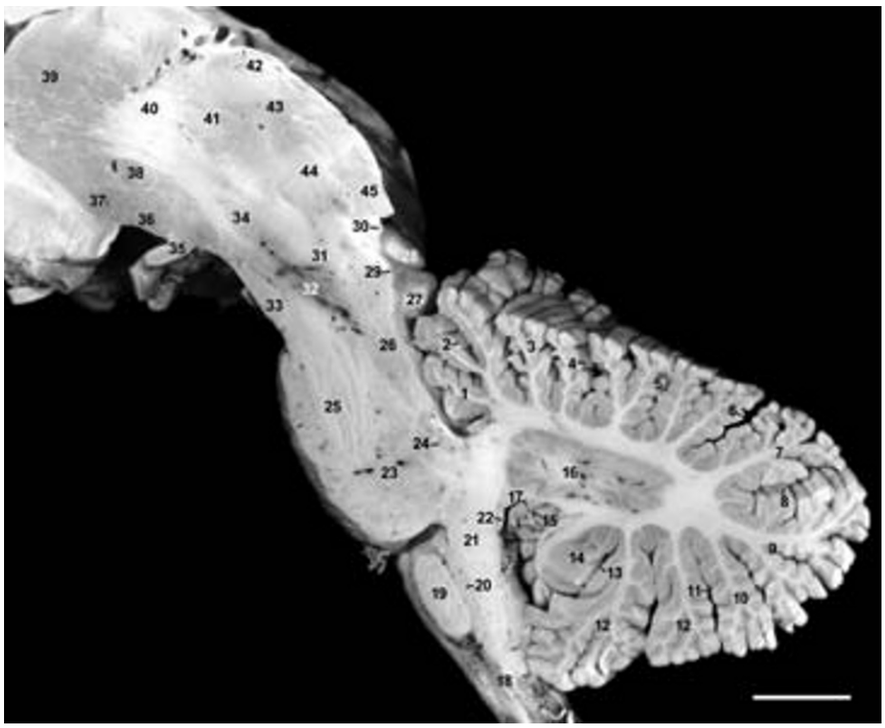

A

Fig. 11.66 (A–C). Sagittal (lateral) section.
A. Sagittal section after removal of the cerebral hemispheres. Bar: 10 mm.
B. Superior oblique view. **C.** Inferior oblique view.

1 Ala of central lobule
2 Postcentral fissure
3 Quadrangular lobule
4 Anterior superior (primary) fissure
5 Simple lobule
6 Posterior superior fissure
7 Superior semilunar lobule
8 Great horizontal fissure
9 Inferior semilunar lobule
10 Gracile lobule
11 Prepyramidal fissure
12 Biventral lobule
13 Postpyramidal (secondary) fissure
14 Tonsil
15 Posterolateral fissure
16 Dentate nucleus
17 Brachium of the flocculus
18 Medulla
19 Inferior olivary nucleus
20 Spinothalamic tract
21 Inferior cerebellar peduncle (restiform body)
22 Acoustic tubercle (dorsal cochlear nucleus) (CN VIII)
23 Pontine nuclei
24 Principal sensory trigeminal nucleus (CN V)
25 Pons, basilar portion (corticospinal tract)
26 Lateral lemniscus
27 Inferior colliculus
28 Superior colliculus
29 Brachium of the inferior colliculus
30 Brachium of the superior colliculus
31 Red nucleus
32 Substantia nigra
33 Crus cerebri (corticospinal tract)
34 Subthalamic nucleus
35 Optic tract (CN II)
35′ Oculomotor nerve (CN III)
36 Anterior perforated substance
37 Nucleus accumbens septi
38 Anterior commissure
39 Caudate nucleus, head
40 Internal capsule, anterior limb
41 Ventral lateral thalamic nucleus
42 Lateral dorsal thalamic nucleus
43 Dorsomedial thalamic nucleus
44 Centromedian thalamic nucleus
45 Pulvinar
46 Pineal gland

B

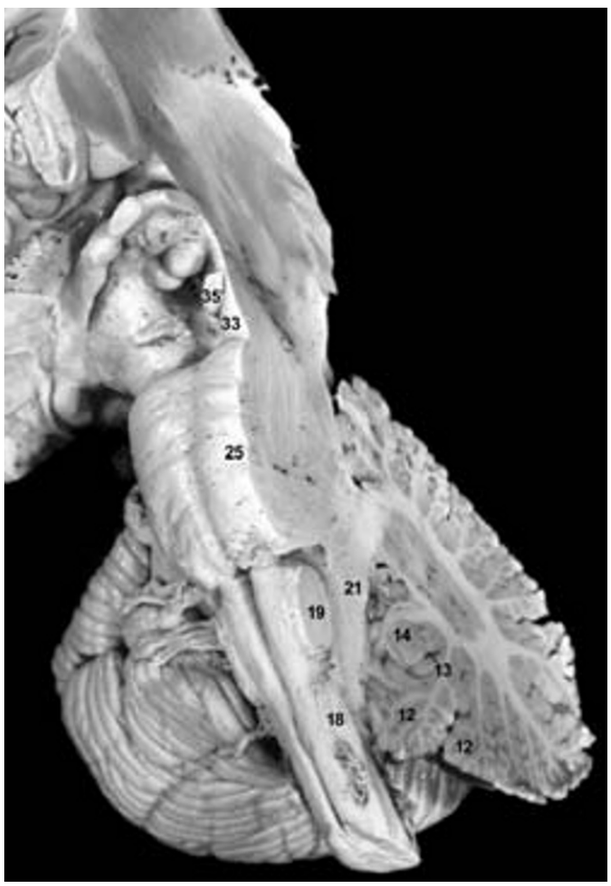

C

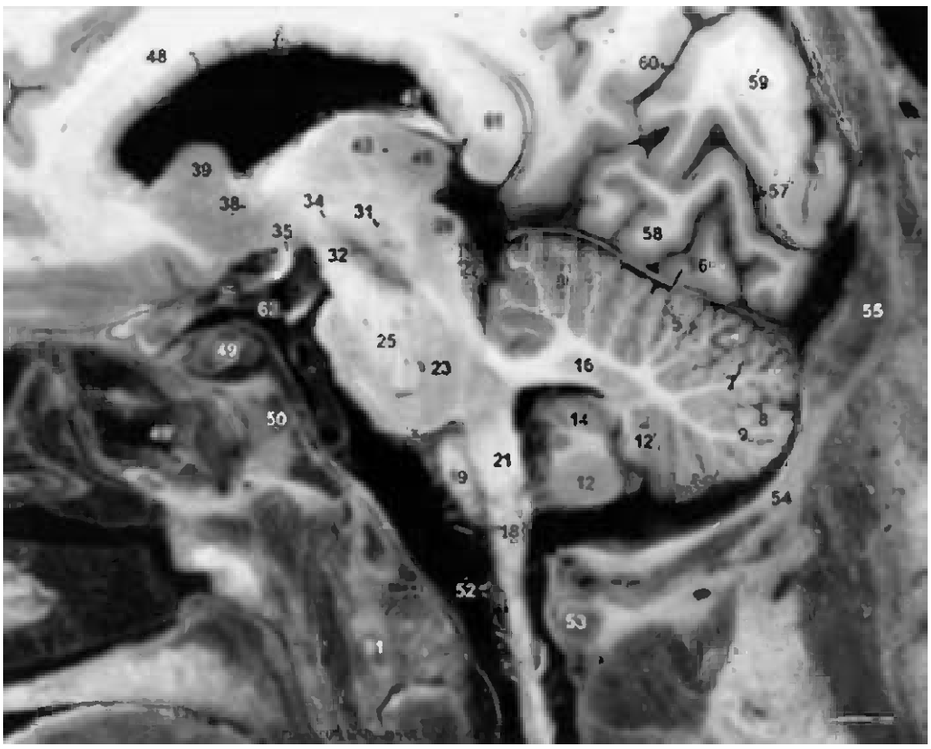

D

Fig. 11.66 (D–F).
D. Sagittal section of the head. Bar: 10 mm.
E–F. 3 Tesla MRI. **E.** T1-weighted MRI. **F.** T2-weighted MRI.

3 Quadrangular lobule
4 Anterior superior (primary) fissure
5 Simple lobule
6 Posterior superior fissure
7 Superior semilunar lobule
8 Great horizontal fissure
9 Inferior semilunar lobule
12 Biventral lobule
14 Tonsil
16 Dentate nucleus
18 Medulla
19 Inferior olivary nucleus
21 Inferior cerebellar peduncle (restiform body)
23 Pontine nuclei
25 Pons, basilar portion (corticospinal tract)
27 Inferior colliculus
28 Superior colliculus
31 Red nucleus
32 Substantia nigra
34 Subthalamic nucleus
35 Optic tract (CN II)
38 Anterior commissure
39 Caudate nucleus, head
43 Dorsomedial thalamic nucleus
45 Pulvinar
47 Crus fornicis
48 Corpus callosum, body
49 Cavernous sinus and internal carotid artery
49′ Sphenoid sinus
50 Clivus
51 Atlas, anterior arch
52 Foramen magnum
53 Atlas, posterior arch
54 Occipital bone, squama
55 External occipital protuberance
56 Tentorium cerebelli
57 Calcarine sulcus and striate cortex
58 Lingual gyrus
59 Cuneus
60 Parieto-occipital fissure
61 Splenium
62 Oculomotor nerve (CN III)

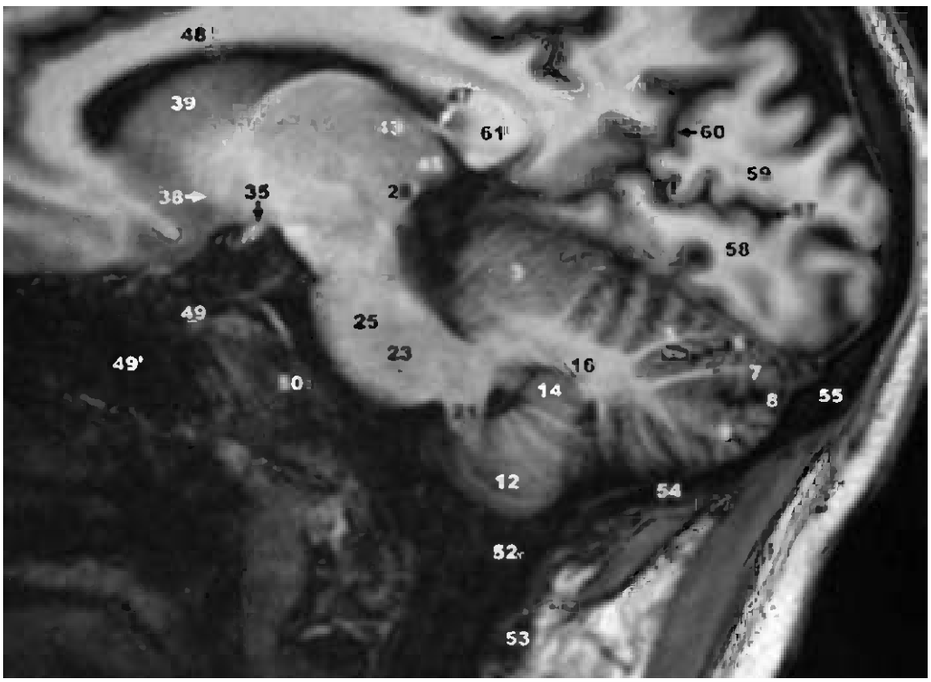
48
39
61
60
59
38
35
58
49
25
23
49'
16
7
14
8
55
12
54
52
53

E

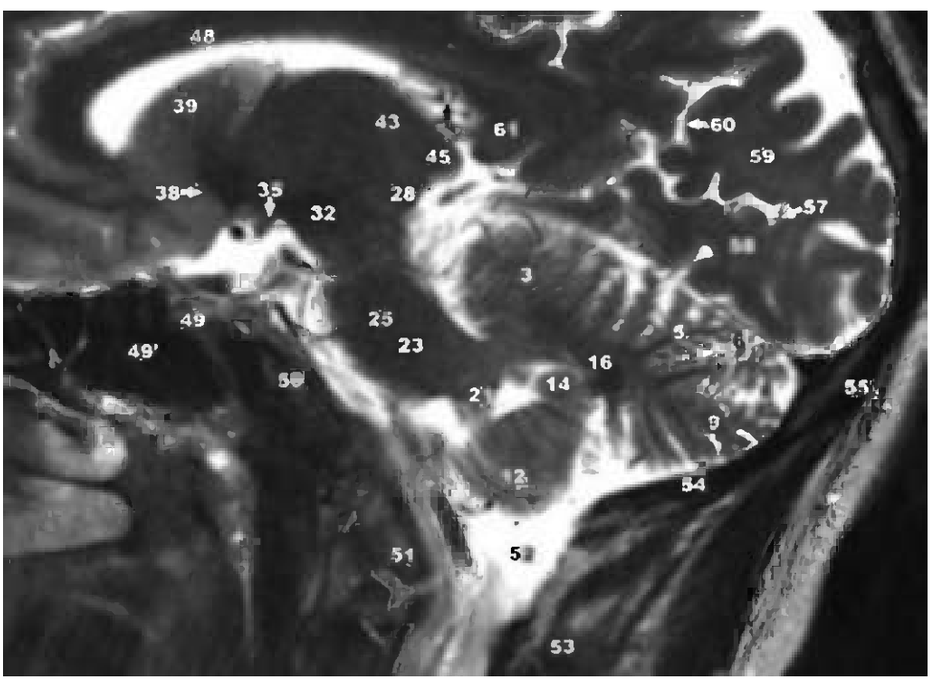
48
39
43
60
45
59
38
35
28
32
57
3
49
25
49'
23
16
14
55
54
51
53

F

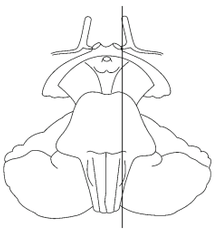

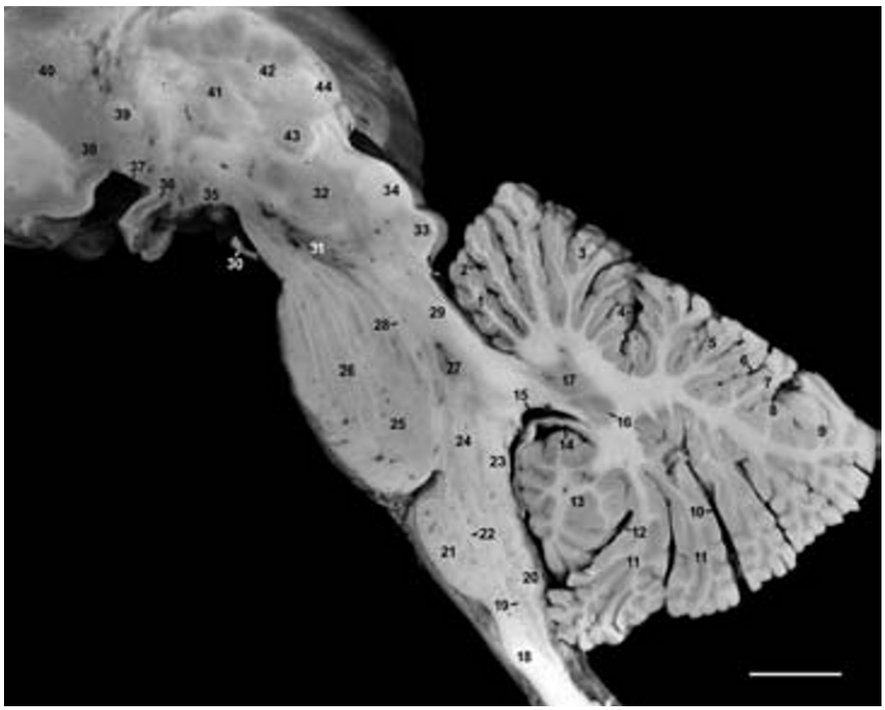

A

Fig. 11.67 (A–C). Sagittal (lateral) section.
A. Sagittal section after removal of the cerebral hemispheres. Bar: 10 mm.
B. Superior oblique view. **C.** Inferior oblique view.

1 Ala of central lobule and central lobule
2 Postcentral fissure
3 Quadrangular lobule and culmen
4 Anterior superior (primary) fissure
5 Simple lobule and declive
6 Posterior superior fissure
7 Superior semilunar lobule
8 Great horizontal fissure
9 Inferior semilunar lobule
10 Prepyramidal fissure
11 Biventral lobule
12 Postpyramidal (secondary) fissure
13 Tonsil
14 Brachium of the flocculus and inferior medullary velum
15 Fourth ventricle, lateral recess
16 Dentate nucleus
17 Emboliform nucleus
18 Pyramid of medulla (corticospinal tract)
19 Spinal trigeminal nucleus (CN V)
20 Lateral cuneate nucleus
21 Inferior olivary nucleus
22 Spinothalamic tract
23 Inferior cerebellar peduncle (restiform body)
24 Spinal trigeminal tract (CN V)
25 Pontine nuclei
26 Pons, basilar portion (corticospinal tract)
27 Motor and principal sensory trigeminal nuclei (CN V)
28 Medial lemniscus
29 Superior cerebellar peduncle (brachium conjunctivum)
30 Oculomotor nerve (CN III)
31 Substantia nigra
32 Red nucleus
33 Inferior colliculus
34 Superior colliculus
35 Lateral tuber of hypothalamus
36 Optic tract (CN II)
37 Anterior perforated substance
38 Nucleus accumbens septi
39 Anterior commissure
40 Caudate nucleus (head)
41 Ventral anterior thalamic nucleus
42 Dorsomedial thalamic nucleus
43 Centromedian thalamic nucleus
44 Pulvinar
45 Pineal gland

B

C

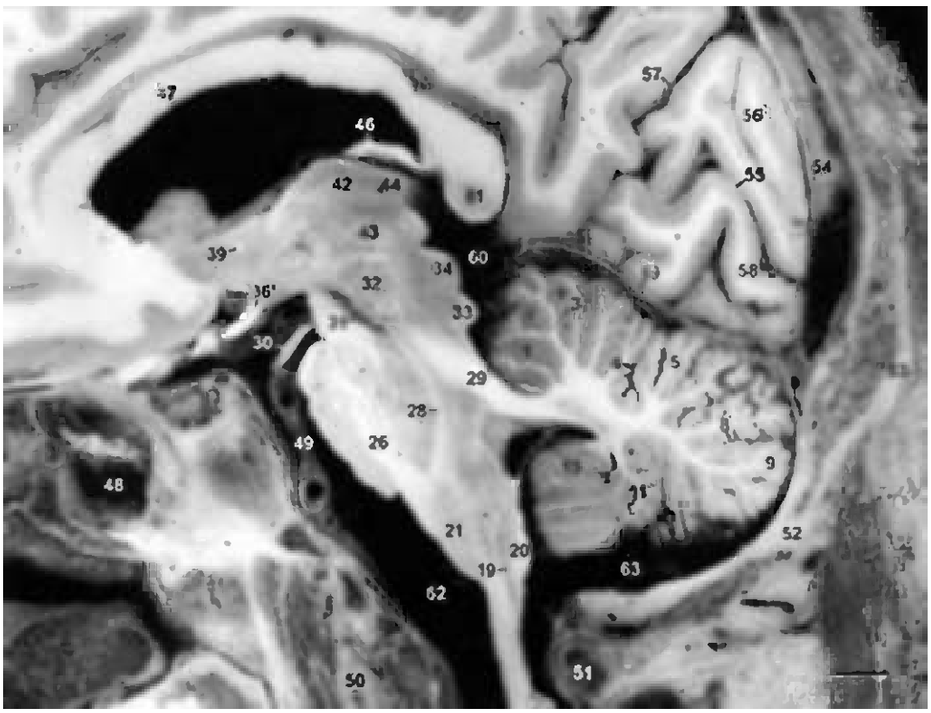

D

Fig. 11.67 (D–F).
D. Sagittal section of the head. Bar: 10 mm.
E–F. 3 Tesla MRI. **E.** T1-weighted MRI. **F.** T2-weighted MRI.

1 Ala of central lobule and central lobule
3 Quadrangular lobule and culmen
4 Anterior superior (primary) fissure
5 Simple lobule and declive
6 Posterior superior fissure
7 Superior semilunar lobule
8 Great horizontal fissure
9 Inferior semilunar lobule
11 Biventral lobule
13 Tonsil
19 Spinal trigeminal nucleus (CN V)
20 Lateral cuneate nucleus
21 Inferior olivary nucleus
26 Pons, basilar portion (corticospinal tract)
28 Medial lemniscus
29 Superior cerebellar peduncle (brachium conjunctivum)
30 Oculomotor nerve (CN III)
31 Substantia nigra
32 Red nucleus
33 Inferior colliculus
34 Superior colliculus
36 Prechiasmal optic nerves leading to optic chiasm (CN II)
36′ Optic chiasm and proximal tract (CN II)
39 Anterior commissure
42 Dorsomedial thalamic nucleus
43 Centromedian thalamic nucleus
44 Pulvinar
46 Crus fornicis
47 Corpus callosum (body)
48 Sphenoid sinus
49 Basilar artery
50 Atlas, anterior arch
51 Atlas, posterior arch
52 Occipital bone, squama
53 External occipital protuberance
54 Superior sagittal sinus
55 Calcarine sulcus
56 Cuneus
57 Parieto-occipital fissure
58 Lingual gyrus
59 Tentorium cerebelli
60 Quadrigeminal cistern
61 Splenium
62 Premedullary cistern
63 Cerebellomedullary cistern (cisterna magna)

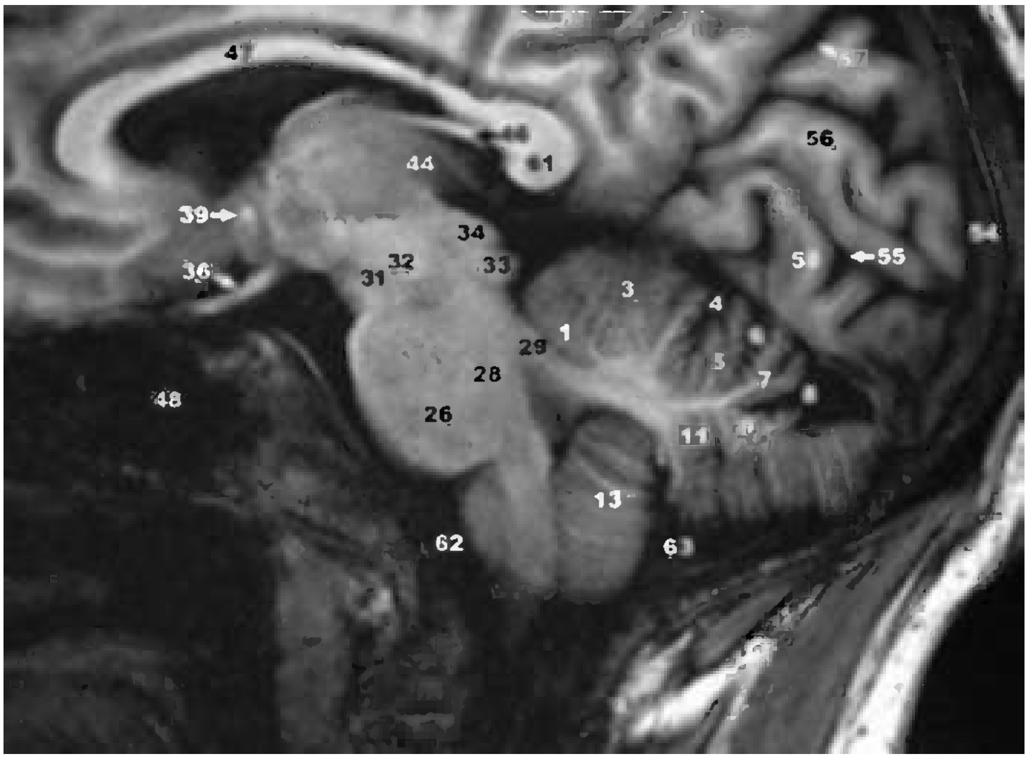
56
44
61
39
34
55
32
33
31
36
3
4
1
29
28
5
7
48
26
11
13
62

E

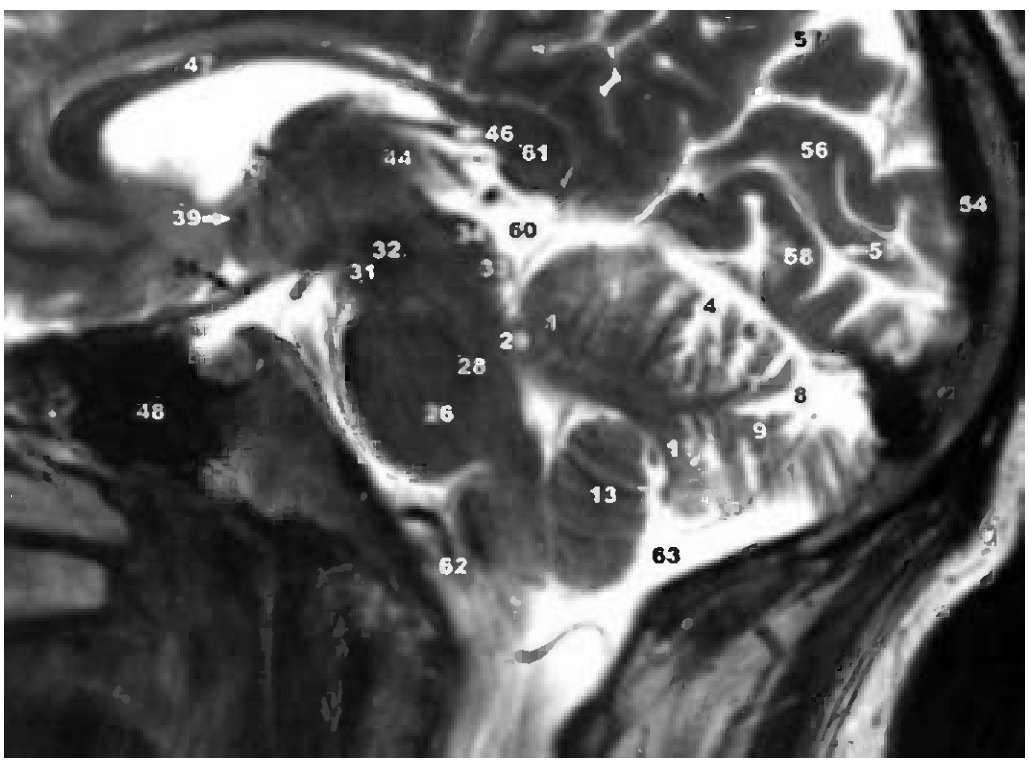
46
44
61
56
54
39
60
32
31
58
4
28
8
48
26
9
13
63
62

F

Fig. 11.68 (A–C). Sagittal (lateral) section.
A. Sagittal section after removal of the cerebral hemispheres. Bar: 10 mm.
B. Superior oblique view. **C.** Inferior oblique view.

1 Central lobule
2 Postcentral fissure
3 Culmen
4 Anterior superior (primary) fissure
5 Declive
6 Posterior superior fissure
7 Superior semilunar lobule
8 Great horizontal fissure
9 Inferior semilunar lobule
10 Prepyramidal fissure
11 Pyramid of vermis
12 Biventral lobule
13 Postpyramidal (secondary) fissure
14 Tonsil
15 Posterolateral fissure
16 Brachium of the flocculus and inferior medullary velum
17 Dentate nucleus
18 Emboliform nucleus
19 Fourth ventricle
20 Corticospinal tract
21 Medial cuneate nucleus
22 Inferior olivary nucleus
23 Nucleus of the solitary tract
24 Vestibular nuclei (CN VIII)
25 Facial nucleus (CN VII)
26 Medial lemniscus
27 Pons, basilar portion (corticospinal tract)
28 Central tegmental tract
29 Superior cerebellar peduncle (brachium conjunctivum)
30 Nucleus ceruleus
31 Inferior colliculus
32 Superior colliculus
33 Pretectal area
34 Red nucleus
35 Substantia nigra
36 Crus cerebri
37 Mammillary body
38 Lateral tuber of hypothalamus
39 Optic tract
40 Lateral hypothalamus
41 Anterior perforated substance
42 Septal nuclei
43 Anterior commissure
44 Anterior column of fornix
45 Anterior thalamic nucleus
46 Dorsomedial thalamic nucleus
47 Mammillothalamic tract
48 Habenular nuclei
49 Pineal gland

B

C

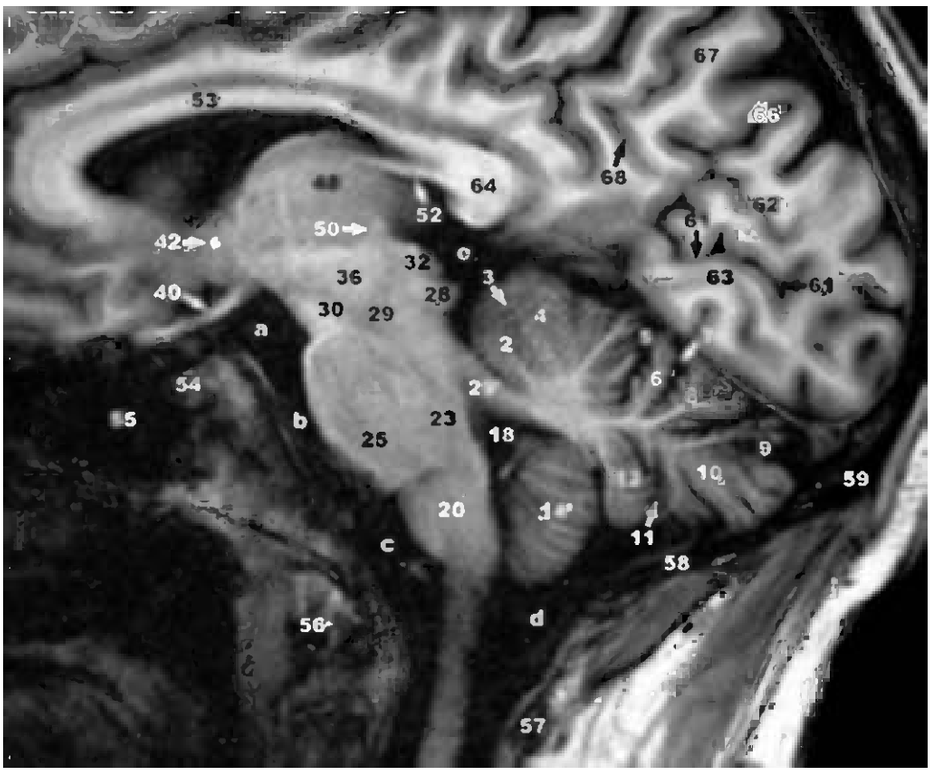

D

Fig. 11.68 (D–E). 3 Tesla MRI.
D. T1-weighted MRI. **E.** T2-weighted MRI.

2 Central lobule
3 Postcentral fissure (preculminate fissure)
4 Culmen
5 Anterior superior fissure (primary fissure)
6 Declive
7 Posterior superior fissure (postclival fissure)
8 Folium
9 Great horizontal fissure
10 Tuber
11 Prepyramidal fissure
12 Pyramid of vermis
14′ Tonsil
18 Fourth ventricle
20 Medulla
23 Medial lemniscus
25 Pons, basilar portion and corticospinal tract
28 Inferior colliculus
29 Decussation of superior cerebellar peduncles
29′ Superior cerebellar peduncle (brachium conjunctivum)
30 Substantia nigra
32 Superior colliculus
36 Red nucleus
40 Optic chiasm (CN II)
42 Anterior commissure
43 Anterior column of fornix
48 Dorsomedial thalamic nucleus
50 Posterior commissure
52 Fornix
53 Corpus callosum, body
54 Sella turcica (hypophyseal fossa and hypophysis)
55 Sphenoid sinus
56 Atlas, anterior arch
57 Atlas, posterior arch

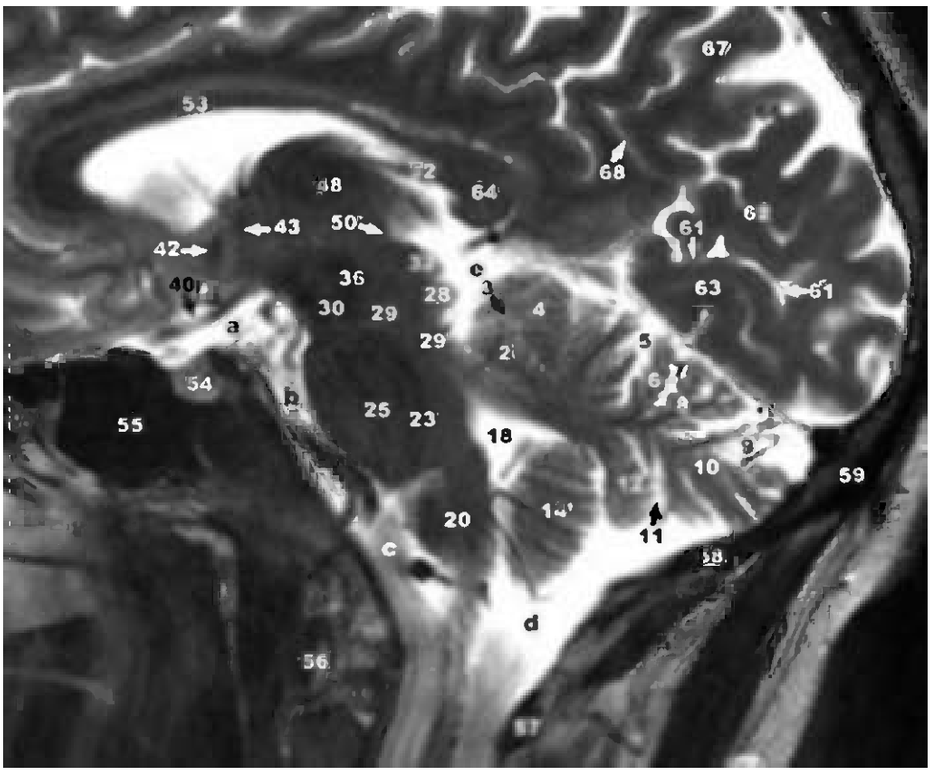

E

58 Occipital bone, squama
59 External occipital protuberance
61 Calcarine sulcus
62 Cuneus
63 Lingual gyrus
64 Splenium
66 Parieto-occipital sulcus
67 Precuneus
68 Subparietal sulcus

Subarachnoid cisterns

a Chiasmatic cistern
b Prepontine cistern
c Premedullary cistern
d Cerebellomedullary cistern (cisterna magna)
e Quadrigeminal cistern

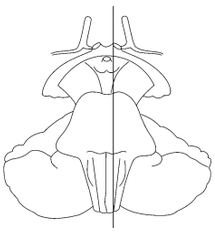

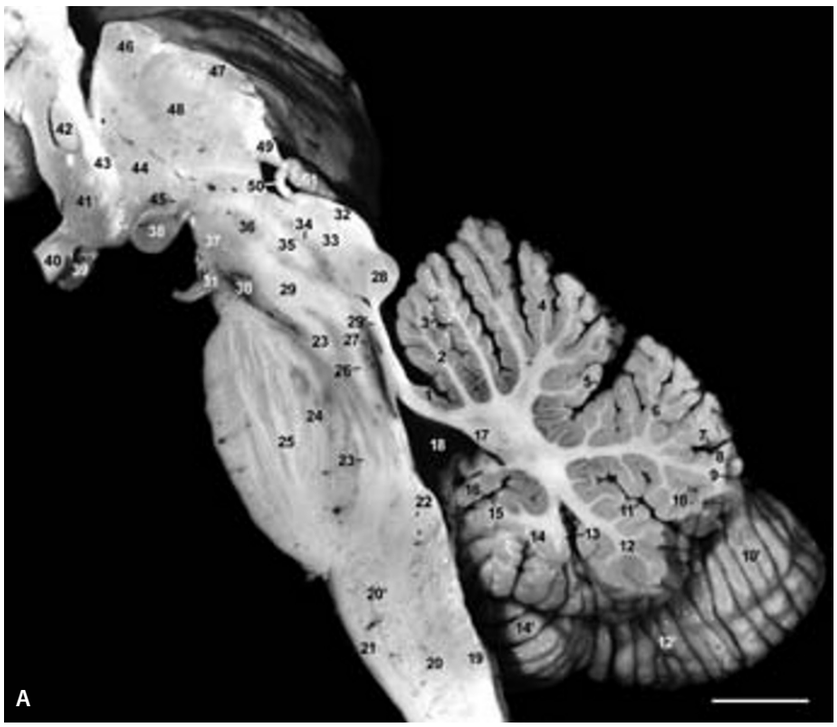

Fig. 11.69 (A–C). Sagittal (lateral) section.
A. Sagittal section after removal of the cerebral hemispheres. Bar: 10 mm.
B. Superior oblique view. **C.** Inferior oblique view.

1 Lingula
2 Central lobule
3 Postcentral fissure (preculminate fissure)
4 Culmen
5 Anterior superior (primary) fissure
6 Declive
7 Posterior superior fissure
8 Folium
8′ Superior semilunar lobule
9 Great horizontal fissure
10 Tuber
10′ Inferior semilunar lobule
11 Prepyramidal fissure
12 Pyramid of vermis
12′ Biventral lobule
13 Postpyramidal (secondary) fissure
14 Uvula
14′ Tonsil
15 Posterolateral fissure
16 Nodulus
17 Fastigial nucleus
18 Fourth ventricle
19 Gracile nucleus
20 Medulla
20′ Accessory medial olivary nucleus
21 Corticospinal tract
22 Abducens nucleus (CN VI)
23 Medial lemniscus
24 Pontine nuclei
25 Pons, basilar portion and corticospinal tract
26 Central tegmental tract
27 Nucleus ceruleus
28 Inferior colliculus
29 Decussation of superior cerebellar peduncles
29′ Superior cerebellar peduncle (brachium conjunctivum)
30 Substantia nigra
31 Oculomotor nerve (CN III)
32 Superior colliculus
33 Periaqueductal gray matter
34 Oculomotor nucleus (CN III)
35 Medial longitudinal fasciculus
36 Red nucleus
37 Ventral tegmental area
38 Mammillary body
39 Hypophyseal stalk
40 Optic chiasm (CN II)
41 Pre-optic area
42 Anterior commissure
43 Anterior column of fornix
44 Hypothalamus
45 Mammillothalamic tract
46 Anterior thalamic nucleus
47 Lateral dorsal thalamic nucleus
48 Dorsomedial thalamic nucleus
49 Habenular nuclei
50 Posterior commissure
51 Pineal gland

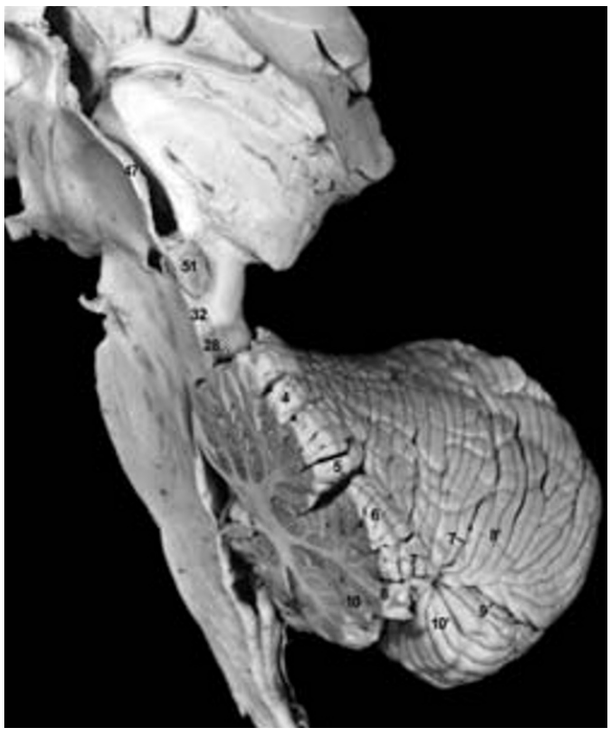

B

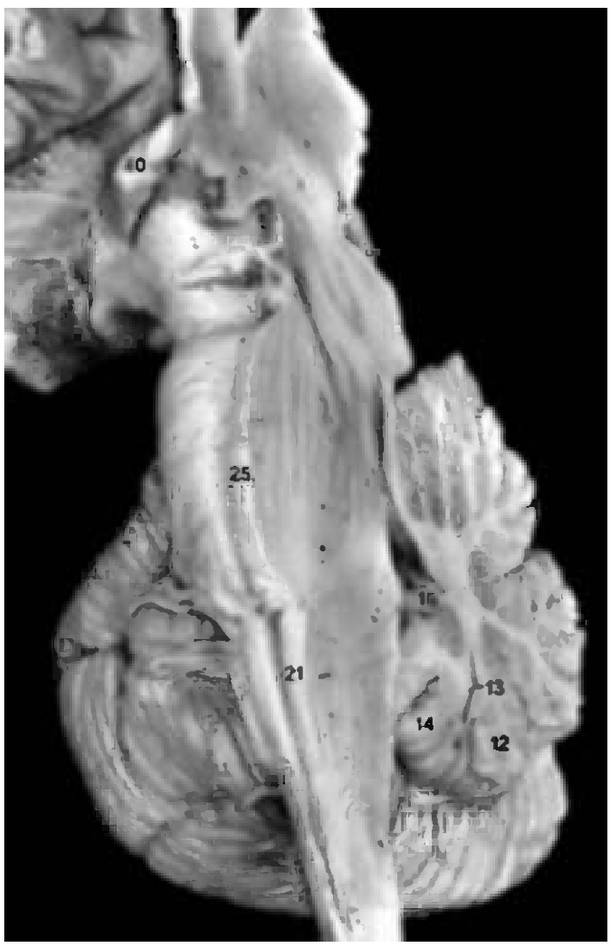

C

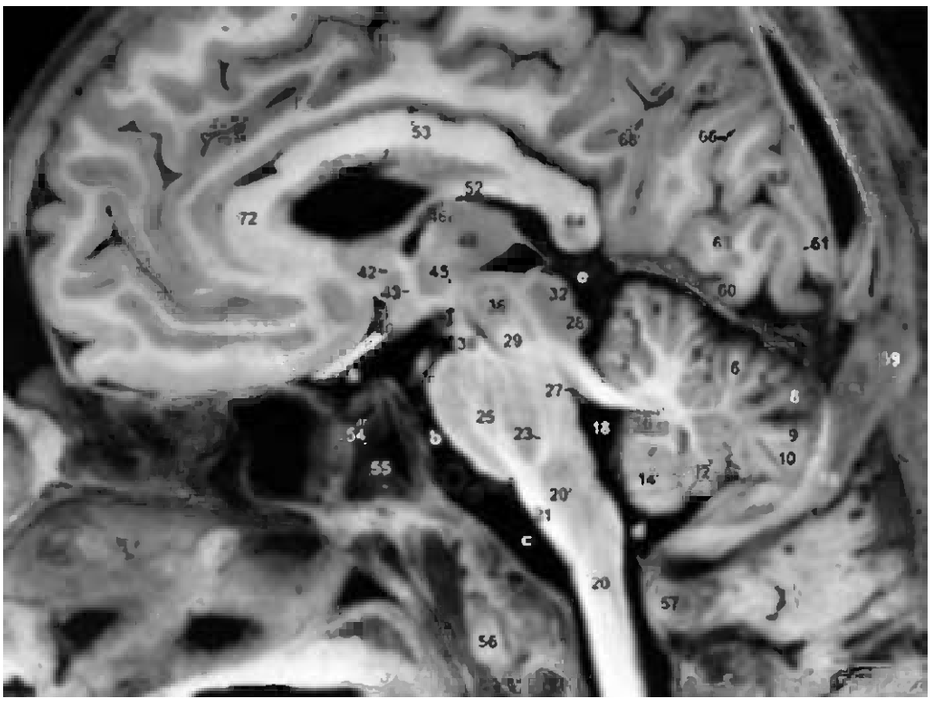

D

Fig. 11.69 (D–F).
D. Sagittal section of the head. Bar: 10 mm.
E–F. 3 Tesla MRI. **E.** T1-weighted MRI. **F**. T2-weighted MRI. In this illustration, the T1- and T2-weighted images depict slightly different paramedian sections. They re-align in the next figure.

2 Central lobule
3 Postcentral fissure (preculminate fissure)
4 Culmen
5 Anterior superior fissure (primary fissure)
6 Declive
7 Posterior superior fissure (postclival fissure)
8 Folium
9 Great horizontal fissure
10 Tuber
11 Prepyramidal fissure
12 Pyramid of vermis
13 Secondary fissure
14 Uvula
14′ Tonsil
16 Nodulus
18 Fourth ventricle
20 Medulla
20′ Medial accessory olivary nucleus
21 Corticospinal tract
23 Medial lemniscus
25 Pons, basilar portion and corticospinal tract
25′ Basilar artery
27 Nucleus ceruleus
28 Inferior colliculus
29 Decussation of superior cerebellar peduncles
29′ Superior cerebellar peduncle (brachium conjunctivum)
30 Substantia nigra
32 Superior colliculus
36 Red nucleus
38 Mammillary body
40 Optic chiasm (CN II)
40′ Anterior cerebral artery
42 Anterior commissure
43 Anterior column of fornix
45 Mammillothalamic tract
46 Anterior thalamic nucleus
48 Dorsomedial thalamic nucleus
50 Posterior commissure
52 Fornix
53 Corpus callosum, body
54 Sella turcica (hypophyseal fossa and hypophysis)
55 Sphenoid sinus
56 Atlas, anterior arch
57 Atlas, posterior arch
58 Occipital bone, squama
59 External occipital protuberance
60 Tentorium cerebelli
61 Calcarine sulcus

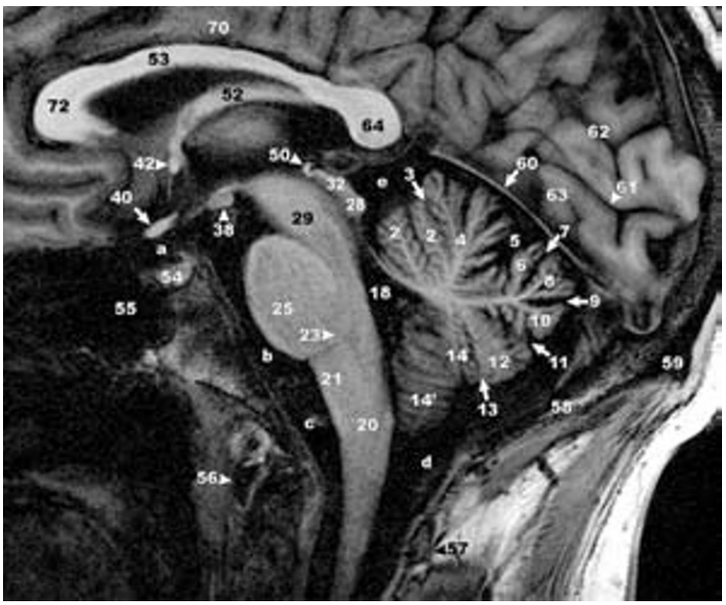

E

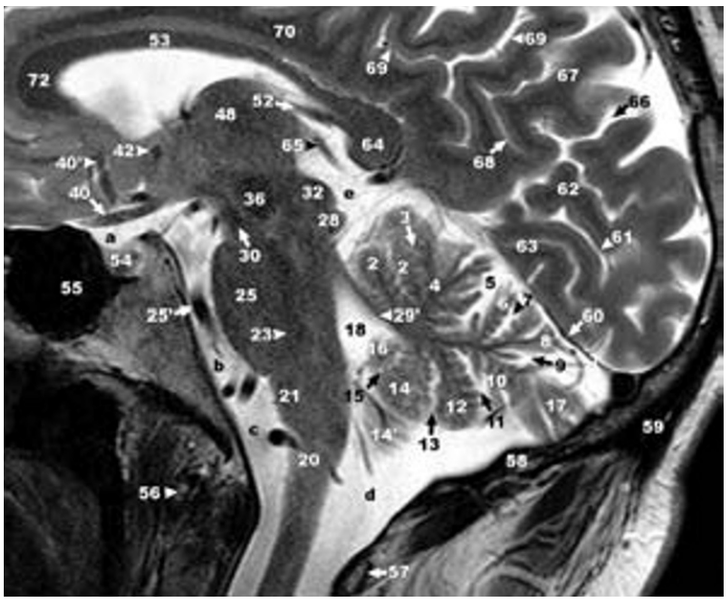

F

62 Cuneus
63 Lingual gyrus
64 Splenium
65 Internal cerebral vein
66 Parieto-occipital sulcus
67 Precuneus
68 Subparietal sulcus
69 Cingulate sulcus (the posterior 69 indicates the pars marginalis)
70 Cingulate gyrus
72 Corpus callosum, genu

Subarachnoid cisterns

a Chiasmatic cistern
b Prepontine cistern
c Premedullary cistern
d Cerebellomedullary cistern (cisterna magna)
e Quadrigeminal cistern

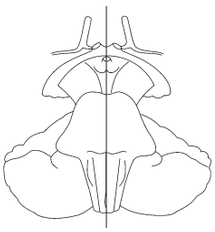

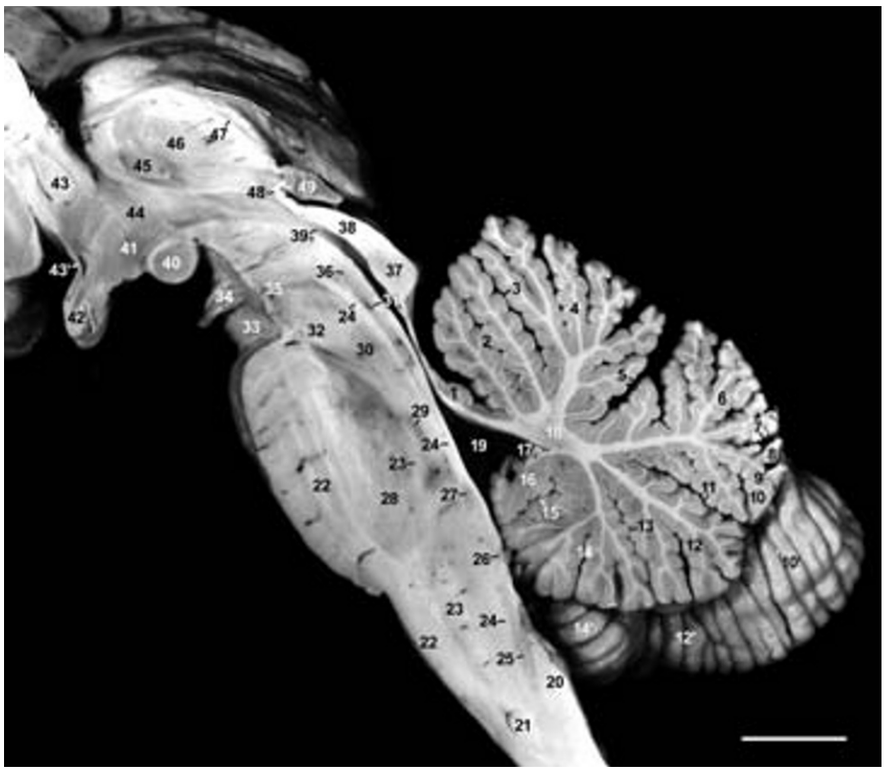

A

Fig. 11.70 (A–C). Sagittal (lateral) section.
A. Sagittal section after removal of the cerebral hemispheres. Bar: 10 mm.
B. Superior oblique view. **C.** Inferior oblique view.

1 Lingula atop superior medullary velum
2 Central lobule
3 Postcentral fissure (preculminate fissure)
4 Culmen
4′ Quadrangular lobule
5 Anterior superior (primary) fissure, separating the anterior from the posterior lobes
6 Declive
6′ Simple lobule
7 Posterior superior fissure
8 Folium
8′ Superior semilunar lobule
9 Great horizontal fissure
10 Tuber
10′ Inferior semilunar lobule
11 Prepyramidal fissure
12 Pyramid
12′ Biventral lobule
13 Postpyramidal (secondary) fissure
14 Uvula
14′ Tonsil
15 Posterolateral fissure (separating the posterior lobe from the flocculonodular lobe)
16 Nodulus
17 Fastigial sulcus
18 Fastigial nucleus
19 Fourth ventricle
20 Gracile nucleus
21 Decussation of the pyramids
22 Corticospinal tract
23 Medial lemniscus
24 Medial longitudinal fasciculus
25 Hypoglossal nucleus (CN XII)
26 Nucleus prepositus hypoglossi
27 Abducens nucleus (CN VI)
28 Pontine nuclei
29 Nucleus reticularis tegmenti pontis
30 Nucleus reticularis centralis superior
31 Trochlear nucleus (CN IV)

B

C

32 Decussation of superior cerebellar peduncles (brachium conjunctivum)
33 Interpeduncular (intercrural) fossa (the medial aspect of the *contralateral* cerebral peduncle is seen through the fossa)
34 Oculomotor nerve (CN III)
35 Ventral tegmental area
36 Oculomotor nucleus (CN III)
37 Inferior colliculus
38 Superior colliculus
39 Cerebral aqueduct
40 Mammillary body
41 Hypothalamus
42 Optic chiasm (CN II)
43 Anterior commissure
43′ Lamina terminalis of the third ventricle
44 Third ventricle
45 Interthalamic adhesion (massa intermedia)
46 Thalamus
47 Stria medullaris thalami
48 Posterior commissure
49 Pineal gland

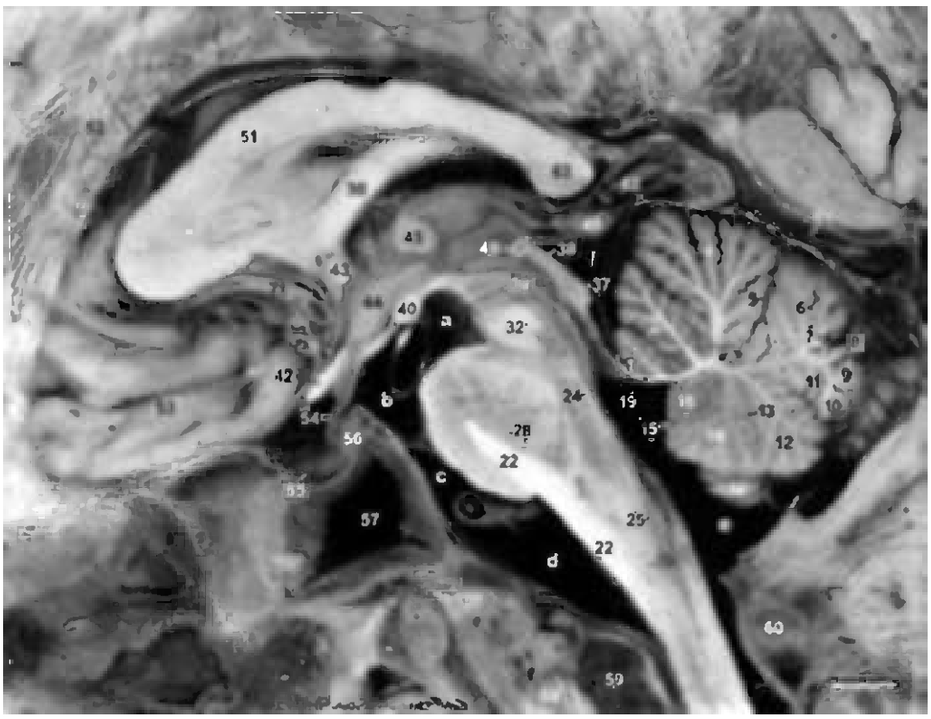

D

Fig. 11.70 (D–F).
D. Sagittal section of the head. Bar: 10 mm.
E–F. 3 Tesla MRI. **E.** T1-weighted MRI. **F**. T2-weighted MRI.

1 Lingula and superior medullary velum
2 Central lobule
3 Postcentral fissure (preculminate fissure)
4 Culmen
5 Anterior superior (primary) fissure
6 Declive
7 Posterior superior fissure
8 Folium
9 Great horizontal fissure
10 Tuber
11 Prepyramidal fissure
12 Pyramid
13 Postpyramidal (secondary) fissure
14 Uvula
14′ Tonsil
15 Posterolateral fissure
16 Nodulus
19 Fourth ventricle
22 Corticospinal tract
24 Medial longitudinal fasciculus
25 Hypoglossal nucleus
28 Pontine nuclei
32 Decussation of superior cerebellar peduncles (brachium conjunctivum)
37 Inferior colliculus
38 Superior colliculus
39 Cerebral aqueduct (of Sylvius)
40 Mammillary body
42 Optic chiasm (CN II)
43 Anterior commissure (midline portion in the anterior wall of the third ventricle)
43′ Lamina terminalis of the third ventricle
44 Third ventricle
45 Interthalamic adhesion (massa intermedia)
48 Posterior commissure
49 Pineal gland
50 Anterior column of fornix
51 Corpus callosum, body
52 Falx cerebri
53 Frontal lobe (medial surface)
54 Hypophyseal stalk
55 Hypophysis, anterior lobe (Adenohypophysis)
56 Hypophysis, posterior lobe (Neurohypophysis)
57 Sphenoid sinus
58 Atlas, anterior arch
59 Dens of axis
60 Atlas, posterior arch
61 Sinus rectus (straight sinus)

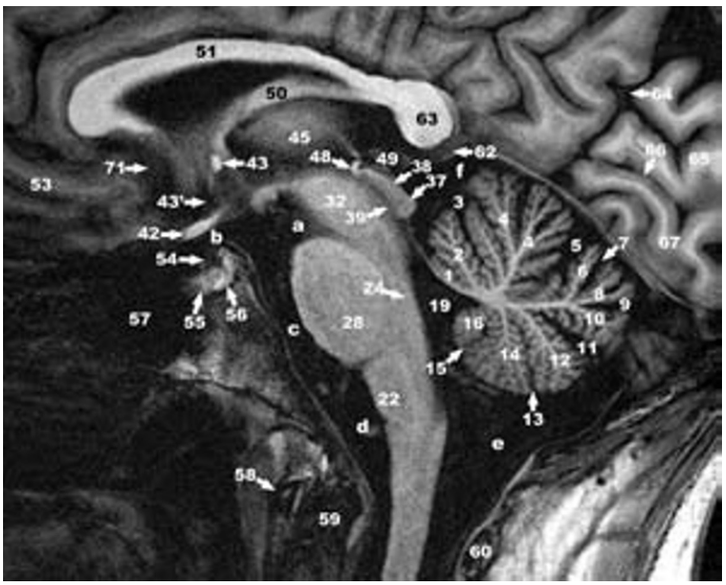

E

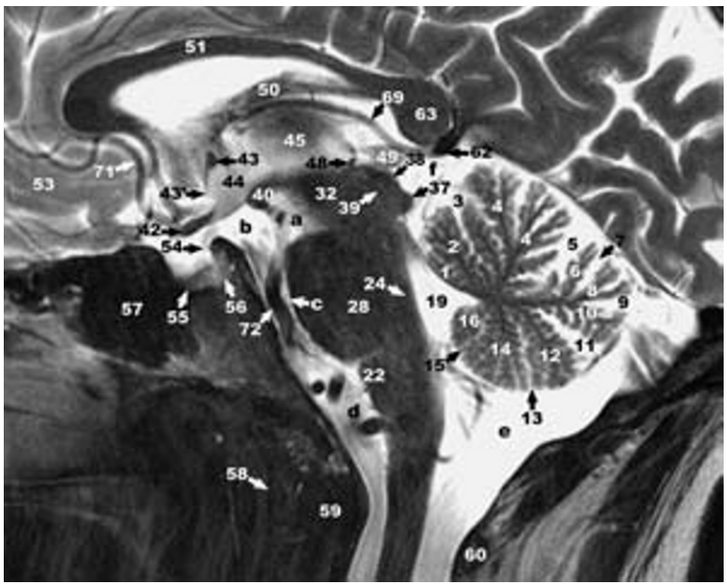

F

62 Great cerebral vein (of Galen)
63 Splenium
64 Parieto-occipital fissure
65 Cuneus
66 Calcarine sulcus
67 Lingual gyrus
69 Internal cerebral vein
71 Pericallosal artery
72 Basilar artery

Subarachnoid cisterns

a Interpeduncular cistern
b Chiasmatic cistern
c Prepontine cistern
d Premedullary cistern
e Cerebellomedullary cistern (cisterna magna)
f Quadrigeminal cistern

References

[1] Aamador LV, Blundell JE, Wahren W (1959) Description of coordinates of the deep structures. In: Schaltenbrand G, Bailey P (eds) Introduction to Stereotaxis with an Atlas of the Human Brain, vol 1. Thieme, Stuttgart, pp 16-28

[2] Abbie AA (1933) The blood supply of the lateral geniculate body, with a note on the morphology of the choroidal arteries. J Anat (London) 67: 491-521

[3] Abbie AA (1933) The clinical significance of the anterior choroidal artery. Brain 56 (3): 233-246

[4] Afshar F, Watkins ES, Yap JC (1978) Stereotaxic atlas of the human brainstem and cerebellar nuclei. A variability study. Raven, New York

[5] Akar ZC, Dujovny M, Gomez-Tortosa E, Slavin KV, Ausman JI (1995) Microvascular anatomy of the anterior surface of the medulla oblongata and olive. J Neurosurg 82: 97-105

[6] Albus JS (1971) A theory of cerebellar function. Math Biosci 10: 25-61

[7] Aleksic S, Budzilovich G (1973) Lateral inferior pontine syndrome. Clinicopathologic study and review of literature. J Neurol Sci 18: 317-322

[8] Alexander L, Suh TH (1937) Arterial supply of lateral parolivary area of the medulla oblongata in man. Arch Neurol Psychiatry 38: 1243-1260

[9] Alezais, D'Astors L (1892) La circulation artèrielle du pèdoncule cèrèbral. Journ de l' Anat et de la physiol (Paris) 28: 519-528

[10] Alezais, D'Astors L (1892) Les artères nourricières des noyaux du moteur oculaire commun et du pathètique CR Soc Biol (Paris) 44: 492-493

[11] Allen JS, Bruss J, Damasio H. (2006) Looking for the Lunate Sulcus: A Magnetic Resonance Imaging Study in Modern Humans. Anat Rec A Discov Mol Cell Evol Biol 288(8): 867-876

[12] Amarenco P, Hauw JJ (1989) Anatomie des arteres cerebelleuses. Rev Neurol (Paris) 145: 267-276

[13] Amarenco P, Hauw JJ, Henin D, Duyckaerts C, Roullet E, Laplane D, Gautier JC, Lhermitte F, Buge A, Castaigne P (1989) Les infarcts du territoire de l'artere cerebelleuse posteroinferieure. Etude clinico-pathologique de 28 cas. Rev Neurol (Paris) 145: 277-286

[14] Andrew J, Watkins ES (1969) A stereotaxic atlas of the human thalamus and adjacent structures. Williams & Wilkins, Baltimore

[15] Angevine JB, Mancall EL, Yakovlev PI (1961) The human cerebellum. An atlas of gross topography in serial sections. Little Brown, Boston

[16] Apkarian AV, Hodge CJ (1989) Primate spinothalamic pathways: I. A quantitative study of the cells of origin of the spinothalamic pathway. J Comp Neurol 288: 447-473

[17] Apkarian AV, Hodge CJ (1989) Primate spinothalamic pathways: II. The cells of origin of the dorsolateral and ventral spinothalamic pathways. J Comp Neurol 288: 474-492

[18] Apkarian A V, Hodge CJ (1989) Primate spinothalamic pathways: III. Thalamic terminations of the dorsolateral and ventral spinothalamic pathways. J Comp Neurol 288: 493-511

[19] Arango V, Ruggiero DA, Callaway JL, Anwar M, Mann JJ, Reis DJ (1988) Catecholaminergic neurons in the ventrolateral medulla and nucleus of the solitary tract in the human. J Comp Neurol 273: 224-240

[20] Arshavsky YI, Gelfand IM, Orlovsky GN (1983) The cerebellum and control of rhythmical movements. Trends Neurosci 6: 417-422

[21] Atkinson WJ (1949) The anterior inferior cerebellar artery. Its variations, pontine distribution, and significance in the surgery of cerebellopontine angle tumours. J Neurol Neurosurg Psychiatry 12: 137-151

[22] Aylward EH, Reiss A (1991) Area and volume measurement of posterior fossa structures in MRI. J Psychiatr Res 25: 159-168

[23] Baeres FM, Moller M (2001) Plastination of dissected brain specimens and Mulligan-stained sections of the human brain. Eur J Morphol 39(5): 307-311

[24] Baker AB (1961) Cerebrovascular disease. IX: The medullary blood supply and the lateral medullary syndrome. Neurology (Minneapolis) 1: 852-861

[25] Baker KG, Tork I, Hornung JP, Halasz P. (1989) The human locus coeruleus complex: an immunohistochemical and three-dimensional reconstruction study. Exp Brain Res 77: 257-270

[26] Baker PC, Bernat JL (1985) The neuroanatomy of vomiting in man: association of projectile vomiting with a solitary metastasis in the lateral tegmentum of the pons and the middle cerebellar peduncle. J Neurol Neurosurg Psychiatry 48: 1165-1168

[27] Baleydier C, Magnin M, Cooper HM (1990) Macaque accessory optic stem: II. Connections with the pretectum. J Comp Neurol 302: 405-416

[28] Bammer R, Auer M, Keeling SL (2002) Diffusion tensor imaging using single-shot-EPI. Magn Reson Med 48(1): 128-136

[29] Bargman W (1943) Die Epiphysis Cerebri. In: Von Mollendorf W (ed) Handbuch der mikroscopischen Anatomie des Menschen, VI – 4. Berlin, Springer, pp 309-349

[30] Barrington FJF (1925) The effect of lesion of the hind- and midbrain on micturition in the cat. J Exp Physiol 15:81-102

[31] Basbaum AI, Fields HL (1978) Endogenous pain control mechanisms: review and hypothesis. Ann Neurol 4: 451-462

[32] Basmajian JV (1975) Grant's method of anatomy, 9th ed. Williams & Wilkins, Baltimore

[33] Bassetti C, Bogousslasky J, Barth A, Regli F (1996) Isolated infarcts of the pons. Neurology 46: 165-175

[34] Batchelor PG, Atkinson D, Hill DL, Calamante F, Connelly A (2003) Anisotropic noise propagation in diffusion tensor MRI sampling schemes. Magn Reson Med 49(6): 1143-1151

[35] Bebin J (1968) The cerebellopontine angle, the blood supply of the brain stem and the reticular formation. Anatomical and functional correlations relevant to surgery of acoustic tumors. Henry Ford Hosp Med J 16: 61-86

[36] Behbehani MM, Zemlan FP (1986) Response of nucleus raphe magnus neurons to electrical stimulation of nucleus cuneiformis: role of acetylcholine. Brain Res 369: 110-118

[37] Bekov DB (1995) Some structural differences among posterolateral tributaries of the great cerebral vein. Fed Proc Suppl 24: 166-170

[38] Belknap DB, McCrea RA (1988) Anatomical connections of the prepositus and abducens nuclei in the squirrel monkey. J Comp Neurol 268: 13-28

[39] Bertram EGM, Moore KL (1982) An atlas of the human brain and spinal cord. Williams & Wilkins, Baltimore

[40] Besson JM (1982) Physiologie de la nociception. J Physiol (Paris) 78: 7-107

[41] Besson JM, Chaouch A (1987) Descending serotoninergic systems. In: Akil H, Lewis JW (eds) Pain and headache, vol. 9. Karger, Basel, 64-100 [Friedmann AP, Granger ME (eds) Pain and headache]

[42] Biemond A (1951) Thrombosis of the basilar artery and the vascularization of the brain stem. Brain 74: 300-317

[43] Blake PY, Mark AS, Kattah J, Kolsky M (1995) MR of oculomotor nerve palsy. AJNR Am J Neuroradiol 16: 1665–1672

[44] Block CH, Estes ML (1990) The cytoarchitectural organization of the human parabrachial nuclear complex. Brain Res Bull 24: 617-626

[45] Bogerts VA (1981) Brainstem atlas of catecholaminergic neurons in man, using melanin as a natural marker. J Comp Neurol 197: 63-80

[46] Bogousslavsky J, Maeder PH, Regli F, Meuli R (1994) Pure midbrain infarction clinical syndromes, MRI, and etiologic patterns. Neurology 44: 2032-2040

[47] Böhnge C (1972) Über die arterielle Versorgung des Gehirns. II. Über die arterielle Blutversorgung der Medulla oblongata. Z Anat Entwickl -Gesch 84: 760-776

[47a] Borges A, Casselman J. (2007) Eur Radiol 17: 2112-2125. Imaging the cranial nerves: Part I: Methodology, infectious and inflammatory, traumatic and congenital lesions. DOI 10.1007/s00330-006- 0575-9

[47b] Borges A, Casselman J. (2007) Eur Radiol 17: 2332-2344. Imaging the cranial nerves: part II: primary and secondary neoplastic conditions and neurovascular conflicts. DOI 10.1007/s00330-006-0572-z

[48] Bossy J (1990) Neuro-anatomie. Springer, Berlin Heidelberg New York Tokyo Paris [Chevrel J-P (ed) Anatomie clinique]

[49] Bourekas EC, Christoforidis GA, Abduljalil AM, Kangarlu A, Chakeres DW, Spigos DG, Robitaille PM (1999) High resolution MRI of the deep gray nuclei at 8 Testa. J Comput Assist Tomogr 23(6): 867-874

[50] Braak H (1970) Über die Kerngebiete des menschlichen Hirnstammes. I: Oliva inferior, Nucleus conterminalis und Nucleus vermiformis corporis restiformis. Z Zellforsch 105: 442-456

[51] Braak H (1970) Über die Kerngebiete des menschlichen Hirnstammes. II: Die Raphekerne. Z Zellforsch 107: 123-141

[52] Braak H (1972) Über die Kerngebiete des menschlichen Hirnstammes. V: Das dorsale Glossopharyngeus und Vagusgebiet. Z Zellforsch 135: 415-438

[53] Bracke-Tolkmitt R, Linden A, Canavan AGM, Rockstroh B, Scholz E, Wessel K, Diener HC (1989) The cerebellum contributes to mental skills. Behav Neurosci 103: 442-446

[54] Bradac GB (1970) The ponto-mesencephalic veins. Neuroradiology 1: 52-57

[55] Brodal A (1981) Neurological Anatomy in relation to Clinical Medicine. Oxford

[56] Bradley WG (1991) MR of the brain stem: a practical approach. Radiology, 179: 319-332

[57] Brass SD, Chen NK, Mulkern RV, Bakshi R (2006) Magnetic resonance imaging of iron deposition in neurological disorders. Top Magn Reson Imaging 17(1): 31-40

[58] Brittenham GM, Farrell DE, Harris JW (1982) Magnetic susceptibility measurements of human iron stores. N Engl J Med 307: 1671-1675

[59] Brody MJ (1986) Central nervous system mechanisms of arterial pressure regulation. Fed Proc FASEB 45: 2700-2706

[60] Brody MJ, Alper RH, O'Neill TP, Porter JP (1986) 1. Central neural control of the cardiovascular system. In: Zanchetti A, Tarazi RC (eds) Handbook of hypertension, vol 8; Pathophysiology of hypertension – regulatory mechanisms. Elsevier, Amsterdam, pp 1–25

[61] Brodal A (1981) Neurological Anatomy in Relation to Clinical Medicine. Oxford University Press, Oxford

[62] Brooks VB (1986) The neural basis of motor control. Oxford University Press, Oxford

[63] Burgel U, Amunts K, Hoemke L, Mohlberg H, Gilsbach JM, Zilles K (2006) White matter fiber tracts of the human brain: three-dimensional mapping at microscopic resolution, topography and intersubject variability. Neuroimage 29(4): 1092-105

[64] Burgess RE, YU Y, Christoforisdis GA, Bourekas EC, Chakeres DW, Spigos D, Kangarlu A, Abduljalil AM, Robitaille PM (1999) Human leptomeningeal and cortical vascular anatomy of the cerebral cortex at 8 Testa. J Comput Assist Tomogr 23 (6): 850-856

[65.] Bullier J (1989) Les deux systemes visuels: resurgences multiples d'une meme idee. MedSci (Montrouge) 5: 575-584

[66] Burde RM, Williams F (1989) Parasympathetic nuclei. Brain Res 498: 371-375

[66a] Burger KM, Tuhrim S, Naidich TP (2005) Brainstem vascular stroke anatomy. [In] Lev MH (ed) Stroke I: overview and current clinical practice. Neuroimaging Clinics of North America 15: 297-324. Saunders, Philadelphia

[67] Buttner-Ennever JA, Holstege G (1986) Anatomy of premotor centers in the reticular formation controlling oculomotor, skeletomotor and autonomic motor systems. Prog Brain Res 64: 89-98

[68] Cabanis EA, Doyon D, Halimi PH, Iba-Zizen MT, Sigal R, Tamraz J (1988) Atlas d'IRM de l'encephale et de la moelle. Masson, Paris

[69] Cabanis EA, Massin M, Iba-Zizen MT, Flament J, Arnaud B (1992) L'imagerie par resonance magnetique (IRM) en ophtalmologie, introduction. Bull Soc Ophtalmol Fr (special issue): 1-472

[70] Cabanis EA, Iba-Zizen MT, Tamraz J, Stoffels C (1984) IRM de la tete et du cou orientee selon le Plan Neuro-Oculaire (P.N.O.): une condition d'efficacite anatomique. Colloque de Medicine Nucleaire de Langue Francaise, Nice, 13-15 September, 1984. J Biophys Med Nucl 8: 48-50

[71] Caillet H, Delvalle A, Doyon D, Sigal R, Francke JP, Halimi PH, Bely N (1991) Les nerfs craniens normaux en IRM. Description et frequence de visualisation. J Radiol 72: 69-78

[72] Ramon y Cajal RS (1909) Histologie du systeme nerveux de l'homme et des vertebres, vol 1. Maloine, Paris

[73] Campbell ACP (1938) The vascular architecture of the cat's brain. A study by vital injection. In: Stanley C, Angud MF, Penfield W, Riley HA (eds) The circulation of the brain and spinal cord. Res Publ Ass Nerv Ment Dis: 18, 69-93

[74] Cannon SC, Rohinson D (1986) The final common integrator is in the prepositus and vestibular nuclei. In: Keller EL, Lee DS (eds) Adaptative processes in visual and oculomotor systems. Pergamon, Oxford, pp 307-311

[75] Capra NF, Anderson L, Putman TJ (1938) Vascular pattern in various lesions of the human central system. Studies with the benzidine stain. Arch Neurol Psychiatr 39, 1550-1202

[76] Capra NF, Anderson KV (1984) Anatomy of the cerebral venous system. In: Kapp JP, Schmidek HH (eds) The cerebral venous system and its disorders. Grune and Stratton, Orlando

[77] Carl JR, Gellman RS, (1986) Adaptative responses in human smooth pursuit. In: Keller EL, Zee DS (eds) Adaptative processes in visual and oculomotor systems. Pergamon, Oxford, pp 335-339

[78] Carpenter MB, Sutin J (1983) Human neuroanatomy, 8th edn. Williams & Wilkins, Baltimore

[79] Carpenter MB (1986) Anatomy of the basal ganglia. In: Vinken PJ, Bruyn GW, Klawans HL (eds) Handbook of clinical neurology, vol 1. Elsevier, Amsterdam, pp 1-18

[80] Cechetto DF (1987) Central representation of visceral function. Fed Proc 16: 17-23

[81] Chalmers J, Pilowsky P (1991) Brainstem and bulbospinal neurotransmitter systems in the control of blood pressure. J Hypertens 9: 675-694

[82] Chaouch A, Besson J (1986) Mecanismes peripheriques et medullaires de la nociception. Rev Neurol (Paris) 142: 173-200

[83] Christoforidis GA, Bourekas EC, Baujan M, Abduljalil AM, Kangarlu A, spigos DG, Chakeres DW, Robitaille PM (1999) High resolution MRI of the deep brain vascular anatomy at 8 Tesla: susceptibility-based enhancement of the venous structures. J Cimput Assist Tomogr 23(6): 857- 866

[84] Ciriello J, Caverson MM, Polosa C (1986) Function of the ventrolateral medulla in the control of the circulation. Brain Res Rev 11: 359-391

[85] Clara M (1959) Das Nervensystem des Menschen, 3rd edn. Barth, Leipzig

[86] Cohen B, Bodis-Wollner I (1990) Vision and the brain. The organization of the central visual system. Raven Press, New York

[87] Cohen B, Raphan T, Waespe W (1986) Vestibulo-cerebellar control of the vestibulo-ocular reflex (VOR). In: Keller EL, Zee DS (eds) Adaptative processes in visual and oculomotor systems. Pergamon, Oxford, pp 277-283

[88] Cools AR (1986) Clinical neuropharmacology of the basal ganglia. In: Vinken PJ, Bruyn GW, Klawans HL (eds) Handbook of clinical neurology, vol 5. Elsevier, Amsterdam, pp 47-63

[89] Cooper HM, Magnin M (1987) Accessory optic system of an anthropoid primate, the gibbon (*Hylobates concolor*): evidence of a direct retinal input to the medial terminal nucleus. J Comp Neural 259: 467-482

[90] Cormier PJ, Long ER, Russel EJ, (1992) MR Imaging of posterior fossa infarctions: vascular territories and clinical correlates. RadioGraphics 12: 1079-1096

[91] Corsellis JAN (1958) Individual variation in the size of the tentorial opening. J Neurol Neurosurg Psychiatry 21: 279-283

[92] Courchesne E, Press GA, Murakami J, Berthoty D, Grafe M, Wiley CA, Hesselink JR (1989) The cerebellum in sagittal plane anatomic-MR correlation: 1. The vermis. AJR Am J Roentgenol 153: 829-835

[93] Cravo SL, Morrison SF, Reis DJ (1991) Differentiation of two cardiovascular regions within caudal ventrolateral medulla. Am J Physiol 261: R985-R994

[94] Craigie EH (1920) On the relative vascularity of various parts of the central nervous system of the albino rat. J Comp Neurol 31: 429-464

[95] Craigie EH (1933) The vascularity of parts of the cerebellum, brain stem, and spinal cord of inbred albino rats. J Comp Neurol 58: 507-516

[96] Craigie EH (1938) The comparative anatomy and embryology of the capillary bed of the central nervous system. In: Stanley C, Angus MF, Penfield W, Reley HA (eds) The circulation of the brain and spinal cord. Res Publ Ass Nerv Ment Dis 18: pp 3-28

[97] Craigie EH (1940) Measurement of vascularity in some hypothalamic nuclei of the albino rat. In: The hypothalamus and central levels of autonomic function. Proc Ass Nerv Ment Disc 20: 310-319

[98] Creutzfeldt OD (1988) Extrageniculate-striate visual mechanisms: compartmentalization of visual functions. Prog Brain Res 75: 307-320

[99] Crosby EC, Humphrey T, Lauer EW (1962) Correlative anatomy of the nervous system. Macmillan, New York

[100] Cusick CG (1988) Anatomical organization of the superior colliculus in monkeys: corticotectal pathways for visual and visuomotor functions. Prog Brain Res 75: 1-15
[101] Daniels DL, Haughton VM, Naidich TP (1987) Cranial and spinal magnetic resonance imaging an atlas and guide. Raven Press, New York
[102] Daniels DL, Mark LP, Ulmer J, Maas EF, Borne JA, Calderwood GW (1998) Understanding the brain stem. Rev Neuroimaging Clin N Am 8(1): 55-68
[103] Daniels DL, Pech P, Pojunas KW, Kilgore DP, Williams AL, Haughton VM (1986) Trigeminal nerve: anatomic correlation with MR imaging. Radiology 159(3): 577-83
[104] Dashner RA, Chakeres DW, Kangarlu A, Schmalbrock P, Christoforidis GA, DePhillip RM (2003) MRI imaging visualization of the cerebral microvasculature: a comparison of live and postmortem studies at 8 T. AJNR Am J Neuroradiol 24:1881-1884
[105] Davidoff RA (1989) The dorsal columns. Neurology 39: 1377-1385
[106] DeArmond SJ, Fusco MM, Dewey MM (1974) A photographic atlas. Structure of the human brain. Oxford University Press, New York
[107] De Chambenoit G, Bugha TN, Duvernoy H, Salamon G (1989) Magnetic resonance imaging of the brain stem. Anatomico-radiological correlations. Surg Radiol Anat 11(2): 155-61
[108] De Smet Y, Brucher JM, Gonsette RE (1984) L'infarctus du territoire olivarie du bulbe. Rev Neurol (Paris) 10: 559-556
[109] Dejerine J (1980) Anatomie des centres nerveux, vol 1. Masson, Paris
[110] Dewulf A (1971) Anatomy of the normal human thalamus. Elsevier, Amsterdam
[111] Diener HC, Dichgans J, Guschlbauer B, Bacher M, Rapp H, Klockgether T (1992) The coordination of posture and voluntary movement in patients with cerebellar dysfunction. Mov Disord 7: 14-22
[112] Diezel PB (1955) Iron in the brain: a chemical and histochemical examination. In: Biochemistry of the developing nervous system. New York, Academic Press, pp 145-152
[113] Diz DI, Barnes KL, Ferrario CM (1987) Functional characteristics of neuropeptides in the dorsal medulla oblongata and vagus nerve. Fed Proc 46: 30-35
[114] Dor P, Salamon G (1970) The arterioles and capillaries of the brain stem and cerebellum: a microangiographic study. Neuroradiology 1: 27-29
[115] Drayer B, Burger P, Darwin R, Riederer S, Herfkens R, Johnson GA (1986) MRI of brain iron. AJR Am J Roentgenol 147(1): 103-10
[116] Dunnings HS, Wolfe HG (1937) The relative vascularity of various parts of the central and peripheral nervous systems of the cat and its relation to function. J Comp Neurol 67: 433-450
[117] Duret H (1873) Sur la distribution des arteres nourricieres du bulbe rachidien. Arch Physiol Norm Pathol 5: 97-113
[118] Duret H (1874) Recherches anatomiques sur la circulation de l'encephale. Arch Physiol Norm Pathol, 2eme Ser 1: 60-91
[119] Duvernoy H (1972) The vascular architecture of the median eminence. In: Knigge KM, Scott DE, Weindl A (eds) Brainendocrine interaction. Median eminence: structure and function. Karger, Basel, pp 79-108 [Int Symposium on Brain-endocrine Interaction]
[120] Duvernoy H (1975) The superficial veins of the human brain. Veins of the brain stem and of the base of the brain. Springer, Berlin Heidelberg New York
[121] Duvernoy H (1995) The Human Brain Stem and Cerebellum. Surface, Structure, Vascularization, and Three-dimensional Sectional Anatomy with MRI. Springer, Wien New York
[122] Duvernoy H (1999) Human brain stem vessels including the pineal gland and information on brain stem infarction, 2nd edn. Springer, Berlin
[123] Duvernoy H, Risold PY (2007) The circumventricular organs: An atlas of comparative anatomy and vascularisation. Brain Research Reviews 56: 119-147
[124] Duvernoy H (2005) The Human Hippocampus Functional Anatomy, Vascularization and Serial Sections with MRI. 3rd edn. Springer, Berlin
[125] Duvernoy H (1999) The Human Brain. Surface, three-dimensional sectional anatomy and MRI. Second Edition. Springer, Wien New York
[126] Duvernoy H, Parratte B, Tatu L, Vuillier F (2000) The Human Pineal Gland. Relationships with surrounding structures and blood supply. Neurological Res 22: 747-790
[127] Duvernoy H, Delon S, Yannson JL (1981) Cortical blood vessels of the human brain. Brain Res Bull 7: 519-579
[128] Duvernoy H, Delon S, Yannson JL (1983) The vascularization of the human cerebellar cortex. Brain Res Bull 11: 419-480
[129] Duvernoy H, Koritke JG, Monnier G (1969) Sur la vascularisation de la lame terminale humaine. Z Zellforsch 102: 49-77
[130] Duvernoy H, Koritke JG, Monnier G (1971) Sur la vascularisation du tuber posterieur chez l'homme et sur les relations vasculaires tuberohypophysaires. J Neurovisc Relat 32: 112-142
[131] Duvernoy H, Koritke JG, Monnier G, Jacquet G (1972) Sur la vascularisation de l'area postrema et la face posterieure du bulbe chez l'homme. Z Anat Entwicklungsgesch 138: 41-66
[132] Eccles JC, Ito M, Szentagothai J (1967) The cerebellum as a neuronal machine. Springer, Berlin Heidelberg New York
[133] Eckmiller R (1987) Neural control of pursuit eye movements. Physiol Rev 67: 797-857
[134] Elster AD (1992) MR contrast enhancement in brainstem and deep cerebral infarction. Am J Neuroradiol 12: 1127-1132
[135] Escourolle R, Hauw JJ, Der Agopian P, Trelles L (1976) Les infarctus bulbaires. Etude des lesions vasculaires dans 26 observations. J Neurol Sci 28: 103-113

[136] Fatterpekar GM, Delman BN, Boonn WW, Gutelkin SH, Fayad ZA, Hoff PR, Naidich TP (2003) MR microscopy of normal human brain. Review. Magn Reson Imaging Clin N Am 11(4): 641-53

[137] Fatterpekar GM, Naidich TP, Delman BN, Aguinaldo JG, Gutelkin SH, Sherwood CC, Hof PR, Drayer BP, Fayad ZA (2002) Cytoarchitecture of the human cerebral cortex: MR microscopy of excised specimens at 9.4 Tesla. AJNR Am J Neuroradiol 23(8): 1313-21

[138] Fazio C, Ferraris M (1949) L'angioarchitettonica del midollo allungato umano e i suoi rapporti con la cito-mieloarchitettonica. Sist Nerv 2: 7-29

[139] Fazio C, Perria L (1940) Primo contributo allo studio della vascularizzazione della pineale dell'uomo. Riv Patol Nerv Ment: 56-104

[140] Ferguson JH, Cole M, Alley K (1977) Is there a decussation of the facial motor nerve root? An experimental neuroanatomical study. Trans Am Neurol Assoc 102: 51-3

[141] Fields HL (1984) Brainstem mechanisms of pain modulation. In: Kruger L, Liebeskind JC (eds) Advances in Pain Research and Therapy, vol 6. Raven, New York, pp 241-252

[142] Fields HL, Heinricher MM (1985) Anatomy and physiology of nociceptive modulatory system. Philos Trans R Soc Lond [Bioi] 308: 361-374

[143] Finley KH (1936) Angio-architecture of the substantia nigra and its pathogenic significance. Arch Neurol Psychiatr 36: 116-127

[144] Finley KH, Cobbs S (1940) The capillary bed of the locus coeruleus. J Comp Neurol 73: 49-58

[145] Fischer B (1986) Express saccades in man and monkey. Progr Brain Res 64: 155-160

[146] Fitzek C, Weissmann M, Speckter H, Fitzek S, Hopf HC, Schulte E, Stoeter P (2001) Anatomy of brain-stem white-matter tracts shown by diffusion-weighted imaging. Neuroradiology 43(11): 953-60

[147] Fix JD, Punte CS (1981) Atlas of the human brain stem and spinal cord. University Park Press, Baltimore

[148] Flannigan BD, Bradley WG, Mazziotta JC, Rauschning W, Bentson JR, Lufkin RB, Hieshima GB (1985) Magnetic resonance imaging of the brainstem: normal structure and basic functional anatomy. Radiology 154: 375-383

[149] Foix CH, Hillemand P (1925) Les arteres de l'axe encephalique jusqu'au diencephale inclusivement. Rev Neurol 2: 705-739

[150] Foix CH, Hillemand P (1925) Irrigation de la protubérance. C R Soc Biol (Paris) 92 (1): 35-36

[151] Foix CH, Hillemand P (1925) Irrigation du pédoncule cérébral. C R Soc Biol (Paris) 92: 608-610

[152] Foix CH, Hillemand P, Schalit I (1925) Irrigation du bulbe. C R Soc Biol (Paris) 92 (1): 33-35

[153] Foix CH, Nicolesco J (1925) Anatomie cerebrale, noyaux gris centraux et region mesencephalo-sous-optique. Masson, Paris

[154] Foreman RD, Blair RW, Ammons WS (1986) Neural mechanisms of cardiac pain. Prog Brain Res 67: 227-243

[155] Fox CA, Siner RS (1967) Progress in Brian Research the Cerebellum. Amsterdam, Elsevier

[156] Fredericks CA, Giolli RA, Blanks RHI, Sadun AA (1988) The human accessory optic system. Brain Res 454: 116-122

[157] Fredrickson JM, Kornhuber HH, Schwarz DWF (1974) Cortical projection of the vestibular nerve. In: Kornhuber HH (ed) Vestibular system. Part I: Basic mechanisms. Springer, Heidelberg New York, pp 565-582

[158] Fuchs AF, Kaneko CRS, Scudder CA (1985) Brainstem control of saccadic eye movements. Annu Rev Neurosci 8: 307-337

[159] Gabrielsen TO, Amundsen P (1969) The pontine arteries in vertebral angiography, Am J Roentgenol 106: 296-302

[160] Galloway J, Greitz T (1960) The medial and lateral choroid arteries. An anatomic and roentgenographic study. Acta Radiol (Stockh) 53: 353-366

[161] Gellman RS, Miles FA (1985) A new role for the cerebellum in conditioning? Trends Neurosci 8: 181-182

[162] Gellman RS, Miles FA (1988) Control of gaze. In: Held R (ed) Sensory systems I, vision and visual systems. Birkhäuser, Boston, p 30

[163] Gillilan LA (1964) The correlations of the blood supply of the human brain stem with clinical brain stem lesions. J Neuropathol Exp Neurol 23: 78-108

[164] Gilman S, Newman SW (2003) Manter and Gatz' Essentials of Clinical Neuroanatomy and Neurophysiology, 10th edn. F.A. Davis Publishers, Philadelphia

[165] Giudicelli G, Faure J, Salamon G (1970) The veins of the thalamus. Neuroradiology I: 92-98

[166] Giudicelli G, Salamon G (1970) The veins of the thalamus. Neuroradiology I: 92-98

[167] Gluhbegovic N, Williams TH (1980) The human brain. A photographic guide. Harper & Row, Hagerstown

[168] Godaux E, Cheron G (1989) Le mouvement. Medsi/McGraw-Hill, Paris

[169] Goddhart SP, Davison C (1936) Syndrome of the posterior inferior cerebellar arteries and of anterior inferior cerebellar arteries and their branches. Arch Neurol Psychiatry 35: 501-524

[170] Gottwald B, Wilde B, Mihajlovic Z, Mehdom HM (2004) Evidence for distinct cognitive deficits after focal cerebellar lesions. J Neurol Neurosurg Psychiatry 75: 1524-1531

[171] Grand W, Budny JL, Gibbons KJ, Sternau LL, Hopkins LN (1997) Microvascular surgical anatomy of the vertebrobasilar junction. Neurosurgery 40: 1219-1225

[172] Greitz T, Lindgren E (1971) Cerebral vascular anatomy. In: Abrams HL (ed) Angiography, vol 1, 2nd edn. Little Brown, Boston, pp 155-281

[173] Greitz T, Sjogren S (1963) The posterior inferior cerebellar artery. Acta Radiol 1: 284-297

[174] Gross PM, Wall KM, Pang JJ, Shaver SW, Wainman DS (1990) Microvascular specializations promoting rapid interstitial solute dispersion in nucleus tractus solitarius. Am J Pysiol 259: R 1131-R 1138

[175] Gunny R, Yousry TA. (2007) Imaging anatomy of the vestibular and visual systems. Review. Curr Opin Neurol 20(1): 3-11

[176] Gyton AC (1991) Textbook of medical physiology, 8th edn. Saunders, Philadelphia

[177] Haacke EM, Xu Y, Cheng, YN, Reichenbach JR (2004) Susceptibility weighted imaging (SWI). MRM 52:612-618

[177a] Habas C, Cabanis EA (2007) Anatomical parcellation of the brainstem and cerebellar white matter: a preliminary probabilistic tractography study at 3 T. Neuroradiology 49: 849-863

[178] Hacker H (1974) Superficial supratentorial veins and dural sinuses. Section I: Normal supratentorial veins and dural sinuses. In: Newton TH, Potts DG (eds). Veins, vol II, book 3. Mosby, St Louis, pp 1851-1877

[179] Haines DE (2004) Neuroanatomy: an atlas of structures, sections, and systems, 6th edn. Lippincott Williams & Wilkins, Philadelphia

[180] Hallgren B, Sourander P (1958) The effect of age on the nonhaemin iron in the human brain. J Neurochem 3: 41-51

[181] Halliday GM, Li YW, John TH, Cotton RGH, Howe PRC, Geffen LB, Blessing WW (1988) Distribution of monoamine-synthesizing neurons in the human medulla oblongata. J Comp Neurol 273: 301-317

[182] Hardy DG, Peace DA, Rhoton AL (1980) Microsurgical anatomy of the superior cerebellar artery. Neurosurgery 6: 10-28

[183] Harvey PH, Gofray CJ (2001) Evolution: A horn ffor an eye. Science 291; 1505-1506

[184] Hasegawa T, Ravens JR, Toole JF (1967) Precapillary arteriovenous anastomoses. "Thoroughfare Channels" in the brain. Arch Neurol 16: 217-224

[185] Hassler O (1967) Venous anatomy of human hindbrain; a stereo-microangiographic study of the venous angio-architecture and the venous areas of drainage. Arch. Neurol 16:404-409

[186] Hassler O (1967) Arterial pattern of human brainstem: normal appearance and deformation in expanding supratentorial conditions. Neurology (Minneapolis) 17: 368-375

[187] Hauw JJ, Der Agopian P, Trelles L, Escourolle R (1976) Les infarctus bulbaires. Etude systematique de la topographie lesionnelle dans 49 cas. J Neurol Sci 28: 83-102

[188] Hayes CE, Tsuruda JS, Mathis CM (1993) Temporal lobes: surface MR coil phased-array imaging. Radiology 189: 918–920

[189] Hayflick SJ, Hartman M, Coryell J, Gitschier J, Rowley H (2006) Brain MRI in neurodegeneration with brain iron accumulation with and without PANK2 mutations. AJNR Am J Neuroradiol 27(6): 1230-3

[190] Helgason CM, Wilbur AC (1991) Basilar branch pontine infarction with prominent sensory signs. Stroke 22: 1129-1136

[191] Henn V, Cohen H, Young LR (1980) Visual vestibular interaction in motion perception and the generation of nystagmus. Neurosci Res Program Bull 18: 459-651

[192] Hess C, Mukerjee P, Han ET, et al (2006) High Angular Resolution Diffusion Tensor Imaging (HARDI). Magn Reson Med 56: 104-117

[193] Hirai T, Jones EG (1989) A new parcellation of the human thalamus on the basis of histochemical staining. Brain Res Rev 14: 1-34

[194] Hirsch WL, Kemp SS, Martinez AJ, Curtin H, Latchaw RE, Wolf G (1989) Anatomy of the brainstem: correlation of in vitro MR images with histologic sections. Am J Neuroradiol 10: 923-928

[195] Hobson JA, Brazier MAB (1980) The reticular formation revisited. Specifying function for a nonspecific system. Raven, New York [International Brain Research Organization Monograph Series, Vol 6]

[196] Hoffman HB, Margolis MT, Newton TH (1974) The superior cerebellar artery. Section I: Normal gross and radiographic anatomy. In: Newton TH, Potts DG (eds) Angiography. Radiology of the skull and brain, vol. 2, book 2: arteries. Mosby, St Louis, pp 1809-1830

[197] Holdorff B, Cervos-Navarro J. (1971) Die Pathologie der inneren pontomesencephalen Venen. Radiologe 12: 465-471

[198] Holstege G, Griffiths D, De Wall H, Dalm E (1986) Anatomical and physiological observations on supraspinal control of bladder and urethral sphincter muscles in the cat. J Comp Neurol 250: 449-461

[199] Hornykiewicz O, Kish SJ (1986) Biochemical pathophysiology of Parkinson's disease. Adv Neurol 45: 19-34

[200] Hoyt WF, Newton TH, Margolis MT (1974) The posterior cerebral artery. Section I: Embryology and developmental anomalies. In: Newton TH, Potts DG (eds) Radiology of the skull and brain. Angiography vol II, book 2. Mosby, St Louis, pp 1540-1550

[201] Huang XF, Tork I, Halliday GM, Paxinos G (1992) The dorsal, posterodorsal, and ventral tegmental nuclei: a cyto- and chemoarchitectonic study in the human. J Comp Neurol 318: 117-137

[202] Huang XF, Tork I, Paxinos G (1993) Dorsal motor nucleus of the vagus nerve: a cyto- and chemoarchitectonic study in the human. J Camp Neural 330: 158-182

[203] Huang YP, Wolf BS (1964) Veins of the white matter of the cerebral hemispheres (the medullary veins): diagnostic importance in carotid angiography. Am J Roentgenol. Radium Ther Nucl Med 92: 739-755

[204] Huang YP, Wolf BS (1965) The veins of the posterior fossa; superior or galenic drainange group. Am J Roentgenol 95: 808-821

[205] Huang YP, Wolf BS (1966) Precentral cerebellar vein in angiography. Acta Radiol [Diagn] 5: 250-262

[206] Huang YP, Wolf BS (1967) The veins of the lateral recess of the fourth ventricle and its tributaries; roentgen appearance and anatomic relationships. Am J Roentgenol Radium Ther Nucl Med 101: 21

[207] Huang YP, Wolf BS, Okudera T (1969) Angiographic anatomy of the inferior vermian vein of the cerebellum. Acta Radiol [Diagn] 9: 327–344

[208] Huang YP, Wolf BS (1974) The basal cerebral vein and its tributaries. In: Newton TH, Potts DG (eds) Radiology of the skull and brain. Angiography, vol II, book 3. Mosby, St. Louis, pp 2111-2154

[209] Huang YP, Wolf BS (1974) Veins of the posterior fossa. In: Newton TH, Potts DG (eds) Radiology of the skull and brain. Angiography, vol II, book 3. Mosby, St. Louis, pp 2155-2219

[210] Huang YP, Wolf BS, Antin SP, Okudera T (1968) The veins of the posterior fossa; anterior or petrosal draining group. Am J Roentgenol 104: 36-56

[211] Hukuhara T (1988) Organization of the brain stem neural mechanisms for generation of respiratory rhythm. Current problems. Jpn J Physiol 38: 753-776

[212] Isaacson RL (1974) The limbic system. Plenum, New York

[213] Ito M (1985) Cerebellar plasticity as the basis of motor learning. In: Eccles JC, Dimitrijevic MR (eds) Recent achievements in restorative neurology 1: Upper motor neuron functions and dysfunctions. Karger, Basel, pp 222-234

[214] Ito M (1988) Oculomotor system, mechanisms. In: Held R (ed): Sensory systems I, vision and visual systems. Birkhäuser, Boston, pp 38-40

[215] Ito M (1990) A new physiological concept on cerebellum. Rev Neurol (Paris) 146: 564-569

[216] Ivry RB, Keele SW, Diener HC (1988) Dissociation of the lateral and medial cerebellum in movement timing and movement execution. Exp Brain Res 73: 167-180

[217] Jaermann T, Crelier G, Pruessmann KP (2004) SENSE-DTI at 3 T. Magn Reson Med 51(2): 230-236

[218] Jansen J, Brodal A (1958) Handbuch der mikroskopischen Anatomie des Menschen, vol 4, part 8: Das Kleinhirn. Springer, Berlin

[219] Javoy-Agid F, Ruberg M, Hirsch E, Cash R, Raisman R, Taquet H, Epelbaum J, Scatton B, S, Marsden CD, Jenner P, Teychenne T (eds) Recent development in Parkinson's disease. Raven, New York, pp 67-83

[220] Jean A (1984) Brainstem organization of the swallowing network. Brain Behav Evol 25: 109-116

[221] Jean A (1991) Le noyau du faisceau solitaire: aspects neuroanatomiques, neurochimiques et fonctionnels. Arch Int Physiol Biochem Biophys 99: A3-A52

[222] Jefferies WA, Brandon MR, Hunt SV, William AF, Gatter KC, Mason DY (1984) Transferrin receptor on endothelium of brain capillaries. Nature 312: 162-163

[223] Jellison BJ, Field AS, Medow J, Lazar M, Salamat MS, Alexander AL (2004) Diffusion tensor imaging of cerebral white matter: a pictorial review of physics, fiber tract anatomy, and tumor imaging patterns. AJNR Am J Neuroradiol 25(3): 356-369

[224] Jhamandas JH, Renaud LP (1987) Neurophysiology of a central baroreceptor pathway projecting to hypothalamic vasopressin neurons. Can J Neurol Sci 14: 17-24

[225] Johanson C (1954) The central veins and deep dural sinuses of the brain. Acta Radiol Supp 107: 5-184

[226] Jordan D, Spyer KM (1986) Brainstem integration of cardiovascular and pulmonary afferent activity. Prog Brain Res 67: 295-314

[227] Justus TC, Ivry RB (2001) The cognitive neuropsychology of the cerebellum. International Review of Psychiatry 13: 276-282

[228] Kahle W, Leonhardt H, Platzer W (1986) Color atlas and textbook of human anatomy, vol 3, nervous system and sensory organs, 3rd rev edn. Thieme, Stuttgart

[229] Kamina P (1990) Petit dictionnaire d'anatomie, d'embryologie et d'histologie. Maloine, Paris

[230] Kamman RL, Go KG, Stomp GP, Hulstaert CE, Berendsen HJC (1985) Changes of relaxation times T1 and T2 after biopsy and fixation. Magn Reson Imaging 3: 245–250

[231] Kaplan HA, Ford DH (1966) The brain vascular system. Elsevier, Amsterdam

[232] Kataoka S, Hori A, Shirakawa T, Hirose G (1997) Paramedian pontine infection. Neurological topographical correlation. Stroke 28: 809-815

[233] Khan NM (1969) The blood supply of the midbrain in man and monkey. PhD thesis, Guy's Hospital Medical School, University of London, London, UK

[234] Kim JS, Lee JH, Choi CG (1998) Patterns of lateral medullary infarction. Vascular lesion - magnetic resonance imaging correlation of 34 cases. Stoke 29: 645-652

[235] Klun B, Prestor B (1986) Microvascular relations of the trigeminal nerve: an anatomical study. Neurosurgery 19: 535-539

[236] Koehler PR, Haughton VM, Daniels DL, Williams AL, Yetkin Z, Charles HC, Shutts D (1985) MR measurement of normal and pathologic brainstem diameters. AJNR Am J Neuroradiol 6(3): 425-7

[237] Komatsu H, Wurtz RH (1989) Modulation of pursuit eye movements by stimulation of cortical areas MT and MST. J Neurophysiol 62: 31-47

[238] Komisaruk BR, Mosier KM, Liu WC, Criminale C, Zaborszky L, Whipple B, Kalnin A (2002) Functional localization of brainstem and cervical spinal cord nuclei in humans with fMRI. AJNR Am J Neuroradiol 23(4): 609-17

[239] Kortike JG, Tournade A, Monnier G, Maillot CL (1970) Les veins superficielles du bulde essai de systematization. Bull Assoc Anat 149: 791-801

[240] Koritke JG, Sick H (1982) Atlas de coupes seriees du corps humain, vol 1. Tete, cou, thorax. Urban & Schwarzenberg, München

[241] Krayenbuehl HA, Yasargil MG (1957) Die vaskularen Erkrankungen im Gebiet der Arteria vertebralis und Arteria basilaris. Thieme, Stuttgart

[242] Krayenbuehl HA, Yasargil MG (1968) Cerebral angiography, 2nd edn. Butterworths, London

[243] Kretschmann HJ, Weinrich, W (2004) Cranial Neuroimaging and Clinical Neuroanatomy, 3rd edn. Thieme, Stuttgart

[244] Krings T, Coenen VA, Axer H, Reinges MH, Holler M, von Keyserlingk DG, Gilsbach JM, Thron A (2001) In vivo 3D visualization of normal pyramidal tracts in human subjects using diffusion weighted magnetic resonance imaging and a neuronavigation system. Neurosci Lett 307(3): 192-6

[245] Kuhlenbeck H (1954) The human diencephalon. Corum Neurol 14 [Suppl]: 1-230

[246] Kumar AJ, Naidich TP, George AE, Linn, JP, Kricheff II (1978) The choroidal artery to the fourth ventricle and its radiological significance. Radiology 126: 431-438
[247] Kuypers HGJM (1982) A new look at the organization of the motor system. Prog Brain Res 57: 381-403
[248] Laget P (1973) Elements de neuro-anatomie fonctionnelle: cervelet, mesencephale, diencephale. Masson, Paris
[249] Laine FJ, Underhill T (2002) Imaging of the lower cranial nerves. Magn Reson Imaging Clin N Am 10(3): 433-49
[250] Lang J (1985) Anatomy of the brainstem and the lower cranial nerves, vessels, and surrounding structures. Am J Otol Suppl: 1-19
[251] Lang J (1981) Klinische Anatomie des Kopfes. Neurokranium, Orbita, kraniozervikaler Übergang. Springer, Berlin, Heidelberg New York
[251a] Lang J (1982) Anatomy, length and blood vessel relations of "central" and "peripheral" paths of intracisternal cranial nerves. Zentralbl Neurochir. 43:217-258
[252] Langhorst P, Lambertz M, Schulz G (1981) Central control and interactions affecting sympathetic and parasympathetic activity. J Autonom Nerv Sys 4: 149-163
[253] Larsell O (1934) Morphogenesis and evolution of the cerebellum. Arch Neurol 31: 373-395
[254] Larsell O (1970) The comparative anatomy and histology of the cerebellum from monotremes through apes. University of Minnesota Press, Minneapolis, p 267
[255] Larsell O, Jansen J (1972) The comparative anatomy and histology of the cerebellum. III. The human cerebellum, cerebellar connections, and the cerebellar cortex. University of Minnesota Press, Minneapolis, p 268
[256] Lasjaunias P, Vallee B, Person H, Brugge KT, Chiu M (1985) The lateral spinal artery of the upper cervical spinal cord. J Neurosurg 63: 235-241
[257] Lazorthes G (1961) Vascularisation et circulation cerebrales. Masson et Cie, Paris
[258] Lazorthes G, Alegre de la Soujeole CH, Espagno J (1949) Note sur les vaisseaux de l'angle ponto-cerebelleux. Variations et rapports avec la racine du trijumeau. C R Ass Anat 57: 437-438
[259] Lazorthes G, Gouaze A, Salamon G (1976) Vascularisation et circulation de l'encephale. Masson, Paris
[260] Leblanc A (2004) Encephalo-Peripheral Nervous System. Vascularisation, Anatomy, Imaging. Springer, Berlin
[261] Le Gros Clark WE (1940) The nervous and vascular relations of the pineal gland. J Anat (Lond) 74: 471-492
[262] Leichnetz GR, Smith DJ, Spencer RF (1984) Cortical projections to the paramedian tegmental and basilar pons in the monkey. J Comp Neurol 228: 388-408
[263] Leiner HC, Leiner AL, Dow RS (1991) The human cerebrocerebellar system: its computing, cognitive, and language skills. Behv Brain Res 44: 113-128
[264] Lierse W, Hortsmann E (1965) Quantitative anatomy of cerebral vascular bed with especial emphasis on homogeneity and inhomogeneity in small parts of the gray and white matter. Acta Neurol Scand [Suppl] 14: 15-19
[265] Liliequist B (1959) The subarachnoid cisterns. An anatomic and roentgenologic study. Acta Radiol [Suppl 185]: 61-71
[266] Lister JR, Rhoton AL Jr, Matsuhima T, Peace DA (1982) Microsurgical anatomy of the posterior inferior cerebellar artery. Neurosurgery 10: 170-199
[267] Loewy AD, Saper CB, Baker RP (1979) Descending projections from the pontine micturition center. Brain Res 172: 533-538
[268] Lofgren FO (1958) Vertebral angiography in the diagnosis of tumours in the pineal region. Acta Radiol (Stockh) 50: 108-124
[269] Louilot A, Taghzouti K, Deminiere JM, Simon H, Le Moal M (1987) Dopamine and behavior: functional and theoretical considerations. In: Sandler M, Feuerstein C, Scatton B (eds) Neurotransmitters interactions. Raven, New York, pp 193-204
[270] Lowe AA (1984) Tongue movements – brainstem mechanisms and clinical postulates. Brain Behav Evol 25: 128-137
[271] Lufkin R, Flannigan BD, Bentson JR, Wilson GH, Rauschning W, Hanafee W (1986) Magnetic resonance imaging of the brains stem and cranial nerves. Surg Radiol Anat 8: 49-66
[272] Mahmood A, Dujovny M, Torche M, Dragovic L, Ausman JL (1991) Microvascular anatomy of the foramen caecum medullae oblongatae. J Neurosurg 75, 299-304
[273] Maillot C (1987) Encephale et moelle epiniere. Atlas d'anatomie macroscopique du systeme nerveux central. JF Bergmann, München
[274] Maillot C, Kortike JG (1970) Les origines du tronc spinal posterieur chez l'homme. CR Ass Anat 149: 837-847
[275] Mamata H, Mamata Y, Westin CF, Shenton ME, Kikinis R, Jolesz FA, Maier SE (2002) High-resolution line scan diffusion tensor MR imaging of white matter fiber tract anatomy. AJNR Am J Neuroradiol 23(1): 67-75
[276] Mangin JF, Poupon C, Cointepas Y (2002) A framework based on spin glass models for the inference of anatomical connectivity from diffusion-weighted MR data – a technical review. NMR in Biomedicine 15(7-8): 481-492
[277] Margolis MT, Newton TH (1974) The posterior inferior cerebellar artery. In: Newton TH, Potts SC (eds) Radiology of the skull and brain. Angiography. Mosby, St Louis, pp 1710-1774
[278] Marinkovic SV, Gibo H (1993) The surgical anatomy of the perforating branches of the basilar artery. Neurosurgery 33(1): 80-87
[279] Marinkovic S, Milisavljevic M, Kovacevic M (1986) Interpeduncular perforating branches of the posterior cerebral artery. Microsurgical anatomy of their extracerebral and intracerebral segments. Surg. Neurol 26, 349-359
[280] Marr D (1969) A theory of cerebellar cortex. J Physiol (Lond) 202: 437-470
[281] Massion J (1988) Red nucleus: past and future. Behav Brain Res 28: 1-8

[282] Matsushima T, Rhoton AL, De Oliveira E, Peace D (1983) Microsurgical anatomy of the veins of the posterior fossa. J Neurosurg 59: 63-105

[282a] Middleton FA, Strick PL. (1998) The cerebellum: an overview. Trends Neurosci 21: 367-369

[283] Maurer J, Mitrovic T, Knollmann FD, Ludtke E, Requardt H (1996) In vitro delineation of human brain-stem anatomy using a small resonator: correlation with macroscopic and histological findings. Neuroradiology 38(3): 217-20

[284] McKinley MJ, McAllen RM, Mendelsohn FAO, Allen AM, Chai SY, Oldfiend BJ (1990) Circumventricular organs: neuroendocrine interfaces between the brain and the hemal milieu. In: Frontiers in Neuroendocrinology 11(2): 91-127. Raven, New York

[285] McKinley MJ, Oldfield BJ (1990) Circumventricular organs. In: Paxinos G. (ed) The human nervous system. Academic Press, San Diego, pp 415–438

[286] McRitchie DA, Tork I (1993) The internal organization of the human solitary nucleus. Brain Res Bull 31: 171-193

[287] Mesulam MM, Geula C, Bothwell MA, Hersh LB (1989) Human reticular formation: cholinergic neurons of the pedunculopontine and laterodorsal tegmental nuclei and some cytochemical comparisons to forebrain cholinergic neurons. J Comp Neurol 281: 611-633

[288] Mettler FA, Cooper I, Liss H, Carpenter M, Noback CH (1954) Patterns of vascular failure in the central nervous system. J Neuropath Exp Neurol 13: 528-539

[289] Meyer P (1958) A propos de l'angle lateral du quatrieme ventricule. C R Ass Anat 99: 495-99

[289a] Middleton FA and Strick PL (1998) The cerebellum: an overview. Trends Neurosci 21: 367-369

[290] Milisavljevic M, Marinkovic S, Lolic-Draganic V, Kovacevic M (1986) Oculomotor, trochlear, and abducens nerves penetrated by cerebral vessels. Microanatomy and possible clinical significance. Arch Neurol 43: 58-61

[291] Miller MJ, Mark LP, Ho KC, Haughton VM (1997) Anatomic relationship of the oculomotor nuclear complex and medial longitudinal fasciculus in the midbrain. AJNR Am J Neuroradiol 18(1): 111-3

[292] Miller MJ, Mark LP, Ho KC, Haughton V (1996) MR appearance of the internal architecture of Ammon's horn. AJNR Am J Neuroradiol 17: 23-26

[293] Miller MJ, Mark LP, Ho KC, Haughton VM, Estkowski L, Wong E (1994) Imaging white matter tracts and nuclei of the hypothalamus: an MR-anatomic comparative study. AJNR Am J Neuroradiol 15: 117–121

[294] Miller RA, Burack E (1982) Atlas of the central nervous system in man, 3rd edn. Williams & Wilkins, Baltimore

[295] Mitchell GAG, Warwick R (1955) The dorsal vagal nucleus. Acta Anat (Basel) 25: 371-395

[296] Mori S, Barker PB (1999) Diffusion magnetic resonance imaging: Its principle and applications. Anat Record 257(3): 102–109

[297] Mori S, Frederiksen K, van Zijl PC, Stieltjes B, Kraut MA, Solaiyappan M, Pomper MG (2002) Brain white matter anatomy of tumor patients evaluated with diffusion tensor imaging. Ann Neurol 51(3): 377–380

[298] Mori S, Kaufmann WE, Davatzikos C, Stieltjes B, Amodei L, Fredericksen K, Pearlson GD, Melhem ER, Solaiyappan M, Raymond GV, Moser HW, van Zijl PCM (2002) Imaging cortical association tracts in the human brain using diffusion-tensor-based axonal tracking. Magn Reson Med 47(2): 215-223

[299] Mori S, van Zijl PC (2002) Fiber tracking: principles and strategies – a technical review. NMR Biomed 15(7-8): 468-480

[300] Morrison SF, Callaway J, Milner TA, Reis OJ (1991) Rostral ventrolateral medulla: a source of the glutamatergic innervation of the sympathetic intermediolateral nucleus. Brain Res 562: 126-135

[301] Mukherjee P, McKinstry RC (2006) Diffusion tensor imaging and tractography of human brain development. Clin N Am 16(1): 19-43, vii

[302] Mukherjee P, Miller JH, Shimony JS, Conturo TE, Lee BCP, Almli CR, McKinstry RC (2001) Normal Brain Maturation during Childhood: Developmental Trends Characterized with Diffusion-Tensor MR Imaging. Radiology 221(2): 349-358

[303] Mukherjee P, Miller JH, Shimony JS, Philip JV, Nehra D, Snyder AZ, Conturo TE, Neil JJ, McKinstry RC (2002) Diffusion-Tensor MR Imaging of Gray and White Matter Development during Normal Human Brain Maturation. AJNR Am J Neuroradiol 23(9): 1445-1456

[304] Muller F, O'Rahilly R (1990) The human rhombencephalon at the end of the embryonic period proper. Am J Anat 189: 127-145

[305] Mustari MJ, Fuchs AF, Wallman J (1986) The physiological response properties of single pontine units related to smooth pursuit in the trained monkey. In: Keller EL, Zee DS (eds) Adaptatiye processes in visual and oculomotor systems. Pergamon, Oxford, pp 253-260

[306] Nagae-Poetscher LM, Jiang H, Wakana S, Golay X, van Zijl PC, Mori S (2004) High-resolution diffusion tensor imaging of the brain stem at 3 T. AJNR Am J Neuroradiol 25(8): 1325-30

[307] Naidich TP, Kricheff, II, George AE, Lin JP (1976) The normal anterior inferior cerebellar artery: anatomic-radiological correlation with emphasis on the lateral projection. Radiology 119: 355-373

[308] Naidich TP, Kricheff, II, George AE, Lin JP (1976) The anterior inferior cerebellar artery in mass lesions: preliminary findings with emphasis on the lateral projection. Radiology 119: 375-383

[309] Naidich TP, Daniels DL, Pech P, Haughton VM, Williams A, Pojunas K (1986) Anterior commissure; anatomic-MR correlation and use as a landmark in three orthogonal planes. Radiology 158: 421-429

[310] Naidich TP, Daniels DL, Haughton VM, Williams A, Pojunas K, Palacios E (1987) The hippocampal formation and related structures of the limbic lobe; anatomic-MR correlation. Part I: Surface features and coronal sections. Radiology 162: 747-754

[311] Naidich TP, Daniels DL, Haughton VM, Williams A, Pojunas K, Palacios E (1987) The hippocampal formation and related structures of the limbic lobe; anatomic-MR correlation. Part II: Sagittal sections. Radiology 162: 755-761

[312] Naidich TP, Daniels DL, Haughton VM, Williams A, Pojunas K, Palacios E (1988) The hippocampal formation and related structures of the limbic lobe; anatomic-magnetic resonance correlation. In: Gouze A, Salamon G (eds): Brians Anatomy and Magnetic Resonance Imaging. Springer, Berlin, pp 32-64

[313] Naidich TP, Hof PR, Gannon PJ, Yousry TA, Yousry I (2001) Anatomic substrates of language emphasizing speech. In: Neuroimaging Clinics of North America. Anatomic basis of functional MR imaging. W.B. Saunders, Philadelphia, pp 305-341

[314] Namin P (1955) L'angiographie vertebrale. Doin, Paris

[315] Nathan PW, Smith MC, Cook AW (1986) Sensory effects in man of lesions of the posterior columns and of some other afferent pathways. Brain 109: 1003-1041

[316] Neil J, Shiran S, McKinstry R, Schefft G, Snyder A, Almli C, Akbudak E, Aronovitz J, Miller J, Lee B, Conturo T (1998) Normal brain in human newborns: apparent diffusion coefficient and diffusion anisotropy measured by using diffusion tensor MR imaging. Radiology 209(1): 57-66

[317] Netsch T, van Muiswinkel A (2004) Quantitative Evaluation of Image-based Distortion Correction in Diffusion Tensor Imaging. IEEE Trans Med Imaging 23(7): 789-798

[318] Newton TH, Potts DG (1974) Radiology of the skull and brain. Angiography, vol II, book 2. Mosby, St. Louis

[319] Newton TH, Potts DG (1974) Radiology of the skull and brain. Angiography, vol II, book 3. Mosby, St. Louis

[320] Niemann K, van den Boom R, Haeselbarth K, Afshar F (1999) A brainstem stereotactic atlas in a three-dimensional magnetic resonance imaging navigation system: first experiences with atlas-to-patient registration. J Neurosurg 90(5): 891-901

[321] Nieuwenhuys R (1985) Chemoarchitecture of the brain. Springer, Berlin Heidelberg New York Tokyo

[322] Nieuwenhuys R, Voogd J, Van Huijzen C (1988) The human central nervous system. A synopsis and atlas, 3rd rev edn. Springer, Berlin Heidelberg New York Tokyo

[323] Noda H, Fujikado T (1987) Topography of the oculomotor area of the cerebellar vermis in macaques as determined by microstimulation. J Neurophysiol 58: 359-378

[324] Nolte J (1988) The human brain. An introduction to its functional anatomy, 2nd edn. Mosby, St Louis

[325] Novak P, Novak V, Kangarlu A, Abduljalil AM, Chakeres DW, Robitaille PM (2001) High resolution MRI of the brainstem at 8 T. J Comput Assist Tomogr 25(2): 242-6

[326] Nudo RJ, Masterton RB (1989) Descending pathways to the spinal cord: II. Quantitative study of the tectospinal tract in 23 mammals. J Comp Neurol, 286: 96-119

[327] Olszewski J, Baxter D (1954) Cytoarchitecture of the human brain stem. Karger, Basel

[328] Olszewski J, Baxter D (1982) Cytoarchitecture of the human brain stem, Karger, Basel 2nd edition

[329] Oliver DL, Shneiderman A (1989) An EM study of the dorsal nucleus of the lateral lemniscus: inhibitory, commissural, synaptic connections between ascending auditory pathways. J Neurosci 9: 967-982

[330] Ono M, Ono M, Rhoton AL, Barry M (1984) Microsurgical anatomy of the region of the tentorial incisura. J Neurosurg 60: 365-399

[331] Palay SL, Chan-Palay V (1974) Cerebellar cortex. Cytology and organization. Springer, Berlin Heidelberg New York

[332] Parent A, Carpenter MB (1995) Human neuroanatomy. Williams & Wilkins, Baltimore

[333] Pasik T, Pasik P (1988) Vision, extrageniculostriate. In: Held R (ed) Sensory systems I, vision and visual systems. Birkhäuser, Boston, pp 67–68

[334] Paturet G (1964) Traite d'anatomie humaine, vol IV: systeme nerveux. Masson, Pars

[335] Paxinos G (1990) The human nervous system. Academic Press, San Diego

[336] Pearson AA (1943) The trochlear nerve in human fetuses. J Comp Neurol 78(1): 29–43

[337] Pedroza A, Dujovny M, Ausman JI, Diaz FG, Cabezudo Artero J, Berman SK, Mirchandani HG, Umansky F (1986) Microvascular anatomy of the interpeduncular fossa. J Neurosurg 64: 484-493

[338] Pfeifer RA (1928) Die Angioarchitektonik der Grosshirnrinde. Springer, Berlin

[339] Pfeifer RA (1930) Grundlegende Untersuchugen für die Angioarchitektonik des menschlichen Gehirns. Springer, Berlin

[340] Pierrot-Deseilligny CH (1985) Circuits oculomoteurs centraux. Rev Neurol (Paris) 141: 349–370

[341] Porrino LF, Goldman-Rakic PS (1982) Brainstem innervation of prefrontal and anterior cingulate cortex in the rhesus monkey revealed by retrograde transport of HRP. J Comp Neurol 205: 63-76

[342] Press GA, Murakami J, Courchesne E (1989) The cerebellum in sagittal plane – anatomic-MR correlation: 2. The cerebellar hemispheres. AJR Am J Roentgenol 153: 837-846

[343] Press GA, Murakami JW, Courchesne E, Grafe M, Hesselink JR (1990) The cerebellum: 3. Anatomic-MR correlation in the coronal plane. Am J Neuroradiol 11: 41-50

[344] Pritchard TC (1991) The primate gustatory system. In: Getchell TV, Doty RL, Bartoshuk LM, Snow JB Jr (eds) Smell and taste in health and disease. Raven Press, New York, pp 109-125

[345] Pruessmann KP, Weiger M, Scheidegger MB, Boesiger P (1999) SENSE: sensitivity encoding for fast MRI. Magn Reson Med 42(5): 952-962

[346] Rakic P (1965) Mesocoelic recess in the human brain. Neurology 15, 709-715

[347] Rapoport M, van Reekum R, Mayberg H (2000) The role of the cerebellum in cognition and behavior: A selective review. J Neuropsychiatry Clin Neurosci 12(2): 193-198

[348] Rasmussen AT (1951) Atlas of cross section anatomy of the brain. Blakiston, Philadelphia

[349] Rasmussen AT (1960) The principal nervous pathways, 4th edn. Macmillan, New York

[350] Rauber A, Kopsch F (1940) Lehrbuch und Atlas der Anatomie des Menschen, vol III, Nervensystem, Sinnesorgane, 15. Aufl. Thieme, Leipzig

[351] Raz N, Torres IJ, Spencer WD, White K, Acker JD (1992) Age-related regional differences in cerebellar vermis observed in vivo. Arch Neurol 49:412-416

[352] Raz N, Dupuis JH, Briggs SD, McGavran C, Acker JD (1998) Differential effects of age and sex on the cerebellar hemisphere and the vermis: a prospective MR study. AJNR Am J Neuroradiol 19:65-71

[353] Raz N, Gunning-Dixon F, Head D, Williamson A, Acker JD (2001) Age and sex differences in the cerebellum and the ventral pons: a prospective MR study of healthy adults. AJNR Am J Neuroradiol 22:1161-1167

[354] Reich DS, Smith SA, Jones CK, Zackowski KM, van Zijl PC, Calabresi PA, Mori S (2006) Quantitative characterization of the corticospinal tract at 3T. AJNR Am J Neuroradiol 27(10): 2168-2178

[355] Reichenbach JR, Venkatesan R, Schillinger DJ, Kido DK, Haacke EM (1997) Small vessels in the human brian: MR venograph with dexyhemoglobin as an intrisnics contrast agent. Radiology 204: 272-277

[356] Reiter RJ (1981) The mammalian pineal glad structure and function. Am J Anat 162, 287-313

[357] Retzius G (1896) Das Menschenhirn. Nordstedt & Soner, Stockholm

[358] Riley HA (1960) An atlas of the basal ganglia, brain stem and spinal cord, based on myelin stained material. Hafner, New York

[359] Robert O, Miachon S, Kopp N, Denoroy L, Tommasi M, Rollet D, Pujol JF (1984) Immunohistochemical study of the catecholaminergic systems in the lower brain stem of the human infant. Human Neurobiol 3: 229-234

[360] Roberts M, Hanaway J (1970) Atlas of the human brain in section. Lea & Febiger, Philadelphia

[361] Rodieck RW (1979) Visual pathways. Annu Rev Neurosci 2: 193-225

[362] Rosenbaum AE, Stein RL (1974) Deep supratentorial veins. II. Abnormal supratentorial deep cerebral veins. In: Newton TH, Potts DG (eds) Radiology of the skull and brain, vol II, book3. Veins, pp 1999–2110. Mosby, St. Louis

[363] Rowbotham GF, Little E (1963) The candelabra arteries and the circulation of the cerebral cortex. Br J Surg 50: 694-697

[364] Ruggiero DA, Meeley MP, Anwar M, Reis DJ (1985) Newly identified ganaergic neurons in regions of the ventrolateral medulla which regulate blood pressure. Brain Res 339: 171-177

[365] Saade NE, Jabbur SJ (1985) Dorsal column influences, through the brainstem, on spinal nociceptive input. In: Rowe M, Willis WD (eds) Development, organization and processing in somatosensory pathways. AR Liss, New York, pp 367-373

[366] Sacco RL, Freddo L, Bello JA, Odel JG, Onesti ST, Mohr JP (1993) Wallenberg's lateral medullary syndrome. Clinical – magnetic resonance imaging correlations. Arch Neurol 50: 609-614

[367] Sadjadpour K, Brodal A (1968) The vestibular nuclei in man. A morphological study in the light of experimental findings in the cat. J Hirnforsch 10(4): 299-323

[368] Saeki N, Rhoton Jr (1977) Microsurgical anatomy of the upper basilar artery and the posterior circle of Willis. J Neurosurg 46: 563-578

[369] Salamon G (1973) Atlas de la vascularisation arterielle du cerveau chez l'homme, 2nd edn. Sandoz, Paris

[370] Salamon G, Huang YP (1976) Radiological anatomy of the brain. Springer, Berlin Heidelberg New York

[371] Salamon N, Sicotte N, Alger J, Shattuck D, Perlman S, Sinha U, Schultze-Haakh H, Salamon G (2005) Analysis of the brain-stem white-matter tracts with diffusion tensor imaging. Neuroradiology 47(12): 895–902

[372] Sartor K (1992) MR imaging of the skull and brain. A correlative text-atlas, Springer, Berlin Heidelberg New York Tokyo

[373] Sasaki M, Shibata E, Tohyama K (2006) Neuromelanin magnetic resonance imaging of locus ceruleus and substantia nigra in Parkinson's disease. Brain Imaging 17: 1215-121

[374] Saunders RL, Bell MA (1971) X-ray microscopy and histochemistry of the human cerebral blood vessels. J Neurosurg 35: 128-140

[375] Savoiardo M, Bracchi M, Passerini A, Visciani A (1987) The vascular territories in the cerebellum and brainstem: CT and MR study. Am J Neuroradiol 8: 199-209

[376] Schaefer GB, Thompson JN Jr., Bodensteiner JB, Gingold M, Wilson M, Wilson D (1991) Age-related changes in the relative growth of the posterior fossa. J Child Neurol 6: 15-19

[377] Schaltenbrand G, Bailey P (1959) Introduction to stereotaxis with an atlas of the human brain, vol I and vol II. Thieme, Stuttgart

[378] Schaltenbrand G, Wahren W (1977) Atlas for Stereotaxonomy of the Human Brain 2nd edn. Thieme, Stuttgart, pp 1-26, plate 50

[379] Scharrer E (1940) Arteries and veins in the mammalian brain. Anat Rec 78: 173-196

[380] Schenck JF, Zimmerman EA (2004) High-field magnetic resonance imaging of brain iron: birth of biomarker? NMR Biomed 17(7): 433-45

[381] Schiller PH (1987) Colliculus, superior. In: Held R (ed) Sensory systems I, vision and visual systems. Birkhäuser, Boston, p 9

[382] Schlesinger B (1976) The upper brainstem in the human, its nuclear configuration and vascular supply. Springer, Berlin Heidelberg New York

[382a] Schmahmann JD. (2004) Disorders of the cerebellum: ataxia, dysmetria of thought, and the cerebellar cognitive affective syndrome. J Neuropsychiatry Clin Neurosci 16: 367-378

[382b] Schmahmann JD, Caplan D. (2006) Scientific Commentaries. Cognition, emotion and the cerebellum. Brain 129: 290-292

[383] Schmahmann JD, Sherman JC (1998) The cerebellar cognitive affective syndrome. Brain 121: 561-579

[383a] Schmahmann JD, Weilburg JB, Sherman JC (2007) The neuropsychiatry of the cerebellum – insights from the clinic. Cerebellum 6: 254-267

[384] Schmidt RF (1978) Fundamentals of sensory physiology. Springer, Berlin Heidelberg New York

[385] Schupert C, Fuchs AF (1988) Development of conjugate human eye movements.Vision Res 28: 585-596

[386] Schwartz JC, Agid Y, Bouthenet ML, Javoy-Agid F, Llorens-Cortex C, Martres MP, Pollard H, Sales N, Taquet H (1986) Neurochemical investigations into the human area postrema. In: Davis CJ, Lake-Bakaar GV, Grahame-Smith DG (eds) Nausea and vomiting: mechanisms and treatment. Springer, Berlin Heidelberg New York Tokyo, pp 19-30

[387] Seeger W (1978) Atlas of topographical anatomy of the brain and surrounding structures. Springer, Wien New York

[388] Seeger W (1984) Microsurgery of cerebral veins. Springer, Wien New York

[389] Segers LS, Shannon R, Lindsey BG (1985) Interactions between rostral pontine and ventral medullary respiratory neurons. J Neurophysiol 54: 318-334

[390] Segraves MA, Goldberg ME, Deng SY, Bruce CJ. Ungerleider LG, Mishkin M (1987) The role of striate cortex in the guidance of eye movements in the monkey. Neurosci 7: 3040-3058

[391] Seifritz E, Di Salle F, Bilecen D, Radu E, Scheffler K (2001) Auditory System: Functional Magnetic Resonance Imaging. Neuroimaging Clinics of North America 11: 275-296

[392] Selim IUM (1976) Extraorganic vessels of the epiphysis of humans and placental mammals in their comparative anatomic aspect. Arch Anat Histol Embryol 71(8): 90-97

[393] Shah SA, Doraiwamy PM, Husain MM, Figiel GS, Boyko OB, McDonald WM, Ellinwood EH Jr., Krishman KR (1991) Assessment of posterior fossa structures with midsagittal MRI: the effect of age. Neurobiol Aging 12:371-374

[394] Shibata E, Sasaki M, Tohyama K (2007) Reduced signal of locus ceruleus in depression on quantitative neuromelanin magnetic resonance imaging. Brain Imaging (in press)

[395] Siegel G, Agranoff B, Albers RW, Molinoff P (1981) Basic neurochemistry, 4th edn. Raven, New York

[396] Singer M, Yakovlev PI (1964) The human brain in sagittal section. CC Thomas, Springfield

[396a] Skinner HA. (1931) Some histological features of the cranial nerves. Arch Neurol Psychiatry 25: 356-372

[397] Smith LH, DeMyer WE (2003) Anatomy of the brainstem. Review. Semin Pediatr Neurol 10(4): 235-40

[398] Sobotta J (1977) Atlas d'anatomie humaine, vol 4: Nomenclature anatomique francaise. Maloine, Paris

[399] Solnitzky O (1940) The angioarchitecture of the cerebral cortex of *Macacus Rhesus*. Anat Rec 76: 52-53

[400] Solsberg MD, Fournier D, Potts DG (1990) MR Imaging or the excised human brainstem: a correlative neuroanatomic study. Am J Neuroradiol 11: 1003-1013

[401] Solsberg MD, Lemaire C, Resch L, Potts DG (1990) High-resolution MR imaging of the cadaveric human spinal cord: normal anatomy. Am J Neuroradiol 11: 3-7

[402] Sourkes TL (1982) Transition elements and the nervous system. In: Pollitt E, Leibel RL (eds) Iron deficiency: brain biochemistry and behavior. Raven Press, New York, pp 1–29

[402a] Standring S, Editor-in-Chief. (2005) Gray's Anatomy. The Anatomical Basis of Clinical Practice, 39th edn. Elsevier Churchill Livingstone, Edinburgh New York

[403] Stein RL, Rosenbaum AE (1974) Normal deep cerebral venous system. In: Newton TH, Potts DG (eds) Radiology of skull and brain, vol II, book 3: veins. Mosby, St. Louis, pp 1904-4998

[404] Stephens RB, Stilwell DL (1969) Arteries and veins of the human brain. CC Thomas, Springfield

[405] Stern K (1938) Note on the nucleus ruber magnocellularis and its efferent pathway in man. Brain 61: 284-289

[406] Stevens RT, Hodge CJ, Apkarian AV *(1989)* Medial intralaminar, and lateral termination of lumbar spinothalamic tract neurons: a fluorescent double-label study. Somatosens Mot Res 6: 285- 308

[407] Stieltjes B, Kaufmann WE, van Zijl PC, Fredericksen K, Pearlson GD, Solaiyappan M, Mori S (2001) Diffusion tensor imaging and axonal tracking in the human brainstem. Neuroimage 14(3): 723-735

[408] Stopford JSH (1916) The arteries of the pons and medulla oblongata. Part I. J Anat Physiol 50: 131-163

[409] Stopford JSB (1916) The arteries of the pons and medulla oblongata. Part II. J Anat Physiol 50: 255-280

[410] Strominger MB, Mincy EJ, Strominger AI, Strominger NL (1986) Bilateral internuclear opthalmoplegia with absence of convergent eye movements. J Clin Neuroopthalmol 6: 57-65

[411] Sumi T (1972) Role of the pontine reticular formation in the neural organization of deglutition. Jpn J Physiol 22: 295-314

[412] Sun MK, Guyenet PG (1985) GABA-mediated baroceptor inhibition of reticulospinal neurons. Am J Physiol 249: R672-R6S0

[413] Swartz JD, Daniels DL, Harnsberger HR, Ulmer JL, Harvey S, Shaffer KA, Mark L (1996) Balance and equilibrium, II: The retrovestibular neural pathway. Review. AJNR Am J Neuroradiol 17(6): 1187-90

[414] Swartz JD, Daniels DL, Harnsberger HR, Ulmer JL, Shaffer KA, Mark LP (1996) Hearing, II: the retrocochlear auditory pathway. AJNR Am J Neuroradiol 17(8): 1479-81

[415] Syka J, Masterton RB (1988) Auditory pathway. Structure and function. Plenum Press, New York

[416] Symms M, Jager HR, Schmierer K, Yousry TA (2004). A review of structural magnetic resonance neuroimaging. Review. J Neurol Neurosurg Psychiatry 75(9): 1235-44

[417] Takahashi M (1977) Atlas of Carotid Angiography. Igaku Shoin Ltd, Tokyo

[418] Takahashi M (1974) Atlas of Vertebral Angiography. University Park Press, Baltimore
[419] Takahashi M (1974) The anterior inferior cerebellar artery. In: Newton TH, Potts SC (eds) Radiology of the skull and brain. Angiography. Mosby, St Louis, pp 1796-1808
[420] Talairach J, David M, Tournoux P, Corredor H, Kvasina T (1957) Atlas d'atomie stereotaxique des moyaux gris centraux. Masson & Cie, Paris
[421] Talairach J, Tournoux P (1988) Co-planar stereotaxic atlas of the human brain. Three-dimensional proportional system: an approach to cerebral imaging. Thieme Medical Publishers, New York
[422] Tamaki N, Fujiwarek, Matsumoto S, Takeda H (1973) Veins draining the pineal body. An anatomical and neuroradiological study of "pineal veins". J Neurosurg 39: 448-454
[423] Tamraz JC, Comair YG (2001) Atlas of Regional Anatomy of the Brain Using MRI with Functional Correlations. Springer, Berlin Heidelberg
[424] Tamraz JC, Comair YG (2006) Atlas of Regional Anatomy of the Brain Using MRI with Functional Correlations. Springer, Berlin Heidelberg
[425] Tamraz J, Saban R, Reperant J, Cabanis EA (1991) A new cephalic reference plane for use with magnetic resonance imaging: the chiasmato-commissural plane. Surg Radiol Anat 13: 197-201
[426] Tapp E (1979) The histology and pathology of the human pineal gland. Prog Brain Res 52: 481-499
[427] Tapp E, Huxley M (1972) The histological appearance of the human pineal glad from puberty to old age. J Pathol 108: 137-144
[427a] Tarlov IM (1937) Structure of the nerve root. I. Nature of the junction between the central and the peripheral nervous system. Arch Neurol Psychiatry 37:555-583
[427b] Tarlov IM (1937) Structure of the nerve root. II. Differentiation of sensory from motor roots; observations on identification of function in roots of mixed cranial nerves. Arch Neurol Psychiatry 37:1338-1355
[428] Tatu L, Moulin T, Bogousslavsky J, Duvernoy H (1996) Arterial territories of human brain: brainstem and cerebellum. Rev Neurology 47(5): 1125-35
[429] Ten Donkelaar HJ, Bangma GC, Barbas-Henry HA, de Boer-van Huizen R, Wolters JG (1987) Review. The brain stem in a lizard, Varanus exanthematicus. Adv Anat Embryol Cell Biol 107: 1-168
[430] Testut L, Latarjet A (1948) Traite d'anatomie humaine, vol 2: angiologie – systeme nerveux central, 9th edn. Doin, Paris
[430a] Thach WT (1998) What is the role of the cerebellum in motor learning and cognition? Trends Cognit Sci 2: 331-337
[431] Thickman DL, Kundel HL, Wolf G (1983) Nuclear magnetic resonance characteristics of fresh and fixed tissue: the effect of elapsed time. Radiology 148: 183–185
[432] Thier P, Koehler W, Buettner UW (1988) Neuronal activity in the dorsolateral pontine nucleus of the alert monkey modulated by visual stimuli and eye movements. Exp Brain Res 70: 496-512
[433] Thomas DL, De Vita E, Roberts S, Turner R, Yousry TA, Ordidge RJ (2004) High-resolution fast spin echo imaging of the human brain at 4.7 T: implementation and sequence characteristics. Magn Reson Med Jun; 51(6): 1254-64
[434] Tomasch J, Ebenessajjade D (1961) The human nucleus ambiguus. A quantitative study. Anat Rec 141: 247-252
[435] Torche M, Mahmood A, Araujo R, Dujovny M, Dragovic L, Ausman JI (1992) Microsurgical anatomy of the lower basilar artery. Neurol Res 14: 259-262
[436] Tournade A, Maillot CI, Koritke JG (1972) Les veins superficielles du tronc cerebral chez l'homme. Essai de systematistion. Arch Hist Embr Norm et Exp 55: 233-281
[437] Toyoda K, Imamura T, Saku Y, Oita J, Ibayashi S, Minematsu K, Yamaguchi AT, Fujishima M (1996) Medullary infarction. Analyses of eleven patients. Neurology 47: 1141-1147
[438] Travers JB, Travers SP, Norgren R (1987) Gustatory neural processing in the hindbrain. Annu Rev Neurosci 10: 595-632
[439] Tusa RJ, Ungerleider LG (1988) Fiber pathways of cortical areas mediating smooth pursuit eye movements in monkeys. Ann Neurol 23: 174-183
[440] Ulchino A, Imada H, Ohno M (1990) MR Imaging of wallerian degeneration in the human brain stem after ictus. Neuroradiology 32: 191-195
[441] Van Buren JM, Borke RC (1972) Variations and connections of the human thalamus. 1 - The nuclei and cerebral connections of the human thalamus. Springer, Berlin Heidelberg New York
[442] Van Buren JM, Borke RC (1972) Variations and connections of the human thalamus. 2 - Variations of the human diencephalon. Springer, Berlin Heidelberg New York
[443] Van Domburg PHMF, Ten Donkelaar HJ (1991) The human substantia nigra and ventral tegmental area. Adv Anat Embryol Cell Biol: 121
[444] Ventre J (1985) Cortical control of oculomotor functions. II. Vestibulo-ocular reflex and visual vestibular interaction. Behav Brain Res 17: 221-23
[445] Villiger E, Ludwig E (1946) Gehirn und Rückenmark. Schwabe, Basel
[446] Vinas FC, Lopez F, Dujovny M (1995) Microsurgical anatomy of the posterior choroidal arteries. Neurol Res 17: 334-343
[447] Virta A, Barnett A, Pierpaoli C (1999) Visualizing and characterizing white matter fiber structure and architecture in the human pyramidal tract using diffusion tensor MRI. Magn Reson Imaging 17(8): 1121-1133
[448] Vollrath L (1981) The pineal organ. Springer, Berlin Heidelberg New York
[449] Vollrath L (1984) Functional anatomy of the human pineal gland. In: Reiter RJ (ed) The pineal gland. Raven, New York, pp 285-322
[450] Vuillemier P, Bogousslavsky J, Regli F (1995) Infarction of the lower brainstem. Clinical, aetiological and MRI-topographical correlations. Brain 118: 1013-1025

[451] Wackenheim A, Braun JP (1970) Angiography of the mesencephalon. Springer, Berlin Heidelberg, New York
[452] Wackenheim A, Braun JP (1978) The veins of the posterior fossa. Normal and pathologic findings. Springer, Berlin Heidelberg New York
[453] Wakana S, Jiang H, Nagae-Poetscher LM, van Zijl PC, Mori S (2004) Fiber tract-based atlas of human white matter anatomy. Radiology 230(1): 77-87
[454] Warwick R (1953) Representation of the extraocular muscles in the oculomotor nuclei of the monkey. J Comp Neurol 98: 449-495
[455] Warwick R, Williams PL (1973) Gray's anatomy, 35th edn. Longman, Edinburgh
[456] Watt JC, McKillop AN (1935) Relation of arteries to roots of nerves in posterior cranial fossa in man. Arch Surg. (Chic) 30: 336-345
[457] Weber JT (1985) Pretectal complex and accessory optic system of primates. Brain Behav Evol 26: 117-140
[458] Welker WI (1990) The significance of foliation and fissuration of cerebellar cortex. The cerebellar folium as a fundamental unit of sensorimotor integration. Arch Ital Biol 128: 87-109
[459] Wheeler-Kingshott CAM, Hickman SJ, Parker GJM, Ciccarelli O, Symms MR, Miller DH, Barker GJ (2002) Investigating Cervical Spinal Cord Structure Using Axial Diffusion Tensor Imaging. NeuroImage 16(1): 93-102
[460] Willis WD (1985) Pain pathways in the primate. Contemporary sensory neurobiology. Prog Clin Biol Res 176: 117-133
[461] Willis WD (1985) Nociceptive pathways: anatomy and physiology of nociceptive ascending pathways. Philos Trans R Soc Lond [Biol] 308: 253-268
[462] Willis WD (1985) Central nervous system mechanisms for pain modulation. Appl Neurophysiol 48: 153-165
[463] Willis WD (1985) Nociceptive transmission in the primate spinal cord. In: Rowe M, Willis WD (eds) Development, organization, and processing in somatosensory pathways. AR Liss, New York, pp 333-345
[464] Willis WD (1986) Visceral inputs to sensory pathways in the spinal cord. Prog Brain Res 67: 207-225
[465] Willis WD (1986) Ascending somatosensory systems. In: Yaksh TL (ed) Spinal afferent processing. Plenum Press, New York, pp 243–274
[466] Willner P, Scheel-Kruger (1991) The mesolimbic dopamine system: from motivation to action. Wiley, Chichester/New York
[467] Wilson-Pauwels L, Akesson EJ, Stewart PA. (1988) Cranial Nerves. Anatomy and Clinical Comments. B. C. Decker, Toronto Philadelphia
[468] Wolf BS, Huang YP (1963) The insula and deep middle cerebral venous drainage system: normal anatomy and angiography. Am J Roentgenol. Radium Ther Nucl Med 90: 472–489
[469] Wolf BS, Huang YP, Newman CM (1963a) The lateral anastomotic mesencephalic vein and other variations in drainage of the basal cerebral vein. Am J Roentgenol Radium Ther Nucl Med 89: 411-422
[470] Wolf BS, Huang YP, Newman CM (1963b) The superficial sylvian venous drainage system. Am J Roentgenol Radium Ther Nucl Med 89: 398-410
[471] Wolf BS, Huang YP (1964) The subependymal veins of the lateral ventricles. Am J Roentgenol. Radium Ther Nucl Med 91: 406-426
[472] Woff HG (1938) The cerebral blood vessels – anatomical principles. In: Stanley C, Angus MF, Penefield W and Riley HA (eds) The circulation of the brain and spinal cord. Res Publ Ass Nerv Ment Dis 18: 29-68
[473] Yamamoto I, Kageyama N (1980) Microsurgical anatomy of the pineal region. J Neurosurg 53: 205-221
[474] Yasargil MG (1984) Microneurosurgery, vol I, microsurgical anatomy of the basal cisterns and vessels of the brain, diagnostic studies, general operative techniques and pathological considerations of the intracranial aneurysms. Thieme, Stuttgart
[475] Yasargil MG (1987) Microneurosurgery, vol III A: AVM of the brain, history, embryology, pathological considerations, hemodynamics, diagnostic studies, microsurgical anatomy. Thieme, Stuttgart
[476] Yasargil MG (1994) Microneurosurgery, vol IV A: CNS tumors: surgical anatomy, neuropathology, neuroradiology, neurophysiology, clinical consideration, operability, treatment options. Thieme, Stuttgart
[477] Young RF, Chambi VI (1987) Pain relief by electrical stimulation of the periaqueductal and periventricular gray matter. J Neurosurg 66: 364-371
[478] Yousry I, Camelio S, Wiesmann M, Schmid UD, Moriggl B, Bruckmann H, Yousry TA (1999) Detailed magnetic resonance imaging anatomy of the cisternal segment of the abducent nerve: Dorello's canal and neurovascular relationships and landmarks. J Neurosurg 91(2): 276-83
[479] Yousry I, Dieterich M, Naidich TP, Schmidt UD, Yousry TA (2002) Superior oblique myokemia: magnetic resonance imaging support for the neurovascular compression hypothesis. Ann Neurol 51: 361-8
[480] Yousry I, Moriggl B, Dieterich M, Naidich TP, Schmid UD, Yousry TA (2002) MR anatomy of the proximal cisternal segment of the trochlear nerve: neurovascular relationships and landmarks. Radiology 223(1): 31-8
[481] Yousry I, Moriggl B, Schmid UD, Wiesman M, Fesl G, Bruckmann H, Naidich TP, Yousry TA (2002) Detailed anatomy of the intracranial segment of the hypoglossal nerve: neurovascular relationships and landmarks on magnetic resonance imaging sequences. J Neurosurg 96(6): 1113-22
[482] Yousry I, Moriggl B, Holtmannspoetter M, Schmid UD, Naidich TP, Yousry TA (2004) Detailed anatomy of the motor and sensory roots of the trigeminal nerve and their neurovascular relationships: a magnetic resonance imaging study. J Neurosurg 101(3): 427-34
[483] Yousry I, Camelio S, Schmid UD, Horsfield MA, Wiesmann M, Bruckmann H, Yousry TA (2000) Visualization of cranial nerves I-XII: value of 3D CISS and T2-weighted FSE sequences. Eur Radiol 10(7): 1061-67

[484] Yousry I, Moriggl B, Schmid UD, Naidich TP, Yousry TA (2005) Trigeminal ganglion and its divisions: detailed anatomy MR imaging with contrast-enhanced 3D constructive interference in the steady state sequences. AJNR Am J Neuroradiol 26: 1128-1135

[485] Zimmermann M (1985) Descending control of somatosensory transmission in the spinal dorsal horn of the cat. In: Rowe M, Willis WD (eds) Development, organization and processing in somatosensory pathways. AR Liss, New York, pp 355-365

[486] Zweig RM, Jankel VVR, Hedreen JC, Mayeux R, Price DL (1989) The pedunculopontine nucleus in Parkinson's disease. Ann Neurol 26: 41-46

[490] Borges A, Casselman J. (2007) Imaging the cranial nerves: Part I: Methodology, infectious and inflammatory, traumatic and congenital lesions. DOI 10.1007/s00330-006-0575-9

[491] Borges A, Casselman J. (2007) Imaging the cranial nerves: part II: primary and secondary neoplastic conditions and neurovascular conflicts. DOI 10.1007/s00330-006-0572-z

[492] Middleton FA and Strick PL (1998) The cerebellum: an overview. Trends Neurosci 21: 367-369

[493] Schmahmann JD (2004) Disorders of the cerebellum: ataxia, dysmetria of thought, and the cerebellar cognitive affective syndrome. J Neuropsychiatry Clin Neurosci 16: 367-378

[494] Schmahmann JD, Caplan D (2006) Scientific Commentaries. Cognition, emotion and the cerebellum. Brain 129: 290-292

[495] Schmahmann JD, Sherman JC (1998) The cerebellar cognitive affective syndrome. Brain 121: 561-579

[496] Schmahmann JD, Weilburg JB, Sherman JC (2006) The neuropsychiatry of the cerebellum – insights from the clinic. Cerebellum 6: 254-267.

[497] Thach WT (1998) What is the role of the cerebellum in motor learning and cognition? Trends Cogn Sci 2: 331-337.

Published abstracts:

A1 Delman BN, Fatterpekar GM, Naidich TP, Itskovich VV, Aguinaldo JG, Tang CY, Fayad ZA, Hof PR, Drayer BP (2002) High Resolution MR Imaging of Brainstem Nuclei at 9.4 T. ASNR Symposium and 40th Annual Meeting, Vancouver, May

A2 Fatterpekar GM, Delman BN, Aguinaldo JG, Itskovich VV, Hof PR, Fayad ZA, Drayer BP, Naidich TP (2002) The Human Spinal Cord: MR Imaging of Excised Specimens at 9.4 T. ASNR Symposium and 40th Annual Meeting, Vancouver, May

A3 Choi PS, Naidich TP, Delman BN, Wolfe DE, Aguinaldo JG, Itskovich VV, Fayad ZA, Hof PR (2003) MR Microscopy of the Medial and Lateral Geniculate Bodies at 9.4T. ASNR Symposium and 41st Annual Meeting, Washington, May

A4 Delman BN, Naidich TP, Fatterpekar GM, Gultekin SH, Itskovich VV, Aguinaldo JG, Fayad ZA, Hof PR (2003) MR Microscopy of Intrinsic Brainstem Vasculature at 9.4 T. ASNR Symposium and 41st Annual Meeting, Washington, May

A5 Naidich TP, Tai AW, Delman BN, Delgado JE, Aguinaldo JG, Perl DP, Wolfe DE, Hof PR, Drayer BP (2004) Nuclei and Tracts of the Human Medulla: MR Microscopy at 9.4 T. ASNR Symposium and 42nd Annual Meeting, Seattle, June

A6 Naidich TP, Delgado JE, Delman BN, Tai AW, Aguinaldo JG, Gultekin SH, Hof PR, Drayer BP (2004) Nuclei and Tracts of the Human Midbrain: MR Microscopy at 9.4
T. ASNR Symposium and 42nd Annual Meeting, Seattle, June

A7 Naidich TP, Delman BN, Byne W, Fatterpekar GM, Hof PR, Tang CY (2007) Internal Architecture of the Thalamus: MR Microscopy of Formalin-fixed Human Cadaver Specimens at 9.4 T ASNR Symposium and 45th Annual Meeting, Chicago, June 11, Paper 30

A8 Naidich TP, Delman BN, Fatterpekar GM, Hof PR, Tang CY (2007) Intrapontine Segments of Cranial Nerves V, VI, VII and VIII. ASNR Symposium and 45th Annual Meeting, Chicago, June 11, 2007 Paper 31

A9 Casselman JW. (2006) The upper and lower cranial nerves. Erasmus course on magnetic resonance imaging. Syllabus, Vienna, Austria 13–17 February

International nomenclature

adhesio interthalamica (interthalamic adhesion)
ala cisternae ambientis (wing of ambient cistern)
ala lobuli centralis (ala of central lobule)
amygdala (amygdala)
ansa lenticularis (ansa lenticularis)
apertura lateralis ventriculi quarti (lateral aperture of fourth ventricle) (foramen of Luschka)
apertura mediana ventriculi quarti (median aperture of the fourth ventricle)
aqueductus cerebri (cerebral aqueduct)
area
  postrema (area postrema)
  pretectalis (pretectal area)
  tegmentalis (field H of Forel)
  tegmentalis ventralis (ventral tegmental area)
  vestibularis (vestibular area)
arteria
  basilaris (basilar artery)
  carotis interna (international carotid artery)
  cerebelli inferior anterior (anterior inferior cerebellar artery)
  cerebelli inferior posterior (posterior inferior cerebellar artery)
  cerebelli superior (superior cerebellar artery)
  ramus lateralis (lateral branch of the superior cerebellar artery)
  ramus medialis (medial branch of the superior cerebellar artery
  cerebri media (middle cerebral artery)
  cerebri posterior (posterior cerebral artery)
  choroidea anterior (anterior choroidal artery)
  choroidea posterior medialis (posteromedial choroidal artery)
  collicularis (collicular artery)
  communicans posterior (posterior communicating artery)
  spinalis anterior (anterior spinal artery)
  spinalis posterior (posterior spinal artery)
  vertebralis (vertebral artery)
articulatio temporo-mandibularis (temporomandi bular joint)
atlas
arcus anterius atlantis (anterior arch of atlas)
arcus posterius atlantis (posterior arch of atlas)
  massa lateralis (lateral mass of atlas)
atrium (atrium)
amiculum olivae (amiculum of the inferior olive)
auris
  interna (internal ear)
  media (middle ear)
axis

basis pedunculi (basis pedunculi)
brachium
  colliculi inferioris (brachium of the inferior colliculus)
  colliculi superioris (brachium of the superior colliculus)
  conjunctivum (brachium conjunctivum)
  pontis (brachium pontis)
bulbus olfactorius (olfactory bulb)

canalis centralis spinalis (central canal)
capsula interna (internal capsule)
  crus anterius (anterior limb)
  crus posterius (posterior limb)
  genu (genu)
  pars retrolenticularis (retrolenticular portion)
caput nuclei caudati (head of caudate nucleus)
cauda nuclei caudati (tail of caudate nucleus)
cavum trigeminale (trigeminal cave)
cellulae mastoideae (mastoid air cells)
chiasma opticum (optic chiasm)
cisterna
  ambiens (ambient cistern)
  cerebellomedullaris (cerebellomed ullary cistern)
  chiasmatis (chiasmatic cistern)
  cruralis (crural cistern)
  fossae lateralis cerebri (sylvian cistern)
  interpeduncularis (interpeduncular cistern)
  laminae terminalis (cistern of the lamina terminalis)
  magna (cisterna magna)
  medullaris
  pars lateralis (lateral medullary cistern)
  pars medialis (premedlillary cistern)
  peri callosa (supracallosal cistern)
  pontis
  pars lateral is (cerebellopontine cistern)
  pars medialis (prepontine cistern)
  pontocerebellaris (cerebellopontine cistern)
  quadrigemina (quadrigeminal cistern)
  veli interpositi (cistern of velum interpositum)
claustrum (claustrum)
clava (clava)
clivus (clivus)
colliculus
  facialis (facial colliculus)
  inferior (inferior colliculus)
  superior (superior colliculus)
columna fornicis (column of fornix)
commissura
  anterior (anterior commissure)
  interhabenularis (habenular commissure)
  posterior (posterior commissure)
condylus occipitalis (occipital condyle)
confluens sinuum (confluens sinuum)
cornu
  ammonis (cornu ammonis)
copia (cornucopia)
corpus
callosum (corpus callosum)
  geniculatum laterale (lateral geniculate body)
  geniculatum mediale (medial geniculate body)
  mamillare (mamilIary body)
  parabigeminum (parabigeminal nucleus)
  pineale (pineal gland)
  pontobulbare (corpus pontobulbare)
  restiforme (restiform body)

- trapezoidum (trapezoid body)
- cortex cerebelli (cerebellar cortex)
- crus
- cerebri (crus cerebri)
  - fornicis (crus fornicis)
  - primum lobuli ansiformis (crus I)
  - secundum lobuli ansiformis (crus II)
- culmen (culmen)
- cuneus (cuneus)

- declive (declive)
- decussatio
  - pedunculorum cerebellarium superium (decussation of superior cerebellar peduncles)
  - pyramidum (decussation of pyramids)
- diencephalon (diencephalon)
- digitationes hippocampi (hippocampal digitations)
- dorsum sellae (dorsum sellae)

- eminentia
  - collateralis (collateral eminence)
  - mediana tuberis (median eminence of tuber)

- falx cerebri (falx cerebri) fasciculus
  - cuneatus (cuneate fasciculus)
  - (gracile fasciculus)
  - lenticularis (lenticular fasciculus)
  - longitudinalis
  - dorsalis (dorsal longitudinal fasciculus)
  - medialis (medial longitudinal fasciculus)
  - thalamicus (thalamic fasciculus)
- fibrae
  - cerebello-thalamicae (cerebello(rubro) thalamic fibers)
  - nervi abducensis (fibers of abducens nerve)
  - nervi facialis (fibers of facial nerve)
  - nervi glossopharyngei (fibers of glossopharyngeal nerve)
  - nervi hypoglossi (fibers of hypoglossal nerve)
  - nervi oculomotorii (fibers of oculomotor nerve)
  - nervi trigemini (fibers of trigeminal nerve)
  - nervi vagi (fibers of vagus nerve)
  - nigrostriatales (nigrostriate fibers)
  - pontocerebellares (pontocerebellar fibers)
  - trigeminocerebellares (trigeminocerebellar fibers)
- fimbria (fimbria)
- fissura
  - ansoparamediana (ansoparamedian fissure)
  - centralis (central fissure)
  - horizontalis (Great horizontal fissure)
  - intraBiventralis (intrabiventral fissure)
  - lateralis (lateral fissure)
  - parieto-occipitalis (parieto-occipital fissure)
  - postcentralis (postcentral fissure)
  - posterolateralis (posterolateral fissure)
  - postnodularis (postnodular fissure)
  - postpyramidalis (postpyramidal fissure)
  - praecentralis (precentral fissure)
  - praeculminata (preculminal fissure)
  - praepyramidalis (prepyramidal fissure)
  - prima (primary fissure)
  - secunda (secondary fissure)
  - superior anterior (anterior superior fissure)
  - superior posterior (posterior superior fissure)
  - transversa cerebri (transverse fissure)
- flocculus (flocculus)
- folium vermis (folium of vermis)
- foramen
  - caecum (foramen caecum)
  - jugulare (jugular foramen)
  - magnum (foramen magnum)
- formatio reticularis (reticular formation)
- fornix (fornix)
- fossa
  - cranii posterior (posterior cranial fossa)
  - interpeduncularis (interpeduncular fossa)
  - rhomboidea (rhomboid fossa)
- fovea
  - inferior (fovea inferior)
  - superior (fovea superior)
  - trigemini (fovea trigemini)
- frenulum veli (frenulum veli)
- funiculus separans (funiculus separans)

- genu nervi facialis (genu of facial nerve)
- globus pallidus (globus pallidus)
  - pars lateralis (globus pallidus, pars lateralis)
  - pars medialis (globus pallidus, pars medialis)
- griseum centrale mesencephali (periaqueductal gray matter)
- gyrus
  - ambiens (gyrus ambiens)
  - cinguli (cingulate gyrus)
  - dentatus (gyrus dentatus)
  - descendens (gyrus descendens)
  - fusiformis (fusiform gyrus)
  - lingualis (lingual gyrus)
  - occipitalis
    - medius (middle occipital gyrus)
  - orbitalis
    - medialis (medial orbital gyrus)
    - posterior (posterior orbital gyrus)
    - parahippocampalis (parahippocampal gyrus)
    - rectus (gyrus rectus)
    - subcallosus (subcallosal gyrus)
  - temporalis
    - inferior (inferior temporal gyrus)
    - medius (middle temporal gyrus)
    - superior (superior temporal gyrus)

- habenula (habenula)
- hippocampus (hippocampus)
- hypophysis
  - lobus anterior (anterior lobe of the hypophysis)
  - lobus posterior (posterior lobe of the hypophysis)

hypothalamus (hypothalamus)
incisura
  praeoccipitalis (temporo-occipital incisure)
  tentorii (incisura tentorii)
infundibulum (infundibulum)
insula (insula)
isthmus gyri cinguli (isthmus)

lamina terminalis (lamina terminalis) lemniscus
lateralis (lateral lemniscus)
  medialis (medial lemniscus)
  trigeminalis (trigeminal lemniscus)
ligula (ligula)
limen insulae
lingula cerebelli (lingula)
lobulus
  ansiformis (ansiform lobule)
  Biventer (biventral lobule)
  centralis (central lobule)
  digastricus (digastric lobule)
  (gracile lobule)
  paramedianus (paramedian lobule)
  quadrangularis (quadrangular lobule)
    pars anterior (anterior quadrangular lobule)
    pars posterior (posterior quadrangular lobule)
  semilunaris inferior (inferior semilunar lobule)
  semilunaris superior (superior semilunar lobule)
  simplex
lobus
  anterior cerebelli (anterior cerebellar lobe)
  flocculonodularis (flocculonodular lobe)
  frontalis (frontal lobe)
  occipitalis (occipital lobe)
  parietalis (parietal lobe)
  posterior cere belli (posterior cerebellar lobe)
  temporalis (temporal lobe)
locus coeruleus (locus coeruleus)

meatus
  acusticus externus (external acoustic meatus)
  acusticus internus (internal acoustic meatus)
medulla oblongata (medulla)
membrana tectoria (membrana tectoria)
mesencephalon (mesencephalon)

neocerebellum (neocerebellum)
nervus
  abducens (abducens nerve)
  accessorius (accessory nerve)
  facialis (facial nerve)
  glossopharyngeus (glossopharyngeal nerve)
  hypoglossus (hypoglossal nerve)
  intermedius (nervus intermedius)
  oculomotorius (oculomotor nerve)
  opticus (optic nerve)
  trigeminus (trigeminal nerve)
    radix motoria (motor root of trigeminal nerve)
    radix sensoria (sensory root of trigeminal nerve)
  trochlearis (trochlear nerve)
  vagus (vagus nerve)
  vestibulocochlearis (vestibulocochlear nerve)
nodulus (nodulus)
nuclei
  pontis (pontine nuclei)
  septi (septal nuclei)
nucleus
  accessorius (accessory nucleus)
  accessorius nervi oculomotorii (accessory oculomotor nucleus)
  accumbens (Nucleus accumbens septi)
  ambiguus (nucleus ambiguus)
  arcuatus (arcuate nucleus)
  caudatus (caudate nucleus)
  coeruleus (nucleus coeruleus)
  cochlearis
    dorsalis (dorsal cochlear nucleus)
    ventralis (ventral cochlear nucleus)
  corporis trapezoidei (nucleus of trapezoid body)
  cuneatus (cuneate nucleus)
    lateralis (lateral cuneate nucleus)
    medialis (medial cuneate nucleus)
  darkschewitschi (nucleus of Darkschewitsch)
  dentatus (dentate nucleus)
  dorsalis motorius nervi vagi (dorsal motor vagal nucleus)
  emboliformis (emboliform nucleus)
  fastigii (fastigial nucleus)
  gelatinosus nervi vagi (nucleus gelatinosus)
  globosus (globose nucleus)
  gracilis (gracile nucleus)
  habenulae (habenular nucleus)
  hypothalami
    dorsomedialis (dorsomedial hypothalamic nucleus)
    paraventricularis (paraventricular hypothalamic nucleus)
    supra-opticus (supra-optic hypothalamic nucleus)
    ventromedialis (ventromedial hypothalamic nucleus)
  intercalatus (nucleus intercalatus)
  intercollicularis (intercollicular nucleus)
  interpeduncularis (interpeduncular nucleus)
  interpositus (nucleus interpositus)
  interstitialis (interstitial nucleus)
  interstitialis rostralis fasciculi longitudinalis
    medialis (rostral interstitial nucleus)
    lacrymalis (lachrymal nucleus)
  lemnisci lateralis (nucleus of lateral lemniscus)
    dorsalis (dorsal nucleus of lateral lemniscus)
    ventralis (ventral nucleus of lateral lemniscus)
mesencephalicus nervi trigemini (mesencephalic trigeminal nucleus)
motorius nervi trigemini (motor trigeminal nucleus)

nervi abducensis (abducens nucleus)
nervi facialis (facial nucleus)
nervi hypoglossi (hypoglossal nucleus)

nervi trochlearis (trochlear nucleus)
oculomotorius (oculomotor nucleus)
  caudalis centralis (caudal central)
  principalis (principal)
olivaris accessorius dorsalis (dorsal accessory olivary nucleus)
olivaris accessorius medialis (medial accessory olivary nucleus)
olivaris inferior principalis (inferior olivary nucleus)
olivaris superior (superior olivary nucleus)
ovalis (nucleus ovalis)

parabrachialis lateralis (lateral parabrachial nucleus)
parabrachialis medialis (medial parabrachial nucleus)
parafascicularis (parafascicular thalamic nucleus)
paralemniscalis (nucleus paralemniscalis)
prepositus hypoglossi (nucleus prepositus)

raphes dorsalis (dorsal nucleus of raphe)
raphes magnus (nucleus raphe magnus)
raphes obscurus (nucleus raphe obscurus)
raphes pallidus (nucleus raphe pallidus)
raphes pontis (nucleus raphe pontis)
reticularis
  centralis superior (nucleus reticularis centralis superior)
  cuneiformis (nucleus reticularis cuneiformis)
  funiculi lateralis (nucleus reticularis funiculi lateralis)
  gigantocellularis (nucleus reticularis giganto cellularis)
  medullae oblongatae centralis (nucleus reticularis medullae oblongatae centralis)
  parvocellularis (nucleus reticularis parvocellularis)
  pedunculopontinus (nucleus reticularis peduncu lopontinus)
  pontis caudalis (nucleus reticularis pontis caudalis)
  pontis oralis (nucleus reticularis pontis oralis)
  tegmenti pontis (nucleus reticularis tegmentipontis)
  retroambiguus (nucleus retroambiguus)
ruber (red nucleus)
  pars magnocellularis (magnocellular portion of red nucleus)
  pars parvocellularis (parvocellular portion of red nucleus)

salivatorius (salivatory nucleus)
  inferior (inferior salivatory nucleus)
  superior (superior salivatory nucleus)
sensorius principalis nervi trigemini (principal sensory trigeminal nucleus)
solitarius (nucleus of the solitary tract)
spinalis nervi trigemini (spinal trigeminal nucleus)
  pars caudalis (pars caudalis of the spinal trigeminal nucleus)
nucleus
spinalis nervi trigemini (spinal trigeminal nucleus)
  pars interpolaris (pars interpolaris of the spinal trigeminal nucleus)
  pars oralis (pars oralis of the spinal trigeminal nucleus)
subcoeruleus (nucleus subcoeruleus)
sublingualis (nucleus sublingualis)
subthalamicus (subthalamic nucleus)
supraspinalis (nucleus supraspinalis)
tegmentalis dorsalis (dorsal tegmental nucleus)
terminalis (terminal nucleus)
thalami
  anterior (anterior thalamic nucleus)
  centromedianus (centromedian thalamic nucleus)
  dorsomedialis (dorsomedial thalamic nucleus)
  lateralis dorsalis (lateral dorsal thalamic nucleus)
  lateralis posterior (lateral posterior thalamic nucleus)
  ventralis anterior (ventral anterior thalamic nucleus)
  ventralis lateralis (ventral lateral thalamic nucleus)
  ventralis posterolateralis (ventral posterolateral thalamic nucleus)
  ventralis posteromedialis (ventral posteromedial thalamic nucleus)
thoracicus (nucleus thoracicus) vestibularis (vestibular nucleus)
  inferior (inferior vestibular nucleus)
  lateralis (lateral vestibular nucleus)
  medialis (medial vestibular nucleus)
  superior (superior vestibular nucleus)

obex (obex)
oliva
  inferior (inferior olive)
  superior (superior olivary nucleus)
organum
  circumventriculare (circumventricular organ)
  subcommissurale (subcommissural organ)

paleocerebellum (paleocerebellum)
paraflocculus (paraflocculus)
paraflocculus accessorius (accessory paraflocculus)
pars
  basilaris ossis occipitalis (occipital basilar portion)
  petrosa ossis temporalis (temporal petrous portion)
pedunculus
  cerebellaris inferior (inferior cerebellar peduncle)
  cerebellaris medius (middle cerebellar peduncle)
  cerebellaris superior (superior cerebellar peduncle)
  flocculi (peduncle of flocculus)
  pes pedunculi (pes pedunculi)
plexus
  basilaris (basilar plexus)
  choroideus ventriculi quarti (choroid plexi of the fourth ventricle)
polus temporalis (temporal pole)
pons (pons)
  Caudatolenticular bridges of gray matter(pontes grisei caudatolenticulares)
processus
  clinoideus anterior (anterior clinoid process)
  condylaris mandibulae (mandibular condyle)
  mastoideus (mastoid process)
pulvinar (pulvinar)
putamen (putamen)

pyramis
  medullae oblongatae (pyramid of medulla)
  vermis (pyramid of vermis)

radix descendens vestibularis (vestibular descending root)
recessus
  infundibuli (infundibular recess)
  latera lis ventriculi quarti (lateral recess of the fourth ventricle)
  mesocoelicus (recessus mesocoelicus)
  pinealis (pineal recess)
  suprachiasmaticus (suprachiasmatic recess)
rhombencephalon (rhombencephalon)

sella turcica (sella turcica)
septum pellucidum (septum pellucidum)
sinus
  cavernosus (cavernous sinus)
  marginalis (marginal sinus)
  petros us superior (superior petrosal sinus)
  rectus (sinus rectus)
  sagittalis superior (superior sagittal sinus)
  sigmoideus (sigmoid sinus)
  sphenoidalis (sphenoidal sinus)
  transversus (transverse sinus)
splenium corporis callosi (splenium)
squama occipitalis (occipital bone, squama)
stria
  medullaris (stria medullaris thalami)
  olfactoria (olfactory stria)
    lateralis (lateral olfactory stria)
    medialis (medial olfactory stria)
  terminalis (stria terminalis)
striae medullares ventriculi quarti (striae medullares)
subiculum (subiculum)
substantia
  innominata (substantia innominata)
  nigra (substantia nigra)
  pars compacta (pars compacta of substantia nigra)
  pars reticulata (pars reticulata of substantia nigra)
  perforate anterior (anterior perforated substance)
  perforata posterior (posterior perforated substance)
sulcus
  basilaris pontis (basilar sulcus)
  calcarinus (calcarine sulcus)
  calcarinus anterior (anterior calcarine sulcus)
  centralis (central sulcus)
  cinguli (cingulate sulcus)
  collateralis (collateral sulcus)
  lateralis mesencephali (lateral mesencephalic sulcus)
  limitans (sulcus limitans)
  lingualis (lingual sulcus)
  occipitalis anterior (anterior occipital sulcus)
  pontomedullaris (pontomedullary sulcus)
  pontomesencephalicus (pontomesencephalic sulcus)
  subparietalis (subparietal sulcus)
  temporalis superior (superior temporal sulcus)
tectum mesencephali (tectum of mesencephalon)
tegmentum
  mesencephali (tegmentum of mesencephalon)
  pontis (pontine tegmentum)
tela choroidea ventriculi quarti (tela choroidea inferior)
telencephalon (telencephalon)
tentorium cerebelli (tentorium cerebelli)
tonsilla cere belli (tonsil)
tuba auditiva (auditory tube)
tractus
  corticobulbaris (corticobulbar tract)
  corticopontinus (corticopontine tract)
  corticonuclearis (corticonuclear tract)
  corticospinalis (corticospinal tract)
  lateralis (lateral corticospinal tract)
  ventralis (ventral corticospinal tract)
  cuneocerebellaris (cuneocerebellar tract)
  frontopontinus (frontopontine tract)
  habenulo-interpeduncularis (habenulo-interpeduncular tract)
  mammillothalamicus (mammillothalamic tract)
  mesencephaIicus nervi trigemini (mesencephalic trigeminal tract)
  olfactorius (olfactory tract)
  opticus (optic tract)
  pari eto tem p orop ontin us (parieto tern porop on tine tract)
  pyramidalis (pyramidal tract)
  reticulospinalis (reticulospinal tract)
  lateralis (lateral reticulospinal tract)
  medialis (medial reticulospinal tract)
  rubrospinalis (rubrospinal tract)
  solitarius (solitary tract)
  spinalis nervi trigemini (spinal trigeminal tract)
  spinocerebellaris (spinocerebellar tract)
    dorsalis (dorsal spinocerebellar tract)
    ventralis (ventral spinocerebellar tract)
  spino-olivaris (spino-olivary tract)
  spinoreticularis (spinoreticular tract)
  spinoreticulothalamicus (spinoreticulothalamic tract)
  spinothalamicus (spinothalamic tract)
  tectospinalis (tectospinal tract)
  tegmentalis centralis (central tegmental tract)
  trigeminothalamicus (trigeminothalamic tract)
  dorsalis (dorsal trigeminothalamic tract)
  ventralis (ventral trigeminothalamic tract)
  vestibulospinalis (vestibulospinal tract)
trigonum
  lemnisci (lemniscal trigone)
  nervi hypoglossi (hypoglossal trigone)
  nervi vagi (vagal trigone)
truncus cerebri (brain stem)
tuber
  cinereum (tuber cinereum)
  vermis (tuber of vermis)

tuberculum
  acusticum (acoustic tubercle)
  nuclei cuneati (cuneate tubercle)
  nuclei gracilis (gracile tubercle)

uncus (uncus)
uvula vermis (uvula)

vallecula cerebelli (vallecula)
velum medullare
  inferius (inferior medullary velum)
  superius (superior medullary velum)
vena
  basilis (basal vein)
  cerebelli anterior (anterior cerebellar vein)
  cerebri interna (internal cerebral vein)
  cerebri magna (great cerebral vein)
  communicans posterior (posterior communicating vein)
  interpeduncularis (interpeduncular vein)
  jugularis interna (internal jugular vein)
vena
  marginalis ventriculi quarti (marginal vein of the fourth ventricle)
  medullaris lateralis (lateral medullary vein)
  medullaris mediana anterior (anterior median medullary vein)
  medullaris mediana posterior (posterior median medullary vein)
  mesencephalica lateralis (lateral mesencephalic vein)
  pedunculi cerebellaris superioris (vein of the superior cerebellar peduncle)
  petrosa superior (superior petrosal vein)
  pontis lateralis (lateral pontine vein)
  pontis mediana anterior (anterior median pontine vein)
  pontis transversa (tranverse pontine vein)
  precentralis (precentral vein)
  sulci pontomedullaris (vein of the pontomedullary sulcus)
  sulci pontomesencephalicus (vein of the ponto mesencephalic sulcus)
ventriculus
  lateralis (lateral ventricle)
  cornu frontale (frontal horn of the lateral ventricle)
  cornu occipitale (occipital horn of lateral ventricle)
  cornu temporale (temporal horn of lateral ventricle)
  quartus (fourth ventricle)
  tertius (third ventricle)
vermis cerebelli (vermis)
vinculum lingulae (vinculum lingulae)

zona incerta (zona incerta)

SUBJECT INDEX

For ease of use, this subject index has been categorized hierarchically. For example, "pulvinar" is not listed as its own entry. Instead, it is listed under the heading "nucleus," first order subheading "thalamic," and second order subheading „pulvinar." This system will enable the reader to more easily find anatomy related to known index structures.

In this index each item may have up to four types of references. These consistently appear in the following order:

1. Section references (**S**).
   These indicate sections or section pages that explain significant aspects of the subject referenced. For example: "S III p97" indicates data in Section III on page 97.
2. Text references (**T**).
   These indicate that text explaining fundamental properties of the subject is contained on a specific page, or within a figure legend. For example: "**T** p34" or "**T** 8.40" indicates that the data are given on page 34 or within the legend of Fig. 8.40.
3. Table references (Table).
   These indicate that the subject is included or summarized in a specific table (e.g., "**Table** 1.2").
4. Figure references (**F**).
   These plentiful references indicate that the structure is specifically labeled on that image. The associated text may be ancil lary or descriptive. For example: "**F** 2.22" indicates that the structure is labeled on Fig. 2.22.

References of each type are grouped together, separated by commas. References of different types are separated by semi-colons. Ranges are indicated with "to." If numerous relevant figures follow the first, the first figure of the series is cited specifically, followed by "ff" (for "following folia"). When a structure runs through many adjacent images, the additional notation "(many)" may follow the "ff."

T